

Acute and Chronic Tubulointerstitial Nephritis

Terminology 1111

Incidence 1112

Etiologic agents, causes, and classification 1112

Clinical features of primary tubulointerstitial nephritis 1112

Pathology of primary tubulointerstitial nephritis 1113

Acute tubulointerstitial nephritis 1113

Chronic tubulointerstitial nephritis 1115

Pathogenesis of tubulointerstitial nephritis 1118

Tubulointerstitial nephritis associated with drug reactions 1119

Clinical features 1119

Pathology 1119

Etiology and pathogenesis 1120

Clinical course 1121

Specific agents 1121

Tubulointerstitial nephritis mediated by immunologic mechanisms 1134

Tubulointerstitial nephritis with anti-tubular basement membrane antibodies 1134

Tubulointerstitial nephritis with immune complexes 1136

Tubulointerstitial nephritis with cellular (mainly T-cell) mechanisms 1143

Tubulointerstitial nephropathy associated with metabolic disorders or monoclonal gammopathies 1146

Tubulointerstitial nephropathy associated with heavy metal exposure 1146

Lead nephropathy 1146

Cadmium nephropathy 1147

Mercury nephropathy 1148

Miscellaneous heavy metal nephropathy 1149

Tubulointerstitial nephropathy associated with hereditary diseases 1150

Familial tubulointerstitial nephritis with hypokalemia 1150

Chronic tubulointerstitial nephritis secondary to mitochondrial abnormalities 1150

Tubulointerstitial nephropathy associated with miscellaneous disorders 1151

Systemic karyomegaly 1151

Balkan endemic nephropathy 1151

Aristolochic acid (Chinese herb) nephropathy 1153

Idiopathic tubulointerstitial nephritis 1154

TERMINOLOGY

Cellular and fluid exudation in the interstitial tissue was noted by Councilman in 1898, while he studied kidneys of patients who died of scarlet fever and diphtheria (1). Councilman also determined that these kidneys did not contain bacteria (they were sterile). He called the condition acute interstitial nephritis (AIN). The term *interstitial nephritis* connotes predominant involvement of the renal interstitium and tubules by inflammatory cells, often with edema or fibrosis and tubular atrophy. Because interstitial nephritis is commonly accompanied by variable tubular damage, the term *tubulointerstitial nephritis* (TIN), or *tubulointerstitial nephropathy*, is preferable and is often used interchangeably with interstitial nephritis. TIN has two common clinical presentations: sudden onset and rapid decline in renal function—*acute TIN*—and protracted onset with slow decline in renal function—*chronic TIN*. Because chronic TIN may present with prominent fibrosis and few inflammatory cells, the term *chronic tubulointerstitial fibrosis*, or *chronic tubulointerstitial nephropathy*, is used by some. *Tubulitis* refers to infiltration of the tubular epithelium by leukocytes, usually mononuclear cells. Acute TIN, with time, can evolve into chronic TIN; therefore, overlaps between these two entities often exist.

The term *primary TIN* refers to cases where the inflammation is essentially limited to the tubules and interstitium; glomeruli and vessels are uninvolved or show minor changes. *Secondary TIN* implies tubulointerstitial inflammation associated with a primary glomerular, vascular, or systemic disease. *Idiopathic TIN* is a primary TIN whose etiologic agent or cause is unknown.

Reactive TIN connotes tubulointerstitial inflammation from the effects of systemic infections; the kidneys usually are sterile. *Infectious TIN* denotes tubulointerstitial inflammation from the effects of localization of live microorganisms in the kidney, where they can be identified and from which they often can be cultured.

Interstitial nephritis is commonly secondary to infection. These include acute and chronic pyelonephritis by bacteria or fungus, viral infection, and protozoal infections. Infection-associated interstitial nephritis is discussed in Chapter 24.

INCIDENCE

The exact incidence of TIN is unknown. Available figures vary by geographical area, entry criteria, and mode of diagnosis. While renal biopsy remains the gold standard for diagnosis of TIN, nephrologists are less likely to biopsy patients with clinical signs and symptoms of TIN than patients with glomerular diseases. Therefore, the diagnosis of TIN is often based on epidemiologic, clinical, and laboratory evaluations rather than renal biopsy findings (2). Also, mild forms of TIN may be overlooked, because of the absence or vagueness of clinical symptoms. Acute TIN accounts for approximately 3% of kidney biopsies, but this figure may be as high as 25% to 27% in adult patients with acute kidney injury (AKI) (3). In children, acute TIN may account for up to 7% of patients with AKI (4).

It is important to establish the diagnosis of TIN through kidney biopsy for the following reasons: (a) Clinical and laboratory data alone often do not differentiate between TIN and other renal diseases attended by renal insufficiency or renal failure; (b) most acute tubulointerstitial nephritides can be successfully treated; (c) untreated acute TIN may result in interstitial fibrosis and irreversible renal injury; and (d) the use of molecular and other techniques discloses possible genetic abnormalities and the underlying mechanisms of tissue injury (5).

ETIOLOGIC AGENTS, CAUSES, AND CLASSIFICATION

TIN is best classified according to the underlying etiology. The classification that we follow in our outline has been modified from those of Churg et al. (6) and Colvin and Fang (7). Some causes of TIN, including infectious etiologies, are covered in other chapters. TIN is often multifactorial, and several etiologic agents or causes, such as concurrent infection and obstruction, may contribute to tubulointerstitial renal disease in the same patient. Drug-induced TIN is the most common type determined by kidney biopsy, accounting for more than two thirds of the cases. Infection-related TIN may account for up to 15% of cases, whereas idiopathic forms of TIN represent approximately 10% of cases (3,8–10). The etiologic agents and causes of TIN are varied but can be grouped into broad categories. Baker and

TABLE 25.1 Main etiologic and pathogenetic factors responsible for TIN

Drug toxicity
Heavy metals
Metabolic disorders
Hereditary disorders
Miscellaneous disorders
Idiopathic
Immunologic mechanisms
Anti-TBM antibodies
Immune complexes
Cellular mechanisms
Hypersensitivity

Pusey (8) pooled their data with two series from the literature (11,12). They found that the most frequent etiology of interstitial nephritis is drug related (71.1%), with antibiotics accounting for about a third of these cases. Infection caused 15.6% of interstitial nephritis cases, and 7.8% were idiopathic. TIN and uveitis syndrome (TINU) was responsible for 4.7% of cases, and only 0.8% of the biopsies were due to sarcoidosis. Similar data were observed by other authors as well (9). Among autoimmune interstitial nephritis, more and more attention is paid to IgG4-related TIN (13). The exact incidence of autoimmune interstitial nephritis, including IgG4-related TIN, is unknown, but it is likely that many of the so-called idiopathic interstitial nephritides represent a form of autoimmune interstitial nephritis.

The main etiologic/pathogenetic factors responsible for TIN are shown on Table 25.1.

CLINICAL FEATURES OF PRIMARY TUBULOINTERSTITIAL NEPHRITIS

Various nonspecific clinical and laboratory findings may occur depending, in part, on the underlying cause or portion of the nephron that is affected. AIN may develop at any age and may be associated with variable degrees of acute renal insufficiency. Acute renal failure tends to be more prominent in the elderly. Systemic manifestations of hypersensitivity, such as erythema, maculopapular skin rash, arthralgias, fever, and peripheral eosinophilia, may occur primarily in drug-induced AIN, but these findings are frequently absent. Urinalysis usually reveals microscopic hematuria. Very rarely, gross hematuria or red blood cell (RBC) casts may be seen. Typically, these patients have white blood cells (WBCs) in the urine, and urine cultures are negative (sterile pyuria). Eosinophils in the urine, particularly if this number is greater than 1% of the cells, are thought to be a very characteristic finding in AIN. However, recent publications suggest that the specificity of urine eosinophils may be overestimated. Thus, out of 62 patients with eosinophiluria, only 13 patients had acute TIN, with the sensitivity of 25% and positive predictive value of 3% (14). Ruffing et al. (15) addressed the diagnostic accuracy of this test. In a selected group of patients, in which the diagnosis of AIN was suspected by the nephrologist, the sensitivity of eosinophiluria was 40% and the specificity was 72% with a positive predictive

value of only 38%. The same authors also examined consecutive patients with WBC in the urine who did not have interstitial nephritis. Four of these patients had urinary eosinophils greater than 1%. Eosinophiluria is not uncommon in secondary forms of interstitial nephritis, particularly in those that are associated with crescentic glomerulonephritis (vasculitis).

Mild proteinuria, usually less than 1 g/24 hours, is frequently seen, but nephrotic-range proteinuria is rare. Nephrotic syndrome may occur if interstitial nephritis is associated with minimal change disease secondary to nonsteroidal anti-inflammatory drugs (NSAIDs). If the inflammation affects primarily the proximal tubule, it may result in renal glucosuria, aminoaciduria, phosphaturia, and uricosuria. If the distal tubule is primarily damaged, potassium secretion and sodium balance regulation suffer. Renal tubular acidosis may follow the damage of both distal and proximal tubules. It is worth noting that in many instances both the proximal and distal tubules are equally undergoing injury. Medullary inflammation may be associated with inappropriate urinary concentration and polyuria.

PATHOLOGY OF PRIMARY TUBULOINTERSTITIAL NEPHRITIS

The details of gross and histologic features underlying the pathology of tubulointerstitial nephritides associated with various agents or conditions are provided in the following sections.

In this section, we present an overview of the pathology of primary TIN. Pyelonephritis and other infection-related interstitial nephritides are discussed in Chapter 24.

Acute Tubulointerstitial Nephritis

Grossly, the kidneys are pale, edematous, and enlarged, with the degree of enlargement proportional to the extent of involvement. The external surface is smooth.

Microscopically, the cellular infiltration and edema are multifocal and vary in intensity. Although neutrophils are common in acute TIN, mononuclear cells, including lymphocytes and macrophages, also participate in inflammation and are usually the predominant cell types (Fig. 25.1). Drug reactions, such as those to antibiotics, are often associated with mononuclear cell infiltrates, including lymphocytes and frequently eosinophils. Most mononuclear cells in the inflammatory infiltrate are T cells (Fig. 25.2) (16,17). Overall, CD4⁺ T cells predominate relative to CD8⁺ T cells (17). However, in the report of Bender et al. (16), nine patients with drug-induced TIN had nephrotic-range proteinuria and predominance of CD8⁺ T cells in the interstitial infiltrate. Similarly, in the report of D'Agati et al. (18), CD8⁺ T cells outnumber CD4⁺ T cells in the interstitium in 22 of 26 biopsies of patients with lupus nephritis. It appears that CD8⁺ T cells are effectors of injury, whereas CD4⁺ cells play a predominantly regulatory role (19). In later stages of progressive tubulointerstitial disease, monocytes/macrophages tend to predominate (20). Eosinophils are

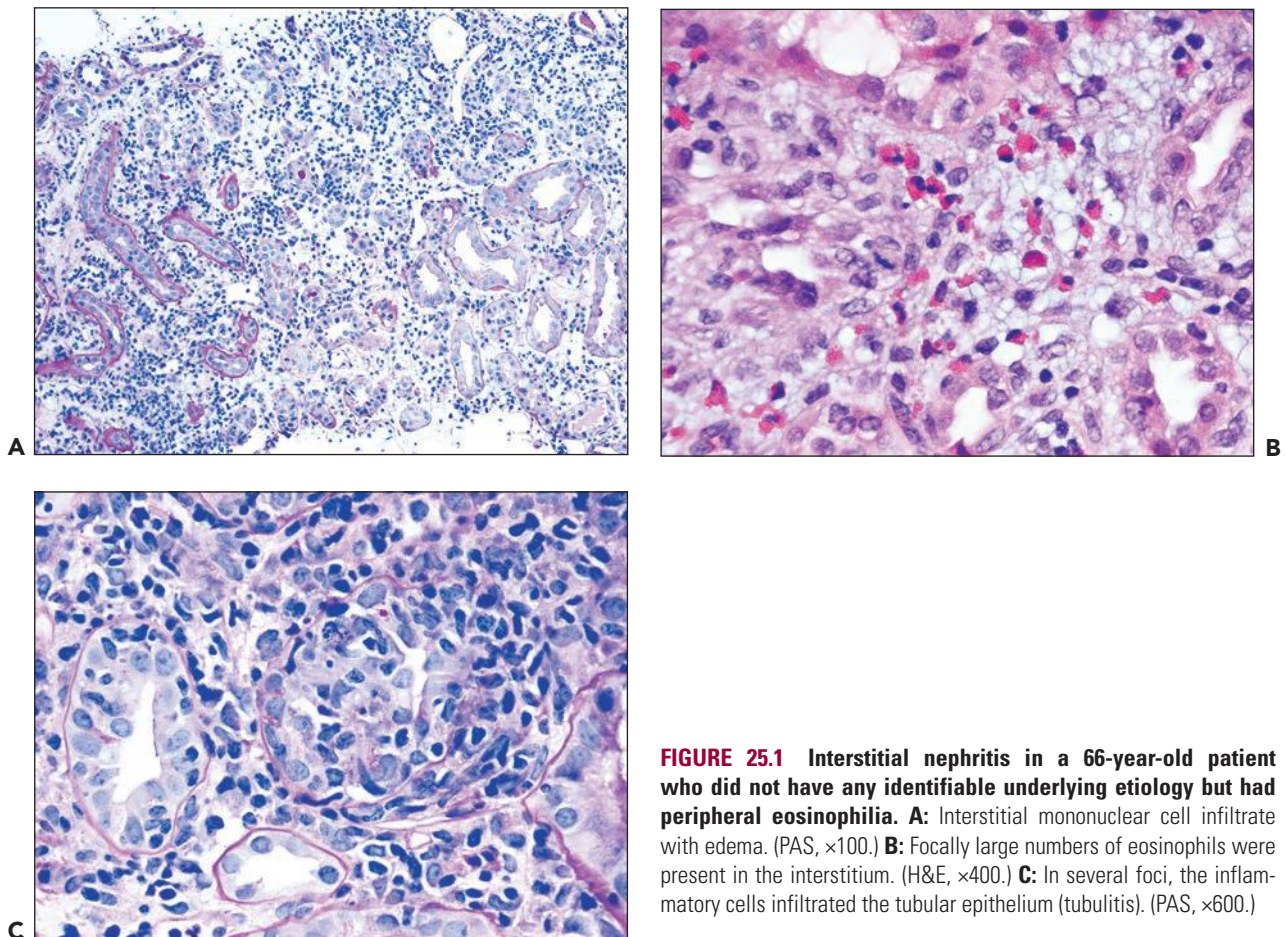


FIGURE 25.1 Interstitial nephritis in a 66-year-old patient who did not have any identifiable underlying etiology but had peripheral eosinophilia. **A:** Interstitial mononuclear cell infiltrate with edema. (PAS, $\times 100$.) **B:** Focally large numbers of eosinophils were present in the interstitium. (H&E, $\times 400$.) **C:** In several foci, the inflammatory cells infiltrated the tubular epithelium (tubulitis). (PAS, $\times 600$.)

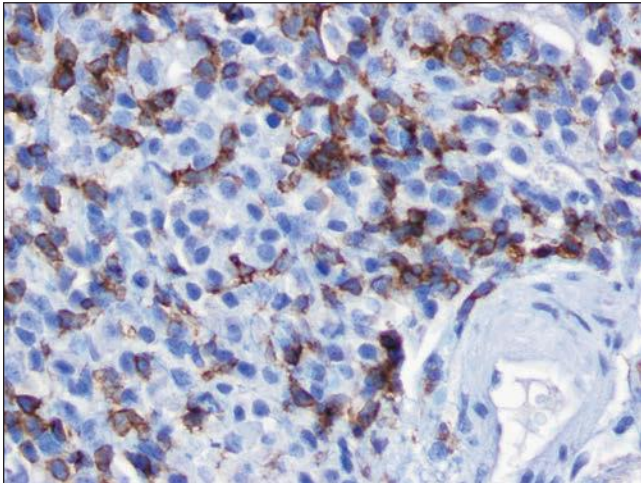


FIGURE 25.2 Immunohistochemistry reveals many T cells in the interstitial inflammatory cell infiltrate in this biopsy from a patient with Sjögren syndrome. (Immunoperoxidase with an anti-CD3 antibody, $\times 400$.)

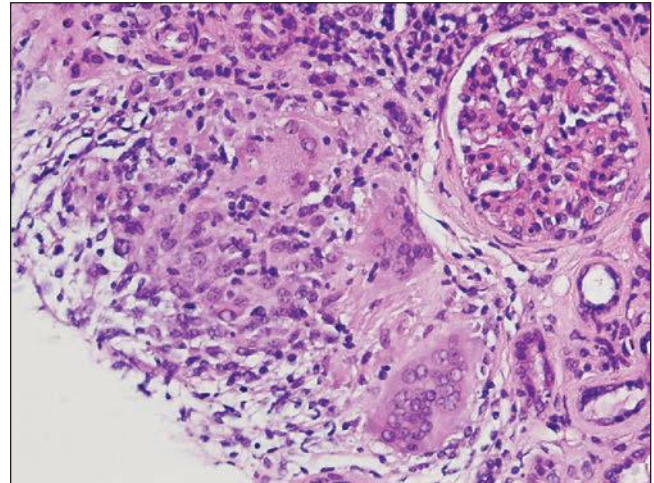


FIGURE 25.4 Granulomatous interstitial nephritis. Well-defined epithelioid granuloma with giant cells in the renal biopsy of a patient with sarcoidosis. (H&E, $\times 100$.)

common in drug-induced cases, but their absence does not exclude a drug-induced form of interstitial nephritis (21). After a few days or weeks have elapsed, a variable accumulation of plasma cells and histiocytes may be present (Fig. 25.3). Although not a common component of acute TIN, granuloma formation may occur in drug reactions, sarcoidosis, and idiopathic forms (Fig. 25.4) (3). If many plasma cells are seen, the diagnosis of IgG4-related interstitial nephritis should be considered, and an immunostain for IgG4 should be performed (13) (Fig. 25.5).

Tubular injury includes tubulitis (see Fig. 25.1C), breaks of tubular basement membrane (TBM), necrosis of tubular cells, and, later, atrophy and loss of tubules, depending on the stage of the disease. According to Ivanyi et al. (22), tubulitis more often involves the distal nephron. Biopsies taken several days after the initial insult show features of tubular cell

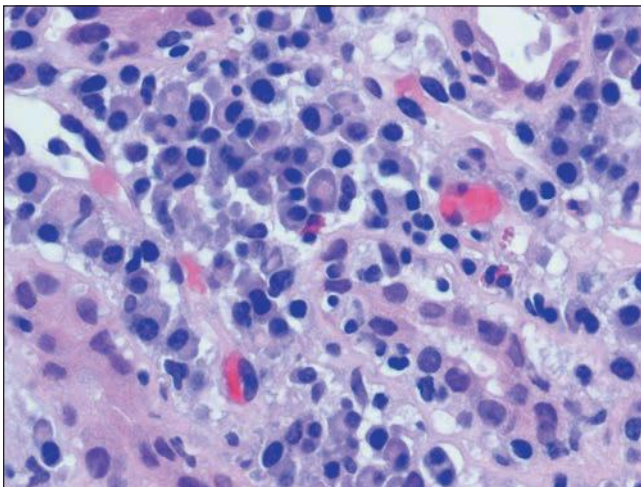


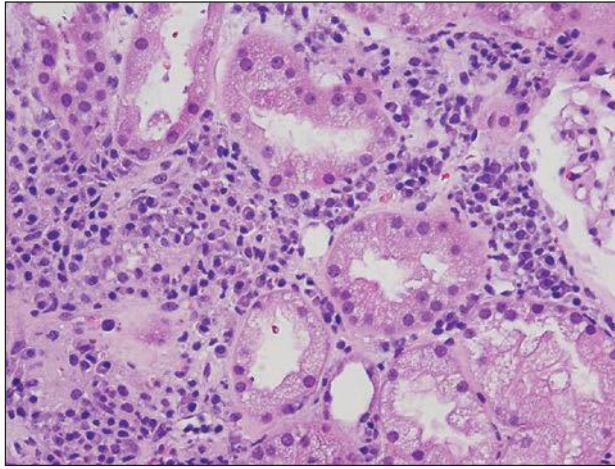
FIGURE 25.3 Many plasma cells in an acute and chronic interstitial nephritis, in a patient with Sjögren syndrome. (H&E, $\times 600$.)

regeneration, manifesting as flattening of the epithelial lining, cytoplasmic basophilia, and enlarged nuclei with frequent and prominent nucleoli. Nuclear changes may also be observed due to direct drug toxicity or in association with viral infections. Although not a common component of acute TIN, some interstitial fibrosis, as a part of the reparative process, may be seen in late biopsies. The presence of monocytes/macrophages and granulomas and some degree of fibrosis, encountered in some forms of acute TIN, emphasizes the overlap that exists between acute and chronic TIN (Figs. 25.4 and 25.6). Tamm-Horsfall protein (THP) may find its way into the interstitium following tubular rupture (Fig. 25.7). Interstitial THP is commonly found in nephron obstruction, but it is not exclusive to obstructive nephropathy.

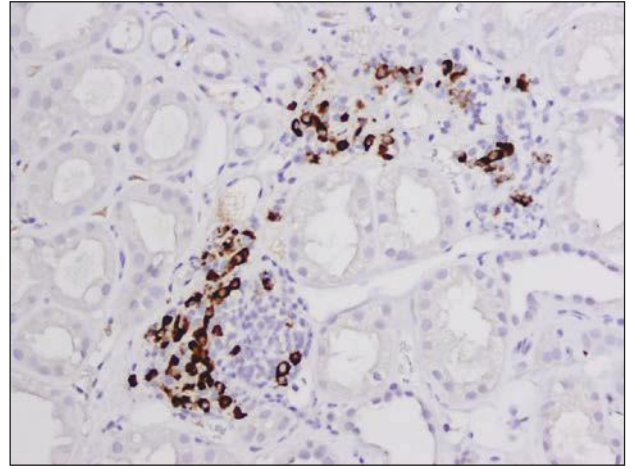
Immunofluorescence and immunohistochemical techniques may be helpful in the determination of the underlying etiology. Linear deposits of an immunoglobulin (usually IgG) and complement along the TBM suggest an antibody directed to or cross-reactive with the TBM. Granular deposits of an immunoglobulin and complement in the TBM, interstitium, or both suggest an immune complex pathogenesis. This is common in systemic lupus erythematosus (SLE) and IgG4-related interstitial nephritis (13,23). However, granular or linear TBM staining for complement (particularly C3) is a frequent nonspecific finding, especially in the basement membrane of atrophic tubules.

Electron microscopy is also of limited value in the diagnosis of interstitial nephritis. Ultrastructural examination may occasionally reveal electron-dense immune-type deposits along the TBM or in the interstitium, particularly if there is underlying SLE or IgG4-related disease. Crystalline inclusions in tubular epithelial cells or finely granular electron-dense deposits along the TBM indicate monoclonal immunoglobulin deposition. Crystalline inclusions may also be seen with cystinosis. Rarely, electron microscopy may be helpful in detecting viral particles in infected tubular epithelial cells.

In acute TIN, the glomeruli are mostly spared. Arterial and arteriolar changes are usually absent. When present in



A



B

FIGURE 25.5 IgG4-related interstitial nephritis. **A:** Numerous plasma cells are seen in interstitial inflammatory cell infiltrates. (H&E, $\times 200$.) **B:** Immunohistochemistry shows multiple IgG4-positive plasma cells. (Immunoperoxidase, $\times 200$.)

older persons, they are unrelated to the primary tubulointerstitial process and reflect aging, associated hypertension, or both.

The morphology of AIN is nonspecific, and only in rare instances is it possible to define the exact etiology. If typical viral inclusions are present or other microorganisms can be identified or if characteristic immune complex deposits are present, an etiologic diagnosis may be possible. A more detailed description of the morphologic findings will be given in this chapter in the section describing the different forms of AIN.

Chronic Tubulointerstitial Nephritis

Common causes of chronic TIN are infections, drug reactions (e.g., analgesics, lithium), urinary tract obstruction, sterile reflux of urine, some forms of immune-mediated TIN, plasma cell dyscrasias, metabolic disorders, exposure to heavy metals, hereditary diseases, and various chronic nephropathies, including idiopathic TIN. Chronic TIN always develops if a progressive

chronic primary glomerular disease is present. It is also a common finding in systemic disorders involving the kidney, including systemic autoimmune diseases, monoclonal gammopathies, and metabolic diseases. Vascular diseases are also frequently associated with chronic TIN, particularly vasculitis and chronic forms of thrombotic microangiopathies, but also ischemia secondary to atherosclerosis and hypertension can induce chronic tubulointerstitial injury with some degree of inflammation.

Grossly, kidneys with chronic TIN appear small, contracted, and pale. Variable papillary involvement, including papillary necrosis, sclerosis, and calcification, may be evident. The external surface is usually scarred, or finely granular from small vessel disease, compensatory hypertrophy of residual nephrons, or both. The corticomedullary junction is usually poorly demarcated. The intrarenal vessels are prominent and may have thickened walls.

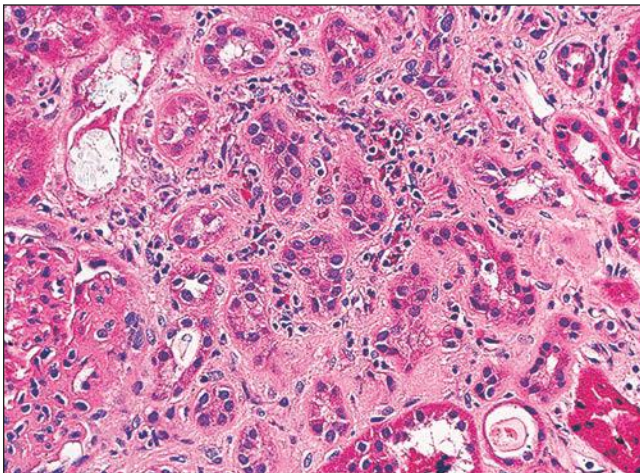


FIGURE 25.6 Active appearing interstitial inflammatory cell infiltrate with eosinophils in the background of interstitial fibrosis and tubular atrophy in a patient with a long history of gout and multiple medication use. (H&E, $\times 200$.)

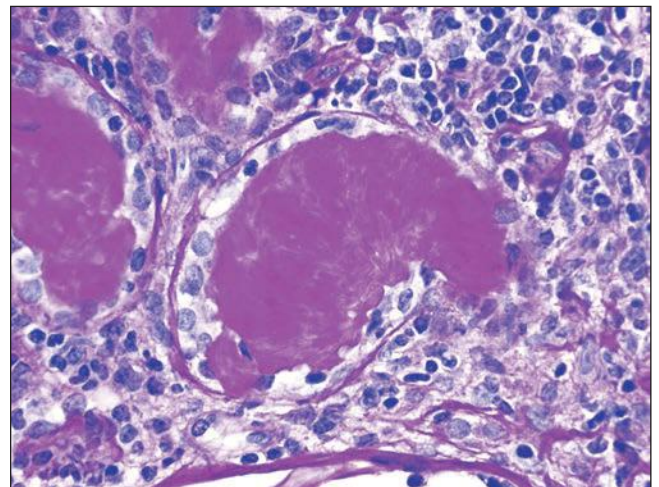


FIGURE 25.7 Tubular rupture with expulsion of Tamm-Horsfall protein from the tubule into the interstitium. Note the interstitial inflammatory cell infiltrate around the Tamm-Horsfall protein. This is a nonspecific finding that can occur in any renal injury with tubular disruption and secondary interstitial Tamm-Horsfall protein deposits. (PAS, $\times 400$.)

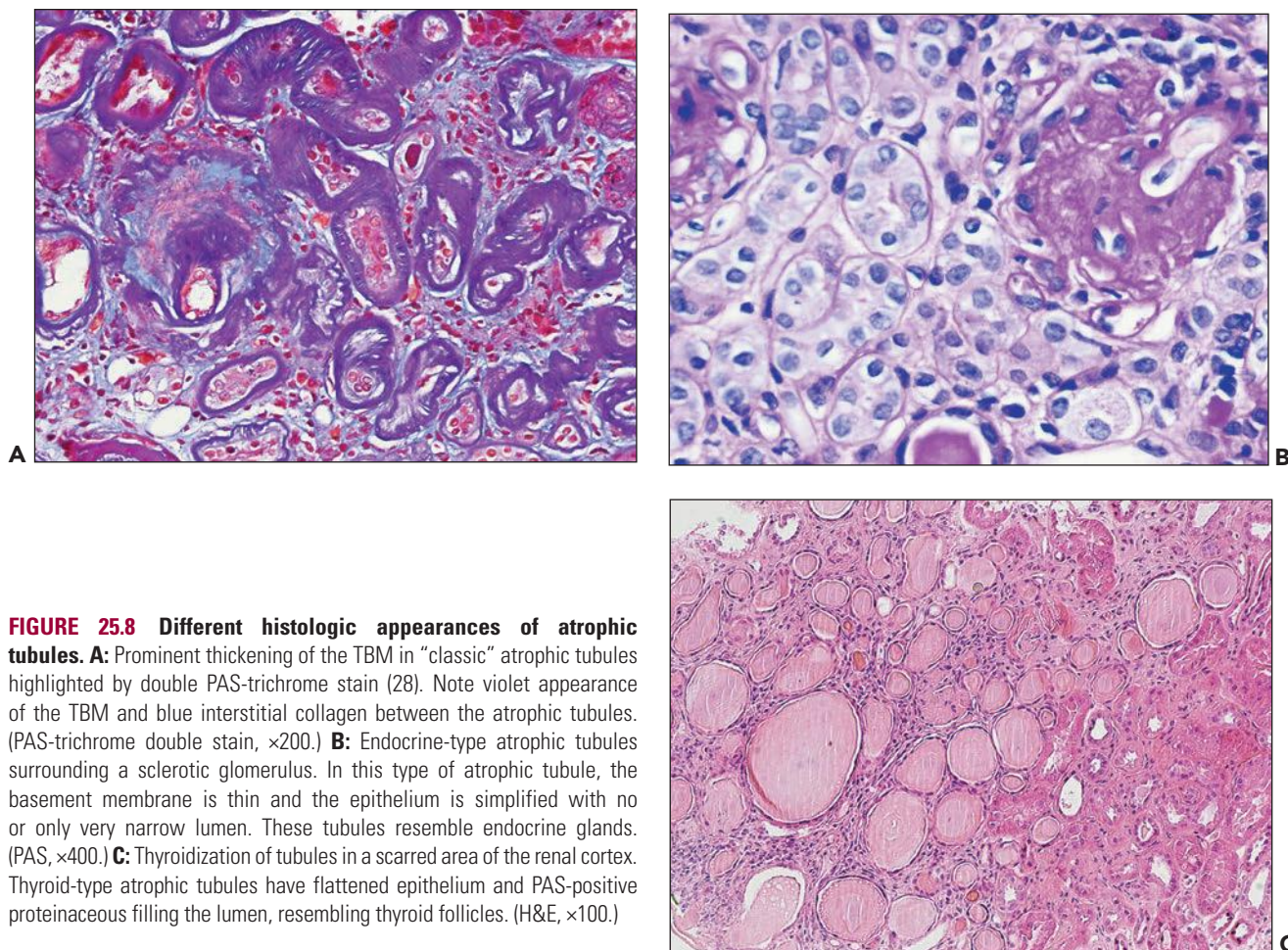


FIGURE 25.8 Different histologic appearances of atrophic tubules. **A:** Prominent thickening of the TBM in “classic” atrophic tubules highlighted by double PAS-trichrome stain (28). Note violet appearance of the TBM and blue interstitial collagen between the atrophic tubules. (PAS-trichrome double stain, $\times 200$.) **B:** Endocrine-type atrophic tubules surrounding a sclerotic glomerulus. In this type of atrophic tubule, the basement membrane is thin and the epithelium is simplified with no or only very narrow lumen. These tubules resemble endocrine glands. (PAS, $\times 400$.) **C:** Thyroidization of tubules in a scarred area of the renal cortex. Thyroid-type atrophic tubules have flattened epithelium and PAS-positive proteinaceous filling the lumen, resembling thyroid follicles. (H&E, $\times 100$.)

Microscopically, the inflammatory cell infiltrates are made up of variable numbers of lymphocytes, monocytes/macrophages, and plasma cells. Granulomas may be seen in TIN associated with drugs; infections with mycobacteria, fungi, and parasites; sarcoidosis; and vasculitis. Some are idiopathic (24–26). Tubular atrophy and interstitial fibrosis are the histologic hallmarks of chronic interstitial nephritis, usually associated with some degree of interstitial mononuclear cell infiltrate. Tubular atrophy has different morphologic subtypes (27) (Fig. 25.8). The most common type is the “classic” type: atrophic tubule with prominently thickened, frequently wrinkled, and lamellated basement membrane (see Fig. 25.8A). The “endocrine”-type atrophic tubule has a narrow lumen or no lumen at all, is usually prominently reduced in diameter, and has simplified epithelium and a thin basement membrane (see Fig. 25.8B). These “endocrine”-type atrophic tubules usually occur in clusters. The “thyroid”-type atrophic tubule has only mildly thickened basement membrane, a simplified flattened epithelium, and a lumen filled with eosinophilic Periodic acid–Schiff (PAS)-positive homogenous proteinaceous material; therefore, the tubule resembles a thyroid follicle (see Fig. 25.8C). These “thyroid”-type atrophic tubules also occur in clusters, and, in occasional cases of renal scarring, the parenchyma resembles thyroid gland. The diagnostic significance of these different types of atrophic tubules is somewhat limited. The endocrine-type atrophic tubule is frequently seen in chronic ischemia,

including renal artery stenosis. The thyroid-type atrophic tubule is a common finding in chronic pyelonephritic scars, but we have also frequently observed thyroidization of tubules in ischemic scars, including kidneys with interstitial fibrosis secondary to antiphospholipid antibodies.

In chronic tubulointerstitial injury, tubules frequently undergo compensatory hypertrophy, whatever the etiology. These hypertrophic tubules are lined usually with tall proximal-appearing tubular epithelial cells. The lumen is dilated and commonly irregular (Fig. 25.9). Microcystic dilation of tubules in scarred interstitial areas may also occur. These microcystic tubules usually have a thin simplified epithelium and are filled by proteinaceous homogeneous material. Sometimes, the microcysts may have a scalloped outline (Fig. 25.10).

Interstitial fibrosis, a characteristic feature of chronic TIN, must be considered according to location. In the cortex, the interstitial volume is uniform and composes approximately 7% of the cortical volume (29), whereas in the medulla, the interstitial space increases from the outer stripe of the inner medulla to the tip of the renal papilla. For example, in the rat kidney, the interstitial space at the base of the inner medulla is about 10% of the medullary space but attains 30% of the interstitial space at the tip of the papilla (30). Interstitial fibrosis may be multifocal or diffuse, and the deposited extracellular matrix is a combination of various types of collagens, including types I, III, and V, derived from interstitial fibroblasts. Other cells,

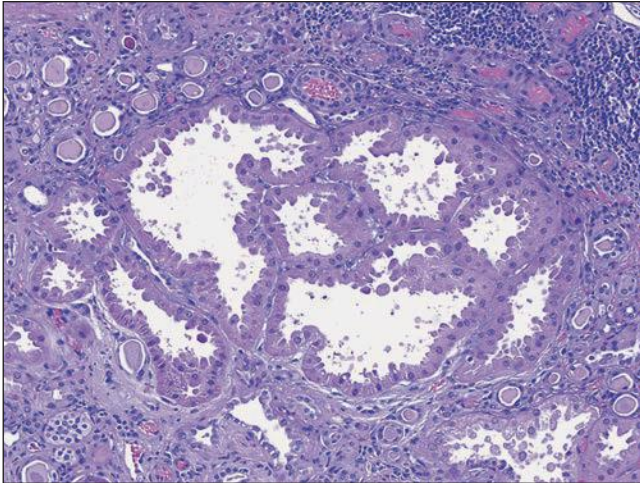


FIGURE 25.9 It is common to see large hypertrophic tubules with thick, hypertrophic epithelial lining in any type of advanced chronic renal injury. (H&E, $\times 100$.)

including tubular epithelial cells and endothelial cells, also contribute to the extracellular matrix deposition by producing fibronectin, type IV collagen, and a variety of other matrix proteins (31). Interstitial fibrosis and tubular atrophy are cardinal features for the diagnosis of chronic TIN because inflammatory cells may be scarce or absent.

Immunofluorescence and immunohistochemical techniques may be helpful in delineation of the pathogenic mechanisms in a few cases, in a manner similar to that already described for acute TIN. Granular deposits of immunoglobulin and complement along the TBM and interstitium may indicate tubulointerstitial injury mediated by immune complexes. But one has to remember that C3 deposition is a very common nonspecific finding in the basement membrane of atrophic tubules. Immunohistochemical techniques

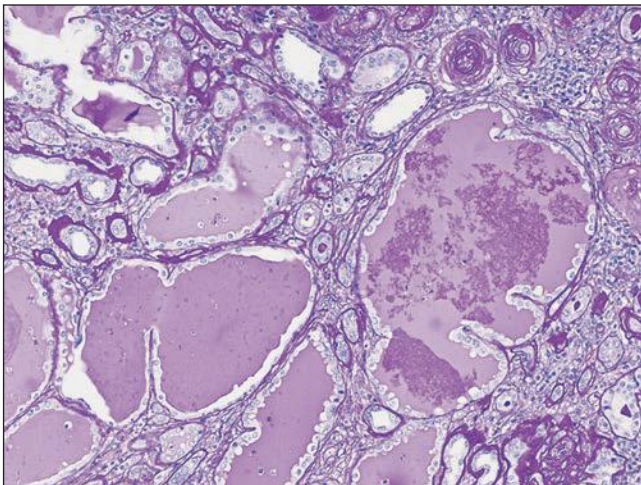


FIGURE 25.10 Microcystic dilation of tubules with scalloped outline. Such tubules can be seen in any kind of chronic tubulointerstitial injury. (PAS, $\times 100$.)

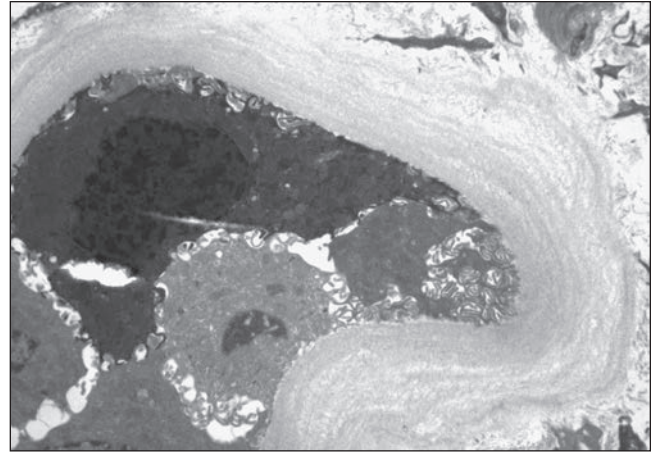


FIGURE 25.11 Thickened lamellated basement membrane of an atrophic tubule. (Uranyl acetate and lead citrate, $\times 3000$.)

also can be used to identify the segment of the nephron that is involved (32) to develop functional correlates of tissue injury. For example, when TIN involves predominantly the proximal tubules, proximal renal tubular acidosis (type II) develops owing to loss of proximal tubule resorbate (e.g., glucose, phosphate, uric acid, organic acids, low molecular weight proteins), with or without Fanconi syndrome. When distal tubules are predominantly involved, distal renal tubular acidosis (type I) develops, caused by failure of lowering the urinary pH, with or without hyperkalemia and salt wasting. When collecting ducts and papillary involvement predominate, water conservation is compromised by the decreased ability to concentrate urine. Molecular techniques have enabled the detection of deletions of genetic material as a possible cause of certain tubulointerstitial nephritides, such as the defect in the tubulointerstitial antigen gene in some children with progressive TIN (see later section in this chapter) (33).

Electron microscopy in chronic TIN has limited diagnostic value, as indicated above in the discussion of AIN. The basement membrane of atrophic tubules is not only thickened on ultrastructural examination but is frequently also lamellated. This lamellation is probably the result of repeated tubular epithelial injury and regeneration. The regenerating renal epithelium probably creates newer and newer thin layers of basement membrane material, which will lend a lamellated pattern to the thickened TBM (Fig. 25.11). Aggregates of granular to microspherical material in the thickened basement membranes of atrophic tubules are not uncommon (Fig. 25.12). This material should not be misinterpreted as immune complex deposition.

In contrast to acute TIN, in which glomeruli are usually spared, glomeruli in chronic TIN often show changes. These glomerular changes are frequently secondary to poor glomerular blood perfusion and include tuft wrinkling and collapse, thickening of the Bowman capsule, periglomerular fibrosis, and glomerular obsolescence. Glomeruli with periglomerular fibrosis are frequently, but not always, atubular (34). Occasionally, segmental glomerulosclerosis may develop. Arterial and arteriolar changes, such as intimal thickening and medial hyperplasia, are usually present and reflect aging and associated hypertension.

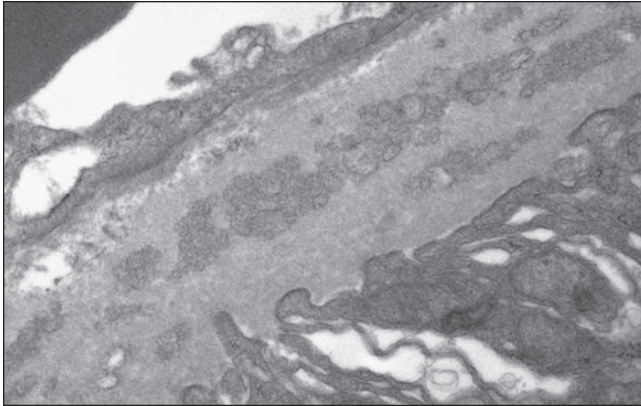


FIGURE 25.12 Deposits of granular to microspherical material in the TBM is a common finding in atrophic tubules. Under low magnification, these structures may be misinterpreted as electron-dense immune-type deposits in the TBM. (Uranyl acetate and lead citrate, $\times 20,000$.)

PATHOGENESIS OF TUBULOINTERSTITIAL NEPHRITIS

The pathogenic mechanisms operative in tubulointerstitial nephritides associated with various agents or conditions are provided in the sections to follow. In this section, we present a brief overview of pathogenic mechanisms that are specific for certain tubulointerstitial nephropathies and that are common to most forms of chronic tubulointerstitial nephropathies.

Reactive TIN appears to result from systemic release of lymphokines that are filtered and reabsorbed by the kidneys, thereby promoting chemoattraction and activation of mononuclear cells in the kidneys (1,7,35,36). *Infectious TIN* results from three basic mechanisms of tissue injury (37): microbial release of degradative enzymes and toxic molecules, direct contact or penetration of host cells by the microbe, and the inflammatory response mediated by antibodies, T cells, or both. The pathogenesis of infectious TIN and vesicoureteral reflux is covered in Chapter 24. *Drug-induced TIN* is most likely immunologically mediated. The most widely accepted theory is that drugs behave as haptens after binding to extrarenal proteins that later will be planted in the kidney or to renal proteins (38). This will be discussed in detail in the following section of this chapter. Drug-induced AIN occurs in only a small percentage of patients taking a medication and is not dose dependent, and exacerbation occurs after reexposure to the drug. Also, systemic signs of hypersensitivity may be evident.

TIN owing to anti-TBM antibodies involves predominantly IgG antibodies directed against different autoantigens in basement membranes, including a 54-kDa protein called TIN antigen, localized to chromosome 6p11.2-12 whose molecular composition has been cloned and sequenced (39). However, in our experience, true anti-TBM antibody-mediated interstitial nephritis is extremely rare, and we believe that the anti-TBM antibodies may form secondary to the tubular damage rather than causing it.

TIN owing to immune complexes involves predominantly IgG antibodies, which probably are generated against a variety of tubular antigens. It is possible that antibodies may form

against THP or megalin (a protein, localized in the brush border of proximal tubular epithelial cells), because immunization of rabbits or rats with those proteins resulted in AIN (40). IgG4-containing immune complexes are present along the TBM in IgG4-related interstitial nephritis; the pathologic role of these immune complexes is unclear (41). Tubulointerstitial injury may depend on complement activation by antibody (42), release of chemoattractants, and activation of leukocytes with release of chemokines, cytokines, proteases, and toxic oxygen radicals (36). In many forms of interstitial nephritis, eosinophils are prominent in the interstitium, which may be related to a chemotactic cytokine, eotaxin, produced locally by renal parenchymal cells (43).

TIN due to cell-mediated mechanisms encompasses two types of reactions. First, delayed-type hypersensitivity reaction, which requires prior sensitization and is caused by CD4⁺ T cells and macrophages, results in production of various lymphokines and may induce a granulomatous reaction. Second, cytotoxic T-cell injury, which requires no prior sensitization, is mediated by CD4⁺ and CD8⁺ T cells (26).

Tubulointerstitial inflammation, fibrosis, and tubular atrophy, common to most chronic tubulointerstitial nephropathies, can be induced by various agents and causes. If the underlying etiology is persistent and cannot be eliminated, eventually all etiologic agents will cause chronic tubulointerstitial injury. Various pathogenetic factors are involved in the generation of interstitial fibrosis and tubular atrophy, including ischemia, reactive oxygen species, toxic agents, or immunologic injury (44). It is likely that an important role in the common final pathway leading to fibrosis can be attributed to the transforming growth factor beta (TGF- β)/Smad3 signaling pathway (45–47). TGF- β is up-regulated in response to injurious stimuli by angiotensin II (47). This accounts, at least in part, for the beneficial effect of angiotensin convertase inhibition slowing the progression of chronic renal injury. TGF- β transmembrane receptors transduce downstream signals via cytoplasmic latent transcription factors called Smad proteins. Smad 2 and 3 are phosphorylated, and they bind to Smad 4 and translocate to the nucleus, where they act as transcriptional regulators of target genes. Disruption of the TGF- β /Smad signaling pathway inhibits interstitial fibrosis in experimental animals (45). Connective tissue growth factor (CTGF) is a downstream mediator of the profibrotic effects of TGF- β . Recent data indicate that CTGF may play a pivotal role in the pathogenesis of TGF- β -dependent interstitial fibrosis (48). There is growing evidence that TGF- β is also capable of inducing epithelial to mesenchymal transdifferentiation of renal tubular epithelial cells (Fig. 25.13) (49,50). The theory is that during tubular injury, activated, injured tubular epithelial cells migrate through TBM ruptures into the interstitium, where they lose their epithelial characteristics and gain mesenchymal markers, such as smooth muscle specific actin, and turn into myofibroblasts. This transdifferentiation process of the injured tubular epithelial cells may be a key pathogenetic step in the development of chronic interstitial nephritis; however, convincing in vivo evidence for tubular epithelial cell to mesenchymal transdifferentiation is still missing (50–52). Based on lineage analysis of mesenchymal cells during nephrogenesis in a mouse model, Humphreys et al. (52) recently proposed that expansion of pericytes is primarily responsible for the development of interstitial fibrosis.

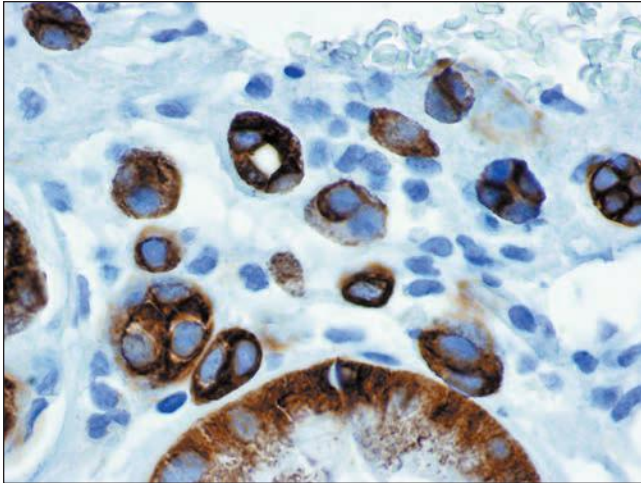


FIGURE 25.13 Scattered cyokeratin-positive cells are commonly found in the fibrotic renal interstitium. It is theoretically possible that these cyokeratin-positive cells represent cells undergoing epithelial-to-mesenchymal transformation. (Immunoperoxidase, $\times 600$.)

TUBULOINTERSTITIAL NEPHRITIS ASSOCIATED WITH DRUG REACTIONS

The kidney is adversely affected by a wide variety of therapeutic and diagnostic agents and toxic compounds. However, there are only a limited number of patterns of injury produced in the kidney. These may affect any of the compartments of the kidney including tubulointerstitial, glomerular, and vascular pathology (53,54). In the following section, we will focus only on acute and chronic TIN induced by drugs. Other patterns of renal injury associated with drug reaction, including acute tubular necrosis (ATN) and glomerular and vascular changes, will be discussed in other chapters.

It should be recognized that it is often difficult to establish a pathogenetic link between a pathologic lesion and a particular drug or toxin. Several factors contribute to this uncertainty, including concurrent factors that may produce renal injury, such as administration of several potentially nephrotoxic drugs at the same time, lack of or inadequacy of morphologic data in reported cases of drug toxicity, and the fact that some drugs may have multiple effects. Moreover, experimental models of toxicity may not be relevant to a particular clinical context because of interspecies variation and markedly different dosing of drugs in these models. In general, we limit our discussion to those drugs for which toxicity has been well documented in humans by disappearance of toxic effects when the drug is withdrawn, reoccurrence of symptoms on rechallenge, or both.

As pointed out earlier, today the most common form of interstitial nephritis is drug induced. Many drugs, including a range of widely used therapeutic agents, produce unpredictable idiosyncratic systemic reactions that may manifest in the kidney primarily as TIN.

Clinical Features

TIN caused by drug or toxin exposure develops in a few patients who receive the drug; reactions can sometimes be predicted if the patient has had a reaction to the same or

a similar agent. The reaction is generally unrelated to the cumulative dose of the drug. Exposure to the offending agent typically occurs days to a few weeks before the clinical presentation (10). Patients may show signs of a systemic syndrome that include fever, skin rash, eosinophilia, and arthralgias. However, only a few patients will have this classic constellation of symptoms (12). Affected individuals may note fluid retention or a fall in urine output, and occasionally, patients may experience back or flank pain (55). Many patients show symptoms of AKI.

Analysis of the urine typically reveals pyuria with numerous mononuclear cells, including lymphocytes and monocytes. There may also be eosinophils, which researchers have touted as a specific marker for allergic interstitial nephritis (56). However, eosinophiluria is not specific for drug-induced interstitial nephritis (14). Eosinophils may best be detected by the use of special stains, such as the Hansel stain (57). Hematuria is not uncommon and is usually microscopic. Mild proteinuria may also be detected, and proteinuria may occasionally be in the nephrotic range, especially in those cases caused by drugs that also produce minimal change disease in the glomeruli. NSAIDs most commonly cause this constellation of symptoms. Urine cultures are routinely negative.

Because the interstitial inflammatory process can result in tubular injury, there may be evidence of tubular dysfunction. Patients may have glycosuria, aminoaciduria, and phosphaturia; occasionally, Fanconi syndrome has been described (58). In addition, tubular acidosis, electrolyte losses, or concentrating defects may be documented. On ultrasound, the kidneys are seen to be of normal size or enlarged. The parenchyma is typically echogenic—a finding that has been correlated with the extent of inflammatory infiltrate (and with the development of long-term changes in the interstitium).

Patients may have renal dysfunction without other accompanying symptoms. Because drug-induced interstitial nephritis is eminently reversible in the early stages, it is important to recognize the etiologic agent, so that long-term damage can be avoided. Some drugs produce more insidious changes, resulting in protracted injury without an obvious acute phase. Classic examples are lithium and analgesic compounds. These patients may show initial signs of salt wasting or acid-base imbalances and evidence of progressive tubular injury.

Pathology

Gross Findings

In acute TIN, the kidney is usually pale and swollen. Areas of congestion and hyperemia may be seen at the corticomedullary junction. In chronic TIN, the kidney is smaller with thinning of the cortex. The surface of the kidney may become granular. Parenchymal cysts may develop as interstitial fibrosis progresses. The cortex may become pale due to a combination of fibrosis and inflammatory cells.

Light Microscopy

GLOMERULI

Glomeruli are typically spared. Occasionally, the interstitial inflammatory infiltrate may breach the Bowman capsule. In later stages of chronic interstitial nephritis, glomeruli may show nonspecific ischemic collapse and sclerosing changes. Periglomerular fibrosis is common in chronic cases.

INTERSTITIUM

In AIN, there are patchy or diffuse edema and inflammatory infiltrates. The infiltrate is predominantly mononuclear (see Fig. 25.1). Both CD4⁺ and CD8⁺ T cells have been detected in varying proportions. B cells and monocyte/macrophages can also be found. Eosinophils typically make up to 10% or less of the infiltrating cells. The eosinophils in the infiltrate may be focal and, rarely, they form clusters resembling a microabscess (see Fig. 25.1B) (56). Eosinophils are typically seen in reactions to antibiotics, especially penicillins, sulfonamides, and rifampicin, more than in response to various other drugs. Neutrophils are usually rare. Mast cells, which are difficult to detect without special stains, have been reported to constitute 1% to 2% of infiltrating cells (59). There is correlation between the number of interstitial mast cells and the degree of interstitial fibrosis in interstitial nephritis (60). Steroid treatment may reduce the severity of the inflammation and, in particular, lessen accompanying edema.

Granulomatous features are seen in the inflammatory reaction to many drugs (Table 25.2) (see Fig. 25.4). Granulomas, typically noncaseating and composed of epithelioid histiocytes, lymphocytes, and giant cells, may be scattered in the interstitium. They resemble the epithelioid granulomas of sarcoidosis, but the granulomas in drug-induced granulomatous interstitial nephritis are frequently less well defined than in sarcoidosis.

TABLE 25.2 Causes of granulomatous interstitial nephritis

Infection (see Chapter 24)
Tuberculosis
Fungal infections
Brucellosis
Parasites
Drugs
Sulfonamides
Penicillins
Fluoroquinolones
Vancomycin
Gentamicin
Nitrofurantoin
Allopurinol
Furosemide
Hydrochlorothiazide
Omeprazole
Lamotrigine
Nonsteroidal anti-inflammatory drugs (NSAIDs)
Bisphosphonates (alendronate)
Diphenylhydantoin
Carbamazepine
Oxycodone
Sarcoidosis
Tubulointerstitial nephritis and uveitis syndrome (TINU)
Granulomatous vasculitis (Wegener's)
Oxalosis (see Chapter 27)
Gout (see Chapter 27)
Cholesterol granuloma
Idiopathic

In chronic drug-induced interstitial nephritis, the defining feature is interstitial fibrosis. An interstitial inflammatory infiltrate often persists, but it is usually mild and composed largely of nonactivated lymphocytes, plasma cells, and macrophages. These infiltrates are often nodular and localized to fibrotic areas. Although drug-induced acute TIN occasionally may persist and lead to chronic interstitial nephritis, some drugs have a propensity to produce subclinical progression to chronic renal failure. These drugs include analgesics, lithium, and calcineurin inhibitors.

TUBULES

Accompanying acute TIN, there may be evidence of tubular cell injury, which may include vacuolation, loss of brush border, and exfoliation and loss of tubular cells. The tubular epithelium is often infiltrated by inflammatory cells, usually lymphocytes (tubulitis) (see Fig. 25.1C). Although these characteristics are often described in the proximal nephron, a few investigators have reported that tubular injury and tubulitis may be more severe in the distal nephron (21,22). With a severe inflammatory reaction, the TBM may be disrupted. In the circumstance of chronic interstitial nephritis, tubular atrophy is typically seen to be associated with fibrosis in the interstitium.

VESSELS

Vessels are usually uninvolved, though a few drugs may produce vasculitis or thrombotic microangiopathy (see Chapters 16 and 18).

Immunopathology

Fibrin is often detected in the interstitium by immunofluorescence, reflecting interstitial edema. IgG and C3 have been reported to be deposited in a linear pattern along the TBM in some cases of apparent drug-induced interstitial nephritis, including cases induced by penicillins (56,61–63) and rifampicin (64). Such linear TBM staining may be nonspecific. Minetti et al. have also reported granular peritubular IgG in one case due to rifampicin (65). In cases of methicillin-induced AIN, a drug antigen has been immunolocalized along the TBM as well (61,62).

Electron Microscopy

Ultrastructural examination is usually of limited informative value in drug-induced interstitial nephritis. Electron microscopy of the interstitium in cases of drug-induced interstitial nephritis reveals edema, infiltrating inflammatory cells, and tubulitis. Olsen et al. (66) have described severe reduction of the proximal tubular brush border and proximal and distal tubular basolateral infoldings in this context, reflecting tubular injury. In some areas, there may be thinning or disruption of the TBM. Electron-dense immune-type deposits are usually not present in TBMs.

Etiology and Pathogenesis

Three major types of immune mechanisms may lead to TIN in response to drugs. These include hypersensitivity/allergic, immune complex, and cell-mediated reactions. Each of these types is discussed in turn. In a few individual cases, mechanisms of action are clearly defined, but for others, pathogenetic mechanisms are assumed, often based on morphologic

and clinical findings. It is possible that several mechanisms of action are at work in an individual patient.

Allergic-type hypersensitivity reactions are idiosyncratic and not related to dose. The reaction to the agent is presumably caused by previous sensitization, and, indeed, patients may give a history of exposure to the ingested drug or a similar compound. The reaction in the kidney is often part of a systemic hypersensitivity reaction, which may include fever, arthralgias, and skin rash. Eosinophils are often a significant component of cells in the inflammatory infiltrate, and, as noted earlier, there is often a peripheral eosinophilia as well.

Reactions involving immune complex deposition are of two types: those with formation of immune complexes that are deposited around tubules and those due to formation of antibodies directed against antigens at or in the TBM. In a few cases, antigens from the drug have been immunolocalized to the TBM. The inciting drug may serve as a hapten, leading to antibody formation. Thus, granular TBM IgG and C3 deposits were reported in a patient after NSAID treatment (67). In a few patients, anti-TBM antibodies have been found; Colvin and Fang (7) reported that these antibodies are frequently found in patients with different forms of AIN if they are sought. In many cases, however, it is unclear whether these antibodies are of clinical significance, and the specificity of the methodologies to detect these antibodies is not always high. The finding of linear staining for IgG along the TBM is not a specific test to detect anti-TBM antibodies; proof of presence of anti-TBM antibodies requires demonstration of the antibody in the serum or renal eluates. Complexing of antibody to antigen may lead to complement binding and activation, triggering a cascade of events that result in inflammatory infiltrates and tissue injury.

Cell-mediated immunity has also been implicated in the genesis of drug-induced interstitial nephritis. The presence of granulomas in the kidney, in a number of cases of interstitial inflammatory reaction to drugs, is consistent with the delayed-type hypersensitivity. Recent data indicate that drug-specific T cells may be activated locally in the kidneys, and this T-cell activation may mediate a local inflammation via secretion of various cytokines, the type of which depends on the cytokine pattern secreted. This T-cell-mediated inflammation may be responsible for the renal damage (17). Cytotoxic lymphocytes, which were reactive against autologous renal cell line, have been isolated from one patient being treated with recombinant interleukin-2 (IL2) (68).

Chronic interstitial nephritis with fibrosis resulting from a prolonged inflammatory process is likely mediated by inflammatory cells and the cytokines released by them. It appears that interstitial mast cells facilitate the development of interstitial fibrosis (60). Some drugs appear to produce persistent tubulointerstitial damage without an acute injury phase. They include analgesics and lithium. Persistent changes produced by analgesics presumably result in part from ischemia produced by imbalances in the vasodilatory versus vasoconstrictor prostaglandins (PGs) over a prolonged period (see later section on "Analgesics and Nonsteroidal Antiinflammatory Drugs"). Chronic TIN is associated with prominent loss of the peritubular capillaries, which may further aggravate the ischemic injury (69). As pointed out earlier, certain cytokines, such as TGF- β , enhance production and release of matrix from epithelial and mesenchymal cells and likely also play a role in bringing about

interstitial fibrosis through promoting epithelial-mesenchymal transdifferentiation of renal tubular epithelial cells (6,7).

Clinical Course

Drug-induced interstitial nephritis is generally reversible by withdrawal of the offending agent. Steroid therapy may enhance the rate of recovery and is frequently given along with withdrawal of the drug. A typical and diagnostic feature of drug-induced interstitial nephritis is its recurrence on reexposure to the drug or a related compound. Although recovery of renal function is the rule if the drug is withdrawn immediately, a study from Germany indicates that permanent renal insufficiency remained in 88% of drug-induced acute TIN cases if the suspected drug was taken for more than a month before the diagnosis of drug-induced interstitial nephritis was made (70). Also, the same authors suggest that NSAID-induced interstitial nephritis has a worse outcome as compared to other drug-induced forms.

Specific Agents

Antimicrobial Agents

CEPHALOSPORINS

The cephalosporin group of antibiotics comprises several "generations" of these useful agents, defined on the basis of antimicrobial activity. The first generation includes cefazolin, cephalothin, and cephalexin. Cefamandole, cefonicid, cefuroxime, cefaclor, cefoxitin, and cefotetan are second generation, whereas the third generation includes ceftazidime, cefotaxime, and ceftriaxone. Cefepime is a fourth-generation cephalosporin more resistant to beta-lactamases than the previous agents. The newest, fifth generation of cephalosporins includes ceftobiprole (with stronger anti-*Pseudomonas* activity) and ceftaroline. These drugs may be nephrotoxic, particularly in patients with preexisting renal insufficiency. Cephaloridine, the most toxic of the group, is no longer available in the United States but is used experimentally for toxicity studies.

Clinical Presentation The cephalosporins are most likely to produce renal failure in patients with preexisting renal insufficiency (71,72), in those with drug overdose (73), and in those receiving other antibiotics (73,74). Patients simultaneously receiving furosemide (73) are also at increased risk, which is probably related to the ability of furosemide to prolong the half-life of the cephalosporins (75). Many of the patients reported to have nephrotoxicity due to cephalosporins are elderly and acutely ill with severe infections.

Cephaloridine has been reported to cause AKI, often as the result of oliguria (75,76). *Cephalothin* given alone (72) or with gentamicin, tobramycin (76,77), or other substances (78) can cause AKI in humans or can worsen preexisting renal insufficiency (71). The AKI is usually reversible. *Cephalexin* is less likely to cause nephrotoxicity than cephaloridine or cephalothin, but hematuria, eosinophilia, and a transient rise in BUN have been reported (79). Clinical features suggest an immunologic basis. Hypersensitivity reactions have been reported in patients treated with *cephalothin* as well (77,80). Rare cases of skin rash, eosinophilia, fever, and renal insufficiency with *ceftriaxone* have been reported (81).

Pathology Renal biopsies have been obtained in relatively few cases of cephalosporin-induced renal injury, usually in those in which the older cephalosporins were given. Biopsies

have shown a picture of interstitial edema with variable numbers of mononuclear cells, accompanied by variable degree of acute tubular injury (76,82,83). Granulomas may be seen in some cases (84). No immunoglobulins or complement have been seen with immunofluorescence techniques.

Pathogenesis Cephalosporins appear to be capable of producing direct toxic injury to tubular cells. Tune and Hsu (85) have shown that cephalosporins interfere with mitochondrial function in the renal tubule. Cephaloridine has structural homology to carnitine, and it has toxic effects on carnitine transport and fatty acid metabolism in rabbit renal cortical mitochondria; *in vivo/in vitro* effects on pyruvate metabolism have been seen, albeit at very high concentrations (85). Cephaloridine also produces lipid peroxidation and acylation and inactivation of some tubular cell proteins. Other cephalosporins, which lack cephaloridine's side group constituents, largely affect tubular cell proteins and especially mitochondrial anionic substrate transporters (85). *In vitro*, proximal tubular cells show evidence of cytotoxicity on exposure to cephaloridine, cephalixin, and cephalothin, whereas distal tubules do not. These studies provide evidence of the role of oxidative stress, cytochrome P450 activation, and mitochondrial dysfunction in tubular cell toxicity (86). It is important to note that preexisting chronic renal failure (the degree of which is not accurately represented by serum creatinine [Scr] levels alone) is a very important risk factor for the development of progressive renal failure following the use of nephrotoxic medications.

In addition, cephalosporins are known to cause hypersensitivity reactions. In some cases, there has been resolution with drug withdrawal and, in a few cases, recurrence on rechallenge (82). The cephalosporins are structurally similar to the penicillins, which produce similar reactions (see later), and cross-reactivity may occur in 1% to 20% of patients (87). No specific cephalosporin is more likely than others to cause such a reaction.

FLUOROQUINOLONES

Clinical Presentation Fluoroquinolones belong to a family of synthetic broad-spectrum antibiotics. *Ciprofloxacin*, the most widely used of these drugs, has been reported to produce AKI with interstitial nephritis. Levofloxacin, norfloxacin, tosfloxacin, and moxifloxacin have also been associated with interstitial nephritis (88–91). There is typically fever, eosinophilia, and skin rash (92–96), but systemic manifestations may not be present (97). Onset of symptoms is generally within 2 to 12 days of beginning either oral or intravenous therapy. Patients have responded to withdrawal of the drug and, generally, concomitant treatment with immunosuppressive agents.

Pathology Renal biopsies in cases of fluoroquinolone-associated renal dysfunction have revealed interstitial nephritis. In a few cases, there were granulomatous features in the interstitial inflammatory infiltrate (69,96,98). Shih et al. have reported a necrotizing vasculitis in the kidney in two patients being treated with ciprofloxacin (96). An interesting case from Japan was reported in which a patient developed crystal-forming chronic interstitial nephritis following long-term exposure to tosfloxacin (90). The crystals were present in interstitial macrophages, but the crystals did not contain immunoglobulin. The patient's renal function improved following discontinuation of the drug.

Pathogenesis The mechanism of pathogenesis appears to be a hypersensitivity reaction, with evidence of a cell-mediated process in the few cases with granulomatous features. As with many drug reactions, the possibility that another drug or underlying disease process may have produced the renal effects cannot be ruled out in several of these cases.

PENICILLINS

In the following section, adverse reactions to ampicillin, methicillin, and penicillin are discussed in detail. AIN has been reported with other penicillins as well, including *cloxacillin* (99) and *piperacillin* (100,101).

Clinical Presentation Several cases are recorded in which ampicillin appears to have provoked renal dysfunction (102–105). Fever, skin rash, and eosinophilia may be found and may antedate renal symptoms. Renal manifestations may be mild, with hematuria and a small amount of proteinuria, or severe, with acute oliguric renal failure. Rapid recovery is the rule. Time to onset varies, but renal symptoms generally appear within a few days of administration of ampicillin; other manifestations, such as fever and skin rash, develop within 24 hours. In several cases, there had been prior treatment with penicillin, methicillin, or tetracycline.

There are many reports of renal damage caused by *methicillin*. Nephrotoxicity with methicillin is not dose dependent. Onset of toxic reactions usually begins within 5 weeks after initiation of the drug. Patients typically manifest fever and skin rash, and 73% of patients in a review of 68 patients were male (106). Patients of all ages are at risk, though renal failure appears to be more common in older patients. Eosinophilia is a typical feature and may reach very high levels (56). Hematuria may occur; it is often the first sign of renal involvement. Proteinuria is seen in some cases but is generally mild. WBCs are frequently found in the urine, which is usually sterile, and eosinophils are present in the urine in a high proportion of patients (56,106). Azotemia occurs in over half of patients and oliguria in one third. Complete recovery of renal function is the rule, though azotemia may persist in less than 10% of patients (107).

Penicillin has been widely used for more than 50 years, and there have been several reports of nephrotoxicity ascribed to the drug. Appel and Neu (108) summarized the reported adverse reactions to penicillin under three main headings: various vascular and glomerular lesions, acute anuric renal failure after a single injection, and AIN. In a number of cases, there is fever, skin rash, and eosinophilia, suggesting a hypersensitivity reaction. The patients have hematuria with varying degrees of proteinuria, and renal failure may ensue.

Pathology Histologic changes in interstitial nephritis associated with penicillin and its derivatives do not differ from other forms of drug-induced interstitial nephritis. Eosinophils, however, are frequently abundant. Occasionally, granulomas (63,109) and vasculitis lesions (56,110) were recorded, but these are rare. Immunofluorescence is usually nonspecific; however, occasional investigators describe linear staining along the TBM for IgG (61,62,111,112). Such staining, in many instances, is probably nonspecific; however, antibodies to TBM antigens were reported in a few cases (62). Ultrastructural examination is also usually noncontributory. Association of minimal change disease with penicillin-induced interstitial nephritis has been

reported (113). A few investigators described fibrillar deposits along distal convoluted tubules and in glomerular epithelial cells (102,105), but the relevance of these fibrils is unclear, and they may merely represent procollagen.

Morphologic examination cannot differentiate between interstitial nephritides caused by different penicillins. In fact, the histology does not even indicate whether the interstitial nephritis is secondary to penicillin or some other drug or injurious agent. Pirani et al. (114) compared beta-lactam–induced interstitial nephritis with NSAID-induced interstitial nephritis and found that the beta-lactam–induced cases contained more eosinophils. Both types contained primarily mononuclear cells with some plasma cells in the infiltrate. Still, these are histologic findings of low specificity.

Pathogenesis Nephrotoxicity of the penicillins is not dose dependent, and the clinical picture overall is that of a hypersensitivity reaction. In several studies, immunofluorescence microscopy raises the possibility that anti-TBM antibodies may play a role in the pathogenesis of TIN, but the evidence is weak (61,62,111). Cell-mediated mechanisms may also be involved in some cases, based on the nature of the inflammatory infiltrate, and the absence of antibody and complement deposition. Gilbert et al. (102) have reported exacerbation of the reaction to methicillin by inadvertent exposure to ampicillin, a closely related drug. In addition, some case histories suggest that ampicillin can trigger a hypersensitivity reaction in patients who might have been sensitized to other penicillins. In one of these cases, antibodies against ampicillin were detected in the patient's serum (104). In some studies, hypocomplementemia provided additional evidence of an immune reaction (102).

RIFAMPICIN

Clinical Presentation Rifampicin is a drug used in the treatment of tuberculosis. When it is given intermittently, it causes various adverse reactions, including fever, chills, dizziness, nausea, and diarrhea (115,116). There have been several reports of acute oliguric renal failure during intermittent rifampicin therapy (115–118). The most common clinical scenario is AKI following a single dose of rifampicin. The average time between the initiation of therapy and clinical presentation is less than 3 weeks (119). Clinical manifestations may include gastrointestinal symptoms. Usually, no skin rashes are observed. Hematuria without any significant proteinuria is common. Anemia is often present, sometimes with associated thrombocytopenia (119). Most patients recover when the drug is withdrawn (116), a few cases have been reported to result in permanent renal damage (119,120).

Pathology Renal biopsies in cases of rifampicin toxicity typically show interstitial edema with variable numbers of mononuclear cells, and eosinophils have also been found (64). Rarely, granulomas may be seen (121). There may be patchy necrosis of the tubular epithelium. Even patchy cortical necrosis has been described (120); in that case, there was residual renal dysfunction. However, the degree of tubular necrosis is often not severe, and in one case, the tubules were described as unaffected (115). In addition, pigmented casts may be evident. Although glomeruli and vessels are usually normal, rarely glomerulonephritis, including crescentic and necrotizing glomerulonephritis, has been noted (64,116). On immunofluorescence

microscopy, it has usually not been possible to establish the presence of immunoglobulins or complement (117,118), although C3 has been found in the mesangium and in the TBM (64,122) (common nonspecific findings).

Pathogenesis Antibodies to rifampicin have been detected in patients (123,124); in one study, they were present in one third of 49 patients (123). The various adverse reactions reported in this series, including renal dysfunction, were found more commonly in patients with antibodies than in patients without them. These authors suggest that the drug acts as a hapten, which, after it has become bound to macromolecules in the plasma, becomes antigenic with the formation of antibodies. The antibodies are considered to be directed against the drug, with formation of hapten-antibody complexes when the drug is given again.

SULFONAMIDES

The sulfonamides have been widely used, with relatively few renal complications. Alleged hypersensitivity reactions in the early days of their use were associated with polyarteritis or AIN (125,126). However, AIN secondary to sulfonamides has become a rare event, and only a few cases have been reported (127,128). In one case, acute oliguric renal failure developed in a patient being treated with *sulfadiazine*. The patient recovered after 6 weeks of oliguria (128). *Cotrimoxazole* (sulfamethoxazole and trimethoprim) has occasionally been found to cause deterioration of renal function (129,130). A case of delayed acute TIN in a patient who developed “drug rash” with eosinophilia and systemic symptoms (DRESS syndrome) secondary to sulfasalazine was described (131).

Patients in whom crystalline precipitates develop with the use of sulfonamides have microscopic or gross hematuria, crystalluria, and renal colic, and in some cases, they become oliguric or anuric (108,132). Occasionally, urolithiasis may evolve. In one series of 40 patients, the urinary bladder was the most common location of stones (133). Sulfasalazine (a combination of 5-amino salicylic acid and sulfapyridine) has been reported to cause obstructive uropathy secondary to calculi (134). Less soluble forms, including sulfapyridine, sulfathiazole, and sulfadiazine, are most frequently associated with crystalline obstruction (135). Fortunately, this complication became rarer when sulfonamides of greater solubility became available. Rapid improvement may take place with discontinuation of the drug, fluid administration, and alkalinization of the urine.

The typical pathologic finding is interstitial nephritis. Eosinophils are a typical component of the infiltrate (127,130,136). Granulomas have occasionally been described (136). In patients with crystallization of sulfonamide in the kidney, some pathologic changes are due to obstruction as a consequence of crystal formation.

VANCOMYCIN

Vancomycin is a glycopeptide antibiotic used increasingly to treat infections caused by organisms resistant to other antibiotics such as methicillin-resistant *Staphylococcus aureus* (MRSA). With the growing number of MRSA infection, the cases of vancomycin-associated TIN have been reported more frequently (137–139). Nephrotoxicity is a known complication of the drugs when given alone or in combination with other drugs, especially aminoglycosides (140,141) or cephalosporins (74). Pediatric patients may be less susceptible to the toxic effects of

vancomycin combination therapy (142). Some patients have an associated rash and eosinophilia, suggesting a hypersensitivity reaction. In addition to these adverse renal effects, in some cases, patients have an anaphylactoid reaction to the drug, with generalized flushing—the so-called red man syndrome.

Pathologic findings in kidney biopsies obtained from patients with vancomycin-associated AKI may include TIN with many eosinophils (137,143). Several case reports described ATN in patients after vancomycin treatment without relevant interstitial inflammation, predominantly in pediatric patients (144–146). Rarely, vancomycin-associated kidney injury may be manifest as granulomatous interstitial nephritis (139). In the last 8 years, we have seen over 50 biopsies with ATN and interstitial nephritis following vancomycin administration. Most of these patients had high vancomycin trough levels and underlying preexisting chronic renal injury. Interestingly, in our experience, the ATN is the predominant finding associated with relatively mild but active interstitial inflammatory cell infiltrate with interstitial edema. In these cases, the lesions are usually reversible unless patients have severe systemic disease, sepsis, or other prominent chronic renal injury such as diabetic nephropathy.

The pathogenesis of renal toxicity is not well defined clinically, but experimental studies suggest that it stems from tubular cell injury. In some patients, the constellation of clinical symptoms and pathologic features indicate a hypersensitivity reaction (147), but many patients do not develop such a syndrome. The potentiation of toxic reactions when vancomycin is used with aminoglycosides may be due, at least in part, to enhancement of aminoglycoside binding to brush border and, presumably, its uptake into tubular cells, with subsequent cellular injury (148).

Analgesics and Nonsteroidal Anti-Inflammatory Drugs

Anti-inflammatory agents can be classified as steroidal and nonsteroidal. However, by convention, the generic term *nonsteroidal anti-inflammatory drugs* (NSAIDs) has come to refer to specific PG synthase (cyclooxygenase [COX]) inhibitors, exclusive of aspirin. This causes some conceptual confusion because aspirin, in fact, is a PG synthase inhibitor. These drugs are used for their analgesic, antipyretic, and anti-inflammatory effects. COX has two isoforms. COX-1 is the constitutive isoform normally expressed in the tissues, and COX-2 is the inducible isoform. The hypothesis was that COX-1–derived PGs are responsible for regulating physiologic functions, whereas COX-2–derived PGs play a more important role in the pathogenesis of inflammation and tissue damage. The older generations of NSAIDs block both COX-1 and COX-2. A new generation of drugs selectively inhibits COX-2, and the assumption was made that these would not be associated with serious gastrointestinal and renal side effects. This led to the finding that constitutive tissue expression is present not only for COX-1 but also for COX-2. COX-2 has been detected in normal renal tissue in the medullary interstitial cells, in the macula densa, in the thick ascending limb of Henle, and also in smooth muscle cells and endothelial cells of arterioles and veins (149–151).

Importantly, more and more data indicate that renal toxicity, including AKI with interstitial nephritis and also heavy proteinuria, may be associated not only with conventional NSAIDs but also with COX-2 inhibitors (152–158).

There is considerable controversy about COX-2 inhibitors and their cardiovascular side effects, which resulted in the withdrawal of rofecoxib (Vioxx) from the US market. However, celecoxib (Celebrex) is still available. The future of these otherwise promising anti-inflammatory medications is currently uncertain.

Under euvolemic conditions, renal PG synthesis is low; however, if the renal blood flow is compromised, PG exerts a compensating influence on renal function. Some PGs induce renal vasodilation that counterbalances vasoconstrictor effects of angiotensin II and norepinephrine. They also affect sodium excretion and, as a consequence of renal vasodilation, they may increase the filtered load of sodium. They also increase medullary blood flow and reduce hypertonicity of the loop of Henle. PGs also have a natriuretic effect by direct inhibition of sodium transport in the loop of Henle and distal nephron, and they also oppose the hydroosmotic effects of vasopressin (150). There are a number of different PGs with diverse effects. The above list of the actions of PGs is not complete, highlighting the complexity of their effect on renal function under normal and pathologic conditions.

Acetaminophen is frequently not classified as an NSAID because it has no anti-inflammatory effect, and it is not a PG synthase inhibitor. It is, however, one of the most widely used analgesic and antipyretic drugs and is discussed under the category of NSAIDs by many pharmacology textbooks. For convenience, we discuss acetaminophen with NSAIDs (Table 25.3). The gastrointestinal toxicity of these agents is well known, but their adverse effect on renal function became apparent only in the past three decades.

INCIDENCE

The incidence of NSAID nephrotoxicity is not well established. Taking into consideration their over-the-counter availability and the frequency with which people take them for pain relief or fever, the incidence appears to be rather low. On the other hand, because of their widespread use and availability, many patients with renal impairment have a history of NSAID use. In a number of such patients, the association of NSAIDs and renal failure is incidental. A causative relationship between NSAIDs and renal impairment should be considered if the initiation of NSAID therapy and the renal impairment show a close temporal association, if other etiologic factors can be excluded, and if renal function improves following discontinuation of NSAIDs.

Approximately 50 million Americans per year are likely to take NSAIDs, and some 500,000 (1%) of them are thought to experience renal side effects (159–161). Murray and Brater (162), in a prospective study, found renal impairment in 18% of patients treated with ibuprofen. Kleinknecht et al. (163), in a prospective study, collected 2160 cases of AKI, 146 of which (6.8%) were attributed to NSAIDs. AKI was defined as a greater than 50% rise in the Scr level or an increase to greater than 2.4 mg/dL from the baseline value. Data from the Boston Drug Surveillance Program on 122,000 hospitalized patients taking NSAIDs indicate that the Scr did not increase compared with levels in patients not receiving NSAIDs (164). A meta-analysis reviewing 1368 patients taking NSAIDs found only 3 patients in whom the Scr concentration increased to greater than 2 mg/dL (165). Corwin and Bonventre (166) reviewed 26 patients with AKI due to NSAID treatment. The Scr increased from a mean value of 1.6 ± 0.1 to 3.3 ± 0.3 mg/dL

TABLE 25.3 Nonsteroidal anti-inflammatory drugs^a

Nonselective PG synthase inhibitors (COX-1 and COX-2)
Carboxylic acids
Salicylic acid derivatives
Aspirin
Salicylates
Diflunisal
Acetic acids
Indomethacin
Sulindac
Tolmetin
Diclofenac
Etodolac
Nabumetone
Ketorolac
Propionic acids
Ibuprofen
Naproxen
Fenoprofen
Ketoprofen
Flurbiprofen
Oxaprozin
Fenamic acids
Mefenamic
Meclofenamic
Flufenamic
Enolic acids
Oxicams
Piroxicam
Selective COX-2 inhibitors
Celecoxib
Rofecoxib ^b
Valdecoxib
Non-PG synthase inhibitors
Para-aminophenols
Acetaminophen
Phenacetin ^b

^aSpecific anti-rheumatoid arthritis agents and antigout agents are not included.

^bWithdrawn from the market.

following 4.2 ± 0.7 days' mean duration of treatment, and the Scr returned to normal following withdrawal of NSAIDs. They estimated the incidence of AKI, defined as the number of recognized cases per inpatient days of therapy, and found it to be 0.001, 0.0003, 0.0001, and 0.0001 for indomethacin, ibuprofen, zomepirac, and sulindac, respectively (166). The incidence may be overestimated in some of these studies because hospitalized patients already represent a selected population and may have risk factors for NSAID toxicity (see later).

CLINICAL PRESENTATION

AKI is the typical clinical presentation and may be accompanied by varying degrees of proteinuria (10,155,166–168). The condition usually develops within a few days to weeks after

initiation of therapy. Sodium retention and edema may occur, and occasionally hyperkalemia may develop, presumably as the result of reduced renal PG production and a subsequent decrease in serum aldosterone (169,170). Calvo-Alen et al. (171) found that prolonged use of NSAIDs leads to subclinical renal failure, which manifests first in decreased renal concentrating capacity and is correlated with the cumulative intake of the drug.

Proteinuria is common among patients with NSAID toxicity, with approximately 10% to 12% of patients with renal impairment due to NSAIDs developing nephrotic-range proteinuria (172,173). A group of researchers from Chicago found that 9% of their adult cases of minimal change nephrotic syndrome were associated with NSAIDs (174). Patients usually take the drugs for several months before the nephrotic syndrome develops. It is worth noting that women appear to be more susceptible (173,174). Rarely, COX-2 inhibitors may also induce nephrotic syndrome as has been reported with celecoxib (155). The proteinuria typically subsides within a few weeks after discontinuation of the NSAIDs but may worsen with reexposure to the drug. The usual glomerular lesion is minimal change disease and is discussed in Chapter 5.

The concurrence of renal insufficiency and severe proteinuria, particularly if the renal failure is nonoliguric, is strongly suggestive of AIN (172,173). Hypersensitivity symptoms (skin rash, eosinophilia) and fever are less frequently noted than in cases of antibiotic-induced AIN (114). Hematuria may also be present. The male-to-female ratio is 1:2. The symptoms usually appear weeks to months after initiation of NSAID therapy and may resolve within days or weeks afterward (114,174,175). Recovery is not always the case for NSAID-associated AIN, and cases of patients who progress to end-stage renal disease (ESRD) have been reported (163,175). Approximately 20% of AIN cases are associated with acetic acid derivatives. However, other NSAIDs, including mefenamic acid, niflumic acid, and many others including COX-2 inhibitors, are reported to induce AIN (114,152–157,174,175).

Oligohydramnios with *congenital renal insufficiency* may follow in utero exposure of the fetus to NSAIDs, which also may cause bleeding diathesis, premature closure of the ductus arteriosus, and ileal perforation. Tubular dysgenesis with incomplete differentiation of the proximal tubules as well as tubular microcystic dilation has been described (176–178), and the renal damage is severe and irreversible. Most reported cases are related to prolonged in utero indomethacin exposure (176,177).

RISK FACTORS

NSAIDs do not alter the glomerular filtration rate (GFR) in healthy, euvolemic individuals (179), but they reduce the GFR in patients with chronic renal disease or with *preexisting impaired renal function* (4,161,179). Elderly and diabetic patients are particularly vulnerable to the toxic effects of NSAIDs (162,180,181), which can be explained by the fact that aging is associated with a progressive decline in the GFR and impaired pharmacokinetics of NSAIDs (168). *Dehydration and decreased cardiac output* are also associated with an increased risk of nephrotoxicity; diminished GFR may be the main risk factor in these conditions as well (166). Patients with *liver cirrhosis* are also at higher risk, which may be related, in part, to the impaired hepatic metabolism of NSAIDs and to renal

impairment associated with chronic hepatic failure (168). In addition, cirrhotic patients have enhanced renal PG-E production, which is vasodilatory. Administration of NSAID to these patients may profoundly reduce renal blood flow and GFR (182).

Certain types of NSAIDs are more likely to cause renal injury than others. It has been reported that fenoprofen causes more than 50% of all NSAID-associated AIN (38). Whelton and coworkers in a randomized trial found that in patients with asymptomatic renal failure, ibuprofen is more frequently associated with AKI than are sulindac and piroxicam (170). There are also data that suggest that sulindac has less nephrotoxic potential than other NSAIDs. Sulindac does not reduce the excretion of urinary PGs and appears to be a safe drug even in patients with preexisting renal failure (168). The kidney has the ability to metabolize sulindac into an inactive sulfone metabolite, thus protecting its own PG metabolism against the drug (168). There is limited literature available regarding nephrotoxicity of COX-2 inhibitors. Ahmad et al. (183) collected data from the U.S. Food and Drug Administration's (FDA's) Adverse Event Reporting System and found that 122 and 142 domestic US cases of celecoxib- and rofecoxib-associated renal failure, respectively, were reported by 2002, suggesting that use of both these drugs is associated with renal effects similar to that of conventional nonselective NSAIDs. Acetaminophen and aspirin are usually not associated with acute renal injury, but large doses of these drugs may cause AKI, especially in a combination with other medications or alcohol (184–187).

PATHOLOGY

In most patients with AKI secondary to NSAIDs, no renal biopsy is performed, and we can assume that in many of these cases, the nephrotoxicity is functional (renal vasoconstriction) and that there are no, or only minor, light microscopic changes. ATN may be present, but the tubular degenerative and regenerative changes are frequently coupled to interstitial nephritis, minimal change disease, or both (Fig. 25.14) (114).

The morphologic features of NSAID-associated AIN are similar to those of other interstitial nephritides and are characterized by a mononuclear interstitial infiltrate. However, minor differences do exist. Pirani et al. compared NSAID and beta-lactam antibiotic-associated renal changes and found that in NSAID-induced interstitial nephritis, there is less intensive infiltrate, and the proportion of eosinophils is substantially smaller. The paucity of eosinophilic cells in the infiltrate was also reported by Bender et al. (16). It is worth noting that routine staining methods may not reveal degranulated eosinophils; thus, the actual number of eosinophils may be underestimated. There are also fewer plasma cells, and tubulitis as well as granulomatous features are less common (114). Although there is agreement that the infiltrate consists mainly of lymphocytes, primarily T lymphocytes, occasionally plasma cells, B lymphocytes, and polymorphonuclear leukocytes may also be present in substantial numbers (16,114,188). There are few data regarding T-lymphocyte subsets, and these are controversial. Initial studies indicated a predominance of cytotoxic/suppressor T cells (16), but other researchers have found a helper/inducer cell predominance (188). The different types of antibodies used and the diverse methodologies, forms of fixation, and selection biases may account for the divergent results.

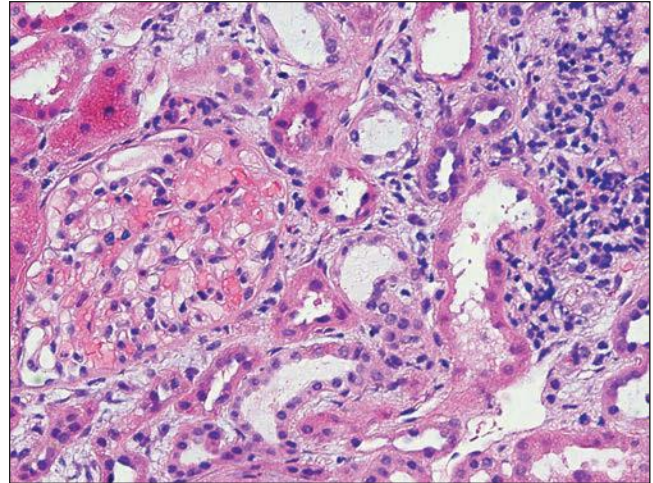


FIGURE 25.14 Mild interstitial edema and inflammation, associated with acute tubular injury, in a patient following NSAID administration. The glomerulus is unremarkable. This patient had nephrotic syndrome and acute renal failure. The renal failure and proteinuria reversed after discontinuation of NSAIDs. (H&E, $\times 200$.)

Occasionally, NSAID-associated interstitial nephritis may have granulomatous features (189). The condition has to be differentiated from sarcoidosis and infectious granulomatous interstitial nephritis, including tuberculosis. The differential diagnosis should not be based on the morphologic characteristics alone, because the histologic changes are usually not distinctive. In NSAID-associated interstitial nephritis, the granulomas are usually, but not always, less distinct than in sarcoidosis. The clinical history is the most important factor in making the correct diagnosis. Discontinuation of NSAIDs usually leads to resolution (189).

Either the glomeruli show no changes on electron microscopy, or, if nephrotic-range proteinuria is present, *minimal change disease* can be seen with the effacement of podocyte foot processes (114,173,174). Baisac reviewed 59 cases of NSAID-induced minimal change nephrotic syndrome and found that interstitial nephritis was also present in 43 patients (190). Occasionally, glomerular lesions other than minimal change disease (e.g., membranous glomerulopathy (191) or glomerular tip lesion (192)) are reported. These NSAID-induced glomerular diseases are discussed in the appropriate chapters (Chapters 5–7).

PATHOGENESIS

There is agreement that NSAIDs exert their toxic effect on the kidney through their interference with renal PG metabolism (149,150). PGI₂ is the most abundant PG in the cortex; it is produced primarily by arterioles and glomeruli. PGE₂ is the most abundant PG synthesized by the tubular epithelium, primarily in the distal nephron segments (distal tubules, collecting ducts) (193). Thromboxane A₂ is produced by the glomeruli, and PGF₂α is produced by the tubules. The effect of PGs on the renal vasculature is primarily vasodilatory (194). Vasoconstrictive mediators, such as angiotensin II, sympathetic stimuli, norepinephrine, arginine vasopressin, and endothelin, also stimulate PGI₂ and PGE₂ synthesis, which, in turn, will counterbalance the vasoconstriction. PGs also inhibit tubular

water and salt reabsorption (168). As mentioned earlier, NSAIDs do not alter the GFR in healthy, euvoletic individuals (179). In contrast, in conditions where the systemic hemodynamic conditions are compromised, NSAIDs may have a deleterious effect on the renal circulation. Owing to the inhibition of COX, the synthesis of vasodilatory PGI₂ and PGE₂ is diminished, and severe, unbalanced renal vasoconstriction may develop, resulting in AKI (168,195).

The development of AIN is probably related to a delayed-type hypersensitivity response to NSAIDs, which is also reflected in the composition of the infiltrate (16,114). This suggestion is also supported by the prolonged exposure and the infrequency of hypersensitivity symptoms. This condition is somewhat different from antibiotic-associated interstitial nephritides, where hypersensitivity signs are more common and eosinophils are more prominent in the infiltrate.

The pathogenesis of NSAID-associated severe proteinuria is unclear. In fact, there is some evidence that NSAIDs may ameliorate glomerular proteinuria (196). Why in certain patients the opposite happens is unresolved. The fact that nephrotic-range proteinuria and interstitial nephritis are frequently present at the same time suggests the role of mediators such as lymphokines released from interstitial or circulating inflammatory cells, which could alter glomerular permeability. In addition, the inhibition of PG synthesis by NSAIDs may hamper the inhibitory effects of PGs on T-cell function, thus intensifying immune activation and cytokine release. The inhibition of COX may also result in a shift of arachidonic acid metabolism toward the lipoxygenase pathway, which may result in the enhanced production of proinflammatory leukotrienes (164,173).

Analgesic Nephropathy

Analgesic nephropathy is a chronic progressive tubulointerstitial disease induced by the prolonged use (abuse) of analgesics and potentially addictive substances, such as caffeine or codeine. Analgesic nephropathy was first described in the 1950s (197) and was further characterized in the following decades (198–202). It became apparent that the chronic use of analgesics, primarily phenacetin, might be associated with the development of renal failure. However, after the withdrawal of phenacetin from the market, the incidence of analgesic nephropathy did not decrease subsequently; therefore, the scientific advisory board of the National Kidney Foundation formed an ad hoc committee who redefined analgesic nephropathy as a disease resulting from the habitual consumption over several years of a mixture containing at least two antipyretic analgesics and usually codeine and caffeine (203).

The definition of analgesic abuse is quite variable and arbitrary in the different studies, but the consumption of daily analgesics for ≥ 1 year or a cumulative intake above 1000 units (tablets) is the minimum criterion required by most investigators. However, true analgesic abuse and subsequent nephropathy are associated with higher cumulative intake (usually above 5000 units).

INCIDENCE

The incidence varies greatly from study to study, depending primarily on the timing of the study and on the region or country where the investigation was performed. In Europe, the percentage of analgesic nephropathy among patients with

ESRD undergoing long-term dialysis varied widely, from only 0.1% in Ireland, Norway, Poland, and Hungary to 18.1% in Switzerland (204). According to the Analgesic Nephropathy Network of Europe study, the average European incidence of analgesic nephropathy among patients who were started on renal replacement therapy in 1991–1992 was 6.4% (199). In Australia and Canada, 11% and 2.5% incidence rates have been reported, respectively (205,206). In the United States, 1.7% to 10% of the ESRD cases are thought to be the result of analgesic nephropathy in various regions (200,207). These large geographic differences may be explained by differences in local habits, psychosocial factors, availability of these drugs, and the frequency of correct diagnosis and reporting.

The removal of phenacetin from the market as well as other regulations (restricting over-the-counter sales and marketing smaller packages) resulted in a decline of the proportion of patients requiring dialysis therapy for analgesic nephropathy in Australia, Sweden, and Germany (206,208,209). Still, the incidence remains high in many countries, indicating that drugs other than phenacetin, such as acetaminophen and NSAIDs, are responsible for the development of the disease (160,198,208). Some authors believe that combination analgesics (acetaminophen and salicylates or aspirin) are more likely to induce analgesic nephropathy than single drug usage (198). Data on analgesic nephropathy in two highly endemic regions, Belgium and New South Wales, Australia, demonstrated that the downward trend and prevalence of analgesic nephropathy were very similar, despite the fact that the sale of only phenacetin was banned in Belgium, while other combined analgesics remained on the market, and in New South Wales not only phenacetin but all combined analgesics were prohibited. Still, the downward trend and prevalence of analgesic nephropathy were very similar during the follow-up period indicating that nonphenacetin mixed analgesics probably do not play a significant role in the development of analgesic nephropathy (210). Because of the relevance of the cumulative dose of analgesics, the effects of restrictions in the sale of combined analgesic medications show only with a delay. Studies from Australia and Belgium (211,212) indicate a recent decline in the incidence of analgesic nephropathy, particularly in the younger population. The cumulative dose of analgesics appears to be an important factor. Perneger et al. (200) have shown that the odds ratio of ESRD is 2 in patients with a cumulative dose of greater than 1000 pills and 2.4 in patients taking greater than 5000 pills of acetaminophen, compared with that in persons taking less than 1000 pills. They also found that the use of NSAIDs is associated with an increased risk of ESRD in patients taking greater than 5000 pills of NSAIDs (odds ratio 8.8), whereas the use of aspirin is not. It appears that the absolute risk of developing ESRD in analgesic abusers is approximately 1.6 to 1.7/1000 per year (198). However, the true incidence of analgesic nephropathy is quite difficult to determine. An Ad Hoc Committee of the International Study Group on Analgesics and Nephropathy critically reviewed the available data of the association between NSAID and renal disease (213). They found that many studies on analgesic nephropathy are inconclusive because of sparse information and substantial methodologic problems. Also, they emphasized that the diagnosis of analgesic nephropathy in different studies can vary and, in many cases, the diagnosis is based primarily on information about drug ingestion without any specific imaging or histologic studies. Therefore, the committee decided that there is no convincing evidence that

nonphenacetin combined analgesics are truly associated with nephropathy (213).

A large autopsy study performed on 616 patients in Switzerland indicates that the autopsy prevalence of analgesic nephropathy decreased from 3% in 1980 to 0.2% in 2000. Similarly, capillary sclerosis of the urinary tract, the initiating event in the pathophysiology of papillary necrosis and analgesic nephropathy and the histologic hallmark of the effect of toxic metabolites of phenacetin in analgesic abusers, decreased from 4% of autopsy cases in 1980 to a 0.2% in 2000. Thus, the classic analgesic nephropathy has practically disappeared some 20 years after the removal of phenacetin from the analgesic market despite the fact that mixed analgesics containing paracetamol, the main metabolite of phenacetin, have continued to be popular and widely used drugs (214). This study later received some critique because it was supported by pharmaceutical companies and the ad hoc committee consisted mainly of researchers from Germany, Switzerland, and Austria. Still, later studies from these three countries further indicate that analgesic nephropathy is disappearing and that non-phenacetin-containing analgesics do not cause analgesic nephropathy (214–216). However, as mentioned above, studies from Belgium and Australia contradict these findings, and, in spite of the declining prevalence of analgesic nephropathy, they state that the continuing use of non-phenacetin-containing analgesics (including paracetamol/phenacetin combined with NSAID, codeine, caffeine) is still associated with the development of analgesic nephropathy (211,212,217). Data from the Physicians' Health Study indicated that analgesic use in healthy male patients is not associated with the risk of subsequent renal failure (218). The study involved 4772 healthy male physicians with normal Scr levels in 1982. During a follow-up period of 14 years, there was no evidence of renal impairment in these patients, not even in those who consumed more than 7000 analgesic pills (218). The studies somewhat contradict previous data, but they emphasize that a preexisting underlying renal condition or other coexisting aggravating pathogenetic factors (such as hypertension, diabetes, obesity) may be important in the pathogenesis of analgesic nephropathy and analgesic intake by itself may not be deleterious to the kidney if no other coexistent or preexistent pathologic factors are present (219). In spite of these contradictory data, considering the widespread use and abuse of analgesics, analgesic nephropathy must be considered an important public health issue.

CLINICAL PRESENTATION

The typical patient is a middle-aged woman with a variety of symptoms, frequently including headaches and some degree of acute and/or chronic renal failure. The decline in the GFR may be due to vasoconstriction, vascular damage, or tubular obstruction (220). Tubular damage is reflected in defects of urinary concentration, acidification, and sodium retention. Microscopic hematuria occurs in 40% of patients (220). Gross hematuria with loin pain and AKI is suggestive of papillary necrosis (221). Occasionally, full-blown papillary necrosis occurs. If the necrotic papilla is sloughed into the renal pelvis, fragments of necrotic papilla segments may cause obstruction or be voided in the urine. Significant proteinuria (greater than 0.3 g/24 hours) is present in half of the patients, but nephrotic-range proteinuria is uncommon (220). Hypertension develops in a substantial number of patients.

The diagnosis of analgesic nephropathy should not be solely based on renal biopsy. Renal imaging techniques, such as

sonography and particularly computed tomography, are the best methods for diagnosis in the appropriate clinical context (199). The Analgesic Nephropathy Network of Europe study showed that shrinkage of renal mass (sensitivity 96%, specificity 37%), bumpy renal contours (sensitivity 57%, specificity 92%), and the presence of papillary calcifications (sensitivity 85%, specificity 93%) are the most useful criteria in diagnosing analgesic nephropathy. The combination of these three criteria resulted in a sensitivity of 85% and a specificity of 93% (199). Radiocontrast examinations may be helpful in the diagnosis of papillary necrosis. The specificity and sensitivity of diagnostic imaging studies have been reviewed by De Broe and Elseviers (222).

PATHOLOGIC FINDINGS

Gross Appearance In the full-blown form, both kidneys are somewhat contracted, and the subcapsular surface shows irregularly alternating depressed areas and raised nodules, the latter sometimes assuming a characteristic ridged form (223,224). The depressed areas correspond to atrophic, scarred portions of the cortex above a necrotic papilla. The nodular areas correspond to the hypertrophic areas of the cortex above the columns of Bertin. The papillae are shrunken and withered and may be pale or brown. Calcification may be present, primarily in the medulla. In early-stage papillary necrosis, yellow stripes radiating outward from the tip of the medulla may be seen, separated by dark zones. This appearance may be confined to the tip or may extend through the entire papilla. Later, the yellow appearance becomes confluent and extends to the border of the inner and outer medullae. In some cases, only the tip of the papilla becomes necrotic. In others, the necrosis is found only in the central part of the papilla. Occasionally, the necrotic papillae become sequestered and may be found lying free in the pelvis. Soft phosphate stones may also be noted in the pelvis in association with papillary necrosis. A characteristic brown pigmentation of the pelvic mucosa may be observed, which is thought to be the result of lipid deposition (225,226).

Light Microscopy The earliest change is the sclerosis (basement membrane thickening) of capillaries beneath the urothelial mucosa (Fig. 25.15) (224,226,227). This suburothelial capillary calcification was demonstrated in phenacetin



FIGURE 25.15 Portion of a kidney with advanced analgesic nephropathy. Note the pale gray-white papilla, representing papillary sclerosis/necrosis.



FIGURE 25.16 Calcium deposits in the basement membranes of the vasa recta in the renal papilla in analgesic nephropathy. (Von Kossa, $\times 200$.)

abuse-associated analgesic nephropathy, and it is not entirely clear whether non-phenacetin-related cases have the same capillary calcification. This capillary sclerosis increases in intensity toward the pelvic-ureteric junction, is most prominent in the proximal ureter, and then gradually decreases (224). At a more advanced stage (in early stages of papillary necrosis),

the capillary sclerosis involves the peritubular capillaries in the papilla and inner medulla. The ascending loop of Henle also exhibits a substantially thickened basement membrane, but the basement membranes of the collecting ducts, descending loop of Henle, and vasa recta are not affected or are only mildly affected. The thickened basement membranes are PAS positive and contain lipid as well as calcium deposits (Fig. 25.16). Ultrastructurally, this basement membrane thickening consists of numerous thin layers of basement membrane material (Fig. 25.17), which probably forms as the result of repeated injury of the capillary endothelium and the epithelium of the thin limb of Henle (224,228). Early on, these changes are confined to the central part of the inner medulla, but as the disease progresses, the affected small foci become confluent and may involve the entire inner medulla.

As full-blown papillary necrosis develops, the collecting ducts and the vasa recta become necrotic as well, and a ghost outline of the original structure is present (Fig. 25.18). Renal papillary necrosis is not associated with an influx of neutrophils into the necrotic areas or the bordering preserved renal parenchyma. There may be focal collections of lymphocytes and macrophages. If the necrotic portion of the papilla sloughs into the lumen of the renal pelvis, the resulting cavity will reepithelialize. The necrotic material may also remain in place, and in such cases, calcification of the necrotic papilla is common, with possible bone formation (Fig. 25.19).

The cortical changes are thought to stem from the alterations in the papilla (229,230). The cortex may be normal in the

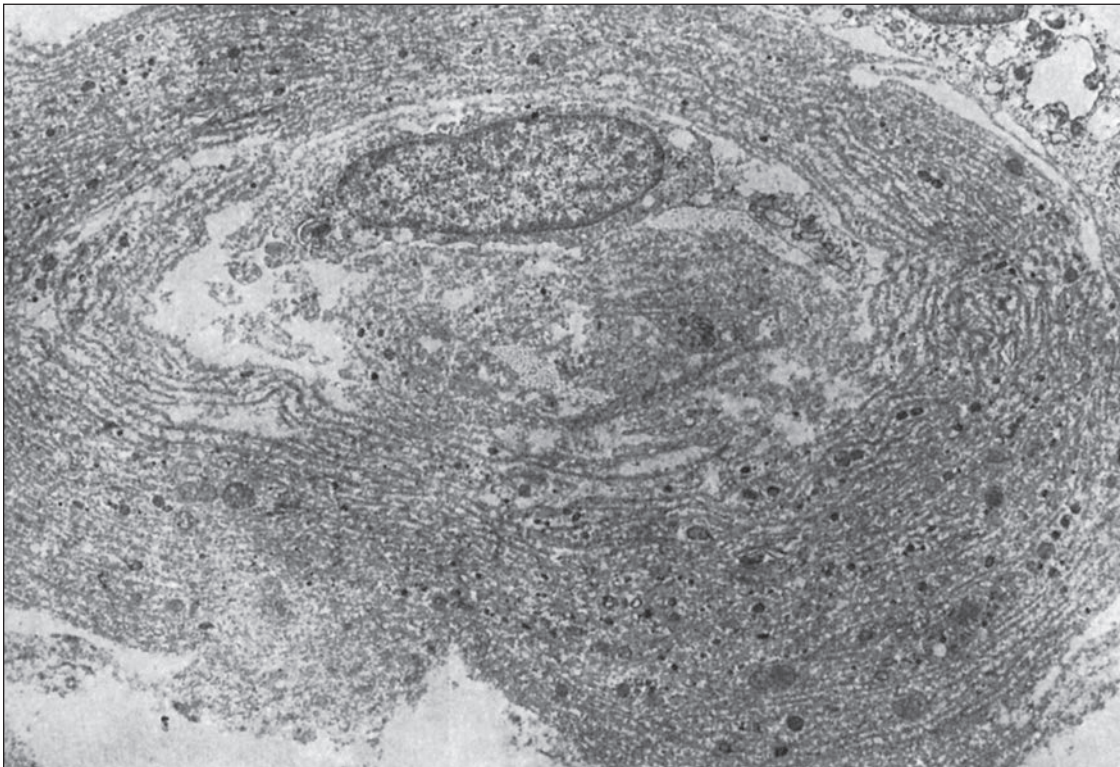


FIGURE 25.17 Electron micrograph of a capillary obtained by biopsy of the renal pelvis of a patient who had abused analgesics. Numerous new basement membrane lamellae have been formed. ($\times 7050$.) (From Mihatsch MJ, et al. The morphologic diagnosis of analgesic (phenacetin) abuse. *Pathol Res Pract* 1979; 164:68.)

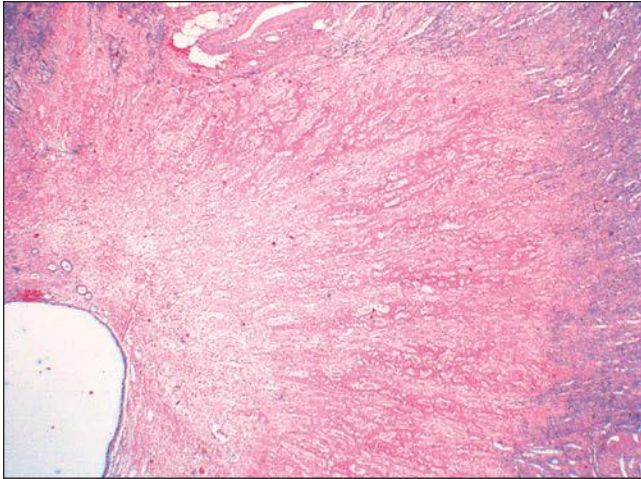


FIGURE 25.18 Low-magnification picture taken from the specimen shown in Figure 25.15. In analgesic nephropathy, typically there is no inflammatory reaction around a necrotic/sclerotic papilla. The ghost structure of the renal papilla is still recognizable. (H&E, $\times 10$.)

early and intermediate forms. The cortical changes consist of tubular loss and tubular atrophy with interstitial fibrosis and a varying degree of interstitial infiltration of chronic inflammatory cells (Fig. 25.20). Lipofuscin accumulation is frequently noted in the epithelium of atrophic tubules. These are nonspecific changes and cannot be reliably differentiated from other forms of chronic tubulointerstitial injury. It appears that the necrotic papilla, in some ways analogous to obstructive nephropathy, is responsible for the cortical changes. This is also supported by the fact that the columns of Bertin are often spared.

The glomerular changes are presumably the result of the tubulointerstitial changes and are quite nonspecific as well. In the atrophic suprapapillary cortex, periglomerular fibrosis, glomerular ischemia, obsolescence, and sclerosis may occur. In the columns of Bertin, where compensatory hypertrophy is common, some glomeruli may undergo segmental hyalinosis and sclerosis (224,231). Zollinger (231) called this change “overload glomerulitis,” which is in fact identical to glomerular hyperperfusion injury. Except for the medullary and pelvic capillary sclerosis, there are no vascular changes characteristic of analgesic nephropathy. Arteriolar hyalinosis and varying degrees of arterial intimal fibrosis may develop,

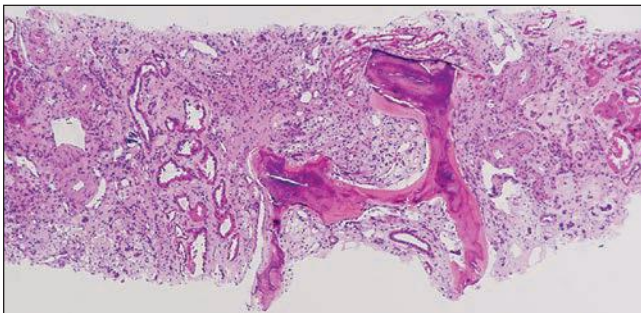


FIGURE 25.19 Bone formation in a necrotic papilla from a patient who had used analgesics for many years. (H&E, $\times 140$.)

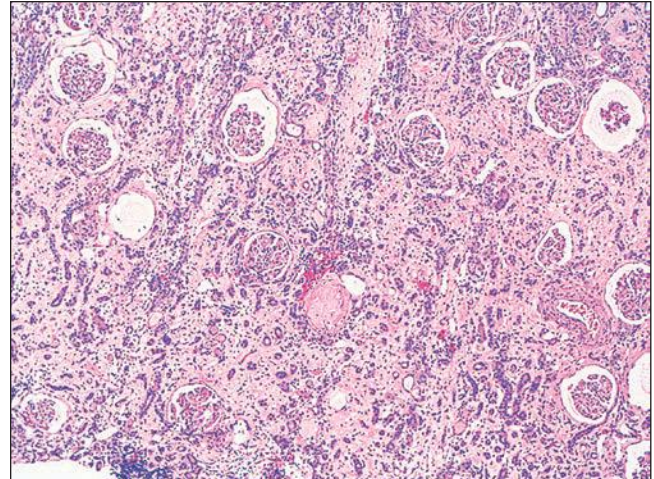


FIGURE 25.20 Interstitial fibrosis and tubular atrophy in the cortex of a kidney with analgesic nephropathy. Note that most glomeruli in this section are preserved; only scattered sclerotic glomeruli are seen. (H&E, $\times 40$.)

particularly in older patients and in patients with arterial hypertension.

DIFFERENTIAL DIAGNOSIS

The key to the differential diagnosis is the clinical history. From the point of view of morphology, the gross findings are at least as characteristic as the histologic appearance. The irregular bumpy cortical contours with underlying papillary necrosis and sclerosis are distinct from the medullary and cortical scarring with caliceal deformities in chronic pyelonephritis/reflux nephropathy. Obstructive uropathy with renal pelvis dilation and parenchymal atrophy is easy to recognize. However, analgesic nephropathy predisposes patients to infections, and acute as well as chronic pyelonephritis is much more common than in the normal population (224). Diabetic nephropathy with papillary necrosis may have a similar gross and microscopic appearance with basement membrane thickening of the loop of Henle and peritubular capillaries. However, the capillary sclerosis beneath the urothelium is not seen. Papillary necrosis may occur in sickle cell disease and, rarely, in vasculitis and SLE (221). In these conditions, as well as in diabetes, the characteristic features of the underlying disease assist in making the diagnosis.

PATHOGENESIS

One theory is that the papillary changes are caused by insufficient blood supply (232,233). Lagergren and Ljungqvist (234) were unable to demonstrate the postglomerular vessels of juxtamedullary glomeruli, indicating decreased blood supply of the papilla. A reduction in number and dimension of the vasa recta in a rat model of analgesic nephropathy was noted by Kincaid-Smith et al. (232) as well. Molland (233) suggested that the reduced medullary blood flow in analgesic nephropathy is the consequence of disturbed autoregulation.

Certainly, capillary sclerosis can compromise the medullary blood flow, but it appears that capillary sclerosis itself is the consequence of toxic effects (235). The concentric lamellated ultrastructure of the thickened basement membranes of the peritubular and pelvic capillaries and the loop of Henle suggests repeated injury and subsequent repair of the capillary endothelium and

loop of Henle epithelium, respectively. Analgesic drugs are highly lipophilic, and they can easily diffuse out of the urine into the medullary and papillary interstitium and cause capillary damage. It has been shown that the concentration of analgesic substances in the renal medulla can be many times higher than in the blood (236). Thus, it appears that the topographic distribution of renal injury is related to the local concentration of analgesics and their metabolites. The primary injury appears to be toxic capillary damage, which in turn, through ischemia, aggravates the injury and leads eventually to papillary necrosis.

The natural history of the medullary/papillary changes is unclear. We had the opportunity to examine a cadaveric donor kidney from a semiprofessional athlete who died because of an automobile accident (Fig. 25.21). Organ donation was considered, but the kidneys were not transplanted because of very poor perfusion on the perfusion pump. Gross examination of the kidney revealed prominent edematous renal papillae (see Fig. 25.21A). Histologically, in the prominently edematous papilla, calcium deposits, including capillary calcification, were noted (Figs. 25.21B and C). Otherwise, the renal parenchyma, including the renal cortex, was normal, and there was no evidence of renal impairment in the donor. After questioning family members, it turned out that the athlete had been taking large amounts of analgesics for several years before his death. There was no evidence of impairment of renal function. Therefore, it is quite possible that this kidney represented an early stage of analgesic nephropathy, which in this particular patient may have been secondary to the combined effect of periodic dehydrations because of the strenuous exercise and the large doses of analgesics.

The pathogenesis of cortical changes is most likely secondary to medullary damage. The nephrons from the columns of Bertin drain into the fornical region of the calyx, which explains their escape from obstruction and subsequent injury in papillary necrosis (223,230). Furthermore, cortical atrophy and chronic interstitial nephritis develop primarily in areas where the underlying papilla remains in situ and undergoes sclerosis with the obstruction of the urine flow. If the separation of the necrotic papilla ensues, the urine flow may persist, and less cortical damage will develop (223,224,230). An alternate theory is that the cortical atrophy in papillary sclerosis/necrosis may be the consequence of the interruption of the limbs of Henle, with subsequent atrophy of the distal and eventually the proximal nephron. The interruption of the peritubular capillaries and vasa recta, by interfering with the blood supply of the tubulointerstitium, may play an important role in the medullary changes and possibly in the cortical changes as well.

The exact pathogenesis of the toxicity of analgesic compounds and the primary target of the toxic reactions are unknown. Inhibition of PG synthesis and immunologic reactions are unlikely causes (224). It is possible that metabolites of phenacetin, aspirin, or paracetamol, under the influence of P450 monooxygenase, bind covalently to cellular proteins and cause toxic damage (220).

Another possible explanation is cellular glutathione depletion with subsequent lipid peroxide production (237). This theory is based on the observation that combination analgesics are more prone to cause damage. Acetaminophen becomes concentrated in the papillae and there undergoes oxidative metabolism, which turns it into a reactive



FIGURE 25.21 Nephrectomy specimen from a young athlete who used large doses of analgesic medications for many years and died of an automobile accident. **A:** Note the edematous papillae. **B:** Histologic examination revealed prominently edematous renal papillae with compression of the vasa recta. (H&E, $\times 100$.) **C:** von Kossa stain revealed finely granular calcium deposits in the basement membranes of the vasa recta and collecting ducts. ($\times 400$.)

quinoneimine that becomes conjugated to glutathione. If acetaminophen is ingested alone, there is sufficient glutathione generated to detoxify the reactive metabolites. If acetaminophen is taken in combination with aspirin or salicylates (aspirin will be converted to salicylate as well), the papillary concentration of salicylates will also be very high. Salicylates potently deplete glutathione, probably through the inhibition of NADPH production. Thus, with the combination of acetaminophen and salicylates or aspirin, glutathione depletion in the papilla may ensue and result in the production of lipid peroxides by the reactive acetaminophen metabolites. This subsequently leads to local tissue damage, resulting in papillary necrosis (237).

There are a few animal models for analgesic nephropathy. Moeckel et al. (238) administered COX-2 inhibitors to mice and found that COX-2 inhibition dramatically reduced osmolyte accumulation in medullary interstitial cells. Exogenous osmolytes reversed COX-2-induced cell death in cultured renal medullary cells. They proposed that the reduction of osmolytes may have a pathogenetic role in analgesic nephropathy (238). In another mouse model of acetaminophen-induced nephrotoxicity, a nitric oxide donor prevented renal injury as measured by blood urea nitrogen levels and renal pathology (interstitial congestion, proximal tubular cell degeneration, and necrosis) (239). The authors proposed that the protective mechanism is secondary to attenuation of lipid peroxidation in the kidney. Ahmed et al. (240) described an animal model with nephropathy following the administration of phenacetin and chloroquine. The renal injury was prevented by the administration of the nitric oxide synthase inhibitor L-nitroarginine methyl ester (L-NAME). A more recent experiment, however, indicated that COX-2 inhibitors may actually be protective against renal injury in an animal model. Administration of COX-2 inhibitor and then an angiotensin 1 receptor inhibitor prevented progressive renal injury in a 5/6 renal ablation model in the rat (241). However, there are clear differences in rodent and human responses to drugs. Chronic aspirin administration can cause renal papillary necrosis in rodents, which has not been reported in humans (242). Therefore, interpreting the somewhat controversial experimental data has to be done with caution. Perhaps nonrodent animals may provide a better model for human analgesic nephropathy.

UROTHELIAL CANCER AND ANALGESIC ABUSE

It is now widely accepted that there is an association between analgesic abuse and transitional cell carcinoma of the renal pelvis and urinary tract (Figure 25.22; (243–245)). The incidence is quite variable, and according to Mihatsch and Knusli (246), it may occur in at least 10% of phenacetin abusers. The latent period can be two or more decades (247). With the decline of phenacetin abuse, the incidence of transitional cell carcinomas of the urinary tract appears to have declined in Australia and Sweden (247,248); however, longer follow-up is needed for definitive proof. Although renal papillary necrosis has been found in a high proportion of patients with transitional cell carcinoma associated with analgesic abuse, it is not a prerequisite for the development of these tumors. Occasional publications also implicate an increased number of renal cell carcinomas in analgesic abusers. However, a study from the National Cancer Institute did not confirm this finding (249).

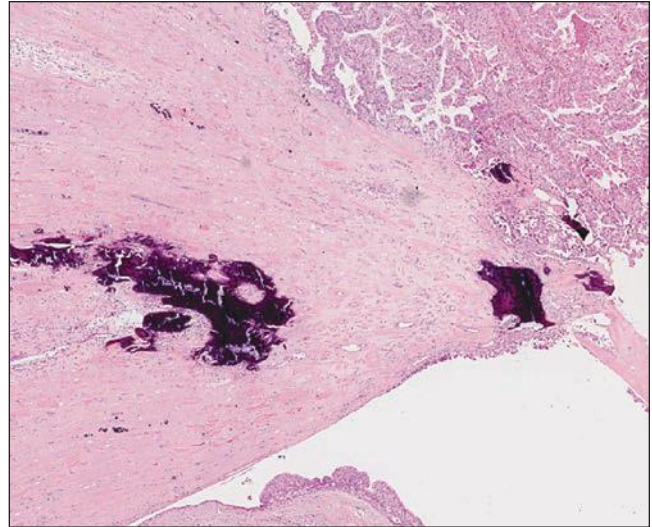


FIGURE 25.22 Transitional cell carcinoma arising in the renal pelvis next to a calcified, sclerotic renal papilla in a patient with end-stage analgesic nephropathy. (H&E, $\times 2$. Section provided by Dr. Bela Ivanyi.)

5-AMINOSALICYLIC ACID

5-Aminosalicylates are anti-inflammatory medications widely used for the treatment of inflammatory bowel disease. Two forms of these medications, mesalazine and sulfasalazine, are used. Based on data from the United Kingdom General Practice Research Database, it appears that the incidence of renal failure in patients on 5-aminosalicylic medications is low (0.17 cases per 100 patients per year) (250). This database indicates that the risk of renal failure is comparable with mesalazine and sulfasalazine use. Examining the renal side effects, Ransford and Langman found that interstitial nephritis was described only following the use of mesalazine (251). This is intriguing because the difference between mesalazine and sulfasalazine is that in sulfasalazine, 5-aminosalicylic acid is combined with sulfapyridine (a sulfonamide). Therefore, theoretically, one might expect a higher prevalence of interstitial nephritis with sulfasalazine. Recently, a case of sulfasalazine-induced hypersensitivity interstitial nephritis was reported (131). Arend and Springate (243) reviewed mesalazine-induced interstitial nephritis, and they concluded that mesalazine-related renal insufficiency occurs in approximately 1 in 100 to 500 patients. In patients with biopsy-proven interstitial nephritis, the frequency of residual renal insufficiency is 61%, and 13% of patients develop ESRD despite discontinuation of the drug (243).

Other Medications

DIPHENYLHYDANTOIN

The drug diphenylhydantoin (Dilantin) is used extensively for the treatment of seizures and arrhythmias. There are several side effects, but adverse reactions involving the kidney are rare. A few cases of oliguric AKI and interstitial nephritis have been reported (244,245,252).

It is well known that vascular changes take place with the use of diphenylhydantoin, and granulomatous arteritis can be seen in patients hypersensitive to this drug (253). Gaffey et al. (253) reviewed eight cases of vasculitis caused by hypersensitivity to Dilantin. The kidney was involved in six cases; three

patients had granulomatous interstitial nephritis. Blood eosinophilia of more than 14% occurred in four patients.

LITHIUM

The widespread use of lithium carbonate in psychiatric practice for the treatment of manic-depressive states has been associated with occasional cases of AKI, the more common occurrence of a diabetes insipidus-like state, and permanent impairment of renal function in others.

Clinical Presentation Nephrogenic diabetes insipidus (polyuria, polydipsia, and impaired renal concentrating capacity) is the most usual renal complication of maintenance lithium therapy (254). Defective distal tubular acidification owing to low fractional excretion of bicarbonate, with normal serum levels of bicarbonate and phosphate and normal ammonia excretion, is also common. Hypercalcemia may also occur (255). These side effects are usually reversible; however, there are reports that chronic irreversible renal injury may develop following maintenance lithium therapy (256).

The frequency with which chronic renal insufficiency and permanent morphologic damage occur in patients receiving long-term lithium therapy has been considered by several authors (257–259). Walker and Edwards (259) summarized the results of seven longitudinal studies between 1981 and 1988 and found little potential for decreased GFR in lithium-treated patients. In a prospective study of 65 lithium-treated patients, Jorkasky et al. (258) found a mild decline in the GFR in men but not in women. They questioned whether the reduction in the GFR was progressive and would lead to clinically significant renal insufficiency. A study from France indicates that the prevalence of lithium nephrotoxicity among ESRD patients is 2 per 1000 dialysis patients (255). They calculated that the lithium therapy duration until ESRD was 19.8 years and the estimated cumulative lithium salt given was 5231 g per patient. Cases of the nephrotic syndrome have been rarely reported (255,260). Interestingly, a study from the Columbia University indicates that 25% of patients who underwent kidney biopsy and were diagnosed to have lithium nephrotoxicity also had nephrotic syndrome (260). These patients had the light microscopic pattern of focal segmental glomerular sclerosis. Lithium nephrotoxicity appears to be a slowly progressive disease, and discontinuation of lithium will result in improved renal function only if the chronic injury is relatively mild.

Pathologic Findings The sparse reports on the renal pathologic features of acute lithium toxicity (261,262) have disclosed little apart from dilated convoluted tubules with some pyknotic nuclei, hyaline droplets, and vacuolated tubular epithelial cells. Chronic lithium nephrotoxicity is associated with progressive chronic TIN.

The original concern about chronic renal disease was raised by the study on the pathologic characteristics of lithium-induced renal disease by Hestbech et al. (256). In this study, renal biopsies were done on 14 patients receiving long-term treatment (1 to 15 years) with lithium carbonate for manic-depressive disease. Thirteen of the biopsies showed pronounced tubular atrophy, interstitial fibrosis, interstitial lymphocytes, and glomerular sclerosis. When the biopsies were assessed by morphometric methods and compared with an age-matched control group without renal disease (transplant donor kidneys

for the most part), the lithium patients had twice the amount of interstitial connective tissue, three times the degree of tubular atrophy, and five times the number of sclerotic glomeruli. The intensity of interstitial mononuclear cell infiltrate was relatively mild, compared with the degree of interstitial fibrosis. In addition, two kidneys from patients taking lithium were seen at autopsy, and those had a granular surface and contained small cortical cysts. Renal cortical microcysts, along with fibrosis, have been described in patients on long-term lithium therapy (Fig. 25.23) (260,263). Markowitz et al. (260), using nephron-specific markers, determined that the microcysts are of distal nephron origin. Other investigators questioned the relevance of these findings (257,264). In spite of these controversial studies, there is now agreement that chronic lithium nephrotoxicity is a cause of chronic TIN with the above-described morphologic changes (254,255,260).

Kincaid-Smith et al. (264) and Walker et al. (265) described a peculiar tubular lesion in biopsies from patients treated with lithium. They found this lesion in the distal convoluted tubules and collecting ducts. It consists of cytoplasmic ballooning or vacuolation with strands of PAS-positive material in the vacuolated cytoplasm, sometimes radiating from the nucleus to the periphery of the cells. The change was regarded as unique; it appeared shortly after the start of lithium therapy and disappeared when treatment was stopped. Other investigators only rarely see this tubular lesion (260).

Glomerular changes are usually secondary and include scattered globally sclerotic glomeruli. Rare cases of minimal change disease and focal segmental glomerular sclerosis have been reported (266,267). Interestingly, Markowitz et al. (260) found that 50% of their biopsies from patients with chronic lithium nephrotoxicity had the glomerular pattern of focal segmental glomerular sclerosis. Half of these patients also had nephrotic syndrome.

None of the above-detailed morphologic changes are specific. A characteristic finding is the microcystic dilation of tubules, which is seen in most cases. One has to remember, however, that microcystic dilation of the tubules is a nonspecific

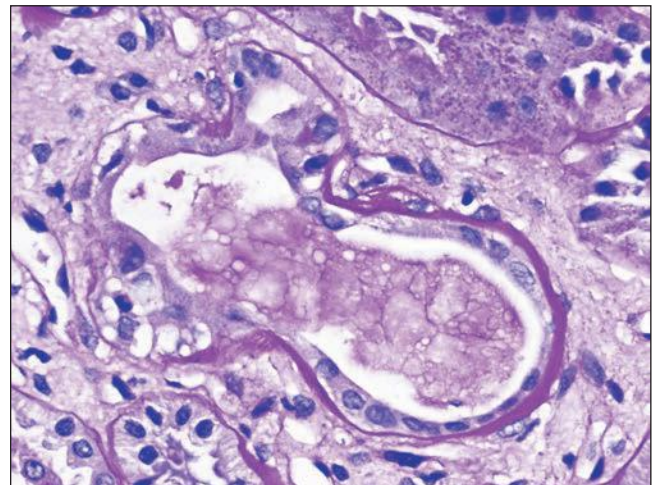


FIGURE 25.23 Dilation of a tubule with vacuolated epithelium, in the background of fibrosis, in a patient who developed chronic renal insufficiency following decades of lithium treatment. (PAS, $\times 400$.)

finding and is commonly seen in any chronic tubulointerstitial disorder. Therefore, obviously, chronic lithium nephrotoxicity is not a renal biopsy diagnosis and the correct diagnosis can be made only following careful correlation of the clinical and morphologic findings.

Pathogenesis The pathogenesis of diabetes insipidus secondary to lithium treatment is most likely the result of the down-regulation of aquaporin-2 expression in the distal nephron (268). The pathogenesis of possible chronic tubulointerstitial injury is much more obscure; it is probably associated with a series of repeated acute injuries and repair. The nephrotic syndrome, seen only occasionally, could be the result of the interaction of lithium with anionic sites on the glomerular basement membranes (GBMs) (267).

PROTON PUMP INHIBITORS

Proton pump inhibitors are commonly used in the treatment of acid peptic disorders. More and more publications indicate that AIN may be a complication of these medications (269–273). Torpey et al. (271) found that in 8 out of 14 drug-related AIN cases at their institution, the etiologic agents were probably proton pump inhibitors. Ray et al. (273) found six cases out of 210 kidney biopsies with AIN that were strongly associated with proton pump inhibitors by either temporal association with the injury or response to stopping the drugs. AIN is diagnosed in an average of 2.7 months following administration of proton pump inhibitors (274). Clinical presentation and the morphologic findings do not differ from other forms of drug-induced interstitial nephritides. Among the proton pump inhibitors, omeprazole appears to be the drug most commonly associated with AIN (274).

PROTEASE INHIBITORS

Protease inhibitors have become the mainstay of current therapy in patients with AIDS. Antiretroviral therapy can contribute to renal dysfunction directly by inducing ATN, AIN, and crystal nephropathy (crystalluria) or indirectly via drug interactions (275). AIN may also be associated with protease inhibitors, primarily with indinavir (276,277). Two patients have been reported who developed AIN with foreign body-type giant cells, presumably secondary to the crystalluria caused by indinavir (278). A few cases of TIN associated with atazanavir and tenofovir use have also been reported (279,280). The kidney biopsies of these patients showed AIN or chronic interstitial nephritis with an acute component. Withdrawal of atazanavir and tenofovir resulted in recovery of renal function (280).

TUBULOINTERSTITIAL NEPHRITIS MEDIATED BY IMMUNOLOGIC MECHANISMS

TIN owing to immune mechanisms may be mediated by antibodies, immune complexes, or T cells. Experimental aspects of TIN have been reviewed by McCluskey (281), Kelly et al. (282), and Wuthrick and Sibalic (283). A brief discussion of immune mechanisms and the various human interstitial nephritides in which such mechanisms are presumed to be operational is offered in this section. In most forms of acute and chronic TIN, immunologic mechanisms are likely to play a pathogenic role, regardless of the initial inciting agent or cause of tissue injury.

Tubulointerstitial Nephritis With Anti-Tubular Basement Membrane Antibodies

The presence of linear deposits of immunoglobulins and complement in the TBM together with tubulointerstitial inflammation is presumptive evidence of anti-TBM antibody disease. However, the significance of TBM deposits of immunoglobulins or complement alone is difficult to ascertain, because such linear TBM staining can occur in diabetes (284) and other advanced chronic renal injuries with tubular atrophy. Complement C3 may be focally present along the TBM even in normal human kidneys (285). Therefore, detection of circulating anti-TBM antibodies in the serum or elution of the antibodies from the renal tissue is necessary to prove the association with interstitial nephritis antibodies. However, the question still remains whether these anti-TBM antibodies are pathogenic or do they merely represent an epiphenomenon secondary to underlying tubular damage. It is theoretically possible that in many forms of severe acute tubulointerstitial injury, tubular and TBM antigens may be exposed, altered, and released in the circulation with subsequent formation of antibodies. Drug-induced TIN with anti-TBM antibodies was discussed earlier in this chapter.

Primary Anti-Tubular Basement Membrane Antibody Nephritis

Primary anti-TBM antibody nephritis is a form of TIN with linear deposits of IgG and complement along the TBM, presence of anti-TBM antibodies in serum, mononuclear cell and neutrophilic infiltration of the interstitium and tubules, and edema and tubular cell injury. Glomeruli and vessels are normal or show nonspecific changes. Very few instances of primary anti-TBM nephritis have been reported. The two patients described by Clayman et al. (286) and Brentjens et al. (287) fulfill the criteria delineated earlier. One of the patients, a 27-year-old woman, presented with nausea, vomiting, fever, and generalized body aches. She became rapidly anuric, and a renal biopsy demonstrated intense inflammatory cell infiltrate in the interstitium with neutrophils and mononuclear cells and linear deposits of IgG, C3, and the terminal components of complement in the TBM. Anti-TBM antibodies were detected in the serum. This patient recovered renal function after intensive steroid therapy, but features of renal tubular acidosis persisted. The other patient, a 36-year-old man, presented with ESRD. Both patients had circulating antibodies that were reactive with a 48- to 58-kDa TBM protein, and in both, this antibody activity could be inhibited with a rodent antibody to a cross-reactive antigen. This protein in the TBM was later called TIN antigen (288). The TIN antigen is an extracellular matrix basement protein, which was originally identified as a target antigen involved in anti-TBM antibody-mediated interstitial nephritis. TIN antigen was mapped to chromosome 6p11.2-12 (39). The essential role of TIN antigen in cell survival by utilizing integrin $\alpha\beta3$ and downstream effectors has recently been demonstrated by Xie et al. (289). The case reported by Bergstein and Litman (290), also an instance of primary anti-TBM nephritis, describes a 6-year-old boy who presented with polydipsia, polyuria, microscopic hematuria, proteinuria, and glucosuria. The renal biopsy demonstrated mononuclear cell infiltrate with occasional lymphoid follicles, pronounced interstitial fibrosis, and tubular atrophy and loss associated with linear deposits of IgG and C3 in the TBM (Fig. 25.24).

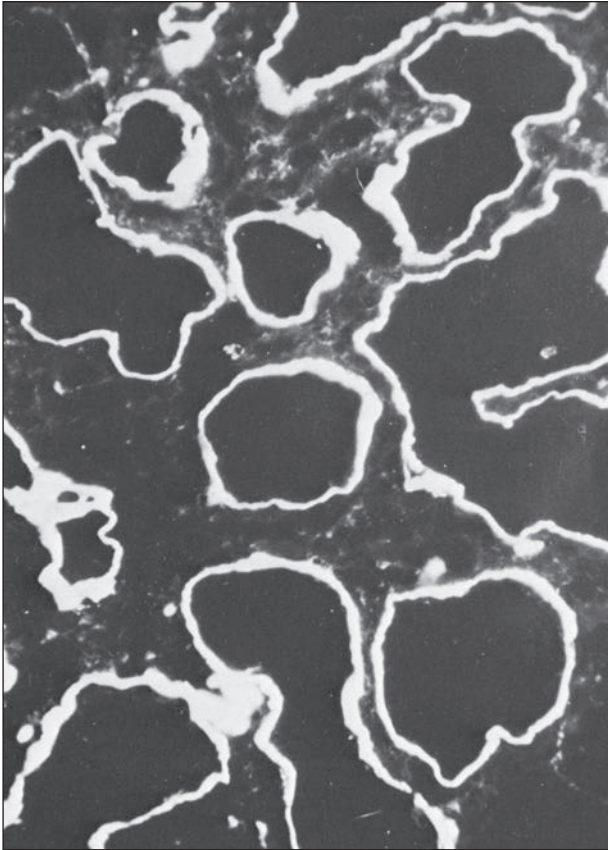


FIGURE 25.24 Primary TIN with anti-TBM antibodies is detected by linear fluorescence for IgG along the TBM. (From Bergstein J, Litman NN. Interstitial nephritis with anti-tubular basement membrane antibody. *N Engl J Med* 1975;292.)

The glomeruli demonstrated no deposits of immunoreactants. Anti-TBM antibodies were demonstrated in the serum and were not reactive with GBM antigens. The reports of Rakotoarivony et al. (291), Freycon et al. (292), and Helczynski and Landing (293) also include instances of primary TIN with anti-TBM antibodies.

Secondary Anti-Tubular Basement Membrane Antibody Nephritis

Included in the category of secondary anti-TBM antibody nephritis are various types of primary glomerulonephritides and allograft nephropathy in which there is an associated component of TIN with linear deposits of IgG and complement in the TBM.

ANTI-GLOMERULAR BASEMENT MEMBRANE ANTIBODY DISEASE

Anti-GBM antibody disease, with or without pulmonary hemorrhage, is an autoimmune disease owing to antibodies reactive exclusively, or principally, with the noncollagenous domain—NC1—of the $\alpha 3$ chain of type IV collagen (294). Anti-TBM antibodies are found in 50% (295) to 70% (296) of patients with anti-GBM nephritis. In general, tubular linear deposits are focal, they are less intense than deposits along the GBM, and they often involve proximal tubules. In the series of Lehman et al.

(285), 23 of 26 patients with Goodpasture syndrome (88.4%) and 13 of 21 patients with anti-GBM antibody disease without pulmonary hemorrhage (61.9%) had linear TBM deposits of IgG, sometimes accompanied by C3. In the series of Graindorge and Mahieu (296), 9 of 11 patients with linear deposits of immunoglobulins along the GBM had anti-TBM antibodies by radioimmunoassay (82%), and 8 of these 9 patients showed linear deposits of IgG along the TBM. Anti-TBM antibodies are detected more frequently in kidney eluates than in serum (285).

Although anti-TBM antibodies are usually of the IgG class, Border et al. (297) reported anti-TBM antibodies of the IgA class in a patient with Goodpasture syndrome. The specificity of anti-TBM antibodies in patients with Goodpasture syndrome is unknown, but they probably are nephritogenic. Andres et al. (295) investigated their relative role in the pathogenesis of TIN in three groups of patients with crescentic glomerulonephritis: group 1 with anti-GBM and anti-TBM antibodies, group 2 with anti-GBM antibodies only, and group 3 with neither anti-GBM nor anti-TBM antibodies. Group 1 had the most severe, group 2 the intermediate, and group 3 the mildest form of TIN. These observations were interpreted to suggest that anti-TBM antibodies contribute to the development of TIN in patients with anti-GBM antibody disease. In our opinion, these observations do not prove the pathogenic role of anti-TBM antibodies in anti-GBM disease.

MEMBRANOUS GLOMERULONEPHRITIS

Some patients with membranous glomerulonephritis may show evidence of anti-TBM antibodies in kidney biopsies, serum, or both (298,299). Males are more often affected than females, and in most patients, the disease occurs before 5 years of age (300). HLA haplotypes B7 and DRw8 provide susceptibility to disease (299). In the publications of Levy et al. (298), Katz et al. (297), and Makker et al. (300), patients presented with proteinuria or the nephrotic syndrome and tubular dysfunction with features of Fanconi syndrome. Some cases have occurred in families (292,293,301). In the report of Makker et al. (300), the putative antigen in glomerular deposits was determined to be human gp330, the Heymann antigen, or megalin (302). However, in most cases, the target antigen in the TBM is the TIN antigen (299,300,303). The disease progresses to chronic renal failure (300,303). Ivanyi et al. (303) reported a child who developed progressive membranous glomerulopathy with circulating antibodies to the TIN antigen. The patient did not develop recurrent disease in his allograft after a 2-year follow-up.

RENAL ALLOGRAFTS

Linear deposits of immunoglobulins and complement in the TBM are found with variable frequency in patients with renal allografts. In the report by Rotellar et al. (304), IgG and complement were present in 18 (2.7%) of 662 biopsies, and they occurred 3 to 13 months after transplantation. Of the 18 patients, circulating anti-TBM antibodies were detected in 10, and in 5 of these 10 patients, anti-TBM antibodies were detected in sera before linear TBM deposits could be found in renal biopsies. Linear deposits of IgG and C3 also were detected in patients who were clinically stable (not rejecting). In 10 of 15 patients who were subjected to sequential biopsies, linear TBM deposits disappeared. Overall, circulating anti-TBM antibodies were detected predominantly in the first 6 months after transplantation; they persisted for an average of 3 months and did not

recur after they disappeared (304). Because graft survival was the same in patients with or without anti-TBM antibodies, the investigators (304) concluded that the presence of anti-TBM antibodies in renal allografts was not contributory to deterioration of graft function. Renal allograft recipients develop anti-TBM antibodies as a result of antigenic polymorphism, and the target antigen is the 48- to 58-kDa TBM protein (296,305). However, TBM staining for IgG and complement is a frequent nonspecific finding in renal allograft biopsies, particularly if chronic injury is already evident. Therefore, such TBM staining has to be interpreted with caution.

MISCELLANEOUS DISEASES

Morel-Maroger et al. (306) reported a patient with crescentic poststreptococcal glomerulonephritis, the nephrotic syndrome, and renal insufficiency. This patient underwent four renal biopsies within 28 weeks, but only the last biopsy revealed linear deposits of IgG and C3 along the TBM. There was also interstitial inflammation with mononuclear cells, tubular atrophy, and interstitial fibrosis. This patient's serum was reactive with the TBM of one of his previous biopsies that had been found to be negative for TBM deposits. Anti-TBM antibodies also have been described in patients with SLE (307), Kimura disease (308), polyglandular autoimmune syndrome (309) and, in isolated cases of IgA nephropathy, focal segmental glomerulosclerosis, lipoid nephrosis, and malignant hypertension (112).

Pathologic Findings

The tubulointerstitium shows variable degree of mononuclear cell infiltrate and, in more advanced stages of the disease, tubular atrophy, and interstitial fibrosis. The light microscopic changes are not different from other forms of tubulointerstitial fibrosis. In primary anti-TBM nephritis, glomeruli are normal or show nonspecific changes. In secondary anti-TBM nephritis, the glomerular changes vary and include crescentic (285,306), membranous (298,299,301,303), lupus (307), or mesangioproliferative glomerulonephritis or focal segmental glomerulosclerosis (112). Arteries and arterioles may show hypertensive or age-related changes. By immunofluorescence, linear deposits of IgG and rarely other immunoglobulins, often with complement, are detected along the TBM (see Fig. 25.24) (112,285,287). Electron microscopy does not reveal electron-dense immune-type deposits along the TBM.

Etiology and Pathogenesis

To establish that TIN is mediated by anti-TBM antibodies, it is necessary to demonstrate linear deposits of immunoglobulins, commonly IgG, and complement along the TBM (281); to detect antibodies specific for TBM antigens in the circulation (281); to demonstrate that antibodies are concentrated severalfold in renal eluates relative to their concentration in plasma; to demonstrate that the antibody activity can be abolished by incubation of plasma or eluate with TBM antigen; and to demonstrate that the antibodies have a pathogenic role, for example, by transferring TIN to syngeneic recipients through injection of antibodies alone. Because only some of these requirements can be satisfied, the diagnosis of human TIN associated with anti-TBM antibodies is inferential and by analogy to data derived from experimental models (281,283). The anti-TBM antibodies may arise because of renal damage, and they recognize antigens present in collagenase digests of TBM. Three antigens have been

identified to date. The major and best-characterized antigen is a 54-kDa protein localized to chromosome 6p11.2-12 (39), which is the target of autoantibodies in idiopathic anti-TBM disease. The latter is called TIN antigen. Earlier, the TIN antigen was referred to as 48- to 54-kDa protein (308,309), 58-kDa protein (310), or 48- to 58-kDa protein (296) and as 3M-1 antigen (311). Purified 3M-1 protein induces antibodies to the TBM and TIN in susceptible hosts; TBM preparations selectively depleted of 3M-1 protein do not (286). Studies by Yoshioka et al. (311) demonstrated that sera from patients with anti-TBM nephritis bind to both 48- and 54-kDa antigens, and the studies of Miyazato et al. (312) demonstrated that the 48- and 54-kDa glycoproteins share the same epitope but are encoded by different mRNA. The protein may contribute to basement membrane assembly and cellular adhesion (313) through interaction with $\alpha 3\beta 1$ and $\alpha v\beta 3$ integrins (314) and also play an important role in renal development (315,316). In spite of its name, it is becoming apparent that TIN antigen may play a more important role in normal renal development than in actual acute TIN later in childhood or in adulthood (33,316–318). Abnormal TIN antigen has been reported in nephronophthisis (317) and renal dysgenesis/chronic TIN in children (33). Transcription of TIN antigen is down-regulated in obstructive nephropathy, and this down-regulation is mediated by CCAAT/enhancer-binding protein beta (C/EBP-beta) (319). The second antigen, a 70-kDa protein, is the target of autoantibodies present in patients with anti-GBM nephritis and in some patients with lupus nephritis. This antigen is present in the GBM and TBM (285). The third antigen, a 45- to 50-kDa protein, is also target of autoantibodies in some patients with anti-GBM disease (320) and of antibodies that developed in one patient with Alport syndrome after renal transplantation (321).

The antibodies involved are predominantly of the IgG class and, rarely, other immunoglobulins (285,287). Interaction of antigen and antibody results in complement activation and deposition of C3 in TBM. That complement is required for inflammatory infiltration, and tubular epithelial cell injury is indicated by the experimental studies of Hatanaka et al. (322). These authors demonstrated that inhibition of complement activation in a rat model of anti-basement membrane (both glomerular and tubular) disease at the C3 convertase level abrogates tubulointerstitial injury and leukocytic infiltration induced by anti-basement membrane antibodies.

Tubulointerstitial Nephritis With Immune Complexes

TIN with immune complexes implies the presence of granular deposits of immunoglobulins and complement in the TBM, interstitium, or both. Deposits often are associated with an underlying renal disease, usually a form of glomerulonephritis mediated by immune complexes, and the incidence of tubulointerstitial immune complex deposits in renal biopsies varies: 1.5% (16 of 1100 biopsies) in the series of Orfila et al. (112), 6.5% (13 of 200 biopsies) in the Lehman et al. series (285), and 42.9% (6 of 14 biopsies) in the study of Levy et al. (298). In these three series, the underlying conditions were various glomerulonephritides (e.g., lupus, membranous, cryoglobulinemic, membranoproliferative, focal proliferative, crescentic, postinfectious, shunt nephritis), minimal change glomerular disease, allograft rejection, graft versus host reaction, idiopathic TIN, hepatitis B infection, and syphilis. We would like to reiterate that complement

and even IgG staining may occur nonspecifically in the TBM, particularly if the tubules are atrophic and if the patient is diabetic. Granular or finely vacuolar deposits are commonly seen in the basement membranes of atrophic tubules by electron microscopy. On low magnification, these nonspecific deposits may appear as discrete immune-type electron-dense deposits. Therefore, before the diagnosis of immune complex deposits in the TBM is made, careful morphologic examination and correlation of the findings with laboratory results are necessary.

Primary Tubulointerstitial Nephritis With Immune Complexes

Primary TIN with immune complexes is very rare because, in most cases of TIN with immune complex deposits, we now recognize the underlying disease. Ellis et al. (323) reported one patient with proximal tubule dysfunction and TIN with granular deposits of immunoglobulins and complement in tubules and interstitium; the glomeruli were normal.

Granular deposits of IgE have been detected in two patients with TIN. The first patient was a 54-year-old woman who presented with anemia, diverticulitis, hypocomplementemia, eosinophilia, and renal insufficiency. The patient had no allergic or drug history and no evidence of systemic connective tissue disease. The kidney biopsy demonstrated TIN with granular TBM deposits for IgE, IgG, IgM, and C3; deposits of IgE predominated (324). The second patient was a 72-year-old man who had a positive antinuclear antibody (ANA) assay but no evidence of SLE. The kidney biopsy demonstrated advanced TIN with prominent granular IgE deposits (7).

Kambham et al. (42) reported eight patients who had interstitial nephritis in their renal biopsies associated with tubulointerstitial immune complex deposition and hypocomplementemia. They used the term “idiopathic hypocomplementemic interstitial nephritis” to designate this entity. None of these patients had evidence of SLE or Sjögren syndrome. In six of their eight patients, complement levels were available. C3 and C4 levels were depressed in all patients except one, in whom C3 was normal and C4 levels were low. In one of their patients, the infiltrate was suggestive of a marginal zone lymphoma, and heavy chain gene rearrangement studies indicated monoclonality (42). Immunofluorescence revealed granular tubular basement deposits for IgG in all cases. C1q was detected in six of eight cases and C3 in only four of the eight cases. Electron microscopy revealed discrete electron-dense immune-type deposits in all biopsies. In two cases, the TBM deposits had a paracrystalline fingerprint-like substructure. None of the patients had evidence of hypocomplementemic urticarial vasculitis syndrome (HUVS). Follow-up data were available in six of their patients, and five of them responded favorably to immunosuppressive medication. Immunosuppression included prednisone and a combination of tacrolimus, prednisone, and mycophenolate mofetil in the patient who had the monoclonal cell population. Rare older and more recent case reports have been published describing very similar primary immune complex tubulointerstitial cases with hypocomplementemia (324–326). Most of these idiopathic hypocomplementemic interstitial nephritis cases probably represent IgG4-related interstitial nephritis (see below).

Markowitz et al. (327) described a patient whose peculiar kidney biopsy showed polyclonal large electron-dense deposits along the TBMs between the tubular epithelial cells and

the basement membrane. These deposits were IgG positive and had a distinctive curvilinear substructure. The patient had underlying diabetic nephropathy, but did not show evidence of active interstitial nephritis.

Secondary Tubulointerstitial Nephritis With Immune Complexes

Included in the category of secondary TIN with immune complexes are various systemic diseases, glomerulonephritides, and other renal diseases in which there is tubulointerstitial inflammation associated with granular deposits of immunoglobulins and complement in the interstitium or TBM.

IgG4-RELATED TUBULOINTERSTITIAL NEPHRITIS

Introduction There is now evidence that some tubulointerstitial nephritides are due to IgG4-related disease. Some patients with IgG4 systemic disease may have TIN with increased number of IgG4-producing plasma cells. Although data are still limited, growing literature suggests that this entity may be overlooked and the number of patients with IgG4-related interstitial nephritis may be substantial.

One of the first reports describing probable cases of IgG4 systemic disease was published more than 50 years ago. Sarles et al. (328) described patients with sclerosing pancreatitis and hyperglobulinemia, and they hypothesized that this may be an autoimmune disease. More recently, this disease was found to be associated with increased IgG4 levels in the serum and the presence of numerous IgG4-positive plasma cells in the affected tissues (329,330). Subsequently, numerous reports described increased number of IgG4-producing plasma cells in a variety of organs associated with IgG4 systemic disease. In addition to “autoimmune pancreatitis,” involvement of the liver (331), lacrimal (332) and salivary (333) glands, lungs (334,335), gastrointestinal system (336), breast (337), lymph nodes (338), retroperitoneum and mediastinum (339,340), and many other organs by IgG4-positive plasma cells was reported. This novel clinical syndrome was proposed to be named IgG4-related disease (41,341). Histologically, patients with IgG4-related disease have infiltration of organs by IgG4-positive plasma cells and progressive fibrosis (342,343). Many questions and problems related to the pathogenesis, diagnostic criteria, and treatment of IgG4-related disease are still to be elucidated. Because of the lack of universal diagnostic criteria, low awareness of the disease among physicians, and high variability of the clinical presentation, the prevalence of IgG4-related disease is unclear. In Japan, the presumed incidence of IgG4-related disease is 0.28 to 1.08/100,000 population (342). Data about incidence and prevalence of the disease elsewhere are scant.

There is growing evidence that the kidney is a frequent target organ in IgG4-related systemic disease (13,344). The main histologic findings in the kidney directly involved by this disease are similar to other organs, namely, TIN with infiltration of the interstitium by IgG4-positive plasma cells and interstitial fibrosis. However, kidney function may also be affected in patients with IgG4-related disease involving retroperitoneum, renal pelvis, or urethra because of urinary outlet obstruction and development of hydronephrosis.

Clinical Presentation Several authors from Japan, Korea, and the United States describe renal involvement in IgG4-related disease and propose diagnostic criteria for its identification (13,345–347).

The average age of patients with IgG4-related tubulointerstitial nephritis is approximately 65 years, ranging from 20 to 83 years (13,346,347). There is a predominance of male patients (from 3:1 in Japan up to 7:1 in the United States). At the time of renal biopsy, the majority of patients have acute or progressive chronic kidney injury. The mean Scr at the time of diagnosis ranges from 1.7 mg/dL (346) to 3.6 mg/dL (13).

Serum total IgG or IgG4 levels are elevated in 79% (13) to 90% (346) of patients. Approximately half of the patients have hypocomplementemia, with decreased C3, C4, or CH50 levels. Peripheral eosinophilia may occur (347). Renal imaging studies reveal different abnormalities, including multiple small low-attenuation lesions, mass lesions, bilaterally markedly enlarged kidneys with bilateral renal swelling, or diffuse thickening of the renal pelvis.

Pathologic Findings

Light microscopy: Histologic findings in renal biopsies and nephrectomy specimens include dense interstitial lymphoplasmacytic infiltrates with some eosinophils and variable degree of interstitial fibrosis in the majority of the cases (see Fig. 25.5A). Focal mononuclear cell tubulitis is common, and some biopsies may show mild focal plasma cell tubulitis (13). The cellular composition of inflammatory infiltrates changes with the progression of interstitial fibrosis; lymphocytes with plasma cells are predominant in early stages of fibrosis, whereas plasma cells become more prominent with increasing fibrosis. Inflammatory cell infiltrates are usually attenuated in extensive fibrosis (347). The interstitial fibrosis is usually zonal with clear demarcation between involved and uninvolved areas (Fig. 25.25A). The fibrosis often extends into the deep medulla and may infiltrate extrarenally, involving the renal capsule and retroperitoneal space. The pattern of interstitial fibrosis is characteristic; the collagenous bundles encircle nests of lymphocytes and plasma cells, resembling the “storiform” pattern

in autoimmune pancreatitis. Some authors refer to this as the “bird’s-eye” pattern (347). The degree of interstitial fibrosis is variable in the biopsy specimens. Nephrectomy specimens with mass lesions show more fibrotic and less inflammatory areas at the center of the mass with more interstitial inflammation and less fibrosis at the periphery. These data indicate that it is very difficult to evaluate the degree of interstitial fibrosis and proportion of involvement of the renal parenchyma based on kidney biopsy findings alone; sampling error is common. Correlation with imaging studies should be performed in each individual case.

The main histologic feature of IgG4-related TIN is the presence of increased number of IgG4-positive interstitial plasma cells (see Figs. 25.5B and 25.25B). There is no clear quantitative approach available, but many authors agree that the presence of more than 10 IgG4-positive plasma cells per high-power field (HPF) in the densest infiltrates is a diagnostic criterion for IgG4-related interstitial nephritis (13,347). A detailed classification proposes that 11 to 30 IgG4-positive plasma cells per HPF should be considered as moderate increase, whereas more than 30 IgG4-positive plasma cells per HPF are marked increase (13). However, increased numbers of IgG4-positive interstitial plasma cells may be noted in other diseases, such as in anti-neutrophil cytoplasmic antibody (ANCA)-associated glomerulonephritis, diabetic nephropathy, idiopathic TIN, membranous glomerulonephritis, and lupus nephritis (348). Therefore, the presence of numerous IgG4-positive plasma cells in a renal biopsy specimen is not a specific diagnostic finding for IgG4-related TIN.

Several proposals to classify the pattern of interstitial fibrosis and inflammation have been made. The Mayo Clinic group proposes the following patterns of tubulointerstitial inflammation and fibrosis: pattern A, AIN with minimal interstitial fibrosis (less than 10%) without expansive interstitial process; pattern B, more dense interstitial inflammatory lesions with

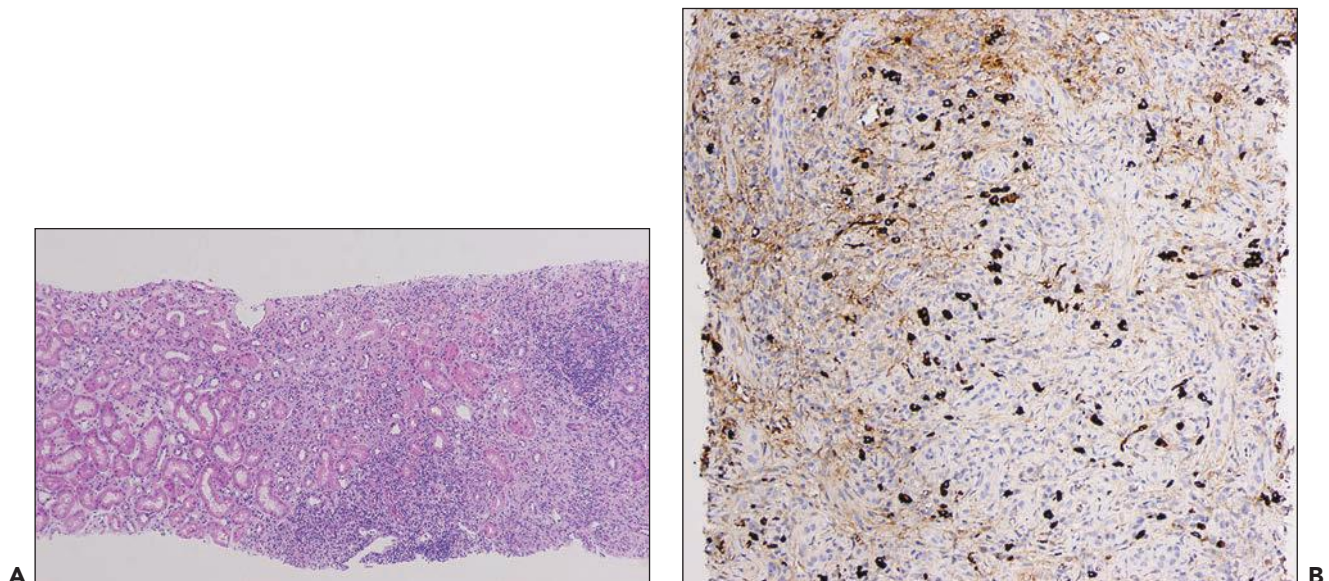


FIGURE 25.25 Light microscopic findings in IgG4-related TIN. **A:** Zonal appearance of mixed interstitial inflammatory cell infiltrate in IgG4-related interstitial nephritis. Note the demarcation between the inflamed and uninvolved renal cortex. (H&E, $\times 40$.) **B:** Numerous IgG4-positive plasma cells in the interstitial inflammatory cell infiltrate. (Immunoperoxidase, $\times 100$.)

expansive interstitial fibrosis; and pattern C, collagen-rich paucicellular fibrosis (13). A four-tier classification of the interstitial fibrosis is proposed by a Japanese group: stage A, active cellular infiltration with fine fibrosis; stage B, active cellular inflammation with mild but distinct interstitial fibrosis; stage C, dominant interstitial fibrosis with mild cellular infiltration; and stage D, advanced interstitial fibrosis with little cellular infiltration (347). According to these authors, electron microscopy is the more valuable tool to classify the degree of interstitial fibrosis, when in the early stages, bundles of fine collagen fibrils are sparse among the infiltrating cells, whereas with more advanced fibrosis (stage C), interstitial-type collagen bundles encase each interstitial inflammatory cell. In the advanced stage (D), interstitial-type collagen bundles become thick, and interstitial inflammatory cells are sparse. Distinct collagen bundles are localized around fibroblasts, which are intermingled with inflammatory cells (347). Regarding the value of ultrastructural studies, one has to consider the problem of sampling error, particularly in a renal tubulointerstitial disease with zonal distribution of changes, because the specimen submitted for electron microscopy is usually small and may not be representative. Whether these ultrastructural findings are truly of diagnostic value awaits confirmation. Outside of the inflammatory lesions, the renal parenchyma usually is normal (13).

Glomeruli usually are unremarkable or show mild mesangial expansion. Several recent reports describe membranous glomerulonephritis in patients with IgG4-related TIN (349,350). Indeed, idiopathic or recurrent membranous glomerulonephritis is characterized by IgG4-predominant deposits along the glomerular capillaries (351,352). Even though this association between membranous glomerulonephritis and IgG4-related disease may be not random, the pathogenetic link between the two diseases is unclear.

No specific vascular lesions are identified that are associated with IgG4-related TIN (13,347).

Immunofluorescence: Immunofluorescence findings are characteristic. Granular TBM staining for IgG is present in the majority of cases (13) (Fig. 25.26). Notably, glomeruli

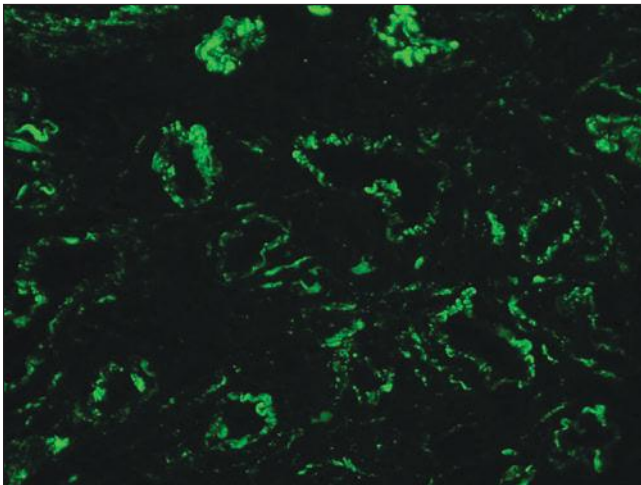


FIGURE 25.26 Immunofluorescence findings in IgG4-related interstitial nephritis. Granular staining for IgG is seen along the TBM. (Direct immunofluorescence, $\times 400$.)

usually do not show IgG staining. The TBM deposits contain predominantly IgG4 (13). TBM staining for both kappa and lambda light chains is present, often associated with some C3 staining as well. A small number of cases have C1q and IgM staining in the TBM. The TBM deposits are usually present in the areas of inflammation, but not in the normal areas, based on the analysis of nephrectomy specimens. The TBM deposits are more commonly found in specimens with more progressive fibrosis (13). Direct immunofluorescence is an excellent method to detect TBM immune complex deposits and the IgG4 dominance in these deposits, but in our experience, direct immunofluorescence to detect and enumerate the interstitial infiltrating IgG4-positive plasma cells is not the optimal method. A more sensitive immunoperoxidase methodology on paraffin sections should be used to quantify the infiltrating IgG4-positive plasma cells in tissue sections.

Electron microscopy: Electron microscopy has limited value in the diagnosis of IgG4-related TIN. Discrete electron-dense immune-type deposits are usually seen within the TBM (Fig. 25.27) (13,347). According to Yamaguchi et al. (347), electron microscopy is a useful tool to determine the degree of interstitial fibrosis (see above). Glomerular changes usually are nonspecific, except for rare cases of membranous glomerulonephritis.

Diagnostic Criteria As mentioned above, the diagnosis of IgG4-related TIN should not be made based on the morphologic findings alone. Several diagnostic criteria were proposed recently in order to render the diagnosis of this disease properly (Table 25.4). The Mayo Clinic group (13) proposes the following criteria for IgG4-related TIN: (a) histologic findings of plasma cell–rich TIN with greater than 10 IgG4-positive plasma cell per HPF in the most concentrated areas, TBM

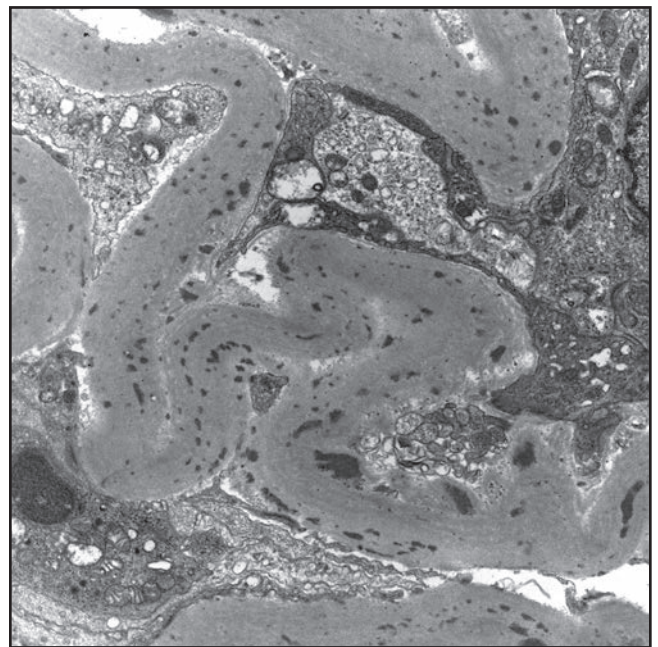


FIGURE 25.27 Electron microscopy findings in IgG4-related interstitial nephritis. Electron-dense immune-type deposits are seen along the TBM. (Uranyl acetate and lead citrate, $\times 10,000$.)

TABLE 25.4 Diagnostic criteria of IgG4-related TIN proposed by two different groups

Findings	Mayo Clinic group	Japanese Society of Nephrology ^a
Light microscopy	Plasma cell–rich interstitial nephritis ^b	Dense lymphoplasmacytic infiltration with greater than 10 IgG4-positive plasma cells per HPF in the most concentrated areas and/or the ratio of IgG4- to IgG-positive plasma cells >40% Characteristic fibrosis surrounding nests of lymphocytes/plasma cells
Immunofluorescence	TBM immune complex deposits ^b	Not included
Immunohistochemistry	>10 IgG4-positive plasma cells per HPF in the most concentrated areas	See light microscopy
Other organ involvement	Autoimmune pancreatitis, sclerosing cholangitis, sialadenitis, inflammatory aortic aneurysm, retroperitoneal fibrosis, inflammatory mass in any organ	Extrarenal organ involvement with characteristic morphologic findings, including >10 IgG4-positive cells per HPF in the most concentrated areas and/or the ratio of IgG4- to IgG-positive plasma cells >40%
Imaging	Small peripheral low-attenuation cortical nodules, round- or wedge-shaped lesions, diffuse patchy involvement of the kidneys, diffuse marked kidney enlargement	Multiple low-density lesions on enhanced computer tomography Diffuse kidney enlargement Hypovascular solitary mass in the kidney Hypertrophic lesions in the renal pelvic wall without irregularity of the renal pelvic surface
Laboratory	Elevated serum IgG4 or total IgG levels	Kidney injury (abnormal urinalysis, decreased kidney function) Hypocomplementemia Elevated serum IgE levels Elevated serum IgG4 levels >135 mg/dL

^aSee the text for diagnostic criteria.

^bMandatory criterion.

immune complex deposits by immunofluorescence, immunohistochemistry, and/or electron microscopy; (b) small peripheral low-attenuation cortical nodules, round- or wedge-shaped lesions, diffuse patchy involvement of the kidneys, or diffuse marked enlargement of the kidneys by imaging studies; (c) elevated serum IgG4 or total IgG levels; and (d) other organ involvement, such as autoimmune pancreatitis, sclerosing cholangitis, inflammatory masses in any organ, sialadenitis, inflammatory aortic aneurysm, lung involvement, and retroperitoneal fibrosis. These authors propose that in order to diagnose IgG4-related TIN, the histologic findings should include plasma cell–rich TIN with increased number of IgG4-positive plasma cells (the mandatory criterion) with at least one of the other criteria. TBM immune complex deposition is a supportive criterion, which is present in more than 80% of cases.

The Japanese Society of Nephrology proposes the following diagnostic criteria for IgG4-related TIN (346): (I) presence of some kidney injury, as manifested by abnormal urinalysis, urine markers, or decreased kidney function with elevated serum IgG levels, hypocomplementemia, or elevated serum IgE levels; (II) abnormal renal radiologic findings, including (a) multiple low-density lesion on enhanced computer tomography, (b) diffuse kidney enlargement, (c) hypovascular solitary mass in the kidney, and (d) hypertrophic lesion of renal pelvic wall without irregularity of the renal pelvis surface; (III) elevated serum IgG4 levels (IgG4 more than 135 mg/dL); (IV) characteristic histologic findings including (a) dense lymphoplasmacytic infiltration with infiltrating IgG4-positive plasma cells greater than 10/HPF and/or the ratio of IgG4- to IgG-positive plasma cells greater than 40% and (b) characteristic fibrosis, surrounding nests of lymphocytes and/or plasma cells; and (c) extrarenal organ involvement with characteristic histologic findings, including

dense lymphoplasmacytic infiltration with infiltrating IgG4-positive plasma cells greater than 10/HPF and/or IgG4/IgG-positive plasma cells greater than 40% in extrarenal organ(s). These authors have criteria for definite, probable, and possible IgG4-related kidney disease. For the definite diagnosis, patients must have criteria 1+3+4 (both 4a and 4b) or 2+3+4 (both 4a and 4b) or 2+3+5 or 1+3+4a+5. If fewer criteria are fulfilled, the diagnosis is probable or possible (346).

These two proposed diagnostic algorithms are slightly different, but they both agree that the diagnosis of IgG4-related TIN cannot be made based on the morphologic findings alone and ancillary studies should always be performed.

Differential Diagnosis A plasma cell–rich interstitial inflammatory cell infiltrate should invariably raise the possibility of IgG4-related TIN, and immunoperoxidase stains for IgG and IgG4 should be performed to determine the number of infiltrating IgG4-positive plasma cells (and perhaps the ratio of IgG-/IgG4-positive plasma cells). As mentioned previously, IgG4-positive plasma cells may occur in other forms of interstitial nephritis as well, not only in IgG4-related interstitial nephritis; therefore, the complex diagnostic criteria mentioned above should be considered. Forms of TIN commonly associated with numerous interstitial plasma cells include Sjögren syndrome; other autoimmune diseases such as lupus nephritis, ANCA-associated vasculitis, and HUVS; and a few cases of drug-induced interstitial nephritis and idiopathic interstitial nephritis. Occasionally, any form of interstitial nephritis can have many interstitial plasma cells. In our experience, sometimes, chronic pyelonephritis can become a differential diagnostic dilemma, particularly in a renal biopsy. In chronic pyelonephritis, the distribution of inflammation is frequently

sharply demarcated and zonal, resembling the pattern of injury in IgG4-related interstitial nephritis. It is likely that most previously diagnosed renal inflammatory pseudotumors in fact represent IgG4-related TIN cases.

Pathogenesis The pathogenesis of IgG4-related disease in general and IgG4-related interstitial nephritis is poorly understood. Most of the available data are observational, and there is no good animal model to study the pathogenesis of this disease. Because of the elevated IgG4 levels in the circulation and in the affected tissue, some authors believe that IgG4-related disease is an autoimmune disease (353). Electron microscopy findings of electron-dense immune-type deposits in the TBM support this hypothesis (354). IgG4 production is controlled primarily by T-helper cells type 2 (Th2) via IL-4 and IL-13 production. Also, interleukin-10 (produced by regulatory T cells), IL-12, and IL-21 shift the balance between IgG4 and IgE production, favoring IgG4 (355,356). Some patients with IgG4-related disease have autoantibodies, including anti-pancreatic trypsin inhibitor, antilactoferrin, and anti-carbonic anhydrase antibodies (41).

An association between *Helicobacter pylori* (*H. pylori*) infection and IgG4-related disease has been proposed (357,358). A specific reactivity with a peptide, having homology with the plasminogen-binding protein of *H. pylori*, was identified in the serum obtained from patients with autoimmune pancreatitis (359). Also, reactivity in the serum from the same patients was found with ubiquitin-protein ligase E3 component n-recognin 2, an enzyme expressed in pancreatic acinar cells. No such reactivity was seen in control serum (359).

Okazaki et al. (360) proposed that the development of autoimmune pancreatitis involves a biphasic reaction, where the first step includes an initial response to autoantigens, such as carbonic anhydrase and lactoferrin, associated with the T-helper cell type 1 (Th1) type cellular immune response. Later, memory T cells, regulatory T cells, and Th2-type cells will predominate and induce increased IL10 production, which eventually will result in B-cell maturation and production of IgG4-producing plasma cells as well as TGF- β production, which will induce progressive fibrosis (360). Proteomic analysis of immune complexes in the serum from patients with IgG4-related disease identified a potential autoantigen, a 13.1-kDa protein, but detailed characteristics of this peptide are not yet available (361).

Several other hypotheses of IgG4-related disease pathogenesis have been advanced, including the possibility of enhanced response of Th2 cells to intestinal microflora (362).

Genetic factors also may play an important role in the pathogenesis of IgG4-related disease. The HLA haplotypes DRB1*0405 and DQB1*0401 are associated with increased susceptibility to IgG4-related disease in the Japanese population (363). In addition, DQB1 with substitution of aspartic acid at position 57 is associated with relapsed autoimmune pancreatitis in a Korean population (364).

Treatment and Outcome IgG4-related TIN usually responds well to steroid or immunosuppressive treatment. Thus, based on the Mayo Clinic data, approximately 90% of the patients who received steroids with or without additional immunosuppressive drugs showed improvement in the Scr levels (13). Approximately 12% of patients with initial response to steroid therapy experienced a relapse with increased Scr upon steroid taper. Approximately 10% of the patients initially treated with steroids progressed to dialysis or expired within 1 year after the

kidney biopsy (13). Similar clinical follow-up data in patients with IgG4-related TIN treated with steroids were reported by the Japanese Society of Nephrology (346). Interestingly, patients with IgG4-related TIN showed significantly better response to treatment compared to patients with TIN not related to IgG4 (365).

In summary, there are still many unanswered questions in the recognition, pathogenesis, and proper treatment of IgG4-related TIN. The critical role of a renal pathologist is to consider this entity based on the morphologic findings and to suggest the possibility of IgG4-related TIN in order to initiate further workup and appropriate treatment.

SYSTEMIC LUPUS ERYTHEMATOSUS

SLE is the most common form of tubulointerstitial disease associated with granular deposits of immunoglobulins and complement. Almost one half of the kidney biopsies from patients with SLE have such deposits. The inflammatory infiltrate is variable but includes large numbers of mononuclear cells and occasional neutrophils, with frequent plasma cells (18,366,367). Deposits are predominantly found in proximal tubules but can also be found in other segments of the nephron (368). The deposits include IgG, IgM, rarely IgA, and complement components C3 and C1q (369). The deposits can be found on various locations: interstitial side of the TBM, intramembranous, around peritubular capillaries, and in the interstitium. Rarely, tubulointerstitial immune complex disease may occur in patients with SLE in the absence of significant glomerular disease. We have found that the IgG subclass composition of the glomerular and extraglomerular immune complex deposits is different (23). Thus, IgG subclass distribution was discrepant between glomerular and TBM deposits in 36/52 biopsies and between glomerular and vascular deposits in 27/40 biopsies. Interstitial inflammation did not correlate with the presence of tubulointerstitial immune complex deposits or with the distribution of IgG subclasses in the TBM, but the IgG subclass staining correlated with C1q staining in all the three compartments. These data suggest that immune complex deposits at different sites do not represent the same preformed immune complexes from the circulation (23). It is likely that glomerular and tubulointerstitial immune complex deposits in lupus nephritis form through different pathogeneses as a response to different antigens and some of them probably form in situ. It has been suggested that immune response and tubulointerstitial inflammation in lupus nephritis are mediated by in situ B cells (370). Renal disease, including interstitial nephritis in SLE, is discussed in Chapter 14.

SJÖGREN SYNDROME

Sjögren syndrome is an immunologic disorder characterized by progressive destruction of the exocrine glands leading to mucosal and conjunctival dryness (i.e., sicca syndrome) associated with autoimmune disease affecting various organs. The disease is discussed in detail in Chapter 14.

Renal changes consist of interstitial inflammation with mononuclear cells including histiocytes, plasma cells, and lymphocytes. Plasma cells may occasionally be abundant (see Fig. 25.3). Several cases have been reported in which immunofluorescence and electron microscopy revealed immune deposits along the TBMs. However, in our experience, and based on literature review, it appears that most cases do not have obvious tubulointerstitial immune complex deposits detectable

by immunofluorescence and/or electron microscopy. Patients with Sjögren syndrome are prone to develop lymphoma, in particular, marginal zone lymphoma (mucosa-associated lymphoid tissue [MALT] lymphoma). The lymphoma primarily involves the salivary glands and head and neck lymph nodes. Involvement of the kidney by lymphoma in Sjögren syndrome is exceptional (371). For more details, see Chapter 14.

MEMBRANOPROLIFERATIVE GLOMERULONEPHRITIS/DENSE DEPOSIT DISEASE

Membranoproliferative glomerulonephritis occasionally may manifest with granular deposits of immunoglobulins or complement in TBM. In dense deposit disease (a form of C3 glomerulopathy), the characteristic very electron-dense ribbon-like deposits may occasionally be seen along the TBM as well.

MIXED CRYOGLOBULINEMIA

Mixed cryoglobulinemia usually manifests with proliferative glomerulonephritis, and some patients can present with focal interstitial inflammation, including mononuclear cells, edema, and tubular cell injury associated with granular IgG and C3 deposits in the TBM (285). In our experience, TBM deposits in cryoglobulinemic glomerulonephritis are rare.

MEMBRANOUS GLOMERULONEPHRITIS

A few patients with membranous glomerulonephritis have tubulointerstitial inflammation with monocytes, plasma cells and eosinophils, and granular deposits of immunoglobulins and complement in the TBM. As mentioned above, many of these patients probably have IgG4-related disease or other autoimmune disease-associated interstitial nephritis and membranous glomerulonephritis.

HYPOCOMPLEMENTEMIC URTICARIAL VASCULITIS SYNDROME

HUVS is an uncommon autoimmune disease resembling SLE. The disease is characterized by recurrent urticarial lesions, complement activation with marked decrease in C1q, anti-C1q antibodies, arthritis, and frequently glomerulonephritis, obstructive lung disease, and other symptoms (372,373). Renal involvement is usually immune complex glomerulonephritis, resembling membranoproliferative glomerulonephritis; sometimes, crescents may also be found. Interstitial nephritis may also occur but usually accompanying the immune complex glomerulonephritis (374,375). A recent publication from Japan describes prominently elevated serum IgG4 level in a patient with HUVS, raising the possibility of an overlap between IgG4-related disease and HUVS (376).

FAMILIAL IMMUNE COMPLEX TUBULOINTERSTITIAL NEPHRITIS

Familial immune complex TIN is a syndrome characterized by familial occurrence of tubulointerstitial immune complex disease, often with membranous glomerulonephritis. Patients present with diarrhea, dermatitis, proteinuria or the nephrotic syndrome, and renal insufficiency (323). TIN is characterized by a mononuclear cell infiltrate, variable tubular atrophy, and interstitial fibrosis. By immunofluorescence, granular deposits of immunoglobulin and complement are found in the TBM. Chronic tubulointerstitial disease and villous atrophy of the small intestine were found in two first cousins (323). Both had proximal tubule dysfunction and malabsorption syndrome

with granular deposits of IgG and C3 in intestinal epithelial cells, and their sera (IgG) were reactive with intestinal epithelial antigen. Membranous glomerulonephritis was detected in only one of these patients; the other had normal glomeruli.

GIANT CELL TUBULITIS WITH TUBULAR BASEMENT MEMBRANE IMMUNE COMPLEX DEPOSITS

Recently, several cases of giant cell tubulitis with TBM immune complex deposits were described (84,377–379). Morphologically, this entity is characterized by acute TIN with numerous giant cells, associated with tubules and TBM immune complex deposits. The TBM deposits contain IgG and C3. Interestingly, all patients had cardiac surgery (aortic valve replacements with mechanical valves, (377); mitral valve replacement with a mechanical valve (378); nonspecified mitral valve repair, (379); multiple cardiac surgeries, (84)) preceding the onset of TIN. The majority of reported patients are adults, but one 15-year-old young patient has been described as well (84). The pathogenesis of this disease is unclear. Hypocomplementemia is common, similar to IgG4-related interstitial nephritis, but no case was worked up for IgG subclass deposition in the TBM, serum IgG4 levels, or other stigmata of IgG4-related disease.

OTHER MISCELLANEOUS DISEASES

Rarely, patients with various types of crescentic glomerulonephritis (295,298), graft versus host disease (380), postinfectious glomerulonephritis, shunt nephritis, hepatitis B, syphilis (298), or fibrillary glomerulonephritis (381) may show TIN with deposits of immunoglobulins or complement in the interstitium, the TBM, or both.

Pathology of Tubulointerstitial Nephritis With Immune Complexes

The kidney size varies and may be normal, enlarged, or reduced, depending on whether TIN is acute or chronic. The interstitial infiltrate is multifocal or diffuse and is composed predominantly of lymphocytes, monocytes, and plasma cells (see Fig. 25.23A) (298). Neutrophils may be present. By immunofluorescence, granular deposits of immunoglobulins, often with complement, are seen in the TBM, the interstitium, or both (see Fig. 25.23B) (112,298). By electron microscopy, dense deposits are usually present in the same location (see Fig. 25.23C). Overall, dense deposits are more frequently seen in biopsies of patients with SLE. The pathology of IgG4-related interstitial nephritis has been detailed previously in this chapter. We would like to reiterate that one has to be careful evaluating the immunofluorescence and electron microscopy findings for TBM deposits because C3 deposits are commonly seen along the TBM, particularly in biopsies with chronic injury and tubular atrophy. Also, granular cell debris in the TBM may mimic electron-dense immune-type deposits on electron microscopy if the TBM is examined only under low magnification (see Fig. 25.11).

Tubular atrophy and interstitial fibrosis are usually absent from early lesions, but are present in patients with chronic renal insufficiency. In primary TIN, glomeruli are normal or show nonspecific changes. In secondary TIN, glomeruli may show crescentic, membranous, proliferative, exudative, or segmental changes according to the primary disease. Arteries and arterioles are normal or show hypertensive or age-related changes.

Pathogenesis of Tubulointerstitial Nephritis With Immune Complexes

To establish that TIN is mediated by immune complexes, the same basic requirements delineated for anti-TBM nephritis apply, except that deposits of antibody, usually IgG, and complement have a granular configuration and localize in the TBM and interstitium, and antigen targets differ and are usually unknown. Because only some of the requirements can be satisfied, the diagnosis of human TIN with immune complexes also is inferential and based on data derived from experimental models.

In an experimental model developed by Hoyer (382), the putative antigen is Tamm-Horsfall glycoprotein, synthesized and secreted by epithelial cells of the thick ascending limb of Henle. Rats and mice immunized with Tamm-Horsfall glycoprotein develop granular TBM deposits of immunoglobulins and complement, electron-dense deposits along the base of tubular cells of thick ascending limb of loops of Henle, and tubulointerstitial mononuclear cell infiltration (382–384). The distribution of THP varies with species, and in mice, immune deposits also are formed in the TBM of distal convoluted tubules (383). Deposits are formed in situ by interaction of circulating antibodies with antigen present on the abluminal side of the tubular cells. Ureteral obstruction in mice promotes the localization of such deposits in extratubular sites and apparently contributes to interstitial inflammation and scarring (385). Tamm-Horsfall glycoprotein does elicit weak antibody response in humans (386), and a component of interstitial inflammation may be related to extravasation of this glycoprotein into the interstitium. Antibodies to *E. coli* that are cross-reactive with Tamm-Horsfall glycoprotein (387) and some anti-DNA antibodies cross-reactive with heparan sulfate (388) provide examples in which autoimmunity may contribute to TIN mediated by immune complexes. However, the exact role of Tamm-Horsfall glycoprotein in humans is still unclear, and whether Hoyer's animal model has a human counterpart is unknown (389,390).

In human TIN with immune complexes, antigens involved, with few possible exceptions (391,392), are unknown. Antibodies are usually of the IgG class and, less frequently, of other classes (285). As discussed above, in IgG4-related interstitial nephritis, a specific subclass of IgG (IgG4) appears pathogenic. Immune deposits may result from immune complexes formed in the circulation, or they may result from local interaction between free antibody and antigen in tissues. Both mechanisms may be operational in SLE, in which immune complexes activate complement, as judged by the presence of C3 and terminal components of complement in electron-dense deposits (369). Complement also can be activated by mechanisms other than those involving immune complexes. For example, ammonia can trigger the alternative pathway of complement activation and cause tubulointerstitial inflammation and injury (393). Based on experimental models, some forms of TIN may require complement activation by antibody, release of chemoattractants, activation of leukocytes, and release of proteases and toxic oxygen radicals (282). Whether such mechanisms play a pathogenic role in human TIN with immune deposits awaits demonstration, particularly because the degree of interstitial inflammation does not always correlate well with the degree of tubulointerstitial immune complex deposition (23).

Tubulointerstitial Nephritis With Cellular (Mainly T-Cell) Mechanisms

TIN in which T-cell mechanisms have been implicated are probably more common than appreciated and include drug reactions; reactions to allograft antigens; systemic disease with renal involvement; reactions to renal localization of various microorganisms, foreign bodies, and crystals; renal involvement in sarcoidosis; and most forms of progressive renal disease.

Primary Tubulointerstitial Nephritis With Cellular (T-Cell) Mechanisms

ALLOGRAFT REJECTION

Most allograft rejections represent a form of TIN that results from disparity of the major histocompatibility complex (MHC) antigens between the recipient and the donor. Allograft rejection is covered in Chapter 29.

TUBULOINTERSTITIAL NEPHRITIS WITH UVEITIS

The syndrome of tubulointerstitial nephritis with uveitis (TINU) was described in 1975 by Dobrin et al. (394). The two patients reported presented with acute renal failure owing to TIN, with predominance of eosinophils in the infiltrate associated with anterior uveitis and granulomas in bone marrow and lymph nodes. These patients were Caucasian females, 14 and 17 years of age. Both recovered renal function, but one required treatment with corticosteroids for about 1 year. The syndrome has been reported mainly in children (395–397), rarely in adults (398–400). It may occur in siblings with identical haplotypes (401) and monozygotic twins (395). Males are affected more often than females (396).

Patients may present with one or more of the following features: proximal tubule dysfunction, including Fanconi syndrome, renal insufficiency and proteinuria, renal failure, and ocular symptoms (402,403). Urinary beta-2 immunoglobulin levels are frequently very high (396). Uveitis may precede or follow renal dysfunction or acute renal failure. Elevated serum levels of autoantibodies against modified C reactive protein may be useful in the diagnosis (403a).

The kidney shows inflammatory infiltrates comprising mononuclear cells, including many lymphocytes and fewer plasma cells and macrophages (Fig. 25.28). Eosinophils, prominent in the initial cases presented by Dobrin (394), are less commonly seen by others. By immunofluorescence, immunoreactants usually are not found in the TBM, and repeat or late biopsies may show variable amounts of interstitial fibrosis and fewer inflammatory cells. Inflammatory cells are mostly T cells, but the predominance of a CD4⁺ or CD8⁺ phenotype varies (404,405). The proximal tubules show the greatest degree of alterations, with circular arrays of infiltrating mononuclear cells. Acute tubular epithelial injury and flattening of the tubular epithelium often occur. Noncaseating granulomas may be found in bone marrow, lymph nodes, and the kidneys (394). We have seen a similar case with giant cells in the kidney biopsy; in such patients, an underlying sarcoidosis should always be considered. Serial kidney biopsies from three pediatric patients showed that acute inflammation diminishes after treatment with prednisone, but the chronic kidney injury increases (406). Morino et al. (401) reported two sisters with TIN and chronic sialadenitis, one of them with recurrent uveitis; this patient also had an immune complex-mediated glomerulonephritis, which is not a component of the syndrome.

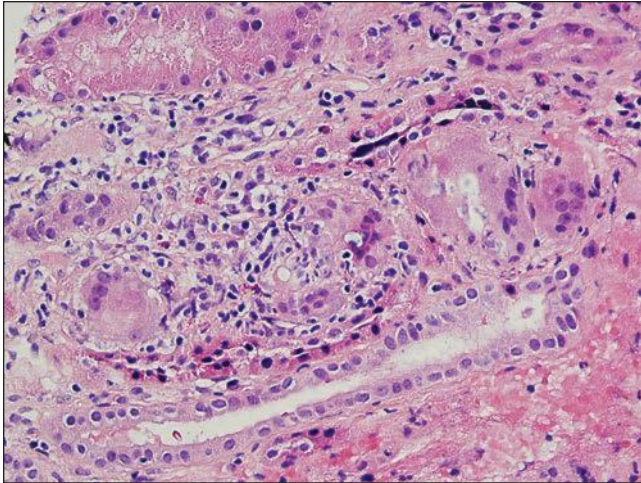


FIGURE 25.28 Interstitial inflammation with giant cells is seen in this young patient with TINU. (H&E, $\times 200$).

It is conceivable that the syndrome encompasses other manifestations, as reported, or that the referenced patient had an overlap syndrome with features of Sjögren syndrome. Recovery by spontaneous remission (394,396) or in response to corticosteroids (404) does occur in children. Some degree of permanent renal dysfunction may remain in adults (407).

The cause of the disease is unknown, but an autoimmune pathogenesis is suspected. Although the association of TINU with IgG4-related disease has been proposed, it appears that most biopsies taken from patients with TINU do not have infiltrating IgG4-positive plasma cells (408). Although uveitis appears to be mediated by immune complexes (401), possibly formed locally, the interstitial inflammation in the kidney has the characteristics of a T-cell-mediated reaction. Lymphocyte reactivity has been detected against antigens from renal tubular epithelia using an assay of inhibition of leukocyte migration (409). One case report describes a patient who had circulating antibodies to a 125-kDa protein localized to the cytoplasm of renal cortical tubular epithelial cells (410). A genetic predisposition to an autoimmune pathogenesis also finds support in the observation that the syndrome has been reported in identical twins (411) and in siblings with identical haplotypes (398). A case of TINU in a mother and her son has been described. The mother was 13 and the son 10 years old at the time of the diagnosis (412). The HLA alleles HLA-DRB1*1401 and HLA-DQB1*0503 haplotype has been observed in patients with TINU (413). An association between HLA-DRB1*0102 and TINU syndrome and bilateral, sudden-onset anterior uveitis has been identified (414). TINU may recur in renal transplants, suggesting a role for circulating autoantibodies in the disease pathology (415). These autoantibodies may be produced against tubular and uveal cells (416). Modified C-reactive protein might be another target autoantigen of TINU syndrome (417). A case of TINU associated with the Chinese herb “Goreisan” has been described in an adult (418).

SARCOIDOSIS

Sarcoidosis is a chronic disorder, involving multiple systems and characterized by accumulation of lymphocytes and other mononuclear cells forming noncaseating epithelioid granulomas. Most

patients present with enlarged lymph nodes, cough, weight loss, fever, dyspnea, polyuria, increased serum calcium concentrations, and occasionally with proteinuria and microscopic hematuria (26,419). Sarcoidosis is more common in males and in blacks, and the peak incidence occurs in the second and third decades of life (26,419). Serum levels of angiotensin-converting enzyme (ACE) are frequently high. Renal involvement, manifested by renal dysfunction, is rare and occurs in only 1% to 2% of all patients with sarcoidosis. For example, of 75 cases of sarcoidosis reviewed by Richmond et al. (420), only 1 patient had TIN (1.3%). However, this low incidence of clinically manifest renal disease is misleading, because in autopsy series, an incidence of 9% to 25% has been reported (419,421,422). A more recent publication from Heidelberg, Germany, describes 46 patients with sarcoidosis and 48% of them had renal abnormalities (422). The patients underwent renal biopsies—6 of these 10 patients had nephrocalcinosis, and only 3 patients had interstitial nephritis; 1 patient had IgA nephropathy. Five of the six patients with nephrocalcinosis had hypercalcemia. These authors found a positive correlation between serum ACE levels and granuloma formation in the renal tissue (422). The most common renal complication in patients with sarcoidosis is related to disturbance in calcium metabolism. Hypercalciuria is present in 50% to 60% of patients with sarcoidosis, and 10% to 20% of them also have hypercalcemia (172,423). Sometimes, AKI may be the first clinical symptom in sarcoidosis interstitial nephritis (424,425), including cases of familial sarcoidosis (426).

In renal sarcoidosis, granulomas are abundant and usually sharply delineated with many epithelioid cells and giant cells (see Fig. 25.4B). The granulomas are associated with an inflammatory infiltrate of mononuclear cells, including many plasma cells and lymphocytes (172,423). Differentiation of sarcoid granulomas from other granulomas causing granulomatous interstitial nephritis, such as drug-induced granulomas, can be difficult; however, drug-induced granulomas may be less distinct (see Fig. 25.4A). Calcifications may occur in and around the interstitial granulomas (Fig. 25.29). Changes of renal sarcoidosis can be focal in nature, and characteristic lesions can be missed in a small-needle core biopsy. Inconclusive renal biopsies

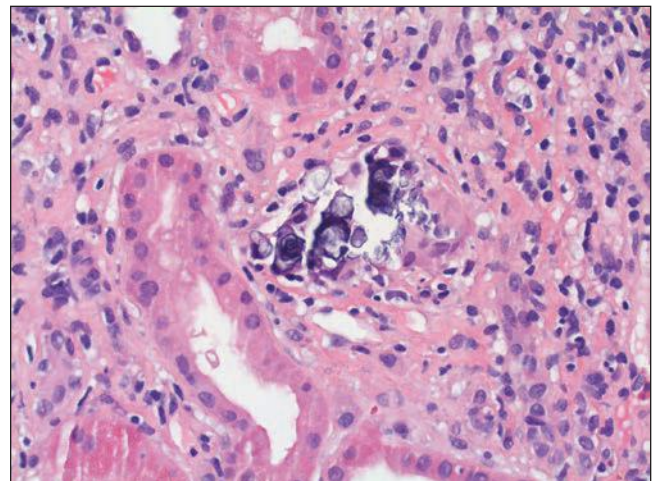


FIGURE 25.29 In sarcoidosis, kidney biopsy often shows calcium phosphate deposits, which may be engulfed by giant cells. (H&E, $\times 400$.)

with only nonspecific findings are frequent in patients with sarcoidosis and AKI. The presence of granulomatous interstitial nephritis in renal biopsy, although classic, is uncommon (427). ACE levels are often high in many patients' sera (428), and they can also be detected in the giant cells and epithelioid cells in the granulomas. Unfortunately, this methodology is not commonly used by renal pathologists to differentiate granulomas in sarcoidosis; we could find only one case report describing ACE-positive epithelioid granulomas in a renal biopsy from a patient with sarcoidosis (429). For the same reason, the specificity of this methodology in renal biopsies cannot be assessed. Renal function may improve after early corticosteroid therapy; however, Scr rarely returns to normal, and long-term follow-up has shown that some patients develop permanent renal dysfunction (430) or chronic renal failure (172,423,431). Current views on the pathogenesis of sarcoidosis implicate an immune mechanism whereby T cells and macrophages are involved (423). Sarcoidosis may recur in renal transplants (432,433).

GRANULOMATOUS TUBULOINTERSTITIAL NEPHRITIS

A list of agents and conditions that can be associated with granulomatous interstitial nephritis is given in Table 25.2. This list is always incomplete because additional causes of granulomatous interstitial nephritis are constantly reported. All these causes should be carefully considered in the differential diagnosis, but one has to remember that, occasionally, granuloma formation can be associated with any etiologic agent causing interstitial nephritis.

The most common cause of granulomatous TIN is exposure to drugs. This was discussed previously in this chapter. For example, in the report by Mignon et al. (434) of 32 patients studied, 28% were owing to drugs, 16% to granulomatosis with polyangiitis (Wegener granulomatosis), and 9% each to tuberculosis and sarcoidosis. Most infectious granulomatous tubulointerstitial nephritides other than tuberculous are caused by infection with bacteria, fungi, or parasites (discussed in Chapter 24). These data may vary in different regions. Joss et al. (26) reported that in Glasgow, the majority of biopsy-proven granulomatous interstitial nephritides (50%) were idiopathic, whereas drug-induced represented only 6% of the cases. Bijol et al. (24) from the Brigham and Women's Hospital in Boston reported that 44.7% of their granulomatous interstitial nephritis cases were drug associated. Sarcoidosis-related granulomas were seen in 28.9% of cases, and 10.5% of the biopsies were diagnosed as idiopathic granulomatous interstitial nephritis (24).

Oxalosis or hyperoxaluria after small intestine bypass is associated with granulomatous reaction to deposited oxalate crystals. In general, the inflammatory reaction is discrete, and granulomas are few and are of the giant cell foreign body type. Other particles or crystals, as may occur in intravenous drug abuse and gout, also can result in granulomatous TIN. Interstitial granulomas may occur in ANCA-associated vasculitis, including granulomatosis with polyangiitis (Wegener granulomatosis). The number of granulomas varies, but in general, few are found in kidney biopsies (435). The granulomas in granulomatous vasculitis are usually localized around glomerular crescents and/or involve arteries.

Several cases of the so-called idiopathic granulomatous interstitial nephritis have been reported (24–26,436). Some authors consider granulomatous idiopathic interstitial nephritis with sarcoid features as cases of isolated renal sarcoidosis (25). They base their assumption on elevated ACE levels in

some patients and a positive response to steroids. However, steroid treatment is not always successful in idiopathic granulomatous interstitial nephritis (25). Interestingly, a case of a good response and recovery of renal function following treatment with an antibody to tumor necrosis factor alpha (infliximab) was described (436).

Secondary Tubulointerstitial Nephritis With Cellular (Mainly T-Cell) Mechanisms

TUBULOINTERSTITIAL NEPHRITIS ASSOCIATED WITH PROGRESSIVE NEPHROPATHIES

Chronic interstitial disease is present in almost all forms of progressive glomerular and vascular disease of the kidney. This subject has been reviewed by several groups, including Pichler et al. (437), Strutz and Neilson (438), and Dodd (439), and is considered here because cell-mediated immunity appears to play a major role in its pathogenesis. Chronic progressive TIN has a diverse etiology, ranging from infection and drugs to immune-mediated, hematologic, metabolic, and hereditary disorders and even chronic ischemia. In other words, several different diseases may result in a common pathologic pathway of progressive interstitial fibrosis and tubular atrophy. Experimental studies revealed several common factors and mechanisms responsible for chronic tubulointerstitial injury, such as activation of peritubular fibroblasts, leukocyte infiltration, release of inflammatory cytokines and growth factors at affected regions, epithelial-mesenchymal transition of tubular epithelium, and apoptosis. The execution of each is mediated by a number of local stimuli, such as filtered albumin, chronic hypoxia, and oxidative stress, in addition to cytokines and growth factors (reviewed 440). Epithelial to mesenchymal transition of tubular epithelial cells may be mediated by hypoxia-inducible factor (HIF) signaling, including HIF-1 and HIF-2 (441). However, as pointed out earlier, the true existence and role of epithelial-mesenchymal transition in kidney fibrosis have been recently questioned (51,52).

Tubulointerstitial inflammation plays a significant role in the pathogenesis of chronic kidney injury (31,442). During the inflammatory phase, inflammatory cells accumulate in the interstitium in response to deposition or local formation of immune complexes or in response to cytokines and other mediators released from injured glomeruli into the filtrate and subsequently to the tubules. Cytokines may also exit the glomeruli through the Bowman capsule, the vascular pole, and the efferent arteriole (437). In response to cytokines and other mediators, adhesion molecules (443) and growth factors (444) are expressed or overexpressed, and inflammatory cells, mostly lymphocytes and macrophages, accumulate in the interstitium. In patients with proteinuria, proximal tubular cells, when exposed to high concentration of proteins, may produce proinflammatory and profibrotic factors. The activation of nuclear factor κ B results in the up-regulation of a variety of cytokines and chemokines, overexpression of adhesion molecules, and interstitial infiltration of inflammatory cells. In many cases, fibrosis is promoted by release of transforming growth factor- β , which induces myofibroblast formation and collagen deposition (442).

Pathology of Tubulointerstitial Nephritis With Cellular (Mainly T-Cell) Mechanisms

The kidneys are usually enlarged and show variable edema, and the inflammatory infiltrate consists of lymphocytes, plasma cells, and few eosinophils. Lymphocytes account for more than

50% of the infiltrating cells, and monocytes/macrophages and plasma cells account for most of the remainder (445). Neutrophils may be seen, but they are infrequently present in large numbers. Granulomas may be found (see above). Tubulitis, tubular cell injury, regenerative epithelial changes, and variable numbers of casts are seen. Tubular atrophy and interstitial fibrosis are variable and more likely to be present in patients who have biopsies late in the course of their disease or in chronic forms. By immunofluorescence, deposits of immune complexes are absent from glomeruli or tubules. Vessels are normal or show hypertension and age-related changes. In secondary TIN with T-cell mechanisms, the glomeruli or vessels may show active, healing, or healed lesions characteristic of the underlying glomerulonephritis and vasculitis.

Pathogenesis of Tubulointerstitial Nephritis With Cellular (Mainly T-Cell) Mechanisms

The mechanism by which inflammatory cells induce fibrosis has been reviewed (45,46,438) and will be discussed here briefly. To establish that TIN is mediated by cellular mechanisms, it is necessary to demonstrate that the transfer of T cells, but not of serum, from a donor with TIN to a normal syngeneic recipient results in TIN in the recipient of T cells or that neonatal thymectomy obviates the expression of TIN (446). Because studies of this type cannot be performed with humans, the diagnosis of cell-mediated TIN is inferential and based on animal models in which T cells have been demonstrated to have a pathogenic role.

Mononuclear cells can mediate TIN by two types of reactions (447). The first, delayed-type hypersensitivity, involves prior exposure and sensitization of the host and is caused by CD4⁺ T cells and macrophages, resulting in production of various lymphokines and a granulomatous reaction. Interstitial lymphocytes interact with monocytes/macrophages, with endothelial cells, and possibly with tubular epithelial cells (448) in antigen presentation, resulting in a delayed-type cell-mediated reaction. IFN- γ augments but is not a necessary requirement for up-regulation of class I and class II molecule expression in renal tubules (449). Some drug reactions and sarcoidosis appear to result from this mechanism. The second, cytotoxic T-cell injury, requires no prior sensitization and involves CD4⁺ T cells and CD8⁺ T cells. Whether a diffuse cellular infiltrate or a granulomatous inflammation develops is also determined by the interplay of cytokines brought into the interstitial microenvironment by T cells (446).

The mechanism of interstitial inflammation involves several biologic events, as discussed previously. Briefly, CD4⁺ T cells become activated by cells expressing class II MHC antigens (450), including tubular epithelial cells (451). Activated T cells, monocytes/macrophages, and renal tubular epithelial cells release chemokines and cytokines (e.g., macrophage colony-stimulating factor [M-CSF], platelet-derived growth factor [PDGF], and TGF- β) that induce chemotaxis of cells to inflammatory sites (315,326,444) and various enzymes that degrade collagens and facilitate fibroblast motility (452). It is now evident that renal tubular epithelial cells are a major site of M-CSF production. Therefore, activated/injured tubular epithelial cells in interstitial nephritis, in turn, may further attract macrophages into the kidney and interstitium, aggravating the disease process (35,36). TGF- β and PDGF activate fibroblasts (453), enhance collagen deposition, and promote fibrogenesis

(45–47). TGF- β was thought to have an important role in the induction of tubular epithelial cell/mesenchymal transdifferentiation, but the pathogenetic significance of this *in vivo* is still debated (51). Other cytokines (IL-1, TNF- α , IFN- γ) modulate inflammation and fibrogenesis (454).

TUBULOINTERSTITIAL NEPHROPATHY ASSOCIATED WITH METABOLIC DISORDERS OR MONOCLONAL GAMMOPATHIES

Tubulointerstitial nephropathy associated with metabolic disorders is reviewed in Chapter 27. Tubulointerstitial nephropathy associated with monoclonal gammopathies is reviewed in Chapter 22.

TUBULOINTERSTITIAL NEPHROPATHY ASSOCIATED WITH HEAVY METAL EXPOSURE

Exposure to heavy metals results in tubular dysfunction and acute or chronic renal disease. The nephropathies caused by chronic exposure to the most abundant toxic metals—lead, cadmium, and mercury—are considered here in some detail; other nephropathies associated with heavy metal exposure are mentioned briefly. Diagnosing chronic heavy metal exposure-associated nephropathy is quite difficult, and the condition is probably frequently overlooked. Contaminating food supply (such as seafood) and possibly also drinking water (possible well water contamination in areas of fracking [hydraulic fracturing during natural gas/petroleum exploration]) is a growing concern and can potentially be the source of low-level chronic heavy metal exposure to certain populations (455). Acute tubular toxicity of heavy metals is discussed in Chapter 26.

Lead Nephropathy

Lead exposure in the form of inhaled fumes and dust is an occupational illness for industrial workers (i.e., painters, printers, welders, foundry workers, and electric storage battery makers). In the form of dust and contaminating fluids and surfaces, it is still of some risk to the general population, in spite of banning lead as an additive in gasoline (456). Soil and paints containing lead are sources of lead exposure, particularly for children (457). Absorbed lead is widely distributed, but the principal sites of long-term storage are the bones, in which 94% of the lead in the body is found. This storage site constitutes a slow-exchange pool, and the biologic half-life of lead in bone is about 16 years (458). Another 4% is present in the blood, tissue fluids, and soft tissues, and these constitute a rapid-exchange pool. The remaining 2% is distributed between actively exchanging parts of the skeleton and soft tissues. Chronic lead intoxication has been widespread, and its history and effects on health are appreciated and well documented as a result of contamination of foods and as an occupational hazard of mining and smelting operation as early as 2500 BCE (459,460). An epidemic of childhood lead poisoning in Queensland, Australia, established lead nephropathy as a recognized clinical and pathologic entity (460,461).

Clinical Presentation

The clinical diagnosis of lead nephropathy is based on history of exposure, evidence of renal dysfunction, and a positive calcium disodium edetate (ethylenediaminetetraacetic acid [EDTA]) mobilization test. The test measures urinary excretion of lead after two 1-g doses of EDTA 12 hours apart (462). The test suggests lead nephropathy if excretion of lead is greater than 650 mg in 24 hours. Because the half-life of circulating lead is about 1 month, the test reflects only recent exposure (457), and the result can be normal for patients with chronic lead toxicity (457,462). The lead concentration can also be measured in tissues (primarily bone) by x-ray fluorescence and neutron activation analyses (458). In addition to its use as a diagnostic test, EDTA has also been advocated as a therapeutic agent (457,462). EDTA causes disruption of the lead inclusions and may contribute to their removal from tissues.

Many studies have confirmed a relationship between lead exposure and chronic renal disease (462–464). However, a well-controlled, prospective study comparing two groups of patients, one with high (more than 100 mg/dL) and the other with low (less than 40 mg/dL) lead concentrations in the blood, failed to show significant differences in blood pressure and in various tests of renal function between these two groups 17 to 23 years after chelation therapy (465). On the other hand, a study from Taiwan recently examined the effect of environmental lead exposure on the progression of chronic renal disease and found that even low-level environmental lead exposure is associated with progressive renal insufficiency (463). One hundred and twenty-one patients were included in the study with a baseline creatinine level between 1.5 and 3.9 mg/dL. Seventeen patients doubled their baseline Scr volume within the follow-up period of 48 months. Blood lead levels and body lead burden at baseline were the most important risk factors to predict progression of renal insufficiency. None of the patients had a history of lead exposure, and all of them had blood lead levels and body lead burden above acceptable levels (463).

Lin et al. (455) demonstrated that even low-level environmental lead exposure accelerates progressive diabetic nephropathy in patients with diabetes mellitus type 2. Thus, thirty patients with type 2 diabetes and diabetic nephropathy (Scr of 1.5 to 3.9 mg/dL) and high-normal body lead burdens (80 to 600 µg) were randomly divided into two groups and received either lead chelation therapy with calcium disodium EDTA weekly until body lead burden fell to less than 60 µg or placebo. The rate of decline in GFR in the chelation group was significantly lower as compared to the control group during a 12-month observation period, suggesting that lead chelation therapy can decrease the rate of diabetic nephropathy progression in patients with lead exposure (455).

Saessen et al. (466) investigated the effects of lead exposure in the general population and found that patients with decreased renal function had increased lead content in the blood and that the decrease in renal function was proportionate to increased lead concentration in the blood. Because of the nature of their study, they could not conclude whether lead exposure resulted in impaired renal function or whether impaired renal function caused increased concentration of lead in the blood. Chronic lead intoxication is manifested by proximal tubular defects, and decreased glucose reabsorptive capacity is an early indicator of tubular cell injury (467). Most

patients have recurrent gout, hyperuricemia, and hypertension (468). Whether hypertension and hyperuricemia are caused by lead exposure, however, is controversial (457,459). Both increased uric acid levels and hypertension are more common in patients with renal insufficiency; therefore, it is difficult to decide whether these are secondary to the lead exposure itself or rather to the subsequent chronic renal injury. However, several studies support the fact that lead can cause decreased renal uric acid excretion and uric acid deposition in the kidney, which may be one important factor in the development of chronic lead nephropathy (468). Also, long-term accumulation of lead in the body is probably an independent risk factor for the development of hypertension (468).

Pathologic Findings

The kidneys are reduced in size, show a finely granular surface with reduction of the cortex, and may weigh one third of normal (461). There is variable multifocal tubular atrophy, tubular loss, and interstitial fibrosis (461,469). Nuclear inclusions seen in acute lead nephropathy (see Chapter 26) are not a common feature. Glomeruli are normal (469), and arteries and arterioles demonstrate medial thickening and luminal narrowing, probably related to hypertension. Urate, in the form of microtophi, may be seen in the medulla (461). Immunofluorescence studies are noncontributory or show only nonspecific findings. The glomeruli and vessels may be spared, except in patients with ESRD, whose kidneys may show features of nephrosclerosis because of the frequently severe hypertension in these patients.

Etiology and Pathogenesis

The pathogenesis of lead nephropathy is not completely understood. Lead in fluids is bound to lead-binding proteins and is taken up by epithelial cells by membrane binding and possibly by passive transport; absorbed lead accumulates preferentially in proximal tubular cells (469,470). A cleavage product of α_2 -microglobulin is the principal component of complexed lead that makes Pb^{2+} available to enzymes (Δ -aminolevulinic acid dehydrase) and mediates intranuclear transport and chromatin binding, resulting in changes in gene expression. Lead interacts with renal membranes and enzymes; disrupts energy production, calcium metabolism, and glucose homeostasis; and interferes with ion transport. Oxidative stress most likely plays a significant role in the pathogenesis because serum levels of oxidative stress markers show a close correlation with lead exposure levels (470). It appears that urine level of alpha-glutathione S-transferase, a marker of proximal tubular injury, may be an early marker of lead nephrotoxicity (470). The clinical usefulness of this marker needs further confirmation.

Cadmium Nephropathy

Cadmium exposure from inhalation of cadmium oxide dust or cadmium fumes is an occupational illness (456) that occurs in the manufacture of pigments, plastics, electric storage batteries, and metal alloys. In the general population, exposure occurs by the oral route through contaminated water or food or inhalation of indoor dust contaminated with cadmium (471). Cigarette smoking is another potential source of exposure, because cadmium aerosol, produced during smoking, facilitates absorption of the metal. The kidney content of cadmium is greater in smokers than in nonsmokers (472). Once absorbed, cadmium binds avidly to metallothionein. Cadmium is stored mainly in

the kidneys and the liver and also in the testes. The half-life of cadmium in the body is 10 to 30 years. (473). Females might be more susceptible than males to cadmium exposure (474).

Clinical Presentation

Cadmium toxicity is manifested by increased excretion of high and low molecular weight proteins, such as β_2 -microglobulin (475), kidney-derived antigens, enzymes, prostanoids, glycosaminoglycans, sialic acid, glucose, and amino acids or the full complement of substances seen in the Fanconi syndrome (476). Subclinical changes in tubular function also occur in the general population above a threshold excretion of urinary cadmium of 2 mg in 24 hours (476). Once manifested, renal injury tends to be progressive, even if exposure is discontinued (477,478). In addition to irreversible dysfunction of proximal tubules, excess cadmium exposure is also known to cause hypercalciuria, nephrolithiasis, and osteomalacia. It has been demonstrated that for each doubling of urinary cadmium concentration, the relative risk for mortality increases by 17% (473). Nogawa (479) reported low-level prolonged environmental exposure to cadmium through contaminated water in the Kakehashi River basin in Japan. Patients in this area suffered from Itai-Itai disease (i.e., ouch-ouch disease), with bone pain from osteomalacia. Hypertension is present in patients with cadmium toxicity (480), but whether cadmium causes hypertension is controversial (472). A study from Sweden examined the effects of occupational and nonoccupational exposure to cadmium on the development of ESRD in a population working in and/or living near a cadmium battery factory (475). They found a 2.3-fold increase in the ratio of ESRD in the population with occupational exposure and a 1.4-fold increase in the patients with low exposure living between 2 and 10 km from the cadmium battery factory. A cross-sectional analysis of 14,778 adults in the United States showed that subjects in the highest quartile of blood cadmium (greater than 0.6 $\mu\text{g/L}$) were almost two times more likely to exhibit albuminuria (greater than 30 mg/g creatinine) and 32% more likely to have reduced GFR (less than 60 mL/min/1.73 m²) (481). Epidemiologic evidence suggests higher susceptibility for persons with diabetes mellitus to develop cadmium-induced kidney injury. A study of 122 adults between 18 and 85 years of age in Australia, who were exposed to cadmium by consuming seafood, found a statistically significant correlation between urinary cadmium levels and albuminuria in individuals with type 2 diabetes, but not in nondiabetic individuals (482). A similar trend was observed in 820 Swedish women, without evidence of environmental cadmium exposure, between the ages of 53 and 64 (483). Increased urinary or blood cadmium levels potentiated diabetes-induced effects on kidney. Even in nondiabetic women, cadmium caused increased urinary acetyl-beta-D-glucosaminidase excretion, at lower cadmium levels than previously documented (483). Cadmium exposure has also been associated with a greater risk of kidney stone formation not only in occupational exposure studies but in the general population as well (484).

Pathologic Findings

Very little is known about the pathologic findings in chronic cadmium nephrotoxicity. Yasuda et al. (485) reported 15 cases of Itai-Itai disease. The kidneys were red-brown, had a granular surface described as sandpaper-like, were decreased

in size, had a hard consistency, and weighed about 60 g each. Microscopically, there were extensive tubular atrophy and interstitial fibrosis involving preferentially the outer cortex. Inflammatory cells were present in small numbers. Some degree of glomerular sclerosis was present. However, five patients in the autopsy series of Smith et al. (486) and three patients in the series of Kazantzis et al. (487), including one autopsy case, showed no significant renal pathology. As judged by excessive mortality from chronic renal failure in areas of environmental cadmium pollution, tissue changes may be proportionate to the quantity of cadmium detected in the tissue (488).

Etiology and Pathogenesis

The pathogenesis of chronic cadmium nephrotoxicity is under investigation. Once absorbed, cadmium is initially deposited in the liver, where it is bound to metallothionein-forming complexes that are released in the circulation and are widely distributed. Filtered by the glomeruli, cadmium-metallothionein complexes are absorbed by proximal tubular epithelial cells and are degraded in lysosomes with release of Cd²⁺ to the cytosol, where it is bound to metallothionein and to non-metallothionein-binding proteins. Cadmium complexed with non-metallothionein-binding proteins probably interferes with biogenesis of lysosomes, because it is this fraction that is temporally associated with cell injury and tubular dysfunction, as denoted by increased numbers of electron-dense lysosomes, decreased lysosomal protease activity, appearance of cellular vesiculation, increased excretion of low molecular weight protein, calciuria, and enzymuria (489). Cadmium may impair reabsorption of proteins by proximal tubular epithelial cells via down-regulation of megalin and chloride channel 5, two key players in albumin receptor-mediated endocytosis (490). Renal excretion of cadmium occurs only after a threshold is exceeded (489). A pathogenetic role for heat shock protein (491,492) and oxidative stress has been raised (470,493,494). The role of kidney injury molecule-1 in the pathogenesis of cadmium toxicity has emerged. Kidney injury molecule-1 is a transmembrane glycoprotein not normally detected in the kidney that is up-regulated and shed into the urine following nephrotoxic injury. Significant elevation of kidney injury molecule-1 in the urine and proximal tubular epithelial cells was detected in Sprague Dawley rats treated with cadmium (495). Urinary excretion of kidney injury molecule 1 levels is correlated with urinary cadmium concentration in an elderly population after long-term, low-dose exposure to cadmium (496).

Cadmium may induce injury in the proximal tubular epithelial cells by accumulation of p53 secondary to down-regulation of the Ube2d4 gene (a member of the ubiquitin-conjugating enzyme Ube2d family), resulting in apoptosis of tubular epithelial cells both in vitro and in vivo (497).

Mercury Nephropathy

Mercury exposure results from accidental or suicidal ingestion of inorganic mercurial compounds (e.g., mercuric chloride), from occupational activity (462) owing to inhalation of mercury vapors in the manufacture of scientific instruments and amalgam handling for dental fillings, from use of various products (e.g., topical ointments, cathartics, cosmetics, paints, pesticides), and from consumption of contaminated food. Mercury salts are methylated by bacteria in the environment, and the product, methyl mercury, finds its way into the food chain

by accumulating in marine life, particularly in fish. Chronic mercury poisoning is becoming uncommon because of the elimination of mercury from most of these compounds. However, environmental pollution and the accumulation of mercury in fish still represent a slight risk. Mercury can be quantified in the kidneys by means of x-ray fluorescence analysis. In 20 exposed workers, excessive deposition of mercury was detected in the kidneys of 9 patients using this method of determination (498). Mercury can cause autoimmune disease in humans and in experimental animals (499).

Chronic mercury poisoning results in kidneys of normal or slightly decreased size. Initially, interstitial edema, inflammatory infiltration with lymphocytes, and tubular cell changes such as necrosis, flattening of epithelium, and desquamation of epithelial cells are present (500–502). Later, there is progressive loss of tubules and interstitial fibrosis (501). Glomerular pathology is limited to membranous nephropathy (503).

Inorganic mercury affects proximal tubules and causes vesiculation and exfoliation of brush border membrane, followed by calcium influx and cell death. Mercury also inhibits water permeability in epithelia stimulated by vasopressin (504) and depolarizes mitochondrial inner membrane, resulting in increased hydrogen peroxide production and oxidative tissue injury and in loss of respiratory function because of interference with the heme biosynthetic pathway in mitochondria. The role of oxidative stress in the pathogenesis of mercury-induced kidney injury was proposed. Thus, melatonin (an antioxidant) protected proximal tubular epithelial cells from mercury-induced injury in rats. The iNOS expression was decreased in animals treated with melatonin and mercury chloride, as compared to mercury chloride–only treated rats (505).

Miscellaneous Heavy Metal Nephropathy

Organic compounds containing *gold* were used in the treatment of rheumatoid arthritis. Gold salts cause various autoimmune diseases in humans (499). Patients chronically exposed to gold compounds develop proteinuria or the nephrotic syndrome (secondary to membranous glomerulonephritis), microscopic hematuria, tubular injury, and chronic TIN with lymphocytic inflammatory infiltrate (506). Gold inclusions are often found in the cytoplasm of epithelial cells and free in the interstitium (506). The pathogenesis of gold nephropathy is unknown. Patients with HLA-DQA haplotype are more susceptible to develop gold nephropathy (see Chapter 7).

Exposure to *copper* and *iron* results in deposits of these metals in tubular cells. Iron may induce tubular cell necrosis and acute renal failure when ingested in large doses as sulfate salts (6). Copper also may cause TIN. In the case reported by Hocher et al. (507), TIN, with diffuse inflammatory infiltration by lymphocytes and eosinophils and renal failure requiring dialysis, was induced by a copper-containing intrauterine device. Removal of the device was followed by near normalization of renal function.

Cis-platinum is a chemotherapeutic agent whose major toxicity is renal (508). Cis-platinum administration results in variable renal dysfunction and tubular cell injury, including flattening of epithelial cells, dilation of tubules, necrosis and desquamation of epithelial cells, and focal edema and interstitial fibrosis. Acute cis-platinum nephrotoxicity is discussed in Chapter 26. Cis-platinum has been associated with contracted

kidneys (508). Studies in which platinum analogs were administered to rats suggest that nephrotoxicity is characterized by early inhibition of protein synthesis and late mitochondrial dysfunction (509).

Intoxication with *arsenic* is uncommon. Arsenic exposure can result in chronic renal injury (510) in the form of TIN with interstitial fibrosis manifesting with the Fanconi syndrome and renal insufficiency (510). The source of arsenic was tentatively traced to consumption of “organic health foods” (511). Diagnosis rests on heavy metal screening. Chronic administration of arsenic impaired renal function in diabetic rats (512).

Chromium copper arsenate (CCA) was used for the protection of wood building materials until 2002, before it was banned by the EPA. Studies in animals demonstrated that this triple-metal compound has more prominent nephrotoxic effect than its component single metals, suggesting a synergistic effect (513).

The nephrotoxicity of *uranium* in humans has been reported (514). The toxicity of the metal depends on several factors, such as sex, age, body mass index (515), and species. Of all the mammals, humans seem to be the least sensitive to uranium (516). People may be exposed to uranium, both acutely and chronically, as a consequence of contamination (e.g., nuclear accidents, war, human dumping), the usual sources of normal exposure with high amounts of uranium arising from the anisotropy of the distribution of the metal in the earth's crust, or from increased contact with the metal, such as in the military and aeronautics or in the fields of mining and industry. Uranium levels in urine are strongly correlated to levels in drinking water from drilled wells in people who used drinking water from private drilled wells located in uranium-rich bedrock, but no significant signs of nephrotoxicity were found (515,517). Nephrotoxicity has been reported in uranium mill workers (518). There is now renewed interest in the toxicity of depleted uranium in soldiers exposed on battlefields. So far, there is no evidence that depleted uranium is associated with nephrotoxicity in human (519).

In 1992, approximately 152 kg of depleted uranium were missing after a cargo aircraft crash near Amsterdam (the Netherlands). It has been suspected that this missed uranium could have been completely oxidized at high temperatures (in the range 600° to 1200°C) that occurred during the fire, resulting in the poorly soluble uranium oxides UO_2 and U_3O_8 . A large study was performed on the health effects of the disaster on professional assistance workers. Data of a historically defined cohort of 2499 (exposed and nonexposed) firefighters, police officers, and hangar workers were collected 8.5 years after the disaster. Albumin-to-creatinine ratio and the fractional excretion of β_2 -microglobulin were calculated in the urine and simultaneous blood samples. Exposed assistance workers were compared with their nonexposed colleagues, and associations between uranium and kidney function data were investigated. No statistically significant differences between exposed and nonexposed workers were found in the uranium concentrations and kidney function (520). Several studies describing uranium nephrotoxicity are experimental (521). Thus, uranium may induce apoptosis in rat kidney proximal cells (522). Uranium affects the expression of vitamin D receptor and X receptor in the rat kidneys after chronic exposure (523). Interestingly, chronic exposure to uranium may lead to accumulation of iron in the kidney (524).

TUBULOINTERSTITIAL NEPHROPATHY ASSOCIATED WITH HEREDITARY DISEASES

The pathology of Alport syndrome is discussed in Chapter 13. Tubulointerstitial diseases in renal developmental defects and cystic diseases, as well as familial metabolic renal diseases, are discussed in Chapters 4 and 27, respectively. In this section, only two somewhat controversial entities will be addressed: familial TIN with hypokalemia and familial TIN secondary to mitochondrial DNA abnormalities.

Familial Tubulointerstitial Nephritis With Hypokalemia

Patients with chronic TIN and hypokalemia have been reported in several families (525,526). The interstitial inflammatory cells are predominantly lymphocytes, and there are associated interstitial fibrosis and variable tubular atrophy. In the report of Gullner et al. (525) of three siblings, a characteristic tubular lesion was described wherein proximal tubular cells stained very darkly with methylene-basic fuchsin stain; TBMs were thickened; and the mitochondria showed dense, flocculent material and appeared enlarged. We have seen a kidney biopsy from a 16-year-old male with familial hyperkalemia who had mild interstitial nephritis and ultrastructural findings similar to those described by Gullner et al. (525) (Fig. 25.30).

Familial TIN with hypokalemia has an autosomal recessive mode of inheritance that is MHC linked, and one or more genes that control potassium reabsorption, present in the short arm of chromosome 6, appear to be involved (526). The pathogenesis is unknown. Although acquired hypokalemia owing to malnutrition or abuse of laxatives has been reported to result in chronic TIN and chronic renal failure (527), this hypothesis is debated (528). Familial chronic TIN with hypokalemia must be differentiated from nonfamilial chronic TIN with secondary hypokalemia. This latter condition is possibly immune mediated, and the loss of potassium may be hormonally driven

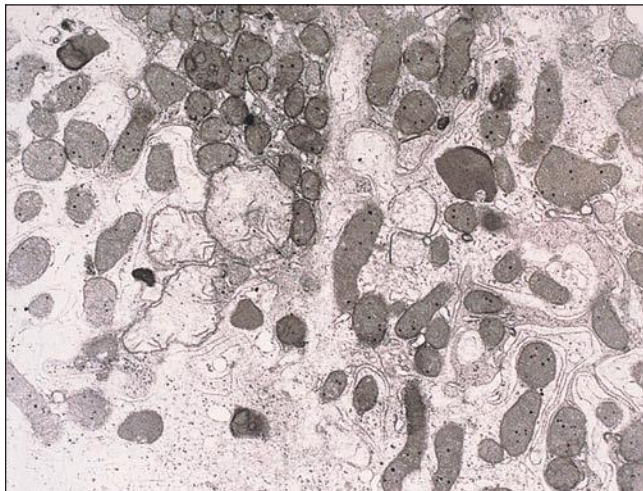


FIGURE 25.30 Abnormally shaped and focally quite swollen mitochondria with flocculent electron-dense inclusions in the mitochondrial matrix in a biopsy from a 16-year-old patient with familial hypokalemic interstitial nephritis. (Uranyl acetate and lead citrate, $\times 20,000$.)

(529). Most affected patients are postpubertal females with systemic features of autoimmune disease (529). In one of the three families reported initially, renal failure developed in three siblings (526).

Chronic Tubulointerstitial Nephritis Secondary to Mitochondrial Abnormalities

In 1994, Szabolcs et al. (529) from Columbia University reported on an 8-year-old girl who had megaloblastic anemia, growth retardation, and progressive renal insufficiency. Renal biopsy revealed chronic tubulointerstitial disease with tubular atrophy and interstitial fibrosis. Ultrastructural examination showed extremely dysmorphic, bizarre mitochondria. Molecular analysis of the mitochondrial DNA detected a 2.7-kb mitochondrial DNA deletion. A year later, a group from France reported a young patient with progressive TIN and leukodystrophy who had a 2.6-kb mitochondrial DNA deletion (530). Consequently, two groups described point mutations in mitochondrial DNA that was associated with progressive interstitial nephritis in three families (531,532). The patients of Zsurka et al. (531) had thoracolumbar scoliosis, muscle weakness, breathing difficulties, mitral prolapse, cardiac conduction defects, pigmented retinopathy, and psychiatric disorders. The patients of Tzen et al. (532) had myopathy and central nervous system abnormalities. Some patients also had Fanconi syndrome.

The morphologic findings in the kidney were dominated by chronic tubulointerstitial injury. The light microscopy and immunofluorescence did not provide a diagnostic clue. Recently, it has been reported that granular swollen epithelial cells among the distal tubules and collecting ducts may be a distinct morphologic feature suggesting mitochondrial nephropathy (533). Ultrastructurally, all patients had bizarre, sometimes curvilinear-appearing mitochondria (530,531,534). The mitochondria also had abnormal cristae and inclusions. One has to keep in mind that dysmorphic, bizarre mitochondria are not necessarily diagnostic of mitochondrial DNA abnormality-associated renal diseases because abnormal mitochondria can occasionally be seen in various conditions, including drug toxicity (e.g., cyclosporine) (Fig. 25.31). Mitochondrial DNA abnormalities are associated not only with chronic progressive tubulointerstitial injury in the kidney, as cases of focal segmental glomerulosclerosis secondary to mitochondrial DNA abnormalities have now been reported (see Chapter 6).

The exact pathogenesis of mitochondrial DNA abnormality-related renal disease is unclear, but it is most likely related to disturbances in the mitochondrial respiratory chain. Renal disease is usually part of a multiorgan disease in these patients, which frequently involves the musculoskeletal system and the central nervous system. Interestingly, it appears that mutation of genes encoding mitochondrial proteins may also be associated with functional and morphologic mitochondrial abnormalities and renal disease, probably both in humans and in experimental animals (535). The *kd/kd* mouse has a mutant allele of a gene encoding a prenyltransferase-like mitochondrial protein (PLMP). The *kd/kd* mouse spontaneously develops severe and progressive nephritis leading to chronic renal failure (535). The mitochondrial defect in *kd/kd* mice primarily affects both the tubular and glomerular visceral epithelium. There is some evidence suggesting that the tubular epithelial defect triggers autoimmune interstitial nephritis, whereas a

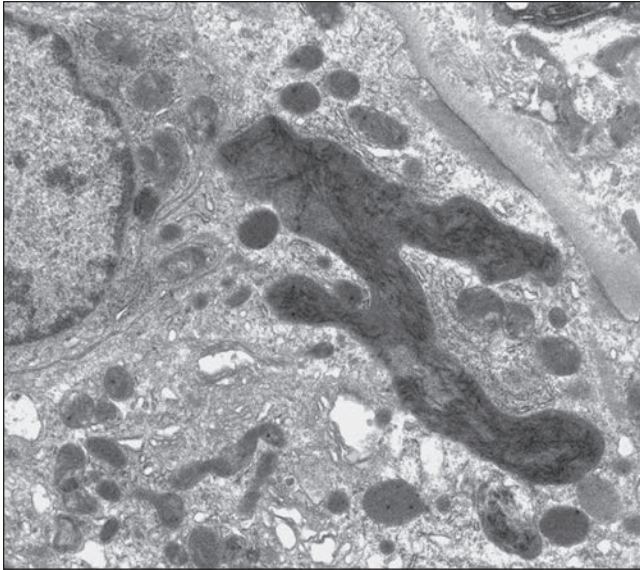


FIGURE 25.31 A bizarre mitochondrion in a tubular epithelial cell in the renal biopsy from a patient with a history of hypertension, rheumatoid arthritis, and obesity. He developed acute renal insufficiency following contrast media administration and NSAID treatment. Light microscopy revealed acute tubular injury, mild to moderate interstitial fibrosis, and enlarged glomeruli. The patient was on many medications in addition to NSAID. Such bizarre mitochondria may occasionally occur in renal biopsies, and they most frequently probably represent toxic injury. (Uranyl acetate and lead citrate, $\times 7000$.)

defect in podocytes leads to proteinuria and glomerulosclerosis (536). Environmental factors play a significant role in the progression of kidney injury in these mice (537).

TUBULOINTERSTITIAL NEPHROPATHY ASSOCIATED WITH MISCELLANEOUS DISORDERS

Systemic Karyomegaly

Mihatsch et al. (538) in 1979 reported chronic TIN manifested by karyomegaly in three patients between 26 and 29 years of age whose TIN progressed to ESRD within 4 to 6 years. Spöndlin et al. (539) reported four additional patients whose presentation in the third decade of life was asymptomatic but later experienced progressive renal failure associated with infections of the upper respiratory tract. Several additional cases have been reported (540,541), some of them in siblings (542).

Renal changes include interstitial infiltration with mononuclear cells, tubular cell injury with focal loss of tubular cells, tubular atrophy, variable interstitial fibrosis, and nuclear changes in proximal and distal tubules. The nuclei are enlarged and measure up to 30 μm in diameter (Fig. 25.32). Enlarged nuclei are found in other cells such as those of bile duct, bronchi, smooth muscle, bowel, vessels, skeletal muscle, and connective tissue (538). The enlarged nuclei are polyploid. By immunofluorescence studies, no deposits of immunoreactants are found, and electron microscopy is not helpful. No convincing viral particles have been found.

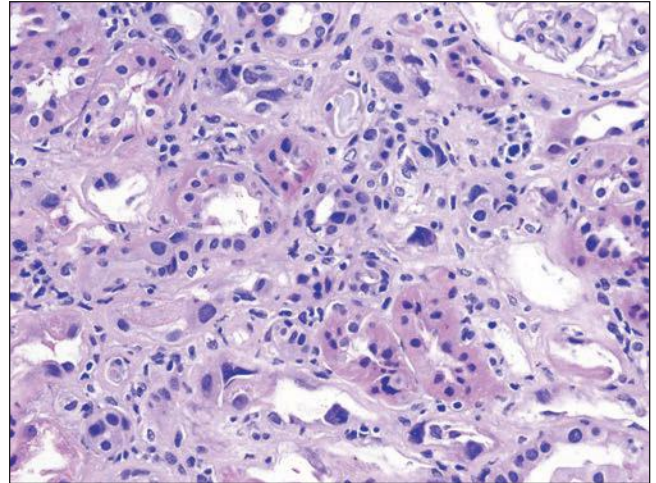


FIGURE 25.32 Karyomegalic interstitial nephritis in the renal biopsy of a patient who underwent bone marrow transplantation and developed progressive renal insufficiency. Note the bizarre, large nuclei primarily in the tubular epithelial cells. Immunostaining for Ki-67 was negative in the nuclei. (H&E, $\times 200$.)

The pathogenesis is unknown. Mihatsch et al. (538) reviewed the various causes of karyomegalic changes and suggested that chemical toxins or viral infections might be implicated. In a report by Hassen et al. (541), high concentrations of ochratoxin, a mycotoxin that interferes with mitotic activity, were found in the blood of affected siblings. Spöndlin et al. (539) studied Ki67 and proliferating cell nuclear antigen in tissues of four patients and concluded that there was inhibition of mitosis in karyomegalic cells. The hypothesis that the karyomegaly is secondary to a block in the G2 phase of the cell cycle has been proposed (539). MHC typing revealed the A9/B35 haplotype, which suggested a genetic defect in chromosome 6 that was linked to the MHC locus. However, the study of Bhandari et al. (543), based on their six patients, did not confirm clustering of A9 or B35.

Balkan Endemic Nephropathy

Balkan endemic nephropathy is found in Croatia, Bosnia, Serbia, Bulgaria, and Romania. In villages where the disease is endemic, the prevalence varies between 2% and 10%. The disease occurs in families but is not hereditary, and most affected persons are farmers (544). The condition is geographically localized and occurs along major tributaries of the Danube river basin. It does not affect children and rarely is seen in patients younger than 20 years of age. Individuals who have lived for a short time in the endemic area do not develop the condition, but individuals from nonendemic areas who spend several years in villages where the condition is endemic may become ill (545). Recent epidemiologic studies from the Kolubara region, the most affected region in Serbia, analyzed the incidence of the disease over a 33-year period from 1977 till 2009 (546). The age-adjusted incidence rates combined for males and females over the period of study fit a significant quadratic (U-shaped) trend ($y = 58.44 - 3.76 + 0.10x^2$), $P = 0.026$). Joinpoint regression analysis showed that the overall age-standardized incidence rates significantly decreased in the first decade of the observed period (1977–1989) by an

average of 10.0% annually, while a nonsignificant increase of 3.9% per year was recorded in the last 2 decades (1989–2009) (547). Some data indicate that in several regions, the incidence of Balkan endemic nephropathy is decreasing (548).

Clinical Presentation

Typical manifestations of the disease occur between 30 and 50 years of age, and the clinical presentation is insidious with weakness, anorexia, anemia, weight loss, copper-yellow skin, orange palms and soles, lumbar pain, mild proteinuria, and microscopic hematuria (544). Hypertension is relatively rare. Renal dysfunction, manifested by tubular proteinuria of usually less than 2 g per day with increased excretion of β_2 -microglobulin, is an early sign of the nephropathy. Proteomic data indicate that 6 proteins, including alpha-1-microglobulin, alpha-2-glycoprotein-1, beta-2-microglobulin, mannose-binding lectin-2, protection of telomeres protein-1, and superoxide dismutase, are found in patients with Balkan endemic nephropathy, but not in patients with AKI, patients with diabetic nephropathy, and healthy volunteers (548). Interestingly, there is a high incidence of upper urothelial carcinoma in patients with Balkan endemic nephropathy. Up to 50% of patients may develop urothelial carcinoma. Transitional cell carcinoma of the renal pelvis and the upper urinary tract can be up to 100 times more frequent in the endemic regions than in the nonendemic regions (549,550).

Pathologic Findings

The kidneys are reduced in size and can weigh as little as 20 g each (551). The external surface is finely granular or smooth, and the cortex is thin (Fig. 25.33). The predominant microscopic changes are in the tubules and interstitium. There are abundant interstitial fibrosis and variable amounts of interstitial inflammatory cells. Nephrons in the superficial cortex are predominantly involved, and there is extensive solidification of glomeruli (552). Based on a study of 50 kidney biopsies, Ferluga et al. (553) described multifocal interstitial fibrosis spreading from the superficial to the deep cortex and tubular atrophy in most of their patients (Fig. 25.34). By immunofluorescence, Ferluga et al. (553) reported prominent glomerular capillary deposits of IgM in 16 of 50 patients. Papillary necrosis is uncommon, but benign and malignant tumors may be found in the pelvis and in the ureters (511,553). About 30% to 48% of Balkan nephropathy patients develop tumors of the upper urothelium, most frequently transitional cell carcinoma. These tumors can be bilateral. Tumors other than transitional cell carcinoma have been reported, including papillomas and squamous cell carcinomas (554).

Pathogenesis

The pathogenesis is unknown. It has been shown that Balkan endemic nephropathy may be associated with the GSTM-1 allele of the glutathione *S*-transferase (555). However, the absence of association with these and other examined alleles has been reported by others (556). Similarly, conflicting data have been published regarding viruses, including the possible role of coronavirus (557). Heavy metals (558), silica (559), low molecular weight proteins (560), and ochratoxin A (561) have been implicated but not substantiated. Pigs fed on barley contaminated with ochratoxin A, which is a fungal metabolite, develop tubular atrophy and interstitial fibrosis comparable to

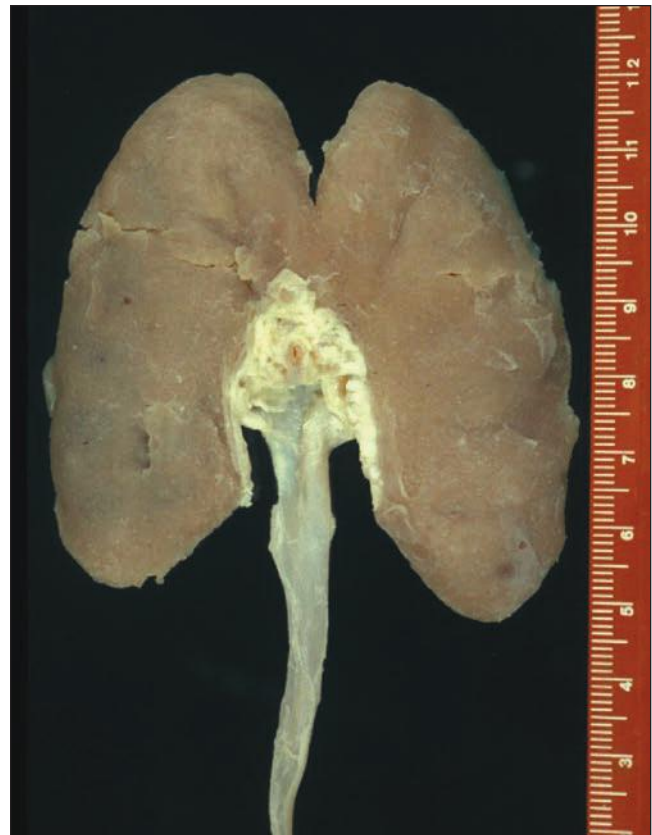


FIGURE 25.33 Gross autopsy specimen of end-stage Balkan endemic nephropathy characterized by a very small shrunken kidney (7 cm in length) with a smooth surface. (Courtesy of Prof. Dr. Dusan Ferluga.)

that seen in Balkan endemic nephropathy (562). The potential etiologic role of ochratoxin A or other mycotoxins as causative agents of Balkan endemic nephropathy is strengthened by the observation that 10% to 20% of cereals, pork meat, and bread from endemic regions are contaminated with ochratoxin A (563).

Another possibility, raised by the similarity of renal changes between Balkan endemic nephropathy and aristolochic acid nephropathy (AAN) (Chinese herb nephropathy), implicates aristolochic acid, a nephrotoxin and carcinogenic agent present in *Aristolochia*, one of the Chinese herbs contaminating herbal preparations taken for weight reduction (564–567). Apparently, *Aristolochia clematis*, which contains aristolochic acid, is common in the endemic areas, and its seeds were found to be contaminants of wheat grains in endemic regions (566). Following metabolic activation, aristolochic acid reacts with genomic DNA to form aristolactam-DNA adducts. Jelakovic et al. (550) found such aristolactam-DNA adducts in 70% of 67 patients who underwent nephroureterectomy for carcinomas of the upper urinary tract in endemic regions for Balkan nephropathy. In contrast, none of the renal tissues from 10 patients from nonendemic regions with carcinomas of the upper urinary tract had such DNA adducts (550). These data suggest a pathogenetic role of aristolochic acid in both Balkan endemic nephropathy and Chinese herb nephropathy (see below). In fact, some investigators suggest

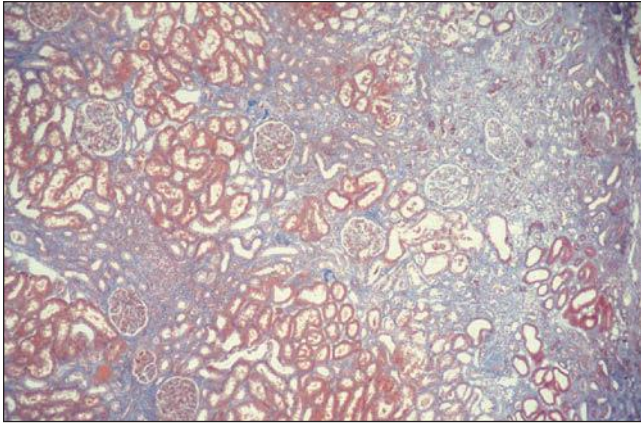


FIGURE 25.34 Balkan endemic nephropathy in a wedge surgical biopsy specimen showing hypocellular interstitial fibrosis and tubular atrophy decreasing from the outer to the inner cortex. The glomeruli are mostly preserved. (Masson trichrome, $\times 40$.) (Courtesy of Prof. Dr. Dusan Ferluga.)

that the names Chinese herb nephropathy and Balkan endemic nephropathy be abandoned and replaced by the term AAN for both diseases (567).

Aristolochic Acid (Chinese Herb) Nephropathy

During 1992 and 1993, an outbreak of rapidly progressive renal failure associated with a slimming regimen containing Chinese herbs occurred in Belgium (568). Withdrawal of the herbs did not prevent progression to chronic renal failure. A large body of subsequent literature appeared on herbal-induced nephropathies, initially mainly from Belgium (564,569,570). Subsequently, series of patients have been reported from Taiwan (571) and Japan (572). It became quickly evident that aristolochic acid (Chinese herb) nephropathy is very similar to Balkan endemic nephropathy (573). There is some controversy about the name of the disease. Some investigators suggested that the term “Chinese herb nephropathy” should be abandoned because most of the cases occurred in Belgium and the term is prejudicial (572). They recommended using the term “aristolochic acid–associated nephropathy.”

In a substantial proportion of patients, transitional cell carcinoma develops. The prevalence of carcinoma was 46% among patients with AAN who underwent nephrectomy (569,574). Because of this high prevalence rate in patients with ESRD secondary to AAN, bilateral nephrectomy may be an appropriate preventive measure.

Clinical Presentation

Most patients present with rapidly progressive renal failure leading to ESRD typically within months. Proteinuria is mild, and microscopic hematuria may be present. Hypokalemia or hyperkalemia may occur, and Fanconi syndrome is common in Japanese patients (572). Most patients in the Belgian studies are female, which may be related to gender differences in taking the diet aid. Males are frequently affected in far Eastern countries (572). Although many aspects of AAN are similar to Balkan endemic nephropathy, the clinical course is clearly different. Balkan endemic nephropathy leads to ESRD after many years (usually 20 years), whereas AAN is rapidly progressive.

Yang et al. (575) describe three clinical subtypes of patients with AAN:

1. AKI (acute AAN) in approximately 4% of the patients
2. Abrupt tubular dysfunction with normal Scr levels occurs in less than 2% of the patients.
3. Chronic tubulointerstitial nephropathy with slowly worsening renal function (in over 90% of cases)

The patients with AKI had the highest aristolochic acid intake per day, and they developed progressive kidney failure during the 1 to 7 years’ follow-up. The patients with isolated tubular dysfunction had the lowest cumulative aristolochic acid intake, and they maintained normal Scr levels during a 2- to 8-year follow-up. The patients with chronic tubulointerstitial nephropathy took the lowest aristolochic acid dose per day, but they used aristolochic acid for the longest period of time (575).

Pathologic Findings

Renal biopsy findings include extensive interstitial fibrosis with tubular atrophy and loss involving predominantly the outer cortex. Interlobular arteries frequently show fibromuroid intimal thickening. In the glomeruli, global sclerosis, collapse, and ischemic changes are common (570,575). The interstitial inflammatory cell infiltrate is usually sparse (hypocellular interstitial fibrosis) (Fig. 25.35). Immunofluorescence and ultrastructural studies are noncontributory. Scattered deposits of C3 may be present in the TBM and interstitium.

Pathogenesis

There is now widespread agreement that AAN is primarily caused by aristolochic acid, which is the constituent of the Chinese herb *Stephania tetrandra* (567,570). Aristolochic acid can form premutagenic aristolochic acid-DNA adducts in the kidney and urothelium and aristolochic acid-DNA adducts have been detected in a renal biopsy by Lo et al. (576). Interestingly, the patient developed transitional cell carcinoma 5 months later. It appears that the cumulative dose of aristolochic acid and the progression rate of renal failure show a

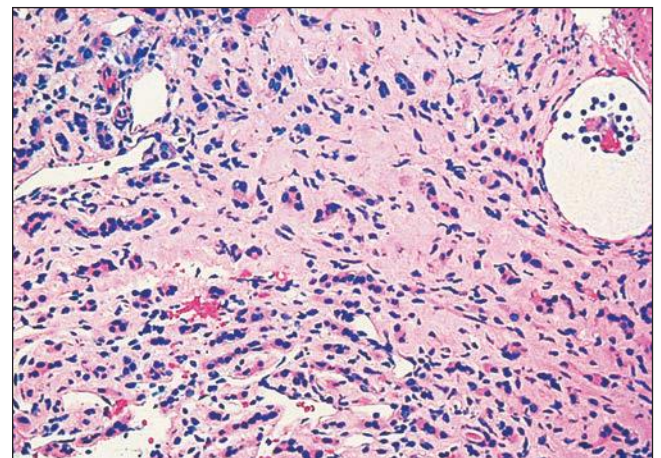


FIGURE 25.35 Prominent hypocellular interstitial fibrosis in the renal biopsy of a patient who developed rapidly progressive renal insufficiency following use of Chinese herbal medications. (H&E, $\times 100$.)

positive correlation (575). The nephrotoxicity of aristolochic acid was also proven in experimental animals (577). However, we would like to note that there are occasional case reports stating that Chinese herb nephropathy develops in the absence of aristolochic acid. In fact, we have encountered a case with typical history and morphology of AAN, but we were unable to prove that the herbal medications the patient was taking contained aristolochic acid.

Idiopathic Tubulointerstitial Nephritis

Idiopathic TIN encompasses a group of diverse conditions. This diagnosis is applied only after known causes or etiologic agents of TIN have been considered and excluded. To exclude every possibility, it is imperative to perform a full renal biopsy workup, including immunofluorescence and electron microscopy. Without immunofluorescence or electron microscopy, the possibility of underlying immune complex disease, anti-TBM disease, monoclonal immunoglobulin deposition disease, mitochondrial abnormalities, and other forms of underlying diseases cannot be excluded. It is also very important to review the clinical history in detail and consider all possible pathogenetic factors to which the patient may have been exposed. The diagnosis of idiopathic TIN reflects only that we are unable to identify the etiologic factor(s).

REFERENCES

- Councilman W. Acute interstitial nephritis. *J Exp Med* 1898;3:393–390.
- Rastegar A, Kashgarian M. The clinical spectrum of tubulointerstitial nephritis. *Kidney Int* 1898;54(2):313–327.
- Praga M, González E. Acute interstitial nephritis. *Kidney Int* 2010;77(11):956–961.
- Uliniski T, Sellier-Leclerc AL, Tudorache E, et al. Acute tubulointerstitial nephritis. *Pediatr Nephrol* 2012;27(7):1051–1057.
- Mezzano S, Droguet A, Burgos ME, et al. Renin-angiotensin system activation and interstitial inflammation in human diabetic nephropathy. *Kidney Int Suppl* 2003;(86):S64–S70.
- Churg J, Cotran R, Siniyah R, et al. *Renal Disease: Classification and Atlas of Tubulointerstitial Diseases*. Tokyo, Japan: Igaku-Shoin, 1985.
- Colvin R, Fang L. Interstitial nephritis. In: Tisher C, Brenner B, eds. *Renal Pathology with Clinical and Functional Correlations*. Vol 1. Philadelphia: JB Lippincott, 1994:723.
- Baker RJ, Pusey CD. The changing profile of acute tubulointerstitial nephritis. *Nephrol Dial Transplant* 2004;19(1):8–11.
- Schwarz A, Krause PH, Kunzendorf U, et al. The outcome of acute interstitial nephritis: Risk factors for the transition from acute to chronic interstitial nephritis. *Clin Nephrol* 2000;54(3):179–190.
- Perazella MA, Markowitz GS. Drug-induced acute interstitial nephritis. *Nat Rev Nephrol* 2010;6(8):461–470.
- Distler A, Keller F, Kunzendorf U, et al. The outcome of acute interstitial nephritis: risk factors for the transition from acute to chronic interstitial nephritis. *Clin Nephrol* 2003;59:65.
- Buysen JG, Houthoff HJ, Krediet RT, et al. Acute interstitial nephritis: a clinical and morphological study in 27 patients. *Nephrol Dial Transplant* 1990;5:94–99.
- Raissan Y, Nasr SH, Larsen CP, et al. Diagnosis of IgG4-related tubulointerstitial nephritis. *J Am Soc Nephrol* 2011;22(7):1343–1352.
- Fletcher A. Eosinophiluria and acute interstitial nephritis. *N Engl J Med* 2008;358(16):1760–1761.
- Ruffing KA, Hoppes P, Blend D, et al. Eosinophils in urine revisited. *Clin Nephrol* 1984;41:163–166.
- Bender WL, Whelton A, Beschoner WE, et al. Interstitial nephritis, proteinuria, and renal failure caused by nonsteroidal anti-inflammatory drugs. Immunologic characterization of the inflammatory infiltrate. *Am J Med* 1984;76:1006–1012.
- Spanou Z, Keller M, Britschgi M, et al. Involvement of drug-specific T cells in acute drug-induced interstitial nephritis. *J Am Soc Nephrol* 2006;17(10):2919–2927.
- D'Agati VD, Appel GB, Estes D, et al. Monoclonal antibody identification of infiltrating mononuclear leukocytes in lupus nephritis. *Kidney Int* 1986;30:573–581.
- Zheng G, Wang Y, Mahajan D, et al. The role of tubulointerstitial inflammation. *Kidney Int Suppl* 2005;94:S96–S100.
- Sean Eardley K, Cockwell P. Macrophages and progressive tubulointerstitial disease. *Kidney Int* 2005;68(2):437–455.
- Hawkins EP, Berry PL, Silva FG. Acute tubulointerstitial nephritis in children: clinical, morphologic, and lectin studies. A report of the southwest pediatric nephrology study group. *Am J Kidney Dis* 1989;14:466–471.
- Ivanyi B, Marcussen N, Kemp E, et al. The distal nephron is preferentially infiltrated by inflammatory cells in acute interstitial nephritis. *Virchows Arch A Pathol Anat Histopathol* 1992;420:37–42.
- Satoskar AA, Brodsky SV, Nadasdy G, et al. Discrepancies in glomerular and tubulointerstitial/vascular immune complex IgG subclasses in lupus nephritis. *Lupus* 2011;20(13):1396–403.
- Bijol V, Mendez GP, Nosé V, et al. Granulomatous interstitial nephritis: a clinicopathologic study of 46 cases from a single institution. *Int J Surg Pathol* 2006;14(1):57–63.
- Robson MG, Banerjee D, Hopster D, et al. Seven cases of granulomatous interstitial nephritis in the absence of extrarenal sarcoid. *Nephrol Dial Transplant* 2003;18:280–284.
- Joss N, Morris S, Young B, et al. Granulomatous interstitial nephritis. *Clin J Am Soc Nephrol* 2007;2(2):222–230.
- Nadasdy T, Laszik Z, Blick KE, et al. Tubular atrophy in the end-stage kidney: a lectin and immunohistochemical study. *Hum Pathol* 1994;25:22–28.
- Brodsky SV, Albawardi A, Satoskar AA, et al. When one plus one equals more than two—a novel stain for renal biopsies is a combination of two classical stains. *Histol Histopathol* 2010;25(11):1379–1383.
- Pfaller W, Rittinger M. Quantitative morphology of the rat kidney. *Int J Biochem* 1980;12:17–22.
- Knepper MA, Danielson RA, Sidel GM, et al. Quantitative analysis of renal medullary anatomy in rats and rabbits. *Kidney Int* 1977;12:313–323.
- Zeisberg M, Neilson EG. Mechanisms of tubulointerstitial fibrosis. *J Am Soc Nephrol* 2010;21(11):1819–1834.
- Silva FG, Nadasdy T, Laszik Z. Immunohistochemical and lectin dissection of the human nephron in health and disease. *Arch Pathol Lab Med* 1993;117:1233–1239.
- Takemura Y, Koshimichi M, Sugimoto K, et al. A tubulointerstitial nephritis antigen gene defect causes childhood-onset chronic renal failure. *Pediatr Nephrol* 2010;25(7):1349–1353.
- Jenkins J, Brodsky SV, Satoskar AA, et al. The relevance of periglomerular fibrosis in the evaluation of routine core renal biopsies. *Arch Pathol Lab Medication* 2011;135:117–122.
- Isbel NM, Hill PA, Foti R, et al. Tubules are the major site of M-CSF production in experimental kidney disease: Correlation with local macrophage proliferation. *Kidney Int* 2001;60:614–625.
- Rovin BH. Beyond a glomerulocentric view of inflammation. *Kidney Int* 2001;60:797–798.
- McAdam AJ, Sharpe AH. Infectious diseases. In: Kumar V, Abbas AK, Fausto N, Aster JC, eds. *Robbins & Cotran Pathologic Basis of Disease*, 8th ed. Philadelphia: WB Saunders Elsevier, 2009:331.
- Rossett J. Drug-induced acute interstitial nephritis. *Kidney Int* 2001;60:804–817.
- Ikeda M, Takemura T, Hino S, et al. Molecular cloning, expression, and chromosomal localization of a human tubulointerstitial nephritis antigen. *Biochem Biophys Res Commun* 2000;268(1):225–230.
- Serafini-Cessi F, Malagolini N, Cavallone D. Tamm-Horsfall glycoprotein: Biology and clinical relevance. *Am J Kidney Dis* 2003;42(4):658–676.
- Stone JH, Zen Y, Deshpande V. IgG4-related disease. *N Engl J Med* 2012;366(6):539–551.
- Kambham N, Markowitz GS, Tanji N, et al. Idiopathic hypocomplementemic interstitial nephritis with extensive tubulointerstitial deposits. *Am J Kidney Dis* 2001;37:388–399.
- Wada T, Furuichi K, Sakai N, et al. Eotaxin contributes to renal interstitial eosinophilia. *Nephrol Dial Transplant* 1999;14:76–80.

44. Boor P, Ostendorf T, Floege J. Renal fibrosis: Novel insights into mechanisms and therapeutic targets. *Nat Rev Nephrol* 2010;6(11):643–656.
45. Sato M, Muragaki Y, Saika S, et al. Targeted disruption of TGF-beta1/Smad3 signaling protects against renal tubulointerstitial fibrosis induced by unilateral ureteral obstruction. *J Clin Invest* 2003;112:1486–1494.
46. Bottinger EP, Bitzer M. TGF-beta signaling in renal disease. *J Am Soc Nephrol* 2002;13:2600–2610.
47. August P, Suthanthiran M. Transforming growth factor beta and progression of renal disease. *Kidney Int Suppl* 2003;(87):S99–S104.
48. Okada H, Kikuta T, Kobayashi T, et al. Connective tissue growth factor expressed in tubular epithelium plays a pivotal role in renal fibrogenesis. *J Am Soc Nephrol* 2005;16:133–143.
49. Lan HY. Tubular epithelial-myofibroblast transdifferentiation mechanisms in proximal tubule cells. *Curr Opin Nephrol Hypertens* 2003;12:25–29.
50. García-Sánchez O, López-Hernández FJ, López-Novoa JM. An integrative view on the role of TGF-beta in the progressive tubular deletion associated with chronic kidney disease. *Kidney Int* 2010;77(11):950–955.
51. Kriz W, Kaissling B, Le Hir M. Epithelial-mesenchymal transition (EMT) in kidney fibrosis: fact or fantasy? *J Clin Invest* 2011;121(2):468–474.
52. Humphreys BD, Lin SL, Kobayashi A, et al. Fate tracing reveals the pericyte and not epithelial origin of myofibroblasts in kidney fibrosis. *Am J Pathol* 2010;176(1):85–97.
53. Silva FG. Chemical-induced nephropathy: a review of the renal tubulointerstitial lesions in humans. *Toxicol Pathol* 2004;32 (Suppl 2):71–84.
54. Markowitz GS, Perazella MA. Drug-induced renal failure: A focus on tubulointerstitial disease. *Clin Chim Acta* 2005;351:31–47.
55. Ra A, Tobe SW. Acute interstitial nephritis due to pantoprazole. *Ann Pharmacother* 2004;38(1):41–45.
56. Galpin JE, Shinaberger JH, Stanley TM, et al. Acute interstitial nephritis due to methicillin. *Am J Med* 1978;65:756–765.
57. Lieske JC, Bonebrake D, Thesing J, et al. Eosinophiluria is common among patients after ileal conduit surgery. *Clin Chem Lab Med* 2011;49(11):1869–1871.
58. Lino M, Binaut R, Noël LH, et al. Tubulointerstitial nephritis and Fanconi syndrome in primary biliary cirrhosis. *Am J Kidney Dis* 2005;46(3):e41–e46.
59. Colvin RB, Burton JR, Hyslop NE Jr, et al. Letter: Penicillin-associated interstitial nephritis. *Ann Intern Med* 1974;81:404–405.
60. Kondo S, Kagami S, Kido H, et al. Role of mast cell tryptase in renal interstitial fibrosis. *J Am Soc Nephrol* 2001;12(8):1668–1676.
61. Baldwin DS, Levine BB, McCluskey RT, et al. Renal failure and interstitial nephritis due to penicillin and methicillin. *N Engl J Med* 1968;279:1245–1252.
62. Border WA, Lehman DH, Egan JD, et al. Antitubular basement-membrane antibodies in methicillin-associated interstitial nephritis. *N Engl J Med* 1974;291:381–384.
63. Olsen S, Asklund M. Interstitial nephritis with acute renal failure following cardiac surgery and treatment with methicillin. *Acta Med Scand* 1976;199:305–310.
64. Gabow PA, Lacher JW, Neff TA. Tubulointerstitial and glomerular nephritis associated with rifampin. Report of a case. *JAMA* 1976;235:2517–2518.
65. Minetti L, Barbiano di Belgioioso G, Busnach G. Immunohistological diagnosis of drug-induced hypersensitivity nephritis. *Contrib Nephrol* 1978;10:15–29.
66. Olsen TS, Wassef NF, Olsen HS, et al. Ultrastructure of the kidney in acute interstitial nephritis. *Ultrastruct Pathol* 1986;10:1–16.
67. Dixit MP, Nguyen C, Carson T, et al. Non-steroidal anti-inflammatory drugs-associated acute interstitial nephritis with granular tubular basement membrane deposits. *Pediatr Nephrol* 2008;23(1):145–148.
68. Vlasveld LT, van de Wiel-van Kemenade E, et al. Possible role for cytotoxic lymphocytes in the pathogenesis of acute interstitial nephritis after recombinant interleukin-2 treatment for renal cell cancer. *Cancer Immunol Immunother* 1993;36:210–213.
69. Choi YJ, Chakraborty S, Nguyen V, et al. Peritubular capillary loss is associated with chronic tubulointerstitial injury in human kidney: Altered expression of vascular endothelial growth factor. *Hum Pathol* 2000;31:1491–1497.
70. Schwarz A, Krause P, Kunzendorf U, et al. The outcome of acute interstitial nephritis: Risk factors for the transition from acute to chronic interstitial nephritis. *Clin Nephrol* 2003;59:65.
71. Benner EJ. Renal damage associated with prolonged administration of ampicillin, cephaloridine, and cephalothin. *Antimicrobial Agents Chemother* 1969;9:417–420.
72. Burton JR, Lichtenstein NS, Colvin RB, et al. Acute renal failure during cephalothin therapy. *JAMA* 1974;229(6):679–682.
73. Foord RD. Cephaloridine, cephalothin and the kidney. *J Antimicrob Chemother* 1975;1:119–133.
74. Plakogiannis R, Nogid A. Acute interstitial nephritis associated with co-administration of vancomycin and ceftriaxone: Case series and review of the literature. *Pharmacotherapy* 2007;27(10):1456–1461.
75. Norrby R, Stenqvist K, Elgefors B. Interaction between cephaloridine and furosemide in man. *Scand J Infect Dis* 1976;8:209–212.
76. Fillastre JP, Kleinknecht D. Acute renal failure associated with cephalosporin therapy. *Am Heart J* 1975;89:809–810.
77. Wade JC, Smith CR, Petty BG, et al. Cephalothin plus an aminoglycoside is more nephrotoxic than methicillin plus an aminoglycoside. *Lancet* 1978;2:604–606.
78. Dodds MG, Foord RD. Enhancement by potent diuretics of renal tubular necrosis induced by cephaloridine. *Br J Pharmacol* 1970;40:227–236.
79. Verma S, Kieff E. Cephalixin-related nephropathy. *JAMA* 1975;234:618–619.
80. Barza M. The nephrotoxicity of cephalosporins: An overview. *J Infect Dis* 1978;137(Suppl):S60–S73.
81. Mancini S, Iacovoni R, Fierimonte V, et al. Drug-induced interstitial nephritis. A case report. *Minerva Pediatr* 1994;46:557–560.
82. Goddard JK, Janning SW, Gass JS, et al. Cefuroxime-induced acute renal failure. *Pharmacotherapy* 1994;14:488–491.
83. Perkins RL, Apicella MA, Lee IS, et al. Cephaloridine and cephalothin: comparative studies of potential nephrotoxicity. *J Lab Clin Med* 1968;71:75–84.
84. Tong JE, Howell DN, Foreman JW. Drug-induced granulomatous interstitial nephritis in a pediatric patient. *Pediatr Nephrol* 2007;22(2):306–309.
85. Tune BM, Hsu CY. Toxicity of cephaloridine to carnitine transport and fatty acid metabolism in rabbit renal cortical mitochondria: Structure-activity relationships. *J Pharmacol Exp Ther* 1994;270:873–880.
86. Lash LH, Tokarz JJ, Woods EB. Renal cell type specificity of cephalosporin-induced cytotoxicity in suspensions of isolated proximal tubular and distal tubular cells. *Toxicology* 1994;94:97–118.
87. Levine BB. Antigenicity and cross-reactivity of penicillins and cephalosporins. *J Infect Dis* 1973;128(Suppl):S364–S366.
88. Zaigraykin N, Kovalev J, Elias N, et al. Levofloxacin-induced interstitial nephritis and vasculitis in an elderly woman. *Isr Med Assoc J* 2006;8(10):726–727.
89. Hadimeri H, Almroth G, Cederbrant K, et al. Allergic nephropathy associated with norfloxacin and ciprofloxacin therapy. Report of two cases and review of the literature. *Scand J Urol Nephrol* 1997;31:481–485.
90. Okada H, Watanabe Y, Kotaki S, et al. An unusual form of crystal-forming chronic interstitial nephritis following long-term exposure to tosuflaxacin tosylate. *Am J Kidney Dis* 2004;44:902–907.
91. Chatzikyrkou C, Hamwi I, Clajus C, et al. Biopsy proven acute interstitial nephritis after treatment with moxifloxacin. *BMC Nephrol* 2010;11:19.
92. Allon M, Lopez EJ, Min KW. Acute renal failure due to ciprofloxacin. *Arch Intern Med* 1990;150:2187–2189.
93. Helmink R, Benediktsson H. Ciprofloxacin-induced allergic interstitial nephritis. *Nephron* 1990;55:432–433.
94. Hootkins R, Fennes AZ, Stephens MK. Acute renal failure secondary to oral ciprofloxacin therapy: A presentation of three cases and a review of the literature. *Clin Nephrol* 1989;32:75–78.
95. Rastogi S, Atkinson JL, McCarthy JT. Allergic nephropathy associated with ciprofloxacin. *Mayo Clin Proc* 1990;65:987–989.
96. Shih DJ, Korbet SM, Rydel JJ, et al. Renal vasculitis associated with ciprofloxacin. *Am J Kidney Dis* 1995;26:516–519.
97. Lo WK, Rolston KV, Rubenstein EB, et al. Ciprofloxacin-induced nephrotoxicity in patients with cancer. *Arch Intern Med* 1993;153:1258–1262.
98. Lien YH, Hansen R, Kern WF, et al. Ciprofloxacin-induced granulomatous interstitial nephritis and localized elastolysis. *Am J Kidney Dis* 1993;22:598–602.
99. Garcia-Ortiz R, Espinoza RS, Silva GR, et al. Cloxacillin-induced acute tubulo interstitial nephritis. *Ann Pharmacother* 1992;26:1241–1242.

100. Soto J, Bosch JM, Alsar Ortiz MJ, et al. Piperacillin-induced acute interstitial nephritis. *Nephron* 1993;65:154–155.
101. Pill MW, O'Neill CV, Chapman MM, et al. Suspected acute interstitial nephritis induced by piperacillin-tazobactam. *Pharmacotherapy* 1997;17:166–169.
102. Gilbert DN, Gourley R, d'Agostino A, et al. Interstitial nephritis due to methicillin, penicillin and ampicillin. *Ann Allergy* 1970;28:378–385.
103. Ruley EJ, Lisi LM. Interstitial nephritis and renal failure due to ampicillin. *J Pediatr* 1974;84:878–882.
104. Tannenber AM, Wicher KJ, Rose NR. Ampicillin nephropathy. *JAMA* 1971;218:449.
105. Woodroffe AJ, Weldon M, Meadows R, et al. Acute interstitial nephritis following ampicillin hypersensitivity. *Med J Aust* 1975;1:65–68.
106. Ditlove J, Weidmann P, Bernstein M, et al. Methicillin nephritis. *Medicine (Baltimore)* 1977;56:483–491.
107. Jensen HA, Halveg AB, Saunamaki KI. Permanent impairment of renal function after methicillin nephropathy. *Br Med J* 1971;4:406.
108. Appel GB, Neu HC. The nephrotoxicity of antimicrobial agents (first of three parts). *N Engl J Med* 1977;296:663–670.
109. Mayaud C, Kanfer A, Kourilsky O, et al. Letter: Interstitial nephritis after methicillin. *N Engl J Med* 1975;292:1132–1133.
110. Minetti L, di Belgiojoso GB, Civati G, et al. Drug induced hypersensitivity nephritis. *Proc Eur Dial Transplant Assoc* 1975;11:526–533.
111. Hansen ES, Tauris P. Methicillin-induced nephropathy. A case with linear deposition of IgG and C3 on the tubular-basement-membrane. *Acta Pathol Microbiol Scand [A]* 1976;84:440–442.
112. Orfila C, Rakotoarivony J, Durand D, et al. A correlative study of immunofluorescence, electron, and light microscopy in immunologically mediated renal tubular disease in man. *Nephron* 1979;23:14–22.
113. Rennke HG, Roos PC, Wall SG. Drug-induced interstitial nephritis with heavy glomerular proteinuria. *N Engl J Med* 1980;302:691–692.
114. Pirani CL, Valeri A, D'Agati V, et al. Renal toxicity of nonsteroidal anti-inflammatory drugs. *Contrib Nephrol* 1987;55:159–175.
115. Flynn CT, Rainford DJ, Hope E. Acute renal failure and rifampicin: danger of unsuspected intermittent dosage. *Br Med J* 1974;2:482.
116. Muthukumar T, Jayakumar M, Fernando EM, et al. Acute renal failure due to rifampicin: A study of 25 patients. *Am J Kidney Dis* 2002;40:690–696.
117. Campese VM, Marzullo F, Schena FP, et al. Acute renal failure during intermittent rifampicin therapy. *Nephron* 1973;10:256–261.
118. Ramgopal V, Leonard C, Bhatena D. Acute renal failure associated with rifampicin. *Lancet* 1973;1:1195–1196.
119. Schubert C, Bates WD, Moosa MR. Acute tubulointerstitial nephritis related to antituberculous drug therapy. *Clin Nephrol* 2010;73(6):413–419.
120. Cochran M, Morrhead PJ, Platts M. Letter: Permanent renal damage with rifampicin. *Lancet* 1975;1:1428.
121. Quinn BP, Wall BM. Nephrogenic diabetes insipidus and tubulointerstitial nephritis during continuous therapy with rifampin. *Am J Kidney Dis* 1989;14:217–220.
122. Minetti L, Barbiano di Belgiojoso G, Civati G, et al. Nephritis caused by drug hypersensitivity [DHN]. Clinicohistological observations in 15 cases. *Minerva Nefrol* 1974;21:197–212.
123. Poole G, Stradling P, Worledge S. Potentially serious side effects of high-dose twice-weekly rifampicin. *Br Med J* 1971;3:343–347.
124. Tomonaga H. Detection of antibody specific to rifampicin metabolite by ELISA—mechanism of sensitization by rifampicin. *Averugi* 1993;42:854–863.
125. French A. Hypersensitivity in the pathogenesis of the histopathologic changes associated with sulfonamide chemotherapy. *Am J Pathol* 1946;22:679.
126. More R, McMillan G, Duff G. The pathology of sulfonamide allergy in man. *Am J Pathol* 1946;22:703.
127. Dry J, Leynadier F, Herman D, et al. Letter: Sulfamethoxazole-trimethoprim combination (cotrimoxazole). Unusual immuno-allergic reaction. *Nouv Presse Med* 1975;4:36.
128. Robson M, Levi J, Dolberg L, et al. Acute tubulo-interstitial nephritis following sulfadiazine therapy. *Isr J Med Sci* 1970;6:561–566.
129. Bailey RR, Little PJ. Deterioration in renal function in association with co-trimoxazole therapy. *Med J Aust* 1976;1:914, 916.
130. Kalowski S, Nanra RS, Mathew TH, et al. Deterioration in renal function in association with co-trimoxazole therapy. *Lancet* 1973;1:394–397.
131. Augusto JF, Sayegh J, Simon A, et al. A case of sulphasalazine-induced DRESS syndrome with delayed acute interstitial nephritis. *Nephrol Dial Transplant* 2009;24(9):2940–2942.
132. Farina LA, Palou Redorta J, Chechile Toniolo G. Reversible acute renal failure due to sulfonamide-induced lithiasis in an AIDS patient. *Arch Esp Urol* 1995;48:418–419.
133. Albala DM, Prien EL Jr, Galal HA. Urolithiasis as a hazard of sulfonamide therapy. *J Endourol* 1994;8:401–403.
134. Russinko PJ, Agarwal S, Choi MJ, et al. Obstructive nephropathy secondary to sulfasalazine calculi. *Urology* 2003;62:748.
135. Dowling H, Lepper M. Toxic reactions following therapy with sulfapyridine, sulfathiazole and sulfadiazine. *JAMA* 1943;121:1190.
136. Cryst C, Hammar SP. Acute granulomatous interstitial nephritis due to co-trimoxazole. *Am J Nephrol* 1988;8:483–488.
137. Htike NL, Santoro J, Gilbert B, et al. Biopsy-proven vancomycin-associated interstitial nephritis and acute tubular necrosis. *Clin Exp Nephrol* 2012;16(2):320–324.
138. Salazar MN, Matthews M, Posadas A, et al. Biopsy proven interstitial nephritis following treatment with vancomycin: A case report. *Conn Med* 2010;74(3):139–141.
139. Hong S, Valderrama E, Mattana J, et al. Vancomycin-induced acute granulomatous interstitial nephritis: Therapeutic options. *Am J Med Sci* 2007;334(4):296–300.
140. Cimino MA, Rotstein C, Slaughter RL, et al. Relationship of serum antibiotic concentrations to nephrotoxicity in cancer patients receiving concurrent aminoglycoside and vancomycin therapy. *Am J Med* 1987;83:1091–1097.
141. Rybak MJ, Albrecht LM, Boike SC, et al. Nephrotoxicity of vancomycin, alone and with an aminoglycoside. *J Antimicrob Chemother* 1990;25:679–687.
142. Nahata MC. Lack of nephrotoxicity in pediatric patients receiving concurrent vancomycin and aminoglycoside therapy. *Chemotherapy* 1987;33:302–304.
143. Hsu SI. Biopsy-proved acute tubulointerstitial nephritis and toxic epidermal necrolysis associated with vancomycin. *Pharmacotherapy* 2001;21:1233–1239.
144. Shah-Khan F, Scheetz MH, Ghossein C. Biopsy-proven acute tubular necrosis due to vancomycin toxicity. *Int J Nephrol* 2011;2011:436856.
145. Wu CY, Wang JS, Chiou YH, et al. Biopsy proven acute tubular necrosis associated with vancomycin in a child: case report and literature review. *Ren Fail* 2007;29(8):1059–1061.
146. Wicklow BA, Ogborn MR, Gibson IW, et al. Biopsy-proven acute tubular necrosis in a child attributed to vancomycin intoxication. *Pediatr Nephrol* 2006;21(8):1194–1196.
147. Kwon HS, Chang YS, Jeong YY, et al. A case of hypersensitivity syndrome to both vancomycin and teicoplanin. *J Korean Med Sci* 2006;21(6):1108–1110.
148. Yano Y, Hiraoka A, Oguma T. Enhancement of tobramycin binding to rat renal brush border membrane by vancomycin. *J Pharmacol Exp Ther* 1995;274:695–699.
149. Harris RC. Cyclooxygenase-2 in the kidney. *J Am Soc Nephrol* 2000;11:2387–2394.
150. Galli G, Panzetta G. Do non-steroidal anti-inflammatory drugs and COX-2 selective inhibitors have different renal effects? *J Nephrol* 2002;15:480.
151. Mungan MU, Gurel D, Canda AE, et al. Expression of COX-2 in normal and pyelonephritic kidney, renal intraepithelial neoplasia, and renal cell carcinoma. *Eur Urol* 2006;50(1):92–97.
152. Rocha JL, Fernandez-Alonso J. Acute tubulointerstitial nephritis associated with the selective COX-2 enzyme inhibitor, rofecoxib. *Lancet* 2001;357:1946–1947.
153. Demke D, Zhao S, Arellano FM. Interstitial nephritis associated with celecoxib. *Lancet* 2001;358:1726–1727.
154. Henao J, Hisamuddin I, Nzerue CM, et al. Celecoxib-induced acute interstitial nephritis. *Am J Kidney Dis* 2002;39:1313–1317.
155. Alper AB Jr, Meleg-Smith S, Krane NK. Nephrotic syndrome and interstitial nephritis associated with celecoxib. *Am J Kidney Dis* 2002;40:1086–1090.

156. Brewster UC, Perazella MA. Acute tubulointerstitial nephritis associated with celecoxib. *Nephrol Dial Transplant* 2004;19:1017–1018.
157. Szalat A, Krasilnikov I, Bloch A, et al. Acute renal failure and interstitial nephritis in a patient treated with rofecoxib: Case report and review of the literature. *Arthritis Rheum* 2004;51:670–673.
158. Fletcher JT, Graf N, Scarman A, et al. Nephrotoxicity with cyclooxygenase 2 inhibitor use in children. *Pediatr Nephrol* 2006;21(12):1893–1897.
159. Taber SS, Pasko DA. The epidemiology of drug-induced disorders: The kidney. *Expert Opin Drug Saf* 2008;7(6):679–690.
160. Whelton A, Hamilton CW. Nonsteroidal anti-inflammatory drugs: Effects on kidney function. *J Clin Pharmacol* 1991;31:588–598.
161. Whelton A. Nephrotoxicity of nonsteroidal anti-inflammatory drugs: Physiologic foundations and clinical implications. *Am J Med* 1999;106:13S–24S.
162. Murray MD, Brater DC. Adverse effects of nonsteroidal anti-inflammatory drugs on renal function. *Ann Intern Med* 1990;112:559–560.
163. Kleinknecht D, Landais P, Goldfarb B. Analgesic and non-steroidal anti-inflammatory drug-associated acute renal failure: A prospective collaborative study. *Clin Nephrol* 1986;25:275–281.
164. Fox DA, Jick H. Nonsteroidal anti-inflammatory drugs and renal disease. *JAMA* 1984;251:1299–1300.
165. Bonney SL, Northington RS, Hedrich DA, et al. Renal safety of two analgesics used over the counter: Ibuprofen and aspirin. *Clin Pharmacol Ther* 1986;40:373–377.
166. Corwin HL, Bonventre JV. Renal insufficiency associated with nonsteroidal anti-inflammatory agents. *Am J Kidney Dis* 1984;4:147–152.
167. Clive DM, Stoff JS. Renal syndromes associated with nonsteroidal anti-inflammatory drugs. *N Engl J Med* 1984;310:563–572.
168. Palmer BF, Henrich WL. Clinical acute renal failure with nonsteroidal anti-inflammatory drugs. *Semin Nephrol* 1995;15:214–227.
169. Marasco WA, Gikas PW, Azziz-Baumgartner R, et al. Ibuprofen-associated renal dysfunction. Pathophysiologic mechanisms of acute renal failure, hyperkalemia, tubular necrosis, and proteinuria. *Arch Intern Med* 1987;147:2107–2116.
170. Whelton A, Stout RL, Spilman PS, et al. Renal effects of ibuprofen, piroxicam, and sulindac in patients with asymptomatic renal failure. A prospective, randomized, crossover comparison. *Ann Intern Med* 1990;112:568–576.
171. Calvo-Alen J, De Cos MA, Rodriguez-Valverde V, et al. Subclinical renal toxicity in rheumatic patients receiving long-term treatment with nonsteroidal anti-inflammatory drugs. *J Rheumatol* 1994;21:1742–1747.
172. Carmichael J, Shankel SW. Effects of nonsteroidal anti-inflammatory drugs on prostaglandins and renal function. *Am J Med* 1985;78:992–1000.
173. Kleinknecht D. Interstitial nephritis, the nephrotic syndrome, and chronic renal failure secondary to nonsteroidal anti-inflammatory drugs. *Semin Nephrol* 1995;15:228–235.
174. Warren GV, Korbet SM, Schwartz MM, et al. Minimal change glomerulopathy associated with nonsteroidal anti-inflammatory drugs. *Am J Kidney Dis* 1989;13:127–130.
175. Lantz B, Cochat P, Bouchet JL, et al. Short-term niflumic-acid-induced acute renal failure in children. *Nephrol Dial Transplant* 1994;9:1234–1239.
176. Kaplan BS, Restaino I, Raval DS, et al. Renal failure in the neonate associated with in utero exposure to non-steroidal anti-inflammatory agents. *Pediatr Nephrol* 1994;8:700–704.
177. van der Heijden BJ, Carlus C, Nancy F, et al. Persistent anuria, neonatal death, and renal microcystic lesions after prenatal exposure to indomethacin. *Am J Obstet Gynecol* 1994;171:617–623.
178. Voyer LE, Drut R, Mendez JH. Fetal renal maldevelopment with oligohydramnios following maternal use of piroxicam. *Pediatr Nephrol* 1994;8:592–594.
179. Ciabattini G, Cinotti GA, Pierucci A, et al. Effects of sulindac and ibuprofen in patients with chronic glomerular disease. Evidence for the dependence of renal function on prostacyclin. *N Engl J Med* 1984;310:279–283.
180. Gurwitz JH, Avorn J, Ross-Degnan D, et al. Nonsteroidal anti-inflammatory drug-associated azotemia in the very old. *JAMA* 1990;264:471–475.
181. Harirforoosh S, Jamali F. Renal adverse effects of nonsteroidal anti-inflammatory drugs. *Expert Opin Drug Saf* 2009;8(6):669–681.
182. Gentilini P. Cirrhosis, renal function and NSAIDs. *J Hepatol* 1993;19:200–203.
183. Ahmad SR, Kortepeter C, Brinker A, et al. Renal failure associated with the use of celecoxib and rofecoxib. *Drug Saf* 2002;25(7):537–544.
184. Blantz RC. Acetaminophen: Acute and chronic effects on renal function. *Am J Kidney Dis* 1996;28:S3–S6.
185. D'Agati V. Does aspirin cause acute or chronic renal failure in experimental animals and in humans? *Am J Kidney Dis* 1996;28:S24–S29.
186. Fruchter LL, Alexopoulos I, Lau KK. Acute interstitial nephritis with acetaminophen and alcohol intoxication. *Ital J Pediatr* 2011;37:17.
187. Jickling G, Heino A, Ahmed SN. Acetaminophen toxicity with concomitant use of carbamazepine. *Epileptic Disord* 2009;11(4):329–332.
188. Cheng HF, Nolasco F, Cameron JS, et al. HLA-DR display by renal tubular epithelium and phenotype of infiltrate in interstitial nephritis. *Nephrol Dial Transplant* 1989;4:205–215.
189. Schwarz A, Krause PH, Keller F, et al. Granulomatous interstitial nephritis after nonsteroidal anti-inflammatory drugs. *Am J Nephrol* 1988;8:410–416.
190. Baisac J, Henrich WL. Nephrotoxicity of nonsteroidal anti-inflammatory drugs. *Miner Electrolyte Metab* 1994;20:187–192.
191. Markowitz GS, Falkowitz DC, Isom R, et al. Membranous glomerulopathy and acute interstitial nephritis following treatment with celecoxib. *Clin Nephrol* 2003;59(2):137–142.
192. Sekhon I, Munjal S, Croker B, Johnson RJ, Ejaz AA. Glomerular tip lesion associated with nonsteroidal anti-inflammatory drug-induced nephrotic syndrome. *Am J Kidney Dis* 2005;46(4):e55–e58.
193. Schlondorff D. Renal prostaglandin synthesis. Sites of production and specific actions of prostaglandins. *Am J Med* 1986;81:1–11.
194. Anderson RJ, Berl T, McDonald KM, et al. Prostaglandins: Effects on blood pressure, renal blood flow, sodium and water excretion. *Kidney Int* 1976;10:205–215.
195. Zambraski EJ. The effects of nonsteroidal anti-inflammatory drugs on renal function: Experimental studies in animals. *Semin Nephrol* 1995;15:205–213.
196. Remuzzi A, Remuzzi G. The effects of nonsteroidal anti-inflammatory drugs on glomerular filtration of proteins and their therapeutic utility. *Semin Nephrol* 1995;15:236–243.
197. Spuhler O, Zollinger Hu. Chronic interstitial nephritis. *Z Klin Med* 1953;151:1–50.
198. Elseviers MM, De Broe ME. A long-term prospective controlled study of analgesic abuse in Belgium. *Kidney Int* 1995;48:1912–1919.
199. Elseviers MM, Waller I, Nenoy D, et al. Evaluation of diagnostic criteria for analgesic nephropathy in patients with end-stage renal failure: results of the ANNE study. Analgesic nephropathy network of Europe. *Nephrol Dial Transplant* 1995;10:808–814.
200. Perneger TV, Whelton PK, Klag MJ. Risk of kidney failure associated with the use of acetaminophen, aspirin, and nonsteroidal anti-inflammatory drugs. *N Engl J Med* 1994;331:1675–1679.
201. Pommer W, Bronder E, Greiser E, et al. Regular analgesic intake and the risk of end-stage renal failure. *Am J Nephrol* 1989;9:403–412.
202. Sandler DP, Smith JC, Weinberg CR, et al. Analgesic use and chronic renal disease. *N Engl J Med* 1989;320:1238–1243.
203. Henrich WL, Agodoa LE, Barrett B, et al. Analgesics and the kidney: summary and recommendations to the Scientific Advisory Board of the National Kidney Foundation from an Ad Hoc Committee of the National Kidney Foundation. *Am J Kidney Dis* 1996;27(1):162–165.
204. Elseviers M, De Broe M. The implication of analgesic in human kidney disease. In: Stewart J, ed. *Analgesic and NSAID-Induced Kidney Disease*. Oxford: Oxford University Press, 1993:32.
205. Gault MH, Wilson DR. Analgesic nephropathy in Canada: Clinical syndrome, management, and outcome. *Kidney Int* 1978;13:58–63.
206. Kincaid-Smith P. Analgesic nephropathy and the effect of non-steroidal anti-inflammatory drugs on the kidney. In: Catto G, ed. *Drugs and the Kidney*. Dordrecht: Kluwer Academic, 1990:1.
207. Gonwa TA, Hamilton RW, Buckalew VM Jr. Chronic renal failure and end-stage renal disease in northwest North Carolina. Importance of analgesic-associated nephropathy. *Arch Intern Med* 1981;141:462–465.
208. Elseviers M, De Broe M. Epidemiology of analgesic nephropathy. *J Nephrol* 1992;5:94.

209. Schwarz A, Preuschhof L, Zellner D. Incidence of analgesic nephropathy in Berlin since 1983. *Nephrol Dial Transplant* 1999;14:109–112.
210. Michielsen P, de Schepper P. Trends of analgesic nephropathy in two high-endemic regions with different legislation. *J Am Soc Nephrol* 2001;12:550–556.
211. Chang SH, Mathew TH, McDonald SP. Analgesic nephropathy and renal replacement therapy in Australia: trends, comorbidities and outcomes. *Clin J Am Soc Nephrol* 2008;3(3):768–776.
212. Lornoy W, Becaus I, Billioux JM, et al. Relationship between nonphenacetin combined analgesics and nephropathy. *Kidney Int* 2001;59:2371–2372.
213. Feinstein AR, Heinemann LA, Curhan GC, et al. Relationship between nonphenacetin combined analgesics and nephropathy: A review. Ad hoc committee of the international study group on analgesics and nephropathy. *Kidney Int* 2000;58:2259–2264.
214. Mihatsch MJ, Khanlari B, Brunner FP. Obituary to analgesic nephropathy—an autopsy study. *Nephrol Dial Transplant* 2006;21(11):3139–3145.
215. Michielsen P, Heinemann L, Mihatsch M, et al. Non-phenacetin analgesics and analgesic nephropathy: Clinical assessment of high users from a case–control study. *Nephrol Dial Transplant* 2009;24(4):1253–1259.
216. Van der Woude FJ, Heinemann LA, Graf H, et al. Analgesics use and ESRD in younger age: a case–control study. *BMC Nephrol* 2007;8:15.
217. De Broe M, Elseviers M. Over-the-counter analgesic use. *J Am Soc Nephrol* 2009;20:2098–2103.
218. Kurth T, Glynn RJ, Walker AM, et al. Analgesic use and change in kidney function in apparently healthy men. *Am J Kidney Dis* 2003;42:234–244.
219. Schnuelle P, Van Der Woude FJ. Analgesics and renal disease in the post-phenacetin era. *Am J Kidney Dis* 2003;42:385–387.
220. Nanra R. Functional defects in analgesic nephropathy. In: Stewart J, ed. *Analgesic and NSAID-Induced Kidney Disease*. Oxford: Oxford University Press, 1993:102.
221. Griffin MD, Bergstralhn EJ, Larson TS. Renal papillary necrosis—a sixteen-year clinical experience. *J Am Soc Nephrol* 1995;6:248–256.
222. De Broe ME, Elseviers MM. Analgesic nephropathy. *N Engl J Med* 1998;338:446–452.
223. Burry A. Pathology of analgesic nephropathy: Australian experience. *Kidney Int* 1978;13:34–40.
224. Mihatsch M, Zollinger H. The pathology of analgesic nephropathy. In: Stewart J, ed. *Analgesic and NSAID-Induced Kidney Disease*. Oxford: Oxford University Press, 1993:67.
225. Berneis K, Korteweg E, Mihatsch MJ. Characterization of the brown pigment of the mucosa of the urinary tract. *Virchows Arch A Pathol Anat Histopathol* 1983;402:203–207.
226. Gloor F. Capillary sclerosis of the urinary tract caused by abuse of an analgesic agent (phenacetin). *Pathologie* 1982;3:132–136.
227. Mihatsch MJ, Hofer HO, Gudat F, et al. Capillary sclerosis of the urinary tract and analgesic nephropathy. *Clin Nephrol* 1983;20:285–301.
228. Mihatsch MJ, Torhorst J, Steinmann E, et al. The morphologic diagnosis of analgesic (phenacetin) abuse. *Pathol Res Pract* 1979;164:68–79.
229. Burry A. The evolution of analgesic nephropathy. *Nephron* 1967;5:185.
230. Kincaid-Smith P. Pathogenesis of the renal lesion associated with the abuse of analgesics. *Lancet* 1967;1:859–862.
231. Zollinger H. *Niere und ableitende harnwege*. Berlin: Springer Verlag, 1966.
232. Kincaid-Smith P, Saker BM, McKenzie IF, et al. Lesions in the blood supply of the papilla in experimental analgesic nephropathy. *Med J Aust* 1968;1:203–206.
233. Molland EA. Experimental renal papillary necrosis. *Kidney Int* 1978;13:5–14.
234. Lagergren C, Ljungqvist A. The intrarenal arterial pattern in renal papillary necrosis. A micro-angiographic and histologic study. *Am J Pathol* 1962;41:633–643.
235. Prescott LF. Analgesic nephropathy: A reassessment of the role of phenacetin and other analgesics. *Drugs* 1982;23:75–149.
236. Duggin GG. Mechanisms in the development of analgesic nephropathy. *Kidney Int* 1980;18:553–561.
237. Duggin GG. Combination analgesic-induced kidney disease: The Australian experience. *Am J Kidney Dis* 1996;28:S39–S47.
238. Moeckel GW, Zhang L, Fogo AB, et al. COX2 activity promotes organic osmolyte accumulation and adaptation of renal medullary interstitial cells to hypertonic stress. *J Biol Chem* 2003;278:19352–19357.
239. Li C, Liu J, Saavedra JE, et al. The nitric oxide donor, V-PYRRO/NO, protects against acetaminophen-induced nephrotoxicity in mice. *Toxicology* 2003;189:173–180.
240. Ahmed MH, Ashton N, Balment RJ. Renal function in a rat model of analgesic nephropathy: Effect of chloroquine. *J Pharmacol Exp Ther* 2003;305:123–130.
241. Goncalves AR, Fujihara CK, Mattar AL, et al. Renal expression of COX-2, ANG II, and AT1 receptor in remnant kidney: Strong renoprotection by therapy with losartan and a nonsteroidal anti-inflammatory. *Am J Physiol Renal Physiol* 2004;286:F945–F954.
242. Schnellmann RG. Analgesic nephropathy in rodents. *J Toxicol Environ Health B Crit Rev* 1998;1:81–90.
243. Arend LJ, Springate JE. Interstitial nephritis from mesalazine: Case report and literature review. *Pediatr Nephrol* 2004;19:550–553.
244. Agarwal BN, Cabebe FG, Hoffman BI. Diphenylhydantoin-induced acute renal failure. *Nephron* 1977;18:249–251.
245. Hyman LR, Ballow M, Knieser MR. Diphenylhydantoin interstitial nephritis. roles of cellular and humoral immunologic injury. *J Pediatr* 1978;92:915–920.
246. Mihatsch MJ, Knusli C. Phenacetin abuse and malignant tumors. An autopsy study covering 25 years (1953–1977). *Klin Wochenschr* 1982;60:1339–1349.
247. Taylor J. Carcinoma of the renal pelvis. In: Stewart J, ed. *Analgesic and NSAID-Induced Kidney Disease*. Oxford: Oxford University Press, 1993:211.
248. McCredie M. Analgesics as human carcinogens: clinical and epidemiological evidence. In: Stewart J, ed. *Analgesic and NSAID-Induced Kidney Disease*. Oxford: Oxford University Press, 1993:211.
249. Chow WH, McLaughlin JK, Linet MS, et al. Use of analgesics and risk of renal cell cancer. *Int J Cancer* 1994;59:467–470.
250. Van Staa TP, Travis S, Leufkens HG, et al. 5-aminosalicylic acids and the risk of renal disease: a large British epidemiologic study. *Gastroenterology* 2004;126(7):1733–1739.
251. Ransford RA, Langman MJ. Sulphasalazine and mesalazine: serious adverse reactions re-evaluated on the basis of suspected adverse reaction reports to the committee on safety of medicines. *Gut* 2002;51:536–539.
252. Matson JR, Krous HF, Blackstock R. Diphenylhydantoin-induced hypersensitivity reaction with interstitial nephritis. *Hum Pathol* 1985;16:94–97.
253. Gaffey CM, Chun B, Harvey JC, et al. Phenytoin-induced systemic granulomatous vasculitis. *Arch Pathol Lab Med* 1986;110:131–135.
254. Alexander MP, Farag YM, Mittal BV, et al. Lithium toxicity: A double-edged sword. *Kidney Int* 2008;73(2):233–237.
255. Presne C, Fakhouri F, Noel LH, et al. Lithium-induced nephropathy: Rate of progression and prognostic factors. *Kidney Int* 2003;64:585–592.
256. Hestbech J, Hansen HE, Amdisen A, et al. Chronic renal lesions following long-term treatment with lithium. *Kidney Int* 1977;12:205–213.
257. Cox M. Lithium in the kidney. *Kidney Int* 1981;19:379.
258. Jorkasky DK, Amsterdam JD, Oler J, et al. Lithium-induced renal disease: A prospective study. *Clin Nephrol* 1988;30:293–302.
259. Walker R, Edwards J. Lithium and the kidney: An update. [editorial]. *Psychol Med* 1989;19:825.
260. Markowitz GS, Radhakrishnan J, Kambham N, et al. Lithium nephrotoxicity: A progressive combined glomerular and tubulointerstitial nephropathy. *J Am Soc Nephrol* 2000;11:1439–1448.
261. Dias N, Hocken AG. Oliguric renal failure complicating lithium carbonate therapy. *Nephron* 1973;10:246–249.
262. Lavender S, Brown JN, Berrill WT. Acute renal failure and lithium intoxication. *Postgrad Med J* 1973;49:277–279.
263. Aurell M, Svalander C, Wallin L, et al. Renal function and biopsy findings in patients on long-term lithium treatment. *Kidney Int* 1981;20:663–670.
264. Kincaid-Smith P, Burrows GD, Davies BM, et al. Renal-biopsy findings in lithium and prelithium patients. *Lancet* 1979;2:700–701.
265. Walker RG, Bennett WM, Davies BM, et al. Structural and functional effects of long-term lithium therapy. *Kidney Int Suppl* 1982;11:S13–S19.
266. Santella RN, Rimmer JM, MacPherson BR. Focal segmental glomerulosclerosis in patients receiving lithium carbonate. *Am J Med* 1988;84:951–954.
267. Tam VK, Green J, Schwieger J, et al. Nephrotic syndrome and renal insufficiency associated with lithium therapy. *Am J Kidney Dis* 1996;27:715–720.

268. Christensen BM, Marples D, Kim YH, et al. Changes in cellular composition of kidney collecting duct cells in rats with lithium-induced NDI. *Am J Physiol Cell Physiol* 2004;286:C952–C964.
269. Delve P, Lau M, Yun K, et al. Omeprazole-induced acute interstitial nephritis. *N Z Med J* 2003;116:U332.
270. Moore I, Sayer JA, Nayar A, et al. Pantoprazole-induced acute interstitial nephritis. *J Nephrol* 2004;17:580–581.
271. Torpey N, Barker T, Ross C. Drug-induced tubulo-interstitial nephritis secondary to proton pump inhibitors: Experience from a single UK renal unit. *Nephrol Dial Transplant* 2004;19:1441–1446.
272. Geevasinga N, Kairaitis L, Rangan GK, et al. Acute interstitial nephritis secondary to esomeprazole. *Med J Aust* 2005;182:235–236.
273. Ray S, Delaney M, Muller AF. Proton pump inhibitors and acute interstitial nephritis. *BMJ* 2010;341:c4412.
274. Myers RP, McLaughlin K, Hollomy DJ. Acute interstitial nephritis due to omeprazole. *Am J Gastroenterol* 2001;96:3428–3431.
275. Kalyesubula R, Perazella MA. Nephrotoxicity of HAART. *AIDS Res Treat* 2011;2011:562790. [Epub 2011 Aug 15]
276. Sarclotti M, Petter A, Zangerle R. Indinavir and interstitial nephritis. *Ann Intern Med* 1998;128:320–321.
277. Olyaei AJ, deMattos AM, Bennett WM. Renal toxicity of protease inhibitors. *Curr Opin Nephrol Hypertens* 2000;9:473–476.
278. Jaradat M, Phillips C, Yum MN, et al. Acute tubulointerstitial nephritis attributable to indinavir therapy. *Am J Kidney Dis* 2000;35:E16.
279. Brewster UC, Perazella MA. Acute interstitial nephritis associated with atazanavir, a new protease inhibitor. *Am J Kidney Dis* 2004;44:e81–e84.
280. Schmid S, Opravil M, Moddel M, et al. Acute interstitial nephritis of HIV-positive patients under atazanavir and tenofovir therapy in a retrospective analysis of kidney biopsies. *Virchows Arch* 2007;450(6):665–670.
281. McCluskey R. Immunologically mediated tubulo-interstitial nephritis. *Contemp Issues Nephrol* 1983;10:121.
282. Kelly C, Tomaszewski J, Neilson E. Immunopathogenic mechanisms of tubulointerstitial injury. In: Tisher C, Brenner B, eds. *Renal Pathology with Clinical and Functional Correlations*. Vol 1. Philadelphia: JB Lippincott, 1994:699.
283. Wuthrich RP, Sibalic V. Autoimmune tubulointerstitial nephritis: Insight from experimental models. *Exp Nephrol* 1998;6:288–293.
284. Miller K, Michael AF. Immunopathology of renal extracellular membranes in diabetes mellitus. specificity of tubular basement-membrane immunofluorescence. *Diabetes* 1976;25:701–708.
285. Lehman DH, Wilson CB, Dixon FJ. Extraglomerular immunoglobulin deposits in human nephritis. *Am J Med* 1975;58:765–796.
286. Clayman MD, Martinez-Hernandez A, Michaud L, et al. Isolation and characterization of the nephritogenic antigen producing anti-tubular basement membrane disease. *J Exp Med* 1985;161:290–305.
287. Brentjens JR, Matsuo S, Fukatsu A, et al. Immunologic studies in two patients with antitubular basement membrane nephritis. *Am J Med* 1989;86:603–608.
288. Nelson TR, Charonis AS, McIvor RS, et al. Identification of a cDNA encoding tubulointerstitial nephritis antigen. *J Biol Chem* 1995;270:16265–16270.
289. Xie P, Kondeti VK, Lin S, et al. Role of extracellular matrix renal tubulo-interstitial nephritis antigen (TINag) in cell survival utilizing integrin (alpha)vbeta3/focal adhesion kinase (FAK)/phosphatidylinositol 3-kinase (PI3K)/protein kinase B-serine/threonine kinase (AKT) signaling pathway. *J Biol Chem* 2011;286(39):34131–34146.
290. Bergstein J, Litman N. Interstitial nephritis with anti-tubular-basement-membrane antibody. *N Engl J Med* 1975;292:875–878.
291. Rakotoarivony J, Orfila C, Segonds A, et al. Human and experimental nephropathies associated with antibodies to tubular basement membrane. *Adv Nephrol Necker Hosp* 1981;10:187–212.
292. Freycon MT, Gilly J, Bouvier B, Braye A. Familial chronic tubulointerstitial nephritis with antibodies to the tubular basement membrane. *Pediatrics* 1982;37:371–381.
293. Helczynski L, Landing BH. Tubulointerstitial renal diseases of children: Pathologic features and pathogenetic mechanisms in Fanconi's familial nephronophthisis, antitubular basement membrane antibody disease, and medullary cyst disease. *Pediatr Pathol* 1984;2:1–24.
294. Kalluri R, Wilson CB, Weber M, et al. Identification of the alpha 3 chain of type IV collagen as the common autoantigen in ant basement membrane disease and goodpasture syndrome. *J Am Soc Nephrol* 1995;6:1178–1185.
295. Andres G, Brentjens J, Kohli R, et al. Histology of human tubulointerstitial nephritis associated with antibodies to renal basement membranes. *Kidney Int* 1978;13:480–491.
296. Graindorge PP, Mahieu PR. Radioimmunologic method for detection of antitubular basement membrane antibodies. *Kidney Int* 1978;14(6):594–606.
297. Border WA, Baehler RW, Bhatena D, et al. IgA ant basement membrane nephritis with pulmonary hemorrhage. *Ann Intern Med* 1979;91:21–25.
298. Levy M, Guesry P, Loirat C, et al. Immunologically mediated tubulointerstitial nephritis in children. *Contrib Nephrol* 1979;16:132–140.
299. Katz A, Fish AJ, Santamaria P, et al. Role of antibodies to tubulointerstitial nephritis antigen in human anti-tubular basement membrane nephritis associated with membranous nephropathy. *Am J Med* 1992;93:691–698.
300. Makker S, Widstrom R, Huang J. Characterization of glomerular antigen of membranous nephropathy (MN) in the syndrome of MN, tubulointerstitial nephritis (TN) and Fanconi syndrome. *J Am Soc Nephrol* 1995;6:925.
301. Tay AH, Ren EC, Murugasu B, et al. Membranous nephropathy with anti-tubular basement membrane antibody may be X-linked. *Pediatr Nephrol* 2000;14:747–753.
302. Kerjaschki D, Farquhar MG. Immunocytochemical localization of the Heymann nephritis antigen (GP330) in glomerular epithelial cells of normal Lewis rats. *J Exp Med* 1983;157:667–686.
303. Ivanyi B, Haszon I, Endreffy E, et al. Childhood membranous nephropathy, circulating antibodies to the 58-kD TIN antigen, and anti-tubular basement membrane nephritis: An 11-year follow-up. *Am J Kidney Dis* 1998;32:1068–1074.
304. Rotellar C, Noel LH, Droz D, et al. Role of antibodies directed against tubular basement membranes in human renal transplantation. *Am J Kidney Dis* 1986;7:157–161.
305. Wilson CB, Lehman DH, McCoy RC, et al. Antitubular basement membrane antibodies after renal transplantation. *Transplantation* 1974;18:447–452.
306. Morel-Maroger L, Kourilsky O, Mignon F, et al. Antitubular basement membrane antibodies in rapidly progressive poststreptococcal glomerulonephritis: Report of a case. *Clin Immunol Immunopathol* 1974;2:185–194.
307. Makker SP. Tubular basement membrane antibody-induced interstitial nephritis in systemic lupus erythematosus. *Am J Med* 1980;69:949–952.
308. Clayman MD, Michaud L, Brentjens J, et al. Isolation of the target antigen of human anti-tubular basement membrane antibody-associated interstitial nephritis. *J Clin Invest* 1986;77:1143–1147.
309. Yoshioka K, Morimoto Y, Iseki T, et al. Characterization of tubular basement membrane antigens in human kidney. *J Immunol* 1986;136:1654–1660.
310. Crary GS, Katz A, Fish AJ, et al. Role of a basement membrane glycoprotein in anti-tubular basement membrane nephritis. *Kidney Int* 1993;43:140–146.
311. Yoshioka K, Hino S, Takemura T, et al. Isolation and characterization of the tubular basement membrane antigen associated with human tubulointerstitial nephritis. *Clin Exp Immunol* 1992;90:319–325.
312. Miyazato H, Yoshioka K, Hino S, et al. The target antigen of antitubular basement membrane antibody-mediated interstitial nephritis. *Autoimmunity* 1994;18:259–265.
313. Kalfa TA, Thull JD, Butkowski RJ, et al. Tubulointerstitial nephritis antigen interacts with laminin and type IV collagen and promotes cell adhesion. *J Biol Chem* 1994;269:1654–1659.
314. Chen Y, Krishnamurti U, Wayner EA, et al. Receptors in proximal tubular epithelial cells for tubulointerstitial nephritis antigen. *Kidney Int* 1996;49:153–157.
315. Kanwar YS, Kumar A, Yang Q, et al. Tubulointerstitial nephritis antigen: an extracellular matrix protein that selectively regulates tubulogenesis vs. glomerulogenesis during mammalian renal development. *Proc Natl Acad Sci U S A* 1999;96:11323–11328.
316. Yoshioka K, Takemura T, Hattori S. Tubulointerstitial nephritis antigen: primary structure, expression and role in health and disease. *Nephron* 2002;90:1–7. doi: 10.1159/000046307.

317. Sugimoto K, Takemura Y, Yanagida H, et al. Renal tubular dysgenesis and tubulointerstitial nephritis antigen in juvenile nephrophtthisis. *Nephrology (Carlton)* 2011;16(5):495–501. doi: 10.1111/j.1440-1737.2011.01442.x.
318. Zhou B, Nelson TR, Kashtan C, et al. Identification of two alternatively spliced forms of human tubulointerstitial nephritis antigen (TIN-Ag). *J Am Soc Nephrol* 2000;11(4):658–668.
319. Xie P, Sun L, Nayak B, et al. C/EBP-beta modulates transcription of tubulointerstitial nephritis antigen in obstructive uropathy. *J Am Soc Nephrol* 2009;20(4):807–819.
320. Yoshioka K, Kleppel M, Fish AJ. Analysis of nephritogenic antigens in human glomerular basement membrane by two-dimensional gel electrophoresis. *J Immunol* 1985;134:3831–3837.
321. Kashtan C, Fish AJ, Kleppel M, et al. Nephritogenic antigen determinants in epidermal and renal basement membranes of kindreds with Alport-type familial nephritis. *J Clin Invest* 1986;78:1035–1044.
322. Hatanaka Y, Yuzawa Y, Nishikawa K, et al. Role of a rat membrane inhibitor of complement in anti-basement membrane antibody-induced renal injury. *Kidney Int* 1995;48:1728–1737.
323. Ellis D, Fisher SE, Smith WI Jr, et al. Familial occurrence of renal and intestinal disease associated with tissue autoantibodies. *Am J Dis Child* 1982;136:323–326.
324. Hyun J, Galen MA. Acute interstitial nephritis. A case characterized by increase in serum IgG, IgM, and IgE concentrations, eosinophilia, and IgE deposition in renal tubules. *Arch Intern Med* 1981;141:679–681.
325. Tokumoto M, Fukuda K, Shinozaki M, et al. Acute interstitial nephritis with immune complex deposition and MHC class II antigen presentation along the tubular basement membrane. *Nephrol Dial Transplant* 1999;14:2210–2215.
326. Takeda S, Haratake J, Kasai T, et al. IgG4-associated idiopathic tubulointerstitial nephritis complicating autoimmune pancreatitis. *Nephrol Dial Transplant* 2004;19:474–476.
327. Markowitz GS, Fine PL, Kunis CL, et al. Polyclonal immunoglobulin G deposition disease: a unique entity. *Am J Kidney Dis* 1998;32:328–333.
328. Sarles H, Sarles JC, Muratore R, et al. Chronic inflammatory sclerosis of the pancreas—an autonomous pancreatic disease? *Am J Dig Dis* 1961;6:688–698.
329. Hamano H, Kawa S, Horiuchi A, et al. High serum IgG4 concentrations in patients with sclerosing pancreatitis. *N Engl J Med* 2001;344(10):732–738.
330. Hamano H, Kawa S, Ochi Y, et al. Hydronephrosis associated with retroperitoneal fibrosis and sclerosing pancreatitis. *Lancet* 2002;359(9315):1403–1404.
331. Uchida K, Satoi S, Miyoshi H, et al. Inflammatory pseudotumors of the pancreas and liver with infiltration of IgG4-positive plasma cells. *Intern Med* 2007;46(17):1409–1412.
332. Yamada K, Kawano M, Inoue R, et al. Clonal relationship between infiltrating immunoglobulin G4 (IgG4)-positive plasma cells in lacrimal glands and circulating IgG4-positive lymphocytes in Mikulicz's disease. *Clin Exp Immunol* 2008;152(3):432–439.
333. Taguchi M, Aridome G, Abe S, et al. Autoimmune pancreatitis with IgG4-positive plasma cell infiltration in salivary glands and biliary tract. *World J Gastroenterol* 2005;11(35):5577–5581.
334. Zen Y, Kitagawa S, Minato H, et al. IgG4-positive plasma cells in inflammatory pseudotumor (plasma cell granuloma) of the lung. *Hum Pathol* 2005;36(7):710–717.
335. Sprangers B, Lioen P, Meijers B, et al. The many faces of Merlin: IgG4-associated pulmonary-renal disease. *Chest* 2011;140(3):791–794.
336. Chetty R, Serra S, Gauchotte G, et al. Sclerosing nodular lesions of the gastrointestinal tract containing large numbers of IgG4 plasma cells. *Pathology* 2011;43(1):31–35.
337. Zen Y, Kasahara Y, Horita K, et al. Inflammatory pseudotumor of the breast in a patient with a high serum IgG4 level: Histologic similarity to sclerosing pancreatitis. *Am J Surg Pathol* 2005;29(2):275–278.
338. Lee LY, Chen TC, Kuo TT. Simultaneous occurrence of IgG4-related chronic sclerosing dacryoadenitis and chronic sclerosing sialadenitis associated with lymph node involvement and Warthin's tumor. *Int J Surg Pathol* 2011;19(3):369–372.
339. Kamisawa T, Nakajima H, Egawa N, et al. IgG4-related sclerosing disease incorporating sclerosing pancreatitis, cholangitis, sialadenitis and retroperitoneal fibrosis with lymphadenopathy. *Pancreatology* 2006;6(1–2):132–137.
340. Zen Y, Sawazaki A, Miyayama S, et al. A case of retroperitoneal and mediastinal fibrosis exhibiting elevated levels of IgG4 in the absence of sclerosing pancreatitis (autoimmune pancreatitis). *Hum Pathol* 2006;37(2):239–243.
341. Takahashi H, Yamamoto M, Suzuki C, et al. The birthday of a new syndrome: IgG4-related diseases constitute a clinical entity. *Autoimmun Rev* 2010;9(9):591–594.
342. Umehara H, Okazaki K, Masaki Y, et al. Comprehensive diagnostic criteria for IgG4-related disease (IgG4-RD), 2011. *Mod Rheumatol* 2012;22(1):21–30.
343. Umehara H, Okazaki K, Masaki Y, et al.; The Research Program for Intractable Disease by Ministry of Health, Labor and Welfare (MHLW) Japan G4 team. A novel clinical entity, IgG4-related disease (IgG4RD): general concept and details. *Mod Rheumatol* 2012;22:1–14.
344. Cornell LD. IgG4-related tubulointerstitial nephritis. *Kidney Int* 2010;78(10):951–953.
345. Otsuki M, Chung JB, Okazaki K, et al.; Research Committee of Intractable Pancreatic Diseases provided by the Ministry of Health, Labour and Welfare of Japan and the Korean Society of Pancreatobiliary Diseases. Asian diagnostic criteria for autoimmune pancreatitis: consensus of the Japan-Korea Symposium on Autoimmune Pancreatitis. *J Gastroenterol* 2008;43(6):403–408.
346. Kawano M, Saeki T, Nakashima H, et al. Proposal for diagnostic criteria for IgG4-related kidney disease. *Clin Exp Nephrol* 2011;15(5):615–626.
347. Yamaguchi Y, Kanetsuna Y, Honda K, et al.; on behalf of the Japanese study group on IgG4-related nephropathy. Characteristic tubulointerstitial nephritis in IgG4-related disease. *Hum Pathol* 2012;43(4):536–549.
348. Houghton DC, Troxell ML. An abundance of IgG4+ plasma cells is not specific for IgG4-related tubulointerstitial nephritis. *Mod Pathol* 2011;24(11):1480–1487.
349. Fervenza FC, Downer G, Beck LH Jr, et al. IgG4-related tubulointerstitial nephritis with membranous nephropathy. *Am J Kidney Dis* 2011;58(2):320–324.
350. Cravedi P, Abbate M, Gagliardini E, et al. Membranous nephropathy associated with IgG4-related disease. *Am J Kidney Dis* 2011;58(2):272–275.
351. Beck LH Jr, Salant DJ. Membranous nephropathy: Recent travels and new roads ahead. *Kidney Int* 2010;77(9):765–770.
352. Kearney N, Podolak J, Matsumura L, et al. Patterns of IgG subclass deposits in membranous glomerulonephritis in renal allografts. *Transplant Proc* 2011;43(10):3743–3746.
353. Divatia M, Kim SA, Ro JY. IgG4-related sclerosing disease, an emerging entity: A review of a multi-system disease. *Yonsei Med J* 2012;53(1):15–34.
354. Deshpande V, Chicano S, Finkelberg D, et al. Autoimmune pancreatitis: a systemic immune complex mediated disease. *Am J Surg Pathol* 2006;30(12):1537–1545.
355. Aalberse RC, Stapel SO, Schuurman J, et al. Immunoglobulin G4: An odd antibody. *Clin Exp Allergy* 2009;39(4):469–477.
356. Rispens T, Ooijevaar-de Heer P, Bende O, et al. Mechanism of immunoglobulin G4 Fab-arm exchange. *J Am Chem Soc* 2011;133(26):10302–10311.
357. Kountouras J, Deretzi G, Zavos C, et al. Association between *Helicobacter pylori* infection and acute inflammatory demyelinating polyradiculoneuropathy. *Eur J Neurol* 2005;12(2):139–143.
358. Guarneri F, Guarneri C, Benvenga S. *Helicobacter pylori* and autoimmune pancreatitis: Role of carbonic anhydrase via molecular mimicry? *J Cell Mol Med* 2005;9(3):741–744.
359. Frulloni L, Lunardi C, Simone R, et al. Identification of a novel antibody associated with autoimmune pancreatitis. *N Engl J Med* 2009;361(22):2135–2142.
360. Okazaki K, Uchida K, Fukui T. Recent advances in autoimmune pancreatitis: concept, diagnosis, and pathogenesis. *J Gastroenterol* 2008;43(6):409–418.
361. Yamamoto M, Naishiro Y, Suzuki C, et al. Proteomics analysis in 28 patients with systemic IgG4-related plasmacytic syndrome. *Rheumatol Int* 2010;30(4):565–568.
362. Akitake R, Watanabe T, Zaima C, et al. Possible involvement of T helper type 2 responses to Toll-like receptor ligands in IgG4-related sclerosing disease. *Gut* 2010;59(4):542–545.

363. Kawa S, Ota M, Yoshizawa K, et al. HLA DRB10405-DQB10401 haplotype is associated with autoimmune pancreatitis in the Japanese population. *Gastroenterology* 2002;122(5):1264–1269.
364. Park do H, Kim MH, Oh HB, et al. Substitution of aspartic acid at position 57 of the DQbeta1 affects relapse of autoimmune pancreatitis. *Gastroenterology* 2008;134(2):440–446.
365. Kim TY, Park KS, Choi JS, et al. Comparative clinical manifestations of IgG4-related and IgG4-negative primary tubulointerstitial nephritis. *Clin Nephrol* 2011;76(6):440–446.
366. Brentjens JR, Sepulveda M, Baliah T, et al. Interstitial immune complex nephritis in patients with systemic lupus erythematosus. *Kidney Int* 1975;7:342–350.
367. Park MH, D'Agati V, Appel GB, et al. Tubulointerstitial disease in lupus nephritis: Relationship to immune deposits, interstitial inflammation, glomerular changes, renal function, and prognosis. *Nephron* 1986;44:309–319.
368. Schwartz MM, Fennell JS, Lewis EJ. Pathologic changes in the renal tubule in systemic lupus erythematosus. *Hum Pathol* 1982;13:534–547.
369. Biesecker G, Katz S, Koffler D. Renal localization of the membrane attack complex in systemic lupus erythematosus nephritis. *J Exp Med* 1981;154:1779–1794.
370. Chang A, Henderson SG, Brandt D, et al. In situ B cell-mediated immune responses and tubulointerstitial inflammation in human lupus nephritis. *J Immunol* 2011;186(3):1849–1860.
371. Pijpe J, Vissink A, Van der Wal JE, et al. Interstitial nephritis with infiltration of IgG-kappa positive plasma cells in a patient with Sjögren's syndrome. *Rheumatology (Oxford)* 2004;43:108–110.
372. Wisnieski JJ, Baer AN, Christensen J, et al. Hypocomplementemic urticarial vasculitis syndrome. Clinical and serologic findings in 18 patients. *Medicine (Baltimore)* 1995;74(1):24–41.
373. Buck A, Christensen J, McCarty M. Hypocomplementemic urticarial vasculitis syndrome: A case report and literature review. *J Clin Aesthet Dermatol* 2012;5(1):36–46.
374. Matsutani H, Mizusawa J, Shimoda M, et al. Severe glomerulonephritis and tubulo-interstitial nephritis accompanied with urticaria and vasculitis. *Child Nephrol Urol* 1990;10(4):214–217.
375. Toprak O, Cirit M, Uzunel H, et al. Hypocomplementaemic urticarial vasculitis syndrome and acute renal failure with cryoglobulin (-) hepatitis C infection. *Nephrol Dial Transplant* 2004;19(10):2680–2682.
376. Wakamatsu R, Watanabe H, Suzuki K, et al. Hypocomplementemic urticarial vasculitis syndrome is associated with high levels of serum IgG4: A clinical manifestation that mimics IgG4-related disease. *Intern Med* 2011;50(10):1109–1012.
377. Chang A, Peutz-Kootstra CJ, Kowalewska J, et al. Giant cell tubulitis with tubular basement membrane immune deposits: A report of two cases after cardiac valve replacement surgery. *Clin J Am Soc Nephrol* 2006;1(5):920–924.
378. Hodgins JB, Whelan J, Markowitz GS, et al. Giant cell tubulitis with immune complex deposits in a patient with lupus nephritis. *Am J Kidney Dis* 2009;53(3):513–517.
379. Lee L, Sevastos J, Rainer S, et al. Giant cell tubulitis and tubular basement membrane immune deposits. *Pathology* 2011;43(4):383–386.
380. Ohsawa I, Ohi H, Fujita T, et al. Glomerular and extraglomerular immune complex deposits in a bone marrow transplant recipient. *Am J Kidney Dis* 2000;36:E3.
381. Adeyi OA, Sethi S, Rennke HG. Fibrillary glomerulonephritis: A report of 2 cases with extensive glomerular and tubular deposits. *Hum Pathol* 2001;32:660–663.
382. Hoyer JR. Tubulointerstitial immune complex nephritis in rats immunized with Tamm-Horsfall protein. *Kidney Int* 1980;17:284–292.
383. Fasth A, Hoyer JR, Seiler MW. Renal tubular immune complex formation in mice immunized with Tamm-Horsfall protein. *Am J Pathol* 1986;125:555–562.
384. Seiler MW, Hoyer JR. Ultrastructural studies of tubulointerstitial immune complex nephritis in rats immunized with Tamm-Horsfall protein. *Lab Invest* 1981;45:321–327.
385. Fasth AL, Hoyer JR, Seiler MW. Extratubular Tamm-Horsfall protein deposits induced by ureteral obstruction in mice. *Clin Immunol Immunopathol* 1988;47:47–61.
386. Benkovic J, Jelakovic B, Cikes N. Antibodies to Tamm-Horsfall protein in patients with acute pyelonephritis. *Eur J Clin Chem Clin Biochem* 1994;32:337–340.
387. Fasth A, Ahlstedt S, Hanson LA, et al. Cross-reactions between the Tamm-Horsfall glycoprotein and *Escherichia coli*. *Int Arch Allergy Appl Immunol* 1980;63:303–311.
388. Faaber P, Rijke TP, van de Putte LB, et al. Cross-reactivity of human and murine anti-DNA antibodies with heparan sulfate. The major glycosaminoglycan in glomerular basement membranes. *J Clin Invest* 1986;77:1824–1830.
389. Thomas DB, Davies M, Williams JD. Tamm-Horsfall protein: An aetiological agent in tubulointerstitial disease? *Exp Nephrol* 1993;1:281–284.
390. El-Achkar TM, Workup XR. Uromodulin in kidney injury: An instigator, bystander, or protector? *Am J Kidney Dis* 2012;59(3):452–461. [Epub 2012 Jan 23]
391. Koffler D, Schur PH, Kunkel HG. Immunological studies concerning the nephritis of systemic lupus erythematosus. *J Exp Med* 1967;126:607–624.
392. Tax WJ, Kramers C, van Bruggen MC, et al. Apoptosis, nucleosomes, and nephritis in systemic lupus erythematosus. *Kidney Int* 1995;48:666–673.
393. Nath KA, Hostetter MK, Hostetter TH. Pathophysiology of chronic tubulo-interstitial disease in rats. Interactions of dietary acid load, ammonia, and complement component C3. *J Clin Invest* 1985;76:667–675.
394. Dobrin RS, Vernier RL, Fish AL. Acute eosinophilic interstitial nephritis and renal failure with bone marrow-lymph node granulomas and anterior uveitis. A new syndrome. *Am J Med* 1975;59:325–333.
395. Howarth L, Gilbert RD, Bass P, et al. Tubulointerstitial nephritis and uveitis in monozygotic twin boys. *Pediatr Nephrol* 2004;19:917–919.
396. Mackensen F, Billing H. Tubulointerstitial nephritis and uveitis syndrome. *Curr Opin Ophthalmol* 2009;20(6):525–531.
397. Thomassen VH, Ring T, Thaarup J, et al. Tubulointerstitial nephritis and uveitis (TINU) syndrome: A case report and review of the literature. *Acta Ophthalmol* 2009;87(6):676–679.
398. Liakopoulos V, Ioannidis I, Zengos N, et al. Tubulointerstitial nephritis and uveitis (TINU) syndrome in a 52-year-old female: A case report and review of the literature. *Ren Fail* 2006;28(4):355–359.
399. Weinstein O, Tovbin D, Rogachev B, et al. Clinical manifestations of adult tubulointerstitial nephritis and uveitis (TINU) syndrome. *Int Ophthalmol* 2010;30(5):621–628.
400. Yasuda K, Sasaki K, Yamato M, et al. Tubulointerstitial nephritis and uveitis syndrome with transient hyperthyroidism in an elderly patient. *Clin Exp Nephrol* 2011;15(6):927–932.
401. Morino M, Inami K, Kobayashi T, et al. Acute tubulointerstitial nephritis in two siblings and concomitant uveitis in one. *Acta Paediatr Jpn* 1991;33:93–98.
402. Koike K, Lida S, Usui M, et al. Adult-onset acute tubulointerstitial nephritis and uveitis with Fanconi syndrome. Case report and review of the literature. *Clin Nephrol* 2007;67(4):255–259.
403. Yao YH, Lin CC, Chung YM, et al. Tubulointerstitial nephritis and uveitis syndrome (TINU) with Fanconi's syndrome. *Clin Nephrol* 2011;75(Suppl 1):75–78.
- 403a. Li C, Su T, Chu R, Li X, Yang L. Tubulointerstitial nephritis with uveitis in Chinese adults. *Clin J Am Soc Nephrol* 2014;9(1):21–28.
404. Hirano K, Tomino Y, Mikami H, et al. A case of acute tubulointerstitial nephritis and uveitis syndrome with a dramatic response to corticosteroid therapy. *Am J Nephrol* 1989;9:499–503.
405. Yoshioka K, Takemura T, Kanasaki M, et al. Acute interstitial nephritis and uveitis syndrome: Activated immune cell infiltration in the kidney. *Pediatr Nephrol* 1991;5:232–234.
406. Yanagihara T, Kitamura H, Aki K, et al. Serial renal biopsies in three girls with tubulointerstitial nephritis and uveitis syndrome. *Pediatr Nephrol* 2009;24(6):1159–1164.
407. Burnier M, Jaeger P, Campiche M, et al. Idiopathic acute interstitial nephritis and uveitis in the adult. Report of 1 case and review of the literature. *Am J Nephrol* 1986;6:312–315.
408. Houghton D, Troxell M, Fox E, et al. TINU (tubulointerstitial nephritis and uveitis) syndrome is not usually associated with IgG4 sclerosing disease. *Am J Kidney Dis* 2012;59(4):582–589.
409. Kikkawa Y, Sakurai M, Mano T, et al. Interstitial nephritis with concomitant uveitis. Report of two cases. *Contrib Nephrol* 1975;4:1–11.

410. Wakaki H, Sakamoto H, Awazu M. Tubulointerstitial nephritis and uveitis syndrome with autoantibody directed to renal tubular cells. *Pediatrics* 2001;107:1443–1446.
411. Gianviti A, Greco M, Barsotti P, et al. Acute tubulointerstitial nephritis occurring with 1-year lapse in identical twins. *Pediatr Nephrol* 1994;8:427–430.
412. Dusek J, Urbanova I, Stejskal J, et al. Tubulointerstitial nephritis and uveitis syndrome in a mother and her son. *Pediatr Nephrol* 2008;23(11):2091–2093.
413. Biester S, Müller C, Deuter CM, et al. Tubulointerstitial nephritis and uveitis in siblings. *Ocul Immunol Inflamm* 2010;18(5):370–372.
414. Mackensen F, David F, Schwenger V, et al. HLA-DRB1*0102 is associated with TINU syndrome and bilateral, sudden-onset anterior uveitis but not with interstitial nephritis alone. *Br J Ophthalmol* 2011;95(7):971–975.
415. Onyekpe I, Shenoy M, Denley H, et al. Recurrent tubulointerstitial nephritis and uveitis syndrome in a renal transplant recipient. *Nephrol Dial Transplant* 2011;26(9):3060–3062.
416. Abed L, Merouani A, Haddad E, et al. Presence of autoantibodies against tubular and uveal cells in a patient with tubulointerstitial nephritis and uveitis (TINU) syndrome. *Nephrol Dial Transplant* 2008;23(4):1452–1455.
417. Tan Y, Yu F, Qu Z, et al. Modified C-reactive protein might be a target autoantigen of TINU syndrome. *Clin J Am Soc Nephrol* 2011;6(1):93–100.
418. Suzuki H, Yoshioka K, Miyano M, et al. Tubulointerstitial nephritis and uveitis (TINU) syndrome caused by the Chinese herb "Goreisan". *Clin Exp Nephrol* 2009;13(1):73–76.
419. Ricker W, Clark M. Sarcoidosis: A clinicopathologic review of 300 cases including 22 autopsies. *Am J Clin Pathol* 1949;19:725.
420. Richmond JM, Chambers B, D'Apice AJ, et al. Renal disease and sarcoidosis. *Med J Aust* 1981;2:36–37.
421. Longcope WT, Freiman DG. A study of sarcoidosis; based on a combined investigation of 160 cases including 30 autopsies from the Johns Hopkins Hospital and Massachusetts General Hospital. *Medicine (Baltimore)* 1952;31:1–132.
422. Bergner R, Hoffmann M, Waldherr R, et al. Frequency of kidney disease in chronic sarcoidosis. *Sarcoidosis Vasc Diffuse Lung Dis* 2003;20:126–132.
423. Gobel U, Ketzritz R, Schneider W, et al. The protean face of renal sarcoidosis. *J Am Soc Nephrol* 2001;12:616–623.
424. Nagaraja P, Davies MR. Granulomatous interstitial nephritis causing acute renal failure: A rare presenting feature of sarcoidosis. *QJM* 2011. [Epub ahead of print]
425. Agrawal V, Crisi GM, D'Agati VD, et al. Renal sarcoidosis presenting as acute kidney injury with granulomatous interstitial nephritis and vasculitis. *Am J Kidney Dis* 2012;59(2):303–308.
426. Pastor E, Arriero JM, Gutiérrez AI, et al. Renal failure as first manifestation of familial sarcoidosis. *Eur Respir J* 2010;36(6):1485–1487.
427. Shah R, Shidham G, Agarwal A, et al. Diagnostic utility of kidney biopsy in patients with sarcoidosis and acute kidney injury. *Int J Nephrol Renovasc Dis* 2011;4:131–136.
428. Mitome J, Kawaguchi Y, Arase S, et al. A case of renal sarcoidosis: A special reference to calcium metabolism as a diagnostic and the therapeutic implications. *Clin Exp Nephrol* 2004;8(4):375–379.
429. Ito Y, Suzuki T, Mizuno M, et al. A case of renal sarcoidosis showing central necrosis and abnormal expression of angiotensin converting enzyme in the granuloma. *Clin Nephrol* 1994;42:331–336.
430. Farge D, Liote F, Turner M, et al. Granulomatous nephritis and chronic renal failure in sarcoidosis. Long-term follow-up studies in two patients. *Am J Nephrol* 1986;6:21–27.
431. Rajakarari R, Sharples EJ, Raftery MJ, et al. Sarcoid tubulo-interstitial nephritis: Long-term outcome and response to corticosteroid therapy. *Kidney Int* 2006;70(1):165–169.
432. Kukura S, Viklicky O, Lácha J, et al. Recurrence of sarcoidosis in renal allograft during pregnancy. *Nephrol Dial Transplant* 2004;19(6):1640–1642.
433. Vargas F, Gedalia A, Craver RD, et al. Recurrence of granulomatous interstitial nephritis in transplanted kidney. *Pediatr Transplant* 2010;14(5):e54–e57.
434. Mignon F, Mery JP, Mougenot B, et al. Granulomatous interstitial nephritis. *Adv Nephrol Necker Hosp* 1984;13:219–245.
435. Fauci AS, Wolff SM. Wegener's granulomatosis: studies in eighteen patients and a review of the literature 1973. *Medicine (Baltimore)* 1994;73:315–324.
436. Thumfart J, Muller D, Rudolph B, et al. Isolated sarcoid granulomatous interstitial nephritis responding to infliximab therapy. *Am J Kidney Dis* 2005;45:411–414.
437. Pichler R, Giachelli C, Young B, et al. The pathogenesis of tubulointerstitial disease associated with glomerulonephritis: The glomerular cytokine theory. *Miner Electrolyte Metab* 1995;21:317–327.
438. Strutz F, Neilson EG. The role of lymphocytes in the progression of interstitial disease. *Kidney Int Suppl* 1994;45:S106–S110.
439. Dodd S. The pathogenesis of tubulointerstitial disease and mechanisms of fibrosis. *Curr Top Pathol* 1995;88:51–67.
440. Tanaka T, Nangaku M. Pathogenesis of tubular interstitial nephritis. *Contrib Nephrol* 2011;169:297–310.
441. Higgins DF, Kimura K, Iwano M, et al. Hypoxia-inducible factor signaling in the development of tissue fibrosis. *Cell Cycle* 2008;7(9):1128–1132.
442. Rodríguez-Iturbe B, García García G. The role of tubulointerstitial inflammation in the progression of chronic renal failure. *Nephron Clin Pract* 2010;116(2):c81–c88.
443. Roy-Chaudhury P, Wu B, King G, et al. Adhesion molecule interactions in human glomerulonephritis: Importance of the tubulointerstitium. *Kidney Int* 1996;49:127–134.
444. Kliem V, Johnson RJ, Alpers CE, et al. Mechanisms involved in the pathogenesis of tubulointerstitial fibrosis in 5/6-nephrectomized rats. *Kidney Int* 1996;49:666–678.
445. Boucher A, Droz D, Adafer E, et al. Characterization of mononuclear cell subsets in renal cellular interstitial infiltrates. *Kidney Int* 1986;29:1043–1049.
446. Neilson EG. The nephritogenic T lymphocyte response in interstitial nephritis. *Semin Nephrol* 1993;13:496–502.
447. McCluskey RT, Bhan AK. Cell-mediated immunity in renal disease. *Hum Pathol* 1986;17:146–153.
448. Rubin-Kelley VE, Jevnikar AM. Antigen presentation by renal tubular epithelial cells. *J Am Soc Nephrol* 1991;2:13–26.
449. Haas C, Ryffel B, Aguet M, et al. MHC antigens in interferon gamma (IFN gamma) receptor deficient mice: IFN gamma-dependent up-regulation of MHC class II in renal tubules. *Kidney Int* 1995;48:1721–1727.
450. Unanue ER, Allen PM. The basis for the immunoregulatory role of macrophages and other accessory cells. *Science* 1987;236:551–557.
451. Kelley VR, Singer GG. The antigen presentation function of renal tubular epithelial cells. *Exp Nephrol* 1993;1:102–111.
452. Postlethwaite A, Seyfer J, Kang A. Chemotactic attraction of human fibroblasts to type I, II, III collagens and collagen-derived peptides. *Proc Natl Acad Sci* 1978;75:871.
453. Tang WW, Ulich TR, Lacey DL, et al. Platelet-derived growth factor-BB induces renal tubulointerstitial myofibroblast formation and tubulointerstitial fibrosis. *Am J Pathol* 1996;148:1169–1180.
454. Bornstein P, Sage H. Regulation of collagen gene expression. *Prog Nucleic Acid Res Mol Biol* 1989;37:67–106.
455. Lin JL, Lin-Tan DT, Yu CC, et al. Environmental exposure to lead and progressive diabetic nephropathy in patients with type II diabetes. *Kidney Int* 2006;69(11):2049–2056.
456. Newman LS. Occupational illness. *N Engl J Med* 1995;333:1128–1134.
457. Ibels LS, Pollock CA. Lead intoxication. *Med Toxicol* 1986;1:387–410.
458. Borjesson J, Mattsson S. Toxicology; in vivo x-ray fluorescence for the assessment of heavy metal concentrations in man. *Appl Radiat Isot* 1995;46:571–576.
459. Bernard BP, Becker CE. Environmental lead exposure and the kidney. *J Toxicol Clin Toxicol* 1988;26:1–34.
460. Chow KM, Liu ZC, Szeto CC. Lead nephropathy: Early leads from descriptive studies. *Intern Med J* 2006;36(10):678–682.
461. Inglis JA, Henderson DA, Emmerson BT. The pathology and pathogenesis of chronic lead nephropathy occurring in Queensland. *J Pathol* 1978;124:65–76.
462. Goyer RA. Effect of toxic, chemical, and environmental factors on the kidney. *Monogr Pathol* 1979;20:202–217.
463. Yu CC, Lin JL, Lin-Tan DT. Environmental exposure to lead and progression of chronic renal diseases: A four-year prospective longitudinal study. *J Am Soc Nephrol* 2004;15:1016–1022.

464. Weaver VM, Jaar BG, Schwartz BS, et al. Associations among lead dose biomarkers, uric acid, and renal function in Korean lead workers. *Environ Health Perspect* 2005;113:36–42.
465. Moel DI, Sachs HK. Renal function 17 to 23 years after chelation therapy for childhood plumbism. *Kidney Int* 1992;42:1226–1231.
466. Staessen JA, Lauwerys RR, Buchet JP, et al. Impairment of renal function with increasing blood lead concentrations in the general population. The Cadmibel Study Group. *N Engl J Med* 1992;327:151–156.
467. Hong CD, Hanenson IB, Lerner S, et al. Occupational exposure to lead: Effects on renal function. *Kidney Int* 1980;18:489–494.
468. Batuman V. Lead nephropathy, gout, and hypertension. *Am J Med Sci* 1993;305:241–247.
469. Cramer K, Goyer RA, Jagenburg R, et al. Renal ultrastructure, renal function, and parameters of lead toxicity in workers with different periods of lead exposure. *Br J Ind Med* 1974;31:113–127.
470. Garcon G, Leleu B, Zerimech F, et al. Biologic markers of oxidative stress and nephrotoxicity as studied in biomonitoring of adverse effects of occupational exposure to lead and cadmium. *J Occup Environ Med* 2004;46:1180–1186.
471. Hogervorst J, Plusquin M, Vangronsveld J, et al. House dust as possible route of environmental exposure to cadmium and lead in the adult general population. *Environ Res* 2007;103:30–37.
472. Scott R, Aughey E, Fell GS, et al. Cadmium concentrations in human kidneys from the UK. *Hum Toxicol* 1987;6:111–120.
473. Nawrot TS, Staessen JA, Roels HA, et al. Cadmium exposure in the population: From health risks to strategies of prevention. *Biometals* 2010;23(5):769–782.
474. Huang M, Choi SJ, Kim DW, et al. Evaluation of factors associated with cadmium exposure and kidney function in the general population. *Environ Toxicol* 2013;28(10):563–570.
475. Hellstrom L, Elinder CG, Dahlberg B, et al. Cadmium exposure and end-stage renal disease. *Am J Kidney Dis* 2001;38:1001–1008.
476. Johri N, Jacquillet G, Unwin R. Heavy metal poisoning: The effects of cadmium on the kidney. *Biometals* 2010;23(5):783–792.
477. Sato R, Kido T, Honda R, et al. Seventeen-year observation on urinary cadmium and beta2-microglobulin in inhabitants after cessation of cadmium-exposure in Japan. *Bull Environ Contam Toxicol* 2010;84(4):363–367.
478. Horiguchi H, Aoshima K, Oguma E, et al. Latest status of cadmium accumulation and its effects on kidneys, bone, and erythropoiesis in inhabitants of the formerly cadmium-polluted Jinzu River Basin in Toyama, Japan, after restoration of rice paddies. *Int Arch Occup Environ Health* 2010;83(8):953–970.
479. Nogawa K. Biologic indicators of cadmium nephrotoxicity in persons with low-level cadmium exposure. *Environ Health Perspect* 1984;54:163–169.
480. Geiger H, Bahner U, Anderes S, et al. Cadmium and renal hypertension. *J Hum Hypertens* 1989;3:23–27.
481. Navas-Acien A, Tellez-Plaza M, Guallar E, et al. Blood cadmium and lead and chronic kidney disease in US adults: A joint analysis. *Am J Epidemiol* 2009;170:1156–1164.
482. Haswell-Elkins M, Satarug S, O'Rourke P, et al. Striking association between urinary cadmium level and albuminuria among Torres Strait Islander people with diabetes. *Environ Res* 2008;106:379–383.
483. Akesson A, Lundh T, Vahter M, et al. Tubular and glomerular kidney effects in Swedish women with low environmental cadmium exposure. *Environ Health Perspect* 2005;113:1627–1631.
484. Ferraro PM, Bonello M, Frigo AC, et al. Cadmium exposure and kidney stone formation in the general population—an analysis of the National Health and Nutrition Examination Survey III data. *J Endourol* 2011;25(5):875–880.
485. Yasuda M, Miwa A, Kitagawa M. Morphometric studies of renal lesions in Itai-Itai disease: Chronic cadmium nephropathy. *Nephron* 1995;69:14–19.
486. Smith J, Smith J, McCall A. Chronic poisoning from cadmium fume. *J Pathol Bacteriol* 1960;80:287.
487. Kazantzis G, Flynn FV, Spowage JS, et al. Renal tubular malfunction and pulmonary emphysema in cadmium pigment workers. *Q J Med* 1963;32:165–192.
488. Lauwers R, De Wals P. Environmental pollution by cadmium and mortality from renal diseases. *Lancet* 1981;1:383.
489. Roels HA, Lauwerys RR, Buchet JP, et al. In vivo measurement of liver and kidney cadmium in workers exposed to this metal: Its significance with respect to cadmium in blood and urine. *Environ Res* 1981;26:217–240.
490. Gena P, Calamita G, Guggino WB. Cadmium impairs albumin reabsorption by down-regulating megalin and CIC5 channels in renal proximal tubule cells. *Environ Health Perspect* 2010;118(11):1551–1556.
491. Woolfson JP, Heikkila JJ. Examination of cadmium-induced expression of the small heat shock protein gene, hsp30, in *Xenopus laevis* A6 kidney epithelial cells. *Comp Biochem Physiol A Mol Integr Physiol* 2009;152(1):91–99.
492. Yang QL, Yao CL, Wang ZY. Acute temperature and cadmium stress response characterization of small heat shock protein 27 in large yellow croaker, *Larimichthys crocea*. *Comp Biochem Physiol C Toxicol Pharmacol* 2012;155(2):190–197.
493. Liu J, Qu W, Kadiiska MB. Role of oxidative stress in cadmium toxicity and carcinogenesis. *Toxicol Appl Pharmacol* 2009;238(3):209–214.
494. Gobe G, Crane D. Mitochondria, reactive oxygen species and cadmium toxicity in the kidney. *Toxicol Lett* 2010;198(1):49–55.
495. Prozialek WC, Vaidya VS, Liu J, et al. Kidney injury molecule-1 is an early biomarker of cadmium nephrotoxicity. *Kidney Int* 2007;72(8):985–993.
496. Pennemans V, De Winter LM, Munters E, et al. The association between urinary kidney injury molecule 1 and urinary cadmium in elderly during long-term, low-dose cadmium exposure: A pilot study. *Environ Health* 2011;10:77.
497. Tokumoto M, Fujiwara Y, Shimada A, et al. Cadmium toxicity is caused by accumulation of p53 through the down-regulation of Ube2d family genes in vitro and in vivo. *J Toxicol Sci* 2011;36(2):191–200.
498. Borjesson J, Barregard L, Sallsten G, et al. In vivo XRF analysis of mercury: the relation between concentrations in the kidney and the urine. *Phys Med Biol* 1995;40:413–426.
499. Bigazzi PE. Autoimmunity and heavy metals. *Lupus* 1994;3:449–453.
500. Burston J, Darmady EM, Stranack F. Nephrosis due to mercurial diuretics. *Br Med J* 1958;14:1277–1279.
501. Joekes AM, Heptinstall RH, Porter KA. The nephrotic syndrome; a study of renal biopsies in 20 adult patients. *Q J Med* 1958;27:495–516.
502. Preedy JR, Russell DS. Acute salt depletion associated with the nephrotic syndrome developing during treatment with a mercurial diuretic. *Lancet* 1953;265:1181–1184.
503. Mandema E, Arends A, Van Zeijst J, et al. Mercury and the kidney. *Lancet* 1963;1:1266.
504. Grosso A, De Sousa RC. Mercury blockage of apical water channels in toad skin (*Bufo marinus*). *J Physiol* 1993;468:741–752.
505. Stacchiotti A, Ricci F, Rezzani R, et al. Tubular stress proteins and nitric oxide synthase expression in rat kidney exposed to mercuric chloride and melatonin. *J Histochem Cytochem* 2006;54(10):1149–1157.
506. Cramer CR, Hagler HK, Silva FG, et al. Chronic interstitial nephritis associated with gold therapy. *Arch Pathol Lab Med* 1983;107:258–263.
507. Hocher B, Keller F, Krause PH, et al. Interstitial nephritis with reversible renal failure due to a copper-containing intrauterine contraceptive device. *Nephron* 1992;61:111–113.
508. Friedman AC, Lautin EM. Cis-platinum (II) diaminedichloride: another cause of bilateral small kidneys. *Urology* 1980;16:584–586.
509. Leibbrandt ME, Wolfgang GH, Metz AL, et al. Critical subcellular targets of cisplatin and related platinum analogs in rat renal proximal tubule cells. *Kidney Int* 1995;48:761–770.
510. Prasad GV, Rossi NF. Arsenic intoxication associated with tubulointerstitial nephritis. *Am J Kidney Dis* 1995;26:373–376.
511. Petronic VJ, Bukurov NS, Djokic MR, et al. Balkan endemic nephropathy and papillary transitional cell tumors of the renal pelvis and ureters. *Kidney Int Suppl* 1991;34:S77–S79.
512. Patel HV, Kalia K. Sub-chronic arsenic exposure aggravates nephrotoxicity in experimental diabetic rats. *Indian J Exp Biol* 2010;48(7):762–768.
513. Matos RC, Vieira C, Morais S, et al. Nephrotoxicity effects of the wood preservative chromium copper arsenate on mice: Histopathological and quantitative approaches. *J Trace Elem Med Biol* 2009;23(3):224–230.
514. Vicente-Vicente L, Quiros Y, Pérez-Barriocanal F, et al. Nephrotoxicity of uranium: Pathophysiological, diagnostic and therapeutic perspectives. *Toxicol Sci* 2010;118(2):324–347.
515. Kurttio P, Harmoinen A, Saha H, et al. Kidney toxicity of ingested uranium from drinking water. *Am J Kidney Dis* 2006;47:972–982.

516. Kathren RL, Burklin RK. Acute chemical toxicity of uranium. *Health Phys* 2008;94:170–179.
517. Seldén AI, Lundholm C, Edlund B, et al. Nephrotoxicity of uranium in drinking water from private drilled wells. *Environ Res* 2009;109(4):486–494.
518. Thun MJ, Baker DB, Steenland K, et al. Renal toxicity in uranium mill workers. *Scand J Work Environ Health* 1985;11:83–90.
519. Sztajnkrzyer MD, Otten EJ. Chemical and radiological toxicity of depleted uranium. *Mil Med* 2004;169:212–216.
520. Bijlsma JA, Slotje P, Huijink AC, et al. Urinary uranium and kidney function parameters in professional assistance workers in the Epidemiological Study Air Disaster in Amsterdam (ESADA). *Nephrol Dial Transplant* 2008;23(1):249–255.
521. Tolson JK, Roberts SM, Jortner B, et al. Heat shock proteins and acquired resistance to uranium nephrotoxicity. *Toxicology* 2005;206:59–73.
522. Thiébaud C, Carrière M, Milgram S, et al. Uranium induces apoptosis and is genotoxic to normal rat kidney (NRK-52E) proximal cells. *Toxicol Sci* 2007;98(2):479–487.
523. Tissandré E, Guéguen Y, Lobaccaro JM, et al. Enriched uranium affects the expression of vitamin D receptor and retinoid X receptor in rat kidney. *J Steroid Biochem Mol Biol* 2008;110(3–5):263–268.
524. Donnadieu-Claraz M, Bonnehogne M, Dhieux B, et al. Chronic exposure to uranium leads to iron accumulation in rat kidney cells. *Radiat Res* 2007;167(4):454–464.
525. Gullner HG, Gill JR Jr, Bartter FC, et al. A familial disorder with hypokalemic alkalosis, hyperreninemia, aldosteronism, high urinary prostaglandins and normal blood pressure that is not "Bartter's syndrome". *Trans Assoc Am Physicians* 1979;92:175–188.
526. Wallace MR, Bruton D, North A, et al. End-stage renal failure due to familial hypokalaemic interstitial nephritis with identical HLA tissue types. *N Z Med J* 1985;98:5–7.
527. Cremer W, Bock KD. Symptoms and course of chronic hypokalemic nephropathy in man. *Clin Nephrol* 1977;7:112–119.
528. Lelamali K, Khunkitti W, Yenrudi S, et al. Potassium depletion in a healthy North-Eastern Thai population: No association with tubulointerstitial injury. *Nephrology (Carlton)* 2003;8:28–32.
529. Wrong OM, Feest TG, MacIver AG. Immune-related potassium-losing interstitial nephritis: A comparison with distal renal tubular acidosis. *Q J Med* 1993;86:513–534.
530. Rotig A, Goutieres F, Niaudet P, et al. Deletion of mitochondrial DNA in patient with chronic tubulointerstitial nephritis. *J Pediatr* 1995;126:597–601.
531. Zsurka G, Ormos J, Ivanyi B, et al. Mitochondrial mutation as a probable causative factor in familial progressive tubulointerstitial nephritis. *Hum Genet* 1997;99:484–487.
532. Tzen CY, Tsai JD, Wu TY, et al. Tubulointerstitial nephritis associated with a novel mitochondrial point mutation. *Kidney Int* 2001;59:846–854.
533. Kobayashi A, Goto Y, Nagata M, et al. Granular swollen epithelial cells: a histologic and diagnostic marker for mitochondrial nephropathy. *Am J Surg Pathol* 2010;34(2):262–270.
534. Szabolcs MJ, Seigle R, Shanske S, et al. Mitochondrial DNA deletion: a cause of chronic tubulointerstitial nephropathy. *Kidney Int* 1994;45:1388–1396.
535. Peng M, Jarett L, Meade R, et al. Mutant prenyltransferase-like mitochondrial protein (PLMP) and mitochondrial abnormalities in kd/kd mice. *Kidney Int* 2004;66:20–28.
536. Madaio MP, Ahima RS, Meade R, et al. Glomerular and tubular epithelial defects in kd/kd mice lead to progressive renal failure. *Am J Nephrol* 2005;25(6):604–610.
537. Hallman TM, Peng M, Meade R, et al. The mitochondrial and kidney disease phenotypes of kd/kd mice under germfree conditions. *J Autoimmun* 2006;26(1):1–6.
538. Mihatsch MJ, Gudat F, Zollinger HU, et al. Systemic karyomegaly associated with chronic interstitial nephritis. A new disease entity? *Clin Nephrol* 1979;12:54–62.
539. Spoendlin M, Moch H, Brunner F, et al. Karyomegalic interstitial nephritis: further support for a distinct entity and evidence for a genetic defect. *Am J Kidney Dis* 1995;25:242–252.
540. Moch H, Spondlin M, Schmassmann A, et al. Systemic karyomegaly with chronic interstitial nephritis. Discussion of the disease picture based on an autopsy case. *Pathologie* 1994;15:44–48.
541. Hassen W, Abid-Essafi S, Achour A, et al. Karyomegaly of tubular kidney cells in human chronic interstitial nephropathy in Tunisia: Respective role of ochratoxin A and possible genetic predisposition. *Hum Exp Toxicol* 2004;23:339–346.
542. Rossini M, Coventry S, Duff DR, et al. Chronic renal failure and abnormal tubular cells in 2 siblings. *Am J Kidney Dis* 2005;46:982–987.
543. Bhandari S, Kalowski S, Collett P, et al. Karyomegalic nephropathy: An uncommon cause of progressive renal failure. *Nephrol Dial Transplant* 2002;17:1914–1920.
544. Radonic M, Radosevic Z. Clinical features of Balkan endemic nephropathy. *Food Chem Toxicol* 1992;30:189–192.
545. Bukvic D, Jankovic S, Maric I, et al. Today Balkan endemic nephropathy is a disease of the elderly with a good prognosis. *Clin Nephrol* 2009;72(2):105–113.
546. Janković S, Bukvić D, Marinković J, et al. Time trends in Balkan endemic nephropathy incidence in the most affected region in Serbia, 1977–2009: The disease has not yet disappeared. *Nephrol Dial Transplant* 2011;26(10):3171–3176.
547. Cvitković A, Vuković-Lela I, Edwards KL, et al. Could disappearance of endemic (Balkan) nephropathy be expected in forthcoming decades? *Kidney Blood Press Res* 2011;35(3):147–152.
548. Pešić I, Stefanović V, Müller GA, et al. Identification and validation of six proteins as marker for endemic nephropathy. *J Proteomics* 2011;74(10):1994–2007.
549. Cukuranovic R, Ignjatovic I, Visnjic M, et al. Characteristics of upper urothelial carcinoma in an area of Balkan endemic nephropathy in south Serbia. A fifty-year retrospective study. *Tumori* 2010;96(5):674–679.
550. Jelaković B, Karanović S, Vuković-Lela I, et al. Aristolactam-DNA adducts are a biomarker of environmental exposure to aristolochic acid. *Kidney Int* 2012;81(6):559–567.
551. Vukelic M, Sostaric B, Fuchs R. Some pathomorphological features of Balkan endemic nephropathy in Croatia. *IARC Sci Publ* 1991;(115):37–42.
552. Hall PW III, Dammin GJ, Griggs RC, et al. Investigation of chronic endemic nephropathy in Yugoslavia. II. Renal pathology. *Am J Med* 1965;39:210–217.
553. Ferluga D, Hvala A, Vizjak A, et al. Renal function, protein excretion, and pathology of Balkan endemic nephropathy. III. Light and electron microscopic studies. *Kidney Int Suppl* 1991;34:S57–S67.
554. Sostaric B, Vukelic M. Characteristics of urinary tract tumours in the area of Balkan endemic nephropathy in Croatia. *IARC Sci Publ* 1991;(115):29–35.
555. Andonova IE, Sarueva RB, Horvath AD, et al. Balkan endemic nephropathy and genetic variants of glutathione S-transferases. *J Nephrol* 2004;17:390–398.
556. Toncheva DI, Von Ahsen N, Atanasova SY, et al. Identification of NQO1 and GSTs genotype frequencies in Bulgarian patients with Balkan endemic nephropathy. *J Nephrol* 2004;17:384–389.
557. Riquelme C, Escors D, Ortego J, et al. Nature of the virus associated with endemic Balkan nephropathy. *Emerg Infect Dis* 2002;8:869–870.
558. Wedeen RP. Environmental renal disease: lead, cadmium and Balkan endemic nephropathy. *Kidney Int Suppl* 1991;34:S4–S8.
559. Radovanovic Z, Markovic-Denic L, Marinkovic J, et al. Well water characteristics and the Balkan nephropathy. *Nephron* 1991;57:52–54.
560. Batuman V. Possible pathogenetic role of low-molecular-weight proteins in Balkan nephropathy. *Kidney Int Suppl* 1991;34:S89–S92.
561. Vrabcheva T, Petkova-Bocharova T, Grosso F, et al. Analysis of ochratoxin A in foods consumed by inhabitants from an area with Balkan endemic nephropathy: A 1 month follow-up study. *J Agric Food Chem* 2004;52:2404–2410.
562. Krogh P, Axelsen NH, Elling F, et al. Experimental porcine nephropathy. Changes of renal function and structure induced by ochratoxin A-contaminated feed. *Acta Pathol Microbiol Scand [A]* 1974;0(Suppl 246):1–21.
563. Krogh P, Elling F. Letter: Fungal toxins and endemic (Balkan) nephropathy. *Lancet* 1976;2:40.
564. Vanherweghem JL. A new form of nephropathy secondary to the absorption of Chinese herbs. *Bull Mem Acad R Med Belg* 1994;149:128–135; discussion 135–140.
565. Yang HY, Wang JD, Lo TC, et al. Occupational kidney disease among Chinese herbalists exposed to herbs containing aristolochic acids. *Occup Environ Med* 2011;68(4):286–290.

566. Pitt JI. Chinese herbal medicines, aristolochic acid and Balkan endemic nephropathy. *Occup Environ Med* 2011;68(4):237.
567. De Broe ME. Chinese herbs nephropathy and Balkan endemic nephropathy: Toward a single entity, aristolochic acid nephropathy. *Kidney Int* 2012;81(6):513–515.
568. Vanherweghem JL, Depierreux M, Tielemans C, et al. Rapidly progressive interstitial renal fibrosis in young women: association with slimming regimen including Chinese herbs. *Lancet* 1993;341:387–391.
569. Nortier JL, Martinez MC, Schmeiser HH, et al. Urothelial carcinoma associated with the use of a Chinese herb (*Aristolochia fangchi*). *N Engl J Med* 2000;342:1686–1692.
570. Vanhaelen M, Vanhaelen-Fastre R, But P, et al. Identification of aristolochic acid in Chinese herbs. *Lancet* 1994;343:174.
571. Chang C, Wang Y, Yang A, et al. Rapidly progressive interstitial renal fibrosis associated with Chinese herbal drugs. *Am J Nephrol* 2001; 21:441.
572. Tanaka A, Nishida R, Yoshida T, et al. Outbreak of Chinese herb nephropathy in Japan: Are there any differences from Belgium? *Intern Med* 2001;40:296–300.
573. Debelle FD, Vanherweghem JL, Nortier JL. Aristolochic acid nephropathy: a worldwide problem. *Kidney Int* 2008;74(2):158–169.
574. Colin P, Koenig P, Ouzzane A, et al. Environmental factors involved in carcinogenesis of urothelial cell carcinomas of the upper urinary tract. *BJU Int* 2009;104(10):1436–1440.
575. Yang L, Su T, Li XM, et al. Aristolochic acid nephropathy: Variation in presentation and prognosis. *Nephrol Dial Transplant* 2012;27(1):292–298.
576. Lo SH, Wong KS, Arlt VM, et al. Detection of herba aristolochia mollissemiae in a patient with unexplained nephropathy. *Am J Kidney Dis* 2005;45:407–410.
577. Sato N, Takahashi D, Chen SM, et al. Acute nephrotoxicity of aristolochic acids in mice. *J Pharm Pharmacol* 2004;56:221–229.

Ischemic and Toxic Acute Tubular Injury and Other Ischemic Renal Injuries

Acute tubular injury 1167

- Historical background 1168
- Clinical presentation 1170
- Pathology of acute renal failure/Acute tubular injury 1175
- Etiology and pathogenesis 1187
- Differential diagnosis 1200
- Clinical course 1201
- Prognosis 1201
- Therapy 1202

Syndromic acute tubular injury 1203

- Acute renal failure in sepsis 1203
- The hepatorenal syndrome 1203
- Acute renal failure and multiple-organ failure 1204
- Cardiorenal syndromes 1204
- Intra-abdominal hypertension and abdominal compartment syndrome 1205

Renal cortical necrosis 1205

- Gross pathology 1205
- Light microscopy 1206

Infarction of the kidney 1207

- Gross pathology 1207
- Light microscopy 1207
- Venous infarction 1208

Atheroembolic disease of the kidney 1208

ACUTE TUBULAR INJURY

Acute tubular injury (ATI) is a major cause of acute renal failure (ARF), a clinical syndrome characterized by rapid deterioration in renal function and glomerular filtration rate (GFR) over a relatively short period of time, ranging from hours to days. The result is a sudden inability to maintain normal fluid and electrolyte homeostasis. The acute reduction in renal

function can be the result of the impairment of blood flow (so-called prerenal failure), obstruction of the urinary collecting system (so-called postrenal failure), or a variety of intrinsic renal diseases ranging from glomerulonephritis to interstitial nephritis to ATI (Fig. 26.1), which is the primary topic of discussion in this chapter. Based on the available literature, which uses somewhat variable definitions, ARF is commonly encountered in hospitalized patients, has a variety of risk factors and etiologies, and is associated with increased mortality (1). Its frequency ranges from 1% at admission to the hospital to as high as 31% in patients undergoing cardiopulmonary bypass or with other high-risk conditions. Clinical manifestations range from mild increase in serum creatinine (sCr) to anuric renal failure (2). A consensus panel of the American Society of Nephrology recommended that “acute renal failure” be replaced by the term *acute kidney injury* (AKI). The term AKI could be used to distinguish early from more advanced stages of kidney disease, in which there is more overt “failure” of clearance by the kidney. Use of the more general term AKI highlights the predictive value of acute or small changes in sCr and facilitates recognition of renal injury and dysfunction at earlier stages of disease, since even transient rise in creatinine is correlated with increased risk of death (3).

In 2004, a consensus definition was published, which included both GFR and urine output criteria (Table 26.1). The earliest phase, *risk of renal dysfunction*, was defined by an increase in sCr by 1.5 times, GFR decrease of more than 25%, or urine output below 0.5 mL/kg/h for 6 hours. *Renal injury* was defined by sCr increase by 2 times, GFR decrease of more than 50%, or urine output less than 0.5 mL/kg/h for 12 hours. *Renal failure* was defined as sCr increase by three times (or over 4 mg/dL), GFR decrease by 75%, urine output below 0.3 mL/kg/h for 24 hours, or anuria for 12 hours. Added to *loss of function* and *end-stage renal disease*, these comprise the “RIFLE” criteria (4). These criteria appear to be clinically relevant and have been widely used (5). They were modified in 2007 as the AKIN (acute kidney injury) criteria, eliminating the *loss-of-function* and *ESRD* categories (6). AKIN criteria defined AKI as “functional or structural abnormalities or markers of kidney damage including abnormalities in blood, urine or tissue tests or imaging studies present for less than 3 months.” However,

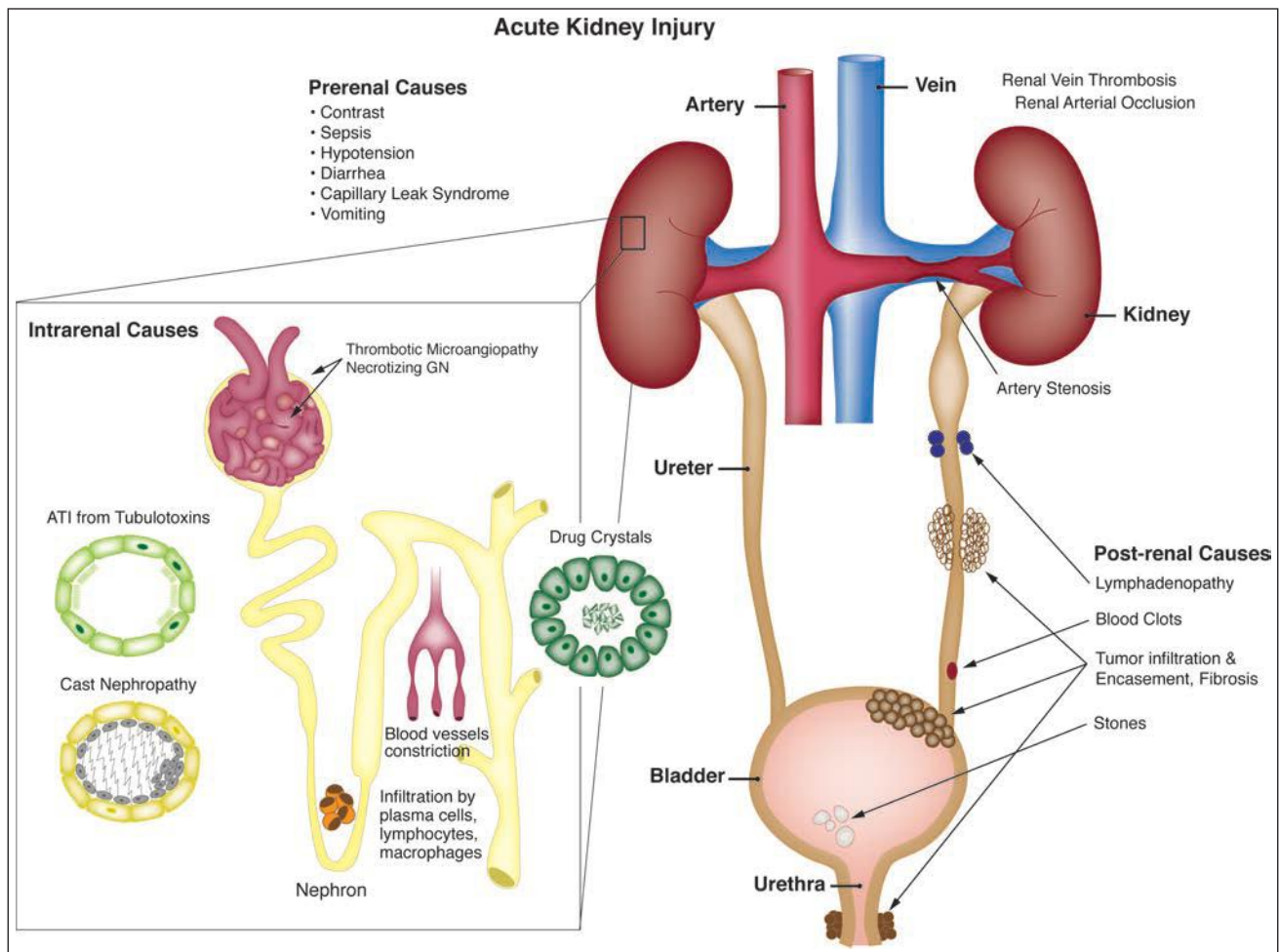


FIGURE 26.1 Causes of acute renal failure. This figure depicts several etiologies that may lead to AKI. Intrarenal causes of tubular injury include tubulotoxins, light chain casts, ischemic injury, and lesions that indirectly affect tubular cell viability through impaired glomerular blood flow (i.e., TMA and necrotizing GN). Other common causes of ATI include drug crystals with associated tubular obstruction, interstitial inflammatory infiltrate by lymphocytes, plasma cells, and macrophages. Prerenal causes include hypotension, diarrhea, vomiting, and contrast. Postrenal causes include lymphadenopathy, tumor infiltration, and urinary outflow obstruction by fibrosis and blood clots and stones.

both classifications use diagnostic criteria of renal impairment (urine output, rise in sCr) that manifest at a late stage of injury and rely on knowledge of baseline creatinine (7). Inclusion of other more sensitive criteria, including biomarkers, may enhance definition criteria (8). There has also been lack of precision in the use of the term *acute tubular injury/necrosis*. The term should be reserved for the clinical pathologic entity of intrinsic renal failure that is the result of either an ischemic or toxic insult to the kidney, with evidence of tubular injury/dysfunction such as altered fractional excretion of sodium (8) and potentially other more specific biomarkers, when other causes have been excluded. As a result of the lack of uniformity in terminology, the percentage of cases of ARF that can be attributed to “acute tubular necrosis/injury” are difficult to accurately ascertain, but the condition is likely responsible for the majority of cases of ARF that require acute renal replacement therapy. The term *acute tubular necrosis* itself is a misnomer, since necrosis, while classically a feature of animal models, is only one morphologic manifestation of clinical ATI. It should

also be noted that morphologic evidence of frank tubular necrosis is not a frequent feature in kidney biopsies obtained in the context of clinical ARF; however, morphologic changes of sublethal tubular injury are usually present. Just as in the clinical classifications, however, morphologic signs of injury appear in a later stage of injury; more sensitive markers are required to identify early tubular cell injury. The term *acute tubular injury* is more accurate and will be used throughout this chapter.

Historical Background

It was not until World War I that acute renal dysfunction was recognized as a distinctive clinical and pathologic entity. Hackradt (9) described what he called “vasomotor nephrosis” following crushing injuries. In a review of autopsy material, Minami (10) described the presence of pigment casts in medullary tubules associated with tubular changes and an interstitial infiltrate and suggested that myohemoglobinuria and subsequent precipitation in the tubules were factors involved in producing the observed anatomic and functional renal abnormalities. Shortly

TABLE 26.1 Clinical phases of AKI

1. Risk of renal dysfunction
Increase in sCr by 1.5 times OR
Decrease in GFR >25% for 6 h OR
Urine output <0.5 mL/kg/h for 6 h
2. Renal injury
Increase in sCr by 2 times OR
Decrease in GFR >50% for 12 h OR
Urine output <0.5 mL/kg/h for 12 h
3. Renal failure
Increase in sCr by 3 times or >4 mg/dL OR
Decrease in GFR by 75% or more for 24 h OR
Urine output <0.3 mL/kg/hr for 24 h OR
Anuria for 12 h

sCr, serum creatinine; GFR, glomerular filtration rate.

Modified from Bellomo R. Defining, quantifying, and classifying acute renal failure. *Crit Care Clin* 2005;21:223.

thereafter, Baker and Dodds (11) studied a rabbit model of ARF and emphasized tubular obstruction as important in the pathogenesis. Progress in the field was relatively dormant until the advent of World War II, when Bywaters and Beall (12) revived interest in ARF as a result of their study of London air casualties. Bywaters and Dible (13) and Dunn et al. (14) described intratubular hemoglobin and myoglobin casts associated with focal necrosis of tubules, interstitial edema, and mild interstitial inflammation localized to specific portions of the nephron in the “crush syndrome or traumatic anuria.” This finding led to the hypothesis that tubular obstruction by necrotic debris and precipitated pigment was the prime cause of the observed oliguria.

Bywaters and Dible (13), however, believed that obstruction alone could not explain all the clinical findings or the abnormal character of the urine that was produced by such patients. Because patients with ARF had urine that was quite abnormal and resembled an unaltered glomerular filtrate, and because there was a marked discrepancy between the degree of anatomic change and the severity of the oliguria, they postulated that other factors must play a part. Lucke (15) emphasized that the discrepancy between structure and function could be related to the observed localization of histologic changes to the distal nephrons, and he coined the term *lower nephron nephrosis*.

Oliver et al. (16) used nephron dissections to study cases of ARF, and they were able to show two distinct types of renal tubular injury. In the first, as a result of the direct cytotoxic effect of a specific nephrotoxin, there was segmental necrosis of the proximal tubular epithelium with denudation of the basement membrane, which remained intact. In the second type, which they termed the *tubulorrhhexic lesion*, there was focal necrosis of tubular cells associated with rupture of the adjacent basement membrane, allowing communication of the tubular lumen with the interstitial tissue, a lesion most commonly seen in the distal portions of the proximal tubule, most likely ischemic in origin. The focal and patchy nature of the necrosis, which was usually not associated with any interstitial reaction, was thought to be the reason that random histologic sections of such kidneys frequently did not demonstrate significant

pathologic change. Oliver et al. suggested that these lesions could lead to the leakage of tubular fluid into the interstitial tissue, diminishing the amount of urine produced. Such leakage could cause a rise in intrarenal pressure, which could further potentiate oliguria by compression of capillaries, resulting in diminished glomerular filtration.

While these investigators were concentrating on the tubular changes, Goormaghtigh (17,18) called attention to the renal arteriolar changes in kidneys of patients with the crush syndrome. He observed considerable hypertrophy and an increase in granularity of the juxtaglomerular cells in the kidneys of patients with ARF and theorized that these cells produced a vasoactive or prevasoactive substance that could act on the renal vasculature. He suggested that the anuria observed in the crush syndrome was the result of vasoconstriction and postulated that glomerular hemodynamic changes would result in the diminution of glomerular filtration, emphasizing decreased glomerular function as a mechanism of oliguria.

Based on direct observation of the kidney as well as angiographic and morphologic studies of intrarenal vascular patterns, Trueta et al. (19) proposed that the fundamental defect in the crush syndrome was a reduction of glomerular filtration as a result of the diversion of blood away from the outer cortical glomeruli through a juxtamedullary shunt. Brun et al. (20,21) produced even more convincing evidence by measuring renal hemodynamics in vivo. Sheehan and Davis (22) and Sevitt (23) also believed that ischemia was important, but they suggested that the mechanisms of action were related to vascular damage following an initial period of ischemia, which prevented adequate reperfusion once blood flow had been established. Hollenberg et al. (24,25) studied patients with ARF following a variety of initiating injuries and noted that it was impossible to see the cortical arteries in such patients; they also documented disappearance of the cortical flow component of xenon washout from the kidney. Munck (26) verified that such a decrease in blood flow was sufficient to result in renal hypoxia. These early studies suggested several physiologic mechanisms of action for the resultant oligoanuria, including tubular obstruction, back leakage of tubular fluid, and changes in hemodynamics resulting in decreasing glomerular filtration.

The advent of micropuncture techniques led to the investigation of several animal models of ARF to identify the pathophysiologic mechanisms of action in greater detail. Oken et al. (27) studied experimental mercury- or glycerol-induced ARF, demonstrating that glomerular filtration progressively diminished as oliguria developed and suggesting that suppressed filtration was the key pathophysiologic factor. Early work in our own laboratory (M.K.) studied two different models of ARF (28), potassium dichromate–induced toxic cellular damage to the early (S_{1-2}) part of the proximal tubule and administration of purified human globin, producing an intrarenal obstructive lesion of the distal nephron. Decrease in urine flow was accompanied by a diminution of the total and individual nephron GFR associated with a decrease in the tubular reabsorptive capacity, and there was evidence of mechanical tubular obstruction, reflected by an elevation of free-flow intratubular pressure. In addition, the glomerular filtration pressure appeared to be diminished, suggesting that the decreased glomerular blood flow and glomerular filtration were the result of preglomerular arteriolar constriction, mediated by activation of the local renin-angiotensin system. Studies of renal blood

flow distribution demonstrated that a diminution of outer cortical flow correlated best with decreased glomerular filtration (29,30). These and other studies led to a proposal that tubular epithelial injury induced either by ischemia or by a toxin could be sublethal but had to be severe enough to result in decreased epithelial transport activity, which then would result in decreased tubular sodium reabsorption and local activation of the renin-angiotensin system. This, in turn, would alter glomerular hemodynamics and result in decreased glomerular filtration. Decreased tubular urine flow associated with the shedding of cellular debris and the presence of Tamm-Horsfall protein would result in tubular obstruction. When combined with focal areas of necrosis, as demonstrated by the microdissection studies of Oliver, this could lead to a back leakage of fluid, all of which contribute to the end result of oliguria. The term *acute renal success* was suggested by Thurau and Boylan (31), interpreting the pathophysiologic changes of decreased glomerular filtration as a defense against loss of intravascular volume caused by the inability of the damaged tubules to reabsorb the glomerular filtrate.

Although these studies primarily focused on pathophysiology and did not address the cellular pathologic characteristics associated with the oliguria of ARF, they did note the discrepancy between structure and function and emphasized the central role of alteration of renal tubular epithelial transport function by ischemic or toxic injury. Studies by Rosen and colleagues on renal pathology in experimental and human ATI have also emphasized the importance of sampling the nephron segments that are most vulnerable to a particular type of injury (32). This section of the chapter will focus on ATI caused by ischemia and/or nephrotoxins. Clinical features, pathology, and pathogenesis will be discussed for ischemia and toxic injury in general and for the major nephrotoxic agents.

Clinical Presentation

Patients with injury to the tubular epithelium have clinical and laboratory evidence of tubular dysfunction that is sometimes quite subtle. Loss of normal resorptive function may lead to polyuria, glucosuria, phosphaturia, or aminoaciduria; Fanconi syndrome has occasionally been reported. With more severe injury, intact and necrotic tubular cells appear in the urine sediment, individually or in cast form. Patients may become oliguric. In some cases, crystals, leukocyturia, and hematuria may also be detected on urinalysis.

Enzymuria is a useful marker for tubular cell injury; it is more sensitive than a rise in sCr and may be used to some extent to gauge the severity of cell injury. Elevated levels of β_2 -microglobulin or enzymes may be detected in the urine and have been used in many clinical studies as markers of tubular toxicity. The presence in the urine of brush border enzymes, such as alkaline phosphatase and gamma-glutamyl transpeptidase, may reflect mild cellular injury. The appearance of lysosomal enzymes, such as *N*-acetyl glucosaminidase, and of cytoskeletal elements reflects more severe injury and cell loss from the tubular epithelium. Measurement of these factors has been used as a noninvasive marker of injury to the renal tubule in both ischemic and toxic tubular injury (33–35). New unbiased genomic and proteomic techniques are leading to the discovery of many potential biomarkers that may be useful in detecting early tubular injury. Biomarkers proposed for early detection of AKI include proteins present in urine (kidney

injury molecule-1 (KIM-1), neutrophil gelatinase-associated ligand (NGAL), IL-18, cysteine-rich-61 (cyr61), Na(+)-H(+) antiporter isoform 3 (NHE3), lipocalin, actin), and, serum (cystin C, tumor necrosis factor- α (TNF- α) receptor, and NGAL) (33,34,36,37). Many of these markers can be found in prerenal azotemia as well as in renal injury, reflecting a continuum of ischemic injury. Differentiation of the two conditions relies on response of creatinine to expansion of circulating volume. Use of biomarkers for this purpose will likely require assay of a panel of candidate markers rather than a single marker.

ATI often results in reduction of GFR, with development of acute renal insufficiency and ARF. The acute reduction in renal function results in both biochemical and clinical abnormalities, related to the inability of the kidney to eliminate water, metabolic by-products, and acids and to regulate electrolyte balance. Oliguria is classically seen as an initial feature of many cases of ATI, but nonoliguric ARF is commonly recognized as well. While altered urine output is part of the definition of AKI, urine output can only be accurately measured in patients with a urinary catheter and is affected by blood volume status and diuretic use (8). Significant laboratory findings include elevations in blood urea nitrogen, sCr, and serum potassium; as noted above, rise in creatinine/fall in creatinine clearance (combined with urine output and other factors) defines AKI. Urinary sodium excretion is markedly amplified, with increased fractional excretion of sodium consistent with a decreased resorptive capacity of the damaged tubules.

Patients with toxic injury to the tubular epithelium also often show signs of renal failure. There is active research on biomarkers of nephrotoxic AKI (34). Hemoglobin and myoglobin are endogenous proteins that can function as nephrotoxins when they are present in large concentrations in the urine. ARF is associated with hemoglobinuria following acute hemolysis in patients with transfusion reactions and in patients with *Plasmodium falciparum* malaria. While the toxicity of hemoglobin may contribute to the pathogenesis of ARF in these instances, ischemia and microcirculatory disturbances probably play a greater role in its development. Myoglobinuria stemming from rhabdomyolysis as a result of trauma, viral infection, or heat stress produces a similar clinical picture. Rhabdomyolysis associated with cocaine abuse has also been demonstrated to result in ATI, as discussed in this chapter in the section on nephrotoxins. High concentrations of filtered light chains may also produce ATI, often with crystalline deposits in tubular cells (see Chapter 22).

A variety of exogenous agents can also cause ATI (Table 26.2). Between 15% and 30% of AKI is caused, at least in part, by exposure to drugs (1,38,39). The use of potentially nephrotoxic drugs such as aminoglycoside antibiotics or nonsteroidal anti-inflammatory drugs, which can accentuate renal ischemia, may predispose seriously ill patients to develop overt ARF. It must be noted that association of a particular drug or toxin with renal injury and dysfunction may be missed or may be difficult to establish as causative, especially in complex clinical settings. Repeated correlation of exposure and injury help to establish nephrotoxicity, and experimental models are often useful in defining the mechanism of injury.

Depending on the specific drug or toxin causing injury, renal dysfunction may occur soon after exposure or after a predictable interval, as is seen with aminoglycosides. Most patients experience a fall in GFR that is detectable on clearance

TABLE 26.2 Drugs that are injurious to renal tubular epithelium

Antiviral agents
Nucleoside analogs
Antiretroviral agents
Antibiotics
Aminoglycosides
Amphotericin B
Cephalosporins
Colistin/polymyxin B
Rifampicin ^a
Sulfonamides ^a
Vancomycin
Immunomodulatory agents
Calcineurin inhibitors
IVIG
Sirolimus
Antineoplastic agents
Cis-platinum
Other
Radiologic contrast media
Narcotics
Anesthetics
Herbal medications

^aDiscussed in Chapter 25.

studies, but only a minority progress to overt renal failure. A few tubular toxins cause injury only at high doses; with other agents, some level of injury can be detected at the usual therapeutic doses in most patients. Pigmented casts or crystals may appear in the urine, providing a clue to the diagnosis; in such cases, oliguria and even anuria may be the presenting feature. Hydration and maintenance of diuresis help prevent renal dysfunction or hasten recovery in cases with intratubular crystals or cast formation. Radiographic studies generally reveal normal-sized kidneys with increased echogenicity. Clinical features of major nephrotoxins are described in the text following; the focus of this chapter is on toxic effects of therapeutic agents. Toxic nephropathies caused by heavy metals and other environmental and food toxins have been reviewed (40).

New imaging techniques are emerging to diagnose and to study AKI, even at early stages. Rapid and accurate measurement of GFR using radioactive and nonradioactive clearance techniques is now possible, even when GFR is not stable. New imaging techniques enable multidimensional kinetic analyses, enhance the study of intrarenal perfusion and oxygenation, and can detect metabolic perturbations and molecular alterations in the kidney in vivo (41–43).

Clinical Features Associated With Specific Toxic Agents

ANTIBIOTICS

Antiviral Agents The nephrotoxicity of antiviral drugs has been reviewed (44–48). Acyclovir, an early nucleoside analog, was reported to be associated with renal dysfunction, and there is a significant incidence of renal dysfunction with newer agents as well. Tubular injury may lead to proximal tubulopathy and even Fanconi-like syndrome (cidofovir, tenofovir, foscarnet),

distal tubular acidosis (foscarnet) and nephrogenic diabetes insipidus (foscarnet, tenofovir). The nucleoside reverse transcriptase inhibitors didanosine, stavudine, and lamivudine have rarely been associated with renal tubular dysfunction with acidosis and hypophosphatemia. Adefovir has been reported to produce proximal tubulopathy in up to 50% of patients at high doses (49). A variety of these agents have been associated with renal failure, including acyclovir (50,51), foscarnet (52), ganciclovir (53), cidofovir (54), indinavir (55,56), tenofovir (57,58), ritonavir (59), and adefovir (49). The widely used agent tenofovir has a rate of renal failure of less than 1% in those without preexisting disease (58), though renal failure is more frequent in those with preexisting disease. Risk factors for toxicity include baseline renal dysfunction, low CD4 counts, low body weight, and concomitant use of lopinavir or didanosine (47). Some agents are associated with crystalluria and/or nephrolithiasis (acyclovir, ganciclovir, indinavir, and much less commonly with the newer protease inhibitors atazanavir, saquinavir, nelfinavir, and lopinavir-ritonavir), and flank or abdominal pain may occur. Incidence may be up to 20% with antiretroviral regimens including indinavir, and more frequent when indinavir is pharmacologically boosted with ritonavir. Crystals are needle shaped and birefringent under polarized light and can be seen in voided urine. Proteinuria has also been described with cidofovir, more commonly than ARF.

Toxicity is dose dependent, and volume depletion may predispose to toxicity. For some agents such as tenofovir, toxicity depends on accumulation of drug in proximal tubular cells and may take weeks to months for injury to be detected (44). Renal failure often resolves rapidly when these drugs are discontinued, and the patient may be rechallenged with a lower dose of the drug without development of renal dysfunction. However, occasional cases of chronic renal failure have been reported in patients receiving cidofovir (60), indinavir (48), and tenofovir (57,61). Renal tubular functional defects may persist as well. Hydration to maintain diuresis may prevent renal toxicity, especially in those agents causing crystalluria. With acyclovir, toxicity has been described frequently with intravenous administration, but cases have been reported with oral administration as well. Combination with other nephrotoxic agents may enhance toxicity (57). Older age and preexisting renal failure are risk factors for ARF in patients receiving acyclovir. Preexisting renal impairment, common in the HIV population, is also a risk factor for ARF induced by tenofovir, cidofovir, foscarnet, indinavir, interferon, and ritonavir, and dosage adjustment is required. Because of renal toxicity, adefovir, cidofovir, and indinavir are not approved/recommended for primary antiretroviral therapy.

Aminoglycosides Aminoglycoside antibiotics have long been recognized as nephrotoxic and ototoxic. They continue to be used, however, because of their efficacy in treating gram-negative infections. The incidence of ARF in patients treated with gentamicin is about 20% (62). The nephrotoxicity of the various aminoglycosides is greatest in those with the largest number of free amino groups (63). Streptomycin, the least toxic, has two amino groups; those with intermediate toxicity, such as gentamicin, tobramycin, and kanamycin, have four to five groups, and neomycin, which is the most toxic, has six free amino groups. Changes in dosing to once-daily administration have evolved to avoid nephrotoxicity. Once-daily dosing

with monitoring of trough levels may enable avoidance of significant renal toxicity, even in elderly patients (64). However, with prolonged treatment, differences between once-daily and twice-daily dosing diminish (65). The toxicity of aminoglycosides may be potentiated by ischemia or other drugs, including thalidomide (66).

Gentamicin is a broad-spectrum antibiotic that has intermediate nephrotoxicity, and kanamycin also has an intermediate potential for nephrotoxicity. In humans, gentamicin alone may cause elevation of serum urea nitrogen (SUN) and sCr, although the incidence is difficult to assess because of a variety of concomitant clinical variables, including advanced age, presence of preexisting renal damage, or administration of other drugs that are potentially nephrotoxic. The frequency with which renal toxicity is reported varies from study to study, in part because of variable criteria for defining significant elevations in SUN and creatinine. Incidences ranging from 8% to 37% have been reported. Identified risk factors include advanced age, poor nutritional status, severe systemic illness, and administration of other drugs, including amphotericin B, vancomycin, methicillin, or cephalosporins, which are themselves potentially nephrotoxic.

Onset of a detectable rise in sCr is typically delayed for 8 to 10 days from initiation of therapy. Renal failure is usually mild, and most patients recover. Enzymuria may be detected in cases without elevations in sCr, suggesting the presence of subclinical injury in many patients. Occasional cases have been reported in which proximal tubular dysfunction is severe enough to produce Fanconi syndrome (67). Neomycin is the most nephrotoxic of the aminoglycoside antibiotics. Because it is poorly absorbed from the gastrointestinal tract, it is used largely as a bowel-sterilizing drug. Neomycin also has been used parenterally and has caused deafness and renal damage. ARF, usually of an oliguric type, has been reported; recovery has been reported in most patients (68,69). ARF occurs most commonly after intravenous or intramuscular administration of the drug, although it has been recorded after oral administration as well (69).

Amphotericin B Nephrotoxicity is the side effect that most commonly limits the use of this important antifungal agent. Renal insufficiency is frequently observed, with a fall in the GFR and renal blood flow. In one large prospective series of patients being treated for cryptococcal meningitis, 26% had an increase in sCr level of more than 2 mg/dL (70). Such renal failure is usually reversible, but renal function may be permanently impaired in 40% of patients who receive more than 5 g of amphotericin (71). In addition, there is a defect in acid excretion by the tubules, resulting in renal tubular acidosis (72), which may precede a significant fall in the GFR and is generally reversible. A common side effect is an impaired ability to concentrate urine (73); this may be present without azotemia. Liposomal and lipid complex formulations may reduce nephrotoxicity (74). The different formulations are probably comparable (75).

Cephalosporins While acute (proximal) tubular injury is rare with the penicillins and uncommon with the current generation of cephalosporins, it is a greater risk with the penems. The cephalosporin group of antibiotics comprises several "generations" of these useful agents, defined on the basis of antimicrobial activity. The first generation includes cefazolin,

cephalothin, and cephalexin. Cefamandole, cefonicid, cefuroxime, cefaclor, cefoxitin, and cefotetan are second generation, while the third generation includes ceftazidime, cefotaxime, and ceftriaxone. Cefepime is a fourth-generation cephalosporin that is more resistant to β -lactamase than the previous agents. Many of these drugs may be nephrotoxic (76). Cephaloridine and cephaloglycin are the most toxic of the group and are no longer used clinically in the United States but are used experimentally for toxicity studies. On the other hand, ceftazidime and cefepime are not nephrotoxic.

The toxic cephalosporins are most likely to produce renal failure in patients with preexisting renal insufficiency, in those with drug overdose, and in those receiving other antibiotics or furosemide, probably related to the ability of furosemide to prolong the half-life of the cephalosporins. Many of the patients reported to have nephrotoxicity owing to cephalosporins are acutely ill with severe infections, and many are elderly. Cephalothin given alone or with gentamicin, tobramycin, or other agents can cause ARF in humans or can worsen preexisting renal insufficiency. The ARF is usually reversible. Cephalexin is less likely to cause nephrotoxicity, but acute renal dysfunction has been reported, with "acute tubular necrosis" (77,78). ARF with tubular proteinuria has been described with a combination of ceftriaxone and acyclovir (79) and cefodizime and vancomycin (80).

Polymyxin B and Colistin Polymyxin B and colistin (polymyxin E) are older antibiotics that are reemerging for treatment of multiple-drug-resistant gram-negative bacteria and are used for "salvage" therapy in critically ill patients. These antibiotics have well-recognized nephrotoxicity. At lower doses, proteinuria, casts, and hematuria may be seen, and at higher doses, renal failure occurs. Reduction in dosing, avoidance of coadministration of other nephrotoxic agents, and other supportive measures likely explain a lower incidence of nephrotoxicity in more recent clinical series compared to older reports (81,82). Incidence of nephrotoxicity in recent studies has been 10% to 24%, with comparable toxicity for colistin and polymyxin B regimens (83–86). When there is preexisting impaired renal function, smaller doses can produce renal symptoms. Renal failure may occur with oliguria. Recovery is usual after withdrawal of the drug.

Vancomycin Vancomycin is a glycopeptide antibiotic that has been associated with nephrotoxicity and ARF since its introduction (87), limiting clinical use of the drug until the advent of methicillin-resistant *Staphylococcus aureus* (MRSA) and other drug-resistant organisms. Nephrotoxicity was initially reported at low rates of $\leq 5\%$ with standard dosing (88), though higher rates were reported with use of concomitant nephrotoxic agents (89). With newer recommendations for use of higher doses for MRSA and hospital-acquired infections, increased rates of nephrotoxicity have been reported over the past decade (90–92). Risk factors include African American race, initial trough level, duration of treatment, and concomitant aminoglycoside use.

IMMUNOSUPPRESSIVE/IMMUNOMODULATORY AGENTS

Cyclosporine Cyclosporine (CsA) is widely used in the prevention and treatment of transplant rejection and to treat autoimmune disease. The major side effect is nephrotoxicity, which is to some extent dose dependent. Both acute and chronic toxic effects have been described (93). With nephrotoxicity broadly

defined to include an asymptomatic mild decline in the GFR, it is likely that many patients treated with immunosuppressive doses of CsA experience nephrotoxicity. When more overt CsA-induced renal failure is superimposed on mild functional toxicity, it may manifest in the form of one or more clinical syndromes: acute reversible renal functional impairment, delayed renal allograft function, tubular cell effects, acute vasculopathy (thrombotic microangiopathy), and chronic nephropathy with interstitial fibrosis.

The occurrence of *acute reversible renal failure*, while not absolutely related to circulating drug levels, is generally seen with serum levels rising above 200 ng/mL and is common at drug levels above 400 ng/mL. Other features may include hyperuricemia, hyperkalemia, hypomagnesemia, sodium retention, and concentrating defects (94–96). These relatively high levels are seen more commonly in heart and liver allograft patients than in patients with renal allografts. ARF may be severe, with polyuria or oliguria (and even rarely anuria). In some cases, renal functional impairment can be rapidly reversed when CsA dosing is reduced (97). This rapid return of function is evidence that there is no direct tubular toxicity, as is the low fractional excretion of sodium, which indicates intact tubular reabsorption. In early phases, the underlying vasoconstriction can be reversed by dopamine (98). Cyclosporine can also produce significant injury to proximal tubule epithelium, potentially related to direct effects as well as to ischemic injury due to prolonged vasoconstriction. In this setting, renal dysfunction is not rapidly reversible on reducing dosage of the drug.

Cyclosporine also has a propensity for producing endothelial cell damage, which can lead to thrombotic microangiopathy. Glomerular thrombi and thromboembolic complications have been described in several series, and a hemolytic uremic type of syndrome (HUS) has been reported, initially in bone marrow transplant recipients and subsequently in other contexts as well (99,100). There may be ischemic tubulointerstitial changes downstream from involved vessels.

Myers et al. (101) were the first to show fibrosis with cyclosporine treatment, and many others have drawn attention to the fact that chronic nephropathy with striped interstitial fibrosis may occur following long-term CsA therapy, particularly in cardiac and other solid organ allograft recipients, as well as in patients receiving chronic CsA for autoimmune disease (102). Proposed risk factors include episodes of clinical toxicity, high CsA trough levels, concurrent administration of other nephrotoxic drugs, acute rejection episodes and therapy, and high variability in CsA levels (103,104). Myers et al. showed significant reductions in the GFR in cyclosporine-treated patients to approximately 50% of that in azathioprine-treated patients (101,105). Patients may also have severe hypertension, mild proteinuria, and evidence of tubular dysfunction. A similar long-term reduction in the GFR has also been reported in liver allograft recipients (106), and comparable changes have been reported in the kidneys of pancreas transplant recipients as well (107). Even low-dose CsA therapy for psoriasis may effect long-term changes (108,109). This type of chronic cyclosporine toxicity may not be reversible. Risk factors for the development of chronic cyclosporine nephrotoxicity include previous episodes of ARF, high-dose treatment, and (for heart transplant patients) increasing age (110,111).

Tacrolimus Tacrolimus (FK506) produces a spectrum of nephrotoxicity very similar to that of CsA (93,94) and is generally dose dependent; toxic reactions are common at or above 20 ng/mL (112) but can occur even when trough levels have been in a lower range (103). Reversible renal dysfunction has been reported with the use of FK506 for prevention of graft versus host disease in bone marrow transplantation and in renal and nonrenal solid organ allografts. Tacrolimus may have a lower nephrotoxic potential than cyclosporine in renal allografts, with less reduction in blood flow (113), and lower sCr and/or higher GFR at doses with comparable efficacy (114–116). Better graft survival has been reported in renal allografts (116,117), and less CRF may occur in other solid organ allografts with tacrolimus versus cyclosporine (118–120). In addition to induction of posttransplant diabetes, patients may develop hypertension (121). Higher incidences of urinary tract infection, of pyelonephritis, and of polyoma virus infection (122) have been reported as well, perhaps owing to the more potent immunosuppressive activity of the drug.

Intravenous Immunoglobulin Intravenous immunoglobulin (IVIG) may produce ARF (123,124). Addition of sugar excipients, and especially sucrose, to IVIG formulations has reduced side effects of pain, fever, chills, and fatigue but may increase the frequency of ARF. Renal failure may be attenuated by slowing the rate of infusion. Renal function generally returns to normal with discontinuation of the drug. Switching to a D-sorbitol-stabilized formulation may prevent toxicity (124). Avoidance of sucrose-stabilized formulations is recommended in patients receiving other nephrotoxins, in the elderly, in those with preexisting dysfunction, and in diabetics.

Sirolimus Nephrotoxic effects of sirolimus have been reported in transplant and native kidneys. Delayed graft function is more common in series of patients treated with sirolimus peritransplant (125,126); another study demonstrated that sirolimus-treated patients were half as likely to resolve delayed graft function (127). A few cases of acute oliguric renal allograft failure associated with combined use of FK506 and sirolimus have been described, apparently owing to ATI (128). In one study of high-risk renal allograft recipients, FK506-treated patients on reduced sirolimus (5 to 10 ng/mL) had a significantly higher incidence of biopsy-proven FK506 toxicity (129). Severe acute renal dysfunction with tubular injury with myoglobin casts has been reported in renal allograft recipients, with ATI, with myoglobin casts noted only in the cohort treated with rapamycin (130), some with elevated creatine phosphokinase and/or serum myoglobin levels. ARF/AKI has also been reported in series of patients treated with rapamycin for chronic glomerulopathy (131); renal biopsies were not performed, but most recovered function after discontinuation of the drug. Some cases of acute renal dysfunction caused by sirolimus have been associated with thrombotic microangiopathy (132).

ANTINEOPLASTIC AGENTS

Several antineoplastic agents produce toxic effects in the kidney. Immunotherapeutic agents, discussed earlier, are among them. In addition, antineoplastic agents that lead to rapid tumor lysis may cause hyperuricemia, with precipitation of uric acid in renal tubules; this syndrome may be largely avoided by hydration and careful monitoring of the patient. Specific agents that are toxic to the kidney are discussed here.

Cis-Platinum Cis-platinum is a chemotherapeutic agent that frequently produces nephrotoxicity and is widely used in animal models of toxic tubular injury. Cis-platinum nephrotoxicity is dose related. In early studies, it was reported in 25% to 30% of patients on single-course therapy and 50% to 75% of patients on multiple courses (133,134) and remains high, affecting about one third of treated patients (135). Patients show gradual signs of elevations in SUN and sCr. Polyuria is a prominent early clinical feature, but even oliguric ARF may be seen. Other presenting symptoms include proteinuria, hyperuricemia, enzymuria, glycosuria, and electrolyte disturbances reflecting tubular dysfunction (136,137). Aggressive hydration, administration of diuretics, or coadministration of thiosulfate or thiophosphate reduces renal toxicity, and novel cytoprotective strategies based on understanding of pathophysiology are being tested in animal models (136–138). Delay of dosing is recommended if renal toxicity occurs. Recovery of renal function following cessation of therapy is the rule, but it may be delayed and incomplete, and subclinical dysfunction may persist (139). Chronic renal dysfunction is best predicted by the cumulative dose administered. Newer platinum derivatives, including carboplatin, spiroplatin, iroplatin, and oxaplatin, and liposome-entrapped platinum compounds appear to have limited nephrotoxicity. However, there is still a degree of nephrotoxicity with some of these formulations (138). Nephrotoxicity may be exacerbated by combination therapy with other agents such as Taxol (140).

Other Chemotherapeutic Agents Nitrosoureas also produce nephrotoxicity. Streptozotocin, a nitrosourea compound, is toxic to pancreatic beta cells and is used to treat metastatic islet cell carcinoma, carcinoid tumors, and lymphoma. Up to 75% of patients experience some degree of nephrotoxicity with prolonged administration (141,142). The alkylating agent cyclophosphamide has only transient effects on water excretion, increasing urine osmolarity and decreasing plasma osmolarity. However, its analog, ifosfamide, has significant renal toxicity. Renal proximal tubular dysfunction is the most common effect, and features of Fanconi syndrome and related electrolyte abnormalities, which may be severe, have been reported (137,138). Distal renal tubular acidosis occurs rarely. Mild decreases in the GFR are common, but severe ARF may occur as well, and irreversible chronic renal failure or continued deterioration after therapy has also been described (143,144). The major risk factor for toxicity is total dose of the drug (143). Other risk factors include age less than 5 years, previous exposure to cisplatin, underlying renal impairment, or tumor infiltrates in the kidney (145). Use of thiophosphates may reduce toxicity (146).

Other chemotherapeutic agents may also be nephrotoxic (137,138). High-dose therapy with mithramycin or methotrexate can result in renal failure, the latter via precipitation of methotrexate and 7-hydroxymethotrexate crystals in tubules. Azacitidine can produce renal symptoms and Fanconi syndrome or mild subclinical tubular dysfunction, which may necessitate bicarbonate and electrolyte supplementation. Imatinib and diaziquone can also produce Fanconi syndrome and AKI. Zolendronate, a bisphosphonate used in conjunction with chemotherapeutic agents, has also been associated with ARF and should be avoided in patients with severe underlying renal disease.

RADIOLOGIC CONTRAST MEDIA

Renal failure is an important complication of contrast media administration; the reported incidence of radiocontrast nephrotoxicity (RN) varies between 2% and 70%, averaging 5% to 10%. In the United States and Europe, RN has been reported to be the cause of 10% of hospital-acquired ARF (147). Differences in reported incidence are in part the result of issues with the definition of RN, optimally defined as “acute impairment in renal function following exposure to radiographic contrast materials.” This impairment is measured by a rise in sCr by most investigators. However, the degree of change in sCr that is considered to be diagnostic of RN shows great variation. Some prospective studies, which measured the sCr levels at regular intervals, diagnosed RN even after relatively small increases. Thus, some of these studies may overestimate the incidence of clinically significant RN. Urinary levels of tubular cell enzymes and markers of oxidative stress rise in the urine of patients with RN (148,149).

Certain underlying conditions predispose to the development of RN; the most important of them is preexisting renal insufficiency (150,151). Moore et al. (152) demonstrated that the incidence of RN in patients with baseline sCr levels between 1.5 and 1.9 mg/dL was 4.7%, the incidence for those with sCr levels between 2.0 and 2.4 mg/dL was 14.3%, and for levels between 2.5 and 2.9 mg/dL, it was 20%. Analogous findings were reported in a large study, with incidence of RN (rise in sCr of more than 0.5 mg/dL) ranging from 2.4% with sCr of 0.1 to 1 mg/dL to 30.6% for sCr above 3 mg/dL (150). A recent study in general ICU patients (153) using only iodinated nonionic low-osmolar or iso-osmolar contrast found an incidence of AKI of 16.4% using standard criteria (22.2% using KDIGO criteria); AKI was stage 3 (severe) in 25% of those who developed AKI. In contrast, with low-risk nonemergent CT, RN is uncommon among outpatients with mild baseline kidney disease (154). Dehydration is a risk factor for RN, which is not surprising because dehydration, and thus hypovolemia, may potentiate the development of renal failure owing to any insult. Effective prophylactic measures, such as rehydration, alleviate this problem. The efficacy of prophylactic hemodialysis and hemofiltration to reduce the incidence of RN in high-risk groups is controversial (151). A variety of protective measures have been proposed, including hydration and sodium bicarbonate, *N*-acetyl cysteine, combination therapy, and statin therapy (155).

Diabetes and *multiple myeloma* are also risk factors for RN. However, it appears that neither condition represents a higher risk if renal function is normal. Identified risk factors for contrast-induced nephropathy after coronary intervention studies include CHF, hypotension, intra-aortic balloon pump, age greater than 75 or 80 years, anemia, diabetes mellitus, contrast volume, and high preprocedural sCr (156). Whether *dosage* and *route of administration* are independent risk factors is a matter of debate. Some studies found a significant correlation between the volume of administered contrast media and the degree of nephrotoxicity, particularly in patients with underlying renal disease such as diabetes mellitus and in the setting of reduced renal function. Other studies did not confirm this relationship. These differences probably reflect biases in selection of patients. Dose may not be a significant risk factor in patients with normal renal function, but dosage as an independent risk factor has not been investigated in most published studies. An equation, to determine maximum acceptable

contrast dose, 5-mL contrast volume \times body wgt (kg)/baseline sCr (mg/dL), has been developed (157). Several recent studies confirm that exceeding this threshold increases the risk for contrast-induced nephropathy (158,159), at least in percutaneous coronary intervention studies. Patients who develop RN reportedly have more frequent adverse events, including myocardial infarction, prolonged hospital stay, worse kidney function at discharge, and higher mortality (153,160).

Following the introduction of nonionic (low-osmolality) contrast media, some studies suggested that such media are less nephrotoxic than the conventional ionic (high-osmolality) contrast media. However, several prospective clinical studies comparing the nephrotoxic effect of low- and high-osmolality contrast media did not find differences in the incidence of nephrotoxicity (152). The randomized prospective multicenter Iohexol Cooperative Study group (161) found that in patients with normal renal function, the incidence rates of RN were not different between patients undergoing cardiac angiography using ionic (sodium diatrizoate) and those patients receiving nonionic (iohexol) contrast media. In contrast, patients with preexisting renal impairment receiving ionic contrast material were 3.3 times more likely to develop RN than patients receiving nonionic contrast material. Thus, it appears that the considerably cheaper conventional ionic contrast media can be safely used in patients with normal renal function, but ionic contrast media should be used with caution in those with preexisting renal insufficiency. Iso-osmolar (e.g., iodixanol) and (less expensive) low-osmolar (iomeprol, iopamidol, ioversol) contrast agents have also been compared in randomized trials. Most show some trend to lower rates of contrast-induced AKI with the iso-osmolar agent, but generally, the difference was not significant (162–164). However, in those receiving high contrast volume (163) or in diabetic patients (164), there may be a lower risk with the iso-osmotic agent.

NARCOTICS

Cocaine has been implicated in both acute and chronic renal failure (165). The clinical symptoms of myoglobinuric ARF associated with narcotic abuse are not different from myoglobinuric ARF of other origins. Patients show signs of ARF, with muscle pain and elevated serum levels of creatine phosphokinase, serum glutamic-oxaloacetic transaminase, serum glutamic-pyruvic transaminase, and lactate dehydrogenase. Hypotension, hypoxia, hypovolemia, and acidosis are common findings. ARF may be polyuric or oliguric and of varying severity and duration (166,167). Only about a third of patients with cocaine-induced rhabdomyolysis develop renal failure; risk factors for ARF include higher creatine phosphokinase levels, hyperthermia, and hypotension (166). With appropriate supportive therapy, the majority of patients recover, but the mortality rate in some cohorts approaches 15% (166). Renal infarction is a rare complication; patients present with flank pain, fever, leukocytosis, elevated lactate dehydrogenase, and hematuria.

ANGIOTENSIN-CONVERTING ENZYME INHIBITORS

Angiotensin-converting enzyme (ACE) inhibitors have become widely used because of their proven beneficial effect on cardiovascular and renal disease. They decrease the GFR through reducing efferent arteriolar vascular tone by antagonizing the angiotensin II effect. There is ample evidence that by reducing glomerular transcapillary hydraulic pressure, ACE inhibitors

slow the progression of chronic renal disease, particularly if it is attributable to glomerular hyperperfusion/hyperfiltration. However, data indicate that ACE inhibitors may induce ARF in some individuals (for review, see Textor (168)). Risk factors include preexisting renal impairment, particularly if it is caused by compromise of the afferent arteriolar blood supply, such as renal artery stenosis. Another unwanted effect of ACE inhibitors is hyperkalemia. Fortunately, in the overwhelming majority of cases, renal failure is reversible, and the benefits of ACE inhibitors appear to far outweigh the risks. These agents may also produce interstitial nephritis and are discussed in detail in Chapter 25.

HERBAL MEDICATIONS

The use of herbal therapies has increased over the past decade in the Western world, and much of the world depends on botanical medicines to treat a variety of health problems (169–172). A number of renal manifestations have been reported with these preparations. These include ARF, Fanconi syndrome, and hypokalemia or hyperkalemia; the focus here will be on tubular injury in this context. Botanical/herbal preparations are inconsistent in composition and effect and, in general, are poorly regulated (173). The use of traditional herbal remedies may underlie about 35% of all cases of ARF in Africa. ARF produced by herbal medications may be a result of direct tubular injury, but may also be part of a systemic reaction or due to interstitial nephritis or urolithiasis. Herbs known to cause ATI/necrosis include *Securida longepedunculata*, *Euphoria matabelensis*, *Callilepis laureola*, *Cape aloes*, *Taxus celebica*, and *Takaout roumia*. Adulteration of herbal preparations by dichromate may underlie toxicity in some cases. Fanconi syndrome has been described with Chinese herbs containing aristocholic acids or adulterated with cadmium (169). Urinary excretion of β_2 -microglobulin and other low molecular weight proteins is increased, and proximal tubular enzymuria has been described with aristocholate exposure (173–175). Cases caused by *Takaout roumia* (paraphenylenediamine) are often associated with rhabdomyolysis (176).

Pathology of Acute Renal Failure/Acute Tubular Injury

Gross Pathology

At a gross level, as a result of extensive interstitial edema, the kidneys become enlarged and swollen. The combined weight of both kidneys is usually increased by about 25% to 30%. On cut section, the tissue bulges above the cut surface and has a flabby consistency. The cortex is widened and pale. The outer medulla may appear as a deep red band, in contrast to the more pale cortex and papillary tip, the result of congestion of the vasa recta. Glomeruli appear as distinct red dots in the pale cortex.

Light Microscopy

ACUTE TUBULAR INJURY

Our understanding of the pathology of human ARF is incomplete, since many cases occur without renal biopsy (177). Autopsy kidneys, even if optimally harvested and processed, often have major preservation artifacts, especially in tubules. Also, premortem ischemia induces tubular injury that is difficult to discern from a previous in vivo insult. Biopsy with rapid processing provides the best histologic preparation, although it has inherent sampling errors. However, while less than ideal, many useful observations have been made with available tissue from cases of ATI.

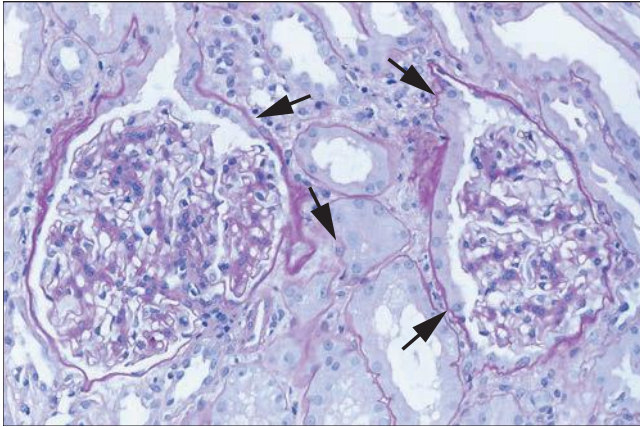


FIGURE 26.2 “Tubularization” of parietal epithelial cells lining the Bowman capsule (arrows). Reactive changes in the proximal tubule extend from the tubular takeoff to involve these epithelial cells, which have marked increase in cytoplasm compared to normal quiescent cells. (H&E; $\times 640$.)

The lesions in both ischemic and toxic ATI primarily involve the tubules; the glomeruli are spared, as indicated by the nomenclature (178). Although no significant changes occur in the glomeruli, the parietal epithelium of the Bowman capsule is often prominent (Fig. 26.2), apparently reflecting

reactive changes in the proximal tubule. Herniation of proximal tubular epithelium into the Bowman’s space is sometimes seen and may be the sole indicator of ATI when tubular epithelial changes are minimal. While these changes may be prominent, they are not specific. Glomeruli may show ischemic collapse, and the Bowman space may appear dilated.

Although “necrosis” has traditionally been included in the clinical term for ARF caused by tubular injury to distinguish this condition from other intrinsic causes of ARF (such as prerenal or postrenal failure or acute glomerular or interstitial nephritis), tubular epithelial cell death is often not evident by light microscopy (179). ATI is generally divided into two subcategories: postischemic ATI and nephrotoxic ATI. Morphologic changes of cellular injury are usually more subtle in the ischemic type, with more obvious cytopathologic changes in the toxic form. In addition, the sites of tubular damage along the nephron differ between the two forms (Fig. 26.3). In the ischemic form, tubular damage is patchy, affecting relatively short lengths of the straight segments of the proximal tubule and focal areas of the ascending limbs of the loop of Henle. In the toxic form, the tubular epithelial damage is more extensive along segments of the proximal tubule; the degree of involvement of the segments varies with the specific toxin. Although there is distal nephron damage, it is less extensive and more inconsistent in location than with ischemic ATI.

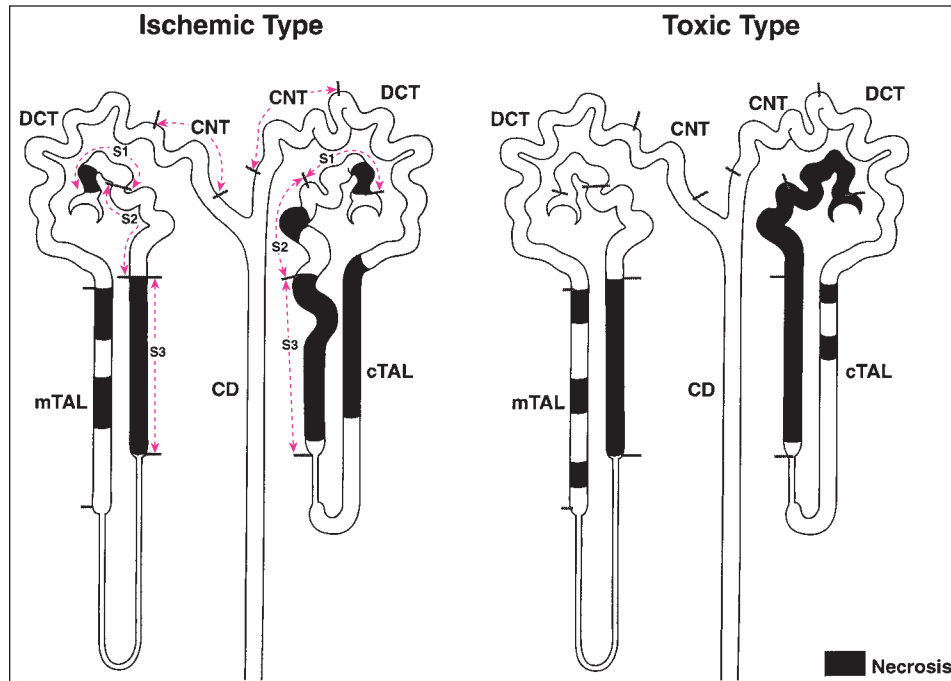


FIGURE 26.3 Cartoon demonstrating the difference in the distribution of lesions between ischemic and classic nephrotoxic tubular injury. In addition to differences in localization along nephron segments, different degrees of damage are visible between cortical and juxtamedullary nephrons. In the ischemic form, the S_3 segments are most severely affected, along with focal areas of the ascending limbs of the loop of Henle. The cortical nephrons show more extensive damage than the juxtamedullary nephrons. In the toxic form, tubular epithelial damage is more extensive. Whereas mercury shows some predilection for the S_3 segment, other heavy metals and organic toxins often show more extensive involvement of all nephron segments, also with a greater predilection for cortical nephrons.

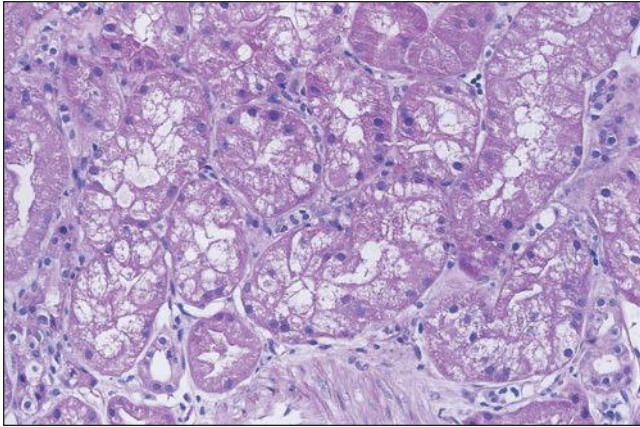


FIGURE 26.4 Tubular cells showing severe cell swelling, in some areas apparently obstructing the tubular lumen. (H&E; $\times 640$.)

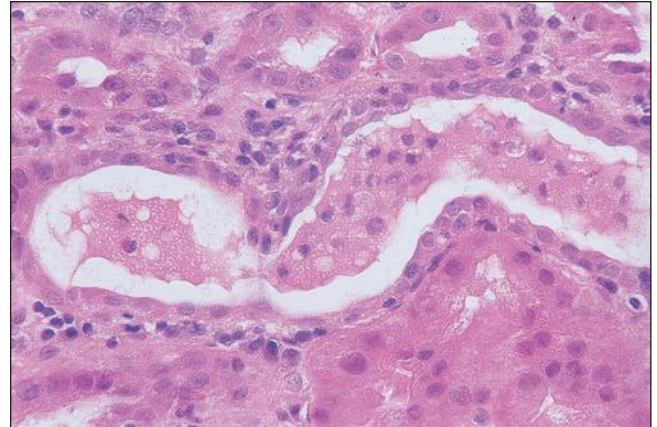


FIGURE 26.6 Intact exfoliated tubular cells in tubular lumen in a kidney with ischemic injury. (H&E; $\times 640$.)

ISCHEMIC ACUTE TUBULAR INJURY

The histologic picture varies with the severity of renal failure and the evolution of the lesion. Early in the course, cellular changes can range from minimal alterations to severe cell swelling (Fig. 26.4) to individual cell necrosis with denudation of the basement membrane (Fig. 26.5). With injury, there may be shedding of both viable (Fig. 26.6) and necrotic epithelial cells (Fig. 26.7) into the tubular lumen. Exfoliated epithelial cells, some viable, can be demonstrated in the urine (Fig. 26.8) (180).

In sections stained with periodic acid-Schiff (PAS), the brush border of proximal tubules is often thinned or absent. Blebs of apical membrane and intact cells shed from their basement membrane anchor are present in the lumen of the tubules (Fig. 26.9). Focal lesions of individual cell necrosis with disruption of the basement membrane also occur in

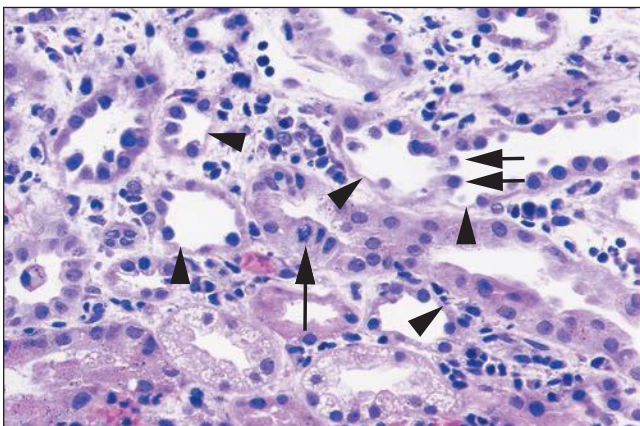


FIGURE 26.5 Areas of single tubular cell loss from a kidney with ischemic injury. Injured cells have detached, leaving areas of tubular basement membrane covered by a thin layer of cytoplasm from adjacent cells (*arrowheads*). A few detached cells can be seen in tubular lumina (*short arrows*). A mitotic figure can be seen in one tubular cell (*long arrow*). There are also interstitial edema and inflammatory cells largely marginating in capillaries. (H&E; $\times 400$.)

the ascending limb of the loop of Henle. Hyaline, granular, cellular, and/or pigmented casts are seen in the distal portions of the nephron and are often particularly prominent in the collecting ducts (Fig. 26.10). These casts consist of Tamm-Horsfall protein, which stains positively with PAS, mixed with cell debris (181). It is the relative prominence of these distal changes that gave rise to the term *lower nephron nephrosis*. In segments of the tubules that do not show significant necrosis, the tubules are often dilated and lined by flattened epithelial cells—so-called tubular simplification (Fig. 26.11). The denuded basement membrane sections are covered by proliferating adjacent viable epithelial cells. There may be evidence of transdifferentiation of tubular cells, which may express vimentin and other mesenchymal markers (Fig. 26.12). There is some evidence that transdifferentiated tubular cells may contribute to fibrogenesis in later stages (182).

As the lesion progresses after the initial injury, evidence of tubular regeneration can be seen. Histologic indicators of cellular proliferation, such as mitoses, hyperchromatic nuclei, and a high nuclear-cytoplasmic ratio, may be seen (Fig. 26.13). Recent studies using genetic fate-mapping techniques in mice after ischemia-reperfusion injury (IRI) showed that most of the injured tubule cells were replaced within 2 days through extensive proliferation by surviving neighboring cells (183). These results indicate that regeneration of injured tubule cells through proliferation of surviving tubule cells is the predominant mechanism of repair after ischemic injury (183). Proliferation can be demonstrated by staining for transcription factors (Fig. 26.14) and other markers.

The injured tubules are separated by sometimes markedly edematous interstitium. There may be a mild interstitial inflammatory infiltrate with small numbers of lymphocytes, macrophages, and neutrophils or, occasionally, eosinophils. The cellular infiltrate tends to be clustered around necrotic and ruptured segments of tubules or where Tamm-Horsfall protein has been extruded, forming small granulomas. It is in these late stages that distinctions have to be made between ischemic ATI and acute tubulointerstitial nephritis, but in general, the infiltrate is much less prominent in cases of ATI.

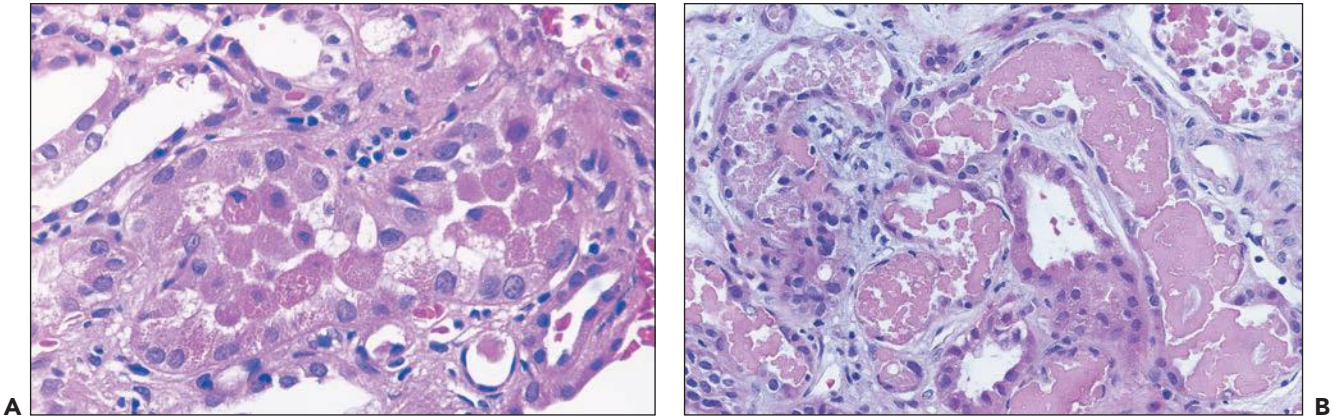


FIGURE 26.7 **A:** Detached necrotic tubular cells, several with pyknotic nuclei, in the lumen of proximal tubule. **B:** Granular casts with necrotic cell debris. Note flattened tubular epithelium in tubules containing necrotic debris. (H&E, $\times 640$.)

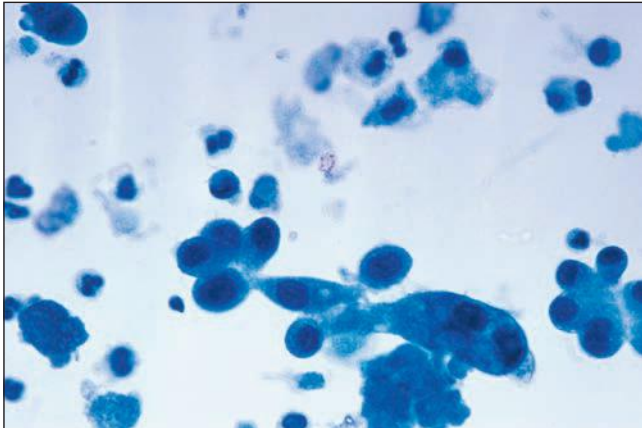


FIGURE 26.8 Intact tubular cells in the urine from a patient with ischemic injury. (Papanicolaou; $\times 1,000$.)

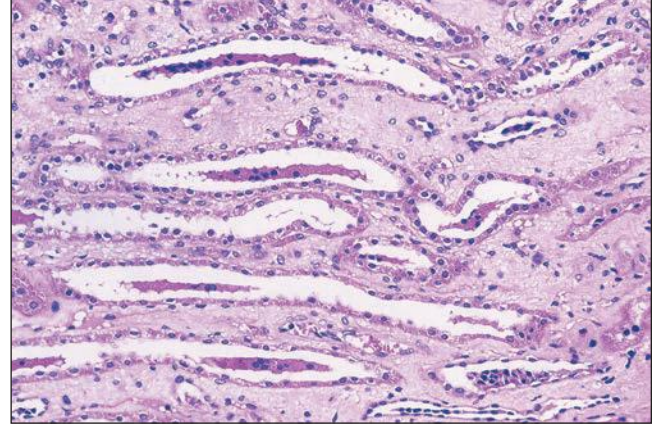


FIGURE 26.10 Tubular cell casts in collecting ducts in papilla. Injured cells have detached from sites in proximal nephron and aggregate into casts, often around a protein core. (H&E; $\times 400$.)

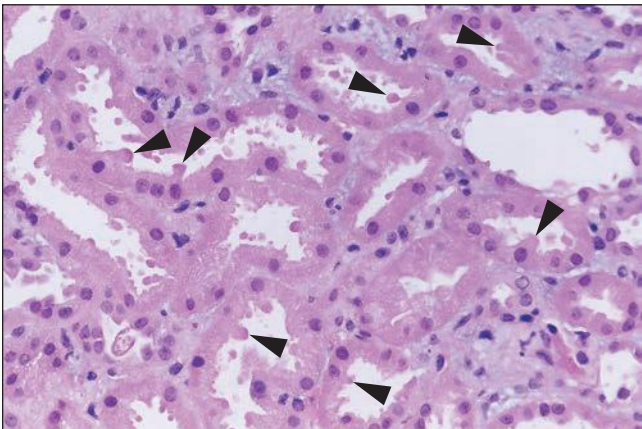


FIGURE 26.9 Apical blebbing from the surface of injured proximal tubular cells (**arrowheads**). Apical cytoplasmic blebs can be seen in tubular lumina. (H&E; $\times 640$.)

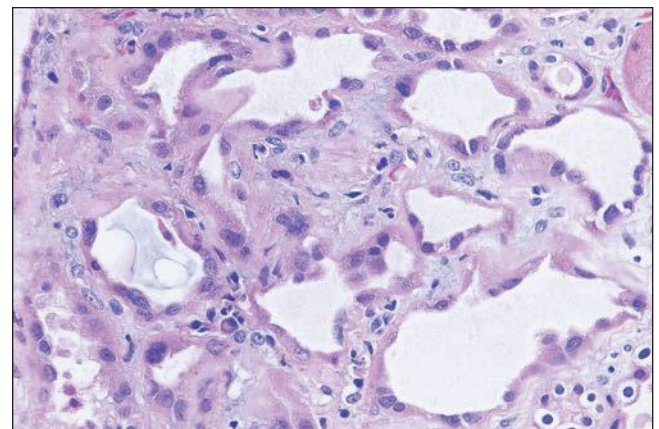


FIGURE 26.11 Dilated tubules with flattened epithelium in the regenerative phase after tubular injury. Marginating inflammatory cells can be seen in capillaries. (H&E; $\times 640$.)

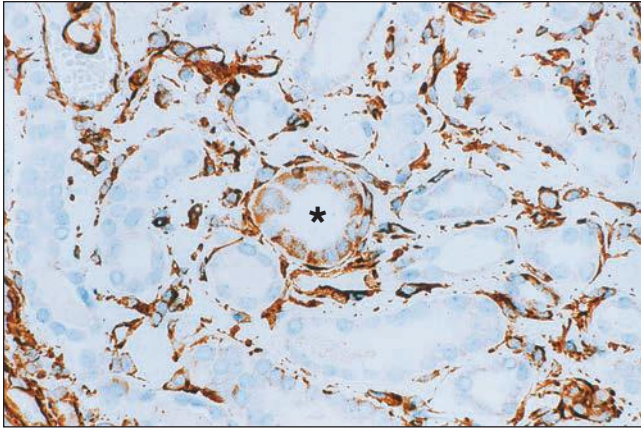


FIGURE 26.12 Injured tubule with cells staining for vimentin (*center*). Adjacent tubules do not stain. Note bright background staining for vimentin in interstitial areas. (Immunoperoxidase; $\times 400$.)

Tubular cell death during ischemia/reperfusion occurs via apoptosis as well as coagulative necrosis and has been documented both in animal models and in clinical renal disease (184–186). It is possible to detect the nuclear and cytoplasmic condensation of cells undergoing apoptosis by light microscopy. Apoptotic cells may appear triangular and may be extruded from the epithelium into the tubular lumen (Fig. 26.15). Apoptotic bodies, representing membrane-bound nuclear fragments, may also be detected in adjacent tubular cells, which have engulfed these cell remnants. However, the most reliable methods of detection are by nick end labeling (TUNEL) of the chromatin that has been cleaved in a characteristic “ladder” pattern by the endonucleases or by staining for apoptosis-associated markers, such as cytochrome c or apoptosis-inducing factor (AIF) (187). Coagulative necrosis is characterized by eosinophilic cytoplasm and pyknosis and eventual disappearance of nuclei (Fig. 26.16).

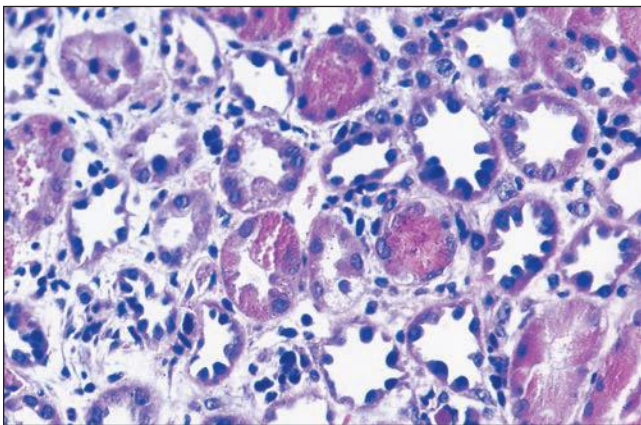


FIGURE 26.13 Striking regenerative changes in tubular cells, with pleomorphic hyperchromatic nuclei, with relatively little cytoplasm. (H&E; $\times 640$.)

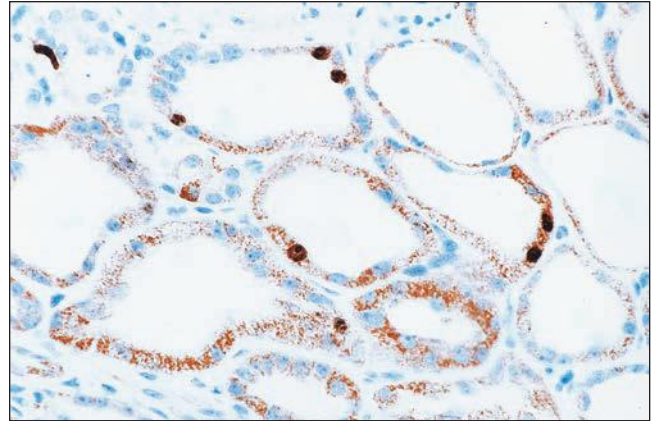


FIGURE 26.14 Immunostain for the transcription factor Ki-67. Note positive nuclear staining in several tubular cells. (Immunoperoxidase; $\times 640$.)

ATI in renal allografts can show changes similar to those found in native kidneys, but more frank necrosis of tubular cross sections may be seen, and calcium oxalate deposits may be numerous in renal tubules (188) (Fig. 26.17). The cellular lesions are most prominent in the S_3 segment of the proximal tubule and tend to be more uniform in character. Apical blebbing may be the only finding in milder forms, whereas the more severe cases also show focal necrosis with rupture of the tubular basement membrane. It is interesting to note that one study has shown a correlation of loss of Na^+, K^+ -adenosine triphosphatase (ATPase) polarity with delayed graft function (189).

Electron microscopy has been helpful in evaluating the tubular epithelial changes in ATI (190–192). In ischemic ATI, scattered epithelial cell changes show a variety of different cytopathic alterations. These include loss of the apical brush border; blebbing of the apical membrane, with shedding of apical membrane blebs into the tubular lumina; high-amplitude swelling, with condensation of the cristae of the mitochondria; individual cell apoptosis, as demonstrated by cell shrinkage

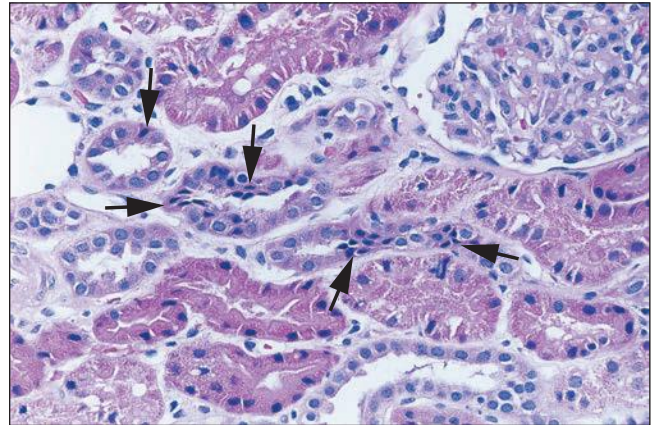


FIGURE 26.15 Focal tubular cell apoptosis, with condensed triangular cells in the epithelium (*arrows*), focally extruding from the epithelium. (H&E; $\times 640$.)

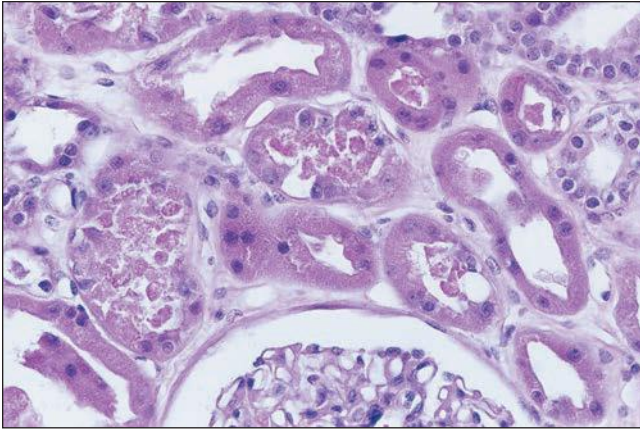


FIGURE 26.16 Coagulative necrosis of focal tubular epithelial cells, with cell debris in the tubular lumina. (H&E; ×640.)

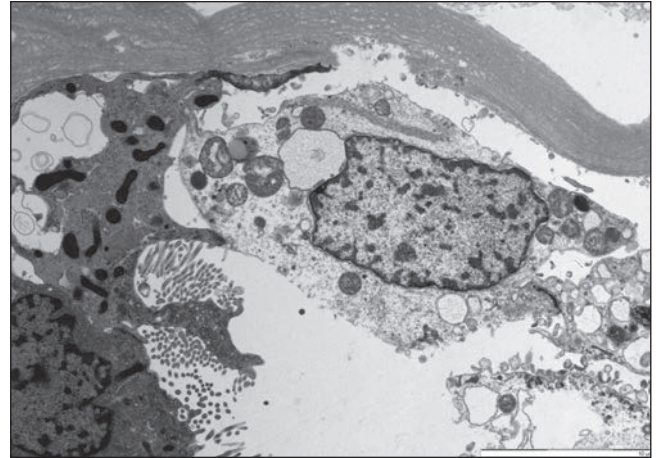


FIGURE 26.18 An electron micrograph shows a tubular epithelial cell in the process of desquamation into the lumen. The cell has separated from the basement membrane but is still adherent to the adjacent epithelial cell through the cell-to-cell junctions. (×3,000.)

with nuclear fragmentation; and a variety of other cytopathic changes leading to necrosis (Fig. 26.18). Detachment of tubular epithelial cells may be seen (Fig. 26.19).

Interstitial inflammation is seen as a response to tubular injury. This inflammation is typically mononuclear and patchy. There is often associated interstitial edema, which may be severe (see Fig. 26.5). A particularly interesting and useful finding in cases of ARF is the accumulation of nucleated cells in the vasa recta of the outer medulla (193,194). This is a very common feature, and in many cases, it is the only histologic clue to the diagnosis of ATI (Fig. 26.20). The nature of the cells changes with progression of the ATI through its three different phases. Lymphocytes are predominant in the first 24 to 48 hours, followed later by immature cells of the myeloid series and eventually by nucleated red cells and red cell precursors. The accumulation of the larger nucleated cells in this location may be merely a reflection of the hemodynamic shifts that occur in ATI, with shifting of blood flow away from the superficial and midcortical glomeruli to the juxtamedullary glomeruli, resulting in a relative increase in blood flow to this nephron population, which gives rise to

the vasa recta. The countercurrent nature of blood flow in the vasa recta would result in dilution of cellular elements as blood flows toward the hairpin turn, resulting in a concentration of cellular elements at the proximal end of the vasa recta vasculature in the outer medulla. There is also some evidence that up-regulation of adhesion molecules on ischemic endothelium leads to accumulation of leukocytes in the microvasculature, which may contribute to stasis and lack of reflow in ischemia-reperfusion injury (see section “The Inflammatory Response in Ischemic Injury”).

At the molecular level in AKI, in addition to transcription factors and markers of cell differentiation/transdifferentiation, there is altered expression of a range of proximal and distal gene products in kidney tissue sections, among which KIM-1 and NGAL are most prominently expressed (195–198). KIM-1 is primarily expressed at the luminal side of dedifferentiated proximal tubules (198). ER stress markers such as CHOP and GRP94 can also be identified in renal tissue in injured cells (199). Tissue (and urine) detection of fibrinogen

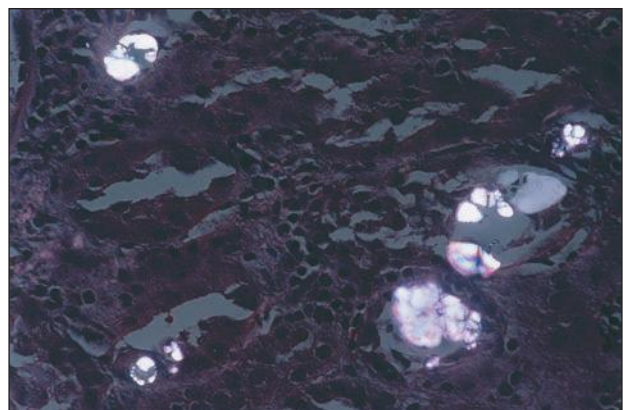
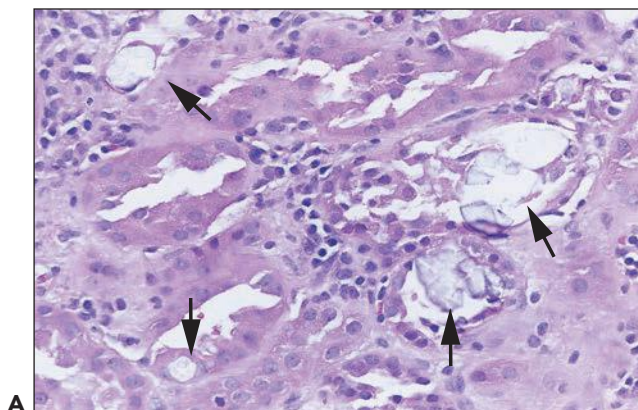


FIGURE 26.17 **A:** Oxalate crystal precipitates (arrows) in ATI in an allograft kidney. **B:** Oxalate crystals in polarized light. (H&E; ×640.)

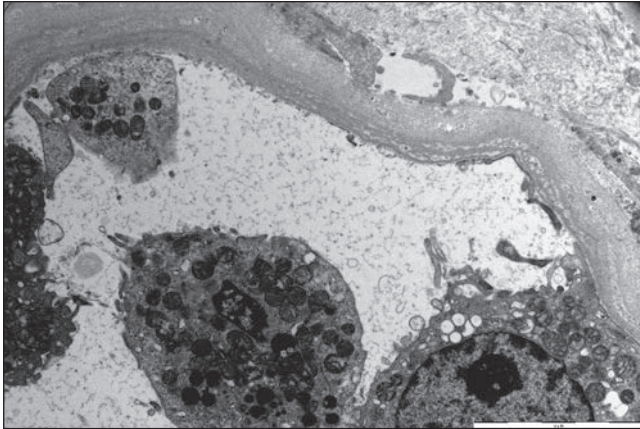


FIGURE 26.19 An electron micrograph demonstrates an area of loss of an array of tubular epithelial cells. ($\times 3,000$.)

has been proposed as a sensitive early marker of AKI, with markedly increased expression (199,200). The L-1 cell adhesion molecule has been identified as a potential biomarker of distal tubular injury in AKI, with loss of normal polarized distribution in the collecting duct, and induction of expression in medullary thick ascending limb and distal tubule with injury (201). Apoptotic cell death, difficult to detect by histology, can be detected in tissue using techniques such as terminal deoxynucleotidyl transferase dUPT nick end labeling (TUNEL) (201). An increase in progenitor cells (e.g., CD133+ CD24+ CD106- cells) can be identified in tissue sections by immunostaining as a correlate of injury (202). Other potential injury markers in tissues are described below in the section on “Pathophysiology.”

NEPHROTOXIC ACUTE TUBULAR INJURY

Tubules Classically, toxic tubular injury may be associated with extensive epithelial necrosis, which tends to involve all nephrons more uniformly than in the ischemic form. However, a range of morphologic changes may be seen in the renal tubules as the result of toxic injury. The extent and severity of the changes will vary depending on the agent, the dose, and the timing of the morphologic assessment. Renal tubular cell changes detectable by light microscopy include the following:

- Alterations in the surface of the cells, including loss of brush border (detectable on PAS), loss of basolateral infoldings, and blebbing of apical cytoplasm
- Cytoplasmic swelling and vacuolation
- Intracellular inclusions
- Extensive tubular cell necrosis
- Loss of individual tubular cells, with gaps along the tubular basement membrane or tubular profiles with fewer and attenuated cells lining the tubule
- Intraluminal proteinaceous cellular debris, casts, or crystals
- Tubular dilation with flattening of tubular epithelium
- Tubular rupture with urinary extravasation
- Regenerative changes, including flattening of epithelial cells, cytoplasmic basophilia, heterogeneity in cell size and shape,

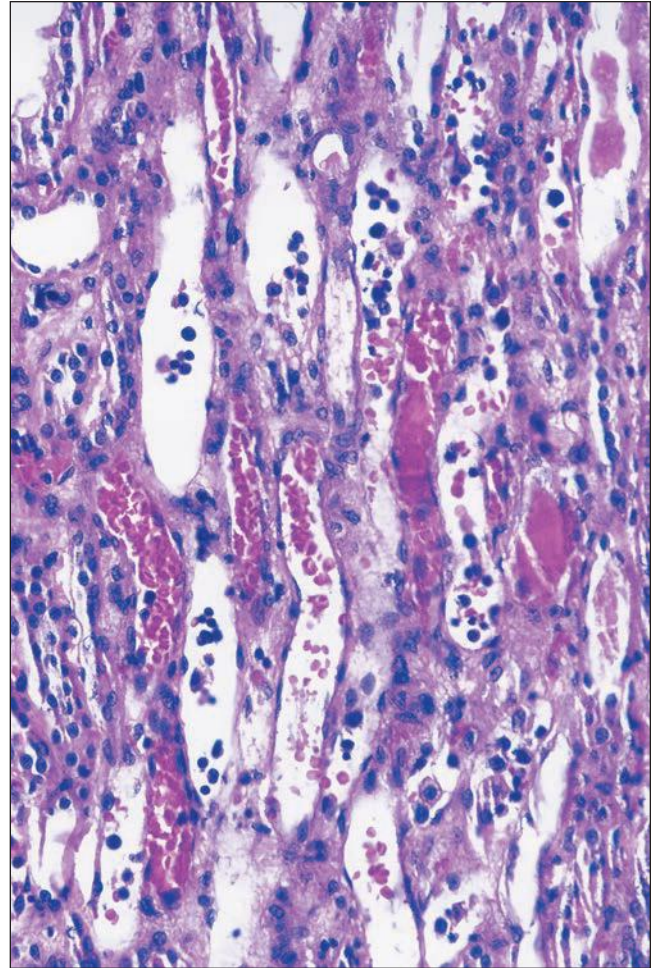


FIGURE 26.20 Erythrocyte congestion and nucleated cells in dilated vasa recta in the outer medulla of a kidney with ischemic injury. (H&E; $\times 400$.)

a higher nuclear-to-cytoplasmic ratio in individual cells, and cellular mitoses

Swelling and vacuolation of proximal tubular cells may be seen; cells appear large and pale and may contain discrete vacuoles of varying size. Hypertonic solutions, including IVIG preparations (203), have been reported to produce severe swelling and vacuolation of renal tubular cells. Intracellular inclusions are occasionally seen in renal tubular cells exposed to drugs. Giant mitochondria, appearing as bright eosinophilic inclusions, have been described after the administration of relatively high doses of CsA to humans. In gold-induced nephropathy, gold can be demonstrated in tubular cells (204). Calcification of tubular cells has been described in cases of severe toxicity caused by amphotericin or bacitracin (205).

Extensive coagulative necrosis of tubular cells has been seen in cases of poisoning by heavy metals such as mercuric chloride, rarely seen today, or in cases of poisoning due to chemicals such as diethylene glycol (206). More often, changes are more subtle, with individual tubular cell necrosis or loss, though there may be more obvious and extensive necrosis than is seen in ischemic

injury (207). It is clear that both necrosis and apoptosis occur in toxic nephropathies in experimental models as well as in clinical tubular injury (208,209). In vitro studies have documented apoptosis in cell culture on exposure to nephrotoxins. For example, LLC-PK1 cells exposed to sublethal doses of mercuric chloride in vitro undergo apoptosis (210), and apoptosis can be induced in Lewis lung cancer-porcine kidney-1 [LLC-PK1] cells by cisplatin as well via activation of caspases (211). Our understanding of the role of apoptosis in the pathogenesis of toxic renal injury has evolved over the past decade. ATI due to cisplatin therapy depends also partially on Fas-mediated apoptosis driven by Fas ligand (FasL) expressed on tubular epithelial cells (212). Moreover, cisplatin down-regulates the expression of the taurine transporter gene *TauT* in LLC-PK1 cells (213). Taurine is one of the organic osmolytes, which have important antiapoptotic properties in the kidney (214). The antiapoptotic function of organic osmolytes in kidney cells is mediated through suppression of efflux of proapoptotic molecules, such as cytochrome c, from the mitochondria.

Tubular casts, which may include cells and cell debris, are frequently seen with toxic tubular injury. In addition, tubular crystalline deposits are found in cases of renal toxicity produced by nephrotoxins. Anesthetic agents, including methoxyflurane and halothane, and antiretroviral agents such as indinavir may produce tubular crystalline deposits. Mechanical obstruction may also result from deposition of intratubular crystals in patients treated with sulfonamides or acyclovir. In addition, radiocontrast agents are uricosuric and oxaluric, and casts and birefringent crystals have been identified following administration of these agents. Uric acid lithiasis with tubular obstruction has been reported with phenylbutazone (215). Finally, pigmented casts may result from hemolysis in rare cases of fulminant drug reactions and with the rhabdomyolysis caused by cocaine.

Vessels Vessels usually show no remarkable features unless there is intercurrent disease. However, newer studies in experimental models have refocused attention on injury to the microvasculature, which may have been underappreciated in clinical specimens. Certainly, vascular congestion in the outer medulla with margination has been noted.

Electron Microscopy Electron microscopy of injured tubules reveals loss of brush border microvilli and basolateral infoldings in the proximal tubules. Cells may show rarefaction of the cytoplasm, with intracellular vacuoles and swollen organelles. Degenerative changes in mitochondria, including swelling and loss of cristae, loss of endoplasmic reticulum, or alterations in lysosomes, are often visible. Within the cells, membrane-bound structures consisting of concentrically arranged whorls of membrane may form, especially with exposure to aminoglycosides; however, these so-called myeloid bodies do not necessarily indicate toxicity.

Pathology of Specific Nephrotoxins

As a preface to this discussion, it should be recognized that it is often difficult to establish a pathogenetic link between a pathologic lesion and a particular drug or toxin. Several factors contribute to this uncertainty, including concurrent factors that may produce renal injury, such as administration of other potentially nephrotoxic drugs, lack of or inadequacy of morphologic data in reported cases, and the fact that some drugs may have multiple effects. Moreover, experimental models of

toxicity may not be relevant to a particular clinical context owing to interspecies variation and markedly different dosing of drug or toxin in these models. In general, we limit our discussion to those drugs for which toxicity has been well documented in humans by disappearance of toxic effects when the drug is withdrawn, recurrence of symptoms after readministration of the drug, or both.

A range of chemotherapeutic agents and other toxins may produce direct injury to the renal tubular epithelium. These agents are outlined in Table 26.2. The focus in this discussion is on primary toxic tubular injury, recognizing that secondary injury to the renal tubule may also occur with other types of toxic renal injury, including tubulointerstitial nephritis, hemodynamic changes, and vascular disease.

ANTIBIOTICS

There have been many reports of renal damage associated with antibiotic therapy. Some drugs are more nephrotoxic and can promote acute renal injury even with brief exposure. One such example is the aminoglycosides (especially neomycin), which are classic nephrotoxins. However, in many cases, there is an association, but the causative role of the antibiotic in the etiology of tubular injury cannot be firmly established. There are several reasons for this. First, the infection for which the drug is being used may damage the kidney directly or indirectly. Second, infections are frequently treated with several agents, making it difficult to implicate a particular drug. Finally, the paucity of renal biopsy studies makes it difficult to define the pathologic changes produced by individual drugs and the pathogenetic mechanisms involved in producing renal injury.

Antiviral Agents In experimental animal models and in humans receiving acyclovir, indinavir, or ganciclovir, renal histologic examination often shows drug crystals in tubules, especially collecting ducts, with dilation of tubules reflecting obstruction (54,55,216,217) (Figs. 26.21 and 26.22). In other cases, there may be tubular dilation and tubular cell injury without detectable crystals in the urine or kidney (218); crystals, of course, might be missed if relatively few collecting ducts are sampled. Proximal tubular injury has been described,

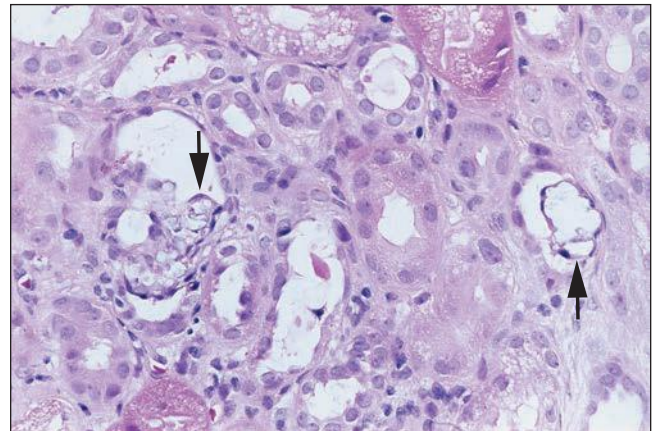


FIGURE 26.21 Crystalline precipitates (arrows) in tubules in a patient treated with intravenous acyclovir. (H&E; $\times 640$.)

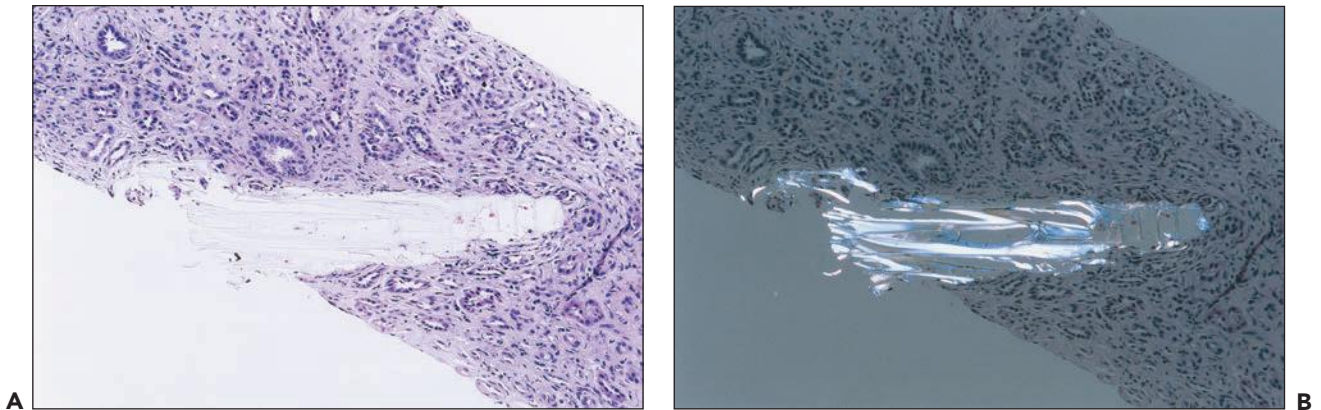


FIGURE 26.22 **A:** Indinavir crystal in papilla of a patient treated long term with highly active antiretroviral therapy. The patient also had crystals in the urine. **B:** Indinavir crystal under polarized light. (H&E; $\times 200$.)

especially with the nucleotide reverse transcriptase inhibitors adefovir and tenofovir, with degenerative changes, thinning and vacuolization of cytoplasm, loss of brush border, and even tubular cell necrosis, with nuclear changes reminiscent of viral inclusions (61,219–221). On electron microscopy, alterations in mitochondria have been observed, with swelling and dysmorphic changes. Changes include variable mitochondrial size, with some small and rounded and others swollen with irregular contours, clumping, loss and disorientation of cristae, and focal marked reduction of mitochondria (61). Giant mitochondria, in some cases, the size of nuclei, fuchsinophilic on trichrome stain but PAS- and silver-negative, may be seen in proximal tubular epithelial cells. Patchy interstitial inflammation has been described without crystals (222), and, occasionally, granulomas have been described. Renal tubular cell apoptosis has been detected in renal biopsy of a patient with irreversible cidofovir toxicity (223), and fibrosis and tubular atrophy have been described with tenofovir (61), with persistent renal dysfunction.

Aminoglycosides Aminoglycosides are classic nephrotoxic agents. Accumulation of high concentrations within lysosomes and release to the cell cytoplasm promotes phospholipid membrane rupture, oxidative stress, and mitochondrial injury. As a consequence, proximal tubule cells develop apoptosis and necrosis. The pathologic lesion most often reported with gentamicin is ATI (224), although in some cases, this lesion has been attributed to concomitant volume depletion and hypotension. Tubulointerstitial inflammation with tubular necrosis also has been reported (225). Myeloid bodies can be seen by ultrastructural examination in the tubular epithelium of patients receiving gentamicin, which predominantly reflect exposure to the drug (224) (Fig. 26.23).

Zager (226) has shown experimentally that gentamicin in a dose that does not by itself cause renal failure will trigger severe renal failure when combined with 1 hour of moderate renal hypoperfusion, which also does not produce renal failure on its own. In those studies, there was tubular necrosis in the S_3 proximal tubule segment, a pattern of injury characteristic of renal ischemia rather than gentamicin toxicity; this suggests that in some instances, gentamicin may worsen ischemic injury rather than causing injury to

the S_1 and S_2 segments, which is more typical of toxic doses of gentamicin (226).

There are few descriptions of renal pathologic lesions in patients receiving kanamycin or tobramycin. In one patient with oliguria who received 21 g of kanamycin over a 2-week period (227), a renal biopsy was done 25 days after the onset of oliguria (21 days after diuresis) and was reported to show some flattening of tubular epithelial cells.

In cases of ARF resulting from a combination of gentamicin and cephalothin, the pathologic features are those of ATI with normal glomeruli and vessels. However, experimental studies in the rat have found no potentiating effect of cephalosporins on gentamicin nephrotoxicity (228).

Amphotericin In human autopsy or biopsy specimens from patients treated with amphotericin, extensive calcification in tubules, presumably developing in the context of severe tubular cell injury, has been reported (229) (Fig. 26.24A). There may be vacuolation of smooth muscle cells in small arteries and arterioles (230) (see Fig. 26.24B). This is a change that potentially reflects direct toxic effects on the arterial wall, some element of intrarenal vasospasm, or both, and it may be very striking.

Cephalosporins Renal biopsies have been obtained in relatively few cases of cephalosporin-induced renal injury, usually in those in which the older cephalosporins were given. In cases of cephaloridine-induced ARF, biopsies have shown a picture of interstitial edema with variable numbers of chronic inflammatory cells accompanied by tubular dilation or necrosis (231). The renal histologic features in these cases showed what is described as ATI, with interstitial fibrosis or edema and infiltration by lymphocytes and mononuclear cells. Pathologic changes in cases induced by cephalothin with or without other potential nephrotoxins consist of interstitial edema with variable numbers of lymphocytes and plasma cells; necrosis, swelling, and evidence of regeneration of tubular epithelium; and only trivial glomerular changes (232,233). Vacuolation of tubular cells has been evident on electron microscopy (232). A case of bilateral renal cortical necrosis (RCN) associated with cefuroxime has been reported (234). ATI has been described in patients treated with cephalixin (77,78).

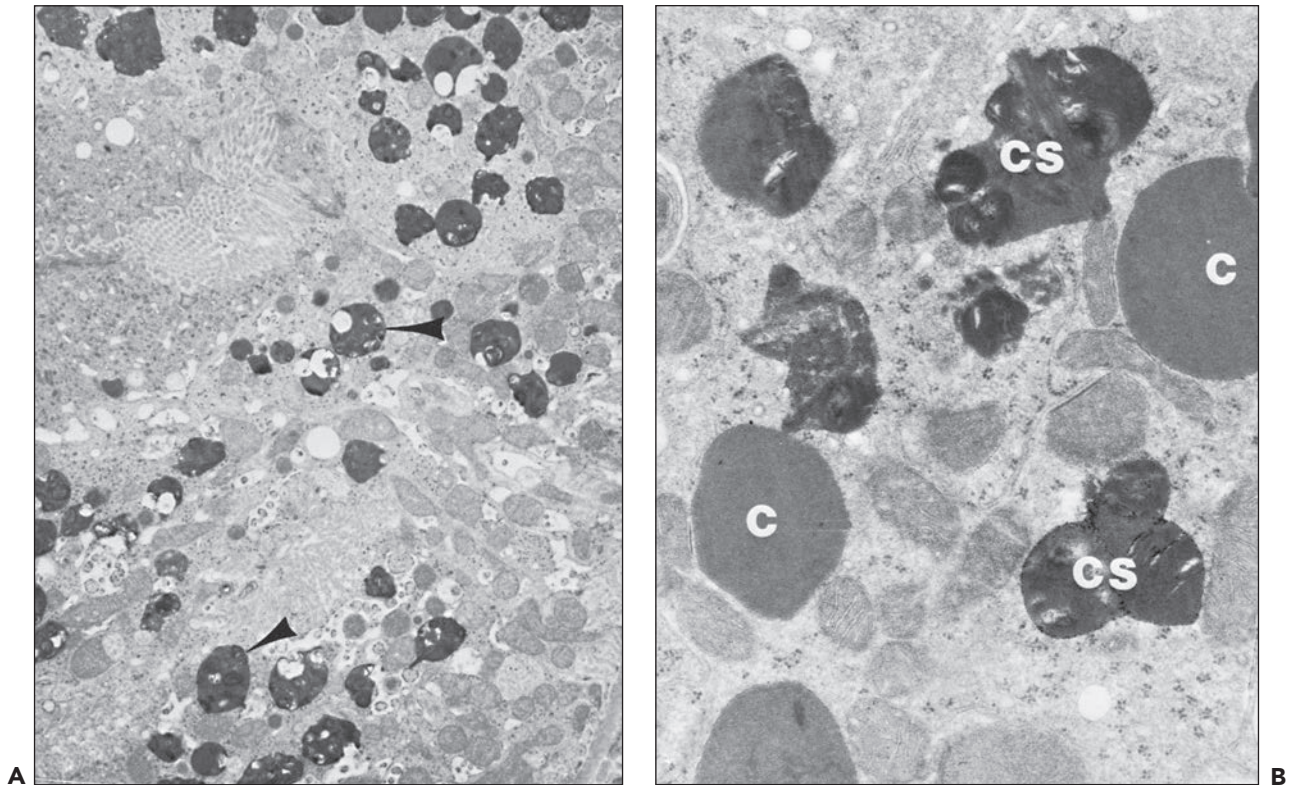


FIGURE 26.23 Electron micrographs of a rabbit killed 14 days after being given a high dose of gentamicin. **A:** Cytosegresomes (*arrowheads*) are scattered throughout the cytoplasm of the proximal convoluted tubule. The brush border can be seen at the top left ($\times 5,700$). **B:** Numerous cytosomes (C) and cytosegresomes (CS) are visible at higher power ($\times 2,800$) (lead citrate and uranyl acetate). (Courtesy of Dr. E. F. Cuppage.)

Polymyxin/Colistin On biopsy of patients treated with polymyxin, there is interstitial edema with eosinophils, plasma cells, lymphocytes, and, occasionally, neutrophils (235). The cellular reaction may have granulomatous characteristics. Tubules show swelling of the epithelium with intramuscular administration of colistin; the lesion described was ATI (236).

Vancomycin While ARF with vancomycin is associated with interstitial nephritis, acute tubulopathy has also been described. Acute tubular necrosis (ATN) with anuria has been described associated with vancomycin and one dose of aminoglycoside (237). Another case with biopsy-proven ATN has been described in a child (238). Another biopsied case in a

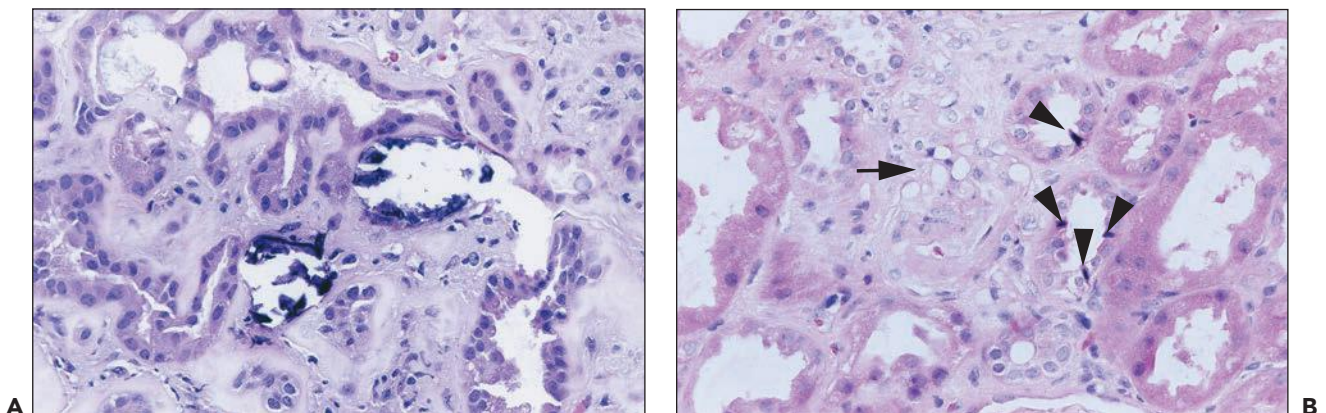


FIGURE 26.24 **A:** Calcification of tubular cells in a patient treated with amphotericin. **B:** Striking vacuolization of smooth muscle cells (*arrow*) in small vessels in the biopsy of a patient treated with amphotericin. Note apoptotic cells (*arrowheads*) in adjacent tubules. (H&E; $\times 640$.)

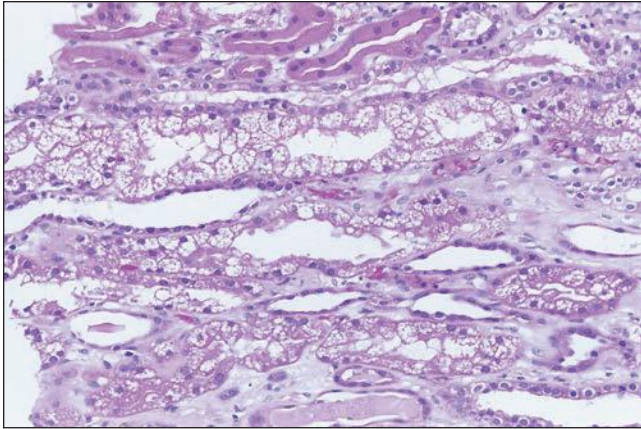


FIGURE 26.25 “Isometric” vacuolization, with many small equal-sized vacuoles in tubular cell cytoplasm, in a patient with high serum levels of calcineurin inhibitor. (H&E; $\times 400$.)

child with elevated vancomycin levels and ARF revealed focal tubular dilation with attenuation of brush border, hyaline casts, and one neutrophil cast without interstitial nephritis (239).

IMMUNOSUPPRESSIVE/IMMUNOMODULATORY AGENTS

Cyclosporine Functional CsA nephrotoxicity can occur without any morphologic changes. The most common morphologic change observed in the kidneys of patients treated with CsA is isometric vacuolation of the proximal tubular cells (Fig. 26.25); this change is characteristic but not specific. Other changes include tubular epithelial cell necrosis with or without calcification, inclusion bodies corresponding to giant mitochondria, and giant lysosomes (240). The megamitochondria and microcalcification in tubular cells of CsA-treated patients do not correlate with dysfunction (241). Strong staining for osteopontin protein and mRNA has been demonstrated in tubular epithelium in clinical CsA toxicity (242).

Vessels in CsA-induced acute renal dysfunction may show only vasospasm and vacuolation of smooth muscle cells, changes that often reflect vasoconstriction. The onset of hyaline arteriolar thickening, especially with nodular accumulation of hyalin in the periphery of the arteriolar wall, has been associated with CsA-induced renal dysfunction, although dysfunction can also exist without this change. The juxtaglomerular apparatus may be hyperplastic; this finding is significantly more prominent in renal transplant patients with CsA nephrotoxicity than in other posttransplant groups, probably indicating activation of the renin-angiotensin system (243). Thrombotic microangiopathy may be seen in particularly severe cases of toxicity.

Descriptions of the pathologic characteristics of both clinical and experimental long-term CsA toxicity have focused on interstitial fibrosis and tubular atrophy, which appears in a “striped” pattern reminiscent of ischemic injury, and hyaline arteriolar change, as described earlier. The fibrosis involves medulla and medullary rays in the cortex (244). Bertani et al. (245) have reported the renal biopsy changes observed in cardiac allograft recipients with renal failure after they had received cyclosporine for 31 to 48 months. Obliterative arteriopathy with ischemic glomerular changes was found. Serial reconstruction of the glomeruli showed the presence of populations of both abnormally small and abnormally large glomeruli. Sclerotic

lesions were confined to the small glomeruli. Myers et al. (246) and Morozumi et al. (247) have also emphasized sclerosing glomerular changes with long-term CsA therapy. The pathologic findings and the differential diagnosis of CsA nephrotoxicity in renal transplant recipients are discussed in detail in Chapter 29.

Tacrolimus Pathologic changes owing to FK506 are very similar to those described for CsA. Changes include tubular cell vacuolization, calcification, myocyte vacuolization, necrotizing arteriolitis, thrombotic microangiopathy, arteriolar hyalinosis, and interstitial fibrosis. Morphologic changes with FK506 toxicity have been compared to those produced by CsA (248,249). Tubular cell vacuoles were small and focally confluent and involved proximal and distal tubules. Morozumi et al. (249) have suggested that FK506-related vacuoles are foamy and nonisometric and present in straight and convoluted portions of the proximal tubules. We have noted involvement of tubules in outer medulla as well (unpublished).

Glomerular capillary and arteriolar thrombi have been seen in renal allograft recipients (250,251) and a few kidney/liver allograft recipients (250). In several of these cases, other factors, including prior CsA therapy in three cases and fungal sepsis in a fourth case, may have contributed to the endothelial injury underlying thrombosis. An HUS-like syndrome with thrombotic microangiopathy may be seen (Fig. 26.26); the estimated incidence is approximately 1% (251), and cases are frequently associated with high serum levels of drug. Hyaline arteriolar change and interstitial fibrosis have been reported with long-term therapy (240).

An increase in BUN and sCr has been documented in rats treated with FK506, with evidence of proximal tubular cell vacuolation and megamitochondria on histologic examination (249). Pathologic changes, including proximal tubular cell vacuolation and tubular regeneration similar to those reported with CsA therapy, also have been reported in canine allografts (252). Stillman et al. (253) developed a rat model of prolonged FK506 toxicity by combining FK506 with a low-salt diet for 6 weeks. In this model, sCr and plasma renin levels were elevated, and there was tubular atrophy and fibrosis in

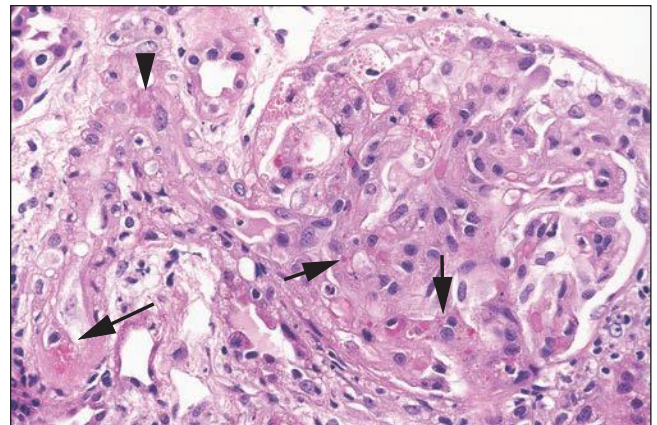


FIGURE 26.26 Thrombotic microangiopathy in a patient on tacrolimus. Note the arteriole with very focal intramural fibrin (*arrowhead*), focal erythrocyte extravasation into the intima (*long arrow*), and focal erythrocyte fragmentation in the glomerulus (*short arrows*). (H&E; $\times 640$.)

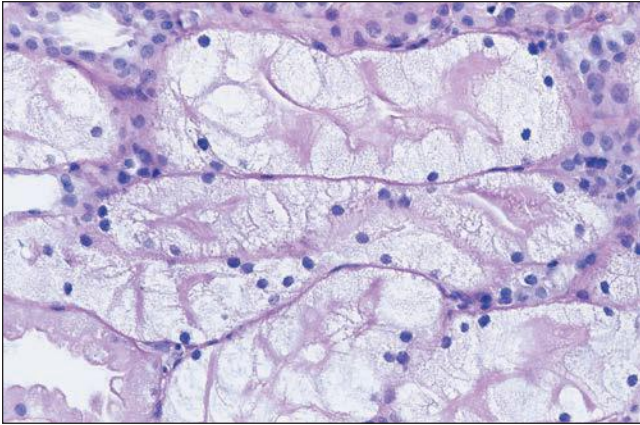


FIGURE 26.27 Severe cell swelling of tubular cells in the biopsy of a patient being treated with IVIG. Note persistence of brush border. (H&E; $\times 640$.)

medullary rays and the inner stripe of the outer medulla. Tacrolimus alone produced increased juxtaglomerular apparatus granularity.

Intravenous Immunoglobulin Intravenous administration of immunoglobulins has been associated with severe swelling of tubular epithelial cells (254) (Fig. 26.27). Of note, the brush border of the cells is generally well preserved. Swelling may be severe enough to occlude the tubular lumen. In one series of transplant patients, isometric vacuolization appeared to precede the more severe cell swelling (255).

Sirolimus Rats given sirolimus (3 mg/kg orally) for 2 weeks on a low-salt diet developed magnesium wasting and structural renal lesions consisting of tubular collapse, vacuolization, and nephrocalcinosis (248). ATI has occasionally been described in patients (128). In one study of sirolimus-treated patients (also on FK506), there was a subset that developed striking intratubular cast formation, reminiscent of myeloma cast nephropathy (125). Vascular changes and glomerular disease have been reported with sirolimus. Some reports have appeared that sirolimus may delay recovery from tubular injury, exacerbate acute FK506 tubular cell toxicity (125,128), or exacerbate chronic calcineurin inhibitor toxicity.

CHEMOTHERAPEUTIC AGENTS

Cis-Platinum In the human kidney, focal necrosis of tubular cells is seen, primarily in the distal tubule and collecting ducts; cast formation and dilation of proximal tubules may be observed (256). In animals, tubular changes are found in the proximal nephron, with or without accompanying distal changes (257). Many patients show continuing damage and fail to regain pretherapy levels of renal function. Dobyen et al. (258) studied the effects of chronic administration in animals and found cyst formation, interstitial fibrosis, and tubular atrophy.

Other The pathologic picture produced by the alkylating agent ifosfamide is that of ATI or chronic tubulointerstitial changes (259). On pathologic examination of kidneys from patients with toxic injury caused by streptozotocin, there is ATI in the proximal tubules, with or without accompanying interstitial inflammation (142).

RADIOCONTRAST AGENTS

Because renal biopsies are not indicated in patients with transient renal failure after contrast media administration, human studies are scant. Patients who undergo biopsy are those who do not recover from renal failure, and in most of these cases, the histologic picture reveals an underlying (and most likely pre-existing) renal disease. The majority of publications describing renal morphologic changes are based on experimental studies. The induction of renal failure in experimental animal models usually requires administration of additional agents (e.g., indomethacin, gentamicin, glycerol), ischemia, water or salt depletion, or a combination of these factors (225,260–263).

The overwhelming majority of both experimental and clinical studies report variable, transient proximal tubular vacuolation, which appears as soon as 30 minutes following administration, disappears within a few days (264,265), and seems to be dose dependent (266). One study emphasizes the selective injury of the thick ascending limb of Henle in the outer medulla after coadministration of indomethacin and iohalmeate to unilaterally nephrectomized, salt-depleted rats (225). They describe mitochondrial swelling, pyknosis, cytoplasmic disruption, calcification, necrosis, and tubular collapse in the thick ascending limb of Henle in areas away from vascular bundles, suggesting hypoxic injury. They also report vacuolation of the proximal convoluted tubules.

Ultrastructural studies indicate that the vacuoles are membrane bound, probably representing lysosomes (225,264). The fine structure of the mitochondria and the endoplasmic reticulum remains intact. Tervahartiala et al. (264) believe that the vacuolation is caused by a nonspecific lysosomal injury and is not the consequence of osmotic diuresis. Autoradiographic and electron microscopic studies failed to demonstrate the presence of iodinated molecules within the vacuoles (225,267).

The most extensive studies in human beings come from the Necker Hospital in Paris, where radiocontrast examination of the kidney was routinely performed before renal biopsies in the 1970s (265,267). This group published the case studies of 211 patients who underwent biopsy within 10 days of urography or renal arteriography using ionic contrast media (267). Tubular vacuolation characteristic of “osmotic nephrosis” was found in 47 patients and was more severe in patients with pre-existing renal failure; however, they did not find a correlation between the extent of tubular vacuolation and the degree of renal functional impairment. The same group later described osmotic nephrosis in 14 of 33 patients who received low-osmolality contrast media before renal biopsy (267). They reported the case of one patient who had evidence of ATI on initial biopsy and showed signs of advanced tubular atrophy and interstitial fibrosis on a second biopsy. Other patients in the Necker Hospital also had evidence of ATI in the renal biopsy, but it appears that these patients had ARF as a preexisting condition. They concluded that tubular vacuolation after radiocontrast administration probably does not represent true osmotic nephrosis and that it is not a reliable morphologic indicator of RN (267).

In 1970, two articles described hemorrhagic necrosis, primarily of the renal medulla, in six infants (268,269). Five of them underwent cardiac catheterization for heart problems, and one had excretory urography because of a flank mass. In these children, there were several confounding variables that might have contributed to the renal necrosis, such as seizures, cardiac developmental abnormalities, and sepsis. All six children died. Although

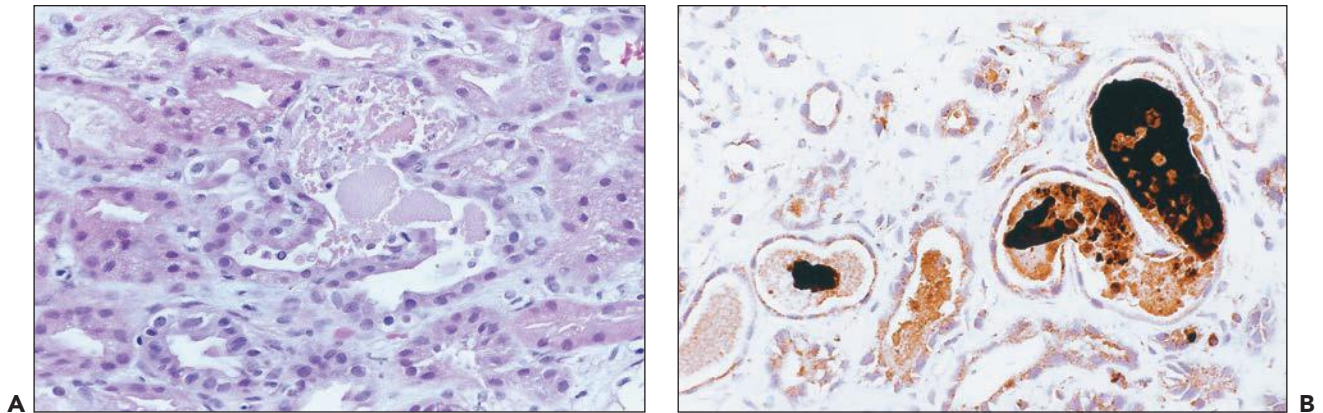


FIGURE 26.28 Pigmented casts in the tubular lumina of a biopsy from a patient with ARF who had overdosed on cocaine. **A:** Light microscopy. (H&E; ×640). **B:** Immunostain for myoglobin. (Immunoperoxidase; ×640.)

ATN has been reported only rarely in patients (265,267,270), recent studies have shown that radiocontrast agents induce apoptosis in proximal tubule cells (271). Increased ceramide synthesis, which stimulates apoptosis, is an important contributing factor to radiocontrast-mediated nephropathy (272).

NARCOTICS AND MYOGLOBINURIC ACUTE RENAL FAILURE

The characteristic finding is the presence of pigmented casts, as in other forms of myoglobinuric ARF. Renal biopsy is rarely performed in affected patients, and for this reason, pathologic reports are uncommon (273,274). The characteristic casts show mild brown pigmentation and usually have a granular appearance with irregular globules. These casts are frequently bright red as seen by trichrome stain. Immunohistochemistry is helpful in identifying myoglobin casts (Fig. 26.28). Hyaline and granular casts not containing detectable myoglobin may be present. Other features of ATI, such as tubular epithelial damage with exfoliation of tubular epithelial cells, thinning of the tubular epithelium, and tubular calcification, are usually noted. Immunofluorescence is typically not helpful. On ultrastructural examination, the myoglobin casts frequently consist of very electron-dense, finely granular globules that may have a somewhat less electron-dense rim (Fig. 26.29). In addition, electron microscopic signs of ATI are readily visible.

ANESTHETICS

The renal lesion consists of interstitial edema with somewhat dilated tubules lined by flattened epithelium. In several cases, a striking degree of intratubular collection of oxalate crystals has been reported (275).

HERBAL MEDICATIONS

There are relatively few reports of biopsy findings in ARF caused by herbal medications. ATI has been described (reviewed by Isnard Bagnis et al. (169)). Pathology of the kidneys in patients with renal failure caused by *Aristolochia* species has shown hypocellular interstitial fibrosis and tubular loss, especially in the outer cortex, in lesions obtained later in the course of the injury (276).

Etiology and Pathogenesis

Although the number of disease entities that have been associated with ATI is large, the basic etiologic factors are very similar

(Table 26.3; Fig. 26.30). Prolonged renal ischemia is the most common cause of ATI (277–279). In the hospital setting, it is frequently associated with major surgery, with extensive trauma such as crushing injuries and burns, or severe congestive heart failure and septic shock (280,281). The widespread use of nonsteroidal anti-inflammatory drugs (NSAIDs), which inhibit renal prostaglandins, is another potential mechanism through which renal ischemia can be initiated, and these drugs have been associated with the development of ARF, particularly in patients who are volume depleted or dehydrated.

The second major category of etiologic agents of AKI is exposure to nephrotoxic drugs. The kidney is uniquely susceptible to toxic injury, because it is the principal excretory organ of the body. Since metabolism and excretion of exogenously administered therapeutic and diagnostic agents are major functions of the kidney, the ingestion of drugs is significantly associated with kidney injury. A number of therapeutic agents have known nephrotoxic potential. Classic examples include antimicrobial agents, chemotherapeutic agents, analgesics, and immunosuppressive agents (44,65,282–286). A problem that has been observed in developing countries is the contamination of commonly used drugs by nephrotoxins during their preparation under less than stringent conditions. Examples include the sudden occurrence of unexplained ARF in children in Pakistan and Haiti, where the cause was found to be contamination of the liquid vehicle of paracetamol with diethylene glycol (287,288). Interaction of herbal products with conventional drugs is also a potential source of toxicity. Examples of nephrotoxic herbal products include aristolochic acid, *Ephedra* species, and *Glycyrrhiza* species (169,289). Adulteration of food products may be another cause of kidney injury. One example is the addition of melamine to baby formula to increase the protein content, which caused AKI and nephrolithiasis in neonates (290). In many cases involving the use of diagnostic and therapeutic agents, the known risk of nephrotoxicity is outweighed by the clinical benefits of using the drug. While the range of injurious compounds is diverse, there are a limited number of patterns of injury produced in the kidney; the focus of this section will be on agents and specifically drugs that produce ATI.

ARF in the newborn may have a prenatal onset associated with maternal hypotension or occur in the setting of congenital diseases, such as renal dysplasia or polycystic kidney disease (279).

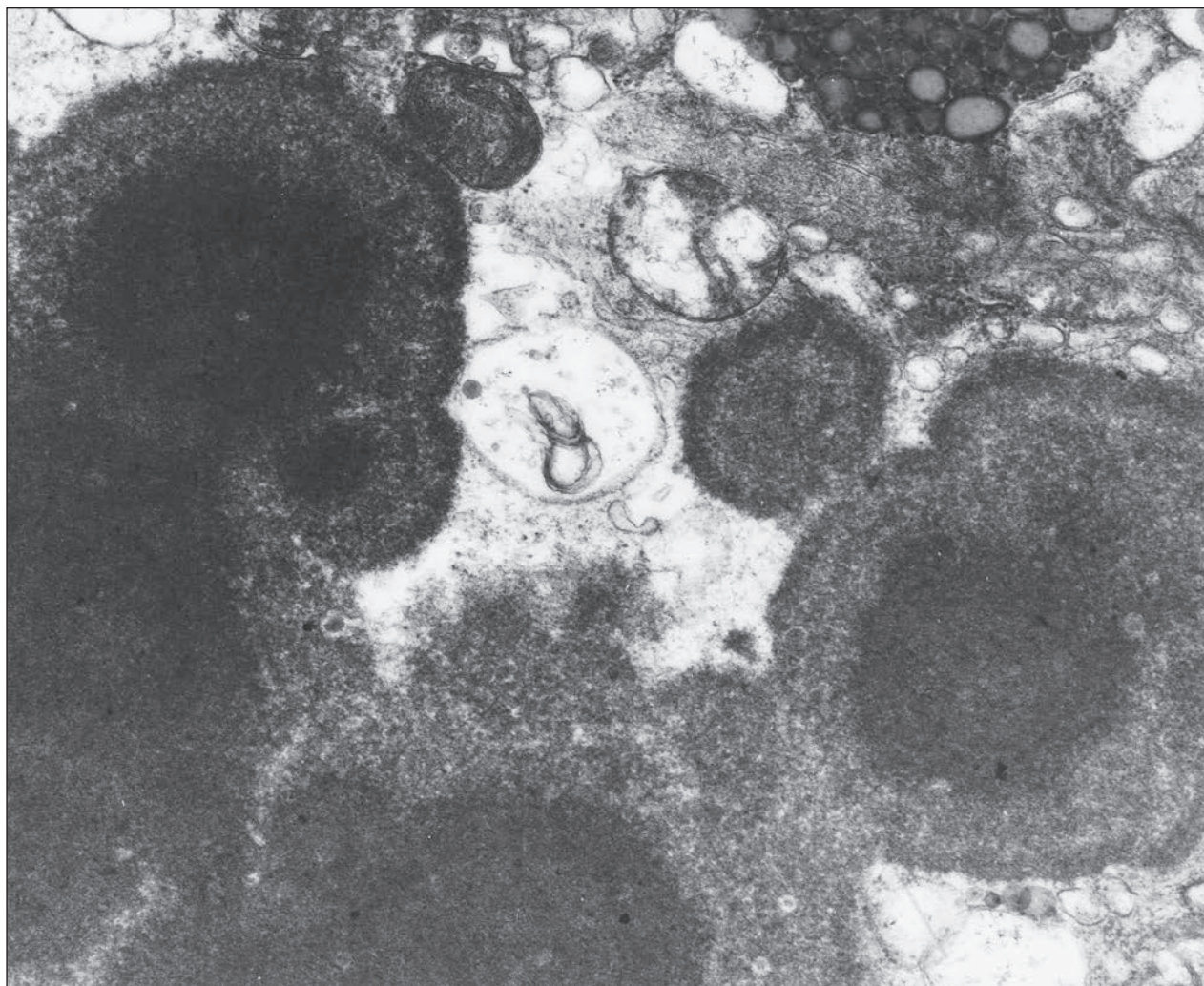


FIGURE 26.29 Ultrastructure of a myoglobin-containing granular cast. Note the electron-lucent periphery relative to the dense core and rim. (Uranyl acetate and lead citrate; $\times 33,800$.)

In the postnatal period, hypoxic/ischemic injury and toxins are the most common etiologies. Toxic ARF is most commonly associated with administration of aminoglycoside antibiotics and NSAIDs given to close a patent ductus arteriosus. Decreased renal function can be documented in about 40% of premature infants receiving indomethacin; the decrease is usually reversible.

In hospitalized patients, ATI/ARF often occurs in the setting of both ischemic and toxic insults. Multiorgan failure, with or without sepsis, is a common scenario. Incidence of ARF increases with enhanced severity from moderate sepsis to septic shock with positive blood cultures (291,292). Clinical course and outcomes will be determined by multiple clinical factors and “cross-talk” between and among affected organs (293) (see Section Acute Renal Failure in Sepsis). ARF occurring in the critically ill has a significant impact on morbidity and mortality (294).

Much of our understanding of ATI and ARF has derived from experimental models, and extrapolation to human ARF may be problematic (295,296). This likely underlies the failure of various therapeutic agents defined in animal models to have clinical efficacy (297). Although they are imperfect, experimental models have provided important insights. New techniques,

including imaging studies, may enable more precise definition of mechanisms of ARF in vivo (298). The rarity of renal biopsies in this setting has contributed to the difficulty of defining the pathobiology in humans (177). However, new techniques will likely make it possible to more precisely define mechanisms in clinical ARF in the future. Micro-magnetic resonance imaging techniques may ultimately be useful in assessing tubular cell function. Detection of renal inflammation may also be possible using these techniques (299). Imaging of subcellular processes, including apoptosis, enzyme markers, and cell pH and calcium, may ultimately be widely applicable in vivo (41–43,298).

Ischemia

MECHANISMS OF INJURY AND CELL DEATH

Alterations in cellular metabolism underlying ischemic cell injury in the kidney are analogous to those in ischemic injury in other organs and have been directly related to the severity of changes in renal cell structure and function regardless of the cause of ATI. Ischemia and reduced oxygen delivery to highly metabolically active tubular epithelial cells reduce oxidative metabolism and cell stores of high-energy phosphate

TABLE 26.3 Causes of acute renal failure

Causes	Examples
Prerenal azotemia (renal hypoperfusion)	Cardiogenic shock, hemorrhage, gastrointestinal loss
Decreased cardiac output	
Diminished intravascular volume	
Postrenal azotemia (obstructive uropathy)	Stone, clot
Intraureteric obstruction	Tumor, fibrosis
Extraureteric obstruction	Urethral occlusion, prostatic disease
Lower urinary tract obstruction	
Renal causes of ARF	
Glomerular/vascular disease	Glomerulonephritis, malignant hypertension, scleroderma, thrombotic thrombocytopenic purpura, emboli, arterial/venous occlusion
Interstitial disease	Drug induced, hypercalcemia, hypokalemia, pyelonephritis, papillary necrosis
Intrarenal tubular occlusion	Crystal (uric acid, oxalic acid), protein (myeloma) deposition
ATI	
Ischemic injury	Severe trauma, aortic cross-clamping, hemorrhage
Nephrotoxic injury	Aminoglycosides, contrast material, heavy metals
Pigment associated	Myoglobinuria, hemoglobinuria

compounds. Reperfusion with return of oxygen delivery enhances generation of oxygen free radicals, with resultant damage to cell components. An increase in intracellular calcium ion related to membrane injury enhances activation of injurious enzymes such as proteases and phospholipases. To some extent, these changes are reversible, but if severe or prolonged, they result in cell death. Definition of molecular mechanisms is a very active area of investigation; some major findings are outlined in the following sections (see Fig. 26.30).

A great deal of attention has focused on alterations in cellular polarity and cytoskeletal assembly that occur as a consequence of renal ischemia; these have been viewed as critical factors in the loss of normal renal epithelial structure and function. Several laboratories have verified that the polar distribution of Na^+, K^+ -ATPase is directed to and maintained in its basolateral location by an interaction with the cortical cytoskeletal proteins ankyrin and fodrin (300). Cellular components involved in the establishment and maintenance of cell polarity include proteins associated with organizing and maintaining cell-to-cell contact, such as E-cadherin, zonula occludens-1 (ZO-1), β -catenin, and other novel proteins at the lateral membranes of the cell and integrins at the basal portions of the cell, where cell-matrix interactions occur (301,302). All of these components have been shown to have interactions with the actin-based cytoskeleton, which may coordinate interactions of the different membrane domains. In the intact proximal

tubule epithelium, actin is primarily associated with the circumferential terminal web of the apical pole. In vivo renal ischemia results in redistribution of actin throughout the cytoplasm, with loss of its interactions with other cytoskeletal components and membrane domains. Indeed, assembly and disassembly of actin filaments are the central steps of actin-dependent cellular processes, such as maintaining cell polarity, cell-cell adhesion, signal transduction, and ion channel activation (303,304). After intracellular ATP depletion in cultured cells, there is a disruption of the actin cytoskeleton and conversion of polymeric filamentous actin (F-actin) to monomeric G-actin with redistribution of residual F-actin from the membrane surface to a perinuclear and cytosolic location (305). Both renal ischemia in vivo and intracellular ATP depletion in vitro induce disruption of this cytoskeletal complex with relocation of apical and basal lateral membrane-specific proteins and lipids into alternate membrane domains (306,307).

The apical microvillar surface of proximal tubule cells is especially sensitive to ischemic insults. After as little as 5 minutes of ATP depletion, there is loss of polarity, degeneration of the microvillar F-actin core with internalization, and blebbing of the apical brush border membranes (305). Renal ischemia in vivo results in increased solubility of Na^+, K^+ -ATPase in rat renal proximal tubule cells, indicating disassembly from the cortical cytoskeleton. Shortly thereafter, basal lateral Na^+, K^+ -ATPase migrates from the basal lateral to the apical membrane. The alterations in cytoskeleton and Na^+, K^+ -ATPase redistribution stemming from ATP depletion result in loss of Na^+, K^+ -ATPase activity and the normal sodium and potassium gradients across the cell. The influx of sodium in conjunction with cytoskeletal disruption results in cell swelling, which has been proposed to also contribute to renal dysfunction (308). Moreover, the mislocation of the Na, K -ATPase leads to increased Na delivery to the distal nephron, which further decreases GFR through the tubuloglomerular feedback mechanism.

The actin-binding protein family of ADF/cofilin proteins plays a critical role in the breakdown of the apical microvilli in response to ischemia (309,310). Ischemia induces rapid activation and relocation of ADF/cofilin from the cytoplasm to the apical cell membrane and membrane-bound vesicles in proximal tubule cells (310). These vesicles shed into the tubular lumen where they aggregate and cause obstruction, leading to increased intratubular pressure and subsequent decrease in GFR.

Reactive oxygen species (ROS) have been implicated as important effectors of cell injury in a variety of systems, including the kidney. Following ischemic injury, ROS generated by the injured tubular epithelium can induce perturbations in cytoskeletal structure and function that largely stem from reduction in ATP levels. ROS contribute to impaired ATP synthesis through several mechanisms. The activation of DNA repair enzyme poly(ADP-ribose) synthetase depletes cellular NAD (311). ROS also compromise mitochondrial respiration and function by impairing the ATP-synthetase complex and other components of the oxidative phosphorylation pathway (312). Moreover, ROS have been shown to act as signal transduction molecules in the regulation of gene transcription and in the activation of transcription factors such as nuclear factor- $\kappa\beta$ (NF- $\kappa\beta$) and activator protein-1 (AP-1), which may lead to cell and tissue pathology (313,314). ROS are also generated by infiltrating leukocytes (315). There is further evidence of ROS-dependent injury up to 72 hours after reperfusion,

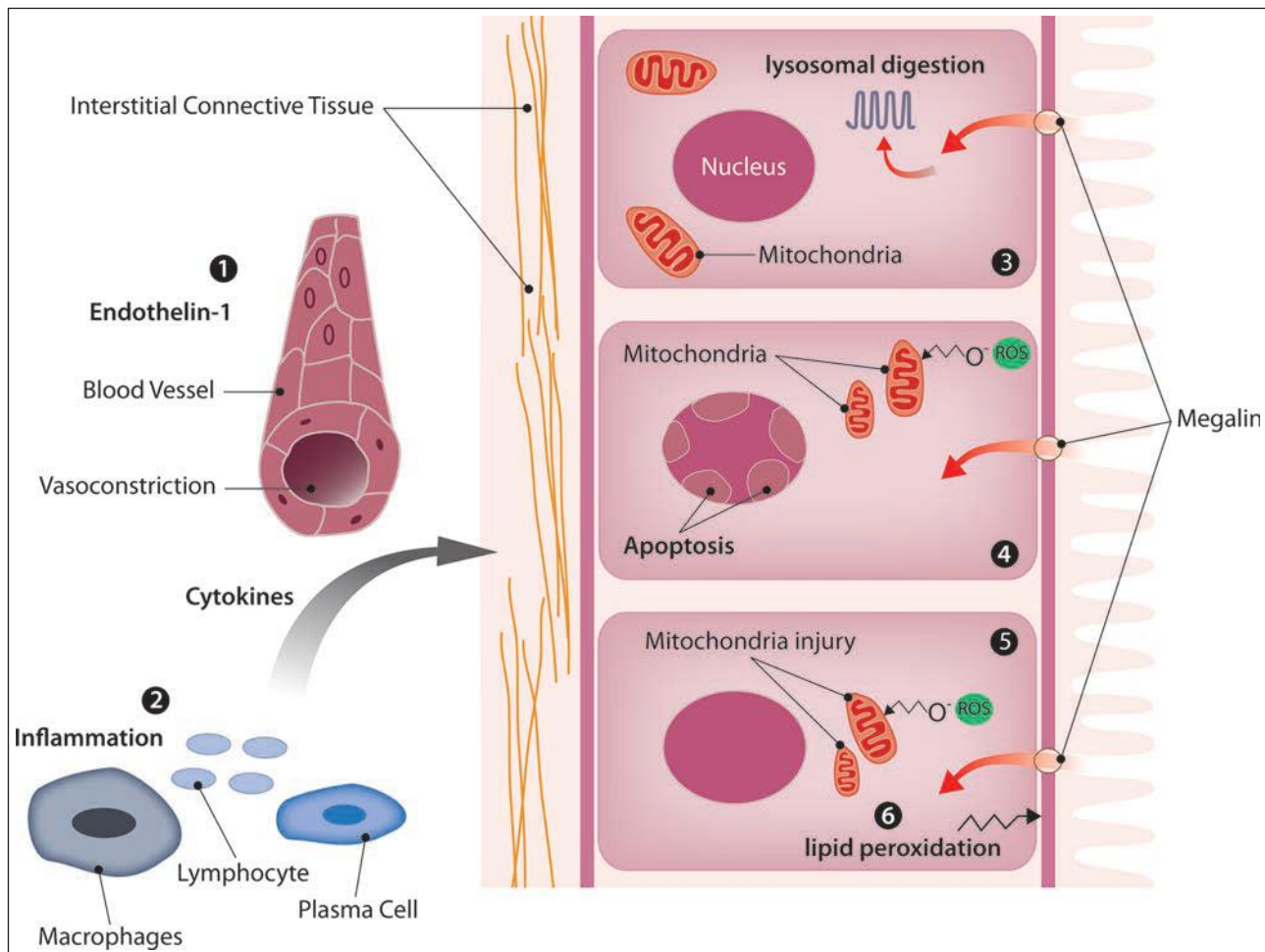


FIGURE 26.30 Graph depicting several important mechanisms of acute tubular cell injury, which are shown in separate parts of the cartoon labeled 1–6: (1) Ischemic injury due to prolonged vasoconstriction, which is mediated through cytokines such as endothelin-1. (2) Tubular cell injury due to cytokines, which are secreted by inflammatory cells, such as macrophages and plasma cells. (3) Lysosomal injury due to enhanced protein uptake by the brush border megalin receptor. (4) ROS-induced mitochondrial injury that may lead to the induction of mitochondrial proapoptotic pathways. (5) Cell death due to mitochondrial injury and subsequent loss of ATP production. (6) Cell injury due to enhanced lipid peroxidation leading to loss of Na⁺,K⁺-ATPase function with subsequent swelling and rupture of proximal tubular cells.

demonstrating long-term complications of reperfusion in addition to the immediate damage by ROS generation (316).

Nitric oxide (NO) plays an important role in the pathogenesis of ATI, but its effects are complex. NO is generated by three separate nitric oxide synthase (NOS) enzyme systems, and its effects depend on site of production, duration of effect, and concomitant levels of other ROS. Endothelial NOS (eNOS) results in transient high-level NO release, activating potentially protective heme-containing enzymes such as guanylate cyclase, mediating vasorelaxation, and triggering an antiapoptotic phenotype. Treatment of mice with L-NAME, which is a non-specific NOS inhibitor, has been reported to worsen ischemic renal injury (317). In contrast, generation of NO by inducible NOS (iNOS) results in sustained NO levels that may lead to lipid peroxidation, DNA damage, and apoptosis. In vitro, NOS inhibition prevents hypoxic damage in fresh proximal tubular preparations (318), and transfection of iNOS antisense oligodeoxynucleotide (AS-ODN) prevented nitrite accumulation and lethal cell injury in cultured green monkey kidney (BSC-1)

cells (319). Proximal tubules isolated from mice with targeted deletion of iNOS were resistant to hypoxia (320). Imbalance between eNOS and iNOS activities is therefore important in the pathophysiology of ARF (321,322). In vivo, oligodeoxynucleotide administration protected renal function and prevented tubular necrosis and decreased loss of brush border and cast formation (323). Effects of superoxide and NO may occur via formation of metabolites such as peroxynitrite and nitrotyrosine that cause tubular damage during ischemia (324,325). α -Melanocyte-stimulating hormone protects against experimental ischemia/reperfusion injury via blockade of both iNOS induction and leukocyte infiltration (326).

MECHANISMS OF APOPTOSIS AND NECROSIS IN ISCHEMIC INJURY

Lethal injury to renal epithelial cells follows the same pathways and mechanisms that result in ischemic cell death in other cell types. Lethal injury can result in coagulative necrosis and/or apoptosis, depending on the nature of the agent and

duration and severity of the insult. There is evidence that these two pathways may be parallel, may be activated by some of the same stimuli, and share common elements, including endonuclease activation, role of mitochondria, and activation of caspases (327). Apoptotic cells are rapidly removed from the environment, modulating the inflammatory responses to injury. Apoptosis may also be important in the tissue remodeling that occurs after tubular epithelial injury. Studies have also focused on the pathways that regulate cell death as potential targets for modulating recovery from acute renal injury (184).

One of the first studies to document apoptosis in ischemic ARF was conducted by Schumer et al. (328). A number of additional studies have described DNA laddering and morphologic changes consistent with apoptosis, which *in vivo* occurs predominantly during the reperfusion period (329–333). A large body of literature has addressed the signaling pathways that initiate or modulate apoptosis. The best characterized surface death receptors are members of the tumor necrosis factor superfamily, including Fas (CD95) and TNFRI (CD120a) (334,335). Mitochondria participate in inducing apoptosis after ischemia and reperfusion injury through multiple pathways, including generation of ROS, release of calcium, altered membrane permeability transition, and release of proapoptotic factors such as cytochrome *c* and AIF. These molecules activate downstream effector caspases that initiate the nuclear changes of chromatin condensation, fragmentation, and marginalization of chromatin. Caspases are cysteine proteinases (336), which can functionally be divided into initiator and effector caspases. The expression and activity levels of caspases are altered after ischemia-reperfusion injury (337). Caspases also affect proapoptotic oncogenes that mediate additional steps in the proapoptotic signaling process. Intracellular proapoptotic oncogenes (p53, *c-myc*, *c-fos*, Bax, Bad) and antiapoptotic oncogenes (Bcl-2 and Bcl-X_i) keep a delicate balance, which determines cell death or cell survival following ischemic injury. Activation of caspase-3 is mediated by Bax translocation from the cytoplasm to mitochondria and subsequent cytochrome *c* release through modification of the mitochondrial permeability transition pore (338,339). Several *in vivo* studies showed up-regulation of p53, *c-myc*, *c-fos*, and *c-jun* in renal tubule cells of ischemic kidneys during reperfusion (329,333,340,341). Bcl-2 mRNA and Bcl-2 protein have been shown in regenerating proximal tubule cells of the outer medullary region, indicating that the expression of antiapoptotic proto-oncogenes correlates well with the regeneration process following ischemic injury (341). Moreover, the proapoptotic oncogene Bax showed increased mRNA and protein expression within 1 to 7 days following ischemic injury in cortical collecting duct and medullary thick ascending limb of the loop of Henle (341). These data show that the regulation of antiapoptotic and proapoptotic oncogenes may vary within different cell types in the kidney, both during the acute phase of kidney injury and during the regeneration process in the recovery phase of the disease.

Actin disassembly and altered adhesion of cells to the tubular basement membranes may trigger apoptosis (342,343). Caspases have also been shown to be able to use the cytoskeletal proteins fodrin and actin as substrates. It is interesting to note that their cleavage appears to have its peak at the same time as the peak of apoptosis during reperfusion after acute ischemia in experimental models, further suggesting the contribution of loss of polar distribution of Na⁺,K⁺-ATPase (and therefore disruption of its function) not only in the development of necrosis but also in apoptosis.

Other cysteine proteases, such as calpain, have been shown to be activated in experimental ischemic/hypoxic injury to tubules *in vitro* (344,345). Inhibition of calpain attenuated hypoxic injury, decreasing lactate dehydrogenase release (346). Calpastatin, an endogenous cellular inhibitor of calpain activation, is down-regulated by caspases during hypoxia (345). Calcium activation of phospholipase A has also been shown to contribute to ischemic renal injury (347). Other mediators of apoptotic cell death include intracellular pH, calcium, free radicals, ceramide, and ATP depletion. Guanosine triphosphate depletion is an independent trigger of apoptosis via p53 (348). Guanosine triphosphate salvage with guanosine or pifithrin- α inhibits apoptosis with a protective effect on experimental ischemic injury (349).

Necrosis has long been thought of as a passive process as a consequence of ATP depletion, subsequently leading to cell swelling, membrane blebbing, and cell rupture. However, recent studies have shown evidence of active signaling steps in the generation of cell necrosis (350,351). A type of programmed necrotic cell death (necroptosis) requires the activity of receptor-interacting protein kinase 1 (RIP1 kinase) (352). Similarly, a programmed necrosis pathway independent of cell death receptor activation can be initiated by the assembly of a protein scaffold in the cytoplasm, termed “ripiosome” (353). The protein complexes found in these pathways contain RIP1 and require its kinase activity but can result in either apoptosis or necrosis. The decision to engage in the necrosis pathway is dependent on the kinase activity of another enzyme, RIP3. RIP1 kinase activity however also contributes to the tubular epithelial damage in a mouse model of ischemia-reperfusion injury (354).

The ROS-mediated volume increase and calcium influx in necrosis are thought to be initiated by binding of free radicals to ion channels including nonselective Ca²⁺ channels, resulting in high intracellular calcium levels. Increased cytoplasmic calcium activates endonucleases to degrade DNA and to activate cellular proteases, such as calpain to degrade structural and signaling proteins, leading to cell collapse (355). Overactivation of poly(ADP-ribose) polymerase (PARP), one of the molecules involved in necrotic cell death, has been demonstrated in renal ischemia (356). This leads to cellular depletion of substrate NAD⁹⁺ and ATP, inducing cell injury. Expression of proinflammatory factors and adhesion molecules is also increased in ischemic kidney with PARP activation. Inhibitors of PARP-1 or gene ablation have been shown to reduce energy depletion and inflammation and improve renal function in ischemic kidney (357). There is evidence that the mitogen-activated protein kinase (MAPK) pathway also plays a role in oxidant injury to the kidney. Up-regulation of extracellular signal-regulated kinase (ERK) by previous ischemic pretreatment has been shown to provide protection against ischemia/reperfusion functional injury and *c-jun* N-terminal kinase (JNK), p38, and MAPK activation (358). In an *in vitro* mouse proximal tubule preparation, inhibition of JNK activation of ERK ameliorated oxidant-induced necrosis (359), an effect mediated by cyclic adenosine monophosphate (AMP) response element-binding protein (360).

THE INFLAMMATORY RESPONSE IN ISCHEMIC INJURY

The inflammatory response to ischemia has been invoked as an amplifier of ischemic injury during the reperfusion period in a variety of organ systems and has been the focus of recent investigation in ARF (361–363). Both innate and adaptive immune responses

play a role in the pathology of ischemic injury. While the innate response involves activation of neutrophils, monocytes/macrophages, and NK cells and usually occurs early after ischemic injury, the adaptive response is initiated within hours and may last over the course of several days after injury. The adaptive response includes dendritic cell maturation and antigen presentation, T-lymphocyte proliferation and activation, and T- to B-cell interaction. The tubular epithelial cell plays an active part in the inflammatory response following ischemic injury by generating proinflammatory and chemotactic cytokines, such as TNF- α , monocyte chemoattractant protein-1 (MCP-1), transforming growth factor- β (TGF- β), and several cytokines (361). Moreover, tubular epithelial cells express Toll-like receptors (TLRs), complement receptors, and other costimulatory molecules that regulate T-lymphocyte activity. TLRs are transmembrane receptors that can bind to either exogenous microbial proteins or endogenous ligands that are released following injury (364,365). Following ischemic injury tubular epithelial cells express increased amounts of TLR2 and TLR4, which modulate a proinflammatory response marked by release of cytokines (366).

Several studies have implicated T cells and B cells in the etiology of ischemic ARE. Marked depletion of T cells using anti-T-cell antibodies in thymectomized mice conferred protection of renal function and structure after ischemia/reperfusion (367). B-cell-deficient mice were also partially protected, with ischemic phenotype restored by serum transfer, but not B-cell transfers (368). However, T- and B-cell-deficient mice (RAG-1 deficient) were not protected from ischemia/reperfusion injury, and adoptive transfer of B cells or T cells into these mice afforded partial protection, indicating complex interactions between T cells and B cells in this setting (369). The proximal tubular epithelium expresses MHCII and can present antigens to T cells and express costimulatory molecules (370). T-cell ligands, such as CD40, induce activation of cell surface receptors in proximal tubule cells (371). CD40 can induce production of the chemotactic cytokine CCL5/RANTES in human tubular epithelial cells, resulting in the recruitment of leukocytes to the place of injury (372).

In addition to T cells, neutrophils, macrophages, and dendritic cells are important contributors to ischemic injury. Neutrophils attach to the endothelium of the peritubular capillaries of the outer medulla within 30 minutes after ischemia/reperfusion (373). Neutrophils enhance the local production of proteases and ROS, which leads to increased endothelial permeability (374). Certain monocyte subsets migrate into the kidney and differentiate into macrophages or dendritic cells, depending on the underlying pathologic condition. Monocyte infiltration is mediated by the CCR2 and CX3CR1 signaling pathways (375,376). Monocytes can differentiate locally into M1 type ("inflammatory") or into M2 type ("repair") macrophages. M1 macrophages produce ROS, nitrogen intermediates, and inflammatory cytokines that enhance the Th1 immune response, while M2 macrophages enhance the Th2 response. Tubular injury can lead to activation of dendritic cells, which then present antigens that activate T cells, thus linking the innate with the adaptive immune response. In both the early and late phase of ischemia-induced AKI, both T lymphocytes and macrophages/dendritic cells can facilitate not only injury but also repair (377). Regulatory T cells are anti-inflammatory lymphocytes that facilitate repair in the ischemia-reperfusion mouse model (378).

Following ischemia-reperfusion injury to the kidney, activation of the complement system is predominantly mediated through the alternative pathway (379). CXC chemokine production by tubular epithelial cells is dependent on the activation of the alternative complement pathway (380). Complement C3 stimulates the expression of adhesion molecules on endothelial cells and leads to maturation of dendritic cells, which leads to activation of the T-cell response (381,382). Inhibition of the alternative pathway protects the kidney against ischemia-reperfusion injury (383,384).

RENAL VASCULATURE IN ISCHEMIC INJURY

Endothelial injury and dysfunction clearly play a role in initiation and especially the maintenance/extension phase of ischemic tubular injury (385). Endothelial cells are crucial in the regulation of vascular tone, leukocyte function, and smooth muscle responsiveness (386). Following ischemic injury, the small arterioles respond strongly to the effects of vasoconstrictive mediators such as endothelin 1, thromboxane A₂, angiotensin II, and sympathetic nerve stimulation (387, 388). Studies have further documented the role of decreased levels of vasodilators, such as acetylcholine and NO in altering blood flow in response to ischemic injury (389,390). Imbalance in iNOS and eNOS, oxidant stress, and generation of peroxynitrite have roles in the pathophysiology (322). The resulting vasoconstrictive effect is further amplified by vasoactive cytokines such as IL-6, IL-12, IL-15, IL-18, IL-32, and endothelin, which are generated as a result of enhanced leukocyte-endothelial adhesion and leukocyte activation that are characteristic of ischemic kidney injury (361). Indeed, administration of a monoclonal antibody to intercellular adhesion molecule type 1 (ICAM1) protected the kidney from perfusion injury both functionally and histologically when administered at the time of bilateral renal ischemia. Furthermore, anti-ICAM1 protected the kidney when administered 0.5 to 2 hours after restoration of blood flow but not after 8 hours. The protection corresponded with the degree of neutrophilic infiltration and suggested that leukocyte-endothelial adhesion and migration do contribute to reperfusion injury in the kidney, as they do in other organs (391). In a complementary study, inhibition of leukocyte adhesion using antibodies to the leukocyte adhesion molecules CD11/CD18 also resulted in a significant protective response (392).

Alteration of regional blood flow is another important factor in the pathogenesis of ischemic kidney injury. Blood flow to the outer medulla is decreased disproportionately to total kidney perfusion in animal models of AKI and in humans following ischemic injury (393). Outer medullary congestion is a vascular hallmark of acute renal ischemia, and it has been proposed that this may worsen hypoxic injury to the S3 segments and medullary thick ascending limbs, which traverse this area of the kidney (393). This congestion and stasis could be the result of altered hemodynamics, increased viscosity, compression by interstitial edema and/or swollen tubular cells, and up-regulation of cell adhesion molecules with stasis of leukocytes. Some toxic agents, including ACE inhibitors, angiotensin 2 receptor blockers, and NSAIDs, exert toxic effects on the kidney via reduction of renal blood flow.

The endothelium further contributes to the pathogenesis of ischemic kidney injury through additional mechanisms. Endothelial cell damage leads to loss of glycocalyx; disruption

of the actin cytoskeleton, which leads to alteration of endothelial cell attachment to adjacent cells and basement membrane; and breakdown of the perivascular matrix leading to increased microvascular permeability and loss of fluid to the interstitium (394,395).

Another detrimental effect of ischemic injury on the renal microvasculature is the decline of peritubular capillary numbers, especially in the outer medulla. This leads to decrease in VEGF synthesis and enhanced production of inhibitors of angiogenesis (394,396). Loss in total number of peritubular capillaries leads to chronic hypoxia, which perpetuates tubular injury and leads to progression of interstitial fibrosis (394) (397). Moreover, there are functional consequences of vascular dropout in the kidney medulla, including the development of salt-sensitive hypertension and altered concentration ability (394).

REGENERATION FOLLOWING TUBULAR INJURY

Reestablishment of normal cell organization comes about during recovery from renal ischemia at a rate dependent on the severity and duration of the insult; it is preceded by restoration of cellular ATP. Restoration of basal lateral Na^+ , K^+ -ATPase localization and of the brush border is a necessary prerequisite for restoration of tubular function (306,307,398). Restored localization of basolateral Na^+ , K^+ -ATPase is not caused by new synthesis of Na^+ , K^+ -ATPase subunits, because the rate of transcription of each subunit decreases in parallel with diminished overall transcription, which occurs with ATP depletion (399). These findings suggest that recycling of misplaced Na^+ , K^+ -ATPase units, rather than increased biosynthesis, is the way in which renal tubule cells repolarize after an ischemic insult. Similar recycling of apical membrane proteins occurs in the restoration of the brush border. The role of heat shock proteins can be invoked in this process, because they can serve as chaperones to protect the misfolded or misplaced proteins from degradation until ATP levels are restored and reorganization can take place (400).

Proper organization of the fodrin cytoskeleton is necessary to maintain Na^+ , K^+ -ATPase in its basolateral location. Fodrin is able to self-associate and bind actin (401), a process modulated by a unique regulatory cascade. Studies have demonstrated that this regulatory cascade appears to be involved in the disruption of the Na^+ , K^+ -ATPase ankyrin-fodrin complex following ischemia in hippocampal neurons as well as in the kidney (300). After 45 minutes of renal ischemia, the presence of fodrin cleavage products can be detected. Cleavage products increase during reperfusion, peaking at 6 hours; afterward, there is a gradual return to a normal pattern, which corresponds to the repolarization of Na^+ , K^+ -ATPase to the basolateral membrane. This temporal pattern suggests that fodrin has a role in the loss and return of Na^+ , K^+ -ATPase polarity after ischemia and during recovery. Cleavage of the cytoskeleton and initiation of the stress response can also result from activation of the enzymes involved in the programmed cell death pathway that leads to apoptosis (342,343,402).

The response of ankyrin to renal ischemia is similar to that of Na^+ , K^+ -ATPase. After ischemia, there is a loss of the normal distribution of ankyrin, and ankyrin is immunodetected in the apical domain and in subapical vacuoles. During recovery, ankyrin codistributes once again with Na^+ , K^+ -ATPase to the basolateral membrane. Examination of ankyrin turnover after

renal ischemia has yielded interesting results that may help in analyzing its role in recovery. Kidney tissue that has been rendered completely ischemic displays a major time-dependent loss of ankyrin that is essentially complete after 2 hours of ischemia (403). This profound loss is not accompanied by the appearance of proteolytic degradation products and was not observed in the ischemic brain or heart. These observations suggest that ischemia causes significant tissue-specific inhibition of ankyrin mRNA transcription, stability, or translation.

Studies of the biosynthetic response of ankyrin during recovery from renal ischemia have revealed that shortly after reperfusion, there is a significant loss of immunodetectable ankyrin associated with a concomitant loss of Na^+ , K^+ -ATPase polarization. However, after 6 hours of reflow, the amount of ankyrin increases to levels close to those of control kidney at a time when restitution of Na^+ , K^+ -ATPase polarity has commenced. After 24 hours of reperfusion, immunodetectable ankyrin levels exceed control levels concomitant with the restitution of Na^+ , K^+ -ATPase polarity. These studies also suggest the potential role of the stress response (or the heat shock response) in ankyrin processing. This could occur by protecting the transcriptional apparatus for ankyrin so that its rapid synthesis can take place at a time when other protein synthesis is restricted. A second possibility is that the loss of ankyrin immunoreactivity is the result of interaction with heat shock protein 70, resulting in a pool of ankyrin available for recycling (399).

Disruption of the cytoskeleton is associated not only with loss of cell polarity of transport proteins but also with relocation of basal integrins, tethered via the cytoskeleton and associated binding proteins in the basolateral domain. For example, nonlethal oxidative stress in cultured mouse tubular cells disrupts focal adhesion sites and is associated with redistribution of integrins to the apical domain (404). This results in disruption of the interaction of the cell with the underlying matrix, with loss of attachment of the epithelial cells from the basement membrane. Both cell-matrix and cell-cell adhesion may be disrupted with ATP depletion (405). Inhibition of cell-matrix adhesion *in vitro* by hydrogen peroxide has been shown to be reversible; recovery was associated with increased α -6 integrin expression (406). Inhibition of integrins during recovery can in turn lead to increase in cell apoptosis (407). Exfoliation of the epithelium into the tubular lumen can occur while the cells are still viable (180). Exfoliated cells and cell debris may interact with other epithelial cells, potentially with Tamm-Horsfall protein as a matrix. Aggregation of the exfoliated cells and adhesion to *in situ* cells can result in tubular obstruction. These exfoliated cells may interact with other cells via surface integrins (408). Arginyl-glycyl-aspartic acid (RGD) peptides, which block these interactions, have been shown to ameliorate ARF *in vivo* (409). Gaps in the tubular epithelial barrier via cell loss or altered tight junctions could also be sites of back leak of glomerular filtrate.

HEAT SHOCK PROTEIN AND OTHER CHAPERONES IN ACUTE TUBULAR INJURY

Heat shock proteins (hsp) are molecular chaperones that play a key role in the adaptive response of cells to stress conditions. Both the gene expression levels and protein abundance of hsp70 and hsp27 increase in response to ischemia (410). The message for inducible hsp70 is found within minutes of an ischemic

insult (410). Hsp70 is a molecular chaperone that is involved in protein folding (411). Since hsp 70 prevents aggregation and refolding of denatured proteins, up-regulation of hsp 70 has been found to be cytoprotective in kidney cells (412). The inducible protein appears shortly after the message and accumulates over several days after the injury. The protein is found in membrane fractions as well as in cytosol, suggesting that it may be complexed with a variety of proteins that have been disassembled or denatured as a result of the ischemic insult (412). Hsp25, the murine homolog of hsp 27, can be detected *in vivo* in renal epithelium, especially in proximal tubular cells.

The induction of hsp70 under stressful conditions has been found to occur rapidly through activation of the heat shock factor (hsf). Hsf is a constitutively active transcription factor that is inhibited by hsp70 under normal conditions. However, increased levels of denatured proteins compete for binding of hsp70 and thereby initiate activation of hsf, resulting in increased transcription of hsp genes (413). While a variety of injurious agents result in protein degradation and hsp activation, the initial mechanisms of induction may differ. Adenosine triphosphate depletion, increases in intracellular calcium, decreases in intracellular pH, activation of phospholipases, and release of arachidonic acid metabolites have been shown to either initiate or modulate the heat shock response in a variety of cell systems.

There is evidence of the importance of hsp during recovery from ischemia (414,415). Following renal ischemia and hsp70 induction, disrupted proteins such as Na,K-ATPase are restored within the cytoskeleton, which correlates with recovery of proximal tubule cells from ischemia (416,417). In ATP-depleted LLC-PK1 cells, inducible up-regulation of hsp70 protects against apoptosis (418). *In vivo*, up-regulation of hsp70 improves recovery from ischemia/reperfusion, associated with protection from apoptosis (419). The protection of cells from apoptosis by heat shock proteins depends on the subunit involved in refolding of damaged proteins and is apparently upstream from the mitochondrial-dependent activation of apoptosis. Heat shock protein 70 also affects signaling pathways for onset of apoptosis. This heat shock factor interacts with protein complexes such as apoptosis signal-regulating kinase 1 (ASK1) and binds to the caspase activator recruitment domain of apoptosis protein-activating factor, preventing activation of caspases and apoptosis.

Other protective mechanisms are also being defined. Caveolae are plasma membrane structures containing proteins. The caveolins are potential participants in protection and repair in both ischemic and toxic renal injury (420). Altered caveolin-1 expression and localization may affect renal cell survival following oxidative stress. Up-regulation of caveolin-1 has been demonstrated in ATI (421,422). More studies are required to determine whether this up-regulation contributes to cell survival or is an epiphenomenon. Lipoxins are lipoxygenase-derived lipid mediators with anti-inflammatory and prorepair properties. There is some experimental evidence that these compounds have therapeutic potential in ARF. Bioactivity of lipoxins is mediated through receptor cross-talk (423). KIM-1 appears in the urine early during AKI and is potentially a reliable and early biomarker of renal damage. The protein contains a novel immunoglobulin-like domain and a mucin domain and is up-regulated in renal injury in dedifferentiated cells undergoing replication (196,424). It is proposed

that shedding of this molecule allows the tubular epithelial cells to move and reconstitute the tubular epithelial barrier (425).

Improved understanding of the interesting interrelationships among alterations of cellular metabolic processes, the integrity of cellular structure and function, and those systems that may serve to protect or repair the injured epithelium will doubtless provide insights into the type of fundamental biologic processes that may be modified therapeutically to modulate the severity of injury and enhance recovery.

STEM CELLS AND GROWTH FACTORS IN TUBULAR EPITHELIAL INJURY AND RECOVERY

While cells that have suffered anoxia-induced sublethal injury can recover, those cells that are lethally injured must be replaced. Renal epithelial cells are stable cells that do not normally divide but must be stimulated by growth factors to undergo mitosis. A number of growth factors have been shown to play an important role during renal development and also in reparative processes following ischemic injury: They include epidermal growth factor (EGF)-like peptide, insulin-like growth factor type 1 (IGF-1), and hepatocyte growth factor (HGF).

EGF is a ubiquitous polypeptide growth factor capable of stimulating proliferation of many different epithelial cells. Administration of EGF to animals with ischemic ATN shortens the recovery time (426). This is likely due to activation of downstream cell survival pathways. In addition to EGF, a number of growth factors are activated in sublethally injured cells following anoxia; they include IGF-1 and HGF. IGF-1 has stimulatory effect on cell growth and regeneration, and its receptor is abundantly expressed in the proximal tubule. Following ischemic injury, expression of IGF-1 is up-regulated in surviving proximal tubule cells (427,428). Although several different mechanisms of action have been proposed, including changes in the GFR, the effect of IGF-1 on enhanced DNA synthesis and its action as an anabolic agent seem most likely to be important in the beneficial effects that are achieved (429). Similar results have been obtained with HGF administration, but whereas IGF-1 has a definite anabolic effect, HGF appears to exert its effects primarily by enhancing DNA synthesis. In animal models of ischemic tubular injury, HGF therapy markedly accelerates renal recovery (430). HGF also promotes adhesion of tubular cells to the basement membrane, decreasing cellular loss and preventing obstruction (431). Moreover, HGF helps to maintain cell polarity through preserved E-cadherin expression (432). It seems likely, therefore, that each of these growth factors contributes in different ways to the recovery process and that they act synergistically to achieve resolution of the injury (429).

Restoration of structure and function following ATI is dependent on the replacement of necrotic or exfoliated tubular epithelial cells by viable epithelium. Several possible mechanisms have been suggested to participate in the regeneration of tubular epithelial cells. Wound healing may occur by extension of adjacent viable epithelial cells to close gaps along the basement membrane through proliferation of existing tubular epithelial cells stimulated by paracrine growth factors. There is evidence from studies of ischemic injury in chimeric mice that restoration of epithelial integrity resulted from intrinsic tubular cell proliferation and not from circulating bone marrow-derived cells (433). Using a genetic tag to label mesenchyme-derived renal epithelial cells, a recent study found that 95% of regenerated

tubular epithelial cells in a model of ischemia-reperfusion carried the genetic tag and that no dilution of cell fate marker was observed (183). These findings indicate that tubular repair is predominantly a function of cell proliferation. However, studies of transplanted kidneys of male patients who received an allograft from a female donor have demonstrated a potential role for recipient-derived cells in reconstituting epithelial damage (434). Other studies have suggested that circulating recipient cells (presumably circulating pluripotent cells) play a role in renal remodeling after injury (435–437). Moreover, experimental studies from several different groups have demonstrated that hematopoietic stem cells are capable of protecting the kidney from ischemic injury and assisting in repair and recovery from ischemia/reperfusion and toxin-induced injury (437–440). In one study, mobilization of bone marrow cells by granulocyte colony-stimulating factor rescued mice from cisplatin-induced renal failure, an effect enhanced by macrophage colony-stimulating factor (M-CSF) (441). While all groups concluded that the majority of tubular repair occurred via proliferation of endogenous renal cells, the exact mechanism by which renotropic stem cells participate in this repair was unclear.

Several studies have demonstrated that administration of *in vitro* expanded stem cells may protect against and/or enhance recovery from ATI (435,436,442–444). Necrotic lesions in the proximal and distal nephron may mediate migration of mesenchymal stem cells (MSC) to the kidney. MSC may have a stimulatory effect on the proliferation rate of residual tubular epithelial cells (443). Moreover, one study found that MSCs injected after ischemia-reperfusion injury had a beneficial effect, but only if conditions favored differentiation of MSCs to endothelial cells (433). These findings indicate that stem cells might have an important role in the regeneration process of tubular epithelial cells through unknown factors, which might act in a paracrine fashion upon injured epithelial cells.

Drug Toxicity and Acute Kidney Injury

In vivo and *in vitro* experimental models have been used to identify the underlying pathogenic mechanisms of renal tubular injury produced by the various types of drugs. Aminoglycoside antibiotics and cis-platinum have been the most widely studied nephrotoxic drugs; pathogenesis of injury owing to these and other agents is discussed in detail later in this chapter. Some drugs and toxins are injurious in their native form. In other cases, metabolic by-products are the actual injurious agents. Drug catabolism may take place in the liver, at other systemic sites, or in the renal epithelium. In the case of many drugs and toxins, injury to the nephron may be zonal, depending on the site of uptake or catabolism. A few agents specifically injure segments of the proximal tubule (e.g., aminoglycosides), whereas others produce effects distally (e.g., lithium).

Polymorphisms of genes encoding proteins involved in the metabolism and renal elimination of drugs have been described and correlate with various levels of drug sensitivity. Loss of function mutations in apical secretory transporters and mutations in kinases that regulate drug carrier proteins can impair drug elimination and promote toxicity by elevating intracellular toxin concentrations (445). Cells of the loop of Henle exist in a relatively hypoxic environment due to the high metabolic rate required to actively transport solutes via the Na⁺,K⁺-ATPase-driven transport. This excess cellular workload and hypoxic environment promote increased sensitivity to injury

when exposure to nephrotoxic substances occurs (446). Elevated tissue concentrations of toxic compounds in the medulla promote toxic injury through direct cell toxicity or by ischemic damage as a result of decreased levels of vasodilatory prostaglandins.

Toxic agents may interfere with normal mitochondrial function and oxidative metabolism, leading to depletion of high-energy phosphate compounds, which causes impairment of ATP-dependent enzymes and cell transport mechanisms. Some alter lysosome function and integrity, causing leakage of digestive enzymes leading to cell membrane injury or disrupted protein synthesis. ROS compounds may be produced by systemic or local metabolism of a drug, by impaired mitochondrial function, or by drug effects on cell metabolism. Free radicals can interact with lipids to produce membrane damage and with proteins to alter cellular enzyme activity. Membrane damage results in loss of critical cell compartmentation, leading to loss of the normal cellular distribution of ions and the breakdown of gradients that drive critical cell processes. Increased concentrations of intracellular ionic calcium result in impaired cell enzyme function and breakdown of cytoskeletal elements, causing loss of the normal cell substructure.

While apoptotic mechanisms play an obvious and important role in ischemia-reperfusion injury, their contribution to toxic nephropathies may be even more complex. Toxins may initiate apoptosis not only through the mitochondrial pathways discussed above but also by directly initiating the signaling pathway for tumor necrosis factor signaling pathway or through p53 via genotoxic stress. Paracetamol toxicity has been linked to the direct activation of Bcl-xL in mouse proximal tubular cells in culture (447). The antiviral drug cidofovir has been shown to induce apoptotic epithelial injury in renal biopsy and human renal tubular cells in culture, via direct effects on epithelial cell membranes (223). Exposure of proximal tubule cells *in vitro* to cisplatin induced phosphorylation of the proapoptotic protein Bad (211).

Some nephrotoxic agents interfere with renal function by altering renal hemodynamics. In some cases, the effects are prerenal, but tubular epithelial cell injury may ensue if vasoconstriction/hypoperfusion persists. In addition, inflammatory cells may play a role in some forms of toxic injury. Finally, mechanisms of recovery are likely analogous to those described for ischemic injury. Removal of the offending agent or significant reduction in dose may be necessary to allow recovery.

There is currently a focus on prediction of nephrotoxic action by identification of toxicity-related biomarkers (448,449). Profiling of gene expression microarray in rats exposed to a range of nephrotoxins revealed clustering based on similarities in severity and type of pathology. A set of potential biomarkers showing time- and dose-response related to progression of proximal tubular toxicity included several transporters: KIM-1, IGF bp-1, osteopontin, α -fibrinogen, and glutathione transferase (Gst- α). Other potential biomarkers include *c-myc*, multidrug resistance gene (MDR-1), clusterin, vimentin, and hepatitis A virus cell receptor (HAVcr-1) (450). Similar studies in cynomolgus monkeys using gentamicin and everninomicin as nephrotoxins confirmed modulation of genes identified in rodent models, including *waf-1*, matrix metalloproteinase-9, and vimentin. Three early gene biomarkers predictive of drug-induced nephrotoxicity included clusterin, osteopontin, and HAV cr-1 (451).

ANTIBIOTICS

Antiviral Agents Tubular cell necrosis is a common consequence of toxic injury due to antiviral drugs (i.e., foscarnet, acyclovir, and cidofovir). However, certain antiviral agents may cause more subtle injury without cell necrosis or apoptosis, resulting in isolated tubular defects such as Fanconi syndrome (cidofovir, tenofovir), distal tubular acidosis (foscarnet), and nephrogenic diabetes insipidus (foscarnet) (284,452). Accumulation of high intracellular concentrations of antiviral drugs is a major mechanism of injury (207). Moreover, intrarenal obstruction occurs due to crystalline deposits that form in the renal tubules in response to acyclovir, ganciclovir, and indinavir therapy (207). Deposition of crystals in the kidney is seen with a variety of these agents, including acyclovir and indinavir (453,454). Several of these agents have relatively low solubility in urine; rapid infusion, volume depletion, and underlying renal insufficiency are important risk factors for crystal formation.

There is experimental evidence that acyclovir has additional direct effects on tubular function. A recent study showed that acyclovir is the substrate for the human breast cancer resistance protein (BCRP) (455). BCRP plays a role in acyclovir transport in human kidney cells and may also play a role in acyclovir-dependent nephrotoxicity. Moreover, increased influx of drug via organic ion transporters, or decreased efflux via the multidrug resistance protein (MRP), may enhance acyclovir cytotoxicity (456,457). Genetic defects in transporters, such as organic anion transporters (OATs) and organic cation transporters (OCTs), or in MRP may induce renal insufficiency. Nucleoside analogs, such as cidofovir, enter the cell by the hOAT or hOCT system (456,458). Increased uptake through this transport mechanism induces proximal tubular injury. Moreover, drug interactions may increase the nephrotoxic potential of certain antiviral drugs. Tubular secretion of lamivudine is significantly impaired by trimethoprim in the isolated perfused rat kidney and in humans, suggesting that the two drugs share a common organic cation transport (459). This leads to increased accumulation of intracellular toxic levels of lamivudine.

Programmed cell death and effects on mitochondrial function have been invoked as potential mechanisms of renal toxicity of antiviral agents (44). Stimulated by tubular cell apoptosis in a renal biopsy of a patient with irreversible ARF caused by cidofovir, Ortiz et al. (223) studied induction of apoptosis in primary cultures and a cell line (HK2) of human proximal tubular cells with time and dose parallel to clinical toxicity. Apoptosis was prevented by probenecid and by an inhibitor of caspase-3. IGF-1 and HGF were protective as well. Additional proapoptotic pathways may be induced when antiviral drugs damage mitochondria. The human equilibrative nucleoside transporter 1 and the apical human concentrative nucleoside transporter 1 in mitochondrial membranes (460,461) are transporters important in mediating the transport of nucleoside and nucleotide (i.e., antiviral and anticancer) drugs across membranes (462). Didanosine, zalcitabine, stavudine, and zidovudine are substrates of human nucleoside transporter, which likely plays a role in intracellular accumulation of these drugs.

Some antiviral agents, such as foscarnet, induce nephrogenic diabetes insipidus by down-regulation of the water channel aquaporin-2 or inhibition of vasopressin responsiveness. The proteinuria seen in patients treated with cidofovir is likely caused by tubular injury and failure of normal resorption.

Aminoglycosides Molecular mechanisms in aminoglycoside toxicity have been reviewed (463,464). Aminoglycosides are freely filtered by the glomerulus and are not metabolized in the body. About 10% of intravenously administered drugs accumulate in the kidney, with little uptake in other tissues. A key aspect of aminoglycoside nephrotoxicity is the tubular toxicity. Treatment of experimental animals results in both apoptosis and necrosis of tubular epithelial cells. Gentamicin toxicity occurs in the epithelial cells of the cortex, especially in the proximal tubule but also in the distal tubule and collecting duct (465). At the brush border of proximal tubular cells, polyanionic inositol phospholipids serve as the binding site. Megalin and cubilin form a giant endocytic receptor complex, which is expressed at the apical membrane of the proximal tubule. This complex plays a major role in binding and transporting these drugs by endocytosis (463). Aminoglycosides then traffic through the endosomal compartment and accumulate in the lysosomes, Golgi apparatus, and endoplasmic reticulum (466). Studies in megalin knockout mice demonstrated almost no renal accumulation of H³-gentamicin, compared to 10.6% of the total dose accumulated in the kidney in control animals (466). Other megalin ligands also have been shown to reduce gentamicin accumulation and nephrotoxicity (467). There is some evidence that gentamicin is trafficked retrogradely through the secretory pathway and is released into the cytosol via the endoplasmic reticulum (468).

Clinical pathologic findings and experimental studies support the direct toxic effects of aminoglycosides on renal tubules. These drugs induce formation of myeloid bodies containing phospholipids and proteins, apparently related to proximate cationic side chains and an apolar ring structure, resulting in a high affinity for the phospholipid components, and especially the acidic phospholipids, of cell membranes. Via binding, aminoglycosides also inhibit lysosomal phospholipases, leading to accumulation of phospholipid myelin figures in the lysosomes. The interaction of the drugs and the membranes leads to lamellar aggregates and lysosomal drug accumulation (469). Membrane aggregation correlates with the toxic potential of aminoglycosides and may contribute to its toxicity (470).

Aminoglycosides have been shown to traffic rapidly to the Golgi complex in cell culture. Cells previously depleted of nucleotides accumulated significantly more gentamicin within a dispersed Golgi complex (471). Destabilization of lysosomal membranes allows escape of enzymes, which cause further cell injury. The lysosome bears the highly active proteases cathepsins, which mediate cell death by directly cleaving execution caspases and inducing the proteolytic activation of the proapoptotic factor Bid (472,473). In addition, aminoglycoside in the cell cytoplasm interacts with mitochondrial membranes and microsomes. There has been evidence for some time that gentamicin inhibits mitochondrial respiration and cellular protein synthesis (474). Aminoglycosides affect protein synthesis as well as protein-protein interactions involving protein disulfide isomerase (PDI). Gentamicin and ribostamycin have been shown to bind to PDI, an enzyme that stabilizes some proteins and participates in mechanisms degrading misfolded proteins in the cell, inhibiting its chaperone activity (475–477). Gentamicin binds to a number of kidney microsomal proteins, including calreticulin, a chaperone protein, and has selective effects on chaperone activity of this molecule *in vitro* (477).

Gentamicin also enhances the generation of reactive oxygen metabolites in renal cortical mitochondria, and many studies suggest that oxygen and hydroxyl radicals have an important role in gentamicin-induced ARF (478). Chelators and antioxidants depress aminoglycoside-induced oxidant stress (479,480). Gentamicin-induced ROS are inhibited by N^G-nitro-L-arginine methyl ester (L-NAME), consistent with a role for endothelin receptor- β /NO pathway in toxicity (481). Aminoglycosides stimulate endothelin 1 and subsequently NO in proximal tubules (482), which can be blocked by L-NAME. Aminoglycosides also increase intracellular calcium levels and ERK activity in proximal tubular cell lines, correlating with cell injury (483). The effects of different aminoglycosides followed the pattern of known *in vivo* toxicity. These changes, and lethal cell injury, presumably result from the mechanisms of action described earlier.

The *N*-methyl-D-aspartate (NMDA) receptor plays a major role in gentamicin-induced ototoxicity, and expression of NMDA receptor has been shown to be increased in gentamicin-induced renal toxicity in rats. Endothelin B receptor expression and urinary nitrite concentration were also significantly increased, with increases in blood pressure, urine pH, and creatinine; an NMDA receptor antagonist ameliorated these effects (484). Calpain isoforms were unaltered by the short-term regimen used.

Mechanisms of fibrosis and progression following gentamicin exposure have been explored. In one study, rats treated with gentamicin were sacrificed at 5 and 30 days after drug injections. Fibronectin, α -smooth muscle actin (myofibroblast marker), ED-1 (monocyte marker), endothelin, angiotensin II, and TGF- β were all increased in renal cortex compared with controls. At 30 days, treated rats also had fibrosis and increased TGF- β content in cortex, despite normalization of creatinine (485).

Amphotericin Amphotericin B has been shown to bind to sterol-containing membranes, causing changes in their permeability via formation of intramembranous pores (486,487). This property, which underlies its antifungal efficacy, may also cause the vascular or tubular toxicity produced by the drug. Studies in rats have shown potentiation of tubular toxicity, as measured by fractional excretion of sodium, with potassium depletion (488). Amphotericin also affects water and urea transport in the inner medullary collecting duct. While amphotericin B causes hypokalemia, which may itself produce a concentrating defect, the defect may be seen with normal serum potassium as well (489). It may also come about in part as the result of the fall in the GFR that can develop in these patients.

In dogs and rats, vasoconstriction has been documented after infusion of amphotericin into the renal artery (490). Experimental studies in the rat have suggested that the vasoconstriction brought about by amphotericin B is in part thromboxane mediated (491) and involves activation of the tubuloglomerular feedback response (492). It appears, however, that the vasoconstriction brought about by amphotericin may also be the result of a direct effect on renal vessels.

CEPHALOSPORINS

Cephalosporins appear to be capable of producing direct toxic injury to tubular cells. Tune and Hsu (493) have shown that cephalosporins interfere with mitochondrial function in the renal tubule via inhibition of substrate transport across the mitochondrial inner membrane. Cephaloridine has structural

homology to carnitine, and it has toxic effects on carnitine transport and fatty acid metabolism in rabbit renal cortical mitochondria *in vivo*; *in vitro* effects on pyruvate metabolism were seen, although only at very high concentrations (493). Cephaloridine also produces lipid peroxidation and acylation and inactivation of some tubular cell proteins. Other cephalosporins that lack cephaloridine's side group constituents largely affect tubular cell proteins and especially mitochondrial anionic substrate transporters. *In vitro*, proximal tubular cells show evidence of cytotoxicity on exposure to cephaloridine (greatest injury), cephalixin, and cephalothin, while distal tubules do not; these studies provide evidence of the role of oxidative stress, cytochrome P450 activation, and mitochondrial dysfunction in tubular cell toxicity (494). Cytochrome C oxidase has been shown to be a target in LLC-PK1 cells (495).

Cephaloridine, ceftazidime, and cefotaxime have also been shown to produce dose-dependent disruption of LLC-PK1 monolayers *in vitro*, as measured by transepithelial potentials, morphologic changes, and enzyme release (496). Cephaloridine was the most toxic and cefotaxime the least toxic, dose for dose. Proximal localization of injury is apparently the result of concentration of drug within these cells; the drug readily enters the cell via the OATs, but it is a poor substrate for efflux porters at the brush border membrane, leading to accumulation in the cell. Despite these experimental findings, clinically significant cases of renal tubular toxicity are rare at the recommended doses of these agents, and newer agents have even less toxic potential.

In addition, cephalosporins are known to cause hypersensitivity reactions. In some cases, there has been resolution with drug withdrawal and, in a few cases, recurrence on rechallenge (497). The cephalosporins are structurally similar to the penicillins, which produce similar reactions, and cross-reactivity may occur in 1% to 20% of patients. No specific cephalosporin is more likely than others to cause such a reaction.

IMMUNOSUPPRESSIVE/IMMUNOMODULATORY AGENTS

Cyclosporine Cyclosporine is very lipophilic, circulating in plasma and erythrocytes and accumulating in the liver and adipose tissue. It is extensively metabolized in the liver; its metabolites are minimally nephrotoxic. Most excretion is in the bile. It interacts with many other drugs through the hepatic cytochrome P450-3A system. Cyclosporine binds in cells to cyclophilin, which interacts with calcineurin to inhibit the enzyme, affecting a wide variety of downstream genes via its substrate, nuclear factor of activated T cells (NFAT). The latter in turn regulates transcription of interleukin-2 (IL-2), TNF- α , and granulocyte-macrophage colony-stimulating factor. Calcineurin also regulates transcription of IL-2 receptor, NO synthase, TGF- β , endothelin-1, collagen types I and II, and Bcl-2 protein (94,498).

Intrarenal vasoconstriction appears to be the central pathogenetic mechanism for most types of CsA nephrotoxicity (95,499). This vasoconstriction can result from a direct vasoconstrictive effect, endothelin mediation (499), increased local production of angiotensin in renal vessels without the usual compensatory release of vasodilatory prostaglandins (500), activation of the sympathetic nervous system, selective impairment of endothelium-dependent relaxation related to prostaglandins or NO release, or increased thromboxane production (93).

Several lines of evidence implicate the role of endothelin in the vascular effects of CsA. Endothelin plasma and urine levels have been shown to be elevated in CsA-treated patients, and in vitro, CsA causes cultured vascular cells to release endothelin (501,502). Antiendothelin antibody or receptor blockade prevents a CsA-induced fall in the GFR in rats (503). Cyclosporine also up-regulates endothelin receptors in the kidney of rats (93). Thromboxane receptor blockade or modulation of thromboxane metabolism has been shown to reduce CsA toxicity in experimental animal models (93). In addition, inhibition of thromboxane synthetase has been demonstrated to improve renal allograft function in patients taking CsA (93). Platelet-derived growth factor, another vasoconstrictor substance, has been found to be increased in arterioles of CsA-treated rats (504). Another intriguing finding is markedly enhanced immunostaining for vascular clusterin after 4 and 6 weeks of CsA treatment in the rat (505). Clusterin has a variety of effects, including chemotactic effects, in injured and regenerating tissue.

The nephrotoxic effect of CsA appears to be tightly linked to its immunosuppressive effects (241). The mechanisms of action of CsA as an immunosuppressive drug involve binding to cyclophilin, a 17-kD basic cytosolic polypeptide with peptidyl-prolyl *cis-trans* isomerase activity. This enzyme is involved in protein folding, an activity that is inhibited by immunosuppressive concentrations of CsA. Kidney androgen-regulated protein (KAP) specifically interacts with cyclophilin B; KAP levels are decreased in CsA-treated rats. Overexpression of KAP in proximal tubular cells significantly decreased toxic effects of CsA, a protective stress response (506). The intracellular target of cyclophilin A-CsA is calcineurin, a protein phosphatase required for signaling via the T-cell receptor (93). Calcineurin regulates both baseline and receptor-activated Na/K-ATPase activity (507). There is evidence that CsA also decreases cell levels of the calcium-binding protein calbindin D (508,509), which increases urinary calcium excretion, promoting intratubular calcifications that can be seen with CsA toxicity.

Administration of cyclosporine and also tacrolimus may lead to the development of thrombotic microangiopathy. The main mechanism is through endothelial damage due to ischemia caused by vasoconstriction. Calcineurin inhibitor-mediated hyperaggregation of platelets contributes also to the activation of prothrombin factors (510). Withdrawal of CsA with conversion to tacrolimus or sirolimus is often a sufficient therapeutic measure (511,512). A variety of additional factors may act together to injure the endothelium; these factors include inflammation and hypertension. Moreover, it has been shown experimentally that at high doses, CsA exhibits direct endothelial toxicity in vitro (513). At lower doses, it may inhibit endothelial repair (514).

The hyaline arteriolar lesions observed in humans have been difficult to reproduce in experimental animal models, with the exception of the spontaneously hypertensive rat. However, Young et al. (515) reported such a model in persistently salt-depleted rats. The lesions, first detected at day 10, began with granular eosinophilic transformation of smooth muscle cells in afferent arterioles, followed by vacuolation of smooth muscle cells and discrete hyaline deposits in vessel walls. Immunocytochemistry and electron microscopy revealed accumulation of renin granules in the smooth muscle cells. It is possible that the lesion is more likely to develop clinically

if the arterioles are abnormal before CsA treatment. Indeed, CsA nephrotoxicity appears to be much more severe in patients with preexisting kidney disease, and age has been identified as an additional risk factor (93). A more recent study attributed the pathogenesis of the arteriolar hyaline lesions to the important role of calcineurin-NFAT in smooth muscle cells (516).

Tubular injury may be enhanced by the antiproliferative effects of CsA on renal tubular cells, an effect which may be explained, in part, by stimulation of TGF- β expression in renal tubular cells (517). In vivo, CsA significantly inhibits H³-thymidine incorporation in a time- and dose-dependent manner; p53 levels increased coincident with cell cycle arrest (518). Oxidants may play a role in tubular cell injury in CsA toxicity. Renal lipid peroxidation has been shown in vivo and in vitro. Acute calcineurin inhibitor toxicity is often associated with cytoplasmic vacuolization, induced by endoplasmic reticulum enlargement and multiplication of lysosomes (247). Cyclosporine induces endoplasmic reticulum stress in tubular cells and endothelial cells, which can contribute to cell death (519–522). Atrial natriuretic factor reduces toxicity in renal cells via cyclic guanine monophosphate and heme oxygenase (523). Melatonin is also protective in isolated perfused rat kidney (524). In vitro exposure of LLC-PK1 cells to CsA increased glucose consumption and pyruvate production, consistent with a shift to glycolysis; interruption of glucose influx and glycolysis increased lactate dehydrogenase release, whereas the *Glut-1* gene was protective (525). In primary cultures of rat renal epithelial cells, CsA-induced increases in mitochondrial Ca²⁺, reduction in mitochondrial membrane potential, and reduction in ATP have been detected; all these changes may play an important role in CsA-related cell cytotoxicity (526). However, while direct treatment of cells in vitro inhibits mitochondrial respiration, cells isolated from CsA-treated rats showed mitochondrial inhibition only at high dose (75 mg/kg/d), not at immunosuppressive doses (527). Cyclosporine-induced apoptosis has been described in a murine cell line in vitro at relatively low doses. However, despite increased expression of apoptosis-stimulating fragment (Fas) and evidence of endoplasmic reticulum stress, the pathway of apoptosis did not involve apoptosis-stimulating fragment ligand (FasL)-induced mechanisms of caspase-12 but instead involved *Bax* translocation to the mitochondria and activation of caspases 2, 3, and 9 (528).

Charuk et al. (529) found that CsA has a high affinity for human renal P-glycoprotein and also described enhanced cell accumulation of the drug and other agents transported by P-glycoprotein. The authors postulated that this binding may competitively inhibit excretion of an endogenous P-glycoprotein substrate (529).

Rosen et al. (530,531) described a model of chronic CsA-induced nephropathy in which CsA (12.5 mg/kg) was injected daily into sodium-depleted rats. Histologic assessment revealed focal atrophy of the thick ascending limb and fibroblast proliferation. Structural lesions and renal functional impairment were less severe in animals, which had been fed a normal sodium diet. Based on this model, Heyman et al. (532) proposed a role for medullary ischemia in CsA-induced lesions.

Young et al. (533) used this model to study the pathogenesis of interstitial fibrosis. Proliferation of tubular and interstitial cells was documented in the medulla by day 5. By day 35, proliferation was maximal, and there was increased

cortical tubular staining for osteopontin, a macrophage adhesion protein. A significant influx of macrophages was detected by day 35, which was associated with maximal cortical interstitial fibrosis. These changes correlated with functional abnormalities, and the authors concluded that these cellular events may be important in the pathogenesis of chronic CsA nephrotoxicity. Studies in rats have implicated angiotensin II in effecting fibrosis with prolonged CsA administration (503). Transforming growth factor- β (TGF- β) also likely plays a role in induction of fibrosis in chronic CsA nephropathy (534). In a rat model of chronic CsA toxicity, administration of anti-TGF- β antibodies reversed most of the CsA-induced renal lesions (535). There is evidence that CsA may bind to the promoter for collagen type III, stimulating collagen expression in renal cells (536). Loss of peritubular capillaries has been demonstrated in chronic CsA toxicity; in an experimental model, vascular endothelial growth factor ameliorated the chronic nephropathy (537). Inappropriate apoptosis and the vascular effects described above leading to chronic vasoconstriction also likely contribute to chronic effects of CsA.

FK506 (Tacrolimus) Tacrolimus appears to have a mechanism of action similar to that of CsA (538). Like CsA, FK506 binds to an intracellular-binding protein, FKBP12; this complex targets calcineurin within the cell (538). Studies have shown inhibition of renal calcineurin in rats treated with FK506, suggesting that renal toxicity is mediated in part by inhibition of the phosphatase activity of calcineurin (539,540). Tacrolimus also binds to FKBP59, a heat shock protein associated with the nucleus, cytoskeleton, and mitotic apparatus (540). Like cyclosporine, FK506 is bound to proteins and erythrocytes in the blood. Like CsA, FK506 is metabolized by the hepatic cytochrome P450 3A4 system, and there is potential for drug interactions (541). Metabolites are generally inactive, and excretion is largely via the biliary tract.

Studies in mesangial cells cultured *in vitro* have shown that FK506 induces release of endothelin-1, an effect that may be mediated by FKBP (542). Clinically, endothelin levels in the urine have been shown to rise with FK506 immunosuppression after liver transplantation, whereas 6-keto-PG1- α levels fell; the changes in levels of these vasoactive substances persisted for 2 years, over a period when the GFR dropped and renal vascular resistance rose (543). In an experimental rat model, 2 weeks of treatment with FK506 produced a rise in SUN and sCr levels, luminal narrowing of arterioles, increases in plasma renin and urine thromboxane, and a decline in urinary 6-keto-PG1- α ; the effects were reversible (544). The drug also induces TGF- β in experimental FK506 toxicity (545), suggesting that the drug may induce renal fibrosis by mechanisms analogous to CsA. Tacrolimus-mediated injury is also related to endoplasmic reticulum stress (546).

Sirolimus Sirolimus has been shown to impair recovery from experimental ARF. A role for cell cycle arrest and apoptosis of tubular cells has been demonstrated (547). This compound has also been studied in a rat model of CsA toxicity (548). The drug potentiated the renal toxicity of low-dose (5 mg/kg/d) CsA. Sirolimus alone increased TGF- β expression by 44%. In the setting of a combination of sirolimus and low-dose CsA, TGF- β mRNA and protein were increased by 121% and 176%.

Lieberthal et al. (548) found that rapamycin inhibits growth factor-induced proliferation of cultured proximal tubular cells and fosters apoptosis by blocking survival effects of the growth factors. The drug also impaired recovery from experimental ARF caused by renal artery occlusion via increased apoptosis and inhibition of regeneration; these effects were attributable to the inhibition of p70 S6 kinase.

Intravenous Immunoglobulin The toxicity of IVIG appears to be osmotic. Highly osmotic, sucrose-stabilized formulations have a disproportionately high rate of ARF compared to non-sucrose-stabilized products (124). Rate of infusion may be an important risk factor for renal tubular injury.

CHEMOTHERAPEUTIC AGENTS

Cis-platinum Cis-platinum is a highly effective chemotherapeutic drug that is used to treat a variety of cancers both as first-line treatment and as adjuvant therapy. Cisplatin chemotherapy is limited by severe toxic side effects, including nephrotoxicity (549). The susceptibility of the kidney to cisplatin is due to accumulation of high concentrations of cisplatin in tubular epithelial cells (550,551). The intestinal secretion of the drug is minimal. Impairment of renal function is seen in 25% to 35% of patients treated and occurs initially predominantly in the proximal tubule. Recently, active transport systems have gained importance in the understanding of mechanism of cisplatin toxicity. The facilitated transport systems associated with cisplatin toxicity are those mediated by the organic cation transporter OCT2 and the copper transporter Ctr1, which foster intracellular accumulation of cisplatin (552,553). OCT1/2 double knockout mice show only mild cisplatin nephrotoxicity (554).

Cisplatin induces both apoptosis and necrosis in proximal tubular epithelial cells. Both mechanisms have been shown *in vivo*. Necrosis has been mainly associated with high doses of cisplatin, whereas apoptosis is associated more commonly with therapeutic doses (550). Both the intrinsic and extrinsic apoptotic pathways have been implicated in cisplatin-mediated toxicity (555,556). Moreover, endoplasmic reticulum stress has been implicated in cisplatin-dependent apoptosis (557).

Inflammatory responses initiated by cisplatin have been shown to be associated with enhanced expression of TNF- α (555,556,558). TNF- α has been shown to activate proinflammatory cytokines and chemokines and recruit leukocytes, thereby causing oxidative stress and amplifying renal damage (559). Moreover, the cytokine-like TGF- β , MCP-1, intercellular adhesion molecule (ICAM), and heme oxygenase 1 have been implicated in cisplatin-induced nephrotoxicity (560). Further evidence that cisplatin induces proinflammatory reactions in the kidney is indicated by the observations that anti-CD54 antibody blockade of leukocyte adhesion is protective (561) and that interleukin-10, an anti-inflammatory cytokine, inhibits cis-platinum-mediated nephrotoxicity (562).

Nitrosoureas The mechanism of injury appears to be direct renal tubular toxicity. Metabolites of the drug ifosfamide may be responsible for the tubular injury induced by that agent (563). Methotrexate also causes direct toxic injury to the proximal tubule. In addition, precipitation of the drug in renal tubules, with resultant obstruction, has been reported.

RADIOCONTRAST AGENTS

Based on the existing clinical and experimental studies, it appears that the tubules and the vasculature of the kidney are the key targets in the development of RN (radiocontrast nephropathy). Increased tubular protein and enzyme excretion have been detected in the urine of patients undergoing radiocontrast studies (150,151), suggesting a direct tubular toxic effect of contrast media. Rise in urinary levels of markers of oxidative stress has been documented (151). The pattern of amplified enzyme and protein excretion (e.g., more urinary brush border enzymes, folate-binding protein) was suggestive of a primarily proximal tubular injury. Mechanisms have been reviewed (564).

In general, it is difficult to induce ARF with contrast media in most animal species, and contrast media alone are not sufficient to cause renal injury in animal models. The combination of unilateral nephrectomy, salt depletion, and administration of indomethacin and other injurious agents is necessary to cause renal injury in animals after contrast media exposure. In this model, apoptosis of medullary tubular cells has been noted, ascribed to hypoxia (565). Some experimental studies describe proximal tubular vacuolation (260). Other investigators have emphasized the selective injury of the thick ascending limb of Henle in a rat experimental model for RN (225,566). However, this thick ascending limb injury appears to have been the consequence of hypoxia rather than direct toxic damage in this model. The thick ascending limb of Henle is the site where Tamm-Horsfall protein is produced, and some data indicate that contrast media may increase the urinary excretion of Tamm-Horsfall protein, an important cast-forming protein (566). Contrast media may also facilitate the urinary excretion of oxalate and urate, but there is no evidence that urinary obstruction by any form of cast plays a role in RN.

There is both human and experimental evidence that vasoconstriction and subsequent ischemic injury may play an important role in RN (567–570). The injection of contrast media causes a biphasic response in the renal blood flow. There is an initial short phase of increased flow followed by a long phase of reduced flow caused by intrarenal vasoconstriction (568,571). Some experimental studies suggest that high endothelin levels, low NO levels, or both are key mediators of this intrarenal vasoconstriction (566,569,570). However, early results with endothelin receptor blockade in clinical trials have not shown benefit (571). Other factors, such as increased adenosine release and decreased prostanoid levels (e.g., owing to the concomitant administration of indomethacin or other prostaglandin synthase inhibitors), may also play a part in pathogenesis (566,567).

More recently developed iso-osmolar contrast media are dimers, while the widely used nonionic, low-osmolar contrast media are monomers. The viscosity of these dimers is higher than that of blood, potentially interfering with flow within the kidney. Experimental studies suggest greater perturbation in renal function with the dimers, although clinical trials have yielded conflicting results (564).

Whereas vascular effects are important, *in vitro* studies demonstrate toxic effects of contrast media on cultured renal epithelial cells (572). Iodinated radiocontrast agents produce cytotoxic effects in glomerular mesangial cells as well as tubular epithelial cells *in vitro*. Exposure of cultured tubular cells to ionic contrast media induces opening of intercellular junctions and redistribution of surface proteins (573,574). More severe injury is usually characterized by cell shrinkage and nuclear

fragmentation, consistent with apoptosis (271,575–577). Most studies utilize the Madin-Darby kidney (MDCK) cell line (predominantly distal phenotype), but changes occur in LLCPK-1 cells (proximal phenotype) as well. There are loss of cellular energy stores, disruption of calcium homeostasis, and disturbance of cell polarity. All agents appear to variably affect mitochondrial function (575). Some experimental evidence has accrued that oxidative stress is an underlying mechanism (578). *In vitro* cell injury is variably correlated with osmolality of the contrast media (576,578).

NARCOTICS

Rhabdomyolysis in drug addicts is associated primarily with the use of opiates and cocaine. The pathogenesis of muscle damage following substance abuse is obscure. Cocaine and opiates may have a toxic effect on the skeletal muscle, but seizures, muscle injury, hyperthermia, and coma-induced ischemic or pressure injury of the muscle may also be important factors (167,273). Once rhabdomyolysis evolves, three major mechanisms are thought to be involved in the development of ARF: direct tubulotoxicity of myoglobin, renal tubular obstructive cast formation, and vasoconstriction/hypoperfusion (for a review, see Zager (167)). Several factors have been implicated in renal infarction induced by narcotics, including intense renal vasoconstriction from adrenergic stimulation, endothelial injury, and platelet activation. Cocaine-induced endothelial injury has also been implicated in the few cases of microangiopathy associated with cocaine use (579).

ANESTHETICS

The toxicity of methoxyflurane may be related to the fluoride ion, but other fluoride-containing anesthetics are not associated with renal failure (580,581).

HERBAL MEDICATIONS

Poisoning caused by these formulations may be a result of the presence of undisclosed drugs or heavy metals, interaction with conventional medications, or misidentified herbal species (169).

Differential Diagnosis

As indicated previously, the causes of ARF are varied, although a significant portion of cases can be attributed to ATI. A similar clinical syndrome is seen in a variety of primary renal diseases, including rapidly progressive glomerulonephritis and thrombotic microangiopathies, though the presence of hematuria, hematologic abnormalities, and other clinical and laboratory data often provides clues to diagnosis in these settings. “Secondary” ATI may occur in these settings due to ischemia, inflammation, and potentially other mechanisms and may contribute to renal dysfunction and ultimate prognosis. Clinical differentiation between ischemic and toxic ATI may be difficult in some settings, especially in hospitalized patients. Morphologically, toxic injury is more strongly associated with frank cellular necrosis. There are some pathologic features, as discussed above, that may make it possible to identify the mechanism and even occasionally a specific agent.

There may be an inflammatory response in ATI. The single most distinguishing feature between ATI and acute interstitial nephritis is the severity and nature of the interstitial infiltrate. Although eosinophils can be present during the recovery phase of some cases of ATI, they are usually low in number and found only in a scattered distribution. The changes associated

with postrenal failure owing to obstruction may lead to tubular dilation and interstitial edema, but the characteristic areas of tubular cell injury are generally absent.

Clinical Course

The clinical course of ATI is usually divided into three phases: the initiation phase, the maintenance phase, and the recovery phase. The *initiation phase*, which usually comprises the initial oliguric symptoms, consists of a rapid decline in renal function followed by stabilization to the maintenance phase, with GFR at a relatively low 5 to 10 mL/min. As noted above, the extent of decrease in GFR correlates with the appearance of oliguria. The *maintenance phase* typically lasts 1 to 2 weeks, but it may be prolonged for several months in individual patients with complications. During the *recovery phase*, patients gradually recover renal function, with normalization of urine output and a fall in sCr. Patients may experience polyuria with significant diuresis, which occasionally can be excessive and require careful management of fluid and electrolyte balance.

The period of renal insufficiency varies from patient to patient, ranging from a few days to as long as several weeks. The morbidity of ATI is largely the result of the multiple possible accompanying complications and the clinical setting in which the ATI occurs. The severity of these complications correlates with mortality (582,583) (Table 26.4). The overall mortality rate for ATI approximates 50% and has changed little since the advent of renal replacement therapy. A variety of pharmacologic agents have been tried in attempts to ameliorate the severity of the failure and to hasten recovery, but none have been shown to be consistently of value. The mortality rates do differ, however, depending on the initiating cause of ARF; trauma and major surgery are associated with the highest mortality rate, and ARF in pregnancy has the lowest rate. In addition, mortality rates are higher in older debilitated people and those with multiple-organ dysfunction. Death is almost inevitable if ARF is associated with failure of more than three other organ systems. As noted above, ARF in itself may play an important role in multiple-organ dysfunction (584).

Prognosis

Patients who survive an episode of ARF generally recover sufficient renal function and do not usually suffer from overt progressive chronic renal deterioration. However, in addition to increased risk of mortality, a minority of patients with AKI may suffer persistent progressive dysfunction. For example, nearly 10% of patients with radiocontrast nephropathy (RN) become dialysis dependent (585). AKI has been shown to be a risk for end-stage renal disease, especially in the elderly (586). Patients with the greatest impairment of renal hemodynamics have the lowest potential for recovery of renal function long term (587), and an accurate estimate of GFR may be of prognostic significance.

Toxic tubular injury will continue as long as there is exposure to the offending agent. Discontinuation of the drug or adjustment of the dosage will allow recovery of tubular cells and of renal function, although permanent damage has been seen with some toxins, and some drugs such as calcineurin inhibitors, lithium, and herbal medications routinely cause fibrosis. Recovery may be incomplete, with persistent decrease in creatinine clearance and urine concentrating ability in 35% to 71% of patients (588), with some evidence of progression of dysfunction after 1 to 5 years in one follow-up study (588).

TABLE 26.4 Complications of acute renal failure

Renal

Chronic renal failure

Metabolic

Hyperkalemia
Metabolic acidosis
Hyponatremia
Hypocalcemia
Hyperphosphatemia
Hypermagnesemia
Hyperuricemia

Cardiovascular

Pulmonary edema
Arrhythmias
Pericarditis
Pericardial effusion
Hypertension
Myocardial infarction
Pulmonary embolism
Pneumonitis

Gastrointestinal

Nausea
Vomiting
Malnutrition
Gastritis
Gastrointestinal ulcers
Gastrointestinal bleeding
Stomatitis or gingivitis
Parotitis or pancreatitis

Neuromuscular irritability

Asterixis
Seizures
Mental status changes
Somnolence
Coma

Hematologic

Anemia
Bleeding

Infectious

Pneumonia
Wound infections
Intravenous line infections
Septicemia
Urinary tract infection

Other

Hiccups
Decreased insulin catabolism
Mild insulin resistance
Elevated parathyroid hormone
Reduced 1,25-dihydroxy- and 25-hydroxyvitamin D
Low total triiodothyronine and thyroxine
Normal free thyroxine

Persistent renal dysfunction has been reported in adults and children (589,590). In the newborn, prognosis and recovery are also dependent upon the underlying etiology. Hypoxic/ischemic and nephrotoxic injury to the developing kidney in the perinatal period can result in a reduced number of nephrons, and monitoring for the late developments of chronic renal insufficiency is recommended. Early ischemic injury in the renal allograft has persistently been shown to predispose to later graft injury and loss (see Chapter 29).

Chronic renal failure and fibrosis have been described in animal models when these animals have been followed long term, and although the renal insults in these models are not completely analogous to those in clinical ARF, these studies provide some insights into mechanisms of progression. Both ischemic injury and cisplatin toxicity have been reported to result in concentrating defects in rats. In the ischemic model, chronic renal insufficiency develops after several months, following recovery of function and morphologic tubular injury, and has been associated with progressive proteinuria (591–593). Early increases in macrophages and myofibroblasts have been documented in early experimental ischemic injury (594) and gentamicin toxicity.

Early postischemia, there are significant alterations in renal blood flow, with reduced and chaotic cortical flow demonstrable by video microscopy (595). Increased capillary leakiness has been documented following ischemia/reperfusion injury by tracking diffusion of fluorescent high molecular weight dextrans by two-photon confocal microscopy (596), associated with disorganization of F-actin in endothelial and vascular smooth muscle cells and loss of E-cadherin-positive tight junction. Late microvascular damage and loss of peritubular capillaries have been documented in animal models with ischemic injury. These changes persist even as tubules recover from the acute insult. In a study using microfil injection, a 30% to 50% reduction in vascular density was demonstrated at 4, 8, and 40 weeks following ischemia/reperfusion injury in the rat (591). It has been hypothesized that rarefaction of peritubular capillaries permanently alters renal function and predisposes to chronic renal insufficiency (592). Other possible mechanisms for progressive decline in renal function include inability of some nephrons to regenerate following ischemic injury (592). Inhibition of B7 costimulatory factor in experimental ischemic injury attenuates the development of progressive renal failure (597), suggesting a role for inflammation, which may be a factor in both ischemic and some types of toxic injury and especially in sepsis (see below). A possible role for endothelin has also been implicated. All of these factors could be interrelated. The hypoxia marker 2-pimonidazole has been used to demonstrate persistent hypoxia in the outer medulla at 5 weeks following experimental ischemia/reperfusion injury, when function and renal tubular structure have recovered. Treatment with L-arginine increased blood flow and attenuated the hypoxia and later interstitial fibrosis (598).

Therapy

Therapy for ARF includes prevention and interventions during or after the insult. Any inciting agents or factors should be removed or corrected. Depending on the toxic agent and severity of injury, recovery may be rapid or prolonged. Careful management of fluid, electrolytes, and acid-base status is critical, especially if renal insufficiency is severe. Renal replacement therapy, including dialysis or other forms of hemofiltration,

may be required (599–602). Intermittent hemodialysis is the most common modality. Peritoneal dialysis is not widely used in adults, and use of this modality is decreasing in pediatric patients, except for neonates and very small infants. Hemofiltration is increasingly common in the pediatric population (603). Dialysis dose is the most critical parameter, regardless of modality (604,605). A number of therapeutic agents and strategies have been efficacious in experimental models to prevent or ameliorate ARF, although many have been generally disappointing in clinical trials.

Prevention of ARF is a goal, and some strategies have been developed, including perioperative hydration, maintenance of perfusion pressure, and avoidance of nephrotoxins or minimization of toxic effects of potential nephrotoxins, to lessen occurrence of ARF (606). Many experimental models have focused on therapies administered before the onset of ARF. However, the efficacy of these approaches is limited to scenarios in which development of ATI can be anticipated, including preoperatively, following myocardial infarction, in sepsis/systemic inflammatory response syndrome (SIRS), prior to use of potential nephrotoxic agents, and in renal transplantation. In humans, some of the best results in prevention of ARF have been seen with RN (607); isotonic sodium bicarbonate infusion, *N*-acetylcysteine combined with hydration (608), and ascorbic acid (609) have been used to prevent RN. However, results have been heterogeneous, and caution is advised in adopting these preventive strategies as standard of care (610). Avoidance of volume depletion and/or volume repletion/expansion may be the most important strategy (611). Prevention of AKI in sepsis focuses on at-risk patients, with prophylactic antibiotics, treatment of hospital-acquired infection, control of blood glucose, and nutritional support. Maintenance of renal blood flow may require support of volume and cardiac output to achieve adequate mean blood pressure and central venous pressure (612,613).

More generally, useful therapies are those that are effective when given during or after the onset of injury and dysfunction. Benefits of low-dose dopamine infusion to produce vasodilation and maintain renal blood flow are equivocal, and some studies have shown worsening of renal perfusion (614). Loop diuretics may reduce the severity of injury and maintain urine output (615), but large clinical trials are needed. A variety of agents, including growth factors, have some efficacy in experimental models. In humans, atrial natriuretic peptide (ANP) has proven efficacious in nonoliguric renal failure (616); however, use of ANP to prevent RN has had variable efficacy, although perhaps with some utility in diabetic patients. Treatment with insulin-like growth factor had no measurable benefit in a randomized clinical trial in ARF patients (617). In general, clinical trials using single agents based on findings in experimental models have not identified significant efficacy. Combination therapies as used in some animal models, for example, use of a vasodilator such as ANP combined with mannitol to maintain tubular flow or ANP and dopamine in combination, could be an optimal approach (618,619).

Removal of inflammatory mediators with plasma therapies and adsorption techniques may have some efficacy in states such as sepsis and multiorgan failure (see Syndromic Acute Tubular Injury below, and see (613) for review). Nutritional support with provision of calories and protein is important in hypercatabolic states such as sepsis. The bioartificial kidney, which combines hemofiltration and a device containing human tubular cells in hopes of replacing some of the metabolic and endocrine

functions of the renal tubules, has been in development for some years (see (620) for review), with some preliminary evidence of efficacy. However, there are technical issues, and these devices have not been approved for clinical use. More recently, based on experimental evidence that extrarenal cells, including bone marrow–derived cells, may have beneficial effect in recovery and repair following renal tubular injury, there has been a focus on how endothelial cells or stem cells might be used to accelerate recovery from ATI. However, intrarenal cells are the primary source for regeneration and repair of tubular epithelium in AKI (433,621). Future strategies in the treatment of ARF include use of growth factors or stem cells and other novel therapies, including anti-inflammatory therapies, especially relevant in septic AKI (588,622–624).

SYNDROMIC ACUTE TUBULAR INJURY

Acute Renal Failure in Sepsis

Clinical definition of sepsis includes fever, high heart and respiratory rates, and elevation in white blood cells and/or immature white blood cell forms in the setting of infection. Severe sepsis is associated with lactic acidosis, and there may be altered mental status. In septic shock, hypotension persists despite adequate fluid replacement. The incidence of ARF is approximately 19% in moderate sepsis, 23% in severe sepsis, and 51% in septic shock with positive blood cultures (291,625). The combination of ARF and shock is associated with 70% mortality (reviewed in (38,626)).

ARF/AKI is one manifestation of acute organ dysfunction occurring in severe sepsis. During sepsis, development of AKI correlates with increased morbidity and mortality, impacts multiple-organ functions, and increases length of stay in the ICU (627). Sepsis is an important contributing factor for AKI in the critically ill (628), and mortality of ARF in sepsis is high. An understanding of mechanisms and development of therapeutic approaches has been hampered by limited histopathologic information and paucity of animal models (626,627).

In an effort to help elucidate mechanisms in sepsis, the pathology of AKI in sepsis has been recently reviewed (201). In a literature review of clinical and experimental studies, while “acute tubular necrosis” occurs, it was seen in only a minority of studies, and “ATN” was described in over 30% of specimens from primates, but in less than 1% of specimens from humans, with rodents intermediate. Human studies were heterogeneous in design, definition of AKI, and histopathology. In one study (629), 82% of biopsied patients showed acute “tubulointerstitial nephropathy,” 7% had acute glomerulonephritis, 3.5% had acute pyelonephritis, and 7% had classic “ATN.” In another large study of patients with severe sepsis (630), 27.5% had nonspecific tubular or glomerular damage, and 22.5% had vascular involvement. This literature review confirmed the paucity of histopathologic material from septic patients, as only a minority were biopsied in each series. As emphasized earlier in this chapter, mild forms of “ATI” are typical rather than “ATN,” even in these severely ill patients. Biomarkers for sepsis-induced AKI include those discussed above for AKI, though excretion of IL-18 is reportedly higher in septic AKI (631).

Pathophysiology of AKI in sepsis is multifactorial, triggered by sepsis-induced activation of the innate immune

response, resulting in cytokine storm, with release of IL-1, IL-6, TNF- α , and other cytokines. This systemic response triggers hemodynamic changes, endothelial dysfunction, infiltration of inflammatory cells, capillary thromboses, and tubular cell injury (reviewed in (627,632)). Patients with severe sepsis may develop prerenal failure as a result of septic shock. Renal vasoconstriction plays a role in sepsis-induced prerenal failure, but arterial vasodilation in sepsis and decrease in renal vascular resistance caused in part by cytokine-mediated vascular effects such as induction of NO synthesis are predisposition to ARF and have been demonstrated in septic states in large animal models (633). Acidosis and decrease in vascular smooth muscle ATP lead to alteration in K⁺ channels and resistance to vasopressin (634). Knockout of eNOS in mice makes the animals very vulnerable to ARF when treated with endotoxin, consistent with a role for endothelial injury in sepsis (635). In a rat model, a specific iNOS inhibitor, L-NIL, protected against ARF (636). The inflammatory cytokine TNF has been implicated in sepsis by studies showing preservation from renal injury in experimental endotoxemia in mice with TNF receptor blockade (637). Other experimental studies have implicated ROS. In animal studies, oxygen radical scavengers, including superoxide dismutase, have been shown to protect against endotoxemia-induced acute renal injury (638). Caspase-1 knockout mice are resistant to ARF induced by endotoxemia (639), implicating this protease in sepsis-associated ARF. A possible role for complement has been proposed in studies documenting the protective effect of blockade of complement component C5a in sepsis (640).

Despite these findings in animal models, clinical trials with anti-TNF antibody and other strategies based on preclinical studies have not shown improved patient survival in these complex patients (641,642). Management of septic AKI includes prophylactic measures, medical and extracorporeal treatment, and support of failing organs (reviewed in (38)). Early diagnosis using standardized criteria for AKI is recommended (8), to optimize management.

The Hepatorenal Syndrome

The term *hepatorenal syndrome* (HRS) is not a definable histopathologic entity of intrinsic renal disease. It describes a clinical syndrome of ARF that may complicate advanced liver disease (643), occurring in up to 40% of cirrhotic patients. Two types have been defined: type 1, with rapid reduction of renal function and frequently associated with failure in other organs and with decreased survival, and type 2, with slowly progressive decline in renal function. The five criteria for HRS, as defined by the International Ascites Club, include severe cirrhosis with ascites; sCr more than 1.5 mg/dL; failure of plasma expansion and diuretic withdrawal to improve renal function, absence of shock, and no current or recent treatment with nephrotoxic drugs; and absence of proteinuria, hematuria, and/or abnormal renal ultrasound. The syndrome is thought to be common, but the incidence is not known, in part because clinical measurements tend to overestimate renal function in cirrhosis (644). In a multivariate retrospective study of 355 patients with cirrhosis and ARF, 58% had prerenal failure (71 of 206 with type 1, the remainder type 2). Forty-two percent had “acute tubular necrosis.” No cases of ARF owing to acute glomerulonephritis were identified (645). This study confirms that the vast majority of cases of ARF in cirrhosis are caused by hypoperfusion injury.

HRS is characterized physiologically by intense intrarenal vasoconstriction and hypoperfusion, resulting in a primary decrease in the GFR, and is a variant of prerenal failure, because it is associated with diminished effective systemic circulatory volume, and splanchnic arterial vasodilation, with some component of cardiac dysfunction (reviewed in (646)). Urinalysis will usually reveal a benign urinary sediment and concentrated urine. In contrast to the chemical composition of the urine in ATI caused by ischemia or nephrotoxins, the sodium concentration is usually low. This finding could be a useful addition to the five criteria for HRS outlined above, helping to differentiate HRS and ATI. The pathogenetic mechanisms of action of the dramatic hemodynamic alterations accompanying severe hepatic disease are incompletely understood. The presence of ascites and other shifts in total body fluid volume are major contributors. Type I HRS usually develops in relationship to precipitating events such as various infections or surgical procedures (647). Gastrointestinal bleeding may underlie the ARF in some of these patients (648). Other risk factors in this setting include vomiting, diarrhea, or diuretic therapy. However, a significant number of cases occur without these antecedents. The renin-angiotensin-aldosterone system, activation of the sympathetic nervous system, and increased ADH activity have all been implicated as possibly playing a role. Treatment of HRS varies between type 1 and type 2 (reviewed in (643,649,650)). The treatment for type 1 HRS is vasoconstrictors and albumin; patients with type 1 HRS have improved renal function after therapy with vasoconstrictors such as terlipressin (645). This response could also serve as an additional diagnostic criterion for HRS (643). Treatment for type 2 HRS is transjugular intrahepatic portacaval shunt or large-volume paracentesis; vasoconstrictors and albumin may be effective, but recurrence rate is high. Prevention of HRS using albumin, prophylactic antibiotics, or TNF inhibitors may be possible in some settings such as bacterial peritonitis. Liver transplantation is the most effective therapy; patients with type 1 HRS have high priority for organ allocation. Recent studies have elucidated a role for intra-abdominal hypertension (IAH) in HRS, and relief of the IAH may have some efficacy (see below).

Because the pathogenesis appears to be primarily hemodynamic, the morphologic changes associated with this syndrome are nonspecific and not distinctive. Although bile-stained casts and crystals can be seen within tubular lumina, the cytologic changes visible in patients with ATI are not consistently present. Relatively few renal biopsy studies have been performed, because the biopsy procedure is often contraindicated in the clinical context of end-stage liver disease. The findings of postmortem studies must be evaluated with consideration of the changes caused by autolysis and other comorbid features. Nevertheless, some authors have emphasized particular histologic findings, including "tubularization" of Bowman capsular epithelium, tubular dilation, interstitial edema, bile-stained intratubular casts, leucine crystals in the tubules and interstitium, and sometimes an interstitial leukocytic infiltrate.

Acute Renal Failure and Multiple-Organ Failure

ARF often occurs in the setting of other acute organ dysfunctions. Potential "cross-talk" between affected organs is emerging as an area of interest for nephrology and critical care medicine (see (584,651) for review). For example, mechanical ventilation may initiate or aggravate ARF. Three mechanisms

have been invoked: permissive hypercapnia or hypoxemia with compromise of renal blood flow, effects on cardiac output, and barotrauma with pulmonary inflammation and release of inflammatory mediators (652). Conversely, ARF may potentiate acute lung injury. ARF leads to macrophage-mediated increase in pulmonary vascular permeability (653). ARF also leads to dysregulation of lung salt and water channels in bilateral ischemic injury or bilateral nephrectomy, though not in unilateral ischemic injury, suggesting a role for "uremic toxins" (654). Mechanisms underlying combined ARF and acute lung injury in the intensive care unit have been reviewed (655).

Cardiorenal Syndromes

The interrelationship between the heart/circulatory system and the kidney is reflected in the cardiorenal syndromes (CRS). The coexistence of cardiac and renal disease increases morbidity and mortality (656–658). A number of definitions and classifications had been developed to describe the syndrome(s) prior to 2008, largely not multidisciplinary (659,660). In 2008, an international multidisciplinary consensus conference was held to consider definition/classification, epidemiology, diagnostic criteria and biomarkers, prevention/protection strategies, management, and therapy. They defined five CRS: type 1 acute cardiorenal, type 2 chronic cardiorenal, type 3 acute renocardiac, type 4 chronic renocardiac, and type 5 secondary CRS (660).

The primary events for type 1 were identified as acute cardiac dysfunction due to acute heart failure/coronary syndrome or cardiogenic shock, resulting in AKI due to hypotension/hypoperfusion and ischemia. Proposed renal biomarkers included serum cystatin C, creatinine and NGAL, and urinary KIM-1, IL-18, NGAL, and NAG. Incidence of this syndrome has been estimated at between 19% and 45% of patients with acute cardiac dysfunction and is associated with increased mortality, hospitalization/readmission, and accelerated progression to CKD (661,662). An association between severity of AKI and risk of death has been noted (663), and even small acute changes in serum creatinine can modify mortality risk (661). Pathology in these cases has not been extensively studied, but is likely that of acute ischemia (see above).

Chronic CRS is due to chronic left ventricular dysfunction, diastolic dysfunction, cardiomyopathy, or other chronic forms of cardiac dysfunction, resulting in chronic kidney disease (CKD). Proposed renal biomarkers for this syndrome include sCr, cystatin C, urea, uric acid, and C-reactive protein. Proposed mechanisms include neurohumoral factors, inflammation, and oxidative injury. Pathology is likely that of chronic ischemia, with "creeping" fibrosis widening interstitial areas between atrophying tubules.

Acute and chronic renocardiac syndromes, CRS types 3 and 4, were also defined. In type 3, acute worsening of kidney function leads to cardiac injury and/or dysfunction. The primary event is AKI, with proposed biomarkers as noted in type 1 CRS. Mechanisms leading to cardiac effects likely include acute sodium and volume overload. In type 4, CKD leads to cardiac injury, disease, and/or dysfunction. Cardiac changes may be due to chronic sodium and volume overload, neurohumoral factors, and/or inflammation, in addition to effects of CKD-associated anemia and mineral/bone abnormalities.

Finally, type 5 (secondary CRS) is due to systemic conditions simultaneously affecting kidney and heart (e.g., sepsis, amyloidosis, autoimmune disease, severe hypertension).

Intra-Abdominal Hypertension and Abdominal Compartment Syndrome

Intra-abdominal hypertension (IAH) is defined as sustained or repeated elevation of intra-abdominal pressure (IAP) to ≥ 12 mm Hg. Abdominal compartment syndrome (ACS) is defined by sustained elevation of IAP greater than 20 mm Hg with new organ dysfunction (664). IAH/ACS increases morbidity and mortality in many patients in medical and surgical intensive care units. While traditionally seen in trauma, major burns, and postabdominal surgery, IAH/ACS is now recognized in patients with a variety of medical conditions, including septic shock and severe acute pancreatitis. Risk factors include conditions in which there is increase in intra-abdominal volume and/or decreased abdominal wall compliance, including sepsis, large-volume fluid resuscitation, multiple transfusions, high-pressure mechanical ventilation, obesity, acidosis, and in abdominal transplantation (reviewed in (665,666)). In mixed medical-surgical intensive care units, IAH occurs in up to 64% and ACS in up to 12% of patients.

Oliguria and AKI are frequent in IAH/ACS and increase morbidity and mortality. IAH/ACS also contributes to renal dysfunction in cardiorenal and hepatorenal syndromes. In one study in patients with advanced heart failure, higher central venous pressure was associated with development of worsening renal function and was a stronger predictor than cardiac index (667), consistent with a role for IAH. Improved GFR and urine flow have been described after reduction of IAP via paracentesis (668).

IAP can be measured using transvesicular pressure monitoring via an indwelling catheter. Abdominal perfusion pressure (APP), defined as the difference between systemic mean arterial pressure (MAP) and the IAP, falls with drop in MAP and/or rise in IAP. A fall in APP is associated with fall in perfusion to organs in or near the abdomen, including the kidneys (669,670). Renal pathology has not been well defined clinically in this syndrome, but is likely that of hypoperfusion. In one study in pigs using pneumoperitoneum to induce IAH, proximal tubular necrosis was described; fluid resuscitation preserved cardiac output, but did not prevent renal tubular injury (or changes in other organs) (670). In rats with ACS, renal tubular cell apoptosis and *bal-2* expression were found, greater with longer duration of ACS. Abdominal decompression has been successful in treatment, and high-volume fluid resuscitation and fluid overload should be avoided or managed with ultrafiltration or diuretics. In general, multidisciplinary integrated management with IAP measurement, preventive measures, and medical and surgical approaches should reduce mortality and costs. Decompressive laparotomy is used if medical treatment is ineffective or if there is rapidly progressive organ dysfunction caused by IAH/ACS. More study is needed by nephrologists and nephropathologists to fully define renal effects of these syndromes.

RENAL CORTICAL NECROSIS

Bilateral RCN is a rare and dramatically unique cause of ARF. The clinical course is similar to that of ATI, except that it almost always presents with anuria or profound oliguria. It most commonly is seen in association with obstetric

accidents (671), such as abruptio placentae, placenta previa, or in septic abortion, but has rarely been reported following elective abortion (672). Coagulopathy associated with abruptio placentae, abortion, or placenta previa is reported as being responsible for 50% to 60% of all cases of acute bilateral RCN. Twin-twin or twin-maternal transfusions with resultant activation of the complement cascade can also lead to cortical necrosis (279). RCN may also occur in the context of HUS/TTP (673) and is also seen in instances of severe trauma, systemic sepsis, postoperative shock, and some specific poisonings, including snake venom, diethylene glycol, and arsenic (672,674–678). Pregnancy-associated HELLP syndrome, with hemolysis, elevated liver enzymes, and thrombocytopenia, is a recognized cause (679,680). Antiphospholipid syndrome has also been associated with RCN (681). A pediatric case has been described in the context of antiprotein S antibodies following varicella infection (682). Acute RCN may also be associated with severe acute pancreatitis (683). In infants and children, the precipitating event is often gastroenteritis with severe vomiting, diarrhea, and dehydration. Overwhelming infection with bacterial sepsis is the other major cause in adults. There are also reports of cortical necrosis related to malarial infection (684). Patchy RCN is also seen in renal allografts, especially with severe antibody-mediated rejection, and is associated with early graft loss (685).

The pathogenesis of cortical necrosis involves microvascular abnormalities. There are several major theories, and they are not mutually exclusive. On the basis of examination of the kidneys from patients who died after abruptio placentae, Sheehan and Davis (22) proposed that vasospasm is the primary event causing cortical necrosis. Alternatively, acute cortical necrosis may result from severe forms of thrombotic microangiopathy, resulting from acute vascular injury followed by activation of coagulation and thrombosis (675,686,687). A third hypothesis suggests that acute cortical necrosis may be the consequence of an immunologic mechanism akin to hyperacute rejection of renal allografts. All of these hypotheses have some supporting evidence, but there is no convincing proof that any one of them fully explains the sequence of events that occurs in human patients.

The clinical course of acute cortical necrosis depends on the extent of involvement. If necrosis is extensive, death occurs within the first few days unless dialysis is undertaken. With timely renal replacement therapy, renal function may recover sufficiently to allow patients to become dialysis independent after a period of 1 to 3 months, and renal function may continue to improve over a period of 1 to 2 years. No specific therapeutic approaches have been successful, although anticoagulants, beta-blockers, cytotoxic drugs, and mannitol have all been tried.

Gross Pathology

Bilateral cortical necrosis in its diffuse form is a condition in which there is widespread destruction of the renal cortex, except for a narrow rim of cortical tissue just underneath the capsule and with relative preservation of the medulla and the adjacent juxtamedullary cortex. This is the most severe form and can be detected on imaging studies (Fig. 26.31A). It is generally recognized on gross examination as large, swollen kidneys in which the necrotic portion of the cortex is pale or yellowish white, with congestion of the

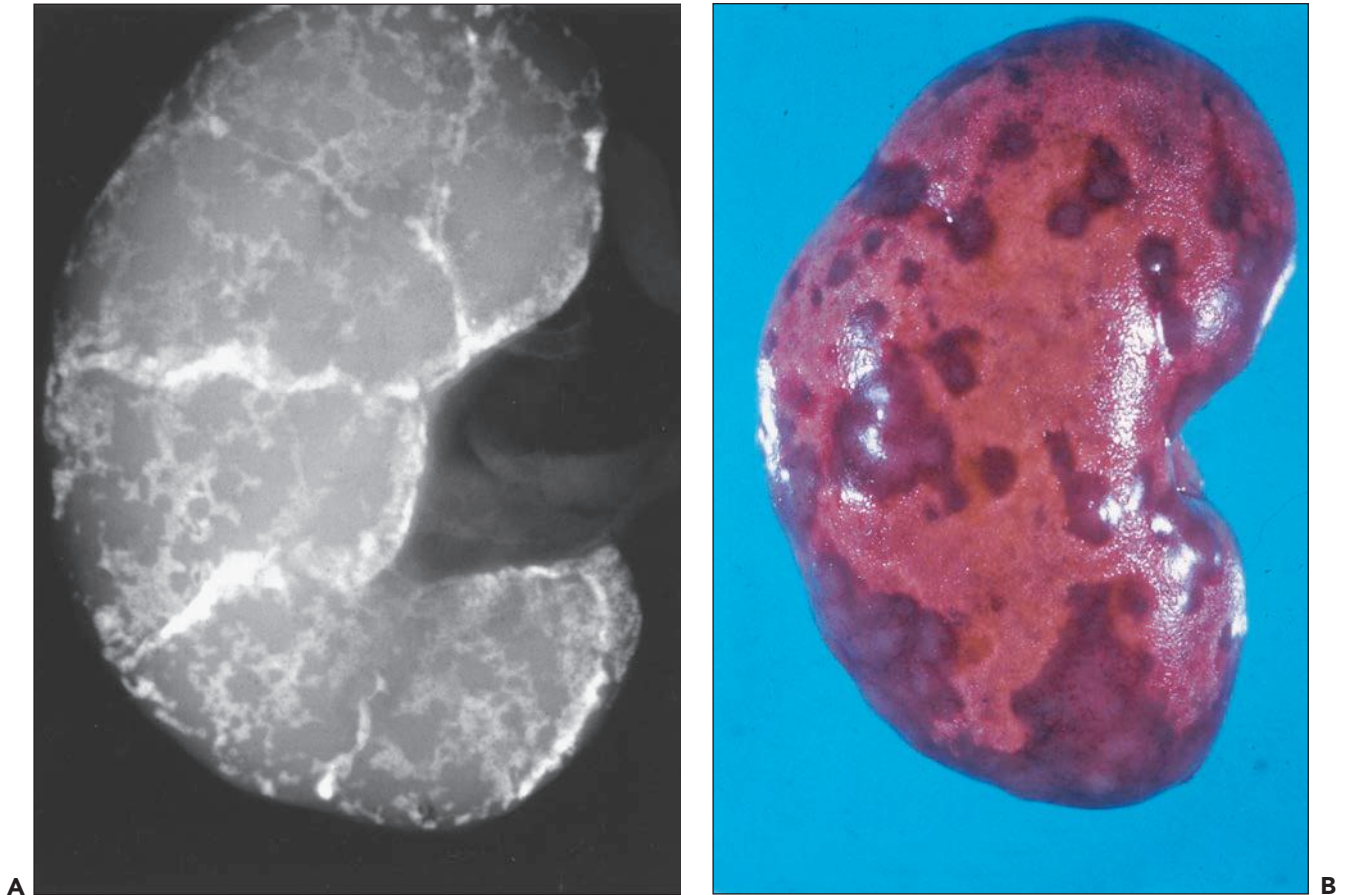


FIGURE 26.31 **A:** Radiograph with contrast of a kidney with cortical necrosis showing hypoperfusion and areas of hemorrhage. **B:** Gross specimen of a kidney with extensive areas of pallor representing the necrotic cortex with intervening areas of congested nonnecrotic parenchyma.

adjacent, relatively well-preserved tissue (see Fig. 26.31B). Patchy and focal forms affect smaller amounts of cortex and appear grossly similar to areas of infarction, except that they are surrounded on all sides by viable tissue and do not have the characteristic wedge-shaped pattern of the classic infarct.

Light Microscopy

By light microscopy, the findings are very similar to those seen with ischemic infarcts. There is coagulation of the central necrotic areas with relative preservation of the architecture of the tubules and the glomeruli but loss of normal cytologic features (Fig. 26.32). The arteries and arterioles are also necrotic

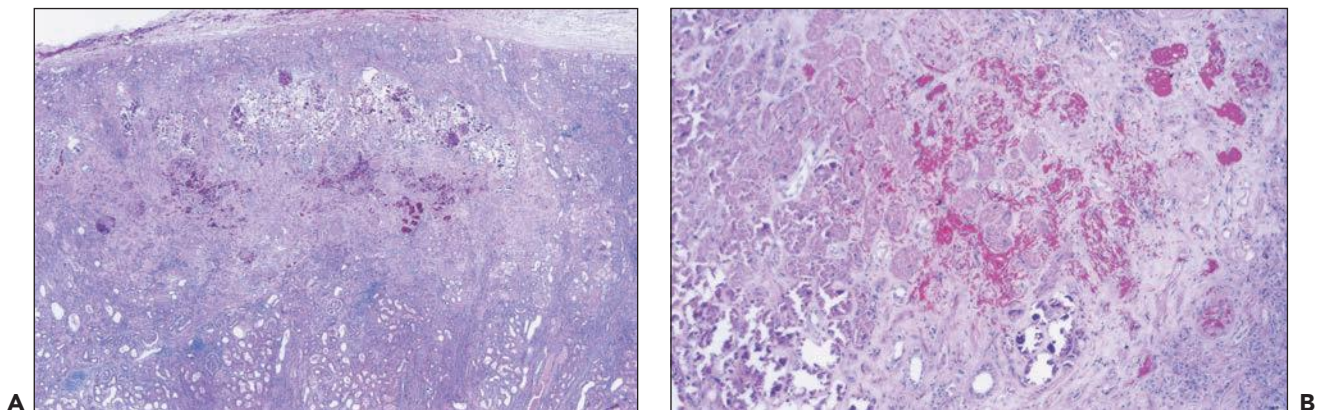


FIGURE 26.32 **A:** Cortical necrosis, with sparing of the subcapsular cortex and medulla. (H&E; $\times 64$.) **B:** Cortical necrosis with coagulative necrosis with focal hemorrhage. (H&E; $\times 200$.)

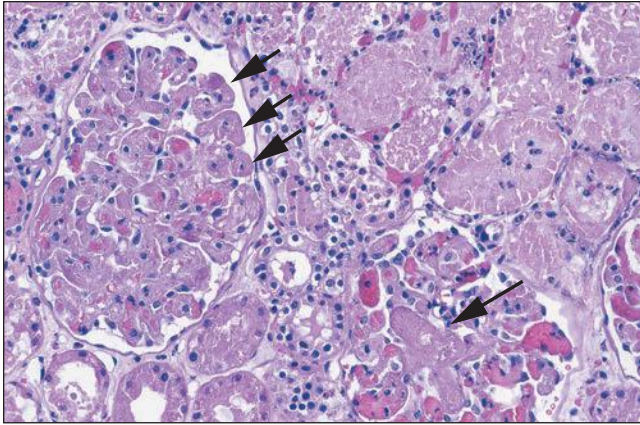


FIGURE 26.33 Cortical necrosis, with thromboses (*arrows*) in glomeruli adjacent to the necrotic area. (H&E; $\times 640$.)

and dilated and frequently contain thrombi. Glomeruli and vessels in the border zones may show evidence of capillary and vascular thrombosis (Fig. 26.33). Biopsy early in the course more often reveals patchy necrosis (688). As the lesion progresses toward healing, leukocytic infiltration, organization, scarring, calcification, and even ossification may take place as the necrotic tissue is gradually replaced by scarring (Fig. 26.34). Patients biopsied late in the course have bland parenchymal fibrosis/sclerosis (689). In cases associated with TMA, characteristic microvascular pathology with thrombosis, endothelial injury, intimal edema, and fibrin and erythrocyte and erythrocyte fragments in small vessels and glomeruli may be seen.

INFARCTION OF THE KIDNEY

Infarction of the kidney results from complete obstruction of major branches of the renal arteries or renal veins, and when it is extensive, it may appear as ARF. Arterial occlusion is more frequently seen as a cause of renal infarction than venous occlusion. It can result from embolism, thrombosis, or vessel wall damage which accompanies malignant hypertension or systemic vasculitis.

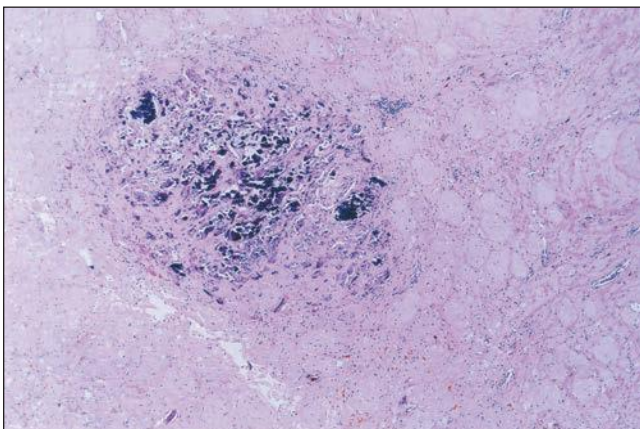


FIGURE 26.34 Chronic cortical necrosis with calcification. (H&E; $\times 80$.)

Renal infarction caused by arterial occlusion is not uncommon, largely because there is little collateral circulation available and because complete occlusion of an arterial branch results in absolute ischemia of the distal parenchyma. The majority of infarcts in adults are often clinically silent and are frequently caused by sudden and complete arterial blockage by emboli, potentially originating from ventricular thrombi or from vegetations on heart valves with verrucous or infective endocarditis or due to atheroemboli (see below). Less commonly, arterial obstruction is produced by thrombosis owing to changes in the wall of the vessel associated with atherosclerosis, systemic sclerosis, malignant hypertension, polyarteritis, or aneurysm formation as a result of dysplastic disease of the renal artery. Renal infarction has also rarely been described as a result of cocaine use (690,691). Cases have also been described with fibromuscular dysplasia involving the renal arteries. Loin or renal fossa pain, hematuria, and/or pyrexia may suggest infection or renal calculi. Renal infarction frequently goes undetected, however, particularly if the area of infarction is small. Large infarcts can be associated with loin pain followed by hematuria and transient proteinuria.

Gross Pathology

The gross appearance of a renal infarct depends on the age of the lesion, the size of the vessel obstructed, and the presence or absence of infection. Initially, the infarct is red and pyramidal in shape, with the apex toward the obstructed artery. Within hours, it becomes gray, with a narrow red rim of adjacent congested parenchyma; as intralésional coagulation occurs, the infarcted area develops a yellow coloration (Fig. 26.35). As necrotic tissue is removed and replaced by collagenous tissue, the area of infarct shrinks and eventually becomes a V-shaped scar. The medulla is generally spared in renal infarction, and the lesions are confined to the cortex. Infarcts resulting from septic embolization are associated with the presence of liquefactive necrosis and abscess formation as a result of digestion by leukocytic enzymes.

Light Microscopy

Histologically, sterile infarcts show the findings of classic coagulative necrosis. Initially, there is marked congestion, followed by cytoplasmic and nuclear changes, where the tubular and glomerular architecture is preserved but gradual loss of viable cytologic

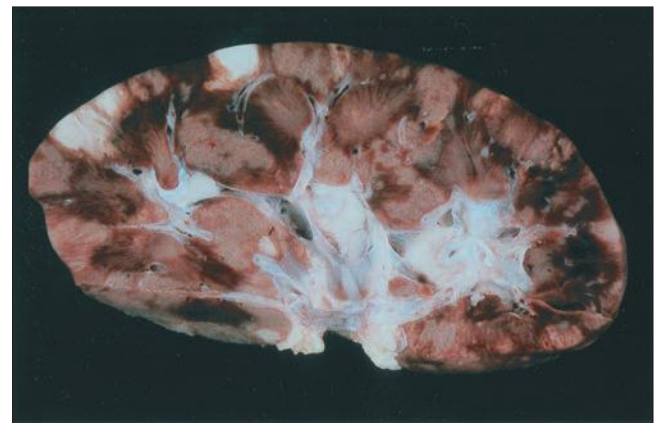


FIGURE 26.35 A kidney with focal, pale, wedge-shaped cortical infarcts. Note congestion at the corticomedullary junction.

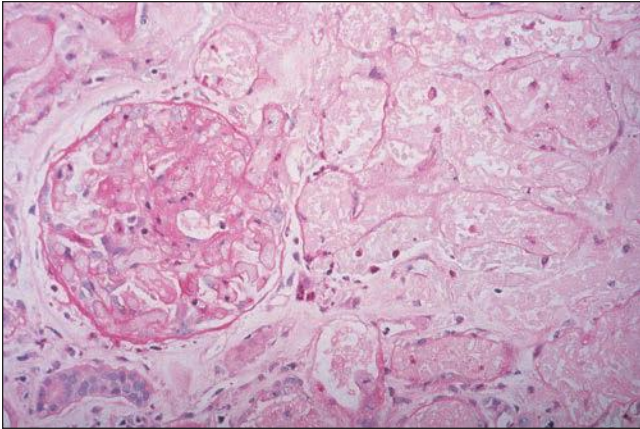


FIGURE 26.36 Renal infarct, with coagulative necrosis of all cellular elements. (H&E; $\times 400$.)

structure occurs. The cytoplasm becomes homogeneous and eosinophilic, and the nuclei demonstrate condensation and karyorrhexis (Fig. 26.36). Peripheral to the central area of necrosis is a marginal zone in which there is a gradual transition from frank necrotic changes to sublethal injury in which glomerular and tubular changes are less striking and are similar to those seen in ATI (Fig. 26.37). As the lesion develops, it is in this zone that polymorphonuclear leukocytic infiltration becomes prominent. As the lesion progresses, the central necrotic area becomes smaller, and organization and regeneration occur around the periphery, with eventual collapse of the central necrotic area and replacement by collagenous scarring. As mentioned previously, the lesions are generally confined to the cortical tissue, and the medulla is spared. This picture helps distinguish scars resulting from infarction from those caused by reflux or pyelonephritis, in which medullary involvement is prominent.

Venous Infarction

Venous obstruction as a cause of infarction is much less common than arterial obstruction. It is seen in infancy as a complication of severe dehydration stemming from diarrheal diseases. Thrombosis

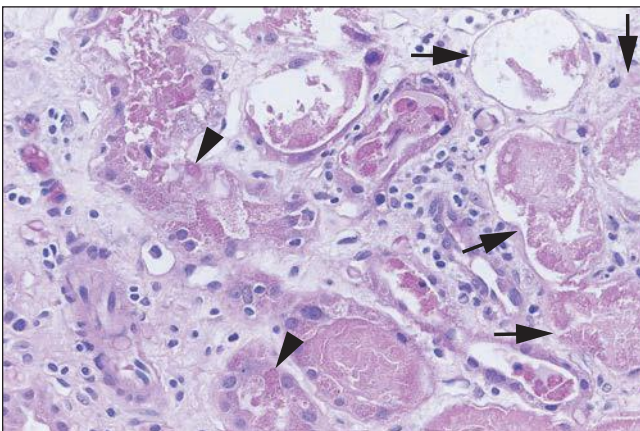


FIGURE 26.37 Transition zone at the edge of a cortical infarct. Note completely necrotic tubules (*arrows*) and relatively intact tubules with individual cell necrosis (*arrowheads*) containing necrotic debris. (H&E; $\times 640$.)

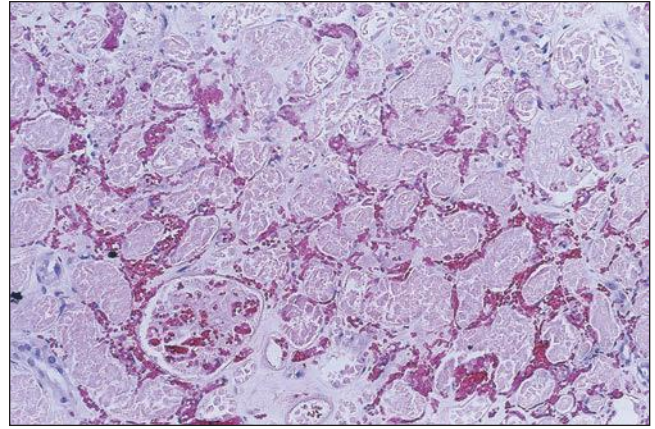


FIGURE 26.38 Hemorrhagic infarct with severe congestion of microvessels. (H&E; $\times 400$.)

of intrarenal veins and, occasionally, of the main renal vein produces an infarct of the hemorrhagic type (Fig. 26.38), as opposed to the relatively bland ischemic infarction that follows arterial occlusion. Whether infarction occurs in the kidney as a result of venous thrombosis depends on the completeness of the occlusion and the speed at which thrombosis and occlusion take place. Sudden, complete occlusions can be associated with infarction in adults, although this is rare; in most instances, thrombosis of the renal vein does not lead to infarction after infancy.

ATHEROEMBOLIC DISEASE OF THE KIDNEY

Embolization of the kidney by fragments of atheromatous plaques is extremely common and is found in nearly 5% of autopsies of men over the age of 50 and 3% of women in the same age group (692–695). Although emboli do appear spontaneously, they more commonly follow invasive arterial procedures, including arteriography, coronary angiography, coronary artery bypass, and repair of aortic aneurysms; they are found in as many as 25% of patients who have undergone such procedures (696). The emboli are usually derived from

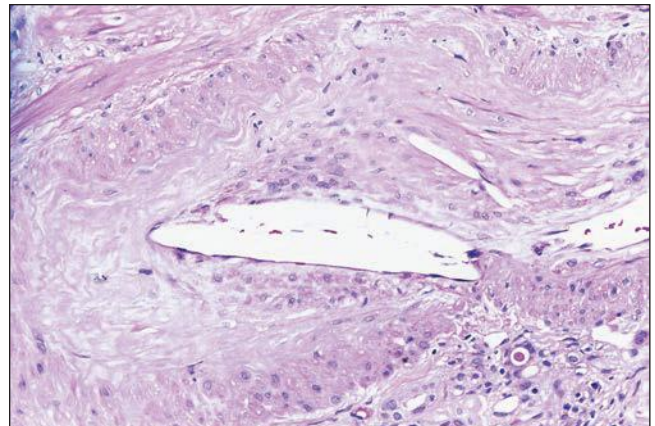


FIGURE 26.39 Atheroembolus in an artery, with cleft-like spaces surrounded by fibrotic reaction. (H&E; $\times 400$.)

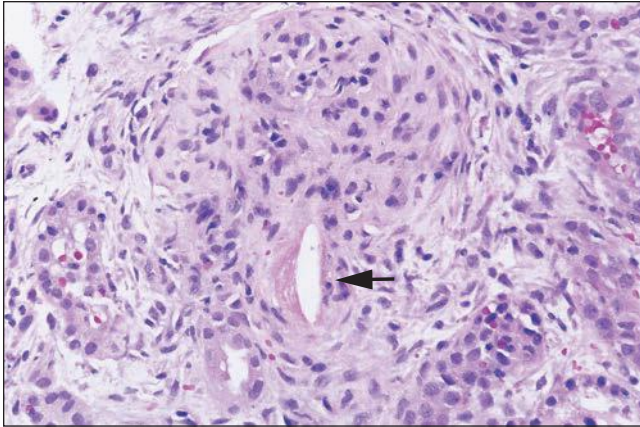


FIGURE 26.40 Atheroembolus in an arteriole. The glomerulus appears ischemic. (H&E; $\times 400$.)

atheromatous lesions of the abdominal aorta that become impacted in intrarenal vessels (Fig. 26.39). Arteriolar and glomerular embolization can also occur (Fig. 26.40). When obstruction is complete, distal areas of infarction and necrosis are evident. Often the obstruction is incomplete, and the distal parenchyma demonstrates only ischemic atrophy (Fig. 26.41).

Cholesterol emboli are identified by the characteristic needle-shaped clefts that remain after the lipid has been dissolved during histologic processing (see Fig. 26.39). In early-stage lesions, the crystals are surrounded by fibrin, occasionally with associated eosinophils. In older embolic lesions, organization is evident, and the crystals are surrounded by fibrous tissue. Renal atheroemboli are frequently part of more generalized atheroembolic disease, resulting from multiple showers of cholesterol-containing microemboli in many organs, including the retina, brain, pancreas, and, in particular, the muscles and skin of the legs in addition to the kidney. Multisystem involvement often mimics systemic vasculitides, such as microscopic polyarteritis. In some instances, showers of emboli may be so extensive as to result in the clinical syndrome of ARE, mimicking the findings of rapidly progressive glomerulonephritis. The presence of eosinophilia, hypocomplementemia, and sometimes eosinophiluria further complicates the clinical recognition of this disease.

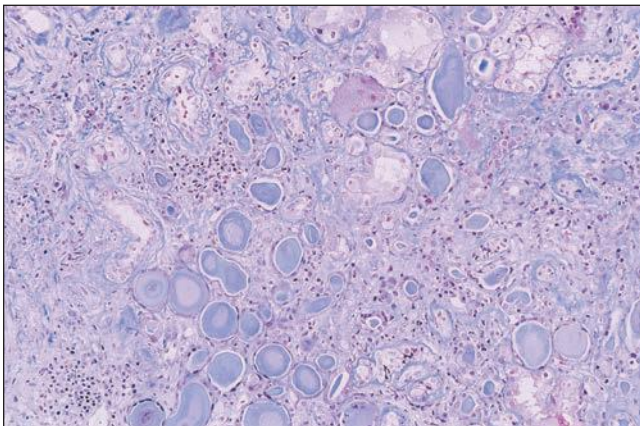


FIGURE 26.41 Ischemic atrophy downstream from chronic arterial atheroembolus. (H&E; $\times 200$.)

REFERENCES

1. Mehta RL, Pascual MT, Soroko S, et al. Spectrum of acute renal failure in the intensive care unit: The PICARD experience. *Kidney Int* 2004;66(4):1613.
2. Hoste EA, Kellum JA. Acute kidney injury: Epidemiology and diagnostic criteria. *Curr Opin Crit Care* 2006;12(6):531.
3. Uchino S, Bellomo R, Bagshaw SM, et al. Transient azotaemia is associated with a high risk of death in hospitalized patients. *Nephrol Dial Transplant* 2010;25(6):1833.
4. Bellomo R, Ronco C, Kellum JA, et al. Acute renal failure - definition, outcome measures, animal models, fluid therapy and information technology needs: The Second International Consensus Conference of the Acute Dialysis Quality Initiative (ADQI) Group. *Crit Care* 2004;8(4):R204.
5. Ricci Z, Cruz D, Ronco C. The RIFLE criteria and mortality in acute kidney injury: a systematic review. *Kidney Int* 2008;73(5):538.
6. Mehta RL, Kellum JA, Shah SV, et al. Acute Kidney Injury Network: Report of an initiative to improve outcomes in acute kidney injury. *Crit Care* 2007;11(2):R31.
7. Bagshaw SM. Acute kidney injury: Diagnosis and classification of AKI: AKIN or RIFLE? *Nat Rev Nephrol* 2010;6(2):71.
8. Ricci Z, Cruz DN, Ronco C. Classification and staging of acute kidney injury: Beyond the RIFLE and AKIN criteria. *Nat Rev Nephrol* 2011;7(4):201.
9. Hackradt A. *Vasomotorische Nephrosen nach Verschuttung*. Munich, Germany: Wagner, 1917.
10. Minami S. Nierenveränderungen nach Verschuttung. *Virchows Arch (Pathol Anat)* 1923;246:1923.
11. Baker SL, Dodds EC. Obstruction of the renal tubules during the excretion of haemoglobin. *Br J Exp Pathol* 1925;6:247.
12. Bywaters EGL, Beall D. Crush injuries with impairment of renal function. *Br Med J* 1941;1:427.
13. Bywaters EGL, Dible JH. The renal lesion in traumatic anuria. *J Pathol Bacteriol* 1942;54:111.
14. Dunn JS, Gillespie M, Niven JSF. Renal lesions in two cases of crush syndrome. *Lancet* 1941;2:549.
15. Lucke B. Lower nephron nephrosis: The renal lesions of the crush syndrome, of burns, transfusions and other conditions affecting the lower segments of the nephrons. *Mil Surg* 1946;99:371.
16. Oliver J, MacDowell M, Tracy A. The pathogenesis of acute renal failure associated with traumatic and toxic injury: Renal ischemia, nephrotoxic damage and the ischemic episode. *J Clin Invest* 1951;30:1307.
17. Goormaghtigh N. Vascular and circulatory changes in renal cortex in the anuric crush-syndrome. *Proc Soc Exp Biol Med* 1945;59:303.
18. Goormaghtigh N. The renal arteriolar changes in the anuric crush syndrome. *Am J Pathol* 1947;23:513.
19. Trueta J, Barclay AE, Daniel PM, et al. *Studies of the Renal Circulation*. Springfield, IL: Charles C. Thomas, 1947.
20. Brun C. *Acute Anuria: A Study Based on Renal Function Tests and Aspiration Biopsy of the Kidney*. Copenhagen, Denmark: E. Munksgard, 1965.
21. Brun C, Crone C, Davidsen HG, et al. Renal interstitial pressure in normal and in anuric man: Based on wedged renal vein pressure. *Proc Soc Exp Biol Med* 1956;91:199.
22. Sheehan HD, Davis JC. Renal ischaemia with failed reflow. *J Pathol Bacteriol* 1959;78.
23. Sevti S. Pathogenesis of traumatic uraemia: A revised concept. *Lancet* 1959;2:135.
24. Hollenberg NK, Adams DF, Oken DE, et al. Acute renal failure due to nephrotoxins: Renal hemodynamic and angiographic studies in man. *N Engl J Med*. 1970;282(24):1329.
25. Hollenberg NK, Epstein M, Rosen SM, et al. Acute oliguric renal failure in man: Evidence for preferential renal cortical ischemia. *Medicine (Baltimore)* 1968;47(6):455.
26. Munck O. *Renal Circulation in Acute Renal Failure*. Oxford: Blackwell, 1958.
27. Oken DE, Arce ML, Wilson DR. Glycerol-induced hemoglobinuric acute renal failure in the rat. I. Micropuncture study of the development of oliguria. *J Clin Invest* 1966;45(5):724.

28. Siegel NJ, Gaudio KM, Katz LA, et al. Beneficial effect of thyroxin on recovery from toxic acute renal failure. *Kidney Int* 1984;25(6):906.
29. Kashgarian M, Siegel NJ, Ries AL, et al. Hemodynamic aspects in development and recovery phases of experimental postischemic acute renal failure. *Kidney Int Suppl* 1976;6:S160.
30. Siegel NJ, Gunstream SK, Handler RI, et al. Renal function and cortical blood flow during the recovery phase of acute renal failure. *Kidney Int* 1977;12(3):199.
31. Thurau K, Boylan JW. Acute renal success. The unexpected logic of oliguria in acute renal failure. *Am J Med* 1976;61(3):308.
32. Heyman SN, Rosenberger C, Rosen S. Acute Kidney Injury: Lessons from experimental models. *Contrib Nephrol* 2011;169:286.
33. Endre ZH, Westhuyzen J. Early detection of acute kidney injury: Emerging new biomarkers. *Nephrology (Carlton)* 2008;13(2):91.
34. Ferguson MA, Vaidya VS, Bonventre JV. Biomarkers of nephrotoxic acute kidney injury. *Toxicology*. 2008;245(3):182.
35. Herget-Rosenthal S, Poppen D, Husing J, et al. Prognostic value of tubular proteinuria and enzymuria in nonoliguric acute tubular necrosis. *Clin Chem* 2004;50(3):552.
36. Haase M, Bellomo R, Devarajan P, et al. Accuracy of neutrophil gelatinase-associated lipocalin (NGAL) in diagnosis and prognosis in acute kidney injury: A systematic review and meta-analysis. *Am J Kidney Dis* 2009;54(6):1012.
37. Molitoris BA, Melnikov VY, Okusa MD, et al. Technology insight: biomarker development in acute kidney injury—what can we anticipate? *Nat Clin Pract Nephrol* 2008;4(3):154.
38. Uchino S, Kellum JA, Bellomo R, et al. Acute renal failure in critically ill patients: A multinational, multicenter study. *JAMA* 2005;294(7):813.
39. Pannu N, Nadim MK. An overview of drug-induced acute kidney injury. *Crit Care Med* 2008;36(4 Suppl):S216.
40. Bacchetta J, Dubourg L, Juillard L, et al. Non-drug-induced nephrotoxicity. *Pediatr Nephrol* 2009;24(12):2291.
41. Szabo Z, Alachkar N, Xia J, et al. Molecular imaging of the kidneys. *Semin Nucl Med* 2011;41(1):20.
42. Sharfuddin AA, Sandoval RM, Molitoris BA. Imaging techniques in acute kidney injury. *Nephron Clin Pract* 2008;109(4):C198.
43. Portilla D, Schnackenberg L, Beger RD. Metabolomics as an extension of proteomic analysis: Study of acute kidney injury. *Semin Nephrol* 2007;27(6):609.
44. Izzedine H, Launay-Vacher V, Deray G. Antiviral drug-induced nephrotoxicity. *Am J Kidney Dis* 2005;45(5):804.
45. Cooper RD, Tonelli M. Renal disease associated with antiretroviral therapy in the treatment of HIV. *Nephron Clin Pract* 2011;118(3):c262.
46. Harris M. Nephrotoxicity associated with antiretroviral therapy in HIV-infected patients. *Expert Opin Drug Saf* 2008;7(4):389.
47. Rodriguez-Novoa S, Alvarez E, Labarga P, et al. Renal toxicity associated with tenofovir use. *Expert Opin Drug Saf* 2010;9(4):545.
48. Daugas E, Rougier JP, Hill G. HAART-related nephropathies in HIV-infected patients. *Kidney Int* 2005;67(2):393.
49. Fisher EJ, Chaloner K, Cohn DL, et al. The safety and efficacy of adefovir dipivoxil in patients with advanced HIV disease: a randomized, placebo-controlled trial. *AIDS* 2001;15(13):1695.
50. Sawyer MH, Webb DE, Balow JE, et al. Acyclovir-induced renal failure. Clinical course and histology. *Am J Med* 1988;84(6):1067.
51. Perazella MA. Crystal-induced acute renal failure. *Am J Med* 1999;106(4):459.
52. Jacobson MA, O'Donnell JJ, Mills J. Foscarnet treatment of cytomegalovirus retinitis in patients with the acquired immunodeficiency syndrome. *Antimicrob Agents Chemother* 1989;33(5):736.
53. Winston DJ, Wirin D, Shaked A, et al. Randomised comparison of ganciclovir and high-dose acyclovir for long-term cytomegalovirus prophylaxis in liver-transplant recipients. *Lancet* 1995;346(8967):69.
54. Lalezari JP, Holland GN, Kramer F, et al. Randomized, controlled study of the safety and efficacy of intravenous cidofovir for the treatment of relapsing cytomegalovirus retinitis in patients with AIDS. *J Acquir Immune Defic Syndr Hum Retroviral* 1998;17(4):339.
55. Tashima KT, Horowitz JD, Rosen S. Indinavir nephropathy. *N Engl J Med* 1997;336(2):138.
56. Boubaker K, Sudre P, Bally F, et al. Changes in renal function associated with indinavir. *AIDS* 1998;12(18):F249.
57. Zimmermann AE, Pizzoferrato T, Bedford J, et al. Tenofovir-associated acute and chronic kidney disease: A case of multiple drug interactions. *Clin Infect Dis* 2006;42(2):283.
58. Cooper RD, Wiebe N, Smith N, et al. Systematic review and meta-analysis: renal safety of tenofovir disoproxil fumarate in HIV-infected patients. *Clin Infect Dis* 2010;51(5):496.
59. Chugh S, Bird R, Alexander EA. Ritonavir and renal failure. *N Engl J Med* 1997;336(2):138.
60. Vandercam B, Moreau M, Goffin E, et al. Cidofovir-induced end-stage renal failure. *Clin Infect Dis* 1999;29(4):948.
61. Herlitz LC, Mohan S, Stokes MB, et al. Tenofovir nephrotoxicity: Acute tubular necrosis with distinctive clinical, pathological, and mitochondrial abnormalities. *Kidney Int* 2010;78(11):1171.
62. Cronin RE, Henrich WL. *Toxic Nephropathies*. Philadelphia, PA: WB Saunders, 2000.
63. Cronin RE. Aminoglycoside nephrotoxicity: Pathogenesis and prevention. *Clin Nephrol* 1979;11(5):251.
64. Raveh D, Kopyt M, Hite Y, et al. Risk factors for nephrotoxicity in elderly patients receiving once-daily aminoglycosides. *QJM* 2002;95(5):291.
65. Rougier F, Ducher M, Maurin M, et al. Aminoglycoside dosages and nephrotoxicity: Quantitative relationships. *Clin Pharmacokinetics* 2003;42(5):493.
66. Montagu C, Bosch F, Villela L, et al. Aminoglycoside-associated severe renal failure in patients with multiple myeloma treated with thalidomide. *Leuk Lymphoma* 2004;45(8):1711.
67. Melnick JZ, Baum M, Thompson JR. Aminoglycoside-induced Fanconi's syndrome. *Am J Kidney Dis* 1994;23(1):118.
68. De Beukelaer MM, Travis LB, Dodge WF, et al. Deafness and acute tubular necrosis following parenteral administration of neomycin. *Am J Dis Child* 1971;121(3):250.
69. Greenberg LH, Momary H. Audiotoxicity and nephrotoxicity due to orally administered neomycin. *JAMA* 1965;194(7):827.
70. Stamm AM, Diasio RB, Dismukes WE, et al. Toxicity of amphotericin B plus flucytosine in 194 patients with cryptococcal meningitis. *Am J Med* 1987;83(2):236.
71. Harbarth S, Pestotnik SL, Lloyd JF, et al. The epidemiology of nephrotoxicity associated with conventional amphotericin B therapy. *Am J Med* 2001;111(7):528.
72. Mccurdy DK, Frederic M, Elkinton JR. Renal tubular acidosis due to amphotericin B. *N Engl J Med* 1968;278(3):124.
73. Yano Y, Monteiro JL, Seguro AC. Effect of amphotericin-B on water and urea transport in the inner medullary collecting duct. *J Am Soc Nephrol* 1994;5(1):68.
74. Ostrosky-Zeichner L, Marr KA, Rex JH, et al. Amphotericin B: Time for a new "gold standard". *Clin Infect Dis* 2003;37(3):415.
75. Safdar A, Ma J, Saliba F, et al. Drug-induced nephrotoxicity caused by amphotericin B lipid complex and liposomal amphotericin B: A review and meta-analysis. *Medicine (Baltimore)* 2010;89(4):236.
76. Tune BM. Nephrotoxicity of beta-lactam antibiotics: mechanisms and strategies for prevention. *Pediatr Nephrol* 1997;11(6):768.
77. Mocan H, Beattie TJ. Acute tubular necrosis associated with cephalixin therapy. *Clin Nephrol* 1985;24(4):212.
78. Longstreth KL, Robbins SD, Smavatkul C, et al. Cephalixin-induced acute tubular necrosis. *Pharmacotherapy* 2004;24(6):808.
79. Vomiero G, Carpenter B, Robb I, et al. Combination of ceftriaxone and acyclovir— an underestimated nephrotoxic potential? *Pediatr Nephrol* 2002;17(8):633.
80. Fiaccadori E, Maggiore U, Arisi A, et al. Outbreak of acute renal failure due to cefodizime-vancomycin association in a heart surgery unit. *Intensive Care Med* 2001;27(11):1819.
81. Falagas ME, Kasiakou SK. Toxicity of polymyxins: A systematic review of the evidence from old and recent studies. *Crit Care* 2006;10(1):R27.
82. Nation RL, Li J. Colistin in the 21st century. *Curr Opin Infect Dis* 2009;22(6):535.
83. Markou N, Apostolakis H, Koumoudiou C, et al. Intravenous colistin in the treatment of sepsis from multiresistant Gram-negative bacilli in critically ill patients. *Crit Care* 2003;7(5):R78.

84. Michalopoulos AS, Tsiodras S, Rellos K, et al. Colistin treatment in patients with ICU-acquired infections caused by multiresistant Gram-negative bacteria: the renaissance of an old antibiotic. *Clin Microbiol Infect* 2005; 11(2):115.
85. Ouderkerk JP, Nord JA, Turett GS, et al. Polymyxin B nephrotoxicity and efficacy against nosocomial infections caused by multiresistant gram-negative bacteria. *Antimicrob Agents Chemother* 2003; 47(8):2659.
86. Sobieszczyk ME, Furuya EY, Hay CM, et al. Combination therapy with polymyxin B for the treatment of multidrug-resistant Gram-negative respiratory tract infections. *J Antimicrob Chemother* 2004; 54(2):566.
87. Hazlewood KA, Brouse SD, Pitcher WD, et al. Vancomycin-associated nephrotoxicity: Grave concern or death by character assassination? *Am J Med* 2010;123(2):182.
88. Wilcox MH, Tack KJ, Bouza E, et al. Complicated skin and skin-structure infections and catheter-related bloodstream infections: Noninferiority of linezolid in a phase 3 study. *Clin Infect Dis* 2009;48(2):203.
89. Downs NJ, Neihart RE, Dolezal JM, et al. Mild nephrotoxicity associated with vancomycin use. *Arch Intern Med* 1989;149(8):1777.
90. Wong-Beringer A, Joo J, Tse E, et al. Vancomycin-associated nephrotoxicity: A critical appraisal of risk with high-dose therapy. *Int J Antimicrob Agents* 2011;37(2):95.
91. Bosso JA, Nappi J, Rudisill C, et al. Relationship between vancomycin trough concentrations and nephrotoxicity: A prospective multicenter trial. *Antimicrob Agents Chemother* 2011;55(12):5475.
92. Cano EL, Haque NZ, Welch VL, et al. Incidence of nephrotoxicity and association with vancomycin use in intensive care unit patients with pneumonia: retrospective analysis of the IMPACT-HAP Database. *Clin Ther* 2012;34(1):149.
93. Naesens M, Kuypers DR, Sarwal M. Calcineurin inhibitor nephrotoxicity. *Clin J Am Soc Nephrol* 2009;4(2):481.
94. Mihatsch MJ, Kyo M, Morozumi K, et al. The side-effects of cyclosporine-A and tacrolimus. *Clin Nephrol* 1998;49(6):356.
95. Rodicio JL. Calcium antagonists and renal protection from cyclosporine nephrotoxicity: Long-term trial in renal transplantation patients. *J Cardiovasc Pharmacol* 2000;35(3 Suppl 1):S7.
96. Clive DM. Renal transplant-associated hyperuricemia and gout. *J Am Soc Nephrol* 2000;11(5):974.
97. Campistol JM, Sacks SH. Mechanisms of nephrotoxicity. *Transplantation* 2000;69(12 Suppl):SS5.
98. Conte G, Dal Canton A, Sabbatini M, et al. Acute cyclosporine renal dysfunction reversed by dopamine infusion in healthy subjects. *Kidney Int* 1989;36(6):1086.
99. Shulman H, Striker G, Deeg HJ, et al. Nephrotoxicity of cyclosporin A after allogeneic marrow transplantation: Glomerular thromboses and tubular injury. *N Engl J Med* 1981;305(23):1392.
100. Young BA, Marsh CL, Alpers CE, et al. Cyclosporine-associated thrombotic microangiopathy/hemolytic uremic syndrome following kidney and kidney-pancreas transplantation. *Am J Kidney Dis* 1996;28(4):561.
101. Myers BD, Ross J, Newton L, et al. Cyclosporine-associated chronic nephropathy. *N Engl J Med* 1984;311(11):699.
102. Zachariae H. Renal toxicity of long-term cyclosporin. *Scand J Rheumatol* 1999;28(2):65.
103. de Mattos AM, Olyaei AJ, Bennett WM. Nephrotoxicity of immunosuppressive drugs: Long-term consequences and challenges for the future. *Am J Kidney Dis* 2000;35(2):333.
104. Levy G, Thervet E, Lake J, et al. Patient management by Neoral C(2) monitoring: an international consensus statement. *Transplantation* 2002; 73(9 Suppl):S12.
105. Myers BD. Cyclosporine nephrotoxicity. *Kidney Int* 1986;30(6):964.
106. McCauley J, Van Thiel DH, Starzl TE, et al. Acute and chronic renal failure in liver transplantation. *Nephron* 1990;55(2):121.
107. Fioretto P, Steffes MW, Mihatsch MJ, et al. Cyclosporine associated lesions in native kidneys of diabetic pancreas transplant recipients. *Kidney Int* 1995;48(2):489.
108. Messana JM, Johnson KJ, Mihatsch MJ. Renal structure and function effects after low dose cyclosporine in psoriasis patients: A preliminary report. *Clin Nephrol* 1995;43(3):150.
109. Zachariae H, Steen Olsen T. Efficacy of cyclosporin A (CyA) in psoriasis: an overview of dose/response, indications, contraindications and side-effects. *Clin Nephrol* 1995;43(3):154.
110. Mihatsch MJ, Steiner K, Abeywickrama KH, et al. Risk factors for the development of chronic cyclosporine-nephrotoxicity. *Clin Nephrol* 1988;29(4):165.
111. Feutren G, Mihatsch MJ. Risk factors for cyclosporine-induced nephropathy in patients with autoimmune diseases. International Kidney Biopsy Registry of Cyclosporine in Autoimmune Diseases. *N Engl J Med* 1992;326(25):1654.
112. McMaster P, Mirza DF, Ismail T, et al. Therapeutic drug monitoring of tacrolimus in clinical transplantation. *Ther Drug Monit* 1995;17(6):602.
113. Nankivell BJ, Chapman JR, Bonovas G, et al. Oral cyclosporine but not tacrolimus reduces renal transplant blood flow. *Transplantation* 2004; 77(9):1457.
114. Kaplan B, Schold JD, Meier-Kriesche HU. Long-term graft survival with neoral and tacrolimus: a paired kidney analysis. *J Am Soc Nephrol* 2003; 14(11):2980.
115. Vincenzi F, Friman S, Scheuermann E, et al. Results of an international, randomized trial comparing glucose metabolism disorders and outcome with cyclosporine versus tacrolimus. *Am J Transplant* 2007;7(6):1506.
116. Ekberg H, Tedesco-Silva H, Demirbas A, et al. Reduced exposure to calcineurin inhibitors in renal transplantation. *N Engl J Med* 2007; 357(25):2562.
117. Webster AC, Woodroffe RC, Taylor RS, et al. Tacrolimus versus cyclosporin as primary immunosuppression for kidney transplant recipients: meta-analysis and meta-regression of randomised trial data. *BMJ* 2005; 331(7520):810.
118. Ojo AO, Held PJ, Port FK, et al. Chronic renal failure after transplantation of a nonrenal organ. *N Engl J Med* 2003;349(10):931.
119. Lucey MR, Abdelmalek MF, Gagliardi R, et al. A comparison of tacrolimus and cyclosporine in liver transplantation: Effects on renal function and cardiovascular risk status. *Am J Transplant* 2005;5(5):1111.
120. Canales M, Youssef P, Spong R, et al. Predictors of chronic kidney disease in long-term survivors of lung and heart-lung transplantation. *Am J Transplant* 2006;6(9):2157.
121. Radermacher J, Meiners M, Bramlage C, et al. Pronounced renal vasoconstriction and systemic hypertension in renal transplant patients treated with cyclosporin A versus FK 506. *Transpl Int* 1998;11(1):3.
122. Ramos E, Drachenberg CB, Papadimitriou JC, et al. Clinical course of polyoma virus nephropathy in 67 renal transplant patients. *J Am Soc Nephrol* 2002;13(8):2145.
123. Itkin YM, Trujillo TC. Intravenous immunoglobulin-associated acute renal failure: case series and literature review. *Pharmacotherapy* 2005; 25(6):886.
124. Chapman SA, Gilkerson KL, Davin TD, et al. Acute renal failure and intravenous immune globulin: occurs with sucrose-stabilized, but not with D-sorbitol-stabilized, formulation. *Ann Pharmacother* 2004;38(12):2059.
125. Smith KD, Wrenshall LE, Nicosia RF, et al. Delayed graft function and cast nephropathy associated with tacrolimus plus rapamycin use. *J Am Soc Nephrol* 2003;14(4):1037.
126. Simon JF, Swanson SJ, Agodoa LY, et al. Induction sirolimus and delayed graft function after deceased donor kidney transplantation in the United States. *Am J Nephrol* 2004;24(4):393.
127. McTaggart RA, Gottlieb D, Brooks J, et al. Sirolimus prolongs recovery from delayed graft function after cadaveric renal transplantation. *Am J Transplant* 2003;3(4):416.
128. Lawsin L, Light JA. Severe acute renal failure after exposure to sirolimus-tacrolimus in two living donor kidney recipients. *Transplantation* 2003; 75(1):157.
129. Lo A, Egidi MF, Gaber LW, et al. Observations regarding the use of sirolimus and tacrolimus in high-risk cadaveric renal transplantation. *Clin Transplant* 2004;18(1):53.
130. Pelletier R, Nadasdy T, Nadasdy G, et al. Acute renal failure following kidney transplantation associated with myoglobinuria in patients treated with rapamycin. *Transplantation* 2006;82(5):645.
131. Fervenza FC, Fitzpatrick PM, Mertz J, et al. Acute rapamycin nephrotoxicity in native kidneys of patients with chronic glomerulopathies. *Nephrol Dial Transplant* 2004;19(5):1288.

132. Sartelet H, Toupance O, Lorenzato M, et al. Sirolimus-induced thrombotic microangiopathy is associated with decreased expression of vascular endothelial growth factor in kidneys. *Am J Transplant* 2005;5(10):2441.
133. Madias NE, Harrington JT. Platinum nephrotoxicity. *Am J Med* 1978; 65(2):307.
134. Lippman AJ, Helson C, Helson L, et al. Clinical trials with cis-diammine-dichloro platinum. *Cancer Chemother Rep* 1973;57:191.
135. Santoso JT, Lucci JA III, Coleman RL, et al. Saline, mannitol, and furosemide hydration in acute cisplatin nephrotoxicity: A randomized trial. *Cancer Chemother Pharmacol* 2003;52(1):13.
136. Pabla N, Dong Z. Cisplatin nephrotoxicity: Mechanisms and renoprotective strategies. *Kidney Int* 2008;73(9):994.
137. Perazella MA, Moeckel GW. Nephrotoxicity from chemotherapeutic agents: clinical manifestations, pathobiology, and prevention/therapy. *Semin Nephrol* 2010;30(6):570.
138. Sahni V, Choudhury D, Ahmed Z. Chemotherapy-associated renal dysfunction. *Nat Rev Nephrol* 2009;5(8):450.
139. Brilllet G, Deray G, Jacquiaud C, et al. Long-term renal effect of cisplatin in man. *Am J Nephrol* 1994;14(2):81.
140. Merouani A, Davidson SA, Schrier RW. Increased nephrotoxicity of combination taxol and cisplatin chemotherapy in gynecologic cancers as compared to cisplatin alone. *Am J Nephrol* 1997;17(1):53.
141. Moertel CG, Lefkopoulo M, Lipsitz S, et al. Streptozocin-doxorubicin, streptozocin-fluorouracil or chlorozotocin in the treatment of advanced islet-cell carcinoma. *N Engl J Med* 1992;326(8):519.
142. Weiss RB. Streptozocin: A review of its pharmacology, efficacy, and toxicity. *Cancer Treat Rep* 1982;66(3):427.
143. Skinner R, Cotterill SJ, Stevens MC. Risk factors for nephrotoxicity after ifosfamide treatment in children: A UKCCSG Late Effects Group study. United Kingdom Children's Cancer Study Group. *Br J Cancer* 2000; 82(10):1636.
144. Skinner R. Chronic ifosfamide nephrotoxicity in children. *Med Pediatr Oncol* 2003;41(3):190.
145. Aleksa K, Woodland K, Koren G. Young age and the risk for ifosfamide-induced nephrotoxicity: A critical review of two opposing studies. *Pediatr Nephrol* 2001;16(12):1153.
146. Hartmann JT, Knop S, Fels LM, et al. The use of reduced doses of amifostine to ameliorate nephrotoxicity of cisplatin/ifosfamide-based chemotherapy in patients with solid tumors. *Anticancer Drugs* 2000;11(1):1.
147. Briguori C, Tavano D, Colombo A. Contrast agent—associated nephrotoxicity. *Prog Cardiovasc Dis* 2003;45(6):493.
148. Erley CM, Duda SH, Rehfuß D, et al. Prevention of radiocontrast-media-induced nephropathy in patients with pre-existing renal insufficiency by hydration in combination with the adenosine antagonist theophylline. *Nephrol Dial Transplant* 1999;14(5):1146.
149. Drager LF, Andrade L, Barros de Toledo JF, et al. Renal effects of N-acetylcysteine in patients at risk for contrast nephropathy: decrease in oxidant stress-mediated renal tubular injury. *Nephrol Dial Transplant* 2004;19(7):1803.
150. Rihal CS, Textor SC, Grill DE, et al. Incidence and prognostic importance of acute renal failure after percutaneous coronary intervention. *Circulation* 2002;105(19):2259.
151. Itoh Y, Yano T, Sendo T, et al. Clinical and experimental evidence for prevention of acute renal failure induced by radiographic contrast media. *J Pharmacol Sci* 2005;97(4):473.
152. Moore RD, Steinberg EP, Powe NR, et al. Nephrotoxicity of high-osmolality versus low-osmolality contrast media: Randomized clinical trial. *Radiology* 1992;182(3):649.
153. Hoste EA, Doom S, De Waele J, et al. Epidemiology of contrast-associated acute kidney injury in ICU patients: A retrospective cohort analysis. *Intensive Care Med* 2011;37(12):1921.
154. Weisbord SD, Mor MK, Resnick AL, et al. Incidence and outcomes of contrast-induced AKI following computed tomography. *Clin J Am Soc Nephrol* 2008;3(5):1274.
155. Brown JR, Thompson CA. Contrast-induced acute kidney injury: The at-risk patient and protective measures. *Curr Cardiol Rep* 2010;12(5):440.
156. Mehran R, Aymong ED, Nikolsky E, et al. A simple risk score for prediction of contrast-induced nephropathy after percutaneous coronary intervention: Development and initial validation. *J Am Coll Cardiol* 2004;44(7):1393.
157. Brown JR, DeVries JT, Piper WD, et al. Serious renal dysfunction after percutaneous coronary interventions can be predicted. *Am Heart J* 2008; 155(2):260.
158. Cigarroa RG, Lange RA, Williams RH, et al. Dosing of contrast material to prevent contrast nephropathy in patients with renal disease. *Am J Med* 1989;86(6 Pt 1):649.
159. Marenzi G, Assanelli E, Campodonico J, et al. Contrast volume during primary percutaneous coronary intervention and subsequent contrast-induced nephropathy and mortality. *Ann Intern Med* 2009;150(3):170.
160. Brown JR, Robb JF, Block CA, et al. Does safe dosing of iodinated contrast prevent contrast-induced acute kidney injury? *Circ Cardiovasc Interv* 2010;3(4):346.
161. Rudnick MR, Goldfarb S, Wexler L, et al. Nephrotoxicity of ionic and nonionic contrast media in 1196 patients: A randomized trial. The Iohexol Cooperative Study. *Kidney Int* 1995;47(1):254.
162. Reed M, Meier P, Tamhane UU, et al. The relative renal safety of iodixanol compared with low-osmolar contrast media: A meta-analysis of randomized controlled trials. *JACC Cardiovasc Interv* 2009; 2(7):645.
163. Wessely R, Koppa T, Bradaric C, et al. Choice of contrast medium in patients with impaired renal function undergoing percutaneous coronary intervention. *Circ Cardiovasc Interv* 2009;2(5):430.
164. Hernandez F, Mora L, Garcia-Tejada J, et al. Comparison of iodixanol and ioversol for the prevention of contrast-induced nephropathy in diabetic patients after coronary angiography or angioplasty. *Rev Esp Cardiol* 2009;62(12):1373.
165. Gitman MD, Singhal PC. Cocaine-induced renal disease. *Expert Opin Drug Saf* 2004;3(5):441.
166. Roth D, Alarcon FJ, Fernandez JA, et al. Acute rhabdomyolysis associated with cocaine intoxication. *N Engl J Med* 1988;319(11):673.
167. Zager RA. Rhabdomyolysis and myohemoglobinuric acute renal failure. *Kidney Int* 1996;49(2):314.
168. Textor SC. Renal failure related to angiotensin-converting enzyme inhibitors. *Semin Nephrol* 1997;17(1):67.
169. Isnard Bagnis C, Deray G, Baumelou A, et al. Herbs and the kidney. *Am J Kidney Dis* 2004;44(1):1.
170. De Smet PA. Herbal remedies. *N Engl J Med* 2002;347(25):2046.
171. Jha V, Chugh KS. Nephropathy associated with animal, plant, and chemical toxins in the tropics. *Semin Nephrol* 2003;23(1):49.
172. Depierreux M, Van Damme B, Vanden Houste K, et al. Pathologic aspects of a newly described nephropathy related to the prolonged use of Chinese herbs. *Am J Kidney Dis* 1994;24(2):172.
173. Marcus DM, Grollman AP. Botanical medicines—the need for new regulations. *N Engl J Med* 2002;347(25):2073.
174. Kabanda A, Jadoul M, Lauwerys R, et al. Low molecular weight proteinuria in Chinese herbs nephropathy. *Kidney Int* 1995;48(5):1571.
175. Nortier JL, Deschodt-Lanckman MM, Simon S, et al. Proximal tubular injury in Chinese herbs nephropathy: Monitoring by neutral endopeptidase enzymuria. *Kidney Int* 1997;51(1):288.
176. Shemesh IY, Mishal Y, Baruchin AM, et al. Rhabdomyolysis in parphenylenediamine intoxication. *Vet Hum Toxicol* 1995;37(3):244.
177. Solez K, Racusen LC. Role of the renal biopsy in acute renal failure. *Contrib Nephrol* 2001;132:68.
178. Dalgaard OZ. An electron microscopic study on glomeruli in renal biopsies taken from human shock kidney. *Lab Invest* 1960;9(3):364.
179. Bohle A, Jahnecke J, Meyer D, et al. Morphology of acute renal-failure—comparative data from biopsy and autopsy. *Kidney Int Suppl* 1976;6:S9.
180. Racusen LC, Fivush BA, Li YL, et al. Dissociation of tubular cell detachment and tubular cell death in clinical and experimental "acute tubular necrosis". *Lab Invest* 1991;64(4):546.
181. Wangsiripaisan A, Gengaro PE, Edelstein CL, et al. Role of polymeric Tamm-Horsfall protein in cast formation: Oligosaccharide and tubular fluid ions. *Kidney Int* 2001;59(3):932.
182. Vongwiwatana A, Tasanarong A, Rayner DC, et al. Epithelial to mesenchymal transition during late deterioration of human kidney transplants: The role of tubular cells in fibrogenesis. *Am J Transplant* 2005; 5(6):1367.
183. Humphreys BD, Valerius MT, Kobayashi A, et al. Intrinsic epithelial cells repair the kidney after injury. *Cell Stem Cell* 2008;2(3):284.
184. Ortiz A, Justo P, Sanz A, et al. Targeting apoptosis in acute tubular injury. *Biochem Pharmacol* 2003;66(8):1589.

185. Gobe GC, Endre ZH. Cell death in toxic nephropathies. *Semin Nephrol* 2003;23(5):416.
186. Castaneda MP, Swiatecka-Urban A, Mitsnefes MM, et al. Activation of mitochondrial apoptotic pathways in human renal allografts after ischemia reperfusion injury. *Transplantation* 2003;76(1):50.
187. Zhang L, Chen D, Chen Z, et al. Hypertonicity-induced mitochondrial membrane permeability in renal medullary interstitial cells: Protective role of osmolytes. *Cell Physiol Biochem* 2010;25(6):753.
188. Solez K, Racusen LC, Marcussen N, et al. Morphology of ischemic acute renal failure, normal function, and cyclosporine toxicity in cyclosporine-treated renal allograft recipients. *Kidney Int* 1993;43(5):1058.
189. Alejandro VS, Nelson WJ, Huie P, et al. Postischemic injury, delayed function and Na⁺/K⁺-ATPase distribution in the transplanted kidney. *Kidney Int* 1995;48(4):1308.
190. Olsen TS, Hansen HE, Olsen HS. Tubular ultrastructure in acute renal failure: alterations of cellular surfaces (brush-border and basolateral infoldings). *Virchows Arch A Pathol Anat Histopathol* 1985;406(1):91.
191. Olsen TS. Ultrastructure of the renal tubules in acute renal insufficiency. *Acta Pathol Microbiol Scand* 1967;71(2):203.
192. Jones DB. Ultrastructure of human acute renal failure. *Lab Invest* 1982;46(3):254.
193. Solez K, Kramer EC, Fox JA, et al. Medullary plasma flow and intravascular leukocyte accumulation in acute renal failure. *Kidney Int* 1974;6(1):24.
194. Solez K, Morel-Maroger L, Sraer JD. The morphology of "acute tubular necrosis" in man: Analysis of 57 renal biopsies and a comparison with the glycerol model. *Medicine (Baltimore)* 1979;58(5):362.
195. Amin RP, Vickers AE, Sistare F, et al. Identification of putative gene based markers of renal toxicity. *Environ Health Perspect* 2004;112(4):465.
196. Ichimura T, Bonventre JV, Bailly V, et al. Kidney injury molecule-1 (KIM-1), a putative epithelial cell adhesion molecule containing a novel immunoglobulin domain, is up-regulated in renal cells after injury. *J Biol Chem* 1998;273(7):4135.
197. Mishra J, Dent C, Tarabishi R, et al. Neutrophil gelatinase-associated lipocalin (NGAL) as a biomarker for acute renal injury after cardiac surgery. *Lancet* 2005;365(9466):1231.
198. van Timmeren MM, van den Heuvel MC, Bailly V, et al. Tubular kidney injury molecule-1 (KIM-1) in human renal disease. *J Pathol* 2007;212(2):209.
199. Zhu XY, Urbietta-Caceres V, Krier JD, et al. Mesenchymal stem cells and endothelial progenitor cells decrease renal injury in experimental swine renal artery stenosis through different mechanisms. *Stem Cells* 2013;31(1):117.
200. Hoffmann D, Bijol V, Krishnamoorthy A, et al. Fibrinogen excretion in the urine and immunoreactivity in the kidney serves as a translational biomarker for acute kidney injury. *Am J Pathol* 2012;181(3):818.
201. Allory Y, Audard V, Fontanges P, et al. The L1 cell adhesion molecule is a potential biomarker of human distal nephron injury in acute tubular necrosis. *Kidney Int* 2008;73(6):751.
202. Angelotti ML, Ronconi E, Ballerini L, et al. Characterization of renal progenitors committed toward tubular lineage and their regenerative potential in renal tubular injury. *Stem Cells* 2012;30(8):1714.
203. Graumann A, Zawada ET Jr. Case report: Acute renal failure after administering intravenous immunoglobulin. *Postgrad Med* 2010;122(2):142.
204. Viol GW, Minielly JA, Bistricki T. Gold nephropathy: Tissue analysis by X-ray fluorescent spectroscopy. *Arch Pathol Lab Med* 1977;101(12):635.
205. Genkins G, Bryer MS. Bacitracin nephropathy: Report of a case of acute renal failure and death. *J Am Med Assoc* 1954;155(10):894.
206. Van Vleet TR, Schnellmann RG. Toxic nephropathy: environmental chemicals. *Semin Nephrol* 2003;23(5):500.
207. Perazella MA. Renal vulnerability to drug toxicity. *Clin J Am Soc Nephrol* 2009;4(7):1275.
208. Bonegio R, Lieberthal W. Role of apoptosis in the pathogenesis of acute renal failure. *Curr Opin Nephrol Hypertens* 2002;11(3):301.
209. Nagothu KK, Bhatt R, Kaushal GP, et al. Fibrate prevents cisplatin-induced proximal tubule cell death. *Kidney Int* 2005;68(6):2680.
210. Duncan-Achanzar KB, Jones JT, Burke MF, et al. Inorganic mercury chloride-induced apoptosis in the cultured porcine renal cell line LLC-PK1. *J Pharmacol Exp Ther* 1996;277(3):1726.
211. Kaushal GP, Kaushal V, Hong X, et al. Role and regulation of activation of caspases in cisplatin-induced injury to renal tubular epithelial cells. *Kidney Int* 2001;60(5):1726.
212. Linkermann A, Himmerkus N, Rolver L, et al. Renal tubular Fas ligand mediates fratricide in cisplatin-induced acute kidney failure. *Kidney Int* 2011;79(2):169.
213. Han X, Chesney RW. Mechanism of TauT in protecting against cisplatin-induced kidney injury (AKI). *Adv Exp Med Biol* 2009;643:105.
214. Moeckel GW, Zhang L, Fogo AB, et al. COX2 activity promotes organic osmolyte accumulation and adaptation of renal medullary interstitial cells to hypertonic stress. *J Biol Chem* 2003;278(21):19352.
215. Weisman JI, Bloom B. Anuria following phenylbutazone therapy. *N Engl J Med* 1955;252(25):1086.
216. Kopp JB, Miller KD, Mican JA, et al. Crystalluria and urinary tract abnormalities associated with indinavir. *Ann Intern Med* 1997;127(2):119.
217. Roberts DM, Smith MW, McMullan BJ, et al. Acute kidney injury due to crystalluria following acute valacyclovir overdose. *Kidney Int* 2011;79(5):574.
218. Fleischer R, Johnson M. Acyclovir nephrotoxicity: A case report highlighting the importance of prevention, detection, and treatment of acyclovir-induced nephropathy. *Case Rep Med* 2010;2010.pii: 602783
219. Tanji N, Tanji K, Kambham N, et al. Adefovir nephrotoxicity: possible role of mitochondrial DNA depletion. *Hum Pathol* 2001;32(7):734.
220. Verhelst D, Monge M, Meynard JL, et al. Fanconi syndrome and renal failure induced by tenofovir: A first case report. *Am J Kidney Dis* 2002;40(6):1331.
221. Creput C, Gonzalez-Canali G, Hill G, et al. Renal lesions in HIV-1-positive patient treated with tenofovir. *AIDS* 2003;17(6):935.
222. Rashed A, Azadeh B, Abu Romeh SH. Acyclovir-induced acute tubulointerstitial nephritis. *Nephron* 1990;56(4):436.
223. Ortiz A, Justo P, Sanz A, et al. Tubular cell apoptosis and cidofovir-induced acute renal failure. *Antivir Ther* 2005;10(1):185.
224. Perazella MA. Toxic nephropathies: Core curriculum 2010. *Am J Kidney Dis* 2010;55(2):399.
225. Heyman SN, Brezis M, Reubinoff CA, et al. Acute renal failure with selective medullary injury in the rat. *J Clin Invest* 1988;82(2):401.
226. Zager RA. Gentamicin nephrotoxicity in the setting of acute renal hypoperfusion. *Am J Physiol* 1988;254(4 Pt 2):F574.
227. Berman LB, Katz S. Kanamycin nephrotoxicity. *Ann N Y Acad Sci* 1958;76(2):149.
228. Harrison WO, Silverblatt FJ, Turck M. Gentamicin nephrotoxicity: Failure of three cephalosporins to potentiate injury in rats. *Antimicrob Agents Chemother* 1975;8(2):209.
229. Wertlake PT, Butler WT, Hill GJ, II, et al. Nephrotoxic tubular damage and calcium deposition following amphotericin B therapy. *Am J Pathol* 1963;43:449.
230. Bullock WE, Luke RG, Nuttall CE, et al. Can mannitol reduce amphotericin B nephrotoxicity? Double-blind study and description of a new vascular lesion in kidneys. *Antimicrob Agents Chemother* 1976;10(3):555.
231. Fillastre JP, Kleinknecht D. Acute renal failure associated with cephalosporin therapy. *Am Heart J* 1975;89(6):809.
232. Perkins RL, Apicella MA, Lee IS, et al. Cephaloridine and cephalothin: Comparative studies of potential nephrotoxicity. *J Lab Clin Med* 1968;71(1):75.
233. Barrientos A, Bello I, Gutierrez-Millet V. Letter; Renal failure and cephalothin. *Ann Intern Med* 1976;84(5):612.
234. Manley HJ, Bailie GR, Eisele G. Bilateral renal cortical necrosis associated with cefuroxime axetil. *Clin Nephrol* 1998;49(4):268.
235. Beirne GJ, Hansing CE, Octaviano GN, et al. Acute renal failure caused by hypersensitivity to polymyxin B sulfate. *JAMA* 1967;202(1):156.
236. Elwood CM, Lucas GD, Muehrcke RC. Acute renal failure associated with sodium colistimethate treatment. *Arch Intern Med* 1966;118(4):326.
237. Sokol H, Vigneau C, Maury E, et al. Biopsy-proven anuric acute tubular necrosis associated with vancomycin and one dose of aminoglycoside. *Nephrol Dial Transplant* 2004;19(7):1921.
238. Wicklow BA, Ogborn MR, Gibson IW, et al. Biopsy-proven acute tubular necrosis in a child attributed to vancomycin intoxication. *Pediatr Nephrol* 2006;21(8):1194.
239. Wu CY, Wang JS, Chiou YH, et al. Biopsy proven acute tubular necrosis associated with vancomycin in a child: Case report and literature review. *Ren Fail* 2007;29(8):1059.
240. Davies DR, Bittmann I, Pardo J. Histopathology of calcineurin inhibitor-induced nephrotoxicity. *Transplantation* 2000;69(12 Suppl):SS11.
241. Foxwell BM, Ruffel B. The mechanisms of action of cyclosporine. *Cardiol Clin* 1990;8(1):107.

242. Hudkins KL, Le QC, Segerer S, et al. Osteopontin expression in human cyclosporine toxicity. *Kidney Int* 2001;60(2):635.
243. Burdmann EA, Andoh TF, Yu L, et al. Cyclosporine nephrotoxicity. *Semin Nephrol* 2003;23(5):465.
244. Fellstrom B. Cyclosporine nephrotoxicity. *Transplant Proc* 2004;36(2 Suppl):220S.
245. Bertani T, Ferrazzi P, Schieppati A, et al. Nature and extent of glomerular injury induced by cyclosporine in heart transplant patients. *Kidney Int* 1991;40(2):243.
246. Myers BD, Newton L, Boshkos C, et al. Chronic injury of human renal microvessels with low-dose cyclosporine therapy. *Transplantation* 1988;46(5):694.
247. Morozumi K, Takeda A, Uchida K, et al. Cyclosporine nephrotoxicity: How does it affect renal allograft function and transplant morphology? *Transplant Proc* 2004;36(2 Suppl):251S.
248. Andoh TF, Burdmann EA, Fransechini N, et al. Comparison of acute rapamycin nephrotoxicity with cyclosporine and FK506. *Kidney Int* 1996;50(4):1110.
249. Morozumi K, Sugito K, Oda A, et al. A comparative study of morphological characteristics of renal injuries of tacrolimus (FK506) and cyclosporin (CyA) in renal allografts: Are the morphologic characteristics of FK506 and CyA nephrotoxicity similar? *Transplant Proc* 1996;28(2):1076.
250. Demetris AJ, Fung JJ, Todo S, et al. Pathologic observations in human allograft recipients treated with FK 506. *Transplant Proc* 1990;22(1):25.
251. Randhawa PS, Tsamandas AC, Magnone M, et al. Microvascular changes in renal allografts associated with FK506 (Tacrolimus) therapy. *Am J Surg Pathol* 1996;20(3):306.
252. Todo S, Ueda Y, Demetris JA, et al. Immunosuppression of canine, monkey, and baboon allografts by FK 506: With special reference to synergism with other drugs and to tolerance induction. *Surgery* 1988;104(2):239.
253. Stillman IE, Andoh TF, Burdmann EA, et al. FK506 nephrotoxicity: morphologic and physiologic characterization of a rat model. *Lab Invest* 1995;73(6):794.
254. Soares SM, Sethi S. Impairment of renal function after intravenous immunoglobulin. *Nephrol Dial Transplant* 2006;21(3):816.
255. Haas M, Sonnenday CJ, Cicone JS, et al. Isometric tubular epithelial vacuolization in renal allograft biopsy specimens of patients receiving low-dose intravenous immunoglobulin for a positive crossmatch. *Transplantation* 2004;78(4):549.
256. Miller RP, Tadagavadi RK, Ramesh G, et al. Mechanisms of Cisplatin nephrotoxicity. *Toxins (Basel)* 2010;2(11):2490.
257. Doby DC, Levi J, Jacobs C, et al. Mechanism of cis-platinum nephrotoxicity: II. Morphologic observations. *J Pharmacol Exp Ther* 1980;213(3):551.
258. Doby DC, Hill D, Lewis T, et al. Cyst formation in rat kidney induced by cis-platinum administration. *Lab Invest* 1981;45(3):260.
259. Berns JS, Haghghat A, Staddon A, et al. Severe, irreversible renal failure after ifosfamide treatment. A clinicopathologic report of two patients. *Cancer* 1995;76(3):497.
260. Yoshioka T, Fogo A, Beckman JK. Reduced activity of antioxidant enzymes underlies contrast media-induced renal injury in volume depletion. *Kidney Int* 1992;41(4):1008.
261. Thomsen HS, Larsen S, Hemmingsen L, et al. Nephropathy induced by intramuscularly administered glycerol and contrast media in rats. A comparison between diatrizoate, iohexol and ioxilan. *Acta Radiol* 1989;30(2):217.
262. Thomsen HS, Golman K, Larsen S, et al. Urine profiles and kidney histology following intravenous diatrizoate and iohexol in the degeneration phase of gentamicin nephropathy in rats. Effects on urine and serum profiles. *Invest Radiol* 1991;26(11):951.
263. Deray G, Martinez F, Cacoub P, et al. A role for adenosine calcium and ischemia in radiocontrast-induced intrarenal vasoconstriction. *Am J Nephrol* 1990;10(4):316.
264. Tervahartiala P, Kivisaari L, Kivisaari R, et al. Contrast media-induced renal tubular vacuolization. A light and electron microscopic study on rat kidneys. *Invest Radiol* 1991;26(10):882.
265. Moreau JF, Droz D, Sabto J, et al. Osmotic nephrosis induced by water-soluble triiodinated contrast media in man. A retrospective study of 47 cases. *Radiology* 1975;115(2):329.
266. Hofmeister R, Bhargava AS, Gunzel P. The use of urinary N-acetyl-beta-D-glucosaminidase (NAG) for the detection of contrast-media-induced 'osmotic nephrosis' in rats. *Toxicol Lett* 1990;50(1):9.
267. Moreau JF, Droz D, Noel LH, et al. Tubular nephrotoxicity of water-soluble iodinated contrast media. *Invest Radiol* 1980;15(6 Suppl):S54.
268. Gilbert EF, Khoury GH, Hogan GR, et al. Hemorrhagic renal necrosis in infancy: relationship to radiopaque compounds. *J Pediatr* 1970;76(1):49.
269. Gruskin AB, Oetliker OH, Wolfish NM, et al. Effects of angiography on renal function and histology in infants and piglets. *J Pediatr* 1970;76(1):41.
270. Whalley DW, Ibels LS, Eckstein RP, et al. Acute tubular necrosis complicating bilateral retrograde pyelography. *Aust N Z J Med* 1987;17(5):536.
271. Hizoh I, Haller C. Radiocontrast-induced renal tubular cell apoptosis: hypertonic versus oxidative stress. *Invest Radiol* 2002;37(8):428.
272. Itoh Y, Yano T, Sendo T, et al. Involvement of de novo ceramide synthesis in radiocontrast-induced renal tubular cell injury. *Kidney Int* 2006;69(2):288.
273. Herrera GA. Myoglobin and the kidney: An overview. *Ultrastruct Pathol* 1994;18(1-2):113.
274. Turbat-Herrera EA. Myoglobinuric acute renal failure associated with cocaine use. *Ultrastruct Pathol* 1994;18(1-2):127.
275. Frascino JA, Vanamee P, Rosen PP. Renal oxalosis and azotemia after methoxyflurane anesthesia. *N Engl J Med* 1970;283(13):676.
276. Hong YT, Fu LS, Chung LH, et al. Fanconi's syndrome, interstitial fibrosis and renal failure by aristolochic acid in Chinese herbs. *Pediatr Nephrol* 2006;21(4):577.
277. de Mendonca A, Vincent JL, Suter PM, et al. Acute renal failure in the ICU: Risk factors and outcome evaluated by the SOFA score. *Intensive Care Med* 2000;26(7):915.
278. Devarajan P. Cellular and molecular derangements in acute tubular necrosis. *Curr Opin Pediatr* 2005;17(2):193.
279. Andreoli SP. Acute renal failure in the newborn. *Semin Perinatol* 2004;28(2):112.
280. Nally JV, Jr. Acute renal failure in hospitalized patients. *Cleve Clin J Med* 2002;69(7):569.
281. Esson ML, Schrier RW. Diagnosis and treatment of acute tubular necrosis. *Ann Intern Med* 2002;137(9):744.
282. Schetz M, Dasta J, Goldstein S, et al. Drug-induced acute kidney injury. *Curr Opin Crit Care* 2005;11(6):555.
283. Kintzel PE. Anticancer drug-induced kidney disorders. *Drug Saf* 2001;24(1):19.
284. Perazella MA. Drug-induced nephropathy: An update. *Expert Opin Drug Saf* 2005;4(4):689.
285. Gambaro G, Perazella MA. Adverse renal effects of anti-inflammatory agents: Evaluation of selective and nonselective cyclooxygenase inhibitors. *J Intern Med* 2003;253(6):643.
286. Lameire NH, Flombaum CD, Moreau D, et al. Acute renal failure in cancer patients. *Ann Med* 2005;37(1):13.
287. Hanif M, Mobarak MR, Ronan A, et al. Fatal renal failure caused by diethylene glycol in paracetamol elixir: The Bangladesh epidemic. *BMJ* 1995;311(6997):88.
288. McKenzie K. Epidemic of acute renal failure in Haiti. *BMJ* 1996;313(7049):70.
289. Blowey DL. Nephrotoxicity of over-the-counter analgesics, natural medicines, and illicit drugs. *Adolesc Med Clin* 2005;16(1):31.
290. Wang IJ, Chen PC, Hwang KC. Melamine and nephrolithiasis in children in Taiwan. *N Engl J Med* 2009;360(11):1157.
291. Riedemann NC, Guo RF, Ward PA. The enigma of sepsis. *J Clin Invest* 2003;112(4):460.
292. Schrier RW, Wang W. Acute renal failure and sepsis. *N Engl J Med* 2004;351(2):159.
293. Bonventre JV. Pathophysiology of ischemic acute renal failure. Inflammation, lung-kidney cross-talk, and biomarkers. *Contrib Nephrol* 2004;144:19.
294. Hoste EA, Kellum JA. Acute renal failure in the critically ill: impact on morbidity and mortality. *Contrib Nephrol* 2004;144:1.
295. Rosen S, Heyman SN. Difficulties in understanding human "acute tubular necrosis": Limited data and flawed animal models. *Kidney Int* 2001;60(4):1220.
296. Lieberthal W, Nigam SK. Acute renal failure. II. Experimental models of acute renal failure: imperfect but indispensable. *Am J Physiol Renal Physiol* 2000;278(1):F1.

297. Kelly KJ, Molitoris BA. Acute renal failure in the new millennium: Time to consider combination therapy. *Semin Nephrol* 2000;20(1):4.
298. Dagher PC, Herget-Rosenthal S, Ruehm SG, et al. Newly developed techniques to study and diagnose acute renal failure. *J Am Soc Nephrol* 2003;14(8):2188.
299. Hauger O, Delalande C, Deminiere C, et al. Nephrotoxic nephritis and obstructive nephropathy: Evaluation with MR imaging enhanced with ultrasmall superparamagnetic iron oxide-preliminary findings in a rat model. *Radiology* 2000;217(3):819.
300. Morrow JS, Cianci CD, Ardito T, et al. Ankyrin links fodrin to the alpha subunit of Na,K-ATPase in Madin-Darby canine kidney cells and in intact renal tubule cells. *J Cell Biol* 1989;108(2):455.
301. Chatterjee PK, Brown PA, Cuzzocrea S, et al. Calpain inhibitor-1 reduces renal ischemia/reperfusion injury in the rat. *Kidney Int* 2001;59(6):2073.
302. Glynne PA, Picot J, Evans TJ. Coexpressed nitric oxide synthase and apical beta(1) integrins influence tubule cell adhesion after cytokine-induced injury. *J Am Soc Nephrol* 2001;12(11):2370.
303. Nelson WJ. Adaptation of core mechanisms to generate cell polarity. *Nature* 2003;422(6933):766.
304. Pollard TD, Borisy GG. Cellular motility driven by assembly and disassembly of actin filaments. *Cell* 2003;112(4):453.
305. Molitoris BA, Geerdes A, McIntosh JR. Dissociation and redistribution of Na⁺,K⁺-ATPase from its surface membrane actin cytoskeletal complex during cellular ATP depletion. *J Clin Invest* 1991;88(2):462.
306. Molitoris BA, Dahl R, Geerdes A. Cytoskeleton disruption and apical redistribution of proximal tubule Na⁺-K⁺-ATPase during ischemia. *Am J Physiol* 1992;263(3 Pt 2):F488.
307. Molitoris BA, Falk SA, Dahl RH. Ischemia-induced loss of epithelial polarity. Role of the tight junction. *J Clin Invest* 1989;84(4):1334.
308. Mason J, Joeris B, Welsch J, et al. Vascular congestion in ischemic renal failure: the role of cell swelling. *Miner Electrolyte Metab* 1989;15(3):114.
309. Ashworth SL, Southgate EL, Sandoval RM, et al. ADF/cofilin mediates actin cytoskeletal alterations in LLC-PK cells during ATP depletion. *Am J Physiol Renal Physiol* 2003;284(4):F852.
310. Ashworth SL, Sandoval RM, Hosford M, et al. Ischemic injury induces ADF relocalization to the apical domain of rat proximal tubule cells. *Am J Physiol Renal Physiol* 2001;280(5):F886.
311. Chatterjee PK, Cuzzocrea S, Thiernemann C. Inhibitors of poly (ADP-ribose) synthetase protect rat proximal tubular cells against oxidant stress. *Kidney Int* 1999;56(3):973.
312. Nath KA, Norby SM. Reactive oxygen species and acute renal failure. *Am J Med* 2000;109(8):665.
313. Araujo M, Welch WJ. Oxidative stress and nitric oxide in kidney function. *Curr Opin Nephrol Hypertens* 2006;15(1):72.
314. Bowie A, O'Neill LA. Oxidative stress and nuclear factor-kappaB activation: A reassessment of the evidence in the light of recent discoveries. *Biochem Pharmacol* 2000;59(1):13.
315. Noiri E, Nakao A, Uchida K, et al. Oxidative and nitrosative stress in acute renal ischemia. *Am J Physiol Renal Physiol* 2001;281(5):F948.
316. Kulah E, Tascilar O, Acikgoz S, et al. Oxidized LDL accumulation in experimental renal ischemia reperfusion injury model. *Ren Fail* 2007;29(4):409.
317. Atanasova I, Burke TJ, McMurtry IF, et al. Nitric oxide synthase inhibition and acute renal ischemia: Effect on systemic hemodynamics and mortality. *Ren Fail* 1995;17(4):389.
318. Yu L, Gengaro PE, Niederberger M, et al. Nitric oxide: A mediator in rat tubular hypoxia/reoxygenation injury. *Proc Natl Acad Sci U S A* 1994;91(5):1691.
319. Peresleni T, Noiri E, Bahou WE, et al. Antisense oligodeoxynucleotides to inducible NO synthase rescue epithelial cells from oxidative stress injury. *Am J Physiol* 1996;270(6 Pt 2):F971.
320. Ling H, Gengaro PE, Edelstein CL, et al. Effect of hypoxia on proximal tubules isolated from nitric oxide synthase knockout mice. *Kidney Int* 1998;53(6):1642.
321. Goligorsky MS, Brodsky SV, Noiri E. Nitric oxide in acute renal failure: NOS versus NOS. *Kidney Int* 2002;61(3):855.
322. Goligorsky MS, Brodsky SV, Noiri E. NO bioavailability, endothelial dysfunction, and acute renal failure: New insights into pathophysiology. *Semin Nephrol* 2004;24(4):316.
323. Noiri E, Peresleni T, Miller F, et al. In vivo targeting of inducible NO synthase with oligodeoxynucleotides protects rat kidney against ischemia. *J Clin Invest* 1996;97(10):2377.
324. Xia Y, Dawson VL, Dawson TM, et al. Nitric oxide synthase generates superoxide and nitric oxide in arginine-depleted cells leading to peroxynitrite-mediated cellular injury. *Proc Natl Acad Sci U S A* 1996;93(13):6770.
325. Wangsiripaisan A, Gengaro PE, Nemenoff RA, et al. Effect of nitric oxide donors on renal tubular epithelial cell-matrix adhesion. *Kidney Int* 1999;55(6):2281.
326. Chiao H, Kohda Y, McLeroy P, et al. Alpha-melanocyte-stimulating hormone protects against renal injury after ischemia in mice and rats. *J Clin Invest* 1997;99(6):1165.
327. Kaushal GP, Basnakian AG, Shah SV. Apoptotic pathways in ischemic acute renal failure. *Kidney Int* 2004;66(2):500.
328. Schumer M, Colombel MC, Sawczuk IS, et al. Morphologic, biochemical, and molecular evidence of apoptosis during the reperfusion phase after brief periods of renal ischemia. *Am J Pathol* 1992;140(4):831.
329. Nakajima T, Miyaji T, Kato A, et al. Uninephrectomy reduces apoptotic cell death and enhances renal tubular cell regeneration in ischemic ARF in rats. *Am J Physiol* 1996;271(4 Pt 2):F846.
330. Yin T, Sandhu G, Wolfgang CD, et al. Tissue-specific pattern of stress kinase activation in ischemic/reperfused heart and kidney. *J Biol Chem* 1997;272(32):19943.
331. Nogue S, Miyazaki M, Kobayashi N, et al. Induction of apoptosis in ischemia-reperfusion model of mouse kidney: Possible involvement of Fas. *J Am Soc Nephrol* 1998;9(4):620.
332. Padanilam BJ, Lewington AJ, Hammerman MR. Expression of CD27 and ischemia/reperfusion-induced expression of its ligand Siva in rat kidneys. *Kidney Int* 1998;54(6):1967.
333. Raafat AM, Murray MT, McGuire T, et al. Calcium blockade reduces renal apoptosis during ischemia reperfusion. *Shock* 1997;8(3):186.
334. Nagata S, Golstein P. The Fas death factor. *Science* 1995;267(5203):1449.
335. Baker SJ, Reddy EP. Modulation of life and death by the TNF receptor superfamily. *Oncogene* 1998;17(25):3261.
336. Thornberry NA, Lazebnik Y. Caspases: enemies within. *Science* 1998;281(5381):1312.
337. Kaushal GP, Singh AB, Shah SV. Identification of gene family of caspases in rat kidney and altered expression in ischemia-reperfusion injury. *Am J Physiol* 1998;274(3 Pt 2):F587.
338. Saikumar P, Dong Z, Patel Y, et al. Role of hypoxia-induced Bax translocation and cytochrome c release in reoxygenation injury. *Oncogene* 1998;17(26):3401.
339. Zhang L, Chen D, Chen Z, et al. Hypertonicity-induced mitochondrial membrane permeability in renal medullary interstitial cells: Protective role of osmolytes. *Cell Physiol Biochem* 2010;25(6):753.
340. Witzgall R, Brown D, Schwarz C, et al. Localization of proliferating cell nuclear antigen, vimentin, c-Fos, and clusterin in the posts ischemic kidney. Evidence for a heterogeneous genetic response among nephron segments, and a large pool of mitotically active and dedifferentiated cells. *J Clin Invest* 1994;93(5):2175.
341. DiMari J, Megyesi J, Udvarhelyi N, et al. N-acetyl cysteine ameliorates ischemic renal failure. *Am J Physiol* 1997;272(3 Pt 2):F292.
342. Chen Z, Naito M, Mashima T, et al. Activation of actin-cleavable interleukin 1beta-converting enzyme (ICE) family protease CPP-32 during chemotherapeutic agent-induced apoptosis in ovarian carcinoma cells. *Cancer Res* 1996;56(22):5224.
343. Stanger BZ. Looking beneath the surface: The cell death pathway of Fas/APO-1 (CD95). *Mol Med* 1996;2(1):7.
344. Edelstein CL, Wieder ED, Yaqoob MM, et al. The role of cysteine proteases in hypoxia-induced rat renal proximal tubular injury. *Proc Natl Acad Sci U S A* 1995;92(17):7662.
345. Shi Y, Melnikov VY, Schrier RW, et al. Downregulation of the calpain inhibitor protein calpastatin by caspases during renal ischemia-reperfusion. *Am J Physiol Renal Physiol* 2000;279(3):F509.
346. Edelstein CL, Ling H, Gengaro PE, et al. Effect of glycine on prelethal and postlethal increases in calpain activity in rat renal proximal tubules. *Kidney Int* 1997;52(5):1271.
347. Choi KH, Edelstein CL, Gengaro P, et al. Hypoxia induces changes in phospholipase A2 in rat proximal tubules: Evidence for multiple forms. *Am J Physiol* 1995;269(6 Pt 2):F846.
348. Dagher PC. Apoptosis in ischemic renal injury: Roles of GTP depletion and p53. *Kidney Int* 2004;66(2):506.

349. Kelly KJ, Plotkin Z, Dagher PC. Guanosine supplementation reduces apoptosis and protects renal function in the setting of ischemic injury. *J Clin Invest* 2001;108(9):1291.
350. Golstein P, Kroemer G. Cell death by necrosis: Towards a molecular definition. *Trends Biochem Sci* 2007;32(1):37.
351. Green DR, Oberst A, Dillon CP, et al. RIPK-dependent necrosis and its regulation by caspases: A mystery in five acts. *Mol Cell* 2011;44(1):9.
352. Degterev A, Huang Z, Boyce M, et al. Chemical inhibitor of nonapoptotic cell death with therapeutic potential for ischemic brain injury. *Nat Chem Biol* 2005;1(2):112.
353. Bertrand MJ, Vandenabeele P. The Ripoptosome: death decision in the cytosol. *Mol Cell* 2011;43(3):323.
354. Linkermann A, Brasen JH, Himmerkus N, et al. Rip1 (Receptor-interacting protein kinase 1) mediates necroptosis and contributes to renal ischemia/reperfusion injury. *Kidney Int* 2012;81(8):751.
355. Wang KK. Calpain and caspase: Can you tell the difference? *Trends Neurosci* 2000;23(1):20.
356. Devalaraja-Narashimha K, Singaravelu K, Padanilam BJ. Poly(ADP-ribose) polymerase-mediated cell injury in acute renal failure. *Pharmacol Res* 2005;52(1):44.
357. Zheng J, Devalaraja-Narashimha K, Singaravelu K, et al. Poly(ADP-ribose) polymerase-1 gene ablation protects mice from ischemic renal injury. *Am J Physiol Renal Physiol* 2005;288(2):F387.
358. Park KM, Chen A, Bonventre JV. Prevention of kidney ischemia/reperfusion-induced functional injury and JNK, p38, and MAPK kinase activation by remote ischemic pretreatment. *J Biol Chem* 2001;276(15):11870.
359. Arany I, Megyesi JK, Kaneto H, et al. Activation of ERK or inhibition of JNK ameliorates H(2)O(2) cytotoxicity in mouse renal proximal tubule cells. *Kidney Int* 2004;65(4):1231.
360. Arany I, Megyesi JK, Reusch JE, et al. CREB mediates ERK-induced survival of mouse renal tubular cells after oxidant stress. *Kidney Int* 2005;68(4):1573.
361. Bonventre JV, Zuk A. Ischemic acute renal failure: an inflammatory disease? *Kidney Int* 2004;66(2):480.
362. Friedewald JJ, Rabb H. Inflammatory cells in ischemic acute renal failure. *Kidney Int* 2004;66(2):486.
363. Ysebaert DK, De Greef KE, De Beuf A, et al. T cells as mediators in renal ischemia/reperfusion injury. *Kidney Int* 2004;66(2):491.
364. Aderem A, Ulevitch RJ. Toll-like receptors in the induction of the innate immune response. *Nature* 2000;406(6797):782.
365. Johnson GB, Brunn GJ, Platt JL. Activation of mammalian Toll-like receptors by endogenous agonists. *Crit Rev Immunol* 2003;23(1-2):15.
366. Jang HR, Ko GJ, Wasowska BA, et al. The interaction between ischemia-reperfusion and immune responses in the kidney. *J Mol Med (Berl)* 2009;87(9):859.
367. Yokota N, Daniels F, Crosson J, et al. Protective effect of T cell depletion in murine renal ischemia-reperfusion injury. *Transplantation* 2002;74(6):759.
368. Burne-Taney MJ, Ascon DB, Daniels F, et al. B cell deficiency confers protection from renal ischemia reperfusion injury. *J Immunol* 2003;171(6):3210.
369. Burne-Taney MJ, Yokota-Ikeda N, Rabb H. Effects of combined T- and B-cell deficiency on murine ischemia reperfusion injury. *Am J Transplant* 2005;5(6):1186.
370. Wühl P, Schoop R, Bilic G, et al. Renal tubular epithelial expression of the costimulatory molecule B7RP-1 (inducible costimulator ligand). *J Am Soc Nephrol* 2002;13(6):1517.
371. Li H, Nord EP. CD40 ligation stimulates MCP-1 and IL-8 production, TRAF6 recruitment, and MAPK activation in proximal tubule cells. *Am J Physiol Renal Physiol* 2002;282(6):F1020.
372. Deckers JG, De Haij S, van der Woude FJ, et al. IL-4 and IL-13 augment cytokine- and CD40-induced RANTES production by human renal tubular epithelial cells in vitro. *J Am Soc Nephrol* 1998;9(7):1187.
373. Awad AS, Rouse M, Huang L, et al. Compartmentalization of neutrophils in the kidney and lung following acute ischemic kidney injury. *Kidney Int* 2009;75(7):689.
374. Jang HR, Rabb H. The innate immune response in ischemic acute kidney injury. *Clin Immunol* 2009;130(1):41.
375. Li L, Huang L, Sung SS, et al. The chemokine receptors CCR2 and CX3CR1 mediate monocyte/macrophage trafficking in kidney ischemia-reperfusion injury. *Kidney Int* 2008;74(12):1526.
376. Oh DJ, Dursun B, He Z, et al. Fractalkine receptor (CX3CR1) inhibition is protective against ischemic acute renal failure in mice. *Am J Physiol Renal Physiol* 2008;294(1):F264.
377. John R, Nelson PJ. Dendritic cells in the kidney. *J Am Soc Nephrol* 2007;18(10):2628.
378. Hume DA. Macrophages as APC and the dendritic cell myth. *J Immunol* 2008;181(9):5829.
379. Thurman JM, Lucia MS, Ljubanovic D, et al. Acute tubular necrosis is characterized by activation of the alternative pathway of complement. *Kidney Int* 2005;67(2):524.
380. Thurman JM, Lenderink AM, Royer PA, et al. C3a is required for the production of CXC chemokines by tubular epithelial cells after renal ischemia/reperfusion. *J Immunol* 2007;178(3):1819.
381. Homeister JW, Lucchesia BR. Complement activation and inhibition in myocardial ischemia and reperfusion injury. *Annu Rev Pharmacol Toxicol* 1994;34:17.
382. Sandor N, Pap D, Prechl J, et al. A novel, complement-mediated way to enhance the interplay between macrophages, dendritic cells and T lymphocytes. *Mol Immunol* 2009;47(2-3):438.
383. Thurman JM, Royer PA, Ljubanovic D, et al. Treatment with an inhibitory monoclonal antibody to mouse factor B protects mice from induction of apoptosis and renal ischemia/reperfusion injury. *J Am Soc Nephrol* 2006;17(3):707.
384. Zheng X, Zhang X, Sun H, et al. Protection of renal ischemia injury using combination gene silencing of complement 3 and caspase 3 genes. *Transplantation* 2006;82(12):1781.
385. Molitoris BA, Sutton TA. Endothelial injury and dysfunction: Role in the extension phase of acute renal failure. *Kidney Int* 2004;66(2):496.
386. Sprague AH, Khalil RA. Inflammatory cytokines in vascular dysfunction and vascular disease. *Biochem Pharmacol* 2009;78(6):539.
387. Kurata H, Takaoka M, Kubo Y, et al. Protective effect of nitric oxide on ischemia/reperfusion-induced renal injury and endothelin-1 overproduction. *Eur J Pharmacol* 2005;517(3):232.
388. da Silveira KD, Pompermayer Bosco KS, Diniz LR, et al. ACE2-angiotensin-(1-7)-Mas axis in renal ischaemia/reperfusion injury in rats. *Clin Sci (Lond)* 2010;119(9):385.
389. Conger JD, Robinette JB, Guggenheim SJ. Effect of acetylcholine on the early phase of reversible norepinephrine-induced acute renal failure. *Kidney Int* 1981;19(3):399.
390. Kwon O, Hong SM, Ramesh G. Diminished NO generation by injured endothelium and loss of macula densa nNOS may contribute to sustained acute kidney injury after ischemia-reperfusion. *Am J Physiol Renal Physiol* 2009;296(1):F25.
391. Kelly KJ, Williams WW Jr, Colvin RB, et al. Antibody to intercellular adhesion molecule 1 protects the kidney against ischemic injury. *Proc Natl Acad Sci U S A* 1994;91(2):812.
392. Rabb H, Mendiola CC, Saba SR, et al. Antibodies to ICAM-1 protect kidneys in severe ischemic reperfusion injury. *Biochem Biophys Res Commun* 1995;211(1):67.
393. Mason J, Torhorst J, Welsch J. Role of the medullary perfusion defect in the pathogenesis of ischemic renal failure. *Kidney Int* 1984;26(3):283.
394. Basile DP. The endothelial cell in ischemic acute kidney injury: Implications for acute and chronic function. *Kidney Int* 2007;72(2):151.
395. Rabelink TJ, de Boer HC, van Zonneveld AJ. Endothelial activation and circulating markers of endothelial activation in kidney disease. *Nat Rev Nephrol* 2010;6(7):404.
396. Basile DP, Fredrich K, Chelladurai B, et al. Renal ischemia reperfusion inhibits VEGF expression and induces ADAMTS-1, a novel VEGF inhibitor. *Am J Physiol Renal Physiol* 2008;294(4):F928.
397. Kwon O, Hong SM, Sutton TA, et al. Preservation of peritubular capillary endothelial integrity and increasing pericytes may be critical to recovery from postischemic acute kidney injury. *Am J Physiol Renal Physiol* 2008;295(2):F351.
398. Spiegel DM, Wilson PD, Molitoris BA. Epithelial polarity following ischemia: A requirement for normal cell function. *Am J Physiol* 1989;256(3 Pt 2):F430.
399. Van Why SK, Mann AS, Ardito T, et al. Expression and molecular regulation of Na(+)-K(+)-ATPase after renal ischemia. *Am J Physiol* 1994;267(1 Pt 2):F75.

400. Van Why SK, Hildebrandt F, Ardito T, et al. Induction and intracellular localization of HSP-72 after renal ischemia. *Am J Physiol* 1992;263(5 Pt 2):F769.
401. Harris AS, Croall DE, Morrow JS. Calmodulin regulates fodrin susceptibility to cleavage by calcium-dependent protease I. *J Biol Chem* 1989; 264(29):17401.
402. Cryns VL, Bergeron L, Zhu H, et al. Specific cleavage of alpha-fodrin during Fas- and tumor necrosis factor-induced apoptosis is mediated by an interleukin-1beta-converting enzyme/Ced-3 protease distinct from the poly(ADP-ribose) polymerase protease. *J Biol Chem* 1996;271(49):31277.
403. Doctor RB, Bennett V, Mandel LJ. Degradation of spectrin and ankyrin in the ischemic rat kidney. *Am J Physiol* 1993;264(4 Pt 1):C1003.
404. Gailit J, Colflesh D, Rabiner I, et al. Redistribution and dysfunction of integrins in cultured renal epithelial cells exposed to oxidative stress. *Am J Physiol* 1993;264(1 Pt 2):F149.
405. Kroshian VM, Sheridan AM, Lieberthal W. Functional and cytoskeletal changes induced by sublethal injury in proximal tubular epithelial cells. *Am J Physiol* 1994;266(1 Pt 2):F21.
406. Nigam S, Weston CE, Liu CH, et al. The actin cytoskeleton and integrin expression in the recovery of cell adhesion after oxidant stress to a proximal tubule cell line (JTC-12). *J Am Soc Nephrol* 1998;9(10):1787.
407. Wijesekera DS, Zarama MJ, Paller MS. Effects of integrins on proliferation and apoptosis of renal epithelial cells after acute injury. *Kidney Int* 1997;52(6):1511.
408. Goligorsky MS, DiBona GF. Pathogenetic role of Arg-Gly-Asp-recognizing integrins in acute renal failure. *Proc Natl Acad Sci U S A* 1993;90(12):5700.
409. Noiri E, Gailit J, Sheth D, et al. Cyclic RGD peptides ameliorate ischemic acute renal failure in rats. *Kidney Int* 1994;46(4):1050.
410. Zhang PL, Lun M, Schworer CM, et al. Heat shock protein expression is highly sensitive to ischemia-reperfusion injury in rat kidneys. *Ann Clin Lab Sci* 2008;38(1):57.
411. Aufricht C. Heat-shock protein 70: Molecular supertool? *Pediatr Nephrol* 2005;20(6):707.
412. Riordan M, Sreedharan R, Wang S, et al. HSP70 binding modulates detachment of Na-K-ATPase following energy deprivation in renal epithelial cells. *Am J Physiol Renal Physiol* 2005;288(6):F1236.
413. Mifflin LC, Cohen RE. Characterization of denatured protein inducers of the heat shock (stress) response in *Xenopus laevis* oocytes. *J Biol Chem* 1994;269(22):15710.
414. Smoyer WE, Ransom R, Harris RC, et al. Ischemic acute renal failure induces differential expression of small heat shock proteins. *J Am Soc Nephrol* 2000;11(2):211.
415. Aufricht C, Ardito T, Thulin G, et al. Heat-shock protein 25 induction and redistribution during actin reorganization after renal ischemia. *Am J Physiol* 1998;274(1 Pt 2):F215.
416. Bidmon B, Endemann M, Muller T, et al. Heat shock protein-70 repairs proximal tubule structure after renal ischemia. *Kidney Int* 2000; 58(6):2400.
417. Bidmon B, Endemann M, Muller T, et al. HSP-25 and HSP-90 stabilize Na,K-ATPase in cytoskeletal fractions of ischemic rat renal cortex. *Kidney Int* 2002;62(5):1620.
418. Wang YH, Knowlton AA, Li FH, et al. Hsp72 expression enhances survival in adenosine triphosphate-depleted renal epithelial cells. *Cell Stress Chaperones* 2002;7(2):137.
419. Yang CW, Kim BS, Kim J, et al. Preconditioning with sodium arsenite inhibits apoptotic cell death in rat kidney with ischemia/reperfusion or cyclosporine-induced injuries. The possible role of heat-shock protein 70 as a mediator of ischemic tolerance. *Exp Nephrol* 2001;9(4):284.
420. Percy C, Waters MJ, Gobe G. Caveolins in the repair phase of acute renal failure after oxidative stress. *Nephrology (Carlton)* 2004;9(6):374.
421. Zager RA, Johnson A, Hanson S, et al. Altered cholesterol localization and caveolin expression during the evolution of acute renal failure. *Kidney Int* 2002;61(5):1674.
422. Mahmoudi M, Willgoss D, Cuttle L, et al. In vivo and in vitro models demonstrate a role for caveolin-1 in the pathogenesis of ischaemic acute renal failure. *J Pathol* 2003;200(3):396.
423. Kieran NE, Maderna P, Godson C. Lipoxins: Potential anti-inflammatory, proresolution, and antifibrotic mediators in renal disease. *Kidney Int* 2004;65(4):1145.
424. Han WK, Bailly V, Abichandani R, et al. Kidney Injury Molecule-1 (KIM-1): A novel biomarker for human renal proximal tubule injury. *Kidney Int* 2002;62(1):237.
425. Bailly V, Zhang Z, Meier W, et al. Shedding of kidney injury molecule-1, a putative adhesion protein involved in renal regeneration. *J Biol Chem* 2002;277(42):39739.
426. Norman J, Tsau YK, Bacay A, et al. Epidermal growth factor accelerates functional recovery from ischaemic acute tubular necrosis in the rat: Role of the epidermal growth factor receptor. *Clin Sci (Lond)* 1990;78(5):445.
427. Matejka GL, Jennische E. IGF-I binding and IGF-I mRNA expression in the post-ischemic regenerating rat kidney. *Kidney Int* 1992;42(5):1113.
428. Tsao T, Wang J, Fervenza FC, et al. Renal growth hormone—insulin-like growth factor-I system in acute renal failure. *Kidney Int* 1995;47(6):1658.
429. Liu KD. Molecular mechanisms of recovery from acute renal failure. *Crit Care Med* 2003;31(8 Suppl):S572.
430. Miller SB, Martin DR, Kissane J, et al. Hepatocyte growth factor accelerates recovery from acute ischemic renal injury in rats. *Am J Physiol* 1994;266(1 Pt 2):F129.
431. Liu ZX, Nickel CH, Cantley LG. HGF promotes adhesion of ATP-depleted renal tubular epithelial cells in a MAPK-dependent manner. *Am J Physiol Renal Physiol* 2001;281(1):F62.
432. Yang J, Liu Y. Blockage of tubular epithelial to myofibroblast transition by hepatocyte growth factor prevents renal interstitial fibrosis. *J Am Soc Nephrol* 2002;13(1):96.
433. Duffield JS, Park KM, Hsiao LL, et al. Restoration of tubular epithelial cells during repair of the posts ischemic kidney occurs independently of bone marrow-derived stem cells. *J Clin Invest* 2005;115(7):1743.
434. Gupta S, Verfaillie C, Chmielewski D, et al. A role for extrarenal cells in the regeneration following acute renal failure. *Kidney Int* 2002; 62(4):1285.
435. Herrera MB, Bussolati B, Bruno S, et al. Mesenchymal stem cells contribute to the renal repair of acute tubular epithelial injury. *Int J Mol Med* 2004; 14(6):1035.
436. Morigi M, Imberti B, Zoja C, et al. Mesenchymal stem cells are renoprotective, helping to repair the kidney and improve function in acute renal failure. *J Am Soc Nephrol* 2004;15(7):1794.
437. de Groot K, Bahlmann FH, Bahlmann E, et al. Kidney graft function determines endothelial progenitor cell number in renal transplant recipients. *Transplantation* 2005;79(8):941.
438. Lin F, Cordes K, Li L, et al. Hematopoietic stem cells contribute to the regeneration of renal tubules after renal ischemia-reperfusion injury in mice. *J Am Soc Nephrol* 2003;14(5):1188.
439. Stokman G, Leemans JC, Claessen N, et al. Hematopoietic stem cell mobilization therapy accelerates recovery of renal function independent of stem cell contribution. *J Am Soc Nephrol* 2005;16(6):1684.
440. Kale S, Karihaloo A, Clark PR, et al. Bone marrow stem cells contribute to repair of the ischemically injured renal tubule. *J Clin Invest* 2003;112(1):42.
441. Iwasaki M, Adachi Y, Minamino K, et al. Mobilization of bone marrow cells by G-CSF rescues mice from cisplatin-induced renal failure, and M-CSF enhances the effects of G-CSF. *J Am Soc Nephrol* 2005;16(3):658.
442. Herrera MB, Bussolati B, Bruno S, et al. Exogenous mesenchymal stem cells localize to the kidney by means of CD44 following acute tubular injury. *Kidney Int* 2007;72(4):430.
443. Lange C, Tögel F, Ittrich H, et al. Administered mesenchymal stem cells enhance recovery from ischemia/reperfusion-induced acute renal failure in rats. *Kidney Int* 2005;68(4):1613.
444. Tögel F, Hu Z, Weiss K, et al. Administered mesenchymal stem cells protect against ischemic acute renal failure through differentiation-independent mechanisms. *Am J Physiol Renal Physiol* 2005;289(1):F31.
445. Ciarrimboli G, Koepsell H, Iordanova M, et al. Individual PKC-phosphorylation sites in organic cation transporter 1 determine substrate selectivity and transport regulation. *J Am Soc Nephrol* 2005;16(6):1562.
446. van de Water B, de Graauw M, Le Devedec S, et al. Cellular stress responses and molecular mechanisms of nephrotoxicity. *Toxicol Lett* 2006; 162(1):83.
447. Lorz C, Justo P, Sanz AB, et al. Role of Bcl-xL in paracetamol-induced tubular epithelial cell death. *Kidney Int* 2005;67(2):592.
448. Huang Q, Dunn RT, 2nd, Jayadev S, et al. Assessment of cisplatin-induced nephrotoxicity by microarray technology. *Toxicol Sci* 2001; 63(2):196.

449. Goodsaid FM. Genomic biomarkers of toxicity. *Curr Opin Drug Discov Dev* 2003;6(1):41.
450. Thukral SK, Nordone PJ, Hu R, et al. Prediction of nephrotoxicant action and identification of candidate toxicity-related biomarkers. *Toxicol Pathol* 2005;33(3):343.
451. Davis JW, 2nd, Goodsaid FM, Bral CM, et al. Quantitative gene expression analysis in a nonhuman primate model of antibiotic-induced nephrotoxicity. *Toxicol Appl Pharmacol* 2004;200(1):16.
452. Schliefer K, Rockstroh JK, Spengler U, et al. Nephrogenic diabetes insipidus in a patient taking cidofovir. *Lancet* 1997;350(9075):413.
453. Perazella MA. Drug-induced renal failure: update on new medications and unique mechanisms of nephrotoxicity. *Am J Med Sci* 2003;325(6):349.
454. Wyatt CM, Morgello S, Katz-Malamed R, et al. The spectrum of kidney disease in patients with AIDS in the era of antiretroviral therapy. *Kidney Int* 2009;75(4):428.
455. Gunness P, Aleksa K, Koren G. Acyclovir is a substrate for the human breast cancer resistance protein (BCRP/ABCG2): Implications for renal tubular transport and acyclovir-induced nephrotoxicity. *Can J Physiol Pharmacol* 2011;89(9):675.
456. Ho ES, Lin DC, Mendel DB, et al. Cytotoxicity of antiviral nucleotides adefovir and cidofovir is induced by the expression of human renal organic anion transporter 1. *J Am Soc Nephrol* 2000;11(3):383.
457. Wijnholds J, Mol CA, van Deemter L, et al. Multidrug-resistance protein 5 is a multispecific organic anion transporter able to transport nucleotide analogs. *Proc Natl Acad Sci U S A* 2000;97(13):7476.
458. Cihlar T, Lin DC, Pritchard JB, et al. The antiviral nucleotide analogs cidofovir and adefovir are novel substrates for human and rat renal organic anion transporter 1. *Mol Pharmacol* 1999;56(3):570.
459. Moore KH, Yuen GJ, Raasch RH, et al. Pharmacokinetics of lamivudine administered alone and with trimethoprim-sulfamethoxazole. *Clin Pharmacol Ther* 1996;59(5):550.
460. Lai Y, Tse CM, Unadkat JD. Mitochondrial expression of the human equilibrative nucleoside transporter 1 (hENT1) results in enhanced mitochondrial toxicity of antiviral drugs. *J Biol Chem* 2004;279(6):4490.
461. Mangravite LM, Xiao G, Giacomini KM. Localization of human equilibrative nucleoside transporters, hENT1 and hENT2, in renal epithelial cells. *Am J Physiol Renal Physiol* 2003;284(5):F902.
462. Griffith DA, Jarvis SM. Nucleoside and nucleobase transport systems of mammalian cells. *Biochim Biophys Acta* 1996;1286(3):153.
463. Nagai J, Takano M. Molecular aspects of renal handling of aminoglycosides and strategies for preventing the nephrotoxicity. *Drug Metab Pharmacokinet* 2004;19(3):159.
464. Mingeot-Leclercq MP, Tulkens PM. Aminoglycosides: Nephrotoxicity. *Antimicrob Agents Chemother* 1999;43(5):1003.
465. Fujiwara K, Shin M, Matsunaga H, et al. Light-microscopic immunocytochemistry for gentamicin and its use for studying uptake of the drug in kidney. *Antimicrob Agents Chemother* 2009;53(8):3302.
466. Schmitz C, Hilpert J, Jacobsen C, et al. Megalin deficiency offers protection from renal aminoglycoside accumulation. *J Biol Chem* 2002;277(1):618.
467. Watanabe A, Nagai J, Adachi Y, et al. Targeted prevention of renal accumulation and toxicity of gentamicin by aminoglycoside binding receptor antagonists. *J Control Release* 2004;95(3):423.
468. Sandoval RM, Molitoris BA. Gentamicin traffics retrograde through the secretory pathway and is released in the cytosol via the endoplasmic reticulum. *Am J Physiol Renal Physiol* 2004;286(4):F617.
469. Laurent G, Kishore BK, Tulkens PM. Aminoglycoside-induced renal phospholipidosis and nephrotoxicity. *Biochem Pharmacol* 1990;40(11):2383.
470. Van Bambeke F, Tulkens PM, Brasseur R, et al. Aminoglycoside antibiotics induce aggregation but not fusion of negatively-charged liposomes. *Eur J Pharmacol* 1995;289(2):321.
471. Sandoval RM, Bacallao RL, Dunn KW, et al. Nucleotide depletion increases trafficking of gentamicin to the Golgi complex in LLC-PK1 cells. *Am J Physiol Renal Physiol* 2002;283(6):F1422.
472. Chwieralski CE, Welte T, Buhling F. Cathepsin-regulated apoptosis. *Apoptosis* 2006;11(2):143.
473. Yin XM. Bid, a BH3-only multi-functional molecule, is at the cross road of life and death. *Gene* 2006;369:7.
474. Sundin DP, Sandoval R, Molitoris BA. Gentamicin inhibits renal protein and phospholipid metabolism in rats: implications involving intracellular trafficking. *J Am Soc Nephrol* 2001;12(1):114.
475. Horibe T, Nagai H, Sakakibara K, et al. Ribostamycin inhibits the chaperone activity of protein disulfide isomerase. *Biochem Biophys Res Commun* 2001;289(5):967.
476. Horibe T, Nagai H, Matsui H, et al. Aminoglycoside antibiotics bind to protein disulfide isomerase and inhibit its chaperone activity. *J Antibiot (Tokyo)* 2002;55(5):528.
477. Horibe T, Matsui H, Tanaka M, et al. Gentamicin binds to the lectin site of calreticulin and inhibits its chaperone activity. *Biochem Biophys Res Commun* 2004;323(1):281.
478. Cuzzocrea S, Mazzon E, Dugo L, et al. A role for superoxide in gentamicin-mediated nephropathy in rats. *Eur J Pharmacol* 2002;450(1):67.
479. Pedraza-Chaverri J, Maldonado PD, Medina-Campos ON, et al. Garlic ameliorates gentamicin nephrotoxicity: Relation to antioxidant enzymes. *Free Radic Biol Med* 2000;29(7):602.
480. Maldonado PD, Barrera D, Rivero I, et al. Antioxidant S-allylcysteine prevents gentamicin-induced oxidative stress and renal damage. *Free Radic Biol Med* 2003;35(3):317.
481. Martinez-Salgado C, Eleno N, Tavares P, et al. Involvement of reactive oxygen species on gentamicin-induced mesangial cell activation. *Kidney Int* 2002;62(5):1682.
482. Notenboom S, Miller DS, Smits P, et al. Role of NO in endothelin-regulated drug transport in the renal proximal tubule. *Am J Physiol Renal Physiol* 2002;282(3):F458.
483. Ward DT, McLarnon SJ, Riccardi D. Aminoglycosides increase intracellular calcium levels and ERK activity in proximal tubular OK cells expressing the extracellular calcium-sensing receptor. *J Am Soc Nephrol* 2002;13(6):1481.
484. Leung JC, Marphis T, Craver RD, et al. Altered NMDA receptor expression in renal toxicity: Protection with a receptor antagonist. *Kidney Int* 2004;66(1):167.
485. Geleilate TJ, Melo GC, Costa RS, et al. Role of myofibroblasts, macrophages, transforming growth factor-beta endothelin, angiotensin-II, and fibronectin in the progression of tubulointerstitial nephritis induced by gentamicin. *J Nephrol* 2002;15(6):633.
486. Hsueh CC, Feingold DS. Selective membrane toxicity of the polyene antibiotics: Studies on natural membranes. *Antimicrob Agents Chemother* 1973;4(3):316.
487. Sawaya BP, Briggs JP, Schnermann J. Amphotericin B nephrotoxicity: The adverse consequences of altered membrane properties. *J Am Soc Nephrol* 1995;6(2):154.
488. Bernardo JF, Murakami S, Branch RA, et al. Potassium depletion potentiates amphotericin-B-induced toxicity to renal tubules. *Nephron* 1995;70(2):235.
489. Sawaya BP, Weihprecht H, Campbell WR, et al. Direct vasoconstriction as a possible cause for amphotericin B-induced nephrotoxicity in rats. *J Clin Invest* 1991;87(6):2097.
490. Tolins JP, Raj L. Adverse effect of amphotericin B administration on renal hemodynamics in the rat. Neurohumoral mechanisms and influence of calcium channel blockade. *J Pharmacol Exp Ther* 1988;245(2):594.
491. Hardie WD, Ebert J, Frazer M, et al. The effect of thromboxane A2 receptor antagonism on amphotericin B-induced renal vasoconstriction in the rat. *Prostaglandins* 1993;45(1):47.
492. Sabra R, Takahashi K, Branch RA, et al. Mechanisms of amphotericin B-induced reduction of the glomerular filtration rate: A micropuncture study. *J Pharmacol Exp Ther* 1990;253(1):34.
493. Tune BM, Hsu CY. Toxicity of cephaloridine to carnitine transport and fatty acid metabolism in rabbit renal cortical mitochondria: Structure-activity relationships. *J Pharmacol Exp Ther* 1994;270(3):873.
494. Lash LH, Tokarz JJ, Woods EB. Renal cell type specificity of cephalosporin-induced cytotoxicity in suspensions of isolated proximal tubular and distal tubular cells. *Toxicology* 1994;94(1-3):97.
495. Kiyomiya K, Matsushita N, Matsuo S, et al. Cephaloridine-induced inhibition of cytochrome c oxidase activity in the mitochondria of cultured renal epithelial cells (LLC-PK1) as a possible mechanism of its nephrotoxicity. *Toxicol Appl Pharmacol* 2000;167(2):151.
496. Steinmassl D, Pfaller W, Gstraunthaler G, et al. LLC-PK1 epithelia as a model for in vitro assessment of proximal tubular nephrotoxicity. *In Vitro Cell Dev Biol Anim* 1995;31(2):94.
497. Fiaccadori E, Maggiore U, Arisi A, et al. Outbreak of acute renal failure due to cefodizime-vancomycin association in a heart surgery unit. *Intensive Care Med* 2001;27(11):1819.

498. Dunn CJ, Wagstaff AJ, Perry CM, et al. Cyclosporin: An updated review of the pharmacokinetic properties, clinical efficacy and tolerability of a microemulsion-based formulation (neoral)1 in organ transplantation. *Drugs* 2001;61(13):1957.
499. Hunley TE, Fogo A, Iwasaki S, et al. Endothelin A receptor mediates functional but not structural damage in chronic cyclosporine nephrotoxicity. *J Am Soc Nephrol* 1995;5(9):1718.
500. Lassila M. Interaction of cyclosporine A and the renin-angiotensin system; new perspectives. *Curr Drug Metab* 2002;3(1):61.
501. Bunchman TE, Brookshire CA. Cyclosporine-induced synthesis of endothelin by cultured human endothelial cells. *J Clin Invest* 1991;88(1):310.
502. Haug C, Duell T, Voisard R, et al. Cyclosporine A stimulates endothelin release. *J Cardiovasc Pharmacol* 1995;26(Suppl 3):S239.
503. Kon V, Hunley TE, Fogo A. Combined antagonism of endothelin A/B receptors links endothelin to vasoconstriction whereas angiotensin II effects fibrosis. Studies in chronic cyclosporine nephrotoxicity in rats. *Transplantation* 1995;60(1):89.
504. Shehata M, el Nahas A, Barkworth E, et al. Increased platelet-derived growth factor in the kidneys of cyclosporin-treated rats. *Kidney Int* 1994;46(3):726.
505. Darby IA, Hewitson T, Jones C, et al. Vascular expression of clusterin in experimental cyclosporine nephrotoxicity. *Exp Nephrol* 1995;3(4):234.
506. Cebrian C, Areste C, Nicolas A, et al. Kidney androgen-regulated protein interacts with cyclophilin B and reduces cyclosporine A-mediated toxicity in proximal tubule cells. *J Biol Chem* 2001;276(31):29410.
507. Ader JL, Rostaing L. Cyclosporin nephrotoxicity: Pathophysiology and comparison with FK-506. *Curr Opin Nephrol Hypertens* 1998;7(5):539.
508. Steiner S, Aicher L, Raymackers J, et al. Cyclosporine A decreases the protein level of the calcium-binding protein calbindin-D 28 kDa in rat kidney. *Biochem Pharmacol* 1996;51(3):253.
509. Aicher L, Meier G, Norcross AJ, et al. Decrease in kidney calbindin-D 28 kDa as a possible mechanism mediating cyclosporine A- and FK-506-induced calciuria and tubular mineralization. *Biochem Pharmacol* 1997;53(5):723.
510. Ponticelli C. De novo thrombotic microangiopathy. An underrated complication of renal transplantation. *Clin Nephrol* 2007;67(6):335.
511. Oyen O, Strom EH, Midtvedt K, et al. Calcineurin inhibitor-free immunosuppression in renal allograft recipients with thrombotic microangiopathy/hemolytic uremic syndrome. *Am J Transplant* 2006;6(2):412.
512. Bren A, Pajek J, Grego K, et al. Follow-up of kidney graft recipients with cyclosporine-associated hemolytic-uremic syndrome and thrombotic microangiopathy. *Transplant Proc* 2005;37(4):1889.
513. Zoja C, Furci L, Ghilardi F, et al. Cyclosporin-induced endothelial cell injury. *Lab Invest* 1986;55(4):455.
514. Lau DC, Wong KL, Hwang WS. Cyclosporine toxicity on cultured rat microvascular endothelial cells. *Kidney Int* 1989;35(2):604.
515. Young BA, Burdmann EA, Johnson RJ, et al. Cyclosporine A induced arteriopathy in a rat model of chronic cyclosporine nephropathy. *Kidney Int* 1995;48(2):431.
516. Nieves-Cintrón M, Amberg GC, Nichols CB, et al. Activation of NFATc3 down-regulates the beta1 subunit of large conductance, calcium-activated K⁺ channels in arterial smooth muscle and contributes to hypertension. *J Biol Chem* 2007;282(5):3231.
517. Wolf G, Thaiss F, Stahl RA. Cyclosporine stimulates expression of transforming growth factor-beta in renal cells. Possible mechanism of cyclosporines antiproliferative effects. *Transplantation* 1995;60(3):237.
518. Lally C, Healy E, Ryan MP. Cyclosporine A-induced cell cycle arrest and cell death in renal epithelial cells. *Kidney Int* 1999;56(4):1254.
519. Pallet N, Rabant M, Xu-Dubois YC, et al. Response of human renal tubular cells to cyclosporine and sirolimus: A toxicogenomic study. *Toxicol Appl Pharmacol* 2008;229(2):184.
520. Bouvier N, Flinois JP, Gilleron J, et al. Cyclosporine triggers endoplasmic reticulum stress in endothelial cells: A role for endothelial phenotypic changes and death. *Am J Physiol Renal Physiol* 2009;296(1):F160.
521. Pallet N, Bouvier N, Bendjallab A, et al. Cyclosporine-induced endoplasmic reticulum stress triggers tubular phenotypic changes and death. *Am J Transplant* 2008;8(11):2283.
522. Han SW, Li C, Ahn KO, et al. Prolonged endoplasmic reticulum stress induces apoptotic cell death in an experimental model of chronic cyclosporine nephropathy. *Am J Nephrol* 2008;28(5):707.
523. Polte T, Hemmerle A, Berndt G, et al. Atrial natriuretic peptide reduces cyclosporin toxicity in renal cells: Role of cGMP and heme oxygenase-1. *Free Radic Biol Med* 2002;32(1):56.
524. Longoni B, Migliori M, Ferretti A, et al. Melatonin prevents cyclosporine-induced nephrotoxicity in isolated and perfused rat kidney. *Free Radic Res* 2002;36(3):357.
525. Dominguez JH, Soleimani M, Batiuk T. Studies of renal injury IV: The GLUT1 gene protects renal cells from cyclosporine A toxicity. *Kidney Int* 2002;62(1):127.
526. Jiang T, Acosta D, Jr. Mitochondrial Ca²⁺ overload in primary cultures of rat renal cortical epithelial cells by cytotoxic concentrations of cyclosporine: A digitized fluorescence imaging study. *Toxicology* 1995;95(1-3):155.
527. Strzelecki T, Kumar S, Khauli R, et al. Impairment by cyclosporine of membrane-mediated functions in kidney mitochondria. *Kidney Int* 1988;34(2):234.
528. Justo P, Lorz C, Sanz A, et al. Intracellular mechanisms of cyclosporin A-induced tubular cell apoptosis. *J Am Soc Nephrol* 2003;14(12):3072.
529. Charuk JH, Wong PY, Reithmeier RA. Differential interaction of human renal P-glycoprotein with various metabolites and analogues of cyclosporin A. *Am J Physiol* 1995;269(1 Pt 2):F31.
530. Rosen S, Brezis M, Stillman I. The pathology of nephrotoxic injury: A reappraisal. *Miner Electrolyte Metab* 1994;20(4):174.
531. Rosen S, Greenfeld Z, Brezis M. Chronic cyclosporine-induced nephropathy in the rat. A medullary ray and inner stripe injury. *Transplantation* 1990;49(2):445.
532. Heyman SN, Fuchs S, Brezis M. The role of medullary ischemia in acute renal failure. *New Horiz* 1995;3(4):597.
533. Young BA, Burdmann EA, Johnson RJ, et al. Cellular proliferation and macrophage influx precede interstitial fibrosis in cyclosporine nephrotoxicity. *Kidney Int* 1995;48(2):439.
534. Shihab FS, Andoh TF, Tanner AM, et al. Role of transforming growth factor-beta 1 in experimental chronic cyclosporine nephropathy. *Kidney Int* 1996;49(4):1141.
535. Islam M, Burke JF, Jr, McGowan TA, et al. Effect of anti-transforming growth factor-beta antibodies in cyclosporine-induced renal dysfunction. *Kidney Int* 2001;59(2):498.
536. Olegginì R, Musante L, Menoni S, et al. Characterization of a DNA binding site that mediates the stimulatory effect of cyclosporin-A on type III collagen expression in renal cells. *Nephrol Dial Transplant* 2000;15(6):778.
537. Kang DH, Kim YG, Andoh TF, et al. Post-cyclosporine-mediated hypertension and nephropathy: amelioration by vascular endothelial growth factor. *Am J Physiol Renal Physiol* 2001;280(4):F727.
538. Dumont FJ. FK506, an immunosuppressant targeting calcineurin function. *Curr Med Chem* 2000;7(7):731.
539. Su Q, Weber L, Le Hir M, et al. Nephrotoxicity of cyclosporin A and FK506: inhibition of calcineurin phosphatase. *Ren Physiol Biochem* 1995;18(3):128.
540. Perrot-Applanat M, Cibert C, Geraud G, et al. The 59 kDa FK506-binding protein, a 90 kDa heat shock protein binding immunophilin (FKBP59-HBI), is associated with the nucleus, the cytoskeleton and mitotic apparatus. *J Cell Sci* 1995;108 (Pt 5):2037.
541. Christians U, Jacobsen W, Benet LZ, et al. Mechanisms of clinically relevant drug interactions associated with tacrolimus. *Clin Pharmacokinet* 2002;41(11):813.
542. Goodall T, Kind CN, Hammond TG. FK506-induced endothelin release by cultured rat mesangial cells. *J Cardiovasc Pharmacol* 1995;26(Suppl 3):S482.
543. Textor SC, Burnett JC, Jr, Romero JC, et al. Urinary endothelin and renal vasoconstriction with cyclosporine or FK506 after liver transplantation. *Kidney Int* 1995;47(5):1426.
544. Mitamura T, Yamada A, Ishida H, et al. Tacrolimus (FK506)-induced nephrotoxicity in spontaneous hypertensive rats. *J Toxicol Sci* 1994;19(4):219.
545. Shihab FS, Bennett WM, Tanner AM, et al. Mechanism of fibrosis in experimental tacrolimus nephrotoxicity. *Transplantation* 1997;64(12):1829.
546. Du S, Hiramatsu N, Hayakawa K, et al. Suppression of NF-kappaB by cyclosporin a and tacrolimus (FK506) via induction of the C/EBP family: Implication for unfolded protein response. *J Immunol* 2009;182(11):7201.

547. Shihab FS, Bennett WM, Yi H, et al. Sirolimus increases transforming growth factor-beta1 expression and potentiates chronic cyclosporine nephrotoxicity. *Kidney Int* 2004;65(4):1262.
548. Lieberthal W, Fuhro R, Andry CC, et al. Rapamycin impairs recovery from acute renal failure: Role of cell-cycle arrest and apoptosis of tubular cells. *Am J Physiol Renal Physiol* 2001;281(4):F693.
549. Wang D, Lippard SJ. Cellular processing of platinum anticancer drugs. *Nat Rev Drug Discov* 2005;4(4):307.
550. Hanigan MH, Devarajan P. Cisplatin nephrotoxicity: Molecular mechanisms. *Cancer Ther* 2003;1:47.
551. Arany I, Safirstein RL. Cisplatin nephrotoxicity. *Semin Nephrol* 2003;23(5):460.
552. Pabla N, Murphy RF, Liu K, et al. The copper transporter Ctr1 contributes to cisplatin uptake by renal tubular cells during cisplatin nephrotoxicity. *Am J Physiol Renal Physiol* 2009;296(3):F505.
553. Ludwig T, Riethmuller C, Gekle M, et al. Nephrotoxicity of platinum complexes is related to basolateral organic cation transport. *Kidney Int* 2004;66(1):196.
554. Ciarimboli G, Ludwig T, Lang D, et al. Cisplatin nephrotoxicity is critically mediated via the human organic cation transporter 2. *Am J Pathol* 2005;167(6):1477.
555. Ramesh G, Reeves WB. TNF-alpha mediates chemokine and cytokine expression and renal injury in cisplatin nephrotoxicity. *J Clin Invest* 2002;110(6):835.
556. Ramesh G, Reeves WB. TNFR2-mediated apoptosis and necrosis in cisplatin-induced acute renal failure. *Am J Physiol Renal Physiol* 2003;285(4):F610.
557. Liu H, Baliga R. Endoplasmic reticulum stress-associated caspase 12 mediates cisplatin-induced LLC-PK1 cell apoptosis. *J Am Soc Nephrol* 2005;16(7):1985.
558. Ramesh G, Reeves WB. p38 MAP kinase inhibition ameliorates cisplatin nephrotoxicity in mice. *Am J Physiol Renal Physiol* 2005;289(1):F166.
559. Szlosarek PW, Balkwill FR. Tumour necrosis factor alpha: A potential target for the therapy of solid tumours. *Lancet Oncol* 2003;4(9):565.
560. Yao X, Panichpisal K, Kurtzman N, et al. Cisplatin nephrotoxicity: A review. *Am J Med Sci* 2007;334(2):115.
561. Kelly KJ, Meehan SM, Colvin RB, et al. Protection from toxicant-mediated renal injury in the rat with anti-CD54 antibody. *Kidney Int* 1999;56(3):922.
562. Deng J, Kohda Y, Chiao H, et al. Interleukin-10 inhibits ischemic and cisplatin-induced acute renal injury. *Kidney Int* 2001;60(6):2118.
563. Rossi R, Helmchen U, Schellong G. Tubular function and histological findings in ifosfamide-induced renal Fanconi syndrome—a report of two cases. *Eur J Pediatr* 1992;151(5):384.
564. Persson PB, Hansell P, Liss P. Pathophysiology of contrast medium-induced nephropathy. *Kidney Int* 2005;68(1):14.
565. Beeri R, Symon Z, Brezis M, et al. Rapid DNA fragmentation from hypoxia along the thick ascending limb of rat kidneys. *Kidney Int* 1995;47(6):1806.
566. Agmon Y, Peleg H, Greenfeld Z, et al. Nitric oxide and prostanoids protect the renal outer medulla from radiocontrast toxicity in the rat. *J Clin Invest* 1994;94(3):1069.
567. Bakris GL, Gaber AO, Jones JD. Oxygen free radical involvement in urinary Tamm-Horsfall protein excretion after intrarenal injection of contrast medium. *Radiology* 1990;175(1):57.
568. Lantz B, Cochat P, Bouchet JL, et al. Short-term niflumic-acid-induced acute renal failure in children. *Nephrol Dial Transplant* 1994;9(9):1234.
569. Oldroyd SD, Haylor JL, Morcos SK. Bosentan, an orally active endothelin antagonist: Effect on the renal response to contrast media. *Radiology* 1995;196(3):661.
570. Schwartz D, Blum M, Peer G, et al. Role of nitric oxide (EDRF) in radiocontrast acute renal failure in rats. *Am J Physiol* 1994;267(3 Pt 2):F374.
571. Wang A, Holsclaw T, Bashore TM, et al. Exacerbation of radiocontrast nephrotoxicity by endothelin receptor antagonism. *Kidney Int* 2000;57(4):1675.
572. Andersen KJ, Christensen EI, Vik H. Effects of iodinated x-ray contrast media on renal epithelial cells in culture. *Invest Radiol* 1994;29(11):955.
573. Haller C, Schick CS, Zorn M, et al. Cytotoxicity of radiocontrast agents on polarized renal epithelial cell monolayers. *Cardiovasc Res* 1997;33(3):655.
574. Schick CS, Haller C. Comparative cytotoxicity of ionic and non-ionic radiocontrast agents on MDCK cell monolayers in vitro. *Nephrol Dial Transplant* 1999;14(2):342.
575. Hardiek K, Katholi RE, Ramkumar V, et al. Proximal tubule cell response to radiographic contrast media. *Am J Physiol Renal Physiol* 2001;280(1):F61.
576. Yano T, Itoh Y, Sendo T, et al. Cyclic AMP reverses radiocontrast media-induced apoptosis in LLC-PK1 cells by activating A kinase/PI3 kinase. *Kidney Int* 2003;64(6):2052.
577. Zager RA, Johnson AC, Hanson SY. Radiographic contrast media-induced tubular injury: evaluation of oxidant stress and plasma membrane integrity. *Kidney Int* 2003;64(1):128.
578. Haller C, Hizoh I. The cytotoxicity of iodinated radiocontrast agents on renal cells in vitro. *Invest Radiol* 2004;39(3):149.
579. Keung YK, Morgan D, Cobos E. Cocaine-induced microangiopathic hemolytic anemia and thrombocytopenia simulating thrombotic thrombocytopenia purpura. *Ann Hematol* 1996;72(3):155.
580. Burchardi H, Kaczmarczyk G. The effect of anaesthesia on renal function. *Eur J Anaesthesiol* 1994;11(3):163.
581. Munday IT, Stoddart PA, Jones RM, et al. Serum fluoride concentration and urine osmolality after enflurane and sevoflurane anesthesia in male volunteers. *Anesth Analg* 1995;81(2):353.
582. Chertow GM, Christiansen CL, Cleary PD, et al. Prognostic stratification in critically ill patients with acute renal failure requiring dialysis. *Arch Intern Med* 1995;155(14):1505.
583. Lima EQ, Dirce MT, Castro I, et al. Mortality risk factors and validation of severity scoring systems in critically ill patients with acute renal failure. *Ren Fail* 2005;27(5):547.
584. Feltes CM, Van Eyk J, Rabb H. Distant-organ changes after acute kidney injury. *Nephron Physiol* 2008;109(4):80.
585. Scanlon PJ, Faxon DP, Audet AM, et al. ACC/AHA guidelines for coronary angiography. A report of the American College of Cardiology/American Heart Association Task Force on practice guidelines (Committee on Coronary Angiography). Developed in collaboration with the Society for Cardiac Angiography and Interventions. *J Am Coll Cardiol* 1999;33(6):1756.
586. Ishani A, Xue JL, Himmelfarb J, et al. Acute kidney injury increases risk of ESRD among elderly. *J Am Soc Nephrol* 2009;20(1):223.
587. Ilic S, Rajic M, Vljakovic M, et al. The predictive value of 131I-hippurate clearance in the prognosis of acute renal failure. *Ren Fail* 2000;22(5):581.
588. Bonomini V, Stefoni S, Vangelista A. Long-term patient and renal prognosis in acute renal failure. *Nephron* 1984;36(3):169.
589. Molitoris BA, Finn WF, eds. *Acute Renal Failure: a Companion to Brenner & Rector's The Kidney*. Philadelphia: W. B. Saunders, 2001.
590. Alon US. Neonatal acute renal failure: The need for long-term follow-up. *Clin Pediatr (Phila)* 1998;37(6):387.
591. Basile DP, Donohoe D, Roethe K, et al. Renal ischemic injury results in permanent damage to peritubular capillaries and influences long-term function. *Am J Physiol Renal Physiol* 2001;281(5):F887.
592. Basile DP. Rarefaction of peritubular capillaries following ischemic acute renal failure: A potential factor predisposing to progressive nephropathy. *Curr Opin Nephrol Hypertens* 2004;13(1):1.
593. Gueler F, Gwinner W, Schwarz A, et al. Long-term effects of acute ischemia and reperfusion injury. *Kidney Int* 2004;66(2):523.
594. Forbes JM, Hewitson TD, Becker GJ, et al. Ischemic acute renal failure: Long-term histology of cell and matrix changes in the rat. *Kidney Int* 2000;57(6):2375.
595. Yamamoto T, Tada T, Brodsky SV, et al. Intravital videomicroscopy of peritubular capillaries in renal ischemia. *Am J Physiol Renal Physiol* 2002;282(6):F1150.
596. Sutton TA, Mang HE, Campos SB, et al. Injury of the renal microvascular endothelium alters barrier function after ischemia. *Am J Physiol Renal Physiol* 2003;285(2):F191.
597. Chandraker A, Takada M, Nadeau KC, et al. CD28-b7 blockade in organ dysfunction secondary to cold ischemia/reperfusion injury. *Kidney Int* 1997;52(6):1678.
598. Basile DP, Donohoe DL, Roethe K, et al. Chronic renal hypoxia after acute ischemic injury: Effects of L-arginine on hypoxia and secondary damage. *Am J Physiol Renal Physiol* 2003;284(2):F338.
599. Quan A, Quigley R. Renal replacement therapy and acute renal failure. *Curr Opin Pediatr* 2005;17(2):205.

600. Palevsky PM, Baldwin I, Davenport A, et al. Renal replacement therapy and the kidney: Minimizing the impact of renal replacement therapy on recovery of acute renal failure. *Curr Opin Crit Care* 2005;11(6):548.
601. Ricci Z, Ronco C. Renal replacement II: Dialysis dose. *Crit Care Clin* 2005;21(2):357.
602. O'Reilly P, Tolwani A. Renal replacement therapy III: IHD, CRRT, SLED. *Crit Care Clin* 2005;21(2):367.
603. Barletta GM, Bunchman TE. Acute renal failure in children and infants. *Curr Opin Crit Care* 2004;10(6):499.
604. Palevsky PM, Zhang JH, O'Connor TZ, et al. Intensity of renal support in critically ill patients with acute kidney injury. *N Engl J Med* 2008;359(1):7.
605. Bellomo R, Cass A, Cole L, et al. Intensity of continuous renal-replacement therapy in critically ill patients. *N Engl J Med* 2009;361(17):1627.
606. Venkataraman R. Prevention of acute renal failure. *Crit Care Clin* 2005;21(2):281.
607. Lin J, Bonventre JV. Prevention of radiocontrast nephropathy. *Curr Opin Nephrol Hypertens* 2005;14(2):105.
608. Pannu N, Manns B, Lee H, et al. Systematic review of the impact of N-acetylcysteine on contrast nephropathy. *Kidney Int* 2004;65(4):1366.
609. Spargias K, Alexopoulos E, Kyzopoulos S, et al. Ascorbic acid prevents contrast-mediated nephropathy in patients with renal dysfunction undergoing coronary angiography or intervention. *Circulation* 2004;110(18):2837.
610. Goldenberg I, Matetzky S. Nephropathy induced by contrast media: pathogenesis, risk factors and preventive strategies. *CMAJ* 2005;172(11):1461.
611. Weisbord SD, Palevsky PM. Prevention of contrast-induced nephropathy with volume expansion. *Clin J Am Soc Nephrol* 2008;3(1):273.
612. Dellinger RP, Carlet JM, Masur H, et al. Surviving Sepsis Campaign guidelines for management of severe sepsis and septic shock. *Intensive Care Med* 2004;30(4):536.
613. Ricci Z, Polito A, Ronco C. The implications and management of septic acute kidney injury. *Nat Rev Nephrol* 2011;7(4):218.
614. Lauschke A, Teichgraber UK, Frei U, et al. 'Low-dose' dopamine worsens renal perfusion in patients with acute renal failure. *Kidney Int* 2006;69(9):1669.
615. Cantarovich F, Rangoonwala B, Lorenz H, et al. High-dose furosemide for established ARF: a prospective, randomized, double-blind, placebo-controlled, multicenter trial. *Am J Kidney Dis* 2004;44(3):402.
616. Rahman SN, Kim GE, Mathew AS, et al. Effects of atrial natriuretic peptide in clinical acute renal failure. *Kidney Int* 1994;45(6):1731.
617. Hirschberg R, Kopple J, Lipsitt P, et al. Multicenter clinical trial of recombinant human insulin-like growth factor I in patients with acute renal failure. *Kidney Int* 1999;55(6):2423.
618. Lieberthal W, Sheridan AM, Valeri CR. Protective effect of atrial natriuretic factor and mannitol following renal ischemia. *Am J Physiol* 1990;258(5 Pt 2):F1266.
619. Conger JD, Falk SA, Yuan BH, et al. Atrial natriuretic peptide and dopamine in a rat model of ischemic acute renal failure. *Kidney Int* 1989;35(5):1126.
620. Saito A, Sawada K, Fujimura S. Present status and future perspectives on the development of bioartificial kidneys for the treatment of acute and chronic renal failure patients. *Hemodial Int* 2011;15(2):183.
621. Lin F, Moran A, Igarashi P. Intrarenal cells, not bone marrow-derived cells, are the major source for regeneration in postschemic kidney. *J Clin Invest* 2005;115(7):1756.
622. Bates CM, Lin F. Future strategies in the treatment of acute renal failure: growth factors, stem cells, and other novel therapies. *Curr Opin Pediatr* 2005;17(2):215.
623. Ricardo SD, Deane JA. Adult stem cells in renal injury and repair. *Nephrology (Carlton)* 2005;10(3):276.
624. Choudhury D. Acute kidney injury: current perspectives. *Postgrad Med* 2010;122(6):29.
625. Rangel-Frausto MS, Pittet D, Costigan M, et al. The natural history of the systemic inflammatory response syndrome (SIRS). A prospective study. *JAMA* 1995;273(2):117.
626. Mori T, Shimizu T, Tani T. Septic acute renal failure. *Contrib Nephrol* 2010;166:40.
627. Zarjou A, Agarwal A. Sepsis and acute kidney injury. *J Am Soc Nephrol* 2011;22(6):999.
628. Bagshaw SM, George C, Bellomo R. Early acute kidney injury and sepsis: a multicentre evaluation. *Crit Care* 2008;12(2):R47.
629. Mustonen J, Pasternack A, Helin H, et al. Renal biopsy in acute renal failure. *Am J Nephrol* 1984;4(1):27.
630. Diaz de Leon M, Moreno SA, Gonzalez Diaz DJ, et al. Severe sepsis as a cause of acute renal failure. *Nefrologia* 2006;26(4):439.
631. Bagshaw SM, Langenberg C, Haase M, et al. Urinary biomarkers in septic acute kidney injury. *Intensive Care Med* 2007;33(7):1285.
632. Hotchkiss RS, Karl IE. The pathophysiology and treatment of sepsis. *N Engl J Med* 2003;348(2):138.
633. Bellomo R, Wan L, Langenberg C, et al. Septic acute kidney injury: New concepts. *Nephron Exp Nephrol* 2008;109(4):e95.
634. Keung EC, Li Q. Lactate activates ATP-sensitive potassium channels in guinea pig ventricular myocytes. *J Clin Invest* 1991;88(5):1772.
635. Wang W, Mitra A, Poole B, et al. Endothelial nitric oxide synthase-deficient mice exhibit increased susceptibility to endotoxin-induced acute renal failure. *Am J Physiol Renal Physiol* 2004;287(5):F1044.
636. Schwartz D, Mendonca M, Schwartz I, et al. Inhibition of constitutive nitric oxide synthase (NOS) by nitric oxide generated by inducible NOS after lipopolysaccharide administration provokes renal dysfunction in rats. *J Clin Invest* 1997;100(2):439.
637. Knotek M, Rogachev B, Wang W, et al. Endotoxemic renal failure in mice: Role of tumor necrosis factor independent of inducible nitric oxide synthase. *Kidney Int* 2001;59(6):2243.
638. Wang W, Jittikanont S, Falk SA, et al. Interaction among nitric oxide, reactive oxygen species, and antioxidants during endotoxemia-related acute renal failure. *Am J Physiol Renal Physiol* 2003;284(3):F532.
639. Wang W, Faubel S, Ljubanovic D, et al. Endotoxemic acute renal failure is attenuated in caspase-1-deficient mice. *Am J Physiol Renal Physiol* 2005;288(5):F997.
640. Czermak BJ, Sarma V, Pierson CL, et al. Protective effects of C5a blockade in sepsis. *Nat Med* 1999;5(7):788.
641. Reinhart K, Menges T, Gardlund B, et al. Randomized, placebo-controlled trial of the anti-tumor necrosis factor antibody fragment afelimomab in hyperinflammatory response during severe sepsis: The RAMSES Study. *Crit Care Med* 2001;29(4):765.
642. Rittirsch D, Hoesel LM, Ward PA. The disconnect between animal models of sepsis and human sepsis. *J Leukoc Biol* 2007;81(1):137.
643. Salerno F, Gerbes A, Gines P, et al. Diagnosis, prevention and treatment of hepatorenal syndrome in cirrhosis. *Gut* 2007;56(9):1310.
644. Mackelaite L, Alsauskas ZC, Ranganna K. Renal failure in patients with cirrhosis. *Med Clin North Am* 2009;93(4):855.
645. Moreau R, Durand F, Poynard T, et al. Terlipressin in patients with cirrhosis and type I hepatorenal syndrome: A retrospective multicenter study. *Gastroenterology* 2002;122(4):923.
646. Guevara M, Arroyo V. Hepatorenal syndrome. *Expert Opin Pharmacother* 2011;12(9):1405.
647. Fasolato S, Angeli P, Dallagnese L, et al. Renal failure and bacterial infections in patients with cirrhosis: Epidemiology and clinical features. *Hepatology* 2007;45(1):223.
648. Cardenas A, Gines P, Uriz J, et al. Renal failure after upper gastrointestinal bleeding in cirrhosis: Incidence, clinical course, predictive factors, and short-term prognosis. *Hepatology* 2001;34(4 Pt 1):671.
649. Angeli P, Morando F, Cavallin M, et al. Hepatorenal syndrome. *Contrib Nephrol* 2011;174:46.
650. Arroyo V, Fernandez J. Management of hepatorenal syndrome in patients with cirrhosis. *Nat Rev Nephrol* 2011;7(9):517.
651. Kielar ML, Rohan Jeyarajah D, Lu CY. The regulation of ischemic acute renal failure by extrarenal organs. *Curr Opin Nephrol Hypertens* 2002;11(4):451.
652. Kuiper JW, Groeneveld AB, Slutsky AS, et al. Mechanical ventilation and acute renal failure. *Crit Care Med* 2005;33(6):1408.
653. Kramer AA, Postler G, Salhab KF, et al. Renal ischemia/reperfusion leads to macrophage-mediated increase in pulmonary vascular permeability. *Kidney Int* 1999;55(6):2362.
654. Rabb H, Wang Z, Nemoto T, et al. Acute renal failure leads to dysregulation of lung salt and water channels. *Kidney Int* 2003;63(2):600.
655. Chien CC, King LS, Rabb H. Mechanisms underlying combined acute renal failure and acute lung injury in the intensive care unit. *Contrib Nephrol* 2004;144:53.

656. Heywood JT. The cardiorenal syndrome: lessons from the ADHERE database and treatment options. *Heart Fail Rev* 2004;9(3):195.
657. Forman DE, Butler J, Wang Y, et al. Incidence, predictors at admission, and impact of worsening renal function among patients hospitalized with heart failure. *J Am Coll Cardiol* 2004;43(1):61.
658. Ronco C, House AA, Haapio M. Cardiorenal syndrome: refining the definition of a complex symbiosis gone wrong. *Intensive Care Med* 2008;34(5):957.
659. Schrier RW. Cardiorenal versus renocardiac syndrome: Is there a difference? *Nat Clin Pract Nephrol* 2007;3(12):637.
660. Ronco C, McCullough P, Anker SD, et al. Cardio-renal syndromes: report from the consensus conference of the acute dialysis quality initiative. *Eur Heart J* 2010;31(6):703.
661. Newsome BB, Warnock DG, McClellan WM, et al. Long-term risk of mortality and end-stage renal disease among the elderly after small increases in serum creatinine level during hospitalization for acute myocardial infarction. *Arch Intern Med* 2008;168(6):609.
662. Smith GL, Vaccarino V, Kosiborod M, et al. Worsening renal function: what is a clinically meaningful change in creatinine during hospitalization with heart failure? *J Card Fail* 2003;9(1):13.
663. Jose P, Skali H, Anavekar N, et al. Increase in creatinine and cardiovascular risk in patients with systolic dysfunction after myocardial infarction. *J Am Soc Nephrol* 2006;17(10):2886.
664. Malbrain ML, Cheatham ML, Kirkpatrick A, et al. Results from the International Conference of Experts on Intra-abdominal Hypertension and Abdominal Compartment Syndrome I. Definitions. *Intensive Care Med* 2006;32(11):1722.
665. Mohmand H, Goldfarb S. Renal dysfunction associated with intra-abdominal hypertension and the abdominal compartment syndrome. *J Am Soc Nephrol* 2011;22(4):615.
666. De Waele JJ, De Laet I, Kirkpatrick AW, et al. Intra-abdominal Hypertension and Abdominal Compartment Syndrome. *Am J Kidney Dis* 2011;57(1):159.
667. Mullens W, Abrahams Z, Francis GS, et al. Importance of venous congestion for worsening of renal function in advanced decompensated heart failure. *J Am Coll Cardiol* 2009;53(7):589.
668. Umgelter A, Reindl W, Franzen M, et al. Renal resistive index and renal function before and after paracentesis in patients with hepatorenal syndrome and tense ascites. *Intensive Care Med* 2009;35(1):152.
669. Dalfino L, Tullo L, Donadio I, et al. Intra-abdominal hypertension and acute renal failure in critically ill patients. *Intensive Care Med* 2008;34(4):707.
670. Wauters J, Claus P, Brosens N, et al. Pathophysiology of renal hemodynamics and renal cortical microcirculation in a porcine model of elevated intra-abdominal pressure. *J Trauma* 2009;66(3):713.
671. Grunfeld JP, Ganeval D, Bournerias F. Acute renal failure in pregnancy. *Kidney Int* 1980;18(2):179.
672. Lim LM, Tsai KB, Hwang DY, et al. Anuric acute renal failure after elective abortion. *Intern Med* 2011;50(16):1715.
673. Gargah T, Cherif M, Goucha-Louzir R, Lakhoua MR. Severe pneumococcal hemolytic uremic syndrome in an 8-month-old girl. *Saudi J Kidney Dis Transpl* 2012;23(5):1024.
674. Geiling E, Cannon P. Pathologic effects of elixir of sulfanilamide (diethylene glycol) poisoning: A clinical and experimental correlation. Final report. *JAMA* 1938;111:9191.
675. McKay D, Jewett J, Reid D. Endotoxin shock and the generalized Shwartzman reaction in pregnancy. *Am J Obstet Gynecol* 1959;78:546.
676. Robboy SJ, Major MC, Colman RW, et al. Pathology of disseminated intravascular coagulation (DIC). Analysis of 26 cases. *Hum Pathol* 1972;3(3):327.
677. Sitprija V. Snakebite nephropathy. *Nephrology (Carlton)* 2006;11(5):442.
678. Kanjanabuch T, Sitprija V. Snakebite nephrotoxicity in Asia. *Semin Nephrol* 2008;28(4):363.
679. Sibai BM, Ramadan MK. Acute renal failure in pregnancies complicated by hemolysis, elevated liver enzymes, and low platelets. *Am J Obstet Gynecol* 1993;168(6 Pt 1):1682.
680. Gupta A, Ferguson J, Rahman M, et al. Acute oliguric renal failure in HELLP syndrome: Case report and review of literature. *Ren Fail* 2012;34(5):653.
681. Kim JO, Kim GH, Kang CM, et al. Bilateral acute renal cortical necrosis in SLE-associated antiphospholipid syndrome. *Am J Kidney Dis* 2011;57(6):945.
682. Larakeb AS, Evrard S, Louillet F, et al. Acute renal cortical necrosis due to acquired antiprotein S antibodies. *Pediatr Nephrol* 2009;24(1):207.
683. Alfonzo AV, Fox JG, Imrie CW, et al. Acute renal cortical necrosis in a series of young men with severe acute pancreatitis. *Clin Nephrol* 2006;66(4):223.
684. Kute VB, Shah PR, Munjappa BC, et al. Outcome and prognostic factors of malaria-associated acute kidney injury requiring hemodialysis: A single center experience. *Indian J Nephrol* 2012;22(1):33.
685. Satoskar AA, Pelletier R, Nadasdy GM, et al. Histopathology and outcome of acute humoral rejection in renal allografts. *Front Biosci (Schol Ed)* 2011;3:919.
686. Raij L, Keane WF, Michael AF. Unilateral Shwartzman reaction: cortical necrosis in one kidney following in vivo perfusion with endotoxin. *Kidney Int* 1977;12(2):91.
687. Marcussen H, Asnaes S. Renal cortical necrosis. An evaluation of the possible relation to the Shwartzman reaction. *Acta Pathol Microbiol Scand A* 1972;80(3):351.
688. Matlin RA, Gary NE. Acute cortical necrosis. Case report and review of the literature. *Am J Med* 1974;56(1):110.
689. Kleinknecht D, Grunfeld JP, Gomez PC, et al. Diagnostic procedures and long-term prognosis in bilateral renal cortical necrosis. *Kidney Int* 1973;4(6):390.
690. Goodman PE, Rennie WP. Renal infarction secondary to nasal insufflation of cocaine. *Am J Emerg Med* 1995;13(4):421.
691. Kramer RK, Turner RC. Renal infarction associated with cocaine use and latent protein C deficiency. *South Med J* 1993;86(12):1436.
692. Modi KS, Rao VK. Atheroembolic renal disease. *J Am Soc Nephrol* 2001;12(8):1781.
693. Cosio FG, Zager RA, Sharma HM. Atheroembolic renal disease causes hypocomplementaemia. *Lancet* 1985;2(8447):118.
694. Kasinath BS, Lewis EJ. Eosinophilia as a clue to the diagnosis of atheroembolic renal disease. *Arch Intern Med* 1987;147(8):1384.
695. Saleem S, Lakkis FG, Martinez-Maldonado M. Atheroembolic renal disease. *Semin Nephrol* 1996;16(4):309.
696. Thurlbeck W, Castleman B. Atheromatous emboli to the kidneys after aortic surgery. *N Engl J Med* 1957;257(10):442.

Renal Disease Caused by Inborn Errors of Metabolism, Storage Diseases, and Hemoglobinopathies

Lipid disorders 1224

- Familial lecithin-cholesterol acyltransferase deficiency 1224
- Lipoprotein glomerulopathy 1225
- Type III hyperlipoproteinemia (familial dysbetalipoproteinemia) 1228

Lysosomal storage diseases 1228

- Fabry disease (angiokeratoma corporis diffusum universale) 1229
- Nephrosialidosis and variants 1235

Vitamin disorders 1236

- Cobalamin C deficiency 1236

Organic acid disorders 1237

- Methylmalonic acidemia 1237

Carbohydrate disorders 1238

- Glycogen storage disease 1238

Peroxisomal disorders 1239

- Zellweger syndrome 1240
- Adult refsum disease 1240
- Primary hyperoxaluria 1241

Membrane transport disorders 1243

- Inherited fanconi syndrome 1243
- Acquired fanconi syndrome 1249
- Specialized heritable tubular defects 1250

Purine metabolism and handling disorders 1250

- Uric acid and the kidney 1250
- Hereditary disorders 1250
- Acute uric acid nephropathy 1255
- Uric acid infarcts 1255

- Chronic uric acid nephropathy 1255
- Urolithiasis 1257

Sickling disorders 1258

- Clinical presentation 1258
- Pathologic changes 1259
- Malignancies 1262
- Etiology and pathogenesis 1264
- Clinical course and prognosis 1265
- Therapy 1266
- Mouse models of sickle cell disease 1268

This chapter covers familial metabolic defects in the kidney, along with more systemic metabolic and hematologic disorders that affect the kidney secondarily. Renal involvement in the first group includes several lysosomal storage diseases caused by deficiencies of lysosomal enzymes in renal tissues as, for example, in Fabry disease. However, not all lysosomal storage diseases primarily affect the kidney; renal involvement in Gaucher disease, for example, results from the entrapment in the kidney of circulating macrophages engorged with glucosyl ceramide. Clearly, secondary renal involvement follows the hyperlipidemia of familial lecithin-cholesterol acyltransferase (LCAT) deficiency, hyperoxaluria of hepatic peroxisomal alanine-glyoxylate aminotransferase deficiency, and the microcirculatory abnormality of hemoglobinopathies. The defect of tubular transport in inherited Fanconi syndrome is intrinsic to the proximal convoluted tubule, although an identical transport abnormality is much more commonly secondary to the renal accumulation of cystine, as the result of a generalized primary defect in lysosomal membrane transport. Therefore, simple categorization of these disorders into primary and secondary groups serves little purpose. The diseases are grouped into broad categories, with descriptions of the genetic basis, molecular and functional abnormalities, and the renal pathologic consequences.

LIPID DISORDERS

Familial Lecithin-Cholesterol Acyltransferase Deficiency

Familial LCAT deficiency (FLD) is an uncommon autosomal recessive disorder resulting from a heritable defect in the esterification of plasma cholesterol. Increased plasma concentrations of unesterified cholesterol, triglycerides, and phosphatidylcholine result in lipid deposition in tissues. The enzyme LCAT is carried by high-density lipoprotein (HDL) with Apolipoprotein (Apo) AI as a cofactor, and it catalyzes the esterification of free cholesterol bound to lipoproteins. Mutations in the LCAT gene, localized to chromosome 16q21-q22, cause classic familial LCAT deficiency (FLD) and fish eye disease (FED). More than 60 mutations have been described, all of which result in greatly reduced concentrations of high-density lipoprotein (HDL). The residual plasma HDL is characterized on electron microscopy by an accumulation of disk-shaped pre- β HDL that may form rouleaux. Other lipid phenotypes include morphologically abnormal low-density lipoprotein (LDL) and very low-density lipoprotein (VLDL) particles and the formation of free cholesterol and phospholipid-rich, triglyceride-poor vesicles known as lipoprotein X (LpX) (1).

Classic FLD is due to the inheritance of homozygous or complex heterozygous deletions that either abolish LCAT production or cause the synthesis of an LCAT enzyme with complete or nearly complete loss of both α -LCAT and β -LCAT activities. The disease, originally described in Norway, appears to be widely distributed. Clinical manifestations of FLD include corneal opacities, hemolytic anemia, accelerated peripheral atherosclerosis, and proteinuria with renal insufficiency. Lipid deposits also occur in the liver, spleen, and bone marrow, in which foam cells (sea-blue histiocytes) are present (2). In contrast to FLD, FED patients, whose lipid/lipoprotein profile overlaps with that seen in FLD, have reduced α -LCAT activity but preserved β -LCAT activity (1). In FED, there are no major clinical manifestations except corneal opacity. Heterozygous carriers may have a lipid/lipoprotein profile intermediate between carriers of two and zero copies of mutant alleles.

Renal involvement, the major cause of morbidity and mortality, commonly begins with proteinuria during childhood (3), and it culminates after several decades of renal insufficiency. The progression of renal disease is variable; some patients show severe proteinuria, and others experience little. Hypertension may appear early in the course or as a late complication of renal insufficiency. Urinalysis usually shows mild hematuria, leukocyturia, and cylindruria. Renal insufficiency is not invariable (1); when present, it usually develops by the fourth decade.

Pathologic Changes

The glomeruli are the principal site of renal injury, undergoing mesangial expansion and a characteristic capillary wall thickening. Foamy lipid is most obvious in thickened capillary walls, which have a bubbly, vacuolated, or honeycomb appearance that is accentuated when stained with toluidine blue (Fig. 27.1). Silver-stained sections show craters in and vacuolization of the glomerular basement membrane (GBM), resembling late-stage membranous glomerulonephritis; double contours are often noted (4–6). Mesangial cellularity is normal

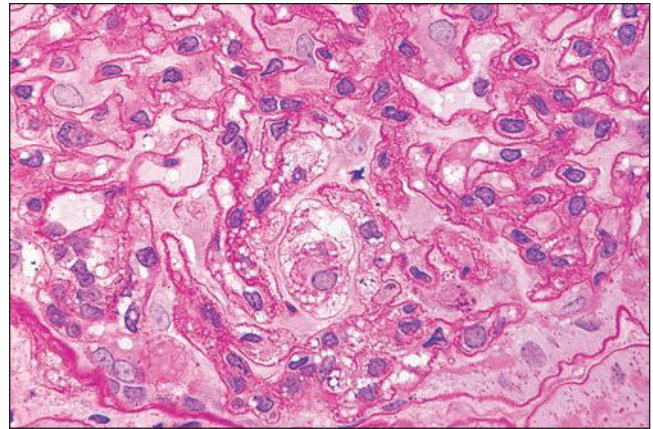


FIGURE 27.1 Glomerulus from a patient with LCAT deficiency. It shows mesangial and focal capillary wall thickening with prominent bubbly lipid interposed between what appear to be two layers of basement membrane (double contours). (Periodic acid-Schiff [PAS]; $\times 400$.)

to mildly increased, and the mesangium is often expanded, with the same vacuolated appearance as the capillary walls. Collections of endocapillary foam cells are an occasional feature. The mesangium also contains an acellular, eosinophilic matrix that accumulates in areas of segmental sclerosis and eventual global sclerosis (Fig. 27.2). Interstitial foam cells may be present, and lipid deposition has been noted in arterial walls. The tubules are generally normal until atrophy accompanies interstitial fibrosis. Immunofluorescence is usually negative for immunoglobulin and complement components, occasionally showing mild, nonspecific changes. The deposits have been shown by immunostaining to contain large amounts of ApoB and ApoE (7).

Electron microscopy has shown a mixture of glomerular epimembranous, intramembranous, subendothelial, and mesangial lipid deposits (Fig. 27.3). One study of sequential biopsy specimens showed early subepithelial and intramembranous deposition, followed by predominantly subendothelial

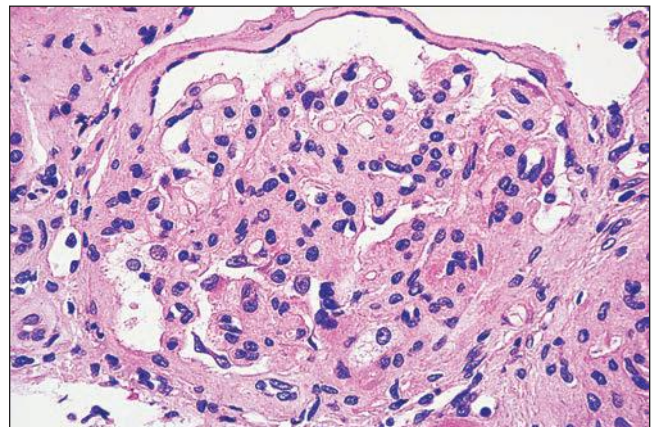


FIGURE 27.2 Glomerulus in LCAT deficiency showing thickened basement membranes and mesangial foam cells (*bottom*) entrapped within increased eosinophilic matrix. (Hematoxylin & eosin [H&E]; $\times 200$.)

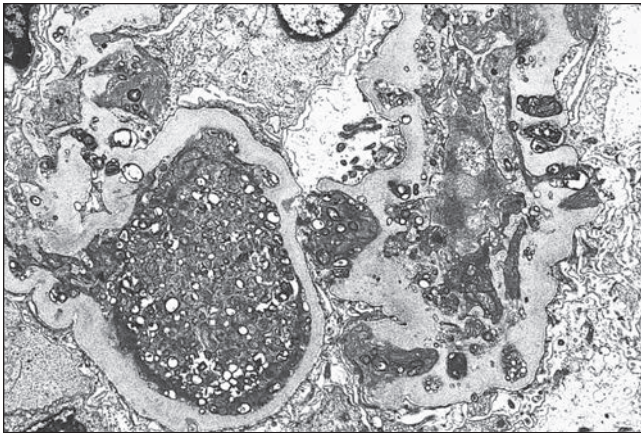


FIGURE 27.3 Electron microscopy in LCAT deficiency shows glomerular epimembranous, intramembranous, subendothelial, and mesangial accumulations of extracellular lipid material with membranous profiles and granules. ($\times 9000$.)

and mesangial deposits (8); these observations contrast with sequential assessment in a kidney allograft where deposits were initially identified in the mesangium (9). The lipid deposits are partly lucent and partly deeply osmiophilic, the latter including cross-striated curvilinear serpiginous fibrils, rounded lamellar densities, and granular densities (5,6). The former two are predominantly in epimembranous and intramembranous deposits, while granular densities are predominantly in subendothelial deposits. Densely osmiophilic basement membrane deposits have resembled the glomerular alterations of dense-deposit disease and may increase basement membrane fragility because focal disruptions are identifiable (10). Mesangial deposits tend to be large and dense, comprising increased matrix and hyaline. Foam cells may be present in the mesangium, as shown by light microscopy; they rarely seem to be endocapillary. Arteriolar endothelial and medial cells may also contain lipid deposits (5). Tubular atrophy and interstitial fibrosis progress variably.

Mesangial lipid deposits recur rapidly in renal allografts (9), sometimes within weeks (Figs. 27.4 and 27.5). The deposits do not necessarily impair renal function, because long-term graft survival has been described (1,11). Renal transplantation has no effect on the systemic metabolic disorder.

The renal abnormality, although distinctive, is not entirely specific, because similar lipid deposits occur in kidneys of patients with chronic liver disease, Alagille syndrome, and cirrhosis of various etiologies, who also have elevated serum lipoprotein (12–14).

Pathogenesis

The cause of renal injury, despite lipid accumulation, has not been completely elucidated. A role for LpX has been supported by animal studies. In vitro experiments have shown up-regulation of monocyte chemoattractant protein-1 mRNA expression and protein levels and increased nuclear activities of nuclear factor κ B in rat mesangial cells, suggesting that LpX may induce a proinflammatory response (15). In the LCAT knockout mouse, high-fat diets produced LpX accumulation, with the development of proteinuria and glomerulosclerosis

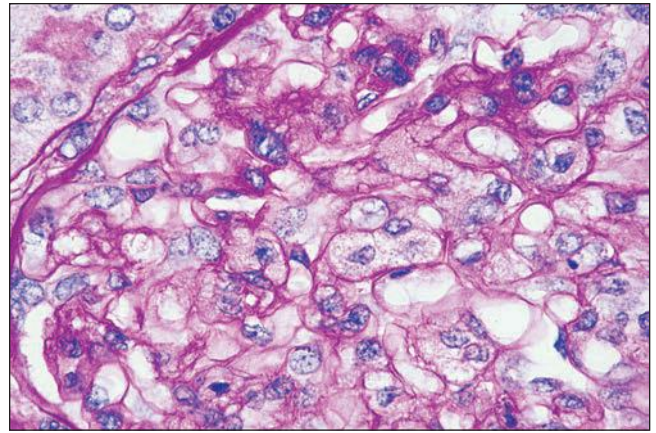


FIGURE 27.4 Glomerulus from renal allograft in a patient with LCAT deficiency, 7 weeks after transplantation, with recurrence of foamy mesangial cells. (PAS; $\times 400$.)

in a subset (16). A more recent analysis circumvented the potentially confounding contribution of coexisting hyperlipidemia in the prior study by generating a novel murine model in which circulating lipoproteins were predominantly LpX. These mice spontaneously developed progressive glomerular lesions that had light and electron microscopic abnormalities similar to those seen in human LCAT deficiency (17). Infusion of recombinant LCAT into LCAT-KO mice rapidly increases HDL cholesterol and lowers cholesterol in fractions containing VLDL and LpX, providing some rationale for enzyme replacement therapy (18). The long-term effect on renal disease of (a) lipid-modifying therapy to change the lipid profile, including lowering LpX; (b) corticosteroid therapy to suppress an inflammatory response; or (c) blockade of the renin-angiotensin system to protect renal function via blood pressure control and reduction of proteinuria has not been adequately assessed in humans (19–21).

Lipoprotein Glomerulopathy

Lipoprotein glomerulopathy (LPG) is a rare disorder associated with distention of glomerular capillaries by lipoprotein thrombi, proteinuria, and progression to renal failure (22). The majority of patients are of Asian ancestry, principally Japanese and Chinese, but occasional cases have been in patients with non-Asian backgrounds (23–29). The disease may present in childhood, and males outnumber females approximately three to two (23,30). Subjects have a characteristic biochemical finding of a twofold to threefold elevation of serum ApoE level, usually accompanied by hyperlipidemia with a predominance of triglycerides (30). Detailed analysis using electrophoresis or ultracentrifugation shows increased very low-density lipoprotein (VLDL) and intermediate-density lipoprotein (IDL) fractions, which resembles type III hyperlipoproteinemia (HLP); however, hyperlipidemia is often milder than in familial type III HLP and not even recognized in some cases (23). Unlike type III HLP, systemic manifestations of hyperlipidemia, corneal arcus, cutaneous xanthomas, and atherosclerosis are very uncommon in LPG. The finding of ApoE2 heterozygosity by isoelectric focusing, rather than ApoE2 homozygosity, typical in type III HLP, also helps to differentiate the diseases.

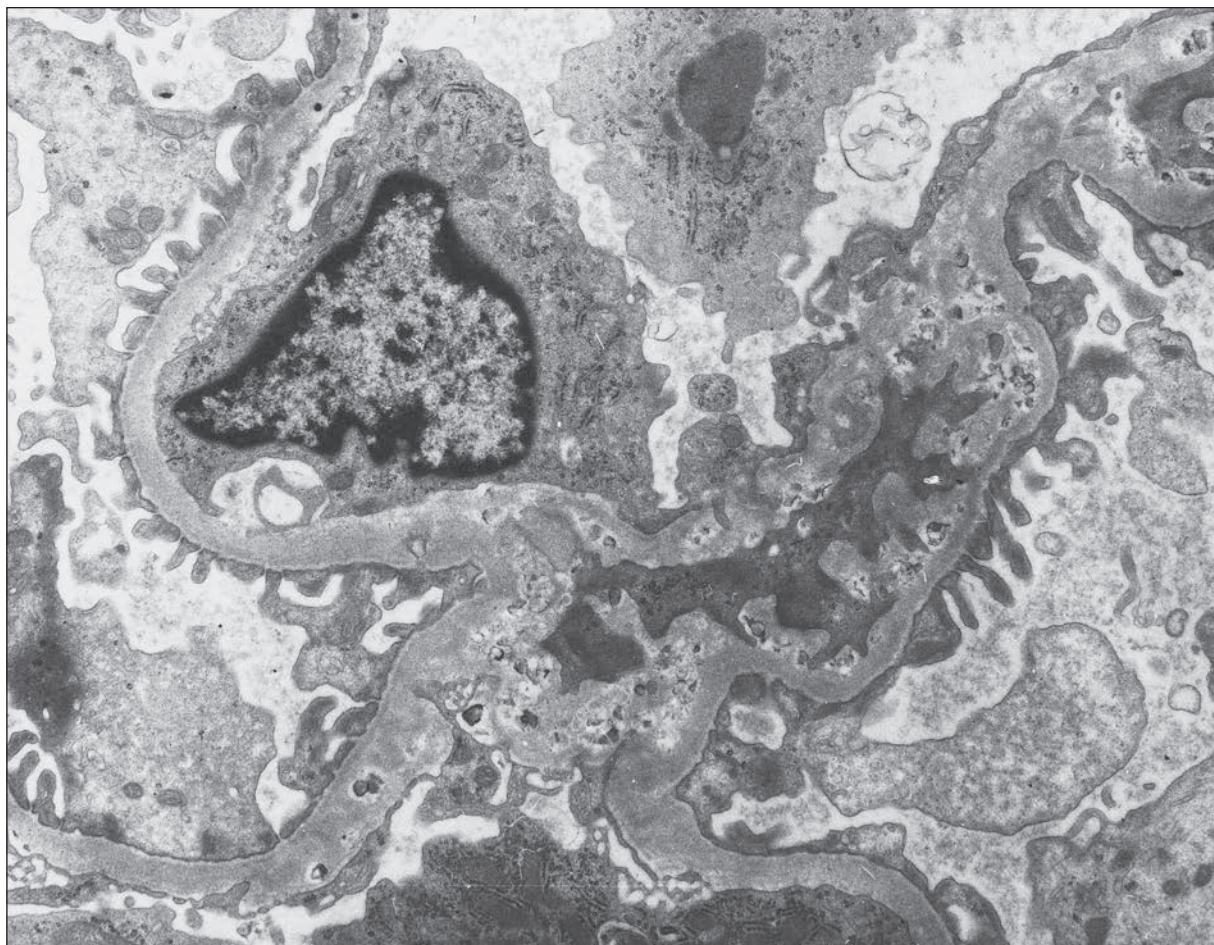


FIGURE 27.5 Electron microscopy shows recurrence of mesangial and subendothelial lipid deposits in renal allograft at 7 weeks after renal transplantation in a patient with LCAT deficiency. ($\times 10,400$.)

Clinical onset is usually marked by proteinuria, and most develop steroid-resistant nephrotic syndrome. Hematuria is not typical. The disease may undergo spontaneous amelioration, but slow progression to renal failure has been observed in half of patients (23).

Pathologic Changes

The glomeruli are large and contain capillaries distended with lipoprotein thrombi (Fig. 27.6). The capillary ectasia is accompanied by mesangiolytic changes. Capillary walls may be at first attenuated, but they often become thickened, with double contour, as in other types of mesangiolytic changes. The thrombi are weakly periodic acid-Schiff (PAS) positive, silver methenamine negative, and pale blue with Masson trichrome, in contrast to the typical fuchsinophilia of fibrin thrombi, with which they might be confused. The lack of congophilia excludes amyloid. The material has a moderately vacuolated and laminated structure under high magnification and is also strongly positive with oil red O and variably sudanophilic in frozen section. Increasing mesangial cellularity and matrix, segmental sclerosis, and hyalinosis progress to global sclerosis (Fig. 27.7). Tubulointerstitial changes are secondary, although interstitial foam cells may appear early in the course. LPG can coexist with other glomerular diseases.

Immunofluorescence shows that the glomerular thrombi contain β -lipoprotein, ApoB, and ApoE. Immunoglobulin M, C1q, and fibrinogen often surround the thrombi. Electron microscopy shows the thrombi to be finely, almost concentrically lamellated, with numerous small lipid vacuoles (Fig. 27.8). In milder cases, lipid deposits may localize to the mesangium and then extend into the subendothelial space. Endothelial hypertrophy may be present in unobstructed capillary segments. Mesangial hypercellularity is associated with segmental interposition and double contours of the GBMs. Effacement of foot processes tends to correlate with proteinuria.

Pathogenesis

Apolipoprotein E plays a major role in lipid and lipoprotein metabolism by functioning as the ligand for receptor-mediated catabolism of chylomicrons, VLDLs, and some HDLs. The *ApoE* gene, located on chromosome 19q13.2, has three common alleles— $\epsilon 2$, $\epsilon 3$, and $\epsilon 4$ —which code the three main isoforms: E2, E3, and E4. Six common polymorphisms are *ApoE2/2*, *ApoE3/3*, *ApoE4/4*, *ApoE3/2*, *ApoE4/2*, and *ApoE4/3*; ApoE3 is the most common with the $\epsilon 3$ allele accounting for 70% to 80% of the gene pool in Caucasians. *ApoE* and its polymorphisms are also instrumental in the pathogenesis of renal disease; they influence the development and progression

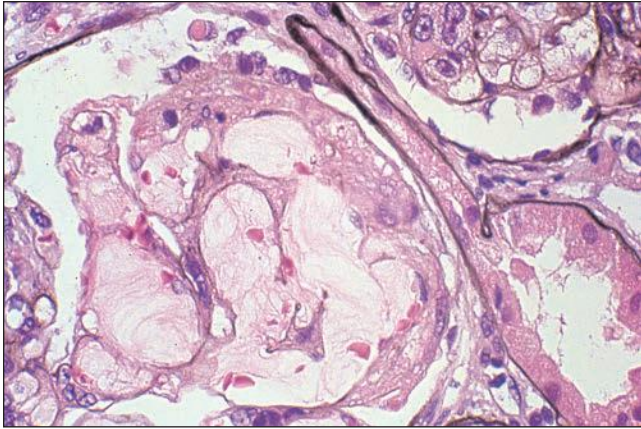


FIGURE 27.6 The glomerulus from a patient with lipoprotein glomerulopathy. The capillaries are distended by pale lipoprotein thrombi that have a vague laminated appearance. Dilatation of the capillary is associated with mesangiolytic changes. (PAS-silver methenamine; $\times 200$.)

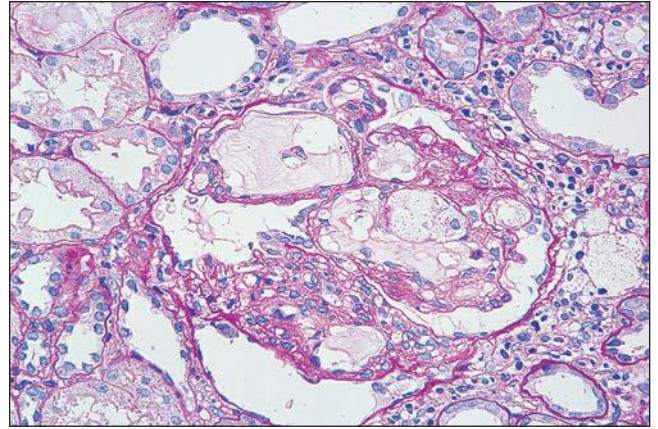


FIGURE 27.7 Capillaries in the glomerulus with lipoprotein glomerulopathy are distended with lipoprotein thrombi. The lobule at the bottom has increased mesangial cellularity and matrix. There are multiple adhesions to Bowman capsule, which will progress with sclerosis and hyalinosis. (PAS; $\times 100$.)

of diabetic nephropathy, the incidence, severity, and response to therapy of various other nephropathies, and the serum lipid profile and the risk of atherosclerosis in end-stage renal disease (ESRD) (30). Novel missense mutations and deletions in the *ApoE* gene are thought to be pathogenic in LPG, and their existence was proven by sequencing after observing

discordant results between restriction fragment genotyping and *ApoE* phenotyping via isoelectric focusing. A growing number of mutant isoforms—*ApoE* Sendai, Kyoto, Tokyo/Maebashi, Tsukuba, Chicago, Okayama, Guangzhou, Hong Kong, Modena, and Las Vegas (each genotype named after the index patient's city of origin) and *ApoE1* and *ApoE5*—have

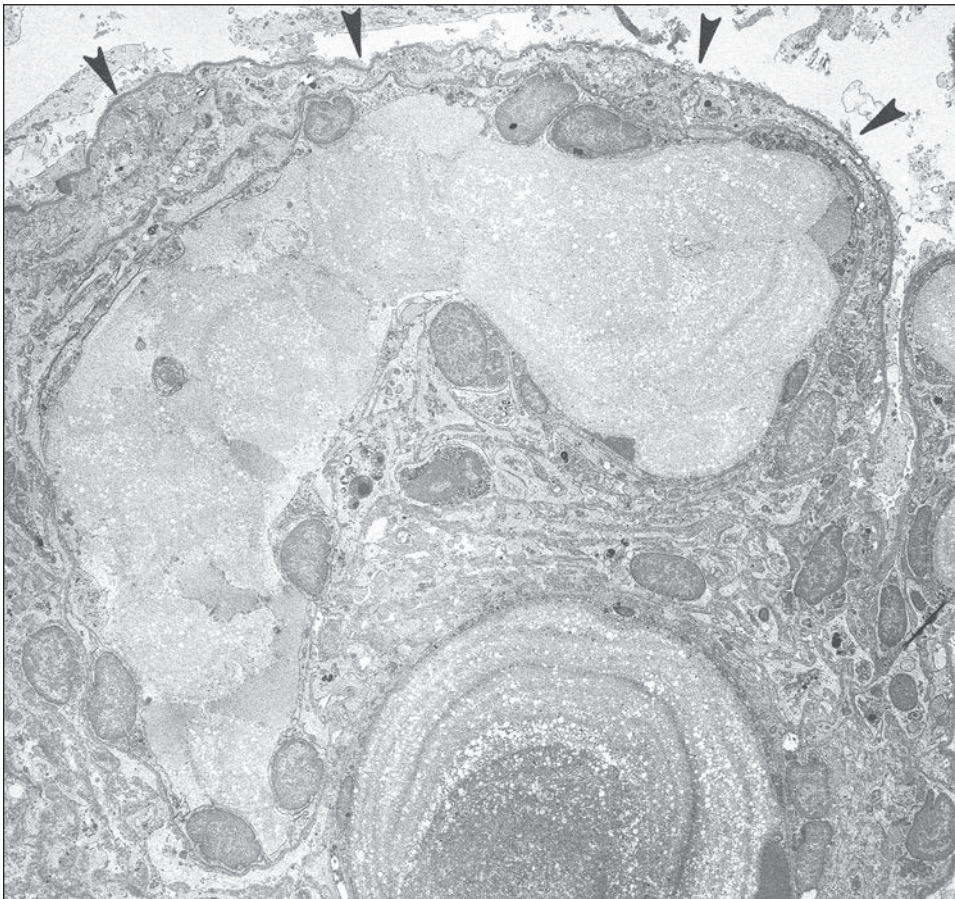


FIGURE 27.8 Electron micrograph shows the glomerular capillary lumina to be filled with partially lamellated, finely vacuolated lipoprotein thrombi. The mesangium is thickened by cell processes and increased matrix. The capillary wall is also thickened, with mesangial interposition and duplication of the glomerular basement membrane (arrowheads). ($\times 1900$.)

been associated with LPG (31), and the development of LPG in *ApoE* Sendai–infected mice suggests an etiologic role for these atypical isoforms (32,33). Some of the mutations can alter the tertiary structure of the variant apolipoprotein, thereby affecting interactions with receptors and cell surfaces that may induce abnormal intraglomerular lipid trafficking (34,35). Multiple family members may carry the same *ApoE* mutation in a heterozygous form, but not all family members with mutant isoforms develop LPG. This observation implies that LPG is a dominantly inherited disease with incomplete penetrance and that other genetic or environmental factors participate in its pathogenesis. For example, alterations in lipoprotein metabolism may be detrimental. The Fc receptor γ on macrophages and mesangial cells is involved in the recognition and clearance of LDL. The development of LPG in Fc receptor γ –deficient mice suggests that a reduction in LDL clearance may induce lipoprotein deposition (36). As lesions are localized to the glomeruli, the role of intrinsic mesangial cells seems paramount. The exact mechanism of the renal disease, however, remains to be defined, but variant *ApoE* appears to be a prerequisite. With one exception, all patients described thus far were found to be heterozygous for *ApoE* gene mutations (37). Although a similar glomerular lesion has been described in two siblings homozygous for nonmutated *ApoE2* (38) and a nonmutated *E2/E3* heterozygote with varying degrees of hyperlipidemia (39), the characteristic layered intraglomerular deposits, considered essential for the diagnosis of LPG (23), were not identified by electron microscopic study; these cases have been considered “LPG-like disease.”

Therapy

Traditional therapies for nephrotic syndrome, such as corticosteroids and immunosuppressive agents, and various alternative treatments, such as anticoagulants and plasmapheresis, have been ineffective. Intensive lipid-lowering therapy, including niceritrol and fibrates, has induced resolution of symptoms and disappearance of glomerular lipoprotein thrombi (40–44). Clinical and histologic improvements have also been achieved by protein A immunoadsorption (45). However, the long-term efficacy of either treatment approach has not been established. Recurrence of the lesion in renal allografts has also been described; stabilization of graft function and reduction of proteinuria were achieved with renin-angiotensin system blockade in several cases (46,47).

Type III Hyperlipoproteinemia (Familial Dysbetalipoproteinemia)

Type III HLP with characteristic xanthomas develops in approximately 10% of patients who are homozygous for *ApoE2/2*, where it is associated with combined and often severe mixed hyperlipidemia caused by the accumulation of β -VLDL, which leads to accelerated atherosclerosis. The $\epsilon 2$ allele is found in approximately 8% of the population (30), and *ApoE2* homozygosity occurs with a frequency of about 1% in Caucasian populations. That only a minority of *ApoE2* homozygotes develop type III HLP implies a multifactorial disorder, and recent studies found an increased incidence of rare *ApoC3* and *ApoA5* alleles in those expressing an abnormal lipid profile (48). Uncommonly, these patients develop glomerular lipidosis, manifested as proteinuria. Renal biopsies have shown large numbers of foam cells in the glomerular mesangium and

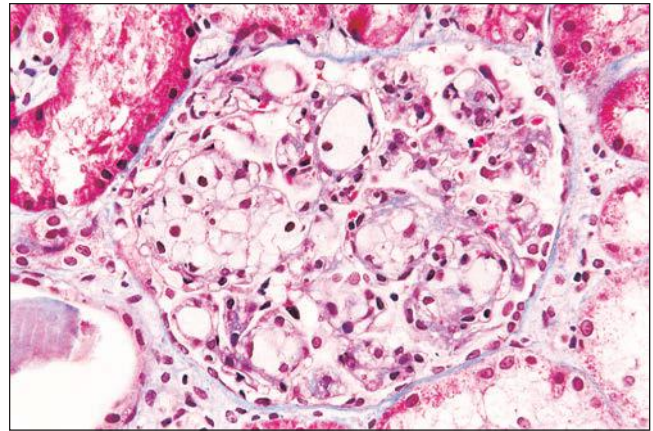


FIGURE 27.9 Glomerulus from a child with type III hyperlipoproteinemia that shows groups of foam cells in the mesangium and distending the capillary lumens. (Masson trichrome; $\times 400$.)

distending glomerular capillaries (Fig. 27.9). Interstitial foam cells have been noted. Lipid vacuoles focally admixed with lamellated electron-dense material and occasional cholesterol clefts have been detected by electron microscopy in the cytoplasm of glomerular intracapillary foam cells, as well as in mesangial, endothelial, and tubular epithelial cells. Podocyte foot processes may be effaced. Renal lipid deposits have cleared with plasmapheresis and lipid-lowering agents. Similar renal pathology including glomerular foam cells was recently described in a patient whose lipid profile was compatible with type III HLP, but whose genotype was *ApoE2/3* and in whom a novel *ApoA5* mutation was discovered (49). “Lipoprotein glomerulopathy-like” disease has also been described in a few patients with type III HLP (38).

LYSOSOMAL STORAGE DISEASES

Several dozen diseases are caused by the pathologic accumulation of naturally occurring molecules inside lysosomes. Taxonomic classification is based on the stored material, which allows organization but does not necessarily reflect a common clinical manifestation. Many lysosomal storage diseases present in infancy or early childhood, although milder adult variants are known. Diagnosis is ascertained by combining the clinical phenotype with biochemical parameters, pathology, and genetic confirmation whenever possible. Fabry disease is the classic example of a lysosomal disorder with primary kidney impairment, and, in a few settings, the diagnosis is made by kidney biopsy. Most lysosomal storage diseases, however, demonstrate only morphologic involvement without clinical renal manifestations; it is unlikely that a renal biopsy in those disorders will lead to the unsuspected diagnosis. More often, these become evident by disturbances of the central nervous and skeletal systems, hepatosplenomegaly, and/or dysmorphic features. In rare cases, clinical renal disease has been described, for example, nephrotic syndrome in children with Hurler syndrome and proximal tubular dysfunction in I-cell disease (50). Several observations about the kidney and lysosomal storage disease are worth noting. Renal involvement in

Gaucher disease, the most common lysosomal storage disease, only becomes symptomatic after splenectomy, a therapeutic procedure in type 1 nonneuropathic disease that is performed less often in the era of enzyme replacement (51–53). Its characteristic “wrinkled paper” appearance allows the diagnosis of Gaucher disease by light microscopy, whereas the pathology of the majority of lysosomal disorders is not distinct. Rather, storage cells are typified by clear and sometimes foamy cytoplasm, the consequence of storage material dissolving with processing (54). Special histochemical staining, especially on frozen sections where water and alcohol-soluble substances are preserved, may help to characterize the stored material, but is frequently nonspecific. Electron microscopy can usually define the disorder further. In most instances, the diagnosis will already be known from the history, laboratory data, and enzyme analysis.

The lysosomal storage diseases that primarily involve the kidney or cause symptoms are briefly discussed below, whereas those that only secondarily involve the kidney appear in Table 27.1. Representative features of I-cell disease and neuronal ceroid lipofuscinosis are illustrated in Figures 27.10 to 27.14. Cystinosis, a lysosomal membrane transport defect, is discussed in the section with Fanconi syndrome.

Fabry Disease (Angiokeratoma Corporis Diffusum Universale)

This condition, described by both Fabry and Anderson in 1898, is a rare metabolic disorder arising from a deficiency of a lysosomal exoglycohydrolase, ceramide trihexosidase, commonly referred to as α -galactosidase A (55). The enzyme catalyzes the cleavage of glycosphingolipids, especially globotriaosylceramide, which is present in most cell membranes. Deficient enzyme activity results in the systemic accumulation of neutral glycosphingolipids with terminal α -linked galactosyl moieties, primarily globotriaosylceramide (Gb3), in plasma and particularly lysosomes of vascular endothelia of the kidneys, heart, brain, and skin.

The disease is uncommon, although it is the second most prevalent inherited lysosomal storage disorder after Gaucher disease. Recent estimates of the frequency range from 1 in 40,000 to 1 in 117,000 births; however, Fabry disease may be more prevalent because of a lack of recognition in patients with isolated renal or cardiac involvement. The prevalence of previously undiagnosed Fabry disease in dialysis patients, with subsequent DNA confirmation, was shown to be 0.33% in men and 0.10% in women undergoing dialysis. Approximately 3% to 4% of patients with left ventricular hypertrophy or cardiomyopathy are discovered to have Fabry disease, and newborn screening programs with subsequent mutational analysis found an incidence of 1 in 3100 to 4700 male infants (56,57). More than 500 mutations of the α -galactosidase gene at Xq22.1 have been described, and most are family specific (55,58). About 5% of the cases are sporadic. Mutations leading to complete loss of gene product are associated with classic forms of the disease, whereas those resulting in amino acid substitutions might occasionally link to a mild phenotype or late manifestation; however, genotype-phenotype correlations are low. The X-linked disease is completely expressed in hemizygous males, but clinical presentation is quite variable, even within families. Most heterozygous females, contrary to historical accounts, are affected. Highly variable levels of enzyme activity in females and the broader range of clinical symptoms can only partly be

accounted for by X inactivation (59). Although renal biopsy may be diagnostic, and EM is a reliable approach to identify the intracellular myeloid bodies, they are not pathognomonic as similar structures are present in silicon nephropathy and pseudolipidosis induced by amiodarone, chloroquine, and hydroxychloroquine (60–63). An aid to diagnosis may be immunofluorescence with a monoclonal anticeraamide trihexoside; this technique has been effectively employed in routinely processed paraffin-embedded tissue (64). Affected males with classic and variant phenotypes are reliably diagnosed by the demonstration of deficient enzyme activity in plasma, leukocytes, cultured cells, or dried blood spots (65). By contrast, female carriers can exhibit normal α -galactosidase A levels, such that exclusion of a carrier status can only be done by mutational analysis of the α -galactosidase A gene. High-throughput PCR-based technologies, such as high-resolution melting analysis, may be cost-effective for newborn screening in females (66). Prenatal diagnosis is possible by amniocentesis, but preferred methods include enzyme and molecular testing on fresh fetal tissue obtained by chorionic villus sampling (67). Diagnosis by molecular probes is typically limited to patients with a positive family history and known mutation; DNA sequencing has proven to be the most reliable strategy for mutation detection. Routine mutational analysis, however, may miss deletions and duplications, which are better detected using quantitative and real-time PCR, multiplex probe amplification and hybridizations, and array comparative genome hybridization (65). New screening tools, based on measurement of urinary Gb3 isoforms via electrospray ionization mass spectrometry, as well as identification of unique proteomic biomarker profiles using capillary electrophoresis coupled to mass spectrometry, may prove relevant for screening females and monitoring response to enzyme replacement therapy (68,69).

Manifestations in hemizygous males may begin in early childhood although storage material has been observed in the prenatal period (70). The earliest and often disabling symptom is acroparesthesia. Gastrointestinal symptoms, nausea, abdominal pain, and diarrhea, commonly appear in childhood and persist into adulthood. Strokes and transient ischemic attacks are not uncommon. Cardiac disease is a well-recognized complication, classically, hypertrophic cardiomyopathy that may initially manifest as arrhythmias in childhood. The skin lesions—angiokeratomas—cluster on the lower trunk and thighs as reddish purple dark spots or papules with dilation of superficial capillaries and variable hyperkeratosis. They typically develop during adolescence and increase with age but are rarely problematic. They remain a valuable clue to the diagnosis because they are seen in only a few rare conditions. Anhidrosis or hypohidrosis and corneal opacities are seen in most patients (71). In addition to the classical phenotype, there are milder variants with residual α -galactosidase A activity that lack the characteristic features. “Cardiac” and “renal” variants present with late-onset manifestations primarily limited to the heart and kidney, respectively (55). Males generally experience onset of symptoms earlier than females, with a median age of 6 years versus 9 years in females.

Progressive nephropathy is a major feature, and ESRD can occur during adolescence (72). Clinical evolution to renal insufficiency and hypertension is variable over several decades and correlates with residual α -galactosidase activity (73). Glomerular pathology may exist, despite the presence of an apparently

TABLE 27.1 Renal involvement by lysosomal storage disorders (without significant functional impairment)

Disease	Stored Material	Enzyme Defect	Storage Location	Light Microscopy	Electron Microscopy	Other
Sphingolipidoses Gaucher disease	Glycosyl ceramide	β -Glucosidase	MC, MI; rare, BM	Gaucher macrophage with "wrinkled" cytoplasm	50-nm tubular bilayers	Renal involvement follows splenectomy.
Niemann-Pick (types A and B)	Sphingomyelin	Sphingomyelinase	P, E, MI, PT, DT	Small, uniform cytoplasmic vacuoles	Myelin-like lamellae	Involved in >50% of cases; red birefringence with polarization
Metachromatic leukodystrophy	Galactocerebroside sulfate	Arylsulfatase A	H, DT, CT, rare PT	15- to 20- μ m cytoplasmic spheroids	6- to 8-nm "stacked disks"; honeycomb pattern opposite plane	Kidney is the major site of pathology in the fetus; green birefringence with polarization
Neuronal ceroid lipofuscinosis	Ceroid (lipofuscin); subunit c of mitochondrial ATP synthase, saposins A and D	Palmitoyl-protein thioesterase 1; tripeptidyl peptidase 1	E, DT, PT, P	Tan, waxy lipid globules	Granular osmiophilic bodies, curvilinear profiles, fingerprints, rectilinear complexes	Yellow-green autofluorescence
Gangliosidosis	Ganglioside (G_{M1})	β -Galactosidase	P, H, M	Clear cytoplasmic vacuoles	Finely granular material with some lipid lamellae	
Sandhoff disease	Ganglioside (G_{M2}) and other sphingolipids	Hexosaminidase- α and hexosaminidase- β	H	Clear cytoplasmic vacuoles	Finely granular material with some lipid lamellae	
Mucopolipidosis I-cell	Sialyl oligosaccharides	<i>N</i> -acetylglucosamine-phosphotransferase deficiency	P, rare PT, fibroblasts	Ballooning of cells with clear cytoplasmic vacuoles	Fibrillogranular	Light microscopy resembles G_{M1} ; defect in multiple enzyme transport
Mucopolysaccharidosis Hurler disease (I)	Heparan sulfate, dermatan sulfate	α -L-iduronidase	P, rare PT	Clear cytoplasmic vacuoles	Sparse fibrillogranular	Reported with nephrotic syndrome
Glycoproteinoses Fucosidosis	Fucosyl oligos	α -Fucosidase	P	Clear cytoplasmic vacuoles	Sparse fibrillogranular and lamellar	
Mannosidosis	Mannosyl oligos	α -Mannosidase, β -mannosidase	P	Clear cytoplasmic vacuoles	Sparse fibrillogranular	
Aspartylglucosaminuria	Aspartylglucosamine	Aspartylglucosaminidase	P	Clear cytoplasmic vacuoles	Sparse fibrillogranular	

PAS, periodic acid-Schiff; SB, Sudan black; AB, Alcian blue; P, podocyte; E, glomerular capillary endothelium; M, mesangial cells; BM, basement membrane; PT, proximal tubular cells; DT, distal tubular cells; H, loop of Henle cells; CT, collecting tubular cells; A, arterial endothelium; MI, interstitial macrophage; MC, circulating and entrapped macrophage; oligos, oligosaccharides.

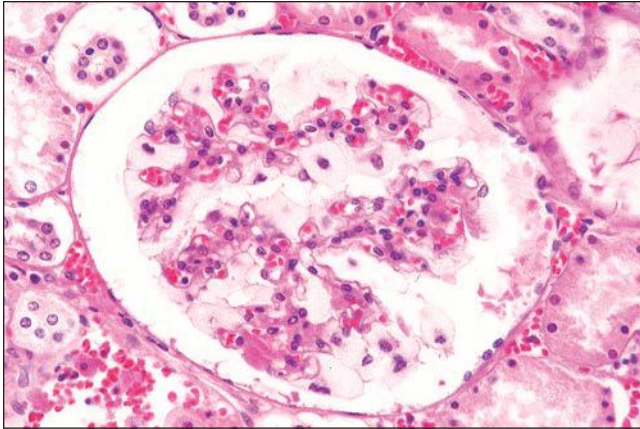


FIGURE 27.10 Glomerulus in I-cell disease has profoundly enlarged, finely vacuolated podocytes. (H&E; $\times 400$.)

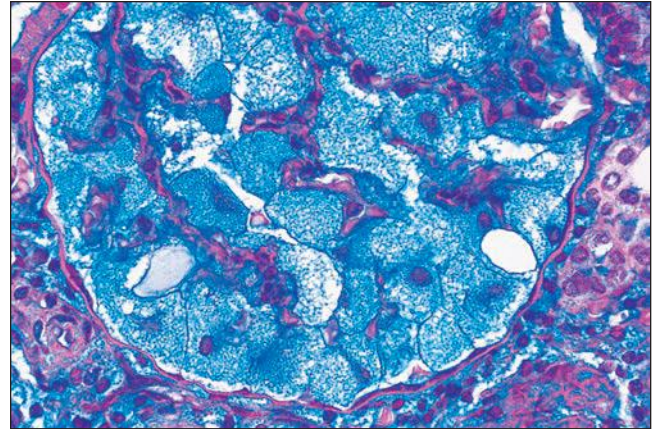


FIGURE 27.11 The vacuolated podocytes in I-cell disease contain abundant glycolipids and acidic glycosaminoglycans. (Hale colloidal iron; $\times 400$.)

normal estimated glomerular filtration rate (GFR), without manifestation of overt proteinuria or even microalbuminuria (74–76). As clinical parameters lack sensitivity, kidney biopsy has been employed by some to assess baseline injury (74,76). Proteinuria seems to be the most important predictor for renal

progression, especially for men, in whom advanced nephropathy is more prevalent and generally occurs earlier (77,78). Most females have slowly progressive kidney disease; however, the subset (15% to 20%) that develops ESRD does so at approximately the same age as men (79). Loss of urine-concentrating

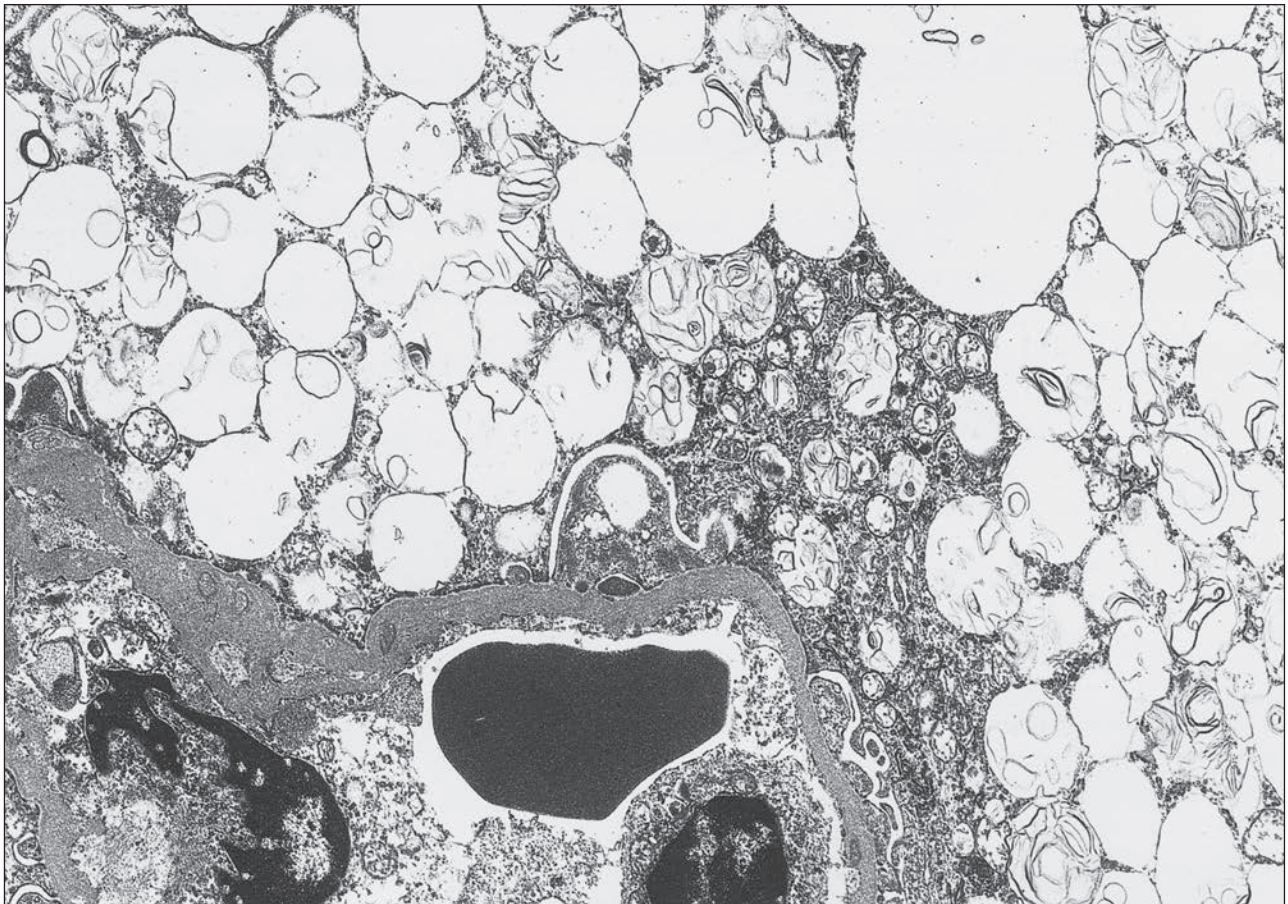


FIGURE 27.12 Electron micrograph of a podocyte in I-cell disease shows that the vacuoles contain a few membranous and lamellated inclusions. The material in the largely “empty” vacuoles may have been dissolved during processing. ($\times 9215$.)

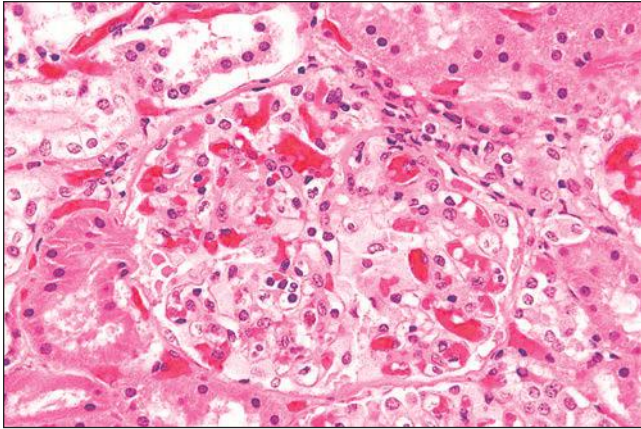


FIGURE 27.13 Glomerulus from a 13-year-old boy with neuronal ceroid lipofuscinosis. The child had severe cerebral atrophy and neurologic impairment but normal renal function. The visceral podocytes are distended with granular ceroid material. (H&E; $\times 200$.)

ability leads to polyuria and polydipsia, and altered tubular functions have also been identified, such as impaired glucose and potassium reabsorption, to a greater degree than can be accounted for by reduced GFR (80). The urine sediment contains lipid globules showing Maltese crosses on polarization and desquamated cells containing myeloid bodies (81).

Pathologic Changes

Gross descriptions of the kidney in Fabry disease are limited, but the kidneys may be enlarged by the accumulation of storage material. Glomeruli may look white on direct examination using stereomicroscopy (74,82). Renal cortical or parapelvic cysts have been demonstrated by ultrasound, magnetic resonance imaging, and computed tomographic imaging in up to 50% of patients studied, which includes classically affected

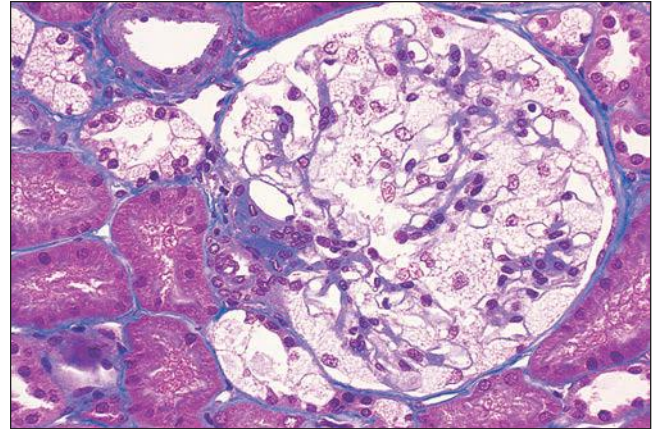
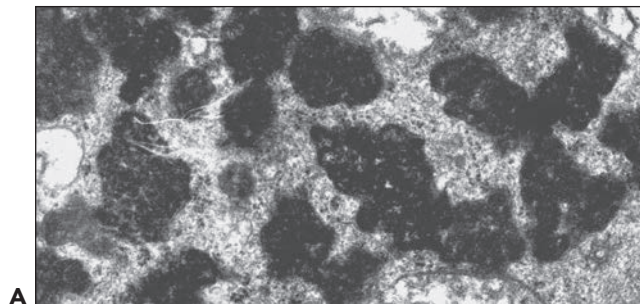


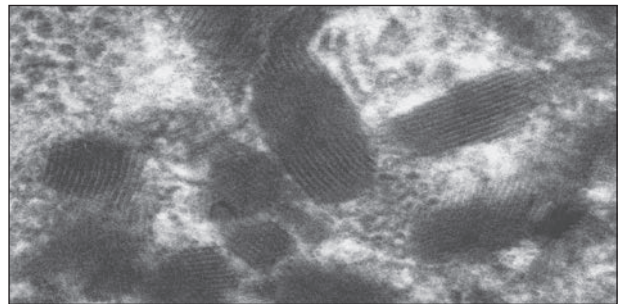
FIGURE 27.15 The glomerular podocytes are swollen and finely vacuolated in a patient with Fabry disease. Epithelial cells of distal tubules are also vacuolated. (Mallory trichrome; $\times 200$.)

hemizygous males, female carriers, and cardiac variants. The prevalence of the cysts increases with age, but their presence does not correlate with residual enzyme activity, mutation type, proteinuria, or kidney function (83,84). The nature and pathogenesis of the cysts remain undetermined.

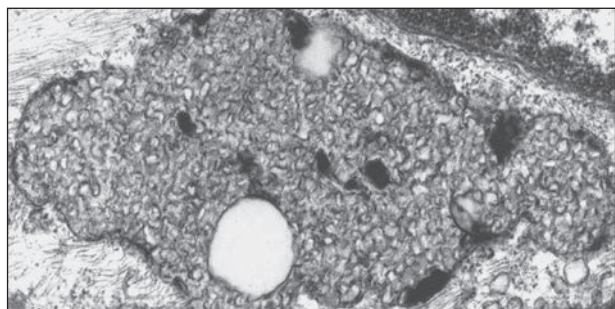
Light microscopic changes are remarkable and can easily yield a diagnosis. The glomerular tuft contains strikingly enlarged and vacuolated glomerular cells, especially podocytes (Fig. 27.15). Similar changes are present to a lesser degree in endothelial and mesangial cells and occasionally in the parietal epithelial cells lining Bowman capsule. They appear empty in paraffin sections because the accumulated glycosides are removed during clearing and paraffin embedding of the tissue. The material is preserved by prior osmification and is easily demonstrated in semithin sections of tissue embedded in epoxy resin (Fig. 27.16). The material in frozen sections, whether fresh



A



B



C

FIGURE 27.14 Electron microscopy of storage material in neuronal ceroid lipofuscinosis showing characteristic granular osmiophilic bodies (A) and fingerprint (B) and curvilinear (C) profiles. ($\times 31,500$.)

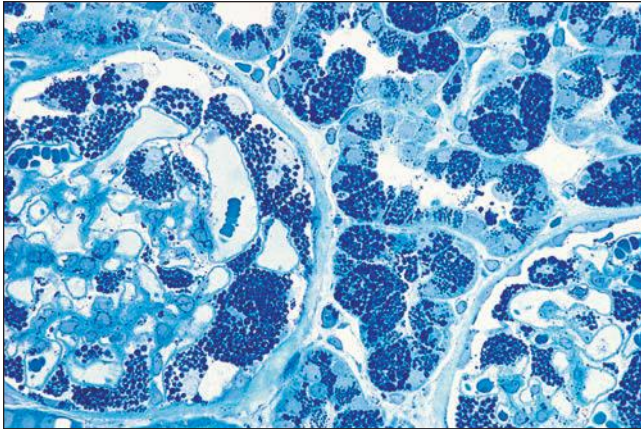


FIGURE 27.16 The intracellular lipid inclusions in Fabry disease are preserved in osmicated, epoxy-embedded tissue. The enlarged podocytes and tubular epithelial cells contain lamellated inclusion bodies (same patient as in Fig. 27.15). (Methylene blue; $\times 250$.)

or formalin fixed, is birefringent, autofluorescent, sudanophilic, and positive to oil red O and PAS. It may also be demonstrated in frozen sections by lectin binding (85). A similar vacuolated appearance, variable in quantity but sometimes considerable, is present in tubular epithelial cells, particularly of the distal tubules and the loop of Henle (Figs. 27.15 and 27.17). Small arteries and arterioles show vacuolation of the endothelial cells and finely vacuolated areas in the smooth muscle (Fig. 27.18). Interstitial foam cells can be seen. Progression of the disease leads to mildly increased mesangial matrix and cellularity with segmental glomerular sclerosis (Fig. 27.19), capillary wall thickening, tubular atrophy, interstitial fibrosis, and arterial and arteriolar sclerosis. Immunofluorescence is negative or nonspecific. Storage of myeloid bodies has been shown also in the liver and spleen (86). Hemizygotes have more severe lipid storage than do heterozygotes (75,87,88).

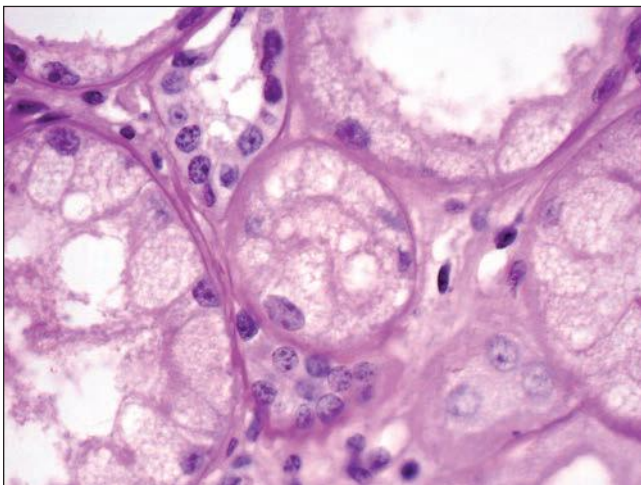


FIGURE 27.17 Fine, foamy vacuolation of tubular cells from a patient with Fabry disease. (PAS; $\times 400$.)

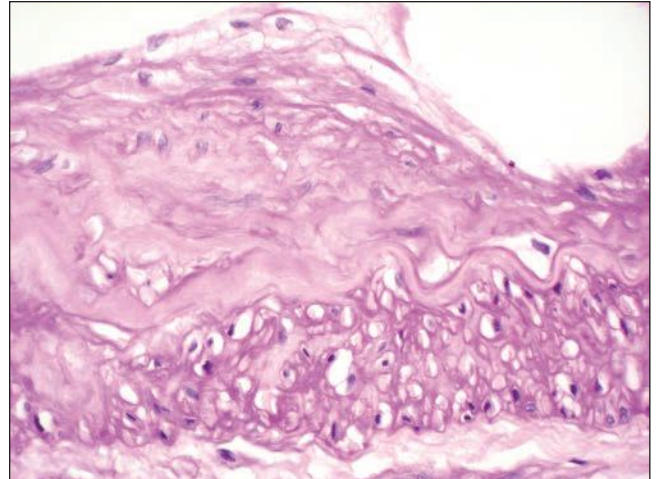


FIGURE 27.18 Renal artery in end-stage Fabry disease has moderate intimal fibroplasia, cleared endothelial cells (*top*), and empty spaces in the media (*bottom*). (PAS; $\times 400$.)

Electron microscopy shows enlarged secondary lysosomes filled with osmiophilic, granular to lamellated membrane structures that have an onion skin–like appearance or parallel dense layers (zebra bodies) (Fig. 27.20) (87,88). The inclusions are present especially in podocytes, parietal epithelium, distal tubular epithelium, and vascular myocytes, although a few inclusions may be present in virtually all renal cells (89). Generally, inclusions within mesangial cells are smallest and those in podocytes the largest. Quantitative stereologic EM methods have documented progressive accumulation of Gb3 inclusions in podocytes with age, but not in endothelial or mesangial cells. This observation may reflect different rates of production or cell turnover (75). The periodicity of the lamellated structures, when measured in plastic thin sections, varies between 3.5 and 5.0 nm but is estimated at 14 to 15 nm when studied by freeze-fracture electron microscopy (90,91).

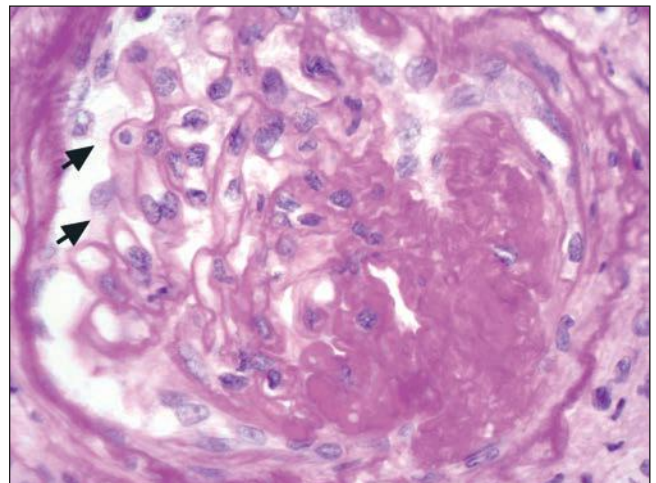


FIGURE 27.19 Glomerulus in Fabry disease shows thickened capillary walls and partial solidification. Fine vacuolation is still evident in a few podocytes (*arrows*) over an intact portion of the tuft. (PAS; $\times 400$.)

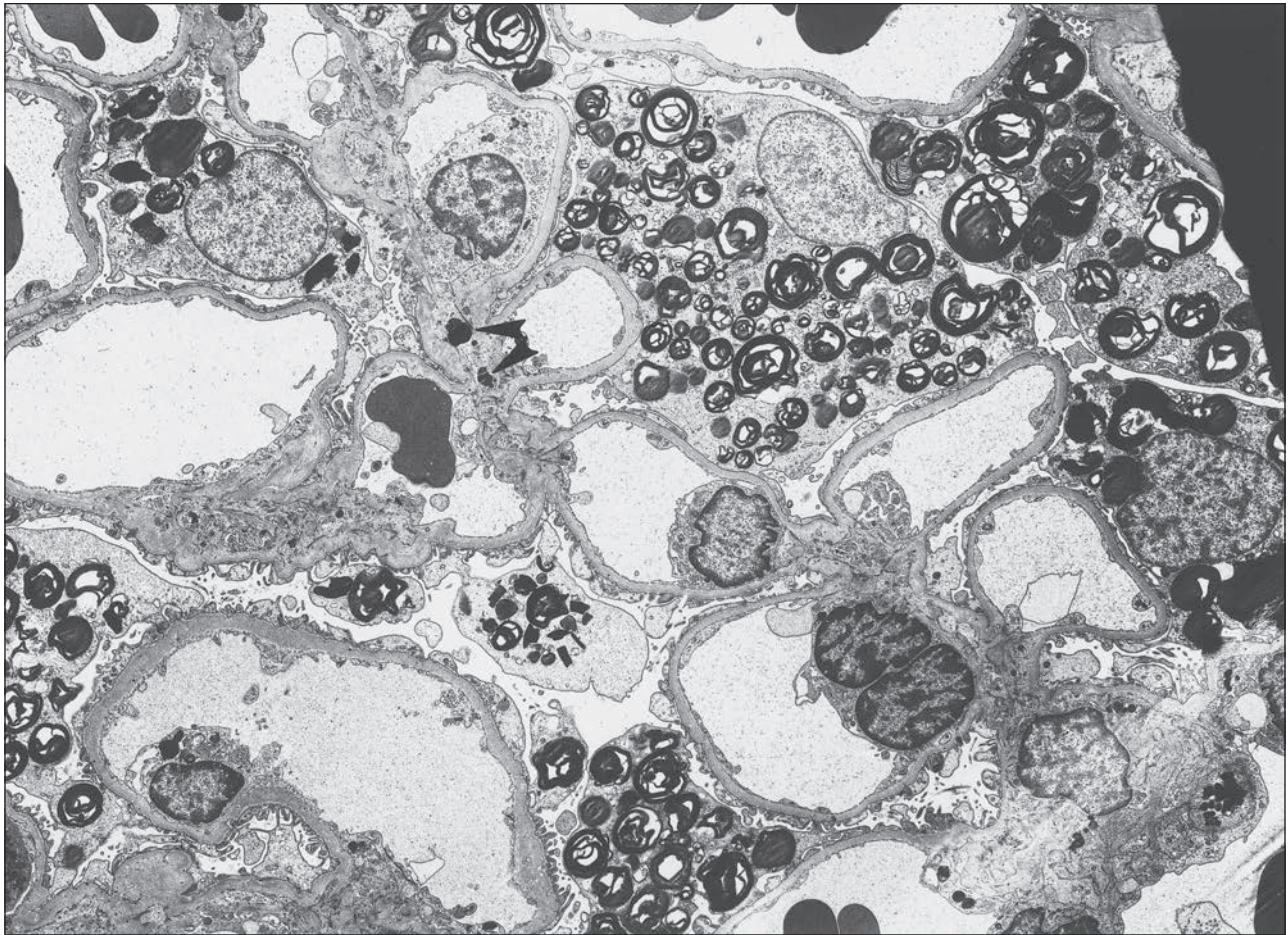


FIGURE 27.20 Electron micrograph of glomerulus in Fabry disease shows lamellated lipid inclusions (“myeloid bodies”) in podocytes. A few mesangial inclusions are also present (*arrowheads*, just above the center). ($\times 3000$.)

Recently described are unique subendothelial deposits associated with basement membrane duplication and composed of membrane-like material arranged in geographic layers (88). Foot process width and the extent of foot process effacement with microvillous transformation correlate with the degree of proteinuria (75,85).

Pathogenesis

Endothelial lipid deposits may be pathogenic in renal disease, as they are absent in the Fabry knockout mouse model that does not develop renal failure (92). Interestingly, deposits are also unapparent in renal endothelial cells from Fabry cardiac variants (93). A putative role for endothelial dysfunction comes from mouse models that demonstrate a prothrombotic and proatherogenic age-dependent phenotype and abnormal vascular reactivity (94–96). Lyso-Gb3 (deacylated Gb3), a bioactive lipid metabolite found at elevated concentrations in Fabry disease, has been shown to increase the expression of TGF- β and CD74 in cultured human podocytes, potentially mediating injury (97). Tubular dysfunction may result from aberrant proteolytic processing and reduced and ectopic expression of uromodulin (UMOD) in epithelial cells with Gb3 storage (98). In addition, cells lacking α -galactosidase A show reduced viability and increased membranous Gb3 expression that could

disrupt cellular signaling (99). Renal manifestations may therefore result from a combination of vascular insufficiency, podocyte toxicity, and tubular damage (85).

Treatment

Kidney transplantation successfully corrects renal failure in Fabry disease, yielding good graft function and patient survival (100,101). Normal renal allografts contain α -galactosidase but do not provide sufficient enzyme for systemic correction of the disorder. Myeloid bodies can appear in the allograft and are usually limited to arteriolar endothelial cells, tubular epithelial cells, and infiltrating monocytes but do not contribute significantly to graft loss or mortality. Asymptomatic living related donors must be screened carefully for heterozygosity (102,103).

Enzyme replacement therapy with recombinant human α -galactosidase (rh α -GAL) has proven to be safe and effective in adult hemizygous male and heterozygous female patients as well as children (76,104–106). Clinical trials have shown an improvement in pain, reduction in left ventricular mass, and a decline in blood and urine Gb3 levels, despite the development of antibodies to rh α -GAL. Interestingly, antibodies are not detected in most women treated with rh α -GAL, likely a consequence of residual native enzyme activity (104).

Stabilization of kidney functional decline has been shown, with consistently better results when therapy is initiated before evidence of significant proteinuria (107,108). Recent efforts are focused on the addition of renin-angiotensin system blockade to augment effectiveness (104). Enzyme replacement therapy in kidney transplant patients with Fabry disease also appears to be safe and often effective against extrarenal involvement (100,106).

Examination of tissues from rh α -GAL-treated patients showed clearing of deposits from the endomyocardium, skin, liver, and kidney. Detailed analysis of sequential kidney biopsies from patients on enzyme replacement therapy showed lipid clearance from mesangial and interstitial cells and endothelium of peritubular capillaries, glomeruli, and arteries at 6 months that was sustained at 54 months (108–111). Initially, only moderate clearance was seen in tubular epithelial cells and vascular smooth muscle, but by 54 months, the tubular cells were cleared (108). Podocytes were most resistant to clearance but continued to improve with therapy. A scoring system of histologic involvement in Fabry nephropathy has recently been validated with potential application to baseline evaluation and therapy response (112).

Nephrosialidosis and Variants

Sialidosis

Sialidosis is an autosomal recessive disorder caused by mutations in the *NEU1* gene on chromosome 6p21, affecting the degradation of glycoprotein. The resulting deficiency of α -neuraminidase activity leads to the accumulation of several sialyl oligosaccharides and glycoproteins, which are excreted in the urine and are useful in diagnosis. Another recently discovered function of α -neuraminidase is to negatively regulate lysosomal exocytosis, a basic physiologic process in many cell types. Therefore, mutations in *NEU1* also exacerbate lysosomal exocytosis that may underlie other phenotypic abnormalities of the disorder (113). Over 40 mutations have been described. The residual catalytic enzyme activity and its subcellular localization (endoplasmic reticulum/Golgi vs. lysosome) appear to influence the clinical severity, with phenotypic heterogeneity even within families. Type 1 sialidosis, the milder form, usually presents in the second decade with visual impairment, generalized myoclonus, ataxia, and epilepsy. Sialidosis type 2 (mucopolidosis I) is divided into three subgroups based on the age of symptom onset: congenital (in utero), infantile (0 to 12 months), and juvenile (approximately 2 to 20 years). Type 2 is distinguished from type 1 by its earlier onset and mucopolysaccharide-like phenotype with abnormal facies, dysostosis multiplex, hepatosplenomegaly, and psychomotor retardation (114). The congenital form is associated with hydrops fetalis and stillbirth or neonatal ascites and early death (115). Infantile sialidosis severely affecting the kidney and causing symptomatic renal disease has been termed *nephrosialidosis*. Macular cherry-red spots, myoclonus, and delayed neurodevelopment soon become manifest. Proteinuria, developing in infancy, progresses to nephrotic syndrome and to early renal insufficiency (116).

Galactosialidosis

Galactosialidosis is closely related to sialidosis and results from a combined deficiency of neuraminidase and β -galactosidase, owing to a defect in another lysosomal protein, the protective protein cathepsin A, with which they are complexed

(113,114). Patients have coarse facies, cherry-red spots, skeletal anomalies, and foam cells in the bone marrow. A juvenile/adult form is characterized by myoclonus, ataxia, and neurologic deterioration and is found predominantly in consanguineous Japanese families, whereas the late infantile form has hepatosplenomegaly, growth retardation, and cardiac valvular disease (116,117). In addition to hydrops, visceromegaly, and skeletal dysplasia, the kidneys are affected in the early infantile form of galactosialidosis, with histopathologic features and progression to renal insufficiency matching that of nephrosialidosis (118).

Free Sialic Acid Storage Disorders (Salla and Infantile Sialic Acid Storage Diseases)

Sialic acid storage disorders are characterized by the lysosomal accumulation of free sialic acid as a result of defects in sialin, encoded by *SLC17A5*, a carrier-mediated lysosomal membrane transport protein (119). The disorder is divided into two phenotypes: the milder Salla disease, nearly unique to the Finnish population, which shows reduced but residual function; and the severe infantile sialic acid storage disease, which is associated with complete loss of sialin activity (120). Patients store in their tissues and excrete in their urine approximately 10 to 100 times the normal amounts of sialic acid. The infantile form can be detected in utero with hydrops fetalis or present at birth with hepatosplenomegaly, failure to thrive, severe mental and motor retardation, coarse facies, and dysostosis multiplex; those with Salla disease are normal at birth but develop psychomotor delay and ataxia during infancy (121). The renal features are similar histopathologically to those of nephrosialidosis and may be associated with steroid-resistant nephrotic syndrome (122).

Pathologic Changes in Nephrosialidosis and Variants

The glomerular podocytes are enlarged by abundant foamy and vesicular cytoplasm (Fig. 27.21) (117,122). Similar histopathologic abnormalities in the podocytes occur in asymptomatic sialidosis. The vesicles in paraffin sections are clear,

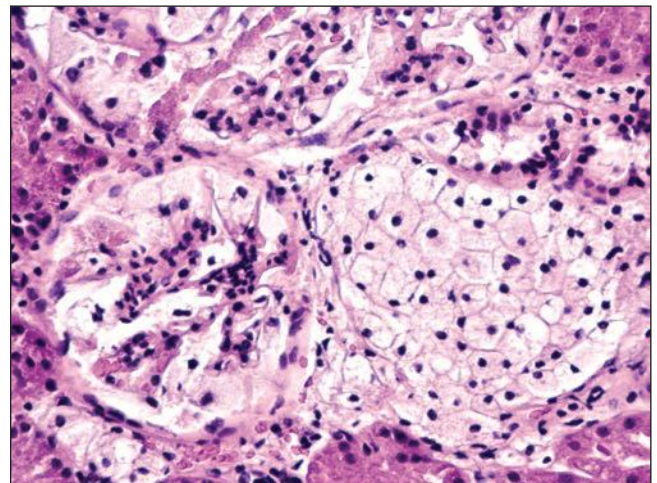


FIGURE 27.21 The glomerulus in nephrosialidosis contains vacuolated podocytes that fill Bowman space. The adjacent interstitium and tubules contain vacuolated storage cells. (H&E; $\times 200$.)

although they stain lightly with colloidal iron, indicating partial preservation of the material during processing. PAS staining shows only a fine granularity. Tubular cells, especially in proximal tubules, and interstitial cells are also vacuolated. Cytoplasmic vacuoles have also been found in endothelial cells of renal vessels (123).

Immunofluorescence may show small, nonspecific glomerular deposits of IgM and C3, reflecting hyalinosis. In sialidosis, some podocyte vacuoles in frozen sections bind concanavalin A and wheat germ agglutinin, demonstrating mannose and sialic acid residues within the stored oligosaccharides.

Electron microscopy shows the vacuoles to be membrane bound and almost empty (Fig. 27.22). Some vacuoles contain granules and membranous profiles of electron-dense material. Similar vacuoles are present in tubules and occasionally in mesangial cells, endothelial cells, or parietal epithelial cells (123). Podocyte changes relate to proteinuria, and renal insufficiency is associated with glomerular collapse and sclerosis.

No specific treatment exists for this rare group of lysosomal storage disorders. A few attempts at bone marrow transplantation have met with limited success, and renal transplantation does not preclude development of systemic abnormalities (124,125).

VITAMIN DISORDERS

Cobalamin C Deficiency

Cobalamin C (CblC) is required for conversion of dietary vitamin B₁₂ to its reduced and methylated forms, which function as coenzymes. Deficiency of cblC is a panethnic disease and the most common inborn error of cobalamin metabolism, with an estimated incidence of 1:100,000 based on expanded newborn screening (126). Cobalamin C defects lead to impaired activities of methylmalonyl-CoA mutase and methionine synthase, resulting in methylmalonic aciduria and homocystinuria. The disorder is inherited as an autosomal recessive trait, and the severity of presentation can vary considerably. CblC-deficient patients typically present in the newborn period with failure to thrive, neurologic and ophthalmologic abnormalities, and hematologic disturbances, especially megaloblastic anemia. Cardiopulmonary and gastrointestinal involvement is not uncommon. Hemolytic uremic syndrome (HUS) is characteristic, and proteinuria may be apparent. Late-onset disease is rarer and milder and can appear at any time from early childhood to adulthood, presenting as neurologic deterioration without systemic symptoms (127,128). Renal damage may be the sole manifestation of late-onset disease (129,130).

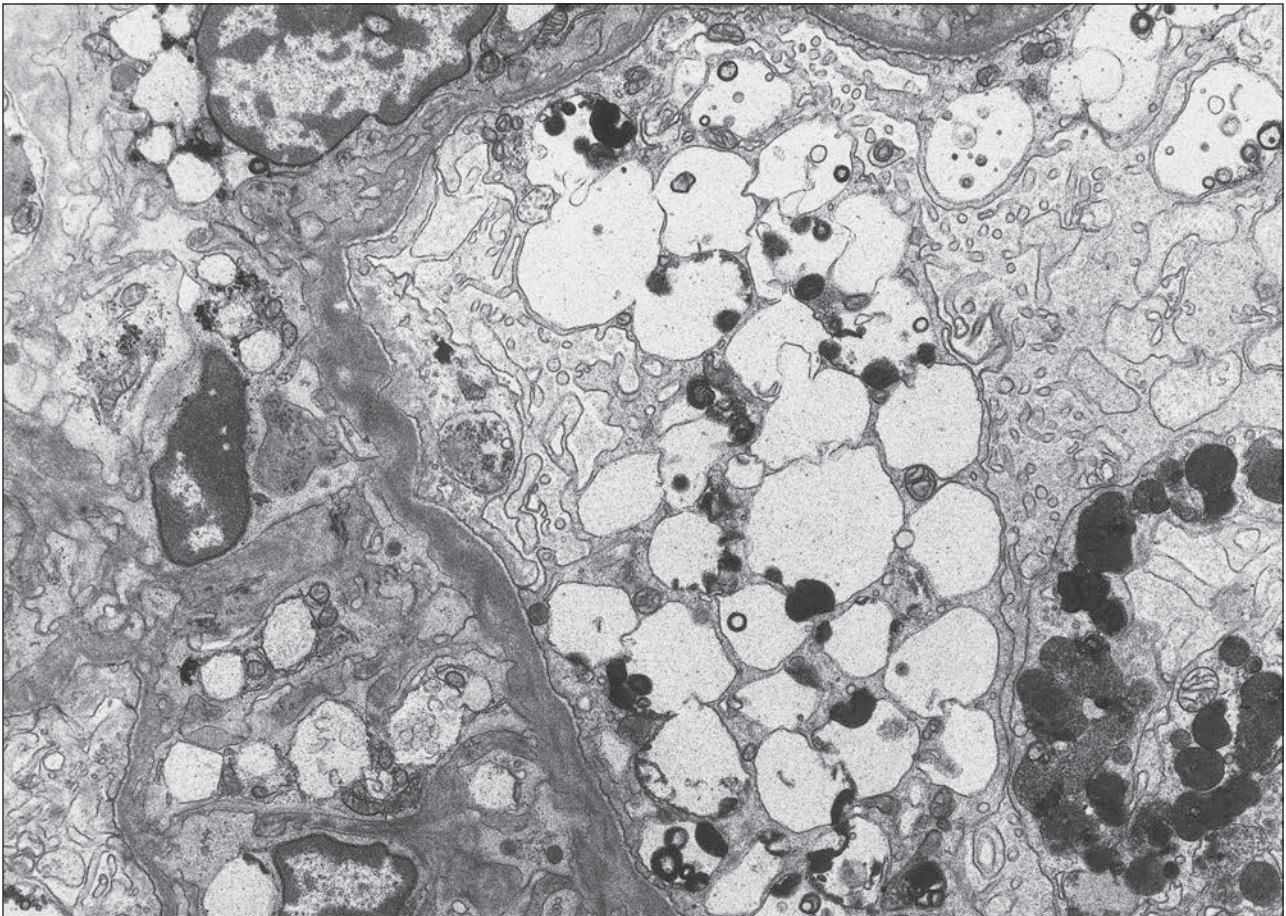


FIGURE 27.22 Electron microscopy of a glomerulus in nephrosialidosis shows vacuolated podocytes and mesangial cells. The vacuoles are partially filled with electron-dense bodies and also contain lucent and finely granular material. (×10,400.) (Courtesy of Drs. C. E. Kashtan and Z. Posalaky.)

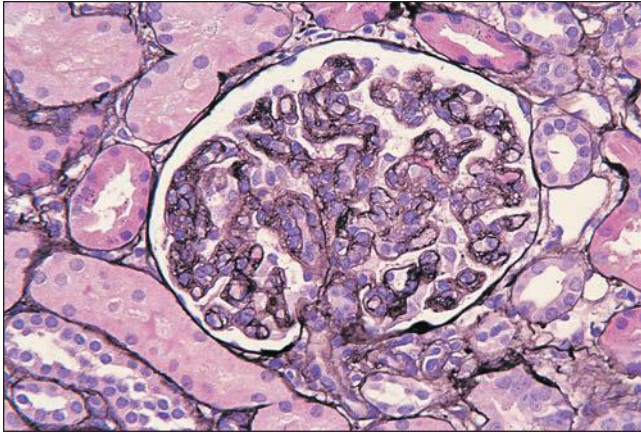


FIGURE 27.23 Mildly hypercellular glomerulus from a 5-year-old boy with cobalamin C deficiency. Chronic microangiopathic changes include thickened and duplicated basement membranes without capillary thrombi. (PAS-silver methenamine; $\times 400$.)

CblC defect can be difficult to diagnose on a clinical basis due to its heterogeneous manifestation but is established by finding the combination of methylmalonic aciduria, homocystinuria, and increased propionylcarnitine with normal serum vitamin B₁₂ and transcobalamin II concentrations.

Renal pathology in this group of patients has most typically been that of thrombotic microangiopathy (129,131). The glomeruli have shown mesangial expansion with mild mesangial and endothelial proliferation, endothelial swelling, capillary dilation, and basement membrane double contours (Fig. 27.23). Intracapillary fibrin or platelet thrombi can be seen. Foot process effacement, endothelial cell detachment, and expansion of the subendothelial space by granular, fibrillary material have been noted by electron microscopy (Fig. 27.24).

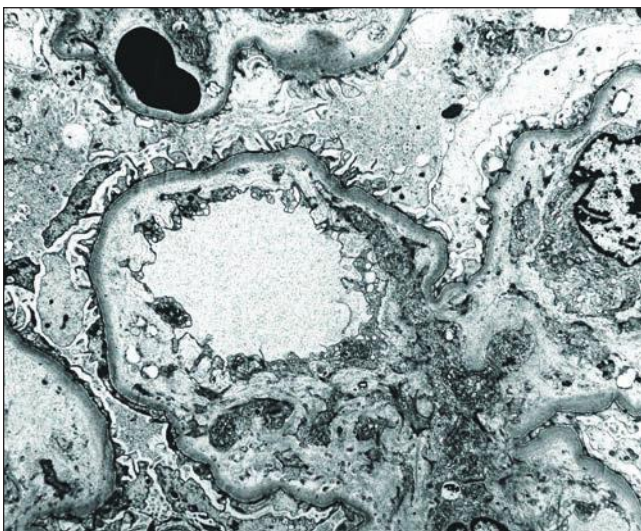


FIGURE 27.24 Electron microscopy in cobalamin C deficiency showing narrowing of the capillary lumen by subendothelial granular and fibrillar material and focal mesangial cell interposition. Foot process fusion is only focal. ($\times 2500$.)

Immunofluorescence is typically negative or nonspecific, but the peripheral glomerular membrane and primarily mesangial C3, C1q, and IgM were found in a single case, which also had widespread electron-dense deposits (131).

Nearly 60 causal mutations have been identified in the recently discovered responsible gene designated *MMACHC*, which maps to chromosome region 1p34.1 (132,133). The protein is involved in binding cobalamin, decyanating cyanocobalamin, and dealkylating alkylcobalamins (134). Presumed mechanisms for the renal pathology include hyperhomocysteine- and hypomethionine-induced vascular damage and methylmalonate-induced proximal tubular injury (128). Successful management requires large amounts of hydroxocobalamin and betaine. Many patients die from severe hemolytic anemia, and in those without HUS, there is often improvement of hematologic, biochemical, visceral, and growth parameters although neurologic and visual complications persist (128).

ORGANIC ACID DISORDERS

Methylmalonic Acidemia

Isolated methylmalonic acidemia is an autosomal recessive disorder of branched-chain amino acid metabolism that has a varied presentation, but neonatal onset is typified by recurrent vomiting, lethargy, dehydration, failure to thrive, hypotonia, and metabolic ketoacidosis that, if untreated, results in multiorgan failure or death. It is caused by a deficiency of the enzyme methylmalonyl-CoA mutase (MCM) due to mutations in the *MUT* gene located on the short arm of chromosome 6 in which approximately 200 mutations have been identified (135). Defects in cobalamin metabolism (cblA, cblB, cblD variant 2) and a deficiency of methylmalonyl-CoA epimerase also yield methylmalonic acidemia (135). Children with complete MCM deficiency are cobalamin nonresponsive and typically develop renal tubular dysfunction that often progresses to ESRD by late childhood or early adolescence; partial enzyme activity correlates with lower urinary methylmalonic acid concentration, which might predict occurrence of renal failure (136,137). Assessment of nonvolatile organic acid patterns, acylcarnitine profiles, and complementation analysis are useful for diagnosis (135). Treatment is centered on dietary control and carnitine supplementation, with emergency support during times of illness.

Chronic organ damage ensues despite improved outcome of the acute metabolic crisis. Impaired renal function occurs in the majority of patients, and kidney pathology has shown tubulointerstitial nephritis with interstitial fibrosis, tubular atrophy, and interstitial mononuclear cell infiltrates (138). Mitochondrial dysfunction has been demonstrated in the MCM-deficient kidney and human proximal tubule cell models and might be implicated in renal perturbation (139,140). Chronic renal failure usually develops in the first or second decade and can be treated with dialysis. Liver transplantation provides enzyme to effectively avoid systemic metabolic derangement, but renal transplantation is required for replacement of localized kidney enzyme; neither prevents the neurologic complications that develop in some patients. The effectiveness of combined kidney and liver transplantation as a therapeutic option remains to be proven (141,142).

CARBOHYDRATE DISORDERS

Glycogen Storage Disease

The glycogen storage diseases are genetic defects that result in the storage of abnormal amounts and/or abnormal forms of glycogen. Some affect several tissues, whereas others may affect only one, most commonly the liver or muscle because of their abundant quantities of glycogen.

Glycogen storage disease type I (GSD-I) is a group of autosomal recessive disorders with an incidence of 1 in 100,000. It includes two major subtypes: GSD-Ia (von Gierke disease), caused by a deficiency of glucose-6-phosphatase alpha (G6Pase- α), which accounts for about 80% of cases; and GSD-Ib, caused by a deficiency in the glucose-6-phosphate transporter (G6PT) (143,144). Glucose-6 transporter translocates glucose-6-phosphate from the cytoplasm into the lumen of the endoplasmic reticulum, where G6Pase- α hydrolyses it into glucose and phosphate; together, these enzymes maintain glucose homeostasis, and their deficiency results in an accumulation of glycogen, as conversion of glucose-6-phosphate to glucose in both glycogenolysis and gluconeogenesis is impaired. Glucose-6-phosphatase- α is expressed in high levels in the gluconeogenic liver and kidney, whereas G6PT is ubiquitous.

Patients with GSD-I commonly become symptomatic in early infancy, presenting with hepatorenomegaly and hyperlactacidemia. They are hypoglycemic, with large abdomens and rounded faces, and some present with seizures. Hyperlipidemia, paralleling that in type IV hyperlipidemia, causes xanthomas; hyperuricemia may cause symptoms of gout in older children. The diagnosis, based on clinical and biochemical findings, is confirmed by measurement of G6Pase- α activity in fresh liver biopsy samples. More recent recommendations for diagnosis combine clinical and biochemical abnormalities with mutational analysis, the latter of which can also be used for carrier testing of at-risk families and prenatal diagnosis (144).

Renal enlargement begins early, and functional impairment is a late complication. Effective renal plasma flow (RPF) and glomerular filtration are increased at first, followed by microalbuminuria with subsequent proteinuria and hypertension. Microalbuminuria and proteinuria have been detected in children less than school age (145). The degree of hyperfiltration correlates with renal size. Patients have an incomplete form of distal tubular acidosis, and they are prone to hypercalciuria with development of nephrocalcinosis and stone disease, which can be demonstrated within the first year of life (146). Hyperuricemia, if untreated, can lead to gout. A form of Fanconi syndrome, originally thought to be associated with GSD-I, is now attributed to Fanconi-Bickel syndrome (see section later in this chapter).

Pathologic Changes

Renal enlargement and glomerular hyperperfusion are associated with twofold to threefold glomerular hypertrophy. The glomeruli may be mildly hypercellular, and they contain large amounts of mesangial lipid. Tubules are lined with large vacuolated cells engorged with glycogen (147) (Fig. 27.25). Frozen tissue or alcohol maintains glycogen to the best advantage, but it is partly preserved with routine formalin processing. Enlarged cells have rarefied or cleared cytoplasm that will stain with PAS and lose their pink blush after treatment with diastase. Progressive renal damage leads to focal segmental and,

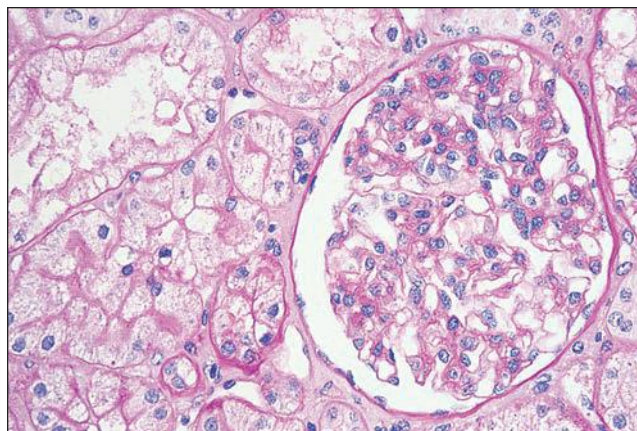


FIGURE 27.25 A glomerulus in a patient with GSD-I is hypertrophied and has mildly increased numbers of prominent mesangial cells. Adjacent tubules show intense vacuolation of epithelial cells. (PAS; $\times 100$.)

eventually, complete glomerular sclerosis (Fig. 27.26), the latter with arteriolar sclerosis, tubular atrophy, and interstitial fibrosis. Immunofluorescence is often positive for immunoglobulin and complement components; it may be positive for ApoAI.

Electron microscopy shows twofold thickening of the GBM, sometimes diffusely. Lamellation and irregular contour, reminiscent of the abnormality in Alport syndrome, occur in areas of severe thickening (Fig. 27.27) (148). Glycogen granules are present among the basement membrane lamellae and focally within mesangial, epithelial, and endothelial cells. Widening of foot processes relates to proteinuria. Mesangial widening and segmental sclerosis are also present. The glomerular abnormality partially resembles that of diabetic nephropathy. Glycogen is present both diffusely and in membrane-bound vesicles in tubular epithelial cells. It is recognized ultrastructurally as aggregates of dense osmiophilic particles, typically small (150 to 200 Å) and monoparticulate but occasionally forming rosettes.

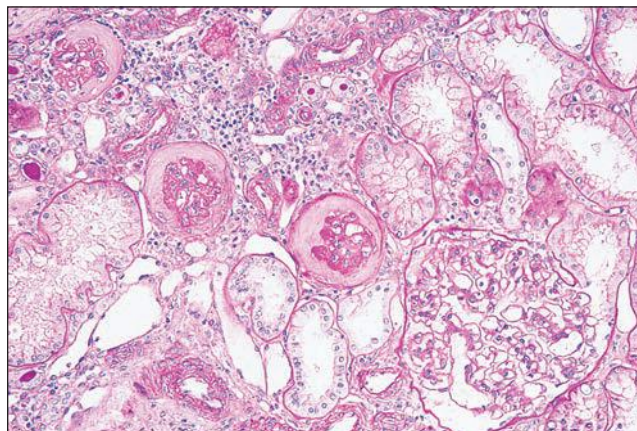


FIGURE 27.26 Nephrectomy kidney from a child with GSD-I shows an enlarged glomerulus and extensive global glomerulosclerosis. Atrophic tubules are associated with interstitial inflammation, fibrosis, and thickened arteries. (PAS; $\times 50$.)

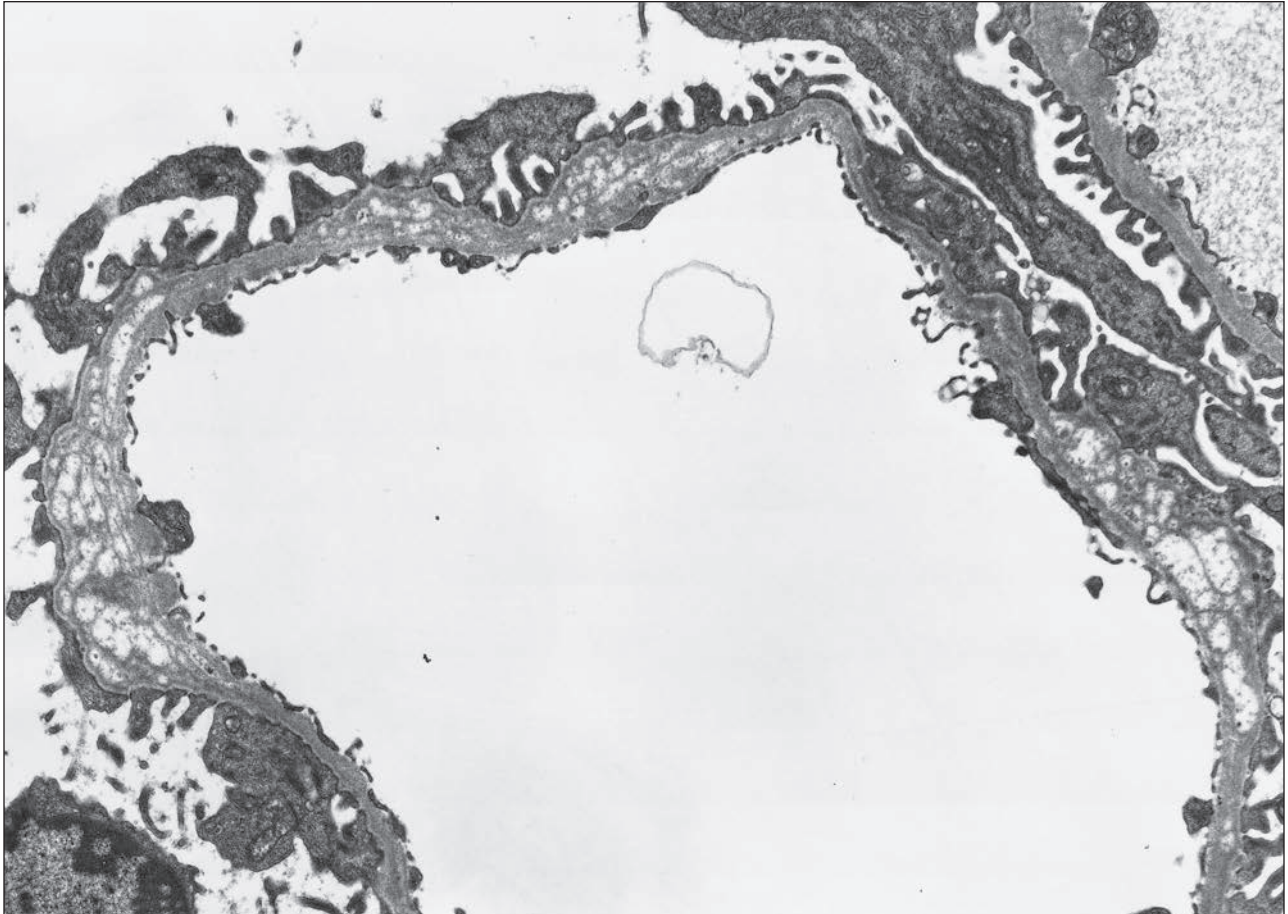


FIGURE 27.27 Electron microscopy shows the glomerular basement membrane in GSD-I to be frequently lamellated, incorporating irregular lucencies and fine granules. ($\times 12,000$.) (Courtesy of Dr. R. Verani.)

Pathogenesis and Treatment

The *G6PC* gene encoding G6Pase- α is located on chromosome 17q21, and more than 85 mutations in the catalytic subunit have been identified in patients with GSD-Ia; a stringent genotype-phenotype correlation does not exist although some missense mutations are associated with partial residual enzyme activity (144,149). More than 81 mutations in the *SLC37A4* gene on chromosome 11q23, which encodes G6PT, are responsible for GSD-Ib (non-Ia) (143). Both conditions result in multiorgan system impairment. Dietary control and uncooked starch may ameliorate dysfunction and promote normal growth but do not prevent all of the long-term complications (144,145,150). G6Pase- α is expressed in the proximal tubules, and impaired energy production due to a defective enzyme can result in epithelial damage, which can lead to elevated TGF- β synthesis; increased tubular TGF- β has been demonstrated in the kidneys from a GSD-I child and G6Pase- α -deficient mice. Renal fibrosis and oxidative stress, mediated by up-regulation of the angiotensin and TGF- β pathway, may contribute to nephropathy in GSD-I, implying a potential benefit from antioxidant therapy (147,151,152). Angiotensin-converting enzyme (ACE) inhibitors decrease the GFR and can slow the progression from glomerular hyperfiltration to microalbuminuria but not to proteinuria, highlighting the importance of early intervention. Kidney transplantation has been used for those

who develop ESRD, although glucose metabolism will not be improved. Conversely, while liver transplantation corrects most metabolic derangements, its effect on renal disease is uncertain. Combined liver/kidney transplantation may be indicated, but posttransplant complications have been noted (153,154). Gene therapy for GSD is currently being explored (155).

Kidney involvement in other GSD subtypes is limited. Renal tubules in GSD-II (acid maltase deficiency) accumulate glycogen without functional impairment. Acute tubular necrosis secondary to rhabdomyolysis has been reported in McArdle disease (GSD-V) (156,157).

PEROXISOMAL DISORDERS

Peroxisomes are single membrane-bound organelles that are found in nearly all cells and participate in β - and α -oxidation of fatty acids; the synthesis of bile acids, cholesterol, and plasmalogens; as well as amino acid and purine metabolism. Disorders are grouped as those that affect single peroxisomal enzymes and as biogenesis disorders (assembly deficiencies) in which the organelle fails to form normally, resulting in defects that involve multiple peroxisomal functions (158). Defects in peroxisomes cause multiorgan disease that often involves the nervous system. Those discussed here include renal abnormalities.

Zellweger Syndrome

Of the peroxisome biogenesis disorders, Zellweger syndrome (ZS) (cerebrohepato-renal syndrome) is the most severe and caused by various mutations in at least 13 different *PEX* genes that encode peroxins, proteins involved in different stages of peroxisomal protein import, and/or the biogenesis of peroxisomes. Peroxisomal enzymes, synthesized in the cytosol, fail to be incorporated into peroxisomes, resulting in a complete deficiency of functional peroxisomes and all peroxisomal functions (159). *PEX1* mutations are most common in ZS, and those that induce premature stop codons correlate with the most severe phenotype and shortest survival (160). Peroxisomes are markedly reduced and sometimes absent in the kidney, liver, and other organs (161). Infants are affected at birth and show severe hypotonia, feeding disability, brain and hepatic dysfunction, periarticular calcifications, and characteristic facies. Elevated very long-chain fatty acids in blood and tissues are diagnostic, but confirmation of “ZS spectrum” patients may require complementation analysis or *PEX* gene testing (162,163).

More than 90% of patients have renal cortical cysts, often of glomerular origin, that may develop in utero and vary from microscopic dimensions to several centimeters in size (Figs. 27.28 and 27.29) (158,164). Most patients die within the 1st year of



FIGURE 27.28 Autopsy kidney from an infant with Zellweger syndrome shows prominent fetal lobulation and numerous small, thin-walled cysts in the peripheral cortex and subcapsular area.

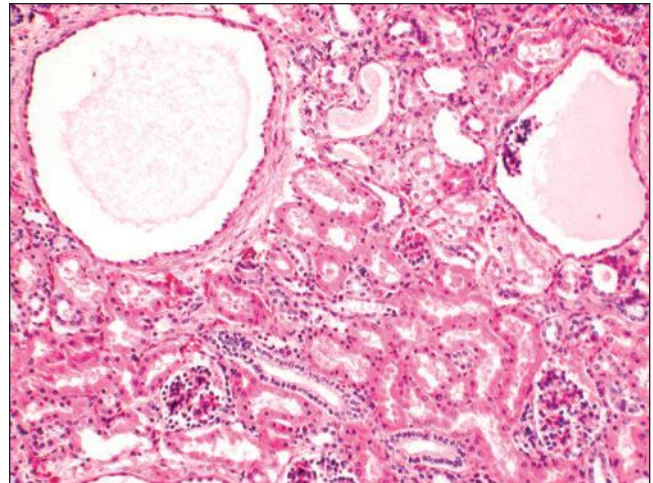


FIGURE 27.29 Microcysts of both tubular and glomerular origin are evident in the cortex of a Zellweger kidney without significant functional implication. (H&E; $\times 100$.)

life. Although the renal cysts are usually asymptomatic and renal function is usually normal, occasional instances of albuminuria, aminoaciduria, and mild azotemia have been described. A high incidence of hyperoxaluria, occasionally associated with urolithiasis and nephrocalcinosis, has been observed (165).

The hypotonia, hepatic dysfunction, facial dysmorphism, and renal cysts of Zellweger could be confused with the entity of glutaric aciduria type 2 (multiple acyl-CoA dehydrogenase deficiency), a mitochondrial electron transfer disorder, but a characteristic organic acid pattern in the urine establishes the latter diagnosis. Renal anomalies in glutaric aciduria type 2 may be dramatic and include extensive cortical and medullary cyst formation, sometimes with dysplastic changes (166).

Adult Refsum Disease

Adult (classic) Refsum disease (heredopathia atactica polyneuritiformis), a rare autosomal recessive disorder, results from an abnormal accumulation of phytanic acid owing to a defect in phytanoyl-CoA hydroxylase (PhyH). Most patients harbor mutations in the *PHYH* gene, although in a subset, mutations have been found in *PEX7*, which encodes the peroxisomal targeting signal receptor that is required for the import of PhyH into peroxisomes (167). Heterozygotes, with approximately 50% enzyme activity, do not accumulate phytanic acid.

Phytanic acid is a 20-carbon, branched-chain fatty acid derived from phytol, a component of chlorophyll. The human source of phytol and phytanic acid is entirely dietary, from dairy products and animal fats. Phytanic acid is stored in plasma and tissues, mostly adipose tissue, liver, kidney, muscle, and nerve, predominantly in triglycerides, and to a lesser extent in phospholipids and cholesterol esters (168). Phytanic acid may cause cellular toxicity by mitochondrial inhibition (169,170).

Clinical symptoms usually present in late childhood as anosmia and night blindness, caused by retinitis pigmentosa. Peripheral neuropathy, cerebellar ataxia, nerve deafness, cardiac arrhythmias, and ichthyosis often occur in the following decades (171). About 35% of patients have bone abnormalities, especially in the hands and feet, that are present at birth but typically are not recognized until other disease manifestations

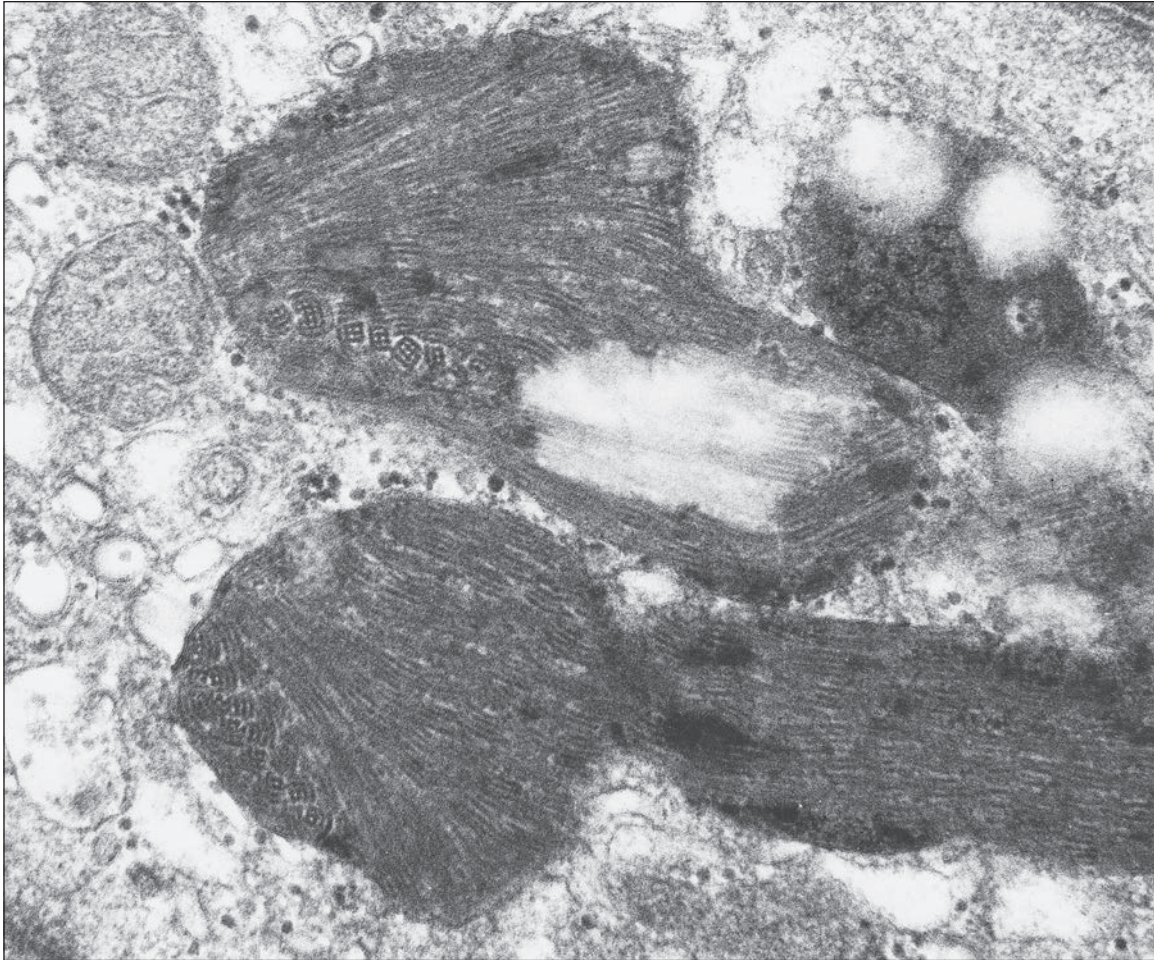


FIGURE 27.30 The tubular epithelial cells in adult Refsum disease contain crystalloid inclusions, with geometric structures. ($\times 77,000$.) (Courtesy of Dr. B. Panner.)

become evident. High concentrations of protein are present in the spinal fluid. Full expression of the disease occurs during the fourth or fifth decade, but it can manifest in childhood.

Renal involvement is demonstrated by proteinuria, mild renal insufficiency, glycosuria, and lipiduria. Elevated plasma phytanic acid esters are demonstrated by gas chromatography, but these elevations are not specific to Refsum disease since they are seen in peroxisome biogenesis disorders; molecular genetic testing is clinically available. The condition is treated by dietary restriction and lipid apheresis (172).

Pathologic Changes

Renal tubular epithelial cells, both proximal and distal, are filled with fine sudanophilic vacuoles. Glomeruli are initially minimally affected, with only mild podocyte vacuolization. Glomerular sclerosis and interstitial fibrosis correlate with renal insufficiency. Electron microscopy shows perinuclear cytoplasmic vacuoles and membrane-bound vesicles in glomerular and tubular epithelial cells. Lancet-shaped inclusions of microtubular material are present within cells of the distal tubules and loop of Henle (173); they are visible in semithin plastic sections. The inclusions resemble mitochondrial paracrystalline structures, but they are not membrane bound. They contain quadrangular microtubular arrays, shown in cross-section

to have geometric patterns (Fig. 27.30) (174). Their origin and composition are unknown, although they may be lipid organized into lamellae.

Primary Hyperoxaluria

Primary hyperoxaluria (PH) is a rare autosomal recessive calcium oxalate kidney stone disease with three recognized molecular causes (175). In type 1 (PH1), which is the most common, continuing renal deposition of calcium oxalate leads to nephrocalcinosis, recurrent nephrolithiasis, and chronic renal insufficiency. The disease is caused by a deficiency of the vitamin B₆-dependent liver-specific peroxisomal alanine-glyoxylate aminotransferase (AGT), which transaminates glyoxylate to glycine. Glyoxylate thus accumulates and is instead oxidized to oxalate and reduced to glycolate. Oxalate is not metabolized further and is eliminated from the body in the urine. Crystallization occurs from highly concentrated solutions, causing urolithiasis or nephrocalcinosis with renal tubulointerstitial damage and progressive renal functional impairment.

Primary hyperoxaluria type 1 is characterized by hyperoxaluria and hyperglycolic aciduria. Renal colic and hematuria, secondary to urolithiasis, often commence in childhood, although there is marked heterogeneity in the onset and severity, even within families. Five clinical presentations have been

recognized: (a) infantile oxalosis with early nephrocalcinosis and kidney failure; (b) childhood recurrent urolithiasis and rapidly progressive renal failure; (c) late onset with only occasional stone passage in adulthood; (d) post-kidney transplantation recurrence; and (e) presymptomatic discovery with family screening (176). Approximately 10% of patients have severe disease, with early infantile onset manifesting as failure to thrive, severe metabolic acidosis, anemia, and rapid progression to renal failure, whereas another 10% may not become symptomatic until the fourth or fifth decades (177). Progressive parenchymal deposition of calcium oxalate impairs renal function, which ultimately leads to systemic oxalosis. Complications include severe deforming osteopathy, arthropathy, cardiomyopathy, retinopathy, neuropathy, and pancytopenia. The kidneys are often small and may feel gritty on cut section (Fig. 27.31). Small, polyhedral or rhomboid, usually transparent, doubly refractile crystals are recognized histologically and accumulate in tubules, where they compress and destroy epithelium. The crystals can extend into the interstitium and induce fibrosis (Fig. 27.32).



FIGURE 27.31 Autopsy kidney of 5-year-old boy with primary hyperoxaluria who presented at 5 months with seizures and failure to thrive. The kidneys were one third the expected weight and had a gritty consistency caused by yellow-tan oxalate crystals. A 0.3-cm calculus occupies a calyx. (Courtesy of J. Siebert, Ph.D., Seattle Children's Hospital, University of Washington.)

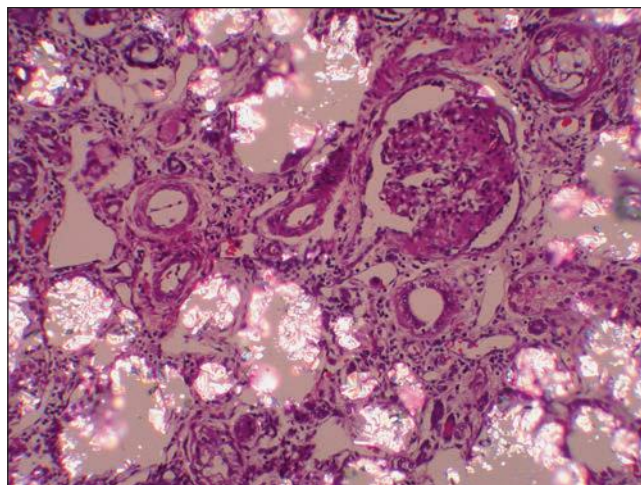


FIGURE 27.32 Renal tubules in primary hyperoxaluria are filled with rhomboid and polyhedral refractile oxalate crystals. A glomerulus is collapsed and segmentally sclerotic (same kidney as Fig. 27.31). (H&E, partial polarization; $\times 200$.)

End-stage kidneys show extensive glomerulosclerosis and widespread interstitial fibrosis that encases abundant crystals (Fig. 27.33). Stone analysis demonstrates virtually pure (>95%) calcium oxalate monohydrate (whewellite) and a whitish or pale-yellow surface with a loose, unorganized center comprised of spherical, variably sized crystal aggregates, approximately 50 μm in diameter, that resemble balls of wool (178).

PH should be suspected in any child with a renal stone, any adult with recurrent stone disease, and anyone with oxalate crystals in tissues or body fluids or with nephrocalcinosis and decreased GFR. Renal ultrasound may disclose stones and possibly medullary or diffuse nephrocalcinosis. Markedly elevated

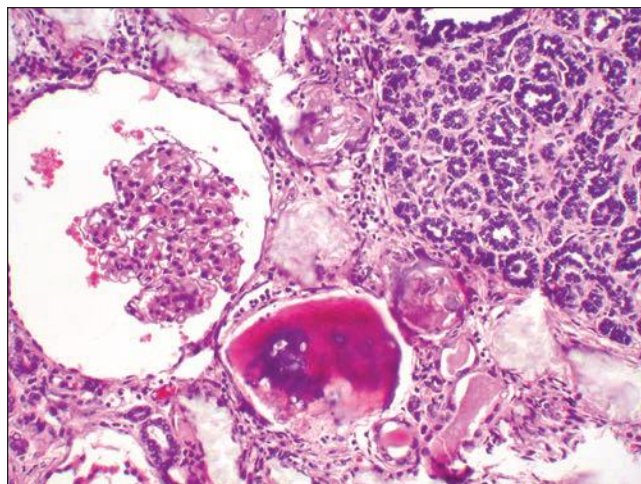


FIGURE 27.33 The end-stage kidney in primary hyperoxaluria has interstitial fibrosis and inflammation that separate crystal-filled tubules. This unique case had marked embryonal hyperplasia characterized by nodular proliferations of small basophilic tubules peppering the cortex; the patient was not dialyzed. Osseous metaplasia is present adjacent to the glomerulus. (H&E; $\times 250$.)

levels of urinary oxalate usually indicate PH in the absence of any likely causes of secondary hyperoxaluria, either increased intake (excessive star fruit and peanut ingestion), increased absorption (“enteric hyperoxaluria” related to orlistat therapy or gastrointestinal disease or surgery), or increased production (ascorbic acid or ethylene glycol ingestion). Histologic demonstration of calcium oxalate deposition in the kidney has been used for diagnosis, but it is not specific for primary disease; determining the AGT activity in a liver biopsy sample has been considered the gold standard for diagnosis. Molecular genetics has now reached a level of sensitivity and specificity that makes it useful for definitive testing and is also considered the preferred method for prenatal testing (179). More than 150 mutations have been identified in the *AGXT* gene, which resides on chromosome 2q37.3 (180,181). Mutations result in accelerated proteolysis, peroxisome-to-mitochondrion targeting defects, intraperoxisomal AGT aggregation, absence of AGT catalytic activity, and absence of both catalytic activity and immunoreactivity. The clinical heterogeneity may relate to great variability in enzymatic activity among patients but is clearly influenced by potential modifier genes, environmental factors, and genetic background, as the genotype-phenotype correlation is limited. However, some mutations that result in AGT mistargeting appear to be associated with responsiveness to pyridoxine treatment (181–186).

Type 2 hyperoxaluria (PH2) is caused by defective cytosolic glyoxylate/hydroxypyruvate reductase (GRHPR) due to mutations in the *GRHPR* gene located on chromosome 9, in which at least 15 mutations have been identified (175,187,188). Type 2 PH is rare and can be distinguished from PH1 by finding elevated glycolate and L-glycerate in addition to high oxalate levels. Clinical manifestations are less severe and consist primarily of urolithiasis, although ESRD has been documented (175,189,190). Liver enzyme analysis confirms the diagnosis. PH3 is caused by mutations in the *HOGAI* gene located on chromosome 10q24. The encoded enzyme, 4-hydroxy-2-oxoglutarate aldolase, catalyzes the synthesis of mitochondrial glyoxylate and is found primarily in the liver and kidney. Patients primarily suffer from urinary stones, but urinary oxalate concentration overlaps with PH1 and PH2. The age of onset is similar, but occasional adult presentation may imply a milder disease (191,192).

Generous fluid intake and drugs that increase the urinary solubility product are important therapeutic measures (193). Pyridoxine (vitamin B₆), which affects AGT expression or activity, lowers urinary oxalate in only about one third of patients (193). Pyridoxamine, by scavenging carbonyl intermediates in the glyoxylate pathway, inhibits oxalate biosynthesis, has been shown to decrease crystal formation in hyperoxaluric animal models, and may offer therapeutic hope for the treatment of PH (194). Combined liver/kidney transplantation, which results in enzyme replacement, has achieved better outcomes than the disappointing early results from isolated kidney transplantation, in which oxalate deposits constantly recurred in the graft (179,195–197). Preemptive liver transplantation may be considered in some settings (198).

MEMBRANE TRANSPORT DISORDERS

Functional tubular abnormalities take the form of both specific defects in solute resorption and generalized disorders of proximal tubular transport. Most specific transport

defects are heritable and are not associated with structural abnormalities.

Fanconi syndrome is a heterogeneous disorder of proximal tubular transport, by definition comprising aminoaciduria, glucosuria, and phosphaturia. Children develop hypophosphatemic, vitamin D-resistant rickets; adults develop osteomalacia. The disorder commonly includes proximal tubular acidosis, impaired urine concentration, and impaired resorption of potassium, urate, and citrate. Fanconi syndrome occurs as a primary idiopathic disease (Lignac-de Toni-Debré-Fanconi syndrome), a heritable tubular defect, or a secondary manifestation of a recognized heritable metabolic disease.

Acquired Fanconi syndrome is the result of a variety of toxic and immunologic renal tubular injuries. The renal manifestations are largely the same in all forms. So-called incomplete Fanconi syndromes with, for example, only renal glycosuria and aminoaciduria may be caused by the same basic tubular disturbances as occur in the complete syndrome.

Fanconi syndrome seems to be the final common manifestation of assorted cellular perturbations that interfere with tubular epithelial function by affecting solute uptake and/or excretion via interference with receptor-mediated endocytosis or passage along the endocytic apparatus (199). Diverse etiologies can affect the delicate balance that maintains tubular function; these include (a) altered energy production, for example, mitochondrial dysfunction that inhibits Na⁺, K⁺-ATPase and thereby impedes Na⁺-dependent transport; (b) abnormal apical or basolateral membrane transport molecules, for example, mutations in *SLC6A19* or *GLUT2*; and (c) interference with membrane trafficking and recycling, for example, *CLCN5* mutations that interrupt the activities of megalin and cubilin. As new discoveries are made, the so-called idiopathic Fanconi syndrome may cease to exist.

Inherited Fanconi Syndrome Idiopathic Fanconi Syndrome

Primary Fanconi syndrome, a diagnosis of exclusion, occurs in both adults and children as familial traits that appear to be predominantly autosomal dominant (200). Sporadic cases without identifiable nephrotoxicity are not necessarily genetic. Although a defined genetic defect is currently unknown, this form of the syndrome can only be diagnosed when no underlying metabolic disease exists and all possible acquired causes have been excluded. The demonstrated absence or partial loss of proximal tubular brush border is common to all forms of Fanconi syndrome. The occurrence of heavy glycogen deposition (Armanni-Ebstein lesion), similar to that in diabetes mellitus, has been described in the pars recta of some patients with Fanconi syndrome (201); this phenomenon is rarely seen in current practice. Clinical manifestations in children include failure to thrive, growth retardation, polydipsia, polyuria, rickets, and unexplained fever. Adults have weakness and bone pain, with polydipsia and polyuria.

Cystinosis

Cystinosis, a rare autosomal recessively inherited lysosomal transport disorder, is the most common identifiable cause of Fanconi syndrome in children. It has an estimated incidence of 1 in 100,000 to 200,000 live births, although higher incidences are reported in some regions of France, Germany, Quebec, and the United Kingdom (202). More than 90 mutations have been

identified in the responsible gene, *CTNS*, which resides on chromosome 17p13 and encodes cystinosin, a ubiquitous lysosomal transmembrane protein that facilitates efflux of cystine from the lysosome (203). It differs thereby from other lysosomal storage diseases, which are caused by deficiencies in lysosomal acid hydrolases. Recently identified is a second cystinosin isoform, cystinosin-LKG, that results from alternative splicing and localizes to lysosomes and other cellular compartments including the plasma membrane, endoplasmic reticulum, and small, nonlysosomal cytoplasmic vesicles (204). All mutations currently described alter the sequence of both isoforms; however, the function of cystinosin-LKG remains unknown.

CLINICAL PRESENTATION

Cystinosis is clinically classified into three forms. Infantile cystinosis is nephropathic, with early onset of Fanconi syndrome and progression to ESRD usually within the first decade of life. Less severe variants probably form a continuum, but two distinct subtypes include (a) intermediate cystinosis (“juvenile” or “late onset”), which causes a mild nephropathy with slow progression of renal impairment, without Fanconi syndrome; and (b) ocular or nonnephropathic cystinosis (“benign” or “adult”), which is characterized by ocular findings without renal involvement.

Free cystine, from lysosomal protein hydrolysis, increases in cells to concentrations between 10 and 1000 times normal. Cystine accumulation and crystal formation vary considerably among tissues and may be related to different rates of protein degradation and cell turnover. The diagnosis can be made either by demonstrating increased concentrations of cystine in peripheral leukocytes and other cells or by demonstrating cystine crystals in the cornea by slit-lamp examination and in bone marrow macrophages, conjunctiva, intestinal mucosa, and kidney by polarization microscopy. In contrast to cystinuria, urinary cystine levels are not elevated. Diagnosis of fetal disease can be made by measurement of cystine in amniotic fluid, amniocytes, or chorionic villi. Molecular analysis of the *CTNS* gene provides confirmation and can be used for prenatal assessment (205).

Children with infantile nephropathic cystinosis develop polyuria, polydipsia, dehydration, and febrile episodes within the first year of life. Features of Bartter syndrome and nephrogenic diabetes insipidus have preceded the development of Fanconi syndrome in occasional patients (206,207). Proximal tubular dysfunction, with aminoaciduria, glycosuria, phosphaturia, and renal tubular acidosis, leads to vitamin D–refractory rickets and growth retardation. Patients may develop muscle weakness as a consequence of myopathy. Glomerular impairment leads to end-stage renal failure by 10 years of age. With renal replacement therapy, widespread end-organ damage may develop from cystine deposition in the eyes, liver, endocrine glands, and muscular and central nervous systems, resulting in late complications of diabetes mellitus, male infertility, hypothyroidism, and coronary artery disease (208–210). Photophobia and abnormal retinal pigmentation are not uncommon and typically the only manifestation in the non-nephronic/adult form. Caucasian children have noticeably less skin and hair pigmentation than their unaffected siblings as a consequence of defective melanin synthesis; the skin and hair of patients from darkly pigmented ethnic groups appear normally pigmented. The juvenile form is uncommon, generally

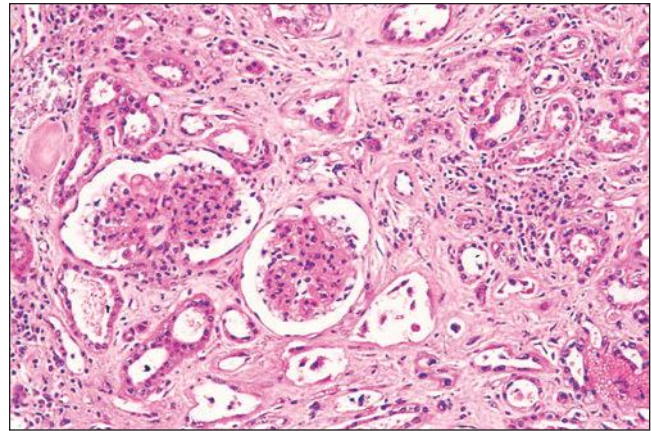


FIGURE 27.34 Renal cortex from an 8-year-old boy with cystinosis showing considerable atrophy of the tubules, interstitial fibrosis, and glomerular solidification. (H&E; $\times 200$.)

presenting after 10 years of age with renal disease ranging from mild proximal tubulopathy to apparent nephrotic syndrome. The renal disease usually progresses more slowly than the infantile form, with ESRD developing in the second or third decade (202,211), although the deterioration rate can differ tremendously among family members (212).

PATHOLOGIC CHANGES

The ultimate histopathologic abnormality in all forms of Fanconi syndrome is tubular atrophy with interstitial fibrosis, variable inflammation, and progressive glomerular sclerosis (Fig. 27.34). Morphologic complications include the occasional development of nephrocalcinosis. The tubular atrophy has been shown by microdissection to be particularly pronounced in the first part of the proximal tubule, in which a shortened and narrow postglomerular segment has been described as the “swan-neck deformity” (Fig. 27.35) (213). This abnormality likely reflects progressive apoptotic cell death and a moderately severe degree of secondary tubular atrophy; it is neither specific to Fanconi syndrome nor an explanation of its functional derangements but may lead to an increased incidence of atubular glomeruli (214). Among the earlier tubular changes, loss of brush border accompanies cell shortening, and the generalized absence of brush border mentioned in the description of idiopathic Fanconi syndrome may well be a secondary phenomenon. Other secondary changes include cellular vacuolization and basement membrane calcification, the latter perhaps a consequence of renal insufficiency and secondary hyperparathyroidism.

Cystinosis is distinguished by the deposition of cystine crystals, predominantly in the interstitium (Fig. 27.36). Large extracellular collections of crystals lie among the tubules in the cortical labyrinth. The crystals, easily dissolved from the tissues in aqueous solutions during tissue processing, are preserved in alcoholic solutions. They have a hexagonal, rhombohedral, or polymorphous configuration; are birefringent; and, even when sparse, are demonstrable by polarization microscopy in frozen sections. A few crystals may be present in tubular and glomerular epithelial cells, and clefts are identified by electron microscopy in podocytes and mesangial cells (Fig. 27.37) (215,216).

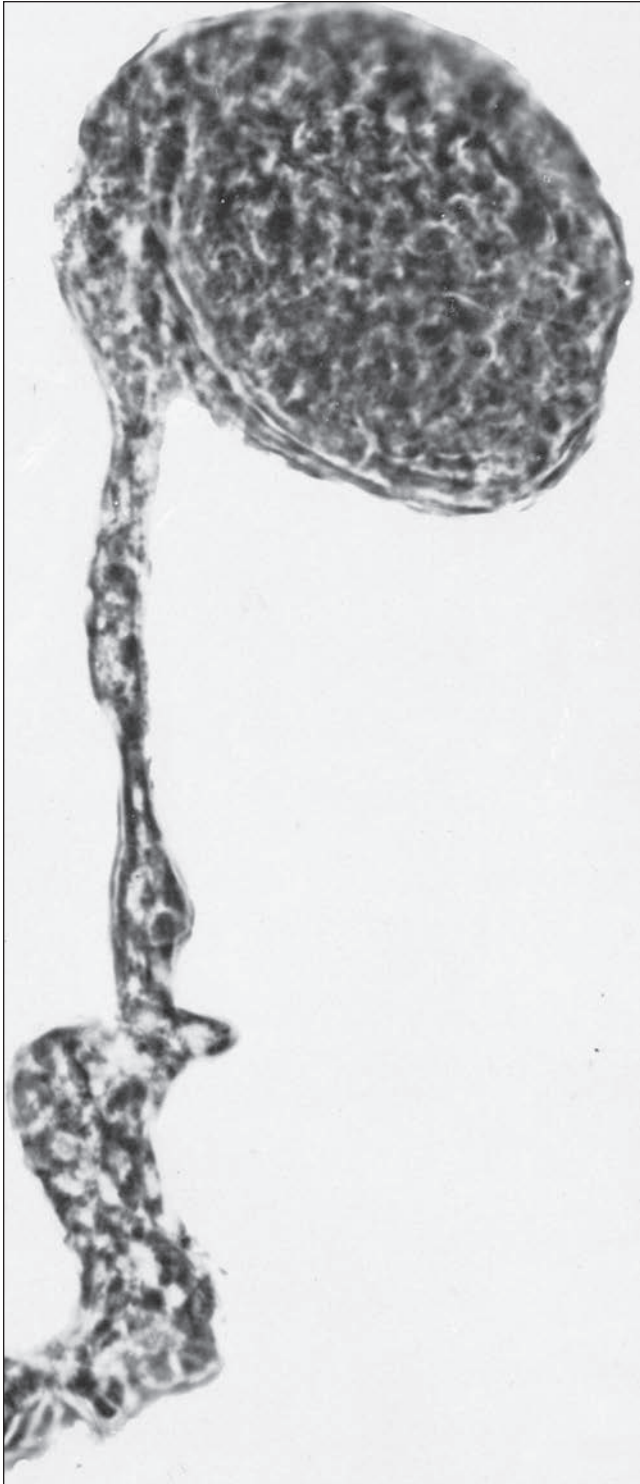


FIGURE 27.35 “Swan-neck” appearance of a dissected proximal convoluted tubule. The thinned early part of the proximal convoluted segment is apparent (glomerulus at top). (Courtesy of Dr. E. M. Darmady.)

Early and distinctive abnormalities in cystinosis are multinucleated podocytes (Fig. 27.38) and, occasionally, tubular and parietal epithelial cells, a finding not unique to cystinosis but helpful in diagnosis (216,217). Similar cells occur in noncystinotic Fanconi syndrome and few other conditions.

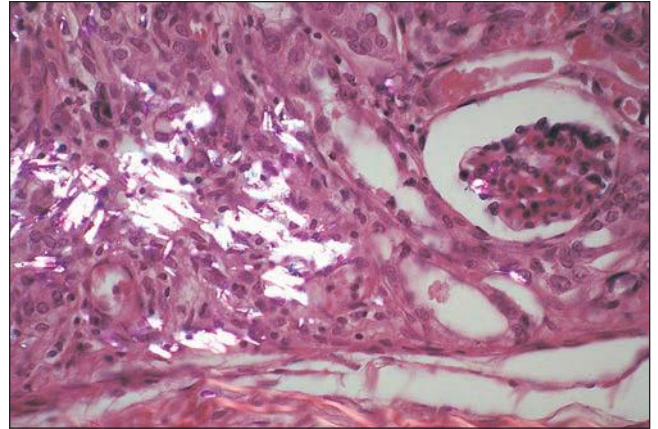


FIGURE 27.36 Alcohol-fixed kidney section from a child with cystinosis showing interstitial deposition of rectangular refractile cystine crystals. A rare crystal is also evident in the glomerulus. (H&E, partial polarization; $\times 100$.)

Glomerular podocytes in cystinosis are sometimes opaque on light microscopic examination of semithin sections of osmicated, plastic-embedded tissue; transmission electron microscopy confirms the observation, showing the dark cells to be filled with electron-dense granular material (215). Dark cells

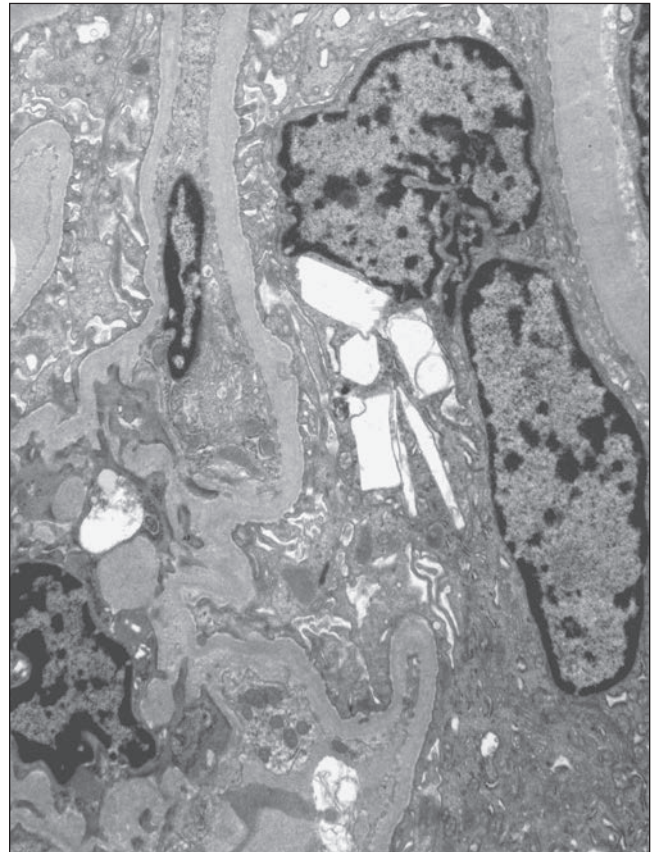


FIGURE 27.37 Electron micrograph shows an epithelial cell from a glomerular tuft that contains rectangular and spindle-shaped clear areas, presumably once occupied by cystine. ($\times 4000$.)

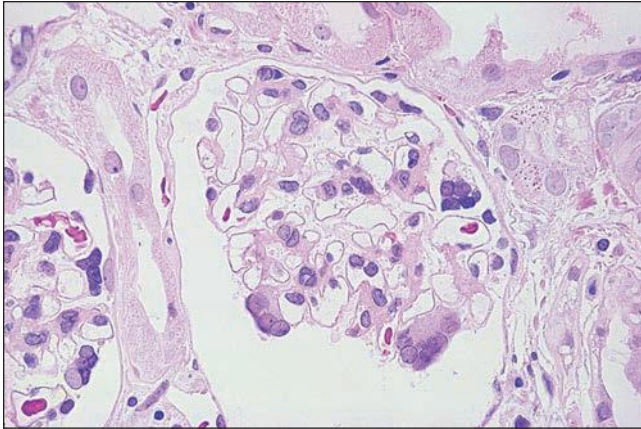


FIGURE 27.38 Glomeruli from a child with cystinosis showing multinucleated visceral epithelial cells. (H&E; $\times 160$.)

are present rarely in tubules and occasionally in the interstitium. The phenomenon is probably caused by a reaction between osmium and intracellular cystine; electron-probe analysis shows that the dark cells contain sulfide, a constituent of cystine. Recently, it was suggested that they represent autophagic vesicles, which are increased in cystinosis (218).

Intermediate, or juvenile, cystinosis causes predominantly glomerular disease, with mesangial hypercellularity, increased matrix, capillary wall thickening, and segmental and global glomerular sclerosis; multinucleated podocytes may be unapparent (212). Crystal deposition may only be detected by electron microscopy, which also demonstrates podocyte foot process effacement.

PATHOGENESIS AND TREATMENT

Cystinosin, a seven-transmembrane-domain protein, is a highly specific H^+ -driven cystine transporter (219). Mutations usually associated with infantile cystinosis cause premature termination of cystinosin and tend to abolish transport of cystine, whereas those associated with milder clinical phenotypes tend to reduce transport (220). The most common mutation is a 57-kilobase deletion found typically in people of northern European descent (203). A minority of patients lack detectable alterations in the *CTNS* gene, implying the presence of mutations in noncoding regions or in other genes that encode proteins with which cystinosin interacts (212). The etiology of Fanconi syndrome in cystinosis is not understood, but cystinotic cells undergo apoptosis at two- to fourfold higher rates than controls, and proposed mechanisms for cell damage include altered cellular oxidation, impaired ATP and glutathione synthesis, and abnormal cysteinylolation of cytosolic enzymes (221–223). Abnormal mitochondria and increased mitochondrial autophagy have been shown in nephropathic cystinotic proximal tubular epithelial cells, which may contribute to increased apoptotic activity (218). Recent demonstration of the cytosolic expression of cystinosin-LKG supports the notion that the disease is not strictly a lysosomal storage disorder (204). Kidney damage results not solely from cystine accumulation but is influenced by yet undetermined modifier genes. Observations supporting this inference include the variable outcome within families, the inconsistent phenotype-genotype correlation, and the dependence upon genetic background for the development of renal dysfunction in the *ctns*^{-/-} mouse (224).

Treatment with oral cysteamine can decrease or significantly delay the complications of cystinosis, although even with early initiation and good compliance, Fanconi syndrome is not prevented and late complications, including ESRD, develop (208,209,225). Kidney transplantation improves survival in cystinosis, although extrarenal deposition of cystine continues. Cystine deposits can appear in allografts but are host mononuclear cell in origin and do not interfere with function. Renal allograft survival has been good, allowing patients to develop other serious cystinotic complications, including vision impairment, peripheral myopathy, and diabetes mellitus (226). Recent demonstration of kidney protection from hematopoietic stem cell therapy in *ctns*^{-/-} mice raises hope for eventual development of bone marrow transplantation or corrected stem cell therapy as new treatment possibilities (227).

Dent Disease

Dysfunction of renal proximal tubules with low molecular weight proteinuria, hypercalciuria, nephrocalcinosis, nephrolithiasis, and rickets characterizes Dent disease. Renal function may begin to decline in the teenage years, and renal failure eventually develops in about two thirds of patients, but the progression is varied (228). Proximal tubular dysfunction is variable but may become evident in the neonatal period. Isolated nephrotic syndrome, notably without hypoalbuminemia, has been reported (229,230). Hypercalciuria, the hallmark of Dent disease, can be detected in the first year of life, but stone formation may not be present in pediatric patients. Some patients complain of night blindness secondary to increased loss of retinol-binding protein in the urine and retinol deficiency, which is responsive to vitamin A supplements (231,232). Hypophosphatemic rickets is not universal but can be one of the first clinical presentations. The disease is generally found in males, but milder features of low molecular weight proteinuria and hypercalciuria are evident in 50% to 75% of female carriers with end-stage renal failure occurring rarely (233). Different clinical features predominated in the original descriptions, but it is now recognized that Dent disease and its “variants”—X-linked recessive hypophosphatemic rickets and X-linked recessive nephrolithiasis—are a single disorder caused by inactivating mutations in the *CLCN5* gene, located on chromosome Xp11.22; nearly 150 mutations have been reported with no apparent genotype-phenotype correlation (234). Interestingly, mutations in *OCRL1*, the gene responsible for Lowe syndrome (see following), have been identified in approximately 15% of patients with a classic Dent disease phenotype (the so-called Dent-2 disease) who lacked mutations in *CLCN5* (233,235,236). Additional genes likely harbor mutations, as normal *CLCN5* and *OCRL1* have been found in 25% to 35% of patients with clinically indistinguishable Dent disease. No mutations have been identified in the *CLC5*-endocytic pathway-associated proteins, *CLC4* and *CFL1*, in the endosomal associated sodium-proton exchanger, *SLC9A6* or *TMEM27*, a proximal tubular protein (233,237).

PATHOLOGIC CHANGES

Light microscopic findings are progressive but nonspecific (238,239). Normal glomeruli and well-preserved tubules are typical in childhood, but medullary tubular calcifications may be seen (239). Pathologic changes in older individuals of both sexes include hyaline casts, tubular epithelial degeneration, tubulointerstitial calcium deposition, mild interstitial

fibrosis with tubular atrophy, and occasionally, glomerular hypercellularity with progressive global glomerulosclerosis and hyalinosis. Rare cases have shown primarily focal segmental glomerulosclerosis (229,230). Electron microscopy fails to show ultrastructural abnormalities in proximal tubular cells, and foot process effacement is usually minimal (229,238).

PATHOGENESIS

The chloride-proton exchanger *CLCN5* is predominantly expressed in the kidney, where it is found in subapical endosomes of cells of the proximal tubule, thick ascending limb (TAL) of the loop of Henle, and intercalated cells of the collecting ducts (240). Small amounts of *CLCN5* are also found on the apical surface of proximal tubule cells where it may engage in endocytosis and microtubular transport (241). *CLCN5* is believed to control the accumulation of chloride ions into endosomes, which could play a crucial role in proximal tubule endocytosis (242). Defects in *CLCN5* impair lysosomal processing and interrupt trafficking in proximal tubule cells, with loss of megalin and cubilin at the brush border and subsequent escape of their ligands in the urine (243,244). Abnormalities in membrane recycling could explain other defects, such as phosphaturia, aminoaciduria, and glycosuria. A loss of *CLCN5* in the TAL, a major site of calcium reabsorption, may account for the hypercalciuria. Alternatively, disturbances in renal phosphate and calcium handling might be secondary to symptoms of impaired renal endocytosis and metabolism of calcitropic hormones (245). Disruption of the interaction between *CLCN5* and H^+ -ATPase appears to alter its polarity or expression in proximal tubular and intercalated cells and may be implicated in urinary acidification deficits in Dent disease (238).

There is no cure for Dent disease, but thiazide diuretics have been helpful in reducing urinary calcium excretion (246,247). Recurrent stone formation has not occurred in renal allografts. The functional disturbances produced by *CLCN5* mutations, analogous to *CFTR* mutations in cystic fibrosis, suggest a possible role for pharmacologic therapy that rescues dysfunctional channels (241).

Mitochondrial Disorders

Oxidative phosphorylation is a ubiquitous metabolic pathway that supplies energy to most tissues. Genetic defects in

oxidative phosphorylation, therefore, produce a variety of clinical symptoms involving multiple organ systems, most typically the neuromuscular system. Renal involvement is noted in 5% to 50% of patients with respiratory chain deficiency, with the first symptoms usually developing in the neonatal period or before age 2 (248–251). The most common kidney presentation in a mitochondrial disorder is a proximal tubulopathy with Fanconi syndrome, although other disorders, including glomerular disease, chronic tubulointerstitial nephritis, and a Bartter-like phenotype have been reported (249,250,252–259).

Effects on active transport in the nephron are not surprising, given the prominence of mitochondria in proximal tubules. Mitochondrial defects result in deficient ATP to drive the sodium-potassium ATPase pump that maintains the sodium gradient across the proximal tubular epithelium and is responsible for all proximal tubular cell activities. Fanconi syndrome in mitochondrial disease is usually part of a multi-system disorder with extrarenal neuropathic, myopathic, endocrine, or cardiac symptoms but can be the initial or isolated presentation (260,261) suggesting that lactaciduria should be investigated in all patients presenting with idiopathic Fanconi syndrome (249). It is occasionally seen with specific syndromes of respiratory chain deficiency, including Leigh, Kearns-Sayre, and Pearson syndromes (249,250).

PATHOLOGIC CHANGES

The renal biopsy in patients with tubulopathy shows generally intact glomeruli with nonspecific tubular changes, including dilation, cast formation, and epithelial atrophy. The so-called “granular swollen epithelial cells” characterized by enlarged cells with fuchsinophilic (Masson trichrome red) PAS-negative cytoplasmic granules have been observed in distal tubules and collecting ducts (262). Histochemical assessment of mitochondrial enzyme activity (cytochrome c oxidase [COX] and succinate dehydrogenase [SDH]) in frozen sections may show a selective decrease in mitochondrial DNA–encoded enzymes, with preservation of nuclear DNA–encoded enzymes, in patients with mtDNA depletion (263). Giant or abnormal mitochondria with paracrystalline arrays or deficient, circular, or otherwise aberrant cristae are often evident with ultrastructural examination; however, their absence does not exclude the diagnosis (Fig. 27.39). Moreover, similar mitochondria,

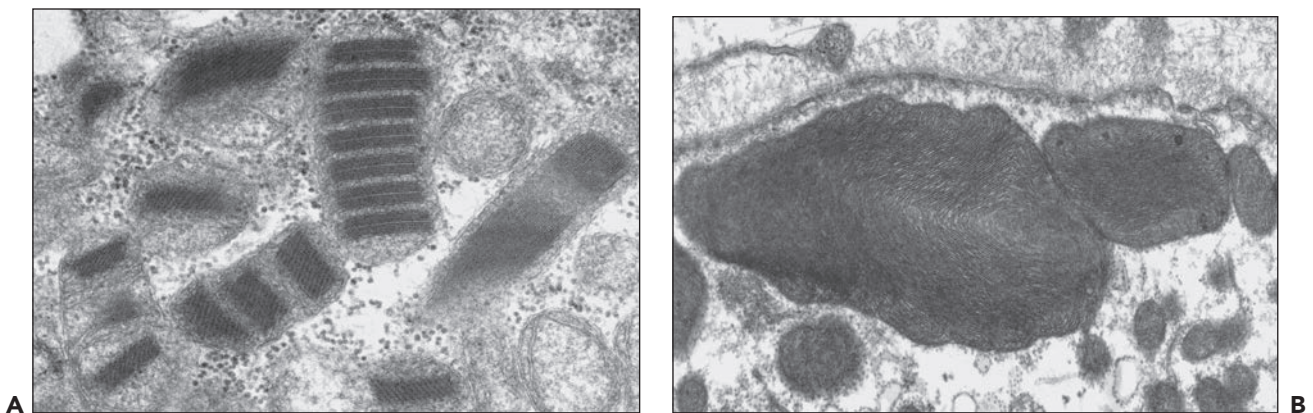


FIGURE 27.39 Tubular epithelial cells in this patient with myopathy and Fanconi syndrome contain enlarged, irregular mitochondria with paracrystalline arrays (**A**) and dense circular cristae (**B**). ($\times 16,000$.)

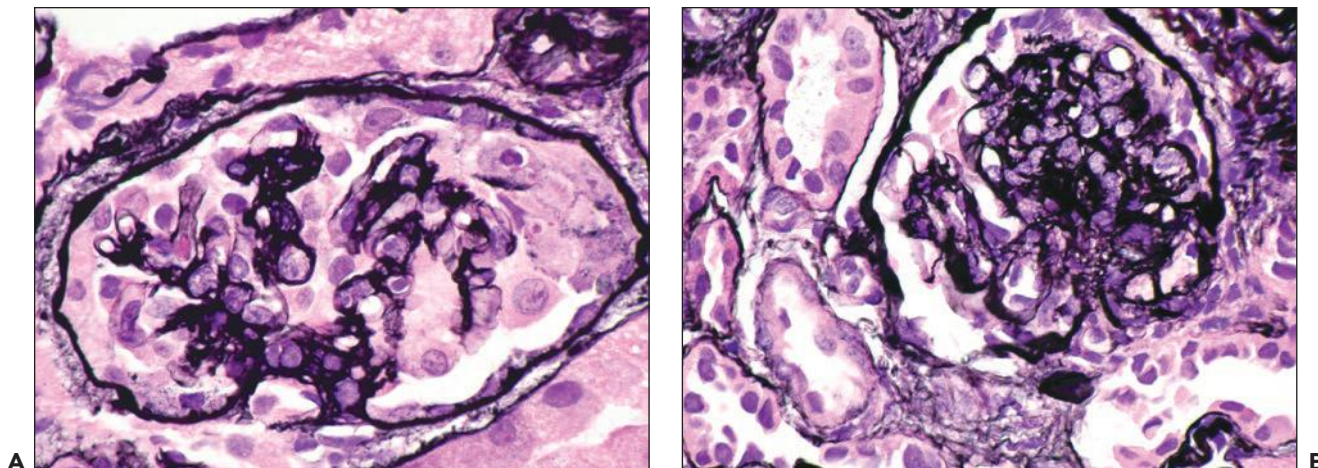


FIGURE 27.40 Glomerular changes in a patient who presented with infantile nephrotic syndrome, congenital sensorineuronal hearing loss, mild hypotonia, and developmental delay include collapse with hyperplasia of the surrounding podocytes (**A**) and mesangial hypercellularity with early sclerosis (**B**). The patient was proven to have primary CoQ10 deficiency. (H&E-silver methenamine;×400.)

with associated tubular dysfunction, can be observed in the presence of certain drugs and toxins, including antiepileptics, antimicrobials, antiretrovirals such as tenofovir, heavy metals and alcohol, as well as systemic illnesses such as diabetes and Wilson disease, and can be induced by hypoxic injury and hypertonic fixatives. Diffuse mesangial hypercellularity and collapsing glomerulopathy in infants (Fig. 27.40) and focal segmental glomerulosclerosis in young children and adults are described in those who present with steroid-resistant nephrotic syndrome (251,258,259,264). Podocytes are hyperplastic or depleted and display dysmorphic mitochondria and variable foot process effacement.

DIAGNOSIS

The diagnosis is suspected in any patient with a complex association of symptoms involving unrelated organs. Renal symptoms are more common in children than in adults. Proximal tubulopathy is often moderate, but isolated hyperaminoaciduria, glycosuria, or hyperphosphaturia has been reported (251). Respiratory chain defects lead to a rise in blood lactate, pyruvate, and ketone bodies. Impaired proximal tubule reabsorption may lower blood lactate to normal levels; urinary lactate is increased in Fanconi syndrome, where the lactate/creatinine ratio is higher than in healthy individuals or those with other renal disease (265). Therefore, a normal plasma lactate concentration does not rule out a mitochondrial disorder. Other methods of evaluation include polarographic and spectrophotometric studies that evaluate isolated mitochondrial oxygen consumption and enzyme activities. Respiratory chain disorders are genetically heterogeneous, and while molecular testing is often viewed as definitive, confirmation remains challenging due to the large number of genes, the two-genome complexity (mitochondrial [mt] DNA—matrilineal inheritance and nuclear DNA—autosomal recessive, autosomal dominant, and X-linked inheritance), and the variable proportion of pathogenic mitochondria (heteroplasmy). The *de novo* mutation rate is high, resulting in apparently sporadic cases (266). Disease-causing mutations have been identified for only a minority of patients. If mtDNA mutational screening is negative,

recognition of a “classic” clinical syndrome can direct further molecular testing. Renal presentation with glomerular involvement may point toward mtDNA mutations in the genes encoding tRNA^{LEU} and CoQ₁₀ biosynthesis defects. Nuclear gene mutations are becoming more recognized and may be responsible for the majority of respiratory chain deficiencies (248,266).

Lowe Syndrome

Lowe oculocerebrorenal syndrome comprises congenital ocular abnormalities, severe cerebral dysfunction, and renal tubular dysfunction similar to that of Fanconi syndrome (267). The ocular abnormalities include microphthalmos, glaucoma, buphthalmos and, most consistently, congenital bilateral cataracts. Cerebral dysfunction results in mental retardation, muscular hypotonia and hyporeflexia, and behavior disorders. Boys often have facial dysmorphism characterized by elongation with microcephaly, deep-set small eyes, and frontal bossing. The renal findings include tubular acidosis, aminoaciduria, tubular proteinuria, and phosphaturia. Glycosuria is usually slight or not detected (268). The renal tubular dysfunction can vary significantly and tends to worsen with age, although the affected children are often rachitic and have growth retardation. Hypercalciuria and nephrocalcinosis have been described (268,269). Proteinuria may dominate, and elevated urinary excretion of low molecular weight proteins is typically the earliest renal manifestation and can be seen in neonates (270). Lowe syndrome is one of the causes of congenital and early infantile nephrotic syndrome. Although the onset is commonly in infancy, slowly progressive disease may lead to renal failure after several decades.

PATHOLOGIC CHANGES

Renal morphologic features may be normal or minimally altered at first, with tubular dilation and loss of brush border (271,272). Mitochondrial swelling in proximal tubules has been described (273). The lesion progresses to tubular atrophy and interstitial fibrosis (274). Glomerular involvement develops early, with basement membrane thickening and splitting, widening of the foot process, and progressive glomerular sclerosis. The changes are secondary and nonspecific.

PATHOGENESIS

The majority of cases in this rare X-linked recessive disorder are boys. Female carriers may have lenticular abnormalities that are detected by slit-lamp exam; full expression in females has been related to a balanced X:autosome translocation (267). At least 100 mutations have been identified in the gene responsible for Lowe syndrome, *OCRL1*, located in the Xq25-26 region (275). Laboratory diagnosis is made by detecting a deficiency of the encoded enzyme, phosphatidylinositol 4,5-bisphosphate 5-phosphatase, in cultured fibroblasts. Molecular genetic testing is clinically available and can be used for confirmation. Assay of enzyme activity is the preferred approach for prenatal testing unless the mutation in the family has been defined previously. Primarily detected on vesicular structures throughout the endosomal system and the Golgi complex, OCRL is also present in plasma membrane at adherens and tight junctions and late-stage endocytic clathrin-coated pits (276). Most recently, OCRL has been shown to localize to the basal body and transition zone of primary cilia, including renal tubule cells and fibroblasts from Lowe patients, where cilia were shortened (277). Human cells deficient in OCRL function have defects in endocytic trafficking, actin polymerization, establishment of cell polarity, cytokinesis, and possibly primary cilia signaling (278). Aberrant trafficking and junctional dysregulation can cause renal tubular disorders (279) and could facilitate progression of tubulointerstitial nephritis to secondary FSGS and ESRD (280). While the exact mechanism is not yet deciphered, the Lowe phenotype is thought to be the consequence of both the enzyme deficiency and the accumulation of phosphatidylinositol (4,5) bisphosphate. Phenotypic heterogeneity is likely influenced by modifying factors (i.e., compensatory phosphatases, interacting proteins, genotypic background) as complete loss of enzyme activity is seen in mild and severe Lowe syndrome and Dent-2 disease. However, most frameshift and nonsense mutations map exclusively to exons 1 to 7 in Dent-2 disease and exons 8 to 23 in Lowe syndrome; complete deletion of the *OCRL* gene results in Lowe syndrome (281).

Fanconi-Bickel Syndrome

Originally described in 1949 and long considered a type of glycogen storage disease, interest in this rare autosomal recessive disorder has been reenergized by the discovery of mutations in the genes for facilitative glucose transporter membrane proteins (282,283). The detection of a genetic defect in the glucose transporter 2 gene (*GLUT2*) helps to disprove the postulated link to an inherited deficiency in phosphoglucomutase and will necessitate redefining “glycogen storage disease type XI.” Patients typically present at 3 to 10 months and have stunted growth, hepatomegaly secondary to glycogen accumulation, glucose and galactose intolerance, fasting hypoglycemia, and severe Fanconi syndrome, with disproportionate glycosuria. Fever, vomiting, and failure to thrive with chronic diarrhea may be evident at a younger age (284–286). Unusual features have included the absence of hepatomegaly, intestinal malabsorption, neonatal cataracts, and glomerular disease (287–289). Older patients typically develop a protuberant abdomen, moon facies, and fat deposits on their shoulders and abdomen. Growth and puberty are severely retarded, and hypophosphatemic rickets is frequent. The clinical spectrum may be broader than initially presumed, as noted in the report of two siblings without organomegaly or failure to thrive who

had only mild tubular dysfunction (290). There is no specific treatment, although symptomatic replacement therapy consisting of supplemental water, electrolytes, and vitamin D, restriction of galactose, and administration of uncooked cornstarch has improved growth.

PATHOLOGIC CHANGES

Renomegaly has been documented by imaging. The kidney may appear normal by light microscopy; however, glycogen accumulation and megamitochondria are evident in proximal tubular epithelial cells by electron microscopy (284). Glomerular disease is reported rarely as increased mesangial matrix and cellularity with segmental fibrosis and swollen podocytes (291).

PATHOGENESIS

Greater than 40 mutations in *GLUT2* (*SLC2A2*), localized to chromosome 3q26.1-q26.3, have been identified, although other genes are potentially involved in Fanconi-Bickel syndrome (288,292,293). No “hot spot” or genotype-phenotype correlation has emerged, making the molecular diagnosis laborious. Affected individuals have either homozygous or compound heterozygous mutations, and possession of a nontruncating mutation in a region predicted to confer residual *GLUT2* activity might yield a milder phenotype (290). The significance of *GLUT2* heterozygosity remains to be established, although elevated fasting glucose levels and isolated renal glucosuria have been observed (294,295).

Glucose transporter 2 is primarily involved in glucose homeostasis through its role in glucose uptake from the intestine, reabsorption by the kidney, sensing in the pancreatic β -cells, and uptake and release by the liver (296). Glucose, reabsorbed by energy-dependent transport at the apical membrane of a proximal tubule cell, is passively released into the circulation via *GLUT2* located in the basolateral membrane. Mutations in *GLUT2* are predicted to yield defective proteins with impaired function and/or localization. Interference with glucose transport out of the cell might cause tubular dysfunction by inducing an osmotic destruction of the cell, by altering driving forces of other substances, or by producing an unspecified energy problem, the latter suggested by the finding of abnormal mitochondria in tubular cells (294).

Other

Fanconi syndrome secondary to other primary diseases is much more common than idiopathic Fanconi syndrome. Additional inborn errors of metabolism that can induce Fanconi syndrome include tyrosinemia, galactosemia, hereditary fructose intolerance, and Wilson disease. In these settings, Fanconi syndrome is reversible with restriction of the offending substrate, respectively, tyrosine or phenylalanine, galactose or lactose, fructose, and copper with chelation.

Acquired Fanconi Syndrome

Acquired causes of Fanconi syndrome include a variety of toxic and immunologic renal tubular injuries that impair net proximal tubular reabsorption. In contrast to those seen with heritable diseases, acquired Fanconi syndrome is primarily an adult disease. These include drug-induced nephropathy, particularly anticancer agents, anticonvulsants, and antimicrobials (antibiotics and antiretrovirals); heavy metal intoxication; nephrotic syndrome; dysproteinemias or multiple myeloma;

and membranous nephropathy with antitubular basement membrane antibodies (297–299). A reversible Fanconi syndrome has followed renal transplantation and been associated with various malignancies, including nonossifying fibroma and lymphomas (200). Mitochondrial derangement, the generation of reactive oxygen species, and induction of apoptosis have been suggested mechanisms of cellular injury in these acquired settings (300–302).

Specialized Heritable Tubular Defects

Heritable defects in specific tubular epithelial cell transporter systems can lead to aminoaciduria, renal tubular acidosis, or phosphaturia, largely without demonstrable morphologic abnormalities. They may, however, be accompanied by secondary morphologic changes. Nephrocalcinosis, with tubulointerstitial damage, occurs early in primary distal tubular acidosis, but it is prevented by therapy to reduce acidemia and hypercalciuria. Stone disease, the common clinical manifestation of classic cystinuria, is ameliorated by bicarbonate therapy to alkalinize the urine and by high fluid intake to maintain high urine volume. Chronic interstitial disease can eventually ensue in some instances. The clinical features range from asymptomatic to life threatening. The major conditions are listed in Table 27.2 (303–313).

PURINE METABOLISM AND HANDLING DISORDERS

Uric acid is the end product of purine metabolism in humans. Purine nucleotides—specifically adenine and guanine—are synthesized from salvaged purines, from dietary purines, or de novo. Endogenous production of purines proceeds by stepwise addition of small molecules on to 5-phosphoribosylpyrophosphate (PP-ribose-P), which is formed from a sugar derivative, D-ribose-5-phosphate, in a process catalyzed by the enzyme PP-ribose-P synthetase. Another enzyme, PP-ribose-P aminotransferase, initiates a series of reactions that lead to inosine monophosphate (IMP), a hypoxanthine nucleotide and the parent compound of purines (314,315). Hypoxanthine-guanine phosphoribosyltransferase (HPRT) catalyzes the salvage synthesis of IMP and guanosine monophosphate from hypoxanthine and guanine, respectively. The absence of this critical enzyme leads to the accumulation of xanthine and hypoxanthine, which are degraded to uric acid by xanthine oxidase.

Hyperuricemia, defined as a concentration of uric acid in blood plasma above 7 mg/dL, may be caused by overproduction, underexcretion, or both. Known causes of hyperproduction include uncommon enzymatic defects, various drugs, ethanol- and protein-rich diets, and diverse disease states such as certain malignancies or obesity (315–317). Decreased excretion because of decreased tubular secretion or increased reabsorption occurs in many situations, such as chronic lead intoxication (saturnine gout), certain drugs (thiazide diuretics, cyclosporine), dehydration, malnutrition, preeclampsia, polycystic kidney disease, chronic renal insufficiency, hypertension, and hyperinsulinemia. Excretion is influenced by age, gender, and race (318). With few exceptions, however, these stimuli seldom result in clinically significant disease. Gout, the best known manifestation of hyperuricemia, is caused mainly by decreased renal excretion (314).

Uric Acid and the Kidney

About two thirds of the daily elimination of uric acid or urate takes place in the kidney, and one third occurs in the gastrointestinal tract (319). The kidney, as the main regulator of serum uric acid, controls renal urate excretion by balancing its reabsorption and secretion. A reduction in renal urate excretion therefore causes hyperuricemia and, likewise, renal hypouricemia is caused by an increased renal urate excretion. New insights into the renal handling of urate have been generated by genome-wide association studies that explore the influence of single nucleotide polymorphisms (SNPs) and disease predisposition. Uric acid is freely filtered by the glomerulus and almost completely reabsorbed in the proximal tubule with resulting excretion of approximately 10% of its filtered load. A model for renal urate absorption proposes a molecular complex, operating as a functional unit, comprised of the major apical transporter URAT1, a urate-anion exchanger, coupled to sodium monocarboxylate cotransporters, SMCT1 and SMCT2, and possibly OAT4, an organic anion-dicarboxylate exchanger, all supported by protein interactions mediated by the scaffold protein PDZK1. Together with the basolateral transporter GLUT9 (URATv1), urate reabsorption progresses from the tubular lumen into the interstitial capillaries. A portion of the reabsorbed urate is secreted back into the urine via facilitators NPT1 and NPT4 at the apical membrane after uptake from plasma into proximal tubule cells mainly by basolateral membrane exchangers OAT1 and OAT3 (319).

If excess urate reaches the collecting ducts, it precipitates from the supersaturated urine because of decreased solubility in the acid medium. The clinical presentation depends on the concentration and the speed of precipitation, which will lead either to ARF with tubular obstruction or to chronic renal disease and gouty nephropathy, with formation of granulomas (microtophi) in the tubules and interstitium around the crystals of urate.

Hereditary Disorders

Enzyme Defects

HYPOXANTHINE-GUANINE PHOSPHORIBOSYLTRANSFERASE DEFICIENCY

Lesch-Nyhan disease (LND) and its attenuated variants result from a deficiency of HPRT, a purine-recycling enzyme that catalyzes guanine and hypoxanthine, and is encoded by the HPRT1 gene located on Xq26-27. Over 400 heterogenous mutations span the whole gene and impart HPRT deficiency by loss of catalytic activity, reduced substrate affinity, reduced enzyme stability, and reduced expression; while residual catalytic activity does not precisely predict phenotype, overall residual activity inversely correlates with clinical severity (320). Classic features of LND include hyperuricemia and its sequelae (gout, nephrolithiasis, and tophi), motor instability (dystonia, chorea, and spasticity), intellectual impairment, and self-injurious behavior. Other cases are unusually mild or incomplete and have been divided into an intermediate group, with overproduction of uric acid and neurologic dysfunction but no self-mutilation, and the least severely affected group that only exhibits the consequences of hyperuricemia (321,322). Few women with LND due to various molecular mechanisms have been reported (323,324).

Patients are normal at birth, and those with total or partial HPRT deficiency can present in infancy with crystalluria (“orange sand” in diaper), stone formation, or acute renal failure (ARF) with obstruction of urine flow (322,325,326).

TABLE 27.2 Heritable intrinsic disorders of renal tubular membrane transport

Disease	Inheritance	Gene	Mechanism	Clinical effects
Cystinuria Type A Type B Type AB	AR AD -ve AD -ve	<i>SLC3A1</i> <i>SLC7A9</i> <i>SLC3A1 and</i> <i>SLC7A9</i>	Impaired reabsorption of cystine and dibasic amino acids (lysine, arginine, ornithine) owing to defective shared b ^{0,+} AT-rBAT system	Urolithiasis secondary to precipitation of highly insoluble cystine
Lysinuric protein intolerance	AR	<i>SLC7A7</i>	Impaired reabsorption of cationic amino acids, especially lysine, owing to defect in γ-LAT1 subunit of cationic amino acid transporter	Aminoaciduria and poor intestinal absorption lead to hyperammonemia, nausea, vomiting, protein malnutrition with hepato-splenomegaly, hypotonia, osteoporosis, occasional mental retardation, respiratory compromise, immunodeficiency.
Dicarboxylic aminoaciduria	AR	<i>SLC1A1</i>	Impaired reabsorption of anionic amino acids (glutamic and aspartic acids) owing to defective EAAT3 transport system	Asymptomatic aminoaciduria
Hartnup disease	AR	<i>SLC6A19</i>	Impaired reabsorption of neutral amino acids owing to defective B ⁰ AT1 transport system	Reduced renal and intestinal absorption of tryptophan, leading to nicotinamide deficiency with pellagra-like rash, ataxia, mental retardation
Iminoglycinuria	AR or AD -ve	<i>SLC36A2, +/-</i> <i>SLC6A20</i>	Impaired reabsorption of proline and glycine owing to defective shared transport system PAT2 and IMINO	Asymptomatic aminoaciduria, rarely associated with nephrolithiasis, mental retardation, hypertension
Glycosuria	AR or AD -ve	<i>SLC5A2</i>	Impaired reabsorption of glucose owing to defect in low-affinity, glucose-specific SGLT2 transporter	Asymptomatic glycosuria
Hypophosphatemic rickets (phosphaturia)	X-linked AD AR AR	<i>PHEX</i> <i>FGF23</i> <i>SLC34A3</i> <i>SLC34A1</i>	Impaired phosphate reabsorption owing to defective phosphate homeostasis and renal vitamin D metabolism or defective sodium phosphate cotransporters	Hypophosphatemia and normocalcemia, growth retardation, rickets, osteomalacia
Primary distal tubular acidosis	AD AR AR	<i>SLC4A1</i> <i>ATP6V0A4</i> <i>ATP6V1B1</i>	Defective membrane transporters owing to dysfunction of anion exchanger AE1 or proton pump vacuolar H ⁺ -ATPase	Hyperchloremic, hypokalemic metabolic acidosis; hypercalciuria; nephrocalcinosis; lithiasis, rickets, or osteomalacia; +/- deafness
Primary proximal tubular acidosis	AR AR	<i>SLC4A4</i> <i>CA2</i>	Impaired bicarbonate reabsorption owing to dysfunction of NBC1 and carbonic anhydrase II (CA2)	Hyperchloremic metabolic acidosis, with ocular abnormalities or osteopetrosis

AD, autosomal dominant; AR, autosomal recessive; ve, variable expressivity; b⁰AT1, b^{0,+} amino acid transport; rBAT, related to b^{0,+} transporter; γ + LAT1, γ-L isoform 1 amino acid transport; EAAT3, excitatory amino acid transporter 3; IMINO, imino acid transporter; NBC1, Na⁺, Na⁺/HCO₃⁻ cotransporter.

Xanthine stones may form in addition to uric acid stones (327). Gross kidney findings at autopsy have included diffuse atrophy and stones. The microscopic changes are a combination of intratubular crystalline deposition and interstitial microtophi. Biopsies in patients with HPRT deficiency have shown intratubular and interstitial amorphous or needle-like crystalline deposition with surrounding giant cells; interstitial fibrosis and tubular atrophy may be present along with an inflammatory response induced by uric acid crystals (325,328). Electron microscopy reveals occasional stacks of needle-like crystals in tubular lumina but not in tubular epithelial cells. Intratubular deposition may lead to tubular obstruction, decline in renal function, and further increase in serum uric acid levels (329). The diagnosis is made by demonstrating hyperuricemia, elevated uric acid:creatinine ratio, decreased HPRT enzyme activity in peripheral blood cells, increased purine metabolites in urine, and mutational analysis (321,322). Allopurinol treatment effectively reduces serum urate and urine uric acid levels but has no influence on neurologic manifestations. Renal function usually remains stable or improves with treatment (330).

5-PHOSPHORIBOSYLPYROPHOSPHATE SYNTHETASE SUPERACTIVITY

5-Phosphoribosylpyrophosphate synthetase hyperactivity, caused by mutations in the *PRPS1* gene located on chromosome X, leads to purine overproduction. As with HPRT deficiencies, the clinical spectrum varies but is typically segregated as a juvenile/adult form with hyperuricemia, gouty arthritis, crystalluria, and renal stone formation and a severe form, with infantile onset that includes the above findings plus sensorineural hearing impairment, hypotonia, and ataxia; female carriers may develop clinical disease (315,331). PP-ribose-P synthetase superactivity is caused by point mutations in *PRPS1* that produce gain of function by interfering with regulatory control of enzyme activity or increased expression of a normally functioning enzyme. The latter may result from alterations in pretranslational mechanisms, since no genetic defects are found in the open reading frame, or untranslated or promoter regions. Increased expression accounts for the milder phenotypes (315). Hyperuricemia and its consequences

can be prevented with allopurinol, which has no effect on hearing or neurologic impairment.

ADENINE PHOSPHORIBOSYLTRANSFERASE DEFICIENCY

Adenine phosphoribosyltransferase (APRT) catalyzes the formation of adenosine monophosphate from adenine. When this enzyme is deficient, adenine is instead converted to 2,8-dihydroxyadenine (2,8-DHA), which is insoluble in urine. APRT deficiency is an autosomal recessive disorder largely described in the Japanese population and likely underrecognized in Caucasians, resulting from mutations in the APRT gene located on chromosome 16q24.3. Mutant alleles have been designated as APRT*Q0 and APRT*J, based on the level of in vitro enzyme activity; complete in vivo enzyme deficiency and similar clinical expression are described in both mutation groups. APRT*J mutations are thus far restricted to patients of Japanese descent (332). The lack of genotype-phenotype correlation, male predominance, and inter- and intrafamilial heterogeneity imply the presence of modifier genes and/or environmental influences.

The disease is limited to the kidney, and most patients present with a history of recurrent nephrolithiasis that can appear at any age but often during childhood. Infants may have recurrent urinary tract infections and red-brown diaper stains. Crystalline nephropathy can lead to acute and typically chronic renal failure (332–334). On occasion, the diagnosis has not been established until recurrence in a renal allograft (335). Allopurinol efficiently treats the majority of patients, reducing crystalluria and while stabilizing or improving renal function. Early initiation of treatment in children and posttransplant can prevent renal disease.

Histologic features of kidney biopsies include acute and chronic tubulointerstitial injury secondary to precipitation of crystals in the tubular lumen, tubular cell cytoplasm, and renal interstitium, predominantly in the cortex; findings have been misinterpreted as oxalate deposition. The strongly birefringent crystals are rod, rhomboid, or irregularly shaped; single or grouped as a fan or radially arranged annuli; and brown to brown-green on H&E and PAS, light blue with Masson trichrome, and black on Jones methenamine silver (Fig. 27.41) (335). The diagnosis can be made by urine analysis with

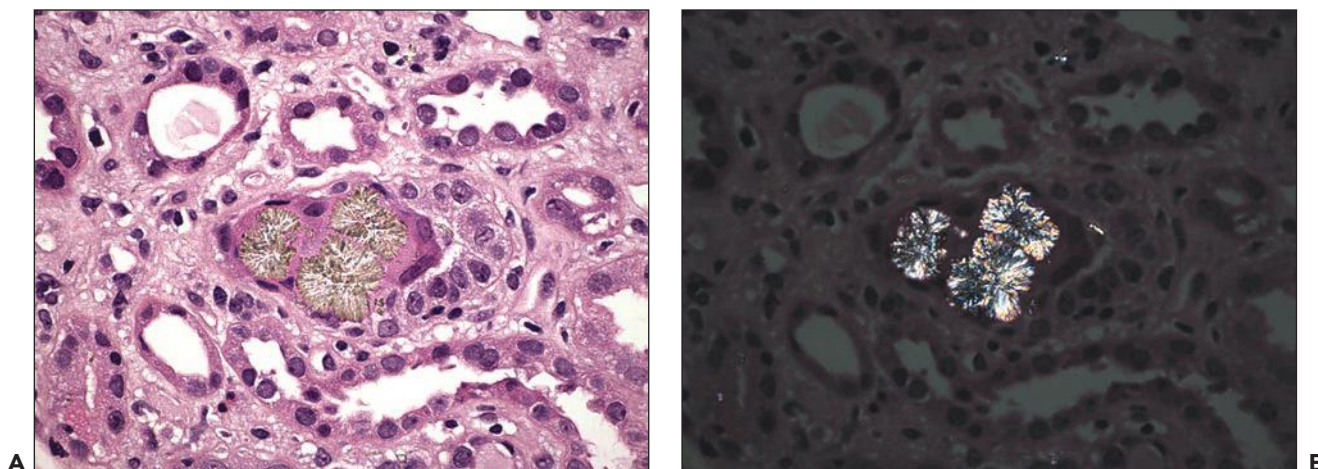


FIGURE 27.41 A renal tubule in adenine phosphoribosyltransferase (APRT) deficiency contains radially arranged rod-shaped, brown-green 2,8-dihydroxyadenine (2,8-DHA) crystals that elicit a foreign body giant cell reaction (**A**). The crystals are strongly birefringent with polarized light (**B**). (H&E; H&E with polarization; $\times 600$.) (Courtesy of Dr. V. D'Agati, Columbia University.)

demonstration of characteristic round, reddish brown crystals with a central Maltese cross when examined with polarized light microscopy. Biochemical stone analysis will not distinguish 2,8-DHA from uric acid; thus, infrared spectroscopy or X-ray crystallography is required. Demonstration of deficient APRT activity in erythrocytes or APRT gene sequencing can confirm the diagnosis (332).

GLUCOSE-6-PHOSPHATASE DEFICIENCY

Glucose-6-phosphatase deficiency, an autosomal recessive trait that is typically found in GSD-I, may cause hyperuricemia and gout. Mechanisms include both an increased rate of purine catabolism and a decreased renal clearance of urate secondary to lactic acidemia and ketonemia (317). The hyperuricemia begins in infancy, and gouty arthritis may occur by the second decade. Chronic renal tubular and glomerular disease are late complications of GSD-I, independent of hyperuricemia (331). Hyperuricemia may also be encountered in type III glycogenosis, with clinical myopathy, as well as types V and VII, although these patients do not have gout (331).

Tubular Defects

HEREDITARY RENAL HYPOURICEMIA

Hereditary renal hypouricemia (HRH) is a rare autosomal recessive renal uric acid transport disorder, with defective urate reabsorption in the proximal tubules that results in increased renal urate clearance and hypouricemia. There is no known pathologic consequence of hypouricemia; thus, the disorder is usually discovered incidentally. While patients are typically asymptomatic, they may present with nephrolithiasis or exercise-induced ARF. Hematuria and idiopathic hypercalciuria have been detected; uric acid or calcium stones are reported in up to 25% of patients (336). The disorder has mainly been described in Japanese, Korean, and non-Ashkenazi Jews. The majority of patients (designated HRH type 1) have homozygous or compound heterozygous loss-of-function mutations in the SLC22A12 gene located on chromosome 11q13.9, which encodes the urate transporter URAT1. GLUT9, a known glucose and fructose transporter encoded by SLC2A9, has recently been shown to possess potent urate transport capacity. Mutations in SLC2A9 have also been linked to renal hypouricemia (designated HRH type 2) (337–344). Patients with HRH type 2 have lower serum uric acid levels and higher fractional excretion of uric acid than those with HRH type 1 presumably because URAT1 dysfunction produces a partial absorption defect given alternative apical uric acid transporters, but loss of GLUT9 function precludes uric acid absorption by all apical uric acid transporters as basolateral uric acid efflux, mediated solely by GLUT9, is also prevented (341).

Individuals with exercise-induced nonmyoglobinuric ARF are more often male and present several hours after exercise with nausea and vomiting. The kidney shows acute tubular necrosis, and despite the need for dialysis, the short-term prognosis seems good. After recovery, most patients had normal creatinine levels, although decreased concentrating abilities have been evident and some have demonstrated progressive interstitial fibrosis, tubular atrophy, and chronic renal dysfunction (345). The proposed mechanisms for ARF include excessive oxidative stress, accelerated ATP degradation, renal vasoconstriction, and acute uric acid nephropathy. The latter

is unlikely given the short lag between exercise and symptoms and the lack of uric acid crystals in biopsies.

UROMODULIN-ASSOCIATED KIDNEY DISEASE

Uromodulin (Tamm-Horsfall protein) is encoded by the *UMOD* gene on chromosome 16p12.3 and synthesized exclusively in the tubular cells of the TAL where it anchors to the luminal membrane from which it is enzymatically cleaved and released into the lumen for eventual excretion as the most abundantly produced protein appearing in normal urine. Uromodulin may also target and be secreted from the basolateral compartment of TAL cells (346). The potential functions of uromodulin include providing water impermeability to the TAL, defense against urinary tract infections and renal calculi, and assistance in maintenance of primary cilia (347). SNPs in the *UMOD* gene have recently been associated with chronic kidney disease, and mutations in the gene have been identified in three phenotypically overlapping autosomal dominant tubulointerstitial nephropathies, medullary cystic kidney disease (MCKD2), familial juvenile hyperuricemic nephropathy (FJHN), and glomerulocystic kidney disease, collectively termed “uromodulin-associated kidney disease” (UAKD) (348–350). Impaired urine-concentrating capability is detected in childhood or adolescence along with hyperuricemia, out of proportion to renal dysfunction, and extreme hypoexcretion of urate; urinary excretion of uromodulin is also decreased but later in the disease course (346,351). HPRT and PP-ribose-P synthetase activities are normal (314). Gout, not invariable, and renal failure develop over the ensuing years leading to ESRD usually around the fourth or fifth decade, although there is significant intra- and interfamilial variability (352,353).

The kidneys show patchy atrophy and loss of tubules associated with inflammation and interstitial fibrosis. Uric acid crystals are almost invariably described as absent (324). There is thickening, reduplication, and attenuation of the basement membranes of distal tubules and collecting ducts. Intracytoplasmic, irregular, pale, and weakly PAS-positive inclusions have been identified within TAL epithelium (Fig. 27.42) (354). Cyst development is inconsistent, and topography is nonspecific, cortical, corticomedullary, or medullary (353). As end-stage disease ensues, one sees thickening of the Bowman capsule, focal and segmental or global glomerular sclerosis, as well as intimal thickening of intrarenal arterioles and arteries. In addition to variable tubulointerstitial nephritis, kidneys with glomerulocystic disease have relatively diffuse and marked dilation of Bowman space with collapsed rudimentary glomeruli (349).

In contrast to normal kidneys where uromodulin shows weak diffuse cytoplasmic localization with pronounced apical membrane staining of TAL and early distal convoluted duct cells, immunohistochemical staining in samples with UAKD shows weak apical membrane staining but intense heterogeneous decoration of the cytoplasm with dense perinuclear aggregates. Rare cases have unusually shown strongly reduced or absent staining (351,355). The dense uromodulin staining in the cytoplasm colocalized with endoplasmic reticulum (ER) markers of stress (351,356). This correlates with ultrastructural demonstration in TAL cells of stacked lamellae, considered hyperplastic ER, focally distended by granular, and moderately electron-dense material consistent with uromodulin

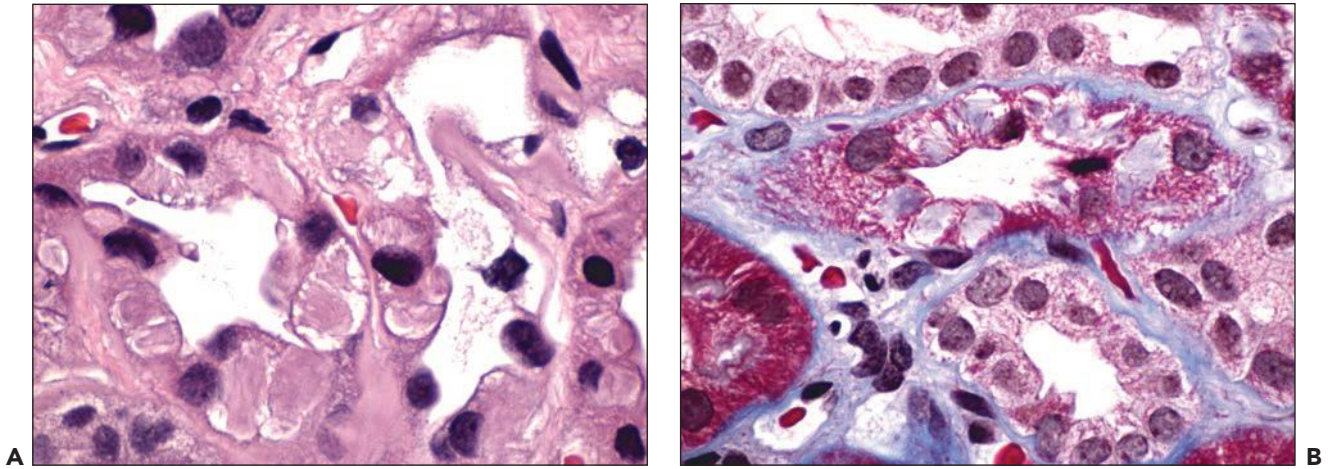


FIGURE 27.42 The kidney of a hyperuricemic woman with a *UMOD* mutation has focal interstitial fibrosis and tubular atrophy. Intracytoplasmic, pale lamellated inclusions displace the nucleus of distal tubular cells and stain weakly eosinophilic (A) and light trichrome blue (B). (H&E; $\times 1000$) (Masson trichrome; $\times 600$.) (Courtesy of Dr. V. D'Agati, Columbia University.)

(Fig. 27.43) (349,351,354). Treatment includes pharmaceutical control of hyperuricemia, but its affect on the progression of renal disease has not been rigorously investigated. Renal transplantation cures UAKD.

Over 50 mutations in *UMOD* have been described, but these are responsible for less than half of the UAKD probands; thus, genetic heterogeneity clearly exists. Mutations in two additional genes, *REN*, encoding renin, and *HNF-1 β* , encoding hepatocyte nuclear factor-1 β , have been demonstrated in some families possessing features of FJHN/MCKD2. Patients with *REN* mutations in addition have early-onset anemia (357), while *HNF-1 β* patients may have early-onset diabetes (358). It is worth noting that hepatocyte nuclear factor-1 β directly controls the expression of *UMOD*; thus, inactivation of *HNF1b* is associated with decreased *UMOD* transcription

(359). Greater than 50% of patients lack mutations in any of these genes, and another locus on chromosome 2p22.1-p21 has recently been linked to MCKD2/FJHN in five of six unrelated families (360).

The etiology of hyperuricemia remains debatable but is postulated to result from increased proximal tubule reabsorption secondary to urine salt wasting (352). The role of *UMOD* mutations in the disease is being defined. Delayed processing and retention of uromodulin in the ER result from mutation-induced alterations in the protein's conformation with decreased uromodulin synthesis and apical expression (361). It is speculated that the resulting ER stress promotes cell death and local inflammation, hence, tubulointerstitial nephritis (362). Additionally, some mutant uromodulin can escape the ER quality control, interfere with wild-type protein

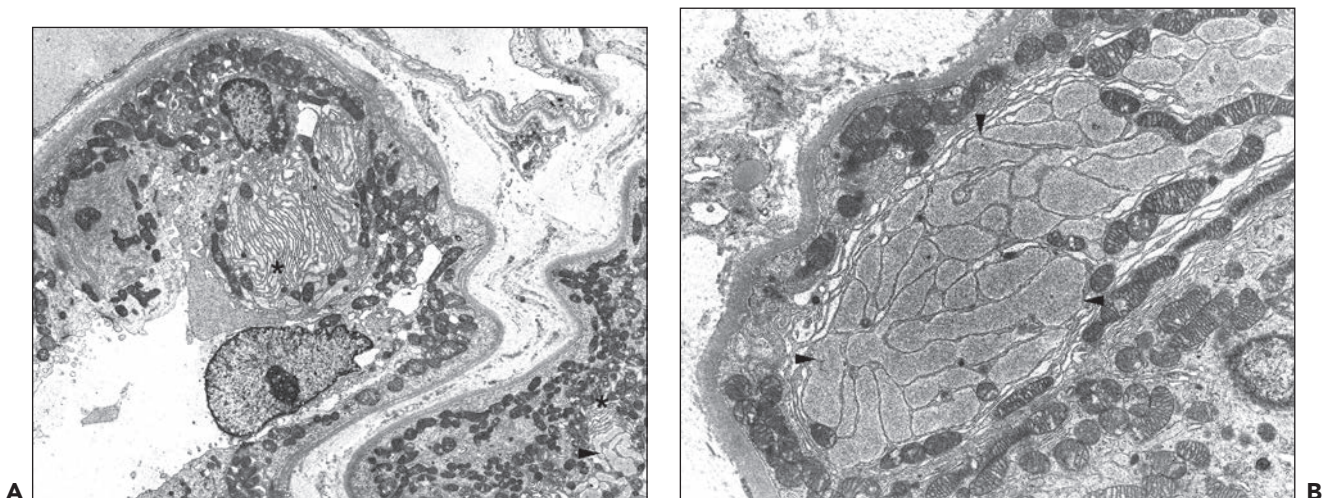


FIGURE 27.43 The distal tubule lining cells in uromodulin-associated kidney disease (same kidney as Fig. 27.42) demonstrate hyperplastic bundles of endoplasmic reticulum (*) (A) ($\times 4000$.) Some cisternae of endoplasmic reticulum are distended with granular moderately electron-dense storage material (arrowheads), consistent with uromodulin (B) ($\times 12,000$.) (Courtesy of Dr. V. D'Agati, Columbia University.)

polymerization, and form large aggregates at the plasma membrane that are secreted into the tubule lumen. The high propensity of mutant uromodulin to aggregate could increase hyaline cast formation leading to tubular obstruction, thereby inducing upstream inflammation and fibrosis. Finally, in contrast to apical secretion, the basolateral release of mutant uromodulin remains as efficient as the normal protein, where it could potentially provoke an inflammatory response (346).

Acute Uric Acid Nephropathy

In contrast to enzymatic defects causing excessive purine and urate biosynthesis, this form of renal injury, caused by uric acid overproduction, typically results from massive tissue destruction, as seen in patients with rhabdomyolysis syndromes or acute tumor lysis syndrome associated with certain hematologic or solid malignancies (363). The onset is usually one of ARF related to the commencement of cytotoxic therapy, which releases large amounts of potassium, phosphorus, and nucleic acids that are metabolized to uric acid. The precipitation of calcium phosphate, uric acid, and xanthine in renal tubules causes inflammation and obstruction. Uric acid can also exert acute proinflammatory and vasoconstriction effects on the kidney, independent of crystal deposition (364,365). Standard preventative measures using vigorous hydration and allopurinol have decreased the incidence of acute hyperuricemic renal failure. Although allopurinol prevents uric acid formation, existing uric acid is still excreted, and xanthine nephropathy may result. Recombinant urate oxidase, which converts uric acid to allantoin, a highly soluble and readily excretable compound, is extremely effective in treating hyperuricemia, but randomized controlled outcome-based trials are still needed to determine appropriate cost-effective use (366).

Pathologic Changes

The kidneys contain linear yellow striations in the medulla and papillae, corresponding to the distribution of the collecting ducts in which precipitation has taken place (Fig. 27.44). The collecting tubules contain large amounts of uric acid that may be accompanied by cellular debris and inflammation (367). This may take the form of amorphous masses or, when frozen sections are examined, of doubly refractile, radially disposed crystals. Some acicular crystals of monosodium urate are present, and these may be seen penetrating the tubular wall, inciting a giant cell reaction and uncommonly in the interstitium. Electron microscopic studies have shown crystals in the epithelium of collecting tubules, accompanied by an increase in lysosomal bodies. Dilatation of the glomerular space and the tubular system proximal to the obstruction plus edema of the cortical interstitium are sometimes present.

Uric Acid Infarcts

Deposits of uric acid crystals may be seen in the kidneys of newborns who die within the first few weeks of life and appear macroscopically as yellow striations along the collecting ducts in the inner medulla, identical in appearance to Figure 27.44. This finding has become less common with better neonatal fluid management and has been held as a normal physiologic state without functional disturbances; it is possibly related to cellular destruction associated with the remodeling of fetal tissues. Histologically, the streaks are amorphous, eosinophilic sediment (368). Renal medullary hyperechogenicity is described in term

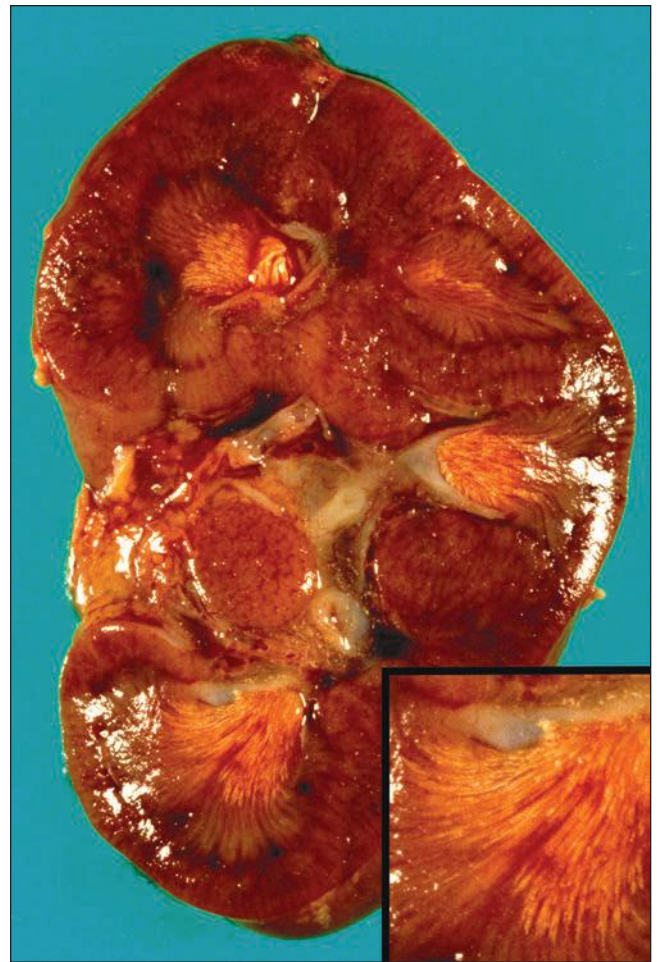


FIGURE 27.44 Gross picture of a kidney from a 3-year-old boy with tumor lysis syndrome and acute urate nephropathy. The papilla (inset) has pale yellow linear streaking that corresponds to the presence of uric acid and urates in the collecting ducts. (Courtesy of J. Siebert, Ph.D., Seattle, Seattle Children's Hospital, University of Washington.)

infants with normal renal function or transient impairment after complicated deliveries in whom hyperuricemia, uric acid crystalluria, and hyperuricemia are demonstrated (369). While hyperuricemia is a known consequence of perinatal asphyxia and tubular obstruction could result from uric acid, an operative role of Tamm-Horsfall protein cannot be excluded.

Chronic Uric Acid Nephropathy

Variation in serum urate levels is influenced by age, sex, body habitus, and ethnic background, and recent evidence for genetic regulation is based on population studies that associate polymorphisms in several uric acid membrane transporters with uric acid levels, including hyperuricemia and gout susceptibility (370,371). That hyperuricemia is a marker of renal dysfunction is understood, but the nature of the association remains debated (372). Support, although not necessarily proof, of a pathogenic role for uric acid in humans is based on hyperuricemia preceding reduced GFRs and a dose-dependent response such that the risk of developing kidney disease is independently influenced by higher uric acid levels (373).

Uric acid in human extracellular fluids exists almost exclusively as a salt, monosodium urate monohydrate. Both uric acid and sodium urate are poorly soluble, and a concentration above 6.8 mg/dL, the limit of solubility at physiologic temperature and pH, promotes deposition in tissue. The majority of chronically hyperuricemic individuals never develop clinical features of gout, and those who do have a reduced renal fractional clearance of urate (374). Nephropathy in gout is associated with the precipitation of sodium urate in the renal tissues, with tubular damage and interstitial granulomatous inflammation (microtophi). Uric acid stones are common. These manifestations of chronic gout were once common but have declined substantially as a result of more effective therapy, particularly uricosurics (probenecid and sulfinpyrazone and benzbromarone) and allopurinol (374).

The prognosis of gouty nephropathy has also changed over the years due to pharmacologic intervention. The historically high incidence of renal insufficiency and end-stage renal disease has been considerably reduced in frequency and severity although a mild reduction of renal function and asymptomatic hypertension can be seen (372). Comorbid states such as hyperlipidemia, hypertension, atherosclerosis, and metabolic syndrome and medications, for example, cyclosporine and

anti-inflammatory drugs, likely contribute to any decline in renal function in patients with hyperuricemia and gout.

Pathologic Changes

The kidneys are affected equally, unless they are asymmetrically obstructed by stones; they are usually reduced in size. Granularity of the subcapsular surface may be accompanied by some coarser scars; the cortex is often reduced in width. The medulla contains small white specks and occasional radiating pale yellow urate deposits. The pelvis may be dilated and contain small uric acid stones; the papillae in these cases are often blunted. In certain cases, the presence of acute infection is apparent grossly. The kidneys occasionally appear normal or even enlarged.

The glomeruli in most cases contain changes attributed to age and chronic hypertension with development of hyalinosis. In the early stages, a distinctive change, similar to thrombotic microangiopathy, has been described that includes uniform fibrillary thickening of the GBM with occasional double contours, mild mesangial matrix, and cellular increase and thickened capillary basement membranes on electron microscopy with focal subendothelial expansion (375,376) (Fig. 27.45). Mechanisms for glomerular pathology could potentially include uric acid-induced endothelial dysfunction,

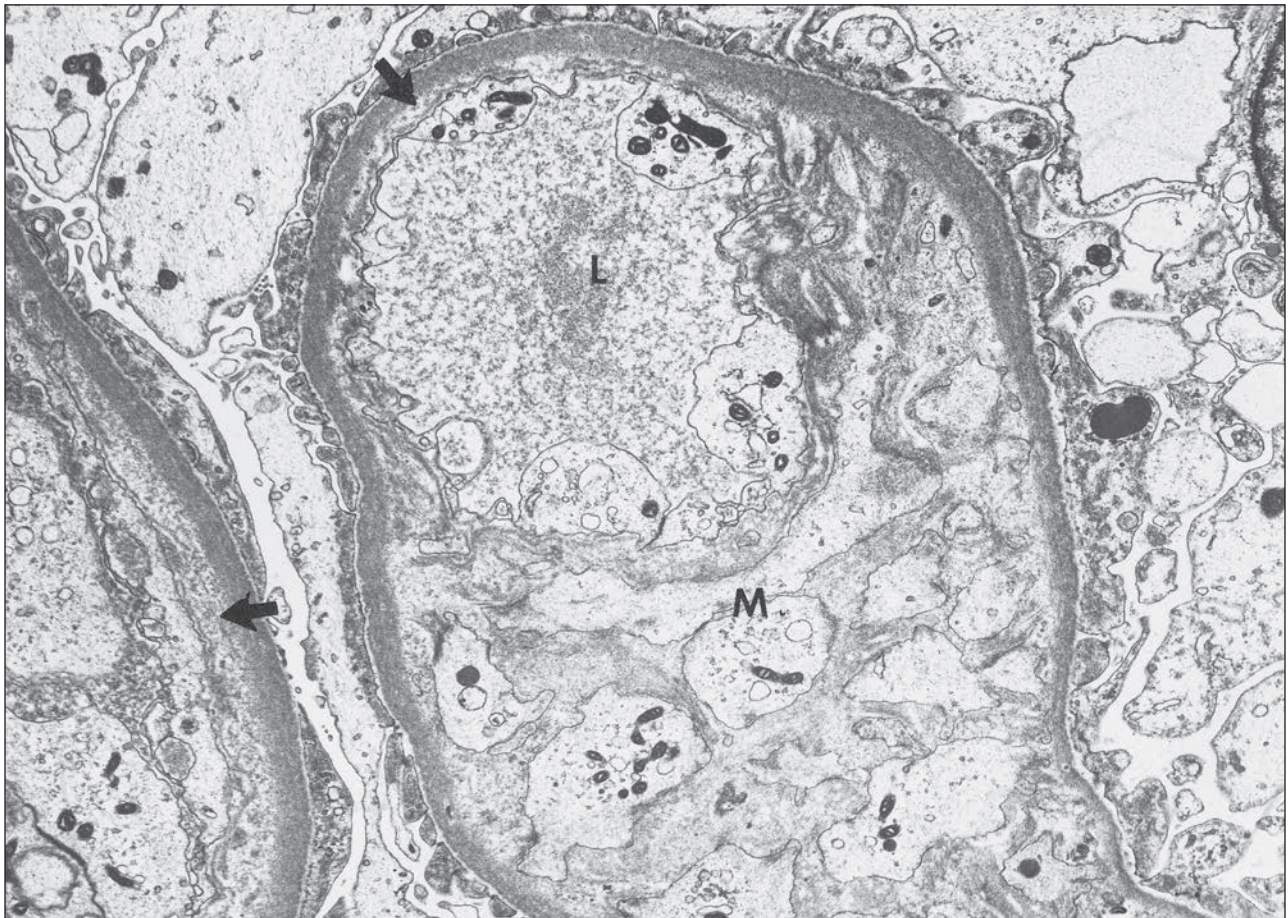


FIGURE 27.45 Electron micrograph of an enlarged glomerulus from a patient with gouty nephropathy. Capillary walls show segmental separation of the endothelium from the basement membranes (*arrow*). The resulting space is filled with granular material similar to that in the capillary lumen. L, capillary lumen; M, mesangium. ($\times 7125$.)

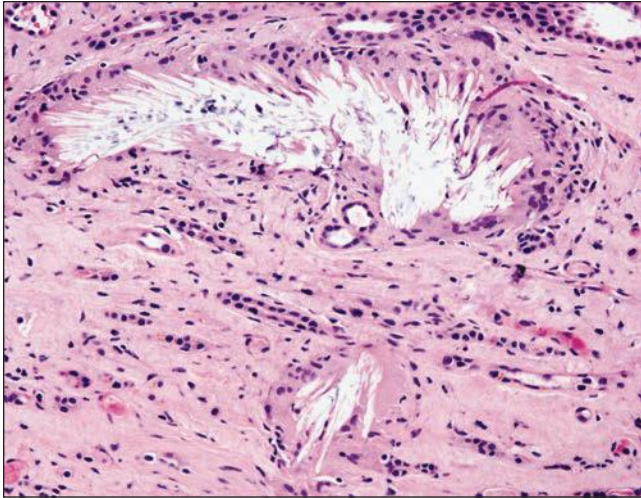


FIGURE 27.46 Collection of elongated urate crystals with a giant cell reaction at the periphery. This collection probably originated in a collecting tubule, the walls of which are no longer apparent. Considerable loss of tubules has occurred. (Formalin fixation; H&E; $\times 400$.) (Specimen courtesy of Dr. K. Smith, University of Washington.)

inflammatory activation, and altered glomerular hemodynamics via activation of the local renin-angiotensin system (377).

The tubules may be atrophic as the result of ischemia, obstruction, or conceivably chronic infection. Dilation of tubules occurs with extensive urate deposition in medullary tubules, rarely in the cortical tubules, or when uric acid stones in the pelvis or ureter cause obstruction. The collecting tubules in the medulla often contain crystals of monosodium urate that are elongated (Fig. 27.46), rectangular, or so fragmented as to be amorphous; inflammation is often associated. The doubly refractile crystals are best seen in alcohol-fixed material but are often surprisingly well preserved with formalin fixation. In many deposits, the crystalline appearance and birefringence are partially lost, and a pale blue, faintly staining, amorphous substance is seen (Fig. 27.47).

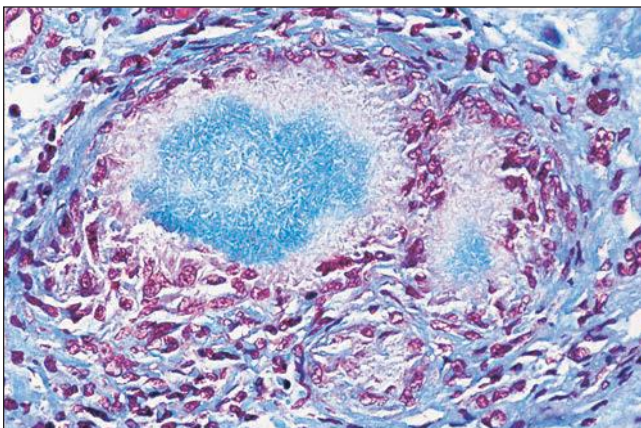


FIGURE 27.47 Urate deposits (microtophi) of amorphous, faintly crystalline material in the medulla with an adjacent narrow zone of inflammatory cells and fibrosis at periphery. (Formalin fixation, Masson trichrome; $\times 200$.)

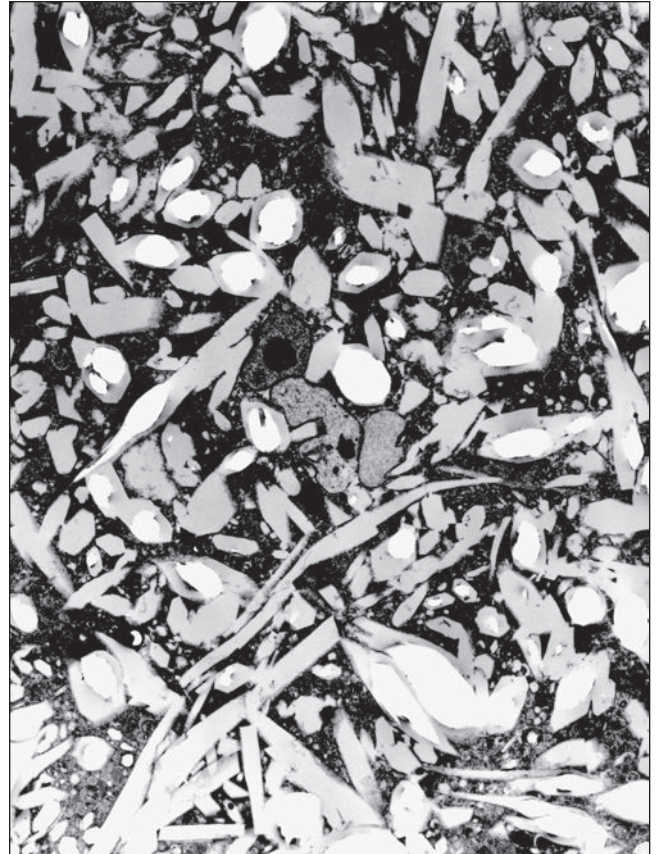


FIGURE 27.48 Electron micrograph of substantial angular and irregularly shaped interstitial urate deposits admixed with inflammatory cells. ($\times 16,000$.) (Specimen courtesy of Dr. K. Smith, University of Washington.)

Some of the crystalline masses in hematoxylin and eosin sections are deep blue, perhaps because of concomitant calcium deposition. The walls of the tubules are frequently deficient, and the crystalline deposits appear to be in the interstitium, outlined by giant cells and other mononuclear cells, beyond which fibrosis replaces resident tubules. Microcalculi have been described in the lumen of tubules. The interstitium may be scarred and contains urate collections with giant cells and acute inflammatory cells (Fig. 27.48). Interstitial deposition of calcium, iron, and phosphate has been seen. In general, interstitial changes have been regarded as secondary to tubular damage. Blood vessels show arterial and arteriolar sclerosis, which is sometimes severe and may contribute to tubular atrophy.

Urolithiasis

Uric acid stones comprise 8% to 25% of kidney stones with variability introduced by race, gender, and geography (378) but accounted for ESRD in only 7 of 7128 dialysis patients in one large series (379). Benjamin Franklin apparently suffered for uric acid stones, which occur in 10% to 25% of patients with gout (314,380). In a US population-based analysis, the frequency of kidney stones in subjects with gout was almost three times greater than that in the general population (381). Stones may occur after the administration of uricosuric drugs (382).

The stones are characteristically radiolucent, but they become radiopaque if covered by calcium salt. Uric acid or monosodium urate crystals are thought to serve as a nidus for stone formation, and heparin sulfate and aspartic and glutamic acids comprise the matrix (382). Changes in dietary habit, including increased consumption of animal proteins and an increasing rate of obesity, metabolic syndrome, and type 2 diabetes, have contributed to the increased incidence of uric acid stones (383,384). Insulin resistance causes impaired renal ammonium excretion with low urine pH that favors the production of uric acid stones (385).

SICKLING DISORDERS

Sickled cells were first reported in the literature by Dr. James Herrick; however, the deadly disease hallmarked by painful episodes was known in Africa for centuries (386,387). A single nucleotide change, from GAG to GTG in the sixth codon of the β -globin gene on chromosome 11p15.5, results in the single amino acid substitution of valine for glutamic acid in the hemoglobin peptide. Although the sickle gene has a genetic advantage of protecting heterozygous carriers from endemic *Plasmodium falciparum* malaria infection, carriers of two gene defects are well known to suffer vasoocclusive pain crises, acute chest syndromes, splenic sequestration, aplastic crises, cerebrovascular accidents, priapism, and chronic organ dysfunction, including effects on the kidney (388–390).

Sickle cell disease (SCD) denotes all genotypes that contain at least one sickle gene. In addition to the homozygous HbSS disease (sickle cell anemia [SCA]) and sickle cell trait (HbAS), other major compound heterozygous genotypes, listed in order of clinical severity, include HbS/ β^0 -thalassemia, HbS/HbC disease, HbS/ β^+ -thalassemia, HbS/HPFH (hereditary persistence of fetal Hb), HbS/HbE syndrome, and additional rare combinations (HbS/Hb β^D -Punjab, HbS/Hb β^O -Arab, HbS/Hb β^D -Leopore). At least 5.2% of the world population carry a significant hemoglobin gene variant, and sickle cell disorders affect approximately 2.3 per 1000 conceptions; around 85% of sickle cell disorders and over 70% of all affected births occur in Africa (391). Based on the National Newborn Screening Information System, the number of individuals in the United States with SCD, when taking into account early mortality, is estimated at 72,000 to 98,000, with an overall prevalence of SCD (1:365) and of SCA (1:601) in the African American birth cohort (392).

SCD manifests in the kidney with both tubular and glomerular effects that culminate as ESRD. Renal involvement is most significant and well characterized in SCA, which is the main focus of this section. In one large series of 310 patients followed in sickle cell clinics, 71% had HbSS, 17% had HbSC, 11% had HbS/ β^+ -thalassemia or HbS/ β^0 -thalassemia, and 1% had hemoglobin S—other (393). Reference below to HbS heterozygotes implies HbS/ β -thalassemia and HbS/HbC.

Clinical Presentation

Sickle cell nephropathy (SCN) includes hematuria, papillary necrosis, urinary concentrating defect, impaired renal acidification and potassium excretion, supranormal proximal tubular function, proteinuria, and renal failure (reviewed by several authors (388,390,394,395)). Renal manifestations of sickling disorders are presented in chronologic order of onset.

Hyposthenuria

The inability to concentrate urine maximally is the most frequent renal abnormality in SCD patients and the earliest evidence of a renal abnormality (396). An impaired capacity to concentrate urine can be demonstrated in patients with SCA as early as 6 months of age. Patients under 10 years of age cannot concentrate their urine greater than 600 to 800 mOsm/kg H₂O. In children, maximum urine osmolality can be increased with blood transfusions; however, this capability is lost with progressive ischemic damage to the renal medulla (397). A maximum urinary osmolality of 400 to 450 mOsm/kg H₂O is typically seen under water deprivation in adults with SCA. By contrast, urine osmolalities on water loading reach significantly lower values in sickle cell patients than in normal subjects, confirming the preservation of the capacity to maximally dilute the urine (398).

In HbS heterozygotes, HbSC, HbS/ β -thalassemia, and HbAS, the defects can be as significant, though typically milder, with more gradual onset that usually becomes apparent later in life (399). In sickle cell trait, the severity of hyposthenuria is heterogeneous and dependent on the percentage of HbS, which is modulated by the α -globin genotype (400).

Hyposthenuria can produce polyuria, thereby increasing the risk of dehydration. High urine volumes may contribute to nocturnal enuresis, a relatively common disorder in children and young adults, with any form of SCD (401). The intensity of enuresis has been linked to the severity of SCD, with a higher incidence in those with anemia and painful crisis and low concentrations of fetal hemoglobin (402,403).

Although intranasal desmopressin has yielded complete or partial resolution of nocturnal enuresis in SCD, the condition is considered multifactorial (404).

Altered Glomerular Function

Children with SCD have supranormal renal hemodynamics, with elevated GFR and RPF. The GFR is usually normal in sickle cell trait, but, like SCA, the filtration fraction is decreased, owing to a small increase in RPF (405). Both GFR and RPF normalize during adolescence but are frequently subnormal in patients with SCD after the age of 40 (406–409). Glomerular hyperfiltration has also been detected in children and young adults with thalassemia; the higher incidence in patients who were not regularly transfused suggests that the elevated GFR could be a consequence of chronic anemia (410).

Proteinuria is an early manifestation of SCN and develops in as many as 20% to 30% of adults with sickle cell trait and 15% to 20% of older children, where it increases with age (406,409,411). Proteinuria is more commonly associated with SCA than other hemoglobinopathies (412). Microalbuminuria is a sensitive marker of preclinical glomerular damage and has been detected in almost 40% of teenagers or adults with HbSS and approximately 30% of those with other sickling hemoglobinopathies (hemoglobin SC, SD, or S/ β -thalassemia) (412). Although it has been documented in children less than 4 years old, the overall incidence of microalbuminuria in HbSS children is about 20% and is usually detectable around 7 years of age (408,413,414). The prevalence of microalbuminuria increases with age, reaching adult incidence in the second decade, but does not correlate with clinical severity of disease (i.e., painful crises, transfusion requirements). Microalbuminuria can also be demonstrated among patients with sickle cell trait, although at a lower frequency (415).

Hyperfunctioning Proximal Tubules

Patients with SCD have lower than normal serum creatinine levels and supranormal proximal tubular function, generating increased secretion of uric acid and creatinine (407,416). The latter can lead to significant overestimation of GFR by creatinine clearance. A discrepancy of 30% was found between creatinine and inulin clearance in a group of patients with SCD with normal GFR (CrCl, 2.57 ± 0.12 mL/s, vs. inulin clearance, 1.98 ± 0.8 mL/s) (417). Homozygous SS patients may actually have a significant deterioration in renal function long before it is detected by traditional measurements of creatinine clearance. Herrera et al. (418), however, recently challenged the notion of increased secretion of creatinine, finding lower baseline tubular secretion of creatinine and impaired response to an intravenous creatinine load in 16 SCA patients versus controls. They argued that a difference in conclusions regarding creatinine secretion between their study and that of de Jong (416) was the result of differences in values between control subjects (418). Nonetheless, alternative measurements or biomarkers of GFR, such as ^{99m}Tc -DTPA or ^{51}Cr -EDTA clearance or serum cystatin C levels, may more accurately reflect renal function (409,419).

Abnormalities of proximal tubular reabsorption include increased reabsorption of phosphate and β_2 -microglobulin, which can lead to elevated serum phosphate (420,421). However, the opposite has been found in children with SCA, who have lower mean serum phosphate and lower maximal tubular phosphate reabsorption values compared to controls, possibly owing to higher parathyroid hormone levels in this age group (422).

Incomplete Renal Tubular Acidosis

In addition to urinary concentrating defects, those with SCD often have impaired distal tubular handling of potassium and hydrogen. Under normal conditions, neither defect of acidification nor potassium secretion is clinically apparent, but either may become so with renal insufficiency or dehydration. During acid loading, HbSS patients were unable to lower their urine pH below 5, but normal renal acidification has been observed in HbAS (405,423). Results similar to those seen in HbSS have been reported for HbS/ β -thalassemia (424).

Homozygous SS patients usually have normal serum potassium concentrations that remain so, even with potassium loading. The defect in potassium excretion is independent of aldosterone deficiency but may be related to a shift of potassium from the extracellular to intracellular compartment (425). The fractional excretion of potassium is also lower in HbSS children, but normal potassium excretion is observed in patients of all ages with sickle cell trait (422,426).

Hematuria

Asymptomatic hematuria is one of the most prevalent features of the disease. Although usually self-limited, it may be dramatic and prolonged, rarely resulting in the passage of clots and severe anemia. Hematuria is often seen with papillary necrosis and is associated with sloughing of the renal papillae, which can produce obstruction to urine outflow and ARF—an outcome that is, however, uncommon, as papillary necrosis is usually a focal disease (417,427,428). Ultrasonography can identify renal papillary necrosis, which can evolve to calcification of the medullary pyramids and may be an incidental

finding in the asymptomatic patient. Contrast-enhanced computed tomography can detect abnormalities at an earlier stage and better differentiate the etiology (428). Other variable presentations of papillary necrosis range from renal colic to symptoms of urinary tract infection or sepsis.

Hematuria occurs at any age in HbSS, HbSC, or HbS/ β -thalassemia and most commonly presents in HbAS patients in the third or fourth decade. It should be cautioned that renal medullary carcinoma (RMC) in sickle cell trait often presents with hematuria (see following).

Hypotension

Individuals with SCD have significantly lower blood pressure than the general population and African American control subjects. The prevalence of hypertension is also less (412,429,430). HbSC patients deviated from normal but to a lesser degree than HbSS patients. Therefore, those with SCD should have their blood pressure monitored, but values obtained must be assessed relative to lower values expected for patients with sickle disease. Indeed, an increasing prevalence of elevated creatinine values was found in patients with relative systemic hypertension compared to other HbSS patients (431).

Acute Renal Failure

ARF is not common in SCD but becomes more probable during periods of acidosis and hypoxia. ARF has been described as part of the multiorgan failure syndrome (dysfunction of at least two major organ systems) that complicates a severe sickle pain episode (432). In SCD, ARF may be related to rhabdomyolysis, sepsis, or general anesthesia, which often accompanies it, but patients generally have good survival and recovery of function without progression to ESRD (433). ARF in the setting of exertional rhabdomyolysis has recently been recognized as a serious complication of sickle cell trait (434).

Pathologic Changes

Gross Pathology

In many instances, the kidneys are of near normal size and have a relatively smooth subcapsular surface. Progressive renal impairment is more common with advancing age, and autopsy studies have shown a negative correlation of kidney weight with age (435). Kidneys typically show papillary changes ranging from blunting to obvious necrosis and scarring, with the more severe changes occurring in those who died of renal failure. An extensive review by Vaamonde (436) showed that renal papillary necrosis is a frequent complication of SCN in HbSS, as well as in heterozygotes, and has an incidence ranging from 15% to 36%. The acute lesion of papillary necrosis is pale infarction of the papillary tip, sometimes accompanied by sloughing (437). Loss of caliceal cupping, irregular renal outline, and cystic extension from the calyx have been demonstrated by intravenous urography and correlate with chronic injury (Fig. 27.49) (438). Renal cortical infarction with subsequent cortical scarring has been observed, and many kidneys show coarsely irregular subcapsular surfaces, which are worse with evidence of uremia, though not to the degree that is common in pyelonephritis (394,435). Generalized cortical thinning is associated with reduced renal weight, and diminished numbers of glomeruli are enlarged and easily visualized on gross examination.

Renal enlargement, however, is apparent in childhood. A baseline study of 197 infants (mean, 12.9 months) with

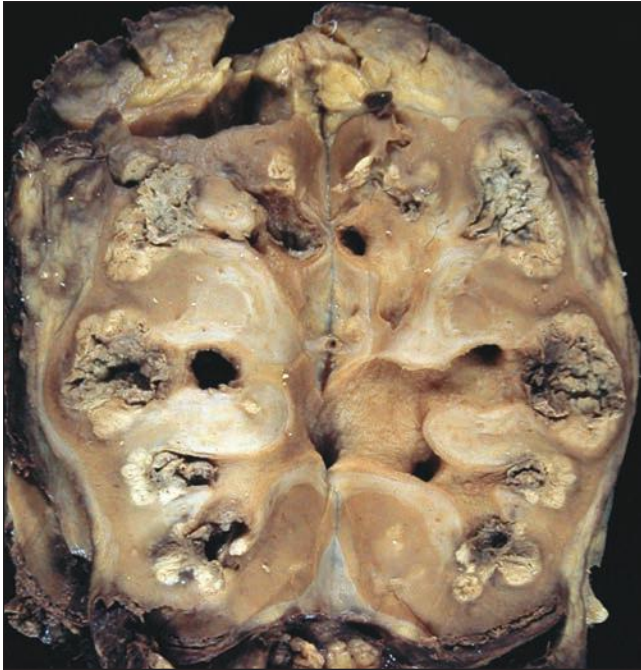


FIGURE 27.49 Bisected kidney from a patient with sickle cell anemia (SS) showing papillary necrosis and destruction with cystically dilated calices. Multifocal pyelonephritis is evident. (Courtesy of Dr. R. Peel, University of Pittsburgh.)

HbSS showed significantly increased renal volume compared with hematologically healthy controls (439). Annual ultrasound evaluation of renal length in 237 subjects between the ages of 6 and 20 years with HbSS showed a significantly greater mean length with age, compared to 147 subjects with HbSC disease and 78 age-matched controls with normal (HbAA) hemoglobin (440). Renal length correlated negatively with hemoglobin levels and correlated positively with reticulocyte counts.

Most of the 21 patients with hematuria in the report of Mostofi et al. (441) were thought to have sickle cell trait. Unilateral nephrectomy specimens showed medullary or cortical hemorrhages as well as necrotic papillae. Renal papillary necrosis usually presents later in HbAS than HbSS, but it may occur in up to 50% of patients with sickle cell trait who present for evaluation of hematuria. Papillary necrosis has been observed radiographically in patients with both HbS-thalassemia and HbSC (442,443).

Microradiographic studies revealed gross lesions of the vessels of the renal medulla with almost complete absence of the vasa recta in SCA; those that remained were spiraled, dilated, and ended blindly (444). The vasa recta in sickle cell trait and HbSC disease were shown to be reduced in number and to have lost the normal bundle architecture.

Microscopic Pathology

VASCULAR ABNORMALITIES

Large blood vessels are usually unremarkable except for sickled erythrocytes. Arterioles and capillaries are dilated and congested with aggregates of erythrocytes without fibrin thrombi

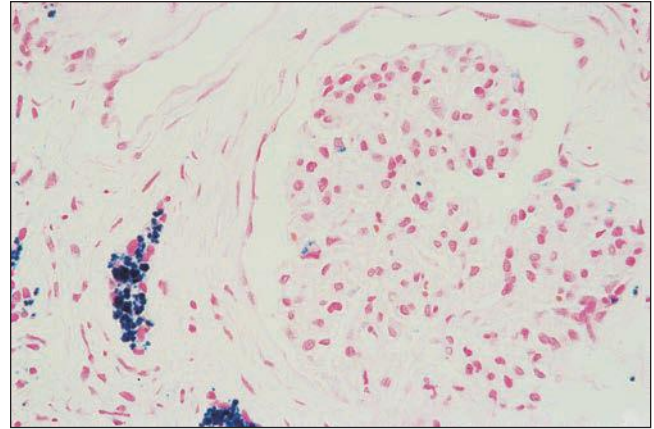


FIGURE 27.50 Tubular epithelial cells in sickle cell anemia kidney contain abundant cytoplasmic iron. Rare granules are evident in glomerular visceral podocytes. (Perls Prussian blue; $\times 400$.) (Specimen courtesy of Dr. A. Chang, University of Chicago.)

(445,446). Only rarely are afferent arterioles or cortical capillaries hyalinized (435,446).

TUBULOINTERSTITIAL ABNORMALITIES

The most frequently reported cortical tubular change is hemosiderin deposition, primarily in proximal tubular epithelial cells (Fig. 27.50) (393,446,447). Early descriptions in children include tubular epithelial necrosis, regeneration, and pigmentation of tubular casts (445,448). Tubular atrophy and interstitial scarring with mononuclear cell infiltrates have also been noted in the cortex of patients with renal failure (435).

Medullary lesions are more prominent, with early changes consisting of edema and telangiectasia (445). Destruction of the vasa recta results in multiple, small infarcts of the papilla that progress to focal scars. Eventually, tubular atrophy and dropout leave only a few surviving collecting ducts within broad areas of inflamed fibrous tissue (Fig. 27.51) (436,449,450).

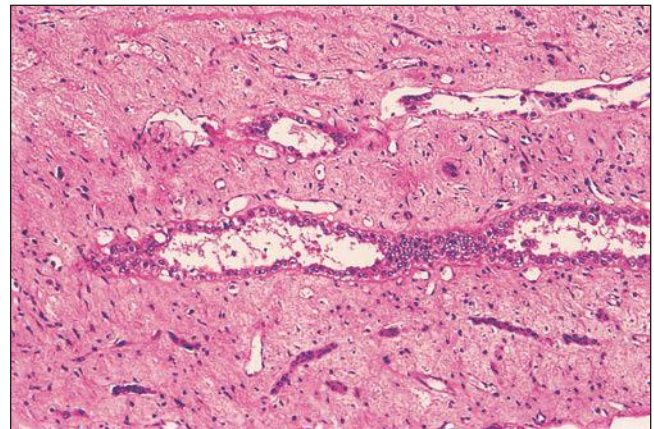


FIGURE 27.51 Sclerotic area of papilla with loss of vasculature and tubular atrophy in an autopsy kidney from a patient with sickle cell disease. (H&E; $\times 200$.) (Specimen courtesy of Dr. E. Mancini, University of South Alabama.)

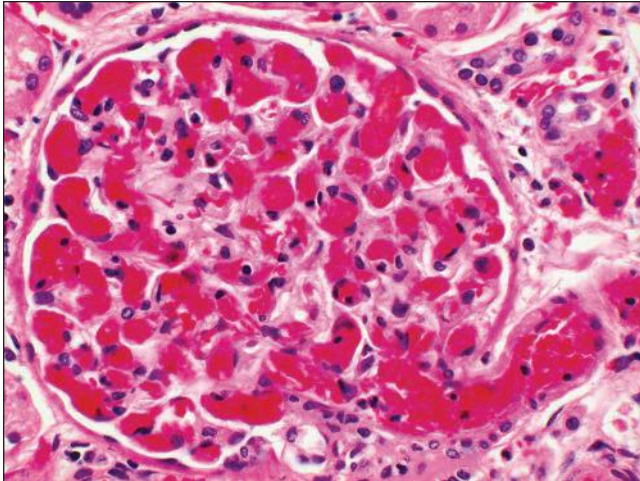


FIGURE 27.52 A glomerulus in a patient with sickle cell anemia has its arteriole and capillaries distended by sickled erythrocytes. (H&E; $\times 400$.) (Specimen courtesy of Dr. E. Mancini, University of South Alabama.)

GLOMERULAR ABNORMALITIES

Hypertrophy Structural changes were first described by Sydenstricker et al. (448) in 1923 as prominent glomeruli distended with blood, though without thrombi. Afferent and efferent arterioles can be dilated and congested with sickled red cells (Fig. 27.52) (445). Nonsclerotic glomeruli are often enlarged, with an increase in the total number of cross-sectioned capillary lumens accompanied by an increase in epithelial, endothelial, and mesangial cells (Fig. 27.53) (445,446,451). Iron deposition is limited and can occasionally be demonstrated in parietal epithelial cells with a lesser amount in visceral epithelial cells (Fig. 27.50) (445,446). Glomerular enlargement, particularly in a juxtamedullary location, to as much as 30% more than normal has been demonstrated in children as young as 2 years of age whose renal function was unknown; glomeruli in

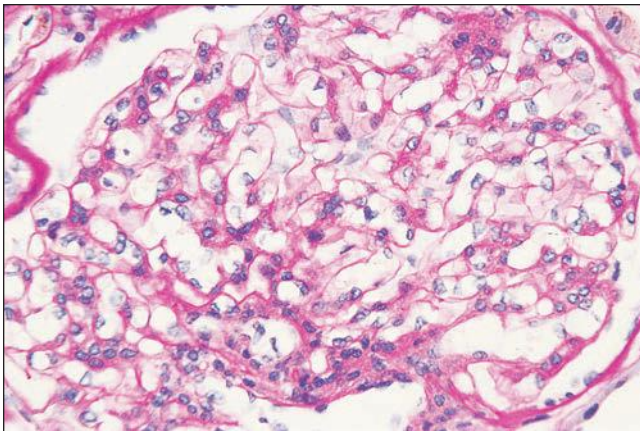


FIGURE 27.53 An enlarged glomerulus from a sickle cell patient has an increased number of capillary lumen cross sections and mild mesangial hypercellularity. (PAS; $\times 400$.) (Specimen courtesy of Dr. A. Chang, University of Chicago.)

even younger children were normal except for variable degrees of congestion (445,446). In adults, glomerular hypertrophy of approximately the same degree has been documented at all cortical levels and exists before evidence of proteinuria. The mean glomerular area increases over a wide age range and has been measured to be more than double that of normal controls (393,435,447,451). No significant difference in glomerular size or densities per unit area of cortex was found in adults with HbAS and controls, as the glomeruli in sickle cell trait can appear virtually normal (451).

Focal Segmental Glomerulosclerosis Glomerular abnormalities can be seen in SCD, with or without proteinuria. The fundamental pathologies in sickle cell glomerulopathy are hypertrophy and focal segmental glomerulosclerosis, sometimes accompanied by global sclerosis (393,447). Tejani et al. (452) described similar lesions in children. The focal segmental glomerulosclerosis is often perihilar in location and typically adherent to the Bowman capsule (Fig. 27.54). Solidification of glomerular tuft segments is associated with hyalinosis, lipid vacuolation, and foam cells, with loss of its capillary bed (393). Bhatena and Sondheimer recognized two patterns, collapsing and expansive; the former was dominated by mesangial atrophy and wrinkling collapse of the capillaries, whereas the obliterated tuft in the latter was characterized by mesangial matrix expansion (447). While their depiction of “collapsing” does not meet current criteria for the “collapsing variant” of FSGS, such a case has been reported in an HIV-negative patient with SSA (453). Application of the Columbia classification (454) to the kidney biopsies from 7 of 18 patients with SSA that demonstrated FSGS resulted in FSGS NOS (3/7), FSGS tip variant (2/7), and FSGS perihilar variant (2/7) (455). Glomerular ischemia and sclerosis are more frequent in HbSS than HbAS.

Immunofluorescent microscopy has shown irregular immunostaining for IgM, C3, and C1q in areas of sclerosis, whereas nonsclerotic segments either are negative or contain trace amounts of IgM, IgG, and C3. Electron microscopy shows focal effacement of podocyte foot processes, no or only

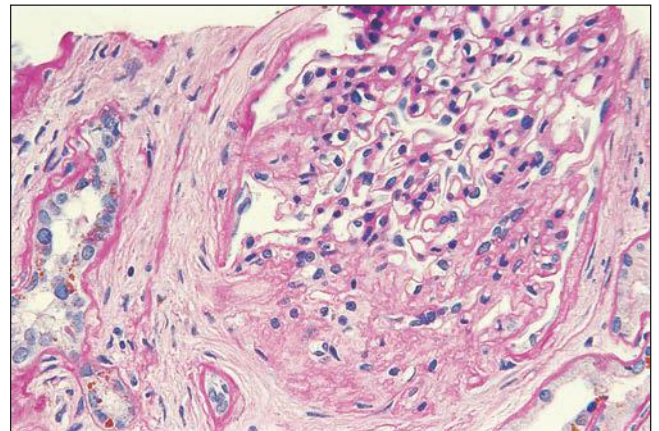


FIGURE 27.54 The enlarged glomerulus has developed segmental sclerosis. The surrounding interstitium is fibrotic, and iron is visible in tubular epithelial cells. (PAS; $\times 400$.) (Specimen courtesy of Dr. A. Chang, University of Chicago.)

rare electron-dense deposits, residual bodies in mesangial cells, and limited mesangial interposition (393,447). Falk et al. (393) noted focal electron-lucent expansion of the subendothelial zone, suggestive of early lesions that could evolve to those in advanced SCN that resemble membranoproliferative glomerulonephritis.

Membranoproliferative Pattern Nine of 12 proteinuric patients studied by Bakir et al. (456) had glomerular lesions that resembled membranoproliferative glomerulonephritis, although the lobular pattern was not as striking. The hypercellular glomeruli had circumferential mesangial expansion, often associated with duplication of the GBM, causing characteristic “tram-tracking” (456). Similar changes, akin to chronic thrombotic microangiopathy have been described by others (435,451,457–459). Normal platelet counts have been observed in most patients with biopsies labeled thrombotic microangiopathy (455). Basement membrane duplication may only be focal, and variable degrees of segmental or global glomerulosclerosis can often accompany this lesion.

Immunofluorescent microscopy is usually negative but can show occasional nonspecific mesangial or capillary loop positivity for C3, IgM, IgG, or even IgA, although staining has typically been very faint (451,456,459). Electron microscopy does not show electron-dense deposits but increased mesangial matrix and mesangial cells. Podocyte foot process effacement is variable. Endothelial cells can be separated from the GBM by electron-lucent material in the subendothelial region (Fig. 27.55). There is often scalloping of the subendothelial aspect of the basement membrane and interposition of mesangial cells between the outer original basement membrane and the new inner basement membrane-like material (457,459). Small siderosomes can be seen in endothelial and mesangial cells. Similar subendothelial zone expansion has been described in a patient with HbSC (460).

Other Only a few instances of potential immune complex-mediated glomerular lesions have been characterized in the literature. Pardo et al. (461) maintained the existence of a normocomplementemic autologous immune complex-mediated process in seven individuals with SCA and proteinuria or nephrotic syndrome. Biopsies from these patients showed enlarged glomeruli with increased mesangial matrix and cellularity, duplication of the GBMs, and progression to sclerosis. Immunofluorescent microscopy demonstrated granular IgG and C3 in the mesangium and GBM in addition to IgM, C2, and C4 in several cases. Antibodies against renal tubular antigen decorated glomeruli in the same pattern in two subjects. Electron microscopy showed electron-dense deposits on the inner aspect of the lamina densa in four patients in addition to mesangial and visceral epithelial siderosomes. Mesangial interposition and basement membrane duplication were noted. Antibody to renal tubular epithelial antigen was detected in the serum of two subjects. Ozawa et al. (462) described similar findings in a patient with sickle cell trait.

Renal biopsy is of value in patients with sickle cell disorders to differentiate the lesions associated with hemoglobinopathies from other acute diseases that may overlap clinically. Coincident diagnoses, including lupus nephritis in patients with HbSS- and HbS-thalassemia (463–465), immunotactoid glomerulopathy in a boy with HbSS (466), and amyloidosis in a patient with SCA and familial Mediterranean fever (467),

have been demonstrated. Amyloidosis of the AA type has also been seen in SS patients, including one child, without a familial predisposition, presumably secondary to frequent sickle cell crises that may provoke recurrent acute inflammation and the development of amyloid A protein (468–470).

Not surprisingly, coexistent immune complex-mediated diseases such as acute poststreptococcal glomerulonephritis can occur (471). Unusual to patients with SCD and acute poststreptococcal glomerulonephritis is a normal complement level, suggested to be secondary to an abnormality of the alternative pathway of complement activation (472). Proliferative segmental glomerulonephritis with immune complexes or microscopic vasculitis has been described in patients with SCD following Parvovirus-induced aplastic crises (473–475).

Malignancies

The incidence of malignancy and SCD deserves further analysis as changes in management offer longer life expectancies with exposure to more medications. A cancer incidence rate of 1.74 cases per 1000 patient years was calculated from a single institution review of 696 patients, results comparable to the Surveillance, Epidemiology, and End Results (SEER) data for age-specific cancer incidence in African Americans (476). Based on genotypic frequencies, however, Baron et al. (477) reported a surprising 16.7-fold excess of HbSS patients and an expected incidence of HbAS patients among those at their institution with renal cell carcinoma. Those with sickle cell trait, it turns out, may have had a tumor other than renal cell carcinoma.

Davis et al. (478) described a rare, highly aggressive neoplasm, which they termed renal medullary carcinoma (RMC), that is almost unique to African Americans with sickle cell trait. Rare cases have been documented in Caucasians and Brazilians (479,480). The tumor occurs in children and young adults and has a slight male predominance. Presenting symptoms most commonly include gross hematuria, abdominal or flank pain, and a palpable mass. Typically, the tumor is widely metastatic at diagnosis to regional lymph nodes and lungs, with spread to the liver, adrenals, and bone reported. The response to therapy including radical surgery and combination chemotherapy has been poor, with most deaths occurring within months of diagnosis (481).

Nearly all patients described to date have HbAS, with rare documented exceptions of HbSS and HbSC (478,479). Isolated cases of RMC have been reported in patients without hemoglobinopathies, confirmed by either electrophoresis or mutational analysis of hemoglobin B gene (482,483).

Pathologic Change

These bulky tumors are poorly circumscribed, occupy the renal medulla and adjacent soft tissue, and spread to the cortex as multiple satellite nodules. Tumor size has ranged from 2 to 18 cm (mean, 7 cm), with hemorrhage and necrosis common. The light microscopic appearance is variable but most commonly includes a cribriform architecture with tumor cell aggregates forming uneven glandular spaces sometimes surrounded by a hypocellular desmoplastic reaction with inflammation (Fig. 27.56). The low-power view is sometimes reminiscent of a yolk sac (endodermal sinus) tumor. Other growth patterns—microcystic with micropapillations, solid, or sarcomatoid—may be present as well as solid sheets of poorly differentiated areas. The tumor cells have large vesicular nuclei

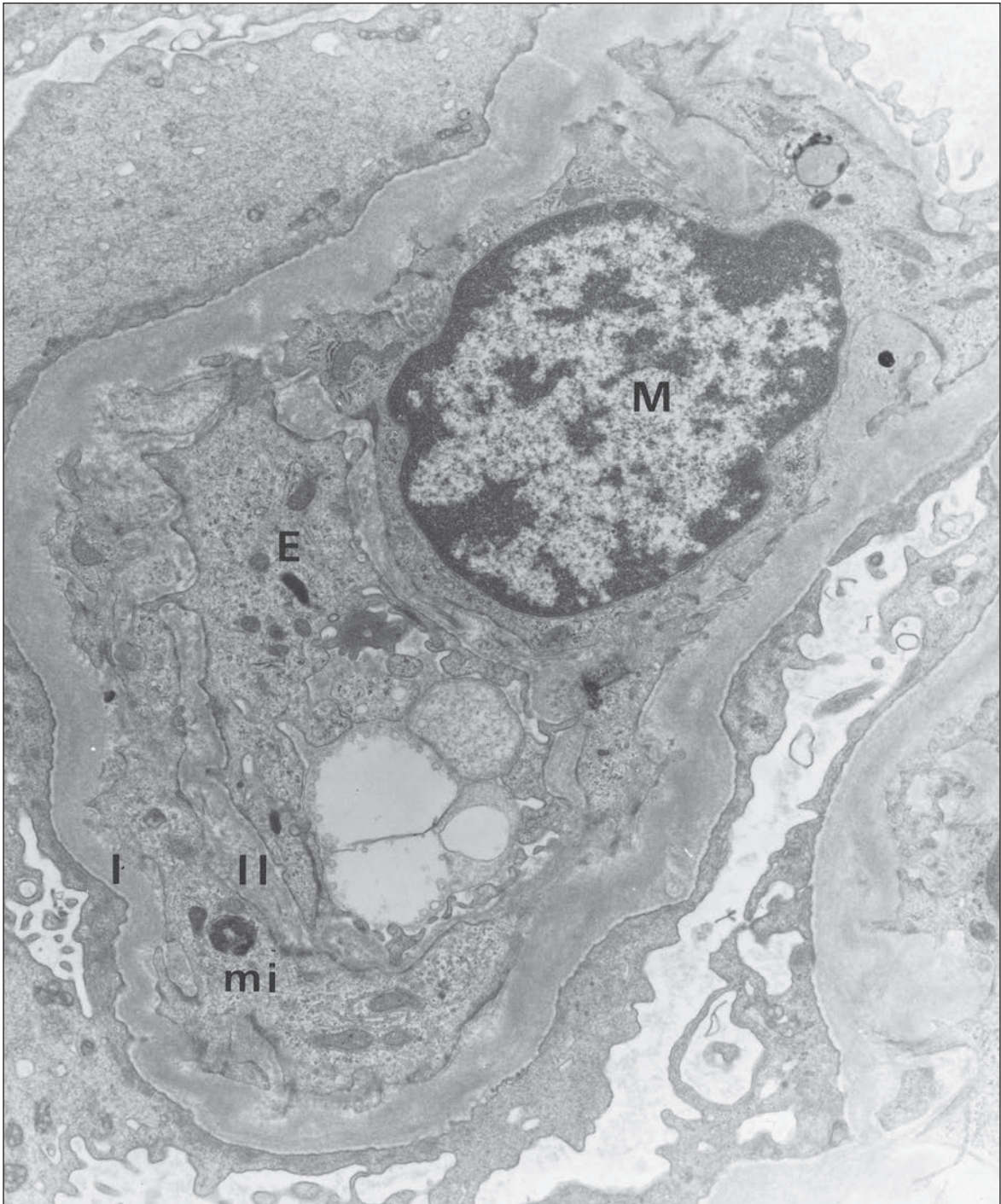


FIGURE 27.55 Electron micrograph from the kidney of a 31-year-old black man with HbSS and nephrotic syndrome (proteinuria 3.1 g/24 h) showing glomerular capillary surrounded by podocytes with effaced foot processes. The capillary is double contoured (I and II) with mesangial interposition (mi). M, mesangial cell nucleus; E, capillary endothelium. ($\times 13,120$.)

with prominent nucleoli and abundant eosinophilic cytoplasm, with cytoplasmic lumina in some cases. Cytoplasmic inclusions resembling rhabdoid tumor are not uncommon (Fig. 27.57). Mitotic activity is highly variable, but lymphatic or vascular invasion is the rule, which occasionally extends into the main renal vein. Tumors coexpress cytokeratin (CAM 5.2 and AE1/AE3) and vimentin (481).

Cytogenetic studies have been limited, but complex hyperdiploidy with numerous structural abnormalities has been demonstrated with no recurring abnormality (479,482). While comparative genomic hybridization demonstrated no genetic gains or losses in eight cases and loss of chromosome 22 in one case (479), more sensitive SNP array assays in two cases demonstrated multiple but distinct segmental chromosomal

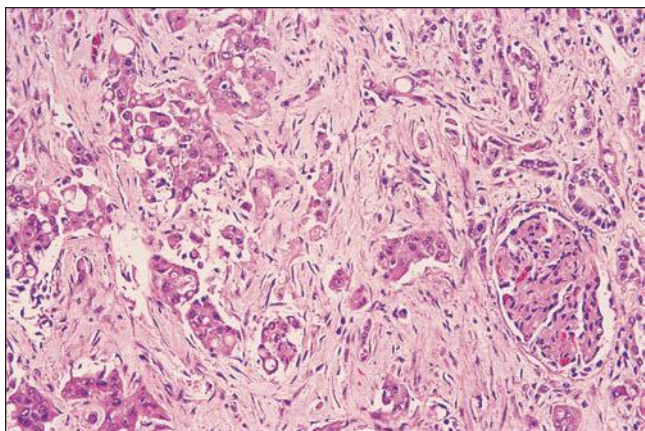


FIGURE 27.56 Renal medullary carcinoma from a 16-year-old African American boy with sickle cell trait. The kidney tumor has glandular structures formed by pleomorphic and mitotically active cells with occasional cytoplasmic lumina. The desmoplastic stroma surrounds tumor cell islands and encases a single sclerotic glomerulus. (H&E; $\times 200$.)

gains and losses (482). Coincident with aggressive behavior, loss of INI-1 (hSNF5/SMARCB1/BAF47) expression was demonstrated in all six cases tested using immunohistochemical analysis, as seen in renal and extrarenal rhabdoid tumors (483,484). The finding of an ALK activating mutation in one tumor (485) and a pericentric inversion of chromosome 2 as the sole cytogenetic abnormality in another tumor (479) might provide rationale for novel treatment using ALK inhibitors.

Differential Diagnosis

RMCs have often been considered a subtype of collecting duct carcinoma (CDC) despite their clinical and pathologic differences. CDC is a rare neoplasm that arises from the medullary collecting ducts and characteristically expresses cytokeratin 34 β -E12 and ulex europaeus agglutinin 1 lectin by immunohistochemical analysis. RMC has been shown to

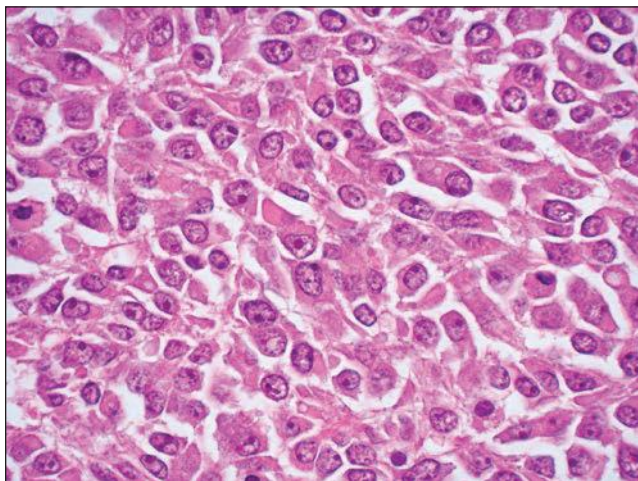


FIGURE 27.57 Renal medullary carcinoma (same patient as Fig. 27.56) with rhabdoid cellular features, including prominent nucleoli and perinuclear cytoplasmic inclusions. (H&E; $\times 400$.)

lack the former and demonstrate only focal staining of ulex europaeus in a minority of cases, supporting the distinctiveness of RMC from CDC (479). Gene expression profiling of two RMCs, however, revealed close clustering with transitional cell carcinoma, perhaps supporting an origin from urothelium of the renal pelvis (486). The perception that CDC is commonly found in young adults is mostly because of its lack of distinction in many references from RMC. CDC may in fact be rare in adolescents, once the diagnosis of RMC is excluded. A single case of CDC in a patient with sickle cell trait was reported in a 61-year-old black woman (487). Recently, the World Health Organization has separately designated CDC and RMC as variants of renal cell carcinoma (488).

Etiology and Pathogenesis

Sickling Cells

The polymerization of HbS is the required event in the molecular pathogenesis of SCD and is enhanced by deoxygenation, low pH, increased intracellular HbS, and decreased intracellular concentration of protective hemoglobins such as HbF and HbA2 (489). The polymer, a rope-like fiber, bundles with others to distort the erythrocyte into a rigid sickled shape, interfering with its usual deformability. The kinetics of polymerization, including a delay time followed by exponential polymerization, is usually longer than the transit time of microcirculation, so that most cells fail to undergo HbS polymerization. Prolongation of erythrocyte transit time is caused by enhanced erythrocyte adhesion to endothelium, cell dehydration, and abnormal vasomotor tone that favors vasoconstriction (388). Microcirculatory obstruction, originally thought to result from impaired capillary transit of sickled cells, is probably caused by trapping of deformed erythrocytes in the slow-flowing venular side and their aggregation with leukocytes and adhesion to endothelium, resulting in obstruction, local hypoxia, increased HbS polymerization, and propagation of the occlusion to adjacent vasculature (490).

Renal Medullary Alterations

Hemoglobin S aggregation and polymerization are the seminal events in the erythrocytes of individuals with the various sickle cell syndromes and the primary pathophysiologic factor in renal injury. The hyperosmolar environment of the renal medulla, with its low O₂ tension and pH, increases the risk of sickling within vessels of the vasa recta leading to diminished perfusion (491). Congestion and sickling produce severe stasis, which leads to peritubular hemorrhage and ischemic necrosis in the medullary pyramids. The resultant hematuria is usually unilateral and more frequently involves the left kidney, perhaps because of the increased venous pressure owing to the greater length of the left renal vein (441).

Impaired local blood flow through the vasa recta decreases the oxygen supply to the tubular cells in the medullary loop of Henle, reducing the ability to absorb sodium from the tubular lumen and resulting in a decrease in the medullary interstitial osmolality (444). The functional defect in the maximal ability of the collecting duct to concentrate urine becomes irreversible with advancing age because sustained ischemia, which produces repeated sludging with thrombosis and progressive infarction, leads to scarring and permanent anatomic alterations including disruption of the vasa recta and countercurrent exchange. While maximum concentrating abilities are lost due to the disappearance of juxtamedullary nephrons and their long loops of

Henle that extend into the inner medulla and renal papillae, the capacity to maximally dilute urine remains intact. This is explained by unimpaired solute reabsorption from the TAL of the loop of Henle, which resides in the outer medullary zone in approximately 85% of nephrons and receives blood via intact patent peritubular capillaries.

Oxidative stress is increased in SCD and originates from multiple sources, including increased levels of tumor necrosis factor- α and interleukin 6, repetitive ischemia-reperfusion, and the generation of oxidants by endothelial cells stimulated by erythrocytes, leukocytes, or the sickled erythrocytes themselves (492,493). The role for oxidative stress in mediating renal tubular damage has been demonstrated. Kidneys from mouse models of SCD and humans with SCA showed increased expression of inducible nitric oxide synthase and increased apoptosis in tubular epithelial cells compared to wild-type control mice and healthy humans (494). Additional data suggest that NO and/or peroxynitrite, an extremely destructive reactive oxygen species, initiates cell damage that leads to apoptosis of epithelial cells and that inhibition of NO-mediated oxidant stress ameliorates renal cellular injury (493,495).

Renal Cortical Alterations

Hyperperfusion of the kidney and supranormal proximal tubular function may be related to the vasorelaxant effects of prostaglandin (398). Ischemia in the medullary region results in altered renal production of prostaglandins, the net effect of which can also lead to vasodilation of afferent glomerular arterioles and to glomerular hypertension (416,450,496). In contrast to controls, prostaglandin inhibitors significantly reduce RPF and GFRs in patients with SCD (398,416). Another vasodilatory agonist, such as heme oxygenase 1, may also contribute to renal hyperperfusion in SCD. Sick cell glomerulopathy appears to be the consequence of focal and segmental glomerular sclerosis superimposed on maximally hypertrophied glomeruli.

Renal hypertrophy commonly occurs in settings of renal hyperperfusion and hyperfiltration, such as diabetes, pregnancy, high dietary protein intake, and subtotal reduction of renal mass. As such, hyperfiltration leads to increased tubular sodium transport, which greatly augments renal oxygen consumption (renal metabolic work) and promotes renal hypertrophy (497). Enlarged glomeruli are vulnerable to injury (498). They experience increased wall tension that may impair glomerular permselectivity, leading to proteinuria and the expression of proinflammatory genes. The mechanical strain placed on podocytes can result in their detachment with subsequent formation of synechiae to Bowman capsule and development of segmental sclerosis (499). An alternative or additive mechanism in SSA, namely, vascular occlusion, could be operative in the development of focal segmental glomerulosclerosis, collapsing variant (453), as has been implicated in collapsing FSGS arising in renal allografts (500).

Glomerular lesions in SCD sometimes resemble those of thrombotic microangiopathy (459). Endothelial dysfunction has been demonstrated in SCD and can be implicated in the pathogenesis of tissue injury and clinical manifestations (497,501). SCA patients exhibit an inflammatory milieu that promotes endothelial activation. They show abnormal responses to shear stress and up-regulation of procoagulants (tissue factor and plasminogen activator inhibitor-1), which

could manifest as thrombotic microangiopathy (502). Other mechanisms have been advanced for the pathogenesis of glomerular injury including increased tissue iron deposition (503). That iron is generally deposited in the interstitium and along the lower nephron rather than glomeruli argues against the theory. Moreover, glomerular lesions of SCA are not seen in other iron overload states such as hemochromatosis or with excessive blood transfusions.

Oxidative stress may also contribute to glomerular damage. The instability of HbS allows degradation to its heme and globin moieties, and increased amounts of heme have been found in the plasma of patients with SCD (504). The bioavailability of NO is reduced in the presence of free heme, impairing important vascular function of NO such as vasodilation, platelet inhibition, and inhibition of endothelin 1, a potent vasoconstrictor in humans that may be involved in the pathogenesis of FSGS (505). Interestingly, up-regulation of heme oxygenase-1 (HO-1), an antioxidant involved in the degradation of heme, has been demonstrated in the kidney vasculature, interstitium, and tubular epithelial cells as well as in circulating endothelial cells in sickle cell patients (506).

Clinical Course and Prognosis

Individuals with SCD have a decreased life expectancy. Historically, mortality in childhood from bacterial sepsis contributed significantly to this shortened survival. Neonatal screening, the introduction of prophylactic penicillin, and effective immunization against *Haemophilus influenzae* type b and *Streptococcus pneumoniae* in early childhood have increased survival into adulthood (>18 years) to nearly 94% (HbSS or HbS β^0) and 98% (HbSC or HbS β^+) in one large American cohort (507). Mortality before adulthood remains high in sub-Saharan Africa where the majority of affected children live (508). The average lifespan in the United States for men and women with HbSS has increased to 42 and 48 years, respectively, compared with ages of 60 and 68 years in those with HbSC disease (509). Improved life expectancy has shifted the focus of clinical problems in developed countries to chronic organ dysfunction. Where optimal medical care is unavailable, for example, in most parts of Africa, life expectancy for affected individuals with SCD is less than 30 years, and it remains the third leading cause of mortality in children receiving hospital care (510).

Multifactorial/Pleiotropic Genes

There is marked variation in clinical severity of SCA, owing in part to environmental, psychosocial, cultural, and even socioeconomic influences. Despite SCA being the first monogenic disease ever described, numerous other genes modify the phenotype. Genetic modification of the expression was originally suspected by notable geographic differences in clinical severity. The HbS gene is found on a genetic background of four major β -globin-like gene cluster haplotypes. Identified by various restriction endonucleases and assigned the name of the geographic area in which they are most frequent, they include the principal African haplotypes—Benin, Central African Republic (CAR or Bantu), and Senegal—in addition to the major Indo-European sickle mutation, Arab-India (511). The CAR haplotype has been associated with the highest incidence of organ damage and renal failure and the poorest HbF response to hydroxyurea (512–514).

Other multigenic influences on clinical presentations include the following: copresence of β -thalassemia or α -thalassemia, pyruvate kinase deficiency, and hereditary spherocytosis; regulators of HbF production such as female sex, polymorphisms in *XmnI-HBG2*, *BCL11A*, and *HBSIL-MYB* and growth factor (erythropoietin, transforming growth factor- β) levels and growth factor modulators (polymorphism in bone morphogenic protein receptor gene, *BMPR1B*) (515); modulators of erythrocyte-endothelial adhesion and leukocyte numbers; and even human leukocyte antigen (HLA) alleles (516–518). A recent large study in African Americans residing in the southeastern United States found that nephropathy risk variants in *APOL1* contribute independently from HbS to the risk of developing nondiabetic ESRD (519). That renal failure occurs in a minority of sickle patients underscores the influence of genetically determined non-SCD genes.

Chronic Renal Failure

Increased lifespan in SCA patients increases the probability of developing chronic renal failure (450,520). Ineffective erythropoiesis with increasingly severe anemia, hypertension, proteinuria, nephrotic syndrome, and microscopic hematuria were shown by Powars (521) to be preazotemic predictors of chronic renal failure. A low hematocrit serves as a protective mechanism in SCD by reducing blood viscosity and thus decreasing vasoocclusive crises; however, an increased number of pain crises do not lead to an increased risk for renal failure (512,522). Severe anemia appears to have an indirect adverse effect on the kidney, as hemoglobin levels have strongly correlated with creatinine clearance, especially in patients over 40 years of age (438,523). Hyposthenuria, unlike glomerular injury, does not correlate with subsequent renal impairment (524).

Compared to other African Americans, patients with SCD have a decrease in life expectancy of 25 to 30 years and a mortality rate that rose from 18% overall to 40% in those with glomerulopathy leading to end-stage renal failure (509). Morphologic evidence of the cause of death in 306 autopsies of SCD (including HbSS, HbSC, HbS/ β -thalassemia) accrued between 1929 and 1996 as part of the National Institutes of Health Centralized Pathology Unit for Sickle Cell Disease found infection to be most common for all ages (33% to 48%). Renal failure was implicated as the cause of death in 4.9% of cases, although additional evidence of chronic renal injury was noted as papillary necrosis (14.5%) and renal infarction and atrophy (23.4%) (525). An autopsy review covering a 26-year span found that renal failure contributed to mortality in nearly 23% of 141 patients with SCD (526). The prospective, 25-year longitudinal demographic and clinical cohort study by Powars et al. showed that 4.2% of patients with SCA (HbSS) and 2.4% with HbSC disease developed renal failure. Once renal failure develops, there is a substantially increased risk for early death. The survival of patients with SCA was 4 years after the onset of ESRD, with a median age at the time of death of 27 years (512). A retrospective analysis of the 1999 United States Renal Data System database revealed a mean age of end-stage renal failure of 40.68 ± 14 years (527).

Renal insufficiency is not typical before age 40, but approximately 30% of patients who survive beyond that age are affected (437,528). Therapeutic advances may be responsible for even fewer patients showing the onset of renal insufficiency in their 20s as compared to earlier studies (523).

Proteinuria is the hallmark of glomerular injury in patients with SCD and the antecedent to renal insufficiency and failure. The distribution of glomerular function and proteinuria in 280 adults with SCD suggests a progressive pattern from early glomerular hyperfiltration and hypertrophy (49%) to microalbuminuria (36%), to macroalbuminuria with preserved GFR (15%), to progressive renal insufficiency with macroalbuminuria, and finally, to ESRD that requires renal replacement therapy (408).

It is apparent that renal involvement begins in childhood and microalbuminuria will likely be a helpful predictor of end-organ damage in SCD, as it is in diabetes and hypertension. Microalbuminuria, as a preclinical marker of glomerular injury, has been documented in about 20% of children under 20 years of age (413,414,529). Early detection may theoretically allow therapeutic intervention to prevent progressive renal insufficiency.

Therapy

Management of SCD requires a concerted team effort addressing pain management, preventative care including prophylactic penicillin, nutritional services, and specialist interventions around pulmonary, ophthalmologic, neurologic, orthopedic, prenatal, and renal issues. Treatment is directed toward prevention of vasoocclusive crises and control of infections that can worsen renal function.

Treatment of Hematuria

Usually bedrest is sufficient for spontaneous resolution of most episodes of gross hematuria. Intravenous hypotonic solutions to decrease medullary tonicity and sodium bicarbonate to alkalinize urine plus hyperbaric oxygen and diuretics can eliminate clots from the bladder, reduce sickling, and potentially prevent papillary necrosis (530). Blood transfusion, the use of aminocaproic acid for fibrinolysis, and irrigation of the pyelocaliceal system may be necessary. Rarely is embolization or nephrectomy required.

Drug Therapy

NONSTEROIDAL ANTI-INFLAMMATORY AGENTS

The use of nonsteroidal anti-inflammatory agents (NSAIDs) as pain management for sickle cell crises carries untoward consequences on renal function. Nonsteroidal anti-inflammatory agents can produce significant declines in creatinine clearance and the rates of glomerular filtration and renal blood flow, owing to the maintenance of GFR by the prostaglandin system (416). Because NSAIDs have a demonstrated antinatriuretic effect and can increase the rate of progression to ESRD, these agents should be avoided in those SCD patients with evidence of SCN (398).

ANGIOTENSIN-CONVERTING ENZYME INHIBITORS

Relative systemic hypertension in patients with SCD appears to be associated with an increased risk of renal dysfunction (431). Urinary protein excretion was shown to decrease with ACE inhibitors, presumably through dilation of the efferent arterioles (393,531,532). Enalapril therapy has also been shown to reduce urinary protein excretion and normalize serum albumin in children (414,533); hyperkalemia resulted in discontinuation of treatment in the minority. The sustained benefit on protein excretion and prevention of renal

insufficiency from long-term ACE inhibitor therapy is anticipated but remains unproven.

HYDROXYUREA

In vivo evidence of mild disease in individuals with SCD with high concentrations of HbF led to the use of hydroxyurea, an S-phase cytologic drug that increases HbF in vivo. Other benefits of hydroxyurea include modulation of sickle erythrocytes' adhesive properties and enhanced NO production. A multicenter study of hydroxyurea in adult SCA, with a 17.5-year follow-up, showed improved survival without accompanying serious adverse events (534). The long-term hematologic efficacy of hydroxyurea at maximal tolerated dose in children with SCD has been demonstrated without adverse effects on growth, increased numbers of acquired DNA mutations, or renal toxicity (535). Early intervention with hydroxyurea may be considered for the prevention of proteinuria and renal disease, because microalbuminuria appears to be associated with a decreased hemoglobin level (413). A retrospective review of 144 children with SCD (123 with HbSS) found those patients treated with hydroxyurea to have the lowest incidence of microalbuminuria (13%) compared to patients on chronic transfusions (26%) or no treatment (24%) (536). Of the 17 pediatric patients with microalbuminuria at baseline, 16 remained free from microalbuminuria, with a mean follow-up period of 1.8 years, and 4 of 9 with microalbuminuria had resolution during treatment with hydroxyurea for nonrenal complications of SSA (414). The addition of hydroxyurea to enalapril therapy in children with proteinuria may further normalize the urine protein/creatinine ratio than enalapril alone (533). An average 2-year follow-up of children (21 to 53 months) treated with hydroxyurea showed prevention of glomerular hyperfiltration (537). These data led to a multicenter placebo-controlled trial of hydroxyurea in infants to prevent chronic organ damage. After 24 months of study, children who received hydroxyurea had better urine-concentrating capacity although no treatment effect was observed on GFR (538). The evaluation of the effect of extended hydroxyurea administration on GFR and the prevention of albuminuria and renal insufficiency remains an import goal.

NOVEL THERAPIES

The complexity of SCD makes it unlikely that a single agent will prevent or treat all sequelae. New agents that act through different mechanisms may yield synergistic benefit. Although the action of hydroxyurea to elevate HbF remains uncertain, increased hemoglobin F levels have been achieved with other drugs (butyrate, decitabine), but their efficacy in preventing end-organ damage has yet to be investigated. Similarly, unproven potential exists for additional novel interventions such as (a) increasing nitric oxide (sildenafil, inhaled NO, 6R-BH4) to modulate vascular tone and improve endothelial function, (b) decreasing inflammation (statins, steroids, sulfasalazine, IVIg) to reduce leukocyte adhesion and improve microvascular flow, (c) preventing RBC dehydration (magnesium supplementation, senicapoc) to avoid HbS polymerization, and (d) blocking endothelin receptor (bosentan) to thwart microvascular congestion (539). A recent trial of senicapoc failed to demonstrate a significant reduction in painful crises; however, clinically significant elevation in creatinine, although uncommon, was more frequent in the placebo group (540). It remains to be seen if improvement in hematologic parameters can modulate clinical outcomes.

RENAL REPLACEMENT THERAPY: DIALYSIS AND RENAL TRANSPLANTATION

Like others with ESRD, the treatment options available to sickle cell patients include dialysis and renal transplantation. Renal replacement therapy in the form of hemodialysis remains the standard management for end-stage SCN, although little is known about the long-term outcome of this group. SCN was the causative factor for 0.11% of the 375,152 patients in the U.S. Renal Data System who started ESRD therapy between 1992 and 1997, and increased the risk of mortality (527). A retrospective cohort study of Saudi Arabian patients revealed a higher mortality and significantly younger age and shorter dialytic age in comparison with ESRD patients without SCD who were receiving long-term hemodialysis, with poor survival attributed to infection (541). There was a trend toward improved survival in African American transplant recipients compared to their dialysis-treated (wait-listed) counterparts (relative risk = 0.14, $P = 0.056$) (542). Information from the year 2000 U.S. Renal Data System showed a far better survival curve—56% versus 14% at 10 years—for transplanted SCD patients compared to those who received only dialysis (390). These data suggest that transplantation is a better option for SCD patients with renal failure and that patients should be encouraged to undergo renal transplantation at an earlier stage.

The conclusions from two sequential national surveys of US transplant centers conducted by Chatterjee were that renal transplantation in patients with sickle cell hemoglobinopathies achieved results comparable to that of other ESRD populations (543,544). Many of these subjects were patients who developed ESRD with HbAS, implying other etiologies for kidney failure (519). The study by Ojo et al. (542) consisted of 22,647 African American end-stage SCN patients who were identified through the U.S. Renal Data System and the United Network of Organ Sharing; 82 (81 HbSS and 1 HbSC) of them received kidney transplantation between 1984 and 1996. There was no difference in the 1-year cadaveric graft survival and no significant effect of SCN on graft loss compared to other causes of ESRD. However, the 3-year cadaveric graft survival tended to be lower in the SCN group, and their adjusted 3-year risk of graft loss was significantly greater. Patient survival in SCN was significantly lower than that of others at 1 year (78% vs. 90%) and 3 years (59% vs. 81%). SCD is a rare cause of ESRD in pediatric patients, accounting for only 0.5% and 0.2% of patients registered in dialysis and transplant arms of the North American Pediatric Renal Transplant Cooperative Study. In this series, 10 transplants in 9 patients (7 HbSS, 1 HbS-thalassemia, 1 HbSC) had a 2-year graft and patient survival of 71% and 89%, respectively, suggesting that renal transplantation is also a viable option for adolescent patients (545).

An important rationale for not offering renal transplantation to those with end-stage SCN is the risk of infections from immunosuppressive therapy in patients who have already undergone splenic involution. Other considerations include the shortage of Afro-Caribbean donors, high panel reactive antibody (PRA) percentage or HLA antibodies due to repeated blood transfusions, poorer survival owing to the systemic nature of the disease, increased frequency of painful crises in association with improved posttransplant hematocrit, avascular osteonecrosis related to steroid therapy, and disease recurrence

in the allograft (546). In summary, results of renal transplantation in patients with ESRD caused by SCN are comparable to those of age- and race-matched recipients with ESRD from other causes. Although the long-term patient and allograft survival is still lagging behind that of other ESRD patients, there is a trend toward better patient survival relative to maintenance dialysis. Some argue that the higher death rates in SCN transplant recipients result from the underlying disease itself rather than an adverse impact of renal transplantation.

HEMATOPOIETIC CELL TRANSPLANTATION

Hematopoietic cell transplantation (HCT) is the only available potentially curative therapy for SCD, and almost 300 patients treated with myeloablative hematopoietic stem cell transplantation from genotypically identical siblings have been described in the literature with nearly a 95% overall survival, a 7% transplant-related mortality, and a 9% graft failure rate with autologous recovery and return to SCA; slightly improved results are noted for thalassemia (547,548). The vast majority of patients transplanted to date are 16 years of age or younger, ideally before end-organ damage occurs although inclusion criteria are still debated. Nonetheless, improved survival of recipients of HCT makes long-term complications, including chronic kidney disease more important. Twenty-three percent of 266 adults without pretransplant renal dysfunction who underwent HCT for hematopoietic disorders developed chronic kidney disease, after a mean of 2.6 years (549).

New developments hold promise including nonmyeloablative conditioning that leads to stable mixed chimerism, novel targeted posttransplantation treatments, and alternative donor sources, including umbilical cord blood and unrelated stem cell donors (550). Whether bone marrow transplantation in the early stage of the disease can reverse or halt the progression of established SCN is currently not known. Gene therapy is regarded with cautious optimism after successful results in the sickle transgenic mouse and a human with β -thalassemia (551).

Mouse Models of Sickle Cell Disease

Mouse models of SCA have been helpful in understanding the pathophysiology of the disease and the development of anti-sickling drugs. Initial models expressing variable degrees of severity include the SAD-1 mouse, which provided information about glomerular abnormalities and the protective effect of human γ -globulin; the Costantini-Fabry-Nagel (NYC1) model, in which it was concluded that increased GFR was not causally related to anemia and that nitric oxide and nitric oxide synthase participate in the pathogenesis of renal abnormalities; and the S + S- Antilles model, where in vivo adhesion of sickle cells to endothelium was first observed. Transgenic models with exclusively human globin chains ("HbS-only models") have been widely used for more than a decade and offer more realistic models. The knockout mice express severe sickle cell syndrome, very low hemoglobin levels, and short survival (552,553). The knockin mice are less severely affected and have longer survival than the knockout models due to replacement of the mouse globin genes by the human β -globin cluster and the γ -gene of fetal hemoglobin (553). These mice are particularly desirable for testing therapeutic gene replacement and stem cell therapy (554).

REFERENCES

1. Calabresi L, Pisciotta L, Costantin A, et al. The molecular basis of lecithin:cholesterol acyltransferase deficiency syndromes: A comprehensive study of molecular and biochemical findings in 13 unrelated Italian families. *Arterioscler Thromb Vasc Biol* 2005;25(9):1972–1978.
2. Naghashpour M, Cualing H. Splenomegaly with sea-blue histiocytosis, dyslipidemia, and nephropathy in a patient with lecithin-cholesterol acyltransferase deficiency: A clinicopathologic correlation. *Metabolism* 2009;58(10):1459–1464.
3. Holleboom AG, Kuivenhoven JA, van Olden CC, et al. Proteinuria in early childhood due to familial LCAT deficiency caused by loss of a disulfide bond in lecithin: Cholesterol acyl transferase. *Atherosclerosis* 2011;216(1):161–165.
4. Hovig T, Gjone E. Familial lecithin: cholesterol acyltransferase deficiency. Ultrastructural studies on lipid deposition and tissue reactions. *Scand J Clin Lab Invest Suppl* 1974;137:135–146.
5. Hirashio S, Izumi K, Ueno T, et al. Point mutation (C to T) of the LCAT gene resulting in A140C substitution. *J Atheroscler Thromb* 2010;17(12):1297–1301.
6. Charlton-Menys V, Pisciotta L, Durrington PN, et al. Molecular characterization of two patients with severe LCAT deficiency. *Nephrol Dial Transplant* 2007;22(8):2379–2382.
7. Ohta Y, Yamamoto S, Tsuchida H, et al. Nephropathy of familial lecithin-cholesterol acyltransferase deficiency: Report of a case. *Am J Kidney Dis* 1986;7(1):41–46.
8. Lager DJ, Rosenberg BF, Shapiro H, et al. Lecithin cholesterol acyltransferase deficiency: Ultrastructural examination of sequential renal biopsies. *Mod Pathol* 1991;4(3):331–335.
9. Strom EH, Sund S, Reier-Nilsen M, et al. Lecithin: Cholesterol Acyltransferase (LCAT) Deficiency: Renal lesions with early graft recurrence. *Ultrastruct Pathol* 2011;35(3):139–145.
10. Sessa A, Battini G, Meroni M, et al. Hypocomplementemic type II membranoproliferative glomerulonephritis in a male patient with familial lecithin-cholesterol acyltransferase deficiency due to two different allelic mutations. *Nephron* 2001;88(3):268–272.
11. Ayyobi AF, McGladdery SH, Chan S, et al. Lecithin: Cholesterol Acyltransferase (LCAT) deficiency and risk of vascular disease: 25 year follow-up. *Atherosclerosis* 2004;177(2):361–366.
12. Habib R, Dommergues JB, Gubler MC, et al. Glomerular mesangiolipidosis in Alagille syndrome (arteriohepatic dysplasia). *Pediatr Nephrol* 1987;1(3):455–464.
13. Davis J, Griffiths R, Larkin K, et al. Glomerular basement membrane lipidosis in Alagille syndrome. *Pediatr Nephrol* 2010;25(6):1181–1184.
14. Benoit G, Sartelet H, Levy E, et al. Mesangiolipidosis in Alagille syndrome—relationship with apolipoprotein A-I. *Nephrol Dial Transplant* 2007;22(7):2072–2075.
15. Lynn EG, Siow YL, Fröhlich J, et al. Lipoprotein-X stimulates monocyte chemoattractant protein-1 expression in mesangial cells via nuclear factor-kappa B. *Kidney Int* 2001;60(2):520–532.
16. Lambert G, Sakai N, Vaisman BL, et al. Analysis of glomerulosclerosis and atherosclerosis in lecithin cholesterol acyltransferase-deficient mice. *J Biol Chem* 2001;276(18):15090–15098.
17. Zhu X, Herzenberg AM, Eskandarian M, et al. A novel in vivo lecithin-cholesterol acyltransferase (LCAT)-deficient mouse expressing predominantly LpX is associated with spontaneous glomerulopathy. *Am J Pathol* 2004;165(4):1269–1278.
18. Rousset X, Vaisman B, Auerbach B, et al. Effect of recombinant human lecithin cholesterol acyltransferase infusion on lipoprotein metabolism in mice. *J Pharmacol Exp Ther* 2010;335(1):140–148.
19. Yee MS, Pavitt DV, Richmond W, et al. Changes in lipoprotein profile and urinary albumin excretion in familial LCAT deficiency with lipid lowering therapy. *Atherosclerosis* 2009;205(2):528–532.
20. Miarka P, Idzior-Walus B, Kuzniewski M, et al. Corticosteroid treatment of kidney disease in a patient with familial lecithin-cholesterol acyltransferase deficiency. *Clin Exp Nephrol* 2011;15(3):424–429.
21. Aranda P, Valdivielso P, Pisciotta L, et al. Therapeutic management of a new case of LCAT deficiency with a multifactorial long-term approach based on high doses of angiotensin II receptor blockers (ARBs). *Clin Nephrol* 2008;69(3):213–218.

22. Saito T, Sato H, Kudo K, et al. Lipoprotein glomerulopathy: Glomerular lipoprotein thrombi in a patient with hyperlipoproteinemia. *Am J Kidney Dis* 1989;13(2):148–153.
23. Saito T, Matsunaga A, Oikawa S. Impact of lipoprotein glomerulopathy on the relationship between lipids and renal diseases. *Am J Kidney Dis* 2006;47(2):199–211.
24. Han J, Pan Y, Chen Y, et al. Common apolipoprotein E gene mutations contribute to lipoprotein glomerulopathy in China. *Nephron Clin Pract* 2010;114(4):c260–c267.
25. Boumendjel R, Papari M, Gonzalez M. A rare case of lipoprotein glomerulopathy in a white man: An emerging entity in Asia, rare in the white population. *Arch Pathol Lab Med* 2010;134(2):279–282.
26. Bombback AS, Song H, D'Agati VD, et al. A new apolipoprotein E mutation, apoE Las Vegas, in a European-American with lipoprotein glomerulopathy. *Nephrol Dial Transplant* 2010;25(10):3442–3446.
27. Rovin BH, Roncone D, McKinley A, et al. APOE Kyoto mutation in European Americans with lipoprotein glomerulopathy. *N Engl J Med* 2007;357(24):2522–2524.
28. Pasquariello A, Pasquariello G, Innocenti M, et al. Lipoprotein glomerulopathy: First report of 2 not consanguineous Italian men from the same town. *J Nephrol* 2011;24(3):381–385.
29. Sam R, Wu H, Yue L, et al. Lipoprotein glomerulopathy: A new apolipoprotein E mutation with enhanced glomerular binding. *Am J Kidney Dis* 2006;47(3):539–548.
30. Liberopoulos E, Siamopoulos K, Elisaf M. Apolipoprotein E and renal disease. *Am J Kidney Dis* 2004;43(2):223–233.
31. Tsimihodimos V, Elisaf M. Lipoprotein glomerulopathy. *Curr Opin Lipidol* 2011;22(4):262–269.
32. Ishigaki Y, Oikawa S, Suzuki T, et al. Virus-mediated transduction of apolipoprotein E (ApoE)-sendai develops lipoprotein glomerulopathy in ApoE-deficient mice. *J Biol Chem* 2000;275(40):31269–31273.
33. Ishimura A, Watanabe M, Nakashima H, et al. Lipoprotein glomerulopathy induced by ApoE-Sendai is different from glomerular lesions in aged apoE-deficient mice. *Clin Exp Nephrol* 2009;13(5):430–437.
34. Hoffmann M, Scharnagl H, Panagiotou E, et al. Diminished LDL receptor and high heparin binding of apolipoprotein E2 Sendai associated with lipoprotein glomerulopathy. *J Am Soc Nephrol* 2001;12(3):524–530.
35. Murano T, Matsumura R, Misawa Y, et al. Interaction of endothelial cells and triglyceride-rich lipoproteins with apolipoprotein E (Arg→Cys) from a patient with lipoprotein glomerulopathy. *Metabolism* 2002;51(2):201–205.
36. Kanamaru Y, Nakao A, Shirato I, et al. Chronic graft-versus-host autoimmune disease in Fc receptor gamma chain-deficient mice results in lipoprotein glomerulopathy. *J Am Soc Nephrol* 2002;13(6):1527–1533.
37. Chen S, Liu ZH, Zheng JM, et al. A complete genomic analysis of the apolipoprotein E gene in Chinese patients with lipoprotein glomerulopathy. *J Nephrol* 2007;20(5):568–575.
38. Sakatsume M, Kadomura M, Sakata I, et al. Novel glomerular lipoprotein deposits associated with apolipoprotein E2 homozygosity. *Kidney Int* 2001;59(5):1911–1918.
39. Karube M, Nakabayashi K, Fujioka Y, et al. Lipoprotein glomerulopathy-like disease in a patient with type III hyperlipoproteinemia due to apolipoprotein E2 (Arg158 Cys)/3 heterozygosity. *Clin Exp Nephrol* 2007;11(2):174–179.
40. Ieiri N, Hotta O, Taguma Y. Resolution of typical lipoprotein glomerulopathy by intensive lipid-lowering therapy. *Am J Kidney Dis* 2003;41(1):244–249.
41. Arai T, Yamashita S, Yamane M, et al. Disappearance of intraglomerular lipoprotein thrombi and marked improvement of nephrotic syndrome by bezafibrate treatment in a patient with lipoprotein glomerulopathy. *Atherosclerosis* 2003;169(2):293–299.
42. Kinomura M, Sugiyama H, Saito T, et al. A novel variant apolipoprotein E Okayama in a patient with lipoprotein glomerulopathy. *Nephrol Dial Transplant* 2008;23(2):751–756.
43. Matsunaga A, Furuyama M, Hashimoto T, et al. Improvement of nephrotic syndrome by intensive lipid-lowering therapy in a patient with lipoprotein glomerulopathy. *Clin Exp Nephrol* 2009;13(6):659–662.
44. Hamatani H, Hiromura K, Kobatake K, et al. Successful treatment of lipoprotein glomerulopathy in a daughter and a mother using nicositol. *Clin Exp Nephrol* 2010;14(6):619–624.
45. Xin Z, Zhihong L, Shijun L, et al. Successful treatment of patients with lipoprotein glomerulopathy by protein A immunoabsorption: A pilot study. *Nephrol Dial Transplant* 2009;24(3):864–869.
46. Foster K, Matsunaga A, Matalon R, et al. A rare cause of posttransplantation nephrotic syndrome. *Am J Kidney Dis* 2005;45(6):1132–1138.
47. Mourad G, Djamali A, Turc-Baron C, et al. Lipoprotein glomerulopathy: A new cause of nephrotic syndrome after renal transplantation. *Nephrol Dial Transplant* 1998;13(5):1292–1294.
48. Henneman P, van der Sman-de Beer F, Moghaddam PH, et al. The expression of type III hyperlipoproteinemia: Involvement of lipolysis genes. *Eur J Hum Genet* 2009;17(5):620–628.
49. Soran H, Charlton-Menys V, Hegele R, et al. Proteinuria and severe mixed dyslipidemia associated with a novel APOAV gene mutation. *J Clin Lipidol* 2010;4(4):310–313.
50. Bocca G, Monnens LA. Defective proximal tubular function in a patient with I-cell disease. *Pediatr Nephrol* 2003;18(8):830–832.
51. Chander PN, Nurse HM, Pirani CL. Renal involvement in adult Gaucher's disease after splenectomy. *Arch Pathol Lab Med* 1979;103(9):440–445.
52. Santoro D, Rosenbloom BE, Cohen AH. Gaucher disease with nephrotic syndrome: Response to enzyme replacement therapy. *Am J Kidney Dis* 2002;40(1):E4.
53. Becker-Cohen R, Elstein D, Abrahamov A, et al. A comprehensive assessment of renal function in patients with Gaucher disease. *Am J Kidney Dis* 2005;46(5):837–844.
54. Renwick N, Nasr SH, Chung WK, et al. Foamy podocytes. *Am J Kidney Dis* 2003;41(4):891–896.
55. Germain DP. Fabry disease. *Orphanet J Rare Dis* 2010;5:30.
56. Nakamura K, Hattori K, Endo F. Newborn screening for lysosomal storage disorders. *Am J Med Genet C Semin Med Genet* 2011;157(1):63–71.
57. Linthorst GE, Bouwman MG, Wijburg FA, et al. Screening for Fabry disease in high-risk populations: A systematic review. *J Med Genet* 2010;47(4):217–222.
58. Saito S, Ohno K, Sakuraba H. Fabry-database.org: Database of the clinical phenotypes, genotypes and mutant alpha-galactosidase A structures in Fabry disease. *J Hum Genet* 2011;56(6):467–468.
59. Maier EM, Osterrieder S, Whybra C, et al. Disease manifestations and X inactivation in heterozygous females with Fabry disease. *Acta Paediatr Suppl* 2006;95(451):30–38.
60. Banks DE, Milutinovic J, Desnick RJ, et al. Silicon nephropathy mimicking Fabry's disease. *Am J Nephrol* 1983;3(5):279–284.
61. Muller-Hocker J, Schmid H, Weiss M, et al. Chloroquine-induced phospholipidosis of the kidney mimicking Fabry's disease: Case report and review of the literature. *Hum Pathol* 2003;34(3):285–289.
62. Albay D, Adler SG, Philipose J, et al. Chloroquine-induced lipidosis mimicking Fabry disease. *Mod Pathol* 2005;18:733–738.
63. Bracamonte ER, Kowalewska J, Starr J, et al. Iatrogenic phospholipidosis mimicking Fabry disease. *Am J Kidney Dis* 2006;48(5):844–850.
64. Valbuena C, Leitao D, Carneiro F, et al. Immunohistochemical diagnosis of Fabry nephropathy and localisation of globotriaosylceramide deposits in paraffin-embedded kidney tissue sections. *Virchows Arch* 2011;460(2):211–221.
65. Oqvist B, Brenner BM, Oliveira JP, et al. Nephropathy in Fabry disease: The importance of early diagnosis and testing in high-risk populations. *Nephrol Dial Transplant* 2009;24(6):1736–1743.
66. Tai CL, Liu MY, Yu HC, et al. The use of high resolution melting analysis to detect Fabry mutations in heterozygous females via dry bloodspots. *Clin Chim Acta* 2012;413(3–4):422–427.
67. Desnick RJ. Prenatal diagnosis of Fabry disease. *Prenat Diagn* 2007;27(8):693–694.
68. Paschke E, Fauler G, Winkler H, et al. Urinary total globotriaosylceramide and isoforms to identify women with Fabry disease: A diagnostic test study. *Am J Kidney Dis* 2011;57(5):673–681.
69. Kistler AD, Siwy J, Breunig F, et al. A distinct urinary biomarker pattern characteristic of female Fabry patients that mirrors response to enzyme replacement therapy. *PLoS One* 2011;6(6):e20534.
70. Vedder AC, Strijland A, vd Bergh Weerman MA, et al. Manifestations of Fabry disease in placental tissue. *J Inher Metab Dis* 2006;29(1):106–111.
71. Zarate YA, Hopkin RJ. Fabry's disease. *Lancet* 2008;372(9647):1427–1435.
72. Desnick RJ, Brady RO. Fabry disease in childhood. *J Pediatr* 2004;144(5 Suppl):S20–S26.

73. Branton MH, Schiffmann R, Sabnis SG, et al. Natural history of Fabry renal disease: Influence of alpha-galactosidase A activity and genetic mutations on clinical course. *Medicine (Baltimore)* 2002;81(2):122–138.
74. Tondel C, Bostad L, Hirth A, et al. Renal biopsy findings in children and adolescents with Fabry disease and minimal albuminuria. *Am J Kidney Dis* 2008;51(5):767–776.
75. Najafian B, Svarstad E, Bostad L, et al. Progressive podocyte injury and globotriaosylceramide (GL-3) accumulation in young patients with Fabry disease. *Kidney Int* 2011;79(6):663–670.
76. Ramaswami U, Najafian B, Schieppati A, et al. Assessment of renal pathology and dysfunction in children with Fabry disease. *Clin J Am Soc Nephrol* 2010;5(2):365–370.
77. Schiffmann R, Warnock DG, Banikazemi M, et al. Fabry disease: Progression of nephropathy, and prevalence of cardiac and cerebrovascular events before enzyme replacement therapy. *Nephrol Dial Transplant* 2009;24(7):2102–2111.
78. Wanner C, Oliveira JP, Ortiz A, et al. Prognostic indicators of renal disease progression in adults with Fabry disease: Natural history data from the Fabry Registry. *Clin J Am Soc Nephrol* 2010;5(12):2220–2228.
79. Wilcox WR, Oliveira JP, Hopkin RJ, et al. Females with Fabry disease frequently have major organ involvement: Lessons from the Fabry Registry. *Mol Genet Metab* 2008;93(2):112–128.
80. Wornell P, Dyack S, Crocker J, et al. Fabry disease and nephrogenic diabetes insipidus. *Pediatr Nephrol* 2006;21(8):1185–1188.
81. Selvarajah M, Nicholls K, Hewitson TD, et al. Targeted urine microscopy in Anderson-Fabry disease: A cheap, sensitive and specific diagnostic technique. *Nephrol Dial Transplant* 2011;26(10):3195–3202.
82. Svarstad E, Iversen BM, Bostad L. Bedside stereomicroscopy of renal biopsies may lead to a rapid diagnosis of Fabry's disease. *Nephrol Dial Transplant* 2004;19(12):3202–3203.
83. Glass RB, Astrin KH, Norton KI, et al. Fabry disease: Renal sonographic and magnetic resonance imaging findings in affected males and carrier females with the classic and cardiac variant phenotypes. *J Comput Assist Tomogr* 2004;28(2):158–168.
84. Ries M, Bettis KE, Choyke P, et al. Parapelvic kidney cysts: A distinguishing feature with high prevalence in Fabry disease. *Kidney Int* 2004;66(3):978–982.
85. Alroy J, Sabnis S, Kopp JB. Renal pathology in Fabry disease. *J Am Soc Nephrol* 2002;13 (Suppl 2):S134–S138.
86. Elleder M. Sequelae of storage in Fabry disease—pathology and comparison with other lysosomal storage diseases. *Acta Paediatr Suppl* 2003;92(443):46–53; discussion 45.
87. Gubler MC, Lenoir G, Grunfeld JP, et al. Early renal changes in hemizygous and heterozygous patients with Fabry's disease. *Kidney Int* 1978;13(3):223–235.
88. Fischer EG, Moore MJ, Lager DJ. Fabry disease: A morphologic study of 11 cases. *Mod Pathol* 2006;19(10):1295–1301.
89. Sessa A, Toson A, Nebuloni M, et al. Renal ultrastructural findings in Anderson-Fabry disease. *J Nephrol* 2002;15(2):109–112.
90. Simon M, Frey H, Gruler H, et al. Glycolipid storage material in Fabry's disease: A study by electron microscopy, freeze-fracture, and digital image analysis. *J Struct Biol* 1990;103(1):40–47.
91. Sessa A, Meroni M, Battini G, et al. Renal pathological changes in Fabry disease. *J Inheret Metab Dis* 2001;24(Suppl 2):66–70; discussion 65.
92. Takahashi H, Hirai Y, Migita M, et al. Long-term systemic therapy of Fabry disease in a knockout mouse by adeno-associated virus-mediated muscle-directed gene transfer. *Proc Natl Acad Sci U S A* 2002;99(21):13777–13782.
93. Desnick RJ, Ioannou YA, Eng CM. Fabry disease. In: Scriver CR, Beaudet AL, Sly WS, et al., eds. *The Metabolic and Molecular Bases of Inherited Disease*. 8th ed. New York: McGraw-Hill, 2001:3733–3774.
94. Eitzman DT, Bodary PF, Shen Y, et al. Fabry disease in mice is associated with age-dependent susceptibility to vascular thrombosis. *J Am Soc Nephrol* 2003;14(2):298–302.
95. Park JL, Whitesall SE, D'Alecy LG, et al. Vascular dysfunction in the alpha-galactosidase A-knockout mouse is an endothelial cell-, plasma membrane-based defect. *Clin Exp Pharmacol Physiol* 2008;35(10):1156–1163.
96. Bodary PF, Shen Y, Vargas FB, et al. Alpha-galactosidase A deficiency accelerates atherosclerosis in mice with apolipoprotein E deficiency. *Circulation* 2005;111(5):629–632.
97. Sanchez-Nino MD, Sanz AB, Carrasco S, et al. Globotriaosylsphingosine actions on human glomerular podocytes: Implications for Fabry nephropathy. *Nephrol Dial Transplant* 2011;26(6):1797–1802.
98. Vylet P, Hulkova H, Zivna M, et al. Abnormal expression and processing of uromodulin in Fabry disease reflects tubular cell storage alteration and is reversible by enzyme replacement therapy. *J Inheret Metab Dis* 2008;31(4):508–517.
99. Thomaidis T, Relle M, Golbas M, et al. Downregulation of alpha-galactosidase A upregulates CD77: Functional impact for Fabry nephropathy. *Kidney Int* 2009;75(4):399–407.
100. Cybulla M, Walter KN, Schwarting A, et al. Kidney transplantation in patients with Fabry disease. *Transpl Int* 2009;22(4):475–481.
101. Shah T, Gill J, Malhotra N, et al. Kidney transplant outcomes in patients with Fabry disease. *Transplantation* 2009;87(2):280–285.
102. Puliya DP, Wilcox WR, Bunnapradist S, et al. Fabry disease in a renal allograft. *Am J Transplant* 2003;3(8):1030–1032.
103. Niaudet P. Living donor kidney transplantation in patients with hereditary nephropathies. *Nat Rev Nephrol* 2010;6(12):736–743.
104. Lidove O, West ML, Pintos-Morell G, et al. Effects of enzyme replacement therapy in Fabry disease—A comprehensive review of the medical literature. *Genet Med* 2010;12(11):668–679.
105. Hughes DA, Barba Romero MA, Hollak CE, et al. Response of women with Fabry disease to enzyme replacement therapy: Comparison with men, using data from FOS—The Fabry Outcome Survey. *Mol Genet Metab* 2011;103(3):207–214.
106. Mignani R, Feriozzi S, Pisani A, et al. Agalsidase therapy in patients with Fabry disease on renal replacement therapy: A nationwide study in Italy. *Nephrol Dial Transplant* 2008;23(5):1628–1635.
107. Feriozzi S, Torras J, Cybulla M, et al. The effectiveness of long-term agalsidase alfa therapy in the treatment of Fabry nephropathy. *Clin J Am Soc Nephrol* 2012;7(1):60–69.
108. Germain DP, Waldek S, Banikazemi M, et al. Sustained, long-term renal stabilization after 54 months of agalsidase beta therapy in patients with Fabry disease. *J Am Soc Nephrol* 2007;18(5):1547–1557.
109. Eng CM, Guffon N, Wilcox WR, et al. Safety and efficacy of recombinant human alpha-galactosidase A—Replacement therapy in Fabry's disease. *N Engl J Med* 2001;345(1):9–16.
110. Thurberg BL, Rennke H, Colvin RB, et al. Globotriaosylceramide accumulation in the Fabry kidney is cleared from multiple cell types after enzyme replacement therapy. *Kidney Int* 2002;62(6):1933–1946.
111. Schaefer RM, Tylki-Szymanska A, Hilz MJ. Enzyme replacement therapy for Fabry disease: A systematic review of available evidence. *Drugs* 2009;69(16):2179–2205.
112. Fogo AB, Bostad L, Svarstad E, et al. Scoring system for renal pathology in Fabry disease: Report of the International Study Group of Fabry Nephropathy (ISGFN). *Nephrol Dial Transplant* 2010;25(7):2168–2177.
113. d'Azzo A, Bonten E. Molecular mechanisms of pathogenesis in a glycosphingolipid and a glycoprotein storage disease. *Biochem Soc Trans* 2010;38(6):1453–1457.
114. Thomas GH. Disorders of glycoprotein degradation: α -mannosidosis, β -mannosidosis, fucosidosis, and sialidosis. In: Scriver CR, Beaudet AL, Valle D, et al., eds. *The Metabolic and Molecular Bases of Inherited Disease*, 8th ed. New York: McGraw Hill, 2001:3507–3533.
115. Caciotti A, Di Rocco M, Filocamo M, et al. Type II sialidosis: Review of the clinical spectrum and identification of a new splicing defect with chitotriosidase assessment in two patients. *J Neurol* 2009;256(11):1911–1915.
116. Strehle EM. Sialic acid storage disease and related disorders. *Genet Test* 2003;7(2):113–121.
117. d'Azzo A, Andria G, Strisciuglio P, et al. Galactosialidosis. In: Scriver CR, Beaudet AL, Valle D, eds. *The Metabolic and Molecular Bases of Inherited Disease*, 8th ed. New York: McGraw Hill, 2001:3811–3826.
118. Matsumoto N, Gondo K, Kukita J, et al. A case of galactosialidosis with a homozygous Q49R point mutation. *Brain Dev* 2008;30(9):595–598.
119. Wreden CC, Wlzl M, Reimer RJ. Varied mechanisms underlie the free sialic acid storage disorders. *J Biol Chem* 2005;280(2):1408–1416.
120. Ruiivo R, Sharifi A, Boubekeur S, et al. Molecular pathogenesis of sialic acid storage diseases: Insight gained from four missense mutations and a putative polymorphism of human sialin. *Biol Cell* 2008;100(9):551–559.

121. Froissart R, Cheillan D, Bouvier R, et al. Clinical, morphological, and molecular aspects of sialic acid storage disease manifesting in utero. *J Med Genet* 2005;42(11):829–836.
122. Ishiwari K, Kotani M, Suzuki M, et al. Clinical, biochemical, and cytochemical studies on a Japanese Salla disease case associated with a renal disorder. *J Hum Genet* 2004;49(12):656–663.
123. Chen W, Yang S, Shi H, et al. Histological studies of renal biopsy in a boy with nephrosialidosis. *Ultrastruct Pathol* 2011;35(4):168–171.
124. Schiff M, Maire I, Bertrand Y, et al. Long-term follow-up of metachronous marrow-kidney transplantation in severe type II sialidosis: What does success mean? *Nephrol Dial Transplant* 2005;20(11):2563–2565.
125. Kiss A, Zen PR, Bittencourt V, et al. A Brazilian galactosialidosis patient given renal transplantation: A case report. *J Inherit Metab Dis* 2008;31(Suppl 2):S205–S208.
126. Weisfeld-Adams JD, Morrissey MA, Kirmse BM, et al. Newborn screening and early biochemical follow-up in combined methylmalonic aciduria and homocystinuria, cblC type, and utility of methionine as a secondary screening analyte. *Mol Genet Metab* 2010;99(2):116–123.
127. Rosenblatt DS, Fenton WA. Inherited disorders of folate and cobalamin transport and metabolism. In: Scriver CR, Beaudet AL, Valle D, et al., eds. *The Metabolic and Molecular Bases of Inherited Disease*, 8th ed. New York: McGraw Hill, 2001:3897–3933.
128. Martinelli D, Deodato F, Dionisi-Vici C. Cobalamin C defect: Natural history, pathophysiology, and treatment. *J Inherit Metab Dis* 2011;34(1):127–135.
129. Guignon V, Fremaux-Bacchi V, Giraudier S, et al. Late-onset thrombotic microangiopathy caused by cblC disease: Association with a factor H mutation. *Am J Kidney Dis* 2005;45(3):588–595.
130. Van Hove JL, Van Damme-Lombaerts R, Grunewald S, et al. Cobalamin disorder Cbl-C presenting with late-onset thrombotic microangiopathy. *Am J Med Genet* 2002;111(2):195–201.
131. Brunelli SM, Meyers KE, Guttenberg M, et al. Cobalamin C deficiency complicated by an atypical glomerulopathy. *Pediatr Nephrol* 2002;17(10):800–803.
132. Lerner-Ellis JP, Tirone JC, Pawelek PD, et al. Identification of the gene responsible for methylmalonic aciduria and homocystinuria, cblC type. *Nat Genet* 2006;38(1):93–100.
133. Lerner-Ellis JP, Anastasio N, Liu J, et al. Spectrum of mutations in MMACHC, allelic expression, and evidence for genotype-phenotype correlations. *Hum Mutat* 2009;30(7):1072–1081.
134. Hannibal L, Kim J, Brasch NE, et al. Processing of alkylcobalamins in mammalian cells: A role for the MMACHC (cblC) gene product. *Mol Genet Metab* 2009;97(4):260–266.
135. Fowler B, Leonard JV, Baumgartner MR. Causes of and diagnostic approach to methylmalonic acidurias. *J Inherit Metab Dis* 2008;31(3):350–360.
136. Horster F, Baumgartner MR, Viardot C, et al. Long-term outcome in methylmalonic acidurias is influenced by the underlying defect (mut0, mut-, cblA, cblB). *Pediatr Res* 2007;62(2):225–230.
137. Cosson MA, Benoist JF, Touati G, et al. Long-term outcome in methylmalonic aciduria: A series of 30 French patients. *Mol Genet Metab* 2009;97(3):172–178.
138. Ha TS, Lee JS, Hong EJ. Delay of renal progression in methylmalonic acidemia using angiotensin II inhibition: A case report. *J Nephrol* 2008;21(5):793–796.
139. Sauer SW, Opp S, Haarmann A, et al. Long-term exposure of human proximal tubule cells to hydroxycobalamin[c-lactam] as a possible model to study renal disease in methylmalonic acidurias. *J Inherit Metab Dis* 2009;32(6):720–727.
140. de Keyzer Y, Valayannopoulos V, Benoist JF, et al. Multiple OXPHOS deficiency in the liver, kidney, heart, and skeletal muscle of patients with methylmalonic aciduria and propionic aciduria. *Pediatr Res* 2009;66(1):91–95.
141. Mc Guire PJ, Lim-Melia E, Diaz GA, et al. Combined liver-kidney transplant for the management of methylmalonic aciduria: A case report and review of the literature. *Mol Genet Metab* 2008;93(1):22–29.
142. Lubrano R, Elli M, Rossi M, et al. Renal transplant in methylmalonic acidemia: Could it be the best option? Report on a case at 10 years and review of the literature. *Pediatr Nephrol* 2007;22(8):1209–1214.
143. Froissart R, Piraud M, Boudjemline AM, et al. Glucose-6-phosphatase deficiency. *Orphanet J Rare Dis* 2011;6:27.
144. Chou JY, Jun HS, Mansfield BC. Glycogen storage disease type I and G6Pase-beta deficiency: Etiology and therapy. *Nat Rev Endocrinol* 2010;6(12):676–688.
145. Martens DH, Rake JP, Navis G, et al. Renal function in glycogen storage disease type I, natural course, and renoprotective effects of ACE inhibition. *Clin J Am Soc Nephrol* 2009;4(11):1741–1746.
146. Lin CC, Tsai JD, Lin SP, et al. Renal sonographic findings of type I glycogen storage disease in infancy and early childhood. *Pediatr Radiol* 2005;35:786–791.
147. Urushihara M, Kagami S, Ito M, et al. Transforming growth factor-beta in renal disease with glycogen storage disease I. *Pediatr Nephrol* 2004;19(6):676–678.
148. Verani R, Bernstein J. Renal glomerular and tubular abnormalities in glycogen storage disease type I. *Arch Pathol Lab Med* 1988;112(3):271–274.
149. Shieh JJ, Terzioglu M, Hiraiwa H, et al. The molecular basis of glycogen storage disease type Ia: Structure and function analysis of mutations in glucose-6-phosphatase. *J Biol Chem* 2002;277(7):5047–5053.
150. Rake JP, Visser G, Labrune P, et al. Glycogen storage disease type I: Diagnosis, management, clinical course and outcome. Results of the European Study on Glycogen Storage Disease Type I (ESGSD I). *Eur J Pediatr* 2002;161(Suppl 1):S20–S34.
151. Yiu WH, Mead PA, Jun HS, et al. Oxidative stress mediates nephropathy in type Ia glycogen storage disease. *Lab Invest* 2010;90(4):620–629.
152. Yiu WH, Pan CJ, Ruef RA, et al. Angiotensin mediates renal fibrosis in the nephropathy of glycogen storage disease type Ia. *Kidney Int* 2008;73(6):716–723.
153. Reddy SK, Austin SL, Spencer-Manzon M, et al. Liver transplantation for glycogen storage disease type Ia. *J Hepatol* 2009;51(3):483–490.
154. Belingheri M, Ghio L, Sala A, et al. Combined liver-kidney transplantation in glycogen storage disease Ia: A case beyond the guidelines. *Liver Transpl* 2007;13(5):762–764.
155. Grinshpun A, Condiotti R, Waddington SN, et al. Neonatal gene therapy of glycogen storage disease type Ia using a feline immunodeficiency virus-based vector. *Mol Ther* 2010;18(9):1592–1598.
156. Walker AR, Tschetter K, Matsuo F, et al. McArdle's disease presenting as recurrent cryptogenic renal failure due to occult seizures. *Muscle Nerve* 2003;28(5):640–643.
157. Delibas A, Bek K, Ezgu FS, et al. Acute renal failure due to rhabdomyolysis in a child with McArdle disease. *Eur J Pediatr* 2008;167(8):939–940.
158. Steinberg SJ, Dodt G, Raymond GV, et al. Peroxisome biogenesis disorders. *Biochim Biophys Acta* 2006;1763(12):1733–1748.
159. Islinger M, Grille S, Fahimi HD, et al. The peroxisome: An update on mysteries. *Histochem Cell Biol* 2012;137(5):547–574.
160. Thoms S, Gronborg S, Rabenau J, et al. Characterization of two common 5' polymorphisms in PEX1 and correlation to survival in PEX1 peroxisome biogenesis disorder patients. *BMC Med Genet* 2011;12:109.
161. Depreter M, Espeel M, Roels F. Human peroxisomal disorders. *Microsc Res Tech* 2003;61(2):203–223.
162. Ebberink MS, Mooijer PA, Gootjes J, et al. Genetic classification and mutational spectrum of more than 600 patients with a Zellweger syndrome spectrum disorder. *Hum Mutat* 2011;32(1):59–69.
163. Krause C, Rosewich H, Gartner J. Rational diagnostic strategy for Zellweger syndrome spectrum patients. *Eur J Hum Genet* 2009;17(6):741–748.
164. Dursun A, Gucer S, Ebberink MS, et al. Zellweger syndrome with unusual findings: Non-immune hydrops fetalis, dermal erythropoiesis and hypoplastic toe nails. *J Inherit Metab Dis* 2009;32:5345–5348.
165. van Woerden CS, Groothoff JW, Wijburg FA, et al. High incidence of hyperoxaluria in generalized peroxisomal disorders. *Mol Genet Metab* 2006;88(4):346–350.
166. Kjaergaard S, Graem N, Larsen T, et al. Recurrent fetal polycystic kidneys associated with glutaric aciduria type II. *APMIS* 1998;106(12):1188–1193.
167. van den Brink DM, Brites P, Haasjes J, et al. Identification of PEX7 as the second gene involved in Refsum disease. *Am J Hum Genet* 2003;72(2):471–477.
168. Jansen GA, Waterham HR, Wanders RJ. Molecular basis of Refsum disease: Sequence variations in phytanoyl-CoA hydroxylase (PHYH) and the PTS2 receptor (PEX7). *Hum Mutat* 2004;23(3):209–218.

169. Schonfeld P, Reiser G. Comment concerning the article: 'Phytanic acid impairs mitochondrial respiration through protonophoric action' by Komen et al.: Branched chain phytanic acid inhibits the activity of the mitochondrial respiratory chain. *Cell Mol Life Sci* 2008;65(14):2266–2269.
170. Komen JC, Distelmaier F, Koopman WJ, et al. Phytanic acid impairs mitochondrial respiration through protonophoric action. *Cell Mol Life Sci* 2007;64(24):3271–3281.
171. Wierzbicki AS, Lloyd MD, Schofield CJ, et al. Refsum's disease: A peroxisomal disorder affecting phytanic acid alpha-oxidation. *J Neurochem* 2002;80(5):727–735.
172. Zolotov D, Wagner S, Kalb K, et al. Long-term strategies for the treatment of Refsum's disease using therapeutic apheresis. *J Clin Apher* 2012;27(2):99–105.
173. Pabico RC, Gruebel BJ, McKenna BA, et al. Renal involvement in Refsum's disease. *Am J Med* 1981;70(5):1136–1143.
174. D'Agrosa MC, Deteix P, Fonck Y, et al. The kidney in Refsum's disease. Clinical, histologic and ultrastructural study of a case. *Nephrologie* 1988;9(6):269–272.
175. Hoppe B, Beck BB, Milliner DS. The primary hyperoxalurias. *Kidney Int* 2009;75(12):1264–1271.
176. Cochat P, Liutkus A, Fargue S, et al. Primary hyperoxaluria type 1: Still challenging! *Pediatr Nephrol* 2006;21(8):1075–1081.
177. Coulter-Mackie MB, Rumsby G. Genetic heterogeneity in primary hyperoxaluria type 1: Impact on diagnosis. *Mol Genet Metab* 2004;83(1–2):38–46.
178. Daudon M, Jungers P, Bazin D. Peculiar morphology of stones in primary hyperoxaluria. *N Engl J Med* 2008;359(1):100–102.
179. Cochat P, Hulton SA, Acquaviva C, et al. Primary hyperoxaluria Type 1: Indications for screening and guidance for diagnosis and treatment. *Nephrol Dial Transplant* 2012;27(5):1729–1736.
180. Danpure CJ. Molecular aetiology of primary hyperoxaluria type 1. *Nephron Exp Nephrol* 2004;98(2):e39–e44.
181. Cellini B, Oppici E, Paiardini A, et al. Molecular insights into primary hyperoxaluria Type I pathogenesis. *Front Biosci* 2012;17:621–634.
182. Pirulli D, Marangella M, Amoroso A. Primary hyperoxaluria: Genotype-phenotype correlation. *J Nephrol* 2003;16(2):297–309.
183. Leumann E, Hoppe B. Primary hyperoxaluria type 1: Is genotyping clinically helpful? *Pediatr Nephrol* 2005;20(5):555–557.
184. Harambat J, Fargue S, Acquaviva C, et al. Genotype-phenotype correlation in primary hyperoxaluria type 1: The p.Gly170Arg AGXT mutation is associated with a better outcome. *Kidney Int* 2010;77(5):443–449.
185. Oppici E, Montioli R, Lorenzetto A, et al. Biochemical analyses are instrumental in identifying the impact of mutations on holo and/or apo-forms and on the region(s) of alanine:glyoxylate aminotransferase variants associated with Primary Hyperoxaluria Type I. *Mol Genet Metab* 2012;105(1):132–140.
186. Fodor K, Wolf J, Erdmann R, et al. Molecular requirements for peroxisomal targeting of alanine-glyoxylate aminotransferase as an essential determinant in primary hyperoxaluria type 1. *PLoS Biol* 2012;10(4):e1001309.
187. Danpure CJ. Primary hyperoxaluria. In: Sciver CR, Beaudet AL, Valle D, et al., eds. *The Metabolic and Molecular Bases of Inherited Disease*, 8th ed. New York: McGraw Hill, 2001:3323–3367.
188. Cregeen DP, Williams EL, Hulton S, et al. Molecular analysis of the glyoxylate reductase (GRHPR) gene and description of mutations underlying primary hyperoxaluria type 2. *Hum Mutat* 2003;22(6):497.
189. Milliner DS, Wilson DM, Smith LH. Phenotypic expression of primary hyperoxaluria: Comparative features of types I and II. *Kidney Int* 2001;59(1):31–36.
190. Johnson SA, Rumsby G, Cregeen D, et al. Primary hyperoxaluria type 2 in children. *Pediatr Nephrol* 2002;17(8):597–601.
191. Belostotsky R, Seboun E, Idelson GH, et al. Mutations in DHAPSL are responsible for primary hyperoxaluria type III. *Am J Hum Genet* 2010;87(3):392–399.
192. Williams EL, Bockenbauer D, Van't Hoff WG, et al. The enzyme 4-hydroxy-2-oxoglutarate aldolase is deficient in primary hyperoxaluria type 3. *Nephrol Dial Transplant* 2012;27:3191–3195.
193. Leumann E, Hoppe B. The primary hyperoxalurias. *J Am Soc Nephrol* 2001;12(9):1986–1993.
194. Chetyrkin SV, Kim D, Belmont JM, et al. Pyridoxamine lowers kidney crystals in experimental hyperoxaluria: A potential therapy for primary hyperoxaluria. *Kidney Int* 2005;67(1):53–60.
195. Gagnadoux MF, Lacaille F, Niaudet P, et al. Long term results of liver-kidney transplantation in children with primary hyperoxaluria. *Pediatr Nephrol* 2001;16(12):946–950.
196. Cibrik DM, Kaplan B, Arndorfer JA, et al. Renal allograft survival in patients with oxalosis. *Transplantation* 2002;74(5):707–710.
197. Bergstralh EJ, Monico CG, Lieske JC, et al. Transplantation outcomes in primary hyperoxaluria. *Am J Transplant* 2010;10(11):2493–2501.
198. Scheinman JI. Liver transplantation in oxalosis prior to advanced chronic kidney disease. *Pediatr Nephrol* 2010;25(11):2217–2222.
199. Sirac C, Bridoux F, Essig M, et al. Toward understanding renal Fanconi syndrome: Step by step advances through experimental models. *Contrib Nephrol* 2011;169:247–261.
200. Bergeron M, Gougoux A, Noel J, et al. The renal Fanconi syndrome. In: Sciver CR, Beaudet AL, Sly WS, et al., eds. *The Metabolic and Molecular Bases of Inherited Disease*, 8th ed. New York: McGraw-Hill, 2001:5023–5038.
201. Bendon RW, Hug G. Glycogen accumulation in the pars recta of the proximal tubule in Fanconi syndrome. *Pediatr Pathol* 1986;6(4):411–429.
202. Gahl WA, Thoene JG, Schneider JA. Cystinosis. *N Engl J Med* 2002;347(2):111–121.
203. Town M, Jean G, Cherqui S, et al. A novel gene encoding an integral membrane protein is mutated in nephropathic cystinosis. *Nat Genet* 1998;18(4):319–324.
204. Taranta A, Petrini S, Citti A, et al. Distribution of cystinosis-LKG in human tissues. *Histochem Cell Biol* 2012;138:351–363.
205. Wilmer MJ, Schoeber JP, van den Heuvel LP, et al. Cystinosis: Practical tools for diagnosis and treatment. *Pediatr Nephrol* 2011;26(2):205–215.
206. Pennesi M, Marchetti F, Crovella S, et al. A new mutation in two siblings with cystinosis presenting with Bartter syndrome. *Pediatr Nephrol* 2005;20(2):217–219.
207. Yildiz B, Durmus-Aydogdu S, Kural N, et al. A patient with cystinosis presenting transient features of Bartter syndrome. *Turk J Pediatr* 2006;48(3):260–262.
208. Brodin-Sartorius A, Tete MJ, Niaudet P, et al. Cysteamine therapy delays the progression of nephropathic cystinosis in late adolescents and adults. *Kidney Int* 2012;81(2):179–189.
209. Nesterova G, Gahl W. Nephropathic cystinosis: Late complications of a multisystemic disease. *Pediatr Nephrol* 2008;23(6):863–878.
210. Gahl WA, Balog JZ, Kleta R. Nephropathic cystinosis in adults: Natural history and effects of oral cysteamine therapy. *Ann Intern Med* 2007;147(4):242–250.
211. Midgley JP, El-Kares R, Mathieu F, et al. Natural history of adolescent-onset cystinosis. *Pediatr Nephrol* 2011;26(8):1335–1337.
212. Servais A, Morinier V, Grunfeld JP, et al. Late-onset nephropathic cystinosis: Clinical presentation, outcome, and genotyping. *Clin J Am Soc Nephrol* 2008;3(1):27–35.
213. Clay RD, Darmady EM, Hawkins M. The nature of the renal lesion in the Fanconi syndrome. *J Pathol Bacteriol* 1953;65(2):551–558.
214. Larsen CP, Walker PD, Thoene JG. The incidence of atubular glomeruli in nephropathic cystinosis renal biopsies. *Mol Genet Metab* 2010;101(4):417–420.
215. Spear GS, Slusser RJ, Tousimis AJ, et al. Cystinosis. An ultrastructural and electron-probe study of the kidney with unusual findings. *Arch Pathol* 1971;91(3):206–221.
216. Stokes MB, Jernigan S, D'Agati VD. Infantile nephropathic cystinosis. *Kidney Int* 2008;73(6):782–786.
217. Chandra M, Stokes MB, Kaskel F. Multinucleated podocytes: A diagnostic clue to cystinosis. *Kidney Int* 2010;78(10):1052.
218. Sansanwal P, Yen B, Gahl WA, et al. Mitochondrial autophagy promotes cellular injury in nephropathic cystinosis. *J Am Soc Nephrol* 2010;21(2):272–283.
219. Kalatzis V, Cherqui S, Antignac C, et al. Cystinosis, the protein defective in cystinosis, is a H(+)-driven lysosomal cystine transporter. *EMBO J* 2001;20(21):5940–5949.
220. Kalatzis V, Nevo N, Cherqui S, et al. Molecular pathogenesis of cystinosis: Effect of CTNS mutations on the transport activity and subcellular localization of cystinosis. *Hum Mol Genet* 2004;13(13):1361–1371.

221. Cetinkaya I, Schlatter E, Hirsch JR, et al. Inhibition of Na(+)-dependent transporters in cystine-loaded human renal cells: Electrophysiological studies on the Fanconi syndrome of cystinosis. *J Am Soc Nephrol* 2002;13(8):2085–2093.
222. Park M, Helip-Wooley A, Thoene J. Lysosomal cystine storage augments apoptosis in cultured human fibroblasts and renal tubular epithelial cells. *J Am Soc Nephrol* 2002;13(12):2878–2887.
223. Wilmer MJ, Emma F, Levtschenko EN. The pathogenesis of cystinosis: Mechanisms beyond cystine accumulation. *Am J Physiol Renal Physiol* 2010;299(5):F905–F916.
224. Nevo N, Chol M, Bailleux A, et al. Renal phenotype of the cystinosis mouse model is dependent upon genetic background. *Nephrol Dial Transplant* 2010;25(4):1059–1066.
225. Greco M, Brugnara M, Zaffanello M, et al. Long-term outcome of nephropathic cystinosis: A 20-year single-center experience. *Pediatr Nephrol* 2010;25(12):2459–2467.
226. Van Stralen KJ, Emma F, Jager KJ, et al. Improvement in the renal prognosis in nephropathic cystinosis. *Clin J Am Soc Nephrol* 2011;6(10):2485–2491.
227. Yeagy BA, Harrison F, Gubler MC, et al. Kidney preservation by bone marrow cell transplantation in hereditary nephropathy. *Kidney Int* 2011;79(11):1198–1206.
228. Knohl SJ, Scheinman SJ. Inherited hypercalciuric syndromes: Dent's disease (CLC-5) and familial hypomagnesemia with hypercalciuria (paracellin-1). *Semin Nephrol* 2004;24(1):55–60.
229. Copelovitch L, Nash MA, Kaplan BS. Hypothesis: Dent disease is an underrecognized cause of focal glomerulosclerosis. *Clin J Am Soc Nephrol* 2007;2(5):914–918.
230. Frisberg Y, Dinour D, Belostotsky R, et al. Dent's disease manifesting as focal glomerulosclerosis: Is it the tip of the iceberg? *Pediatr Nephrol* 2009;24(12):2369–2373.
231. Becker-Cohen R, Rinat C, Ben-Shalom E, et al. Vitamin A deficiency associated with urinary retinol binding protein wasting in Dent's disease. *Pediatr Nephrol* 2012;27:1097–1102.
232. Sethi SK, Ludwig M, Kabra M, et al. Vitamin A responsive night blindness in Dent's disease. *Pediatr Nephrol* 2009;24(9):1765–1770.
233. Wu F, Reed AA, Williams SE, et al. Mutational analysis of CLC-5, cofilin and CLC-4 in patients with Dent's disease. *Nephron Physiol* 2009;112(4):53–62.
234. Devuyt O, Thakker RV. Dent's disease. *Orphanet J Rare Dis* 2010;5:28.
235. Hoopes RR Jr, Shrimpton AE, Knohl SJ, et al. Dent Disease with mutations in OCRL1. *Am J Hum Genet* 2005;76(2):260–267.
236. Shrimpton AE, Hoopes RR Jr, Knohl SJ, et al. OCRL1 mutations in Dent 2 patients suggest a mechanism for phenotypic variability. *Nephron Physiol* 2009;112(2):27–36.
237. Tosetto E, Addis M, Caridi G, et al. Locus heterogeneity of Dent's disease: OCRL1 and TMEM27 genes in patients with no CLCN5 mutations. *Pediatr Nephrol* 2009;24(10):1967–1973.
238. Moulin P, Igarashi T, Van der Smissen P, et al. Altered polarity and expression of H⁺-ATPase without ultrastructural changes in kidneys of Dent's disease patients. *Kidney Int* 2003;63(4):1285–1295.
239. Hodgins JB, Corey HE, Kaplan BS, et al. Dent disease presenting as partial Fanconi syndrome and hypercalciuria. *Kidney Int* 2008;73(11):1320–1323.
240. Devuyt O, Christie PT, Courtoy PJ, et al. Intra-renal and subcellular distribution of the human chloride channel, CLC-5, reveals a pathophysiological basis for Dent's disease. *Hum Mol Genet* 1999;8(2):247–257.
241. Lourdel S, Grand T, Burgos J, et al. CLC-5 mutations associated with Dent's disease: A major role of the dimer interface. *Pflugers Arch* 2012;463(2):247–256.
242. Novarino G, Weinert S, Rickheit G, et al. Endosomal chloride-proton exchange rather than chloride conductance is crucial for renal endocytosis. *Science* 2010;328(5984):1398–1401.
243. Christensen EI, Devuyt O, Dom G, et al. Loss of chloride channel CLC-5 impairs endocytosis by defective trafficking of megalin and cubilin in kidney proximal tubules. *Proc Natl Acad Sci U S A* 2003;100(14):8472–8477.
244. Christensen EI, Gburek J. Protein reabsorption in renal proximal tubule-function and dysfunction in kidney pathophysiology. *Pediatr Nephrol* 2004;19(7):714–721.
245. Gunther W, Piwon N, Jentsch TJ. The CLC-5 chloride channel knock-out mouse—An animal model for Dent's disease. *Pflugers Arch* 2003;445(4):456–462.
246. Blanchard A, Vargas-Poussou R, Peyrard S, et al. Effect of hydrochlorothiazide on urinary calcium excretion in dent disease: An uncontrolled trial. *Am J Kidney Dis* 2008;52(6):1084–1095.
247. Raja KA, Schurman S, D'Mello RG, et al. Responsiveness of hypercalciuria to thiazide in Dent's disease. *J Am Soc Nephrol* 2002;13(12):2938–2944.
248. Rotig A, Munnich A. Genetic features of mitochondrial respiratory chain disorders. *J Am Soc Nephrol* 2003;14(12):2995–3007.
249. Martin-Hernandez E, Garcia-Silva MT, Vara J, et al. Renal pathology in children with mitochondrial diseases. *Pediatr Nephrol* 2005;20(9):1299–1305.
250. Neiberger RE, George JC, Perkins LA, et al. Renal manifestations of congenital lactic acidosis. *Am J Kidney Dis* 2002;39(1):12–23.
251. Emma F, Bertini E, Salviati L, et al. Renal involvement in mitochondrial cytopathies. *Pediatr Nephrol* 2012;27(4):539–550.
252. Tzen CY, Tsai JD, Wu TY, et al. Tubulointerstitial nephritis associated with a novel mitochondrial point mutation. *Kidney Int* 2001;59(3):846–854.
253. de Lonlay P, Valnot I, Barrientos A, et al. A mutant mitochondrial respiratory chain assembly protein causes complex III deficiency in patients with tubulopathy, encephalopathy and liver failure. *Nat Genet* 2001;29(1):57–60.
254. Hotta O, Inoue CN, Miyabayashi S, et al. Clinical and pathologic features of focal segmental glomerulosclerosis with mitochondrial tRNA^{Leu}(UUR) gene mutation. *Kidney Int* 2001;59(4):1236–1243.
255. Yamagata K, Muro K, Usui J, et al. Mitochondrial DNA mutations in focal segmental glomerulosclerosis lesions. *J Am Soc Nephrol* 2002;13(7):1816–1823.
256. Rotig A. Renal disease and mitochondrial genetics. *J Nephrol* 2003;16(2):286–292.
257. Emma F, Pizzini C, Tessa A, et al. “Bartter-like” phenotype in Kearns-Sayre syndrome. *Pediatr Nephrol* 2006;21(3):355–360.
258. Gucer S, Talim B, Asan E, et al. Focal segmental glomerulosclerosis associated with mitochondrial cytopathy: Report of two cases with special emphasis on podocytes. *Pediatr Dev Pathol* 2005;8(6):710–717.
259. Goldenberg A, Ngoc LH, Thouret MC, et al. Respiratory chain deficiency presenting as congenital nephrotic syndrome. *Pediatr Nephrol* 2005;20(4):465–469.
260. Kuwertz-Broking E, Koch HG, Marquardt T, et al. Renal Fanconi syndrome: First sign of partial respiratory chain complex IV deficiency. *Pediatr Nephrol* 2000;14(6):495–498.
261. Au KM, Lau SC, Mak YF, et al. Mitochondrial DNA deletion in a girl with Fanconi's syndrome. *Pediatr Nephrol* 2007;22(1):136–140.
262. Kobayashi A, Goto Y, Nagata M, et al. Granular swollen epithelial cells: A histologic and diagnostic marker for mitochondrial nephropathy. *Am J Surg Pathol* 2010;34(2):262–270.
263. Szabolcs MJ, Seigle R, Shanske S, et al. Mitochondrial DNA deletion: A cause of chronic tubulointerstitial nephropathy. *Kidney Int* 1994;45(5):1388–1396.
264. Diomedes-Camassei F, Di Giandomenico S, Santorelli FM, et al. COQ2 nephropathy: A newly described inherited mitochondriopathy with primary renal involvement. *J Am Soc Nephrol* 2007;18(10):2773–2780.
265. Thirumurugan A, Thewles A, Gilbert RD, et al. Urinary L-lactate excretion is increased in renal Fanconi syndrome. *Nephrol Dial Transplant* 2004;19(7):1767–1773.
266. Wong LJ, Scaglia F, Graham BH, et al. Current molecular diagnostic algorithm for mitochondrial disorders. *Mol Genet Metab* 2010;100(2):111–117.
267. Nussbaum RL, Suchy SF. The oculocerebrorenal syndrome of Lowe (Lowe syndrome). In: Scriver CR, Beaudet AL, Sly WS, et al., eds. *The Metabolic and Molecular Bases of Inherited Disease*, 8th ed. New York: McGraw-Hill, 2001:6257–6266.
268. Bockenbauer D, Bokenkamp A, van't Hoff W, et al. Renal phenotype in Lowe Syndrome: A selective proximal tubular dysfunction. *Clin J Am Soc Nephrol* 2008;3(5):1430–1436.
269. Cho HY, Lee BH, Choi HJ, et al. Renal manifestations of Dent disease and Lowe syndrome. *Pediatr Nephrol* 2008;23(2):243–249.
270. Laube GF, Russell-Eggitt IM, van't Hoff WG. Early proximal tubular dysfunction in Lowe's syndrome. *Arch Dis Child* 2004;89(5):479–480.

271. Van Acker KJ, Roels H, Beelaerts W, et al. The histologic lesions of the kidney in the oculo-cerebro-renal syndrome of Lowe. *Nephron* 1967;4:193.
272. Witzleben CL, Schoen EJ, Tu WH, et al. Progressive morphologic renal changes in the oculo-cerebro-renal syndrome of Lowe. *Am J Med* 1968;44(2):319–324.
273. Ores RO. Renal changes in oculo-cerebro-renal syndrome of Lowe. Electron microscopic study. *Arch Pathol* 1970;89(3):221–225.
274. Tricot L, Yahiaoui Y, Teixeira L, et al. End-stage renal failure in Lowe syndrome. *Nephrol Dial Transplant* 2003;18(9):1923–1925.
275. Leahey AM, Charnas LR, Nussbaum RL. Nonsense mutations in the OCRL-1 gene in patients with the oculocerebrorenal syndrome of Lowe. *Hum Mol Genet* 1993;2(4):461–463.
276. Grieve AG, Daniels RD, Sanchez-Heras E, et al. Lowe Syndrome protein OCRL1 supports maturation of polarized epithelial cells. *PLoS One* 2011;6(8):e24044.
277. Luo N, West C, Murga-Zamalloa C, et al. OCRL localizes to the primary cilium: A new role for cilia in Lowe syndrome. *Hum Mol Genet* 2012;21:3333–3344.
278. Pirruccello M, De Camilli P. Inositol 5-phosphatases: Insights from the Lowe syndrome protein OCRL. *Trends Biochem Sci* 2012;37(4):134–143.
279. Lee DB, Huang E, Ward HJ. Tight junction biology and kidney dysfunction. *Am J Physiol Renal Physiol* 2006;290(1):F20–F34.
280. Izu A, Sugimoto K, Fujita S, et al. Nonfunction of the ECT2 gene may cause renal tubulointerstitial injury leading to focal segmental glomerulosclerosis. *Clin Exp Nephrol* 2012;16:875–882.
281. Hichri H, Rendu J, Monnier N, et al. From Lowe syndrome to Dent disease: Correlations between mutations of the OCRL1 gene and clinical and biochemical phenotypes. *Hum Mutat* 2010;32(4):379–388.
282. Fanconi G, Bickel H. Die chronische aminoacidurie (amino-saure-diabetes oder nephrotisch-glukosurischer Zwergwuchs) bei der Glykogenose und der Cystinkrankheit. *Helv Paediatr Acta* 1949;4:359–396.
283. Santer R, Schneppenheim R, Dombrowski A, et al. Mutations in GLUT2, the gene for the liver-type glucose transporter, in patients with Fanconi-Bickel syndrome. *Nat Genet* 1997;17(3):324–326.
284. Manz F, Bickel H, Brodehl J, et al. Fanconi-Bickel syndrome. *Pediatr Nephrol* 1987;1(3):509–518.
285. Mohandas Nair K, Sakamoto O, Jagadeesh S, et al. Fanconi-Bickel syndrome. *Indian J Pediatr* 2012;79(1):112–114.
286. Su Z, Du ML, Chen HS, et al. Two cases of Fanconi-Bickel syndrome: First report from China with novel mutations of SLC2A2 gene. *J Pediatr Endocrinol Metab* 2011;24(9–10):749–753.
287. Berry GT, Baker L, Kaplan FS, et al. Diabetes-like renal glomerular disease in Fanconi-Bickel syndrome. *Pediatr Nephrol* 1995;9(3):287–291.
288. Santer R, Groth S, Kinner M, et al. The mutation spectrum of the facilitative glucose transporter gene SLC2A2 (GLUT2) in patients with Fanconi-Bickel syndrome. *Hum Genet* 2002;110(1):21–29.
289. Furlan F, Santer R, Vismara E, et al. Bilateral nuclear cataracts as the first neonatal sign of Fanconi-Bickel syndrome. *J Inherit Metab Dis* 2006;29(5):685.
290. Grunert SC, Schwab KO, Pohl M, et al. Fanconi-Bickel syndrome: GLUT2 mutations associated with a mild phenotype. *Mol Genet Metab* 2012;105(3):433–437.
291. Berry GT, Baynes JW, Wells-Knecht KJ, et al. Elements of diabetic nephropathy in a patient with GLUT 2 deficiency. *Mol Genet Metab* 2005;86(4):473–477.
292. Fukumoto H, Seino S, Imura H, et al. Sequence, tissue distribution, and chromosomal localization of mRNA encoding a human glucose transporter-like protein. *Proc Natl Acad Sci U S A* 1988;85(15):5434–5438.
293. Ozer EA, Aksu N, Uclar E, et al. No mutation in the SLC2A2 (GLUT2) gene in a Turkish infant with Fanconi-Bickel syndrome. *Pediatr Nephrol* 2003;18(4):397–398.
294. Santer R, Steinmann B, Schaub J. Fanconi-Bickel syndrome—A congenital defect of facilitative glucose transport. *Curr Mol Med* 2002;2(2):213–227.
295. Leturque A, Brot-Laroche E, Le Gall M. GLUT2 mutations, translocation, and receptor function in diet sugar managing. *Am J Physiol Endocrinol Metab* 2009;296(5):E985–E992.
296. Brown GK. Glucose transporters: Structure, function and consequences of deficiency. *J Inherit Metab Dis* 2000;23(3):237–246.
297. Izzedine H, Launay-Vacher V, Isnard-Bagnis C, et al. Drug-induced Fanconi's syndrome. *Am J Kidney Dis* 2003;41(2):292–309.
298. Ma CX, Lacy MQ, Rompala JF, et al. Acquired Fanconi syndrome is an indolent disorder in the absence of overt multiple myeloma. *Blood* 2004;104(1):40–42.
299. Dauchy FA, Lawson-Ayayi S, de La Faille R, et al. Increased risk of abnormal proximal renal tubular function with HIV infection and antiretroviral therapy. *Kidney Int* 2011;80(3):302–309.
300. Tanji N, Tanji K, Kambham N, et al. Adefovir nephrotoxicity: Possible role of mitochondrial DNA depletion. *Hum Pathol* 2001;32(7):734–740.
301. Thevenod F. Nephrotoxicity and the proximal tubule. Insights from cadmium. *Nephron Physiol* 2003;93(4):87–93.
302. Watanabe T, Yoshikawa H, Yamazaki S, et al. Secondary renal Fanconi syndrome caused by valproate therapy. *Pediatr Nephrol* 2005;20(6):814–817.
303. Shah GN, Bonapace G, Hu PY, et al. Carbonic anhydrase II deficiency syndrome (osteopetrosis with renal tubular acidosis and brain calcification): Novel mutations in CA2 identified by direct sequencing expand the opportunity for genotype-phenotype correlation. *Hum Mutat* 2004;24(3):272.
304. Zhu Q, Kao L, Azimov R, et al. Topological location and structural importance of the NBCe1-A residues mutated in proximal renal tubular acidosis. *J Biol Chem* 2010;285(18):13416–13426.
305. Fry AC, Su Y, Yiu V, et al. Mutation conferring apical-targeting motif on AE1 exchanger causes autosomal dominant distal RTA. *J Am Soc Nephrol* 2012;23:1238–1249.
306. Vargas-Poussou R, Houillier P, Le Pottier N, et al. Genetic investigation of autosomal recessive distal renal tubular acidosis: Evidence for early sensorineural hearing loss associated with mutations in the ATP6V0A4 gene. *J Am Soc Nephrol* 2006;17(5):1437–1443.
307. Mohebbi N, Vargas-Poussou R, Hegemann S, et al. Homozygous and compound heterozygous mutations in the ATP6V1B1 gene in patients with renal tubular acidosis and sensorineural hearing loss. *Clin Genet* 2012;83:274–278.
308. Prie D, Friedlander G. Genetic disorders of renal phosphate transport. *N Engl J Med* 2010;362(25):2399–2409.
309. Camargo SM, Bockenbauer D, Kleta R. Aminoacidurias: Clinical and molecular aspects. *Kidney Int* 2008;73(8):918–925.
310. Bailey CG, Ryan RM, Thoeng AD, et al. Loss-of-function mutations in the glutamate transporter SLC1A1 cause human dicarboxylic aminoaciduria. *J Clin Invest* 2011;121(1):446–453.
311. Calado J, Santer R, Rueff J. Effect of kidney disease on glucose handling (including genetic defects). *Kidney Int Suppl* 2011(120):S7–S13.
312. Broer S, Bailey CG, Kowalczyk S, et al. Iminoglycinuria and hyperglycinuria are discrete human phenotypes resulting from complex mutations in proline and glycine transporters. *J Clin Invest* 2008;118(12):3881–3892.
313. Claes DJ, Jackson E. Cystinuria: Mechanisms and management. *Pediatr Nephrol* 2012;27:2031–2038.
314. Becker MA. Hyperuricemia and gout. In: Scriver CR, Beaudet AL, Valle D, et al., eds. *The Metabolic and Molecular Bases of Inherited Disease*, 8th ed. New York: McGraw Hill, 2001:2513–2535.
315. de Brouwer AP, van Bokhoven H, Nabuurs SB, et al. PRPS1 mutations: Four distinct syndromes and potential treatment. *Am J Hum Genet* 2010;86(4):506–518.
316. Rho YH, Zhu Y, Choi HK. The epidemiology of uric acid and fructose. *Semin Nephrol* 2011;31(5):410–419.
317. Chen Y-T. Glycogen storage disease. In: Scriver CR, Beaudet AL, Valle D, et al., eds. *The Metabolic and Molecular Bases of Inherited Disease*. New York: McGraw Hill, 2001:1521–1552.
318. Bieber JD, Terkeltaub RA. Gout: On the brink of novel therapeutic options for an ancient disease. *Arthritis Rheum* 2004;50(8):2400–2414.
319. Wright AF, Rudan I, Hastie ND, et al. A 'complexity' of urate transporters. *Kidney Int* 2010;78(5):446–452.
320. Fu R, Jinnah HA. Genotype-phenotype correlations in Lesch-Nyhan disease: Moving beyond the gene. *J Biol Chem* 2012;287(5):2997–3008.
321. Jinnah HA, Ceballos-Picot I, Torres RJ, et al. Attenuated variants of Lesch-Nyhan disease. *Brain* 2010;133(Pt 3):671–689.
322. Torres RJ, Puig JG. Hypoxanthine-guanine phosphoribosyltransferase (HPRT) deficiency: Lesch-Nyhan syndrome. *Orphanet J Rare Dis* 2007;2:48.
323. Rinat C, Zoref-Shani E, Ben-Neriah Z, et al. Molecular, biochemical, and genetic characterization of a female patient with Lesch-Nyhan disease. *Mol Genet Metab* 2006;87(3):249–252.

324. Cameron JS, Simmonds HA. Hereditary hyperuricemia and renal disease. *Semin Nephrol* 2005;25(1):9–18.
325. Wong H, Feber J, Chakraborty P, et al. Novel HGPRT 293 A>G point mutation presenting as neonatal acute renal failure. *Pediatr Nephrol* 2008;23(2):317–321.
326. Pela I, Donati MA, Procopio E, et al. Lesch-Nyhan syndrome presenting with acute renal failure in a 3-day-old newborn. *Pediatr Nephrol* 2008;23(1):155–158.
327. Sikora P, Pijanowska M, Majewski M, et al. Acute renal failure due to bilateral xanthine urolithiasis in a boy with Lesch-Nyhan syndrome. *Pediatr Nephrol* 2006;21(7):1045–1047.
328. Singal R, Krishnamurthy S, Narayanan P, et al. Urate nephropathy associated with impaired kinetic properties of hypoxanthine phosphoribosyl transferase in a 45-day-old infant. *Clin Exp Nephrol* 2012;16(1):164–167.
329. Marangella M. Uric acid elimination in the urine. Pathophysiological implications. *Contrib Nephrol* 2005;147:132–148.
330. Torres RJ, Prior C, Puig JG. Efficacy and safety of allopurinol in patients with hypoxanthine-guanine phosphoribosyltransferase deficiency. *Metabolism* 2007;56(9):1179–1186.
331. Nyhan WL. Inherited hyperuricemic disorders. *Contrib Nephrol* 2005;147:22–34.
332. Bollee G, Dollinger C, Boutaud L, et al. Phenotype and genotype characterization of adenine phosphoribosyltransferase deficiency. *J Am Soc Nephrol* 2010;21(4):679–688.
333. Harambat J, Bollee G, Daudon M, et al. Adenine phosphoribosyltransferase deficiency in children. *Pediatr Nephrol* 2012;27(4):571–579.
334. Edvardsson V, Palsson R, Olafsson I, et al. Clinical features and genotype of adenine phosphoribosyltransferase deficiency in Iceland. *Am J Kidney Dis* 2001;38(3):473–480.
335. Nasr SH, Sethi S, Cornell LD, et al. Crystalline nephropathy due to 2,8-dihydroxyadeninuria: An under-recognized cause of irreversible renal failure. *Nephrol Dial Transplant* 2010;25(6):1909–1915.
336. Sperling O. Hereditary renal hypouricemia. *Mol Genet Metab* 2006;89(1–2):14–18.
337. Enomoto A, Kimura H, Chairoungdua A, et al. Molecular identification of a renal urate anion exchanger that regulates blood urate levels. *Nature* 2002;417(6887):447–452.
338. Iwai N, Mino Y, Hosoyamada M, et al. A high prevalence of renal hypouricemia caused by inactive SLC22A12 in Japanese. *Kidney Int* 2004;66(3):935–944.
339. Takahashi T, Tsuchida S, Oyama T, et al. Recurrent URAT1 gene mutations and prevalence of renal hypouricemia in Japanese. *Pediatr Nephrol* 2005;20(5):576–578.
340. Dinour D, Gray NK, Campbell S, et al. Homozygous SLC2A9 mutations cause severe renal hypouricemia. *J Am Soc Nephrol* 2010;21(1):64–72.
341. Dinour D, Gray NK, Ganon L, et al. Two novel homozygous SLC2A9 mutations cause renal hypouricemia type 2. *Nephrol Dial Transplant* 2012;27(3):1035–1041.
342. Matsuo H, Chiba T, Nagamori S, et al. Mutations in glucose transporter 9 gene SLC2A9 cause renal hypouricemia. *Am J Hum Genet* 2008;83(6):744–751.
343. Cheong HI, Kang JH, Lee JH, et al. Mutational analysis of idiopathic renal hypouricemia in Korea. *Pediatr Nephrol* 2005;20(7):886–890.
344. Dinour D, Bahn A, Ganon L, et al. URAT1 mutations cause renal hypouricemia type 1 in Iraqi Jews. *Nephrol Dial Transplant* 2011;26(7):2175–2181.
345. Kikuchi Y, Koga H, Yasutomo Y, et al. Patients with renal hypouricemia with exercise-induced acute renal failure and chronic renal dysfunction. *Clin Nephrol* 2000;53(6):467–472.
346. Jennings P, Aydin S, Kotanko P, et al. Membrane targeting and secretion of mutant uromodulin in familial juvenile hyperuricemic nephropathy. *J Am Soc Nephrol* 2007;18(1):264–273.
347. Zaucke F, Boehnlein JM, Steffens S, et al. Uromodulin is expressed in renal primary cilia and UMOD mutations result in decreased ciliary uromodulin expression. *Hum Mol Genet* 2010;19(10):1985–1997.
348. Hart TC, Gorry MC, Hart PS, et al. Mutations of the UMOD gene are responsible for medullary cystic kidney disease 2 and familial juvenile hyperuricemic nephropathy. *J Med Genet* 2002;39(12):882–892.
349. Rampoldi L, Caridi G, Santon D, et al. Allelism of MCKD, FJHN and GCKD caused by impairment of uromodulin export dynamics. *Hum Mol Genet* 2003;12(24):3369–3384.
350. Kottgen A, Hwang SJ, Larson MG, et al. Uromodulin levels associate with a common UMOD variant and risk for incident CKD. *J Am Soc Nephrol* 2010;21(2):337–344.
351. Vylet' al P, Kublova M, Kalbacova M, et al. Alterations of uromodulin biology: A common denominator of the genetically heterogeneous FJHN/MCKD syndrome. *Kidney Int* 2006;70(6):1155–1169.
352. Scolari F, Caridi G, Rampoldi L, et al. Uromodulin storage diseases: Clinical aspects and mechanisms. *Am J Kidney Dis* 2004;44(6):987–999.
353. Bollee G, Dahan K, Flamant M, et al. Phenotype and outcome in hereditary tubulointerstitial nephritis secondary to UMOD mutations. *Clin J Am Soc Nephrol* 2011;6(10):2429–2438.
354. Nasr SH, Lucia JP, Galgano SJ, et al. Uromodulin storage disease. *Kidney Int* 2008;73(8):971–976.
355. Benetti E, Caridi G, Vella MD, et al. Immature renal structures associated with a novel UMOD sequence variant. *Am J Kidney Dis* 2009;53(2):327–331.
356. Adam J, Bollee G, Fougeray S, et al. Endoplasmic reticulum stress in UMOD-related kidney disease: A human pathologic study. *Am J Kidney Dis* 2012;59(1):117–121.
357. Beck BB, Trachtman H, Gitman M, et al. Autosomal dominant mutation in the signal peptide of renin in a kindred with anemia, hyperuricemia, and CKD. *Am J Kidney Dis* 2011;58(5):821–825.
358. Bingham C, Ellard S, van't Hoff WG, et al. Atypical familial juvenile hyperuricemic nephropathy associated with a hepatocyte nuclear factor-1beta gene mutation. *Kidney Int* 2003;63(5):1645–1651.
359. Gresh L, Fischer E, Reimann A, et al. A transcriptional network in polycystic kidney disease. *EMBO J* 2004;23(7):1657–1668.
360. Piret SE, Danoy P, Dahan K, et al. Genome-wide study of familial juvenile hyperuricemic (gouty) nephropathy (FJHN) indicates a new locus, FJHN3, linked to chromosome 2p22.1-p21. *Hum Genet* 2011;129(1):51–58.
361. Williams SE, Reed AA, Galvanovskis J, et al. Uromodulin mutations causing familial juvenile hyperuricemic nephropathy lead to protein maturation defects and retention in the endoplasmic reticulum. *Hum Mol Genet* 2009;18(16):2963–2974.
362. Choi SW, Ryu OH, Choi SJ, et al. Mutant Tamm-Horsfall glycoprotein accumulation in endoplasmic reticulum induces apoptosis reversed by colchicine and sodium 4-phenylbutyrate. *J Am Soc Nephrol* 2005;16(10):3006–3014.
363. Howard SC, Jones DP, Pui CH. The tumor lysis syndrome. *N Engl J Med* 2011;364(19):1844–1854.
364. Shimada M, Johnson RJ, May WS Jr, et al. A novel role for uric acid in acute kidney injury associated with tumour lysis syndrome. *Nephrol Dial Transplant* 2009;24(10):2960–2964.
365. Shimada M, Dass B, Ejaz AA. Paradigm shift in the role of uric acid in acute kidney injury. *Semin Nephrol* 2011;31(5):453–458.
366. Bose P, Qubaiah O. A review of tumour lysis syndrome with targeted therapies and the role of rasburicase. *J Clin Pharm Ther* 2011;36(3):299–326.
367. Kim YG, Huang XR, Suga S, et al. Involvement of macrophage migration inhibitory factor (MIF) in experimental uric acid nephropathy. *Mol Med* 2000;6(10):837–848.
368. Manzke H, Eigster G, Harms D, et al. Uric acid infarctions in the kidneys of newborn infants. A study on the changing incidence and on oxypurine ratios. *Eur J Pediatr* 1977;126(1–2):29–35.
369. Makhoul IR, Soudack M, Smolkin T, et al. Neonatal transient renal failure with renal medullary hyperechogenicity: Clinical and laboratory features. *Pediatr Nephrol* 2005;20(7):904–909.
370. Dehghan A, Kottgen A, Yang Q, et al. Association of three genetic loci with uric acid concentration and risk of gout: A genome-wide association study. *Lancet* 2008;372(9654):1953–1961.
371. Taniguchi A, Urano W, Yamanaka M, et al. A common mutation in an organic anion transporter gene, SLC22A12, is a suppressing factor for the development of gout. *Arthritis Rheum* 2005;52(8):2576–2577.
372. Kang DH, Chen W. Uric acid and chronic kidney disease: New understanding of an old problem. *Semin Nephrol* 2011;31(5):447–452.
373. Obermayr RP, Temml C, Gutjahr G, et al. Elevated uric acid increases the risk for kidney disease. *J Am Soc Nephrol* 2008;19(12):2407–2413.
374. Neogi T. Clinical practice. Gout. *N Engl J Med* 2011;364(5):443–452.
375. Gonick HC, Rubini ME, Gleason IO, et al. The renal lesion in Gout. *Ann Intern Med* 1965;62:667–674.

376. Bernstein J, Chung J. Heritable metabolic diseases. In: Jennette JC, Olson JL, Schwartz MM, et al., eds. *Heptinstall's Pathology of the Kidney*, 5th ed. Philadelphia: Lippincott-Raven, 1998:1287–1320.
377. Filiopoulos V, Hadjiyannakos D, Vlassopoulos D. New insights into uric acid effects on the progression and prognosis of chronic kidney disease. *Ren Fail* 2012;34(4):510–520.
378. Lopez M, Hoppe B. History, epidemiology and regional diversities of urolithiasis. *Pediatr Nephrol* 2008;25(1):49–59.
379. Ounissi M, Gargueh T, Mahfoudhi M, et al. Nephrolithiasis-induced end stage renal disease. *Int J Nephrol Renovasc Dis* 2010;3:21–26.
380. Finger S, Hagemann IS. Benjamin Franklin's risk factors for gout and stones: From genes and diet to possible lead poisoning. *Proc Am Philos Soc* 2008;152(2):189–206.
381. Kramer HM, Curhan G. The association between gout and nephrolithiasis: The National Health and Nutrition Examination Survey III, 1988–1994. *Am J Kidney Dis* 2002;40(1):37–42.
382. Shekariz B, Stoller ML. Uric acid nephrolithiasis: Current concepts and controversies. *J Urol* 2002;168(4 Pt 1):1307–1314.
383. Stamatelou KK, Francis ME, Jones CA, et al. Time trends in reported prevalence of kidney stones in the United States: 1976–1994. *Kidney Int* 2003;63(5):1817–1823.
384. Daudon M, Traxer O, Conort P, et al. Type 2 diabetes increases the risk for uric acid stones. *J Am Soc Nephrol* 2006;17(7):2026–2033.
385. Sakhæe K, Adams-Huet B, Moe OW, et al. Pathophysiologic basis for normouricosuric uric acid nephrolithiasis. *Kidney Int* 2002;62(3):971–979.
386. Herrick JB. Peculiar elongated and sickle-shaped red blood corpuscles in a case of severe anemia. *Arch Intern Med* 1910;6:517–521.
387. Onwubalili JK. Sickle-cell anaemia: An explanation for the ancient myth of reincarnation in Nigeria. *Lancet* 1983;322(8348):503–505.
388. Stuart MJ, Nagel RL. Sickle-cell disease. *Lancet* 2004;364:1343–1360.
389. Malowany JI, Butany J. Pathology of sickle cell disease. *Semin Diagn Pathol* 2012;29(1):49–55.
390. Scheinman JI. Sickle cell disease and the kidney. *Nat Clin Pract Nephrol* 2009;5(2):78–88.
391. Modell B, Darlison M. Global epidemiology of haemoglobin disorders and derived service indicators. *Bull World Health Organ* 2008;86(6):480–487.
392. Hassell KL. Population estimates of sickle cell disease in the U.S. *Am J Prev Med* 2010;38(4 Suppl):S512–S521.
393. Falk RJ, Scheinman J, Phillips G, et al. Prevalence and pathologic features of sickle cell nephropathy and response to inhibition of angiotensin-converting enzyme. *N Engl J Med* 1992;326(14):910–915.
394. Pham PT, Pham PC, Wilkinson AH, et al. Renal abnormalities in sickle cell disease. *Kidney Int* 2000;57(1):1–8.
395. Ataga KI, Orringer EP. Renal abnormalities in sickle cell disease. *Am J Hematol* 2000;63:205–211.
396. Miller ST, Wang WC, Iyer R, et al. Urine concentrating ability in infants with sickle cell disease: Baseline data from the phase III trial of hydroxyurea (BABY HUG). *Pediatr Blood Cancer* 2010;54(2):265–268.
397. Sundaram N, Bennett M, Wilhelm J, et al. Biomarkers for early detection of sickle nephropathy. *Am J Hematol* 2011;86(7):559–566.
398. Allon M, Lawson L, Eckman JR, et al. Effects of nonsteroidal anti-inflammatory drugs on renal function in sickle cell anemia. *Kidney Int* 1988;34(4):500–506.
399. Weatherall DJ, Clegg JB, Higgs DR, et al. The hemoglobinopathies. In: Sciver CR, Beudet AL, Sly WS, et al., eds. *The Metabolic and Molecular Bases of Inherited Disease*, 8th ed. New York: McGraw-Hill, 2001:4571–4636.
400. Tsaras G, Owusu-Ansah A, Boateng FO, et al. Complications associated with sickle cell trait: A brief narrative review. *Am J Med* 2009;122(6):507–512.
401. Portocarrero ML, Portocarrero ML, Sobral MM, et al. Prevalence of enuresis and daytime urinary incontinence in children and adolescents with sickle cell disease. *J Urol* 2012;187(3):1037–1040.
402. Barakat LP, Smith-Whitley K, Schulman S, et al. Nocturnal enuresis in pediatric sickle cell disease. *J Dev Behav Pediatr* 2001;22(5):300–305.
403. Mabilia Babela JR, Loumingou R, Pemba-Loufoua A, et al. Enuresis in children with sickle cell disease. *Arch Pediatr* 2004;11(10):1168–1172.
404. Jordan SS, Hilker KA, Stoppelbein L, et al. Nocturnal enuresis and psychosocial problems in pediatric sickle cell disease and sibling controls. *J Dev Behav Pediatr* 2005;26(6):404–411.
405. Oster JR, Lespier LE, Lee SM, et al. Renal acidification in sickle-cell disease. *J Lab Clin Med* 1976;88(3):389–401.
406. Wigfall DR, Ware RE, Burchinal MR, et al. Prevalence and clinical correlates of glomerulopathy in children with sickle cell disease. *J Pediatr* 2000;136(6):749–753.
407. Thompson J, Reid M, Hambleton I, et al. Albuminuria and renal function in homozygous sickle cell disease: Observations from a cohort study. *Arch Intern Med* 2007;167(7):701–708.
408. Haymann JP, Stankovic K, Levy P, et al. Glomerular hyperfiltration in adult sickle cell anemia: A frequent hemolysis associated feature. *Clin J Am Soc Nephrol* 2010;5(5):756–761.
409. Aygun B, Mortier NA, Smeltzer MP, et al. Glomerular hyperfiltration and albuminuria in children with sickle cell anemia. *Pediatr Nephrol* 2011;26(8):1285–1290.
410. Quinn CT, Johnson VL, Kim HY, et al. Renal dysfunction in patients with thalassaemia. *Br J Haematol* 2011;153(1):111–117.
411. McPherson Yee M, Jabbar SF, Osunkwo I, et al. Chronic kidney disease and albuminuria in children with sickle cell disease. *Clin J Am Soc Nephrol* 2011;6(11):2628–2633.
412. Guasch A, Navarrete J, Nass K, et al. Glomerular involvement in adults with sickle cell hemoglobinopathies: Prevalence and clinical correlates of progressive renal failure. *J Am Soc Nephrol* 2006;17(8):2228–2235.
413. McBurney PG, Hanevold CD, Hernandez CM, et al. Risk factors for microalbuminuria in children with sickle cell anemia. *J Pediatr Hematol Oncol* 2002;24(6):473–477.
414. McKie KT, Hanevold CD, Hernandez C, et al. Prevalence, prevention, and treatment of microalbuminuria and proteinuria in children with sickle cell disease. *J Pediatr Hematol Oncol* 2007;29(3):140–144.
415. Abo-Zenah H, Moharram M, El Nahas AM. Cardiorenal risk prevalence in sickle cell hemoglobinopathy. *Nephron Clin Pract* 2009;112(2):c98–c106.
416. de Jong PE, de Jong-Van Den Berg TW, Sewrajsingh GS, et al. The influence of indomethacin on renal haemodynamics in sickle cell anaemia. *Clin Sci* 1980;59(4):245–250.
417. Allon M. Renal abnormalities in sickle cell disease. *Arch Intern Med* 1990;150(3):501–504.
418. Herrera J, Avila E, Marin C, et al. Impaired creatinine secretion after an intravenous load is an early characteristic of the nephropathy of sickle cell anaemia. *Nephrol Dial Transplant* 2002;17(4):602–607.
419. Barros FB, Lima CS, Santos AO, et al. ⁵¹Cr-EDTA measurements of the glomerular filtration rate in patients with sickle cell anaemia and minor renal damage. *Nucl Med Commun* 2006;27(12):959–962.
420. De Jong PE, De Jong-Van Den Berg LTW, Statius van Eps LW. The tubular reabsorption of phosphate in sickle-cell nephropathy. *Clin Sci Mol Med* 1978;55:429–434.
421. de Jong PE, de Jong-van den Berg LTW, Sewrajsingh GS, et al. Beta-2-microglobulin in sickle cell anaemia. *Nephron* 1981;29:138–141.
422. Bayazit AK, Noyan A, Aldudak B, et al. Renal function in children with sickle cell anemia. *Clin Nephrol* 2002;57(2):127–130.
423. Oster JR, Lee SM, Lespier LE, et al. Renal acidification in sickle cell trait. *Arch Intern Med* 1976;136(1):30–35.
424. Katopodis KP, Elisaf MS, Pappas HA, et al. Renal abnormalities in patients with sickle cell-beta thalassemia. *J Nephrol* 1997;10:163–167.
425. DeFronzo RA, Taufield PA, Black H, et al. Impaired renal tubular potassium secretion in sickle cell disease. *Ann Intern Med* 1979;90(3):310–316.
426. Oster JR, Lanier DC Jr, Vaamonde CA. Renal response to potassium loading in sickle cell trait. *Arch Intern Med* 1980;140(4):534–536.
427. da Silva GB Jr, Liborio AB, Daher Ede F. New insights on pathophysiology, clinical manifestations, diagnosis, and treatment of sickle cell nephropathy. *Ann Hematol* 2011;90(12):1371–1379.
428. Jung DC, Kim SH, Jung SI, et al. Renal papillary necrosis: Review and comparison of findings at multi-detector row CT and intravenous urography. *Radiographics* 2006;26(6):1827–1836.
429. Ernst AA, Weiss SJ, Johnson WD, et al. Blood pressure in acute vaso-occlusive crises of sickle cell disease. *South Med J* 2000;93(6):590–592.
430. Karayaylali I, Onal M, Yildizer K, et al. Low blood pressure, decreased incidence of hypertension, and renal cardiac, and autonomic nervous system functions in patients with sickle cell syndromes. *Nephron* 2002;91(3):535–537.

431. Gordeuk VR, Sachdev V, Taylor JG, et al. Relative systemic hypertension in patients with sickle cell disease is associated with risk of pulmonary hypertension and renal insufficiency. *Am J Hematol* 2008;83(1):15–18.
432. Hiran S. Multiorgan dysfunction syndrome in sickle cell disease. *J Assoc Physicians India* 2005;53:19–22.
433. Audard V, Homs S, Habibi A, et al. Acute kidney injury in sickle patients with painful crisis or acute chest syndrome and its relation to pulmonary hypertension. *Nephrol Dial Transplant* 2010;25(8):2524–2529.
434. Makaryus JN, Catanzaro JN, Katona KC. Exertional rhabdomyolysis and renal failure in patients with sickle cell trait: Is it time to change our approach? *Hematology* 2007;12(4):349–352.
435. Morgan AG, Shah DJ, Williams W. Renal pathology in adults over 40 with sickle-cell disease. *West Indian Med J* 1987;36(4):241–250.
436. Vaamonde CA. Renal papillary necrosis in sickle cell hemoglobinopathies. *Semin Nephrol* 1984;4:48–64.
437. Falk RJ, Jennette JC. Sickle cell nephropathy. *Adv Nephrol Necker Hosp* 1994;23:133–147.
438. Morgan AG, Serjeant GR. Renal function in patients over 40 with homozygous sickle-cell disease. *Br Med J (Clin Res Ed)* 1981;282(6271):1181–1183.
439. McCarville MB, Luo Z, Huang X, et al. Abdominal ultrasound with scintigraphic and clinical correlates in infants with sickle cell anemia: Baseline data from the BABY HUG trial. *AJR Am J Roentgenol* 2011;196(6):1399–1404.
440. Walker TM, Beardsall K, Thomas PW, et al. Renal length in sickle cell disease: Observations from a cohort study. *Clin Nephrol* 1996;46(6):384–388.
441. Mostofi FK, Vorder Bruegge CF, Diggs LW. Lesions in kidneys removed for unilateral hematuria in sickle-cell disease. *Arch Pathol* 1957;63(4):336–351.
442. Zadei G, Lohr JW. Renal papillary necrosis in a patient with sickle cell trait. *J Am Soc Nephrol* 1997;8(6):1034–1039.
443. Pandya KK, Koshy M, Brown N, et al. Renal papillary necrosis in sickle cell hemoglobinopathies. *J Urol* 1976;115(5):497–501.
444. Stadius van Eps LW, Pinedo-Veels C, de Vries GH, et al. Nature of concentrating defect in sickle-cell nephropathy. Microradiographic studies. *Lancet* 1970;1(7644):450–452.
445. Bernstein J, Whitten CF. A histologic appraisal of the kidney in sickle cell anemia. *Arch Pathol* 1960;70:407–418.
446. Pitcock JA, Muirhead EE, Hatch FE, et al. Early renal changes in sickle cell anemia. *Arch Pathol* 1970;90:403–410.
447. Bhatena DB, Sondheimer JH. The glomerulopathy of homozygous sickle hemoglobin (SS) disease: Morphology and pathogenesis. *J Am Soc Nephrol* 1991;1(11):1241–1252.
448. Sydenstricker VP, Mulherin WA, Houseal RW. Sickle cell anemia: Report of two cases in children, with necropsy in one case. *Am J Dis Child* 1923;26:132–154.
449. Alleyne GA. The kidney in sickle cell anemia. *Kidney Int* 1975;7(6):371–379.
450. de Jong PE, Stadius van Eps LW. Sickle cell nephropathy: New insights into its pathophysiology. *Kidney Int* 1985;27(5):711–717.
451. Elfenbein IB, Patchefsky A, Schwartz W, et al. Pathology of the glomerulus in sickle cell anemia with and without nephrotic syndrome. *Am J Pathol* 1974;77(3):357–376.
452. Tejani A, Phadke K, Adamson O, et al. Renal lesions in sickle cell nephropathy in children. *Nephron* 1985;39(4):352–355.
453. Nasr SH, Markowitz GS, Sentman RL, et al. Sickle cell disease, nephrotic syndrome, and renal failure. *Kidney Int* 2006;69(7):1276–1280.
454. D'Agati VD, Fogo AB, Bruijn JA, et al. Pathologic classification of focal segmental glomerulosclerosis: A working proposal. *Am J Kidney Dis* 2004;43(2):368–382.
455. Maigne G, Ferlicot S, Galacteros F, et al. Glomerular lesions in patients with sickle cell disease. *Medicine (Baltimore)* 2010;89(1):18–27.
456. Bakir AA, Hathiwala SC, Ainis H, et al. Prognosis of the nephrotic syndrome in sickle glomerulopathy. A retrospective study. *Am J Nephrol* 1987;7(2):110–115.
457. McCoy RC. Ultrastructural alterations in kidney of patients with sickle cell disease and the nephrotic syndrome. *Lab Invest* 1969;21:85–95.
458. Arakawa M, Kimmelstiel P. Circumferential mesangial interposition. *Lab Invest* 1969;21(3):276–284.
459. Vogler C, Wood E, Lane P, et al. Microangiopathic glomerulopathy in children with sickle cell anemia. *Pediatr Pathol Lab Med* 1996;16:275–284.
460. Freedman BI, Burkart JM, Iskandar SS. Chronic mesangiolytic glomerulopathy in a patient with SC hemoglobinopathy. *Am J Kidney Dis* 1990;14:361–363.
461. Pardo V, Strauss J, Kramer H, et al. Nephropathy associated with sickle cell anemia: An autologous immune complex nephritis. II. Clinicopathologic study of seven patients. *Am J Med* 1975;59(5):650–659.
462. Ozawa T, Mass MF, Guggenheim S, et al. Autologous immune complex nephritis associated with sickle cell trait; diagnosis of the hemoglobinopathy after renal structural and immunologic studies. *Br Med J* 1976;1:369–371.
463. Flanagan G, Packham DK, Kincaid-Smith P. Sickle cell disease and the kidney. *Am J Kidney Dis* 1993;21:325–327.
464. Kanodia KV, Vanikar AV, Goplani KR, et al. Sickle cell nephropathy with diffuse proliferative lupus nephritis: A case report. *Diagn Pathol* 2008;3:9.
465. Saxena VR, Mina R, Moallem HJ, et al. Systemic lupus erythematosus in children with sickle cell disease. *J Pediatr Hematol Oncol* 2003;25(8):668–671.
466. Aviles DH, Craver R, Warriar RP. Immunotactoid glomerulopathy in sickle cell anemia. *Pediatr Nephrol* 2001;16:82–84.
467. Akar H, Keven K, Nergizoglu G, et al. Renal amyloidosis in a patient with homozygous sickle cell anemia and M694V/M694V mutation. *Nephron* 2000;86:383–384.
468. Win N, Brozovic M, Gabriel R. Secondary amyloidosis accompanying multiple sickle cell crises. *Trop Doct* 1993;23:45–46.
469. Simsek B, Bayazit AK, Ergin M, et al. Renal amyloidosis in a child with sickle cell anemia. *Pediatr Nephrol* 2006;21(6):877–879.
470. Balal M, Paydas S, Seyrek N, et al. Different glomerular pathologies in sickle cell anemia. *Clin Nephrol* 2004;62(5):400–401.
471. Assar R, Pitel PA, Lammert NL, et al. Acute poststreptococcal glomerulonephritis and sickle cell disease. *Child Nephrol Urol* 1988–1989;9:176–179.
472. Johnston RP, Newton SL, Struth AG. An abnormality of the alternate pathway of complement activation in sickle-cell disease. *N Engl J Med* 1973;288(16):803–808.
473. Iskandar SS, Morgann RG, Browning MC, et al. Membranoproliferative glomerulonephritis associated with sickle cell disease in two siblings. *Clin Nephrol* 1991;35(2):47–51.
474. Wierenga KJJ, Pattison JR, Brink N, et al. Glomerulonephritis after human parvovirus infection in homozygous sickle-cell disease. *Lancet* 1995;346(8973):475–476.
475. Tolaymat A, Al Mousily F, MacWilliam K, et al. Parvovirus glomerulonephritis in a patient with sickle cell disease. *Pediatr Nephrol* 1999;13:340–342.
476. Dawkins FW, Kim KS, Squires RS, et al. Cancer incidence rate and mortality rate in sickle cell disease patients at Howard University Hospital: 1986–1995. *Am J Hematol* 1997;55(4):188–192.
477. Baron BW, Mick R, Baron JM. Hematuria in sickle cell anemia—not always benign: Evidence for excess frequency of sickle cell anemia in African Americans with renal cell carcinoma. *Acta Haematol* 1994;92(3):119–122.
478. Davis CJ Jr, Mostofi FK, Sesterhenn IA. Renal medullary carcinoma. The seventh sickle cell nephropathy. *Am J Surg Pathol* 1995;19(1):1–11.
479. Swartz MA, Karth J, Schneider DT, et al. Renal medullary carcinoma: Clinical, pathologic, immunohistochemical, and genetic analysis with pathogenetic implications. *Urology* 2002;60(6):1083–1089.
480. Watanabe IC, Billis A, Guimaraes MS, et al. Renal medullary carcinoma: Report of seven cases from Brazil. *Mod Pathol* 2007;20(9):914–920.
481. Davis CJ. Renal medullary carcinoma. In: Eble JN, Sauter G, Epstein JI, et al., eds. *Tumours of the Urinary System and Male Genital Organs*. Lyon: IARC Press, 2004:35–36.
482. Gatalica Z, Lilleberg SL, Monzon FA, et al. Renal medullary carcinomas: Histopathologic phenotype associated with diverse genotypes. *Hum Pathol* 2011;42(12):1979–1988.
483. O'Donnell PH, Jensen A, Posadas EM, et al. Renal medullary-like carcinoma in an adult without sickle cell hemoglobinopathy. *Nat Rev Urol* 2010;7(2):110–114.

484. Cheng JX, Tretiakova M, Gong C, et al. Renal medullary carcinoma: Rhabdoid features and the absence of IN11 expression as markers of aggressive behavior. *Mod Pathol* 2008;21(6):647–652.
485. Marino-Enriquez A, Ou WB, Weldon CB, et al. ALK rearrangement in sickle cell trait-associated renal medullary carcinoma. *Genes Chromosomes Cancer* 2010;50(3):146–153.
486. Yang XJ, Sugimura J, Tretiakova MS, et al. Gene expression profiling of renal medullary carcinoma: Potential clinical relevance. *Cancer* 2004;100(5):976–985.
487. Yip D, Steer C, al-Nawab M, et al. Collecting duct carcinoma of the kidney associated with the sickle cell trait. *Int J Clin Pract* 2001;55(6):415–417.
488. Eble JN, Sauter G, Epstein JI, et al., eds. *Pathology and Genetics of Tumours of the Urinary System and Male Genital Organs*. Lyon: IARC Press, 2004.
489. Barabino GA, Platt MO, Kaul DK. Sickle cell biomechanics. *Annu Rev Biomed Eng* 2010;12:345–367.
490. Kaul DK, Finnegan E, Barabino GA. Sickle red cell-endothelium interactions. *Microcirculation* 2009;16(1):97–111.
491. Kaul DK, Fabry ME. In vivo studies of sickle red blood cells. *Microcirculation* 2004;11(2):153–165.
492. Kaul DK, Hebbel RP. Hypoxia/reoxygenation causes inflammatory response in transgenic sickle mice but not in normal mice. *J Clin Invest* 2000;106(3):411–420.
493. Nur E, Biemond BJ, Otten HM, et al. Oxidative stress in sickle cell disease; pathophysiology and potential implications for disease management. *Am J Hematol* 2011;86(6):484–489.
494. Aslan M, Ryan TM, Townes TM, et al. Nitric oxide-dependent generation of reactive species in sickle cell disease. Actin tyrosine induces defective cytoskeletal polymerization. *J Biol Chem* 2003;278(6):4194–4204.
495. Bank N, Kiroycheva M, Singhal PC, et al. Inhibition of nitric oxide synthase ameliorates cellular injury in sickle cell mouse kidneys. *Kidney Int* 2000;58(1):82–89.
496. de Jong PE, Saleh AW, de Zeeuw D, et al. Urinary prostaglandins in sickle cell nephropathy: A defect in 9-ketoreductase activity? *Clin Nephrol* 1984;22(4):212–213.
497. Nath KA, Katusic ZS, Gladwin MT. The perfusion paradox and vascular instability in sickle cell disease. *Microcirculation* 2004;11(2):179–193.
498. Hostetter TH. Hyperfiltration and glomerulosclerosis. *Semin Nephrol* 2003;23(2):194–199.
499. D'Agati VD, Kaskel FJ, Falk RJ. Focal segmental glomerulosclerosis. *N Engl J Med* 2011;365(25):2398–2411.
500. Nadasdy T, Allen C, Zand MS. Zonal distribution of glomerular collapse in renal allografts: Possible role of vascular changes. *Hum Pathol* 2002;33(4):437–441.
501. Belhassen L, Pelle G, Sediame S, et al. Endothelial dysfunction in patients with sickle cell disease is related to selective impairment of shear stress-mediated vasodilation. *Blood* 2001;97(6):1584–1589.
502. Nath KA, Katusic ZS. Vasculature and kidney complications in sickle cell disease. *J Am Soc Nephrol* 2012;23:781–784.
503. Hirschberg R. Glomerular hyperfiltration in sickle cell disease. *Clin J Am Soc Nephrol* 2010;5(5):748–749.
504. Reiter CD, Wang X, Tanus-Santos JE, et al. Cell-free hemoglobin limits nitric oxide bioavailability in sickle-cell disease. *Nat Med* 2002;8(12):1383–1389.
505. Chen HC, Guh JY, Chang JM, et al. Plasma and urinary endothelin-1 in focal segmental glomerulosclerosis. *J Clin Lab Anal* 2001;15(2):59–63.
506. Nath KA, Grande JP, Haggard JJ, et al. Oxidative stress and induction of heme oxygenase-1 in the kidney in sickle cell disease. *Am J Pathol* 2001;158(3):893–903.
507. Quinn CT, Rogers ZR, McCavit TL, et al. Improved survival of children and adolescents with sickle cell disease. *Blood* 2010;115(17):3447–3452.
508. Makani J, Cox SE, Soka D, et al. Mortality in sickle cell anemia in Africa: A prospective cohort study in Tanzania. *PLoS One* 2011;6(2):e14699.
509. Platt OS, Brambilla DJ, Rosse WF, et al. Mortality in sickle cell disease. Life expectancy and risk factors for early death. *N Engl J Med* 1994;330(23):1639–1644.
510. Diallo D, Tchernia G. Sickle cell disease in Africa. *Curr Opin Hematol* 2002;9(2):111–116.
511. Powars DR. β^S -gene-cluster haplotypes in sickle cell anemia. *Hematol Oncol Clin North Am* 1991;5(3):475–492.
512. Powars DR, Elliott-Mills DD, Chan L, et al. Chronic renal failure in sickle cell disease: Risk factors, clinical course, and mortality. *Ann Intern Med* 1991;115(8):614–620.
513. Steinberg MH, Lu ZH, Barton FB, et al. Fetal hemoglobin in sickle cell anemia: Determinants of response to hydroxyurea. Multicenter Study of Hydroxyurea. *Blood* 1997;89(3):1078–1088.
514. Bakanay SM, Dainer E, Clair B, et al. Mortality in sickle cell patients on hydroxyurea therapy. *Blood* 2005;105(2):545–547.
515. Nolan VG, Ma Q, Cohen HT, et al. Estimated glomerular filtration rate in sickle cell anemia is associated with polymorphisms of bone morphogenetic protein receptor 1B. *Am J Hematol* 2007;82(3):179–184.
516. Chui DH, Dover GJ. Sickle cell disease: No longer a single gene disorder. *Curr Opin Pediatr* 2001;13(1):22–27.
517. Nagel RL. Pleiotropic and epistatic effects in sickle cell anemia. *Curr Opin Hematol* 2001;8(2):105–110.
518. Steinberg MH. Predicting clinical severity in sickle cell anaemia. *Br J Haematol* 2005;129:465–481.
519. Hicks PJ, Langefeld CD, Lu L, et al. Sickle cell trait is not independently associated with susceptibility to end-stage renal disease in African Americans. *Kidney Int* 2011;80(12):1339–1343.
520. Serjeant GR. Sickle-cell disease. *Lancet* 1997;350(9079):725–730.
521. Powars DR. Sickle cell anemia and major organ failure. *Hemoglobin* 1990;14:573–598.
522. Faulkner M, Turner EA, Deus J, et al. Severe anemia: A risk factor for glomerular injury in sickle cell disease. *J Natl Med Assoc* 1995;(87):209–213.
523. McKerrrell TDH, Cohen HW, Billett HH. The older sickle cell patient. *Am J Hematol* 2004;76:101–106.
524. Lonsdorfer A, Comoe L, Yapo AE, et al. Proteinuria in sickle cell trait and disease: An electrophoretic analysis. *Clin Chim Acta* 1989;181(3):239–247.
525. Manci EA, Culbertson DE, Yang YM, et al. Causes of death in sickle cell disease: An autopsy study. *Br J Haematol* 2003;123(2):359–365.
526. Darbari DS, Kple-Faget P, Kwagyan J, et al. Circumstances of death in adult sickle cell disease patients. *Am J Hematol* 2006;81(11):858–863.
527. Abbott KC, Hypolite IO, Agodoa LY. Sickle cell nephropathy at end-stage renal disease in the United States: Patient characteristics and survival. *Clin Nephrol* 2002;58(1):9–15.
528. Sklar AH, Campbell H, Caruana RJ, et al. A population study of renal function in sickle cell anemia. *Int J Artif Organs* 1990;13(4):231–236.
529. Datta V, Ayengar JR, Karpate S, et al. Microalbuminuria as a predictor of early glomerular injury in children with sickle cell disease. *Indian J Pediatr* 2003;70(4):307–309.
530. de Santis Feltran L, de Abreu Carvalhaes JT, Sesso R. Renal complications of sickle cell disease: Managing for optimal outcomes. *Paediatr Drugs* 2002;4(1):29–36.
531. Aoki RY, Saad ST. Enalapril reduces the albuminuria of patients with sickle cell disease. *Am J Med* 1995;98(5):432–435.
532. Foucan L, Bourhis V, Bangou J, et al. A randomized trial of captopril for microalbuminuria in normotensive adults with sickle cell anemia. *Am J Med* 1998;104(4):339–342.
533. Fitzhugh CD, Wigfall DR, Ware RE. Enalapril and hydroxyurea therapy for children with sickle nephropathy. *Pediatr Blood Cancer* 2005;45:982–985.
534. Steinberg MH, McCarthy WF, Castro O, et al. The risks and benefits of long-term use of hydroxyurea in sickle cell anemia: A 17.5 year follow-up. *Am J Hematol* 2010;85(6):403–408.
535. Zimmerman SA, Schultz WH, Davis JS, et al. Sustained long-term hematologic efficacy of hydroxyurea at maximum tolerated dose in children with sickle cell disease. *Blood* 2004;103:2039–2045.
536. Lebensburger J, Johnson SM, Askenazi DJ, et al. Protective role of hemoglobin and fetal hemoglobin in early kidney disease for children with sickle cell anemia. *Am J Hematol* 2011;86(5):430–432.
537. Thornburg CD, Dixon N, Burgert S, et al. A pilot study of hydroxyurea to prevent chronic organ damage in young children with sickle cell anemia. *Pediatr Blood Cancer* 2009;52(5):609–615.
538. Alvarez O, Miller ST, Wang WC, et al. Effect of hydroxyurea treatment on renal function parameters: Results from the multi-center placebo-controlled baby hug clinical trial for infants with sickle cell anemia. *Pediatr Blood Cancer* 2012:668–674.
539. Ataga KI. Novel therapies in sickle cell disease. *Hematology Am Soc Hematol Educ Program* 2009:54–61.

540. Ataga KI, Reid M, Ballas SK, et al. Improvements in haemolysis and indicators of erythrocyte survival do not correlate with acute vaso-occlusive crises in patients with sickle cell disease: A phase III randomized, placebo-controlled, double-blind study of the Gardos channel blocker senicapoc (ICA-17043). *Br J Haematol* 2011;153(1):92–104.
541. Saxena AK, Panhotra BR, Al-Ghamdi AM. Should early renal transplantation be deemed necessary among patients with end-stage sickle cell nephropathy who are receiving hemodialytic therapy? *Transplantation* 2004;77(6):955–956.
542. Ojo AO, Govaerts TC, Schmouder RL, et al. Renal transplantation in end-stage sickle cell nephropathy. *Transplantation* 1999;67(2):291–295.
543. Chatterjee SN. National study on natural history of renal allografts in sickle cell disease or trait. *Nephron* 1980;25(4):199–201.
544. Chatterjee SN. National study in natural history of renal allografts in sickle cell disease or trait: A second report. *Transplant Proc* 1987;19(2 Suppl 2):33–35.
545. Warady BA, Sullivan EK. Renal transplantation in children with sickle cell disease: A report of the North American Pediatric Renal Transplant Cooperative Study (NAPRTCS). *Pediatr Transplant* 1998;2(2):130–133.
546. Nath J, McDaid J, Bentall A, et al. Sickle cell and renal transplant: A national survey and literature review. *Exp Clin Transplant* 2012;10(1):1–7.
547. Khoury R, Abboud MR. Stem-cell transplantation in children and adults with sickle cell disease: An update. *Expert Rev Hematol* 2011;4(3):343–351.
548. Bhatia M, Walters MC. Hematopoietic cell transplantation for thalassaemia and sickle cell disease: Past, present and future. *Bone Marrow Transplant* 2008;41(2):109–117.
549. Kersting S, Hene RJ, Koomans HA, et al. Chronic kidney disease after myeloablative allogeneic hematopoietic stem cell transplantation. *Biol Blood Marrow Transplant* 2007;13(10):1169–1175.
550. Hsieh MM, Fitzhugh CD, Tisdale JF. Allogeneic hematopoietic stem cell transplantation for sickle cell disease: The time is now. *Blood* 2011;118(5):1197–1207.
551. Cavazzana-Calvo M, Payen E, Negre O, et al. Transfusion independence and HMGA2 activation after gene therapy of human beta-thalassaemia. *Nature* 2010;467(7313):318–322.
552. Nagel RL, Fabry ME. The panoply of animal models for sickle cell anaemia. *Br J Haematol* 2001;112:19–25.
553. Beuzard Y. Mouse models of sickle cell disease. *Transfus Clin Biol* 2008;15(1–2):7–11.
554. Hanna J, Wernig M, Markoulaki S, et al. Treatment of sickle cell anemia mouse model with iPS cells generated from autologous skin. *Science* 2007;318(5858):1920–1923.

Renal Changes With Aging and End-Stage Renal Disease

Manifestations of end-stage renal disease 1283

- Clinical features 1283
- Cardiovascular system 1283
- Lung 1286
- Beta-2-microglobulin amyloidosis 1286
- Gastrointestinal tract and pancreas 1287
- Hematopoietic system 1288
- Chronic hepatitis and hepatic iron overload 1289
- Central nervous system 1289
- Secondary parathyroid hyperplasia 1289
- CKD-mineral bone disorder and renal osteodystrophy 1289
- Hypertension in end-stage renal disease 1291

Functional changes of the aging kidney 1291

- Renal hemodynamics 1291
- Glomerular filtration rate 1292
- Tubular function 1293
- Endocrine and metabolic function 1293

Pathology of the aging kidney 1294

- Gross pathology 1294
- Microscopic pathology 1294

Pathology of the end-stage kidney 1297

- Gross pathology 1297
- Light microscopy 1298
- Acquired renal cystic disease 1306
- Renal cell tumors of acquired renal cystic disease 1308

Etiology and pathogenesis 1309

- Pathogenesis of renal aging 1309
- Etiology and pathogenesis of end-stage renal disease 1311

Management and outcome 1312

- Management and outcome of end-stage renal disease 1312
- Dialysis therapy in the elderly 1313

The growth in the proportion of older adults is unmatched in the history of humankind. Improvements in prevention and medical treatment of diseases have led to increased life expectancies all over the world, resulting in an absolute increase in the numbers of the elderly. In addition, the lower population growth rates in the developed world have led to a relative increase in the elderly, leading to an inversion of the population pyramid. By 2030, there will be 72 million adults aged 65 years and older in United States accounting for approximately 20% of the US population (1). Aging is accompanied by a higher rate of morbidity, with a consequent impact on economic and human resources. Compared to younger individuals, it costs three to five times to provide health care for an American older than 65 years and treatment for this population accounts for 66% of the U.S. healthcare budget (1). It is well known that advancing age per se is associated with deterioration of renal function. The presence of diverse chronic diseases in older individuals could accelerate the age-related decline in renal function. Thus, the prevalence of chronic kidney disease (CKD) is greatest in the elderly, and the older population has the fastest-growing segment of end-stage renal disease (ESRD) (2).

Mirroring the elderly populace, the world population has lately experienced an exponential growth of ESRD requiring renal replacement therapy (RRT). The 2013 United States Renal Data System (USRDS) report showed more than 50% increase in the prevalent dialysis population between 2000 and 2011 (2). There were 615,899 ESRD patients in 2011, and with an annual growth of 3.2%, the ESRD population is projected to grow to more than 700,000 dialysis patients by 2020 (2). While ESRD comprises only 1% of total Medicare population, it consumes 8.1 % of the Medicare budget and \$49.27 billion in total spending (2). With extensive efforts made to prevent or slow progression of renal disease, there has been a recent reduction of the overall ESRD incidence (2). Nevertheless, the incidence of ESRD continues to grow particularly among elderly patients. Since 2000, there has been a 7.1% growth in the incidence rate of ESRD in patients over 75 years of age. Moreover, as of 2011, the incidence rate was four times higher in patients over 65 years of age compared to the overall incidence rate of ESRD in the US population (2). Furthermore, the total number of elderly patients 65 years and older with ESRD has increased by

68%, since 2000 (2). Currently, one in four patients starting dialysis in the United States is over the age of 75 years (2). An increase in the prevalence of associated comorbidities such as diabetes and hypertension as well as improved survival from cardiovascular (CV) disease may explain the increase in ESRD incidence among the elderly. This increase in the numbers of ESRD patients has obvious social and economic dimensions that are even more pronounced in the case of older patients (2,3).

ESRD is the terminal phase of CKD caused by a progressive deterioration of kidney function to the point of requiring RRT. The Kidney Disease Outcomes Quality Initiative (K/DOQI) defines CKD as kidney damage or glomerular filtration rate (GFR) less than 60 mL/min/1.73 m² for 3 months or more, irrespective of cause (4). By this definition, 11% of the United States adult population (more than 20 million individuals) has been estimated to have CKD (5). CKD is subclassified into five stages according to the level of GFR (Table 28.1) (6). Individuals with stage 5 CKD (GFR less than 15 mL/min/1.73 m²) that require dialysis are termed ESRD patients. It has been recently observed that the lifetime risk of ESRD at the age of 40 is significantly higher in patients with reduced kidney function (eGFR 44 to 59 mL/min/1.73 m²) compared with individuals with normal kidney function (7). ESRD is sometimes diagnosed when patients undergo renal biopsy for unexplained renal failure. The recognition that a final point has been reached in a disease process allows patients to be placed on dialysis and to avoid unneeded diagnostic or therapeutic measures. In addition, the specific disease that has led to the renal failure can often be identified. When patients have been supported by dialysis for several years, the original renal disease may be obscured by the advanced degree of tissue changes. But even among these cases, the cause can often be assigned to at least one of five major categories of disease (hypertension, diabetes, glomerulonephritis, interstitial nephritis, or ischemic nephropathy). It also may be possible to discriminate specific forms of glomerulonephritis and interstitial nephritis. It is important to realize that, while structural and functional changes of the kidney occur ubiquitously with aging, there is no specific disease confined only to the geriatric population. In general, the types of renal diseases seen in the elderly are similar to those encountered in the general population, although certain disorders such as diabetes and hypertension may have an increased prevalence and accelerate the development of CKD in this population (Table 28.2) (8,9). Therefore, the approach

TABLE 28.1 Stages of chronic kidney disease

Stages	Description	GFR (mL/min/1.73 m ²)
1	Kidney damage with normal or elevated GFR	≥90
2	Kidney damage with mildly decreased GFR	60–89
3	Moderately decreased GFR	30–59
4	Severely decreased GFR	15–29
5	Chronic kidney failure	<15 or dialysis

Adapted from Kidney Disease Outcome Quality Initiative (K/DOQI). Part 4. Definition and classification of stages of chronic kidney disease. *Am J Kidney Dis* 2002;39(Suppl):S46–S75.

TABLE 28.2 Diseases that commonly affect the aging kidney

Systemic diseases
Hypertension
Diabetes mellitus
Dyslipidemia
Atherosclerosis
Atheroemboli
Myeloma cast nephropathy
Amyloidosis
Light-chain deposition disease
Vasculitides
Glomerular diseases
Membranous GN
Mesangial proliferative GN (including IgA nephropathy)
Pauci-immune crescentic GN
Anti-GBM disease
Minimal change disease
Focal segmental glomerulosclerosis
Acute renal failure
Hypovolemic and cardiovascular shock
Septic shock
Nephrotoxic injury
Nonsteroidal anti-inflammatory agents
Antibiotics (penicillins, cephalosporins, sulfonamides, rifampin, ciprofloxacin)
Diuretics (furosemide, potassium-sparing diuretics)
Contrast media
Cancer chemotherapy
Allopurinol
Cimetidine
Captopril
Interstitial nephritis
Urinary tract infection
Renal stones
Obstructive uropathy
Benign causes
Nodular hyperplasia of prostate
Neurogenic bladder
Renal stones
Obstructive pyelonephritis/papillary necrosis
Urethral stricture
Malignant causes
Prostate cancer
Bladder cancer
Pelvic tumors
Colonic tumors
Retroperitoneal tumors
Renal tumors
Primary
Metastatic
Simple renal cysts

GN, glomerulonephritis; GBM, glomerular basement membrane

Adapted from Zhou XJ, Rakheja D, Yu XQ, et al. The Aging Kidney. *Kidney Int* 2008;74:710–720.

to the interpretation of renal biopsies in the elderly is similar to that of the general population. However, given the high prevalence of type 2 diabetes mellitus and hypertension in the elderly, these two disorders should be ruled out before ascribing any morphologic changes to aging.

MANIFESTATIONS OF END-STAGE RENAL DISEASE

Clinical Features

Patients with CKD most often present with nonspecific complaints or are asymptomatic and are referred to a nephrologist because of abnormal blood or urinary findings (10). In symptomatic patients with CKD, often symptoms have been present for months or years (4). Urinary symptoms suggesting CKD include difficulty with urination, history of urinary tract infections, passage of kidney stones, dysuria, and nocturia.

A common early sign of uremic encephalopathy is sleep disturbance. Typically, patients have difficulty falling asleep, awaken during the night, and again have difficulty falling asleep, with subsequent early morning awakening accompanied by daytime sleeping. Subsequent loss of short-term memory, difficulty concentrating, and episodes of confusion can occur.

Another early sign of CKD is dependent edema that presents first as ankle or periorbital edema. Uremic patients frequently develop congestive heart failure, in which case dependent edema becomes increasingly severe and may progress to anasarca. The skin of uremic patients has a sallow, yellow appearance because it is pigmented with carotene. When blood urea levels are greatly elevated, urea is secreted through the skin where it can dry into a white uremic frost. The patient's breath has a urinous odor because of urea being metabolized to ammonia by mouth bacteria. In terminal stages, uremic patients become delirious and lapse into coma before death. Because of the nearly universal access to RRT, cases of fully developed uremia are rare. Nevertheless, ESRD patients have a high prevalence of nonrenal comorbid disease. With prolonged survival on dialysis, pathologic changes occur in virtually all systems of the body.

Cardiovascular System

CKD is an independent risk factor for CV disease and all-cause mortality. Observational studies indicate that rates of both stroke and myocardial infarction are higher in patients with CKD before the development of ESRD. For example, Go et al. (11) reported on the risk of all-cause mortality and CV hospitalizations among 1.2 million participants in the Northern California Kaiser Permanente health care system. They found a graded increase in mortality and CV hospitalizations as estimated GFR declined. This association was independent of traditional CV risk factors such as age, blood pressure, diabetes, hypercholesterolemia, and proteinuria and suggests that CKD may be an independent risk factor for coronary heart disease (11).

CKD markedly increases the risk of CV death from cardiac events and stroke (2). The mortality risk in CKD patients with CVD is 10- to 30-fold higher than that in normal, age-matched populations. Median survival after an acute myocardial infarction in patients undergoing dialysis is less than 18 months, even in the thrombolytic era. Hypertensive

patients with elevated serum creatinine are at higher risk of myocardial infarction and stroke, and diabetic patients with proteinuria are at greater risk for fatal myocardial infarction and stroke (2). Prevalence of left ventricular hypertrophy (LVH) and congestive heart failure is strikingly elevated in patients with CKD stages 2 through 5, including those undergoing dialysis (12). Morbidity and mortality for congestive heart failure and coronary heart disease are also excessive in CKD. Moreover, presence of coronary artery disease increases the risk of progression to ESRD in CKD patients. McClellan et al. (13) observed that patients hospitalized for myocardial infarction or congestive heart failure who also had CKD had a high rate of progression to ESRD in a 12-month period following the cardiovascular event. Current clinical practice guidelines target the treatment of the risk factors of hypertension, hyperlipidemia, and tobacco use not only for the prevention of CV disease but also to retard the progression of CKD (6).

Cardiomyopathies of End-Stage Renal Disease

The cardiomyopathies of ESRD are classified into dilated or hypertrophic cardiomyopathy (14). Dilated cardiomyopathy is characterized by enlargement of the chamber of the left ventricle but without an increase in the thickness of the left ventricular free wall or interventricular septum. It is clinically associated with impaired systolic function and a low left ventricular ejection fraction. Dilated cardiomyopathy precedes dialysis in 16% of ESRD patients and develops in another 15% during the course of dialytic therapy (14). Dilated cardiomyopathy seems to occur most frequently in hypertensive patients who have hyperparathyroidism and high-turnover bone disease. It is suggested that an excessive entry of calcium into myocardial cells limits their capacity to hypertrophy in response to elevated blood pressure. To compensate for the increased workload, the heart is forced to dilate to maintain cardiac output.

Hypertrophic cardiomyopathy is characterized by LVH. Concentric LVH is the most common form of hypertrophic cardiomyopathy in the patient with ESRD and consists of an increased thickness of both the interventricular septum and left ventricular free wall. Eccentric hypertrophy and asymmetric septal hypertrophy do occur but are less common. LVH affects up to 70% of patients during intermediate stages of CKD and approaching 90% of patients with ESRD (15,16). Using magnetic resonance imaging, Patel et al. (17) observed 63.8% prevalence of LVH among 246 HD patients. Independent predictors of LVH were predialysis blood pressure and diastolic LV volume (suggesting volume overload) and the calcium phosphorus product but not anemia. LVH among these patients was associated with LV systolic and diastolic dysfunction. The study suggests the role of preload and afterload in causing LVH and confirms some of the previous studies done with the echocardiograms in HD patients that noted a similar prevalence of LVH (15–17). However, LVH has been seen in some patients whose blood pressure appears to be adequately controlled, and the regression of LVH after transplantation suggests that other CKD-specific risk factors are involved (16). To this end, recent studies have shown that circulating concentrations of FGF23 were markedly elevated in patients with advanced CKD and the elevated FGF23 was independently associated with greater left ventricular mass and greater prevalence of

LVH (18–20). FGF23 functions as an endocrine hormone that regulates phosphorus homeostasis through binding to the FGF receptor (FGFR) and Klotho (its coreceptor) in the kidney and parathyroid glands (21). The authors demonstrated that FGF23 directly induces pathologic hypertrophy of isolated rat cardiomyocytes and that mice develop LVH after intraventricular or intravenous injection of FGF23. In addition, FGFR blocker attenuates the severity of LVH in 5/6 nephrectomized rats without affecting blood pressure (18). Thus, chronically elevated FGF23 levels may contribute directly to high rates of LVH and mortality in individuals with CKD. Recent studies have also demonstrated the possible role of activation of the mammalian target of rapamycin (mTOR) pathway in LVH. To this end, LVH associated with uremia can be mitigated or even reversed by rapamycin administration in a mouse model of chronic renal failure. LVH also can be modulated by microRNAs, which regulate cardiac growth by degradation of mRNA or inhibition of translocation. The histone acetylation/deacetylation pathway can also modulate the development of LVH (22). Acetylation relaxes chromatin structure and allows access of transcription factors, whereas deacetylation produces opposite effects.

Atherosclerotic Coronary Artery Disease

Atherosclerotic CV disease is the principal cause of morbidity and mortality in ESRD patients. This largely reflects the prevalence of hypertension and diabetes mellitus in this population and the severity of the atherosclerotic vascular disease that is part of the natural history of these diseases. Nevertheless, severe atherosclerosis can be seen at an unusually young age. In addition, oxidative stress, inflammation, and HDL deficiency and dysfunction contribute to the pathogenesis of accelerated atherosclerosis and CV disease in the ESRD population (23,24). In a retrospective analysis of transplantation candidates with no active symptoms of coronary artery disease (CAD), noninvasive imaging revealed abnormalities suggestive of ischemia in 30.7% of patients and coronary angiography showed obstructive disease in 54.1% of the same cohort (25). Braun et al. (26) measured cardiac and coronary artery calcification by electron-beam computed tomography to assess coronary artery disease in 49 chronic hemodialysis (HD) patients aged 39 to 74 years. The results were compared with 102 age-matched nondialysis patients with known coronary artery disease who had undergone coronary angiography. A 2.5- to 5-fold higher coronary artery calcification score was found in the dialysis patients, and the scores significantly increased when the patients were reexamined after 1 year.

The high CV mortality in patients with CKD is closely associated with vascular calcification (27). The severity of calcification in atherosclerotic plaques can be related to plaque size (28). Although calcification can be found in small plaques, it is most pronounced in larger, complicated plaques having a necrotic lipid core and varying amounts of inflammation (29). Calcification also occurs along the media of coronary arteries as Mönckeberg medial calcific sclerosis, in which there is little intimal thickening or luminal narrowing (30). The bone matrix proteins osteopontin, osteocalcin, and osteoblastic differentiation factor (Cbfa1) are expressed in areas of medial and plaque calcification. The presence of these locally produced bone matrix-stimulating factors indicates that metastatic calcification is an active, cell-mediated process similar to osteogenesis

rather than a passive deposition of minerals (31,32). Moe et al. (32,33) and Chen et al. (31) have suggested that chronic uremia may up-regulate the local deposition of bone matrix proteins and promote atherosclerotic plaque growth.

Hypertension, dyslipidemia, diabetes, and elevated plasma phosphate, homocysteine, and osteoprotegerin levels are risk factors for vascular calcification (34). Defects in endogenous anticalcification factors may also play a role (35). In a recent study, Hu et al. showed that CKD is associated with Klotho deficiency, which contributes to soft tissue calcification (36). By enhancing phosphaturia, preserving glomerular filtration, and directly inhibiting phosphate uptake by vascular smooth muscle, Klotho can mitigate vascular calcification in CKD.

Sudden cardiac death is the single most common cause of death in ESRD patients and accounts for one quarter to one third of all deaths (2). In an analysis of outcomes of 102 cardiac arrests in HD units in the Seattle area, it was observed that ventricular fibrillation (65%) and pulseless electrical activity (23%) were the two most common reasons of cardiac arrests in HD patients. More than one third of patients died in the dialysis unit, only approximately one quarter were discharged alive from the hospital, and only 15% were alive at 1 year (37). The possible risk factors for sudden death in dialysis patients include hyper-/hypokalemia and hypervolemia, LVH and heart failure, myocardial fibrosis, QT dispersion, sympathetic overactivity, hyperphosphatemia, and possibly sleep apnea (38). Unlike nondialysis patients, underlying ischemic heart disease is not an important contributor to sudden cardiac death in the dialysis population (39). It is unknown whether preventing or treating any of the aforesaid risk factors will reduce the incidence of sudden death in dialysis patients.

Valvular Calcification

The cardiac valves of ESRD patients are frequently abnormal. Valvular calcification is closely related to coexisting atherosclerotic coronary artery disease, and the extent of valvular calcification has been found to predict CV mortality (26,40–42). The mitral valve is calcified in 10% to 59% and the aortic valve in 28% to 55% of dialysis patients. The calcification most severely affects the annulus (Figs. 28.1 and 28.2). Although involvement of the aortic valve cusps and mitral leaflets can produce clinically significant stenosis, this is not common, and the relationship between valvular calcification and cardiac death is primarily owing to the close association of valvular calcification with coronary artery disease (26,42). Calcification of the mitral valve can cause heart block or other arrhythmias when the calcification of the annulus extends into the adjacent ventricular wall. Oxalosis is sometimes found in the hearts of ESRD patients as a result of the secondary oxalosis of advanced CKD. It can extensively involve the coronary arteries or be deposited in the AV node and conducting bundles.

Calcemic Uremic Arteriopathy

Calcemic uremic arteriopathy (CUA) or calciphylaxis is an uncommon clinical condition that occurs in some patients with long-standing ESRD. Calcification of arterioles in the dermis and subcutaneous tissues produces painful red skin nodules that frequently undergo ischemic necrosis and ulceration (Fig. 28.3) and is most commonly found on the thighs, buttocks, and abdomen. When the hands or feet are affected, there may be gangrene of the fingers or toes. Involvement of the mesenteric



FIGURE 28.1 Nodular calcification of the annulus and base of the mitral valve in a 55-year-old hemodialysis patient.

artery has also been reported. Histologically, the skin shows medial calcification and intimal fibrosis of arterioles and small arteries. The intimal fibrosis may be occlusive or accompanied by thrombosis, and coagulative necrosis is found in the dermis

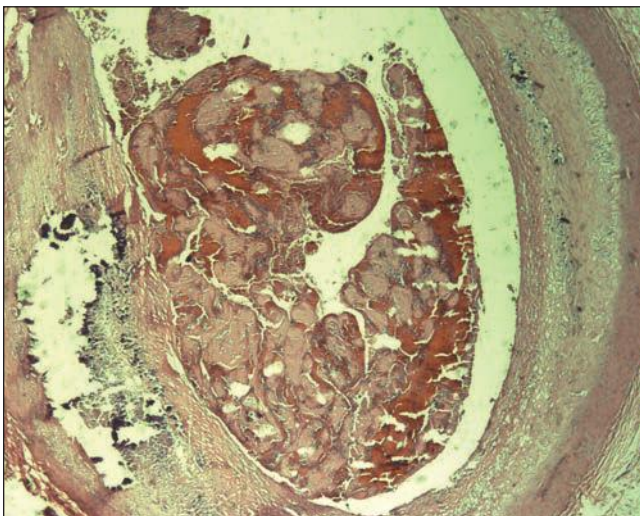


FIGURE 28.2 Thrombosis over a calcified plaque of the left anterior descending coronary artery in the hemodialysis patient with the mitral valve calcification shown in Figure 28.1. Note the fissuring of the plaque over the necrotic and calcified core. (H&E, $\times 400$.)

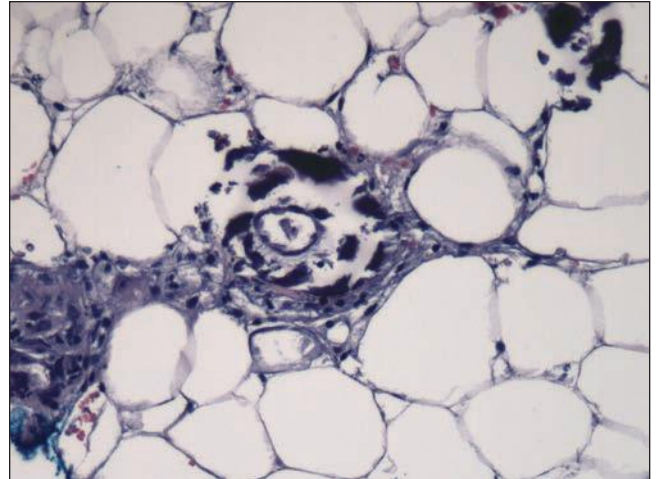


FIGURE 28.3 Calcemic uremic arteriopathy. An arteriole in the dermis of a painful skin nodule on the lower leg of a hemodialysis patient is calcified. (H&E, $\times 400$.)

and subcutaneous tissue. Ulceration frequently develops, and a necrotizing panniculitis is sometimes seen that is often complicated by septicemia. Studies have reported incidences ranging from 1% to 4% in chronic HD patients. A case-control study of 67 Japanese patients with CUA identified warfarin therapy, low serum albumin level, elevated plasma glucose level, and increased serum calcium level at the time of diagnosis to be significantly associated with CUA (43). However, no significant associations were found with female sex, vitamin D analog therapy, serum phosphate level, adjusted calcium-phosphate products, or serum alkaline-phosphatase level. This study suggests that in high-risk patients with poor control of blood sugar and calcium levels, warfarin therapy should be undertaken only with great caution. Treatment of CUA is unsatisfactory. Therapeutic strategies include removing medications thought to contribute to calciphylaxis (calcium-based phosphate binders, active vitamin D analogs, and warfarin) as well as aggressive wound management and antibiotic therapy, supplemented by intensified HD, intravenous sodium thiosulfate, and attempted oxygen therapy including hyperbaric oxygen (44). Bisphosphonates or cinacalcet may also be helpful in selected patients (45). There are no randomized control trials, and most of the literature is anecdotal, and results are variable (46).

Pericardium

Uremia appears to increase the permeability of small blood vessels and allows a fibrinous exudate to leak across the pericardium leading to *uremic pericarditis* (47,48). The gross examination of the heart shows easily broken bands of fibrin producing the classical bread and butter appearance (Fig. 28.4). The histopathology of uremic pericarditis reveals a fibrinous exudate accompanied by sparse inflammatory cells covering the visceral and parietal surfaces of the pericardium.

A fibrinous pericarditis can also be seen in acute renal failure and occasionally in adequately dialyzed patients. When it occurs 1 month or more after beginning dialysis, it is diagnosed as dialysis-associated pericarditis (47,48). It is generally held that dialysis-associated pericarditis and uremic



FIGURE 28.4 Dialysis-associated pericarditis from an autopsy of a 58-year-old diabetic hemodialysis patient who died of septicemia. The heart is coated with a fibrinous exudate.

pericarditis represent the same pathologic condition. It is often seen when dialysis patients become infected or when they are under increased metabolic stress, such as following surgery. In most cases, dialysis-associated pericarditis clears after treatment schedules are intensified (47,48). In long-standing pericarditis, the fibrinous exudate is organized into fibrous tissue that produces a constrictive pericarditis, which is usually a complication of ESRD, but has also been described with acute renal failure following a single episode of pericarditis. Typically, uremic or dialysis-associated pericarditis is associated with pleuritic chest pain and, if a significant amount of fluid accumulates, with cardiac tamponade (47,48). Hemorrhage can occur into the pericardium and is an additional cause of cardiac tamponade in the uremic patient.

Lung

The cardiomyopathy of ESRD frequently decompensates into congestive heart failure as a result of anemia, fluid retention, and hypertension. Congestive heart failure is one of the most common causes of death among ESRD patients. Patients develop pulmonary edema when the passive accumulation of blood within the pulmonary vasculature causes alveolar intracapillary hydrostatic pressure to exceed oncotic pressure. Grossly, the lungs involved by pulmonary edema are heavy, and their sectioned surfaces are covered by frothy, blood-tinged fluid. Microscopically, alveolar capillaries are distended with blood. The perivascular interstitium and interlobular septa are edematous, and lymphatics are dilated. Alveoli become filled with amorphous, slightly eosinophilic edema fluid that can contain a few red blood cells. If patients have been in congestive heart failure for several days, some hyaline membrane formation may be present (49,50).

In advanced uremia, proteinaceous fluid sometimes leaks into the alveoli, producing what has been referred to as *uremic*

pneumonitis, which is a form of pulmonary edema caused by injury to and increased permeability of the alveolar capillaries (49–51). It has been suggested that IL-6 is a direct mediator of uremia-induced increase in vascular permeability (52). Grossly, the lungs have a stiff, rubbery consistency, and the sectioned surfaces have a dark, reddish color. Histologically, the earliest stage reveals a hemorrhagic fibrinous fluid filling the alveoli with hyaline membranes being formed along alveolar walls and alveolar ducts. If the process does not resolve, fibrin in the alveolar fluid and hyaline membranes is organized into whorls of fibrous tissue referred to as *Masson bodies* (50).

When ESRD is complicated by metastatic calcification, it is usually found in the lung. The calcification may be focal or diffuse and tends to affect the upper lobes most severely. Both lungs can be involved. Metastatic pulmonary calcification is usually clinically asymptomatic, and the pattern of deposition may be so delicate that it will not be detected by routine chest radiographs. Nevertheless, if the calcification is extensive, it can lead to respiratory failure. Grossly, the involved areas of lung have a firm but brittle consistency and a fine net-like appearance that exaggerates the outlines of open alveoli. The areas are gray to pale yellow in color and typically contrast sharply with the adjacent normal or congested lung. They are gritty to the touch. Histologically, linear calcifications outline basement membranes within the alveolar septae. Calcifications also are seen along the elastica of arteries, veins, bronchi, and bronchioles and in fibrotic nodules within the lung parenchyma (50).

Beta-2-Microglobulin Amyloidosis

Beta-2-microglobulin is the light chain of class I HLA molecules, which enters the bloodstream when HLA molecules are degraded and shed from the surfaces of cell membranes. Beta-2-microglobulin accumulates in the plasma of ESRD patients and is deposited as insoluble amyloid fibrils in the articular surfaces of bone, in periarticular connective tissue (Fig. 28.5), and in

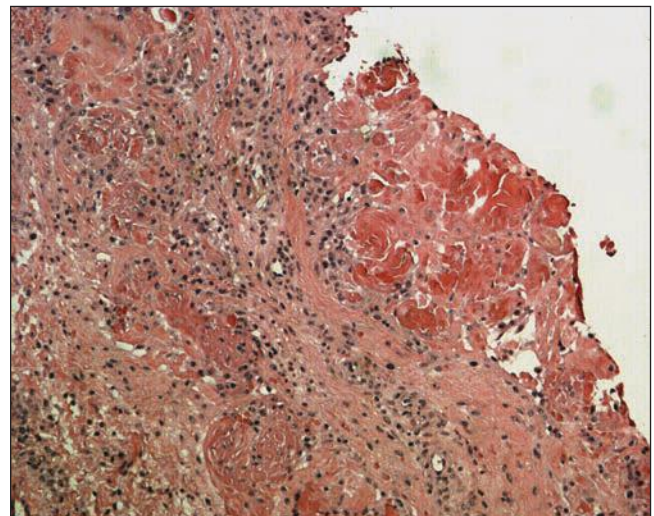


FIGURE 28.5 Beta-2-microglobulin-related amyloidosis in the synovium from the right hand of a 54-year-old long-term hemodialysis patient who had a several-week history of interphalangeal joint pain and swelling. Nodular deposits of amorphous hyaline material are seen in the synovial connective tissue. (H&E, $\times 200$.)

nerve sheaths in as many as 80% of HD patients after 10 years of treatment (53). It causes carpal tunnel syndrome and a destructive arthropathy of medium- and large-sized joints, mainly of the shoulders and knees (53,54). Dialysis-associated amyloid tumors of breast and ovary, nodular skin masses particularly of the buttocks and shoulder area, and nodules of the tongue are additionally described (55–58). Beta-2-microglobulin amyloid was found in the hearts of 7 of 18 HD patients who had been dialyzed for more than 10 years (59). Amyloid was present in the endocardium and myocardium of the left atrium. In the left ventricle, it was localized to the walls of blood vessels and around areas of calcification of the mitral valve. Rarely, amyloid deposits can occur in the intestinal wall (60,61).

Beta-2-microglobulin amyloid is found within bone of 19% of HD patients after 10 years of treatment (62). These bone deposits are responsible for cysts that develop in the carpal bones, femur, and femoral head and possibly for the unusually high prevalence of pathologic femoral neck fractures in HD patients (Figs. 28.6 and 28.7). Onishi et al. (62) observed that 62% of patients had femoral neck fractures when periosteal amyloid deposits were found in posterior iliac crest bone biopsies. Only 4% of a control group of HD patients having biopsies who did not show periosteal amyloid had femoral neck fractures.

Beta-2-microglobulin amyloid shows Congo red–positive staining and apple-green birefringence under polarized light. By electron microscopy, it is composed of fine fibrils 8 to 10 nm in diameter having a curvilinear structure that is thought to be characteristic of beta-2-microglobulin (Fig. 28.8) (62).



FIGURE 28.6 Beta-2 microglobulin–related amyloidosis of the femoral head removed from a 37-year-old long-term hemodialysis patient who had a femoral neck fracture. A necrotic cyst surrounded by a rim of solid white material is present beneath the insertion of the ligamentum teres.

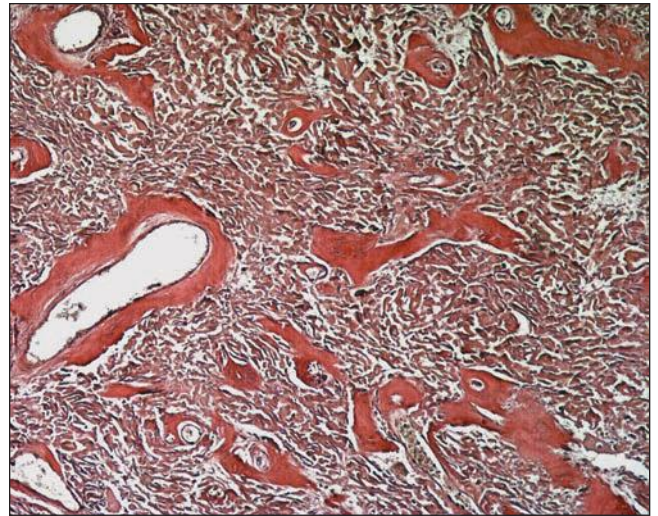


FIGURE 28.7 Histologic section from the solid area surrounding the femoral head cyst shown in Figure 28.6. Amyloid is present in the walls of blood vessels and in the interstitium. (Congo red, $\times 100$.)

Since beta-2-microglobulin is cleared to some extent through the peritoneum and PD patients often have more residual renal function, amyloidosis does not seem to be as prevalent with CAPD as it is with HD (53). The addition of beta-2-microglobulin adsorption columns in tandem with HD reduces the radiolucency of bone cysts in the wrist joints and improves clinical symptoms associated with dialysis-related amyloidosis (63). A successful renal transplantation often results in marked symptomatic improvement and may arrest the growth of the cysts (64).

Gastrointestinal Tract and Pancreas

Terminal uremia is accompanied by edema, inflammation, mucosal erosions, and ulcerations of the entire gastrointestinal tract. Gastrointestinal bleeding is a common clinical problem

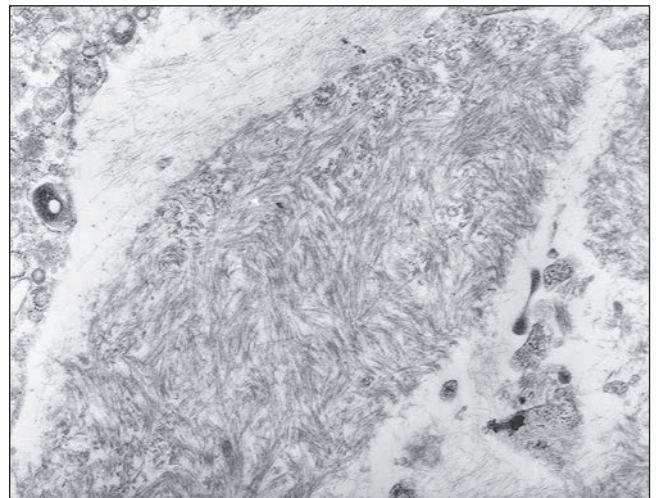


FIGURE 28.8 Electron microscopic photomicrograph of the synovial tissue shown in Figure 28.5. Curvilinear fibrils characteristic of beta-2-microglobulin amyloidosis are demonstrated. ($\times 18,000$.)

among dialysis patients and most frequently originates in a hemorrhagic gastritis (65). Many dialysis patients have a mild gastritis, duodenitis, or peptic ulcer disease in which *Helicobacter pylori* can sometimes be found; although, these findings may not be any more common than in the general population (66).

Colonic bleeding can originate from cecal ulcers, stercoral ulcers, angiodysplasia, diverticulosis, or ischemic colitis (65,67). Multiple shallow ulcers attributed to uremia may be found in the cecum and ascending colon. Constipation and fecal impaction, resulting from the use of oral phosphate binders as well as other medications, produce stercoral ulcers in the transverse and rectosigmoid colon. Angiodysplasia consisting of clusters of abnormally dilated mucosal and submucosal blood vessels is found primarily in the cecum and ascending colon. Angiodysplasia is more prevalent in dialysis patients than in the general population, and in some series, it is the most frequent cause of gastrointestinal hemorrhage among ESRD patients (65,67,68). Diverticulosis, diverticulitis, pericolic abscesses, and colonic perforation may be more common in autosomal dominant polycystic kidney disease (ADPKD) than with other categories of renal disease (69).

The severe atherosclerosis of diabetes and hypertension places ESRD patients at high risk for ischemic colitis and intestinal infarction (67). HD patients with beta-2-microglobulin amyloidosis may have amyloid deposited in the connective tissue and small blood vessels of the mucosa and submucosa of the GI tract (60). The gastrointestinal amyloid is usually an incidental finding, but massive involvement of the muscularis propria of the colon has been identified as a cause of bleeding and intestinal infarction (61).

Systemic inflammation is a constant feature and a major mediator of CV disease and numerous other complications in the ESRD population. Systemic inflammation is associated with and, in part, mediated by endotoxemia, which is invariably present in ESRD patients in the absence of clinically detectable infection (70). Until recently, little attention had been paid to the role of gastrointestinal tract and its microbial flora in the pathogenesis of the CKD-associated inflammation. However, recent studies have demonstrated marked disintegration of the gastric, small intestinal and colonic epithelial tight junction (71) and extensive alteration of the composition of colonic bacterial flora in humans and animals with advanced chronic renal failure (72). More recent *in vitro* studies have revealed the role of urea and its conversion to ammonia by microbial flora as a major cause of the uremia-induced disintegration of colonic epithelial tight junction and barrier dysfunction (73). Discovery of the disruption of gastrointestinal epithelial tight junction complex has helped to elucidate the underlying mechanism of endotoxemia and contribution of the intestinal tract to the local and systemic inflammation in ESRD (70). In addition, via the disruption of the normal symbiotic relationship, the ESRD-associated profound changes in the composition and function of the intestinal microbial flora can contribute to local and systemic inflammation and uremic toxicity. In fact, recent studies have documented the role of colonic bacteria as the primary source of several well-known proinflammatory/prooxidant uremic toxins as well as many as-yet unidentified retained compounds in ESRD patients (74).

Patients dying of uremia may develop an acute pancreatitis in which pancreatic ductules and acini are dilated and contain

inspissated eosinophilic material (75). The dilated acini become disrupted and surrounded by an acute inflammatory reaction. Pancreatitis is also seen in patients who are well maintained on long-term peritoneal and hemodialysis (76). The pancreas may show focal or generalized fibrosis. Sometimes, fibrosis may be the sequela of episodes of acute pancreatitis, but it has also been related to hyperphosphatemia and to ischemic atrophy secondary to the marked arteriolosclerosis that is often found in the small pancreatic arteries (75). Nephrogenic or dialysis-associated ascites occurs in a small proportion of HD patients (77). Some of these patients had been previously treated by peritoneal dialysis (PD), and histologic studies of the peritoneum have shown fibrosis and chronic inflammation.

Hematopoietic System

Anemia is a highly prevalent complication in CKD patients. Contributing factors include erythropoietin (EPO) deficiency, frequently coexistent iron deficiency, and shortened erythrocyte life span. In addition to common causes of iron deficiency that occur in the general population, CKD and more so ESRD patients are at further risk because of impaired gastrointestinal iron absorption, blood loss during the HD, and enhanced incorporation of iron stores into hemoglobin by erythropoietin-stimulating agents (ESAs) (78). A shortened red blood cell life span also contributes to the anemia of CKD. This is reflected in peripheral blood smears that show numerous poikilocytes resulting from extrinsic factors that fragment or metabolically alter the erythrocyte. The anemia of CKD is usually normocytic and normochromic. Since red blood cell production and iron utilization are low, bone marrow examinations of patients with the typical anemia of CKD show normal to increased amounts of iron. Gastrointestinal bleeding and poor dietary intake, however, can lead to iron deficiency and a microcytic hypochromic anemia. Aluminum toxicity causes a microcytic hypochromic anemia in which adequate iron stores are present (79). Correction of anemia provides relief from many of the debilitating symptoms of ESRD (80). These include improvement in sleep, cognitive function, and exercise tolerance. The response to EPO is poor in some ESRD patients, and they require high doses of EPO to raise their hemoglobin levels. There are disease differences in EPO requirements. Patients with IgA nephropathy and polycystic kidney disease have lower requirements than other patients, and patients with hypertension appear to need higher doses than diabetics. The differences may be partly explained by underlying inflammatory conditions or infections. Patients with ESRD owing to SLE, vasculitis, and AIDS require relatively high doses, and EPO resistance is more common in African American patients. The hypertrophic cardiomyopathy of ESRD has been observed to regress after EPO therapy, and hemodynamic improvement has been seen with dilated cardiomyopathy (81). However, administration of high doses of EPO to achieve hemoglobin levels ≥ 12 g/dL has been shown to increase morbidity and mortality in patients with ESRD and CKD patients not requiring dialysis. These adverse effects are primarily due to the non-erythropoietic actions of high doses of EPO and intravenous iron preparations (78,82). Hemorrhage into skin, mucous membranes, and gastrointestinal tract is a common problem in the patient with ESRD. The bleeding tendency is attributed to platelet dysfunction. Platelets are normal in number but appear unable to adequately adhere to damaged blood vessels

and form hemostatic plugs (83). The ESRD-associated platelet dysfunction is in part due to impaired calcium signaling, which is ameliorated by EPO therapy (84). In addition, EPO administration increases platelet production and can potentially cause thrombosis in ESRD patients (85).

Chronic Hepatitis and Hepatic Iron Overload

Hepatitis C virus is the most common cause of chronic liver disease in ESRD. In December 2002, all US chronic HD centers were surveyed regarding selected patient care practices and dialysis-associated diseases. Routine testing for antibody to hepatitis C virus (anti-HCV) was performed on patients at 64% of centers; anti-HCV was found in 7.8% of patients (86). The prevalence of seropositivity is related to the number of transfusions that the patients have received. Liver biopsies have demonstrated chronic liver disease in 50% to 100% of anti-HCV–positive patients (87). Martin et al. (87) found mild or moderate necroinflammatory changes in all of 28 anti-HCV–positive patients who had liver biopsies while being referred for transplantation. Fibrosis was seen in 79%, and 3 of the 28 (11%) had cirrhosis. Hepatitis C infection does not seem to change mortality rates of dialysis patients (88). The other common liver abnormality in the ESRD population is iron overload, which was due to frequent use of blood transfusion in the preerythropoietin era and is caused by excessive use of intravenous iron preparations in recent years (89).

Central Nervous System

Central nervous system disorders in ESRD have been defined clinically as uremic encephalopathy, dialysis disequilibrium syndromes, and dialysis dementia (50,90). The clinical manifestations of uremic encephalopathy are lethargy, confusion, obtundation, and coma (90). The signs and symptoms can evolve rapidly in patients with acute renal failure and are less often seen in patients who slowly progress to chronic renal failure. If patients have been severely hypertensive, the brain at autopsy may show fibrinoid necrosis of small arteries and provide evidence of a hypertensive encephalopathy. Otherwise, the brain may reveal only nonspecific changes of cerebral edema, or if patients have been dehydrated, the brain may be dry and reduced in size. The dialysis disequilibrium syndrome is rarely seen in current nephrology practice. The clinical symptoms are caused by elevated intracranial pressure such as nausea, vomiting, tremor, muscle cramps, dizziness, and blurred vision (90). Dialysis dementia is caused by the chronic toxicity of aluminum absorbed from oral phosphate binders or dialysate water. Aluminum exposure is now closely controlled, and dialysis dementia has virtually disappeared as a clinical syndrome (90).

Secondary Parathyroid Hyperplasia

In early-stage CKD, plasma fibroblastic growth factor 23 (FGF23), a bone-derived phosphaturic hormone, is increased to maintain neutral phosphate balance through down-regulation of sodium-phosphate cotransporters and suppression of renal production of 1,25(OH)₂D (or calcitriol) by inhibiting 1- α -hydroxylase and stimulating 24-hydroxylase (91). Calcitriol normally acts through the vitamin D receptor to inhibit parathyroid hormone (PTH) transcription and growth of parathyroid cells. Via loss of this inhibitory activity, low serum levels of calcitriol directly contribute to the increased secretion of PTH and promote parathyroid hyperplasia.

In addition, low calcitriol reduces the intestinal absorption of calcium and further contributes to secondary parathyroid hyperplasia. In ESRD, dietary phosphate overwhelms the compensatory mechanisms of elevated FGF23, resulting in overt hyperphosphatemia. Hyperphosphatemia together with decreased 1,25(OH)₂D and resulting hypocalcemia contributes to further stimulation of PTH secretion and parathyroid cell proliferation (91).

Grossly, all four parathyroid glands and any accessory glands are enlarged in cases of secondary hyperplasia, although there can be considerable variation in the size of each gland. Single-gland weights can range from less than 100 mg to more than 2 g (normal combined gland weight is 50 to 300 mg). The enlargement may be diffuse or nodular. Histologically, the hyperplasia is composed of a mixture of chief cells and oxyphil cells with chief cells usually predominating (Fig. 28.9). In cases of refractory secondary hyperparathyroidism, clonal chromosomal changes have been detected in the parathyroid glands of 61% of dialysis patients (92). The most common abnormality was a deletion of 1p that was found in 71% of the glands having chromosomal abnormalities. A deletion of 1p is the most common cytogenetic abnormality found in parathyroid adenomas, and the recurring clonality of the deletion in secondary hyperplasia suggests a neoplastic process and the involvement of a tumor suppressor gene (92).

CKD-Mineral Bone Disorder and Renal Osteodystrophy

CKD-mineral bone disorder is defined as a systemic condition of mineral and bone metabolism due to CKD manifested by either one or a combination of the following: (a) abnormalities of calcium, phosphorus, PTH, and vitamin D metabolism; (b) abnormalities in bone turnover, mineralization, volume, linear growth, or strength; and (c) vascular or other soft tissue calcification (93). The term *renal osteodystrophy* is used exclusively to define alterations in bone morphology associated with CKD, which can be further assessed by histomorphometry (93).

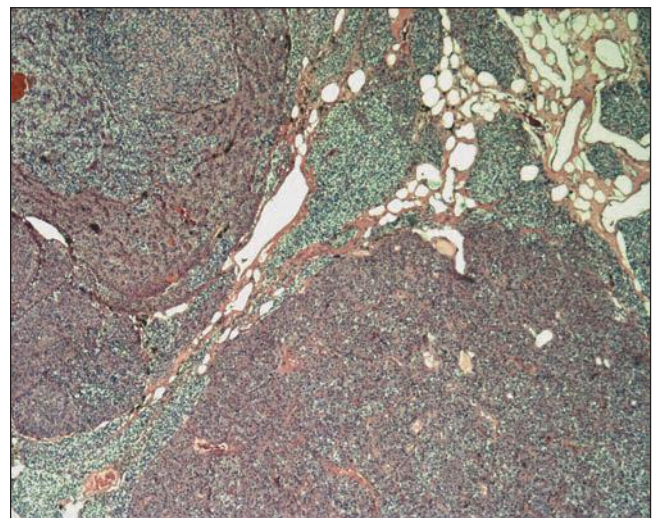


FIGURE 28.9 Secondary parathyroid hyperplasia in a 47-year-old chronic hemodialysis patient. Nodules of oxyphil cells are separated by chief cells in a parathyroid gland that weighed 1.12 g. (H&E, $\times 40$.)

It encompasses the following disorders: osteitis fibrosa cystica, osteomalacia, mixed patterns of osteitis fibrosa and osteomalacia, and adynamic bone disease (94). Osteitis fibrosa cystica is caused by secondary hyperparathyroidism. It is characterized by a high rate of bone formation and resorption and is referred to as *high-turnover bone disease*. PTH activates bone remodeling by stimulating marrow stromal cells to proliferate and differentiate into osteoblasts and fibroblasts (94). PTH also promotes proliferation of osteoclasts either directly or through cytokines and growth factors produced by marrow stromal cells and osteoblasts (95). The most important of these locally produced factors appear to be macrophage colony-stimulating factor, IL-6, osteoprotegerin, and receptor activator of NF- κ B ligand (RANKL).

The bones then undergo a continuing process of resorption and deposition that is not under the normal control of local mechanical strain. The cortex of long bones becomes more porous, and the trabecular bone of the medulla becomes thicker as a result of an increase in unmineralized woven bone or osteoid. Histologically, bone biopsies show an increased number of trabeculae composed of lamellar, mineralized bone of irregular shape and thickness lined by increased amounts of osteoid (94) (Fig. 28.10). Osteoblasts are prominently clustered along the osteoid. Trabeculae are surrounded by fibrous tissue and are scalloped by osteoclasts within the Howship lacunae (Fig. 28.11). Unconnected trabecular islands can be seen within the medullary fibrous tissue emphasizing the lack of organization to the remodeling. The bones are susceptible to spontaneous fractures and, in advanced cases, develop medullary cysts and become markedly deformed.

Osteomalacia is a low-turnover bone disease and, in most cases, is the result of aluminum toxicity (50,94). Osteomalacia softens the bones that can then become deformed and fracture with mild mechanical stress. Bone biopsies show normal numbers of abnormally thickened trabeculae (50,94). The trabeculae consist of a core of irregularly thickened and thinned lamellar bone surrounded by a markedly widened

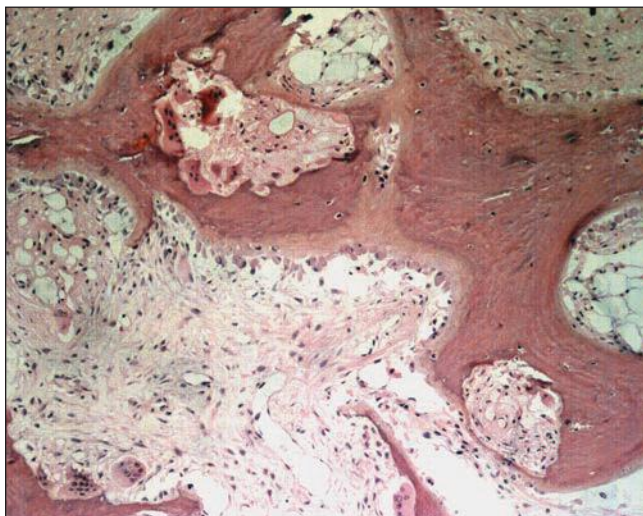


FIGURE 28.10 Osteitis fibrosa in a 27-year-old hemodialysis patient with secondary hyperparathyroidism. Fibrous tissue surrounds irregularly shaped trabeculae with numerous multinucleated osteoclasts. Undecalcified section. (H&E, $\times 100$.)

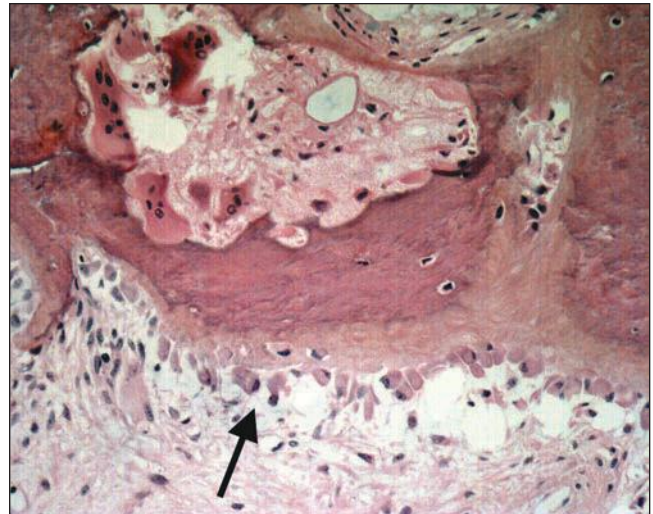


FIGURE 28.11 Higher magnification of Figure 28.10. Irregularly shaped trabeculae with a widened zone of unmineralized osteoid are lined on the lower edge by osteoblasts (arrow). Osteoclasts are identified in the Howship lacunae in the center. Undecalcified section. (H&E, $\times 200$.)

zone of osteoid (Fig. 28.12). Osteoblasts and osteoclasts are reduced below the number found in normal bone and are sparsely seen in histologic sections. Mixed bone disease shows a background of osteomalacia with foci of osteitis fibrosa in which there is increased osteoblastic and osteoclastic activity (50,94). Histochemical stains such as alizarin red react stoichiometrically with aluminum. Aluminum bone disease can be diagnosed when a biopsy shows osteomalacia or normal to thinned bone, a low rate of bone turnover, and aluminum histochemical staining over 25% or more of the trabecular surfaces (96) (Fig. 28.13).

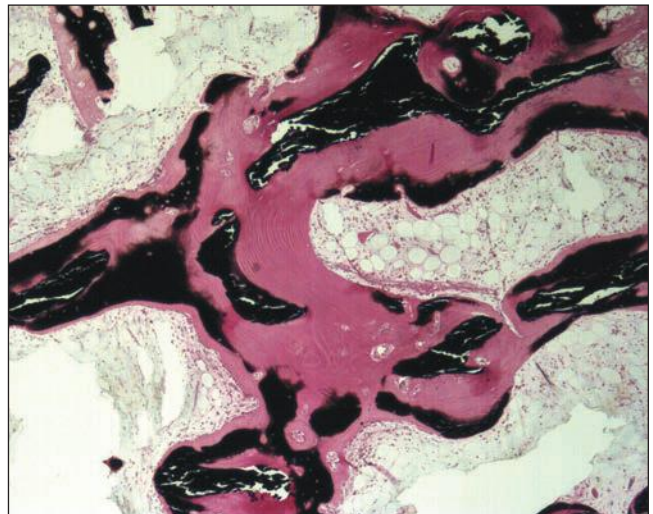


FIGURE 28.12 Osteomalacia in a long-term hemodialysis patient with low-turnover bone disease. There is a marked excess of pink-staining osteoid and no osteoblastic or osteoclastic activity. The mineralized parts of the trabeculae are stained black. Undecalcified section. (von Kossa, $\times 100$.)

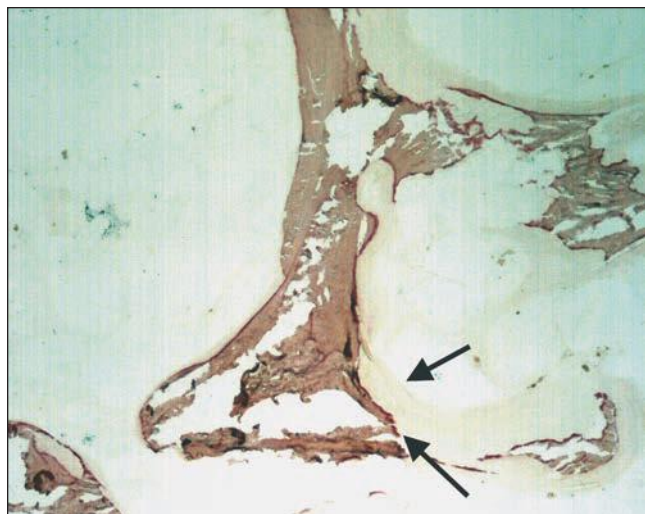


FIGURE 28.13 Iliac crest bone biopsy stained for aluminum. Osteomalacia is diagnosed by the wide osteoid seams, represented by the pale-staining areas outside the mineralized bone (arrows). The aluminum histochemical reaction product is the red line at the interface between mineralized bone and osteoid. Undecalcified section. (Alizarin red, $\times 200$.)

Adynamic bone disease is also a low-turnover state (50,94). The underlying mechanism is oversuppression of PTH. It also can be caused by aluminum overload (97). Patients with adynamic bone disease have bone pain of uncertain cause. In some patients, pain may be the result of microfractures of trabecular bone. In cases of aluminum overload, bone pain can sometimes be rapidly relieved by treatment with deferoxamine. Bone biopsies of adynamic bone disease show normal to decreased numbers of normal-appearing or thinned trabeculae composed of lamellar bone with reduced numbers of osteocytes (94,96,97). The trabeculae show little or no osteoid and few osteoblasts or osteoclasts.

The principal therapeutic approaches for CKD bone and mineral disease include control of hyperphosphatemia/phosphate retention with phosphate binders, administration of vitamin D sterols to suppress PTH, calcimimetic therapy in selected cases of secondary hyperparathyroidism, and parathyroidectomy in refractory cases. All of these measures need to be conducted with attention to the calcium burden since such therapeutic maneuvers can increase the risk of calcium overload with accompanying soft tissue and vascular calcification particularly when using calcium containing phosphorus binders (calcium carbonate and calcium acetate) and vitamin D sterols. Hence, vitamin D administration is not recommended if serum calcium, corrected for albumin, is greater than 9.5 mg/dL or serum phosphorus is more than 4.5 mg/dL (98). Consequently, novel therapeutic strategies are being developed that utilize calcium-free phosphorus binders (lanthanum carbonate and sevelamer carbonate/chloride) and calcimimetic agents (cinacalcet) to reduce serum phosphorus and suppress PTH without increasing calcium burden (99).

Hypertension in End-Stage Renal Disease

Ninety percent of patients with CKD experience hypertension (defined as a BP of greater than 130/80 mm Hg) during the course of the disease. Uncontrolled hypertension

accelerates the rate of progression regardless of the cause of renal failure. Clinical trials and epidemiologic studies indicate that hypertension is a major risk factor for progressive kidney disease. Evaluation of subjects screened in a multiple risk factor intervention trial who were monitored over a 16-year period showed that (a) higher blood pressure was a strong and independent risk factor for the development of ESRD and (b) the relative risk for ESRD increased with rising systolic blood pressure independent of diastolic blood pressure. In patients with type 2 diabetes mellitus, there is almost a linear relationship between increase in mean arterial blood pressure and yearly decrease in GFR. Analysis of the National Health and Nutrition Evaluation Survey (NHANES) III data suggests that adequate blood pressure control is achieved in only 11% of patients with hypercreatininemia (serum creatinine greater than 1.5 mg/dL) (100). Analysis of the NHANES IV indicates that only 37% of hypertensive patients with CKD have blood pressure controlled to a level of less than 130/80 mm Hg. Risk factors for uncontrolled hypertension included age older than 65, black race, and presence of albuminuria (101). In general, older people with hypertension are unaware of their blood pressure elevation, and the majority of those who are aware have poor control rates. CKD prevalence is higher in older age groups, in which systolic hypertension is very common (2). The importance and potential benefit of blood pressure control in renal outcome cannot be overemphasized.

FUNCTIONAL CHANGES OF THE AGING KIDNEY

Renal Hemodynamics

Several studies conducted in elderly individuals without significant renal disease have demonstrated that renal blood flow (RBF) decreases with advancing age. Total RBF was well maintained through approximately the fourth decade and, progressively, declined by approximately 10% per decade thereafter (102). In a study of 207 healthy kidney donors, Hollenberg et al. (103) demonstrated an explicit and progressive reduction in mean blood flow per unit kidney mass with advancing age, suggesting that the decrease in RBF does not simply reflect the decline in the renal mass with aging. The fall in renal perfusion with aging is most profound in the cortex, with relative sparing of flow to the medulla. This redistribution of blood flow from the cortex to medulla may explain the slight increase in filtration fraction observed in the elderly population. The precise mechanisms of reduced RBF with aging are incompletely understood. Aging is associated with changes in vascular tone, which is determined by the balance between vasoconstrictors and vasodilators. In aging, there is an attenuated responsiveness to vasodilators such as nitric oxide (NO), endothelial-derived hyperpolarizing factor (EDHF), and prostacyclin and enhanced responsiveness to vasoconstrictors such as angiotensin II (Ang II) (104). This may result in enhanced vasoconstrictive responses in aging that can potentially cause renal damage and ultimately a fall in GFR. Although the renin-angiotensin system (RAS) is suppressed in aging, the intrarenal RAS may be relatively spared. In particular, aging-associated oxidative stress can reduce NO availability by inactivation of NO, inhibition of NO synthase (NOS) via depletion of NOS cofactor tetrahydrobiopterin, uncoupling of endothelial NOS,

accumulation of the endogenous NOS inhibitor asymmetric dimethylarginine, and limiting uptake of the NOS substrate L-arginine by endothelial cells via down-regulation of cationic amino acid transporter-1 (105).

Elastic arteries undergo two distinct aging-related physical changes, namely dilation and stiffness due to fatigue and fracture of the medial elastin with little aging change in distal muscular arteries (106,107). Thus, dilation and stiffening are most marked in the proximal aorta and its major branches, namely the brachiocephalic, carotid, and subclavian arteries. Increased arterial stiffening results in an increase in pulse wave velocity (PWV), which is the speed with which pulse wave travels along the artery (108). A typical value is 5 m/s in a 20-year-old and 12 m/s in an 80-year-old person representing a 2.5-fold increase in 60 years (109). The elastic properties of the aorta in the young serve to partially store blood volume and pressure during systole and release them during diastole via the recoiling process. This phenomenon helps to protect the vital organs by sustaining blood flow during diastole and blunting the damaging effects of high-pressure waves during systole. In addition, the microcirculation, which comprises small arteries, arterioles, and capillaries and constitutes the greatest resistance to blood flow, participates in transforming pulsatile flow to steady flow by reflecting the pulsations that enter from the larger arteries. With aortic stiffening and consequent increase in aortic PWV, transmission of flow pulsations downstream into various organs, principally the brain and kidney, can damage the microvessels (110,111). The lesions comprise damage to medial smooth muscle and endothelium (not attributable to atherosclerosis) and, in their chronic form, are described as "lipohyalinosis" (112). The renal afferent arterioles and glomeruli are exposed to the same high pulsatile microvascular stress and strain as in the brain. Recent studies have shown that independent of conventional brachial systolic and diastolic pressure values, measures of arterial stiffness are closely related to outcomes attributable to microvascular damage to vital organs, particularly the brain and kidney. Furthermore, measures of large artery stiffness are closely related to the effects of microvascular changes in the kidney, including albuminuria (110,111).

Glomerular Filtration Rate

The GFR gradually increases after birth approaching adult levels by the end of the second decade. It remains stable until age of 30 to 40 years and then usually declines linearly at an average rate of about 8 mL/min/decade, a phenomenon that can be partially explained by age-associated glomerulopenia (8,113,114). Thus, inulin clearance, an excellent measure of the GFR, is about 20 mL/min at birth and gradually rises to around 120 mL/min by the age of 30 years. It is a generally accepted dogma that the GFR declines with increasing age after the age of about 30 years, when it starts dropping at an average rate of 1 mL/min/yr, resulting in an inulin clearance of 65 mL/min at the age of 90 years (114). However, in the Baltimore longitudinal study of aging among 254 "normal" subjects, although the mean decline in creatinine clearance was 0.75 mL/min/yr, 36% of the subjects showed no aging-related decrease in creatinine clearance, and a few of these actually showed an increase in their creatinine clearance (115). Creatinine clearance, of course, is influenced by the nutritional status, protein intake, and muscle mass and is, therefore, an inferior method of estimating GFR in the elderly. Healthy elderly subjects with daily

ingestion of more than 1 g of protein per kilogram body weight had a creatinine clearance of 90 to 100 mL/min/1.73 m², while those with diets poorer in protein had lower creatinine clearances (116). In addition, the creatinine production gradually declines with age, in proportion with the decreasing muscle mass and body weight. Therefore, the urinary creatinine output also shows a corresponding decline. This is the reason why the plasma creatinine does not rise with increasing age, despite the aging-related reduction in the creatinine clearance (117). Thus, a modestly elevated plasma creatinine is often of greater significance in the elderly than in a younger patient.

Since one third of elderly individuals show no change in GFR (115), factors other than aging may be responsible for the apparent reduction in renal function. For instance, an increase in blood pressure (still within the normotensive range) is associated with accelerated age-related loss of renal function. The use of creatinine clearance in a timed urinary collection is commonly used to estimate GFR. Inulin and iothalamate clearances are very accurate measurements of GFR but are clinically cumbersome to perform (118). To obviate the need for a timed urine collection, various equations have been developed and are increasingly used to estimate GFR. In adults, creatinine clearance is often estimated by the Cockcroft-Gault (CG) equation and GFR by the Modification of Diet in Renal Disease (MDRD) formula (119,120).

Cockcroft-Gault formula:

$$C_{Cr} \text{ (mL/min)} = \frac{(140 - \text{age} \times \text{weight})}{72 \times S_{Cr}} \times (0.85 \text{ if female})$$

MDRD formula:

$$\text{GFR (mL/min/1.73m}^2) = 186 \times (S_{Cr})^{-1.154} \times (\text{age})^{-0.203} \times (0.742 \text{ if female}) \times (1.210 \text{ if African-American})$$

It is important to point out that the CG equation estimates GFR in mL/min, while the MDRD formula expresses GFR in mL/min/1.73 m². However, neither MDRD nor CG equation was developed for elderly individuals, and reduced reliability would be expected when used in this population. The MDRD equation generally yielded higher estimates of GFR than the CG equation (121). A new creatinine-based equation was developed by the Chronic Kidney Disease Epidemiology Collaboration (CKD-EPI). It reported a more accurate estimation of GFR than the MDRD equation, particularly at higher levels of estimated GFR (eGFR) (122). However, the performance of the serum creatinine-based estimating equations remains insufficiently evaluated in older patients, in whom there may be a high prevalence of chronic disease associated with alterations in muscle mass and diet, resulting in overestimation of measured GFR and underestimation of severity of CKD. Recently, cystatin C, a filtration marker that is less related to muscle mass than creatinine, is found to have a particular advantage in the estimation of GFR in the elderly population (123). In a study involving 11,909 patients, risk of death, CV events, and kidney failure were compared in patients with GFR less than 60 mL/min/1.73 m² (CKD) to those with GFR greater than 60 mL/min/1.73 m² estimated by creatinine and cystatin C measurements. The survey showed that cystatin

C–based estimates were better predictors of adverse outcomes among adults with CKD, suggesting that cystatin C may be useful in identifying patients with CKD who have higher risks of complications (124).

Tubular Function

Renal Concentrating and Diluting Ability

The Baltimore longitudinal study of aging evaluated urine concentrating ability in healthy people aged between 20 and 79 years by assessing maximum urine osmolality, minimal urine flow rate over a period of 12 hours, and ability to concentrate solutes (or reabsorb sodium and urea). Compared to younger age groups, individuals aged 60 to 79 years had approximately 20% reduction in maximal urine osmolality, a 100% increase in minimal urine flow rate, and a 50% decrease in the ability to conserve solutes (125). These changes could not be explained by the reduction in GFR. No significant differences in ADH levels have been observed between the elderly and the younger cohorts suggesting that the defect is likely due to ADH resistance as opposed to ADH deficiency (126). A decrease in the abundance of aquaporin and urea transporter proteins, as observed with aging in the kidneys of animals, likely accounts for the reduced urinary concentrating capacity in the elderly. Experimental studies suggest that the abundance of aquaporins 2 and 3 is reduced by 80% and 50%, respectively, in the aged rats' renal medullary collecting ducts (127,128). Besides the decrease in aquaporin 2, there is impairment of its phosphorylation, which may interfere with trafficking and insertion of aquaporin 2 in the apical membrane of the collecting duct. Together, these defects diminish the urine-concentrating ability by decreasing water reabsorption in the collecting ducts. In addition, aging results in decreased abundance of the major urea transporters (UT-A1 and A2) in the inner medullary collecting duct (127–129) and reduced NaCl transporter NKCC2/BSC1 in the thick ascending limb of the loop of Henle (128,130). These changes can reduce urine concentrating ability in the elderly by limiting urea and sodium reabsorption and, hence, inner medullary osmolality.

Although much less data are available on renal diluting capacity, existing studies suggest a mild impairment of renal diluting ability in the elderly due to reduced GFR. There is no evidence for impaired function of the diluting segment or altered suppressibility of vasopressin in the pathogenesis of this disorder. Reduced renal diluting capacity renders the older individuals more susceptible to the development of dilutional hyponatremia in the setting of excess water load; stress situations such as surgery, fever, acute illness; or administration of drugs such as diuretics or those that enhance vasopressin production and action. These events may act alone or in concert to impair the renal diluting ability and render the elderly patients susceptible to water intoxication.

Fluid and Electrolyte Balance

Age has no effect on basal plasma electrolyte concentrations or the ability to maintain normal extracellular fluid volume. However, structural changes in the elderly kidney have an impact on the adaptive mechanisms responsible for maintaining homeostasis of extracellular fluid volume and composition. In the elderly, the capacity to conserve sodium in response to reduced sodium intake is impaired (131). The exact mechanism is not known, but reduction in the number of functioning

nephrons with increased sodium load per each remaining nephron as well as reduced aldosterone secretion in response to sodium depletion are plausible explanations. Nevertheless, inability to conserve sodium may predispose the elderly to hemodynamic instability in the setting of sodium loss. This, along with other structural and functional changes, makes older patients more prone to develop acute kidney injury (132). In addition to impaired sodium conservation, the elderly are also prone to volume expansion when challenged with a sodium load, which is due to a diminished capacity of renal sodium excretion (133). Additionally, the elderly seem to have more sodium excretion at nighttime compared to daytime, suggesting an impaired circadian variation (134). Impaired pressure natriuresis and altered response to Ang II are apparent mechanisms involved (135). Elderly subjects also show abnormalities in renal potassium and calcium handling, which are discussed in the next section.

Endocrine and Metabolic Function

Renin-Angiotensin-Aldosterone System

The baseline plasma renin activity in the elderly is 40% to 60% lower than that in younger adults (136,137). This difference becomes even more pronounced under conditions that stimulate renin release because of the blunted renal response in the elderly (138). The lower renin levels in the elderly result in 30% to 50% reductions in plasma aldosterone levels (139). Age-related decrease in renin and aldosterone levels contributes to the development of various fluid and electrolyte abnormalities. Through action on distal tubules, aldosterone increases sodium reabsorption and facilitates potassium excretion, thereby protecting against hyperkalemia after a potassium load (136). Decrease in the production of renin-angiotensin-aldosterone and the reduced GFR impair the ability of the elderly to handle large potassium loads. Potassium levels can be seriously elevated after a potassium-loading event such as gastrointestinal bleeding, transfusion reaction, or the administration of oral or intravenous potassium. The tendency toward hyperkalemia can be further enhanced by certain inorganic metabolic acidosis or by the administration of medications that inhibit potassium excretion (such as potassium-sparing diuretics, ACEI, ARB, nonsteroidal anti-inflammatory agents, direct renin inhibitors, or beta-blockers). Given their higher susceptibility to hyperkalemia, caution should be exercised in prescribing such medications to the elderly.

While the RAS is suppressed in aging, the intrarenal RAS may be relatively intact. Ang II has several hemodynamic and nonhemodynamic effects on the kidney affecting not only filtration pressure and proximal tubular sodium and water transport but also tubular and glomerular cell growth, NO synthesis, immunomodulation, growth factor induction, production of reactive oxygen species, inflammation, cell migration, apoptosis, as well as extracellular matrix (ECM) protein accumulation that can work in concert to accelerate age-related glomerulosclerosis and tubulointerstitial fibrosis (140,141). Preferential Ang II–dependent efferent arteriolar vasoconstriction of older nephrons maintains adequate filtration pressure. However, this may also promote intraglomerular hypertension and glomerulosclerosis (142). Furthermore, Ang II activates proinflammatory and profibrotic pathways including transforming growth factor- β (TGF- β) and collagen IV transcription, monocyte-macrophage influx, mRNA and protein expression of chemokine RANTES

promoting fibrosis, and endothelial plasminogen activator inhibitor-1 (PAI-1) stimulation increasing matrix accumulation (143,144). Interestingly, physiologic intrarenal down-regulation of both renin mRNA and ACE in the elderly may be protective toward long-term sclerosis, and the processes that increase Ang II response with age can hasten kidney aging (145).

Erythropoietin

While there are many causes of anemia in the elderly, normocytic normochromic anemia may be related to reduced EPO production by the kidney (146). The InCHIANTI study showed an association between advancing age, declining renal function, reduced EPO production, and anemia. After adjusting for confounding variables, the subjects with a creatinine clearance of 30 mL/min or lower had a higher prevalence of anemia and lower plasma EPO levels compared to those with a creatinine clearance higher than 90 mL/min. Additionally, a trend toward an increase in the prevalence of anemia with decreasing renal function was observed in subjects with creatinine clearance higher than 30 mL/min (147). Serum EPO levels rise with age in healthy subjects, perhaps a compensation for aging-related subclinical blood loss, increased red blood cell turnover, or increased EPO resistance of red cell precursors (148). On the other hand, the serum EPO levels are unexpectedly lower in the elderly with anemia compared to young subjects with anemia, suggesting a blunted response to low hemoglobin (149).

Calcium, Vitamin D, and Klotho

Levels of 1,25-dihydroxy vitamin D₃ and its receptor VDR are highly expressed in the kidney and decrease with age. Evidence suggests that vitamin D₃ and its analogs suppress renin and the absence of VDR gene results in a predisposition for high renin hypertension, cardiac hypertrophy, and thrombogenicity. Recent studies also demonstrate that VDR can decrease renal fibrosis (150). Vitamin D and its analogs can also attenuate glomerulosclerosis and tubulointerstitial fibrosis mediated by proinflammatory, profibrotic, and oxidant stress via suppression of NF- κ B (151). Vitamin D deficiency in those with CKD appears to be an independent predictor of renal disease progression (152). In addition to reduced levels and impaired activation of vitamin D, elderly individuals demonstrate increased renal calcium loss due to reduced calcium reabsorption in the distal convoluted and connecting tubules (153). Distal calcium reabsorption is facilitated by the transient receptor potential ion channel, TRPV5, in the tubular apical membrane (154). TRPV5 gene expression is regulated by 1,25-dihydroxy vitamin D and PTH (155). The antiaging hormone, Klotho, has been shown to play a role in the regulation of distal calcium reabsorption by deglycosylating *N*-glycans on the surface of TRPV5 (156). Klotho deficiency is associated with a phenotype resembling aging in experimental animals (157). Thus, impaired Klotho activity in the elderly may well be responsible for reduced calcium reabsorption via TRPV5.

PATHOLOGY OF THE AGING KIDNEY

Gross Pathology

On gross examination, the kidneys from elderly subjects are symmetrically contracted with a finely granular texture of the subcapsular surface. The average kidney weight increases

from birth to about age 40 to 50 years and then progressively declines with a dramatic decrease of 20% to 30% occurring between 70 and 90 years of age. This loss of kidney mass affects the renal cortex more than the medulla leading to thinning of the renal cortical parenchyma (8,9,158). In addition to the loss of renal mass, almost 50% of the subjects over the age of 40 years have one or more acquired renal cysts (159). The cysts are usually round to oval and unilocular, contain clear yellowish fluid, and are believed to arise either from dilated tubules or glomeruli or from tubular diverticula that are found in increasing incidence with aging.

Microscopic Pathology

The Aging Glomerulus

Many morphologic changes have been noted in the human glomerulus with aging (8,9,158,160,161). The numbers of glomeruli (and therefore nephrons) in each kidney vary from 333,000 to 1,100,000 with a mean of 620,000 \pm 250,000 (25th percentile at 500,000 and 75th percentile at 740,000) (162). The average female has 15% fewer glomeruli than the average male (163). Consistent with the decrease in the kidney weight and thinning of the cortical ribbon with increasing age, the glomeruli also decrease in number and size with aging (162,163). At birth, the number of nephrons is directly and linearly proportional to the birth weight, with regression coefficient analysis predicting an increase of 257,426 glomeruli per kilogram increase of birth weight (164). In adult, there is a considerable variation (up to eightfold) in glomerular volume, which shows a strong inverse correlation with the number of glomeruli (165).

Many studies have shown that the development of focal segmental glomerulosclerosis and the percentage of glomeruli showing global glomerulosclerosis increase with age. Standard morphometric techniques and multiple linear regression analysis have shown a direct correlation between the number/percentage of globally sclerotic glomeruli and increasing age. There is also an inverse correlation between global glomerulosclerosis and intrarenal arterial lumen area (166). In this autopsy study, the glomerular size was best directly correlated with heart weight and coronary artery atherosclerosis, rather than with global glomerulosclerosis. The latter correlated directly with aortic atherosclerosis (166). In addition, the percentage of globally sclerotic glomeruli that can be considered "normal" depends on the patient's age. Thus, up to 10% of the glomeruli may be globally sclerotic in a subject younger than 40 years; beyond 40 years, the estimation of "normal" sclerotic glomeruli is difficult as the effects of diseases such as diabetes and hypertension confound such estimation (167). It has been suggested that the renal pathologist should consider "pathologic" glomerulosclerosis when the number of globally sclerotic glomeruli exceeds the number calculated by the formula: (patient's age/2) - 10 (168).

The globally sclerotic glomeruli may be underestimated on hematoxylin and eosin (H&E)-stained sections. Special histochemical stains, such as periodic acid-Schiff (PAS), silver methenamine, and Masson trichrome, are helpful in recognizing shrunken globally sclerotic glomeruli that may merge imperceptibly with the adjacent, usually scarred, and sometimes inflamed interstitium. Some have suggested that the vascular/ischemic changes seen in the aging kidneys first cause cortical glomerulosclerosis and consequent juxtamedullary glomerular

hypertrophy, followed by juxtamedullary glomerulosclerosis. However, other authors note that the superficial cortical glomeruli are 20% larger than the juxtamedullary glomeruli in 12 adult males aged 51 to 69 years, suggesting that the loss of glomeruli in the superficial cortex might shift perfusion to adjacent functional glomeruli within the peripheral vascular supply of the superficial cortex and promote their enlargement (169). Besides segmental or global glomerulosclerosis, the aging glomeruli may show mesangial sclerosis and thickening of the GBM, which are nonspecific changes that may also be seen in many conditions including hypertension and diabetes mellitus. On the other hand, some studies do not show consistent mesangial sclerosis or GBM thickening with aging (170).

The Aging Tubules and Interstitium

Many parameters of renal function such as serum creatinine, creatinine clearance, and urine osmolality correlate with changes in the tubulointerstitium rather than with changes in the glomeruli or vessels (171,172). Morphologically, three types of tubular atrophy have been described: classic atrophy, endocrine tubules, and tubular thyroidization (Fig. 28.14) (173). Classic atrophy is the most common and consists of tubules with small lumens containing eosinophilic and PAS-positive hyaline casts. The tubular basement membrane is thick and often duplicated. The epithelium of classic atrophic

tubules is cuboidal, and the cytoplasm often contains lipofuscin pigment. Lectin histochemistry has shown that the cells of most of these tubules stain with markers that in the normal kidney bind preferentially with proximal renal tubules (173). A few of the tubules of classic atrophy demonstrate staining with distal tubular markers.

Endocrine tubules consist of cells having pale to slightly granular cytoplasm that are surrounded by thin basement membranes. Lumens are inconspicuous, and epithelial cell nuclei have a round to slightly oval appearance with finely granular chromatin and small nucleoli. Endocrine tubular cells stain primarily with distal tubular markers, but proximal tubular staining is also seen occasionally (173). The endocrine tubule is named after similar appearing tubules that develop in the two-kidney, one-clip model of hypertension in the rat (173). The clipped kidney is reduced in size and becomes the endocrine kidney. Tubules lose their proximal and distal tubular histologic features and acquire a uniform appearance consisting of cords of pale cells that do not form perceptible lumens. The tubules of this experimental model were initially thought to be the source of a pressor substance that caused the hypertension. The pressor substance was subsequently shown to be renin derived from the juxtaglomerular apparatus of glomeruli in the ischemic kidney. The name “endocrine tubule” has been retained, but the tubules do not have neurosecretory granules and are not known to have any endocrine function.

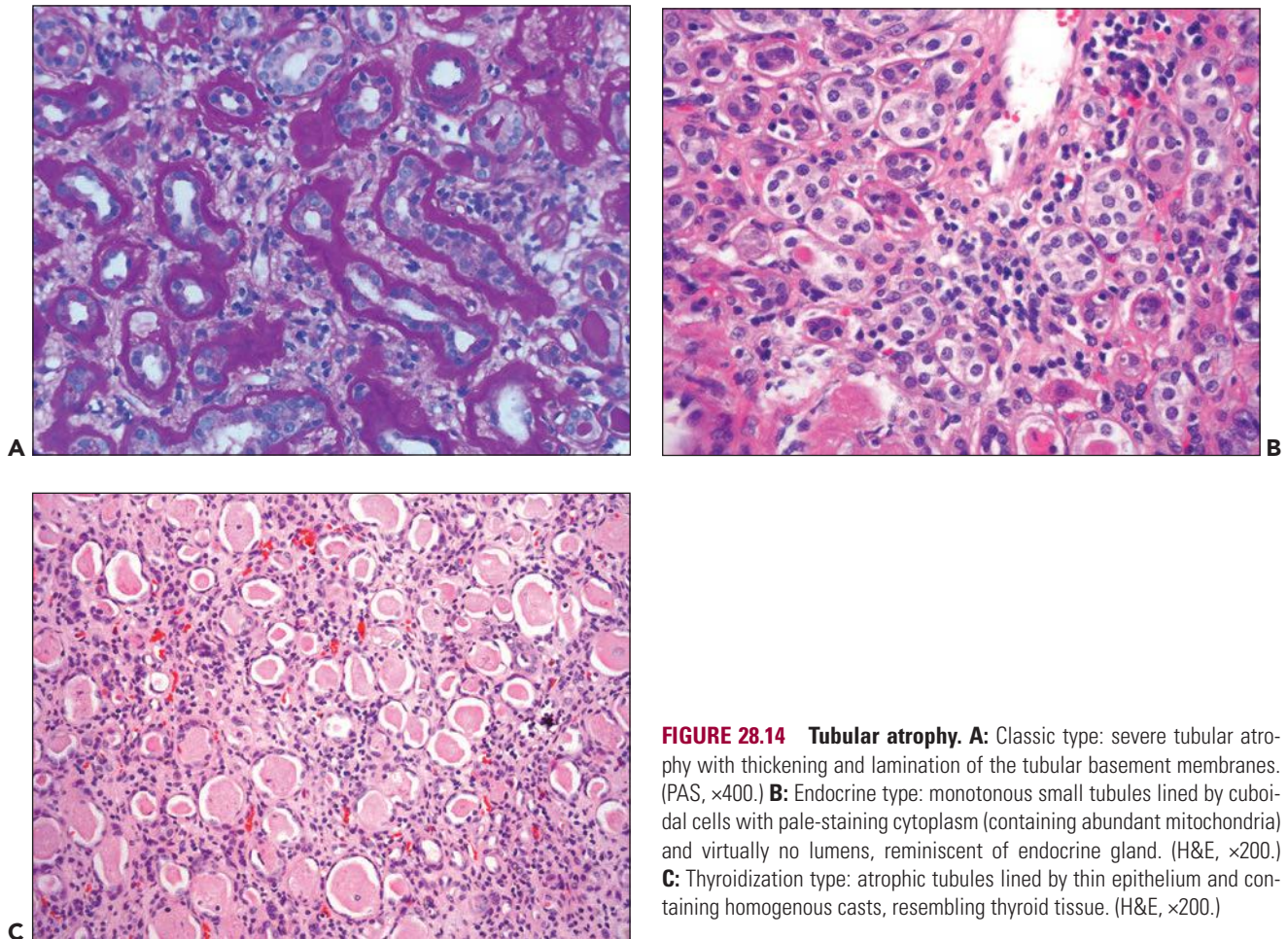


FIGURE 28.14 Tubular atrophy. **A:** Classic type: severe tubular atrophy with thickening and lamination of the tubular basement membranes. (PAS, $\times 400$.) **B:** Endocrine type: monotonous small tubules lined by cuboidal cells with pale-staining cytoplasm (containing abundant mitochondria) and virtually no lumens, reminiscent of endocrine gland. (H&E, $\times 200$.) **C:** Thyroidization type: atrophic tubules lined by thin epithelium and containing homogenous casts, resembling thyroid tissue. (H&E, $\times 200$.)

Thyroid tubules are small, round cystic structures filled with eosinophilic colloid, resembling follicles of the thyroid gland (173). Thyroid tubules are lined by a flattened simple epithelium and are surrounded by a basement membrane that is normal to slightly increased in thickness. Thyroidization is often a conspicuous feature of chronic pyelonephritis, but it is not diagnostic of this condition. It is found in the late stages of all chronic renal diseases.

The tubular atrophy in the aging kidney is accompanied by an increased degree of interstitial fibrosis and an influx of infiltrating macrophages and myofibroblasts. The fibrosis is caused, at least in part, by the deposition of collagen types I and III, mediated by the local expression of TGF- β .

The Aging Renal Vasculature

A number of changes in the renal vasculature have been documented in the aging human kidney (8,9,158,160), none of which are specific for aging. "Arteriosclerosis" or "arterial intimal fibrosis" denotes thickening of the arterial wall and narrowing of the vascular lumen produced by fibrotic intimal thickening and replication of the internal elastic lamina (Fig. 28.15). This lesion may be seen with hypertension, diabetes mellitus, and aging, and its frequency increases with increasing age (8,9,158,160,174). The intima is expanded by myofibroblasts and fibroblasts and an accumulation of the collagenous matrix coupled with concentric collagenous laminae

that are best seen with elastic stains. Intimal fibrosis/fibroplasia may be associated with thinning of the media and is found uniformly in the older kidneys with or without underlying CV disease. Intimal fibroplasia is seen primarily in arteries that are 80 to 300 μm in diameter such as the interlobular arteries. The regional heterogeneity of intimal hyperplasia may account for the heterogeneity of ischemic nephrons. While the etiology of aging-associated intimal fibroplasia is not entirely clear, it starts early in life and is accelerated by hypertension. Intimal hyperplasia in the interlobular arteries may allow the transmission of the pulse wave abnormally into the smaller distal branches leading to arteriolar hyaline changes, which may themselves accelerate the proximal intimal fibrosis. Global glomerulosclerosis appears to be associated with arterial intimal fibrosis rather than with arteriolar hyaline change (175–178).

Another common feature of the aging kidney is hyaline arteriosclerosis that refers to plasmatic insudation or accumulation of plasma proteins in the afferent arteriolar walls (vessel 10 to 30 μm in diameter), a change that is better correlated with arterial intimal fibrosis than with systemic hypertension in most studies. The hyaline material is eosinophilic, strongly PAS positive, Jones methenamine silver negative, and fuchsinophilic with trichrome stain (Fig. 28.15). It may also be seen with diabetes mellitus; in fact, it is most striking and severe in patients with uncontrolled diabetes mellitus with or without hypertension (160). The aging kidney is also associated with a high

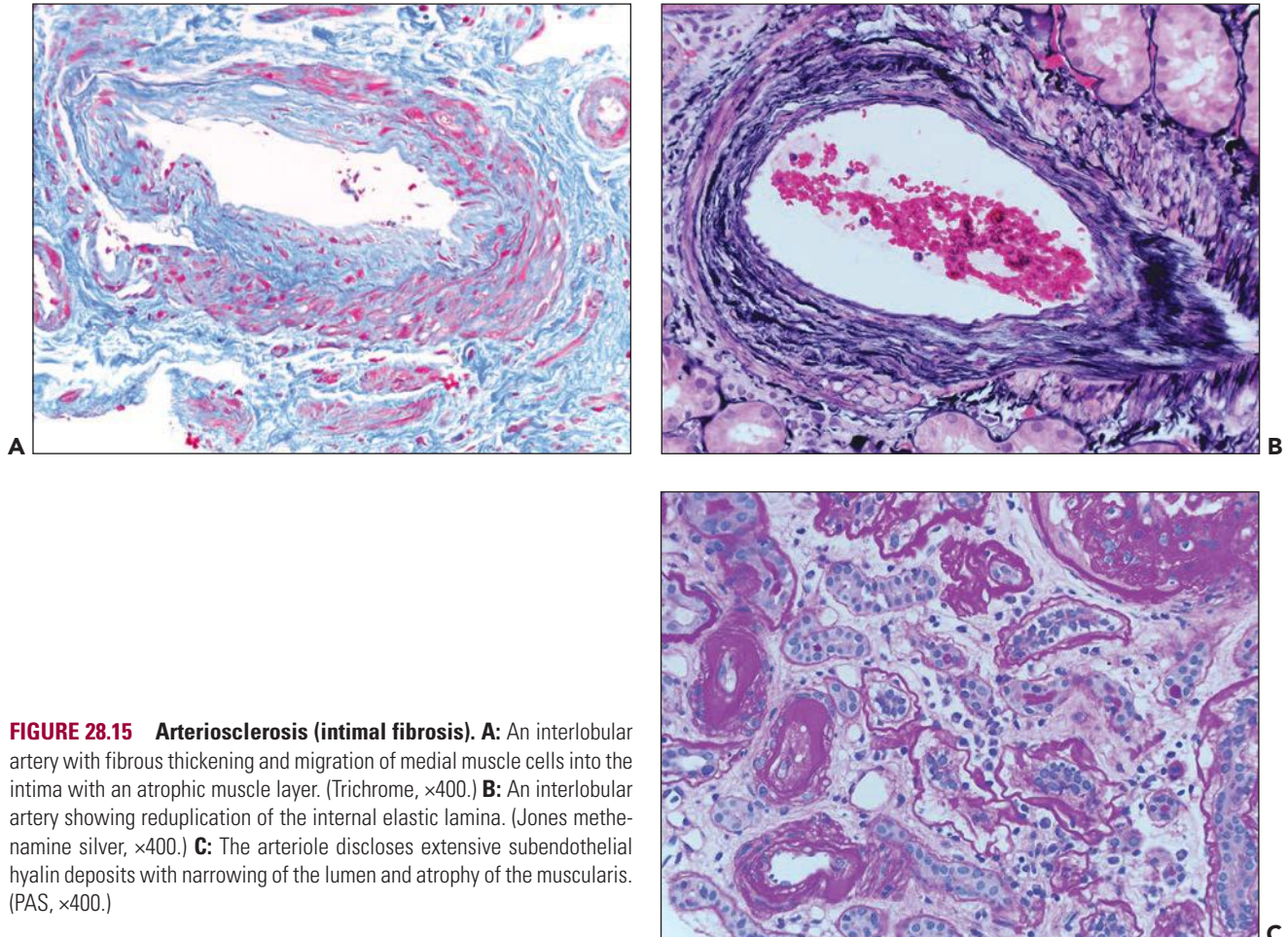


FIGURE 28.15 Arteriosclerosis (intimal fibrosis). **A:** An interlobular artery with fibrous thickening and migration of medial muscle cells into the intima with an atrophic muscle layer. (Trichrome, $\times 400$.) **B:** An interlobular artery showing reduplication of the internal elastic lamina. (Jones methenamine silver, $\times 400$.) **C:** The arteriole discloses extensive subendothelial hyalin deposits with narrowing of the lumen and atrophy of the muscularis. (PAS, $\times 400$.)

percentage of afferent and efferent arterioles that communicate directly with each other because of loss of glomeruli, particularly the juxtamedullary glomeruli (“aglomerular arterioles”) (174). A morphometric study of the aging kidneys showed dilation of the afferent arterioles, glomerular capillary lumens (especially hilar), and enlarged glomeruli that suggested a dysregulation between the afferent and efferent arterioles (179).

The aging-related vascular changes of intimal fibrosis and hyaline arteriosclerosis in interlobular arteries usually precede rather than follow systemic hypertension. As a result of such changes, microischemia in scattered nephrons ensues. Consequently, mean blood pressure rises, usually by 1.6 mm Hg for each 1- μ m increase in intimal thickness in a 100- μ m-diameter artery. This source of hypertension may account for the rise of blood pressure with age (175–178). Increase in hypertension is a strong independent risk factor for ESRD, especially in African Americans. Hypertensive and morphologic vascular changes of aging are not easily separable at this time (7–9,160,175–178).

PATHOLOGY OF THE END-STAGE KIDNEY

Gross Pathology

Unless involved by acquired renal cystic disease (ARCD), end-stage kidneys are usually reduced in size and weigh in the range of 40 to 120 g, but some are very small (50,180). The kidneys frequently contain cysts filled with clear yellow to cloudy green fluid. Some of the subcapsular cysts project through the renal capsule, and many will rupture if the capsules are stripped from the kidneys.

Hypertension, Diabetes, and Glomerulonephritis

The kidneys from patients with hypertension, diabetes, and glomerulonephritis have a granular surface that is produced by depressed areas of atrophy that alternate with the cortex having normal or hypertrophied nephrons (Fig. 28.16). End-stage diabetic kidneys are frequently larger than expected and may show no apparent reduction in size. In contrast, the kidneys of



FIGURE 28.16 Kidney from a patient with end-stage chronic glomerulonephritis. Both kidneys were markedly reduced in size (40 g each). The subcapsular surface is coarsely granular.

patients with end-stage glomerulonephritis are often severely contracted and can weigh as little as 5 g (180). In all three conditions, the kidneys have conically shaped renal pyramids and a pelvicaliceal system that is not dilated and that is lined by a normal transitional mucosa. Kidneys removed for malignant hypertension may show some hemorrhages in the subcapsular cortex and pelvic mucosa, but more often, such hemorrhages are inconspicuous or are not present in the end-stage kidney (50). Small arteries stand out prominently at the corticomedullary junction and as radially oriented cord-like structures in the lower cortex. The main renal artery of kidneys from younger patients may not be appreciably thickened, but atherosclerotic plaques are frequently noted in the proximal parts of the main renal artery in kidneys from patients with diabetes and hypertension. In patients with hypercholesterolemia, yellow atheromatous plaques may be seen in segmental and interlobar arteries.

Ischemic Nephropathy

Ischemic nephropathy is caused by renal vascular disease, frequently due to aortic or renal artery atherosclerosis. It is also seen with large vessel vasculitis (Takayasu disease and giant cell arteritis), polyarteritis nodosa, fibromuscular dysplasia, and Kawasaki disease in children (181,182). Aortic atherosclerosis, with or without an abdominal aneurysm, can produce stenosis of the renal artery ostia, and atherosclerotic narrowing of the proximal renal artery can reduce and, in some cases, completely obstruct the flow of blood to the kidneys. Atherosclerotic renal artery stenosis is often bilateral, but one kidney typically is affected more severely than the other (182,183). Ischemic nephropathy produces irregular scarring of the renal cortex (Fig. 28.17). Kidneys with accessory renal arteries show



FIGURE 28.17 Ischemic nephropathy. The patient died of a myocardial infarct after being treated for renal failure by hemodialysis for 3 months. Parts of both kidneys are contracted or scarred owing to bilateral atherosclerotic renal artery stenosis above a large abdominal aneurysm.

marked contraction of the part of the kidney supplied by a narrowed or occluded artery and preservation or relative preservation of the part supplied by a nonstenotic accessory artery. Atheromatous material mechanically disrupted by operative or invasive intravascular procedures or spontaneously dislodged from the surface of ulcerated atheromatous plaques can embolize into the kidney (184). These emboli can be associated with deep, broad-based cortical scars that in some instances represent old infarcts and in other instances reveal areas of ischemic atrophy.

Interstitial Nephritis

Tubulointerstitial nephritis consists of a long list of disorders, and this section will consider the pathology of those diseases that cause a substantial number of cases of ESRD. Chronic pyelonephritis is the late result of bacterial infections that have reached the kidney from the lower urinary tract (185). As a cause of ESRD, chronic obstructive pyelonephritis is most common in older males with benign hyperplasia or carcinoma of the prostate. It is seen with bladder stones, and in women, it is a frequent complication of uterine malignancy. The kidneys of chronic obstructive pyelonephritis show dilation of the ureter, renal pelvis, and caliceal system (Fig. 28.18). The collecting system is lined by a transitional mucosa thickened by chronic inflammation and fibrosis (185). Renal pyramids entering the dilated calices are blunted, and the overlying renal cortex is contracted into broad-based scars owing to chronic tubulointerstitial inflammation.

Nephrolithiasis is responsible for 0.2% of ESRD patients in the United States. Patients with chronic nonobstructive pyelonephritis have vesicoureteral reflux, but they do not have obstruction to urine flow in the lower urinary tract (2). Struvite renal stones are commonly present in the chronically infected kidney, and large staghorn calculi are formed in some cases (186,187). The kidney shows dilation of one or more calices



FIGURE 28.18 End-stage chronic obstructive pyelonephritis. Ureters and the pelvicaliceal system are thickened and dilated. The renal papillae are blunted, and the renal cortex is markedly thinned.

and large, flattened scars deforming the overlying cortex. This most commonly occurs at the poles of the kidney where compound papillae drain fused renal lobes (185).

Analgesic nephropathy is occasionally seen in patients who over time consume hundreds of grams or thousands of pills of an analgesic (188,189). The condition was originally described in phenacetin abusers, but after phenacetin was removed from a large part of the world market in the 1970s, analgesic nephropathy continued to be seen with mixtures containing acetaminophen and aspirin (189,190). It can be seen with acetaminophen alone and in patients who take large amounts of nonsteroidal anti-inflammatory drugs (189–191). Cigarette smoking, excessive caffeine consumption, and chronic alcoholism have been suggested as contributing factors (189). A large cohort of US patients suggests that analgesic nephropathy accounts for about 1% of the ESRD population (192). The gross appearance of analgesic nephropathy can be similar to that of chronic nonobstructive pyelonephritis. Both are characterized by scarring and inflammation of the renal cortex and by alterations of the underlying papillae. In analgesic nephropathy, papillary necrosis is invariably present, and most of the pyramids are involved. Some are partially necrotic and show a central pale discoloration. Others are completely necrotic and may have sloughed from the kidney, leaving a cavitory defect beneath the cortex. Necrotic remnants of papillae may be found lying free within the pelvis. Necrotic papillae that remain attached to the kidney often contain gross calcifications.

Light Microscopy

The end-stage kidney is characterized by advanced glomerulosclerosis, tubular atrophy, and some degree of cystic change. There is extensive interstitial fibrosis with various degrees of inflammation. Many end-stage kidneys contain extensive oxalate crystal deposits. In some cases of chronic glomerulonephritis, there is a diffuse pattern of glomerular solidification with generalized tubular atrophy and loss in which the cortex is smooth rather than granular (Fig. 28.19). The renal arteries disclose significant intimal fibrosis.

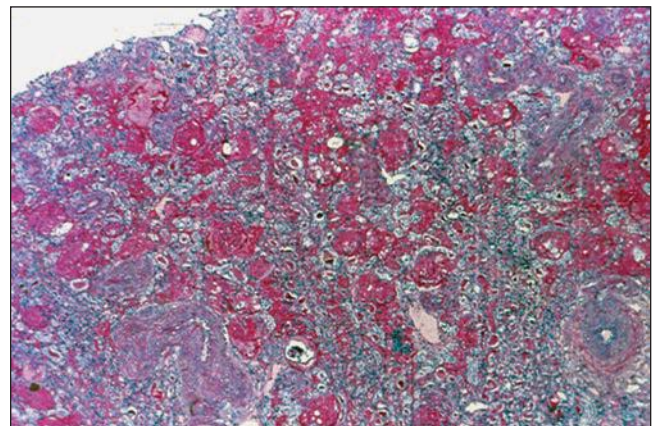


FIGURE 28.19 Low-power view of kidney with great reduction in size. There is diffuse glomerular solidification and generalized tubular atrophy. From a 22-year-old woman with end-stage glomerulonephritis who had been on dialysis for 15 months. She had been anuric for a year and had developed accelerated hypertension. (H&E, $\times 40$.)

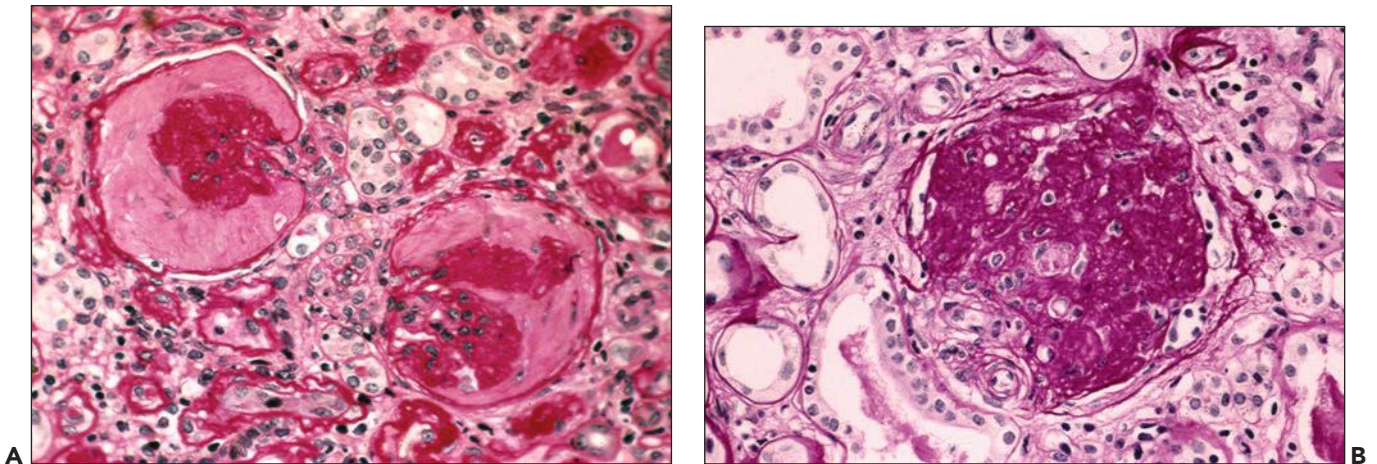


FIGURE 28.20 Global glomerulosclerosis. **A:** Late stage of ischemic glomerular obsolescence. The tufts of two glomeruli are contracted into small hyaline knots and are surrounded by lightly staining collagen that has formed inside of the Bowman capsule. (PAS-hematoxylin stain, $\times 200$.) **B:** Solidified glomerulus in a patient with focal segmental glomerulosclerosis. The glomerular tuft is expanded by an increase in the mesangial matrix that effaces the glomerular capillaries. The basement membrane of the Bowman capsule is fragmented, and the solidified tuft merges with the surrounding connective tissue. (PAS-hematoxylin stain, $\times 200$.)

Glomeruli

Chronically diseased kidneys show patterns of glomerulosclerosis that lead to the effacement of normal glomerular capillary structure. This is referred to as glomerular obsolescence, and the final structure is termed a *hyalinized* or *obsolete glomerulus*. Different patterns of glomerular obsolescence as well as pathologic changes in less severely involved glomeruli can be used to classify the renal disease that has led to ESRD.

HYPERTENSION AND ISCHEMIC GLOMERULAR OBSOLESCENCE

Hypertension and ischemic nephropathy produce a type of glomerular loss termed *ischemic glomerular obsolescence* (Fig. 28.20) (193). In its early stages, glomerular capillary basement membranes are thickened because of wrinkling. The glomerular tuft then contracts toward the hilar pole and becomes simplified into fewer capillary loops. At the same time, fibrous connective tissue builds up on the inside of the basement membrane of the Bowman capsule. This process, termed *intracapsular fibrosis*, eventually fills the Bowman space with acellular fibrous tissue having the staining characteristics of collagen. The structure of the ischemic glomerulus is best studied with the PAS stain. The intracapsular fibrosis is pale pink and is encircled by the bright magenta staining basement membrane of the Bowman capsule. The glomerular tuft also stains a deep magenta and is contracted into a small hyalinized knot at the vascular pole where it is surrounded by the intracapsular fibrosis. The basement membrane of the Bowman capsule remains relatively intact until the late stages of glomerular obsolescence when it becomes disrupted into small fragments as the glomerulus gradually disappears.

In hypertensive patients, perfusion of the renal cortex is reduced due to arteriosclerosis of the interlobular and arcuate arteries (166,194). This leads to the development of scars in the subcapsular cortex that contain clusters of glomeruli showing ischemic obsolescence. These areas of scarring may be small and identified only by the presence of a few obsolete glomeruli, or they can be larger and show increased amounts of interstitial

fibrous tissue where tubules have been lost. Atrophic, colloid-containing tubules are found in the fibrous scars, and adjacent tubules are frequently hypertrophic and dilated. Some chronic inflammation is usually present. It may be quite intense and notably conspicuous beside hyalinized glomeruli.

ISCHEMIC NEPHROPATHY

Ischemic nephropathy is caused by the reduction of RBF through the large renal arteries. Histologically, the grossly angular or broad-based cortical scars of an ischemic nephropathy show wide areas of atrophy that contain many ischemic glomeruli reflecting the larger size of the involved vessels. Evidence of cholesterol embolization may be seen (Fig. 28.21), and sometimes, cortical infarcts are found (184). Patients with ischemic nephropathy frequently have secondary renovascular hypertension, or they may have coexisting essential hypertension (182), which, in turn, accelerates intimal thickening in the interlobular and arcuate arteries and exacerbates renal ischemia.

DIABETIC GLOMERULOSCLEROSIS

The glomeruli not in an advanced state of obsolescence show diffuse thickening of glomerular capillary basement membranes, increased mesangial matrix, and an expansion of the mesangial matrix into mesangial (Kimmelstiel-Wilson) nodules (Fig. 28.22). As these diabetic changes progress, they solidify glomeruli into large hyalinized structures about the size of a normal glomerulus (193). With a PAS stain or with the Jones methenamine silver method, Kimmelstiel-Wilson nodules and hyalinosis lesions can be observed in glomeruli in late stages of obsolescence. In addition to large solidified glomeruli, a variable number of hyalinized glomeruli are noted that are contracted and show ischemic changes. Arterio- and arteriosclerosis are severe in the late-stage diabetic kidney. Both afferent and efferent arteriolar hyalinization can be seen. In diabetes, the renal tubules show basement membrane thickening. The degree of tubular loss and atrophy usually corresponds to the severity of the glomerulosclerosis.

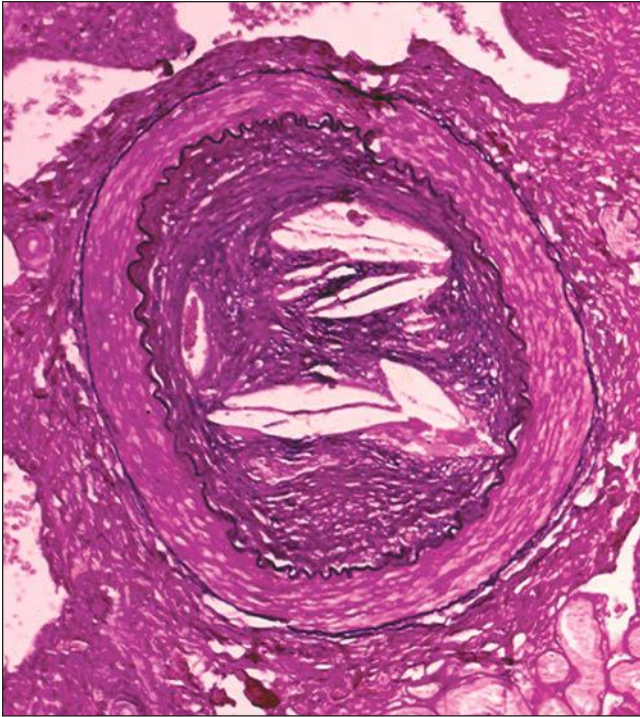


FIGURE 28.21 Atheroembolus. Kidney from a patient with renal failure owing to ischemic nephropathy showing an arcuate artery occluded by cholesterol emboli and intimal fibrous tissue. (Aldehyde fuchsin-van Gieson, $\times 100$.)

GLOMERULONEPHRITIS

Unlike ischemic obsolescence, glomerulonephritis results in a pattern of obsolescence that solidifies glomerular tufts in a manner that results in little reduction in their size (52,193). During the development of the solidified glomerulosclerosis,

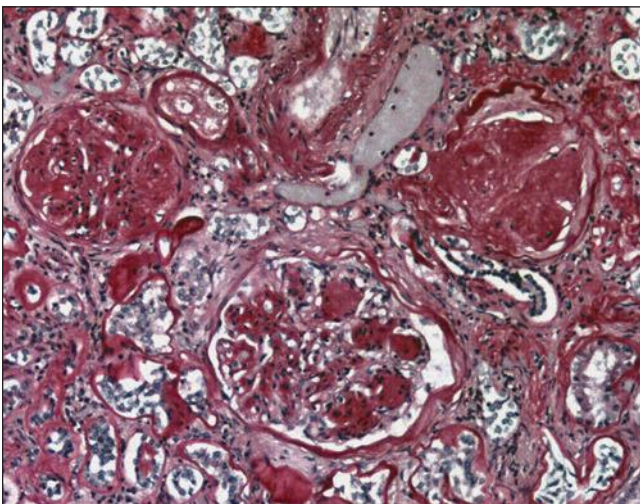


FIGURE 28.22 Glomerular obsolescence in an end-stage diabetic nephropathy. Solidified glomeruli lie beside a less severely involved glomerulus showing basement membrane thickening, expansion of the mesangium, and Kimmelstiel-Wilson nodules. (PAS, $\times 150$.)

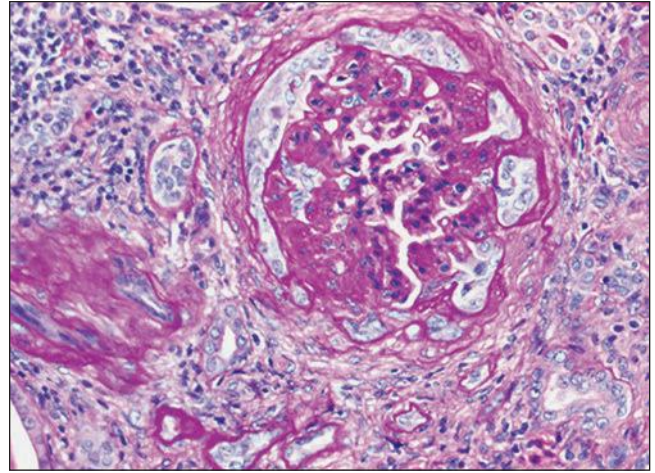


FIGURE 28.23 Sclerotic, partially solidified glomerulus from a case of end-stage glomerulonephritis. Tubule-like structures lined by epithelial cells are present over the sclerotic tuft and separated by adhesions to the Bowman capsule. (Alcian blue-PAS, $\times 200$.)

the basement membrane of the Bowman capsule is fragmented and partially lost, and the sclerotic glomerulus becomes surrounded by small tubular structures termed *pseudotubules* or *adenomatoid lesions* (also known as tubularization of the Bowman space) (Fig. 28.23). Cases of membranous glomerulopathy sometimes retain glomeruli showing diffuse basement membrane thickening within an open Bowman space, while the tubulointerstitial compartment is severely atrophic. Silver stains may reveal spikes or holes in the glomerular basement membranes. Membranoproliferative glomerulonephritis often shows a prominent lobular pattern into late stages of obsolescence. Immunofluorescence and electron microscopy are helpful in making a definitive diagnosis. For example, IgA nephropathy shows predominant or codominant staining for IgA by immunofluorescent microscopy and prominent mesangial electron-dense deposits on electron microscopy. Idiopathic focal segmental glomerulosclerosis displays many hyalinosis lesions and lack of electron microscopic and immunofluorescent findings. However, hyalinosis lesions may be seen in most forms of glomerular disease and show immunofluorescence staining with IgM and C3. The diagnostic immunofluorescence and electron microscopic features of a specific type of glomerular disease are found in the parts of glomeruli still retaining patent capillary loops away from the hyalinosis lesions.

PYELONEPHRITIS

In chronic pyelonephritis, prominent periglomerular fibrosis is frequently seen. The Bowman space is open, and the glomerular tuft and parietal epithelium are not notably changed, but the basement membrane of the Bowman capsule is thickened and surrounded by loose layers of connective tissue in a lamellar arrangement. Arteriosclerosis of large and small renal arteries is invariably present in long-standing chronic pyelonephritis, and a considerable amount of glomerular loss is the result of ischemic glomerular obsolescence. Focal and segmental glomerulosclerosis with hyalinosis can be seen, particularly if the patient has significant proteinuria. Cases of end-stage chronic pyelonephritis

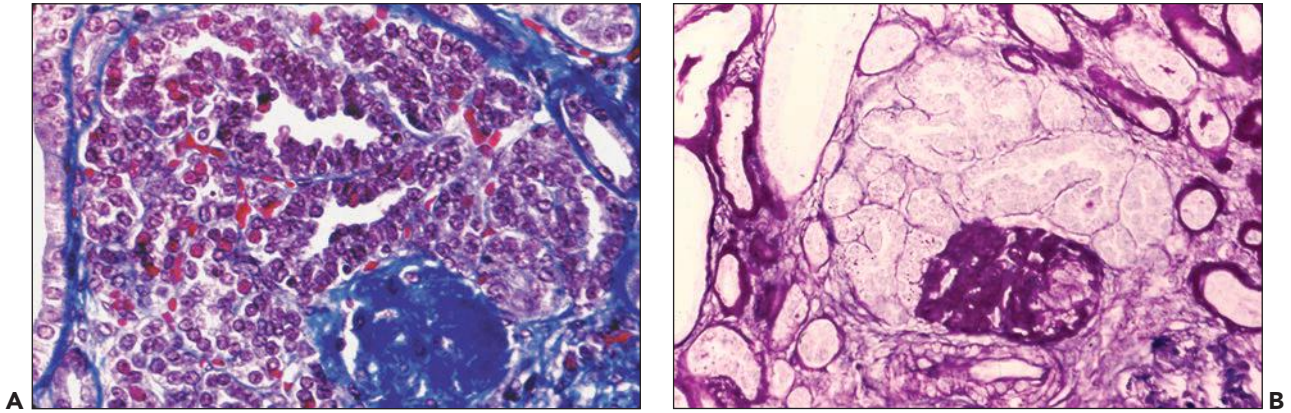


FIGURE 28.24 Embryonal hyperplasia of Bowman capsular epithelium. **A:** EHBCE forms delicate tubulopapillary structures beside a hyalinized glomerulus. (Luxol fast blue-hematoxylin, $\times 200$.) **B:** The hyalinized remnant of the glomerulus is emphasized in this micrograph, which shows the EHBCE surrounding an obsolete glomerular tuft. (PAS, $\times 200$.)

as well as other diseases complicated by malignant hypertension can show fibrinoid necrosis of glomeruli, and some of the affected glomeruli develop cellular crescents.

EMBRYONAL HYPERPLASIA OF THE BOWMAN CAPSULAR EPITHELIUM

As many as one third of end-stage kidneys reveal a proliferation of small dark embryonal-appearing cells that surround obsolete glomeruli (195) (Fig. 28.24). These cellular proliferations have been termed *embryonal hyperplasia of the Bowman's capsular epithelium* (EHBCE). In early stages, the cells line pseudotubular structures, but larger lesions form cell clusters that can be more than twice the size of a normal glomerulus (195). Serial histologic sections may be needed to demonstrate the association of EHBCE with a remnant of a glomerulus. De Silva et al. (196) reported EHBCE in the bilateral nephrectomies of a 9-year-old male with end-stage FSGS. A 1-cm tumor was present in one kidney that resembled a metanephric adenoma. The authors observed that EHBCE morphologically, immunohistochemically, and ultrastructurally resembled the metanephric adenoma and proposed that both originated from the

same cell type. Interstitial epithelial proliferations composed of small dark cells indistinguishable from those of EHBCE are found in tubules that seem to have no association with obsolete glomeruli. Ogata (197) identified these interstitial lesions in one third of pediatric end-stage kidneys.

Unusual Epithelial Growth or Endothelial Metaplasia

McManus et al. (198,199) studied serial sections of end-stage kidneys and found unusual patterns of cell growth. They described a complex lesion that resembled EHBCE, which grew within a tubule lumen creating branching nests of cells with multiple outpouchings and blind ends. The same kidney contained a tubule that grew along and then into a large myelinated renal nerve at the renal hilum and formed nests of loosely cohesive and mitotically active cells (Fig. 28.25). Another kidney demonstrated metaplastic squamous epithelium in tubules adjacent to an infarct (199). By itself, this would not be an unexpected response in the urinary tract since it commonly occurs in the prostate gland. But more remarkable was the presence of cells resembling cuboidal tubular

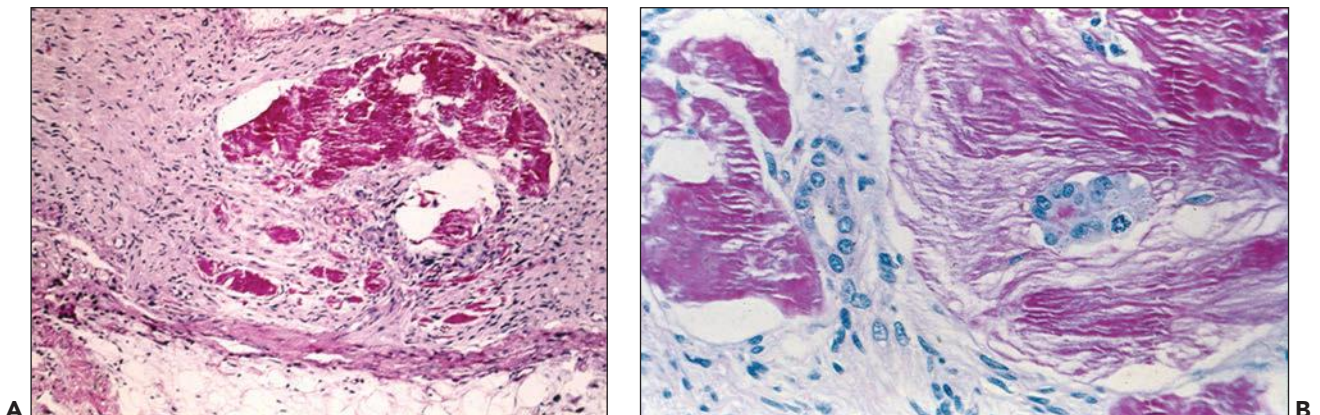


FIGURE 28.25 Nerve containing epithelial inclusions within an extracellular PAS-positive material. **A:** The section was taken from the hilum of an end-stage kidney of a patient on hemodialysis for more than 2 years. (PAS-hematoxylin, $\times 100$.) **B:** High magnification of the nerve showing a gland-like inclusion with a mitotic figure within the PAS-positive mucinous material. (PAS-hematoxylin, $\times 400$.)

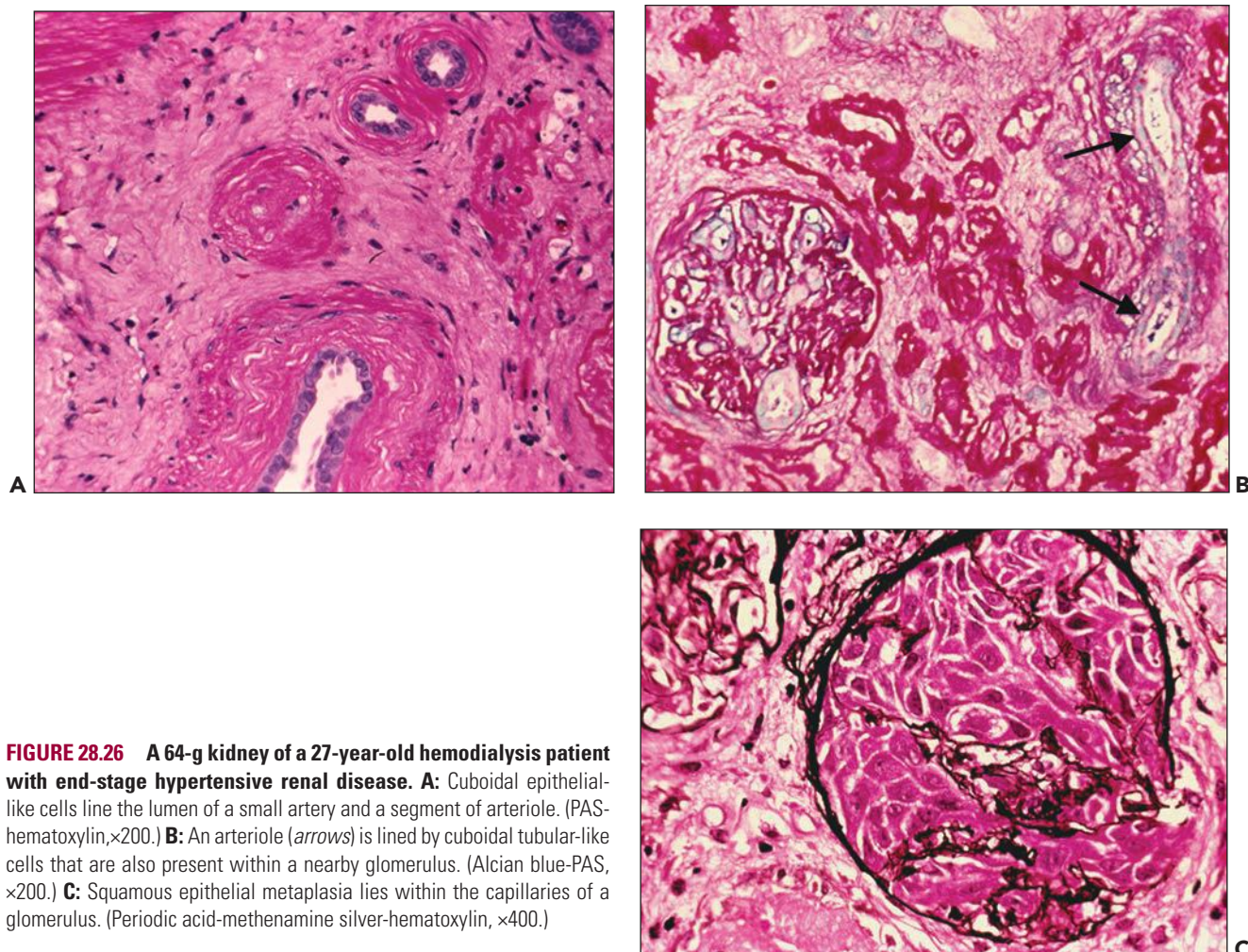


FIGURE 28.26 A 64-g kidney of a 27-year-old hemodialysis patient with end-stage hypertensive renal disease. **A:** Cuboidal epithelial-like cells line the lumen of a small artery and a segment of arteriole. (PAS-hematoxylin, $\times 200$.) **B:** An arteriole (arrows) is lined by cuboidal tubular-like cells that are also present within a nearby glomerulus. (Alcian blue-PAS, $\times 200$.) **C:** Squamous epithelial metaplasia lies within the capillaries of a glomerulus. (Periodic acid-methenamine silver-hematoxylin, $\times 400$.)

epithelium that lined the lumen of an artery (Fig. 28.26). From the artery, the epithelial-like cells extended into the more peripheral arterioles and then into the lumens of the glomerular capillaries. In some glomeruli, the intracapillary cells assumed features of squamous epithelium with distinct intercellular bridges.

Juxtaglomerular Apparatus

End-stage kidneys removed from patients with malignant hypertension and high plasma renin levels show hyperplasia of granular cells in the juxtaglomerular apparatus of obsolete glomeruli (200) (Fig. 28.27). Granules can also be seen in hypertrophied smooth muscle cells along most of the length of afferent arterioles where the modification of cells is termed *granular cell metaplasia*. Faraggiana et al. (201) studied the immunohistochemical staining and distribution of renin in the nondiabetic end-stage kidneys of five patients who had severe hypertension that could not be readily lowered by dialysis. Also studied were three cases of end-stage diabetic glomerulosclerosis in which patients were mildly hypertensive. Intense renin immunoreactivity was found in the glomeruli and afferent arterioles of the patients with severe dialysis-resistant hypertension. In two of the cases, the degree of renal atrophy was so advanced that most of the glomeruli had disappeared. In

these cases, many arterioles showed the strong renin staining. In contrast, the kidneys of diabetic patients demonstrated only minimal renin immunoreactivity that was even less than the staining in normal control kidneys (201). This anatomic finding correlates with the clinical observation that diabetics rarely develop high plasma renin activity and malignant hypertension (202).

Blood Vessels

The intrarenal arteries of end-stage kidneys develop *obliterative intimal fibrosis* because of the concentric thickening of the arterial intima by collagenous connective tissue containing moderate numbers of spindle cells. Obliterative intimal fibrosis is considered to be an adaptive change to increased vascular resistance resulting from the loss of the peripheral microvascular bed. The spindle cells are identified as myointimal cells by their positive immunohistochemical staining for smooth muscle actin. Electron microscopy of the intimal cells demonstrates thin cytoplasmic filaments and cytoplasmic membrane-dense bodies characteristic of smooth muscle.

The intrarenal arteries of the kidneys removed for severe hypertension show a pronounced intimal thickening composed of mucoid ground substance and many myointimal cells (200,203) (Fig. 28.28). If there has not been a history of chronic

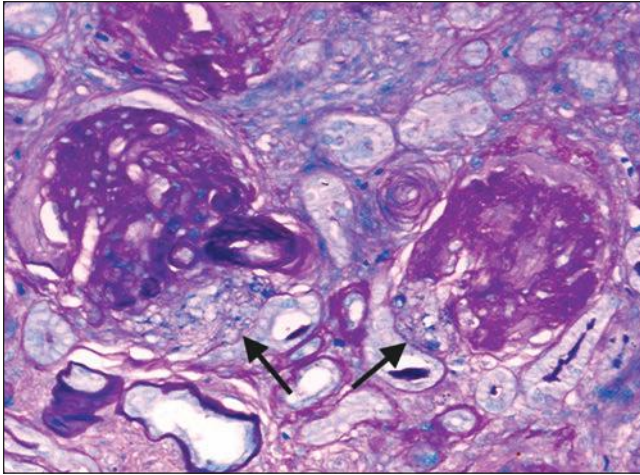


FIGURE 28.27 Prominent granular cells (arrows) are seen in the hyperplastic juxtaglomerular apparatus of two obsolete glomeruli. The specimen was from a bilateral nephrectomy performed to treat pharmacologically intractable malignant hypertension. The patient had been treated by hemodialysis for 6 weeks and had very high plasma renin levels. (Luxol fast blue-PAS, $\times 200$.)

hypertension, the internal elastic lamina may show minimal, if any, duplication. Mucoïd ground substance focally involves the media, and in such areas, medial smooth muscle cells can be found crossing the internal elastic lamina where they appear to be migrating into the intima. Intimal smooth muscle frequently is oriented tightly around the narrowed arterial lumen in the fashion of a new internalized media (204) (Fig. 28.29). This type of vascular change was termed *musculomucoïd intimal hyperplasia* (203). The histopathology resembles or is identical to the arterial pathology of malignant hypertension and scleroderma renal crisis. The arteries most severely affected in scleroderma and malignant hypertension, however, measure less than 200 μm in diameter (distal arcuate and interlobular

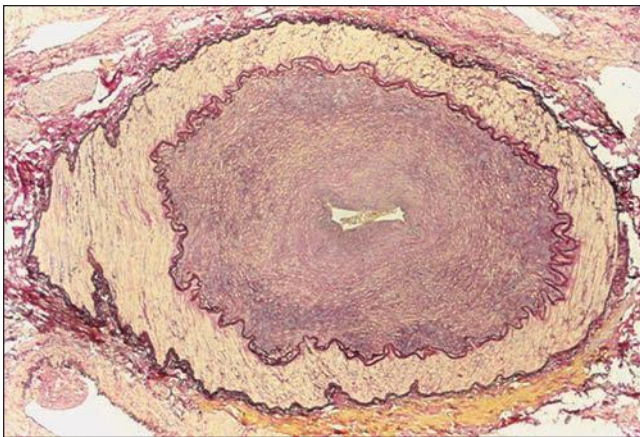


FIGURE 28.28 Musculomucoïd intimal hyperplasia of an interlobular artery. The intima is markedly thickened by dark-staining mucoïd ground substance. There is minimal reduplication of the internal elastic lamina. (Aldehyde fuchsin-Weigert hematoxylin-van Gieson, $\times 100$.)

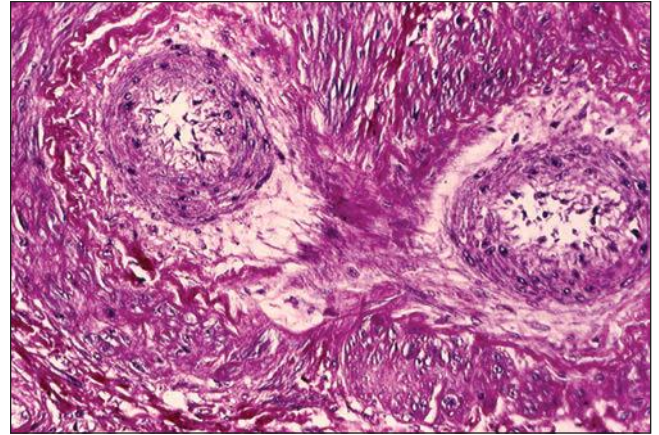


FIGURE 28.29 Remodeling or remedialization of an interlobular artery in a hemodialysis patient. Smooth muscle is rearranged within the intima to form a collar of cells resembling a second media around the lumen. (H&E, $\times 400$.)

arteries), whereas musculomucoïd intimal hyperplasia in dialysis kidneys involves intrarenal arteries of all sizes (51). In musculomucoïd intimal hyperplasia with arterial necrosis, the interlobular arteries show an insudate of fibrin and red cells that dissects along the mucoïd intima and focally extends into the media (200,204). Fibrinoid necrosis is found in afferent arterioles, and in some arterioles, the cells of the vessel wall proliferate to form arteriolar nodules (Fig. 28.30). Many are solid smooth muscle nodules and resemble small leiomyomas. Others are vascular and resemble the plexiform lesions of the lung that are found in the small pulmonary arteries of patients with high-grade pulmonary hypertension. Arteriolar nodules are also seen in organs other than the kidney (pancreas, adrenal capsule, heart, paravertebral ganglia) of patients with treated malignant hypertension (205) (Fig. 28.31).

Obliterative intimal fibrosis and musculomucoïd intimal hyperplasia probably represent a continuum of arterial pathology rather than different types of vascular disease. Musculomucoïd intimal hyperplasia is likely to change into the picture of obliterative intimal fibrosis when myointimal cells begin to synthesize increased amounts of collagen and the intimal mucopolysaccharide content is reduced. The veins of end-stage kidneys are thickened by bundles of smooth muscle and fibrous tissue (204). The bundles of smooth muscle are frequently oriented parallel to the long axis of the vein in a configuration that has been termed *nodular phlebosclerosis*. The walls of the thickened veins sometimes enclose tubules lined by cuboidal clear cells (Fig. 28.32). The tubules seem to be entrapped atrophic tubules, although the epithelium sometimes demonstrates mitoses (204).

Tubules and Interstitium

Injury to the tubules and interstitium can be primary when the disease is directed toward the tubulointerstitium or secondary when the initiating pathology principally involves glomeruli and blood vessels. In either case, the kidneys of ESRD patients show marked interstitial fibrosis, tubular atrophy, and some amount of chronic interstitial inflammation.

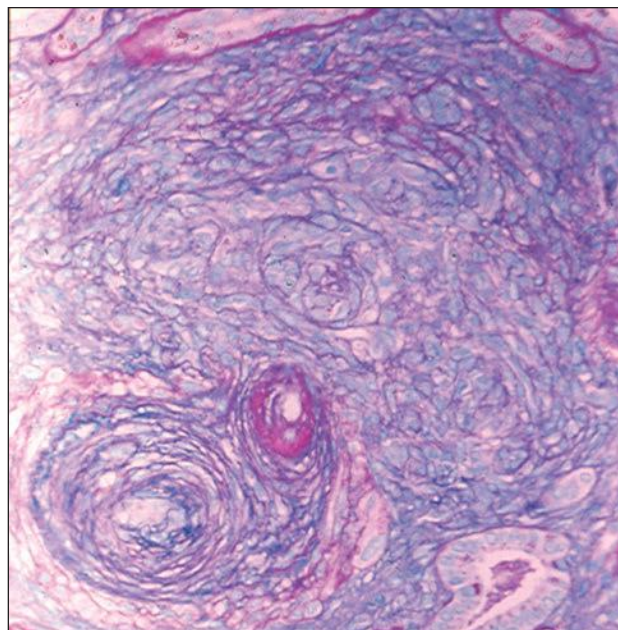
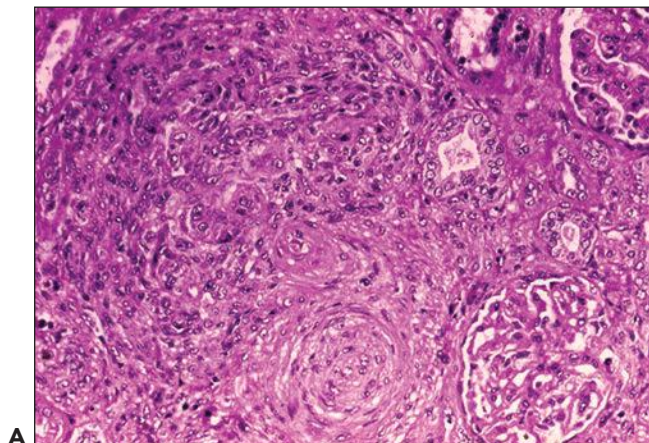


FIGURE 28.30 The kidney of a hemodialysis patient with malignant hypertension. **A:** A cellular arteriolar nodule originates in an arteriole at the bottom of the micrograph. (H&E, $\times 200$.) **B:** The origin of another nodule is demonstrated in an arteriole showing fibrinoid necrosis. (Alcian blue-PAS, $\times 200$.)

INTERSTITIAL NEPHRITIS AND DIFFERENTIAL DIAGNOSIS

Chronic pyelonephritis shows inflammation of the renal parenchyma that consists mainly of lymphocytes, macrophages, and plasma cells (185). The characteristic feature is a “pyelitis” consisting of lymphoplasmacytic inflammation in the mucosa of the pelvis and calices and blunting of the associated renal papillae (185). The lymphoid infiltrate is frequently arranged in follicles with prominent germinal centers. Some eosinophils are present, and in some cases, neutrophils may be numerous. The inflammation is primarily interstitial, but neutrophil infiltrates and casts may be found in the tubules.

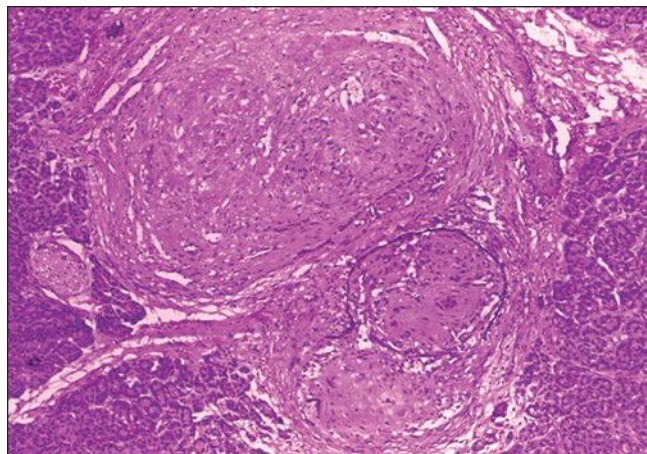


FIGURE 28.31 Arteriolar nodule. Arteriolar nodule in the pancreas of a hemodialysis patient with poorly controlled malignant hypertension. (Aldehyde fuchsin-hematoxylin, $\times 100$.)

Areas of chronic inflammation are seen that contain atrophic tubules having a thyroid-like appearance. Tamm-Horsfall protein extravasates from tubules into the interstitium and elicits an inflammatory reaction consisting of mononuclear cells and eosinophils. The protein can be identified as an amorphous to fibrillar eosinophilic material that stains brightly with the PAS stain. If there is no pelvicaliceal inflammation, other forms of interstitial nephritis should be considered, including antibody and cell-mediated immune diseases. If a large number of eosinophils or granulomas are present, the differential diagnosis should include a drug-induced hypersensitivity disease. Sarcoidosis and tuberculosis need to be ruled out when the inflammation is granulomatous. It should be noted that the inflammatory changes are not specific for chronic pyelonephritis. However, chronic inflammation usually is not striking in hypertension or diabetes unless there is coexisting pyelonephritis, but collections of small lymphocytes can be prominent in ischemic nephropathy. Chronic inflammation with many plasma cells is frequently pronounced in the renal cortex of glomerulonephritis. In both glomerulonephritis and ischemic nephropathy, the intensity of the inflammation can lead to a mistaken diagnosis of chronic pyelonephritis.

Papillary necrosis is often present in cases of analgesic nephropathy (190). Histologically, the necrotic papillae show ghost-like remnants of collecting tubules and a deeply eosinophilic staining interstitium. In long-standing cases, the necrotic papillae are frequently calcified, and heterotopic bone formation may be present. In analgesic nephropathy, there is little or no inflammation adjacent to the necrotic papillae, and in most cases, there is a pronounced thickening of the capillary walls in the submucosa of the renal pelvis and ureter. The thickened capillary wall consists of concentric lamellae of basement membrane material that stain brightly with the PAS

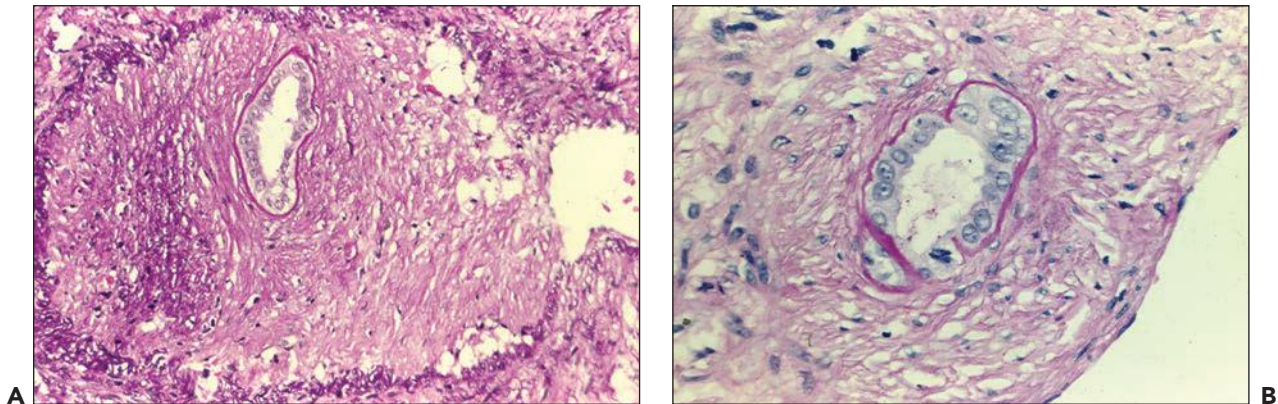


FIGURE 28.32 Thickened vein wall in an end-stage kidney of a chronic hemodialysis patient. A: A tubule is enclosed within the thickened vein whose original wall is outlined by elastic tissue. (Aldehyde fuchsin-hematoxylin, $\times 200$.) **B:** A mitotic figure is seen in the tubule in further sections of the vein shown in A. (H&E, $\times 200$.)

method (see Chapter 25). Renal papillary necrosis is also found in acute pyelonephritis and is particularly common in diabetics. In these kidneys, there is a band of intense acute inflammation in the upper papillae between the viable and necrotic tissue. These kidneys also show interstitial and intratubular collections of neutrophils as additional evidence of acute pyelonephritis. Acute interstitial nephritis is not a feature of analgesic nephropathy unless there is a superimposed infection.

Malacoplakia and xanthogranulomatous pyelonephritis are forms of chronic pyelonephritis that present special histologic features (206,207). In xanthogranulomatous pyelonephritis, sheets of large foamy histiocytes efface the renal parenchyma. This often has a tumorous appearance that can be confused with clear cell carcinoma of the kidney. In malacoplakia, histiocytes with somewhat granular basophilic cytoplasm are found in the renal interstitium. The histiocytes contain PAS-positive Michaelis-Gutmann bodies that are calcospherites and stain with the von Kossa technique for calcium.

TUBULAR ATROPHY

Tubular atrophy is classified into three types (classic atrophy, endocrine tubules, and tubular thyroidization), which have been described earlier. In addition to atrophic tubules, the end-stage kidney contains tubules that are hypertrophied and dilated (173). These are mainly proximal tubules, and they display proximal tubular staining with lectin stains and by immunohistochemistry (173). These tubules are lined by columnar eosinophilic cells sometimes containing hyaline protein resorption droplets (173,174). The droplets frequently collect at the apex of cells and are shed into the tubular lumens in a manner similar to apocrine secretory activity. The nuclei contain prominent nucleoli, and the chromatin is margined along the nuclear membranes.

OXALOSIS

Oxalate crystals can be seen in most end-stage kidneys and, in some kidneys, the crystal deposits can be quite extensive. Oxalate deposits are found within tubule lumens, embedded within interstitial connective tissue, or intermixed with the epithelium of cysts and tubules. The crystals are birefringent with polarized light in routinely processed histologic sections

and can be stained histochemically with Alcian blue. Oxalate is normally excreted by the kidneys, and plasma oxalate levels become elevated with uremia. The severity of the oxalate deposition has been related to the duration of chronic renal failure (50). Oxalate may be seen in disorders such as primary hyperoxaluria and ethylene glycol intoxication (acute and chronic), and ESRD can be a complication of these conditions.

MISCELLANEOUS INTERSTITIAL CHANGES

In some cases with well-advanced atrophy, aldehyde fuchsin, orcein, and Verhoeff-van Gieson stains show areas of interstitial fibrosis having the staining properties of elastic tissue. By means of aldehyde fuchsin and Giemsa stains, large numbers of mast cells are frequently seen within interstitial inflammatory infiltrates (200). Occasional end-stage kidneys contain focal collections of interstitial myxoid connective tissue. Metaplastic cartilage and woven bone can be seen in such foci (Fig. 28.33) (204).

The renal medullae of chronically diseased kidneys are often fibrotic. Interstitial fibrosis in which collagen fibril formation appeared to be derived from medullary interstitial

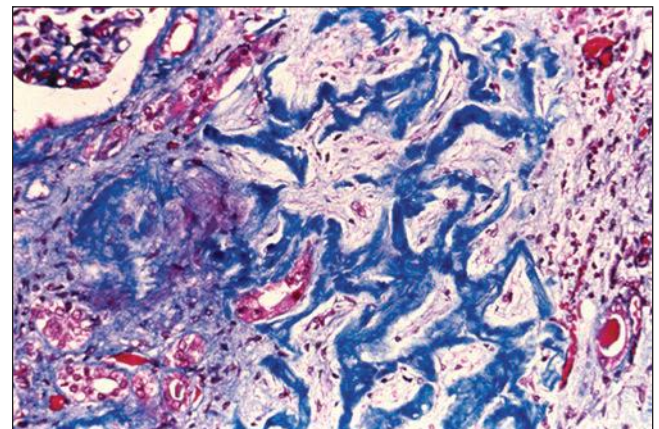


FIGURE 28.33 Osteoid forming within a focus of myxoid tissue in the interstitium of an end-stage dialysis kidney. (Masson trichrome, $\times 200$.)

cells was described in benign nephrosclerosis by Haggitt et al. (208). In this study, medullary fibrosis increased with age, blood pressure, and the degree of arterioarteriosclerosis. The loss of the normal loose ground substance and medullary interstitial cells that compose the medullary interstitium may be pathophysiologically significant, because the renal medulla plays an important role in regulating sodium and fluid homeostasis and blood pressure (209). Medullary fibrosis is seen in many end-stage kidneys, but in some kidneys, the renal medulla is occupied by spindle cells having features of smooth muscle that tend to be oriented circumferentially around collecting ducts (210).

Acquired Renal Cystic Disease

Radiologic studies of HD patients have shown that during the 3 years after beginning dialysis, diseased kidneys continue to atrophy, but that at approximately 4 years, the size of the kidneys increases as ARCD begins to develop (211–213). Kidney enlargement due to ARCD reached a plateau 21 years after the start of HD in male patients (212). ARCD has been reported to occur in 20% to 90% of dialysis patients (214,215). Older age, male gender, dialysis, and greater kidney calcifications are risk factors for ARCD (212,213). Radiologically, ARCD has been defined as the presence of five or more cysts in each kidney in some studies and three or more cysts in others (216). For the pathologist, Feiner et al. (217) suggested that ARCD should be defined as the cystic change of at least 40% of the volume of the kidney. This creates some discrepancy between radiologic and pathologic diagnoses, which might account for differences in the frequency with which ARCD is reported by different observers. ARCD develops in both HD and CAPD patients. Park et al. (216) investigated the prevalence of ARCD by ultrasonography in 49 HD and 49 CAPD patients. ARCD developed in 31% of patients at an average duration of 74 months, and no difference in prevalence was seen between the methods of dialysis. Intrarenal hemorrhage has been observed in 17% of cystic end-stage kidneys (211). Hemorrhage has been associated with heparinization during HD, but it is actually seen more frequently between dialysis periods when patients are not heparinized. In these cases, platelet dysfunction secondary to uremia is suggested as the etiologic factor. In some patients, intrarenal hemorrhage ruptures into the retroperitoneum and can be life threatening (211).

The pathogenesis of acquired cystic disease (ACD) is not known. It has been proposed that following a loss of renal tissue, a renotropic growth factor is produced that promotes renal hypertrophy (214). In the end-stage kidney, the factor or factors may act on remaining tubular segments and stimulate cyst growth. Hepatocyte growth factor and its receptor *c-met* are protooncogenes involved in the regulation of epithelial cell growth (218). Konda et al. (219) have shown that both hepatocyte growth factor and *c-met* are overexpressed in the cystic epithelium of ARCD with the increased expression being predominantly in hyperplastic, multilayered cysts. Inhibition of apoptosis by the increased expression of *bcl-2* was also thought to play a role in cyst growth (219). In addition, protooncogene *c-Jun* activation may also have a role in the aberrant proliferation of hyperplastic atypical cells in ARCD and subsequent development of renal cell carcinoma (RCC) (220).

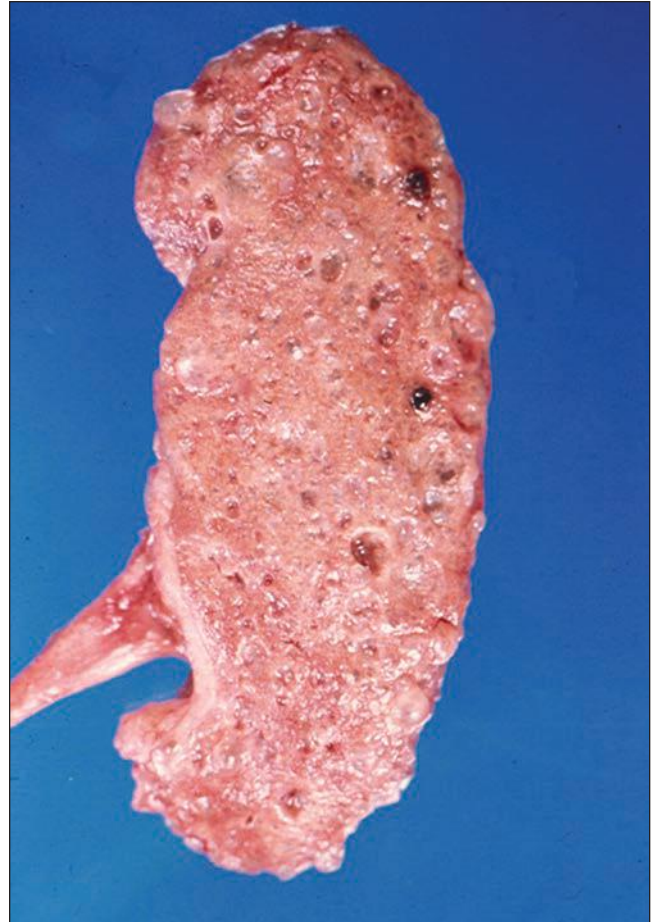


FIGURE 28.34 Acquired cystic disease in a 42-year-old man supported by hemodialysis for 4 years. This 120-g kidney contained many small cysts.

Gross Pathology

Hughson et al. (180) reviewed published case series and noted that the single kidney involved by ARCD weighs 134 g on average with a range of up to 800 g. In some cases, the cysts are small and evenly distributed, giving the kidney a spongy texture (Fig. 28.34). Cysts can be localized or involve the entire kidney. Extensive cystic transformation is not uncommonly accompanied by the development of RCC (Fig. 28.35). Cysts are located mainly in the cortex but can be found in the renal medulla. Most cysts are filled with clear to slightly cloudy straw-colored serous fluid, but the contents may have a gelatinous consistency. When there has been intrarenal hemorrhage, cysts are filled with liquid or clotted blood.

Although rare ARCD can resemble ADPKD, the size of the kidneys in the two conditions is quite different (221). In symptomatic ADPKD, the single kidney weighs from 2000 to 4000 g (222), whereas the largest kidneys reported for ARCD are just at 800 g, and the great majority are less than 300 g (180). To help discriminate between the two diseases, the anatomic findings should be correlated with the clinical history. Cases of ARCD are found in patients with chronic renal failure who have not reached the point of requiring dialysis, but most patients have been on dialysis for many months and more often



FIGURE 28.35 Acquired cystic disease in a man supported by hemodialysis for 9 years. The kidneys are enlarged by extensive cystic change and had a combined weight of 680 g. The kidney on the right has two renal cell carcinomas. A small tumor is in the lower pole. (Courtesy of Dr. M.S. Dunnill, Oxford University.)

years (223,224). A prior history of noncystic renal disease will establish a diagnosis of ARCD, and a family history of autosomal dominant disease inheritance will allow ADPKD to be diagnosed. The presence of cysts in the liver and pancreas can be helpful, but liver cysts have been described with ARCD (221).

Microscopic Pathology

Most cysts of ARCD are lined by a flat, nondescript epithelium (Fig. 28.36). Some are lined by tall proximal tubular cells containing prominent hyaline droplets that are identical to those seen in hypertrophied tubules (Fig. 28.37). Other cysts are lined by small cuboidal cells resembling distal tubular epithelium,

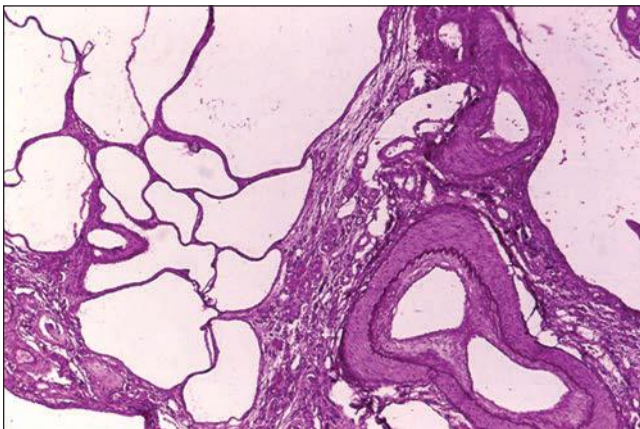


FIGURE 28.36 Micrograph from a case of acquired cystic disease. The cysts are lined by a flattened simple epithelium. (H&E, $\times 100$.)



FIGURE 28.37 Acquired cystic disease. This cyst is lined by proximal tubular cells that contain hyalin colloid droplets. The cells focally pile on one another along the cyst's wall. (H&E, $\times 200$.)

and the small cuboidal cells stain with lectins or immunohistochemical markers (*Arachis hypogaea* and epithelial membrane antigen) that bind preferentially with distal tubule in the normal kidney (225). In some cases, cystic dilation of glomeruli is widespread and contributes to the cystic appearance of the kidneys. Cysts lined by both tall columnar and small cuboidal cells often develop a papillary and multilayered hyperplasia (Fig. 28.38). These hyperplastic, multilayered cysts, or atypical cysts, are seen in approximately 30% of end-stage kidneys (226). The epithelium of atypical cysts frequently shows dysplastic cytologic features and loss of nuclear polarity. Atypical cysts are seen with increased frequency in the kidneys with renal cortical tumors and appear to be preneoplastic lesions (226).

Cysts of ARCD are derived from both proximal and distal tubules, and many cysts begin as outpouchings or sacculations of intact tubular segments (225,227). Histologically, nodules of collagen, elastic tissue fibers, and duplicated tubular basement

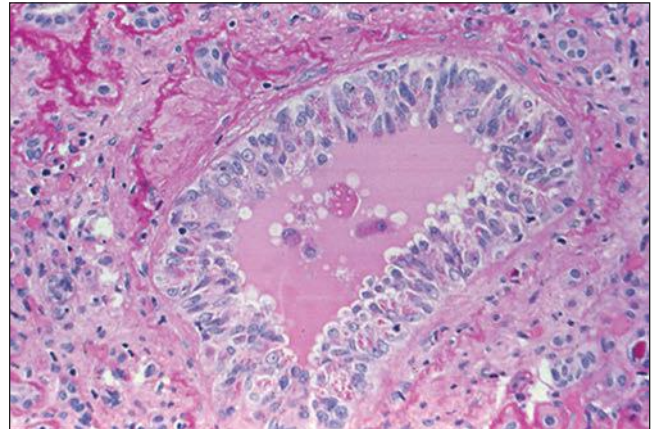


FIGURE 28.38 An atypical cyst in a dialysis kidney. The cyst is lined by hyperplastic cells showing loss of stratification. (PAS-hematoxylin, $\times 200$.)

membranes are formed at points of cyst outpouching (226). As a result of old intracystic hemorrhage, some cysts contain a large amount of hemosiderin in the epithelium and connective tissue of the cyst wall. The kidneys of ARCD invariably show the background of obsolete glomeruli, tubular atrophy, and obliterative intimal fibrosis of arteries that characterize end-stage kidneys. The renal parenchyma between the cysts of ADPKD, in contrast, remains remarkably normal, even when patients are becoming uremic. After dialysis, however, secondary atrophic changes are seen in ADPKD, and the microscopic differences between ADPKD and ARCD become obscure (228). The cysts of ADPKD, like those of ARCD, are derived from all levels of the nephron, and immunohistochemical studies do not distinguish between the two types of cystic diseases (227).

Renal Cell Tumors of Acquired Renal Cystic Disease

ESRD is associated with an increased incidence of RCC, which occurs in both cystic and noncystic kidneys, but patients with ARCD appear to develop RCC approximately 100 times more frequently than the general population (180,211,215,226,229). Schwarz et al. (213) studied the native kidneys of 561 patients who received renal transplantation and found 4.8% had RCC. The prevalence of RCC increased to 19.4% in the patients who had ARCD. In an analysis of data from the United States, Europe, Australia, and New Zealand registries, Stewart et al. (230) calculated the risk for kidney cancer among dialysis patients as standardized incidence ratios (SIR) of the background risk in those countries. The SIR of all dialysis patients was 3.6 and increased from 3.2 during the first year of dialysis to 6.8 after 10 years. The increased risk was seen in all renal diseases but was greatest for congenital diseases, toxic and analgesic nephropathies, and Balkan nephropathy, with the SIR of analgesic nephropathy being 16.7 and Balkan nephropathy 26.2. The type of kidney cancer was not specified, and the very high SIR for analgesic and Balkan nephropathy was probably owing to the increased prevalence of transitional cell carcinoma of the renal pelvis that is seen in these conditions (230).

It has been shown that approximately 40% of RCCs arising in ESRD are of the more common histologic types identical to sporadically occurring neoplasms (215,229) (Figs. 28.39

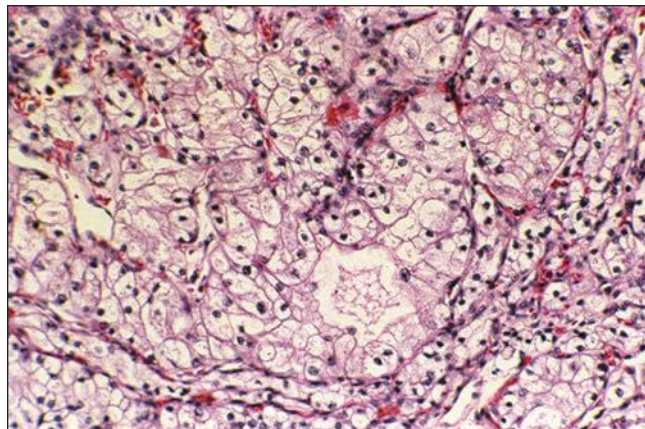


FIGURE 28.39 Clear cell renal cell carcinoma. This clear cell carcinoma developed in a dialysis kidney that was also involved by acquired cystic disease. (H&E, $\times 100$.)

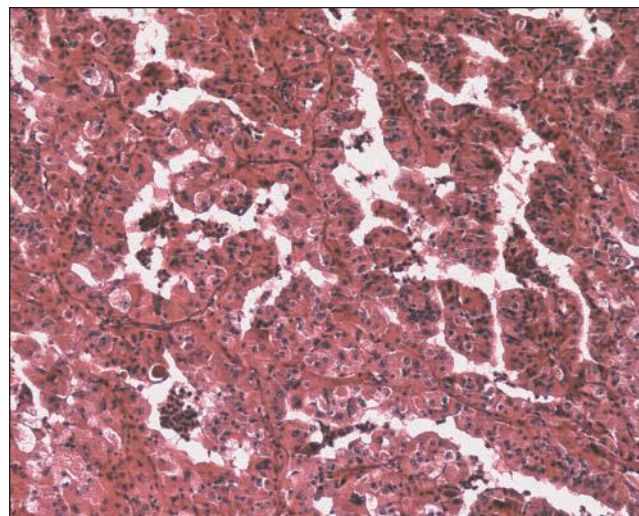


FIGURE 28.40 A papillary renal cell carcinoma that had developed in acquired cystic disease. This tumor is composed of columnar, eosinophilic cells. (H&E, $\times 100$.)

and 28.40). The remaining approximately 60% consists of two subtypes of RCC that appear quite unique to ESRD. Papillary RCCs are overrepresented in the end-stage kidney compared with clear cell carcinomas (213,215,229) ranging from 42% to 71%. However, papillary RCC represents only 10% to 15% of sporadically occurring RCC. Cases of ESRD-associated oncocytoma, oncocytomatosis, and chromophobe carcinoma have been reported (215). There are two specific forms of RCC arising in kidneys affected by ARCD (229). The first variant has been designated as “acquired cystic disease (ACD)-associated RCC,” which appears to be specific to ARCD and is not found in ESRD without cystic changes. ACD-associated RCCs are usually well circumscribed, many of which are arising from the cysts. It is characterized by a typical microcystic architecture, eosinophilic cytoplasm with Fuhrman grade 3 nuclei, and frequently associated with intratumor oxalate crystals (Fig. 28.41). The second variant, designated as “clear cell papillary RCC of the end-stage kidneys,” is much less common than ACD-associated RCC and occurs both in ARCD and noncystic ESRD. Half of these tumors may be seen arising within a cystic structure. The deposition of oxalate appears to be a feature unique to renal cancer occurring in ESRD and ARCD and perhaps pathogenetically related to carcinogenesis (Fig. 28.42) (215,229). Thus, a broad spectrum of RCC exist in ESRD, only some of which resemble the sporadic RCC. ACD-associated RCC is the most common tumor subtype in ESRD, and its biologic behavior appears to be more aggressive than the other tumor subtypes in ESRD.

Genetic analyses have been performed on several papillary RCC of ESRD (231,232). Chudek et al. (232) found trisomies of chromosomes 3, 5, 7, 8, or 16 in four of five tumors but trisomy of 17 in only one. Hughson et al. (231) identified duplications of 7 and/or 17 in 6 of 14 tumors with 8 of the 14 papillary RCC showing involvement of neither chromosome 7 nor 17. Deletions of 3p have been detected in 8 of 16 ESRD clear cell RCC. This represents the number analyzed in three separate studies of ESRD tumors (232–234).

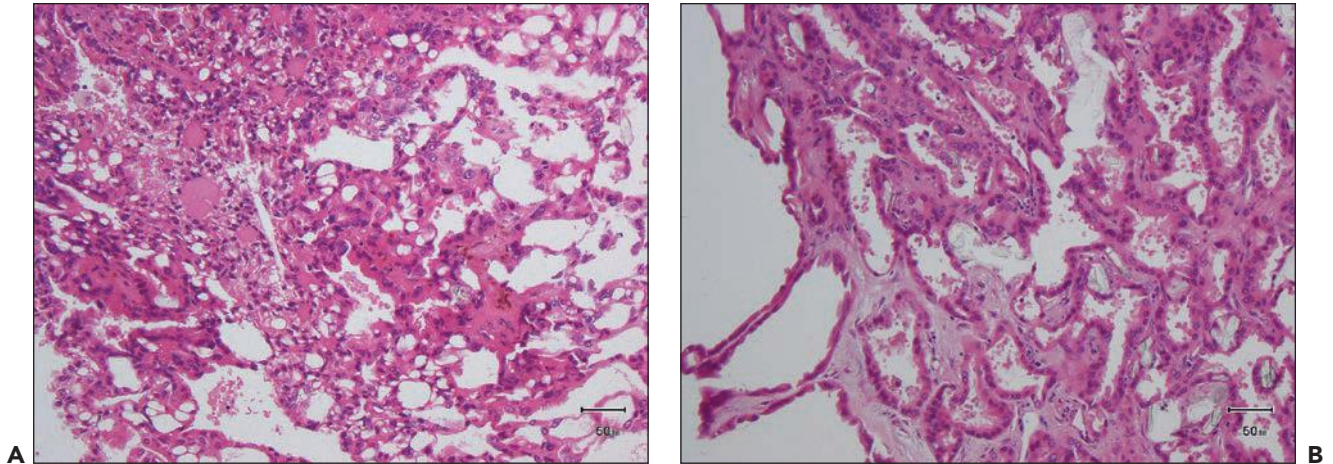


FIGURE 28.41 Acquired cystic disease-associated renal cell carcinoma (ACD-associated RCC). **A:** The tumor shows a variegated architecture, including papillary, solid, and clear cell–like areas. (H&E, $\times 200$.) **B:** Abundant oxalate crystals are seen in this tumor with prominent tubular architecture. The tumor cells are predominantly large, with abundant eosinophilic, granular cytoplasm and Fuhrman grade 3 nuclei. (H&E, $\times 400$.) (Courtesy of Dr. S. Tickoo, Memorial Sloan-Kettering Cancer Center.)

The high prevalence of papillary RCC in ESRD suggests that an increased frequency of nondisjunction may be the abnormal event leading to tumor development (234). The presence of extra gene copies, or increased gene dosage owing to the increased number of chromosomes, may provide a selective growth advantage and result in a transformed cell type (234). More recently, Inoue et al. (235) studied the genetic profiles of 63 ESRD patients with RCC by analyzing genomic copy number aberrations. Using unsupervised hierarchical clustering analysis, the 63 cases can be divided into two groups, cluster A and B. Cluster A was composed of mainly clear cell RCC, whereas cluster B consisted of papillary RCC, ACD-associated RCC, and clear cell papillary RCC. On the basis of genomic profiles, the molecular pathogenesis of clear cell RCC in ESRD resembled that of sporadic clear cell RCC. Similarly,

the molecular pathogenesis of the various histologic subtypes of non–clear cell RCC in ESRD resembled those of sporadic clear papillary RCC.

ETIOLOGY AND PATHOGENESIS

Pathogenesis of Renal Aging

While kidneys of the elderly are affected by diseases like hypertension, diabetes mellitus, and sporadic insults such as infections, which can themselves accelerate the “natural” process of aging, it appears that renal aging does occur in the absence of systemic or local diseases. The molecular basis of the phenomenon of renal aging is poorly understood but under active investigation. Here, we review some of the

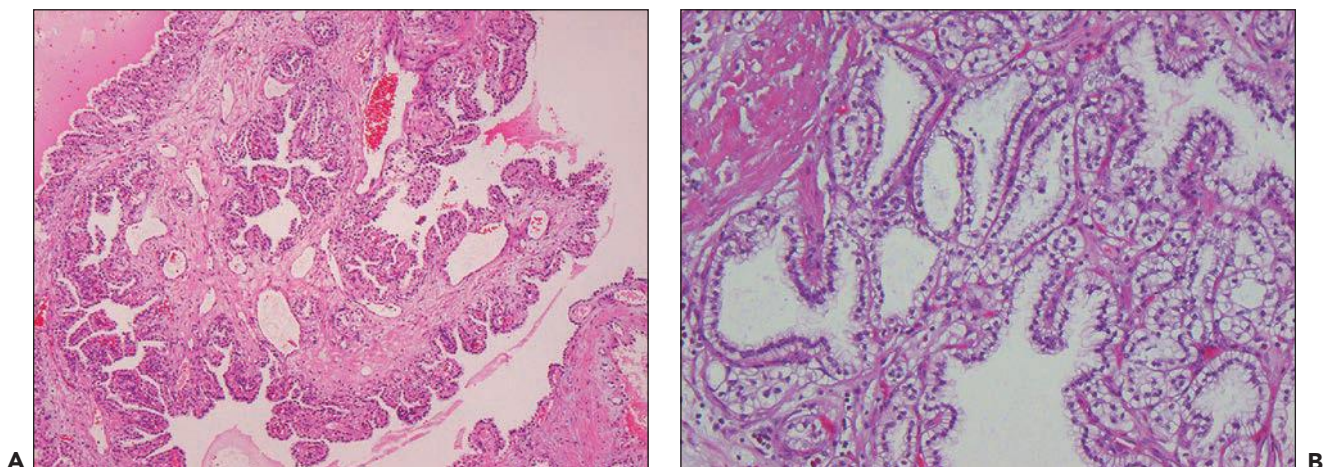


FIGURE 28.42 Clear cell papillary RCC of end-stage kidneys. **A:** Most tumors are multicystic with a prominent papillary architecture and composed of entirely clear cells. (H&E, $\times 200$.) **B:** The nuclei are usually arranged in a linear fashion and away from the basement membranes. (H&E, $\times 400$.) (Courtesy of Dr. S. Tickoo, Memorial Sloan-Kettering Cancer Center.)

promising results from the investigations directed specifically at renal aging.

Telomeres

DNA-protein complexes located at the ends of chromosomes, called telomeres, protect the chromosomes from fusing with each other. The enzyme telomerase synthesizes the telomeric DNA, which are repeats of the sequence TTAGGG. However, most somatic cells do not synthesize telomerase, and therefore telomeres shorten with each cell division. Ultimately, the cells are left with chromosomes that have critically shortened telomeres. The cellular machinery senses the short telomeres as DNA strand breaks, which leads to the activation of p53 and p16 and induction of cell cycle arrest and replicative senescence (236). It has been shown that telomeres shorten with increasing age in the kidney, especially in the renal cortex, where 0.24% to 0.25% telomere shortening occurs every year (237).

Oxidative Stress

Cumulative oxidative stress is believed to play a major role in the process of cellular aging. The increase in oxidative stress and lipid peroxidation in the aging kidney correlates with an increase in the advanced glycosylation end products (AGE) and their receptors (RAGE) that can cross-link adjacent proteins. This, along with reactive oxygen species that can activate ubiquitin-proteasome, may degrade hypoxia-inducible factor-1 α (HIF-1 α) and limit the capacity of the aging cells to form hypoxia-inducible factor-1 (HIF-1)-DNA hypoxia-responsive recognition element (HRE) complexes (HIF-1-HRE complexes) (238,239). In the kidney, the consequent decrease in the ability of the cells to respond to hypoxia could explain the attenuated anemia-induced secretion of EPO as well as the decreased hypoxia-induced production of vascular endothelial growth factor leading, respectively, to reduced erythropoiesis and angiogenesis. In addition, oxidative stress causes telomere shortening (240) and lowers NO bioavailability (see below), further accelerating the process of renal aging.

Nitric Oxide Deficiency and Intrarenal Activation of the Renin-Angiotensin System

NO deficiency also has a role in the renal changes of aging (241). NO deficiency can be caused by several mechanisms: (a) accumulation of endogenous NOS inhibitors such as asymmetric dimethylarginine; (b) reduced abundance or activity of NOS enzymes; and (c) oxidative stress that lowers NO bioavailability. It has been shown that both endothelial and neuronal NOS are reduced in the aging kidney and the latter is associated with renal injury. The RAS, via its effects on the angiotensin receptor AT1, may induce the synthesis of reactive oxygen species and TGF-1 that produce fibrosis. Indeed, angiotensin-converting enzyme inhibitors (ACE inhibitors) and angiotensin receptor blockers ameliorated the aging-related renal damage in rats leading to a decline in glomerular sclerosis and mesangial expansion, tubular atrophy, interstitial fibrosis, and mononuclear infiltration (242). The effect of ACE inhibitors may be mediated by their positive modulation of aging-related dysfunction and ultrastructural changes in the mitochondria, the cell organelles involved in energy metabolism, and production of reactive oxygen species (243).

Klotho, FGF23 and Phosphate Toxicity

A defect in the expression of the gene *Klotho* leads to the development of an aging-like syndrome in mice, while overexpression of the Klotho protein leads to suppression of age-related organ degeneration and elongation of the life span in mice (244). Similarly, *FGF23*-deficient mice are phenotypically identical to that of *Klotho*-deficient mice leading to the discovery that Klotho forms a constitutive binary complex with FGF receptors and functions as an obligatory coreceptor for FGF23 (245). It has been shown that the aging-like phenotypes can be rescued by reversing hyperphosphatemia associated with Klotho or FGF23 deficiency and can be induced by dietary phosphate overload indicating phosphate retention/toxicity is responsible for the aging-like phenotypes (246–248). Klotho may also be involved in vitamin D, calcium, and phosphate metabolism via its proposed enzymatic glucuronidase action on steroid glucuronides and the calcium channel transient receptor potential vallinoid-5 (TRPV5). Klotho is highly expressed in the human kidney, where it colocalizes with TRPV5 in the distal tubular cells (249). *Klotho* gene polymorphisms have been associated with variations in bone mineral density in women (250) and decreased longevity (251). Recently, a homozygous missense mutation in the *Klotho* gene was reported in a 13-year-old girl with severe tumoral calcinosis with dural and carotid artery calcifications (252).

Mitochondria and Autophagy

Mutations in mitochondrial DNA (mtDNA) accrue in various tissues of aging mammals. These mtDNA mutations may provide selective advantage among fast replicating mitochondrial variants leading to clonal expansion of predominantly large defective mitochondria (termed “malignant” mitochondria) that carry mutated mtDNA and resist autophagy. Glomerular injury and glomerular aging are associated with decreased expression of proteins involved in autophagy (253). Inhibition of autophagy, as happens with aging, might create a permissive environment for accumulation of giant and nonactive mitochondria in various organs. This permissive intracellular environment is TOR dependent. TOR inhibits autophagy, thus potentially allowing the “malignant” mitochondria to accumulate. Inhibition of TOR by agents such as rapamycin or metformin may reverse accumulation of defective mitochondria and simultaneously retard the aging process (254).

MicroRNAs (MiRNAs)

The microRNAs (miRNA) are small noncoding RNAs that negatively regulate gene expression at the posttranscriptional level. They have an ability to degrade the target gene or repress its expression without completely silencing it. miRNAs are now believed to play a pivotal role in various cellular processes such as cell proliferation, differentiation, and apoptosis through up-regulation of specific groups of miRNAs to suppress unwanted gene expressions or by down-regulation of other miRNAs whose target genes' expression is necessary for cellular function. The equilibrium between these two groups of miRNA expressions largely determines the function of particular cell types. Recent data suggest that during aging, there is a trend of up-regulation of unwanted miRNA expressions, which in turn down-regulate their target gene products such as proteins mediating the insulin/IGF1 and TOR signaling in *C. elegans*, both of which play crucial roles in the aging process. (255).

Understanding age-dependent changes of miRNA expression and their target genes may open new vistas to understand the mechanism of the aging process and identify new therapeutic targets to delay aging and extend healthy life span.

Calorie Restriction and Sirtuins

Several potential mechanisms have been proposed to account for the beneficial effects of calorie restriction on longevity. Among them are an increase in the activity of sirtuins and adenosine monophosphate (AMP)-activated protein kinase (AMPK) signaling and a decrease in mTOR and S6K1 signaling (256). Sirtuins are members of the silent information regulator 2 (Sir2) family (a family of class III histone/protein deacetylases). There are several mammalian sirtuins of which Sirtuin 1 (SIRT1) has been extensively studied. SIRT1, silent hormone regulator 1, is present in subcellular compartments and regulates expression of various genes and proteins involved in cell survival, differentiation, metabolism, DNA repair, inflammation, and longevity (257). They can mediate NAD⁺-dependent histone deacetylase activity. Calorie restriction appears to increase SIRT1 activity in most tissues including the kidney. This is based on the observations that SIRT1 knockout mice are resistant to the beneficial effects of calorie restriction and that transgenic SIRT1 mice exhibit the same phenotype as calorie-restricted mice on unrestricted calorie intake (258). Interestingly, a plant polyphenol, resveratrol, is a potent activator of SIRT1 activity and has been shown to have renoprotective effects in several models of nephrotoxic and ischemic renal injury (259). In a small pilot study conducted in 10 subjects (mean age 72 years) with impaired glucose tolerance, resveratrol was shown to improve insulin sensitivity and reduce post-meal plasma glucose (260). In a recent study, however, caloric restriction in rhesus monkeys had no effect on longevity (261).

Etiology and Pathogenesis of End-Stage Renal Disease

Diabetes mellitus and hypertension together account for 72% of patients being treated for ESRD (2,5). Other common causes are glomerulonephritis, interstitial nephritis, hereditary conditions, and malignancy. Very rarely ESRD is the result of irreversible acute renal injury such as cortical necrosis or chemical nephrotoxicity. Primary glomerulonephritis may be the most common cause of CKD outside of North America, Europe, and Australia, but hypertension and diabetes are becoming commonplace throughout Asia, Latin America, and large parts of sub-Saharan Africa (5). The percentage of the diseases leading to entry into ESRD programs and the racial and gender differences as reported in the USRDS 2013 Annual Data Report are shown in Table 28.3 (2).

The etiology and pathogenesis of specific glomerular, tubulointerstitial, and vascular diseases are discussed in various chapters throughout the book. However, it is believed that regardless of the initial injury to the kidney, there may be a final common pathway to progressive renal failure after enough nephrons are lost (262–264). As discussed earlier, renal aging disturbs both renal structure and function and provides a natural window of opportunity to probe the mechanisms of renal fibrosis and the progression of renal diseases. The pathogenesis of glomerulosclerosis is not completely understood and is likely multifactorial. Inflammation and increasing oxidative stress that accompanies CKD and aging can result in endothelial dysfunction and changes in vasoactive mediators resulting in atherosclerosis, hypertension, and glomerulosclerosis. Furthermore, changes in CV hemodynamics, such as reduced cardiac output and systemic hypertension, may contribute to glomerular changes. Moreover, impaired autoregulation of the afferent and efferent arterioles may increase glomerular plasma flow, glomerular capillary pressure, and “hyperfiltration” leading to mesangial matrix accumulation and podocyte injury, which ultimately

TABLE 28.3 Incidence of reported ESRD, by primary diagnosis, 2007–2011 combined

Disease	Age (year)	Male (%)	All Races (%)	White (%)	African American (%)	Native American (%)	Asian (%)
All	64	56.74	—	65.5	28.0	1.2	4.87
Diabetes	63	55.0	45.7	65.4	27.4	1.8	5.2
Hypertension/large vessel disease	69	58.1	29.1	59.41	36.3	0.5	4.1
Glomerulonephritis	54	61.2	6.7	67.5	23.4	1.3	7.7
Secondary glomerulonephritis/vasculitis	49	34.0	2.1	64.4	29.6	1.1	4.8
Interstitial nephritis/pyelonephritis	65	58.4	3.0	82.3	13.1	0.6	3.8
Cystic/hereditary/congenital disease	51	56.9	3.3	79.7	13.2	0.7	6.2
Neoplasms/tumors	69	64.4	2.0	79.0	18.3	0.67	2.0
Miscellaneous	63	60.1	6.3	73.5	23.4	0.7	2.3
Cause uncertain	65	58.9	3.8	73.0	21.4	0.8	4.7
Cause missing	61	58.6	1.4	43.5	21.5	1.9	8.5

From the U.S. Renal Data System 2013 Annual Data Report [www.usrds.org]. The data reported here have been supplied by the United States Renal Data System. The reporting of these data is the responsibility of the author and should not be seen as an official policy or interpretation of the US government.

causes segmental glomerulosclerosis (264). The vascular adaptations to functional or structural nephron loss may help preserve GFR by producing hyperperfusion and hyperfiltration in the surviving nephrons. This local glomerular hypertension and hypertrophy may lead to cytokine-mediated mesangial matrix expansion and eventually glomerulosclerosis. Such hyperperfusion-associated glomerular injury is seen with oligomeganephronia, diabetic nephropathy, morbid obesity, sickle cell anemia, and reflux nephropathy. The rate of progression of glomerulosclerosis and ischemic glomerular obsolescence in CKD is critically dependent on systemic blood pressure, and control of hypertension has been shown to be crucial in slowing the rate of progression to ESRD. Although systemic blood pressure control is vital, individual glomerular capillary pressure may increase independently of systemic blood pressure. Treatment with inhibitors of the RAS reduces glomerular capillary pressure and systemic blood pressure and interferes with TGF- β , helping to preserve functioning nephrons (265,266).

The molecular mechanisms leading to tubular atrophy and interstitial fibrosis are complex and incompletely understood. Genetic polymorphisms and epigenetic modifications determine the susceptibilities to develop ESRD in individual patients (263). The ECM and multiple cell types including fibroblasts/myofibroblast, fibrocytes, tubular epithelial cells, inflammatory cells (lymphocytes, macrophages, dendritic cells, and mast cells), endothelial cells, and the microvasculature are involved in this process. Excessive production/accumulation of the ECM (predominantly collagens type I/III and fibronectin) is the defining feature of tubulointerstitial fibrosis. The accumulation of the ECM replaces peritubular capillaries and tubules leading to atubular glomeruli (i.e., open capillary tufts without attached tubules), contributing to decline in GFR. ECM production is regulated by multiple factors including TGF- β and the RAS. In addition, there is inadequate/decreased production of factors, which degrade matrix proteins including matrix metalloproteinase (MMP). However, the antifibrotic effects of MMPs are complex and inconsistent in most studies (262). Likewise, the effects of the plasminogen-plasmin system on renal fibrosis are equally complex with both pro- and antifibrotic activities (262).

The accumulation of fibroblasts/myofibroblasts in the damaged tissue is associated with increased risk of renal fibrosis (262). Tubular epithelial cells can contribute to renal fibrosis through the process of epithelial-to-mesenchymal transition (EMT), which describes a phenotypical change where epithelial cells lose their defined cell-cell-basement membrane contacts and their structural polarity to become spindle shaped and morphologically similar to mesenchymal/myofibroblast cells (267). The role of EMT in renal fibrosis is well documented in both animal models and human biopsy specimens including renal transplantation (267–270) although this is controversial (267). EMT is induced by numerous factors including cytokines (IL-1, oncostatin M), growth factors (TGF- β , basic fibroblast growth factor, connective tissue growth factor), Angiotensin II, proteases (MMP-2, tissue-type plasminogen activator plasmin), and microenvironmental stresses (hypoxia, oxidative stress, advanced glycation end products). Similarly, many factors in the peritubular microenvironment suppress EMT. For instance, hepatocyte growth factor and bone morphogenic protein-7 prevent or even reverse EMT and renal fibrosis by directly targeting TGF- β /Smad signaling. Angiotensin II receptor blocker, statin, rapamycin, and vitamin

D exert their antifibrotic effects, at least in part, by suppressing EMT. More recently, it has been demonstrated that miRNAs are involved in the regulation of EMT and renal fibrosis (271,272). Progressive renal injury leads to rarefaction of the peritubular capillaries resulting in hypoxia, which induces the endothelial-mesenchymal transition (EndoMT) (267). It has been shown that allograft dysfunction is associated with decreased peritubular capillaries at 3 months postrenal transplantation and predicts loss of renal function at 1 year (273).

Renal inflammation plays a major role in renal fibrogenesis. Increased T cells, macrophages, and natural killer cells, but not B cells, are associated with tubulointerstitial fibrosis in renal transplantation (274,275). Increased dendritic cells and mast cells are also associated with interstitial fibrosis (276,277). However, the role of macrophages and mast cells in renal fibrosis is more complex; both have been shown to exert antifibrotic effects (278,279).

MANAGEMENT AND OUTCOME

Management and Outcome of End-stage Renal Disease

ESRD ensues when CKD has progressed to the point at which the kidneys are no longer able to function at a level needed for day-to-day life. It typically occurs when eGFR is less than 10 to 15 mL/min (6). The management of ESRD is aimed to replace, albeit partially, kidney function by treatments collectively termed as renal replacement therapies (RRTs) including renal transplantation, hemodialysis (HD), and peritoneal dialysis (PD). While renal transplantation remains the RRT of choice, the proportion of ESRD patients receiving renal transplants has not changed in the past decade (2). Thus, the majority of ESRD patients depend upon various dialysis modalities for sustaining life. Renal transplantation will not be discussed further in this chapter.

Despite technologic advances in dialysis techniques, the mortality of patient on dialysis remains excessive. In 2011, the annual mortality of dialysis patients in the United States, from day 90 of initiation, was 19.6% (2). Moreover, there are substantial racial disparities in risk for death in the dialysis population. Even though ESRD is substantially more common in African American individuals, Caucasian individuals have a higher risk for death; in 2011, the adjusted 5-year survival rates for Caucasian individuals, African American individuals, and other racial groups were 34%, 42%, and 47%, respectively (2). This has led some to propose that this may be “survivor bias”: The sickest African American patients die early during the course of CKD, and only the healthiest survive and live long enough to reach ESRD. Consistent with this hypothesis, two studies have now shown that in individuals with CKD not on dialysis, the risk for death for African American patients is higher than that among Caucasian patients (280,281). Hispanic individuals now constitute the largest minority group in the United States; their risk for ESRD is higher than that seen among non-Hispanic individuals, and the number of Hispanic dialysis patients has doubled since 1996 (282). Although still unacceptably high, there has been a progressive decline in the overall mortality rate of dialysis patients, particularly since 2000, when the annual mortality rate was 22% (2).

While utilization of HD has progressively increased, there has been a steady decline the PD usage over the last two decades, with about 7.25% of the total US dialysis patients receiving PD

in 2011 (2). In contrast, PD is employed much more frequently elsewhere in the world and is the primary mode of dialysis therapy in Mexico (2). Complex psychosocial and economic factors, pre-ESRD education, patient preference, nephrology and surgery training patterns, as well as skills and bias are examples of the many confounding factors influencing the crucial selection of the best RRT modality for the individual patient (283–287). In situations where timely, accurate, and perhaps passionate pre-ESRD education is given to the patient, a significantly higher number of CKD patients (40%) choose PD, and only a small fraction start HD with a temporary catheter (285–287). In the ideal world, the impending ESRD diagnosis is proactively managed with a preemptive living donor kidney transplant (CKD stage 4 to 5). In sharp contrast, only a small fraction of dialysis patients (3.6% or 17,671) (2) in the US received a kidney transplant in 2011. Thus, appropriate planning is of utmost importance to the proper selection and timely initiation of RRT, in order to prevent serious uremic complications, avoid the use of dialysis catheters, and improve patient outcome and quality of life in a cost-effective way (288).

Dialysis Therapy in the Elderly

With a more liberal utilization of RRT, the greatest increases in the incidence and prevalence of ESRD have been seen among the elderly, particularly among those who are older than 75 years (2). As expected, the mortality rate of elderly patients who undergo dialysis therapy is high (2,289,290). PD is frequently viewed as unfeasible in elderly patients, perhaps due to a negative image on the part of physicians and nurses in some dialysis centers. When patients with advanced kidney disease are adequately informed, the number of patients starting on PD increases (291). In a large Dutch prospective multicenter study, entitled the Netherlands Cooperative Study of the Adequacy of Dialysis (NECOSAD), out of the 64% of patients who were given a choice, 27% of the patients older than 70 years of age chose PD (286). Excellent median patient and PD technique survival have been observed in an old ESRD population (292) suggesting that PD is a suitable RRT modality for elderly patients. Notwithstanding dialysis modalities, the outcome of dialysis among the elderly remains poor, suggesting that alternative paths, such as a decision for conservative management (nondialysis therapy), should be incorporated in discussions in the predialysis setting (293). No randomized trials have compared the outcomes of maximum conservative treatment with dialysis therapy among the elderly. In a single-center study from the United Kingdom comprising of 202 individuals aged 70 years or more, 29 chose maximum conservative treatment (294). The median survival was almost threefold higher among those who were treated with dialysis, suggesting that dialysis therapy prolongs life even among the elderly (294). However, the patients who were treated with dialysis were almost twice as likely to be hospitalized, and the time spent at home was similar between the two groups (294). In another study, the clinical course of 3702 nursing home residents who started dialysis during a 2-year period (1998 through 2000) was described (295). By 12 months, 87% of patients had either died or experienced a significant functional decline (295). One has to be careful in making broad conclusions about the appropriateness of dialysis therapy among the elderly. When developing a therapeutic plan, a physician should recognize that a patient's functional status and expectations about lifestyle and

the therapy are probably more important than the chronologic age. Moreover, when informed about the anticipated morbidity and mortality, it is possible that many elderly patients may choose maximum conservative treatment rather than long-term RRT. This reinforces the importance of patient education as well as shared decision making (296).

REFERENCES

1. CDC. The State of Aging and Health in America 2013 Atlanta, GA: CDC, US Department of Health & Human Services; 2013; Available from: <http://www.cdc.gov/aging/>
2. United States Renal Data System: Annual Data Report 2013: www.usrds.org. Accessed January 14, 2014.
3. Tonelli M, Riella MC. Chronic kidney disease and the aging population. *Kidney Int* 2014;85:487–491.
4. Levey AS, Eckardt KU, Tsukamoto Y, et al. Definition and classification of chronic kidney disease: A position statement from Kidney Disease: Improving Global Outcomes (KDIGO). *Kidney Int* 2005;67:2089–2100.
5. Coresh J, Astor BC, Greene T, et al. Prevalence of chronic kidney disease and decreased kidney function in the adult US population: Third National Health and Nutrition Examination Survey. *Am J Kidney Dis* 2003;41:1–12.
6. Kidney Disease Outcome Quality Initiative (K/DOQI). Part 4. Definition and classification of stages of chronic kidney disease. *Am J Kidney Dis* 2002;39(Suppl):S46–S75.
7. Turin TC, Tonelli M, Manns BJ, et al. Lifetime risk of ESRD. *J Am Soc Nephrol* 2012;23:1569–1578.
8. Zhou XJ, Rakheja D, Silva FG. The aging kidney. In: Zhou XJ, Laszik Z, Nadasdy T, et al., eds. *Silva's Diagnostic Renal Pathology*. New York, NY: Cambridge University Press; 2009:488–501.
9. Zhou XJ, Rakheja D, Yu XQ, et al. The aging kidney. *Kidney Int* 2008;74:710–720.
10. Rahman M, Smith MC. Chronic renal insufficiency: A diagnostic and therapeutic approach. *Arch Intern Med* 1998;158:1743–1752.
11. Go AS, Chertow GM, Fan D, et al. Chronic kidney disease and the risk of death, cardiovascular events, and hospitalization. *N Engl J Med* 2004;351:1296.
12. Middleton RJ, Parfrey PS, Foley RN. Left ventricular hypertrophy in the renal patient. *J Am Soc Nephrol* 2001;12:1079–1084.
13. McClellan WM, Langston RD, Presley R. Medicare patients with cardiovascular disease have a high prevalence of chronic kidney disease and a high rate of progression to end-stage renal disease. *J Am Soc Nephrol* 2004;15:1912.
14. Foley RN, Parfrey PS, Hartnett JD, et al. Clinical and echocardiographic disease in patients starting end-stage renal disease therapy. *Kidney Int* 1995;47:186.
15. Paoletti E, Bellino D, Cassotana P, et al. Left ventricular hypertrophy in nondiabetic predialysis CKD. *Am J Kidney Dis* 2005;46(2):320–327.
16. Vlahakos DV, Hahalis G, Vassilakos P, et al. Relationship between left ventricular hypertrophy and plasma renin activity in chronic dialysis patients. *J Am Soc Nephrol* 1997;8:1764.
17. Patel RK, Oliver S, Mark PB, et al. Determinants of left ventricular mass and hypertrophy in hemodialysis patients assessed by cardiac magnetic resonance imaging. *Clin J Am Soc Nephrol* 2009;4:1477–1483.
18. Faul C, Amaral AP, Oskoueï B, et al. FGF23 induces left ventricular hypertrophy. *J Clin Invest* 2011;121:4393–4408.
19. Isakova T, Wahl P, Vargas GS, et al. Fibroblast growth factor 23 is elevated before parathyroid hormone and phosphate in chronic kidney disease. *Kidney Int* 2011; 79:1370–1378.
20. Gutierrez OM, Januzzi JL, Isakova T, et al. Fibroblast growth factor 23 and left ventricular hypertrophy in chronic kidney disease. *Circulation* 2009;119:2545–2552.
21. Wolf M. Forging forward with 10 burning questions on FGF23 in kidney disease. *J Am Soc Nephrol* 2010;21:1427–1435.
22. Ritz E. Left ventricular hypertrophy in renal disease: Beyond preload and afterload. *Kidney Int* 2009;75:771–773.
23. Kahn MR, Robbins MJ, Kim MC, et al. Management of cardiovascular disease in patients with kidney disease. *Nat Rev Cardiol* 2013;10:261–273.

24. Vaziri ND, Norris K. Lipid disorders and their relevance to outcomes in chronic kidney disease. *Blood Purif* 2011;31:189–196.
25. Kahn MR, Fallahi A, Kim MC, et al. Coronary artery disease in a large renal transplant population: implications for management. *Am J Transplant* 2011;11:2665–2674.
26. Braun J, Oldendorf, Moshage W, et al. Electron beam computed tomography in the evaluation of cardiac calcifications in chronic dialysis patients. *Am J Kidney Dis* 1996;27:394.
27. Parikh NI, Hwang SJ, Larson MG, et al. Chronic kidney disease as a predictor of cardiovascular disease (from the Framingham Heart Study). *Am J Cardiol* 2008;102:47–53.
28. Rumberger JA, Simons DB, Fitzpatrick LA, et al. Coronary artery calcium area by electron-beam computed tomography and coronary atherosclerosis plaque area: a histopathologic correlative study. *Circulation* 1995;93:2157.
29. Gotlieb AI, Silver MD. Atherosclerosis: Pathology and pathogenesis. In: Silver MD, Gotlieb AI, Schoen FJ, eds. *Cardiovascular Pathology*, 3rd ed. New York: Churchill Livingstone, 2001:68.
30. McCullough PA, Soman S. Cardiovascular calcification in patients with chronic renal failure. Are we on target with this risk factor? *Kidney Int* 2004;66(Suppl 90):S18.
31. Chen NX, O'Neill KD, Duan D, et al. Phosphorus and uremic serum up-regulate osteopontin expression in vascular smooth muscle cells. *Kidney Int* 2002;62:1724.
32. Moe SM, O'Neill KD, Duan D, et al. Medial artery calcification in ESRD patients is associated with deposition of bone matrix proteins. *Kidney Int* 2002;61:638.
33. Moe SM, Duan D, Doehle BP, et al. Uremia induces the osteoblastic differentiation factor Cbfa 1 in human blood vessels. *Kidney Int* 2003;63:1003.
34. Mizobuchi M, Towler D, Slatopolsky E. Vascular calcification: the killer of patients with chronic kidney disease. *J Am Soc Nephrol* 2009;20:1453–1464.
35. Stubbs JR, Liu S, Tang W, et al. Role of hyperphosphatemia and 1,25-dihydroxyvitamin D in vascular calcification and mortality in fibroblastic growth factor 23 null mice. *J Am Soc Nephrol* 2007;18:2116–2124.
36. Hu MC, Shi M, Zhang J, et al. Klotho deficiency causes vascular calcification in chronic kidney disease. *J Am Soc Nephrol* 2011;22:124–136.
37. Davis TR, Young BA, Eisenberg MS, et al. Outcome of cardiac arrests attended by emergency medical services staff at community outpatient dialysis centers. *Kidney Int* 2008;73:933–939.
38. Ritz E, Wanner C. The challenge of sudden death in dialysis patients. *Clin J Am Soc Nephrol* 2008;3:920–929.
39. Herzog CA, Strief JW, Collins AJ, et al. Cause-specific mortality of dialysis patients after coronary revascularization: Why don't dialysis patients have better survival after coronary intervention? *Nephrol Dial Transplant* 2008;23:2629–2633.
40. Adler Y, Vaturi M, Herz I, et al. Nonobstructive aortic valve calcification: A window to significant coronary artery disease. *Atherosclerosis* 2002;161:193.
41. Raggi P, Boulay A, Chasan-Taber S, et al. Cardiac calcification in adult hemodialysis patients: A link between end-stage renal disease and cardiovascular disease? *J Am Coll Cardiol* 2002;39:695.
42. Wang AY, Wang M, Woo J, et al. Cardiac valve calcifications as an important predictor for mortality and cardiovascular mortality in long-term peritoneal dialysis patients: a prospective study. *J Am Soc Nephrol* 2003;13:159.
43. Hayashi M, Takamatsu I, Kanno Y, et al. For the Japanese Calciphylaxis Study Group: A case-control study of calciphylaxis in Japanese end-stage renal disease patients. *Nephrol Dial Transplant* 2012;27:1580–1584.
44. Baldwin C, Farah M, Leung M, et al. Multi-intervention management of calciphylaxis: a report of 7 cases. *Am J Kidney Dis* 2011;58:988–991.
45. Ross EA. What is the role of using sodium thiosulfate or bisphosphonates in the treatment for calciphylaxis? *Semin Dial* 2011;24:434–436.
46. Vedvyas C, Winterfield LS, Vleugels RA. Calciphylaxis: A systematic review of existing and emerging therapies. *J Am Acad Dermatol* 2012;67:e253–e260.
47. Rostand SG, Rutsky EA. Pericarditis in end-stage renal disease. *Clin Clin* 1990;8:701.
48. Alpert MA, Ravenscraft MD. Pericardial involvement in end-stage renal disease. *Am J Med Sci* 2003;325:228–236.
49. Groshong SD, Tomashefski Jr JF, Cool CD. Pulmonary vascular diseases. In: Tomashefski JF Jr, ed. *Dail & Hammar's Pulmonary Pathology*, 3rd ed. New York: Springer-Verlag, 2008:1032.
50. Hughson MD. End-stage renal disease. In: Jennette JC, et al., ed. *Heptinstall's Pathology of the Kidney*, 6th ed. Philadelphia: Lippincott Williams & Wilkins, 2007:1308.
51. Hammar SP. Nonneoplastic pleural diseases pulmonary vascular diseases. In: Dail DH, Hammar SP, eds. *Dail & Hammar's Pulmonary Pathology*, 3rd ed. New York: Springer-Verlag, 2008:1139.
52. Klein CL, Hoke TS, Fang W-F, et al. Interleukin-6 mediates lung injury following ischemic acute kidney injury or bilateral nephrectomy. *Kidney Int* 2008;74:901–909.
53. Dember LM, Jaber BL. Dialysis-related amyloidosis: Late finding or hidden epidemic? *Semin Dial* 2006;19:105–109.
54. Fenves AZ, Emmett M, White MG, et al. Carpal tunnel syndrome with cystic bone lesions secondary to amyloidosis in chronic hemodialysis patients. *Am J Kidney Dis* 1986;2:130–134.
55. Fleury AM, Buetens OW, Campassi C, et al. Pathologic quiz case: A 77-year-old woman with bilateral breast masses. Amyloidosis involving the breast. *Arch Pathol Lab Med* 2004;128:e67.
56. Mount SL, Eltabbakh GH, Hardin NJ. β 2-Microglobulin amyloidosis presenting as bilateral ovarian masses: A case report and review of the literature. *Am J Surg Pathol* 2002;26:130.
57. Mendoza PD, Fenves AZ, Punar M, et al. Subcutaneous β 2-microglobulin amyloid shoulder nodules in a long-term hemodialysis patient. *Proc (Bayl Univ Med Cent)* 2010;23:139–141.
58. Yusa H, Yoshida H, Kikuchi H, et al. Dialysis-related amyloidosis of the tongue. *J Oral Maxillofacial Surg* 2001;59:947.
59. Takayama F, Miyazaki S, Morita T, et al. Dialysis related amyloidosis of the heart in long-term dialysis patients. *Kidney Int* 2001;78(Suppl):8172.
60. Takahashi S, Morita T, Koda Y, et al. Gastrointestinal involvement of dialysis-related amyloidosis. *Clin Nephrol* 1988;30:168.
61. Choi H-S, Heller D, Picken MM, et al. Infarction of the intestine with massive amyloid deposition in two patients on long-term hemodialysis. *Gastroenterology* 1989;96:230.
62. Onishi S, Andress DL, Maloney NA, et al. Beta-2-microglobulin deposition in bone in chronic renal failure. *Kidney Int* 1991;39:990.
63. Kuragano T, Inoue T, Yoh K, et al. Effectiveness of β (2)-microglobulin adsorption column in treating dialysis-related amyloidosis: A multicenter study. *Blood Purif* 2011;32:317–322.
64. Yamamoto S, Gejyo F. Historical background and clinical treatment of dialysis-related amyloidosis. *Biochimica et Biophysica Acta* 2005;1753:4–10.
65. Milito G, Taccone-Galluci M, Brancaleone C, et al. The gastrointestinal tract in uremic patients on long-term hemodialysis. *Kidney Int* 1985;28:S157.
66. Rowe PA, El Nujumi AM, Williams C, et al. The diagnosis of *Helicobacter pylori* in uremic patients. *Am J Kidney Dis* 1992;20:574.
67. Vaziri ND, Dure Smith B, Miller R, et al. Pathology of the gastrointestinal tract in chronic hemodialysis patients: An autopsy study of 78 cases. *Am J Gastroenterol* 1985;80:608.
68. Navab F, Masters P, Siubrami R, et al. Angiodysplasia in patients with renal insufficiency. *Am J Gastroenterol* 1989;84:1297.
69. Scheff RT, Zuckerman G, Hartner H, et al. Diverticular disease in patients with chronic renal failure due to polycystic kidney disease. *Ann Intern Med* 1980;92:202.
70. Vaziri ND. CKD impairs barrier function and alters microbial flora of the intestine—a major link to inflammation and uremic toxicity. *Curr Opin Nephrol Hypertens* 2012;21(6):587–592.
71. Vaziri ND, Yuan J, Nazertehrani S, et al. Chronic kidney disease causes disruption of gastric and small intestinal epithelial tight junction. *Am J Nephrol* 2013;38:99–103.
72. Vaziri ND, Wong J, Pahl MV, et al. Chronic kidney disease alters the composition of intestinal microbial flora. *Kidney Int* 2013;83(2):308–315.
73. Vaziri ND, Yuan J, Norris K. Role of urea in intestinal barrier dysfunction and disruption of epithelial tight junction in CKD. *Am J Nephrol* 2012;37(1):1–6.
74. Aronov PA, Luo FJ, Plummer NS, et al. Colonic contribution to uremic solutes. *J Am Soc Nephrol* 2011;22(9):1769–1776.
75. Avram RM, Iancu M. Pancreatic disease in uremia and parathyroid hormone excess. *Nephron* 1982;32:60–62.

76. Lankisch PG, Weber-Dany B, Maisonneuve P, et al. Frequency and severity of acute pancreatitis in chronic dialysis patients. *Nephrol Dial Transplant* 2008;23:1401.
77. Han SH, Reynolds TB, Fong TL. Nephrogenic ascites. Analysis of 16 cases and review of the literature. *Medicine* (Baltimore) 1998; 77:233–245.
78. Van Buren P, Velez R, Vaziri ND, et al. Iron overdose: a contributor to adverse outcomes in randomized trials of anemia correction in CKD. *Int Urol Nephrol* 2012;44:499–507.
79. Eschbach JW, Adamson JW. Anemia of end-stage renal disease (ESRD). *Kidney Int* 1985;28:1.
80. Eschbach JW, Egrie JC, Downing MR, et al. Correction of the anemia of end-stage renal disease with recombinant erythropoietin: Results of a combined phase I and phase II trial. *N Engl J Med* 1987;316:73.
81. Hayashi T, Suzuki A, Shoji T, et al. Cardiovascular effect of normalizing the hematocrit during erythropoietin therapy in predialysis patients with chronic renal failure. *Am J Kidney Dis* 2000;35:250.
82. Vaziri ND, Zhou XJ. Potential mechanisms of adverse outcomes in trials of anemia correction with erythropoietin in chronic kidney disease. *Nephrol Dial Transplant* 2009;24:1082–1088.
83. Galbusera M, Remuzzi G, Boccardo P. Treatment of bleeding in dialysis patients. *Semin Dial* 2009;22:279–286.
84. Zhou XJ, Vaziri ND. Defective calcium signaling in uremic platelets and its amelioration with long-term erythropoietin therapy. *Nephro Dial Transpl* 2002;17:992–997.
85. Vaziri ND. Thrombocytosis in erythropoietin-treated dialysis patients may be mediated by erythropoietin rather than iron deficiency. *Am J Kidney* 2009;53:733–736.
86. Finelli L, Miller JT, Tokars J, et al. National surveillance of dialysis-associated diseases in the United States, 2002. *Semin Dial* 2005;18: 52–61.
87. Martin P, Carter D, Fabrizi F, et al. Histopathologic features of hepatitis C in renal transplant candidates. *Transplantation* 2000;69:1479.
88. Roth D. Hepatitis C virus: The nephrologist's view. *Am J Kidney Dis* 1995;25:3.
89. Vaziri ND. Epidemic of iron overload in dialysis population caused by intravenous iron products: A plea for moderation. *Am J Med* 2012;125(10):951–952.
90. Lien YH. Nervous system manifestations of renal disease. In: Coffman TM et al., ed. *Schrier's Diseases of the Kidney*, 9th ed. Philadelphia: Lippincott Williams & Wilkins, 2013:2277.
91. Komaba H, Kakuta T, Fukagawa M. Diseases of the parathyroid gland in chronic kidney disease. *Clin Exp Nephrol* 2011;15:797–809.
92. Alphonso S, Santamaria I, Guinsburg ME, et al. Chromosomal aberrations, the consequence refractory hyperparathyroidism: Its relationship with biochemical parameters. *Kidney Int* 2003;63(Suppl 85):S32.
93. Moe S, Druke T, Cunningham J, et al. Definition, evaluation, and classification of renal osteodystrophy: A position statement from kidney disease: improving global outcomes (KDIGO). *Kidney Int* 2006;69:1945–1953.
94. Chauhan V, Kelepouris E, Chauhan N, Vaid M. Current concepts and management strategies in chronic kidney disease—mineral and bone disorder. *South Med J* 2012;105:470–485.
95. Boyce BF, Xing L, Shakespeare W, et al. Regulation of bone remodeling and emerging breakthrough drugs for osteoporosis and osteolytic bone metastasis. *Kidney Int* 2003;63(Suppl 85):S2.
96. Pei Y, Herez G, Greenwood C, et al. Non-invasive prediction of aluminum bone disease in hemo- and peritoneal dialysis patients. *Kidney Int* 1992;41:1374.
97. Coburn JW. Mineral metabolism and renal bone disease: Effects of CAPD versus hemodialysis. *Kidney Int* 1993;43(Suppl 40):S92.
98. Coburn JW, Maung HM. Use of active vitamin D sterols in patients with chronic kidney disease, stages 3 and 4. *Kidney Int* 2003;63(Suppl 85):S49.
99. Cozzolino M, Mazzaferro S, Brandenburg V. The treatment of hyperphosphataemia in CKD: Calcium-based or calcium-free phosphate binders? *Nephrol Dial Transplant* 2011;26:402–407.
100. Coresh J, Wei GL, McQuillan G, et al. Prevalence of high blood pressure and elevated serum creatinine level in the United States: Findings from the third National Health and Nutrition Examination Survey (1988–1994). *Arch Intern Med* 2001;161:1207–1216.
101. Perlata CA, Hicks LS, Chertaw GM, et al. Control of hypertension in adults with chronic kidney disease in the United States. *Hypertension* 2005;45:1119–1124.
102. Wesson Jr LG. Renal hemodynamics in physiological states. In: *Physiology of the Human Kidney*. New York: Grune & Stratton, 1969: 309–316.
103. Hollenberg NK, Adams DF, Solomon HS, et al. Senescence and the renal vasculature in normal man. *Circ Res* 1974;34(3):309–316.
104. Long DA, Mu W, Price KL, Johnson RJ. Blood vessels and the aging kidney. *Nephron Exp Nephrol* 2005;101(3):e95–e99.
105. Delp MD, Behnke BJ, Spier SA, et al. Ageing diminishes endothelium-dependent vasodilatation and tetrahydrobiopterin content in rat skeletal muscle arterioles. *J Physiol* 2008;586(4):1161–1168.
106. Virmani R, Avolio AP, Mergner WJ, et al. Effect of aging on aortic morphology in populations with high and low prevalence of hypertension and atherosclerosis. Comparison between occidental and Chinese communities. *Am J Pathol* 1991;139:1119–1129.
107. Boutouyrie P, Laurent S, Benetos A, et al. Opposing effects of ageing on distal and proximal large arteries in hypertensives. *J Hypertens Suppl* 1992;10(6):S87–S91.
108. Laurent S, Cockcroft J, Van Bortel L, et al. Expert consensus document on arterial stiffness: Methodological issues and clinical applications. *Eur Heart J* 2006;27(21):2588–2605.
109. Nichols WW, O'Rourke MF, Vlachopoulos C. *McDonald's Blood Flow in Arteries: Theoretical, Experimental and clinical principles*, 6th ed. London: Hodder Arnold, 2011.
110. Verhage JC, Fesler P, du Cailar G, et al. Elevated pulse pressure is associated with low renal function in elderly patients with isolated systolic hypertension. *Hypertension* 2005;45(4):586–591.
111. O'Rourke MF. Arterial aging: Pathophysiological principles. *Vasc Med* 2007;12(4):329–341.
112. Fisher CM. Lacunar strokes and infarcts: A review. *Neurology* 1982;32(8):871–876.
113. Tan JC, Busque G, Workeneh B, et al. Effects of aging on glomerular function and number in living kidney donors. *Kidney Int* 2010;78(7):686–692.
114. Morrissey PE, Yango AF. Renal transplantation: Older recipients and donors. *Clin Geriatr Med* 2006;22(3):687–707.
115. Lindeman RD, Tobin J, Shock NW. Longitudinal studies on the rate of decline in renal function with age. *J Am Geriatr Soc* 1985;33(4):278–285.
116. Kimmel PL, Lew SQ, Bosch JP. Nutrition, ageing and GFR: Is age-associated decline inevitable? *Nephrol Dial Transplant* 1996;11(Suppl 9):85–88.
117. Musch W, Verfaillie L, Decaux G. Age-related increase in plasma urea level and decrease in fractional urea excretion: Clinical application in the syndrome of inappropriate secretion of antidiuretic hormone. *Clin J Am Soc Nephrol* 2006;1(5):909–914.
118. Maher FT, Nolan NG, Elveback LR. Comparison of simultaneous clearances of 125-I-labeled sodium iothalamate (Glofil) and of inulin. *Mayo Clin Proc* 1971;46(10):690–691.
119. Cockcroft DW, Gault MH. Prediction of creatinine clearance from serum creatinine. *Nephron Exp Nephrol* 1976;16(1):31–41.
120. Levey AS, Coresh J, Balk E, et al. National Kidney Foundation practice guidelines for chronic kidney disease: Evaluation, classification, and stratification. *Ann Intern Med* 2003;139(2):137–147.
121. Berman N, Hostetter TH. Comparing the Cockcroft-Gault and MDRD equations for calculation of GFR and drug doses in the elderly. *Nat Clin Pract Nephrol* 2007;3(12):644–645.
122. Levey AS, Stevens LA, Schmid CH, et al. A new equation to estimate glomerular filtration rate. *Ann Intern Med* 2009;150(9):604–612.
123. Ognibene A, Mannucci E, Caldini A, et al. Cystatin C reference values and aging. *Clin Biochem* 2006;39(6):658–661.
124. Peralta CA, Katz RK, Sarnak MJ, et al. Cystatin C identifies chronic kidney disease patients at higher risk for complications. *J Am Soc Nephrol* 2011;22:147–155.
125. Rowe JW, Shock NW, DeFronzo RA. The influence of age on the renal response to water deprivation in man. *Nephron* 1976;17(4):270–278.
126. Preisser L, Teillet L, Aliotti S, et al. Downregulation of aquaporin-2 and -3 in aging kidney is independent of V(2) vasopressin receptor. *Am J Physiol Renal Physiol* 2000;279(1):F144–F152.

127. Combet S, Teillet L, Geelen G, et al. Food restriction prevents age-related polyuria by vasopressin-dependent recruitment of aquaporin-2. *Am J Physiol Renal Physiol* 2001;281(6):F1123–F1131.
128. Sands JM. Urine concentrating and diluting ability during aging. *J Gerontol A Biol Sci Med Sci* 2012;67:1352–1357.
129. Combet S, Geffroy N, Berthouaud V, et al. Correction of age-related polyuria by dDAVP: Molecular analysis of aquaporins and urea transporters. *Am J Physiol Renal Physiol* 2003;284:199–208.
130. Tian Y, Riazi S, Khan O, et al. Renal ENaC subunit, Na-K-2Cl and Na-Cl cotransporter abundances in aged, water-restricted F344 x Brown Norway rats. *Kidney Int* 2006;69(2):304–312.
131. Epstein M, Hollenberg NK. Age as a determinant of renal sodium conservation in normal man. *J Lab Clin Med* 1976;87(3):411–417.
132. Musso CG, Liakopoulos V, Ioannidis I, et al. Acute renal failure in the elderly: Particular characteristics. *Int Urol Nephrol* 2006;38(3–4):787–793.
133. Luft FC, Grim CE, Fineberg N, et al. Effects of volume expansion and contraction in normotensive whites, blacks, and subjects of different ages. *Circulation* 1979;59(4):643–650.
134. Luft FC, Weinberger MH, Fineberg NS, et al. Effects of age on renal sodium homeostasis and its relevance to sodium sensitivity. *Am J Med* 1987;82(1B):9–15.
135. Baylis C. Renal responses to acute angiotensin II inhibition and administered angiotensin II in the aging, conscious, chronically catheterized rat. *Am J Kidney Dis* 1993;22(6):842–850.
136. Weidmann P, De Myttenaere-Bursztein NS, Maxwell MH, et al. Effect on aging on plasma renin and aldosterone in normal man. *Kidney Int* 1975;8(5):325–333.
137. Tsunoda K, Abe K, Goto T, et al. Effect of age on the renin-angiotensin-aldosterone system in normal subjects: Simultaneous measurement of active and inactive renin, renin substrate, and aldosterone in plasma. *J Clin Endocrinol Metab* 1986;62(2):384–389.
138. Weidmann P, Beretta-Piccoli C, Ziegler WH, et al. Age versus urinary sodium for judging renin, aldosterone, and catecholamine levels: studies in normal subjects and patients with essential hypertension. *Kidney Int* 1978;14(6):619–628.
139. Skott P, Ingerslev J, Damkjaer Nielsen M, et al. The renin-angiotensin-aldosterone system in normal 85-year-old people. *Scand J Clin Lab Invest* 1987;47(1):69–74.
140. Maric C, Aldred GP, Antoine AM, et al. Effects of angiotensin II on cultured rat renomedullary interstitial cells are mediated by AT1A receptors. *Am J Physiol* 1996;271(5 Pt 2):F1020–F1028.
141. Conti S, Cassis P, Benigni A. Aging and the renin-angiotensin system. *Hypertension* 2012;60:878–883.
142. Anderson S, Brenner BM. Effects of aging on the renal glomerulus. *Am J Med* 1986;80(3):435–442.
143. Inserra F, Romano LA, de Cavanagh EM, et al. Renal interstitial sclerosis in aging: Effects of enalapril and nifedipine. *J Am Soc Nephrol* 1996;7(5):676–680.
144. Vaughan DE, Lazos SA, Tong K. Angiotensin II regulates the expression of plasminogen activator inhibitor-1 in cultured endothelial cells. A potential link between the renin-angiotensin system and thrombosis. *J Clin Invest* 1995;95(3):995–1001.
145. Jung FF, Kennefick TM, Ingelfinger JR, et al. Down-regulation of the intrarenal renin-angiotensin system in the aging rat. *J Am Soc Nephrol* 1995;5(8):1573–1580.
146. Berliner N. Anemia in the elderly. *Trans Am Clin Climatol Assoc* 2013;124:230–237.
147. Ble A, Fink JC, Woodman RC, et al. Renal function, erythropoietin, and anemia of older persons: The INCHIANTI study. *Arch Intern Med* 2005;165(19):2222–2227.
148. Ershler WB, Sheng RC, McKelvey J, et al. Serum erythropoietin and aging: A longitudinal analysis. *J Am Geriatr Soc* 2005;53(8):1360–1365.
149. Ferrucci L, Guralnik JM, Bandinelli S, et al. Unexplained anaemia in older persons is characterised by low erythropoietin and low levels of pro-inflammatory markers. *Br J Haematol* 2007;136(6):849–855.
150. Zhang Z., Sun L, Wang Y, et al. Renoprotective role of the vitamin D receptor in diabetic nephropathy. *Kidney Int* 2008;73(2):163–171.
151. Zhang Y, Kong J, Deb DK, et al. Vitamin D receptor attenuates renal fibrosis by suppressing the renin-angiotensin system. *J Am Soc Nephrol* 2010;21(6):966–973.
152. Ravani P, Malberti F, Tripepi G, et al. Vitamin D levels and patient outcome in chronic kidney disease. *Kidney Int* 2009;75(1):88–95.
153. Mensenkamp AR, Hoenderop JG, Bindels RJ. Recent advances in renal tubular calcium reabsorption. *Curr Opin Nephrol Hypertens* 2006;15(5):524–529.
154. Clapham DE, Julius D, Montell C, et al. International Union of Pharmacology. XLIX. Nomenclature and structure-function relationships of transient receptor potential channels. *Pharmacol Rev* 2005;57(4):427–450.
155. Hoenderop JG, Muller D, Van Der Kemp AW, et al. Calcitriol controls the epithelial calcium channel in kidney. *J Am Soc Nephrol* 2001;12(7):1342–1349.
156. Chang Q, Hoefs S, van der Kemp AW, et al. The beta-glucuronidase klotho hydrolyzes and activates the TRPV5 channel. *Science* 2005;310(5747):490–493.
157. Kuro-o M, Matsumura Y, Aizawa H, et al. Mutation of the mouse klotho gene leads to a syndrome resembling ageing. *Nature* 1997;390(6655):45–51.
158. Silva FG. The aging kidney: A review—part I. *Int Urol Nephrol* 2005;37(1):185–205.
159. Tada S, Yamagishi J, Kobayashi H, et al. The incidence of simple renal cyst by computed tomography. *Clin Radiol* 1983;34(4):437–439.
160. Zhou XJ, Laszik ZG, Silva FG. Anatomical changes in the aging kidney. In: Macias-Nunez JF, Cameron JS, Oreopoulos DG, eds. *The Aging Kidney in Health and Disease*. New York, NY: Springer, 2007:39–54.
161. Wiggins JE. Aging in the glomerulus. *J Gerontol A Biol Sci Med Sci* 2012;67:1358–1364.
162. Nyengaard JR, Bendtsen TF. Glomerular number and size in relation to age, kidney weight, and body surface in normal man. *Anat Rec* 1992;232(2):194–201.
163. Hughson MD, Douglas-Denton R, et al. Hypertension, glomerular number, and birth weight in African Americans and white subjects in the southeastern United States. *Kidney Int* 2006;69(4):671–678.
164. Hughson M, Farris AB III, Douglas-Denton R, et al. Glomerular number and size in autopsy kidneys: The relationship to birth weight. *Kidney Int* 2003;63(6):2113–2122.
165. Keller G, Zimmer G, Mall G, et al. Nephron number in patients with primary hypertension. *N Engl J Med* 2003;348(2):101–108.
166. Kasiske BL. Relationship between vascular disease and age-associated changes in the human kidney. *Kidney Int* 1987;31(5):1153–1159.
167. Kaplan C, Pasternack B, Shah H, et al. Age-related incidence of sclerotic glomeruli in human kidneys. *Am J Pathol* 1975;80(2):227–234.
168. Smith SM, Hoy WE, Cobb L. Low incidence of glomerulosclerosis in normal kidneys. *Arch Pathol Lab Med* 1989;113(11):1253–1255.
169. Samuel T, Hoy WE, Douglas-Denton R, et al. Determinants of glomerular volume in different cortical zones of the human kidney. *J Am Soc Nephrol* 2005;16(10):3102–3109.
170. Steffes MW, Barbosa J, Basgen JM, et al. Quantitative glomerular morphology of the normal human kidney. *Lab Invest* 1983;49(1):82–86.
171. Nath KA. Tubulointerstitial changes as a major determinant in the progression of renal damage. *Am J Kidney Dis* 1992;20(1):1–17.
172. Eknoyan G, McDonald MA, Appel D, et al. Chronic tubulo-interstitial nephritis: Correlation between structural and functional findings. *Kidney Int* 1990;38(4):736–743.
173. Nadasdy T, Laszik Z, Blick KE, et al. Tubular atrophy in the end-stage kidney: A lectin and immunohistochemical study. *Hum Pathol* 1994;25:22.
174. Takazakura E, Sawabu N, Handa A, et al. Intrarenal vascular changes with age and disease. *Kidney Int* 1972;2(4):224–230.
175. Tracy RE, Ishii T. What is 'nephrosclerosis'? Lessons from the US, Japan, and Mexico. *Nephrol Dial Transplant* 2000;15(9):1357–1366.
176. Tracy RE. Renal vasculature in essential hypertension: A review of some contrarian evidence. *Contrib Nephrol* 2011;169:327–336.
177. Tracy RE, Newman WP III, Wattigney WA, et al. Histologic features of atherosclerosis and hypertension from autopsies of young individuals in a defined geographic population: The Bogalusa Heart Study. *Atherosclerosis* 1995;116(2):163–79.
178. Tracy RE, Parra D, Eisaguirre W, et al. Influence of arteriolar hyalinization on arterial intimal fibroplasia in the renal cortex of subjects in the United States, Peru, and Bolivia, applicable also to other populations. *Am J Hypertens* 2002;15(12):1064–1073.

179. Hill GS, Hedes D, Bariety J. Morphometric study of arterioles and glomeruli in the aging kidney suggests focal loss of autoregulation. *Kidney Int* 2003;63:1027–1036.
180. Hughson MD, Buchwald D, Fox M. Renal neoplasia and acquired cystic disease in patients receiving long-term dialysis. *Arch Pathol Lab Med* 1986;110:592.
181. Mailloux LV, Napolitano B, Bellucci AG, et al. Renal vascular disease causing end-stage renal disease, incidence, clinical correlates, and outcomes: A 20 year experience. *Am J Kidney Dis* 1994;24:662.
182. Moody WE, Edwards NC, Chue CD, et al. Arterial disease in chronic kidney disease. *Heart* 2013;99:365–372.
183. Adamczak M, Wiecek A. Ischemic nephropathy—pathogenesis and treatment. *Nefrologia* 2012;32:432–438.
184. Saric M, Kronzon I. Cholesterol embolization syndrome. *Curr Opin Cardiol* 2011;26:472–479.
185. Meehan SM, Nadasdy T. Tubulointerstitial diseases. In: Zhou XJ et al., eds. *Silva's Diagnostic Renal Pathology*. New York: Cambridge University press, 2009:407–435.
186. Rule AD, Krambeck AE, Lieske JC. Chronic kidney disease in kidney stone formers. *Clin J Am Soc Nephrol* 2011;6:2069–2075.
187. Keddiss MT, Rule AD. Nephrolithiasis and loss of kidney function. *Curr Opin Nephrol Hypertens* 2013;22:390–396.
188. Perneger TV, Whelton PK, Klag MJ. Risk of kidney failure associated with the use of acetaminophen, aspirin, and nonsteroidal antiinflammatory drugs. *N Engl J Med* 1994;331:1675.
189. Henrich WL. Analgesic nephropathy. *Trans Am Clin Climatol Assoc* 1998;109:147–158.
190. Buckalew Jr VM, Shey HM. Renal disease from habitual antipyretic analgesic consumption: An assessment of the epidemiological evidence. *Medicine* 1986;11:291.
191. Henrich WL, Agoda LE, Barrett B, et al. National Kidney Foundation position paper: Analgesics and the kidney: Summary and recommendations to the Scientific Advisory Board of the National Kidney Foundation. *Am J Kidney Dis* 1996;27:162.
192. Henrich WL, Clark RL, Kelly JP, et al. Non-contrast-enhanced computerized tomography and analgesic-related kidney disease: Report of the National analgesic nephropathy study. *J Am Soc Nephrol* 2006;17:1472–1480.
193. Hughson MD, Johnson K, Young RJ, et al. Glomerular size and glomerular sclerosis: Relationship to disease categories, glomerular solidification, and ischemic obsolescence. *Am J Kidney Dis* 2002;39:649.
194. Tracy RE. Blood pressure related separately to parenchymal fibrosis and vasculopathy of the kidney. *Am J Kidney Dis* 1992;20:2.
195. Hughson MD, McManus JF, Hennigar GR. Studies on end-stage kidneys. II. Embryonal hyperplasia of Bowman's capsular epithelium. *Am J Pathol* 1978;91:71.
196. DeSilva K, Tobias V, Kainer G, et al. Metanephric adenoma with embryonal hyperplasia of Bowman's capsular epithelium: Previously unreported association. *Pediatr Dev Pathol* 2000;3:472.
197. Ogata K. Clinicopathologic study of kidneys from patients on chronic dialysis. *Kidney Int* 1990;37:1333.
198. McManus JFA, Hughson MD, Hennigar GR, et al. Dialysis enhances renal epithelial proliferations. *Arch Pathol Lab Med* 1980;104:192.
199. McManus JFA, Hughson MD. Studies on end-stage kidneys. V. Unusual epithelial activity or remarkable endothelial metaplasia: Findings in a dialyzed kidney. *Am J Surg Pathol* 1979;3:229.
200. McManus JF, Hughson MD, Fitts CT, Williams AV. Studies on end-stage kidneys. I. Nodule formation in intrarenal arteries and arterioles. *Lab Invest* 1977;37:339.
201. Farraggiana T, Venkatesheshan VS, Inagami T, et al. Immunohistochemical localization of renin in end-stage kidneys. *Am J Kidney Dis* 1988;12:194.
202. Van Buren PN, Toto RD. The pathogenesis and management of hypertension in diabetic kidney disease. *Med Clin North Am* 2013;97:31–51.
203. Pitcock JA, Johnson JG, Share L, et al. Malignant hypertension due to musculo-mucoid intimal hyperplasia of intrarenal arteries. *Circ Res* 1975;36(Suppl 1):S33.
204. Hughson MD, Fox M, Garvin AJ. Pathology of the end-stage kidney after dialysis. *Progress Reprad Urinary Tract Pathol* 1990;2:157.
205. Hughson MD, Harley RA, Hennigar GR. Cellular arteriolar nodules: their presence in heart, pancreas, and kidney of patients with treated malignant hypertension. *Arch Pathol Lab Med* 1982;106:71.
206. Dobyan DC, Truong LD, Eknayan G. Renal malakoplakia reappraised. *Am J Kidney Dis* 1993;33:243.
207. Li L, Parwani AV. Xanthogranulomatous pyelonephritis. *Arch Pathol Lab Med* 2011;135:671–674.
208. Haggitt RC, Pitcock JA, Muirhead EE. Renal medullary fibrosis in hypertension. *Hum Pathol* 1971;2:587.
209. Zhuo JL. Renomedullary interstitial cells: A target for endocrine and paracrine actions of vasoactive peptides in the renal medulla. *Clin Exp Pharmacol Physiol* 2000;27:465–473.
210. Hughson MD, McManus JFA, Fitts CT, et al. Studies on end-stage kidneys. III. Glycogen deposition in interstitial cells of the renal medulla. *Am J Clin Pathol* 1979;72:400.
211. Levine E, Slusher SL, Grantham JJ, et al. Natural history of acquired renal cystic disease in dialysis patients: A prospective longitudinal CT study. *Am J Radiol* 1991;156:501.
212. Ishikawa I, Hayama S, Morita K, et al. Long-term natural history of acquired cystic disease of the kidney. *Ther Apher Dial* 2010;14:409–416.
213. Schwarz A, Vatandaslar S, Merkel S, et al. Renal cell carcinoma in transplant recipients with acquired cystic kidney disease. *Clin J Am Soc Nephrol* 2007;2:750–756.
214. Grantham JJ. Acquired cystic kidney disease. *Kidney Int* 1991;40:143.
215. Flamming S. Renal cell carcinoma in acquired cystic kidney disease. *Histopathology* 2010;56:395–400.
216. Park JH, Kim YO, Park JH, et al. Comparison of acquired cystic disease between hemodialysis and continuous ambulatory peritoneal dialysis. *Korean J Med* 2000;15:51.
217. Feiner HD, Katz LA, Gallo GR. Acquired cystic disease of the kidney in chronic dialysis patients. *Urology* 1981;12:260.
218. Lubensky IA, Schmidt L, Zhuang Z, et al. Hereditary and sporadic papillary renal cell carcinomas with *c-met* mutations share a distinct morphologic phenotype. *Am J Pathol* 1999;155:517.
219. Konda R, Sato H, Hatafuku F, et al. Expression of hepatocyte growth factor and its receptor c-met in acquired renal cystic disease associated with renal cell carcinoma. *J Urol* 2004;171:2166.
220. Oya M, Mikami S, Mizuno K, et al. C-jun activation in acquired cystic kidney disease and renal cell carcinoma. *J Urol* 2005;174:726.
221. Bakir AA, Hasnain M, Young S, et al. Dialysis associated renal cystic disease resembling autosomal dominant polycystic kidney disease: A report of two cases. *Am J Nephrol* 1999;19:519.
222. Liapis H, Winyard P. Developmental defects and cystic diseases of the kidney. In: Jennette JC, Olson JL, Silva FG, D'Agati V, eds. *Heptinstall's Pathology of the Kidney*, 7th ed. Philadelphia: Lippincott-Raven Publishers, 2014.
223. Chung-Park M, Ricanati E, Lanckerani M, et al. Acquired renal cysts and multiple renal cell and urothelial tumors. *Am J Clin Pathol* 1983;141:238.
224. Hogg RJ. Acquired renal cystic disease in children prior to the start of dialysis. *Pediatr Nephrol* 1992;6:176.
225. Deck MA, Verani R, Silva FG, et al. Histogenesis of renal cysts in end-stage renal disease (acquired cystic kidney disease): An immunohistochemical and lectin study. *Surg Pathol* 1988;1:391.
226. Hughson MD, Hennigar GR, McManus JF. Atypical cysts, acquired cystic disease and renal cell tumors in end-stage dialysis kidneys. *Lab Invest* 1980;42:475.
227. Farraggiana T, Bernstein J, Strauss L, et al. Use of lectins in the study of histogenesis of renal cysts. *Lab Invest* 1985;53:575.
228. Zeir M, Fehrenbach P, Geberth S, et al. Renal histology in polycystic disease with incipient and advanced renal failure. *Kidney Int* 1992;42:1259.
229. Tickoo SK, dePeralta-Venturina MN, Harik LR, et al. Spectrum of epithelial neoplasms in end-stage renal disease: an experience from 66 tumor-bearing kidneys with emphasis on histologic patterns distinct from those in sporadic adult renal neoplasia. *Am J Surg Pathol* 2006;30:141–153.
230. Stewart JH, Buccianti G, Agoda L, et al. Cancers of the kidney and urinary tract in patients on dialysis for end-stage renal disease: An analysis of data from the United States, Europe, and Australia and New Zealand. *J Am Soc Nephrol* 2003;14:197.
231. Hughson MD, Bigler S, Dickman K, et al. Renal cell carcinoma of end-stage renal disease: An analysis of chromosomes 3, 7, and 17 abnormalities by microsatellite amplification. *Mod Pathol* 1999;12:301.

232. Chudek J, Herbers J, Wilhelm M, et al. The genetics of renal tumors of end-stage renal dialysis differs from those occurring in the general population. *J Am Soc Nephrol* 1998;9:1045.
233. Yoshida M, Yao M, Ishikawa I, et al. Somatic von Hippel-Lindau disease gene mutations in clear-cell carcinomas associated with end-stage renal disease/acquired cystic disease of the kidney. *Genes Chromosomes Cancer* 2002;35:359.
234. Hughson MD, Schmidt L, Zbar B, et al. Renal carcinoma of end-stage renal disease: A histopathologic and molecular genetic study. *J Am Soc Nephrol* 1996;7:2461.
235. Inoue T, et al. Genomic profiling of renal cell carcinoma in patients with end-stage renal disease. *Cancer Sci* 2012;103:569–576.
236. Sahin E, dePinho RA. Axis of aging: Telomeres, P53 and mitochondria. *Nat Rev Mol Cell Biol* 2012;13:397–404.
237. Melk A, Ramassar V, Helms LM, et al. Telomere shortening in kidneys with age. *J Am Soc Nephrol* 2000;11(3):444–453.
238. Frenkel-Denkberg G, Gershon D et al. The function of hypoxia-inducible factor 1 (HIF-1) is impaired in senescent mice. *FEBS Lett* 1999;462:341–344.
239. Labunsky VM, Gladyshev VN. Role of reactive oxygen species-mediated signaling in aging. *Antioxid Redox Signal* 2013;19:1362–1372.
240. Houben JM, Moonen HJ, van Schooten FJ, et al. Telomere length assessment: Biomarker of chronic oxidative stress? *Free Radic Biol Med* 2008;44:235–246.
241. Baylis C. Sexual dimorphism: The aging kidney, involvement of nitric oxide deficiency and angiotensin II overactivity. *J Gerontol A Biol Sci Med Sci* 2012;67:1365–1372.
242. Basso N, Paglia N, Stella I, et al. Protective effect of the inhibition of the renin-angiotensin system on aging. *Regul Pept* 2005;128(3):247–252.
243. de Cavanagh EM, Piotrkowski B, Basso N, et al. Enalapril and losartan attenuate mitochondrial dysfunction in aged rats. *FASEB J* 2003;17(9):1096–1098.
244. Kurosu H, Yamamoto M, Clark JD, et al. Suppression of aging in mice by the hormone Klotho. *Science* 2005;309:1829–1833.
245. Urakawa I, Yamazaki Y, Shimada T, et al. Klotho converts canonical FGF receptor into a specific receptor for FGF23. *Nature* 2006;444:770–774.
246. Hu MC, Shiizaki K, Kuro-o M, et al. Fibroblast growth factor 23 and klotho: Physiology and pathophysiology of an endocrine network of mineral metabolism. *Annu Rev Physiol* 2013;75:503–533.
247. Ohnishi M, Nakatani T, Lanske B, et al. In vivo genetic evidence for suppressing vascular and soft-tissue calcification through the reduction of serum phosphate levels, even in the presence of high serum calcium and 1,25-dihydroxyvitamin D levels. *Circ Cardiovasc Genet* 2009;2(6):583–590.
248. Ohnishi M, Razzaque MS. Dietary and genetic evidence for phosphate toxicity accelerating mammalian aging. *FASEB J* 2010;24(9):3562–3571.
249. Torres PU, Prie D, Molina-Bletry V, et al. Klotho: An antiaging protein involved in mineral and vitamin D metabolism. *Kidney Int* 2007;71(8):730–737.
250. Yamada Y, Ando F, Niino N, Shimokata H. Association of polymorphisms of the androgen receptor and klotho genes with bone mineral density in Japanese women. *J Mol Med* 2005;83(1):50–57.
251. Arking DE, Krebsova A, Macek M Sr, et al. Association of human aging with a functional variant of klotho. *Proc Natl Acad Sci U S A* 2002;99(2):856–861.
252. Ichikawa S, Imel EA, Kreiter ML, et al. A homozygous missense mutation in human KLOTHO causes severe tumoral calcinosis. *J Clin Invest* 2007;117(9):2684–2691.
253. Hartleben B, et al. Autophagy influences glomerular disease susceptibility and maintains podocyte homeostasis in aging mice. *J Clin Invest* 2010;120:1084–1096.
254. Blagosklonny MV. Program-like aging and mitochondria: Instead of random damage by free radicals. *J Cell Biochem* 2007;102:1389–1399.
255. Grillari J, Grillari-Voglauer R. Novel modulators of senescence, aging, and longevity: Small non-coding RNAs enter the stage. *Exp Gerontol* 2010;45:302–311.
256. Mair W, Dillin A. Aging and survival: The genetics of life span extension by dietary restriction. *Annu Rev Biochem* 2008;77:727–754.
257. Finkel T, Deng CX, Mostoslavsky R. Recent progress in the biology and physiology of sirtuins. *Nature* 2009;460:587–591.
258. Imai S. SIRT1 and caloric restriction: An insight into possible trade-offs between robustness and frailty. *Curr Opin Clin Nutr Metab Care* 2009;12:350–356.
259. Lagouge M, Argmann C, Gerhart-Hines Z, et al. Resveratrol improves mitochondrial function and protects against metabolic disease by activating SIRT1 and PGC-1alpha. *Cell* 2006;127:1109–1122.
260. Crandall JP, Oram V, Trandafirescu G, et al. Pilot study of resveratrol in older adults with impaired glucose tolerance. *J Gerontol A Biol Sci Med Sci* 2012;67:1307–1312.
261. Mattison JA, Roth GS, Beasley TM, et al. Impact of caloric restriction on health and survival in rhesus monkeys from the NIA study. *Nature* 2012;489:318–321.
262. Zeisberg M, Kalluri R. Cellular mechanisms of tissue fibrosis. 1. Common and organ-specific mechanisms associated with tissue fibrosis. *Am J Physiol Cell Physiol* 2013;304:C216–C225.
263. Tampe B, Zeiberger M. Contribution of genetics and epigenetics to progression of kidney fibrosis. *Nephrol Dial Transplant* 2013 Aug 23 [Epub ahead of print].
264. Komers R, Meyer TW, Anderson S. Pathophysiology and nephron adaptation in chronic kidney disease. In: Coffman TE, et al., eds. *Schrier's Diseases of the Kidney*. 2013:P2214–P2237.
265. Aldigier JC, Kanjanbuchi T, Ma LJ, et al. Regression of existing glomerulosclerosis by inhibition of aldosterone. *J Am Soc Nephrol* 2005;16:3306–3314.
266. Macconi D. Targeting the renin angiotensin system for remission/regression of chronic kidney disease. *Histol Histopathol* 2010;25:655–668.
267. Quaggin SE, Kapus A. Scar wars: Mapping the fate of epithelial-mesenchymal-myofibroblast. *Kidney Int* 2011;80:41–50.
268. Hertig A, Aglicheay D, Verine J, et al. Early epithelial phenotypic changes predict graft fibrosis. *J Am Soc Nephrol* 2008;19:1584–1591.
269. Rastaldi MR, Ferrario F, Giardino L, et al. Epithelial-mesenchymal transition of tubular epithelial cells in human renal biopsies. *Kidney Int* 2002;62:137–146.
270. Attanasio M, Uhlenhaut NH, Sousa VH, et al. Loss of GLIS2 causes nephronophthisis in human and mice by increased apoptosis and fibrosis. *Nat Gen* 2007;39:1018.
271. Oba S, Kumano S, Suzuki E, et al. miR-200b precursor can ameliorate renal tubulointerstitial fibrosis. *PLoS ONE* 2010;5:e13614.
272. Lorenzen JM, Haller H, Thum T. MicroRNAs are mediators and therapeutic targets in chronic kidney disease. *Nat Rev Nephrol* 2011;7:286–294.
273. Steegh FM, Gelens MA, Nieman FH, et al. Early loss of peritubular capillaries alter kidney transplantation. *J Am Soc Nephrol* 2011;22:1024–1029.
274. Ascián MJ, Maluf DG, Archer KJ, et al. Gene expression changes are associated with loss of kidney graft function and interstitial fibrosis and tubular atrophy: Diagnosis versus prediction. *Transplantation* 2011;91:657–665.
275. Khan F, Sar A, Gonul I, et al. Graft inflammation and histologic indicators of kidney chronic allograft failure: Low expressing interleukin-10 genotypes cannot be ignored. *Transplantation* 2010;90:630–638.
276. Snelgrove SL, Kausman JY, Lo C, et al. Renal dendritic cells adopt a proinflammatory phenotype in obstructive uropathy to activate T cells, but do not directly contribute to fibrosis. *Am J Pathol* 2012;180:91–103.
277. Veerappan A, Reid AC, O'Connor N, et al. Mast cells are required for the development of renal fibrosis in the rodent unilateral ureteral obstruction model. *Am J Physiol Renal Physiol* 2012;302:F192–F204.
278. Semedo P, Donizetti-Oliveira C, Burgos-Silva M, et al. Bone marrow mononuclear cells attenuate fibrosis development after severe acute kidney injury. *Lab Invest* 2010;90:685–695.
279. Kim DH, Moon SO, Jung YJ, et al. Mast cells decrease renal fibrosis in unilateral ureteral obstruction. *Kidney Int* 2009;75:1031–1038.
280. Mehrotra R, Kermah D, Fried L, et al. Racial differences in mortality among those with CKD. *J Am Soc Nephrol* 2008;19:1403–1410.
281. Derose SF, Rutkowski MP, Levin NW, et al. Incidence of end-stage renal disease and death among insured African Americans with chronic kidney disease. *Kidney Int* 2009;76:629–637.
282. Frankenfield DL, Krishnan SM, Ashby VB, et al. Differences in mortality among Mexican-American, Puerto Rican, and Cuban-American dialysis patients in the United States. *Am J Kidney Dis* 2009;53:647–657.
283. Stack AG. Determinants of modality selection among incident dialysis patients: Results from a national Study. *J Am Soc Nephrol* 2002;13:1279–1287.

284. Mehrotra R, Blake P, Berman N, et al. An analysis of dialysis training in the United States and Canada. *Am J Kidney Dis* 2002;40:152–160.
285. Golper T. Patient education: Can it maximize the success of therapy? *Nephrol Dial Transplant* 2001;16(Suppl 7): S20–S24.
286. Jager KJ, Korevaar JC, Dekker FW, et al. The effect of contraindications and patient preference on dialysis modality selection in ESRD patients in the Netherlands. *Am J Kidney Dis* 2004;43:891–899.
287. Korevaar JC, Boeschoten EW, Dekker FW, et al. What have we learned about PD from recent major clinical trials? *Perit Dial Int* 2007;27: 11–15.
288. Levin A, Lewis M, Mortiboy P, et al. Multidisciplinary predialysis programs. Quantification and limitations of their impact on patient outcomes in two Canadian settings. *Am J Kidney Dis* 1997;29: 533–540.
289. Poppel DM, Cohen LM, Germain MJ. The renal palliative care initiative. *J Palliat Med* 2003;6:321–326.
290. Coresh J. CKD prognosis: Beyond the traditional outcomes. *Am J Kidney Dis* 2009;54:1–3.
291. Goovaerts T, Jadoul M, Goffin E. Influence of a pre-dialysis education programme (PDEP) on the mode of renal replacement therapy. *Nephrol Dial Transplant* 2005;20:1842–1847.
292. Castrale C, Evans D, Verger C, et al. Peritoneal dialysis in elderly patients: report from the French Peritoneal Dialysis Registry (RDPLF). *Nephrol Dial Transplant* 2010;25:255–262.
293. Carson RC, Juszcak M, Davenport A, et al. Is maximum conservative management an equivalent treatment option to dialysis for elderly patients with significant comorbid disease? *Clin J Am Soc Nephrol* 2009;4:1611–1619.
294. Jassal SV, Chiu E, Hladunewich M. Loss of independence in patients starting dialysis at 80 years of age or older. *N Engl J Med* 2009;361:1612–1613.
295. Kurella Tamura M, Covinsky KE, Chertow GM, et al. Functional status of elderly adults before and after initiation of dialysis. *N Engl J Med* 2009;361:1539–1547.
296. Chandna SM, Silva-Gane MD, Marshall C, et al. Survival of elderly patients with stage 5 CKD: Comparison of conservative management and renal replacement therapy. *Nephrol Dial Transplant* 2011;26:1608–1614.

tahir99 - UnitedVRG

Renal Transplant Pathology

Introduction 1322

- Brief historical background 1322
- Surgical procedure 1323
- Standard immunosuppression 1323
- Clinical outcome 1324

The renal allograft biopsy 1325

- Diagnostic value 1325
- Sensitivity and specificity 1325
- Safety 1326
- Diagnostic approach to biopsies 1326

Donor biopsies: procurement and zero-hour implantation 1327

- Procurement/harvest biopsies 1328
- Zero-hour implantation biopsies 1330

T-cell-mediated rejection 1331

Acute T-cell-mediated rejection 1332

- Pathologic findings 1332
- Molecular studies 1343
- Etiology and pathogenesis 1344
- Differential diagnosis 1348
- Clinical course, prognosis, therapy, and clinicopathologic correlations 1350

Chronic T-cell-mediated rejection 1351

Antibody-mediated rejection 1352

Hyperacute rejection 1356

- Introduction and clinical presentation 1356
- Pathologic changes 1356
- Etiology and pathogenesis 1357
- Clinical course, prognosis, therapy, and clinicopathologic correlations 1358

Acute antibody-mediated rejection 1359

- Introduction 1359

- Prevalence, clinical presentation, and risk factors 1359

- Pathologic findings 1359

- Differential diagnosis 1366

- Pathogenesis 1367

- Clinical course, prognosis, therapy, and clinicopathologic correlations 1368

Chronic antibody-mediated rejection 1371

- Prevalence, clinical presentation, and risk factors 1371

- Pathologic changes 1372

- Molecular studies 1379

- Etiology and pathogenesis 1379

- Risk factors, prognosis, and differential diagnosis 1379

- Variants of AMR 1381

- Natural history, therapy, and outcome 1381

Late graft biopsies 1383

- Differential diagnosis 1383

Protocol biopsies, surrogate endpoints, accommodation, and tolerance 1385

- Protocol biopsies 1385

- Surrogate endpoints 1387

- Molecular Studies 1388

- Accommodation, acceptance, and tolerance 1388

Acute ischemic injury 1389

- Pathologic findings of acute ischemic injury and differential diagnosis 1390

- Pathogenesis 1390

- Molecular Studies 1390

- Clinical presentation, prognosis, and therapy 1391

Calcineurin inhibitor toxicity 1391

- Introduction 1391
- Light microscopy 1391
- Immunofluorescence microscopy 1398
- Electron microscopy 1398
- Etiology and pathogenesis 1398
- Differential diagnosis 1399
- Clinical presentation, prognosis, and therapy 1400

Other drug-induced disease in allografts 1402

- Drug-induced acute tubulointerstitial nephritis 1402
- Rapamycin-/sirolimus-associated toxic effects 1402

Infections 1403

- Polyomavirus nephropathy 1403
- Cytomegalovirus 1410
- Adenovirus 1411
- Acute pyelonephritis 1413

Surgical and miscellaneous complications 1413

- Ureteral obstruction/leak/reflux 1413
- Lymphocele 1413
- Arterial or venous thrombosis 1414
- Arterial stenosis 1414
- Graft rupture 1414

De novo and recurrent renal diseases 1415

- De novo glomerular diseases 1415
- Recurrent glomerular diseases 1418

Posttransplant lymphoproliferative disorders and other neoplasia 1424**Molecular transplantation pathology: methods and applications 1428****INTRODUCTION**

Renal transplantation provides a cost-effective therapy worldwide that improves survival and quality of life for patients with end-stage renal disease (1). Over the last 5 years, an average of 16,000 patients per year received renal transplants in the United States, but over 100,000 patients wait for a donor (2). While overall survival is excellent, a substantial fraction of patients experience episodes of graft dysfunction, for which management is based primarily on renal biopsy findings (3). These biopsies provide urgent and perplexing challenges for the pathologist, because there is little time for consultation, several diseases can impinge on the graft simultaneously, and a wide range of potent therapy is possible, whose appropriate selection rests firmly on the accuracy of the diagnosis. We hope that this chapter will provide a practical resource to pathologists and clinicians trying to solve clinical dilemmas and to investigators seeking innovative solutions to prevent graft loss.

Brief Historical Background

The first public demonstration of a successful renal transplant was by Emerich Ullmann, on March 7, 1902, in the lecture hall of the Society of Physicians in Vienna (4). He showed a

dog with an autotransplant in the neck that produced visible urine for 5 days from the ureter in the skin; 12 days later, he reported his findings in the medical literature (5). In 1902, Dr. Ullmann also attempted the first kidney transplant (from a pig) to a patient, but this was technically unsuccessful (6). Alexis Carrel, working in Lyons, France, developed the end-to-end vascular suture techniques in 1902 that are widely used in transplantation and, for this and his subsequent work on organ preservation at the Rockefeller Institute in New York, received the Nobel Prize in 1912 (7). In 1906, Mathieu Jaboulay, also from Lyons, used Carrel's technique to transplant a xenograft kidney (pig or goat) to the limbs of two patients with chronic renal failure; both failed within an hour (8). Three years later, Ernest Unger in Berlin transplanted a monkey kidney to a girl dying of renal failure; no urine was produced, and Unger concluded that the biochemical barrier was insoluble (9). Working in some obscurity, Dr. Yu Yu Voronoy, in 1936 in Kherson, Ukraine, transplanted the first human kidney. The donor died from a head injury, and the recipient had acute renal failure from mercuric chloride poisoning. The kidney was ABO incompatible (B to O), and the kidney never worked, but the vessels were patent at autopsy 2 days later (10).

In 1945, Drs. David Hume, Charles Hufnagel, and Ernest Landsteiner at the Peter Bent Brigham Hospital and Harvard Medical School in Boston transplanted a human cadaver kidney to the axilla of a young woman comatose from acute renal failure due to septicemia (11). The kidney worked for several days and was then removed after the woman regained consciousness; her own kidneys then made a full recovery. In 1951–1953, Dr. Hume continued this approach, transplanting kidneys into the thighs of nine patients without immunosuppression; one graft functioned for 6 months (12). In 1952, N. Oeconomos and J. Hamburger performed the first living kidney transplant. A mother donated a kidney to her son, whose congenital single kidney had to be removed due to a traffic accident injury. The kidney functioned without any immunosuppression for 21 days before developing anuria (13).

Mastery of the surgical aspects encouraged the surgeons to begin transplanting kidneys from identical twins, who do not require immunosuppression. The first such operation was performed on December 23, 1954, by Drs. Hume, Joseph Murray, and Hartwell Harrison (14). The recipient survived 8 years, succumbing to recurrent disease, the major risk in twin recipients.

Broad clinical application awaited the definition of the underlying immunologic events and the means to thwart immunologic rejection. The need for skin graft treatment of war burn wounds motivated the scientific efforts of the young Peter Medawar to ponder “why it was not possible to graft skin from one human being to another, and what could be done about it.” Medawar did indeed do something about it, showing in 1953 that injection of lymphoid cells in neonatal mice sometimes established a lifelong, specific tolerance to subsequent transplanted skin from the same donor, for which he received the Nobel Prize in 1960 (15). The discovery of the immunosuppressive ability of 6-mercaptopurine by Robert Schwartz and William Damesheck in Boston in 1959 (16) was soon applied in humans in 1960. Gertrude Elion and George Hitchings (Nobel Prize 1988) at Burroughs Wellcome discovered azathioprine that Roy Calne in Cambridge proved beneficial and less toxic in dog kidney grafts (17). Joseph

Murray (Nobel Prize 1992) first tried azathioprine in humans and added corticosteroids to the regimen (14). The improved results obtained by combination of azathioprine with corticosteroids ushered in the era of clinical renal transplantation in the early 1960s, through the successful studies of Thomas Starzl (18) and Murray et al. (14). Innovative therapies, such as antithymocyte globulin (ATG or ALG) (1970s), cyclosporine and anti-CD3 monoclonal antibody (OKT3) (1980s), mycophenolate, tacrolimus (1990s), and others, have markedly increased success. Recent clinical trials with protocols to induce mixed or complete chimerism have shown promise of achieving Medawar's goal of specific tolerance without immunosuppression (19–21).

The pathologic literature on renal grafts began with the photomicrographs of canine allograft rejection, published by Carl Williamson of the Mayo Clinic in 1926. He illustrated a “marked lymphocytic infiltration” and “intense glomerulitis” in the dog and attributed graft loss to “atypical glomerular nephritis” (22). He noted that recipients responded differently to autografts and allografts and hoped that “in the future it may be possible to work out a satisfactory way of determining the reaction of the recipient's blood serum or tissues.” Subsequent work reported in 1953 by William Dempster in London (23) and Morten Simonsen in Denmark (24) showed that canine grafts are infiltrated by pyroninophilic mononuclear cells, which they concluded were donor-derived plasma cells and their precursors, a “response of the renal mesenchyma to the recipients' individual-specific antibodies and antigens” (25). The infiltrating cells were later shown to be of recipient origin using radiolabeled cells (26). Simonsen illustrated an example of endarteritis in a small artery in a dog, but did not appreciate its distinctiveness, interpreting the lesions, which also had fibrinoid necrosis, as “periarteritis nodosa” (24).

The first renal transplant biopsy in a patient was in 1952, when a living donor kidney developed anuria on day 21. The slides were recently discovered at the Necker Hospital and, upon review, show a combination of T-cell- and antibody-mediated rejection (Fig. 29.1) (27). Appreciation of the general pathology of human renal transplants began in the 1960s, particularly by Gustav Dammin at Harvard and Kendrick Porter at St. Mary's Hospital in London. Among the early discoveries were the descriptions of endarteritis in acute rejection by Dammin, which he attributed correctly to recipient mononuclear cells (28), chronic transplant arteriopathy (29) and chronic transplant glomerulopathy by Porter (30,31), the relationship of the arteriopathy to anti-human leukocyte antigen (HLA) antibodies by Paul Russell et al. (32), and the pathology of hyperacute rejection and its relationship to humoral antibodies by Kissmeyer-Nielsen et al. (33). The recurrence of glomerulonephritis in transplants was first described in isografts by Richard Glasscock, Dammin, and colleagues (34). Perhaps most important to pathologists, Priscilla Kincaid-Smith demonstrated the value of the renal biopsy in clinical management, concluding that “the renal biopsy provides a clear-cut diagnosis of rejection and indicates which patients should receive prompt treatment for rejection” (35). Our goal is to make this always true!

Surgical Procedure

The donor kidney is usually placed in the right iliac fossa, which has the advantages of simplicity and accessibility for observation and biopsy. The main renal artery is anastomosed

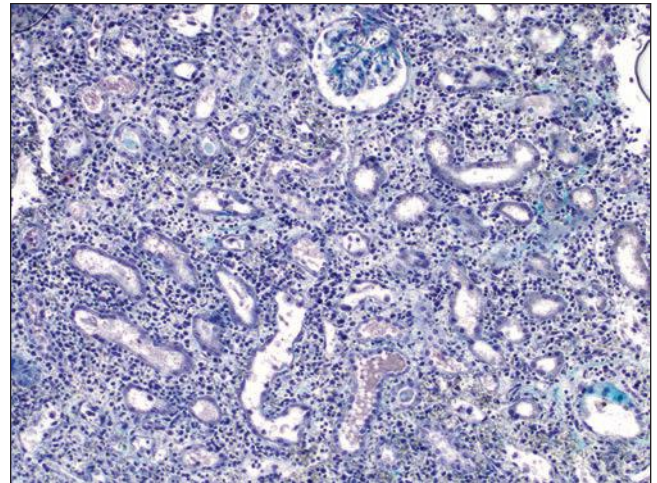


FIGURE 29.1 Photomicrograph of the first renal transplant biopsy (27). A living related kidney transplant (mother to son) was done under no immunosuppression in Paris in 1952 at the Necker Hospital under the supervision of Jean Hamburger. The biopsy was done for anuria on day 21 and shows a diffuse infiltrate of activated mononuclear cells, capillaritis with intracapillary neutrophils, glomerulitis, interstitial hemorrhage, and severe tubular injury, typical of combined acute TCMR (T-cell mediated rejection) and AMR. Trichrome-stained slide. (Courtesy of Christophe Legendre, Paris.)

end to end to the right hypogastric artery (or end to side to the iliac artery with a cuff of donor aorta). When the renal arteries are multiple, various procedures have been devised, making sure the lower pole artery is not sacrificed, because it usually also supplies the ureter. Endarterectomy may be necessary in atherosclerotic vessels. The renal vein is anastomosed end to side to the iliac vein. Two alternative techniques are commonly used for the ureter, either implantation of the donor ureter into the recipient bladder or anastomosis of the donor pelvis to the recipient ureter. The advantages of the former are that the recipient kidney does not have to be removed and a normal recipient ureter is not required. The main disadvantage is that the blood supply to the upper ureter (which comes from the kidney) can be compromised, and later, stenosis can result; reflux may also develop. The pyeloureteral anastomosis minimizes the risk of ureteral ischemia and stenosis, but urine leaks are more common, if not done properly. Pyeloureteral anastomosis requires a recipient nephrectomy, which provides the potential benefit to determine the primary disease and exclude malignancy in the end-stage kidney. Double kidney transplants from marginal donors have also been performed with success.

Standard Immunosuppression

Calcineurin inhibitors (CNIs, cyclosporine or tacrolimus) are the mainstay of most standard protocols, usually with corticosteroids (prednisolone or prednisone) and mycophenolate mofetil (MMF) or azathioprine (“triple therapy”). The drugs are tapered in the initial 3 to 6 months to baseline maintenance levels, which in adults are typically approximately 100 ng/mL of cyclosporine and 5 to 15 ng/mL of tacrolimus at the trough level, depending on the other drugs in the regimen and the immunologic risk (36). ATG can substitute for CNIs in

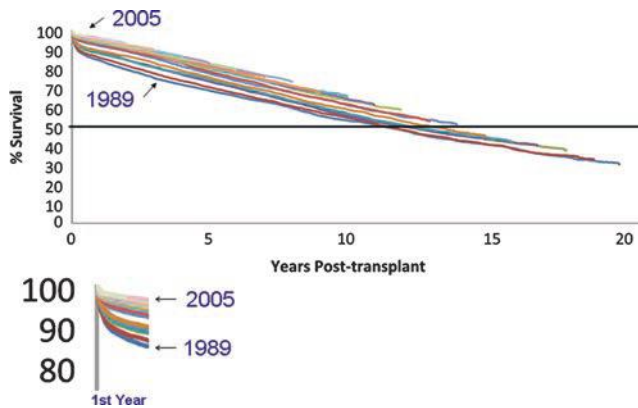
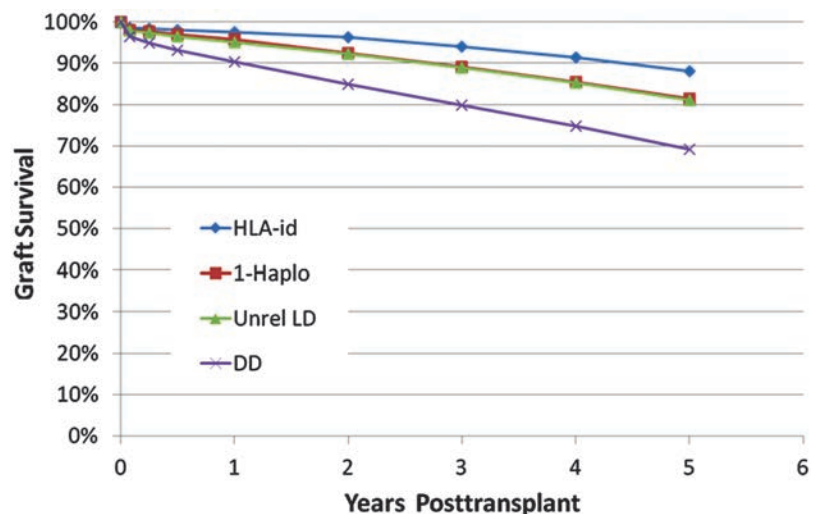


FIGURE 29.2 Kaplan-Meier plot of kidney graft failure by year of transplantation from 1989 to 2005 for 140,900 standard criteria deceased donor kidneys, censored for death due to other causes (38). Each colored line is a single year cohort from transplant year 1989 on the bottom to 2005 on the top. The half-life is indicated by the horizontal line at 50%. Most of the improved survival during this time period occurred in the first year posttransplant (shown in the **insert**). The slopes after 1 year are close to parallel, indicating little or no change in the rate of late graft loss. (Reprinted with permission from Lamb KE, Lodhi S, Meier-Kriesche HU. Long-term renal allograft survival in the United States: A critical reappraisal. *Am J Transplant* 2011;11(3):450–62; copyright 2011, John Wiley and Sons.)

patients with delayed graft function (DGF). For treatment of acute rejection episodes, the usual first defense is a short course (2 to 3 days) of high-dose steroids orally (prednisolone) or intravenously (methylprednisolone), followed if necessary by rescue with ATG. Additional FDA-approved drugs include rapamycin (sirolimus, a blocker of IL-2 signaling and cell proliferation) and monoclonal antibodies to the IL-2 receptor (basiliximab [Simulect]), CD52 (daclizumab, CAMPATH1) and CD20 (rituximab [Rituxan]), and inhibitors of costimulatory signals (belatacept). All of these drugs have the potential for complications related to immunosuppression, and some cause nephrotoxicity, especially CNI.

FIGURE 29.3 Graft survival according to the HLA match and type of donor. Survival of HLA-identical sibling grafts (HLA-id) is better than for related grafts with one HLA haplotype match (1-Haplo), demonstrating the importance of complete HLA matching. However, living unrelated grafts (Unrel LD) have better survival than deceased donor grafts (DD), indicating the state of the graft itself is also important. Living unrelated grafts have similar survival as one HLA haplotype-matched living grafts. Figure provided by Michael Cecka (University of California at Los Angeles) based on data from the Renal Transplant Registry of the Organ Procurement and Transplantation Network and United Network of Organ Sharing as of March 2011. N, Number of patients and $T_{1/2}$, calculated half-life in years.



Clinical Outcome

The outcome of the graft depends on the source of the graft (deceased, living related, living nonrelated) and the histocompatibility between the donor and recipient (Fig. 29.2) (37). Graft and patient survival curves have improved dramatically over the last two decades (Fig. 29.3) (38). The biggest improvement is in the first year, with a lower frequency of rejection, improved response to antirejection therapy, and fewer infectious complications. The long-term loss of grafts has shown only modest improvement, with almost parallel curves of attrition in the last decade.

Living Donors

Isografts (between monozygotic twins) are not immunologically rejected, and no immunosuppression is required. However, isografts are lost from recurrence of the original disease. In the largest compilation, 5-year graft survival was 70% (39). After 5 years, the graft survival was quite stable, with 55% surviving 27 years. Eight of the graft failures (27%) were due to recurrent glomerulonephritis or vasculitis 3 months to 20 years after transplantation, and 18% were lost in the first year.

Human leukocyte antigen (HLA)-identical grafts from siblings have identical major histocompatibility complex (MHC) genes on both chromosomes 6, but differ randomly in non-MHC (minor) histocompatibility antigens encoded by genes that segregate independently. These grafts do well, with a 91% 5-year graft survival, compared with 79% 5-year survival of non-HLA-identical sibling grafts (40). HLA-identical grafts do develop acute T cell mediated rejection (TCMR) (46% to 54%) (40,41) and rarely acute antibody mediated rejection (AMR) (42,43); chronic rejection occurs in about 2% over 10 years, about half the rate of haploidentical grafts (44–46). These results demonstrate that non-MHC antigens can elicit a strong recipient immune response for acute TCMR, but have relatively little role in chronic rejection.

HLA-haploidentical grafts (from parent, child, or sibling) have a common chromosome 6 region of one MHC locus but differ in the other MHC and non-MHC antigens. These grafts have a half-life of 17 years, significantly worse than the HLA-identical grafts ($T_{1/2}$ 29 years). The 10-year survival difference compared with MHC-identical grafts demonstrates the

importance of the MHC as a target in the immune response in chronic rejection.

Living unrelated grafts, typically from a spouse or friend, have results almost as good as haploidentical grafts, with a half-life of 17 years and much better than deceased donor grafts of similar MHC mismatch ($T_{1/2}$ 10 years). Thus, the condition of the donor (living vs. deceased) is more important than the MHC match.

Deceased Donors

Deceased donors represent the majority of grafts used worldwide. Five-year graft survival for first kidney transplants performed in 1999–2003 is 71% to 75% for white recipients in the United States aged 20 to 64 years with lower survival for older (57%) and black recipients (60% to 61%) and higher survival among recipients in Europe (77% to 82%) (37). Living donor grafts had about an 8% increase in 5-year survival in the same series. Graft survival is also a function of the number of mismatched antigens (see Fig. 29.3) (47). With zero HLA-A, HLA-B, and HLA-DR mismatches, the long-term survival approaches living donors, with a graft half-life of 14 years, compared with six mismatches with a half-life of 8 years. The estimated overall improvement of survival justifies the cost of HLA matching by the United Network for Organ Sharing (UNOS).

Because of the shortage of donors, the standards for accepting a graft are becoming less stringent. Expanded criteria donors (ECDs) are defined by UNOS as those over age 60 years or age 51 to 59 with any two additional risk factors (cerebrovascular death, hypertension, serum creatinine level greater than 1.5 mg/dL). Grafts from these donors have a poorer outcome, but still have a 70% 1-year graft survival (48). Selection of older donor kidneys based on histologic criteria leads to graft survival equivalent to grafts from young donors. Kidneys from donors whose heart stopped before the kidney is harvested (asystolic donors) have a striking increase in the requirement of dialysis posttransplant (DGF) (93% vs. 17%), but a satisfactory long-term outcome (49). Protocol biopsies at 6 to 12 months show these kidneys have no increase in fibrosis compared with those from heart-beating deceased donors (50).

Factors That Affect Graft Survival

In addition to the type of immunosuppression, kidney source, and MHC match, the key factors that affect outcome are acute rejection episodes, presensitization, DGF, donor and recipient

race and age, and transplant center. DGF is an adverse complication primarily due to the associated increased risk of acute rejection (51), although this has been questioned in recent series (51a). Black race of recipient is an adverse risk factor, whether the donor is white or black. The survival of HLA-identical sibling kidneys is the same in blacks as whites, but survival of grafts with a one-haplotype match is no different than deceased donor grafts. Outcome varies by institution (“the center effect”) with a 10% to 15% difference in 1-year graft survival, arising in part from different levels of comorbidity among the recipients. The nature of the primary disease influences graft survival through recurrence and extrarenal complications (e.g., diabetes, hypertension, oxalosis, hemolytic uremic syndrome [HUS]).

THE RENAL ALLOGRAFT BIOPSY

Diagnostic Value

Renal biopsies remain the gold standard to determine the cause of graft dysfunction, which occurs in about 30% of recipients early after transplant and at a rate of 2% to 4% per year after the first year (3,52). Biopsies are particularly useful to guide treatment in ambiguous clinical situations and are used in combination with other diagnostic tests, including imaging and laboratory tests. Biopsies best distinguish acute rejection, acute tubular necrosis, infections such as polyomavirus nephropathy (PVN), thrombotic microangiopathy (TMA), recurrence of original disease, CNI toxicity, and chronic rejection (53,54). Biopsy findings change the clinical diagnosis in an average of 36% of patients (27% to 46%) and therapy in 59%, with no obvious diminishing value in the last 20 years (53–60) (Table 29.1). Biopsy results change therapy in both the early and late (greater than 1 year) posttransplant periods with approximately equal frequency (58,59). Most importantly, biopsy findings lead to reduced immunosuppression in 22% (19% to 39%) of patients.

Sensitivity and Specificity

The sensitivity of the biopsy depends on the size, number, and content of the cores. In a study of 130 biopsies with multiple cores, acute rejection was found in only one of two cores in 10% of the cases (61). Thus, the sensitivity of a single core is approximately 90%. Similarly, 10% of 79 paired biopsy cores had one core that was insufficient for the diagnosis of rejection (62). The sensitivity

TABLE 29.1 Clinical impact of the renal allograft biopsy

No. of biopsies	Changed clinical diagnosis	Changed therapy	Avoided immunosuppression	References
89	46%			(55)
35	46%	46%		(54)
64	42%	42%	30%	(53)
240		83%		(56)
95	30%	38%	18%	(57)
263		55%		(58)
100	27%			(60)
82		42%	19%	(59)
Total 968	36%	59%	22%	

of “*n*” biopsy cores can be calculated as $1 - (1 - \text{sensitivity of a single core})^n$. Accordingly, if one core has a sensitivity of 90%, two cores have a predicted sensitivity of 99%, substantiating the conventional wisdom that recommends two cores.

The specificity of the biopsy is impossible to measure because no higher standard for comparison is available. The short-term clinical course or response to therapy is not the final arbiter, because rejection may be occult or delayed. One study showed a specificity of 87% compared with a blinded retrospective clinical review (63). The results that show the biopsy results correlate with the clinical course in 80% to 89% of cases are also reassuring (56,61). Molecular testing for gene expression may increase the specificity and sensitivity of the biopsy and is a subject of active investigation.

Safety

Most renal biopsies are done with ultrasound-guided biopsy “guns” and 16- to 18-gauge needles (64,65). These have an excellent record of safety in experienced hands. None of the large series in adults reported any deaths due to biopsy (0/5026) and few graft losses (1/3996, 0.03%) (56,64–68). A multicenter audited series of 2127 protocol biopsies reported no patient deaths and one potentially avoidable graft loss (68). Pediatric transplant biopsies have a similar low complication rate: 0/212 biopsies from 19 centers led to death or graft loss, and only one required surgical exploration for bleeding (69). The types of complication are the same as from biopsies of native kidneys, namely, hematuria, ureteral obstruction from clots, hemorrhage, shock, and arteriovenous fistula. Follow-up showed 75% of the fistulas spontaneously closed, and none had an impact on renal function requiring intervention (70).

Ultrasound guidance increases the probability of obtaining cortex from 75% to 91%; guidance by on-site examination with a dissecting microscope increases adequacy to 100% (71). Transfemoral vein renal biopsies offer an alternative method for patients who are deemed unsuitable for percutaneous biopsy. These yield adequate tissue in 51% of the biopsies (10 or more glomeruli) with rare major complications (1/58 causing obstruction from hematuria) (72). A 16-gauge needle appears to be the best compromise between tissue yield and complications. Among 1171 protocol biopsies in adults with an automated 16- or 18-gauge needle, no graft losses occurred (73). The 16-gauge needle had no worse major complication rate (73,74) and a better yield of tissue than the 18-gauge needle (76% vs. 53% yielded greater than 7 glomeruli and ≥ 1 artery) (73). The 16-gauge needle had a higher hematoma rate than did the 18-gauge needle in children (75).

Diagnostic Approach to Biopsies

Typically, two cores are divided for light and immunofluorescence microscopy, with most of both cores going for light microscopy. Most biopsies taken after 1 year are processed for electron microscopy. Electron microscopy is important if glomerular disease or chronic rejection is suspected. We prepare about 15 sections stained with hematoxylin and eosin (H&E) (three levels) and five for trichrome and five cut at 2 to 4 μm and stained with periodic acid-Schiff reagent (total of five slides); Jones silver stain is an alternative. Elastin stains are recommended for evaluation of intimal fibrosis. Each section is carefully examined for (a) the nature and degree of the interstitial cellular infiltrate (e.g., activated mononuclear cells, edema,

intracapillary cells); (b) arterial and arteriolar lesions (e.g., endarteritis, myocyte necrosis, thrombi, nodular hyaline); (c) tubular injury, inflammation (tubulitis), and viral inclusion bodies; and (d) glomerular lesions. Further levels are obtained if no diagnosis is evident. We recommend that all biopsies be assessed for C4d, as well as IgG, IgA, IgM, C3, lambda, kappa, albumin, and fibrin by immunofluorescence microscopy or by immunohistochemistry (IHC) when frozen sections are not available. Frozen sections for light microscopy are of limited value, but can be prepared in urgent situations; the diagnostic accuracy was reported to be 89% compared with permanent sections (76). Rapid (2 to 4 hours) permanent sections are an alternative used at our centers and provide quite satisfactory preparations.

Adequacy

The recommended requirements are at least 10 nonsclerotic glomeruli and 2 arteries (with two or more medial layers) (61,77). However, the adequacy of the biopsy sample depends entirely on the lesions seen. One artery with endarteritis is sufficient for the diagnosis of acute rejection, even if no glomerulus is present; similarly, immunofluorescence or electron microscopy of one glomerulus is adequate to diagnose membranous glomerulonephritis. In contrast, a large portion of cortex with 10 glomeruli and a minimal infiltrate does not exclude rejection. A normal medulla also does not rule out rejection (78), because medulla has a lower sensitivity for rejection than cortex (77%) (79). However, when a prominent mononuclear infiltrate and tubulitis are present in the medulla, rejection is highly likely, provided infection, obstruction, and drug allergy are excluded (79). The minimal adequacy for C4d scoring is for viable cortical or medullary tissue. No glomeruli are required. This means that if tissue is sparse, the portion with medulla can be used for C4d staining. Necrotic and scarred areas are not sufficient, since they are commonly negative, even in samples positive elsewhere.

Diagnostic Classification

Jean Hamburger emphasized that graft rejection could not be attributed merely to different intensities of a single type of immune response (80). This has proved to be true, with many different immunologic mechanisms of injury to each of the cellular targets in the graft. The principal alloreactive initiators of graft rejection are T cells and antibodies, which trigger a variety of secondary mediators (e.g., activation of macrophages, complement). The ideal diagnostic classification should be based on pathogenesis, have therapeutic relevance, and be reproducible. The classification in Table 29.2 is our current attempt to meet these criteria.

Banff Criteria and Scoring System

Several grading systems have been proposed over the years to codify renal allograft rejection. At the present time, the most widely used system is called the “Banff working schema” (“Banff” for short). Banff started as a collaborative effort of investigators meeting in Banff, Canada, with the leadership of Kim Solez, Philip Halloran, and Lorraine Racusen, to achieve a consensus that would be acceptable to the FDA for drug trials and useful for routine diagnostic use (77). This system has gone through a number of significant revisions and modifications over the years since it was published in 1993. The most important of these were the incorporation of the NIH Cooperative Clinical Trials in Transplantation (CCTT) criteria (61) in 1999, which separated the category of endarteritis (81), and

TABLE 29.2 Pathologic classification of renal allograft diseases**I. Immunologic rejection**

- A. T-cell–mediated rejection^a
 - 1. Acute
 - i. Tubulointerstitial (Banff type I and borderline/suspicious)
 - ii. Endarteritis (Banff type II)
 - iii. Arterial transmural inflammation or fibrinoid necrosis (Banff type III)
 - 2. Chronic
 - i. Tubulointerstitial inflammation and fibrosis
 - ii. Transplant arteriopathy
- B. Antibody-mediated rejection^a
 - 1. Hyperacute
 - 2. Acute^d
 - i. Acute tubular injury (Banff type I)
 - ii. Capillaritis (Banff type II)
 - iii. Arterial fibrinoid necrosis (Banff type III)
 - 3. Chronic
 - i. Transplant glomerulopathy
 - ii. Multilamination PTC basement membranes
 - iii. Transplant arteriopathy
 - 4. Variants
 - i. Smoldering/indolent (mononuclear capillaritis)
 - ii. C4d deposition without evidence of active rejection
 - iii. C4d-negative (mostly chronic or smoldering)

II. Auto/alloantibody-mediated diseases

- A. De novo membranous glomerulonephritis
- B. Anti-GBM disease in Alport recipients
- C. Anti-nephrin disease in recipients with congenital nephrosis (Finnish type)
- D. Anti-TBM disease in TBM antigen–deficient recipients
- E. Anti-angiotensin II type 1 receptor antibody syndrome

III. Nonalloimmune injury

- A. Acute ischemic injury (ATN)
- B. Drug toxicity
 - 1. CNI toxicity (cyclosporine, tacrolimus)
 - 2. mTOR inhibitor toxicity (rapamycin, sirolimus)
 - 3. Antiviral drug tubular toxicity (foscarnet, adefovir, tenofovir)
 - 4. Acute allergic tubulointerstitial nephritis
- C. Infection
 - 1. Viral^b
 - i. Polyomavirus
 - ii. Adenovirus
 - iii. Cytomegalovirus
 - iv. Herpes simplex
 - 2. Bacterial/fungal^b
 - i. Acute/chronic pyelonephritis
 - ii. Tuberculosis
 - iii. Malakoplakia
- D. Major vessel disease
 - i. Arterial/venous thrombosis
 - ii. Arterial dissection
 - iii. Arterial stenosis
 - iv. Atheromatous emboli
- E. Pelvis/ureter
 - 1. Urine leak
 - 2. Obstruction
- F. De novo glomerular disease^b: focal segmental glomerulosclerosis, diabetic nephropathy
- G. Neoplasia: Post-transplant lymphoproliferative disease
- H. Idiopathic: interstitial fibrosis and tubular atrophy, not otherwise classified (IF/TA, NOS)^c

IV. Recurrent primary disease^b

- A. Immunologic: IgA nephropathy, lupus nephritis, anti-GBM disease
- B. Metabolic: amyloidosis, diabetes, oxalosis
- C. Other: dense deposit disease, focal segmental glomerulosclerosis

^aOften, T-cell and AMR concur. Many features, such as transplant glomerulopathy or the multilamination of PTC basement membranes, can be induced by antibodies and/or T cells.

^bPartial list.

^cFormerly termed chronic allograft nephropathy, or CAN.

^dBanff 2013 includes endarteritis and thrombotic microangiopathy as potential manifestations of acute AM or mixed TCMR and AMR.

the addition of AMR in 2003 (82). Banff scores the individual elements of the biopsy by light microscopy and uses these to classify rejection (Table 29.3). Combinations of individual scores are then used to define various categories of acute and chronic rejection. While many details are still being refined, Banff has had a beneficial effect in the standardization of definitions for publications and provides a stimulus for consensus development and translational research.

The criteria for diagnosis of rejection are not absolute, but based on clinicopathologic correlations in patients on standard immunosuppressive therapy. Drugs have the ability to modify rejection, for example, a decrease in the intensity of infiltrate and edema with cyclosporine or a decrease in eosinophils with steroids. Some of the newer drugs may have other effects. For example, CAMPATH1, which profoundly depletes T and B cells, can lead to episodes that clinically behave like rejection,

yet do not meet the criteria of Banff, due to sparse mononuclear infiltrates (83). To the extent that our criteria correspond to mechanisms of the rejection process itself (tubulitis, endarteritis, capillaritis), the criteria will be robust. Nonetheless, we have to be prepared to identify novel features and mechanisms of rejection that might occur with new drugs.

DONOR BIOPSIES: PROCUREMENT AND ZERO-HOUR IMPLANTATION

Grafts typically had a previous “life,” and they often show some signs of hypertension-induced so-called arterionephrosclerosis and, occasionally, even other renal diseases. Both procurement and zero-hour implantation biopsies designate tissue samples obtained at the time of grafting to assess donor disease.

TABLE 29.3 Banff scores of individual features

Feature	Banff term	Banff Score			
		0	1	2	3
Interstitial inflammation (% of nonfibrotic cortex) ^a	i	<10%	10%–25%	26%–50%	>50%
Total inflammation (% all cortex)	ti	<10%	10%–25%	26%–50%	>50%
Tubulitis (maximum mononuclear cells/tubule) ^b	t	0	1–4	5–10	>10
Arterial inflammation (% lumen endarteritis) ^c	v	None	<25%	≥25%	Transmural or necrosis
Glomerulitis (% glomeruli involved) ^d	g	None	<25%	25%–75%	>75%
Capillaritis (cells per cortical PTC ^e ; requires >10% of PTC to be affected for scoring)	ptc	(<10%)	<5/PTC	5–10/PTC	>10/PTC
C4d deposition in PTC (% positive) ^f	C4d	0%	1%–9%	10%–50%	>50%
Interstitial fibrosis (% of cortex)	ci	≤5%	6%–25%	26%–50%	>50%
Tubular atrophy (% cortex)	ct	0%	≤25%	26%–50%	>50%
Arterial intimal thickening (% narrowing lumen of most severely affected artery) ^g	cv	0%	≤25%	26%–50%	>50%
Transplant glomerulopathy (% of capillaries with duplication in most severely affected glomerulus) ^h	cg	0%	≤25%	26%–50%	>50%
Arteriolar hyalinosis (number with focal or circumferential hyaline)	ah	None	1 focal	>1 focal	1 circumferential
Mesangial matrix increase (% affected glomeruli) ⁱ	mm	0%	≤25%	26%–50%	>50%

^aExcludes perivascular, nodular, and subcapsular infiltrates.

^bExcludes atrophic tubules; for longitudinal sections, count per 10 epithelial nuclei.

^cMononuclear cells in intima (v1,2) or media (v3).

^dThreshold for number of cells/glomerulus not defined.

^ePTC, peritubular capillary; note whether cells are only mononuclear cells or include neutrophils.

^fNote whether frozen or fixed tissue used. Requires at least 5 high-power fields of sample.

^gNote if lesions are characteristic of chronic rejection or fibroelastosis.

^hcg1 with duplication in >1 glomerular capillary loop in one glomerulus; cg1a changes seen by EM only, cg1b changes seen by light microscopy (according to 2013 updates to the Banff scoring scheme) (481).

ⁱIncrease defined as >2 mesangial cells in width in at least 2 glomerular lobules.

Procurement biopsies are primarily collected to give information on the organ suitability for transplantation, and implantation biopsies provide insight into preexisting diseases relevant for comparative analyses posttransplantation; thus, the diagnostic implications of both biopsy types are similar. Since procurement biopsies are often evaluated on a rush basis by general surgical pathologists during off-hours in the frozen section laboratory and recorded under the donor's name, the analysis is commonly rudimentary, and the results are often unavailable for subsequent graft management under the "new" recipient's name. In some cases, both procurement and zero-hour implantation biopsies are collected. In general, guidelines for the interpretation and recording of donor biopsies have not been definitively established. Often, Banff scoring criteria are used, which can, unfortunately, easily lead to subsequent confusion during the evaluation of diagnostic graft biopsies since the scoring results of "old preexisting donor lesions" versus "new de novo posttransplant changes" are not distinguished from each other using ci, ct, and cv scores.

Procurement/Harvest Biopsies

The pathologist may be asked to advise whether a particular kidney from a deceased donor is suitable for transplantation, sometimes in the middle of the night. The most common

questions are (a) the degree of scarring in the "marginal" donor, (b) the presence of active renal disease, and (c) the clinical significance of incidentally discovered neoplasms.

The question of donor vascular disease (hypertensive and age-related arterionephrosclerosis) arises more often now due to increasing use of older donors (84). The utilization of procurement biopsies increases with donor age: 5% at age 20, to 20% at age 45, 40% at age 55, and 60% at age 65 (85). Most studies show a correlation of glomerulosclerosis (86), interstitial fibrosis (87), and intimal fibrosis (88,89) with donor age. Up to 40 years of age, 54% of deceased donor biopsies are normal, while only 7% of donor kidneys 40 years or older are normal (90). However, even septuagenarians can have kidneys with relatively minor glomerulosclerosis that varies from 1.5 to 23% (91). Among a group of "marginal" donors aged 60 to 75 years, 57% had less than 10% glomerulosclerosis (89). Thus, age alone is only an imperfect predictor of the overall degree of nephrosclerosis and the suitability of an organ for transplantation.

Most examinations of procurement biopsies are limited to frozen sections of subcapsular wedges, which have numerous pitfalls in the interpretation. Conventional frozen sections (with the exception of biopsies carefully frozen in precooled isopentane) have prominent artificial interstitial spaces, which can be

mistaken for fibrosis or edema. Glomerular cellularity cannot be reliably assessed, although thrombi and crescents can be identified. The minimum number of glomeruli needed to correlate with outcome was found to be 25, and the minimum number required to obtain consistent results from paired biopsies was 15 (92). In our opinion, at least 25 glomeruli should be studied, from as deep in the cortex as is feasible. If a scar is sampled, as indicated by clusters of globally sclerotic glomeruli, this area should be noted, but it should be treated separately in the analysis to avoid overstating the percent sclerosis. Most importantly, a wedge biopsy is not representative, since it includes mostly outer cortex, the zone where glomerulosclerosis and fibrosis due to vascular disease is most severe. Intimal fibrosis, in contrast, most prominently affects arcuate and larger-caliber arteries and therefore is underrepresented in a wedge biopsy (93–95). If needle core biopsy samples are obtained on isolated/procured kidneys by the surgeons in the operating room with a so-called biopsy gun, then the tissue cores may show predominately renal medulla thereby limiting the diagnostic yield considerably. This problem can be avoided by “shooting” tangentially rather than perpendicularly into the “naked procured” organ. Good results were also reported using skin punch biopsy tools (94). In general, procurement biopsies are examined with H&E stains only; serial step sections and special stains (including trichrome incubation for the evaluation of sclerosis) are usually not performed, thereby further limiting the diagnostic yield.

Thus far, no study has established an absolute, validated threshold of glomerular sclerosis, fibrosis, or arteriosclerosis beyond which a donor kidney must not be used. It is clear that some abnormalities do not measurably affect long-term prognosis, in part due to other more severe causes of graft loss (e.g., rejection, cardiovascular disease, infection). Glomerulosclerosis as an indicator for organ suitability has been evaluated in many studies with contradictory results. A seminal report showed that allografts with good function at 6 months had less global glomerulosclerosis in the donor biopsy than did those with poor function (2% vs. 20%) (86). A threshold of less than 20% glomerulosclerosis characterized the group with a lower rate of DGF (33% vs. 87%) and graft loss (7% vs. 38%), and as a result, the proposed 20% cutoff has had some subsequent support. Graft survival was strikingly diminished in recipients of grafts with greater than 20% glomerulosclerosis, compared with those having 0% (35% vs. 80% 5-year graft survival rate) (96). However, a large study of 387 donor biopsies found that donor glomerulosclerosis was not an independent predictor of outcome if age was included in a multivariate analysis (97). In a large, well-analyzed UNOS study of 3444 deceased donor kidney biopsies, glomerulosclerosis greater than 20% predicted decreased graft survival only when associated with decreased creatinine clearance in the donor and, even then, only to a minor degree (3.4% more graft loss) (98). According to this result, glomerulosclerosis should not be the sole criterion for discarding donor kidneys. A recent well-conducted single-center series from Baltimore analyzed 371 donor biopsies, mainly collected from an “expanded donor organ pool” with relatively long ischemia times, kidneys that had been declined by other transplant centers. In this cohort of mostly “marginal donor organs,” five histologic features (global glomerulosclerosis, periglomerular fibrosis, arteriosclerosis, arteriolosclerosis, and scar formation) were weighted and incorporated into a cumulative chronic histologic scoring index. Overall, graft

survival was 90% at 1 year, and at 5 years, it ranged from 53% in organs with high cumulative indices up to 90% in those with low indices (99). Thus, in this study, more than 50% of organs with relatively marked sclerosis and chronic injury functioned 5 years postgrafting and kept patients off dialysis. Data from Baltimore underscore that even marginal donor organs can be beneficial for some recipients, particularly in “old for old” or dual organ transplantation programs (100–103). Another study found a high donor-recipient age ratio, that is, old donor organ into young recipient, to be associated with increased risk for subsequent allograft failure; the age of the donor organ (greater than 55 years with presumed higher degrees of chronic injury) was, however, not in and of itself an independent risk factor for poor long-term prognosis (104). Whether the recently proposed baseline “Leuven sum score” (donor age and glomerulosclerosis, interstitial fibrosis, tubular atrophy evaluated at time of procurement/transplantation), indeed, helps to better predict 5-year graft survival and allocation of donor organs remains to be seen (105–107). Thus chronic renal injury including the percentage of globally sclerotic glomeruli does not provide universal guidelines for the suitability of donor kidneys for transplantation.

At present, 19% of all kidneys recovered in the United States are discarded. The Organ Procurement and Transplantation Network reports that in 2011 in the United States, while there were 940,000 patients waitlisted for a kidney or kidney/pancreas transplant, only 17,600 transplants were performed. According to the National Kidney Foundation, the largest (and growing) reason for discard of donor organs is an abnormal biopsy finding that led to 42.8% of kidney discards during the period 2005–2009, up from 37.2% during 1995 to 1999. Compared to dialysis costs, each transplanted kidney saves tens of thousands of health care dollars over costs for dialysis and typically improves the recipient’s quality of life. There is great concern that rigid and arbitrarily set morphologic criteria for the evaluation of procurement biopsies result in needless discard of kidneys (100,108). In the future, great efforts will have to be made by transplant pathologists to develop optimal criteria for the evaluation of procurement biopsies and to use precious donor kidneys wisely (106,108).

With regard to tumors, among the pitfalls in the frozen section interpretation of a possible clear cell carcinoma are epithelioid angiolipoma, intrarenal adrenals (109), and cystic renal cell carcinoma with scant epithelial lining. The detection of a renal cell carcinoma is not necessarily an absolute contraindication against transplantation (110). Completely resected, well-differentiated (Fuhrman grade 1 to 2) renal cell carcinomas less than 1 cm in diameter have an estimated minimal risk of less than 0.1% for tumor transmission, tumors greater than 1 and ≤ 2.5 cm have a low risk of 0.1% to 1%, and those between 4 and 7 cm have an intermediate risk of 1% to 10% (110). In a recent review, Nalesnik et al. identified 64 organ donors with confirmed renal cell carcinomas that resulted overall in 7 (11%) tumor transmissions in the organ recipients and 1 (1.6%) carcinoma-related recipient death (111). Organs from patients with metastatic disease (including invasive breast, neuroendocrine, and colon carcinomas; malignant melanoma; leukemia; sarcomas; and lung cancer [stages I to IV]) carry a high risk (greater than 10%) of disease transmission, and they should not be transplanted (110).

In some procurement biopsies, thrombi may be encountered. While massive generalized thrombosis of intrarenal

vessels constitutes a contraindication to renal transplantation, organs with focal fibrin thrombi limited to the microvasculature can have an excellent prognosis, although these grafts may experience an initial period of DGF. Glomerular thrombi are found in 3% to 7% of donor biopsies, particularly in those originating from patients with head trauma (97,112,113). Thrombi in less than 50% of glomeruli after reperfusion had no effect on graft outcome in one series (114), but in another series of nine donor kidneys with glomerular thrombi (of unspecified extent), three had primary nonfunction (PNF) (97). Thrombi disappeared in five recipients with subsequent biopsies as soon as 8 days post-grafting, and long-term outcome was unaffected even in cases with "severe" microthrombosis (113). It is likely that unaltered fibrinolysis in the recipient results in full restoration of blood flow postgrafting. TMAs, in contrast, affecting small arteries with intramural vascular injury, extravasation of fragmented red blood cells, intimal remodeling, and swelling are poor prognostic indicators and should preclude transplantation. Anecdotal reports and personal experience suggest that eclamptic kidneys can fully recover (112). It is not established whether an occasional cholesterol embolus is a contraindication. However, donor-derived atheroembolization is often multifocal and associated with a high graft failure rate (115,116).

Zero-Hour Implantation Biopsies

Zero-hour implantation biopsies are performed either prereperfusion or, more frequently, postreperfusion. In general, the same aspects concerning tissue sampling (wedge biopsy vs. needle core biopsy) apply as discussed above for "procurement biopsies." Often, needle biopsies are obtained by the transplant surgeons with only minor complications (0.5% of biopsies resulted in minor bleeding episodes at the University of North Carolina). Implantation biopsies are best evaluated following standard protocols including the analysis of multiple step sections, special stains, and elastic tissue stains. In general, immunofluorescence and electron microscopic evaluations are least helpful.

Implantation biopsies are primarily intended to provide information on the overall condition of the transplanted organ for subsequent comparative biopsy analyses. They may also provide some prognostic information, although prediction of long-term graft function in an implantation biopsy is somewhat limited since many factors encountered down the road (such as rejection, hypertension-induced de novo arterionephrosclerosis, or recurrence of renal disease) may influence outcome (105–108). The presence of acute tubular injury in an implantation biopsy—if not extreme—only poorly predicts subsequent episodes of DGF.

Chronic, hypertension-induced donor-derived arterionephrosclerosis is common. It mainly affects arterioles, arteries, and, to a much lesser degree, the tubulointerstitial and glomerular compartments. We found evidence of arterionephrosclerosis in approximately 68% of our conventional donor pool organs; in 19% of the cases, there were moderate to severe changes at a mean donor age of 37 years. Unexpected moderate to severe arteriosclerosis was also found in 19% of organs of living donation, which is suggestive of clinically undiagnosed episodes of hypertension in the donor. Moderate to severe arteriosclerosis was correlated in our analyses with inferior graft function during the first 12 months posttransplantation; however, it was not associated with an increased risk of graft failure at 1 year. Similar findings were also made by others (117).

Several studies have attempted to correlate the presence of neutrophils in a postperfusion biopsy with outcome. Older reports found that neutrophils in both glomerular and peritubular capillaries (PTC) predicted hyperacute rejection: Neutrophils in PTC predicted acute rejection, and neutrophils in glomeruli correlated with cold ischemia time and subsequent graft loss (114). Experience in recent years seems to be different. In the experience of one of the authors (VN) in a cohort of conventional transplant recipients polymorphonuclear leukocytes in the microvasculature (mainly in glomerular capillaries) are uncommon; if present, usually, only few polymorphonuclear leukocytes are detected that do not carry any diagnostic or prognostic significance. Also, rare platelet microthrombi are occasionally seen (finely granular and relatively pale staining material); they typically resolve rapidly during follow-up. In an implantation postperfusion biopsy, the presence of the complement degradation product C4d along PTC is uncommon, but when observed predicts subsequent antibody-mediated acute rejection in some presensitized ABO-compatible transplant recipients (118). The presence of intratubular casts or tubular degeneration correlates with increased ischemic time but not with DGF (88).

The zero-hour implantation biopsy also provides a unique view of other subclinical renal lesions in healthy individuals. These lesions might require more extensive morphologic and clinical workup. The most common glomerular finding is IgA deposition, which was present in 11% of 108 living donors (two had mesangial sclerosis, and the others were normal by light microscopy) (119) and in 9% of deceased donors (120). In a large series from Nanking, 24% of 342 donor kidneys had IgA deposits (121). This suggests either that subclinical IgAN is quite common or that mesangial IgA without proliferation is not a disease. Donor-derived IgA disappears within weeks to few months on follow-up biopsies (112,122–124), and graft survival is no different from those without IgA (121).

Rarely, kidneys with membranous glomerulonephritis have been transplanted; one survived at least 3 years (125), and another case showed signs of resolution and GBM remodeling at 20 months posttransplant (126). Other donor renal diseases that resolved without obvious ill effects include lupus nephritis (127), acute postinfectious glomerulonephritis (128), membranoproliferative glomerulonephritis (type I) (129), and hepatorenal syndrome (130). In one anecdotal report, a graft with 25% crescent formation showed good function during a 2-year follow-up, whereas the contralateral kidney with 90% crescents failed (131).

In an unpublished but instructive case from the University of North Carolina, very small, scattered, dense mononuclear inflammatory cell aggregates were noted in the interstitial compartment of a zero-hour implantation biopsy. These infiltrates proved to represent extranodal involvement of a small lymphocytic lymphoma and resulted in subsequent graft removal.

Molecular Studies

Organ donation (donor events, procurement, storage, reperfusion) induces a significant molecular disturbance in the donor tissue, which is more intense in deceased donors (132,133). Over recent years, attempts have been made to assess gene expression profiles in donor organs and to develop possible adjunct strategies to determine organ quality and predict outcome postgrafting.

At the transcriptional level, the response to renal injury manifests as a decreased expression of functional genes (e.g., solute carrier transcripts), up-regulation of cell cycle, repair and tissue remodeling transcripts, embryonic pathways like *unt* and *notch*, and injury-associated genes (e.g., cytoprotective heat shock proteins, HMGB1) (134,135).

Donor kidneys with impaired renal function (GFR < 45 mL) at 1-year postgrafting showed a distinctively different gene expression profile when compared to a set of well-functioning organs (GFR > 45 mL) including the up-regulation of genes in the functional classes of immunity, signal transduction, and oxidative stress (136). Interestingly, microarray analysis in a small series of implantation biopsies also found altered gene expression in those donor organs procured by laparoscopic nephrectomy including pneumoperitoneum as compared to open nephrectomy, indicating that certain systemic, surgically induced stress factors might already alter the molecular profile in a donor organ (137). Larger series are needed to further validate this finding. In another study, microarray results of 87 consecutive time-zero biopsies taken postreperfusion in 42 deceased and 45 living donor kidneys were compared to clinical and histopathology-based scores. Unsupervised analysis separated the kidneys into three groups at risk for DGF: living donors, low-risk deceased donors, and high-risk deceased donors. Neither clinical nor histopathologic risk scores discriminated high-risk from low-risk deceased donors. In contrast, 1051 transcripts were differentially expressed in the two deceased donor risk groups; however, no transcript clearly separated grafts with delayed function from those with immediate function. Further analysis revealed a continuum starting from living donors, moving to low-risk deceased donors, and ending with high-risk deceased donors, that is, from best to poorest functioning kidneys (132). In a consecutive study, the same group analyzed microarray results from implantation biopsies of deceased donors only. Two definitions of early dysfunction were used: serum creatinine greater than 265 $\mu\text{mol/L}$ at day 7 posttransplantation or need for dialysis in the first week. The strongest correlate with early dysfunction was the mean expression of a set of 30 injury-associated gene transcripts primarily expressed by tubular epithelial cells such as osteopontin M receptor, integrin beta 6, lipocalin 2, versican, cathepsin S, and cadherin 6 (135,138). Prediction of early dysfunction was best when the injury gene expression profile was combined

with donor or recipient age, thereby presumably taking chronic injury such as donor-derived arteriosclerosis into account. Of note, the injury transcripts did not predict late graft function.

T-CELL-MEDIATED REJECTION

Traditionally, rejection has been divided on clinical grounds and the temporal occurrence postgrafting into hyperacute, acute, and chronic episodes. In this context, hyperacute and acute rejection is considered an early event characterized by relatively rapid deterioration of graft function, whereas chronic rejection is a late event months or years after transplantation often associated with creeping functional deteriorating and proteinuria. Over the years, this simple point of view has caused much confusion. Many physicians interpreted acute/active rejection and chronic rejection as separate entities without much overlap. Chronic rejection was often viewed as “end-stage transplant disease” with marked scarring unresponsive to therapy. Nowadays, rejection episodes with acute/active and concurrent chronic features are defined as chronic active rejection category 2 or 4 in the “Banff” scheme (139). Of note, inactive/burnt-out chronic rejection remains unclassified in the Banff scheme (139).

In the following sections, we will separate rejection-induced changes for didactic purposes into acute/active and chronic, “cell” (= T-cell-mediated rejection, TCMR) and “antibody” mediated rejection (AMR). The reader should, however, be aware that these categories show vast overlap (Fig. 29.4). For example, active/acute rejection can show varying degrees of concurrent minor or major chronic rejection that can be induced by cellular- and/or antibody-mediated injury (140–142). Since grafts “had a preceding life,” all rejection episodes can be superimposed on preexisting donor disease, such as hypertension-induced arterionephrosclerosis, glomerulonephritides, etc. (108). Thus, the picture can be complex, and the analysis of renal allograft biopsies requires a high level of expertise; a true challenge for the transplant pathologist! In the future, our understanding will further evolve, and new immunohistochemical marker sets, electron microscopy, and molecular assays including gene expression profiles will be incorporated into the standard diagnostic interpretation of an allograft biopsy.

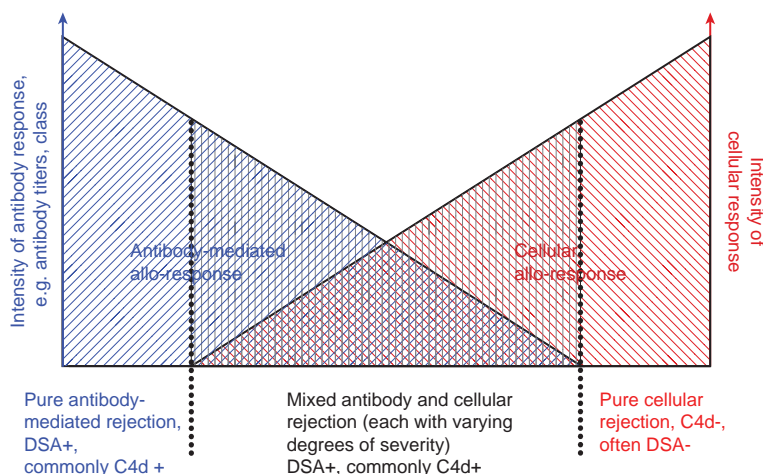


FIGURE 29.4 Schema of acute/active rejection. Acute rejection episodes can either be pure antibody- or pure cell-mediated events or also represent mixed rejection with varying degrees of antibody and cellular components.

ACUTE T-CELL-MEDIATED REJECTION

Acute T-cell-mediated rejection (i.e., acute TCMR, Banff category 4 types 1 to 3) is the form of rejection that develops most commonly in the first few months after transplantation with sharply decreasing frequencies thereafter. Acute TCMR can occur as early as 6 days and as late as decades posttransplantation (143,144). It can involve the tubulointerstitial compartment, arteries, and glomeruli individually or in various combinations thereby reflecting differences in clinical presentation and outcome. The classical clinical features of severe acute TCMR are an abrupt rise in serum creatinine that progresses over several days, a decline of urine output, weight gain, fever, malaise, graft tenderness, and swelling (these symptoms are often muted or lacking in compliant patients under modern immunosuppression). Hematuria (mainly due to hemorrhage into injured tubules or infarction) and proteinuria (possibly induced by severe transplant glomerulitis and diffuse acute tubular injury) are very unusual presentations in acute TCMR. Of note, although typical, allograft dysfunction is by no means a *sine qua non* for the diagnosis of acute TCMR that is defined by histologic changes in the allograft. Rejection episodes detected in allografts with stable function are referred to as “subclinical”—a term not meant to imply a benign long-term prognosis if left untreated (145). The primary risk factors for acute rejection, T-cell and/or antibody mediated, are the degree of histocompatibility between the donor and the recipient, the level of presensitization (previous graft, pregnancy, blood transfusions), immunosuppressive drug protocols, and, last not least, the level of patient compliance with daily therapy (85,146). Other factors of importance are recipient age, race, and sex. Current immunosuppression regimens with CNIs, steroids, and MMF have considerably reduced the frequency of acute cellular rejection (147). For the transplant period 2005–2009, only 11.6% of patients with cadaveric and 10% of patients with living donor kidneys experienced acute rejection (cell or antibody mediated) by 1 year postgrafting (148). In the so-called DeKaf study, 34% of early diagnostic biopsies (mean sampling 12 months postgrafting) showed acute TCMR and 19% of late biopsies (149).

Pathologic Findings

T cells, some of them reactive to donor histocompatibility antigens in the graft, affect the interstitium, tubules, vessels, and glomeruli, individually or in various combinations. The approximate relative frequencies of the different patterns of acute cellular rejection are 45% to 70% tubulointerstitial (Banff category 4, type 1), 30% to 55% vascular (Banff category 4, type 2 or 3), and 2% to 4% glomerular (not specifically used for categorization of rejection in the Banff scheme). Percentages show considerable center variations. Approximately 20% to 40% of acute TCMR episodes, dependent on the histologic type, show C4d positivity along PTC, that is, evidence of concurrent antibody-mediated injury (Fig. 29.4) (142,150–152). Mixed AMR and acute TCMR episodes are more severe (152) and constitute an independent risk factor for graft failure (140,153). Mixed acute cellular- and AMR episodes are not well categorized in the currently employed Banff scheme of allograft rejection (142).

Gross Pathology

Gross specimens from kidneys with severe acute rejection (mainly mixed TCMR and AMR) are swollen due to interstitial edema and hemorrhage (Fig. 29.5). The failed allografts can increase up to threefold in weight (154) and sometimes rupture. In cross section, the cortex is of normal thickness or expanded with a geographic, mottled appearance showing areas of normal parenchyma, yellowish pale zones of ischemic infarction, and adjacent hemorrhage/hemorrhagic infarction. In most severe cases, early after transplantation, interlobar arteries may contain thrombi (then usually associated with AMR). If veins are affected by thrombus formation at the anastomotic site, then the differential diagnosis includes other underlying conditions such as coagulopathies. Extrarenal graft tissue including the ureter and perirenal adipose tissue is usually also affected and can show necrosis, hemorrhage, and inflammation including extrarenal/extraparenchymal transplant endarteritis.

The so-called pale rejection of the early days of transplantation due to pure tubulointerstitial cellular rejection (Banff category 4, type 1) does not occur anymore with modern immunosuppression.

Light Microscopy

The usual major finding in acute TCMR is infiltration of activated T lymphocytes, macrophages, and also to a lesser degree B cells, plasma cells, polymorphonuclear and eosinophilic



FIGURE 29.5 This transplant failed within few weeks postgrafting due to severe rejection with fibrinoid arterial wall necrosis (v3 lesion) and presumed mixed acute antibody- and cell-mediated rejection. Segments of hemorrhagic infarction in the cortex and medulla border on zones with normal-appearing renal parenchyma. Large arterial cross sections show some degree of arteriosclerosis but no gross evidence of thrombus formation.

TABLE 29.4 Banff types of acute T-cell–mediated rejection

Suspicious/ borderline ^a	Any tubulitis + infiltrate of 10%–25%, or Any infiltrate of $\geq 10\%$ + tubulitis of 1–4 cells/tubule
Type I ^b	Tubulitis >4 /tubule + infiltrate $>25\%$ A: with 5–10 cells/tubule (t2), or B: with >10 per tubule (t3)
Type II	Mononuclear cells under arterial endothelium A: $<25\%$ luminal area or B: $\geq 25\%$ luminal area
Type III	Transmural arterial inflammation or fibrinoid arterial necrosis with accompanying tubu- lointerstitial lymphocytic inflammation

^aAll cases should be analyzed for C4d deposition. If C4d is present, an additional diagnosis of concurrent antibody-mediated rejection is made.

^bCases with types I–III rejection can be due to concurrent alloantibody-induced injury. To use as a category of TCMR requires C4d in PTC to be negative.

From Racusen LC, Colvin RB, Solez K, et al. Antibody-mediated rejection criteria - an addition to the Banff 97 classification of renal allograft rejection. *Am J Transplant* 2003;3(6):708-14.

leukocytes into a mildly edematous interstitium and into the tubules (so-called tubulointerstitial cellular rejection; Banff category 4, type I rejection). In some cases, plasma cells dominate, that is, the so-called plasma cell–rich cellular rejection. The infiltrate can in more severe TCMR episodes also (or occasionally solely) affect arteries (so-called transplant endarteritis; Banff category 4, type II rejection) and glomeruli (so-called transplant glomerulitis; not specifically categorized in the Banff classification scheme). Inflammation is accompanied by

signs of injury of the target cells, such as endothelial swelling, tubular cell activation, or apoptosis. Acute cellular rejection is often patchy and typically affects the cortex. Rejection-induced inflammation in the medulla is only seen in pronounced cases as a “spillover effect.” In general, medullary inflammation might have many etiologies such as PVN, pyelonephritis, allergic interstitial nephritis, etc., and it is least specific for rejection-induced injury. Diffuse and pronounced interstitial edema or hemorrhage is only seen in most severe forms of acute TCMR involving arteries and glomeruli. Such cases often also show concurrent AMR and C4d positivity.

It is important to remember that minimal threshold levels for the diagnosis of C4d-negative tubulointerstitial cellular rejection (Banff category 4, type 1 rejection) are controversially debated (61,141,155,156). The Banff criteria for tubulointerstitial cellular rejection seem high (Table 29.4). The Banff category 3 of the so-called borderline changes suspicious for TCMR is problematic; it is occasionally used as a “waste basket” that may even contain unrecognized cases of severe rejection episodes including missed transplant endarteritis/type 2 rejection.

GLOMERULI

In a minority of cases with acute TCMR, approximately 5% to 10%, a distinct form of glomerular inflammation is seen, called transplant glomerulitis. It typically occurs in the first 1 to 4 months posttransplant (157–161) although it may as well arise years after grafting and is then often associated with signs of chronic rejection and transplant glomerulopathy (162,163). Transplant glomerulitis is often focal and segmental and less frequently diffuse and global. It is characterized by dilatation of glomerular capillaries “occluded” by three or more mononuclear cell elements, that is, monocytes, lymphocytes, and activated and swollen endothelial cells (Fig. 29.6A) (141,161). Rarely, mitotic figures may be detected and, in severe forms, also

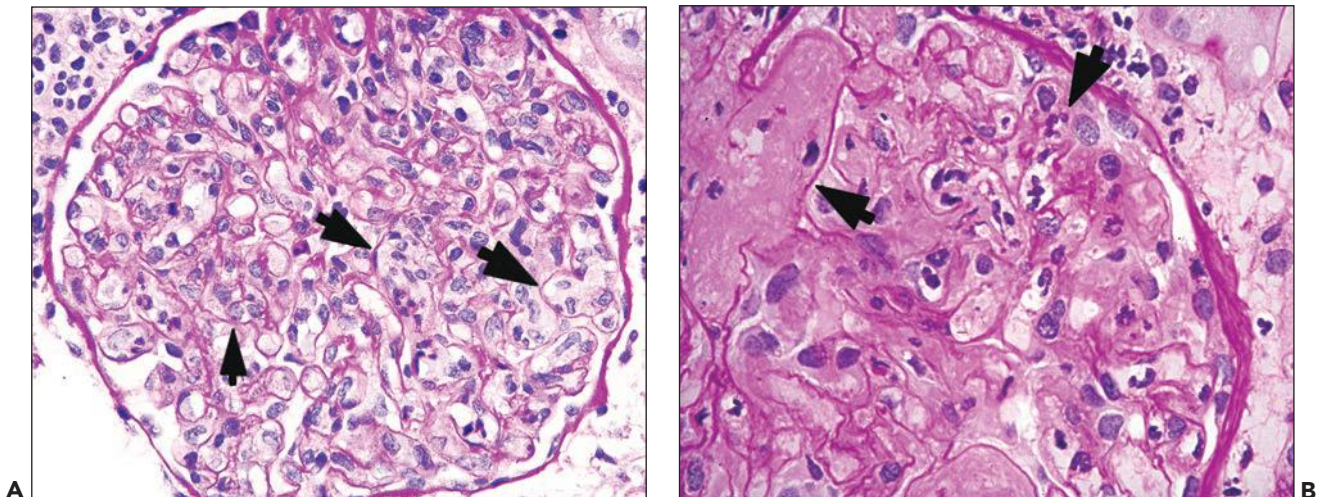


FIGURE 29.6 Transplant glomerulitis. A: Acute cellular rejection with transplant glomerulitis 6 days posttransplantation. Peripheral glomerular capillaries are dilated and “occluded” by mononuclear cell elements and swollen endothelial cells (arrows). The biopsy also showed transplant endarteritis and tubulointerstitial cellular rejection. This case of acute TCMR was not associated with acute AMR. The acute TCMR episode responded fully to thymoglobulin therapy. **B:** In comparison, a case of acute AMR, C4d-positive with transplant glomerulitis. This case shows mainly intracapillary polymorphonuclear leukocytes and fibrin microthrombi (compare to figure A); this case did not show concurrent acute CR. (PAS, $\times 500$.)

mesangiolytic. Intracapillary polymorphonuclear leukocytes and small fibrin thrombi can occasionally be seen; these latter features are more prominent in C4d-positive cases with (concurrent) AMR (Fig. 29.6B). Fibrinoid tuft necrosis, crescent formation, or GBM duplications are not features of rejection-induced glomerulitis. Glomerular lesions are best appreciated in 2- μ m PAS-stained sections or silver stains with a good nuclear counterstain (GBM duplication characterizes transplant glomerulopathy and chronic rejection that can be associated with transplant glomerulitis in chronic active rejection episodes). Transplant glomerulitis with endothelial cells as a target of the cellular immune response occurs in approximately 60% of cases combined with other acute rejection-induced vascular lesions, that is, transplant endarteritis (53,157–159,163–166). In one series of 12 patients, 92% had associated endarteritis (165). In exceptionally rare cases, glomeruli can be solely affected without rejection-induced changes in other renal compartments (157,161,163). We found that approximately 20% of biopsies with transplant glomerulitis are “pure” Banff category 4 cellular rejection episodes lacking concurrent acute AMR/C4d positivity that is detected in the remaining cases. The predominance of intraglomerular monocytes (glomerular monocyte/T-cell ratio greater than 1) is more typical of acute AMR-induced transplant glomerulitis (167,168). In nonhuman primates protracted transplant glomerulitis evolved into chronic rejection/transplant glomerulopathy within 6 weeks (164).

Scattered circulating intraglomerular mononuclear cells in nondilated capillary loops are present in relatively many biopsies with acute TCMR (169) (Fig. 29.7) (157,163,170,171). These circulating mononuclear cells are not considered diagnostic for transplant glomerulitis. Currently, attempts are under way to better define morphologic features characterizing transplant glomerulitis and the potential significance of intraglomerular monocytes (172–174).

TUBULES

In acute TCMR, T cells and macrophages invade tubules and insinuate between tubular epithelial cells inside the basement membrane, a process termed “tubulitis” (Fig. 29.8). This is

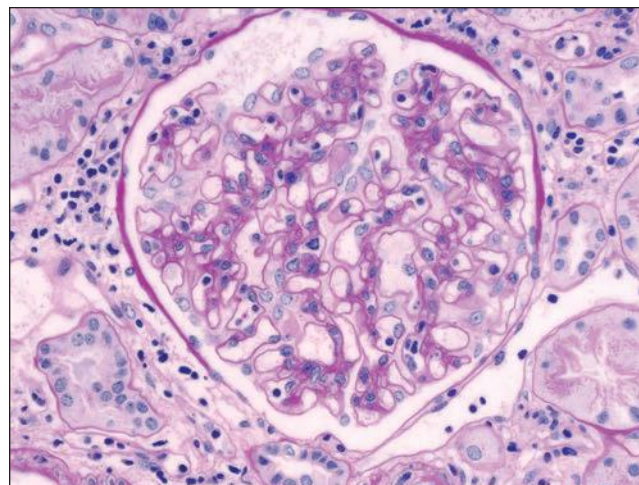


FIGURE 29.7 Several mononuclear cells are present in glomerular capillaries. This is below the threshold of transplant glomerulitis. (PAS stain, 400 \times original magnification.)

best demonstrated in PAS- or trichrome-stained slides highlighting the TBM. Tubulitis is usually recognized by increased numbers of small dark nuclei often arranged along the inner aspect of the tubular basement membrane and occasionally surrounded by small clear spaces/halos (Fig. 29.9). Normal tubular epithelial cells have larger and less dense nuclei than do lymphocytes and tend to be located more apical toward the tubular lumens. However, it can sometimes be difficult to distinguish infiltrating mononuclear cells from apoptotic or degenerating tubular epithelial cells; then, “halos” surrounding nuclei of lymphocytes can help in identifying tubular cross sections with tubulitis. Also, CD3 and CD68 stains may be combined with a PAS incubation to help demonstrate tubulitis. Mononuclear cell elements constituting tubulitis can undergo proliferation based on the expression of Ki-67/MIB-1. Tubulitis affects mostly distal tubular segments in the

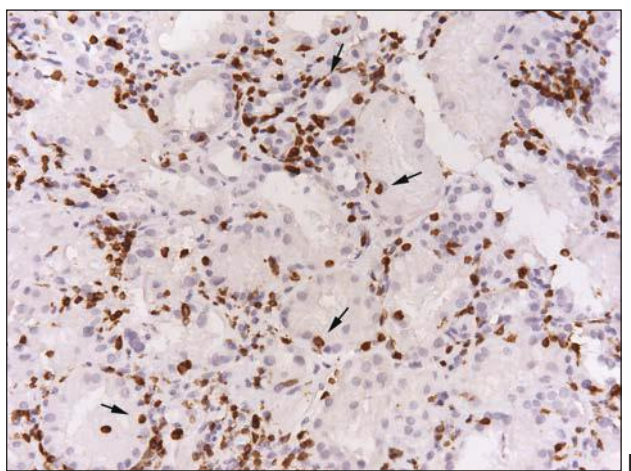
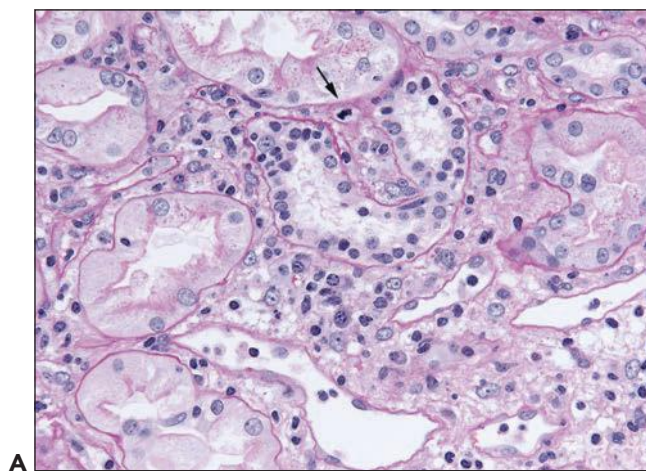


FIGURE 29.8 Acute tubulointerstitial cellular rejection with tubulitis. **A:** Activated mononuclear cells and edema are present in the interstitium. A mitotic figure is present in the infiltrate (arrow). ($\times 40$ PAS) **B:** A CD3 stain in another case shows abundant T cells in the interstitial and intratubular compartments/foci of tubulitis (arrows). (PAS stain, 40 \times original magnification. Immunoperoxidase $\times 200$.)

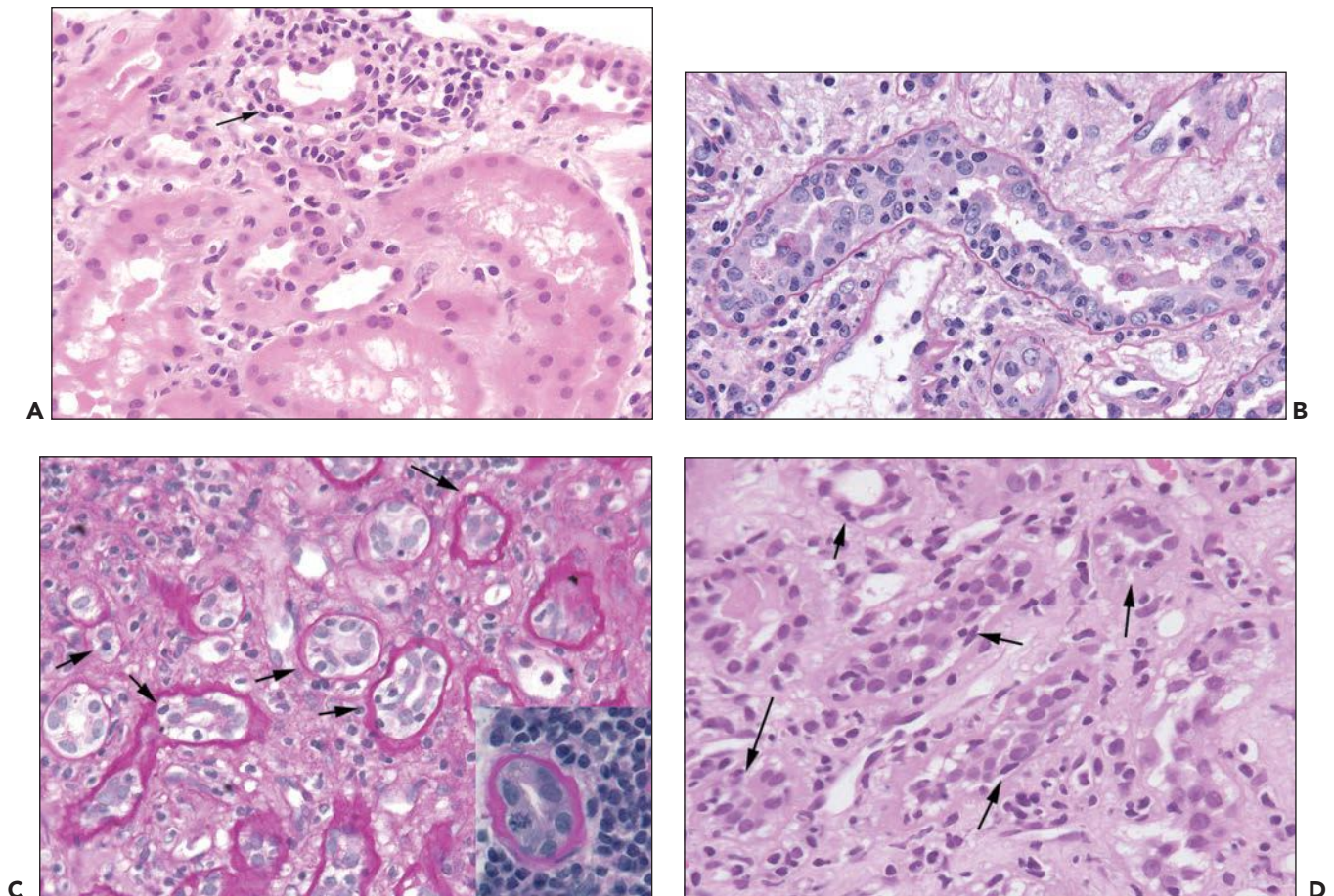


FIGURE 29.9 Diagnostic and nondiagnostic tubulitis. **A:** Diagnostic tubulitis: Over 10 mononuclear cells are in one tubular cross section (*arrow*). Surrounding tubules have zero to two infiltrating cells. (H&E $\times 400$.) **B:** Diagnostic tubulitis: extreme tubulitis (t3) in a longitudinal section. (PAS $\times 400$.) **C:** Nondiagnostic tubulitis: Inflammation in severely atrophic tubules is currently considered to be a nondiagnostic observation. Mononuclear cells (*arrows*) are in small tubules with thickened basement membranes. (PAS $\times 400$.) The presence of occasional mitotic figures in “atrophic” tubules belies their designation of atrophy. (*Insert*, original magnification $\times 600$.) **D:** Likely diagnostic tubulitis: Tubulitis is present in these smaller tubules with simplified, clear cytoplasm. However, the tubular diameters do not seem to be markedly reduced, and the TBM is not severely thickened. This focus of tubulitis possibly represents active rejection. (H&E $\times 400$.)

cortex; proximal tubules are often spared and collecting ducts in the medulla hardly ever involved (175–177). Although plasma cells found in the so-called plasma cell–rich cellular rejection can be abundant in the interstitium (subtype of Banff category 4, type I rejection), they rarely invade tubules, and “plasma cell” tubulitis is uncommon. Occasionally scattered neutrophils can be seen in tubular lumens as a sign of acute injury. Small interstitial granulomas form adjacent to ruptured tubules and leakage of Tamm-Horsfall protein (uromodulin) into the interstitium (Fig. 29.10); this feature is nondiagnostic and can occur in many forms of tubular injury. Tubulitis in atrophic tubules, that is, less than 50% of the original diameter and markedly thickened TBM, is currently considered to be a nondiagnostic sign of parenchymal scarring; at present, this feature is not used to establish a diagnosis of acute TCMR (see Fig. 29.9C). However, this view may change in the future since there is increasing evidence that all tubulitis (in atrophic and nonatrophic tubules) and all interstitial inflammation (in scarred and nonscarred regions) is a sign of TCMR (see

Fig. 29.9D) (149,178,179). The newly introduced Banff scoring entity of “total inflammatory (ti) score” may help assess the significance of tubulointerstitial inflammatory cell infiltrates (139). In some cases of acute TCMR, marked reactive atypia of tubular epithelial cells including multinucleation is seen. Such regenerative, ischemia-induced changes often occur in the setting of protracted severe rejection with marked edema, transplant endarteritis, and/or concurrent acute AMR/C4d positivity. Very pronounced tubular epithelial atypia is usually inconsistent with a diagnosis of “pure” tubulointerstitial cellular rejection, Banff category 4 type 1.

INTERSTITIUM

Acute TCMR has a pleomorphic interstitial infiltrate of mononuclear cells (lymphocytes, macrophages), varying degrees of CD20-expressing B cells, plasma cells, and, occasionally, scattered polymorphonuclear leukocytes in areas of severe tubular injury (180). Inflammation typically surrounds nonatrophic tubules in a finger-like fashion. Eosinophils can be focally

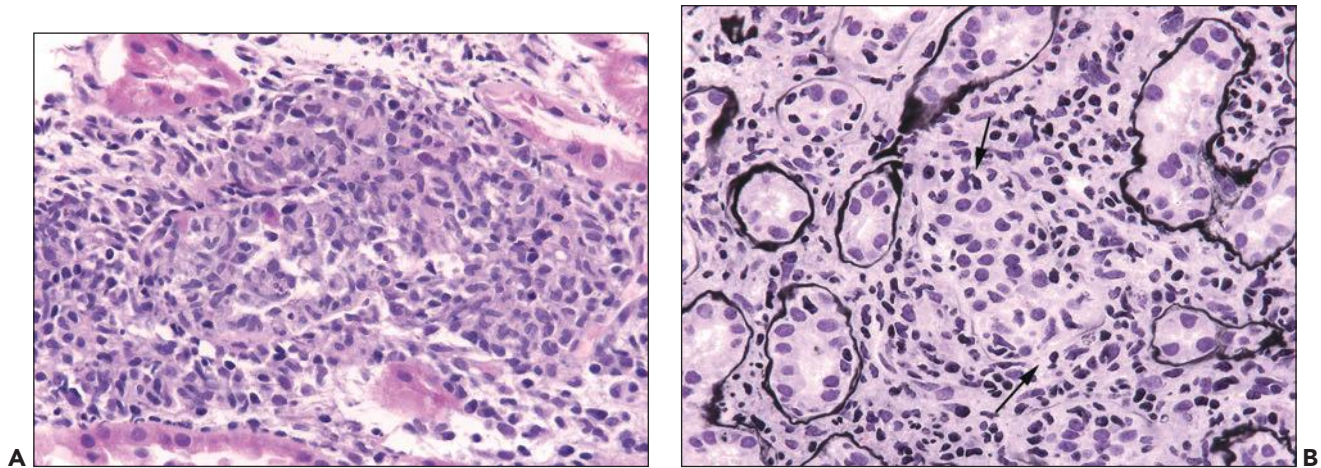


FIGURE 29.10 Severe tubulitis. **A:** Acute cellular rejection with tubular rupture and granuloma formation. (H&E $\times 400$.) **B:** Partial dissolution and rupture of the tubular basement membrane can be appreciated in periodic acid-silver stains (arrows). ($\times 400$.)

prominent and may indicate the presence of transplant endarteritis (Fig. 29.11). Inflammation in the setting of tubulointerstitial rejection (Banff category 4, type 1) is associated with relatively mild and often focal edema; marked diffuse edema usually indicates endothelial injury seen in cases with transplant endarteritis (Banff category 4, type II rejection) and/or concurrent acute AMR with C4d positivity. In acute TCMR, edematous regions often show dilatation of PTC and so-called PT capillaritis with intracapillary mononuclear cell elements (181). Polymorphonuclear PT capillaritis is rare and usually indicates acute AMR.

The infiltrating mononuclear cells are predominately T cells and macrophages (see Fig. 29.8). The T cells are typically activated (lymphoblasts), with increased basophilic cytoplasm, occasional nucleoli, and very rare mitotic figures, indicative of increased synthetic and proliferative activity.

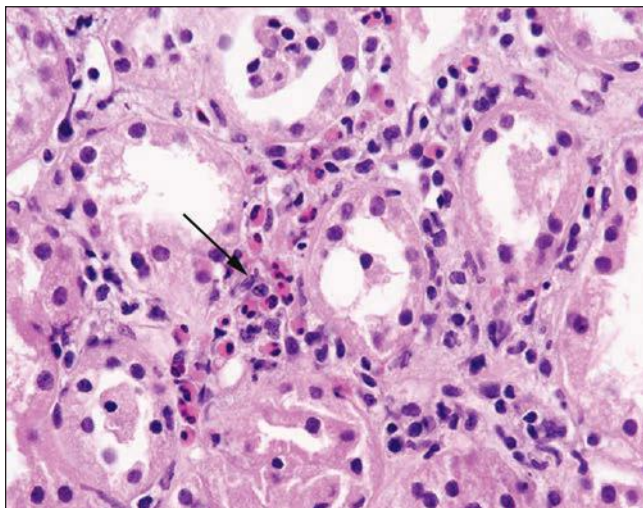


FIGURE 29.11 Acute cellular rejection with abundant eosinophils. Eosinophils (arrow) are about 20% of the infiltrate in this field. (H&E $\times 400$.)

Small lymphocytes with dense nuclear chromatin and little cytoplasm are also present. Macrophages can already be seen in early acute TCMR and can account for up to half of the inflammatory cell infiltrates (170,182). On occasion, they may even constitute the major cell type, in particular if T-cell-depleting agents such as CAMPATH1 are used (183). Low numbers of B cells (CD20+) can also be detected. Whether their presence in acute TCMR indicates unfavorable long-term prognosis as suggested by some authors is undetermined (184–187). Plasma cells can be prominent, especially in acute rejection episodes that occur months after transplantation (188–192), and they often mark “steroid unresponsiveness” (185). Plasma cells only rarely invade tubules/cause tubulitis, and plasma cell–rich rejection is often C4d/DSA-negative (Fig. 29.12). Mast cells are present in increased numbers in acute rejection, as judged by tryptase content, and correlate with edema (193).

In acute TCMR, scattered granulocytes can be present in the interstitium; they are typically located adjacent to severely injured tubules. When neutrophils are abundant, the possibility of an acute AMR or pyelonephritis should be considered. Eosinophils are present in about 30% of biopsies with acute rejection, but are rarely more than 2% to 3% of the infiltrate (see Fig 29.11) (194–198). Focally abundant eosinophils are associated with the presence of transplant endarteritis, that is, they can mark Banff category 4 type 2 rejection (199,200). Basophils comprise a minor component of the infiltrate; these cells can also invade tubules and make up to 5% of the infiltrate (201).

The degree of interstitial inflammation and tubulitis does not correlate tightly with the severity of TCMR or the presence or absence of transplant endarteritis (196), that is, little inflammation does not necessarily equal minimal rejection. This observation is particularly important when interpreting small graft biopsies and considering a diagnosis of “borderline/suspicious for rejection” (Banff category 3).

VESSELS

Infiltration of mononuclear cells under enlarged and “activated” arterial endothelial cells (mainly arcuate caliber vessels or interlobular arteries, less often arterioles) is a typical lesion

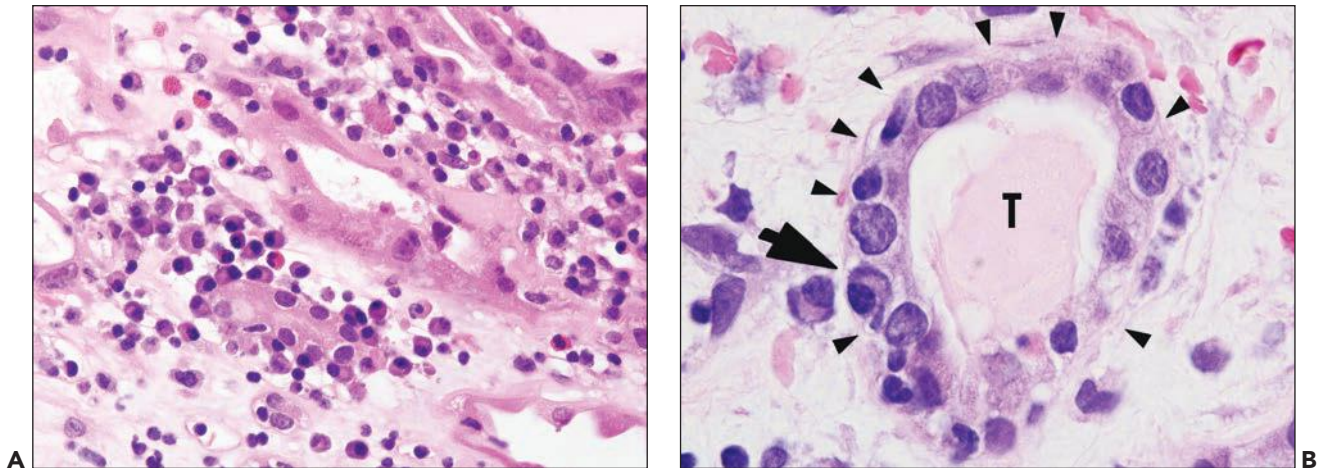


FIGURE 29.12 Plasma cell-rich acute TCMR. **A:** Acute tubulointerstitial cellular rejection rich in plasma cells (Banff category 4, type 1; C4d-negative, no DSA, no transplant endarteritis, no polyomavirus nephropathy) 8 years posttransplantation. Note abundant plasma cell aggregates in the edematous interstitium accompanied by scattered eosinophilic leukocytes. Plasma cells are “hugging” tubules, but they do not invade, that is, they do not cause “plasma cell” tubulitis. (H&E, $\times 640$ oil.) **B:** This case of acute TCMR (C4d-negative, no DSA, no polyomavirus nephropathy) rich in plasma cells shows plasma cell tubulitis with one plasma cell (*arrow*) located inside the basement membrane (*arrowheads*) between tubular epithelial cells (T, tubular cross section). Plasma cell tubulitis is relatively uncommon. (H&E $\times 400$.)

of acute TCMR (Fig 29.13). Many terms have been used for this process, including endothelialitis, endotheliitis, endovasculitis, intimal arteritis, infiltrative and proliferative transplant vasculopathy, or endarteritis. We prefer endarteritis, because it emphasizes the type of vessel involved and the site of inflammation; also, more than the intima can be affected in some cases. The biologic and diagnostic significance of endarteritis was probably first noted and illustrated by Dammin in 1960 (28). The importance of this lesion has been emphasized for many years (202), and it is widely accepted as a feature of acute TCMR, particularly if transplant endarteritis is accompanied by tubulointerstitial cellular rejection (61,81,196). However, a considerable proportion of acute TCMR with transplant endarteritis also has concurrent acute AMR (142,150,151,153).

On occasion, endarteritis can occur as an isolated event without tubulointerstitial changes. Since the endothelial cell layer is a key immunologic target in transplant endarteritis, the close association between endarteritis and glomerulitis is not surprising, and the detection of glomerulitis should always raise suspicion for transplant endarteritis.

Endarteritis has been reported in 18% to 56% of renal biopsies with acute TCMR (61,196,203–206). The prevalence of endarteritis in biopsies is affected by the sample size, the timing of the biopsy with respect to antirejection therapy, HLA matching, and the level of immunosuppression. Endarteritis tends to affect larger arteries preferentially (196,207). If biopsy samples are small and do not contain arcuate caliber vessels, then transplant endarteritis may remain undetected. This

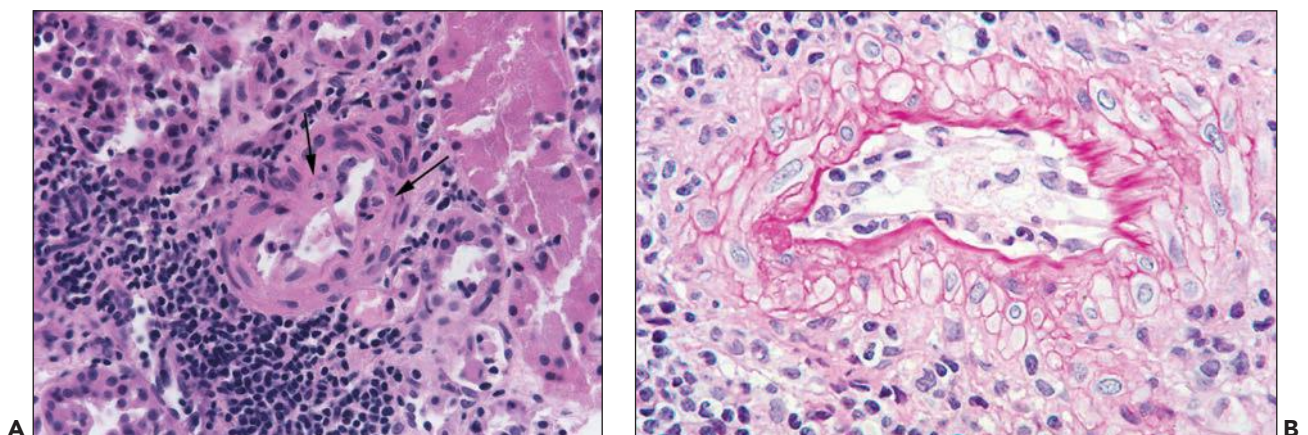


FIGURE 29.13 A, B: Acute cellular rejection with transplant endarteritis (Banff category 4, type 2 rejection). **A:** Small artery with few subendothelial mononuclear cells (*arrows*). (H&E $\times 400$.) **B:** Small artery with many subendothelial mononuclear cells. The endothelial layer is not clearly defined and is probably partially denuded. Note: no thrombus formation and no inflammation in the medial smooth muscle layer. (PAS $\times 400$.)

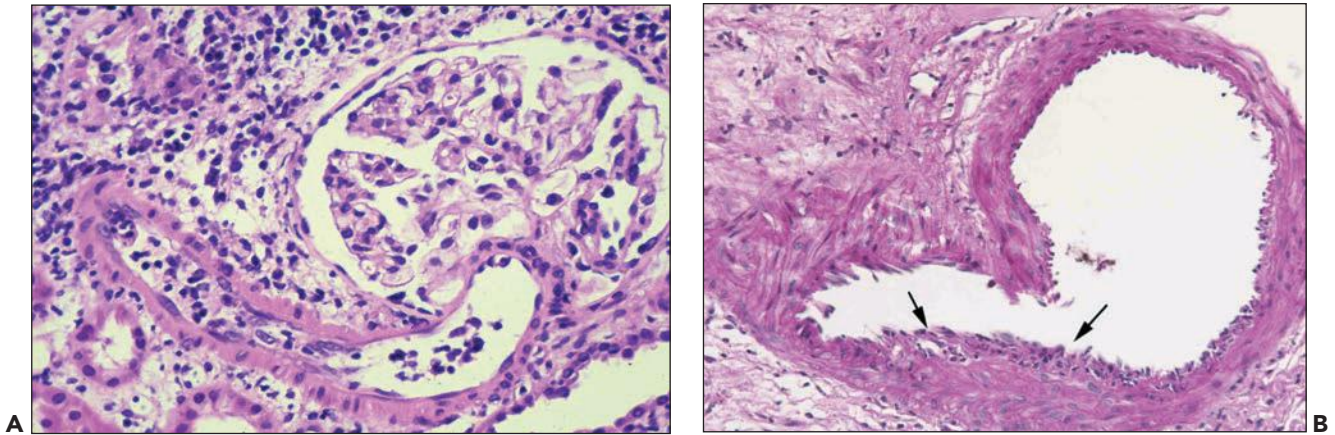


FIGURE 29.14 Acute cellular rejection with transplant endarteritis (Banff category 4, type 2 rejection). **A:** An afferent arteriole has a prominent mononuclear inflammatory cell infiltrate. This finding in a small-caliber artery is of similar significance as endarteritis affecting larger arteries; compare with B. (H&E $\times 400$.) **B:** Arcuate size artery with endarteritis (arrows). (PAS $\times 200$.)

becomes a major problem if endarteritis occurs as an isolated rejection event.

In cases of endarteritis, endothelial cells are usually activated with basophilic cytoplasm and show lifting from the supporting elastic interna/stroma by infiltrating inflammatory cells (Figs. 29.13 to 29.16) (164,196,208). Very rarely, endothelial cells are apoptotic or show mitotic figures. One inflammatory cell under the arterial endothelium is considered to be sufficient for the diagnosis of transplant endarteritis (see Fig. 29.15) (61,81) that is often patchy, that is, only few arteries are affected, and segmental, that is, not the entire intimal circumference is inflamed. The infiltrating cells are typically mononuclear cell elements, T lymphocytes, macrophages, and varying numbers of myofibroblasts that produce collagens and promote intimal sclerosis/chronic vascular rejection in protracted cases (Fig. 29.17) (164). Although mitotic figures are uncommon, the infiltrating cells show proliferative activity based on Ki-67/MIB-1 expression (Fig. 29.18D) (164). The inflamed subendothelial

intimal zones contain early matrix proteins including fibrinogen and fibronectin and in persistent cases within 3 to 4 weeks also collagen types 1 and 3 (164). Eosinophils can on occasion be found in the inflamed intimal zones; CD20-expressing B cells and plasma cells are exceptionally rare. Despite the obvious endothelial injury, thrombosis is conspicuously absent.

Mononuclear inflammatory cells that are solely adherent to the luminal surface of endothelial cells are insufficient for rendering a diagnosis of Banff category 4 type 2 rejection/transplant endarteritis (see Fig. 29.15B). Since many donor organs show preexisting hypertension-induced arteriosclerosis, transplant endarteritis is not infrequently superimposed on varying degrees of donor-derived intimal fibroelastosis (Fig. 29.18) that can sometimes be confused with chronic vascular rejection. Usually, elastic tissue stains allow for easy detection since hypertension-induced arterial intimal fibroelastosis gives an intense staining reaction that is lacking in cases of “chronic vascular rejection” (also see below). In

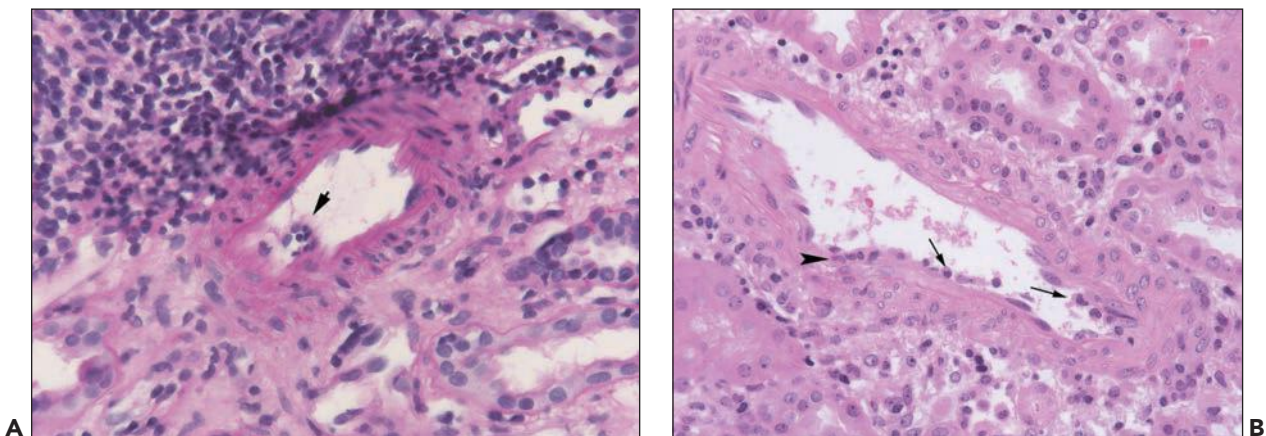


FIGURE 29.15 Acute cellular rejection with transplant endarteritis (Banff category 4, type 2 rejection). **A:** Minimum endarteritis. A single subendothelial infiltrating inflammatory cell is evident; endothelial cells are activated but intact. (PAS $\times 400$.) **B:** Mononuclear cells mainly stick to the endothelium (arrows) and are only focally underneath the endothelium (arrowhead). Only subendothelial mononuclear inflammatory cells are diagnostic for transplant endarteritis. (H&E $\times 300$.)

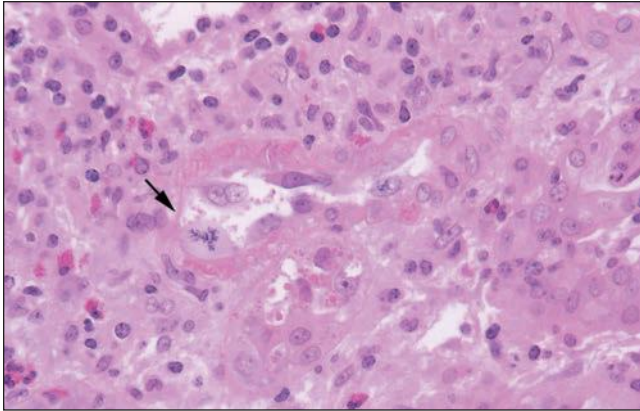


FIGURE 29.16 Acute cellular rejection with transplant endarteritis (Banff category 4, type 2 rejection). Small artery with reactive, enlarged, basophilic endothelial cell cytoplasm. An endothelial mitosis is present (arrow). Eosinophils are seen in the surrounding mixed mononuclear interstitial infiltrate. (H&E $\times 600$.)

transplant endarteritis, inflammation is typically limited to the intima/subendothelial zone sparing the medial smooth muscle layer. Transmural inflammation involving all layers of arterial walls including segmental fibrinoid necrosis can occur in severe cases of acute TCMR (Banff category 4 type 3 rejection) (Fig. 29.19); however, this feature is more often seen in biopsies with (concurrent) acute AMR and C4d positivity (150). Arteries located in or adjacent to the renal capsule can also be affected by endarteritis; however, diagnostic interpretation is challenging due to the altered blood flow in intracapsular vessels of allografts.

In acute TCMR, PT capillaries are often dilated and contain increased numbers of mononuclear cells even in the absence of concurrent AMR (82,181,209). Capillaritis reflects trafficking of inflammatory cells from the blood into the inflamed tubulointerstitial compartment and the fact that the capillary endothelium is a target of TCMR. Some evidence suggests that PT capillaritis with a predominance of monocytes (monocyte/T-cell ratio greater than 1) is an indicator of acute AMR (167). On rare occasions, polymorphonuclear leukocytes

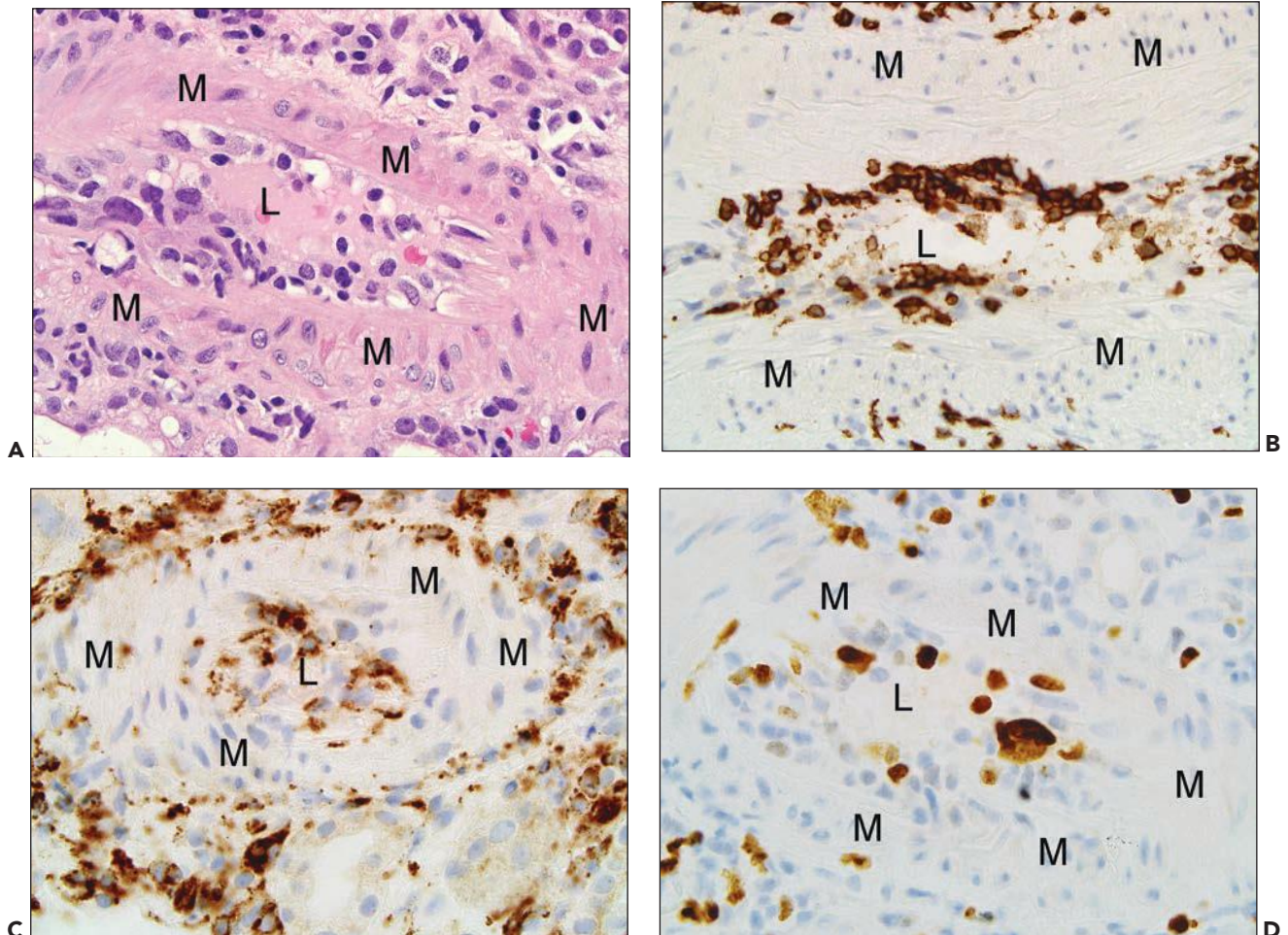


FIGURE 29.17 Acute cellular rejection with transplant endarteritis (Banff category 4, type 2 rejection). Seven days posttransplantation, this patient experienced diffuse tubulointerstitial cellular rejection, marked diffuse transplant glomerulitis, and marked transplant endarteritis (Banff type IIB rejection, C4d-negative). The patient was not sensitized, crossmatch and PRA negative with no DSA at the time of biopsy. Inflammation along the intimal layer of an interlobular artery (A) is rich in CD3 (B) and, to a lesser degree, also CD68 (C)-expressing cells that are mitotically active (Ki-67/MIB-1 positivity, D).

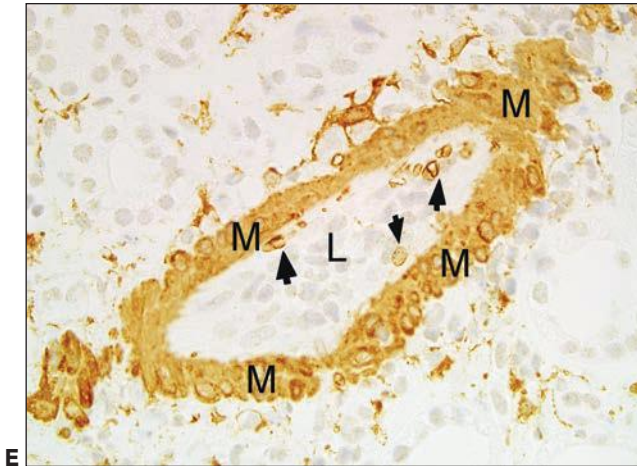


FIGURE 29.17 (Continued) Note: Even in cases of early transplant endarteritis, intimal inflammation contains scattered myofibroblasts expressing smooth muscle actin (SMA, arrows, E). Myofibroblasts can synthesize collagens and promote chronic vascular rejection in protracted/suboptimally treated rejection episodes. This patient responded fully to thymoglobulin therapy. ((A) H&E, (B–D) IHC on formalin-fixed and paraffin-embedded tissue, (B) anti-CD3, (C) anti-CD68, (D) Ki-67/MIB-1, (E) anti- α smooth muscle actin, $\times 600$ oil. L, arterial lumen; M, medial smooth muscle layer.)

are the dominant cell type in PT capillaritis suggesting in our experience concurrent acute AMR.

Infiltration of mononuclear cells into the wall of veins or lymphatics is found in about 10% of biopsies with acute TCMR. This is a sign of inflammatory cell trafficking in areas of inflammation without direct diagnostic significance (210). Not surprisingly, these lesions can be found in inflammatory processes other than rejection.

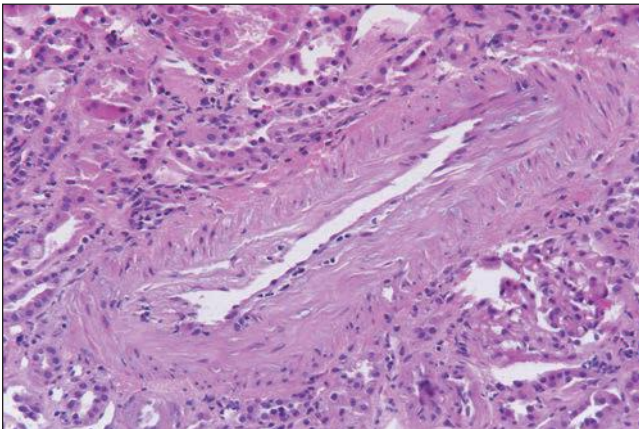


FIGURE 29.18 Acute cellular rejection with transplant endarteritis (Banff category 4, type 2 rejection). Subendothelial mononuclear cells are present in an artery (= acute rejection) superimposed upon pre-existing arteriosclerosis (donor disease). This pattern can be confused with chronic rejection; elastic tissue stains usually help making a distinction (strong staining in cases of hypertension-induced arteriosclerosis vs. chronic vascular rejection largely lacking elastic tissue accumulations). (H&E $\times 200$.)

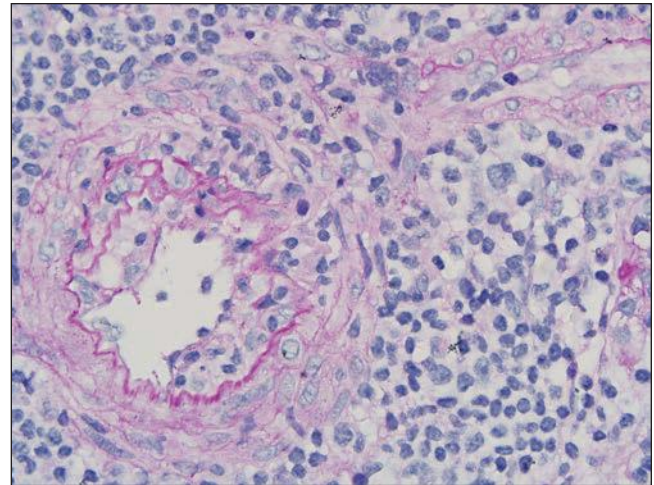


FIGURE 29.19 Acute cellular rejection with severe transplant endarteritis (Banff category 4, type 3 rejection). An interlobular artery has segmental transmural inflammation including destruction of the lamina elastica interna (at 10 o'clock; v3 in the Banff scoring system). There was no evidence of DSA, and a C4d stain was negative confirming the diagnosis of a TCMR process. The rejection episode responded to therapy. (PAS $\times 600$ oil.)

URETER AND PELVIS

All transplanted tissues (i.e., renal parenchyma, renal pelvis, ureter, and extrarenal vessels/tissue) can be involved by acute rejection. Lymphocytes and plasma cells infiltrate the urothelium and ureteral walls (Fig. 29.20) (154,164,211,212). Small arteries in the ureter can be affected by endarteritis and fibrinoid necrosis (154,164,213). Of 26 ureters from irreversibly rejected kidneys, 80% had acute rejection-induced injury (211). Endarteritis in peripelvic adipose tissue can result in fat necrosis occasionally mimicking neoplastic growth in imaging studies (see Fig 29.51). The inflammatory reaction in extrarenal structures usually corresponds to the severity of rejection found in the renal cortex.

Immunofluorescence Microscopy

Little, if any, immunoglobulin deposition is found by immunofluorescence in acute cellular rejection. Extravascular fibrin is typically present in the edematous interstitium. C3 and non-diagnostic C4d deposits can be prominent along the TBM, mainly along tubular segments undergoing atrophy. By definition, in pure acute cellular rejection (Banff category 4), PTC in the cortex and medulla lack any linear C4d deposition; the presence of C4d indicates a component of concurrent AMR/mixed acute TCMR and AMR.

GLOMERULI

In transplant glomerulitis, fibrin and scant IgM and C3 deposits are found along the GBM (161). C4d is usually detected in mesangial regions (by IF only; no mesangial staining by IHC) and, on occasion, with a linear or granular staining pattern along the GBM. In the absence of PTC C4d staining, these isolated glomerular C4d deposits are nondiagnostic for AMR- or antibody-induced glomerular injury. MHC class II/HLA-DR is usually strongly expressed by infiltrating inflammatory cells in segments with glomerulitis.

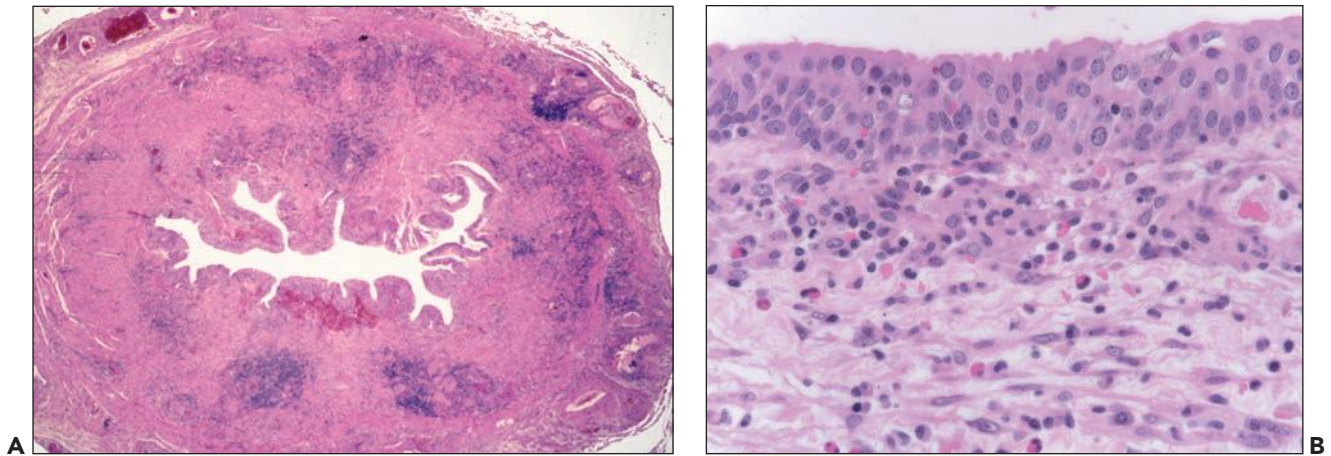


FIGURE 29.20 **A:** Ureter with acute cellular rejection. At low power, dense lymphocytic submucosal infiltrates are seen. (H&E $\times 25$.) **B:** Urothelial invasion of mononuclear cells in acute rejection, involving the calyceal mucosa. Lymphocytes and eosinophils are in the submucosa. (H&E $\times 400$.)

TUBULES

In acute TCMR, MHC class II/HLA-DR antigens and intercellular adhesion molecules are expressed stimulated by the release of interferon-gamma in inflamed regions (Fig. 29.21) (142,214). The detection of MHC class II in the cytoplasm of tubular epithelial cells by IF on frozen tissue samples may be used as an adjunct marker to establish a diagnosis of acute TCMR, in particular if the so-called Banff borderline changes (Banff category 3) are seen by standard light microscopy in

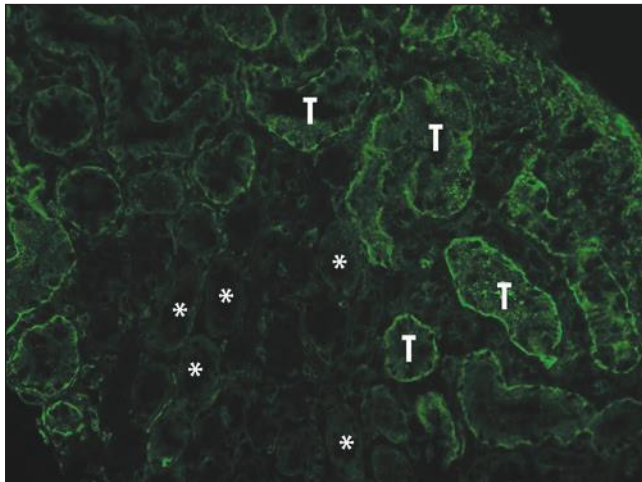


FIGURE 29.21 In cases of acute TCMR, the release of interferon-gamma stimulates the expression of MHC class II (HLA-DR) in the cytoplasm of tubular epithelial cells best detected by immunofluorescence staining (T, tubular cross sections with MHC class II expression; asterisk, tubules without class II). The detection of tubular MHC class II can serve as an adjunct diagnostic parameter to establish a diagnosis of acute TCMR, in particular if Banff borderline changes (Banff category 3) are present or to confirm the concurrence of AMR and acute TCMR. (Direct immunofluorescence microscopy on frozen tissue with an antibody directed against MHC class II, $\times 200$.)

corresponding formalin-fixed tissue sections (141,142,156). Tubules, in particular those with some evidence of atrophy, show prominent linear staining along basement membranes for C3 and, to a lesser degree, also C4d, C5b-9, and IgM. C3 is largely derived from tubular cells, as judged by C3 allotype antibodies; donor-specific C3 mRNA can be detected in rejecting renal allografts by PCR (215). Proximal tubular cells in culture synthesize C3 in vitro in response to IL-2 (216). The origin of C4d and C5b-9 is less well understood.

INTERSTITIUM

Fibrin is typically present in the edematous interstitium (217) and likely a promoter for the development of the so-called scleredema in protracted cases of acute TCMR that is increasing accumulation of matrix proteins including collagens in an edematous stroma. The fibrin deposition derives from leakage of PTC walls and activation of the clotting system, probably by cytokine induction of macrophage procoagulants (218).

VESSELS

Most investigators find no significant immunoglobulin deposits in the arterial vessels in acute TCMR with or without transplant endarteritis (208); fibrin deposition is sometimes seen in inflamed intimal segments and in vessels with fibrinoid necrosis. Infiltrating cells in foci of endarteritis strongly express MHC class II/HLA-DR. Diffuse PTC C4d deposits or the exceptional event of arterial IgG deposits is evidence for concurrent acute AMR (219). C4d, C3, and, to a lesser degree, IgM are typically seen in arteriolar hyalinosis as a nondiagnostic staining pattern.

Electron Microscopy

Electron microscopy is generally not performed for diagnostic purposes in acute rejection; however, it may be indicated if the glomeruli are notably involved.

GLOMERULI

Transplant glomerulitis typically shows dilated capillary lumens filled with activated and enlarged endothelial cells as well as other mononuclear cell elements, mainly monocytes.

Polymorphonuclear leukocytes, platelets, and fibrin strands are occasionally seen. Mitotic figures can be detected but are usually rare. Glomerular endothelial cells are reactive, with a marked increase in cytoplasmic organelles (ribosomes, mitochondria, endoplasmic reticulum) and nuclei show open chromatin and prominent nucleoli (Fig. 29.22). The endothelial cells typically lose their fenestrations and are often separated from the GBM by a widened lamina rara interna. Rudimentary thin subendothelial new lamina densa formation can occasionally be seen as an early ultrastructural sign of evolving transplant glomerulopathy (220) scored in the Banff 2013 update as “cg1a” (see Fig. 29.22D). The mesangium has loose matrix and sometimes monocytes. Podocytes primarily those overlying segments with glomerulitis usually show foot process effacement.

TUBULES

Lymphocytes in the tubules accumulate between the epithelium and the TBM, frequently surrounded by a clear zone (221). The tubular epithelial cells remain in contact with the basement membrane, whereas the lymphocytes are often separated from it by a thin layer of epithelial cytoplasm. Breaks in the TBM are rarely found by electron microscopy (Fig. 29.23) (175). Leakage of Tamm-Horsfall protein into the interstitium through fractured TBM segments can occur; these deposits contain 4-nm-thick filaments arranged in parallel clusters and

sometimes herniating into vessels (222). The tubular epithelial cells in the vicinity of mononuclear cells often show signs of injury, including vacuolization (221), necrosis, or apoptosis (175). Tubular basement membranes, especially those with evidence of atrophy, are thickened and can contain nondiagnostic small electron-dense particles, mainly complement products.

INTERSTITIUM

The interstitium is expanded by edema and a mixed infiltrate of activated lymphocytes and macrophages. Granulocytes are occasionally encountered. The fibroblasts may appear active with fibrils, typical of myofibroblasts.

VESSELS

Mononuclear cells accumulate in the PTC lumens in areas of interstitial inflammation and edema, sometimes to the point of apparent capillary occlusion. The intracapillary cells mostly consist of lymphocytes and monocytes, which are sometimes in contact with the endothelium or emigrating through the capillary walls (223). The endothelium shows signs of activation, as judged by nuclear enlargement; increased ribosomes, endoplasmic reticulum, mitochondria, and Golgi apparatuses; and loss of fenestration (223). The endothelial hypertrophy has been compared with normal postcapillary venules that are not anatomically recognized in the kidney (223). Which of these

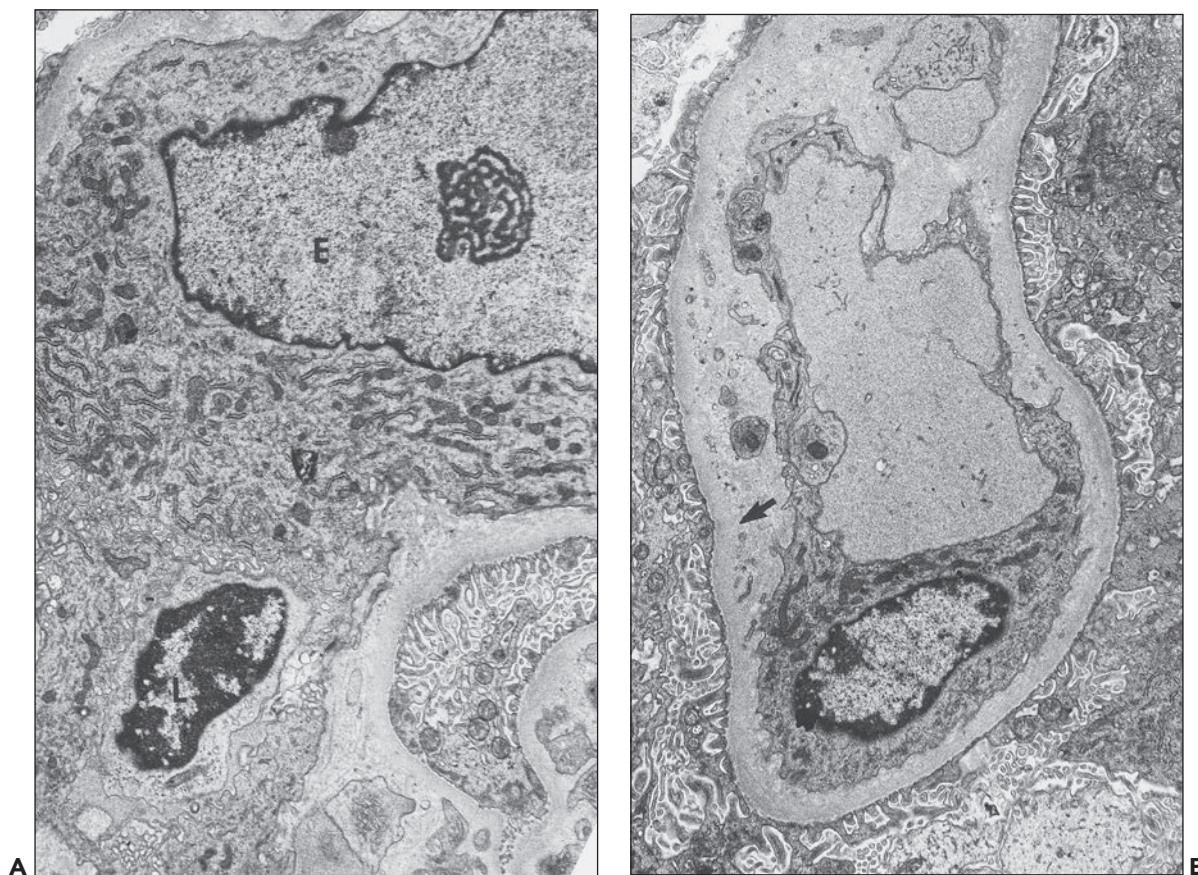


FIGURE 29.22 Transplant glomerulitis. A: A lymphocyte (L) is in contact with an activated glomerular endothelial cell (E). **B:** An activated endothelial cell has lost fenestrations and is separated from the original basement membrane (arrow) by an expanded subendothelial space/lamina rara interna that contains loose matrix, cell processes, and debris.

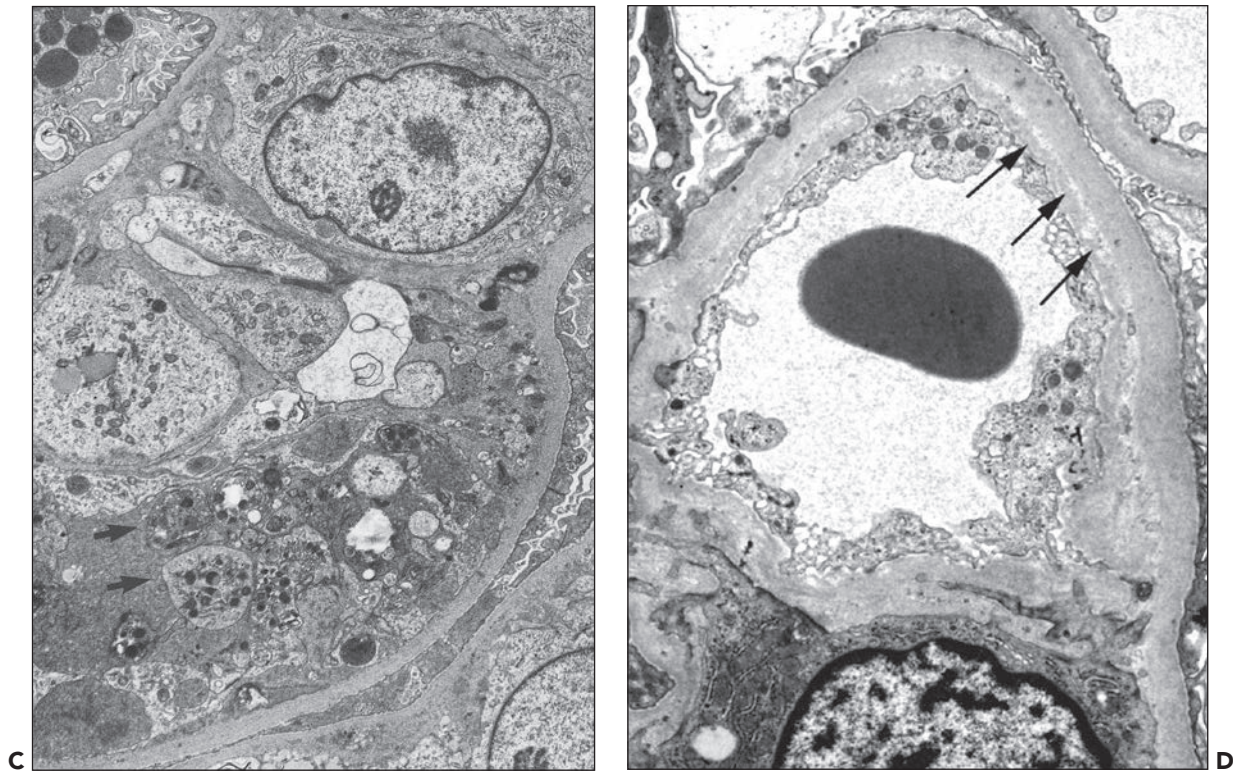


FIGURE 29.22 (Continued) **C:** Platelets are numerous in a capillary loop that has denuded endothelium. **D:** Activated endothelial cells are overlying a widened lamina rara interna containing rudimentary new dense as a sign of early, ultrastructural evidence of GBM remodeling and duplication (arrows). Light microscopy in this case showed focal minimal glomerulitis without transplant glomerulopathy. Early ultrastructural GBM remodeling/minimal duplication as illustrated in **D** is scored in the 2013 update of the Banff classification scheme as “cg1a”. (Electron micrographs. (A) $\times 6360$, (B) $\times 5225$, (C) $\times 6000$, (D) $\times 5500$.)

features are specifically related to TCMR versus AMR has not been determined. Multilaminations of PTC basement membranes are typically minor but can become prominent with 5 to 7 basement membrane layers seen in 10% to 20% of late acute TCMR rejection episodes occurring post-year 1 (224). Such pronounced multilaminations in cases of acute TCMR (C4d-negative) represent protracted endothelial injury and evidence of early chronic rejection (224). The endarteritis lesions have been little studied ultrastructurally, because of the difficulty in sampling these very focal lesions.

Molecular Studies

The molecular phenotype in renal allografts with acute TCMR, mainly tubulointerstitial cellular rejection, Banff category 4, type 1, primarily comprises transcripts expressed by various subsets of activated lymphocytes and other inflammatory cell elements: cytotoxic T lymphocytes (granzyme B, perforin, and Fas ligand), effector memory T cells, T helper cells, regulatory T cells (225–236), and macrophages (237,238). Also, increased levels of transcripts regulated by interferon-gamma (TGF- β , TNF- α , RANTES, MIP-1 α , HLA class I and II molecules, CXCL9, CXCL10, and CXCL11) and for T-bet, a master transcription factor for T cells, are found (229,239–242). As expected, successful treatment of rejection is followed by a significant decrease of all molecular signals/transcripts (228,239).

Complement components are also expressed during rejection, such as C3 and C1q, but probably this phenomenon reflects a “nondiagnostic” rejection-induced injury response (229,243–245). Tissue injury results in down-regulation of numerous transcripts associated with various physiologic functions, such as solute carriers and membrane transporters with high constitutive expression levels in normal tubular epithelium (233,234,240,246).

Recently, the Edmonton group used their comprehensive collection of human renal allograft mRNA microarray data to construct a hypothetical cellular rejection classifier (239,247). This classifier assigns to each biopsy a probability score for the presence of cellular rejection according to the detected molecular expression profile. Interestingly, IFN- γ and inducible or cytotoxic T-cell-associated transcripts, for example, CXCL9, CXCL11, GBP1, and INDO, were most predictive in this algorithm (239). A comparison of molecular marker expression with histologic Banff categories revealed discordant diagnoses in 20% of biopsies. Potential explanations for the observed discrepancies include an inadequate molecular test performance, sampling differences, treatment prior to biopsy that suppresses all molecular signals while histologic lesions might still be present, presence of isolated histologic lesions not reflected by major shifts in the gene expression profile, etc. However, a concordance rate of 100% can hardly be expected comparing different tests, and the reported findings are very encouraging emphasizing the value of biopsy diagnoses. In biopsies with

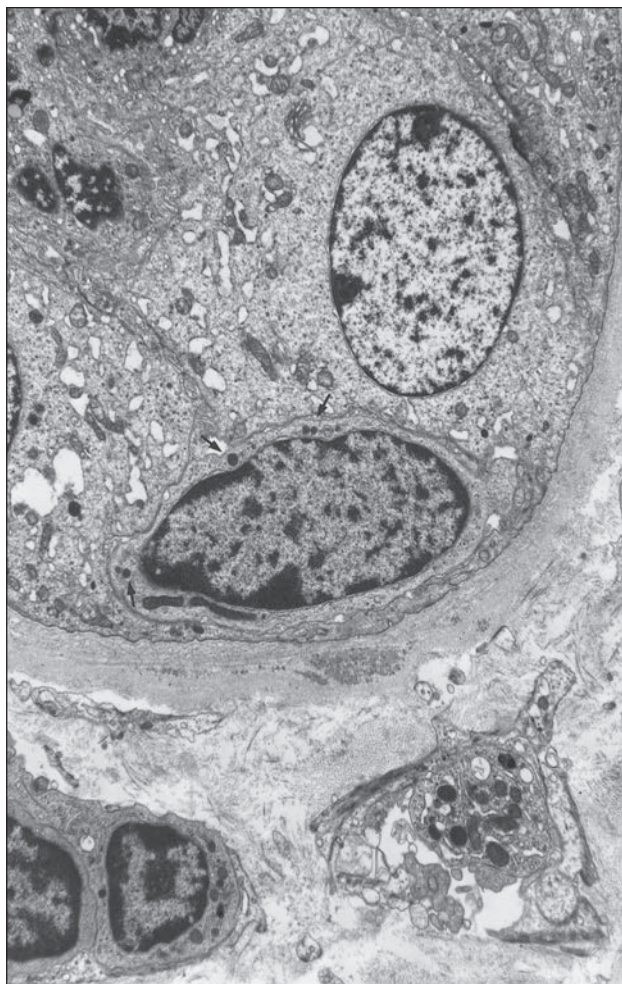


FIGURE 29.23 Acute cellular rejection. A tubule is invaded by a lymphocyte with a few dense cytototoxic granules (arrows) that are oriented toward the epithelial cells. The tubular basement membrane has fine laminations but does not appear disrupted. (Electron micrograph; $\times 5200$.)

Banff category 3 “borderline” changes, 33% of cases showed a molecular phenotype similar to TCMR, while 67% were nonrejection-like, underscoring on a molecular level the diagnostic heterogeneity of this group. The tightest association was between molecular phenotype and Banff total inflammatory (ti) score, indicating that the molecular phenotype is largely due to tubulointerstitial inflammation.

Suthanthiran et al. pioneered work on mRNA profiles from urinary cells that reflect events in the renal allograft (248). Elevated levels of mRNA for OX40, OX40L (costimulatory proteins), PD-1 (programmed death-associated protein), and Foxp3 (master regulatory protein in regulatory T cells) indicate acute rejection (249). More recently in a large cohort of 485 kidney graft recipients, Suthanthiran et al. analyzed 4300 urine samples and found a 3-gene signature of CD3- mRNA, IP-10 mRNA, and 18S rRNA levels to be diagnostic of acute TCMR (250). Similar efforts are made with RNA retrieved from peripheral blood leukocytes (251).

Elevated expression levels of both microRNAs (miRNA) and mRNAs were found in acutely rejecting grafts. Profiling

urinary microRNA expression levels of stable transplant patients and patients with acute rejection revealed micro R-10b and micro R-210 to be down-regulated and micro R-10a to be up-regulated in acute rejection compared to the control cohort. Only micro R-210 differed between patients with acute rejection compared to stable transplant recipients with urinary tract infections and, thus, may potentially serve as a biomarker of acute rejection (252). These preliminary data suggest that microRNA expression patterns correlate with mRNA profiles. They might possibly be of diagnostic value due to their stability, especially in body fluids and after formalin fixation and paraffin embedding of tissue samples (253,254).

Etiology and Pathogenesis

Antigens

The primary T-cell allograft response is to the antigens encoded in the MHC, present in all vertebrates. Genetic experiments in mice showed that one genetic locus (the MHC) was the major determinant of graft survival. Two chemically and functionally different classes (I and II) of histocompatibility molecules are encoded in the MHC. Disparity of either alone is sufficient to cause graft rejection in mice (255). The exquisite sensitivity of the immune system to these antigens has been elegantly demonstrated using Kbm mutant mice. Skin grafts from donors that differ from the recipient in only 1 to 3 amino acids in a single MHC molecule are promptly rejected (255,256). The human MHC (termed HLA for human leukocyte antigen) spans 4000 kb on the short arm of chromosome 6 and contains multiple genes (257). The dominance of HLA antigen mismatch in determining outcome is supported by the observation that grafts from an HLA-identical sibling survive longer on average than those from a non-HLA-identical sibling (see Fig. 29.3).

Class I MHC antigens consist of highly polymorphic transmembrane 45-kDa glycoprotein α -chains associated with monomorphic 12-kDa $\beta 2$ -microglobulin. About 100 alleles of the A, B, or C class I loci have been defined with alloantibodies and over 1000 with genetic probes (256). Class I antigens are widely distributed on all nucleated cells, but their concentration on the cell surface varies widely, even to the point of undetectability by standard immunohistochemical techniques (e.g., placental and Langerhans cells). In normal human tissues, the vascular endothelium (arteries, veins, capillaries) stains most intensely for class I antigens; the parenchymal cells are moderately positive (258).

Class II MHC antigens contain noncovalently associated transmembrane α - and β -chains of 25 to 28 and 29 to 34 kDa, with most of the polymorphism on the smaller β -chain. Three gene families (DP, DQ, DR), each with multiple α - and β -genes, have been identified. Class II antigens are more restricted in distribution than class I and vary by species and class II family. In humans, class II antigens are normally found on B cells, dendritic cells, capillary endothelium, monocytes, Langerhans cells, and activated T cells (258). DR but not DQ is demonstrable on capillary endothelium; both are on dendritic cells. Parenchymal cells normally have less intense staining for HLA-DR and no DQ or DP (157,259,260). Normal arterial endothelium has little or no detectable class II antigens.

The expression of MHC molecules is regulated on the cell surface, under the control of inflammatory mediators, such as the interferons and tumor necrosis factor (261,262).

IFN- γ , produced by antigen-activated T cells and NK cells, induces both class I and class II MHC antigens on epithelial and endothelial cells (263). Increased surface density of MHC molecules enhances the susceptibility to T-cell-mediated lysis and the ability to present antigen (264). However, induction of graft MHC molecules is not necessary to promote rejection. IFN- γ -deficient mice reject kidney allografts as quickly as normal mice without induction of MHC molecules (265). Paradoxically, class I- and class II-deficient grafts are also rejected efficiently, with MHC expression undetectable by immunoperoxidase techniques (266,267).

The normal function of MHC class I and II molecules is to “present” antigen to T cells. MHC molecules bind certain peptide antigens more avidly and thereby present these antigens more effectively. T cells are positively selected in the thymus for recognition of self-MHC molecules, so that they are normally “restricted” to antigen presented by self-MHC antigens. Cells with a high reactivity to self-MHC or no affinity for MHC are deleted. The T cells recognize an altered conformation of self-MHC molecules plus the associated antigen. Graft rejection thus occurs in part because the T cells recognize the foreign MHC antigens as if they were self-MHC molecules altered by association with some “X” antigen (the altered self-hypothesis) (268) or because of their intrinsic affinity for the MHC. These theories explain the high clonal frequency of T cells directly reactive to nonrelated individual cells and why the MHC is the “major” determinant of allograft survival (269).

Direct recognition of HLA antigens on graft cells can result in cell-mediated cytotoxicity and release of cytokines. T cells can also react with MHC alloantigens from the graft that are processed and presented by autologous dendritic cells or infiltrating macrophages, as with other protein antigens (270). This response is termed the “indirect” pathway to distinguish it from the “direct” recognition of antigens on the donor cell surface. Indirect responses cause rejection by the action of lymphokines or through activation of B cells or macrophages associated with dendritic cells.

NON-MHC ANTIGENS

Non-MHC histocompatibility antigens (“minor antigens”) are defined simply by their ability to elicit graft rejection and a genetic locus outside the MHC. These antigens are responsible for graft rejection between MHC-identical congenic mice and HLA-identical siblings. Their chemical nature and distribution are largely unknown. In the mouse, 30 to 50 minor loci are calculated to trigger skin graft rejection (271). Graft-infiltrating T cells can be isolated that recognize minor antigens on donor tubular epithelium (272). The vascular endothelium expresses polymorphic non-MHC histocompatibility antigens, which have not yet been well characterized at a molecular level.

Antigen Response by T Cells

Engagement of MHC-associated antigen by the specific T-cell receptor leads to expression of IL-2 receptor on the cell surface. Second (costimulatory) signals from the antigen-presenting cell are required to move the T cell to produce T-cell growth factors, such as IL-2, IL-4, or IL-15. Costimulatory signals, including CD86, CD40, and OX40L, are provided by “professional” antigen-presenting

cells, such as dendritic cells and monocytes. These bind to CD28, CD40L (CD154), and OX40 on T cells, respectively. T cells that see antigen without the second signal are rendered anergic, that is, refractory to specific antigen stimulus in the future. The conditions that promote such an outcome are of considerable clinical interest as a potential strategy to produce tolerance.

Upon recognition of antigen on a cell surface with sufficient costimulatory signals, the T cells make two types of responses: secretion of cytokines and chemokines, which affect the behavior of nearby cells, and the development of cytotoxic effector functions that kill cells that express the relevant MHC. Delayed-type hypersensitivity to exogenous protein antigens is mediated by the former mechanism, while resistance to viral infection is dependent on the latter. These are the two nonexclusive mechanisms proposed for acute graft rejection.

T cells are heterogeneous in function. CD4 cells, which recognize peptide antigens (typically antigens exogenous to the cell) presented by self-class II molecules, are critically important for graft rejection. Deficiency of CD4 cells prevents heart or skin graft rejection in mice (273). CD4 cells can be divided according to their cytokine production into Th1 and Th2 cells, as proposed by Mosmann et al. (274), although some cells have overlapping cytokine profiles. Th1 cells produce IFN- γ , IL-2, and TNF- α and express CXCR3 and CCR5 chemokine receptors. Th1 cells activate macrophages, mediate delayed hypersensitivity reactions, mediate cytotoxicity via Fas ligand/Fas, and are typically present in the infiltrate of acutely rejecting grafts. IFN- γ and TNF- α activate macrophages to produce nitric oxide, which causes vasodilation and edema, reactive oxygen species, and more TNF- α . TNF- α in turn induces apoptosis via activation of caspases. IL-12 produced by other cells (e.g., dendritic cells and macrophages) promote Th1 cell activity and inhibit Th2 cytokines. IL-10 and IL-13 produced by macrophages and other cells promote Th2 activity and inhibit production of Th1 cytokines.

Th2 cells synthesize IL4, IL-5, IL-10, and TNF- α and have the chemokine receptors CCR3, CCR4, and CCR8. These cells provide help for B cells and production of IgE and IgG4 antibodies (275). Th2 cytokines promote eosinophil production and infiltration. IL-4 and IL-13 stimulate the production of eotaxins (CCL11, CCL24, CCL26) by parenchymal cells, including endothelial cells (276). Th2 cells are sufficient to mediate cardiac allograft rejection in mice and promote a heavy infiltrate of eosinophils (277). It is likely that some of the variation in morphology of acute graft rejection is due to differences in the proportionate contribution of Th1 and Th2 cells in the infiltrate.

CD8 cells, which recognize peptide antigens presented by class I MHC molecules, produce IFN- γ and mediate direct cytotoxicity via granzymes A and B and perforin and by Fas ligand (278,279). Perforin forms a membrane channel that allows the granzymes into the target cell cytoplasm, where they activate Bid and caspases that trigger apoptosis (280). Expression of granzyme B, but not perforin, depends upon IL-12 and correlates strongly with cytolytic activity. Across an isolated class I mismatch, perforin deficiency prolongs survival of heart or skin grafts (281). However, fully mismatched recipients that lack either perforin or granzymes A and B reject kidneys with equal efficiency and develop tubulitis and endarteritis, arguing against a necessary role for either mediator (282).

A subpopulation of T cells, termed regulatory T cells (Treg), inhibits activation of effector T cells. Treg are antigen specific and can suppress memory CD8 cells, apparently via a CD30-dependent pathway (283). Activation of Treg function requires engagement of the TCR (i.e., is antigen specific), but can affect other cells through soluble mediators (antigen nonspecific). Most Treg are CD4⁺CD25⁺CD152⁺ and produce IL-10 and TGF- β , but not IL-2 or IL-4 (284,285). Differentiation into Treg is promoted by TGF- β and is mediated by the master transcription factor, Foxp3, which continues to be expressed in Treg cells and serves as a distinctive marker of these cells in tissues.

Chemokines

A burgeoning, complex, and confusing literature is emerging on the role of chemokines in transplantation. In acutely rejecting human kidney grafts, a variety of chemokines are produced (IP-10, RANTES, MIP-1 α , MIP-1 β , lymphotactin, MCP-1), and the infiltrating cells express several chemokine receptors (CXCR4, CXCR3, CCR5, CCR2, and others) (286–291). CCR5 is mostly in the diffuse infiltrate (287), while CXCR4 is in nodular aggregates of mononuclear cells (292). The pattern of expression suggests a predominance of Th1 over Th2 cells (i.e., CCR5 and not CCR3 or CCR8) (287). Tubules synthesize RANTES (293), IL-8 (294), CXCL1 (292), and IL-6 (295) in acute rejection; none of these are detected in normal kidneys. These may be a response to local T-cell production of IL-17 (296). MCP-1, MIP-1 α , MIP-1 β , and RANTES are increased in the basolateral surface of tubules (289,293,297). Heparan sulfate in the TBM may provide sites for chemokines, such as CCL4, to bind and create gradients (298). MCP-1 and MIP-1 β levels are higher in type 2 than in type 1 rejection (297).

Pathogenetic Mechanisms

The various components of the kidney are affected to differing degrees in individual episodes of acute rejection. While each of these targets is believed to be affected by T cells, macrophages, and cytokines, the pathogenesis may vary somewhat. IHC in situ hybridization, and laser capture microdissection are yielding new insights into the cells and molecules that participate in rejection.

INFILTRATING CELLS

Both CD8⁺ and CD4⁺ T-cell subsets are present in varying proportions, as well as a minor population of CD4⁺CD8⁺ cells (299,300). Typically, the CD8⁺ cells are enriched in the graft and are found permeating diffusely in the renal cortex (157,301,302). CD4⁺ cells are usually selectively concentrated in perivascular aggregates (157,301,303). T cells in the infiltrate express the CD45RO isoform of activated/memory cells (304). Most infiltrating CD3⁺ T cells express the usual α/β -TCR (305,306); in a minority of specimens, over 10% of T cells are γ/δ ⁺ (306). A skewed distribution of TCR gene rearrangements has been reported, suggesting local selection of specificities (307–311).

Many infiltrating T cells express cytotoxic molecules, namely, perforin (312,313), FasL (314), granzymes A and B (315–317), and TIA-1/GMP-17 (317,318) (Fig 29.24). About 30% of the infiltrating cells are TIA-1/GMP-17⁺ (318); most of these express CD8, but 12% are CD4 (318). Thus, some

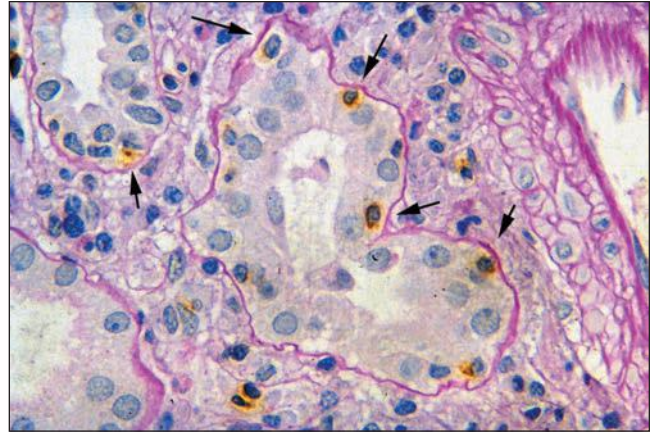


FIGURE 29.24 Acute tubulointerstitial cellular rejection (Banff category 4, type 1). Lymphocytes in tubules express the cytotoxic granule associated protein TIA-1 (GMP17). (PAS combined with anti-TIA-1 antibody/immunoperoxidase technique $\times 400$.)

cytotoxicity may be mediated by CD4⁺ T cells, consistent with the observation that donor-specific cytotoxic CD4⁺ T cells can be cultured from grafts (319). The infiltrating cells also express TNF- β (lymphotoxin) and TNF receptors (320).

Foxp3⁺ cells, presumably Tregs, are present in variable numbers in the infiltrate (321) (Fig. 29.25). Foxp3⁺ Treg cells are known to suppress cell-mediated reactions and serve to dampen T-cell-mediated graft rejection as recently shown in mice (322). Supporting this role in vivo, Foxp3⁺ cells infiltrate grafts in certain experimental conditions that promote tolerance (323) and specific depletion of Foxp3 cells triggers acute TCMR in the mouse (322). The presence of Foxp3⁺ cells in the graft has no correlation with the outcome of TCMR (321,324,325). However, Foxp3⁺ cells are more prevalent in borderline than TCMR biopsies (326). In stable grafts Foxp3⁺ infiltrates have been associated with donor hyporesponsiveness in vitro (327) and decreased Cr at 2-3 years (328). Grafts with subclinical rejection without Foxp3 cells had a significantly worse prognosis at 5 years than those with Foxp3⁺ cells, even among those with fibrosis (329). Further studies are warranted to assess their significance.

Activation of the infiltrating T cells has been demonstrated by the presence of IL-2 (320) and its receptor CD25 (182,330,331). In situ hybridization studies show cytokines are typically synthesized by a minority of the cells (presumably the specific alloreactive cells) (332). IFN- γ is synthesized in the graft (189,244,333) and is detected in lymphocytes scattered throughout the infiltrate (330). Other markers of activation expressed by the infiltrate are the transferrin receptor (334), CD38 (171), and CD69 (335). Some CD8 cells express CD152, and a few CD4 cells express CD40L.

Apoptosis of the infiltrating T cells can be demonstrated with the TdT-uridine nick end label (TUNEL) technique (318,336–338) and may occur at a frequency comparable to that in the normal thymus (1.8% of cells in a section) (318). Apoptosis probably occurs in infiltrating T cells as a result of activation-induced cell death and would thereby serve to limit the immune reaction (318).

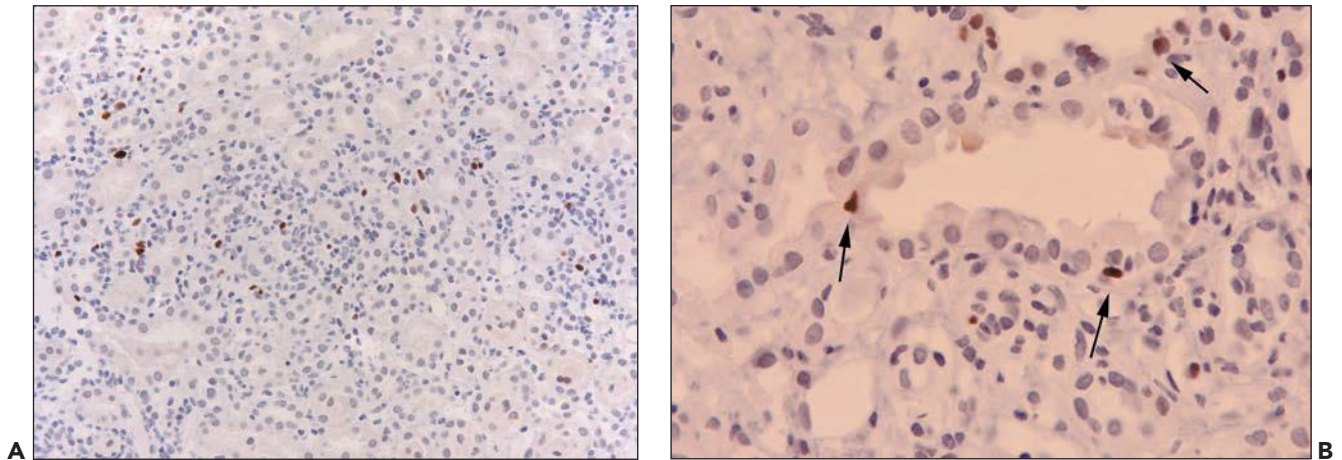


FIGURE 29.25 Acute tubulointerstitial cellular rejection (Banff category 4, type 1). **A:** Cells in the infiltrate stain for Foxp3, a transcription factor for T regulatory cells. **B:** Foxp3 cells are present in the tubules (arrows). (Anti-Foxp3 immunoperoxidase, (A): $\times 200$, (B) $\times 600$.)

Macrophages expressing CD14 or CD68 sometimes rival T cells in abundance and may be the predominant leukocyte (302,339,340). Macrophages display markers of activation, including the tissue factor procoagulant-related antigen (182,341), receptors for VCAM-1 and fibronectin (CD49d, VLA-4), and Fas ligand (342). Macrophages expressing the tissue procoagulant-related antigen are associated with interstitial fibrin deposits (182). Endothelin, IL-6, and VEGF can also be detected in macrophages in rejection (295,343,344). Macrophages express costimulatory molecules CD80 and CD86, but not CD40 (331). Plasminogen activator inhibitor-1 (PAI-1) synthesis is detected in infiltrating cells, especially in hemorrhagic areas, perhaps serving a protective role (345). Urokinase plasminogen activator and its receptor are also produced by the infiltrating cells (346).

B cells can be present, even in early biopsies. The local synthesis of CXCL13 and expression of its receptor CXCR5 in B-cell clusters have been noted in patients who developed rejection in the first 9 days (347). About 2% to 30% of the infiltrating mononuclear cells have been reported to express CD57 (HNK-1) (157,182,259,302). Numerous CD56⁺ cells (also considered to be NK cells) have been reported (315), but using a panel of three “NK” antibodies (PEN 5, CD57, and CD56), positive mononuclear cells were rare (less than 1%) (318); similar results were noted by others (348).

TUBULES

Tubulitis is an important mechanism of graft rejection that involves both CD8⁺ and CD4⁺ cells (157). Intratubular T cells with cytotoxic granules accumulate selectively in the tubules, compared with the interstitial infiltrate (318) (see Fig. 29.24). These cells account for 65% of the mononuclear cells in tubules compared with about 30% of the interstitial cells. Lymphocytes expressing perforin mRNA and perforin protein are closely associated with tubular epithelial cells (349). Intratubular T cells express CD103 ($\alpha E\beta 7$), the integrin that binds to E-cadherin, which is normally on the surface of tubular cells (350–352). CD103⁺ cells are found exclusively in the tubules (352). CD103 probably contributes to their concentration within tubules (318): Mouse T cells deficient in CD103 do not effectively mediate tubulitis or tubular injury

(353). Surprisingly, cyclosporine increases the expression of CD103 in the infiltrate (353). CD4 cells with Foxp3 expression are relatively concentrated in the tubules (321). T cells proliferate once inside the tubule, as judged by the marker Ki-67 (MIB-1), which labels 15% of the intratubular lymphocytes (354).

Increased numbers of TUNEL⁺ tubular cells are present in acute rejection, compared with normal kidneys (318,336,338); CNi toxicity; or ATN (318). Tubular cells have increased Bax and p53 and less Bcl-2 (355). The degree of apoptosis correlates with the number of cytotoxic cells and macrophages in the infiltrate, consistent with a pathogenetic relationship (318). Apoptosis of murine tubular cells can be induced in vitro by IL-2 or IFN- γ , both present in acute rejection (356). Tubular epithelial cell proliferation can also be detected with Ki 67, which labels 1.5% \pm 2.3% of the epithelial cells (354).

Tubular cells can process and present antigen to activated T cells in vivo and in vitro (357) and express MHC class II and the costimulatory molecules CD80 and CD86 in acute rejection (358). Increased tubular epithelial cell expression of HLA-DR is typical, but not by itself diagnostic, of acute cellular rejection since it can also be seen in cases such as pyelonephritis (170,259,334,359–362) (see Fig. 29.21). Increased tubular HLA-DR antigen expression correlates strongly with the presence of a T-cell infiltrate and presumably is a local response to IFN- γ produced by these cells (156,170,244,259). Proximal and distal tubules express the IFN- γ receptor, detectable with immunoperoxidase in acute rejection (320,363). Tubular synthesis of C3 (215) correlates with local IFN- γ production (244) and exposure to IL-17 (296). Tubules also synthesize TNF- α (364), TGF- $\beta 1$, IL-15, osteopontin, and VEGF (344,351,363). Expression of osteopontin correlates with CD68⁺ cell infiltration and tubular cell regeneration (Ki 67+).

Several adhesion molecules are increased on tubular cells during acute rejection. ICAM-1 (CD54) is increased (365–367) and closely correlated with HLA-DR. VCAM-1 is increased, mostly on the basal surface of tubular cells, and correlates with the degree of T-cell infiltration (339) and CD25⁺ cells (366). Decreased staining for urokinase and antithrombin III occurs in proximal tubular cells (368). Tubules also produce urokinase plasminogen activator and its receptor (346).

Some molecules and cells in tubules have the potential to inhibit acute rejection. Protease inhibitor-9 (PI-9), an inhibitor of granzyme B, is synthesized by tubules in acute rejection, suggesting this may suppress tubular injury by cytotoxic T cells (316). IL-15 produced by tubular cells inhibits expression of perforin (351). Tubules also produce the complement inhibitor clusterin (369), which is colocalized in the TBM with the C5b-9 complex and vitronectin (370).

VESSELS

Endarteritis is a common and significant manifestation of cellular rejection, observed in all solid allograft organs. There is good support for a T-cell-mediated type of injury in transplant endarteritis. The cellular arteritis occurs in the absence of antibodies (B-cell knockout mice) (Fig. 29.26) (371). As further evidence, in humans, rejection with intimal infiltrates can usually be reversed with antibody preparations mainly targeting T cells (204,372,373). However, antibodies can elicit endarteritis in mice (374) and may co-stimulate with TCMR arterial inflammation in humans. The cells infiltrating the endothelium and intima are T cells and monocytes/histiocytes, but not B cells (157,164,208). Both CD8⁺ and CD4⁺ cells invade the intima in early grafts, but later, CD8⁺ cells predominate (157), suggesting that class I antigens are the primary target. Some of the T cells express a cytotoxic phenotype (318,375). TNF receptors are detectable in the endothelium of arteries (320). Apoptosis of vascular endothelial cells can be detected in sites of endarteritis (318,336), and increased numbers of endothelial cells appear in the circulation (376).

Normal arterial endothelial cells express class I antigens, weak ICAM-1, and little or no class II antigens, or VCAM-1. During acute rejection, the endothelium of arteries expresses increased HLA-DR (157,259) and ICAM-1 and VCAM-1 (365,367), and endothelial synthesis of ICAM-1 and VCAM-1 can be demonstrated by *in situ* hybridization (377). Endothelium also up-regulates ligands for L selectin (sialyl Lewis X and lactosamine) (378). The endothelium of arteries with acute cellular rejection shows a striking increase in PDGF A-chain mRNA and protein (379). In endarteritis, PDGF B chain, in contrast, is largely limited to the CD68⁺ inflammatory cells, probably macrophages, under the endothelium; it probably promotes myofibroblast proliferation. IL-6 is also

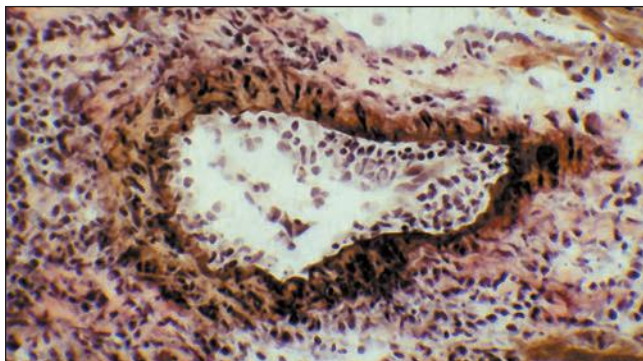


FIGURE 29.26 Endarteritis in a cardiac allograft in a mouse deficient in B cells. This shows that endarteritis lesions can occur without the participation of antibody (371). (Elastic tissue stain of a cryostat section, $\times 400$.)

increased in the media and endothelium of vessels in acute rejection (295). In transplant endarteritis, the endothelium expresses PAI-1 mRNA (345) and the urokinase plasminogen activator receptor (346); the arterial media shows increased urokinase plasminogen activator (346).

Normal PTC endothelial cells express prominent HLA-DR, HLA class I antigens, LFA-3 (CD58), PECAM-1 (CD31), factor VIII antigen, and low levels of ICAM-1 and ICAM-2 (348,366,380). During acute cellular rejection, the capillary pattern for HLA-DR and ICAM-1 antigens is lost, probably due to disruption and necrosis of the endothelium (348,380). This was confirmed using a monoclonal antibody that reacted selectively with donor class I (HLA-A2) in six cases (380). Endothelial cells also have decreased endothelin expression in rejection with endarteritis, but not in tubulointerstitial rejection (381).

GLOMERULI

In transplant glomerulitis, intraglomerular mononuclear cells are primarily CD8⁺ (157,382) accompanied by macrophages (see Fig. 29.6A). The lymphocytes have an activated phenotype, as judged by expression of CD25 and HLA-DR. The glomeruli have increased staining for HLA class I antigens (157). TNF- α protein is detectable in glomerular endothelial cells (364), which normally have TNF receptors (320). Thromboxane synthetase and IL-6 increase in glomeruli in rejection, probably due to intraglomerular macrophages (295,383).

It is not known why rejection often becomes focused on specific anatomic compartments. Transplant glomerulitis may only involve some glomeruli and occasionally spares the tubulointerstitial and arterial compartments completely.

Differential Diagnosis

Tubulointerstitial Inflammation

Interstitial mononuclear inflammation and tubulitis occur in a variety of diseases other than acute rejection, such as infection, posttransplant lymphoproliferative disease (PTLD), and drug-induced allergic tubulointerstitial nephritis, and are not sufficient per se to prove the existence of rejection. Interstitial inflammation and sclerosis in the subcapsular cortex are common in renal transplant biopsies and not evidence for rejection.

INFECTION

Viral infection is suggested by nuclear inclusions and confirmed by specific viral stains (e.g., polyomavirus, cytomegalovirus [CMV], adenovirus, Epstein-Barr virus [EBV]). Features that favor a polyomavirus infection are prominent tubular cell lysis and occasionally a vaguely granulomatous inflammatory infiltrate with "intratubular" granuloma formation, that is, dilated tubules containing abundant epithelial cells and histiocytic cell elements. Tubular HLA-DR expression typical for cellular rejection is generally not found in cases of uncomplicated polyomavirus infections (362). Some light microscopic clues that can suggest a viral infection are listed in Table 29.10. Neutrophils forming not only casts in injured tubules but also being present between tubular epithelial cells and in the edematous interstitium suggest a diagnosis of pyelonephritis. Frank abscesses (collections of abundant neutrophils with destruction of tissue) do not occur in rejection but rather are signs of "destructive" pyelonephritis. However, neutrophils in PTC, that is, neutrophilic capillaritis, and in tubules can be found in AMR and in cases of ischemia and reperfusion injury or potentially even indicate an

antineutrophil cytoplasmic antibody (ANCA)-associated small-vessel vasculitis. In contrast to pyelonephritis, all these latter diagnoses typically lack dense intratubular polymorphonuclear cast material and polymorphonuclear leukocytes between injured tubular epithelial cells. Granulomas are extremely rare in allograft biopsies due to rejection alone, although they may occur in response to ruptured tubules. Granulomas have been associated with miliary tuberculosis, adenovirus, *Escherichia coli* urinary tract infection/pyelonephritis, and *Candida albicans*, generally with the organism demonstrable in the lesions (384). Drug allergy or sarcoidosis may also produce granulomatous interstitial nephritis.

POSTTRANSPLANT LYMPHOPROLIFERATIVE DISEASE

PTLD is fully discussed later in this chapter. In contrast to acute cellular rejection, PTLT typically has a more monotonous often vaguely nodular mononuclear cell infiltrate of enlarged lymphocytes (with few macrophages and granulocytes) and little edema. Tubulitis, endarteritis, transmural vascular inflammation, and even necrosis can occasionally be found in PTLT (385). In contrast to cellular rejection, the infiltrate is largely comprised of CD20- and PAX5-expressing B cells. EBV infection can usually be demonstrated by in situ hybridization for EBER.

DRUG ALLERGY

Definitive distinction between drug allergy and cellular rejection is not generally possible. If eosinophils are prominent (greater than 5%), if eosinophils invade tubules, or if inflammation is centered at the corticomedullary junction and not in the renal cortex, then the possibility of drug allergy should be considered (in the absence of transplant endarteritis and lack of PTC C4d staining).

CALCINEURIN INHIBITOR TOXICITY AND ISCHEMIC INJURY

If tubular injury extends widely outside areas of cell infiltrates, other causes should be considered (vascular compromise with ischemia, obstruction). Compared with tubular injury in general, inflammation and tubulitis are by far more prominent in rejection (176), and tubular expression of MHC class II (HLA-DR) is more pronounced (156,334). Isometric tubular epithelial cell vacuolization is not a feature of rejection-induced injury and usually suggests, in the right clinical setting, a diagnosis of concurrent CNI-induced toxicity that can coincide with rejection (386). CNI toxicity is discussed in detail below.

Vascular Lesions

Detection of endarteritis permits a definitive diagnosis of active/acute rejection (203,299). The issue is exactly what constitutes endarteritis. When lymphocytes only adhere to the surface of the endothelium, a definitive diagnosis of type 2 rejection cannot be rendered. This change similar to the detection of reactive endothelial cells (enlarged nuclei) or interstitial hemorrhage is suspicious but not diagnostic for type 2 rejection and should prompt an intensive search including the evaluation of step sections into the paraffin block to find possible diagnostic changes (196). Lymphocytes also commonly surround vessels, a nonspecific feature, unless the lymphocytes also invade deep into the media. Transplant endarteritis is most common in branches of arcuate caliber vessels, and it can easily be missed in small biopsy samples containing only few small interlobular arteries. The diagnostic accuracy of type 2

rejection improves with increasing numbers of arteries (196). Using the probability of 27% per artery sampled, a negative biopsy does not rule out endarteritis with a $P < 0.05$, unless 10 or more arteries are included ($p_{\text{no arteries involved}} = (1 - 0.27)^n$, where n = number of arteries sampled) (61). Of course, the usual biopsy sample contains far fewer arteries.

Endarteritis with intimal inflammation (so-called Banff v1 and v2 scores) must not be confused with necrotizing arteritis or transmural inflammation (so-called Banff v3 score), which is more often seen with antibody-mediated/C4d-positive rejection. Fibrinoid arterial necrosis may be found in the absence of circulating DSA (20% to 50% of cases with fibrinoid necrosis in our experience), presumably due to severe cell-mediated inflammation. ANCA-associated cases of small-vessel vasculitides may present with fibrinoid vascular necrosis that in comparison to rejection-induced lesions often shows a sunburst type of extension into the adventitial space. Of course, ANCA cases typically have a crescentic glomerulonephritis. TMA can also resemble endarteritis, because rare mononuclear cells may be present in the edematous and widened intima (Fig 29.27), or a TMA may show fibrinoid vascular necrosis thereby resembling a “v3” lesion associated with Banff category 4, type 3 rejection. As a general rule, a diagnosis of “TMA” can be made based on lack of significant vascular inflammation, presence of entrapped and fragmented red blood cells, mucoid intimal changes, predominant involvement of glomerular vascular pole regions, and absence of PTC C4d deposits. Also, TMAs are typically found in small vessels in contrast to endarteritis typically seen in larger arterial cross sections. On occasion, early transplant biopsies with preexisting donor-derived intimal fibroelastosis can show during ischemia-reperfusion injury peculiar activation and enlargement of intimal fibrocytes giving rise to a “busy

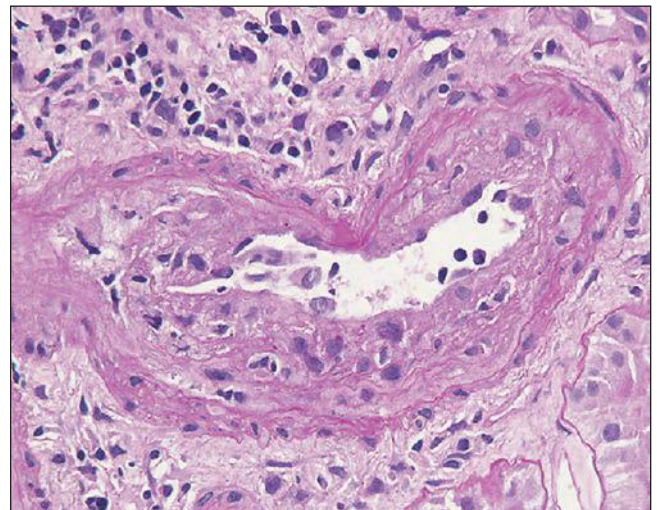


FIGURE 29.27 The differential diagnosis of endarteritis includes thrombotic microangiopathy (TMA) as illustrated in this case. The loose, thickened intima of TMA might contain rare mononuclear cells amidst abundant and dominating myofibroblasts that may resemble lymphocytes or macrophages at first glance. Clues that favor TMA over transplant endarteritis are insignificant inflammation, trapped and fragmented red blood cells, mucoid intimal changes, lack of C4d staining along PTC, and involvement of the glomerular vascular pole regions. (PAS $\times 400$.)

appearance” of the intima. These changes are of no diagnostic and prognostic significance; they should not be misinterpreted as evidence of transplant endarteritis.

Glomerular Lesions

Transplant glomerulitis is found as a TCMR phenomenon in approximately 20% to 30% of cases (the remaining cases of transplant glomerulitis, are associated with AMR and peritubular C4d deposits) (150,169,387–389). The differential diagnosis mainly includes a glomerulonephritis with intracapillary proliferations and hypercellularity. Of course, the presence of fibrinoid glomerular tuft necrosis and crescent formation confirms the diagnosis of “glomerulonephritis.” Generally, immunofluorescence or immunohistochemical studies, electron microscopy, the clinical presentation with an abnormal urinalysis, and the absence of other rejection-induced changes including the lack of peritubular C4d deposits allow for a distinction between “glomerulonephritis” and “transplant glomerulitis.”

Clinical Course, Prognosis, Therapy, and Clinicopathologic Correlations

The first-line treatment for acute cellular rejection, that is, rejection in the absence of C4d staining and/or circulating DSA, is bolus steroids for up to 3 days; this therapeutic approach works well in patients with T-cell–mediated tubulointerstitial rejection (i.e., Banff category 4, type 1). In patients who do not respond, mainly those with transplant endarteritis and glomerulitis, the standard rescue therapy is thymoglobulin. Antibody treatment is continued typically for 10 days. If the acute cellular rejection episode is concurrent with C4d positivity/AMR (mixed Banff category 2 and category 4 rejection), then often intravenous immunoglobulin (IVIG) or plasmapheresis is added to the therapeutic regimen. Future treatment options for antibody-mediated components of acute mixed rejection episodes may also include rituximab (an anti-CD20 antibody) or bortezomib (targeting activated plasma cells) (390).

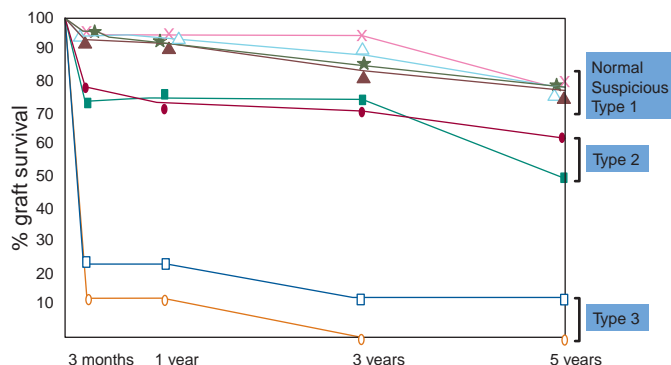
Following treatment of acute cellular rejection with pulse steroids, or thymoglobulin, a marked decrease in the interstitial infiltrate occurs, although the intratubular cells/tubulitis may remain, along with edema. Also, endarteritis may persist (although at lower levels of activity) in posttreatment biopsies suggesting an inadequate response to therapy and smoldering ongoing rejection. However, systematic studies of “postrejection treatment” protocol biopsies are lacking, and our overall understanding of the “morphologic” response to antirejection therapy and the significance of residual inflammatory cell infiltrates is incomplete.

FIGURE 29.28 The Banff types of rejection correlate well with graft survival (206). Type I does not significantly affect prognosis, but both type II and especially type III do diminish graft survival. This study was done before C4d stains were widely used or routine posttransplantation DSA testing was performed. A recent single-center observation suggests that C4d/DSA negative type II rejection has a favorable prognosis (similar to type 1 rejection) compared to cases with a concurrent antibody-mediated rejection component (153). (Adapted from Bates WD, Davies DR, Welsh K, et al. An evaluation of the Banff classification of early renal allograft biopsies and correlation with outcome. *Nephrol Dial Transplant* 1999;14(10):2364–2369.)

Certain pathologic features of acute cellular rejection have prognostic significance either individually or in combination. The most important predictors of outcome are the arterial lesions. Endarteritis, which defines type 2 rejection, has an adverse effect on prognosis, compared with tubulointerstitial rejection without arterial involvement. Several studies have demonstrated decreased survival or reversibility of type 2 rejection. Bates and colleagues studied the outcome in 293 patients with biopsies (206). Those with type 2 rejection had a 75% one-year graft survival versus greater than 90% among those with type 1, suspicious, or no rejection. Endarteritis was the only determinate in the Banff classification to predict graft failure (hazard ratio of 1.85) (391), similar to that in another series, in which endarteritis doubled the rate of graft loss (31% vs. 15%) (392). A large multicenter trial found that endarteritis increased the risk of a clinically severe rejection sixfold (61). Graft survival at 1 year (71% to 75%) versus (51% to 58%) (204) is higher for type 1 than type 2 rejection, and steroid resistance is more often found in the latter (196,393,394). Those with $\geq 25\%$ of the luminal area involved (Banff type 2B) have a worse response to antirejection therapy and a twofold increased risk of graft loss, compared with those with endarteritis involving less than 25% of the luminal area (395). This is likely in part due to the presence of myofibroblasts in the inflamed intimal zones that can, in protracted cases, cause intimal sclerosis, that is, rejection-induced chronic sclerosing transplant vasculopathy (164,396,397). Arteriolitis is associated with endarteritis and has a similar adverse effect on prognosis (207). Type 3 rejection (necrotizing or transmural arteritis) has much worse prognosis than intimal type 2 endarteritis (20% to 32% 1-year survival) (196,206,264,394,398), in particular cases mediated by antibodies.

It is important to remember that most historic reports on outcome do not separate between acute TCMR and mixed cellular- and AMR episodes (mixed Banff category 2 and category 4 rejection) due to the lack of C4d staining results and data on circulating DSA titers in previous years. Thus, in old studies, the “mixed rejection cases” were mostly classified as acute TCMR and received, based on current standards, suboptimal therapy. Consequently, all historic outcome studies are nowadays difficult to interpret and need reevaluation (Fig. 29.28). A good example of increased insight is the lack of adverse outcome of endarteritis if C4d is negative (151) or donor specific antibodies are not present (153).

Infarction is an ominous finding in graft biopsies, if surgical trauma including malperfusion through small accessory arteries can be excluded (399,400). It is often caused by severe



rejection episodes with arterial thrombus formation and the presence of DSA/C4d positivity. Occasionally, infarction can be associated with infections, especially CMV or productive adenovirus (see below) (401). Old infarcts are occasionally found in well-functioning grafts, dating from the time of transplantation; these are of no significance (402).

The intensity of the interstitial infiltrate or tubulitis for that matter has no correlation with the severity of the rejection episode (55,61,196,372,393,398,399,403,404). Of note, Banff category 4 type 2 rejection with transplant endarteritis can lack any significant interstitial inflammation. Consequently, Banff category 3 so-called borderline/suspicious for rejection is a very problematic and controversially debated entity. Many, but not all, of these “borderline” cases are, indeed, rejection. Two large studies have shown that 75% to 88% of patients with suspicious/borderline changes and graft dysfunction at time of biopsy functionally improved with increased immunosuppression (405,406), comparable to the overall response rate in type 1 rejection (86%) (405). Untreated “borderline cases” can progress to frank rejection during follow-up (406,407). If there is any evidence that favors rejection (e.g., marked interstitial edema incompatible with “borderline” rejection, peritubular capillaritis, glomerulitis, C4d positivity, a rise in creatinine), a diagnosis of rejection should be made and therapy initiated. We find in “borderline cases” that the tubular expression of MHC class II/HLA-DR by immunofluorescence microscopy can be helpful to establish a definitive diagnosis of “rejection” (156).

The intensity of the inflammatory cell infiltrate lacks prognostic significance and so does the expression profile of CD3⁺ or CD2⁺ cells in the interstitium (170,334,408). In some studies, greater numbers of CD3- and CD2-expressing cells even had a better outcome than those with focal infiltrates. Thus, grading the rejection on the basis of the extent of the infiltrate is of dubious value. The proportion of CD8⁺ cells correlates with a poorer response to immunosuppressive therapy in some (157,170,301) but not all studies (372). By multivariate analysis, type 1 tubulointerstitial rejection with diffuse cortical CD8⁺ infiltrates was associated with a 46-fold increase in risk of graft loss within 10 weeks (301). Expression of granzyme B by greater than 2% or CD40 by greater than 25% of the infiltrating cells has been associated with shorter allograft survival (317). The reason for this is not clear; the CD8⁺ cells may be relatively resistant to immunosuppressive drugs or mediate more severe injury. Eosinophil-rich infiltrates (greater than 2%) have been associated with graft loss (86% vs. 37%) (194). One explanation may be the strong association of eosinophils with transplant endarteritis/type 2 rejection. An increased number of interstitial macrophages has also been associated with an adverse outcome (335). Plasma cell-rich acute rejection has been reported to have a poorer prognosis in most (188–191), but not all, series (192). When three studies (188,191,409) are combined in a meta-analysis, plasma cell infiltrates in acute rejection affect prognosis only in the first 6 months (increasing graft loss from 23% to 53%); after 6 months, the outcomes of acute rejection with or without plasma cells are equally poor (graft loss in 67% to 68%) (409). Some tubulointerstitial cellular type 1 rejection episodes are “rich” in CD20-positive B-cell clusters shown in some (184,187,410) but not all (180,411) studies to indicate poor outcome. Future trials have to determine whether monoclonal anti-CD20 antibody therapy, such as rituximab, may be of beneficial therapeutic value in CD20-rich rejection episodes (412,413).

The prognostic significance of transplant glomerulitis in pure TCMR has not been settled. Most studies report a poor prognosis, for example, 67% graft loss (157–159,161,165), likely due to the tight association of transplant glomerulitis and transplant endarteritis/type 2 rejection.

CHRONIC T-CELL-MEDIATED REJECTION

It is clear that single, severe acute rejection episodes or, more frequently, smoldering and recurrent rejection lead to chronic alloinjury with increased fibrosis and tissue remodeling termed chronic rejection. Chronic rejection is characterized by: sclerosing transplant arteriopathy without elastosis, transplant glomerulopathy, severe multilamination of peritubular capillary basement membranes in three PTC (≥ 7 circumferential layers in one and ≥ 5 layers in the remaining capillaries as defined by Liapis et al. (224)), and, to some extent, also by interstitial fibrosis and tubular atrophy (IFTA). If these lesions are detected in a graft biopsy, in particular in combination, then a diagnosis of chronic rejection can be rendered, and descriptive diagnostic terms such as “interstitial fibrosis and tubular atrophy” or the now outdated term “chronic allograft nephropathy” can be avoided. Chronic rejection is often associated with other “chronic” lesions such as hypertension-induced arterionephrosclerosis (Fig. 29.29), preexisting donor disease, or possibly CNI toxicity making the diagnostic workup of a late graft biopsy challenging for the pathologist.

The etiology of chronic rejection-induced changes in late graft biopsies, particularly if significant activity is lacking, is often difficult to determine: Were the lesions induced by cellular and/or antibody-induced injury? Interestingly, Liapis and colleagues showed that especially mixed chronic active cellular and concurrent AMR induced severe “chronic” changes to the microvasculature with marked multilaminations of peritubular capillary basement membranes. This feature carried a positive predictive value for chronic TCMR of 17% and for chronic AMR of 49% (negative predictive values for chronic rejection of any type, i.e., absence of severe PTC multilaminations, approximately 90%). In Liapis’ series of 40 cases with transplant glomerulopathy, 18% were interpreted as secondary to chronic TCMR, 10% as secondary to pure AMR, and 32% as mixed TCMR and concurrent AMR (224). Thus, both cellular and/or antibody-induced tissue injury and fibrosis are common.

Chronic rejection-induced changes are currently only imperfectly reflected in the Banff classification scheme, and strict defining criteria have to be established in the future. Although Banff recognizes the entity of chronic active rejection in categories 2 and 4, “burnt-out” inactive chronic rejection remains unclassified. Careful chart review and correlation with historic data is required to reach the most appropriate diagnosis in late graft biopsies with chronic changes including evidence of chronic rejection.

One histologic feature of chronic rejection that is mainly but not exclusively driven by smoldering TCMR is so-called chronic active sclerosing transplant arteriopathy (see Fig. 29.29). It is characterized by intimal widening due to de novo accumulation of collagens I and III lacking elastosis and varying degrees of intimal inflammation with mononuclear inflammatory cells (ranging from absent to prominent). This peculiar form of intimal sclerosis can be most prominent at arterial branching points in arcuate

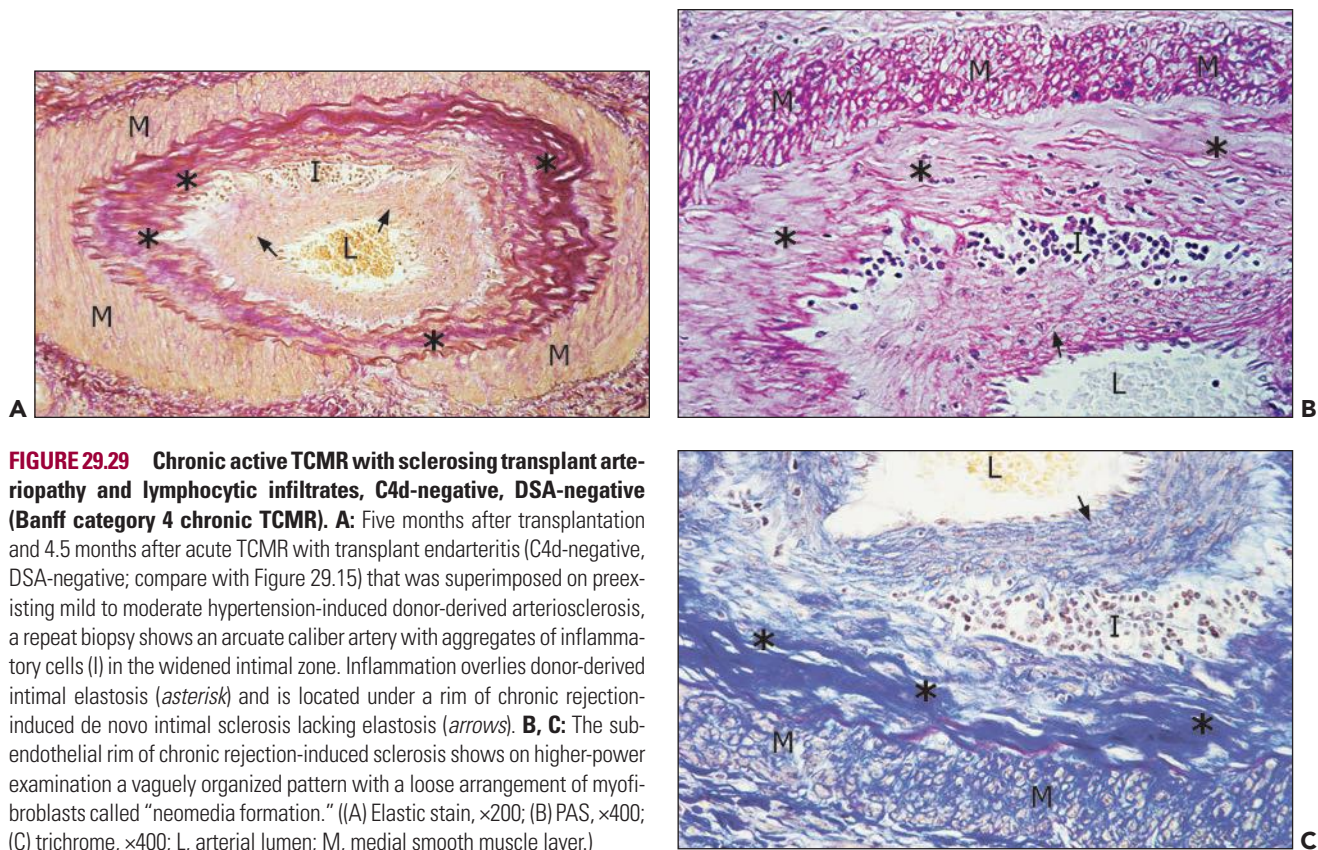


FIGURE 29.29 Chronic active TCMR with sclerosing transplant arteriopathy and lymphocytic infiltrates, C4d-negative, DSA-negative (Banff category 4 chronic TCMR). **A:** Five months after transplantation and 4.5 months after acute TCMR with transplant endarteritis (C4d-negative, DSA-negative; compare with Figure 29.15) that was superimposed on preexisting mild to moderate hypertension-induced donor-derived arteriosclerosis, a repeat biopsy shows an arcuate caliber artery with aggregates of inflammatory cells (I) in the widened intimal zone. Inflammation overlies donor-derived intimal elastosis (*asterisk*) and is located under a rim of chronic rejection-induced de novo intimal sclerosis lacking elastosis (*arrows*). **B, C:** The sub-endothelial rim of chronic rejection-induced sclerosis shows on higher-power examination a vaguely organized pattern with a loose arrangement of myofibroblasts called “neomedial formation.” ((A) Elastic stain, $\times 200$; (B) PAS, $\times 400$; (C) trichrome, $\times 400$; L, arterial lumen; M, medial smooth muscle layer.)

caliber vessels and is typically found as a sequela of transplant endarteritis (396). In sclerosing transplant arteriopathy, the intima usually contains varying numbers of myofibroblasts, occasional foam cells, and, in active disease stages, scattered, often clustered mononuclear inflammatory cells that can be most prominent along the inner elastic lamina. Potentially, even eosinophilic leukocytes play a role in the development of intimal sclerosis (414). Endothelial cells are often enlarged with reactive nuclei sometimes overlying an ill-defined ring of smooth muscle cells, that is, so-called neomedial formation (see Fig 29.29B and C). The inner elastic lamina usually remains intact without major breaks that are only prominent in cases with preceding transmural inflammation (Banff v3 lesions). The differential diagnosis of sclerosing arteriopathy includes TMAs (see Fig 29.27) and hypertension-induced arteriosclerosis characterized by marked arterial intimal fibroelastosis and a lack of intimal inflammation.

Since chronic tissue injury due to rejection, regardless whether T-cell and/or antibody mediated, shows specific changes in glomeruli, arteries, and PTC, detailed features are discussed for didactic purposes in the section “chronic antibody-mediated rejection” below.

ANTIBODY-MEDIATED REJECTION

AMR was first recognized in 1966 in the form of hyperacute rejection in patients with pretransplant DSA (33). In 1970, chronic rejection was linked to posttransplant DSA (32). Evidence of antibody binding to the graft was sparse, and the

concept of acute and chronic AMR was not widely accepted until the 1990s. DSA, largely reactive to HLA antigens, are now recognized by pathologists and clinicians as a significant cause of early and late graft dysfunction and failure (415). The primary reasons for increased appreciation of AMR are the improved diagnosis afforded by detection of the complement fragment, C4d, and improved sensitivity and specificity of the solid-phase antibody assays. AMR arises in three major forms, hyperacute, acute, and chronic rejection (see Table 29.5). These and the known variants (C4d-negative AMR, smoldering AMR, and accommodation) are discussed in this section. General aspects of pathogenesis and diagnosis will be considered first; more specific aspects will be discussed with each category. The reader should bear in mind that AMR (acute or chronic) often coincides with TCMR (acute or chronic).

Antigens

MHC ANTIGENS

Class I and II HLA antigens are by far the most common targets of AMR, just as they are for TCMR. Production of HLA alloantibodies depends on exposure to HLA antigens from pregnancy, blood transfusion or transplantation; these antibodies are predominately IgG. Acute AMR is mediated by either class I or class II donor-reactive antibodies (DSA) (416–418), while the chronic form is largely associated with class II DSA (419–422). The microvasculature in the human, in contrast to the mouse, constitutively expresses class II MHC.

In addition, the nonclassical polymorphic MHC antigen MICA (MHC class I–related chain A) is a potential endothelial target. MICA is induced on the endothelium and other cells under conditions of cellular stress and is a ligand for the NK receptor NKG2D. The glomerular capillary wall is the main site of MICA localization in normal and rejecting kidneys, rather than PTC (423). Preexisting antibodies to MICA can be detected in 7% to 10% of renal allograft recipients unrelated to pregnancy or previous transplant and are associated with acute rejection and lower graft survival (424–426). However, the donor specificity and mechanism of rejection is not clear. Three cases of acute AMR have been attributed to MICA antibodies in the absence of HLA DSA (427,428).

NON-MHC ANTIGENS

ABO blood group antigens are the best characterized of the non-MHC polymorphic endothelial target in renal transplantation. Other antigens are potentially important, as evidenced by the occasional HLA-identical grafts that develop AMR (42,43) or hyperacute rejection (429,430) and the elution of alloantibodies from rejected HLA-identical kidneys (431). Antibodies to H-Y antigens have been detected in females with male kidney grafts and are associated with acute rejection and plasma cell infiltrates, although not C4d deposition (432). Most putative non-MHC antigens have not been characterized at the molecular level nor are approved diagnostic tests available (415).

Autoantigens may provide an additional target of AMR. Autoantibodies to angiotensin II type 1 receptor (AT1R) have been linked to malignant hypertension and graft dysfunction, fibrinoid necrosis of arteries, and acute rejection with C4d in 33% of the cases (433). AT1R antibodies do not affect vessels in native organs, suggesting a component of rejection is necessary. AT1R antibodies were detected in 86% (6/7) of patients with acute AMR and negative HLA DSA (434). Autoantibodies to glutathione S-transferase T1 have also been detected in acute AMR (428). De novo development of antibodies to unknown and probably nonpolymorphic antigen(s) on umbilical vein endothelial cells was associated with glomerulitis and capillaritis, but not C4d deposition (435). Autoantibodies to agrin, a proteoglycan component of the GBM, have been reported in patients with transplant glomerulopathy (436), as have autoantibodies to peroxisomal trans-2-enoyl-CoA-reductase (437). B cells derived from grafts with chronic AMR produce a variety of polyreactive autoantibodies (438), and protein microarray studies have revealed a wide variety of autoantibodies to normal renal urothelium and glomeruli in patients with allograft rejection (439). Their role, if any, is unproved.

The enigma of autoantibodies is how the graft would be selectively affected. A clue comes from experimental studies in rodents that proved endothelial damage in ischemic organs is mediated by natural IgM autoantibodies to externalized membrane components (440). Perhaps, the graft specificity of autoantibodies in humans is similarly due to increased expression or exposure of the antigen in tissue injured from other causes, for example, rejection or drug toxicity. However, studies exploring the role of these autoantibodies in nontransplanted but severely injured organ as a control (e.g., acute kidney failure) are lacking.

B Cells and Plasma Cells

High-affinity IgG alloantibody response requires CD4⁺ T-cell reactivity through the indirect pathway (441), particularly the T follicular helper cell (442). Activated T cells provide help

for B-cell memory, isotype switching, and affinity maturation through various T-cell–derived cytokines and costimulatory factors that recognize receptors on B cells (such as CD80/CD86, CD40L, and ICOS). The B-cell response leads to the production of long-lived plasma cells, which migrate to the bone marrow and continue to produce antibodies indefinitely, without requiring T-cell help (443). It is not known whether antibodies specific for graft antigens are maintained owing to the longevity of plasma cells or to the continuous generation of new memory B, although alloantibody-secreting plasma cells are detectable in the bone marrow (444). B cells also provide antigen presentation and help for T cells, in part due to binding of antigen on B-cell surface immunoglobulin (445,446). IgM alloantibodies specific for MHC antigens and carbohydrate antigens (ABO) may not require T-cell help (447).

ASSAYS FOR DSA

The testing for antibodies to MHC antigens has markedly evolved over the last decade from panels of living lymphocytes as targets by cytotoxicity or flow cytometry (panel reactive antibodies, PRA) to solid-phase assays with purified antigen on plates (ELISA) or fluorescent beads (Luminex) (415). The advantages of the solid phase are high sensitivity, high specificity, and lack of dependence on donor cells. Both class I and class II single-antigen beads are available. The disadvantages of the solid-phase assay are that the antigens are not on their natural surface and may not have their normal conformation (415). Indeed, normal individuals can have antibodies reacting to HLA-coated beads that do not react to living lymphocytes of the same HLA type (448). The solid-phase assays are FDA approved for determining the presence or absence of DSA, not for quantitation. Some of the factors that confound quantitation by using the mean fluorescence intensity (MFI) have been described and include variable coating of the antigens on the beads, batch differences, interlaboratory variation, saturation, and the difficulty in combining results across beads (415). Before transplantation, donor blood lymphocytes are tested with serum from the potential recipient for donor reactivity by cytotoxicity and/or flow cytometry (crossmatch). A “virtual” crossmatch is done with solid-phase beads with the putative donor HLA antigens. This can narrow down the list of potential recipients and reveal compatibility that would otherwise be missed (415).

Effector Mechanisms

There are three major pathways by which antibodies can affect the endothelium (Fig 29.30) (449).

DIRECT EFFECTS OF ANTIBODY TO MHC

Antibody to MHC acting alone in vitro on cultured endothelium promotes proliferation and activation of multiple signaling pathways (450). Studies by Reed et al. have shown that antibodies to MHC molecules on cultured endothelial cells elicit strong responses that include proliferation and activation of intracellular signaling pathways (451–456) and exocytosis of Weibel-Palade bodies with release of von Willebrand factor and P selectin (457). Among the changes noted was increased phosphorylation of ERK (pERK), indicative of increased ERK activity (458), a pathway that promotes cellular proliferation (459,460).

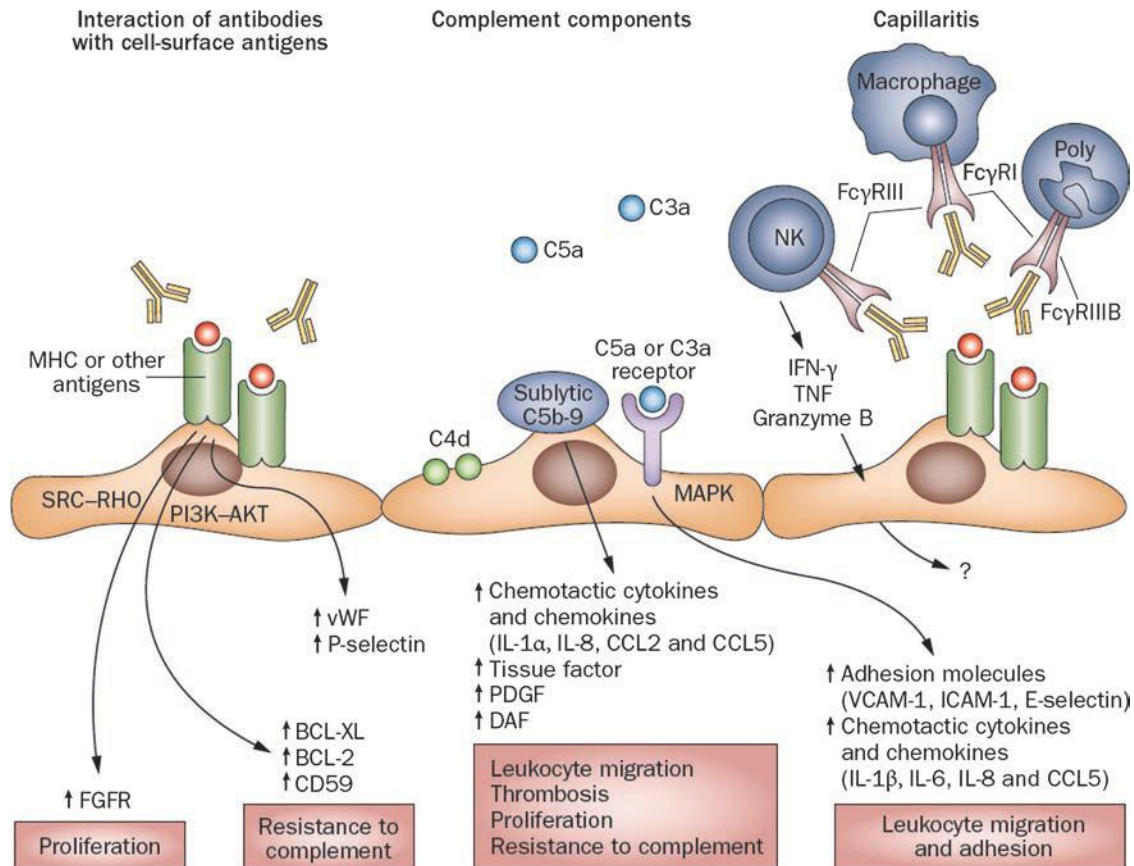


FIGURE 29.30 Three major pathways by which antibody can affect the endothelium. (1) Antibody to MHC acting alone in vitro on cultured endothelium promotes proliferation and activation of multiple signaling pathways. (2) Complement activation by DSA can attract inflammatory cells through C3a and C5a and cause lysis of endothelial cells (462) and expression of adhesion and procoagulant molecules. (3) DSA can potentially mediate endothelial injury and activation via Fc receptors on NK cells, monocytes, and granulocytes. (Reprinted from Farkash EA, Colvin RB. Pathology: Diagnostic challenges in chronic antibody-mediated rejection. *Nat Rev Nephrol* 2012;8(5):255–257.)

COMPLEMENT FIXATION

Complement activation by DSA at the surface of the endothelium can have profound effects via a variety of complement components. The pathways that lead to complement activation and C4d deposition are diagrammed in Figure 29.31 (461). Complement mediates acute graft injury by attracting inflammatory cells mainly through the chemoattractants C3a and C5a and by lysis of endothelial cells (462). C3a also promotes vasospasm through the release of PGE₂ from macrophages, and C5a causes edema through the release of histamine from mast cells. Both cause endothelial cell release of IL-6, IL-8, IL-1 α , and CCL5 and increased expression of adhesion molecules E-selectin, VCAM-1, and ICAM-1 (463,464). Membrane attack complex (MAC) causes lysis and apoptosis of endothelial cells, a process dependent on C6 (465,466). In sublytic concentrations, soluble MAC increases expression of adhesion molecules, such as E-selectin, ICAM-1, and VCAM-1 on cultured endothelial cells and synthesis and secretion of IL-8, MCP-1, CCL2, and CCL5 and triggers endothelial synthesis of tissue factor (467–470).

CELLULAR FC RECEPTORS (FCR)

NK cells, monocytes, and granulocytes, via DSA and Fc receptors, can potentially mediate endothelial injury and activation (a process known as antibody-dependent cell-mediated cytotoxicity,

ADCC) (471,472) and provide a third, relatively neglected, pathway of DSA-mediated graft injury. Complement-independent mechanisms may be relevant to the pathogenesis of AMR, particularly those cases with little or no C4d deposition. NK cells express the low-affinity Fc γ RIII (CD16), and monocytes express in addition the high-affinity Fc γ RI. Interaction of effector cells with target cells via Fc receptors and antibody can lead to lysis of the target and/or production of cytokines and chemokines such as IFN- γ , TNF- α , MCP-1, and others (473,474). Monocytes cultured with endothelial cells and DSA stimulate the production of MCP-1 and IL-6 (475). NK cells, via their Fc receptors, are necessary for hyperacute xenograft rejection mediated by non-complement-fixing anti-Gal antibodies (476). Depletion of NK cells with anti-asialo-GM1 prolongs survival of mouse to rat cardiac xenografts, arguing for their participation in acute AMR (477). Antibody-induced chronic allograft vasculopathy in the mouse also depends on NK cells and the Fc portion of the DSA and is independent of complement fixation (374).

Diagnostic Evaluation of Antibody Interaction With the Graft With C4d Stains

At present, C4d deposition in PTC is the most specific indicator in biopsies of the presence of circulating DSA and its interaction with endothelial cells in the graft (142,478,479).

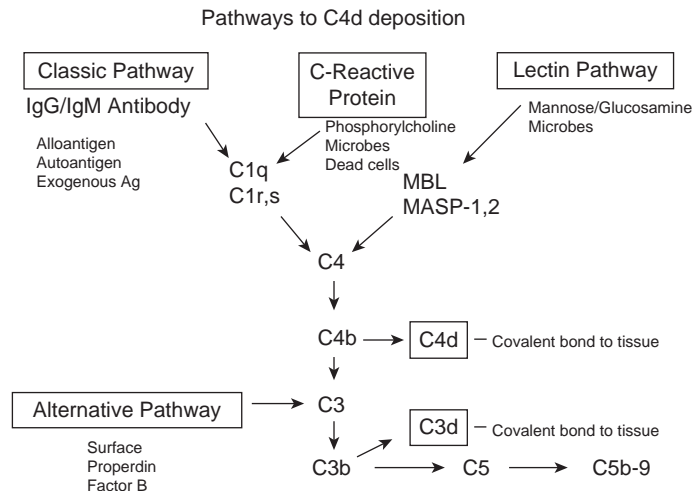


FIGURE 29.31 Pathways of C4 activation (389). Activation of C1 (composed of C1q, C1r, and C1s) is initiated by interaction of C1q with IgG or IgM bound to epitopes on the graft endothelium. C4 is cleaved by C1s into C4a and C4b, exposing a sulfhydryl group. The reactive sulfhydryl group of C4b rapidly forms an ester or amide bond with nearby molecules containing hydroxyl or amino groups. C4b combines with the enzymatically active fragment C2a to form C4bC2a, which is known as the classical pathway C3 convertase. C4bC2a cleaves C3 into C3a and C3b (which also has a reactive sulfhydryl group) and with the C3b molecule covalently deposited in the immediate vicinity and forms the C5 convertase C4bC2aC3b. Cleavage of C5 releases a bioactive peptide C5a and C5b. C5b initiates formation of the membrane attack complex (MAC; membrane-bound C5b-9), which causes cell lysis (435). The lectin pathway is stimulated when mannan-binding lectin (MBL), L-ficolin, or H-ficolin binds to the appropriate carbohydrate (typically on pathogens or apoptotic cells) (467). MBL binds to mannose (or glucosamine), and the ficolins bind to *N*-acetylglucosamine. L-ficolin also binds to elastin and lipoteichoic acid, and H-ficolin also binds to *N*-acetyl galactosamine. MBL, L-ficolin, and H-ficolin (all homologous to C1q and fibrinogen) activate C4 via their associated serine proteases, MASP-1 and MASP-2 (homologous to C1r and C1s). C4 is also activated via the binding of C-reactive protein (CRP) to the carbohydrate, phosphorylcholine with participation of C1q (1303). Little or no terminal components (C5b-9) are generated, because CRP simultaneously recruits Factor H, and may thus provide an anti-inflammatory effect. (From Rotman S, Collins AB, Colvin RB. C4d deposition in allografts: Current concepts and interpretation. *Transplant Rev* 2005;19:65.)

In the older literature, about 85% to 90% of the patients with C4d⁺ had positive tests for circulating DSA, but these tests were less sensitive than current solid-phase assays. In recent protocol biopsies of presensitized patients, all biopsies with C4d had circulating DSA by solid-phase assay, arguing against the hypothesis that the kidney could absorb enough DSA to render this highly sensitive serologic test negative (480). The deposition of C4d in the absence of detectable DSA to MHC is strong presumptive evidence for non-MHC endothelial target antigens.

A positive C4d stain with the immunofluorescence technique (IF) was defined as “widespread, strong linear circumferential PTC staining in cortex or medulla, excluding scar or necrotic areas,” according to a consensus at the 2003 Banff Conference. For positivity with IHC on paraffin-embedded tissues, strong staining is not required, as tissue pretreatment influences staining intensity. At present, there is debate on the appropriate threshold for positivity in the Banff consensus; 2+ staining intensity (on a scale of 0–4) seems to be a reasonable threshold level for “C4d positivity” by IHC. The 2013 Banff consensus conference proposed that the threshold for C4d positivity should be >10% for IF (C4d2) and >0 for IHC (C4d1) (481). Early biopsies with even one C4d⁺ cluster of 3 or more PTC with acute rejection were associated with DSA (57%) and grafts failed by 1 year in 38%. The DSA rate was somewhat lower than in patients with biopsies with greater than 50% C4d⁺ capillaries (86% DSA), but graft failure of the latter was similar (31% at 1 year) (482). Late biopsies with focal C4d (10% to 50%) in paraffin sections had a worse graft survival compared

with negative C4d biopsies (483). Among 368 biopsies, focal C4d in frozen sections (10% to 50%) was intermediate in graft survival compared to negative and diffusely positive C4d and intermediate in association with DSA (484). Taken together, it appears that even focal C4d is sufficient to diagnose AMR.

Several pitfalls of C4d staining must be mentioned. Arterial endothelial surfaces and thickened intima in arteriosclerosis and hyaline arteriolar deposits in native kidneys are often C4d-positive in frozen sections or, to a lesser degree, also by IHC. The mechanism is not known. Granular staining of PTC by IHC is of doubtful significance (485). Interpretation of glomerular staining in frozen sections is complicated by the normal presence of C4d in the mesangium, which is therefore not specific for AMR. Additional staining along the GBM occurs in acute AMR, but is difficult to score, and we do not use it as evidence of AMR. In fixed, paraffin-embedded tissues, however, normal glomeruli are entirely negative (486). This difference may be due to fixation blocking access to C4d embedded in the mesangial matrix or GBM (as opposed to cell surfaces). Granular glomerular C4d is typical in immune complex diseases (e.g., membranous glomerulonephritis).

IF in frozen sections remains the technique of choice (487), with the triple layer IF technique probably the most sensitive (488). The sensitivity of immunofluorescence using monoclonal antibody to C4d in frozen sections (IF) is greater than immunoperoxidase stains using polyclonal antibody in paraffin-embedded tissue (IHC) (388,487–489). IHC demonstrated a substantially lower prevalence (31% to 87%) and extent (36%)

of C4d deposition in PTC and had a lower reproducibility than IF (κ 0.3 vs. 0.9, respectively) (487). Furthermore, there is considerable interinstitutional variability in IHC results, as shown by an international quality assurance project involving 73 centers (490). Some variation was attributed to techniques. Heat-induced epitope recovery (pH 6 to 7, 20 to 30 minutes, citrate buffer) with polyclonal antibody incubation (less than 1:80, greater than 40 minutes) appeared to be the best practice (490). Not uncommonly, the plasma in the capillaries is fixed by the formalin processing and also stains for C4d by IHC, which interferes with interpretation. Extravasation of C4d into the connective tissue is also common and should not be mistaken for capillary wall deposition. If extensive, these samples are not interpretable.

The sensitivity of C4d deposition for AMR is probably around 80%, as judged by patients who have other evidence of AMR, such as DSA with capillaritis or increased levels of endothelial gene expression (491,492). Capillaritis with DSA and little or no C4d is more common in “smoldering” and chronic AMR than acute AMR, although the frequency in the last category has not been reported.

HYPERACUTE REJECTION

Introduction and Clinical Presentation

Hyperacute rejection refers to immediate rejection of the kidney upon perfusion with recipient blood (typically within 60 minutes). Hyperacute rejection is a variant of acute AMR, in which donor-specific antibody titers are sufficient at the time of transplantation to cause immediate rejection. The graft rapidly becomes cyanotic and flaccid, despite good pulses at the hilum and swells poorly on venous compression (493). In the first 10 minutes, the graft sequesters platelets, neutrophils, complement, fibrinogen, and coagulation factors, and the level of circulating DSA decreases (494). The clinical signs are anuria, high fever, and no perfusion on renal scan. Microangiopathic hemolytic anemia with thrombocytopenia and increased circulating fibrin split products can develop and reverses on removal of the graft (495). Fortunately, hyperacute rejection is now rare, due to effective crossmatch screening, and is encountered in less than 0.1% of transplants (496).

Pathologic Changes

Gross

The kidney becomes livid, mottled, and cyanotic soon after reperfusion in the operating room (33,497–499). The kidney is initially flabby and soft, but subsequently swells and develops widespread hemorrhagic cortical necrosis, with medullary congestion (Fig. 29.32). The large vessels are sometimes thrombosed.

Light Microscopy

The pathologic features are the same as severe acute AMR (Fig. 29.33). Neutrophil and platelet margination occurs in the first hour along damaged endothelium of glomerular and PTC, and the capillaries fill with sludged, compacted red cells and fibrin (493). Neutrophils form “chain-like” figures within the PTC without obvious thrombi (493). The endothelium is stripped off the underlying basal lamina, and the interstitium becomes edematous and hemorrhagic. Intravascular coagulation occurs, and cortical necrosis ensues over 12 to 24 hours. The medulla is relatively spared, but is ultimately affected as the whole kidney becomes necrotic (33). Widespread

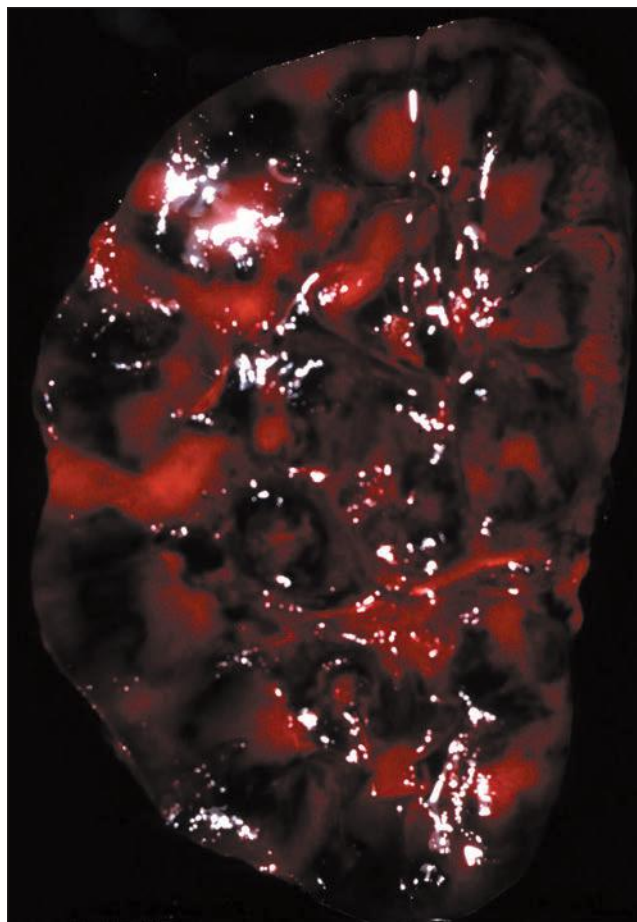


FIGURE 29.32 Hyperacute rejection, nephrectomy. The cut surface of the markedly swollen kidney is grossly hemorrhagic and glistening with edema fluid (hence the reflections).

microthrombi are usually found in the arterioles and glomeruli and can be detected even in totally necrotic samples. The larger arteries may be spared, but small arteries often also show neutrophilic infiltration or fibrinoid necrosis. Mononuclear cell infiltrates are typically sparse. One case showed CD3⁺ cells in the adventitia of small arteries and in the surrounding interstitium, probably indicating a component of TCMR (497).

Immunofluorescence Microscopy and Immunohistochemistry

Fibrin, IgM, and C3 are occasionally quite prominent in the vascular and glomerular lesions (493,497). The nature of the antigen influences the distribution of the staining and the isotype of the antibody. ABO antibodies are primarily IgM and deposit in all vascular endothelia. Antibodies to HLA class I or II cause little or no IgG or IgM deposition in the microvasculature (500,501).

C4d is deposited in the PTC and glomeruli, as in acute AMR (see Fig. 29.33) and is more useful diagnostically than immunoglobulin deposition. Occasional cases biopsied at the time of operation may be negative for C4d (502), perhaps related to focally decreased perfusion, necrosis, or insufficient time to generate substantial amounts of C4d. Careful search for viable tissue, in particular in the medulla, can sometimes reveal areas of

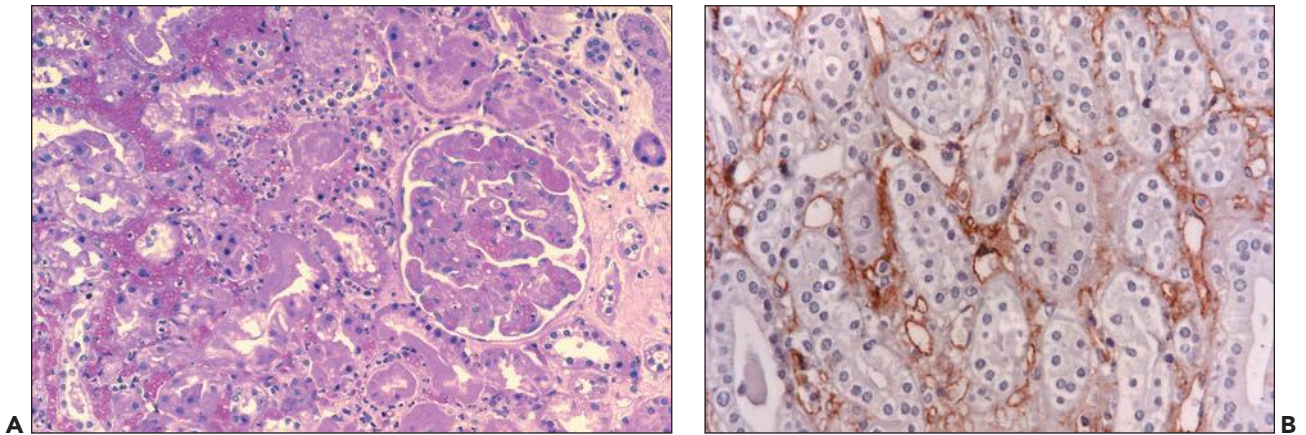


FIGURE 29.33 Hyperacute rejection due to preexisting antidonor class II HLA antibodies (509). **A:** Interstitial edema and hemorrhage are conspicuous as are neutrophils in PTC. Glomeruli are congested and have lost endothelial nuclei. (H&E, original magnification 200 \times .) **B:** C4d on paraffin section shows widespread, circumferential deposition along the PTC (stain done on an unstained paraffin section stored for 25 years). (C4d IHC, original magnification 400 \times .)

C4d positivity along PTC. Lack of C4d deposition in one case of hyperacute rejection was attributed to non-complement-fixing donor-specific antiendothelial antibodies (502).

Electron Microscopy

Neutrophils are abundant in the glomerular and PTC (i.e., in the microcirculation), where they seem to attach to injured endothelial cells (493) (Fig. 29.34). Electron-dense deposits are rare or absent (493). The endothelium is swollen, separated from the GBM by a lucent space. Capillary loops and PTC are often bare of endothelium. Platelet, fibrin thrombi, and trapped erythrocytes occlude capillaries.

Etiology and Pathogenesis

Antigens

ABO blood group antigens were the first identified target of hyperacute rejection (493,499). Eluates from the rejected kidney contain anti-ABO IgM or IgG antibodies (503). HLA class I (33,493,498,499,504) and class II (417,501) antigens can also be targets of hyperacute rejection, and DSA have been eluted from hyperacutely rejected kidneys (505). The rapid graft destruction in humans by anti-MHC antibodies contrasts with that in rodents and may be explained by the fact that normal murine endothelium has less class I and class II antigen expression and a less efficient complement system.

Occasional cases of hyperacute rejection still arise despite a negative lymphocyte crossmatch. These have been attributed to non-HLA antigens on endothelium (205,502,506). These recipients are typically multiparous females or recipients of prior transplants (497), and some have received HLA-identical kidneys (429,430). The nature of the antigen(s) has not been determined in most cases, even whether they are allospecific. In one instance, selective reactivity to donor endothelial cells in contrast to donor lymphocytes was demonstrated (502). Antibodies have been eluted from hyperacutely rejected kidneys that stain the endothelium of PTC and arterioles (507,508). Some of these cross-react with monocytes (508), and others do not (502,507). Testing of the pretransplant serum on the donor kidney sometimes shows binding of immunoglobulin to

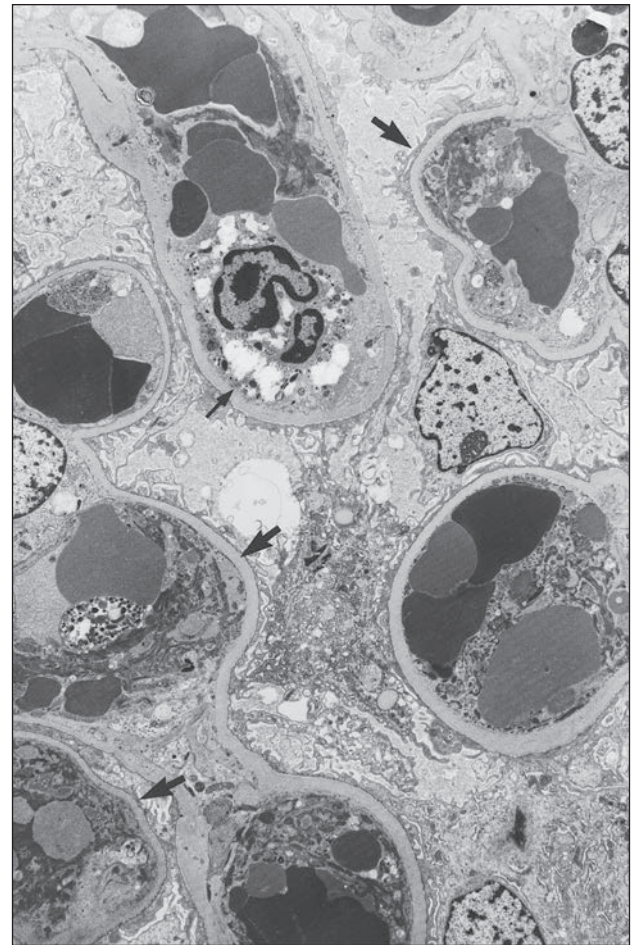


FIGURE 29.34 Hyperacute rejection due to anti-HLA-DR antibodies, biopsied at 24 hours after transplantation. Electron micrograph of glomerular capillaries shows fibrin platelet thrombi (*thick arrows*), a degranulated neutrophil (*arrow*), and compacted red cells; the endothelium is absent from most of the GBM. ($\times 5000$.)

the PTC in patients with antiendothelial antibodies (205,507). Preexisting donor kidney reactive antibodies were detected by immunoperoxidase techniques in 19% of 70 patients who had a negative T-cell cytotoxic crossmatch, and 50% reacted with endothelium (some also with epithelium) (509).

Other antibodies include cold-reactive IgM agglutinins reactive with recipient red cells in kidneys that are not rewarmed before blood flow is reestablished (510,511). These cause immediate graft dysfunction due to intravascular aggregation of recipient erythrocytes and thrombosis, as described in five cases (512). Exogenous antibodies can also cause hyperacute rejection. Perfusion of the donor kidney with third-party human plasma-containing donor-reactive cytotoxic antibodies is a rare cause of hyperacute rejection (513,514), which provides proof that antibody alone is sufficient to initiate this injury, even a single exposure. ATG has been implicated in rare instances, in one of which the batch of rabbit ATG (Thymoglobulin) reacted with activated endothelial cells; no C4d was detected in PTC in that case (515). Equine ATG (Atgam) was also implicated in early acute AMR in two cases; these had C4d deposition in PTC and no DSA (515).

Effector Mechanisms

Hyperacute rejection is caused by binding of circulating antibodies to the surface of endothelial cells, complement fixation, platelet activation, lysis of the endothelium, and activation of the clotting system with thrombosis. The sequence of events is similar, if not identical, to that in acute AMR, only developing more rapidly and vigorously, in a setting with no opportunity for the endothelium to develop resistance (accommodation).

Renal allografts in monkeys presensitized to donor antigens develop a marked reduction in renal blood flow due to vasoconstriction, as the earliest and most abnormal finding (516). At 5 minutes, endothelial immunoglobulin and faint C3 deposits were detectable but never became prominent; fibrin formation was sparse at all times. Glomeruli were the most sensitive, and arterial injury became more prominent at higher antibody titers. Early red cell sequestration and stasis were marked, followed by progressive aggregation of platelets and infiltration of neutrophils. Renal venous studies revealed marked consumption of C3 but no evidence of intrarenal activation of the coagulation, fibrinolytic, or kinin-forming systems. Platelet aggregates in glomeruli and arteries and IgM deposition on the surface of glomerular endothelial cells were beautifully demonstrated by electron microscopy in hyperacute rejection in rabbits (517). Increased expression by endothelial cells of leukocyte adhesion molecules CD31 (PECAM-1) and CD62E (E-selectin); increased production of tissue factor, PAI, and platelet-activating factor; and decreased thrombomodulin also occur (517,518). A similar sequence occurs in discordant xenografts (i.e., those in which the recipient has preformed "natural" IgM antibodies) (519).

In general, only the complement-fixing antibodies mediate hyperacute rejection. IgG3 (4% of circulating IgG) and IgM are better complement-fixing antibodies than IgG1 (65% of circulating IgG) or IgG2 (25% of IgG); IgG4 (5% of IgG) does not fix complement. Sera that are positive in microcytotoxicity assays (complement fixation required) contain predominantly IgG3 with or without other IgG iso-

types; sera negative by microcytotoxicity but positive by flow cytometry (only antigen binding required) contain predominantly IgG2 and IgG4. About 80% of patients with high titers of antidonor cytotoxic antibodies in pretransplant crossmatch tests reject their kidney hyperacutely (520). IgM antibodies to HLA antigens curiously do not always trigger hyperacute rejection; only about half of those with IgM anti-class I antibodies have hyperacute rejection. One reason may be low affinity, as some only react in the cold or dissociate after multiple washes. IgA antibodies have not been associated with hyperacute rejection.

Hyperacute rejection does rarely occur in the absence of demonstrable antidonor antibody, presumably due to primed cytotoxic T cells present in the circulation at the time of transplantation. Such a phenomenon has been described in presensitized pigs, which reject renal allografts hyperacutely, but have no detectable humoral antibody (521). The first visible lesion within 30 minutes consists of lymphocytes attached to the arterial endothelium; after a few hours, the graft develops florid mononuclear infiltrate and necrosis. T-cell-mediated hyperacute rejection of mouse heart allografts has also been described in the absence of preexisting donor-reactive antibodies (522). Hyperacute rejection was occasionally reversed in humans by anti-T-cell antibody (OKT3), arguing for a T-cell-mediated component in rare cases (497).

Differential Diagnosis

The differential diagnosis of hyperacute rejection includes perfusion injury and major vascular thrombosis. Perfusion injury has prominent loss of endothelium and rare thrombi but generally no significant hemorrhage and necrosis. Increased neutrophils in PTC are associated with hyperacute rejection, but not ischemic injury (114). Grafts lost secondary to thrombosis of extrarenal arteries due to technical complications, or hypercoagulable states typically show necrosis with little or no hemorrhage, no thrombi, in intraparenchymal vessels, and no accumulation of neutrophils in PTC and glomeruli. Renal vein thrombosis shows marked congestion and relatively little neutrophil response and is not a feature of hyperacute rejection but rather raises the possibility of an underlying coagulopathy. Antiphospholipid antibodies can predispose to the thrombotic events (523).

Clinical Course, Prognosis, Therapy, and Clinicopathologic Correlations

Removal of the necrotic graft is often necessary to prevent the development of systemic toxicity. Recovery is extraordinarily rare, but has been reported (497,524). In one case, a follow-up biopsy at 30 days showed resolution of the glomerular thrombi (497). In another case, transplant glomerulopathy was evident at 39 days posttransplant (524).

Preventive desensitization protocols are now being tried that involve various combinations of plasmapheresis, IVIG, rituximab, and immunosuppressive drugs (525,526). New drugs that block complement activation, such as eculizumab, are under evaluation (527). Splenectomy is also added in some protocols and immunoabsorption with antigen (ABO) or protein A columns (528,529). If the titer of antibodies diminishes to low or undetectable, transplantation has been safely undertaken, even though antibodies were previously present (525,530). In some patients, the antibodies return with either

an episode of acute rejection or no immediate effect on graft function (accommodation). The long-term outcome of these recipients is unknown but of great interest.

ACUTE ANTIBODY-MEDIATED REJECTION

Introduction

Acute antibody-mediated rejection (acute AMR or acute humoral rejection) became a well-defined diagnostic category in 2003 (82). Acute AMR occurs in patients who either develop a threshold level of antidonor antibodies after transplantation or were presensitized and transplanted after desensitization. The histologic features of acute AMR are not absolutely specific and quite variable and thus not sufficient alone for definitive diagnosis (141,150,219,531). Detection of C4d in graft endothelium and the new solid-phase methods for detecting antidonor antibody have led to better diagnosis of this condition.

Halloran and colleagues described a short-term worse outcome in patients who developed acute rejection in the presence of circulating antibodies to donor HLA class I antigens (416,500). Certain morphologic features (neutrophils in PTC, thrombi, fibrinoid necrosis) were more common in patients with anti-HLA antibodies, but no histologic feature was a specific or sensitive indicator of circulating DSA (169). Furthermore, deposition of immunoglobulin or C3 was not conspicuous in these cases. The first diagnostically useful immunologic marker of AMR was identified by Feucht in the early 1990s, who reported that deposition of complement split fragments C4d and C3d in PTC could be detected in the majority of transplanted kidneys with “cell-mediated rejection” (532,533). C4d deposition was associated with “high immunologic risk” (i.e., previous transplants or high levels of PRA) and with a poor prognosis. They suggested that humoral rejection should be considered, despite negative crossmatch before transplantation and paucity of immunoglobulin deposition. The C4d deposition in PTC, circulating DSA, and neutrophils in capillaries were later documented as the diagnostic triad for acute AMR (387,418,534). However, peritubular capillaritis rich in mononuclear cell elements (macrophages, lymphocytes) rather than neutrophils is common in acute AMR, and the lack of neutrophils or even PT capillaritis does not argue against a diagnosis of acute AMR. On the other hand PT capillaritis, in particular in early graft biopsies, can occur in the absence of acute AMR (478). These observations have been confirmed in many centers, and the criteria are now widely accepted Banff consensus (82,461). As outlined above, the reader should also be aware that AMR often concurs with TCMR with overlapping histologic changes.

Prevalence, Clinical Presentation, and Risk Factors

The clinical presentation of acute AMR is generally that of severe rejection, with more frequent oliguria (35% vs. 10% without antibodies) and need of dialysis (40% vs. 10%), compared with rejection in the absence of HLA class I antibodies (416). However, there is no clinical feature that permits distinction from pure T-cell-mediated acute rejection. Acute AMR is most common 1 to 3 weeks after transplantation in

TABLE 29.5 Conditions caused by antibody-induced graft injury^a

Major Forms
Hyperacute rejection
Acute antibody-mediated rejection
Chronic antibody-mediated rejection
Variants
Smoldering/indolent antibody-mediated rejection ^b
Accommodation ^c

^aMost of these have C4d deposition in PTC and circulating DSA to HLA antigens. Variants with DSA but little or no C4d (\leq C4d 1 by IF and C4d 0 by IHC) have also been described, particularly for the chronic AMR and smoldering AMR. These are indicated as “C4d-negative” added to the diagnostic category, for example, C4d-negative chronic AMR.

Antibody induced graft injury, especially acute, smoldering and chronic antibody-mediated rejection, can show concurrent T-cell mediated rejection (acute and/or chronic).

^b“Smoldering” refers to biopsies with mononuclear cell capillaritis and/or glomerulitis without chronic or acute changes.

^c“Accommodation” is defined here as C4d deposition in PTC or DSA without evidence of active rejection.

particular in desensitized patients, but can develop suddenly at any time (150). In one series, the mean day of onset was 15 ± 11 days (earliest 3 days), not different from that of acute cellular rejection (14 ± 10 ; earliest 6 days) (387). The latest case reported was 30 years after transplant (535). Late onset is often associated with iatrogenic or patient-initiated decreased immunosuppression (536,537).

The primary risk factor for acute AMR is presensitization (blood transfusion, pregnancy, prior transplant) as judged by a historical positive crossmatch or high levels of PRA (538). About 24% of biopsies for acute rejection meet the criteria for acute AMR (either solely mediated by antibodies or with a concurrent T-cell component) (Table 29.5). The overall frequency of acute AMR in transplant recipients is about 6%. However, among presensitized patients with DSA, the frequency increases to 28% (range 8% to 43% among 11 centers) (539). Some crossmatch-negative patients in the past with acute AMR would be reclassified as presensitized with the current more sensitive DSA assays (540). The risk of acute AMR is increased if the pretransplant sera DSA fix complement in vitro as judged by C1q or C4d deposition on Luminex beads (541) or if the levels of DSA are higher as judged by the mean fluorescence channel in solid-phase assays (540,542). Acute AMR occurs with all traditional drug regimens, even in protocols that cause profound T-cell depletion (538,543,544). Experience with the newer agents, such as belatacept, is still limited, but there is a suggestion that alemtuzumab (anti-CD52) induction is associated with a higher frequency of acute AMR (543,545).

Pathologic Findings

Gross Pathology

The kidneys are swollen and congested; in severe cases, widespread hemorrhage and patchy infarction are present (Fig. 29.35).

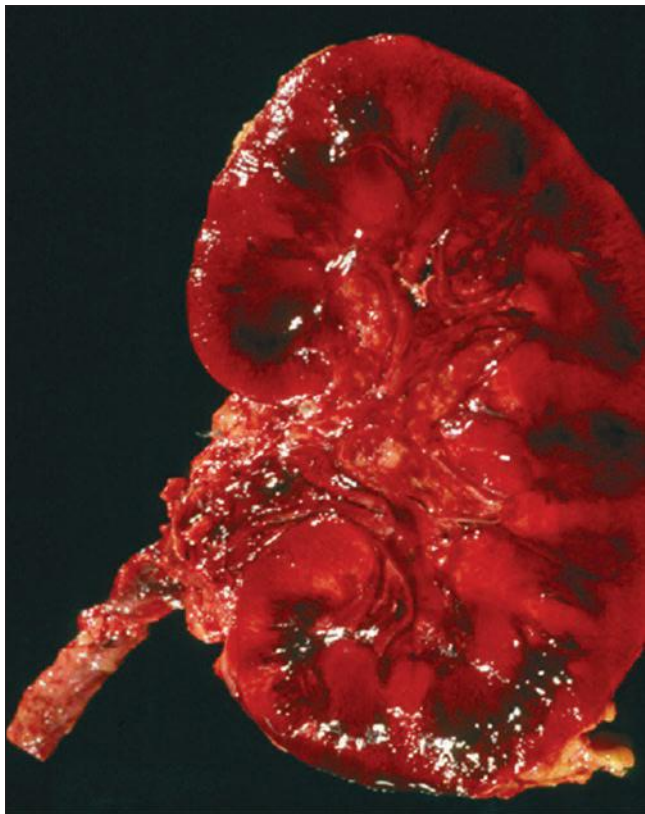


FIGURE 29.35 Gross appearance of an allograft with severe acute AMR 16 days after transplantation that failed after initially functioning for several days; ABOi graft (A2 into O).

Light Microscopy

Acute AMR has been divided into three types based on light microscopy (82,387): type I, acute tubular injury; type II, microcirculation inflammation with neutrophils and mononuclear cells in capillaries; and type III, fibrinoid necrosis of arteries (82). Acute AMR commonly is accompanied by features of TCMR, that is, these cases are classified as mixed acute TCMR and AMR, but AMR can occur in isolation. Acute AMR in late biopsies is typically superimposed on chronic AMR or TCMR (546).

GLOMERULI

Glomerular capillaries have neutrophils in 10% to 55% of cases (169,387,388,416) and mononuclear glomerulitis in 19% to 90% (150,169,387,388) (Fig. 29.36). Intraglomerular mononuclear cells are mostly monocytes/macrophages (CD68+) (389,547), in contrast to T-cell predominance in acute TCMR (168). Fibrin thrombi are present in about 20% of cases (169,387,416).

TUBULES

Evidence of acute tubular injury is common (loss of brush borders, thinning of cytoplasm, paucity of nuclei); in one series, these were found in 75% of cases (387). Indeed, acute tubular injury may be the only manifestation of acute AMR (Fig. 29.37) (387). Focal coagulative necrosis of tubules can be found in a minority of cases (Fig. 29.38) (387). Neutrophilic tubulitis is found in rare cases of acute AMR (Fig. 29.39) (387). Mononuclear tubulitis

is seen in 30% to 80% of cases and is considered evidence of a concurrent T-cell-mediated component (150,169,387,388), as is increased expression of HLA-DR (142,531).

INTERSTITIUM

In cases with pure acute AMR, edema with a scant mononuclear infiltrate may be present in the interstitium, insufficient for the diagnosis of (concurrent) acute TCMR following current Banff criteria. In one series, the majority fell within the Banff “suspectious/borderline” range (Banff category 3) (388). Whether this represents a component of TCMR or is caused by the antibody/complement interaction with the tissue is not known. Interstitial hemorrhage and edema can be prominent, but is not necessarily indicative of an antibody component (387,409). Frank cortical infarction is present in a minority of cases (5%) (387). B cells can be present in aggregates, and plasma cells can be detected (Figs. 29.40 and 29.41); these latter features are not diagnostic for acute AMR and can also be seen in TCMR.

VESSELS

Trpkov et al. (169) pointed out the association of neutrophils in PTC with class I DSA, a feature long recognized in hyperacute rejection (Fig. 29.42). In three series totaling 78 cases, 54% had neutrophils in PTC (169,387,548). However, neutrophils were rarely (less than 3%) found in a series from Vienna (388). Mononuclear cells, especially monocytes/macrophages, are also present in PTC. The PTC are often markedly dilated (169). Capillaritis can be present with little or no C4d deposition, which may follow a few days later (549).

In about 25% of cases, the arterial media shows myocyte necrosis, fragmentation of elastica, and accumulation of brightly eosinophilic material called “fibrinoid” with little mononuclear infiltrate in the intima or adventitia (Fig. 29.43). This lesion is not dissimilar to microscopic polyangiitis. Among the patients with anti-class I antibody, 25% had fibrinoid necrosis (vs. 5% of those without such antibodies) (169). Another study noted 53% of 17 patients had either fibrinoid necrosis (24%) or transmural arterial inflammation (18%), or both (12%) (550). Arterial thrombosis is uncommon. However, acute AMR may also manifest as TMA, with mucoid intima thickening and trapped red cells. These cases have a higher risk of graft loss than those without TMA (551). Epidemiologic evidence argues that endarteritis with mononuclear cells in the arterial intima may in some cases be mediated by antibody (153), a feature also noted in experimental studies with adoptive transfer of DSA (374). Approximately 40% to 50% of acute rejection episodes with transplant endarteritis (many also with tubulo-interstitial cellular rejection) are C4d positive and have a component of concurrent AMR (142,150,151,153,532). Whether the cellular component of transplant endarteritis in AMR is different from that due to TCMR is not apparent.

Immunofluorescence Microscopy and Immunohistochemistry

GLOMERULI

Glomerular staining for C4d is considered nondiagnostic in frozen sections (Fig. 29.44). In fixed tissue stained by IHC, about 30% of cases have glomerular C4d (388) (Fig. 29.45A), while normal glomeruli do not stain (Fig. 29.45B). No distinctive patterns are found by immunofluorescence for immunoglobulins

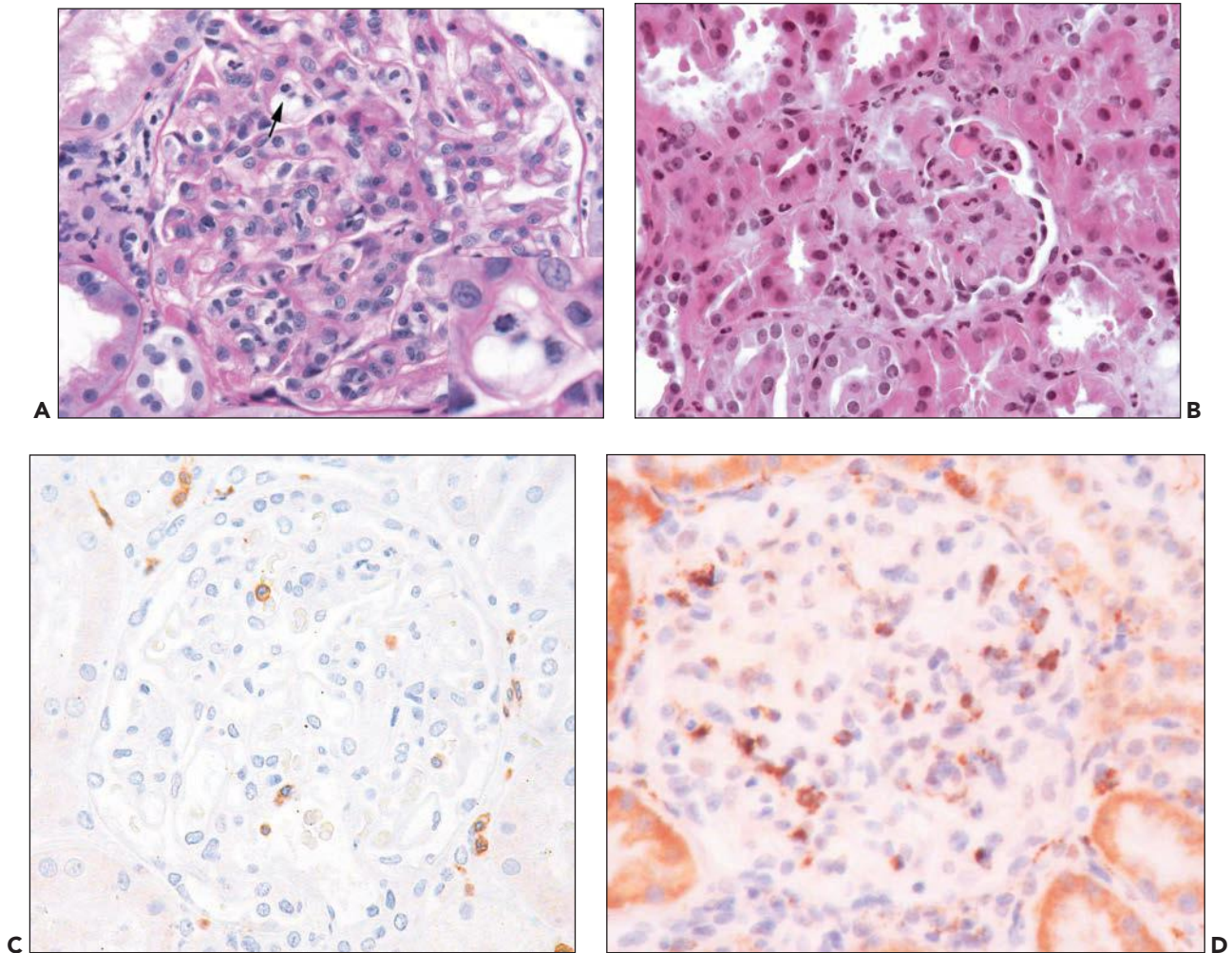


FIGURE 29.36 Acute AMR with glomerular inflammation (compare to Figure 29.7). **A:** Transplant glomerulitis with mononuclear cells, neutrophils, and reactive endothelial cells. An endothelial mitosis is shown (*arrow, insert*) C4d stain along PTC was positive. (PAS stain, original magnification 400 \times .) **B:** Transplant glomerulitis with neutrophils and thrombi. (H&E original magnification 20 \times .) **C:** Transplant glomerulitis in acute AMR with a few CD3⁺ cells (T cells). (Immunoperoxidase stain.) **D:** Same graft showing many CD68 cells (macrophages). The graft had prominent C4d deposition along PTC. (Immunoperoxidase stain.) (C, D courtesy of Alex Magil, Vancouver.)

(387). Mesangial IgM and IgG may be more prominent than in non-AMR, but the difference (43% vs. 17%) is not diagnostically useful (169).

TUBULES

C3 and C5b-9 (MAC) deposits have been reported primarily in tubular basement membranes, rather than PTC. The reason for this is not clear, but may relate to the ability of tubules to activate the alternative complement pathway (552). C5b-9 and C3 also are deposited in TCMR along the TBM. C4d is occasionally present segmentally along the TBM, in both acute AMR and TCMR, often in cases with tubular atrophy and TBM thickening.

PERITUBULAR CAPILLARIES

Immunoglobulin is usually not demonstrable in PTC (150); however, in a small minority of anti-class I antibody cases, IgM and IgG may be detectable (169,387). IgM is usually present in ABO-incompatible (ABOi) grafts with acute AMR (553).

Intense immunofluorescence staining for C4d is usually detected in a widespread, uniform distribution in the PTC of the cortex and medulla (142,150,531,532,534) (Fig. 29.46). Focal deposition may also be found. In classic cases, at low power, the smaller oval and elongated ring-like fluorescent profiles of dilated PTC are readily evident between the larger, negative tubular cross sections although dilated PTC may mimic tubular cross sections by IF. The capillary staining is crisp, linear, and continuous, but also may have a finely granular pattern at high power, which extends into the lumen from the more linear deposits. Medullary vessels are typically positive and can be the only place of C4d positivity in some cases with marked edema and cortical injury (141,531). In IHC, C4d has a similar pattern, diffuse, linear, and circumferential in the PTC wall, although the intensity typically is less and variable (see Fig. 29.45). Intraluminal and interstitial C4d may also be seen, but is an artifact of fixation. C4d-negative cases of acute AMR have been described, although

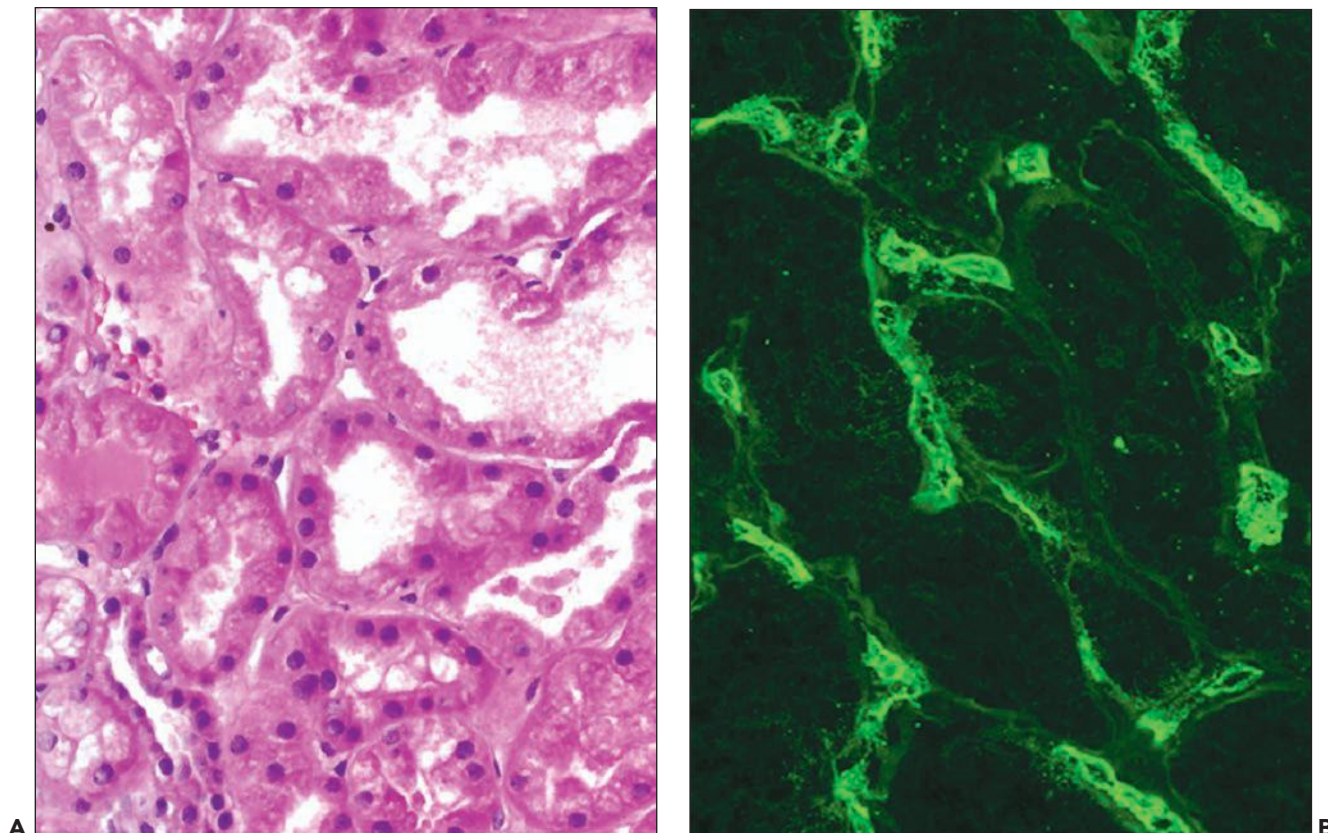


FIGURE 29.37 Acute AMR present on day 9 of DGF. **A:** Pattern of acute tubular injury, without evidence of inflammation. (H&E stain, original magnification 400 \times .) **B:** Immunofluorescence C4d stain on cryostat section shows widespread staining of PTC. (Original magnification, 400 \times .)

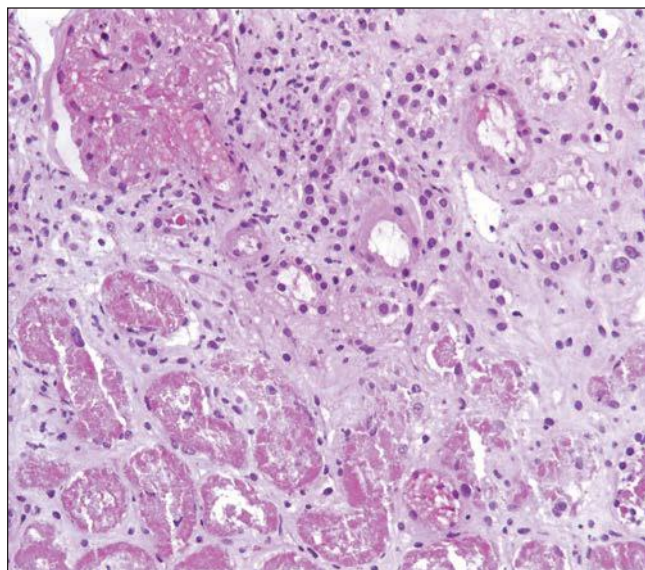


FIGURE 29.38 Acute AMR with glomerular and tubular necrosis. (H&E original magnification 200 \times .)

the frequency is uncertain. In a series with serial biopsies of presensitized patients, C4d became positive later after the capillaritis had been present for several days (549).

C4d is present in most PTC, even those that lack endothelial cell markers, and colocalizes with anti–type IV collagen and endothelial cells in frozen tissue (531,534). This location fits with the known ability of C4b to crosslink to nearby proteins at the site of complement activation. The covalent linkage of C4d to structural proteins may explain why C4d remains for several days after alloantibody disappears, since antibody binds to cell surface antigens that can be lost by modulation, shedding, or cell death. C4d can be detected on the surface of the endothelial cells and in intracytoplasmic vesicles by immunoelectron microscopy (554). Reduced CD34 expression has been described as well as platelet fragments that stain for CD61 (also found in acute TCMR) (555).

Protocol biopsies have shown that C4d deposition can precede histologic evidence of acute AMR. Haas et al. (118) found focal or diffuse C4d staining in two of eighty-two 1-hour biopsies taken at the time of transplantation after reperfusion. Both patients later developed an acute AMR (days 5 and 34) (118). The recipients had been treated with plasmapheresis before transplantation because of a positive crossmatch and had a weakly positive

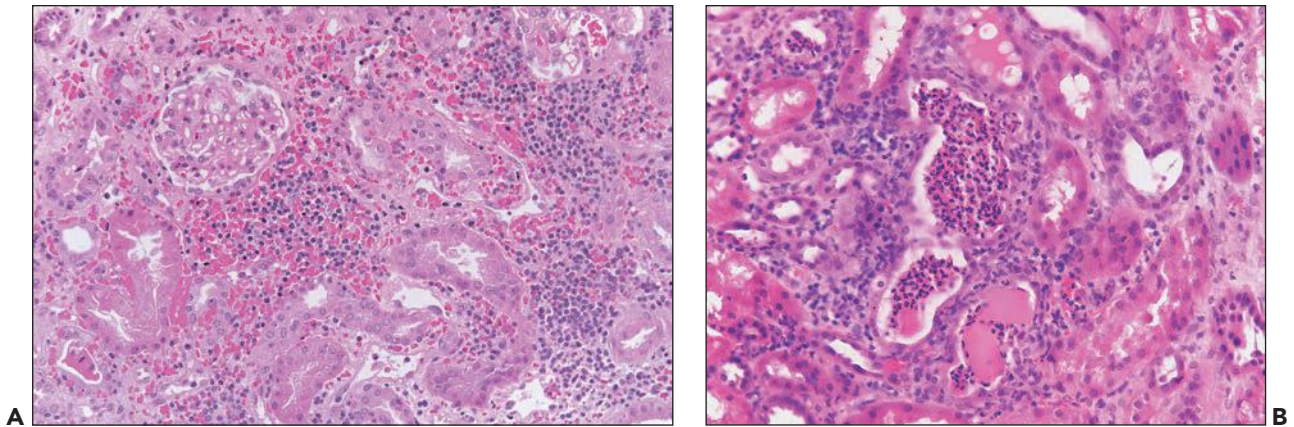


FIGURE 29.39 Acute AMR **(A)** Widespread interstitial hemorrhage is present. **B:** Neutrophils are in tubules, resembling acute pyelonephritis. (H&E, original magnification 400× (A) and 200× (B).)

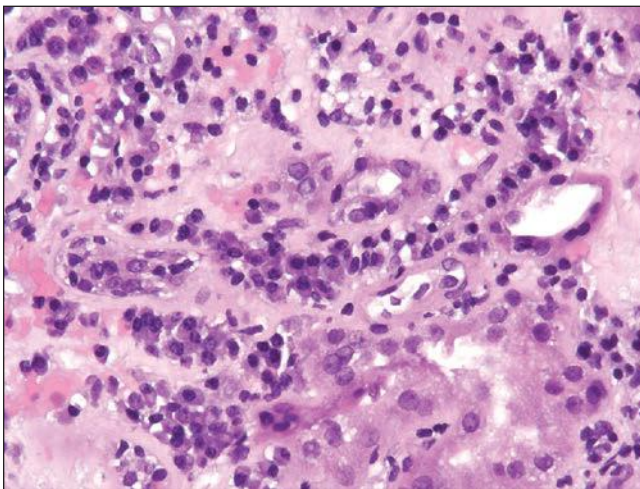


FIGURE 29.40 Plasma cell-rich late acute TCMR, C4d-positive (compare to Figure 29.13). The combination of plasma cell infiltrates, that is, acute plasma cell-rich TCMR and acute AMR, is a very rare occurrence that seems to carry a poor prognosis. (H&E original magnification 400×.)

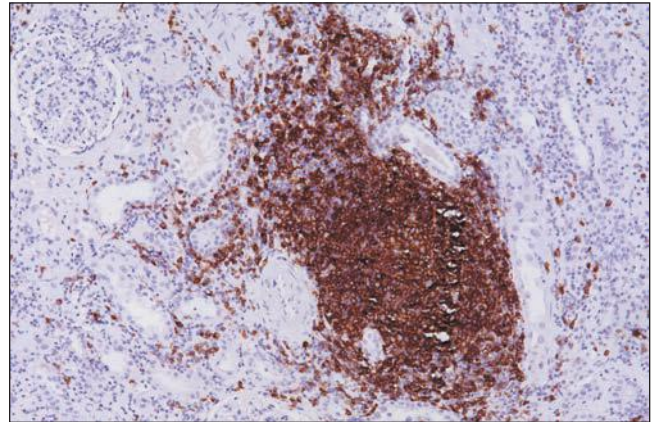


FIGURE 29.41 Acute AMR with a nodule of B cells, a finding that has been reported by some to carry an adverse prognostic significance. At present, there is no linkage between B cells in the interstitial infiltrate and the presence of antidonor antibodies. (Immunohistochemical stain for CD20, original magnification 100×.)

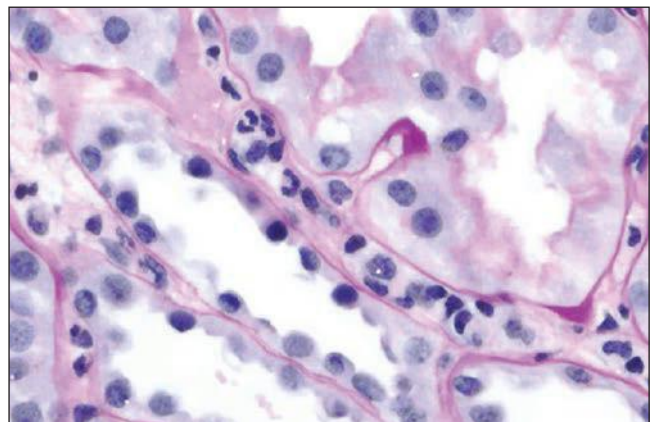
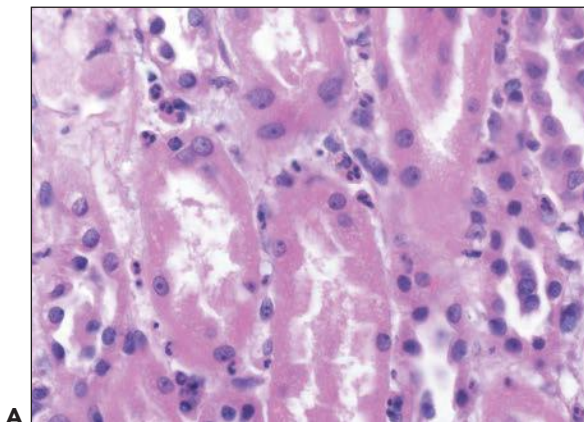


FIGURE 29.42 Acute AMR with characteristic intraluminal PTC leukocytes. Primarily neutrophils **(A)** and primarily mononuclear **(B)** cells. (H&E (A) and PAS (B). Original magnification 400× (A) and 600× (B).)

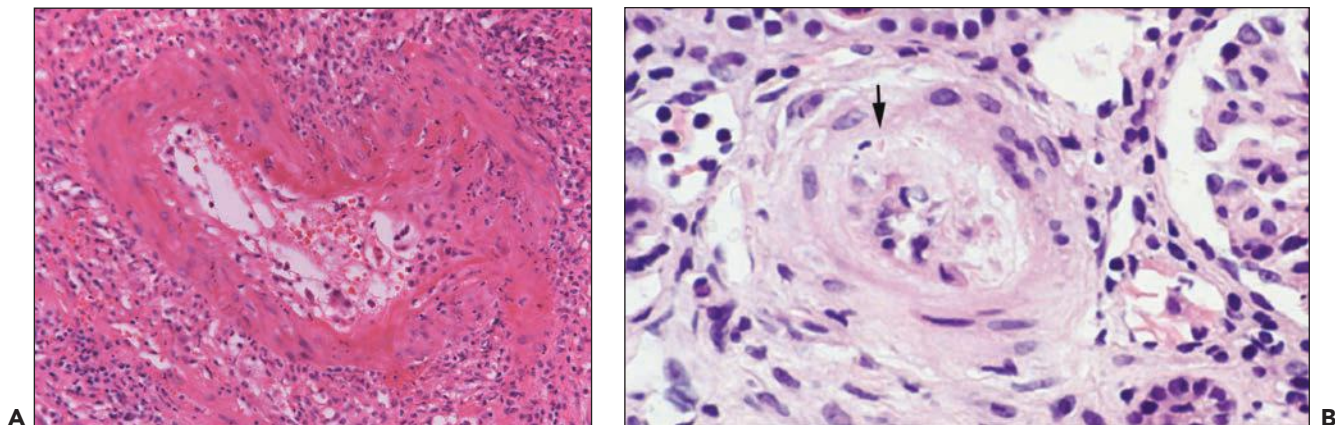


FIGURE 29.43 Acute AMR **(A)** Fibrinoid arterial necrosis (Banff type III). Neutrophils and fibrin are seen in the wall of the arcuate sized artery. Nephrectomy specimen. (C4d stain–positive. H&E original magnification 200 \times .) **(B)** Mucoic intimal thickening resembling TMA. Patient had anti–class I antibodies (134). Red cell fragment in intima (*arrow*). (H&E, original magnification unknown.) (Courtesy of Kim Solez.)

flow crossmatch at the time of transplantation (118). In 1-week protocol kidney biopsies, Sund showed PTC endothelial C4d deposition in 30% of cases; 33% of these did not meet histologic criteria of acute rejection, but 82% developed rejection during further follow-up. Koo reported C4d in 13% of 48 one-week protocol biopsies (556). C4d was present in 33% of samples with rejection and 3% of samples without rejection; all 5 with C4d

and rejection had DSA (556). Outcome at 1 year was not affected by C4d status at 7 days, despite the lack of specific treatment.

The precise time course of C4d clearance and relationship to DSA levels has not been documented in humans. C4d deposition disappears a few days after treatment, provided the antibody disappears, as judged by sporadic repeat biopsies and experimental studies. Loss of C4d has been observed in as early

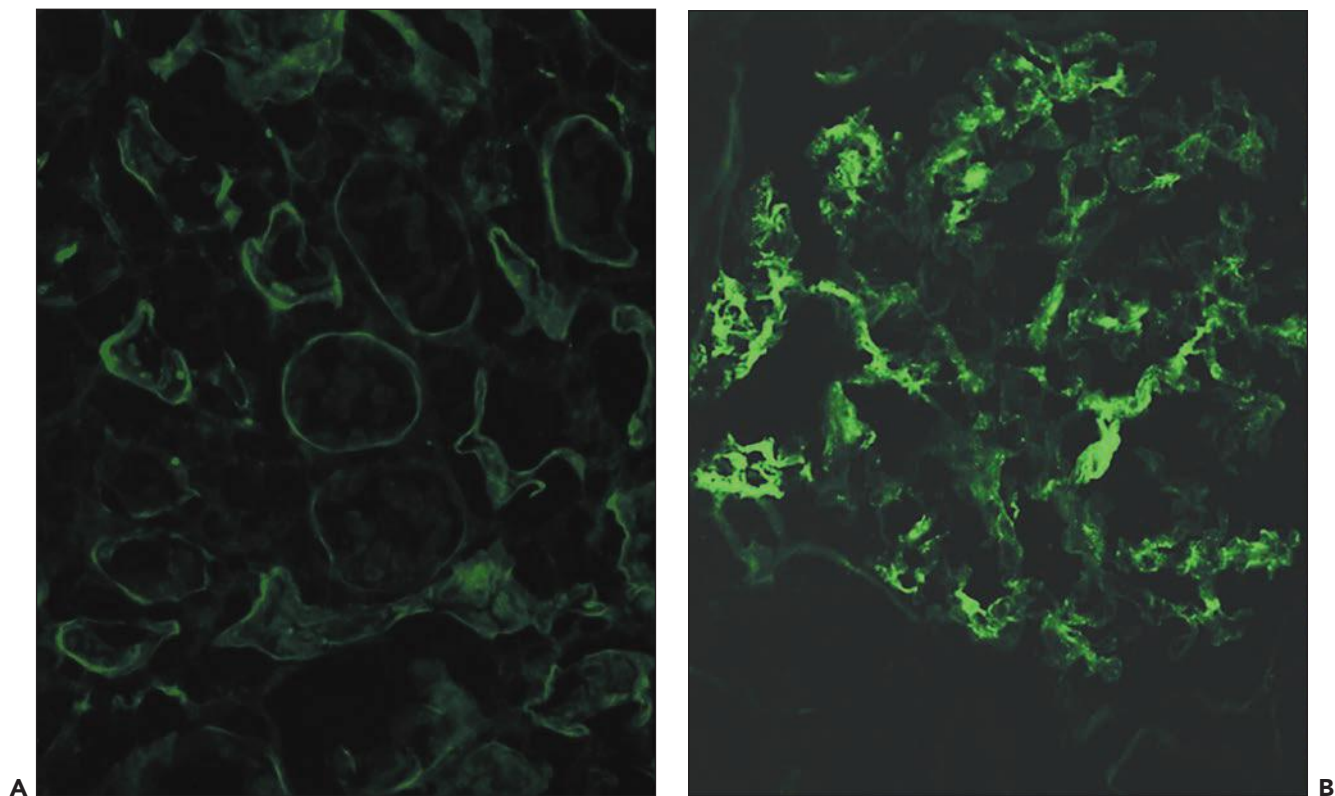


FIGURE 29.44 Normal kidneys stained for C4d using a monoclonal antibody cryostat sections. **A:** Negative PTC and faint staining along the TBM. **B:** Prominent mesangial deposits are present in normal glomeruli. (Original magnifications 400 \times .)

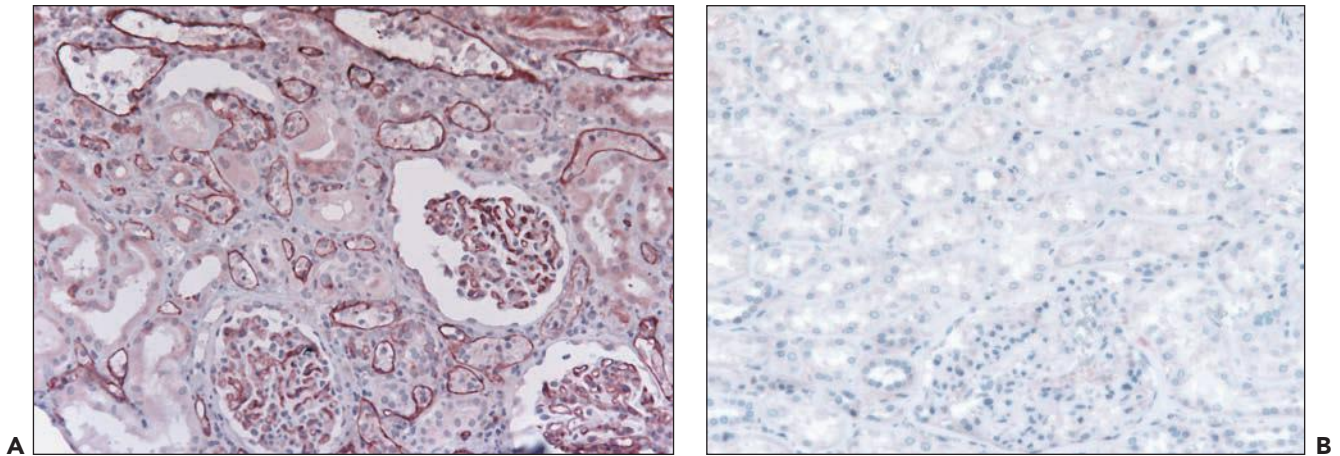


FIGURE 29.45 Paraffin sections stained using a polyclonal anti-C4d (347). **A:** Acute AMR showing widespread, circumferential deposits in characteristically dilated PTC containing leukocytes. The glomerular capillary walls also stain prominently. **B:** Normal kidney stained with the same technique demonstrates the absence of C4d in the glomeruli in paraffin sections (compare with Fig. 28-45B). (Original magnification 200 \times .)

as 7 to 8 days after a positive biopsy (150) and in rat heart transplants in 5 days (557).

C3d, produced by the classical pathway after C4b, has been suggested as an indicator of more complete complement activation. However, the normally high background of C3 deposition in the tubular basement membranes makes C3d much harder to interpret than C4d (558). Two series found C3d in 44% to 60% cases of C4d+ acute AMR (534); a minority had C3d without C4d. In other studies, C3d in PTC was not associated with neutrophils in PTC (548,558) or DSA (548).

ARTERIES

Fibrinoid necrosis in arteries usually stain for IgG and/or IgM, C3, C4d, and fibrin (217,534). Nondiagnostic C4d deposition occurs along endothelial surfaces of arteries and arterioles, in the thickened intima of arteries and in arteriolar hyaline,

whether or not acute AMR is present; this staining pattern is seen also in native kidneys.

Electron Microscopy

GLOMERULI

The appearance may resemble TMA, with platelets, fibrin, and neutrophils in glomerular capillaries (Fig. 29.47). The glomerular endothelium is reactive with loss of fenestrations. Endothelial cell swelling (88%), separated from the GBM by a widened lucent space (100%) and early GBM duplication (76%), was present in C4d+ biopsies within the first 3 months in a series mostly of presensitized patients (559). Similar ultrastructural changes were seen with little or no C4d deposition in patients with DSA and glomerulitis/capillaritis. These changes are more evident in allografts that later develop transplant glomerulopathy (220,560).

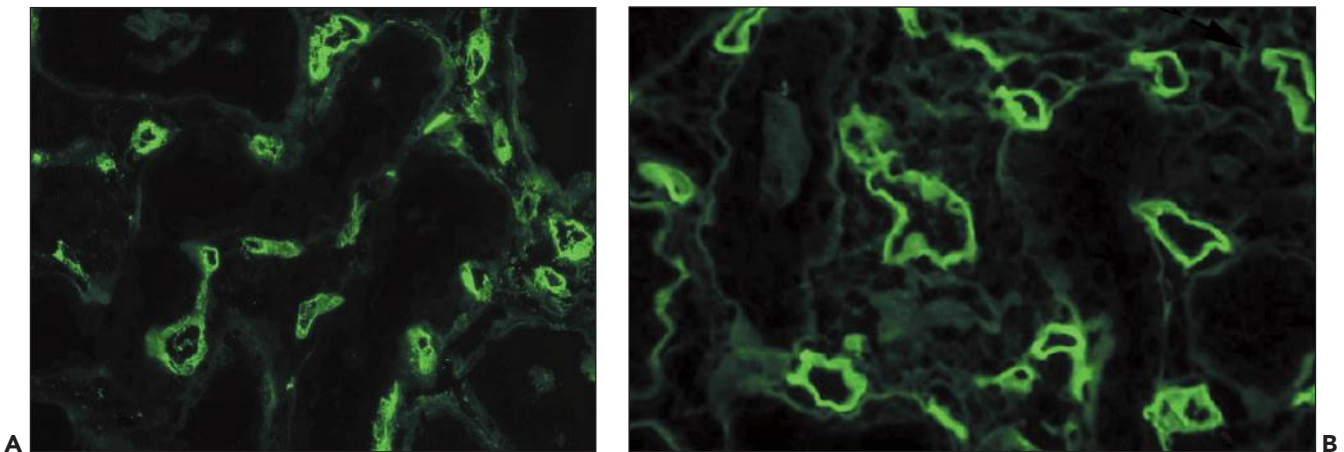


FIGURE 29.46 Acute AMR, C4d stain using monoclonal antibody to C4d in cryostat sections. Bright widespread, circumferential staining is present in **(A)** and **(B)**. **A:** Has a slightly granular appearance, and **(B)** is purely linear. Both patients had antibodies to donor HLA antigens. (Original magnification 400 \times .)

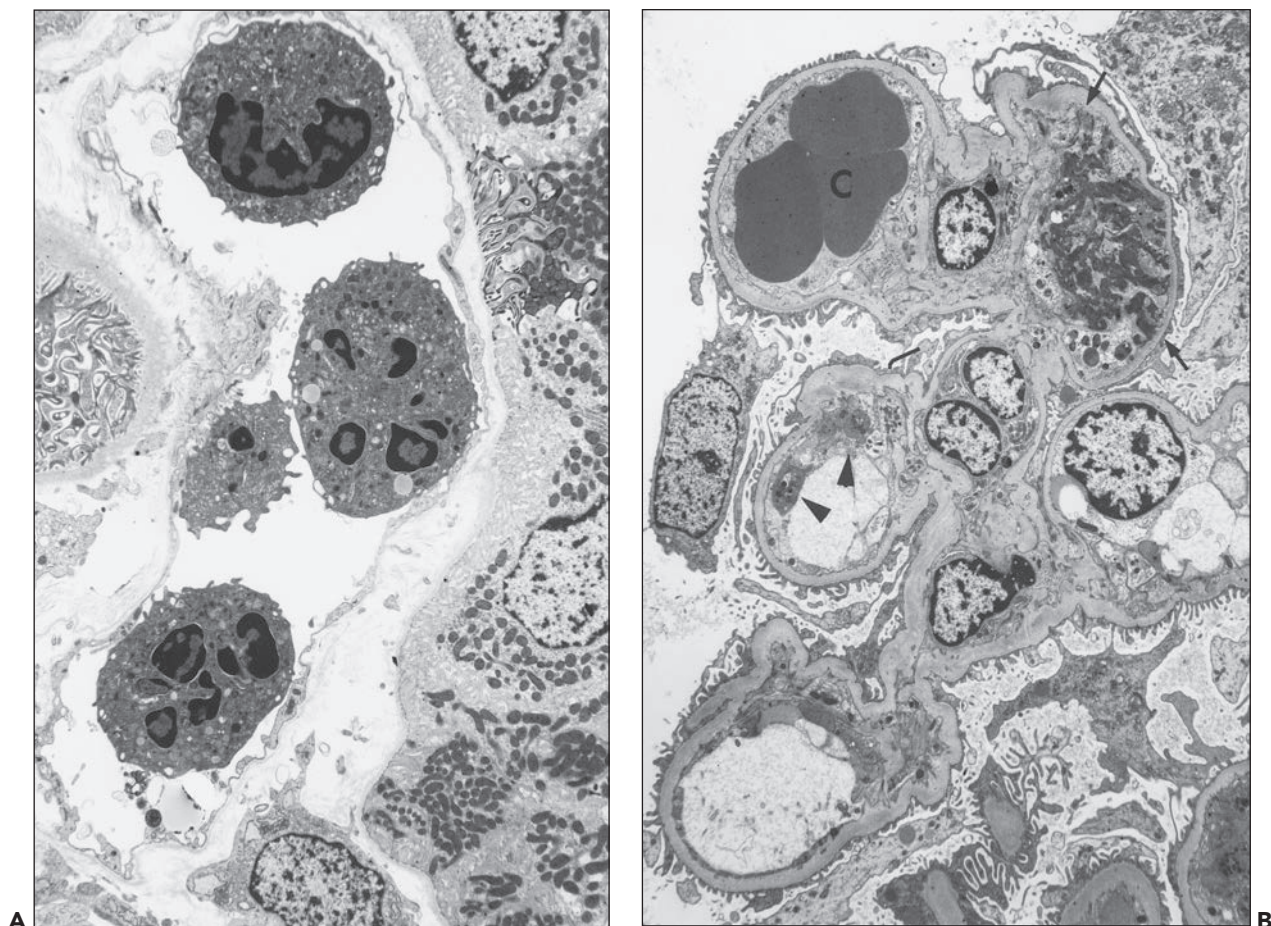


FIGURE 29.47 Acute AMR. A: Neutrophils are in PTC whose endothelium shows the subtle changes of injury (loss of fenestrations). **B:** A glomerulus has one capillary plugged with fibrin (arrows) and another filled with compacted red cells surrounded by a reactive endothelial cell (C); a third loop has a few platelets (arrowheads). (Electron micrographs. (A) $\times 3,700$; (B) $\times 3,300$.)

PERITUBULAR CAPILLARIES

Neutrophils and monocytes are found in PTC with platelets, and fibrin (560,561). Interstitial edema and red cell extravasation can be found. Intact platelets are few, but microvesicles presumably derived from platelets are common (555). Endothelial cells show swelling, detachment, and expansion of the subendothelial space with electron-lucent “fluffy” material and sometimes trapped red cells (561). Lysis, apoptosis, and fragmentation of endothelial cells are evident (560). These changes are more severe and extensive than the endothelial swelling and apoptosis that occurs in ischemic renal injury (560). Apparent new capillary sprouts have been illustrated (560). After 2 to 4 weeks, the endothelial cells show cytoplasmic processes extending into the lumen and early multilayering of the basement membrane (560,561). Liapis et al. (224) showed in approximately 30% of late biopsies with acute AMR or with mixed acute TCMR and AMR evidence of severe PTC multilamination, that is, ultrastructural evidence of chronic rejection (as judged by ≥ 7 circumferential layer in one PTC and greater than five layers in two additional PTC). These observations illustrate that electron microscopy can uncover signs of chronic rejection before they become more prominent and detectable by standard light

microscopy. In severe cases, after 2 to 3 months, some capillaries are completely destroyed, with disappearance of the endothelial lining and remnants of the basement membrane; those that remain have a thickened, multilayered basement membrane (561).

ARTERIES

The small arteries with fibrinoid necrosis show marked endothelial injury and loss, smooth muscle necrosis and deposition of fibrin tactoids.

Differential Diagnosis

The diagnostic triad for acute AMR proposed by Mauiyyedi et al. (387) was incorporated with minor modification by Banff (82) (Table 29.6). These include (a) histologic evidence of acute injury (neutrophils and/or monocytes in capillaries, acute tubular injury, fibrinoid necrosis), (b) evidence of antibody interaction with tissue (typically C4d in PTC), and (c) serologic evidence of circulating antibodies to antigens expressed by donor endothelium (typically HLA or ABO). If only two of the three major criteria are established (e.g., when no DSA assay is available or when C4d staining is not done or is negative), the diagnosis should be considered suspicious for acute

TABLE 29.6 2013 Banff criteria for acute/active ABMR^{a,b}

1. Histologic evidence of acute tissue injury, including one or more of the following:
 - Microvascular inflammation ($g > 0^c$ and/or $ptc > 0$)
 - Intimal or transmural arteritis ($v > 0$)^d
 - Acute thrombotic microangiopathy, in the absence of any other cause
 - Acute tubular injury, in the absence of any other apparent cause
2. Evidence of current/recent antibody interaction with vascular endothelium, including at least one of the following:
 - Linear C4d staining in peritubular capillaries (C4d2 or C4d3 by IF on frozen sections, or C4d > 0 by IHC on paraffin sections)^e
 - At least moderate microvascular inflammation ($[g + ptc] \geq 2$)^f
 - Increased expression of endothelial activation and injury transcripts (ENDATs) or other gene expression markers of endothelial injury in the biopsy tissue, if thoroughly validated
3. Serologic evidence of donor-specific antibodies (HLA or other antigens)

^aAs reported by Haas et al. (481).

^bAll three major criteria must be present for diagnosis. Biopsies showing two of the three features may be designated as “suspicious” for acute/active ABMR, except those with DSA and C4d without histologic evidence of active rejection (also known as accommodation). TCMR may also be present as in Table 29.5.

^cRecurrent/de novo glomerulonephritis should be excluded.

^dArterial lesions may be indicative of ABMR, TCMR, or mixed ABMR/TCMR. “v” lesions are scored in arteries having continuous media having two or more smooth muscle layers.

^eReports should specify whether the lesion is C4d positive or negative and the technique used.

^fIn the presence acute TCMR, borderline infiltrates, or evidence of infection, $ptc \geq 2$ alone is not sufficient to define moderate microvascular inflammation and g must be ≥ 1 .

AMR. A negative C4d stain or a negative serology does not rule out acute AMR. Histology by itself is insufficient to rule acute AMR in or out, and the diagnosis can be complicated by other pathology, such as concurrent acute TCMR (82,142,150,562).

Biopsies that meet the criteria for both acute AMR and TCMR type I or II are considered to have both forms of rejection; these mixed rejection episodes are quite common. Lesions that favor an antibody mediated component of the rejection episode are neutrophils in PTC (46% to 65% vs. 5% to 9%), fibrinoid necrosis of arteries (25% vs. 0% to 5%), glomerulitis (35% to 55% vs. 4% to 20%), thrombi (20% to 46% vs. 0% to 15%), and infarction (5% to 38% vs. 0% to 2%) (150,169,219). Of these criteria, peritubular neutrophils are the most useful. However, neutrophils can be observed in PTC in acute TCMR, sepsis, ANCA associated small vessel vasculitis or pyelonephritis, even to a quite prominent degree, with no circulating DSA.

Fortunately, other diseases in the differential are negative for C4d (141,461,479). Acute tubular necrosis in native kidneys has no C4d deposition in PTC (563). In ANCA-related glomerulonephritis in native kidneys, we also found no examples of PTC C4d deposition (461). One of the common diagnostic dilemmas in transplant biopsies is the

distinction between TMA. Fortunately, C4d is negative in PTC in TMA in native kidneys, including cases with lupus anticoagulant and antiphospholipid antibodies (461). In five reported cases of recurrent HUS in a transplant, C4d was also negative (564). Thus, although the arterial and glomerular lesions overlap, PTC C4d provides a useful discriminator between acute AMR and TMA/HUS (Fig. 29.48) (388). The only condition that occasionally has bright PTC C4d staining is lupus nephritis, but that is typically in a granular pattern and associated with glomerular deposits (461,565) and due to immune complexes.

Fibrinoid necrosis of arteries often occurs in association with C4d deposition in PTC (50% to 73% of cases) (566) and can serve as a potential diagnostic sign of acute AMR. However, fibrinoid necrosis is also seen in acute TCMR and may respond to OKT3 therapy (372). Other causes of fibrinoid necrosis are malignant hypertension/TMA and recurrent polyangiitis. As described above, antibodies to the AT1R have been implicated in fibrinoid necrosis in acute rejection, in the absence of C4d deposition in capillaries (433).

Differential diagnosis is more challenging in C4d-negative AMR. Presence of DSA and microcirculation inflammation in the absence of immune complexes in glomeruli and tubular basement membranes make AMR the most likely diagnosis despite absence of C4d, as long as acute TCMR can be excluded as the cause. This has been incorporated as an alternative criterion for antibody interaction with the vessels (Table 29.6).

Pathogenesis

Most cases of acute AMR have detectable DSA to donor class I and/or II antigens (543,550). DSA react with MHC expressed on donor endothelium, particularly in peritubular and glomerular capillaries, and sometimes target arteries and arterioles. Whether other donor antigen-expressing cells in the allograft can be targeted (such as epithelial cells, smooth muscle) is unknown. A small minority (less than 5%) have evidence of reactivity to non-MHC or other endothelial antigens (567), for example, the rarely reported acute AMR in HLA-identical sibling grafts (42,43). The nature of these antigens is unknown, with the exception of autoantibodies to the angiotensin 1 receptor (567). These autoantibodies may act by amplifying the damage initiated by MHC antibodies, as shown for AT1R antibodies experimentally (433).

Several lines of evidence support an important role for complement fixation in the pathogenesis of acute AMR. Complement-fixing antibody isotypes are required for passive transfer of acute AMR in mouse cardiac allografts (568). Blocking the terminal complement pathway with anti-C5 antibodies prevents acute AMR of kidney or heart allografts in mice (569,570). In presensitized patients, the ability of DSA to fix complement in vitro (C4d on HLA-coated beads) predicts early graft loss (559,571). Presensitized patients with DSA treated with eculizumab (which blocks activation of C5) have a significantly reduced frequency of acute AMR compared with historical controls (572). Protocol biopsies in these patients showed C4d in the PTC, without inflammation or endothelial injury, evidence that C5 activation is necessary for these features (573). Genetic deficiency of complement regulatory factors may intensify acute AMR. A patient deficient in factor H-related protein 3/1 developed severe acute AMR, which was reversed with eculizumab therapy (574).

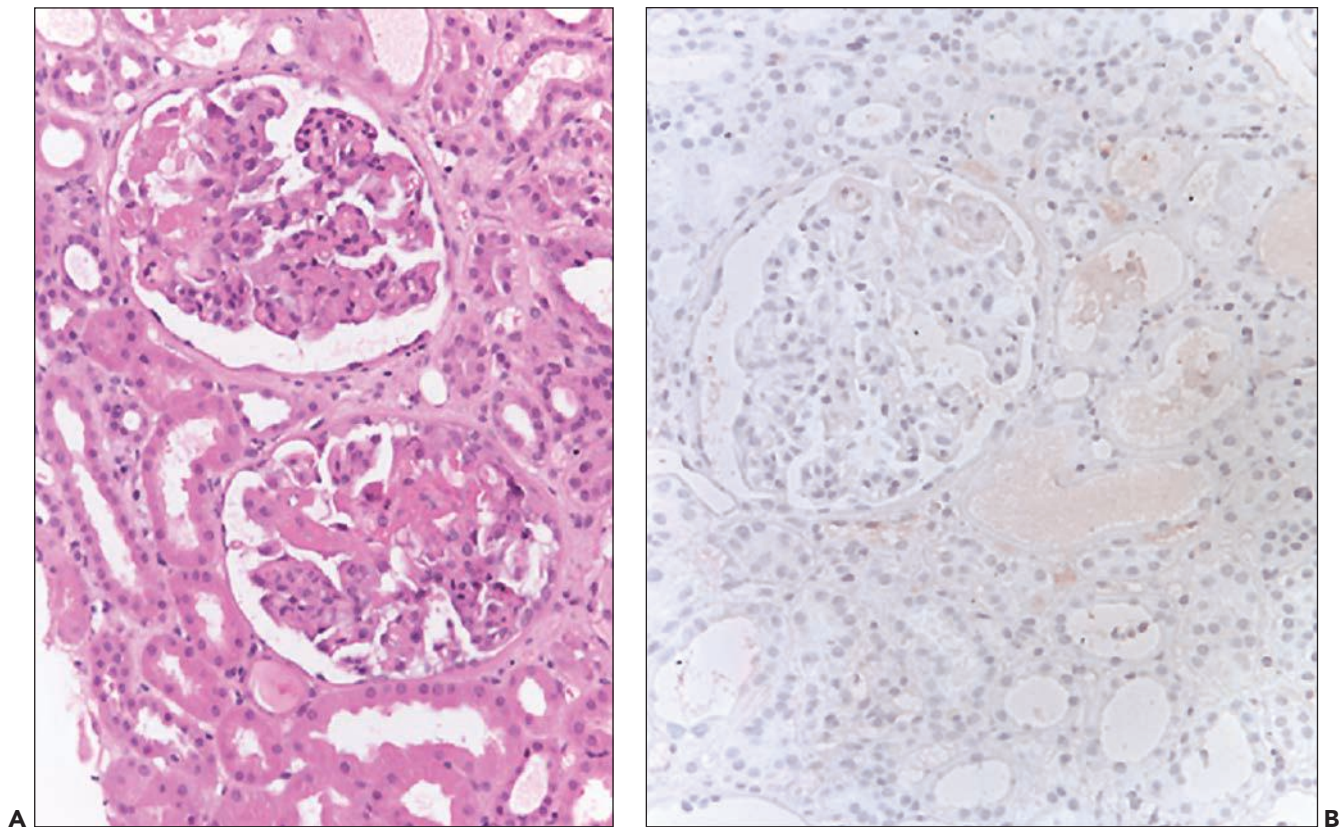


FIGURE 29.48 Allograft with TMA. **A:** Fibrin thrombi in glomeruli. H&E. **B:** C4d stain by IHC (paraffin section). No C4d is detected in PTC or glomeruli. (Both original magnifications 200 \times .)

Clinical Course, Prognosis, Therapy, and Clinicopathologic Correlations

The outcome of acute AMR is considerably worse than acute TCMR. The worst prognosis is, however, often seen in cases with mixed acute TCMR and AMR (140). The presence of C4d strikingly and adversely impacted the outcome of either type 1 or 2 acute TCMR and is an independent predictor of graft outcome in patients with acute rejection (151,531,575) (Fig. 29.49).

Among various reports, 16% to 50% of C4d+ acute AMR grafts were lost in a year, compared with 3% to 7% loss after a C4d-negative acute rejection episode (151,387,486,540,543,576). The difference is minimal in some series (150). In a series of 469 non-presentation patients treated with alemtuzumab, 10% developed acute AMR, and 20% of these lost their graft within a year (543). In another large series of 402 crossmatch-negative patients, 8% developed acute AMR; 1- and 5-year graft survival rates were 87% and 54%, respectively (540). DSA were detectable in pretransplant serum in many of these patients using the more sensitive solid-phase assays. Either HLA class I- or class II-reactive DSA pretransplant is a risk factor for acute AMR and graft loss (540). The risk of acute AMR and poorer outcome correlates with the level of MFI of the DSA in Luminex assays (540,577). DSA that fix complement, as judged by uptake of C4d or C1q on HLA-coated beads, is a risk factor for acute AMR, compared with DSA that do not fix complement, whether measured pretransplant (559) or posttransplant (578,579). When the patients

are known to be presensitized, close monitoring and aggressive treatment can minimize the graft loss. Among a group of 51 presensitized patients treated with desensitization, the risk of acute AMR was 41%, but only 4% of the grafts were lost within a year (572). In addition to early graft loss, the long-term effects of acute AMR include a fivefold high risk of chronic AMR with transplant glomerulopathy (419).

The pathologic feature historically correlated with increased graft loss in acute rejection is fibrinoid necrosis of arteries (type III) (196), with about 25% graft survival at 1 year (206). Type III rejection is often C4d-positive (in approximately 50% of cases (150)), but the older studies did not include that test. Type III acute AMR has a lower graft survival than type I (tubular injury) or type II (capillaritis), but in a recent series, 1-year graft survival of type III was 75%, a considerable improvement over past results (543).

Treatment of acute AMR is still evolving; randomized controlled trials of therapies are sparse (580). The most common strategies are based on the quick reduction of antibody titers with plasmapheresis, IVIG, and thymoglobulin to treat any concurrent TCMR (142,580,581). The best evidence supporting the use of plasmapheresis and IVIG come from studies of desensitization (441,582). IVIG has a variety of immunomodulatory effects, especially on B cells, antibody, and complement (583). Splenectomy has also been used as a last resort, with beneficial results thought to be due to the abundant plasma cells present (584). Immunoabsorption with protein A, which

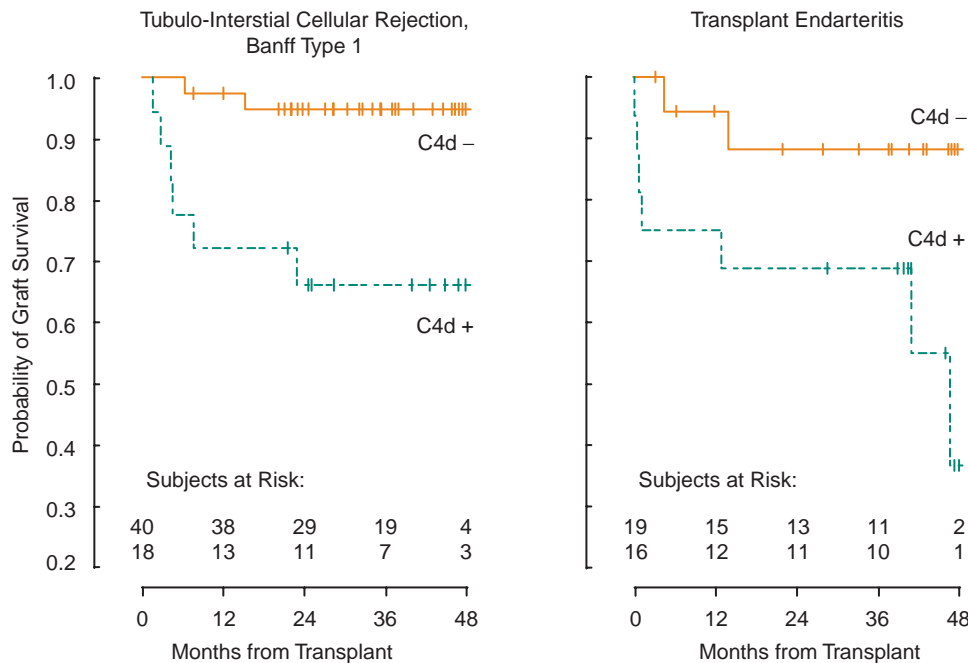


FIGURE 29.49 Graft survival as a function of the type of rejection (Banff category 4, type I or II cellular) and the presence or absence of concurrent acute AMR/C4d deposition in PTC (353). In both types of TCMR, concurrent C4d is a poor prognostic feature. (Adapted from Hertzberg AM, Gill JS, Djurdjev O, et al. C4d deposition in acute rejection: An independent long-term prognostic factor. *J Am Soc Nephrol* 2002;13:234.)

binds mainly to IgG, was subject to a randomized trial that was prematurely terminated due to a dramatically better outcome in the treated group (585). Eculizumab, an antibody to C5 that blocks the terminal complement pathway, has shown evidence of efficacy in nonrandomized pilot trials (586) and in isolated cases (574). Infusion of soluble (587) or membrane-targeted complement regulators (588) as well as C5a receptor antagonists (589) also deserve study.

Other therapies commonly considered are anti-B-cell agents, such as anti-CD20. Rituximab reacts with CD20 on pre- and mature B cells and leads to transient B-cell depletion with B-cell recovery after 6 to 9 months. Drugs directed at modulating B-cell and plasma cell function are still under investigation but are already frequently used off-label in treatment of AMR. Bortezomib, a proteasome inhibitor used in the treatment of multiple myeloma for plasma cell depletion, has been tried in a small cohort with acute AMR with evidence of success (590,591). Agents that inhibit B-cell and plasma cell growth factors, such as belimumab, a human monoclonal antibody that inhibits B-cell activating factor (BAFF), have been approved for use in autoimmune diseases and will likely be tried in transplantation.

ABO-Incompatible Grafts

ABOi grafts have special features that warrant separate consideration. Blood group antigens, most importantly the A and B antigens, are carbohydrate epitopes on glycolipids and glycoproteins in most tissues, including erythrocytes and the endothelium. In the kidney, ABO antigens are on the endothelium and distal convoluted tubules (and on the collecting ducts of secretors) (592). Antibodies to A or B antigens (isoagglutinins) arise “naturally” in normal individuals without A or B blood groups in response to similar bacterial antigens in the environment and are of the IgM and IgG isotype.

Much of the experience with ABOi grafts comes from Japan, where they represent about 30% of the living donor grafts (593). Several groups in Japan (593–595), as well as

in the United States (596–598), have reported excellent results. Pretransplant removal of circulating ABO antibodies by plasmapheresis has permitted successful transplantation of ABOi kidneys without hyperacute rejection. Initially, these protocols required splenectomy (599), but more recently, rituximab has been substituted with success (594) and so has standard immunosuppression (600). Extracorporeal immunoabsorption (601) is another strategy, using ABO carbohydrate columns, which can reduce IgM and IgG antibodies. This approach does not remove all of the ABO specificities (602) and reduces antibodies to bacterial polysaccharides (603).

A minority of desensitized recipients of ABOi grafts develop clinical acute AMR, ranging from 4% to 30% depending on the regimen (594,604). The primary risk of acute AMR is in the first month, particularly the first 2 weeks, with the risk of acute rejection 2.3 times that of ABO-compatible grafts (596). The pathologic features are similar to acute AMR due to HLA DSA, although IgM is more often detected in the capillaries (Fig. 29.50) (553). One-hour postperfusion biopsies have shown C4d in 57% of ABOi grafts, usually also with IgM (88%) and occasionally with IgG (40%); however, only 37% of patients with C4d deposition developed acute rejection in the first month. Subclinical acute AMR manifested by glomerular thrombi was diagnosed by protocol biopsies in 12% of patients (604). At 6 to 12 months, 28% of protocol biopsies showed subclinical rejection (605). However, only few of these studies in ABOi patients reported detailed data regarding simultaneous development of de novo anti-HLA antibodies. Recovery from acute AMR in ABOi grafts correlates with a decrease in ABO titer, but not with a disappearance of C4d, in contrast to acute AMR caused by HLA antibodies in which recovery is associated with both loss of antibody titer and C4d (606). Protocol biopsies show that C4d deposition continues in most patients, with 94% positive at 1 year (605). As judged by protocol biopsies at 1 year, the frequency of transplant glomerulopathy is higher in ABOi

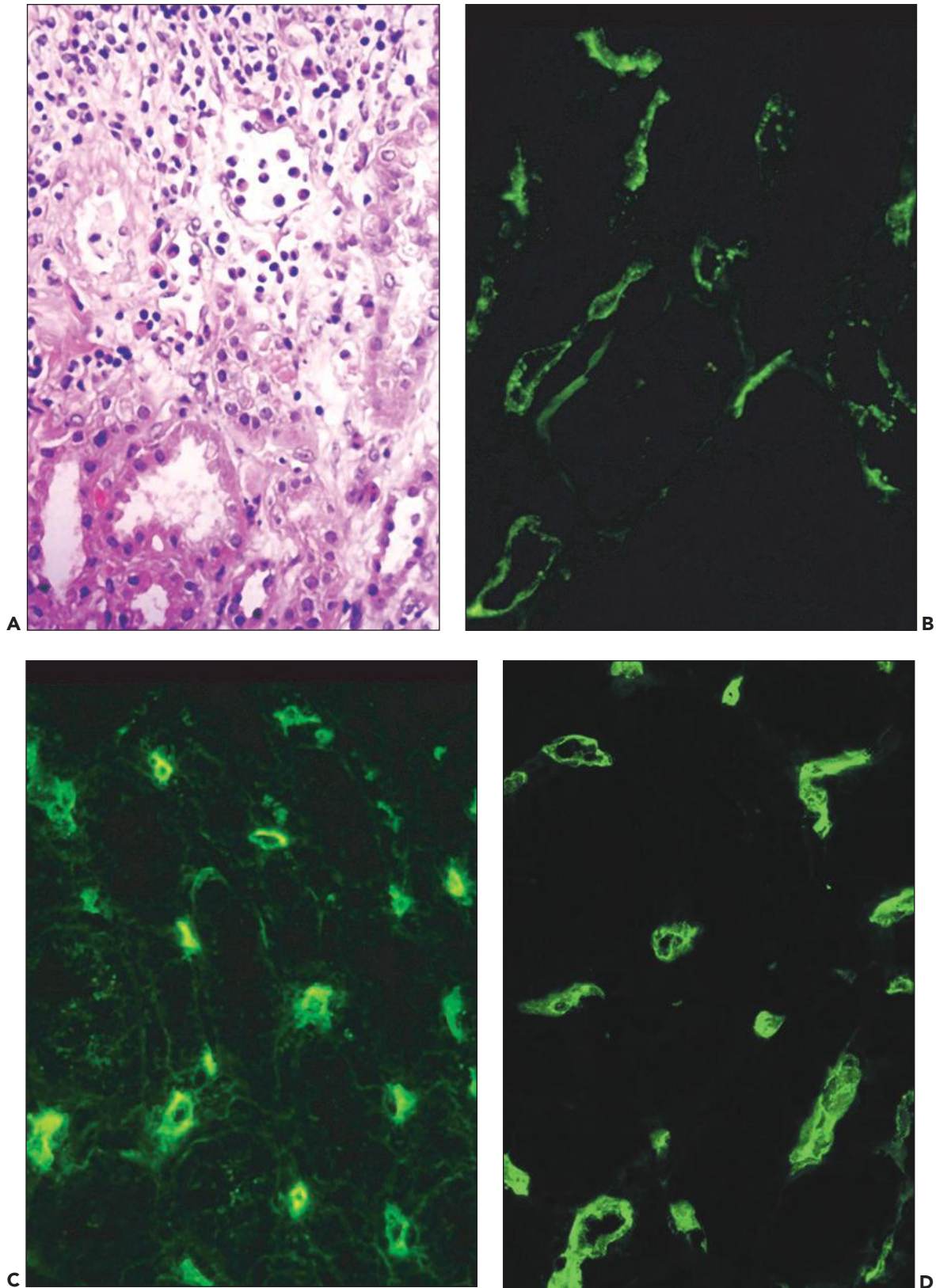


FIGURE 29.50 ABOi graft with Acute AMR. **A:** Neutrophils are prominent in dilated PTC. IgM **(B)**, **(C)** C3, and **(D)** C4d are deposited in PTC, as shown by immunofluorescence stains of cryostat sections.

grafts compared with ABO-compatible grafts (13% to 15% vs. 7% to 8%, respectively), a difference that reaches statistical significance when the two series are combined ($P < 0.001$) (597,605). The major risk factors for TG were prior acute AMR (597,607) and the presence of HLA DSA, indicating the importance to rule out concomitant anti-HLA DSA in ABOi patients (605,607).

A striking difference between ABOi and compatible grafts is the common presence of C4d in the PTC in the former, in the absence of inflammation or graft dysfunction, a state termed “accommodation.” One possible explanation of the lack of pathology in C4d-positive ABOi grafts might be the lack of Fc receptors for the dominant IgM isotype of blood group antigens. This and the observation of C4d without graft pathology suggest that accommodation to ABO antibodies may be more easily achieved than to HLA antibodies. Some have even suggested that accommodation to ABO antibodies may protect against the effects of HLA antibodies (608).

ABOi grafts have close to the same survival rate as ABO-compatible grafts, with 1-year survival of 95% and 5-year survival of 91% (593,595,596). The major risk factor is whether acute AMR develops in the first 3 months, which lead to a lower 5-year graft survival (84% vs. 95% in the absence of early AMR). The risk of AMR is increased in patients with higher levels of ABO antibodies, but survival has been achieved even though high titers of IgG and IgM antibodies returned in the circulation after 1 year (598). Antibodies to blood group A2, which accounts for about 20% of type A, are present at lower levels, and tissues express less of the A2 blood group glycolipid, making allografts less vulnerable to rejection than other ABOi allografts.

CHRONIC ANTIBODY-MEDIATED REJECTION

In the last decade, it has become clear for the first time that late graft failure is often due to chronic antibody-mediated rejection (chronic AMR, also known as chronic humoral rejection, CHR) (537,609,610). Chronic AMR is a clinicopathologic entity that can be separated from other causes of late graft dysfunction, but it shows considerable histologic overlap with chronic TCMR. Often, mixed rejection episodes, that is, TCMR and AMR, show most pronounced chronic changes. The original evidence that acute AMR leads to chronic rejection came from combining serologic, clinical, and pathologic data (554,611). According to an NIH-sponsored consensus conference (536) and a subsequent Banff conference (612), three elements should be present: histologic evidence of chronic injury, immunopathologic evidence of antibody action in the graft (e.g., C4d deposition), and serologic evidence of donor-reactive antibody (Table 29.7). Chronic AMR is distinguished from acute AMR by chronic lesions (particularly transplant glomerulopathy, duplication of PTC basement membranes, and chronic allograft arteriopathy) and lack of acute inflammation (neutrophils, edema, necrosis, thrombosis). A concurrent component of (acute or chronic) cell-mediated rejection is often present.

Prevalence, Clinical Presentation, and Risk Factors

About 60% of late graft failure is due to chronic AMR (609,610). In a large multicenter biopsy study of 173 patients with late-onset graft dysfunction, 57% had evidence of chronic AMR, including 41% with DSA and 39% with C4d (610). Of those 23% with C4d deposition and DSA, 50% lost the

TABLE 29.7 2013 Banff criteria for chronic, active ABMR^{a,b}

1. Morphologic evidence of chronic tissue injury, including one or more of the following:
 - Transplant glomerulopathy (cg >0)^c, if no evidence of chronic TMA
 - Severe peritubular capillary basement membrane multilayering (requires EM)^d
 - Arterial intimal fibrosis of new onset, excluding other causes^e
2. Evidence of current/recent antibody interaction with vascular endothelium, *including at least one of the following*:
 - Linear C4d staining in peritubular capillaries (C4d2 or C4d3 by IF on frozen sections, or C4d > 0 by IHC on paraffin sections)^f
 - At least moderate microvascular inflammation ([g + ptc] ≥ 2)^g
 - Increased expression of endothelial activation and injury transcripts (ENDATs) or other gene expression markers of endothelial injury in the biopsy tissue, if thoroughly validated
3. Serologic evidence of donor-specific antibodies (HLA or other antigens)

^aAs reported in (481).

^bAll three major criteria must be present. Lesions of chronic, active ABMR can range from primarily active lesions with early transplant glomerulopathy evident only by electron microscopy to those with advanced transplant glomerulopathy and other chronic changes in addition to active microvascular inflammation. In the absence of evidence of current/recent antibody interaction with the endothelium (those features in section 2), the term active should be omitted; in such cases, DSA may be present at the time of biopsy or at any previous time posttransplantation.

^cIncludes GBM duplication by electron microscopy only (cg1a) or GBM double contours by light microscopy.

^d≥7 layers in 1 cortical peritubular capillary and ≥5 in 2 additional capillaries (229), avoiding portions cut tangentially.

^eWhile leukocytes within the fibrotic intima favor chronic rejection, these are seen with chronic TCMR as well as chronic ABMR and are therefore helpful only if there is no history of TCMR. An elastic stain may be helpful as absence of elastic lamellae is more typical of chronic rejection and multiple elastic lamellae are most typical of arteriosclerosis, although these findings are not definitive.

^fReports should specify whether the lesion is C4d positive or negative and the technique used.

^gIn the presence acute TCMR, borderline infiltrates, or evidence of infection, ptc ≥ 2 alone is not sufficient to define moderate microvascular inflammation and g must be ≥1.

graft within 18 months, slightly worse than those with C4d and no DSA (40%) and substantially worse than those with no C4d with or without DSA (20% and 10%, respectively). No adverse effect of the cellular infiltrate was evident. In another series, 17/27 late graft failures (63%) were attributed to chronic AMR, and 25% of these failed within 3 years of the biopsy (609).

Chronic AMR typically presents insidiously several years after transplantation. The average time of biopsy for graft dysfunction was 7.3 years posttransplant in one series (610). A definitive study by Wiebe et al. (537) followed 365 non-sensitized patients prospectively with protocol biopsies and serum samples for DSA. Overall, 15% developed de novo DSA, at a mean time of 4.6 years posttransplant (6 to 130 months). Most patients developed DSA to HLA class II (94%); only 6% had antibodies to donor class I alone. The pretransplant risk factors for DSA were younger age and a higher number of HLA mismatches (especially HLA-DR β 1). The main posttransplant risk factor was nonadherence (49% among DSA-positive patients versus 8% in those without DSA). Acute TCMR in the first 6 months was also a risk factor for chronic AMR (28% vs. 13%). The patients who developed de novo DSA presented with three distinct clinical phenotypes in about equal proportions: 38% indolent dysfunction (39% C4d+), 30% acute dysfunction (80% C4d+), and 32% stable function (57% C4d+). Most with dysfunction and DSA had proteinuria of ≥ 0.5 g/d (86%). Those with indolent dysfunction had a 53% frequency of nonadherence and a 40% graft failure rate. Those with acute dysfunction were all nonadherent (100%), and 57% of those grafts failed. In this group, clinical dysfunction was detected at about the same time as the DSA. Most of the graft loss in the DSA-positive patients was chronic AMR (84%). The stable function with DSA had a nonadherence rate of 6% and no proteinuria, and none of these grafts were lost within the follow-up period (0 to 128 months, mean 19 months), the same as those with stable function without DSA.

Pathologic Changes

Gross

Whether the cause is antibody, cellular rejection, or a combination, a chronically rejected kidney is typically pale and fibrotic with a dense, thickened, adherent capsule (Fig. 29.51). The cortical surface is typically smooth, indicating uniform atrophy, and the cortex and medulla are proportionately affected. The thickened, obliterated arcuate and interlobar arteries can often be appreciated at the corticomedullary junction. It is not uncommon to reduce immunosuppression in patients before graft nephrectomies; therefore, superimposed acute rejection changes can be observed as well, including infarcts and hemorrhage. As illustrated in Figure 29.51 rejection induced changes can also be seen in extraparenchymal tissues.

Light Microscopy

GLOMERULI

The most characteristic feature of chronic AMR is transplant glomerulopathy (TG, also known chronic allograft glomerulopathy), defined by widespread duplication or multilayering of the GBM, in the absence of specific de novo or recurrent glomerular disease or evidence of thrombotic microangiopathies (Figs. 29.52 and 29.53).

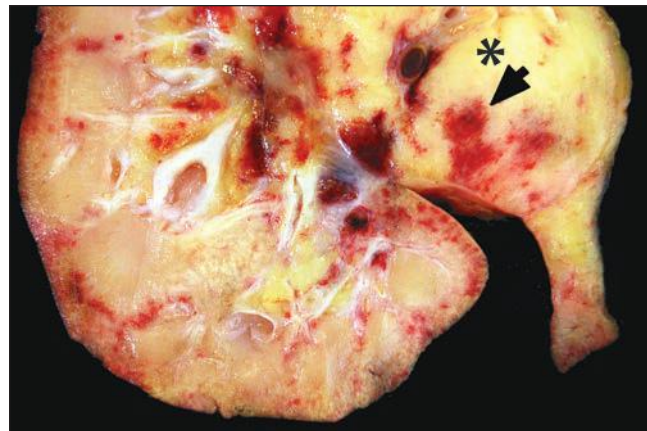


FIGURE 29.51 This graft was removed 10 years after transplantation due to severe chronic active, likely cell-mediated rejection (C4d- and DSA-negative). Multiple foci of anemic and hemorrhagic infarcts (arrow) are seen in intra- and extraparenchymal sites including the perihilar adipose tissue (asterisk). Clinically, a mass lesion suspicious for an extranodal lymphoma was suspected.

Glomerular abnormalities were first recognized in long-term grafts and related to rejection by Porter et al. (30). The term “transplant glomerulopathy” probably was first used by Zollinger, who described the duplication of basement membranes of glomeruli and PTC, and presciently thought the two were related and due to an immune reaction to the endothelium (613).

The duplicated GBM, best seen on PAS or silver stains, is involved segmentally or globally and can have mesangial cell interposition (see Fig. 29.52). Transplant glomerulopathy closely resembles chronic TMA. Mesangial hypercellularity and increased matrix is typically mild (614). The glomeruli can develop global or segmental sclerosis and adhesions, either as a secondary phenomenon or as a direct result of the glomerular damage. Glomerular hypertrophy can also be sometimes marked. In addition to these chronic features, signs of activity are often present, with prominent mononuclear cells in capillary loops with endothelial swelling (transplant glomerulitis) (see Fig. 29.53) (615). The cells are primarily monocytes, with few T cells. Transplant glomerulopathy may occur with little or no tubulointerstitial disease (421).

TUBULES

There is no known specific tubular lesion in chronic AMR. Tubular atrophy is often found focally or diffusely and is likely to be caused by ischemia due to loss of PTC and glomerular lesions.

INTERSTITIUM

The interstitium has no specific lesions for chronic AMR, but frequently has fibrosis, in association with tubular atrophy and a variable mononuclear infiltrate, with small lymphocytes, plasma cells, and mast cells (201,616,617). Such changes are seen in many chronic conditions, and they are nondiagnostic. The fibrosis can have many different patterns: dense and focal, diffuse and fine, striped, or subcapsular. The lymphocytes generally do not appear activated, and edema is not conspicuous (unless there is a component acute TCMR). Lymphocytes may

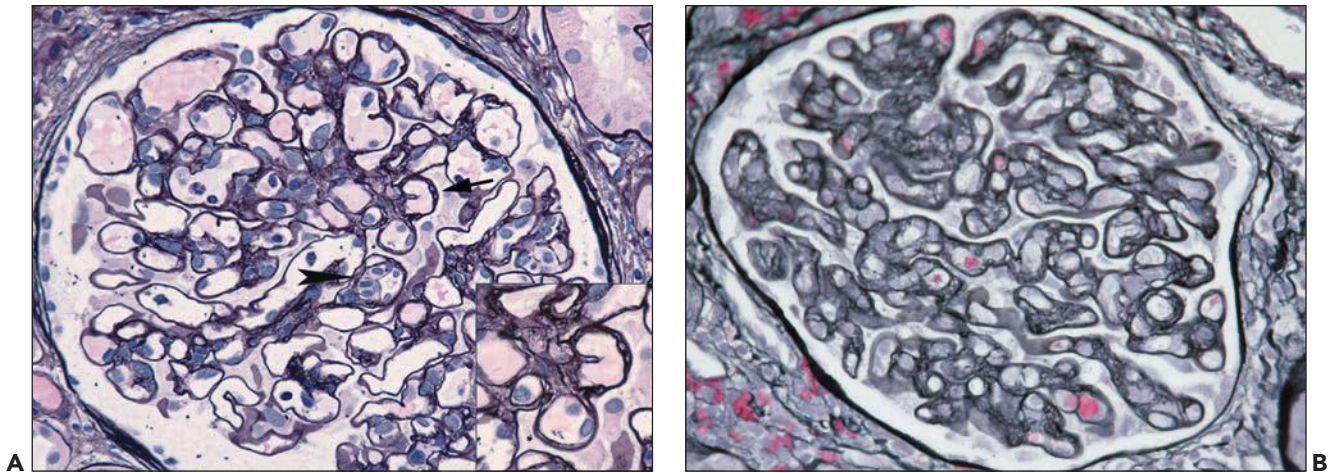


FIGURE 29.52 Transplant glomerulopathy. A: Segmental duplication of the GBM (*arrow*, shown at higher power in the insert) accompanied by mild mesangial hypercellularity and intracapillary mononuclear cells and reactive endothelial cells (*arrowhead*). **B:** Widespread duplication of the GBM affecting greater than 90% of the capillaries associated with positive C4d deposition (chronic AMR). Capillaries are compromised by reactive endothelial cells. The mesangium is mildly increased. (Periodic acid-silver stain, original magnification 400× (A and B).)

be present in areas with or without fibrosis. Nodular aggregates of lymphoid cells, sometimes with germinal centers, can occur around small arteries, especially at the corticomedullary junction and associated with increased lymphatic vessel density (Fig. 29.54) (618). Abundant plasma cells may also be present, but their presence may indicate concurrent (active) TCMR (Fig. 29.55) (409). Mast cells, readily detected with tryptase or *c-kit* antibodies, are associated with fibrosis and are often degranulated (617,619).

PERITUBULAR CAPILLARIES

Two lesions in PTC are strongly linked to chronic AMR, multilamination of the PTC basement membrane, and capillaritis. In favorable silver- or PAS-stained sections, thickening

and lamination of the basement membrane may be appreciated by light microscopy (Fig. 29.56). When the thickness is similar or thicker than nonatrophic tubular basement membrane, it correlates well with multilamination on EM (620,621) and is a specific (98% but not very sensitive [61%]) indicator of chronic AMR (224,621). However, multilamination is optimally evaluated by EM. PTC mononuclear cell capillaritis in late biopsies is strongly correlated with DSA, glomerulitis, and C4d deposition (478,622). The cells stain for markers of monocyte/macrophages and NK cells (623). The PTCs are often dilated, as they are in acute AMR.

PTCs are depleted, sometimes leaving only occasional traces of the original basement membrane behind (380,624).

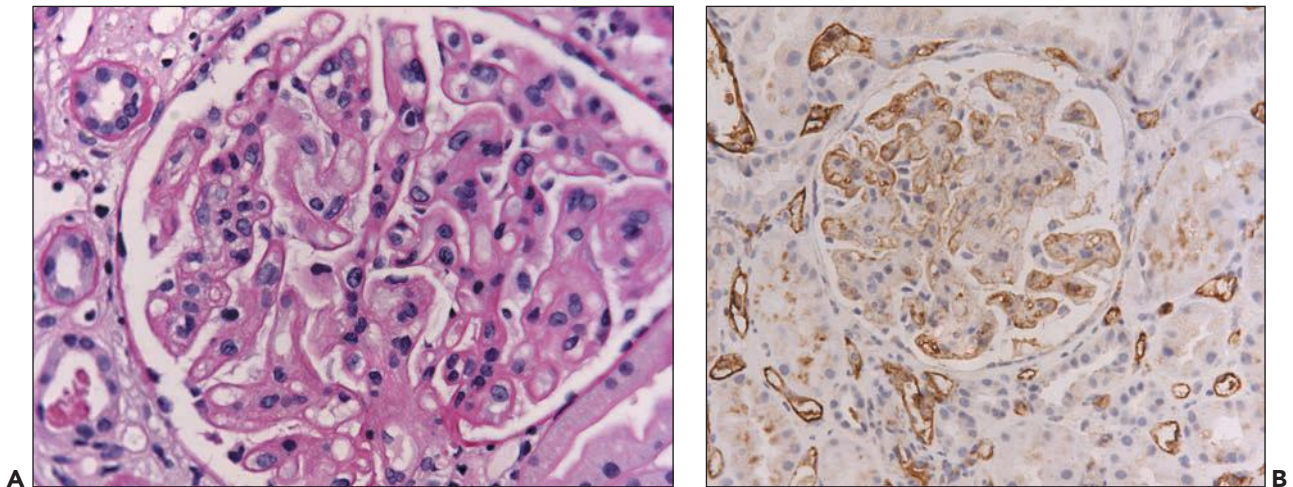


FIGURE 29.53 Transplant glomerulopathy with **(A)** prominent mononuclear cells in capillary loops, that is concurrent transplant glomerulitis, and duplication of the GBM and **(B)** C4d deposition in glomerular and PTC. (A: PAS stain, original magnification 400×, B: C4d immunohistochemical stain on paraffin section, original magnification 200×.)

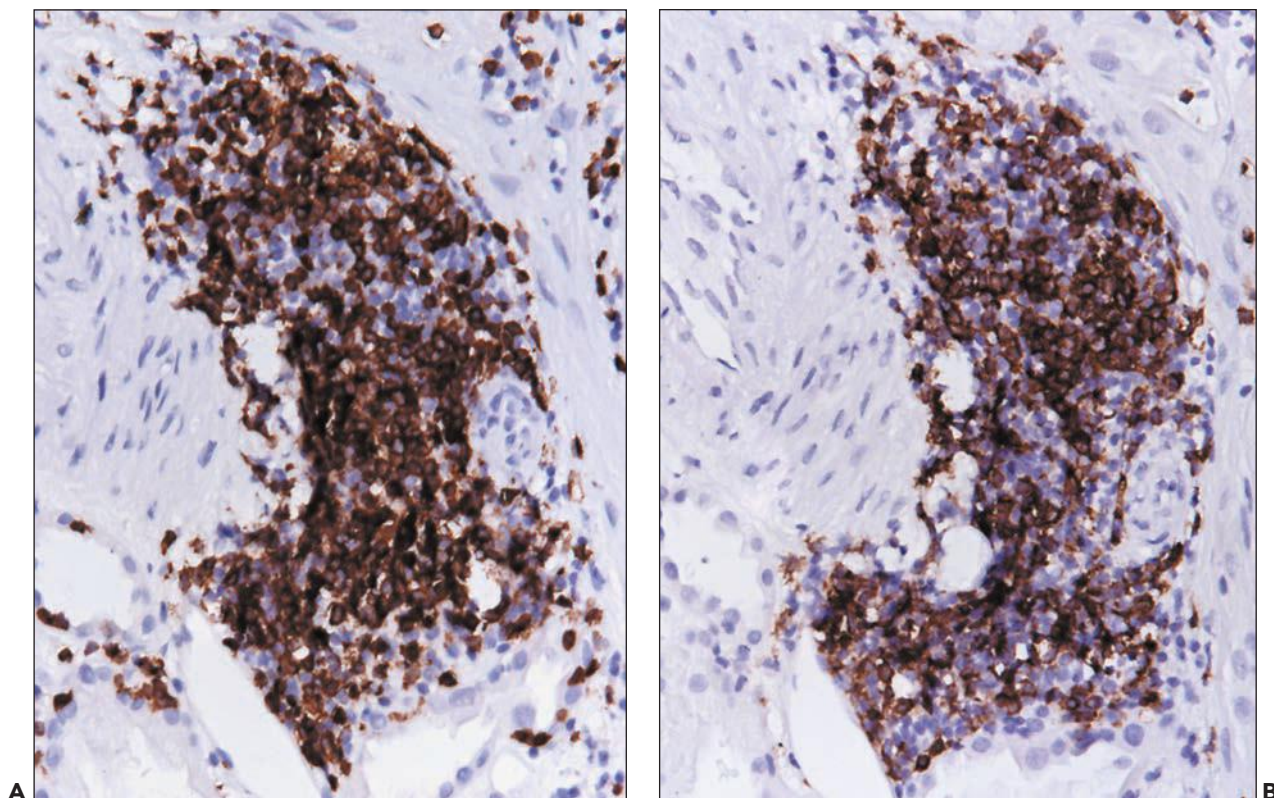


FIGURE 29.54 Nodular aggregate of CD3-positive T cells (**A**) and CD20-positive B cells (**B**) in a graft with chronic AMR (C4d-positive). Some of the small vessels may be lymphatics.

Decreased density of PTC per unit area in late graft biopsies correlates with the extent of interstitial fibrosis and graft dysfunction, although this has not been related specifically to chronic AMR (624). Loss of PTC can be appreciated as early as 3 months posttransplant in protocol biopsies, probably independent of DSA (625) and may be related at least in part to ischemia (626).

ARTERIES

Arterial vascular stenosis is a typical feature of rejection in late grafts and has been variously termed “chronic allograft vasculopathy,” “sclerosing transplant vasculopathy,” “graft atherosclerosis,” and “transplant arteriopathy.” These lesions are

thought to be caused by antibody or T cells (or both). Chronic transplant vasculopathy is typically preceded by transplant endarteritis arguing for a (major) T-cell–mediated pathogenesis in most cases (164).

The intimal change is most prominent in the larger arteries, but extends from the main renal artery to the interlobular arteries, the same distribution as endarteritis in acute rejection. The intima shows pronounced, concentric or eccentric, fibrous thickening without prominent elastic fiber accumulation, in contrast to the multilayering of elastica typical of hypertensive and involutive arteriosclerosis (fibroelastosis) (Fig. 29.57). The elastica interna generally remains intact. The matrix is generally loose, somewhat pale in

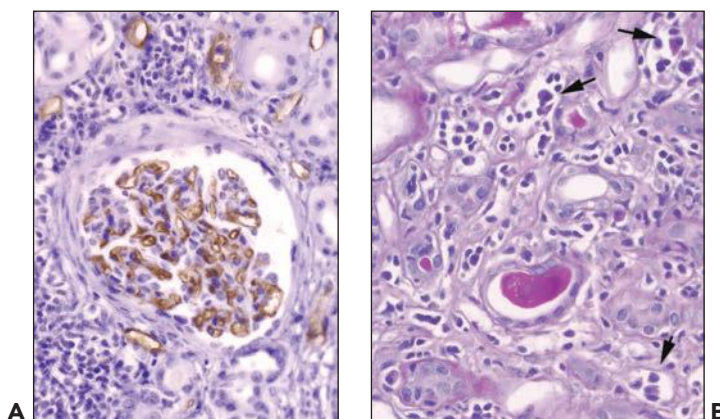


FIGURE 29.55 Chronic AMR with (**A**) C4d deposition and (**B**) prominent plasma cells in the infiltrate, some of which are in capillaries (*arrows*). This pattern is uncommon. (A: C4d IHC original magnification 200 \times ; B: H&E, original magnifications 400 \times .)

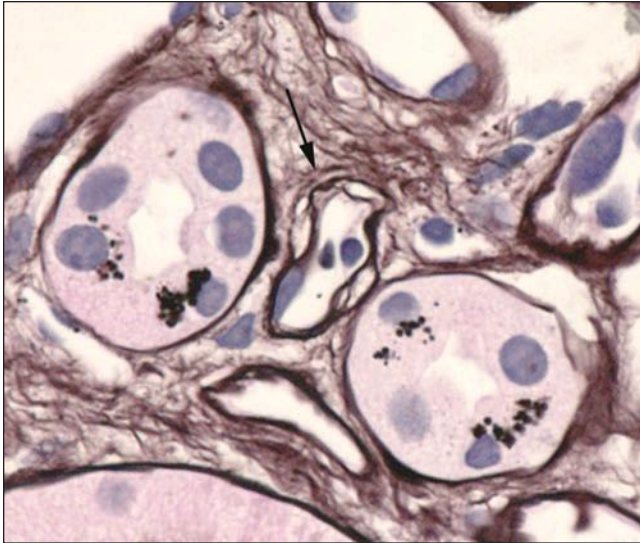


FIGURE 29.56 Chronic AMR with duplicated basement membrane of PTC evident by light microscopy (arrow). Silver positive protein reabsorption droplets are in the tubules. (Periodic acid-silver stain, original magnification 600 \times .)

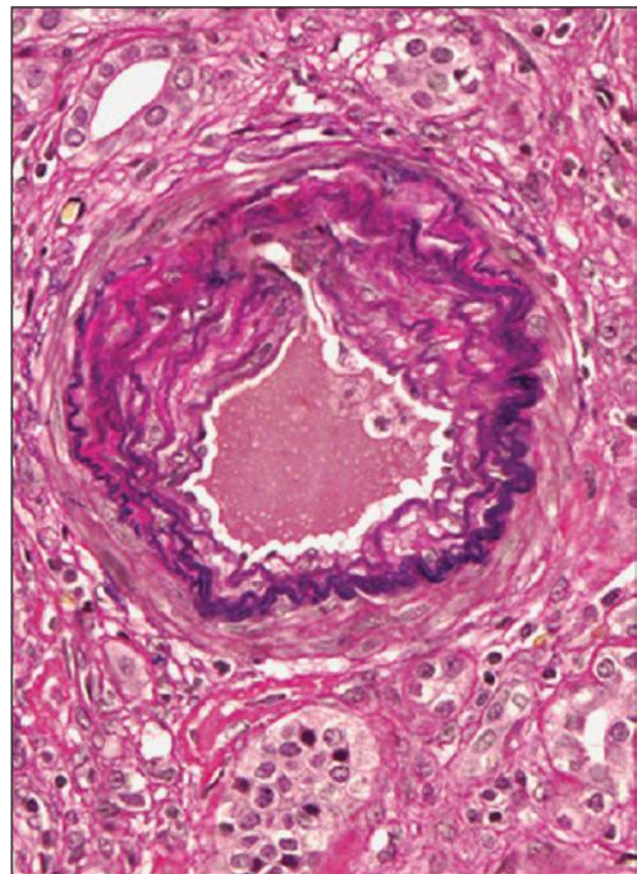
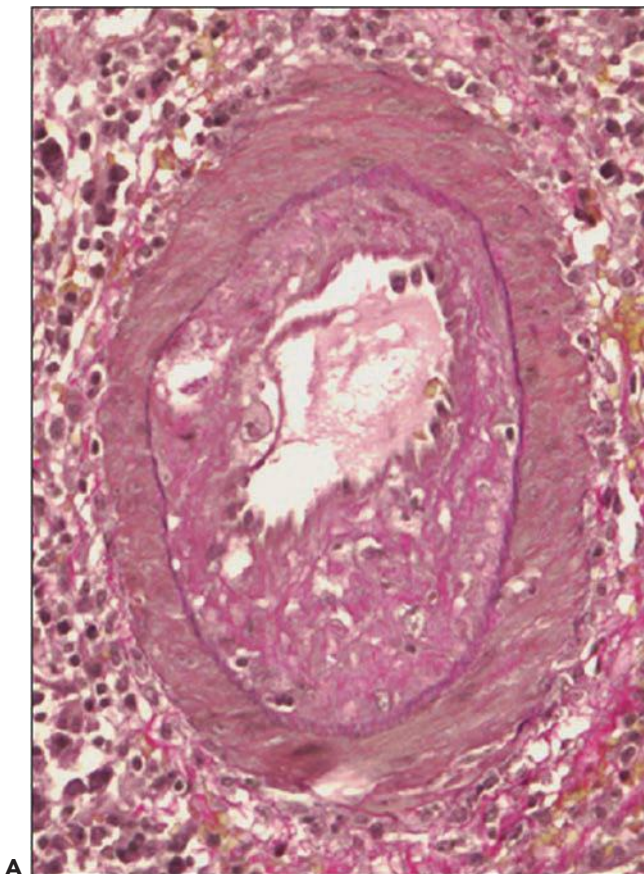
H&E-stained sections, and contains acid mucopolysaccharides, collagen, and increased hyaluronic acid (627). The media generally shows no obvious abnormality aside from focal loss of smooth muscle.

Arterioles do not show intimal changes, but may have hyaline deposits. Such lesions are regarded as due to donor disease, diabetes, hypertension, aging, or chronic CNI toxicity, rather than rejection, although it is not inconceivable that hyalinosis could result from repeated immune injury to the endothelium, as suggested by Hill (628).

Immunofluorescence Microscopy and Immunohistochemistry

GLOMERULI

C4d deposition along the GBM is present in a minority of cases (6% in one series) (554). Glomerular C4d is best appreciated in paraffin-embedded tissues, since glomeruli have no background C4d staining with this technique in contrast to frozen sections (Fig. 29.58). Immunofluorescence shows few or no granular deposits of immunoglobulin, except for IgM often present in the mesangium and/or along the GBM, sometimes with C3 (31,160,614,629). Deposits of IgG or IgA are unusual and indicate recurrent or de novo glomerulonephritis (31,34,630).



A

B

FIGURE 29.57 Comparison of chronic arterial sclerosis due to aging/arterial hypertension (arteriosclerosis) and chronic TCMR and/or AMR. (Sclerosing transplant arteriopathy.) **A:** Artery from a graft shows a neointima formation without prominent elastic fibers and with a few scattered mononuclear cells. **B:** Artery from a native kidney shows neointima with marked duplication of the internal elastica (fibroelastosis) and no inflammatory cells. (Elastic tissue stain, original magnification 400 \times .)

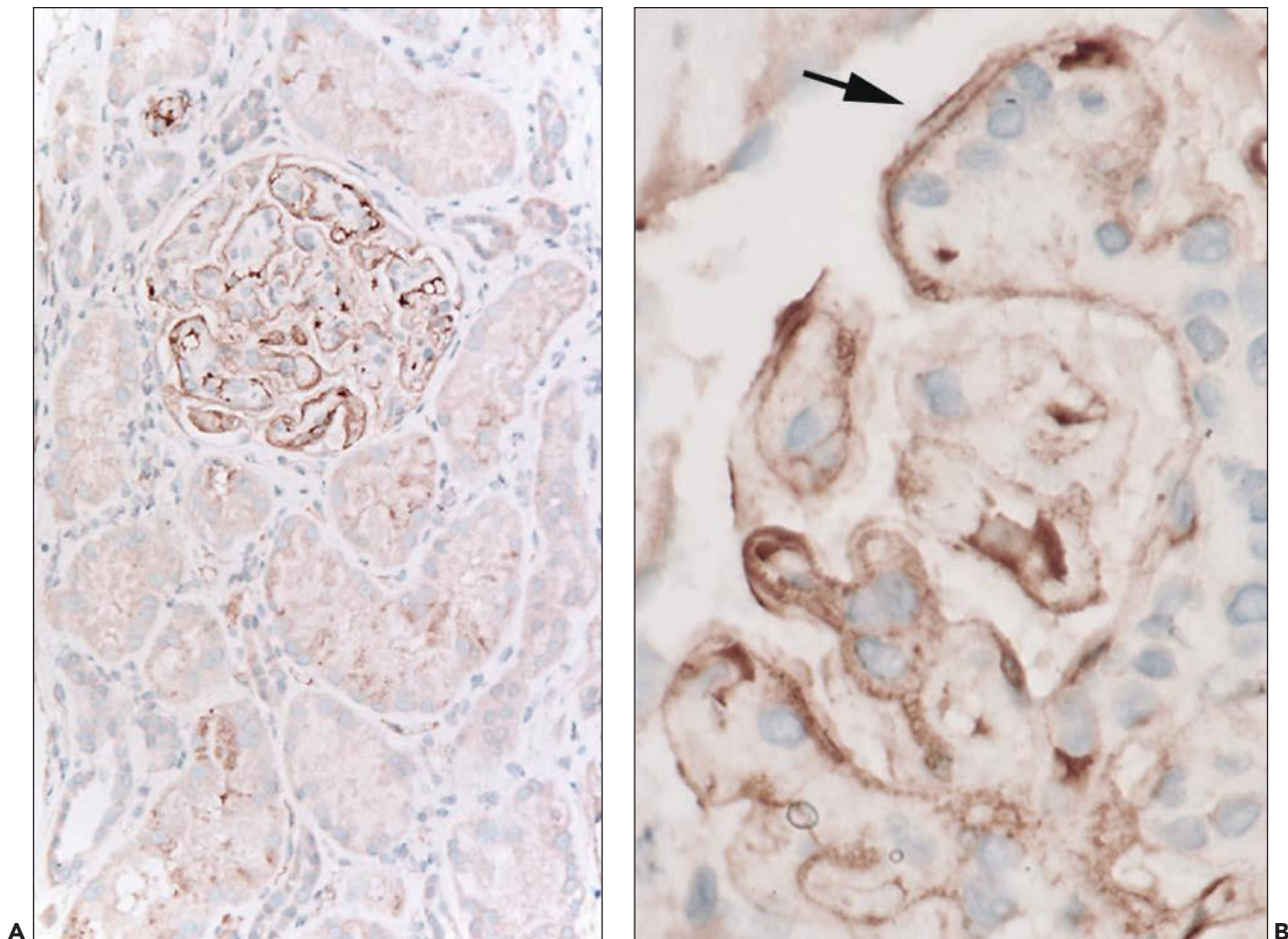


FIGURE 29.58 Chronic AMR, with C4d deposition in glomerular but not PTC (A). A double contour of C4d deposition is evident in some of the glomerular capillaries (B, arrow). The isolated detection of C4d in glomeruli is of undetermined clinical significance, and it cannot be used as a histologic sign for AMR or C4d positivity. (C4d IHC original magnification 200× (A) and 600× (B).)

TUBULES

There is no specific immunofluorescence finding in the tubules in chronic AMR. The tubular basement membrane not uncommonly has deposition of C3 in a broad segmental pattern and to a lesser degree also IgM and C4d. This is an exaggeration of similar changes found in normal kidneys and probably represents a residue from prior episodes of tubular injury and remodeling/atrophy with TBM thickening or possibly persistent chronic injury.

PERITUBULAR CAPILLARIES

PTC have deposition of C4d in about 50% of the grafts with either transplant arteriopathy or glomerulopathy (Fig. 29.59) (150,554,631–634). The association is greatest for transplant glomerulopathy. The pattern is linear and circumferential, similar to that in acute AMR; however, fewer positive capillaries are found, and the “widespread” pattern is not so common. The reasons for the difference are not known, but contributing factors may include decreased antigen expression, endothelial complement inactivation, lack of complement fixation by the DSA, and/or loss of PTC. C4d staining may be most prominent in the renal medulla where chronic injury is usually only mild. In some cases with marked chronic changes

in the cortex, C4d positivity may only be detected in the medulla (personal observation). Cases, which have little or no C4d (C4d0-1) but demonstrate other features of chronic

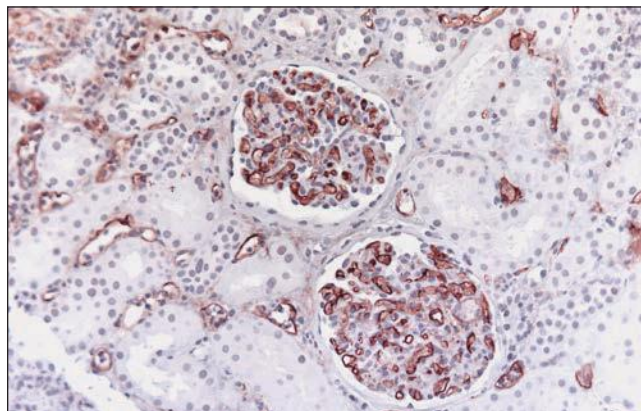


FIGURE 29.59 Chronic AMR with both peritubular and glomerular C4d deposition. C4d IHC, original magnification. Capillaritis is also evident. (200×.)

AMR (DSA, capillaritis, transplant glomerulopathy), are now called according to latest Banff consensus (481) C4d-negative chronic AMR (153,635). This is discussed separately below with other variants. In human and mouse cardiac allografts, increased endothelial expression of phosphorylated signaling proteins in the AKT pathway has been described in chronic AMR (636,637).

ARTERIES

There is no specific immunofluorescence feature in the arteries that indicate chronic AMR. IgG, IgM, C3, and fibrin can be found in the intima and media, as a diffuse blush or as focal granular deposits (32,638). It is not clear whether this is due to specific antibody deposition. C4d is also present in the intima, but does not indicate AMR, since native kidneys also have C4d in arteriosclerotic intimal fibrosis.

Electron Microscopy

GLOMERULI

The characteristic feature of transplant glomerulopathy is widespread duplication of the GBM (30,613,639,640) (Fig. 29.60), sometimes with multiple lamina extending around the circumference of the capillary, internal to the original GBM and extending between the endothelium and the mesangium, where the GBM is normally absent (Figs. 29.61 and 29.62). These changes are very similar to those seen in chronic TMA and are caused by repetitive or persistent injury to the glomerular endothelium. The underlying etiology of such endothelial injury is diverse; if other features of rejection are present, such as transplant arteriopathy, severe multilamination of PTC basement membranes, or C4d positivity, chronic AMR is most likely. Electron microscopy detects 40%

more cases of transplant glomerulopathy than light microscopy (641). Endothelial cell “dedifferentiation” is characteristically present, as manifested by a loss of the normal fenestrations (30,639,642). Another sign of endothelial damage is the ectopic location of the endothelial nuclei on the free side of the capillary loops; they are normally mainly on the mesangial side of the capillaries. Glomerular endothelial cells show increased expression of plasmalemma-associated protein-1, found in caveoli, which correlates with the severity of the glomerulopathy and proteinuria (643). The mesangial matrix is often increased, and sometimes, mesangiolytic is present, manifested by dissolution of the mesangial matrix, leaving a loose reticular web (639). Mesangial cells may be interposed between the GBM layers (see Fig. 29.62). Focal effacement of foot processes is common and may be extensive (639). Of note, none of the changes is pathognomonic for chronic AMR or chronic TCMR but rather reflect persistent TMA like GBM remodeling.

Transplant glomerulopathy develops in stages best seen by electron microscopy and well described by Zollinger (613). These stages have been related to chronic AMR in recent studies (220,644). Among seven patients followed prospectively with surveillance biopsy who developed transplant glomerulopathy, the earliest lesions, seen at a mean of 39 days posttransplant, were vacuolation and hypertrophy of glomerular endothelial cells and serration and expansion of lamina rara interna (220). Endothelial cells contained numerous mitochondria, prominent Golgi apparatus, and ribosomes. Later changes were loss of fenestrations, mesangial matrix expansion, and foot process effacement. Light microscopic evidence of transplant

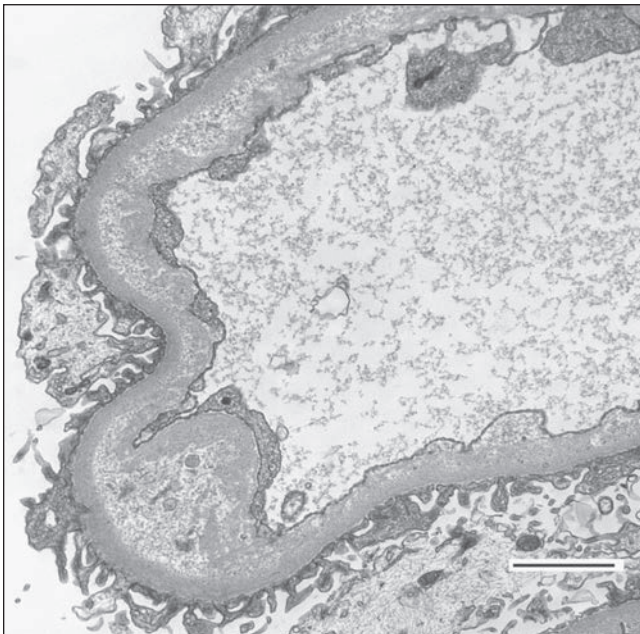


FIGURE 29.60 Transplant glomerulopathy with duplication of the GBM separated by loose matrix and some cell debris. The podocytes are normal, and the endothelium shows segmental loss of fenestrations. Electron micrograph. Bar = 2000 nm.

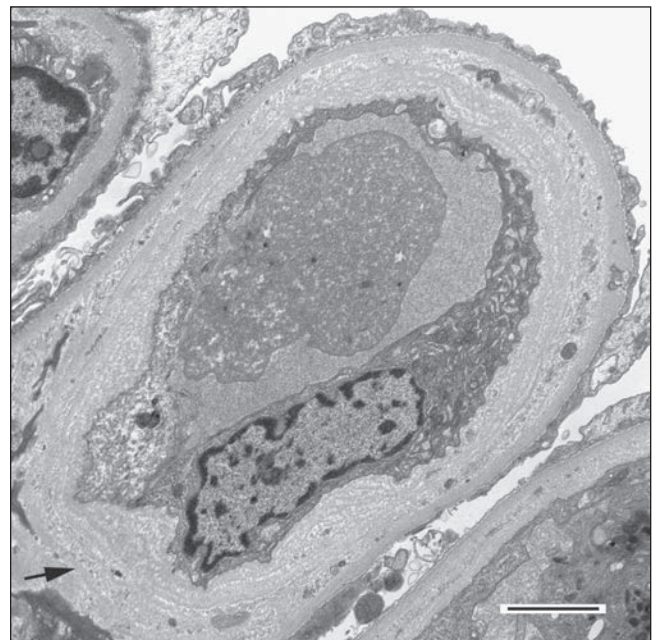


FIGURE 29.61 Transplant glomerulopathy with multilamination of the GBM that extends circumferentially around the capillary lumen, including the region that normally has no basement membrane, between the endothelium and the mesangium (arrow). The endothelium is reactive (expanded endoplasmic reticulum) with loss of fenestrations. Podocytes show focal loss of foot processes. Biopsy showed focal C4d positivity. Same case as Fig. 29.60. Electron micrograph. Bar = 2000 nm.

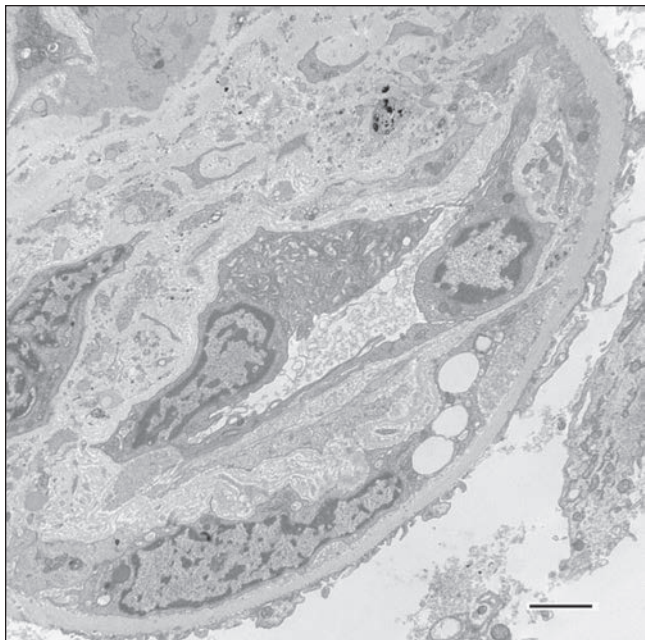


FIGURE 29.62 Transplant glomerulopathy. GBM duplication and mesangial cell interposition are present, with marked endothelial cell hypertrophy and loss of fenestrations. No electron-dense deposits are evident. C4d was present focally along the GBM (not shown). Electron micrograph. Bar = 2000 nm.

glomerulopathy occurred only much later (2 to 3 years post-transplant). The specificity of these ultrastructural features was documented in indication biopsies taken within 3 months of transplantation (644). Glomerular endothelial swelling, subendothelial widening, and early glomerular basement membrane duplication were present in 65% of 17 patients with DSA and C4d deposition, 50% of 16 patients with DSA and no C4d

deposition, and 0% of 65 patients without DSA. In follow-up biopsies, 40% of 20 patients with DSA developed transplant glomerulopathy, 3.5 to 30 months posttransplant.

PERITUBULAR CAPILLARIES

Sequential biopsies have shown that endothelial cell activation occurs in PTC before basement membrane multilamination (220). Multilayering of the basement membrane (Fig. 29.63) was first noted by Monga et al. (645,646) and associated with chronic AMR by Regele et al. (554). Each ring of basement membrane surrounding a PTC probably represents the residue of one previous episode of endothelial injury going from oldest (outer) to most recent (inner). PTC lamination correlates with transplant glomerulopathy (224,613,641,646). However, similar to other histologic changes including transplant glomerulopathy, PTC multilamination is not pathognomonic for AMR.

Several studies have sought to define the threshold and specificity of PTC basement membrane multilamination. Ivanyi assessed a median of 14 capillaries/case and found that biopsies with three or more PTC with 5 to 6 circumferential layers or one PTC with seven or more circumferential layers were found only in patients with other features of chronic rejection (641). In that series, 59% of biopsies (27/46) with chronic rejection had such features, and 85% were accompanied by GBM duplication, but DSA or C4d status was not reported. A subsequent comprehensive study by Liapis compared native and transplant kidneys (224). In this study, higher threshold levels were set to define severe PTC lamination (15 PTC capillaries examined and the 3 most affected ones used for scoring; severe PTC lamination defined as ≥ 7 layers in one capillary and ≥ 5 layers in the remaining two capillaries). Among 360 native kidney biopsies, severe PTC lamination was exceedingly uncommon and, if present, mainly seen in chronic TMA. In contrast, 23% of 187 transplant biopsies had severe PTC lamination in the setting of TCMR, AMR, or CNI toxicity. The association with C4d and, to a lesser degree, also transplant

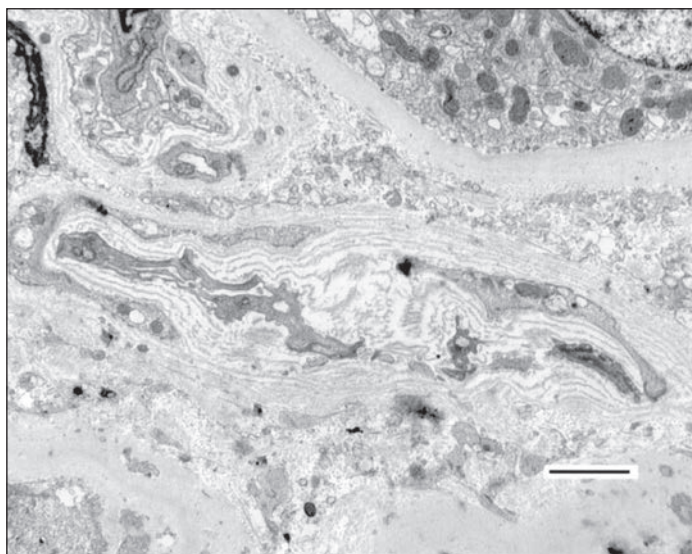
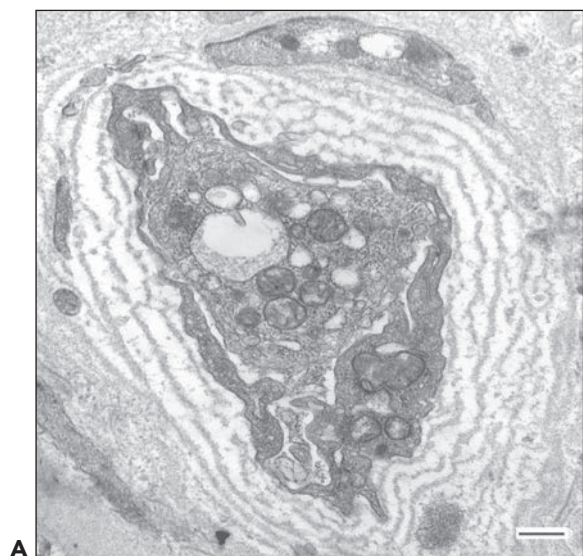


FIGURE 29.63 PTC with marked multilayering of the basement membrane. More than six layers are seen. **A,B:** Electron micrographs. Bar = 500 nm (A) or 2000 nm (B).

glomerulopathy was strong (60% of C4d+ and 50% of cases with glomerulopathy). However, severe PTC laminations were also detected in 15% of C4d-negative biopsies after 1 year, 9% of C4d-negative/DSA-negative cases, 30% of chronic TCMR, and 20% of cases with CNI toxicity as well as cases of acute TCMR. The authors concluded that evaluation of PTC basement membrane multilamination is useful, although not specific for chronic AMR (positive predictive value for chronic AMR, approximately 50%). Based on these observations, it is fair to assume that if severe PTC lamination is accompanied by other signs of rejection, for example, C4d positivity or capillaritis, a diagnosis of chronic AMR is likely. Interestingly, the absence of marked circumferential PTC laminations is a powerful parameter to exclude chronic AMR from the list of differential diagnoses (224).

ARTERIES

No specific features have been described in arteries in chronic AMR compared with chronic rejection of presumed T-cell mediation. Scanning electron microscopy shows endothelial cell injury, disorganization of the endothelium, and gaps between endothelial cells, often with leukocytes and platelets. The thickened arterial intima consists of smooth muscle cells, collagen fibrils, basement membrane material, and a loose amorphous electron-lucent ground substance (642). Scattered lymphocytes and macrophages are present, the latter sometimes filled with fine lipid droplets, corresponding to the foam cells by light microscopy. Smooth muscle cells also may contain fat droplets in lysosomes (647). With time, the cellularity diminishes and the amount of collagen increases (164,648).

Molecular Studies

Interaction between antibodies and endothelial cells leads to significant molecular changes in the endothelium of the microcirculation, that is, PTC and glomeruli. Sis et al. (491) were the first to employ a set of transcripts with primary expression in endothelial cells. In biopsies from patients with DSA a median of 16 months posttransplant, a significant up-regulation of endothelium-specific mRNA encoding VWF, melanoma cell adhesion molecule (CD146/MCAM), cadherin 5, selectin E (CD62e), platelet/endothelial cell adhesion molecule 1 (PECAM1/CD31), CD34 molecule, and caveolin 1 (CAV1) was observed.

mRNA species relatively specific for NK cells were associated with capillaritis and glomerulitis and the presence of DSA (623,649). By comparing the intragraft gene expression from patients with DSA to those without DSA, the following NK cell transcripts were identified: fractalkine receptor (CX3CR1), myeloblastosis viral oncogene homologue (MYBL1), fibroblast growth factor-binding protein 2 (FGFBP2), killer cell lectin-like receptor F1 (NKP80), and SH2 domain containing 1B (also known as EAT2). Transcripts encoding the cytotoxic molecule granzysin showed high expression in NK cells but were also expressed in T cells.

Biopsies with focal/diffuse C4d positivity showed increased expression of genes related to the immune response, interferon- γ and rejection-induced, cytotoxic T-cell, macrophage-associated, and endothelial cell transcripts. However, increased expression of endothelial and NK cell transcripts in the presence of DSA and AMR pathology was independent of C4d staining results (490). Thus, adding quantitative

molecular assessments to cases with DSA has the potential to increase diagnostic precision for C4d-negative AMR.

The Mayo group studied intragraft gene expression profiles in protocol biopsies of positive crossmatch kidney transplant recipients who develop transplant glomerulopathy and those who did not. Microarrays showed few differentially expressed genes between paired biopsies from recipients before and after the diagnosis of transplant glomerulopathy. However, the glomerulopathy group had significantly altered expression for greater than 2000 genes at 4 to 24 months posttransplantation compared with the controls (no glomerulopathy or negative crossmatch). The differentially expressed genes were in pathways associated with innate and adaptive immune responses, including some NK cell transcripts and numerous endothelial cell-associated transcripts (650).

The transcripts that distinguish AMR from other diagnoses are mostly expressed in endothelial cells or NK cells or are IFN- γ inducible and have been incorporated into a “molecular AMR score” suggested by Halloran et al. (651). The AMR score correlated with capillaritis, DSA levels, and the consensus diagnosis for AMR among pathologists. The molecular AMR score also strongly predicted future graft loss. The fact that the molecular classifier independently uses endothelial cell- and NK cell-associated transcript for diagnosing AMR corroborates the previous observations by others that such transcripts are specifically increased in renal allografts with AMR. As the consequence the 2013 Banff classification now includes besides histology and C4d molecular measurements as potential diagnostic criteria for AMR.

Etiology and Pathogenesis

Endothelium is the major, but perhaps not the only, target of chronic rejection mediated by antibodies. The mechanisms by which the DSA cause chronic lesions are not clear. In particular, it is not known which of the three pathways in Fig. 29.30 are responsible: antibody alone, complement fixation, or cellular Fc receptors or a combination. Nor is it clear why DSA of similar levels cause either acute or chronic injury. Presumably, this is related to differences in the resistance of the endothelium (accommodation) or possibly difference in functional activity of antibodies themselves. For unknown reasons, class II DSA are by far the predominant specificity in chronic AMR. Since many cases also have concurrent injury caused by TCMR, the etiology of chronic remodeling and rejection is complex.

Whatever the mechanism, the endothelium responds by repeated synthesis of basement membrane, analogous to the response of other basement membrane producing cells. Loss of PTC is found with or without evidence of currently active T-cell- or antibody-mediated injury and may be a sequela of prior episodes of acute or subacute rejection (624). Loss of PTC correlates with fibrosis and graft dysfunction (presumably because the glomerular capillaries are also affected) (624).

Risk Factors, Prognosis, and Differential Diagnosis

Transplant Glomerulopathy

The median time of diagnosis of transplant glomerulopathy by indication biopsies is 5 to 8 years (422,634). Transplant glomerulopathy is found in a small minority (3%) of protocol biopsies at 1 year by light microscopy and increases almost linearly to 20% of protocol biopsies at 5 years in non-presentation

patients (421,652). Lesions can be seen by electron microscopy before 3 months (644) and in patients with acute or hyperacute AMR (524). Circulating DSA are found in 36% to 60% of patients (422,653). The risk of transplant glomerulopathy is increased by the presence of higher levels of class II DSA (419), particularly those reactive to HLA-DQ (654) and that fix C1q in vitro (579). A history of acute AMR (419) and presensitization also increase the risk. In one series, 76% of the patients who developed transplant glomerulopathy had pretransplant sera that retrospectively had DSA by solid-phase bead assay (421). Transplant glomerulopathy is often preceded by transplant glomerulitis, and glomerulitis coincides with glomerulopathy in approximately 50% of cases.

Transplant glomerulopathy has a poor prognosis, particularly when accompanied by C4d deposition (419,655,656). In biopsies 10 years or more after transplantation, a majority (70%) of grafts with transplant glomerulopathy and C4d deposition failed within 1 year of biopsy, a much worse failure rate than grafts with transplant glomerulopathy without C4d (15%) or grafts with C4d and no glomerulopathy (less than 5%). The presence of C4d was an independent risk factor for graft loss in another series (419) and for rapid decline in GFR (656). Among those in whom subclinical transplant glomerulopathy was detected in a 1-year protocol biopsy, the 3-year graft survival was 85%, worse than those with normal biopsies or only interstitial fibrosis (657,658). Duplication of the GBM ($\geq 10\%$ of loops) correlated with decline in GFR better than the percentage of sclerosed glomeruli (652). The presence of PTC basement membrane multilamination and interstitial fibrosis was an adverse risk factor for graft failure in patients with transplant glomerulopathy (656).

Patients with transplant glomerulopathy commonly have proteinuria, often in the nephrotic range (659) and can develop secondary FSGS. In one series, 61% of patients with transplant glomerulopathy had greater than 1 g/d proteinuria, more than those whose grafts had just IFTA (25%) (653). Proteinuria itself is associated with decreased graft survival in proportion to the degree of proteinuria (660,661). The rate of graft loss in the presence of 1 g/d of proteinuria is 25% in the first year and 62% by 5 years (662). Proteinuria due to recurrent or de novo glomerulonephritis had a better prognosis (17% graft loss in 5 years).

Transplant glomerulopathy is not a specific diagnosis but a pattern of glomerular endothelial injury resembling TMA in native kidneys. Three partially overlapping etiologies accounted for 84% of transplant glomerulopathy: chronic C4d+ AMR (48%), hepatitis C virus infection (36%), and TMA (32%). Also chronic CNI toxicity (often without apparent TMA) and chronic TCMR can induce transplant glomerulopathy. DSA were detected in only 36% of 36 patients with transplant glomerulopathy in one series, arguing for mechanisms independent of MHC antibodies in the development of transplant glomerulopathy (653). In any case, it is important to distinguish these mechanisms, as they may have different prognostic and therapeutic implications. Features that favor chronic AMR include C4d deposition (most useful), capillaritis (glomeruli or PTC), and severe multilamination of the PTC basement membranes.

The other major diagnoses to consider are recurrent or de novo glomerular disease. If immune complex deposits are more than occasional or if in a subepithelial location, recurrent or de novo glomerulonephritis should be suspected. Recurrent membranoproliferative glomerulonephritide (MPGN) type I typically

has prominent mesangial hypercellularity, subendothelial electron-dense deposits, and C3 staining greater than IgM, in contrast to transplant glomerulopathy (663).

Transplant Arteriopathy

Arterial lesions are common in allografts, caused by chronic rejection (including AMR and TCMR), hypertension, and donor disease. Features favoring rejection are the lack of intimal fibroelastosis (Weigert elastin stain) and the presence of mononuclear cells including foam cells in the intima (usually sparse and best appreciated by IHC).

Considerable evidence implicates DSA as a contributing factor in the pathogenesis of transplant arteriopathy in some cases; most cases, however, are induced by chronic TCMR or mixed chronic AMR plus TCMR. DSA induce transplant arteriopathy in experimental animals in the absence of T cells (374,664). Transplant arteriopathy is associated with DSA in kidney (627,665) and heart transplants in humans (666,667). DSA may also promote banal arteriosclerosis, as judged by the progression of severity in allografts from patients with DSA (629). More severe arteriosclerosis was significantly associated with capillaritis, glomerulitis, and interstitial inflammation (628).

Transplant arteriopathy is uncommon in the first 6 months after transplantation, but increases to 36% to 41% in protocol biopsies at 1 to 2 years (658,668). Rarely, chronic arteriopathy has been reported as early as 1 month posttransplant (669). In nonhuman primates on little or no immunosuppression, the lesions can develop within 2 to 3 months (164,670). In the past, arteriopathy influenced long-term survival more than interstitial fibrosis (671). However, a recent large series showed no prognostic effect of arteriopathy in 1-year biopsies, separate from interstitial fibrosis, inflammation, or glomerulopathy, a finding attributed to reduced severity of arteriopathy under current drug regimens (658).

Capillaritis

Regele first noted the link between mononuclear capillaritis and chronic AMR (554). Gibson was a strong advocate for this otherwise neglected lesion and proposed a scoring system, which has since been incorporated into the Banff system (622). Capillaritis is scored only in the cortex, and only when more than 10% of the PTC are involved. Areas of necrosis, pyelonephritis, subcapsular cortex, longitudinal vessel sections, and vessels around nodular aggregates are not included. The scores are the highest number of cells in a single PTC (see Table 29.3). In a survey of 688 indication and protocol biopsies in the first year, the most common pattern was 5 to 10 luminal cells, involving 10% to 50% of PTC, with a majority of mononuclear cells (622). Capillaritis was strongly associated with glomerulitis and C4d+: 24% of C4d negative biopsies compared with 75% of C4d+ biopsies showed capillaritis. However, capillaritis was not specific for AMR (50% of biopsies with borderline or acute TCMR showed capillaritis), and the interobserver reproducibility was only fair to moderate. Nonetheless, diffuse capillaritis in early protocol biopsies had significant negative prognostic impact in terms of glomerular filtration rate 2 years later. Further work on the specificity and sensitivity of capillaritis by Sis and colleagues in 329 indication biopsies (478) revealed peritubular capillaritis in 75% of acute and chronic AMR biopsies, but also in acute TCMR and acute tubular necrosis. Interestingly, PT capillaritis in early graft biopsies was not significantly associated

with AMR; associations were mainly noted in late biopsies. The authors concluded that C4d+ was the most specific biopsy finding for DSA, but capillaritis plus glomerulitis (ptc + g scores) was more sensitive for DSA and is useful diagnostically in late graft biopsies (without acute TCMR or ATN).

Variants of AMR

C4d-Negative AMR

Several studies have provided convincing evidence that antibodies can injure grafts with little or no detectable C4d deposition in PTC at the time of biopsy although strict and uniform criteria for “C4d negativity” were not applied (491,492,644,672,673). The evidence consists of demonstrating pathologic lesions that are otherwise typical of C4d+ AMR in the presence of DSA. Most commonly, these lesions are mononuclear cell capillaritis in PTC and/or glomeruli, termed “microcirculation inflammation” (MI), the sum of Banff ptc and g scores. Capillaritis without C4d has been demonstrated in 3-month protocol biopsies in presensitized patients and is a risk factor for transplant glomerulopathy at 1 year (492,673). C4d deposition was an even stronger risk factor for later transplant glomerulopathy (up to 18-fold), but capillaritis remained predictive even after correction for C4d status (up to sixfold). Another study mostly in presensitized patients showed indication biopsies with capillaritis in biopsies taken before 3 months had a greater rate of graft loss, especially when not treated (644). Late indication biopsies can also show capillaritis in the absence of C4d and presence of DSA (478). In this setting, capillaritis is a risk factor for graft failure. Late biopsies with MI scores (microvascular injury score; Banff ptc + g) of 3 or more had a 24-fold increased rate of graft loss within 4 years compared with those with an MI score of 0 (17% vs. 96% 4-year graft survival). Higher MI scores were associated with DSA and C4d deposition, but even when adjusted for C4d status, high MI scores were a strong risk factor for later graft failure (21-fold) (672). Another way to detect evidence of C4d-negative AMR is by molecular testing. Increased endothelium-specific and NK cell gene transcripts can be detected in association with DSA, as described above in Molecular Studies.

A wide range of the prevalence of C4d-negative chronic AMR is reported, ranging from 31% to 61% of patients with DSA. The frequency of C4d-negative acute AMR is unknown. Several factors contribute to the heterogeneity: the threshold of “C4d-negativity” used (less than 50%, less than 10% or 0%), the technique (fixed paraffin sections vs. frozen sections), and the nature of the biopsy (protocol vs. indication, early vs. late). Nonetheless, even with the most sensitive immunofluorescence technique, about 20% of late indication biopsies have DSA and capillaritis without any C4d deposition (481). Additional possibilities for negative C4d stain are complement regulation at the level of the endothelium and properties of the DSA itself. Some of the difference in C4d deposition resides in the ability of DSA to fix complement, as judged by the *in vitro* C1q fixation test, which in turn may relate to antibody titer. There are significant therapeutic implications if C4d negativity implies complement-independent mechanisms being responsible for the injury. The capillaritis might be a manifestation of the accumulation of Fc receptor bearing mononuclear cells (monocytes and NK cells) that are the actual mediators of the endothelial activation/injury. However, many questions remain. C4d often fluctuates on serial biopsies (positive to negative to positive),

and it may be that the injury itself occurs during the C4d-positive phase. Alternatively, C4d deposition may somehow protect the endothelium or be irrelevant to the injury.

The criteria for C4d negative (“complement poor”) have been proposed in the 2013 Banff consensus report (481). MI scores play an important diagnostic consideration. However, as well noted by Sis, capillaritis is common in early biopsies with acute TCMR in the absence of DSA, so capillaritis is not as specific as C4d. The consensus proposal is that a g + ptc score of ≥ 2 as evidence of AMR in the absence of C4d (defined as C4d ≤ 1 by IF or C4d0 by IHC) (Tables 29.6 and 29.7).

Smoldering/Indolent AMR

To date, the Banff diagnostic criteria recognize four categories of DSA-associated graft pathology (see Table 29.5). Because of the increased use of protocol biopsies, a fifth category has been identified (although not yet incorporated into Banff). This category lacks the features of acute AMR (neutrophils, necrosis, thrombosis) or chronic AMR (increased matrix accumulation), but does have signs of activity, namely, capillaritis (ptc + g) with or without C4d deposition in the presence of DSA. This has been shown to be a precursor for chronic AMR over months to years in surveillance biopsies (537,635,665). Some have termed this smoldering or indolent (536,635) AMR. In any case, this category should be recognized as an intermediate stage in the development of chronic AMR. Optimal treatment is yet uncertain.

C4d Deposition Without Evidence of Active Rejection

As noted above, ABOi grafts commonly have C4d deposition in PTC with no apparent consequence. ABO-compatible, nonsensitized patients show C4d deposition in 2% to 4% of protocol biopsies in the first year with no immediate effect on graft survival (Fig. 29.64) (674,673). This appears to be a form of accommodation to DSA, although the long-term stability, particularly in the setting of HLA-incompatible grafts, is dubious (674). The Banff classification terms this state “C4d deposition without evidence of active rejection” and recommends careful monitoring of patients with this pattern (155). Indeed, this has been documented to be an early stage of chronic AMR, at least in the setting of HLA-incompatible grafts (see below).

Natural History, Therapy, and Outcome

Chronic AMR develops through a series of stages over many months to years, schematically diagrammed in Fig. 29.65 and first documented in nonhuman primates (676). Regele showed that patients with C4d+ biopsies in the first year posttransplant had a higher frequency of transplant glomerulopathy in later biopsies (554). A similar sequence was noted by Loupy in 3-month protocol biopsies in sensitized patients, in which C4d+ or capillaritis predicted transplant glomerulopathy 9 months later. In non-presensitized patients, *de novo* DSA preceded the onset of proteinuria by an average of 9 months and the onset of an elevated Cr by 12 months (537). The whole sequence beginning with DSA, C4d deposition, and later transplant glomerulopathy and graft dysfunction has also been described in a limited number of individual cases (665,677). Further studies are needed to identify the risk factors for progression through the stages and the optimal therapy.

Treatment of chronic AMR remains to be established (415). The primary focus should be to insure the patients are

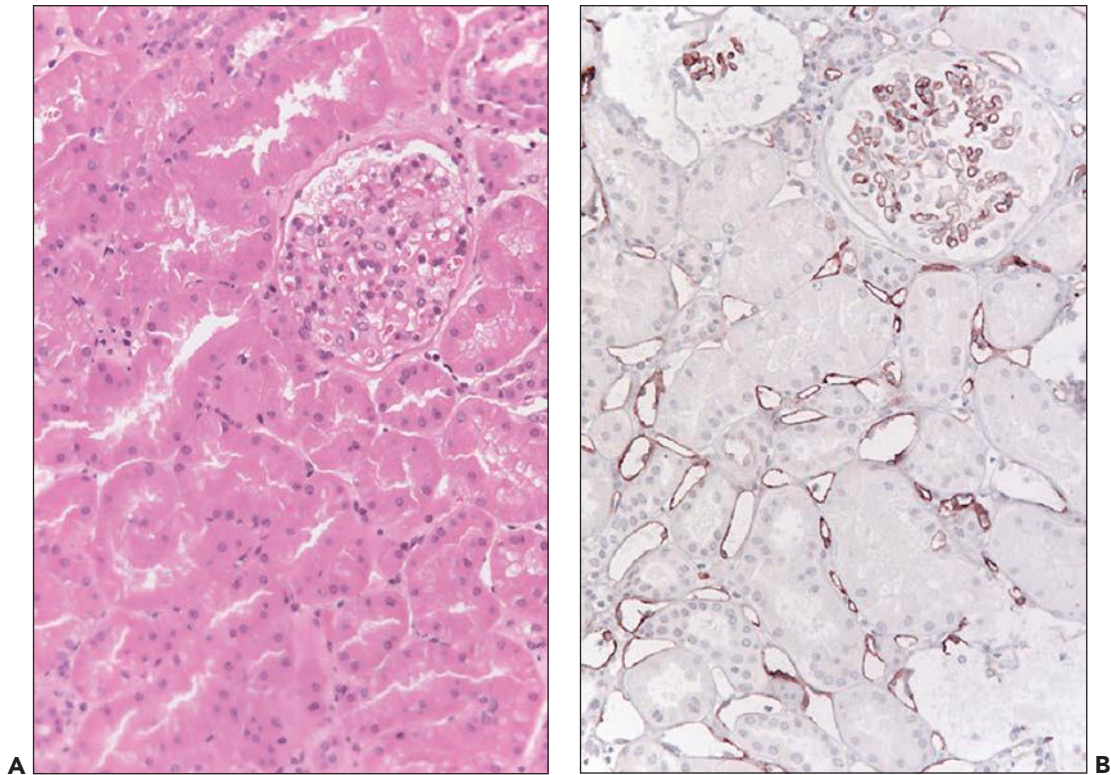


FIGURE 29.64 Surveillance biopsy with normal graft histology but with prominent accumulation of C4d in peritubular and glomerular capillaries (corresponding to stage II in A). (A, H&E; B, C4d IHC, original magnifications 200 \times .)

adherent to their maintenance immunosuppressive regimen. Some strategies (none with controlled randomized trials) include IVIG and rituximab (678,679) and bortezomib (680). Whether complement inhibition will be useful remains to be determined. One would expect that earlier treatment would

have greater success. Indeed, that seems to be the case for early glomerulopathy (644). Regular monitoring of DSA and appropriate surveillance biopsies are recommended (415). Of course, the best intervention is prevention, which remains elusive to achieve.

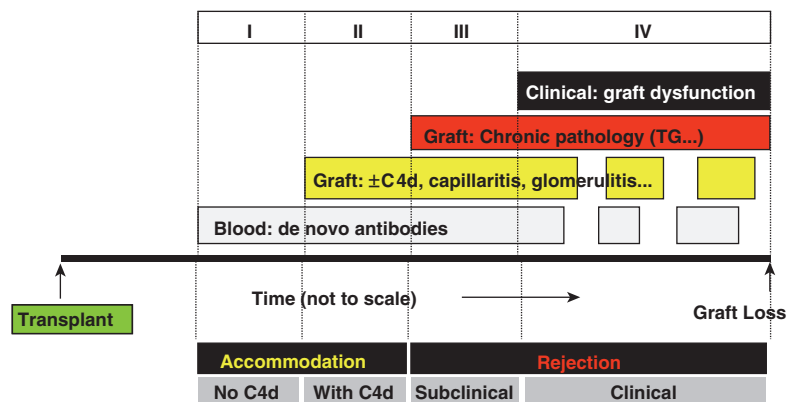


FIGURE 29.65 Postulated stages (or states) of chronic AMR. The process begins with antibody production, followed by C4d fixation in the tissue (if sufficient amounts of complement-fixing antibodies are formed). These two stages have no graft pathology or dysfunction and are therefore states of "accommodation" to antibody rather than "rejection." Microcirculatory inflammation (capillaritis, glomerulitis) can be seen in the early stage with or without C4d and, if present, is better termed "smoldering AMR" rather than accommodation, since it clearly portends graft dysfunction. The third stage has chronic pathologic lesions, such as transplant glomerulopathy (classically, TG and multilamination of the PTC) followed by the fourth stage when graft dysfunction becomes clinically evident. The inevitability of progression has not been proved in humans, although these stages occur in nonhuman primates without immunosuppression. C4d deposition fluctuates and may be negative at any given point. Data from (462,537,670).

LATE GRAFT BIOPSIES

Late graft failure develops at a rate of about 2% to 4% per year, which has changed little over the last decade, despite dramatic improvements in short-term graft survival (see Fig. 29.2) (681). Patients with progressive loss of renal function commonly have hypertension and proteinuria, often in the nephrotic range (640). Both alloimmune-mediated and non-immune-mediated mechanisms contribute to late graft loss (Table 29.8). While these may be coexistent and even synergistic, the active mechanisms in a graft need to be distinguished whenever possible to choose appropriate therapy (682–684). By 10 years after transplantation, about 20% of the grafts have been lost to chronic rejection, 8% to recurrent glomerulonephritis, 4% to acute rejection, and 15% to death with a functioning graft (685). While some have argued that the renal biopsy is not useful in analyzing graft dysfunction after 1 year, published studies show that the biopsy leads to a change in management that improved renal function in 8% to 38% of patients (58,59).

Considerable confusion reigns in the nomenclature of the pathology of late graft loss, largely related to the difficulty in diagnosis and the common occurrence of multiple diseases. We recommend that “chronic rejection” be defined specifically as graft injury due to immunologic reaction to donor antigens. “Chronic” (chronos, time) does not mean “inactive,” as some have used the term, but, rather, that the process progresses slowly (months to years) due to persistent or recurrent activity. This definition requires evidence in the biopsy for *ongoing* immunologically activity due to T cells and/or alloantibodies, as well as evidence of tissue injury (e.g., tubular atrophy, loss of capillaries) or abnormal production of new tissue components (e.g., fibrosis, new basement membrane).

Few pathologically terms are misused more than chronic allograft nephropathy (CAN), which entered the medical literature in 1993 as a category in the Banff classification “because it is often impossible to define the precise cause or causes of chronic allograft damage.” CAN became the generic term for chronic renal allograft dysfunction and fibrosis, or as a synonym for “chronic rejection.” The 2005 Banff conference agreed by consensus to abolish the term CAN and replace it with a term more clearly descriptive, such as “interstitial

fibrosis and tubular atrophy (IFTA), not otherwise specified” (612). In addition, the criteria for chronic AMR and TCMR were proposed. An instructive series from the Mayo Clinic sought identifiable causes of late graft failure (496). Among 153 graft failures (from 1317 recipients) due to intrinsic renal disease, 37% had glomerular disease: recurrent (15%), de novo (7%), or transplant glomerulopathy (15%, probably mainly chronic AMR). IFTA was dominant in 31%, with specific causes that included PVN (7%), T-cell- and/or AMR (16%), pyelonephritis (5%), and CNI toxicity (1%).

Unfortunately, a significant minority of biopsies taken for late graft dysfunction cannot be assigned to a specific diagnosis, in particular small biopsies lacking arterial cross sections. An estimate of this can be derived from a Mayo study that found 19% of late graft failures had nonspecific IFTA (496). This percent is consistent with our experience. This residual group is rightfully defined as “IFTA, NOS,” until further specific pathologic or pathogenetic features are identified.

Differential Diagnosis

The diagnosis of late graft damage first requires evaluation of whether an active alloimmune process is responsible. Among the established measures of immunologic activity are those related to injury mediated by T cells (tubulitis, interstitial inflammation, infiltration of arterial intima, and glomerulitis) and antibody (C4d deposition in PTC). Other assessments are likely to be useful in the future. Many of these have shown promise in research studies, such as markers of cell death (TUNEL), cell proliferation (Ki 67, PCNA), IFN- γ action (HLA-DR and other IFN- γ -triggered gene expression) (150,156), matrix synthesis (mRNA for collagen types, matrix-related proteases, and their inhibitors), and cytokines (e.g., TGF- β). Molecular markers will potentially enhance detection of ongoing activity and determine which signaling pathways are most appropriate for therapeutic intervention (see below).

In addition to a careful analysis of the late biopsy itself, other pieces of information are helpful in identifying the cause of late graft injury. A review of previous biopsies may reveal more easily appreciated diagnostic features in the early, active stages of the disease as well as underlying donor disease. DSA levels may point to an antibody-mediated process. Imaging studies sometimes reveal etiologic vascular or ureteral problems. The late biopsy should be worked up just as a native kidney biopsy (light, immunofluorescence, and electron microscopy), since glomerular diseases are commonly present. Knowledge of the primary cause of renal failure is obviously essential to distinguish recurrent from de novo glomerular diseases.

The late pathologic features that are generally attributed to repeated or persistent immunologic attack on graft target cells are elastin-free arterial intimal fibrosis (with or without T cells in the intima) and glomerular and/or PTC basement membrane duplication (with or without corresponding C4d deposition) (224,396,682). Isolated IFTA that also have signs of immunologic activity, such as a mononuclear infiltrate or C4d deposition in PTC, might also be considered sufficient. Indeed, the presence of inflammation in areas of fibrosis is a better predictor of later graft loss than either inflammation or fibrosis alone (178,658,686). These features are discussed fully in the sections on chronic TCMR and chronic AMR.

TABLE 29.8 Causes of slowly deteriorating graft function^a

Chronic Rejection
T cell mediated
Antibody mediated
Structural CNI toxicity
Infection (e.g., polyomavirus nephropathy/PVN)
Recurrent disease
De novo disease (e.g., diabetic nephropathy)
De novo arteriosclerosis (hypertensive vascular disease)
Renal artery stenosis
Unclassified (interstitial fibrosis and tubular atrophy, not otherwise specified)
Progression of donor disease (arteriosclerosis, fibrosis)

^aDeath with a functioning graft is responsible for about 22% to 25% of graft failures.

Molecular Studies

Early application of targeted PCR mRNA expression analysis to late allograft biopsies showed that increased TGF- β , but not IL-2, IFN- γ , IL-4, IL-10, granzyme B, or perforin, correlated with concurrent fibrosis (230,687). TGF- β and laminin- β 2 mRNA were higher in chronic CNI toxicity than chronic rejection. The mRNA species that predict later graft loss include increased CD3- γ (688); increased FGF-1, type 1 angiotensin II receptor (689), and cytokeratin 15; and decreased TGF- β 1 (690). The last finding fits with the observation that high TGF- β 1 in acute rejection predicts later lack of chronic rejection (perhaps related to induction of Treg cells) (691).

Using microarrays for assessing late biopsies, the strongest molecular correlates of the extent of IFTA were mast cell- and B-cell-associated transcripts (692). In addition, the expression of plasma cell-associated transcripts (i.e., immunoglobulin heavy chain transcripts) and also Foxp3 increased with time posttransplantation. These findings were confirmed by IHC in corresponding biopsies showing increased accumulation of cells staining for CD20, IgG4, Foxp3, or CD117 in areas with IFTA (325,692,693).

A molecular classifier for the prediction of allograft failure in indication biopsies after 1 year was developed and, in initial studies, was superior to clinical (creatinine, proteinuria, GFR) and morphologic (Banff lesion scores) risk factors for predicting allograft failure (694). Interestingly, the classifier utilized genes part of the molecular injury response as the main source for prediction, suggesting that an ongoing, active molecular injury response of the tissue due to progressive diseases like chronic AMR or GN is the main correlate for functional deterioration in late allograft biopsies (694). Increased expression of a gene set reflecting the acute injury response in the kidney parenchyma correlated with poor function and with inflammation in areas of fibrosis, but not with fibrosis without inflammation (695). Confirming the predictive value of the survival classifier, the molecular injury signal in late kidney transplant biopsies strongly predicted future graft loss in multivariate survival analysis. Many individual transcripts expressed in late biopsies were shared between the injury gene set (135,695) and the molecular risk score, for example, integrin- β 6 (ITGB6), versican (VCAN), and nicotinamide *N*-methyltransferase (NNMT). The molecular injury signal correlates with allograft function at time of biopsy (696) and was a better predictor of future graft loss than extent of interstitial fibrosis, total inflammation, or expression of collagen genes.

miRNA alterations associated with IFTA in kidney allografts may point toward pathologic mechanisms. Using small RNA sequencing in eight human kidney allograft biopsies (four IFTA and four normal) guided selection of miRNAs accompanying IFTA, which were quantified in 18 biopsies using real-time quantitative PCR. Total miRNA content was 50% lower in IFTA compared with normal biopsies. Several miRNAs including miR-21, miR-142-3p, and miR-5p and the cluster comprising miR-506 on chromosome X had twofold to sevenfold higher expression in IFTA compared with normal biopsies, whereas miRNAs miR-30b and miR-30c were lower in IFTA biopsies. However, no specific diagnoses were assigned to the IFTA cases, not allowing further understanding of potential specific disease mechanisms. Using RT-PCR, the levels of miRNAs were found to be associated with allograft function and survival (697).

Suthanthiran et al. describe a noninvasive diagnostic test for fibrosis based on mRNA measurements in urine by RT-PCR (249). In 114 urine specimens from 114 renal allograft recipients (48 with IFTA in their biopsy), levels of the following mRNA were significantly associated with IFTA: vimentin, hepatocyte growth factor, α -smooth muscle actin, fibronectin, perforin, PAI-1, TGF- β 1, TIMP1, granzyme B, fibroblast-specific protein 1, CD103, and collagen 1A1. A four-gene model composed of the levels of mRNA for vimentin, NKCC2, and E-cadherin and of 18S ribosomal RNA provided the most accurate diagnostic model of IFTA with a sensitivity of 93.8% and a specificity of 84.1% (698).

Using DNA microarrays, tandem mass spectroscopy proteomics and bioinformatics in peripheral blood specimens of 77 kidney transplant patients with biopsy-documented IFTA compared to specimens from patients with normal histology revealed over 2400 genes for mild IFTA and over 700 for moderate/severe IFTA to be differentially expressed. No further histologic subtyping of the IFTA cases was provided. Blood proteomic profiles showed over 500 candidate molecules each, for both stages of IFTA including 302 proteins unique to mild and 509 unique to moderate/severe IFTA (699). In a follow-up study, the same group acquired proteomic data using tandem mass spectrometry with subsequent quantification, analysis of differential protein expression, validation, and functional annotations to known molecular networks through parallel genome-wide expression profiling in human renal allograft biopsies. More than 1400 proteins were associated with the progression from normal transplant biopsies to biopsies with mild to moderate and severe IFTA. Multiple sets of proteins were mapped to pathways associated with immune responses, inflammatory cell activation, and apoptosis primarily consistent with chronic rejection as the cause for IFTA. The most dominant pathways were associated with the alternative rather than the classical complement pathway, actin cytoskeleton, and cell signaling of the acute-phase response (700).

Thus, a stereotyped acute molecular injury signal, comprising numerous individual transcripts identical to those observed during acute kidney injury (AKI), is present in late biopsies with many different diseases as a reflection of parenchymal stress. Progression to failure is primarily a function of ongoing parenchymal injury by specific diseases and not non-specific, progressive fibrogenesis.

Morphologic Scoring Systems for Chronic Lesions

The Banff system for chronic lesions grades cortical fibrosis, vascular intimal fibrosis, tubular atrophy, glomerular GBM duplication, total inflammation, mesangial matrix, and hyalinosis (see Table 29.3). These are grades and not diagnoses. Banff does not distinguish between specific causes of "cv," such as rejection or hypertension, and "cg," such as recurrent TMA, CNI toxicity, or etiologies of rejection. The reproducibility of Banff chronic scores is not high (kappa scores of 0.195 to 0.375). Reproducibility improved substantially for intimal fibrosis and hyalinosis when photomicrographs were used, indicating that one problem was identifying the relevant lesion in the slides. The reproducibility of interstitial fibrosis did not improve with practice or by supplying photomicrographs (701), indicating that there is a problem with the definition. A small group of pathologists who had worked together had better kappas (0.53 to 0.65) evaluating protocol biopsies for interstitial fibrosis, but transplant glomerulopathy scoring was not reproducible (702).

If Masson trichrome stains are used, areas with interstitial edema may show increased staining and result in overinterpretation of fibrotic interstitial remodeling, that is, Banff ci scores. Sampling problems must also be considered. It has been estimated that 25% of biopsies are over- or underscored for fibrosis by sampling, based on the observation that 12% of protocol biopsies show a decrease in fibrosis on subsequent sampling, even when 7 or more glomeruli are in the sample (703). Two cores may reduce this problem. Sampling is a greater problem in evaluating vascular lesions, since few arteries are included and branches of arcuate caliber vessels are often absent.

MORPHOMETRY

For clinical research and trials, a variety of techniques have been employed to obtain more precise quantitation (704,705). Most morphometry studies have focused on interstitial fibrosis, which is amenable to morphometry and may be less subject to sampling error than vascular lesions. The markers used for fibrosis include antibodies to collagen I or III (706) and Masson/Mallory trichrome (707) and Sirius/picrosirius red (708,709). Digital images and computerized data analysis are used to calculate cortical interstitial volume fraction (V_{IF}). Errors due to interpretation (but not sampling) can be minimized by using morphometric analysis, although selection of the threshold for positive staining (segmentation) is itself subjective (710). Since interobserver segmentation thresholds vary, a computer program has been developed, which sets the segments automatically for Sirius red staining of interstitial and mesangial areas (710). In our experience, the best reproducibility of fibrosis extent was achieved by morphometry with collagen III-stained sections and visual evaluation of trichrome stains (705). Both correlated better with eGFR than Sirius red stains.

The definition of percent fibrosis itself is subject to differences in interpretation: the percentage of the cortex that has increased fibrosis of any degree (the usual interpretation of pathologists) or an estimate of the percentage of the cortical area that is the fibrotic tissue itself (as with point counting in morphometry, with or without excluding glomeruli and large vessels or subtracting the normal amount of fibrous tissue). For example, the amount of “fibrous tissue” in normal kidneys by point counting is 26% of cortical volume, which the pathologist would score as 0% “fibrosis” (711). How is “chicken-wire”-type fibrosis surrounding nonatrophic tubules accounted for in the Banff ci-scoring approach? The area of fibrosis could be related to the number of glomeruli in the sample, which would serve to mark the area of the original cortex (like surgical clips). Curiously, in a study of 1-year protocol biopsies, the visual scores of fibrosis were superior to Sirius red morphometry in predicting serum creatinine at 8 to 10 years or late graft loss (712). A multicenter study by the Banff working group has concluded that the interobserver variability is high and emphasizes the need for morphometric analysis on digital images (virtual microscopy) (107).

COMBINED SCORES

Some propose combining the scores for multiple pathologic features to assess the degree of chronic renal damage. For example, the “Chronic Allograft Damage Index” (CADI) is the arithmetic sum of the six scores for interstitial fibrosis, tubular atrophy, glomerular mesangial expansion, intimal fibrosis, interstitial infiltrates, and glomerulosclerosis (all 0-3). CADI scores correlate

with graft loss at 3 years (713); the extent of interstitial fibrosis at 6 months was the most predictive of graft loss by multivariate analysis (713). Previous acute cellular rejection predicted elevated CADI at 3 years, and the latter predicted inferior graft function at 5 years. Other combined scores have been used. A chronic graft damage score at 6 months, calculated from the degree of vascular intimal hyperplasia, glomerular mesangial changes, focal lymphocytic infiltration, focal and diffuse interstitial fibrosis, and tubular atrophy, was also strongly associated with graft loss 2 to 3 years after transplantation (714). The Banff chronic sum (calculated as the sum of cg, ci, ct, and cv) was not correlated with morphometric analysis of Sirius red staining, but did correlate with graft failure (708). When predictive variables are combined arithmetically to give a single score, as in the CADI or the Banff chronicity grade, the individual predictors should ideally be independent, strongly correlated to outcome, and provide some unique contribution to the assessment of the score (715). Several studies with protocol biopsies have shown that the combination of inflammation with fibrosis is correlated with later graft loss (178,658,686). These markers need to be validated in long-term follow-up to see if changes in the scores correlate with changes in late outcome. Which markers might qualify as surrogate indicators for graft failure? Answers are much needed in clinical trials to shorten the time needed to assess efficacy.

PROTOCOL BIOPSIES, SURROGATE ENDPOINTS, ACCOMMODATION, AND TOLERANCE

Protocol Biopsies

Protocol (surveillance) biopsies are taken at predetermined times, in contrast to the usual biopsies taken to diagnose graft dysfunction (“indication” or “for cause” biopsies). Protocol biopsies can be done safely and have become a common component of multicenter clinical trials, and many centers routinely perform protocol biopsies (68,73). However, their definitive clinical value is still debated (716–718). Protocol biopsy studies have shown repeatedly that considerable graft pathology can be present before graft dysfunction is clinically evident and that inflammation in the graft generally portends a worse prognosis. Protocol biopsies thus have the potential to improve clinical care by prompting early interventional therapy (including both increase and decrease of immunosuppression). They also are valuable to elucidate initiating pathogenetic mechanisms before the pathologic features become nonspecific or inactive. However, a large proportion of protocol biopsies taken in a standard/low-risk population shows no relevant pathology (719) and therefore maybe considered needless. Therefore, the prevalence of relevant subclinical pathologies depends on the risk profile of the protocol biopsy population and the time posttransplantation. For example, in presensitized patients with an increased risk for AMR, early protocol biopsies show a high prevalence of subclinical AMR lesions, which are of prognostic value in this setting (492).

Subclinical Rejection

SUBCLINICAL CELL-MEDIATED REJECTION

Protocol biopsies have demonstrated that a mononuclear interstitial infiltrate and tubulitis can be present in stable patients (299,720). When the biopsy findings meet the pathologic

criteria for acute rejection in a patient with normal graft function, the term “subclinical rejection” is used. Depending on the immunosuppressive protocol, in the first 1 to 6 months, an average of 12% to 17% of patients have subclinical rejection, and 21% to 28% have borderline/suspicious inflammation (657,721–729) and declining thereafter. The wide variation among studies is related to not only differences in immunosuppression but also HLA match, sensitization, and donor organ type. Among 190 patients, acute rejection was detected as often in protocol biopsies (17%) as biopsies taken for graft dysfunction (13%) (724). Subclinical or clinical acute rejection was a predictor of IFTA at 12 months. In another study of 120 recipients on CsA and azathioprine, subclinical rejection by Banff criteria was common, detected in about 25% at 1 to 2 years and in 5% to 10% thereafter (726). Among a group of patients treated with either tacrolimus or cyclosporine, the prevalence of acute rejection in 2-year protocol biopsies was 8.9% and 9.2%, respectively (730). With more recent triple immunosuppressive maintenance therapy (tacrolimus, MMF, prednisone), significant lower rates of subclinical acute TCMR (4.6%) are observed (731). Very early protocol biopsies in the first 1 to 2 weeks have revealed acute rejection in 5% to 25% and borderline/suspicious inflammation in 9% to 38%. Focal interstitial infiltrates, TBM rupture, peritubular macrophages, or C4d each increased the risk of a clinical rejection episode by two- to threefold (556,732). Those with subclinical acute rejection at 2 weeks had lower graft survival at 1 to 10 years (657). Acute rejection was more common in patients with DGF than those with initial function (18% vs. 4%), a strong argument for biopsies in this setting (722).

Subclinical cell-mediated rejection is considered a risk factor for progression of IFTA, arguing that immunologic rejection is a major pathogenetic factor. Among 128 grafts at 2 years, 30% had diffuse inflammation, which correlated with later development of reduced function (668). Similarly, patients who had the least infiltrate in sequential protocol biopsies from 1 to 12 months posttransplant had the best graft function at 12 months (720). In patients with IFTA in protocol biopsies at 1 year, 50% had subclinical acute rejection; these patients had a worse graft survival at 5 years than those with IFTA without subclinical acute rejection. These findings were confirmed by a study of 292 recipients with 12-month surveillance biopsies: Subsequent graft survival was predicted by fibrosis with inflammation (Fig. 29.66). Even in a low-risk cohort of patients, the combination of fibrosis and inflammation in 1-year protocol biopsies was associated with reduced graft function and survival as well as a rejection-like gene expression signature (733). These data argue that more than a minimal infiltrate in a long-term graft is pathologic, but most of these studies did not take into consideration the actual course of graft failure and therefore merely describe associations between subclinical inflammation and outcome but not with the development of specific disease processes. A more recent randomized, multicenter study with the aim to determine whether treatment of subclinical rejection with increased corticosteroids results in beneficial outcomes in renal transplant patients receiving tacrolimus, MMF, and prednisone found no benefit. Actually in the 6-month protocol biopsies, 34.8% of the patients undergoing protocol biopsies but only 20.5% of those not undergoing protocol biopsies had a ci + ct score ≥ 2 , while no significant difference in allograft function was observed (731). In protocol

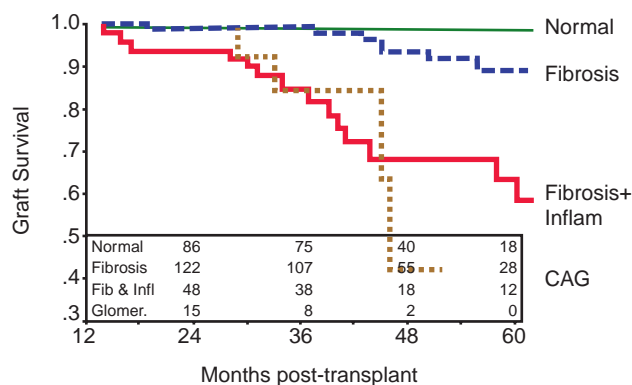


FIGURE 29.66 One-year protocol biopsies with both fibrosis and inflammation have a worse prognosis than fibrosis alone; the latter have little difference compared with no fibrosis (734).

These data argue that the inflammation is related to progression and that cases with both fibrosis and inflammation are a form of chronic rejection. Transplant glomerulopathy also has a poor prognosis. (Adapted from Cosio FG, Grande JP, Wadei H, et al. Predicting subsequent decline in kidney allograft function from early surveillance biopsies. *Am J Transplant* 2005;5(10):2464–2472.)

biopsies from patients under current triple immunosuppression chronic histologic changes are generally mild at 1 and 5 years posttransplantation and are similar in deceased and living donor kidneys. In patients with both 1- and 5-year protocol biopsies, mild fibrosis present at 1 year progressed to more severe forms at 5 years in 23% of allografts. The prevalence of moderate or severe arteriolar hyalinosis was similar in tacrolimus and CNi-free immunosuppression. These results in the recent era of transplantation demonstrate fewer, less severe, and less progressive chronic histologic changes in the first 5 years after transplantation than previously reported (735). Protocol biopsies from 315 consecutive renal transplants without pretransplant DSA and under current triple immunosuppression revealed the presence of subclinical inflammation, including borderline findings, was associated with the later development of DSA (537).

SUBCLINICAL ANTIBODY-MEDIATED REJECTION

Protocol biopsies help identify early events mediated by antibodies, including those that lead to accommodation. In a large European multicenter study with 551 protocol biopsies from crossmatch-negative patients, 4.4% had PTC deposits of C4d (2.0% diffuse, greater than 50% of capillaries; 2.4% focal, 25% to 50% of capillaries) (675). C4d was associated with retransplants and inflammation in peritubular and glomerular capillaries, similar to the C4d associations in indication biopsies. However, C4d had no immediate impact on allograft survival during the time of observation (approximately 1 year). In ABOi, crossmatch-negative grafts, the frequency of C4d+ biopsies from stable grafts was 25% (604).

Histologically normal protocol biopsies may show C4d deposition (see Fig. 29.64). Further follow-up and correlations with circulating antibody will be needed to interpret the clinical significance of “incidental” C4d deposition. At least, we can conclude that incidental C4d deposition does not portend acute AMR and probably represents accommodation as long

no DSA are found and the crossmatch is negative using sensitive detection methods. In stable grafts, endarteritis is found rarely (0.3% in one series) (675) and fibrinoid necrosis never (299,736). In one instance, endarteritis was present in a protocol biopsy, and the patient developed clinically evident rejection 3 days later (736). We have seen only three cases in which endarteritis was present in a biopsy with no clinical evidence of rejection at the time of biopsy or later.

TG was diagnosed in 10% of patients based on protocol biopsies in well-functioning grafts. The cumulative incidence of TG increased over time to 20% at 5 years. The prognosis of subclinical TG was equally as poor as TG diagnosed with graft dysfunction, with progressive worsening of histopathologic changes and function. TG was associated with acute rejection, pretransplant hepatitis C positivity, and anti-HLA antibodies (especially anti-class II), with the risk increasing if the antibodies were donor specific (421).

The findings are significantly different in protocol biopsies from presensitized patients undergoing transplantation after desensitization. Retrospective analysis of 83 patients who received HLA-incompatible renal allografts following desensitization showed ten patients with subclinical AMR on protocol biopsies defined as stable SCr, peritubular capillaritis, diffuse C4d deposition, and positive DSA during the first year posttransplantation. Three patients had a subsequent rise in SCr and an associated biopsy for cause with AMR. However, the mean increase in chronic Banff scores (cg + ci + ct + cv) from those biopsies showing subclinical AMR to follow-up biopsies was significantly greater than that in recipients of HLA-incompatible grafts with no AMR over a similar interval, suggesting that subclinical AMR contributes to the development of IFTA and TG (737). In 157 protocol biopsies from 80 DSA-positive patients obtained at 3 months and 1 year posttransplant, Banff C4d scores were associated with significant increments of microcirculation inflammation, worse TG and higher class II DSA-MFI. A total of 54% of patients had variation of C4d score between 3 months and 1 year posttransplant. Cumulative (3 months + 1 year) C4d scores correlated with long-term renal function worsening. Multivariate analysis demonstrated that the presence of microcirculation inflammation and class II DSA at 3 months was associated with a fourfold increased risk of progression to chronic AMR independently of C4d (492). Protocol biopsies performed 12 months posttransplant in crossmatch-positive, ABOi, and conventional allografts revealed that all three groups had only minimal histologic changes, but that TG was significantly increased in crossmatch-positive patients and correlated with prior AMR episodes. Patients with a prior history of AMR also had a significant increase in IFTA (597).

An important concept emerging from these protocol biopsy studies done in patients with either preexisting or de novo anti-HLA DSA is that the natural course of AMR is a dynamic, continuous process with significant fluctuations in the DSA status, C4d deposition, and Banff scores for microcirculation inflammation (635). This concept is supported by findings from very early protocol biopsies in patients with DSA showing only by EM detectable features of microcirculation injury (endothelial swelling, subendothelial widening, and beginning basement membrane duplication and multilayering), which were associated with later manifestation of overt TG (220,644).

Other Subclinical Diseases

Protocol biopsies at 3 and 12 months have revealed polyomavirus nephropathy (PVN) in about 1.2% of recipients (738). These patients had an outcome better than those 1.5% first diagnosed with graft dysfunction, reflecting favorable long-term outcome in early polyomavirus disease stages (see section on Infections below). Arteriolar hyalinosis as a potential feature of subclinical CNI toxicity was typically found in protocol biopsies at 3 years and beyond, reaching 100% of recipients at 7 to 10 years; other features that may be related to CNI toxicity, striped fibrosis, and tubular microcalcification were found in 88% and 79%, respectively. However, despite showing subclinical features potentially consistent with chronic CNI toxicity, these allografts had an excellent long-term survival (726,739). Acute, reversible CNI toxicity (tubulopathy) was found usually in the first 6 months (739).

Nephrocalcinosis in protocol biopsies was a predictor of later IFTA (73,740). Intratubular calcium oxalate crystals were found in 52% of biopsies in the first 3 months and were associated with prior acute tubular injury, graft dysfunction, and decreased 10-year graft survival (50% vs. 74%) (741). Tubular calcification was progressively more common in protocol biopsies taken from 6 weeks (6%) to 6 months (18%) and was correlated with higher serum parathormone and calcium levels, rather than rejection, acute tubular injury, or CNI toxicity. Tubular calcification with high parathormone levels predicted inferior graft function 1 year after transplantation (740).

Surrogate Endpoints

Protocol biopsies have also been used to predict outcome, with the potential benefit of shortening the follow-up time needed to evaluate efficacy in drug trials (742,743). Candidates for an early surrogate marker of long-term graft survival rely on protocol biopsies at a time relatively close to transplant, that is, 3 to 6 months. Among the documented predictors of graft loss at 2 to 10 years are arterial intimal fibrosis and interstitial fibrosis, detected on biopsy at 3 to 6 months posttransplant (671,713,728,744) and CADI scores at 1 year (716). One example of this approach is the finding that patients who had early withdrawal of steroids had increased interstitial fibrosis at 12 months (745). The use of CNI is generally guided by drug levels. In an analysis from the Mayo Clinic, two groups of kidney transplant recipients were compared: In the first ($n = 245$), tacrolimus levels were significantly higher than in the second ($n = 330$). The recipient and donor demographics were not statistically different between the two groups. At 1 year posttransplant, the low tacrolimus group had (a) lower incidence of PVN, (b) lower fasting glucose levels, (c) higher GFR, and (d), on 1-year protocol biopsies, lower incidence and severity of IFTA, while the incidence and severity of acute rejection episodes was similar between both groups (746).

It should be emphasized that the outcome of a graft is not predetermined by early events alone, but is also influenced by subsequent events that are not always predictable, such as non-compliance, drug toxicity, infections, and recurrent or de novo diseases (743). Routine biopsies at late intervals (1 to 5 years) are recommended in investigative therapeutic trials, since the pathologic lesions may be silent, and the risk of protocol biopsies is minimal (73,747).

Molecular Studies

Subclinical rejection has gene expression profiles quantitatively different, but qualitatively similar to clinically evident acute rejection, which argues that the process is indeed rejection (748). Many of the same potentially injurious molecules are elevated: perforin, granzyme B, IFN- γ , TNF- β , and TNF- α , as well as the chemokines, RANTES, and MIP-1 α and the costimulatory molecules CD154 (CD40L) and inducible costimulator molecule (ICOS) (229,748,749). The only up-regulated genes that distinguished clinical from subclinical rejection in one study were T-bet, Fas ligand, and CD152 (CTLA4) (229). Using microarrays and pathogenesis-based transcript sets on protocol biopsies taken 6 weeks posttransplantation confirmed quantitative differences and qualitative similarities between subclinical and clinical rejection episodes.

Microarray analysis of 3-month protocol biopsies showed overexpression of several genes that are important in the T- and B-cell activation and immune response and profibrotic processes in patients that developed IFTA at 6 months. Furthermore, several genes with transporter and metabolic functions showed decreased expression in the progressors in the 3-month biopsies. These results suggest that gene expression profiling of early protocol biopsies might potentially give clues that help to predict IFTA (598,750). Similar findings are described from microarray analysis of sequential protocol biopsies taken at 1, 3, and 12 months posttransplantation (751). Changes in gene expression predated histologic damage, suggesting a possible adjunct role in early diagnostic testing. However, mRNA expression was correlated with time after transplantation. Transcripts associated with the immune response peaked at 1 month, while fibrotic expression at 3 months, injury and remodeling, and cell proliferation-repair processes were activated between 3 and 12 months, whereas macrophage-related gene expression occurred late by 12 months. Protocol biopsies developing IFTA displayed 262 differentially expressed genes compared with at implantation, dominated by up-regulated injury-repair and immune-related genes. Injury-repair and remodeling genes were expressed before interstitial fibrosis was observed by histology.

Accommodation, Acceptance, and Tolerance

Acute rejection episodes become less frequent with time, for largely unknown reasons. Graft acceptance probably involves events in the graft and changes in the immune response.

Events in the Graft

It has been hypothesized that events in the graft are critical to the development of tolerance. Not all infiltrates in the graft lead to graft injury, and some may actually promote acceptance. Individual patients can have biopsies that meet the histologic criteria for rejection, yet remain stable for 6 months even without increased immunosuppression (752). Grafts in animals that are developing tolerance typically have graft infiltrates, which has been termed the "acceptance reaction" (753). In certain class I disparate murine and pig renal allografts, the intense infiltrate spontaneously disappears and is followed by indefinite graft survival (754,755). Graft biopsies reveal a T-cell and macrophage infiltrate with tubulitis. However, the acceptance infiltrate differed from that in rejecting grafts in certain features, including less infiltration by CD3⁺ T cells and macrophages, less T-cell activation (CD25, PCNA), absent

endarteritis, and less apoptosis of graft cells. Long-lasting apoptosis of graft-infiltrating T cells occurred, which may have contributed to the limitation of the immune response. The grafts also expressed less IFN- γ and more IL-10 than rejecting grafts (755). Acceptance reactions associated with donor-specific transfusions in rats had mRNA levels for cytotoxic proteins similar to that in rejection reactions (756), suggesting that cytotoxic cells were present but blocked in their effects. Treg cells (identified by the transcription factor Foxp3) were more numerous in mice undergoing certain forms of tolerance induction (costimulatory blockage with anti-CD40L) (323). Foxp3⁺ cells have also been detected in accepted grafts in humans and mice (20,322,327). On the other hand, Foxp3⁺ cells have also been observed in human grafts with acute cellular rejection. Thus, the significance of Foxp3⁺ cells is still not fully determined; it is possible that high numbers of such Treg cells are beneficial, in view of their known regulatory functions. Indeed, depletion of Foxp3⁺ cells from allografts in mice precipitates an acute TCMR (322).

Accommodation

Accommodation is defined as an acquired state in which an organ resists the assault of humoral or cellular rejection. For example, grafts from recipients with donor-reactive alloantibodies are considered to show complete accommodation if they show no pathologic changes, such as interstitial fibrosis, glomerulopathy, or arteriopathy. At a cellular level, accommodation may occur via multiple mechanisms, including internalization, down-regulation, inactivation, or inhibition of the target antigen. Binding of human natural antibodies to porcine endothelial cells triggers the induction of inducible nitric oxide synthase (iNOS), Bcl-2, and Bcl-xl, which in turn confer resistance to apoptosis (757). Accommodation may also be induced by immunosuppressive regimens notably after intravenous gamma-globulin (IVIG) in pig to primate xenografts (758). In a small study of pig to baboon renal xenografts, lack of histologic injury was associated with C4d deposition in the absence of C5b or MAC, both of which were present in rejecting grafts (759), suggesting truncation of complement activation was a feature of accommodation. Expression of complement regulatory proteins, CD59 and CD55, is increased in some cases of chronic rejection (760). Microarray gene expression analysis of stable ABOi renal allografts showed differences in signaling pathways and cytokines, but no detectable increase in mRNA for the antiapoptotic molecules (761).

Endothelial Repopulation

One of the proposed mechanisms for accommodation is the replacement of donor endothelium by recipient cells. This has been documented in human organ allografts, but recipient endothelial repopulation is neither common nor predictable. In human renal allografts, 8% had detectable, focal recipient endothelium, as judged by the development of Barr bodies in male to female kidney transplants (762). The Barr body technique is limited, because not all sections are in the right plane and the interpretation is difficult. As judged by the expression of ABO blood group antigens, 23% had partial endothelial replacement (763). The ABO antigen is not an ideal marker, since the carbohydrate epitopes might be converted on the cell by enzymes supplied by the recipient.

Studies of long-standing renal grafts (26 to 29 years) showed only donor endothelium of vessels, as judged by IHC for donor HLA class I antigens in four cases and Y chromosome in situ hybridization in two cases (764). Only one case had evidence of recipient cells in glomeruli. Studies using XY FISH techniques in 26 sex-mismatched renal allografts showed a strong correlation between the percentage of recipient endothelial cells in the PTC and Banff category 4 type 2 rejection with transplant endarteritis; grafts without a history of rejection had only sporadically recipient endothelial cells (765). These data suggest that endothelium damaged by vascular rejection is repaired by circulating cells from the recipient. Low levels of tubular epithelial chimerism (2% to 7%) have been detected by XY FISH or laser capture/short tandem repeat analysis in 88% of patients (766). Lymphatic endothelial chimerism also can be detected by FISH in long-standing grafts (767). Chimerism in tubules had no correlation to outcome or graft morphology. The main pitfall of the FISH technique is that infiltrating leukocytes need to be excluded by combining FISH with a cell lineage marker.

Clinical Tolerance Induction

Specific immunologic tolerance can be defined as acceptance of a histoincompatible graft without immunosuppressive agents while retaining full immunologic competence for other antigens. While this can be done predictably in rodents, it has been achieved only sporadically in patients (768,769). In patients, the term “operational tolerance” is preferred, because proof of tolerance by rechallenge with donor and third-party grafts cannot be done. A great need is an assay that will predict a state of operational tolerance, to guide immunosuppressive reduction.

A few protocols are currently undergoing clinical development and testing. The most promising at the time of writing is induction of mixed chimerism, using bone marrow cells from the kidney donor and nonmyeloablative treatment that spares the recipient marrow (770–773). Stable, fully chimeric recipients of bone marrow transplants have successfully been transplanted years later with kidneys from the same donor without immunosuppression (774) or the converse (769). In most mixed chimerism protocols, short-term immunosuppression is given at the time of transplantation (CNI, anti-T-cell antibody, cyclophosphamide). In HLA-identical recipients who had end-stage renal failure due to myeloma cast nephropathy, the approach has shown promise, with six patients off immunosuppression with functioning grafts at up to 7 years (771). In HLA-haploidentical living donor recipients, long-term graft survival has been achieved off immunosuppression in seven of ten patients (Fig. 29.67) (20,775). Stem cell transplant combined with a kidney transplant from the same donor has also reported to be successful in short-term pilot studies (21). Mixed chimerism protocols are being refined in nonhuman primates, with the expectation that a combination of costimulatory blockade and other measures might make this approach work, even after an organ has been transplanted under conventional immunosuppression (776).

Molecular Markers of Operational Tolerance

Brouard et al. described a “tolerant footprint” of 49 genes in peripheral blood cells from patients with stable grafts off immunosuppression. The gene signature comprised transcripts of reduced costimulatory signaling, immune quiescence,

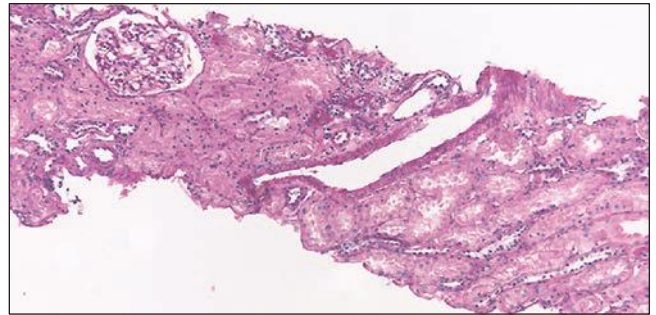


FIGURE 29.67 Protocol biopsy from an operationally tolerant patient induced by the mixed chimerism protocol. Biopsy taken 18 months after transplantation, with over a year off all immunosuppression. The blood vessels, glomeruli, interstitium, and tubules are normal. There was no interstitial infiltrate. (H&E, original magnification 100 \times .)

apoptosis, and memory T-cell responses; 27% of the genes were known to be regulated by TGF- β (777). Recently, two large consortia from Europe and North America reported independently a B-cell signature in peripheral blood as specific for operational tolerance. In the European study, tolerant patients presented with a combination phenotype of an expansion of peripheral blood B and NK lymphocytes, fewer activated CD4⁺ T cells, a lack of donor-specific antibodies, donor-specific hyporesponsiveness of CD4⁺ T cells, and a high ratio of Foxp3 to alpha-1,2-mannosidase gene expression (603). In a collaborative study in the United States, tolerant subjects showed increased expression of multiple B-cell differentiation genes, and a set of just three of these genes distinguished tolerant from nontolerant recipients. This B-cell signature was associated with up-regulation of CD20 mRNA in urine and elevated numbers of peripheral blood naive and transitional B cells in tolerant participants compared with those receiving immunosuppression (778). Thus, noninvasive testing for this signature may allow in the future more tailored immunosuppression in the individual patients avoiding the side effects of over-immunosuppression in some and inappropriate withdraw of immunosuppression in others. However, none of these studies were designed to predict who could safely go off immunosuppression. Thirty percent of the patients off immunosuppression from one of the series showed over time slow deterioration of allograft function with development of DSA and in some cases histologic features of chronic AMR, indicating that they are rather having slowly smoldering rejection than truly being tolerant (779). This highlights the delicate balance between over- and under-immunosuppression in transplant patients.

ACUTE ISCHEMIC INJURY

Allografts inevitably undergo a period of ischemia that results in graft injury. If transient dialysis is required during the first week posttransplantation, the term “delayed graft function” (DGF) is used, whereas “primary nonfunction” (PNF) indicates that a graft never functioned. DGF is very rare after living donation but not uncommon in deceased donor kidneys, which are preserved in the cold for 24 to 48 hours and even more common

in donation after cardiac death. Among 457 adult recipients of primary deceased donor allografts at Minnesota, the incidence of DGF was 23% and 42% to 84% in asystolic donors, while PNF occurs in 7% to 18% (780–783). PNF occurs in 2% to 3% of conventional deceased donor grafts (781,783). In a series from the University of North Carolina, DGF occurred in 19% of kidneys from deceased donors and 2% in those from living donors. The average duration of DGF is 10 to 15 days, with a declining prevalence with time (14% at 2 weeks, 9.5% at 3 weeks, and 1.7% at 4 weeks posttransplantation) (784).

It is important to understand that DGF is purely a clinical term (785). While the initial pathogenesis is usually acute ischemic injury, numerous other causes may contribute such as drug toxicity and rejection. Therefore, if allograft function remains poor posttransplantation, a diagnostic biopsy is indicated to render a specific diagnosis. This is critical for assessing the significance of DGF on long-term outcome of a renal allograft, which mainly depends on the cause for DGF (786).

Pathologic Findings of Acute Ischemic Injury and Differential Diagnosis

As in native kidneys, ATN in renal allografts is characterized by dilatation of proximal tubules accompanied by flattening of the epithelial cell layer, loss of the brush border, and activation of epithelial cell nuclei containing prominent nucleoli. Mitotic figures are sometimes conspicuous in later biopsies (787). Ischemic tubular injury is commonly associated with nonisometric tubular cell vacuolization. The interstitium can show edema and minimal inflammation and, especially in the medulla, dilatation of PTC filled with mononuclear cells, sludged erythrocytes, and neutrophils. Changes can be most prominent in the vasa recta of the outer medulla and increase over the first days postgrafting.

In a retrospective study including 329 deceased donor transplantations, DGF occurred in 28% of recipients. The percentage of patients with ≥ 1 allograft biopsy within the first year posttransplant was similar between the DGF patients and those with immediate graft function. Also, the cumulative 1-year incidence of biopsy-proven clinical and subclinical rejection was not different between the groups. Furthermore, there were no differences regarding rejection phenotypes/severities and time frame of occurrence. By multivariable analysis, DSA, younger recipient age, and immunosuppressive regimens were independent predictors for clinical rejection, while DGF was not, suggesting that DGF is not a major risk factor for rejection (51a).

Arteries, arterioles, and glomeruli typically only show minor “nonspecific” abnormalities (788). Ischemic injury and ATN are typically not associated with the deposition of C4d along PTC (118,150,789). If C4d is found in the setting of ischemia-reperfusion injury, AMR has to be considered as the primary cause for graft dysfunction.

Several differences between ATN in native and transplant kidneys have been described. Proliferation in proximal tubular epithelium is higher in transplanted kidneys (8.0%) than in native kidneys (4.4%) (790). ATN in transplanted kidneys had tubular injury affecting short tubular segments, with necrotic tubular cells, a finding seldom seen in ATN in native kidneys. Intratubular cellular debris and scattered neutrophils may be found that resembles acute pyelonephritis. In cases of pyelonephritis, however, the neutrophil casts are typically densely packed, and neutrophils are additionally found in the adjacent interstitium.

DGF may also be the result of glomerular injury. The changes associated with ice storage include endothelial swelling and vacuolization with obliteration and collapse of glomerular capillary lumens (791). In addition, intraglomerular fibrin thrombi, for example, in the setting of a disseminated intravascular coagulopathy in the donor, may contribute to delayed function; however, they did not predict poor outcome (114), presumably due to rapid lysis by the normal host fibrinolytic system.

Pathogenesis

There is mounting evidence that the inflammatory response in ATN significantly contributes to disease severity and outcome. Recent developments in the understanding of how the immune system responds to dying cells are relevant to ATN in the transplant setting; in particular, NLRP3 inflammasome and complement activation and IL-1 β -mediated neutrophil recruitment are likely to play a key role and may provide novel therapeutic targets for immunotherapy in ATN (792). Furthermore, T cells, in particular CD4+ lymphocytes, natural killer cells, and IFN- γ , have a crucial role in the development of ischemia-reperfusion injury likely due to direct “cross talk” of activated T lymphocytes with the endothelium of the microvasculature and up-regulation of adhesion molecules (see Chapter 26). T-cell activation and the up-regulation of adhesion molecules may explain the association between ATN, and increased detection of graft infiltrates in biopsies during DGF.

Molecular Studies

Although ATN (also termed AKI for “acute kidney injury”) is a relevant problem in native kidneys, biopsies are obtained infrequently, most likely due to the recoverability of AKI. However, kidney transplantation offers a unique opportunity to study the injury-repair response of the tissue because all transplants experience AKI to some extent and biopsies are obtained in great frequency to exclude rejection. Numerous new AKI markers such as neutrophil gelatinase-associated lipocalin, interleukin-18, cystatin C, and kidney injury molecule 1 (KIM-1) have been proposed as early detection markers of AKI in the urine and/or blood. Since AKI is often multifactorial and heterogeneous in origin, it seems likely that not one single marker but a panel of biomarkers will be required to detect and subtype AKI. Despite description of numerous noninvasive AKI biomarker candidates in single-center studies, validation in the multicenter setting is still lacking.

By comparing microarray mRNA expression profiles from clinically indicated renal allograft biopsies with histologic features of AKI and no rejection to time-matched protocol biopsies, a molecular profile of AKI was identified (135). This approach allowed subtraction of the ubiquitous injury changes every transplant is experiencing from clinically relevant AKI. Kidneys with AKI showed increased expression of 394 transcripts associated with the repair response to injury, suggesting a massive coordinated response of the kidney parenchyma to acute injury. This included among the top 30 transcripts many previously identified as AKI biomarkers (793): epithelium-expressed injury molecules (FOS, EGR1, integrin- $\beta 6$ and integrin- $\beta 3$), tissue remodeling molecules (AKAP12, versican, ADAMTS1, ADAM9), and inflammation-associated transcripts (SERPINA3, lipocalin 2, FCGR3A) (135,794). Many other genes also correlated with the molecular

phenotype, including the acute injury biomarkers HAVCR1 (KIM-1) and IL18, but showed quantitatively less extensive changes in the gene expression. The molecular AKI score, calculated as the geometric mean of all related transcripts, correlated with reduced graft function, future functional recovery, brain death, and need for dialysis, but not with future graft loss. Whether a molecular marker profile in patients suffering from ischemic injury can help as an adjunct prognostic tool to histology remains to be shown. Interestingly, the expression of KIM-1 was inversely correlated with eGFR at the time of biopsy (795). KIM-1 is increased in procurement biopsies of deceased donor kidneys compared with living donors, but its expression did not predict DGF (796).

Clinical Presentation, Prognosis, and Therapy

Patients are maintained on dialysis as needed, and CNIs are generally used sparingly in the setting of DGF. Patients with DGF require less dialysis when CNIs are withheld. New treatment strategies for ischemia-reperfusion injury include antioxidants as well as anti-inflammatory drugs (785). Unexpectedly slow functional improvement of DGF warrants a renal biopsy in order to rule out other causes.

By multivariate analysis, DGF by itself is not a significant risk factor for decreased graft survival for patients without rejection (51,797). Rather, it appears that the adverse prognosis associated with DGF is related to underlying cause, in particular acute rejection (51,797,798). Approximately 95% to 98% of grafts with DGF recover: 50% within 10 days and 83% within 20 days postsurgery (785). In organs from donors after cardiac death, 10% of the episodes of DGF last for more than 4 weeks (780). In most instances, ATN and ischemia-reperfusion injury heal with *restitutio ad integrum*. Although DGF is most frequently found in organs from asystolic donors, the 6-year death-censored graft survival does not differ significantly from conventional deceased donors (781).

CALCINEURIN INHIBITOR TOXICITY

Introduction

Drugs that inhibit calcineurin have tremendously improved allograft survival of all organs. Cyclosporine (cyclosporine A, CsA, Neoral) increased 1-year deceased donor kidney graft survival from less than 60% to more than 80% during the decade of its clinical introduction in the 1980s (799). CsA, the first CNI, is a cyclic, lipophilic undecapeptide isolated from a soil fungus (*Tolypocladium inflatum Gams*) (800). The peptide was relegated to obscurity as a mediocre antifungal agent until the screening system of Jacques Borel documented its potent immunosuppressive activity in 1976 (801). Clinical trials were soon reported by Calne, Powles, and colleagues in kidney and bone marrow transplant recipients (802,803). The results confirmed the promising animal studies; however, high doses of CsA (20 mg/kg/d) caused profound oliguric renal failure (803,804). Over the years, CsA drug preparations, as well as dosing and monitoring protocols, have undergone significant adaptations (805). The second widely used CNI is tacrolimus (FK506, Prograf), a macrolide isolated from the fungus *Streptomyces tsukubaensis* in Japan. It was introduced into clinical transplantation in the early 1990s as an alternative to CsA. Tacrolimus does not share any

structural similarities with CsA, but it has similar therapeutic mechanisms and toxicity.

CNIs play a major role in the immunosuppression of allograft recipients. Currently, in the United States, tacrolimus is administered more often than CsA. Tacrolimus is favored by many because it seems to reduce the incidence of acute rejection episodes, and it has a lower incidence of hirsutism and gingival hyperplasia (806–808).

Both CsA and tacrolimus have the same nephrotoxic side effects with indistinguishable histologic lesions primarily involving tubules, arterioles, and glomeruli (739,808,809). Thus, toxic changes are better referred to as CNI-induced toxicity. A histologic diagnosis of CNI toxicity was made in 61% of renal allograft biopsies in one series from the early 1980s (203) and in 38% almost a decade later (56). Under modern therapeutic regimens, classical signs of toxicity have dramatically decreased. Graft losses due to CNI toxicity are exceptionally rare (0.6% in one series) (496).

There are two major forms of toxicity: functional (due to vasospasm and without morphologic changes) and structural (with various early or late histologic alterations, typically associated with functional toxicity; Fig. 29.68). Nephrotoxicity also occurs in native kidneys of patients treated with CsA or tacrolimus, such as recipients of heart or bone marrows or patients with autoimmune diseases (810). The pioneering studies of Michael Mihatsch in Basel have defined most of the key histopathologic features of CNI toxicity, most notably, the structural changes in arterioles and glomeruli, which Mihatsch termed “cyclosporine-type arteriolopathy” and “cyclosporine-type glomerulopathy” (811–814). We will modify his terms to “calcineurin inhibitor–induced” arteriolopathy and glomerulopathy, since they also apply to tacrolimus.

Functional toxicity is typically not associated with any characteristic morphologic changes and is fully reversible (815). Often, allograft biopsies display a normal architecture, and the diagnosis of “functional toxicity” is made by exclusion. Signs of acute tubular injury and necrosis can be seen in some instances.

Most structural nephrotoxic effects of CNI in arterioles and glomeruli may best be regarded as manifestations of TMAs, with different patterns and degrees of severity (813). The TMA-like toxic changes range from insidious and limited renal forms (hyaline arteriolopathy) to full-blown florid variants of the HUS. Mild forms are without great clinical significance; they are fully or partially reversible on dose reduction. Severe variants with systemic TMA/HUS can result in graft failure. Both CNI arteriolopathy and glomerulopathy can develop within days to few weeks, rendering terms such as “acute” and “chronic” toxicity inaccurate. Tubules and the interstitial compartment also show pathologic lesions, but these are of only limited diagnostic use. The following pathology description focuses on structural toxicities. In this context, it is important to remember that although certain lesions are suggestive of CNI toxicity, none is specific.

Light Microscopy

Glomeruli

Glomeruli can be affected by CNI therapy due to toxic endothelial cell injury that can be minor or severe. Downstream to arterioles with marked CNI toxicity, that is, marked late structural CNI arteriolopathy (Fig. 29.69), glomeruli can undergo sclerosis. Intraglomerular fibrin thrombi, typically in a focal

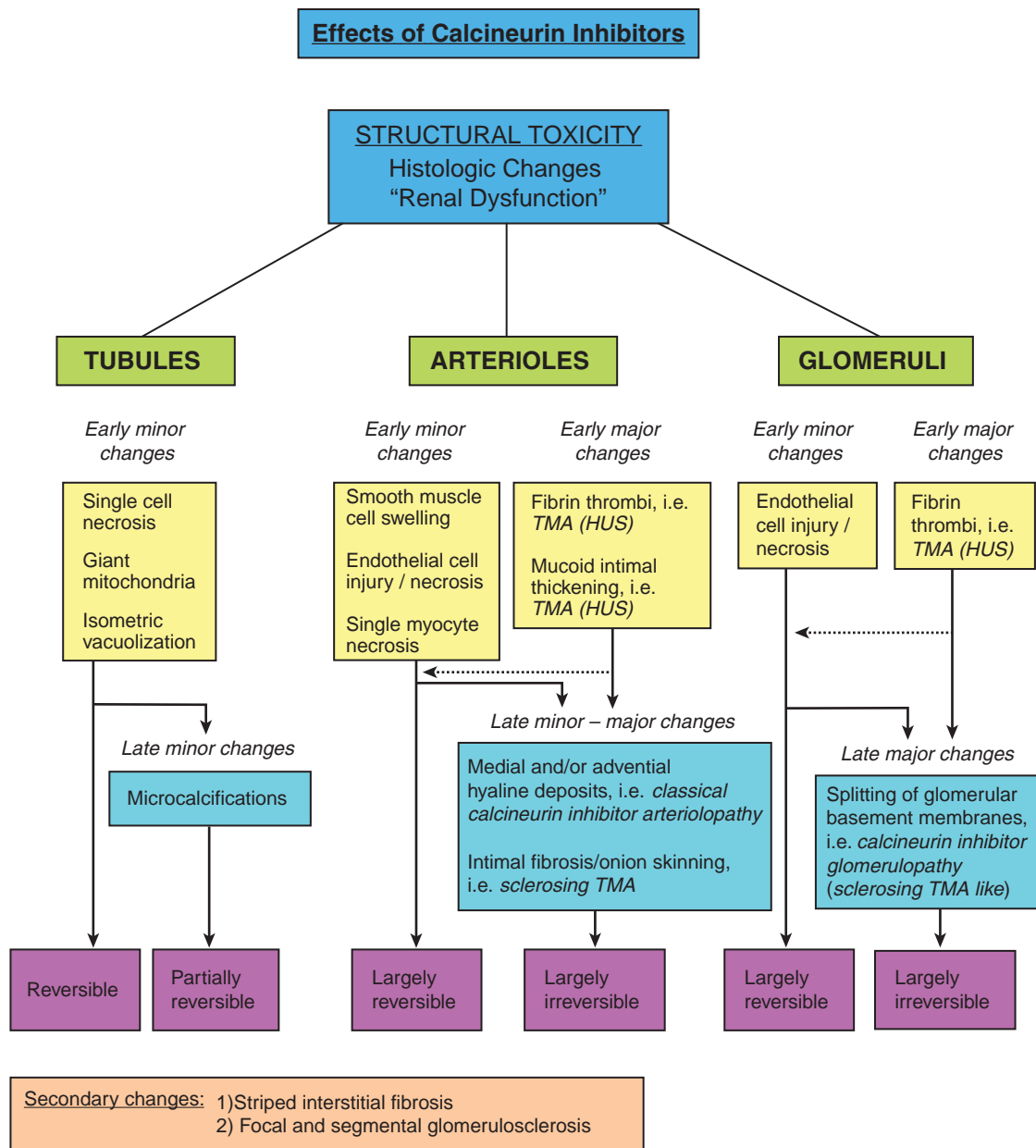


FIGURE 29.68 Schematic of CNi-induced structural toxicity. (TMA, thrombotic microangiopathy; HUS, hemolytic uremic syndrome.)

and segmental distribution pattern, are found in cases of most severe CNi-induced toxic glomerulopathy with florid TMA (Fig. 29.70), occasionally associated with mesangiolytic. The thrombi may undergo resolution (Fig. 29.71C), or they may stimulate basement membrane remodeling with duplication of peripheral glomerular capillary walls (identical to other forms of a TMA).

Often, however, protracted or recurrent glomerular endothelial cell injury caused by CNIs does not lead to a florid TMA. Rather, the endothelium gets "activated" with widening of the lamina rara interna, subendothelial new lamina densa formation, and, ultimately, GBM duplication (i.e., so-called late toxic CNi glomerulopathy; Figs. 29.71 and 29.72). GBM

duplication is typically focal and segmental, and mesangial regions are often slightly expanded due to matrix deposition. This lesion has been termed "CNi glomerulopathy." The glomerular capillary lumens can contain scattered mononuclear cells. However, capillary dilatation with conspicuous intracapillary inflammatory cell aggregates and prominent cell interposition along duplicated capillary walls are not characteristic in CNi glomerulopathy (in contrast to transplant glomerulitis or recurrent glomerulonephritis) (see Table 29.9). Identical toxic glomerular changes occur in native kidneys in heart and bone marrow transplant recipients on CNIs (814). CNi glomerulopathy is characteristically associated with arteriopathy, often most severe in afferent arterioles feeding affected glomeruli

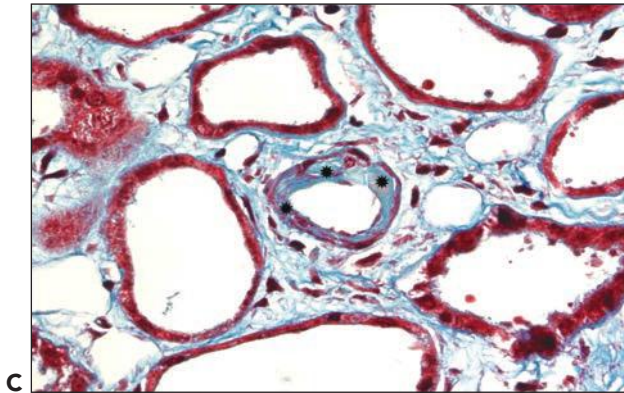
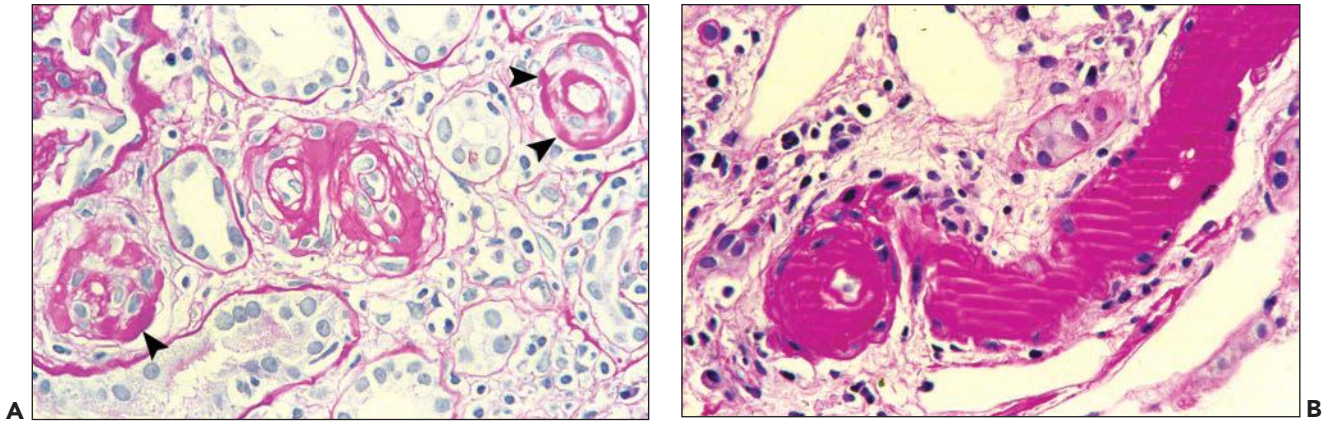


FIGURE 29.69 Arteriopathy suggestive of late CNI-induced toxicity (A and B) with PAS-positive hyaline deposits deep in the medial smooth muscle layers. Note the “string of pearl”-like arrangement of hyaline nodules along the adventitial aspect in some arterioles (*arrowheads* in A); figure (B) shows an example with very severe transmural and circumferential hyaline accumulations. The illustrated changes resemble those induced by TMAs of etiologies other than CNI toxicity, such as severe malignant range hypertension. In contrast, ordinary hypertension-induced arteriosclerosis (C) typically demonstrates subendothelial hyaline deposits (*asterisk*) surrounded by (sometimes atrophic) medial smooth muscle cells. ((A and B) PAS, original magnification $\times 400$; (C) trichrome stain, original magnification $\times 400$.)

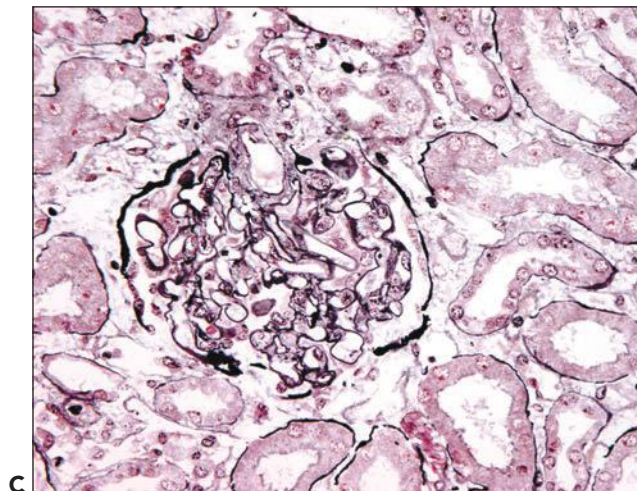
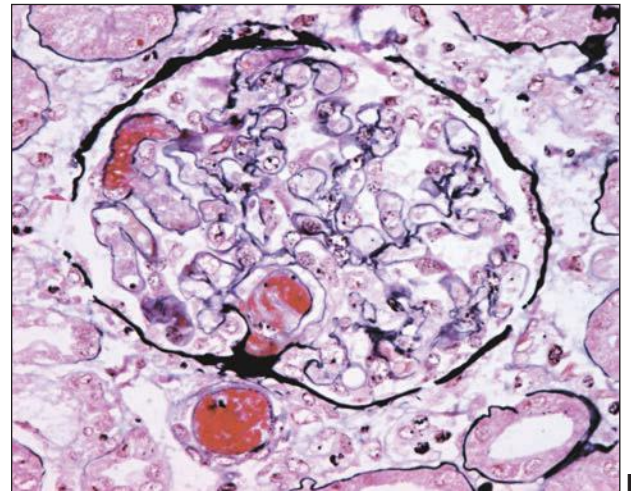
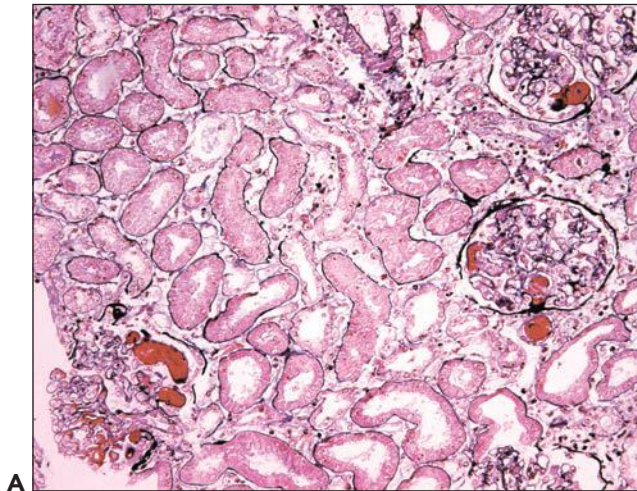


FIGURE 29.70 A CNI induced florid TMA (hemolytic uremic syndrome, A and B). The patient clinically presented on day 11 after transplantation with new onset anuria and anemia. The graft biopsy shows fibrin thrombi in glomerular capillaries and arterioles at the glomerular vascular poles. The discontinuation of CsA therapy resulted in rapid and complete resolution of the TMA within 5 days. A repeat biopsy (C) reveals normal parenchyma without thrombi. Renal function in the patient remained stable with a serum creatinine level of 1 mg/dL 7 months post-grafting. ((A–C) Methenamine silver, (A) original magnification 100 \times , (B) original magnification 250 \times , (C) original magnification 200 \times .) (Courtesy of Alenka Vizjak and Dusan Ferluga, Ljubljana, Slovenia.)

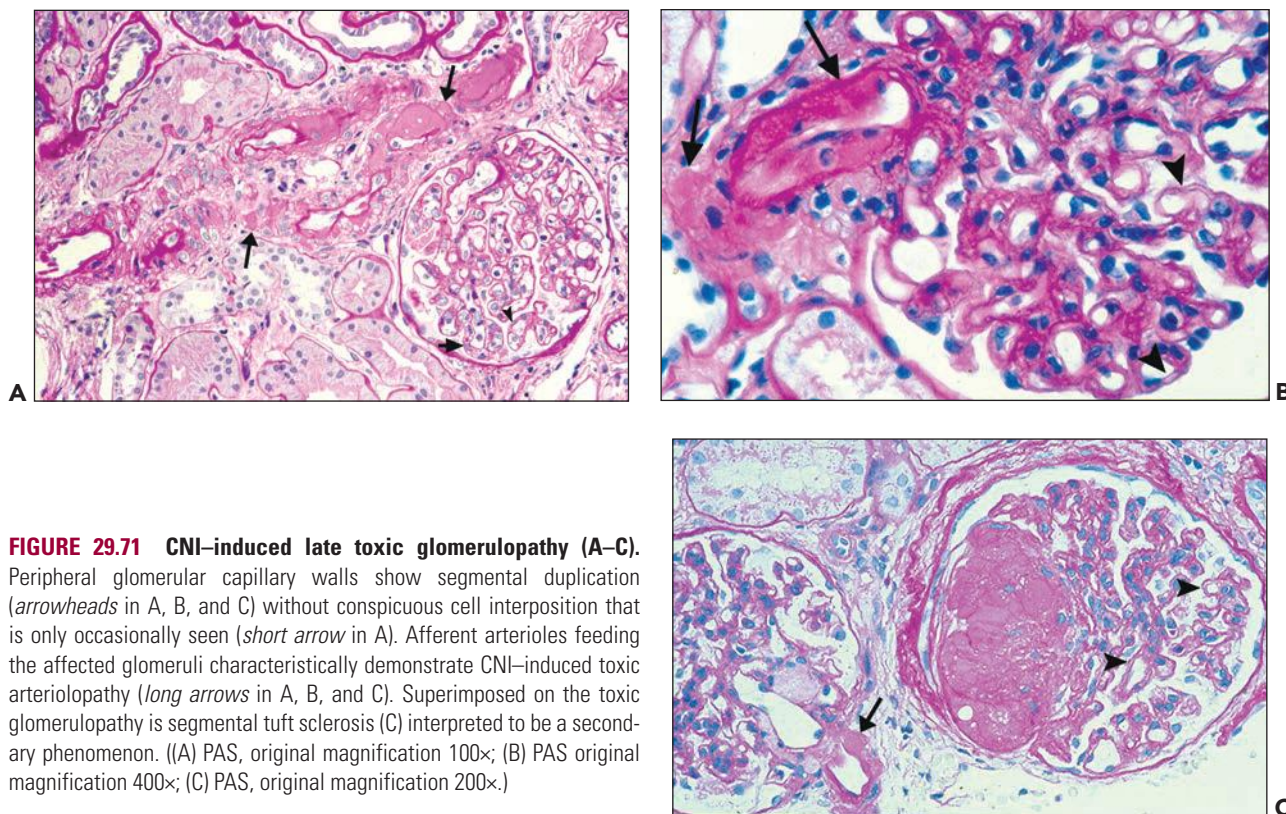


FIGURE 29.71 CNI-induced late toxic glomerulopathy (A–C). Peripheral glomerular capillary walls show segmental duplication (arrowheads in A, B, and C) without conspicuous cell interposition that is only occasionally seen (short arrow in A). Afferent arterioles feeding the affected glomeruli characteristically demonstrate toxic arteriopathy (long arrows in A, B, and C). Superimposed on the toxic glomerulopathy is segmental tuft sclerosis (C) interpreted to be a secondary phenomenon. ((A) PAS, original magnification 100 \times ; (B) PAS original magnification 400 \times ; (C) PAS, original magnification 200 \times .)

(see Fig. 29.71). In biopsies with CNI arteriopathy, CNI glomerulopathy occurred in 65% of those diagnosed as severe CNI arteriopathy, 25% to 45% of those diagnosed as mild to moderate, and in none of the biopsies lacking evidence of CNI arteriopathy (814,816). Other glomerular lesions possibly related to CNIs include FSGS that is most often seen in the setting of pronounced interstitial fibrosis, hyaline arteriopathy, or CNI glomerulopathy and most probably represents “secondary FSGS” due to nephron loss and “overload glomerulopathy” (see Fig. 29.71C). Distal to afferent arterioles with severe (stenosing) arteriopathy (i.e., aah-3), glomeruli might reveal atrophy, global sclerosis, or occasionally even collapsing FSGS (817) likely as a sign of ischemic podocyte injury (Fig. 29.73).

Tubules

The most common morphologic change linked to CNI toxicity is isometric vacuolization of the tubular epithelial cell cytoplasm that shows uniformly sized, small vacuoles (Fig. 29.74). The vacuoles, much smaller than the nucleus, contain clear aqueous fluid (unstained by H&E or PAS) and represent on electron microscopy dilated portions of the smooth endoplasmic reticulum (818). Tubular brush borders can remain intact. Although typically the entire cytoplasm of an affected tubular cell is densely packed with equal size vacuoles, they can be less abundant in the early phase of toxic injury. Under current therapeutic dose regimens, cytoplasmic vacuolization most often involves only scattered proximal tubules with predominance of the straight portion (818); the convoluted portion and parietal epithelial cells lining the Bowman space are only infrequently affected. Tubular epithelial cells with isometric vacuolization suggestive of toxic tubulopathy can occasionally

also be found in urine cytology specimens (819,820). The degree of vacuolization does not correlate well with CNI blood levels: the lesions are readily reversible under dose reduction.

Two other pathologic features in tubules have been linked to CNI toxicity, but they have little diagnostic value: giant mitochondria and dystrophic microcalcifications. Giant mitochondria are rare, even in cases with marked toxicity (814). They can be seen by light microscopy but are more easily appreciated by electron microscopy in proximal tubular segments (Fig. 29.75). Giant mitochondria, typically one per cell, are heterogeneously distributed in tubules and are characteristically absent in epithelial cells with isometric toxic vacuolization. They are often located close to the nucleus and can reach half its size. The diagnostic utility of the detection of giant mitochondria is marginal (814). Dystrophic microcalcifications (often not bigger than a tubular cell) can occasionally be found scattered throughout the nephron. They typically have a round or layered, “eggshell” appearance and are believed to arise as dystrophic calcifications from intratubular Tamm-Horsfall protein or secondary to toxicity-induced single epithelial cell necrosis (814); they are rather uncommon under modern CNI doses (821) and are nondiagnostic residues of acute tubular injury.

Interstitial

In acute toxicity, the interstitium is often normal and lacks inflammation or edema. If marked mononuclear inflammatory cells, tubulitis, and marked peritubular capillaritis are found, a concurrent acute rejection episode has to be considered.

CNI therapy contributes to scarring with striped interstitial fibrosis, tubular atrophy, and glomerulosclerosis that is mainly seen in biopsies with conspicuous CNI arteriopathies

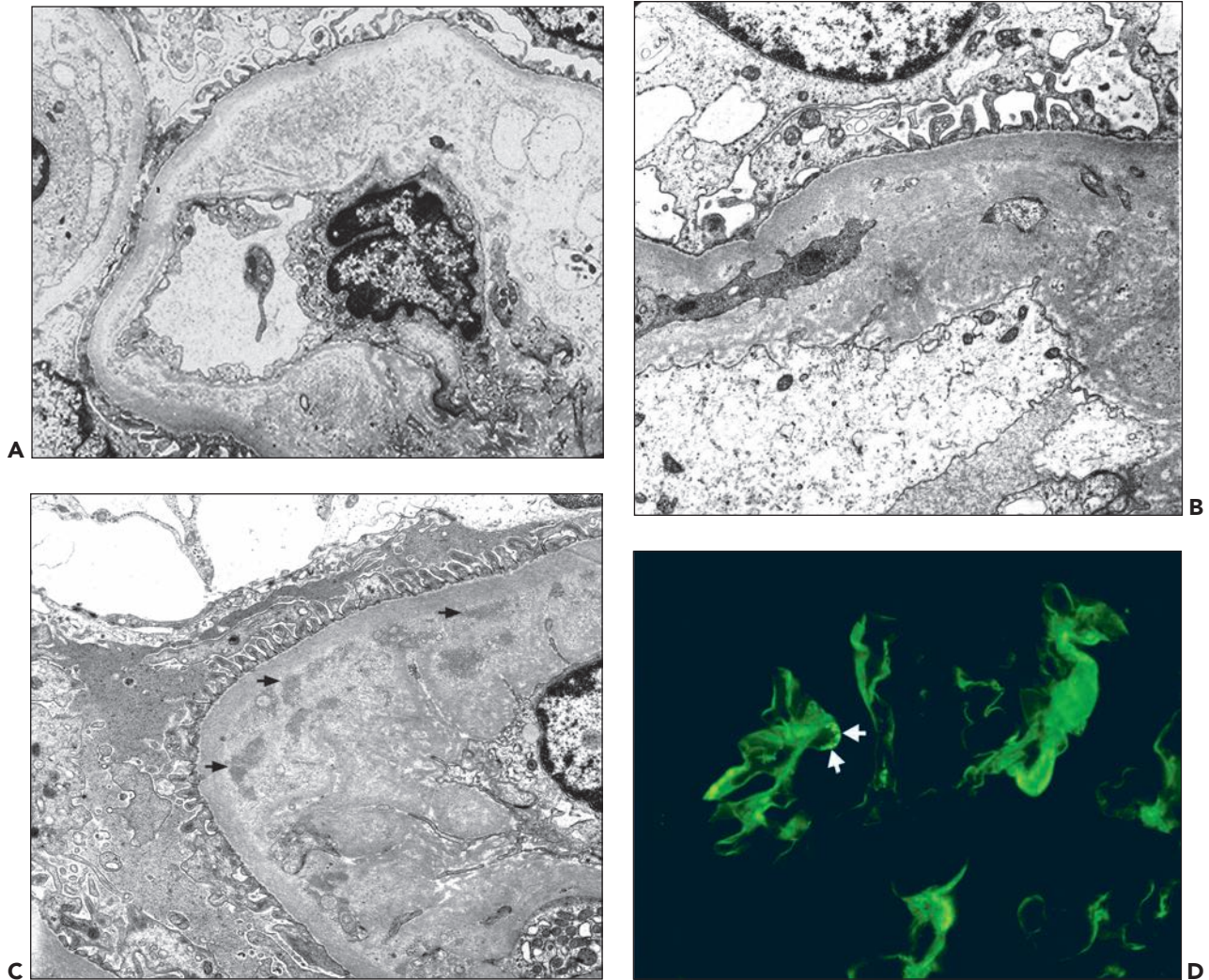


FIGURE 29.72 CNI-induced late toxic glomerulopathy. By electron microscopy, widening of the subendothelial compartment, the accumulation of flocculent material, and new basement membrane formation (sometimes wavy appearing, **B**) are noted. Occasionally, small, focal, and segmental electron-dense deposits are seen (*arrows* in **C**) associated with segmental minimal IgG staining by immunofluorescence microscopy (*arrows* in **D**). The deposits are characteristically inconspicuous and should not be misinterpreted as evidence of an immune complex-mediated glomerulonephritis. The overall changes of toxic glomerulopathies are reminiscent of the remodeling phenomena seen in cases of TMAs (e.g., the hemolytic uremic syndrome). (Electron photomicrographs: (A) 6500 \times , (B) 10,000 \times (C) 7500 \times . (D) Immunofluorescence microscopy with an antibody directed against IgG, original magnification 400 \times . (B, C, and D and Figure 29.74A are from the same case.)

and glomerulopathies (808,810,814). In native renal biopsies from patients suffering from psoriasis or uveitis under CsA therapy, significant IFTA were found when compared with age- and sex-matched controls (822). However, even though CNI-associated (striped) fibrosis is clinically significant and contributes to graft dysfunction, these changes are likely often caused by nephron loss of various etiologies and lack any diagnostic specificity (823).

Arterioles and Arteries

CNI-induced vascular lesions are found most characteristically in afferent arterioles. The arteriolar lesions can extend in severe cases into the glomerulus (i.e., signs of CNI-induced glomerulopathy) and into small arteries with up to two layers

of smooth muscle cells (824–826). Arcuate arteries are characteristically spared. Proliferative arterial intimal fibrosis, fibroelastosis, and transplant endarteritis are not features of toxicity.

Early CNI-induced arteriolar changes can show marked swelling, the so-called “ballooning”, of medial smooth muscle cells obscuring the normal vascular architecture (Fig. 29.76). The cytoplasm of the medial cells contains very large, clear vacuoles, caused by marked dilatation of the endoplasmic reticulum. These early changes are fully reversible on dose reduction. They can, however, progress to “classical” CNI arteriolar pathology with intramural hyaline deposits (see Fig. 29.68). Arteriolar medial “ballooning” as a sign of early CNI-induced toxicity should only be evaluated

TABLE 29.9 Differential diagnosis of calcineurin inhibitor–induced toxicity

CNI toxicity feature	Differential diagnosis	Features helping to exclude CNI toxicity
Tubulopathy with isometric vacuolization	Osmotic nephrosis	Clinical history of previous medications, for example, mannitol, IVIG solutions Electron microscopy showing phagolysosomes
Thrombotic microangiopathy (TMA)	Other causes of a TMA Antibody-mediated rejection	Clinical history of native kidney disease, other risk factors for TMA (e.g., drugs such as sirolimus) C4d positivity Marked peritubular capillaritis Detection of circulating DSA
CNI arteriopathy	Diabetes mellitus Hypertension Preexisting donor disease Chronic so-called vascular rejection Fabry disease	Clinical history Other diabetic changes, for example, nodular glomerulosclerosis, capsular drops Clinical history Concurrent arterial intimal fibroelastosis Dominant subendothelial arteriolar hyaline deposits Findings in zero-hour implantation biopsies Chronic rejection typically affects arteries, not afferent arterioles History and glomerular changes
CNI glomerulopathy	Other causes of a TMA Chronic TCMR/AMR (transplant glomerulopathy) Membranoproliferative glomerulonephritis	Clinical history of native kidney disease, other risk factors for a TMA (e.g., radiation, drugs) Concurrent chronic allograft arteriopathy (= chronic vascular rejection) Concurrent transplant glomerulitis Absence of marked CNI arteriopathy C4d positivity along peritubular capillaries Peritubular capillaritis Pronounced glomerular hypercellularity, proliferative changes, and cell interposition Marked immune complex–type deposits (often complement factor C3 dominant) Sometimes crescent formation Hematuria Marked proteinuria Decreased serum complement levels

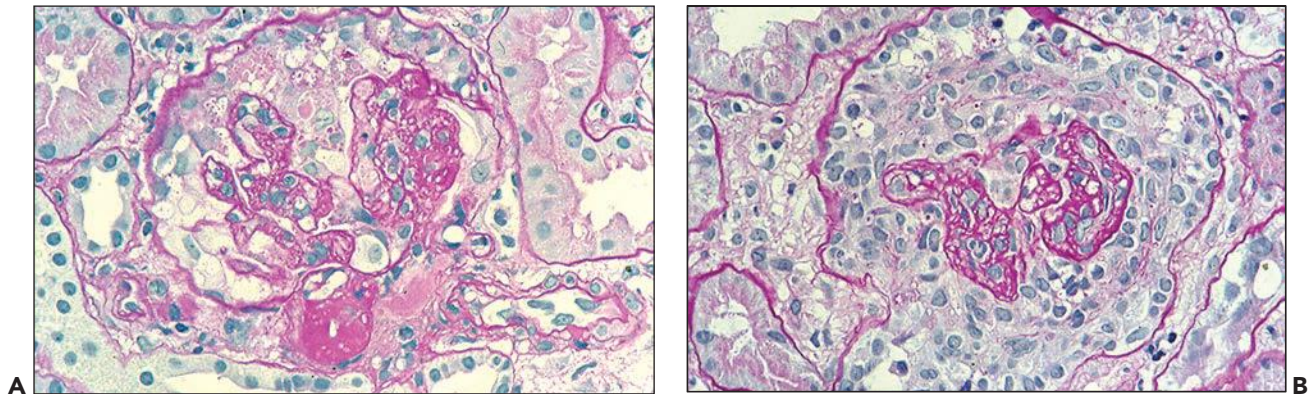


FIGURE 29.73 De novo collapsing focal and segmental glomerulosclerosis (A and B) in a patient with marked CNI–induced toxic arteriopathy 35 months after grafting. Glomerular capillary tufts appear condensed and collapsed with marked activation of the overlying podocytes (illustrated in B is a so-called pseudocrescent caused by podocyte crowding and proliferation). ((A and B) PAS, $\times 200$.)

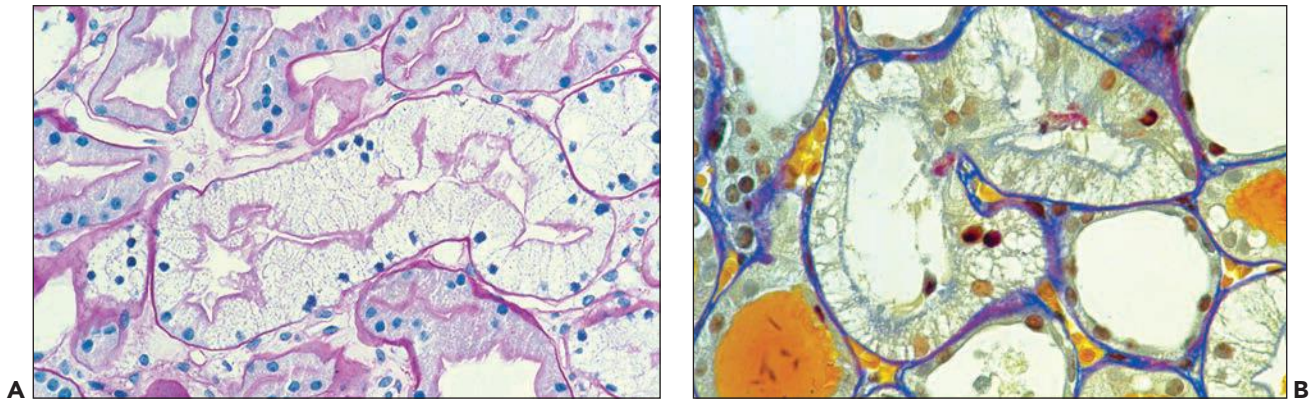


FIGURE 29.74 CNI-induced toxic tubulopathy (A) with isometric vacuolization of the proximal tubular epithelial cell cytoplasm. In comparison, ischemia-induced tubular injury (B) with nonisometric vacuolization of the tubular cytoplasm; this change should not be mistaken for toxic tubulopathy. ((A) PAS, original magnification 150 \times ; (B) trichrome stain, original magnification 250 \times .)

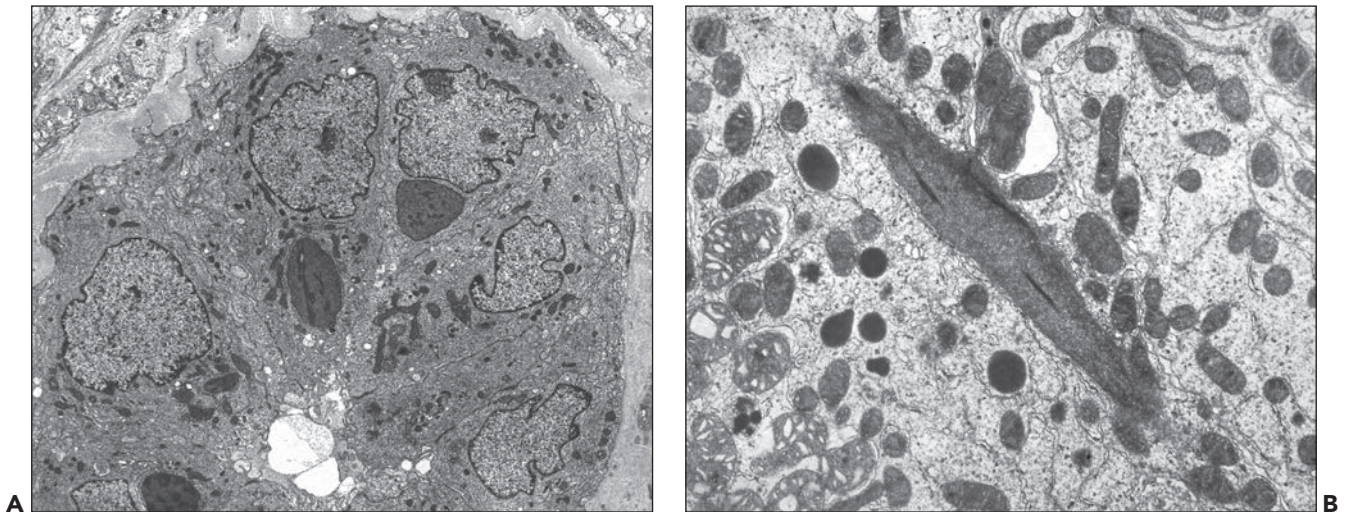


FIGURE 29.75 CNI-induced toxic tubulopathy with megamitochondria (typically one per cell). The mitochondria reach approximately one half the size of the nucleus (A) and display distorted cristae (B). Electron photomicrographs. ((A) original magnification 3000 \times ; (B) original magnification 14,000 \times .) (Courtesy of Michael Mihatsch, Basel, Switzerland.)

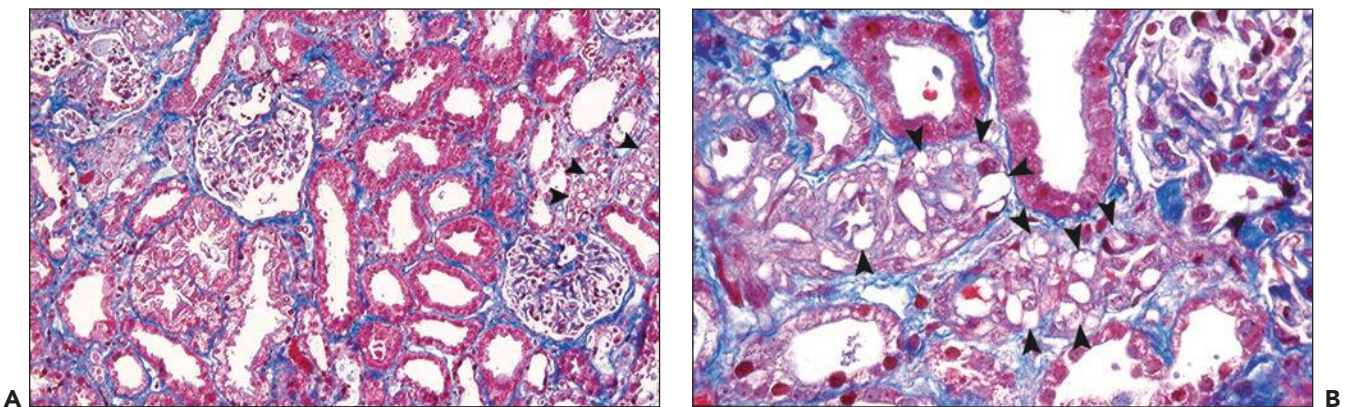


FIGURE 29.76 CNI-induced early toxic arteriopathy with swelling (so-called ballooning) of medial smooth muscles cells obscuring the vascular architecture (arrowheads in A and B). In this case, early toxic arteriolar changes are associated with isometric vacuolization of the tubular cytoplasm (A). ((A) trichrome, original magnification 100 \times ; (B) trichrome, original magnification 400 \times .)

in normal-appearing parenchymal zones, since identical changes are seen in severe ischemic renal injury or in some cases of the nephrotic syndrome presenting with nonselective proteinuria.

The classical morphology of late CNI arteriopathy has been described as “nodular protein deposits replacing single necrotic smooth muscle cells of the media...” (813), with a further descriptor of “occasionally in a pearl-like pattern” (see Fig. 29.69A) (825). Intramural hyaline nodules stain strongly in PAS incubations and can be most pronounced along the adventitial layer of renin-producing (afferent) arterioles. The severity of CNI arteriopathy varies considerably, even in the same biopsy. Some vessels may show only mild changes with few intramural/adventitial hyaline nodules, whereas others demonstrate advanced arteriopathy with segmental or circumferential hyalinosis, complete loss of medial smooth muscle cells, and stenosis (see Fig. 29.69). We now know that these changes are far less specific for CNI toxicity than originally thought (735,827,828).

The endothelial cell layers remain usually intact, even in severe cases, and fibrin thrombi are absent. Extensive fibrinoid arteriolar wall necrosis or inflammation is typically absent, and if present, a TMA or severe acute rejection has to be considered in the differential diagnosis. Identical arteriolar lesions presumed to represent CNI toxicity develop in native kidneys of patients who receive CsA or tacrolimus (707,810,829). There is no generally accepted scheme for scoring the severity of CNI-induced hyaline arteriopathy/toxicity; the “Banff 2007” ah-scoring system may be best suited for the task (Table 29.3) (155).

CNI arteriopathy with medial hyaline nodules can develop quickly over days to weeks; we saw an exceptional case as early as day 15 posttransplantation. Over time, CNI arteriopathy becomes more apparent (830) reaching an estimated 100% prevalence at year 10 in one historic series, that is, all transplants showed presumed structural CNI toxicity (739). However, under current low-dose CNI therapy, the overall prevalence of toxic arteriopathy has markedly decreased.

In most severe cases, CNI can induce a florid TMA with focal fibrin and platelet thrombi at glomerular vascular poles extending proximally into afferent arterioles and distally into glomerular capillaries (see Fig. 29.70A and B). Medial smooth muscle layers can show segmental necrosis. Other morphologic changes of toxicity, mainly arteriolar mucoid intimal thickening and edematous swelling, can occur but are uncommon. Similar to other forms of a TMA, vascular lesions can undergo remodeling with intimal sclerosis and occasionally even onion skinning. Toxic TMA with fibrin thrombi can resolve with *restitutio ad integrum* (see Figs. 29.68 and 29.70C).

Immunofluorescence Microscopy

By immunofluorescence microscopy, glomeruli with CNI glomerulopathy show nondiagnostic IgM and complement factor C1q, C3, C4d, and C5b-9 deposits. On rare occasions, focal and segmental minimal to mild (nondiagnostic) granular IgG, IgA, or light chains accumulate along peripheral basement membranes (Fig. 29.72D); such minor changes should not be misdiagnosed as evidence of an immune complex-mediated glomerulonephritis. Also in arteries, immunofluorescence microscopy is rather nonspecific with the accumulation of

IgM and the complement factors C1q, C3, C5b-9, and C4d in arteriolar hyaline deposits. In cases of CNI-induced TMA, fibrin deposits can be seen in the microvasculature. C4d is not detected along PTC. If peritubular C4d is found (and/or other histologic evidence of acute rejection such as transplant endarteritis), a diagnosis of concurrent acute rejection has to be considered.

Electron Microscopy

Ultrastructurally, glomeruli and arterioles show in the setting of CNI toxicity varying degrees of TMA-like remodeling ranging from minimal to marked (see Fig. 29.72). Most common are minor abnormalities. The endothelium of glomeruli is reactive with loss of fenestration. The lamina rara interna is widened and subendothelial new basement membrane/lamina densa-like material is formed, sometimes with a layered appearance due to repetitive endothelial cell injury (the ultrastructural correlate of GBM duplication seen by light microscopy). The newly formed subendothelial compartment can contain cell processes and occasional small, ill-defined (nondiagnostic) electron-dense deposits (see Fig. 29.72C). Glomerular injury in severe cases shows microthrombi and segmental mesangiolytic typical for florid stages of a TMA. In approximately 20% of cases of structural CNI toxicity and CNI glomerulopathy (lacking evidence of rejection), additional injury in PTC is seen with marked multilaminations of capillary basement membranes (224). Severe tubular CNI toxicity is ultrastructurally characterized by enlarged and irregularly outlined mitochondria with only few cristae and occasional crystalline material. The electron microscopic correlate for isometric tubular epithelial vacuolation seen by light microscopy is the presence of dilated smooth (and to a lesser degree rough) endoplasmic reticulum (818). CNI arteriopathy reveals ultrastructurally single smooth muscle cell necrosis. The necrotic cells are “replaced” by amorphous dense, granular material that protrudes into the adventitial layer (the ultrastructural correlate of hyaline nodules seen by light microscopy) (824,825,831).

Etiology and Pathogenesis

CsA and tacrolimus bind to intracytoplasmic receptor proteins, the immunophilins, a family of peptidyl-prolyl cis-trans isomerases that include the cyclophilins (for binding of CsA) and FK-binding proteins (for tacrolimus), both with rotamase activity (832–838). The immunophilin/CsA or tacrolimus complexes have a high affinity to bind and thereby inhibit calcineurin, a phosphatase (838). Calcineurin physiologically dephosphorylates intracytoplasmic nuclear regulatory proteins in lymphocytes (i.e., NFAT, nuclear factors of activated T cells) and hence facilitates their translocation into the nucleus and activation as intranuclear transcription factors for various mediators (such as IL-2, IL-4, interferon-gamma, and tumor necrosis factor- α). Calcineurin typically promotes T-cell activation. In therapeutic doses, CsA and tacrolimus block approximately 50% of the calcineurin activity. They do not affect neutrophils, phagocytosis, or the bone marrow, thus still allowing for an effective overall immune response.

A key question is whether the immunosuppressive and nephrotoxic effects of CNIs are related to inhibition of the isomerase enzymatic activity of calcineurin. Elegant studies with dozens of CsA analogs showed that immunosuppression

potency and acute nephrotoxicity are inseparable. These data suggest that the transduction pathways important for immunosuppressive activity are similar to the ones that cause nephrotoxicity and that there is little hope for finding a variant that separates these effects (839). The likely common mechanism of action for both immunosuppression and toxic side effects is the inhibition of calcineurin.

Overall nephrotoxicity correlates best with peak CNI blood levels (739) and less with trough levels (815). CsA trough levels above 400 ng/mL predicted CsA toxicity with a specificity of 89%, but a sensitivity of only 32%. Of note, 63% of episodes of nephrotoxicity and 59% of the acute rejection episodes occurred at “therapeutic” CsA levels of 150 to 400 ng/mL. Al-Awwa et al. (60) reported that more than 75% of all histologic diagnoses of either CsA or tacrolimus-induced structural toxicity were made in the clinical setting of low or therapeutic blood drug levels. The imperfect correlation between trough levels and histologically diagnosed structural toxicity may be because the biopsy diagnosis of “late” structural toxicity is established long after peak toxic drug levels caused injury to arterioles and glomeruli. In addition, individuals differ in metabolism, absorption, and sensitivity to the toxic side effects. Factors known to contribute include polymorphism of P-glycoprotein (840) or variation in the level of cytochrome p450 (841–842). A further contributing factor is the relative difficulty with which a firm diagnosis of structural CNI toxicity is made, particularly in mild cases, thereby hampering correlative studies.

CNI significantly affects smooth muscle cells of the media leading to vasoconstriction, which can already be seen after the first oral dose. CsA can cause a slow contraction of isolated aortic smooth muscle cells, which can be inhibited by a calcium channel blocker. CsA causes hypersensitivity to angiotensin II, by increasing the permeability of the plasma membrane to Ca^{2+} (843), which can be inhibited with atrial natriuretic peptide *in vitro* and by a calcium channel blocker (diltiazem) *in vivo* (844,845). The elevation of cytosolic free calcium is associated with an increase in the production of endothelin (844). CsA stimulates the synthesis and release of endothelin 1, a vasoconstrictor, from cultured human and rat vascular endothelial and smooth muscle cells (846–849) and the transcription of endothelin 1 mRNA in the rat renal medulla (850). In isolated rat arterioles, CsA induces endothelin-mediated vasoconstriction (851), whereas the blockage of endothelin receptors counteracts the vasoconstrictive effects (851–853). Cultured endothelial cells secrete increased amounts of endothelin in response to 100 ng/mL CsA (847).

CNI can cause necrosis of individual smooth muscle cells, as shown in animal studies (854). In one model of CNI-induced toxicity, injury to muscle cells was first detected at day 10 as an accumulation of eosinophilic granular material in afferent arterioles (855). The disease process progressed over the next 25 days with focal smooth muscle cell vacuolization and the accumulation of discrete hyaline deposits in vessel walls (855,856). Electron microscopy demonstrated an increased accumulation of renin granules in the smooth muscle cell cytoplasm, corresponding to the eosinophilic granular transformation seen histologically. Increased renin was also demonstrated by immunocytochemistry. The inhibition of type I angiotensin II receptors with losartan (but not other antihypertensives, hydralazine, and furosemide) inhibited the development of CNI-induced arteriopathy in rats (857).

Regeneration of medial smooth muscle cells in arterioles is typically very limited. Thus, CNI-induced necrosis of single medial smooth muscle cells is usually repaired by insudation of plasma proteins into the necrotic foci. This gives rise to intramural hyaline deposits and the classical morphology. In native kidneys, structural CNI-induced arteriopathy may potentially be enhanced due to the intact sympathetic innervation (810).

CNI also affects the endothelium since it shifts the balance of arachidonate pathways toward vasoconstriction and thrombosis (increased thromboxane A2 levels) and decreased vasodilation and antithrombosis (decreased prostaglandin and prostacyclin levels) (858,859). Experimentally, CsA toxicity is inhibited by thromboxane A2 antagonists. The rise in circulating levels of von Willebrand factor including the unusually large multimer secreted by endothelial cells (860), tissue plasminogen activator, and PAI-1 was correlated with the severity of TMA in bone marrow recipients on CNI therapy (861). Further evidence that CsA causes endothelial injury was the finding of elevation of plasma concentrations of factor VIII-related antigen in renal allograft recipients during CNI nephrotoxicity, which fell toward normal as the dose of CsA was reduced (862). In cultured renal tubular cells, CsA promotes the so-called epithelial-mesenchymal transformation, including the increased production of TGF- β and activation of the protein kinase C pathways (863).

Differential Diagnosis

The major differential diagnoses of CNI structural toxicities are listed in Table 29.9. In order to establish the cause of arteriolar hyalinosis, implantation/zero-hour and early post-transplant biopsies should be reviewed for potential preexisting hypertension-induced donor disease. Biopsies taken years after grafting often show combined hypertensive and toxic CNI arteriopathies (i.e., a combination of subendothelial and medial/adventitial hyaline deposits). When considering a diagnosis of CNI toxicity, it is important to remember, as pointed out in a recent editorial comment, that there is “...no such thing as a specific histological diagnosis of structural CNI toxicity...” and findings have to be interpreted in the clinical context (864). Toxic changes can coincide with other diseases, such as rejection, infections (PVN), or glomerulonephritides. C4d is characteristically not detected along PTC in CNI-induced toxicity including TMAs; its presence in ABO-compatible grafts indicates AMR (865).

Glomerulopathy

The detection of duplicated GBM in renal transplants raises three major differential diagnoses (see Table 29.9): a late phase of a TMA not induced by CNI (e.g., recurrent disease or caused by other drugs), MPGNs, and transplant glomerulopathy in the setting of chronic TCMR or AMR. TMA of other causes can only be diagnosed on clinical grounds including detailed knowledge of the underlying native kidney disease that had resulted in renal failure. MPGN is characterized by glomerular hypercellularity, an accentuation of the tuft lobulation including conspicuous cell interpositions, and the accumulation of abundant immune complex-type deposits detected by immunofluorescence and electron microscopy (Fig. 29.77). The urine sediment is often active with dysmorphic hematuria. Transplant glomerulopathy in the setting of chronic rejection is very similar, but not identical, to CNI-induced

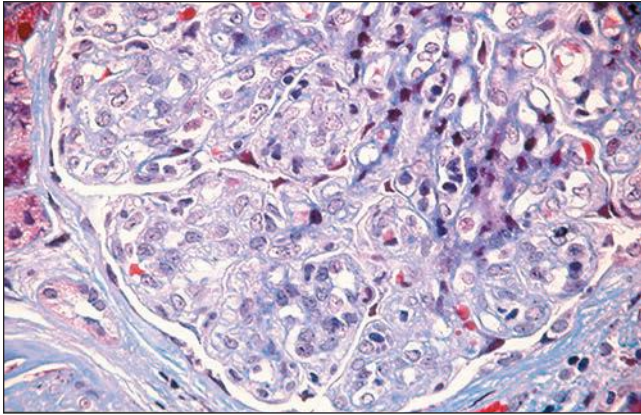


FIGURE 29.77 Membranoproliferative glomerulonephritis type I (MPGN-I). The differential diagnosis of a CNI-induced late toxic glomerulopathy includes a MPGN that usually presents with global hypercellularity of glomerular capillary tufts, accentuation of the tuft lobulation, and conspicuous cell interpositions along duplicated GBM segments. The MPGN pattern is commonly quite different from a toxic glomerulopathy. (Trichrome, 400× original magnification.)

glomerulopathy. Rejection-induced transplant glomerulopathy often also shows other evidence of rejection-induced injury, such as transplant endarteritis, transplant glomerulitis (57% to 90% of cases), peritubular capillaritis, or C4d deposits along PTC (36% to 53% of cases) (150,160,634). CNI-induced toxic glomerulopathy typically does not show evidence of active rejection, but rather demonstrates marked CNI arteriolopathy in the afferent arterioles. Marked multilaminations of PTC basement membranes are more common in rejection-induced transplant glomerulopathy (approximately 70% to 80% of cases) as compared to CNI toxicity and glomerulopathy (approximately 10% to 20% of cases). The absence of marked PTC basement membrane multilaminations in a graft biopsy could be used to suggest absence of chronic rejection and thereby indirectly favor a potential diagnosis of CNI glomerulopathy in the right setting (224). Combination of chronic TCMR or AMR and CNI toxicity also occurs and can be diagnosed by the presence of the distinctive lesions of each type.

Tubular Lesions

Isometric tubular epithelial vacuolization is characteristic, but not pathognomonic of CNI-induced tubulopathies, because identical light microscopic changes can be seen in a variety of diseases, including fatty changes in the setting of the nephrotic syndrome or cases of osmotic nephrosis following therapy with plasma expanders (such as mannitol or dextran), contrast media, sucrose-rich hyperimmune globulin, or IVIG solutions (866–868). In contrast to CNI-induced tubulopathy, however, these cases typically demonstrate dilated phagolysosomes rather than a dilated endoplasmic reticulum by electron microscopy. Phagolysosomes in nephrotic syndrome contain fat. Nonisometric and irregular intracytoplasmic tubular vacuoles of different sizes should not be interpreted as evidence of toxic tubulopathy (see Fig. 29.74); they are commonly seen in various forms of tubular injury, mainly ischemia. Late after grafting, tubular vacuolization may be seen in scattered

atrophic-appearing tubules located in zones of fibrosis; these changes are of undetermined etiology and significance.

Several other morphologic changes can be seen in patients treated with CNI that are considered to be nondiagnostic of structural toxicity. Acute tubular injury and congested peritubular capillaries containing mononuclear cell elements pronounced at the corticomedullary junction are often seen in acute renal failure of different etiologies (869). Giant mitochondria in tubular epithelial cells are present in ischemia; they typically appear “lysed and empty.” Dystrophic calcifications can be seen after pronounced ischemic acute tubular injury and necrosis (donor disease and/or posttransplantation following ischemia/reperfusion injury), in the setting of hypercalcemia or possibly even subsequent to bowel cleansing procedures with phosphate-rich solutions (a treatment strategy now abandoned) (740,870,871). In these latter conditions, the calcifications are often large and irregular, and they sometimes even involve basement membranes.

Arteriopathy

Arteriolar hyalinosis is very common in patients suffering from long-standing hypertension or diabetes mellitus. Arteriosclerosis in the setting of hypertension often (but not always) differs from late CNI-induced arteriolopathy, because it has predominately subendothelial hyaline deposits that are commonly covered by an intact although sometimes atrophic medial smooth muscle layer (Fig. 29.69C). Intramedial and transmural hyaline deposits can occur in patients suffering from hypertension, but they are less frequent (827,828).

Peripheral/adventitial arteriolar hyaline nodules are suggestive of CNI-induced toxicity (814), although they are not pathognomonic. These nodules can be relatively rare, and detection may require meticulous study of multiple sections. When the arteriolar hyalinosis has discrete nodules of similar size and location of medial smooth muscle cells, then CNI-type toxicity should be considered. Peripheral/adventitial nodules are rarely found in nontransplant cases not treated with CNI; the only other settings are untreated cases of Fabry disease or TMAs of etiologies other than CNI toxicity including malignant range hypertension (personal observations). Since kidney transplant recipients treated with CNIs often also suffer from arterial hypertension or diabetes mellitus, injury can be synergistic and lead to combination lesions. Michael Mihatsch refers to such late changes as “arteriopathies of the mixed conventional hypertensive and toxic CNI types” (personal communication). Arterial intimal sclerosis (in vessels larger than arterioles) and inflammation are not features of CNI toxicity.

Clinical Presentation, Prognosis, and Therapy

Patients treated with CNI commonly present with a decreased glomerular filtration rate and evidence of arterial hypertension, and patients with CNI-type glomerulopathy with proteinuria. Functional and early structural toxicities often reverse upon reduction or discontinuation of CNI therapy, and even toxicity with protracted oliguria (for 21 to 83 days posttransplantation) usually vanishes (872). Isometric vacuolization is readily reversible (see Fig. 29.68) (873).

Chronic renal failure can occur after long-term use of CNIs (825); it was more prevalent in previous years under higher CNI doses. In pediatric heart transplant patients, 3.2% of 125 recipients developed chronic renal failure years

postgrafting (874). Ojo et al. (875) found chronic renal failure (defined as a glomerular filtration rate of ≤ 29 mL/min/1.73 m² of body surface area) in 16.5% of 69,321 recipients of nonrenal organ transplants during the period of 1990–2000; 29% of these patients (3,297) went on to end-stage renal disease (dialysis or transplantation). The cumulative rate of chronic renal failure was 20% and 25% at 10 years for heart and liver transplant recipients, respectively. However, no pathology was provided, so that the cause of renal failure was not proved to be CNI toxicity. Other studies indicate that hypertension and hyperlipidemia are probably factors contributing to chronic renal failure in the setting of CNI therapy (810,875).

Regression of CNI hyaline arteriolopathy has been reported (739,876,877). In mild to moderate forms, discontinuation of CsA is followed by arteriolar remodeling and morphologic resolution of the intramural hyaline deposits in a substantial number of patients (55% of 20 renal allografts), as judged by repeat biopsies after 6 to 18 months (Fig. 29.78) (877). This arteriolar remodeling is characterized by structural irregularities in the medial smooth muscle layer and an increased deposition of basement membrane–like material (“unorganized appearance”; see Fig. 29.78B). Even circumferential arteriolar hyaline deposits may occasionally undergo resolution and repair (876). The most convincing evidence of regression of CNI-induced arteriolopathy was demonstrated in rats following the discontinuation of CsA for 2 months (856).

CNI arteriolopathy does not necessarily indicate poor long-term prognosis. Serum creatinine levels improve in most patients on dose reduction (likely in part due to functional toxicity and vasoconstriction), and drastic changes to the immunosuppressive drug regimens are not imperative. In a recent pathology-based series, CNI toxicity accounted for less than 1% of all renal allograft losses (496).

CNI-induced TMA is generally an early event occurring within the first few weeks postgrafting (range, 2 to 56 days) (878–880) with only sporadic cases later (881,882). While the precise mechanisms are not known, a causal role of CNI is clear, in that rechallenge with CsA can precipitate a recurrence of the

TMA (883). In kidney transplant recipients, a CNI-induced TMA may be limited to the renal allograft without systemic symptoms (i.e., absence of hemolysis, schistocytes, or low platelet counts), and it can present clinically with rapid onset of graft dysfunction (884). Among reported cases, thrombocytopenia was present in 33% to 64% and hemolytic anemia in 86%; LDH elevation occurred in 95% (879). Sometimes, TMA-like symptoms induced by CNI therapy can clinically be missed before biopsy if not specifically sought (879).

The incidence of TMA has significantly diminished since CsA was introduced (865). CsA-associated TMA caused graft loss in 8% of 200 consecutive renal allografts in the early 1980s (accounting for 40% of those that failed) (885). Series of patients from the last 20 years reported an incidence of 0.9% to 14% (879,880,884,886–889), representing 26% of all cases of TMA after renal transplantation (acute rejection, probably AMR, accounted for 53% and recurrent TMA for 16%) (887). Similar findings were recently reported from the Ohio State University with de novo TMA diagnosed in 6.1% of renal allograft recipients, mainly caused by AMR (55% of cases) (865).

The treatment of CNI-induced TMA includes the discontinuance or reduction of CsA/tacrolimus (sometimes with a switch to sirolimus) and, occasionally, therapeutic intervention with plasmapheresis, IVIG, or thrombolytic agents (878,879,889,890), with an overall graft salvage rate of 80% to 90% (878,880,890). If outcome is stratified into renal-limited forms of a TMA and systemic generalized variants, graft survival rates were 100% in the former group (with reduction, temporary discontinuation, or conversion of CNI therapy) and 62% to 90% in the latter cohort (including plasmapheresis as a treatment option) (886,889). CNI-induced TMA is (sometimes) fully reversible with resolution of fibrin thrombi and restitutio ad integrum as demonstrated in follow-up repeat biopsies (873,880) (see Fig 29.70). In one study, even onion skin arteriolar lesions disappeared in three of three patients in repeat biopsies and three of five patients showed loss of subendothelial fibrin deposits (873). Other series, however, reported less favorable outcome (even in renal-limited forms of CNI-induced

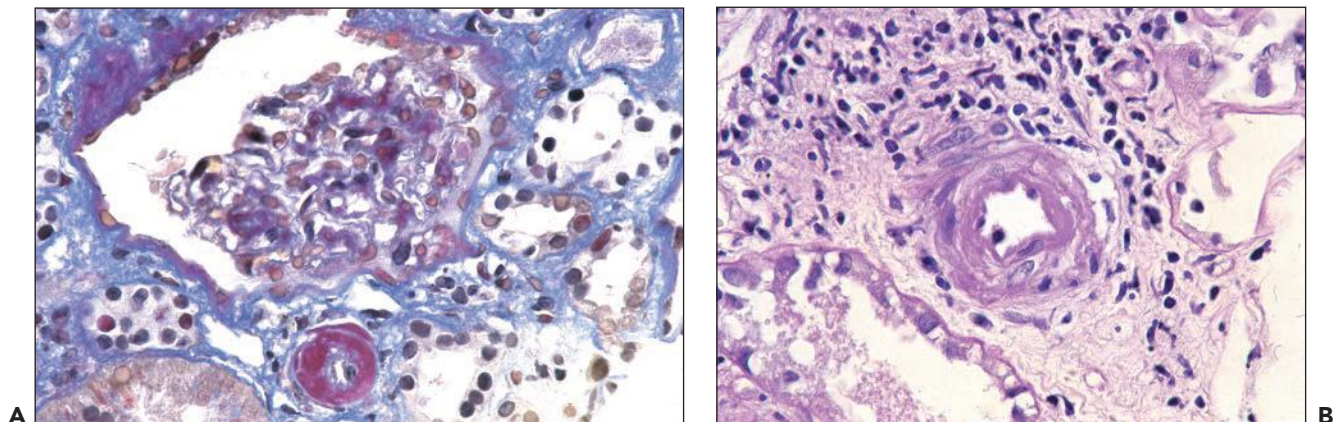


FIGURE 29.78 Regression of a CNI-induced late toxic arteriolopathy (A and B). Forty weeks after transplantation, typical signs of a toxic arteriolopathy are seen (*red* staining hyaline deposits in A) in a patient treated with CsA. Discontinuation of CsA therapy resulted in almost complete resolution of the hyaline deposits (B). The repeat biopsy was taken 92 weeks after transplantation; it shows arteriolar wall remodeling with structural changes including irregularly arranged medial smooth muscle cells. ((A) Trichrome, original magnification 200 \times ; (B) PAS, original magnification 400 \times .) (Courtesy of Michael Mihatsch, Basel, Switzerland.)

TMA) with an overall graft survival rate of only 69% (884). Surprisingly, most renal transplant recipients (60% to 90%) tolerate the reintroduction of CNI (878,880,889,891–894), and some were successfully converted to tacrolimus, with an overall salvage rate of 92%. It is curious that switching from CsA to tacrolimus is sometimes successful in treating a TMA, even though both drugs act via very similar pathways (884,888,895).

OTHER DRUG-INDUCED DISEASE IN ALLOGRAFTS

All drugs known to have nephrotoxic side effects in the native kidneys can induce identical changes in the renal allograft (see Chapter 25 on tubulointerstitial nephritis in native kidneys). Drugs, such as IVIG or hyperimmune globulin solutions (due to the high sucrose content) as well as mannitol or dextran, can induce isometric vacuolization of tubular epithelial cells (i.e., osmotic nephrosis) very similar to the type of changes seen with CNI-induced toxic tubulopathies (867,896). Here, we will provide limited information relevant for the interpretation of kidney transplant specimens.

Drug-Induced Acute Tubulointerstitial Nephritis

In general, allergic types of acute interstitial nephritides induced by various drugs (such as trimethoprim-sulfamethoxazole and others) can cause great problems for the pathologist since the morphologic changes are identical to those seen in cases of tubulointerstitial cellular Banff type I rejection. This is one reason why acute allergic interstitial nephritis is rarely recognized after kidney transplantation (897). The other reason is that steroids used for immunosuppression inhibit allergic reactions. The temporal relationship between drug administration and the onset of allograft dysfunction and the development of rash, fever, or eosinophilia may provide clues for differentiating allergic nephritis from rejection. Close clinical correlation in the truest sense is required.

Both allergic interstitial nephritis and tubulointerstitial cellular rejection demonstrate patchy mononuclear cell infiltrates (often with small clusters of plasma cells), eosinophils in variable numbers, edema, some degree of peritubular capillaritis, tubulitis, and tubular injury. Acute cellular rejection occasionally has a prominent eosinophilic infiltrate, particularly in the setting of transplant endarteritis (194,195,197,198,898,899), or can be rich in plasma cells; conversely, drug-induced interstitial nephritis may have no eosinophils but plasma cells instead, especially in cases due to nonsteroidal anti-inflammatory drugs. If the inflammatory cells predominate at the corticomedullary junction/outer medulla (and spare the cortex), allergic interstitial nephritis is most likely (897). The detection of ill-formed, small, nonnecrotizing granulomas may serve as a further diagnostic clue for the diagnosis of allergic nephritis in some cases. If tubulointerstitial inflammation, even with abundant eosinophils, is accompanied by additional typical signs of rejection (e.g., transplant endarteritis, glomerulitis, C4d accumulation along PTC), then a diagnosis of rejection must be made. Often, however, it is impossible to make a clear distinction based on morphologic criteria. In those cases, it seems best to “err on the side of rejection” and initiate antirejection therapy with bolus steroids that will help to decrease all tubulointerstitial inflammatory cell infiltrates and will prevent the long-term detrimental effects of untreated rejection.

Rapamycin-/Sirolimus-Associated Toxic Effects

Rapamycin (sirolimus, everolimus, rapamune) is a newer immunosuppressive agent increasingly used since the late 1990s to permit lower steroid and/or CNI exposure and to potentially limit chronic graft injury with fibrosis by inhibiting the proliferation of mesenchymal cells (900–902). Rapamycin is a macrolide antibiotic that was isolated from *Streptomyces hygroscopicus*. Rapamycin, in conjunction with the FK-binding protein, binds to a protein named mTOR (mammalian target of rapamycin), a kinase that controls the phosphorylation of proteins and thereby regulates mRNA translation of cell cycle regulators. Various cytokine- and growth factor-stimulated signals on cell proliferation (mainly, the progression from G1 to S phase) and on cell differentiation are inhibited (903). Rapamycin blocks the production of vascular endothelial growth factor (VEGF) via mTOR, and it can induce endothelial cell death and thrombosis in tumor vessels (904–906). Potentially, alterations of the VEGF expression in podocytes can promote the development of proteinuria seen in some patients (907). By IHC mTOR was found ubiquitously in epithelial, mesenchymal, and epithelial renal cells with the highest staining intensity in tubular cells of the distal nephron (784).

In 2003, Smith and coworkers reported a new type of tubular injury that they had observed in 55% (12 of 22) of patients under rapamycin therapy (Fig. 29.79) (784). All of the patients had experienced prolonged episodes of DGF of more than 3 weeks duration without signs of acute rejection. The tubules demonstrated histologic signs of acute injury, intratubular amorphous eosinophilic cast material with fracture lines, influx of histiocytes, and the formation of multinucleated giant cells, closely resembling “myeloma cast nephropathy.” However, in contrast to myeloma, the casts contained keratin (remnants of epithelial cells) rather than light chains. Upon withdrawal of rapamycin and tacrolimus, resolution of the casts and functional recovery were noted after 2 weeks in 3 of 3 patients. This

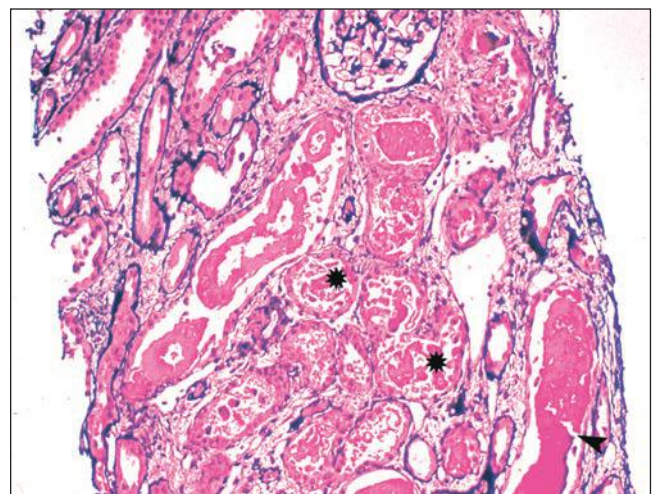


FIGURE 29.79 Toxic changes associated with rapamycin therapy. The tubules show signs of acute injury and contain abundant amorphous, proteinaceous cast material, partially coarsely granular (*asterisk*), partially cylindrical with a fracture line (*arrowhead*). (Methenamine silver, original magnification 100 \times .) (Courtesy of Kelly Smith, Seattle, WA.)

side effect seems to be exceptionally rare (we have not seen any cases in our practice) and most likely represents a combined toxic effect of two drugs: rapamycin and a CNI.

Proteinuria is another complication attributed to rapamycin with an unknown mechanism. Reversible proteinuria occurs in about 30% of patients and can be in the nephrotic range (907,908). Some patients on mTOR inhibitors have developed FSGS (909). One case showed no foot process effacement and no tubular reabsorption droplets, arguing for a tubular mechanism of the proteinuria (910). This fits with the tubular toxicity noted above and studies of protein overload in the rat, in which rapamycin increases cast formation (911).

Rapamycin is also associated with TMA (912), possibly secondary to decreased renal production of VEGF (913). On the other hand, rapamycin has been successful in preventing recurrent TMA/HUS (914). Rapamycin can show various other side effects, including leukopenia, anemia and thrombocytopenia, hyperlipidemia, diarrhea, mouth ulcers, cardiac arrhythmias, and impaired wound healing (900,915,916).

INFECTIONS

Many infections can affect immunosuppressed renal allograft recipients either as systemic or organ-limited disease. Some infections, such as PVN, are restricted to the kidney transplant. The following section will focus on the most important infections found in renal allografts; posttransplant lymphoproliferative disorders (PTLD) are discussed later in this chapter.

Polyomavirus Nephropathy

Introduction

Polyomaviruses are double-stranded, nonenveloped DNA viruses of approximately 5300 base pairs with substantial gene homology. Polyomaviruses are ubiquitous and have specifically

adapted to their hosts during evolution. After primary infections, polyomaviruses commonly establish lifelong clinically asymptomatic latency, often in renal tubular and transitional cells (renal pelvis, ureters, urinary bladder).

In recent years, transitional and renal cell carcinomas associated with polyoma BK virus have been described in few patients. These tumors arise in renal allograft recipients either in the transplanted kidney or along the urothelium, such as the bladder. The tumors strongly express the polyoma T antigen; however, there is no compelling evidence of productive BK virus replication, that is, VP polyomavirus capsid proteins are not expressed, and electron microscopy does not show mature virions in tumor cells. These neoplasms are currently under further investigation. The intriguing observations may potentially provide evidence for the oncogenic role of polyoma BK virus in some patients (917–921).

Better characterized are inflammatory disease processes caused by the replication of polyomaviruses in intensely immunocompromised patients, especially in kidney transplant recipients (polyomavirus nephropathy, PVN) and in AIDS patients (progressive multifocal leukoencephalopathy) (922). PVN has also been found in animals (923,924).

PVN is defined morphologically and pathologists play a crucial role in patient management (141). A diagnosis requires histologic evidence of an intrarenal, productive polyomavirus infection in the medulla and/or cortex. Polyomavirus replication can be identified by standard light microscopy and the presence of intranuclear viral inclusion bodies or in early disease stages lacking inclusions also solely by IHC or alternatively by in situ hybridization (Table 29.10 and below). In rare cases, only electron microscopy might show evidence of polyomavirus replication and allows for a diagnosis (925). Thus, a definitive diagnosis of PVN is not established by laboratory tests, such as the level of viremia, but rather requires a renal biopsy. The definition of PVN and the diagnostic approach

TABLE 29.10 Histology of selected viral lesions in allografts: diagnostic clues

	Polyomavirus ^a	Cytomegalovirus	Adenovirus	EBV-PTLD
Viral inclusion type				
Smudgy/ground-glass nuclear	++ ^b	+	++	–
Central nuclear with halo	+ ^b	+++	+	–
Cytoplasmic	–	+	±	–
Sites of viral replication/ staining				
Tubular epithelial cells	+++	+++	+++	–
Endothelial cells	–	++	–	–
Inflammatory cells	–	±	++	+++
Acute tubular injury/necrosis	absent –+++	+ –+++	+++	±
Focal parenchymal necrosis	–	±	+ –+++	± –+++
Interstitial hemorrhage	–	–	+	±
Granuloma formation	absent –+ ^c	±	+ –+++	–
Interstitial inflammation	absent –++	+ –+++	+ –+++	+++

^aPolyomavirus infections are mainly caused by the BK virus strain, rarely by JC virus, and hardly ever by SV40 virus.

^bSome early cases of polyomavirus nephropathy do not show intranuclear viral inclusion bodies; evidence of polyomavirus replication is only found by IHC (positive SV40-T staining) or by in situ hybridization.

^cPolyomavirus nephropathy can show ill-defined nonnecrotizing granulomas, sometimes located in injured and distended tubules.

Modified from Singh HK, Nickeleit V. Kidney disease caused by viral infections. *Curr Diag Pathol* 2004;10:11–21.

follow paradigms previously established for other viral infections, in particular CMV (926). Possibly in the future, a new biomarker for PVN, the urinary polyomavirus-Haufen test, can allow for a noninvasive diagnosis without a biopsy procedure (927). Since potent antiviral drugs to treat PVN are not available, much emphasis is placed on patient screening and a diagnosis in an early disease stage that responds favorably to reduction of maintenance immunosuppression.

Pathologic Findings

GROSS PATHOLOGY

Kidneys lost to polyomavirus infections are generally slightly decreased in size and firm with an ill-defined corticomedullary junction and a granular surface. The gross abnormalities are nondiagnostic and similar to other disease entities resulting in diffuse fibrosis and atrophy.

LIGHT MICROSCOPY

Two histologic changes are commonly seen in PVN: (i) intranuclear viral inclusion bodies in epithelial cells and (ii) virally induced tubular epithelial cell injury and lysis (362,928–931). Polyomaviruses use the proliferative “machinery” of the host cells for replication. Thus, intranuclear viral inclusion bodies in tubular and collecting duct epithelial cells are a typical sign of a productive viral infection found in the majority of cases (see Table 29.10) (928,929,931). Cytoplasmic viral inclusions are not found. Four distinct types of virally induced nuclear changes exist that can be seen side by side and next to many “hybrid variants” (362,929,930) (Fig. 29.80): type 1, an amorphous basophilic ground-glass inclusion body (the most common form); type 2, a central, eosinophilic, granular inclusion surrounded by a mostly incomplete halo (a rare form); type 3, a finely granular variant without a halo; and type 4, a

vesicular variant with coarsely clumped, intranuclear virions. These changes are (at least in part) due to different patterns of intranuclear viral aggregation, that is, evenly dispersed virions cause type 1 inclusions and crystalloid aggregates are the ultrastructural correlate of “coarsely clumped material” seen in type 2 and 4 alterations (Fig. 29.81). Most easily discernible by light microscopy are type 1 and 2 inclusions. PVN typically involves renal tubules and collecting ducts in a focal fashion, and occasionally, virally induced changes are limited to distal nephrons and the medulla. In one study, 37% of biopsies with multiple cores had cores discordant for virus expression further underscoring the focal distribution pattern of PVN (932) and the need for adequate biopsy material consisting of two cores including medulla.

Most important for the course of PVN is virally induced injury to tubules. Viral replication ultimately results in the lysis of host cells and the denudation of basement membranes, that is, PVN shows varying degrees of virally induced acute tubular necrosis (Fig. 29.82A and C). Despite marked epithelial damage, however, the tubular basement membranes usually remain intact. They can serve as the structural skeleton for subsequent regeneration once the viral replication ceases. Parietal epithelial cells lining the Bowman capsule can, on occasion, also show signs of viral replication, sometimes in association with the formation of small “pseudocrescents” (929,933). Replication of polyomaviruses in podocytes is exceptionally rare; the authors are aware of one such case.

Attempts have been made to subclassify PVN in order to obtain additional diagnostic, clinical, and prognostic information. A recent multicenter international trial organized by the Banff working group on PVN has defined three clinically significant disease grades based on the degree of intraparenchymal polyomavirus replication (histologic viral load levels) and the degree of

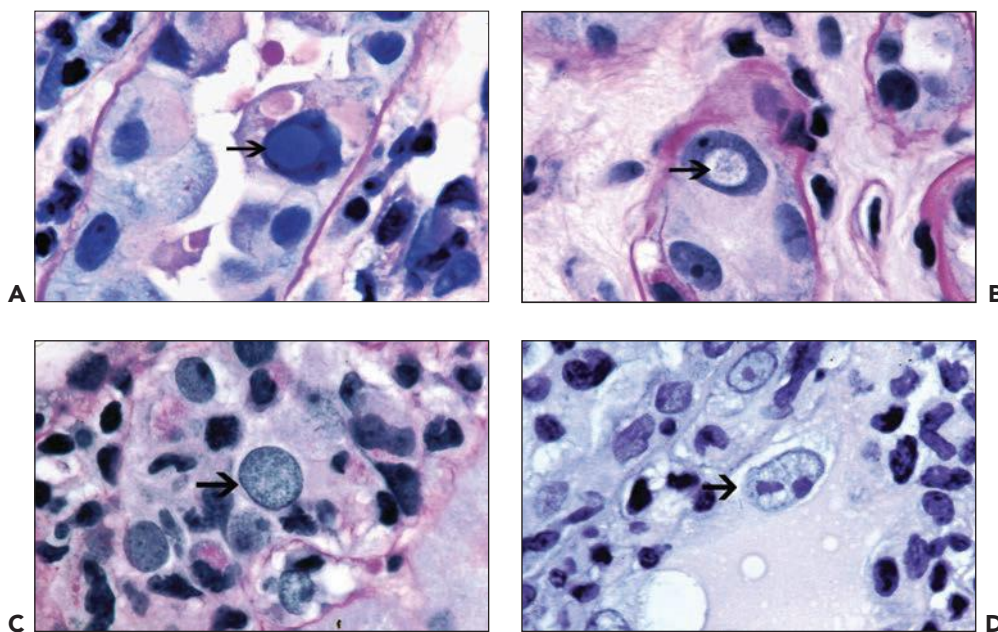


FIGURE 29.80 Polyomavirus nephropathy. Viral replication in epithelial cells can induce different nuclear changes: (A) an amorphous ground-glass inclusion body (type 1), (B) a central eosinophilic granular inclusion surrounded by a halo (type 2), (C) finely granular nuclear alterations (type 3), and (D) vesicular changes with coarsely clumped viral inclusions (type 4). ((A–C) PAS and (D) H&E; original magnification 600 \times .)

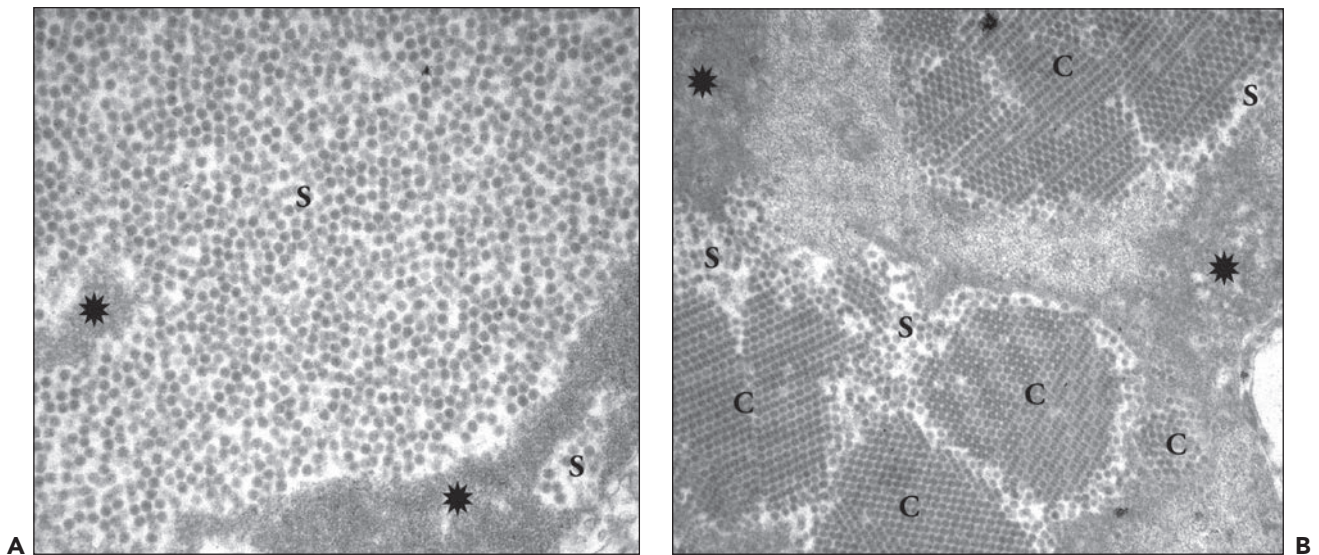


FIGURE 29.81 Ultrastructurally, polyomaviruses (30 to 50 nm in diameter) are found in the nuclei as single viral particles (S) or in crystalloid arrays (C) surrounded by chromatin (asterisk). Changes illustrated in (A) are the ultrastructural correlate for amorphous ground-glass type of inclusions (compare this figure with Fig. 29.80A); crystalloid viral aggregates (B) can be associated with types 2 and 4 nuclear changes (compare with Fig. 29.80B and D).

interstitial fibrosis: PVN grade 1 (minimal evidence of polyomavirus replication in less than 1% of the biopsy cores and interstitial fibrosis less than 25%), PVN grade 2 (varying replication and fibrosis levels different from grades 1 and 3), and PVN grade 3 (marked evidence of polyomavirus replication greater than 10% of the biopsy cores and greater than 25% interstitial fibrosis).

PVN is associated with varying degrees of interstitial cortical and/or medullary inflammation and fibrosis that can vary from absent to marked (see Fig. 29.82) (932,934,935). During the early disease stage, that is, PVN grade 1, tubules can look unremarkable, typical intranuclear inclusions may be absent, and interstitial inflammation can be minimal or even lacking. In such early cases, polyomavirus replication is only detected by IHC. Florid PVN is characterized by marked tubular injury and intranuclear viral inclusion bodies, denudation of the tubular basement membranes secondary to lysis of infected epithelial cells, and interstitial edema with a mixed, mild to marked inflammatory cell infiltrate (B and T lymphocytes, macrophages, and plasma cells). Plasma cells, often predominately expressing IgM (936), can be prominent and cause plasma cell tubulitis. Of note, inflammation represents in some cases concurrent allograft rejection (see below). Polymorphonuclear leukocytes can be prominent adjacent to severely injured tubules and are likely a sign of urine back leak. Inflammation is commonly associated with marked tubulitis in tubules with and without signs of polyomavirus replication.

On occasion (in ~15% of cases), vaguely formed nonnecrotizing interstitial granulomas are found; giant cells of the Langhans type are rare (Fig. 29.83A). Interstitial granuloma formation is usually accompanied by peculiar “intratubular granulomas,” that is, markedly distended tubules occluded by inflammatory, epithelial, and histiocytic cell elements often lacking intranuclear viral inclusion bodies (see Fig. 29.83B) (141). Granuloma formation is likely due to the rupture of TBM and leakage of Tamm-Horsfall protein into the interstitial compartment as seen

in other forms of acute tubular injury. “Intratubular” granulomas, however, are uncommon in rejection, and their presence can be a diagnostic hint to intensely search for PVN.

Signs of a productive polyomavirus infection are also found in the transitional cell layer lining the renal pelvis, the ureters, and/or the urinary bladder (929). Viral inclusion bodies in the urothelium, however, are not part of the histologic hallmarks defining PVN that is characterized by intraparenchymal renal changes. Mesenchymal, inflammatory, and endothelial cells do not reveal any cytopathic alterations, and glomerular capillary tufts as well as blood vessels are unaltered. Glomerulitis, transplant glomerulopathy, and endarteritis are not features of PVN; if present, these latter changes support a diagnosis of concurrent allograft rejection (see below).

IMMUNOFLUORESCENCE AND IMMUNOHISTOCHEMISTRY

Polyomavirus replication is readily detected with commercially available antibodies to the SV40 T antigen (“large” T antigen) that cross-reacts with all polyomaviruses pathogenic in humans (i.e., BK-, JC-, and SV40) and works in paraffin sections (see Fig. 29.82). The nuclear expression and detection of the large T antigen is a sign of polyomavirus replication and found during the early stages of viral replication; it does not indicate the actual presence of virions. Thus, strong staining signals can be seen in normal-appearing nuclei, while those with typical viral inclusion bodies, for example, type 1 or 2, can be SV40 T antigen negative (362,929,930,937). Crisp nuclear polyoma T antigen expression (IHC staining intensity ≥ 2 on a scale of 0 to 4) in one (or more) intraparenchymal renal epithelial cells always indicates clinically significant viral replication, that is, PVN, and it can be the first sign of viral nephropathy in PVN disease grade 1 lacking intranuclear inclusions, inflammation and allograft dysfunction. Viral replication can also be detected by in situ *hybridization* or with antibodies directed against virus capsid proteins.

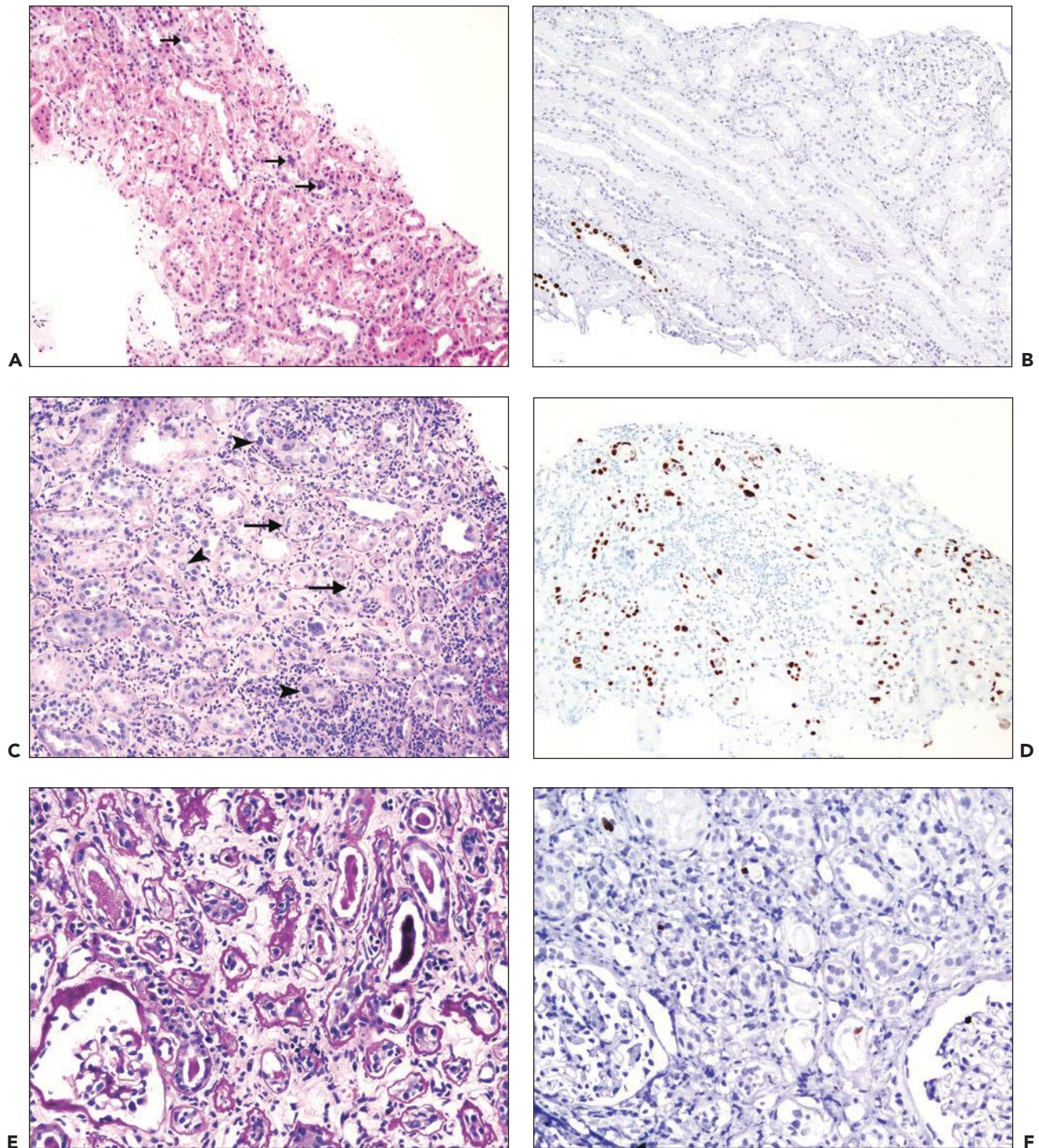


FIGURE 29.82 Histologic stages of polyomavirus nephropathy (A–F). PVN grade 1 (early phase) with only few intranuclear inclusion bodies (*arrows* in A) and minimal tubular injury (A and B); the interstitium is without significant changes. PVN grade 2 (florid phase) with marked viral replication (*arrowheads* in C) involving many tubules (D), severe tubular injury, and focal denudation of tubular basement membranes (*arrows* in C). There is a diffuse inflammatory cell infiltrate in the interstitium and associated tubulitis. PVN grade 3 (sclerosing phase) with marked IFTA (E and F). IHC (F) demonstrates only very focal evidence of viral replication with scattered positive (*brown*) staining signals in tubular nuclei. (A, C, E) H&E and PAS original magnifications 100 \times , 200 \times , and 250 \times ; (B, D, F) IHC to detect the SV40 T antigen shows intranuclear staining in epithelial cells, 100 \times and 250 \times original magnifications. (A, B, E, and F are from biopsies of the same patient taken 10 weeks apart.)

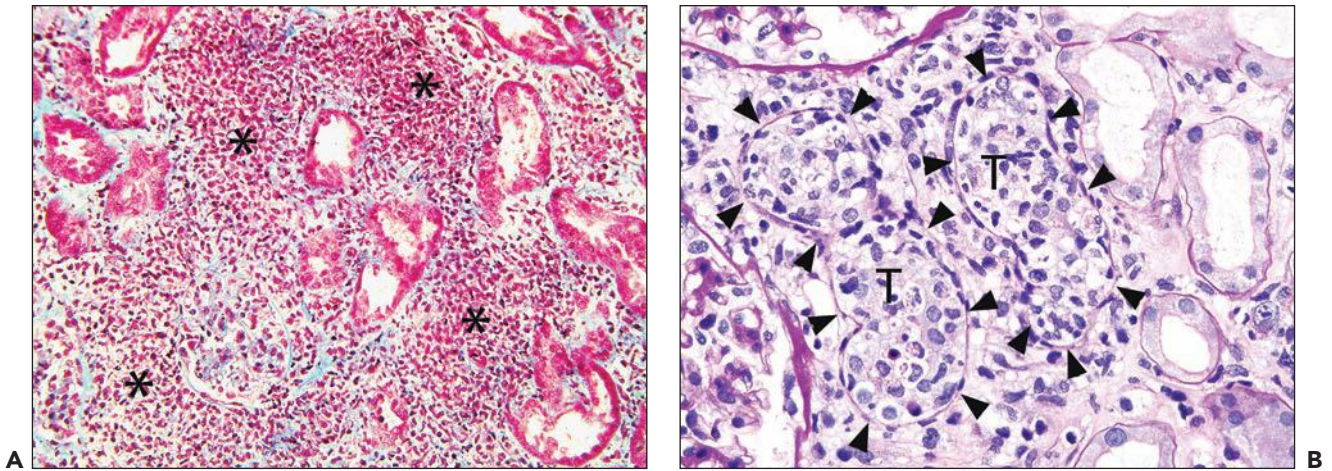


FIGURE 29.83 PVN with granulomatous inflammation. (A) shows a nodular inflammatory cell infiltrate in the interstitium rich in histiocytes forming vague granulomas (*asterisk*). (B) illustrates peculiar “intratubular granuloma formation” with markedly distended tubular cross sections entirely filled with and occluded by epithelial, histiocytic, and other inflammatory cell elements (T, tubular cross section; *arrowheads* outline TBM); typical intranuclear viral inclusion bodies are not seen. (A: 200× original magnification (trichrome), B: 400× magnification (PAS).)

In rare patients, PVN demonstrates focal granular TBM staining (immunoglobulins, light chains, and complement components including C4d; Fig. 29.84) (938,939). This finding is of undetermined biologic and clinical significance, however it may be diagnostically useful. In PVN, the complement degradation product C4d is not detected along PTC (150,940,941). Viral replication in tubular cells is not associated with marked tubular expression of MHC class II (HLA-DR); its detection by immunofluorescence microscopy might serve as an adjunct marker of concurrent cellular rejection, in particular in the setting of endarteritis, glomerulitis, or C4d positivity

(362,940,942). However, tubular HLA-DR expression is not in and by itself a rejection marker (943). In PVN, no diagnostic IF/IHC staining pattern is noted in glomeruli applying a standard panel of antibodies.

ELECTRON MICROSCOPY

Polyomaviruses present as viral particles of 30 to 45 nanometers in diameter, occasionally forming crystalloid structures (see Fig. 29.81). Viral particles are primarily found in the nucleus and rarely in membrane-bound structures in the cytoplasm. On occasion, immune complex–type deposits are detected

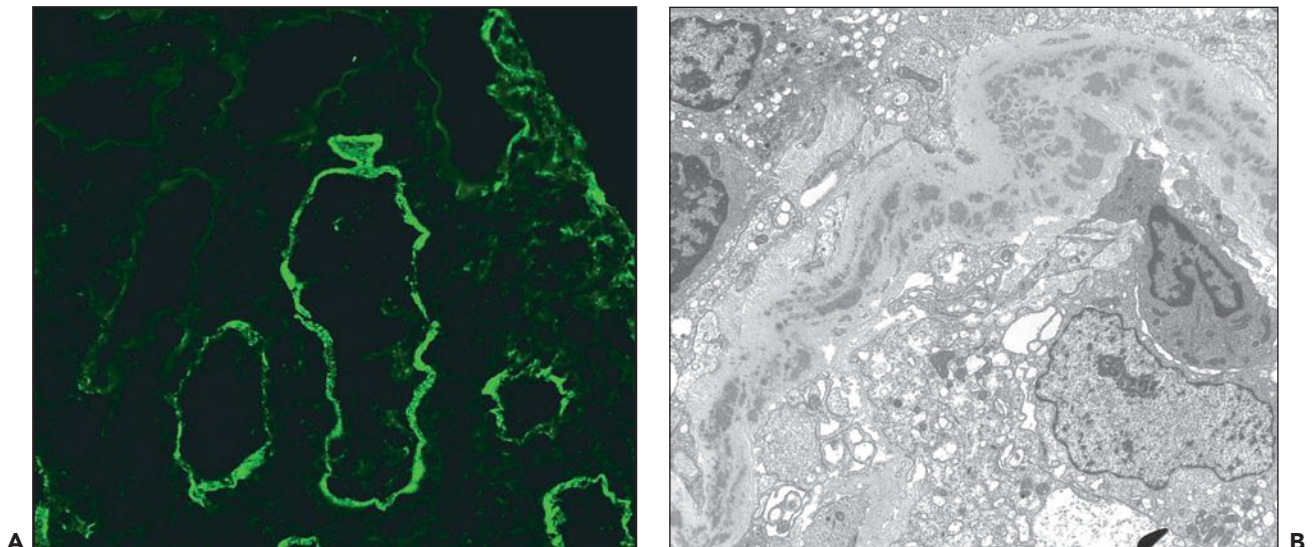


FIGURE 29.84 Polyomavirus nephropathy with focal immune complex–type deposits along tubular basement membranes; this finding is rare and of undetermined biologic and clinical significance. A: Immunofluorescence microscopy with an antibody directed against IgG demonstrates granular deposits along some tubular basement membranes; (400× original magnification.) B: Electron microscopy from the same case shows immune complex–type deposits in the TBM. (1000× original magnification.)

along tubular basement membranes, the ultrastructural correlates for granular staining seen by immunofluorescence microscopy (see Fig. 29.84B) (141,939). In PVN, glomerular immune complex-type deposits are not seen.

ETIOLOGY AND PATHOGENESIS

PVN is nearly always caused by a productive infection with the BK virus strain. Only a minority of cases (approximately 10% to 20%) show minor coactivation of polyoma JC virus in the kidneys with no direct clinical or prognostic significance. PVN solely caused by productive JC or SV40 virus infections is exceptionally rare (944–949).

It is assumed that the reactivation of latent BK virus infections in the transplanted donor organ causes disease, that is, PVN is most likely donor derived (362,929,950–952). After a primary infection, BK viruses are generally not completely eliminated from the body but rather establish lifelong latency in permissive tissues, in particular in renal tubular and urothelial cells (950,953–955).

PVN affecting a kidney transplant was first described as a case report by the pathologist Mackenzie in 1978 (956). Subsequently, under cyclosporine-based immunosuppression, PVN was largely “forgotten” (929) possibly in part due to the inhibitory effect of cyclosporine on polyomavirus replication (957). The clinical scenario changed dramatically in the mid-1990s when new immunosuppressive drugs were introduced into the routine management of kidney transplant recipients worldwide. Intense immunosuppression, especially high doses of tacrolimus and mycophenolate mofetil and possibly also pretransplant desensitization protocols, seems to promote viral reactivation (362,929,951,958–962). The graft microenvironment promotes the development of PVN as evidenced by the rarity of PVN in native kidneys in recipients of non-renal allografts. A window of opportunity for polyomaviruses to replicate might be provided in injured and regenerating tubular cells found in conditions such as ischemia or rejection (362,930,963). However, overall risk factors associated with PVN are only incompletely defined (951), and potentially even transplantation into a BK virus antibody-negative recipient, natural killer cell-related genetic predisposition with insufficient killer cell activation in the recipient, or dendritic cell abnormalities may promote PVN (964–966). Mutations or gene rearrangements of BK viruses have been reported in PVN; however, their pathogenetic significance remains undetermined (967,968).

Polyomaviruses adhere to their host cells via binding of viral capsid proteins to cell surface receptors (involving an N-linked glycoprotein containing an α (2,3)-linked sialic acid as a receptor) (969). After cell entry via caveola-mediated endocytosis (970), the viruses migrate through the cytoplasm/microtubules (971,972) and the nuclear pores into the host cell nucleus, where the large T antigen is expressed as an initial step in viral replication. BK virus infection and replication is dependent on a regulatory network requiring nuclear factor of activated T cells (NFAT) (973). The host cell is ultimately reprogrammed to produce viral particles, and daughter virions are assembled in the nucleus with formation of intranuclear viral inclusion bodies identified by light microscopy (974). Infection of tubular cells, in particular of collecting duct cells, seems to induce an inflammatory microenvironment with expression of IL-6 and IL-8 via activation of the

double-stranded RNA sensor toll-like receptor 3 (triggered by double-stranded intracytoplasmic polyomavirus RNA during the viral replicative cycle) (975). As last step during viral replication, inclusion-bearing host cells are lysed and mature daughter virions released into tubular lumens. A critical factor for control of BK virus replication and recovery from PVN is cell-mediated immunity (976,977).

Only few studies have examined intragraft gene expression profiles in PVN. One study confirmed on a molecular level the presence of transcripts associated with inflammation and demonstrated, similar to histology, gene expression profiles overlapping with those of cellular rejection. Transcripts described in cellular rejection including CD8, IFN- γ , CXCR3, and perforin were even higher in PVN when compared to rejection cases. In PVN, the transcription of molecules associated with extracellular matrix proteins including collagens, TGF- β , and MMPs was significantly increased (978). One group reported elevated granzyme B and protease inhibitor-9 mRNA levels in urinary cells from patients with PVN and subsequent decline of renal function compared to PVN patients with stable serum creatinine levels. Interestingly, the level of granzyme B expression in the PVN cohort with functional deterioration was similar to a control group with acute rejection (979). Future studies will have to correlate molecular findings with the histologic PVN disease grades.

DIFFERENTIAL DIAGNOSIS

Although histologic changes including intranuclear viral inclusion bodies are relatively characteristic for PVN, viral infections caused by herpes simplex virus, adenovirus, or CMV must be considered in the differential diagnosis (see Table 29.10). Diagnostic confirmation of PVN is achieved by IHC with antibodies directed against the polyomavirus T antigen, VP capsid proteins; by *in situ hybridization*; and/or by electron microscopy. PCR techniques may also be utilized to demonstrate viral DNA or RNA in tissue samples and to confirm the diagnosis of PVN (980,981). However, such PCR results must be interpreted with great caution. Only strong amplification signals of viral DNA (greater than 60 to 100 BK virus copies per “cell equivalent”), in the setting of histologically or immunohistochemically demonstrable virally induced cytopathic changes, can be used to prove the diagnosis of PVN and to distinguish clinically significant productive from clinically insignificant latent infections (950,953,954,981,982). PVN is hardly ever seen in association with a concurrent second viral infection of the kidney. We are only aware of exceptionally few anecdotal cases with dominant productive infections of either adenovirus (983) or CMV (984) and only focal apparently minor evidence of polyomavirus coactivation.

PVN (mainly PVN grade 1) without distinct intranuclear viral inclusion bodies is difficult to diagnose, and a high level of suspicion is needed. Plasma cell-rich inflammation primarily in the medulla, granulomatous inflammation, and, in particular, “intratubular” granuloma formation should always raise suspicion of PVN; positive intranuclear staining for SV40 T antigen can be diagnostically confirmatory. As a general rule, we recommend immunohistochemical incubations to detect the SV40 T antigen and to establish a potential diagnosis of PVN in all equivocal cases with atypical-appearing tubular epithelial nuclei and in patients at increased risk, such as those

shedding urinary decoy cells or presenting with viremia. We currently do not recommend SV40-T incubations on a routine basis in all graft biopsies.

Either cellular and/or AMR can concur with PVN (362,930,940,985–987). Rejection can be treated since a transient increase of immunosuppression and antirejection therapy, even with lymphocyte antibodies, does not seem to result in “explosive” polyomavirus replication or a significant increase in viremia (940,986), and patients might benefit. Rejection should be diagnosed if transplant endarteritis, transplant glomerulitis, significant tubulitis in areas without viral inclusion bodies, tubular expression of MHC class II (HLA-DR), and/or C4d along PTC is found (940,941). IHC phenotyping of the inflammatory cells in PVN has shown plasma cell (CD138), B-cell (CD20), T-cell (CD3), or monocyte-dominant infiltrates, so that IHC is not diagnostically helpful to distinguish rejection from virally induced nephritis (978,988,989). Mihatsch and colleagues suggested that in plasma cell–rich PVN (greater than 15% of inflammatory cells), a predominance of IgM-containing plasma cells may suggest viral nephropathy (vs. rejection with IgG dominance) (936). While Banff acute C4d-positive AMR or acute TCMR with transplant endarteritis can be diagnosed easily, a diagnosis of PVN and concurrent acute TCMR with tubulointerstitial cellular rejection only is challenging (942,943).

Few reports on specific histologic findings encountered during the resolving/healing phase of PVN show increased, mostly transient inflammation interpreted to represent in part a form of polyomavirus-associated interstitial nephritis or reconstitution type of inflammation during low-dose immunosuppression rather than cellular rejection (942,943,977). Larger multicenter studies are needed to better understand these phenomena.

CLINICAL PRESENTATION, PROGNOSIS, AND THERAPY

PVN is currently by far the most important infection involving kidney transplants with an incidence of around 4% (reported by the Banff working group on PVN); a 12% incidence was noted in one recent Brazilian study and a 20% incidence in desensitized immunologically high-risk graft recipients (958). ABOi grafts seem to be at high risk for PVN (incidence 18%) (990). PVN in native kidneys, even in patients with solid organ transplants other than kidneys, is very rare.

Except for very rare systemic forms of BK virus infections in severely immunocompromised patients, PVN is typically limited to the kidneys/renal allograft (922,929,930,991,992). PVN presents 6 days to many years posttransplantation (930,944,993). In general, PVN grade 1 is diagnosed early, that is, on average 4 to 5 months postgrafting, whereas the sclerosing disease grade 3 is detected much later, that is, on average after 13 months. Graft failure rates depend on the PVN disease grade: approximately 15% in grade 1, 25% in grade 2, and 50% in PVN grade 3 (data collected by the Banff working group on PVN). If kidney allografts are lost due to progressive viral nephropathy, retransplantation is an option. Small case series have provided encouraging results: Recurrent PVN was only observed in approximately 6% to 10% of all repeat allografts (994–997).

Although allograft dysfunction with elevated serum creatinine levels can be seen at time of initial diagnosis, clinical signs are generally nonspecific. Hematuria and proteinuria are

typically absent. General signs of an infection (e.g., fever, leukocytosis) are lacking, and multiorgan involvement is practically never seen (with only one exception) (992). PVN with viral replication limited to the medulla typically presents with unaltered serum creatinine levels. In these patients, a diagnosis may only be incidentally established in a protocol biopsy (737) or in a biopsy triggered by targeted risk assessment (see below). The therapeutic goal is to limit viral replication and tubular injury, to promote tubular epithelial cell regeneration, and to prevent disease progression to irreversible scarring.

Antiviral treatment strategies are poorly defined; they usually include the reduction of immunosuppression, in particular tacrolimus and mycophenolate, potentially combined with leflunomide or cidofovir (932,985,998–1003). Whether treatment with cidofovir, leflunomide, fluoroquinolone, or IVIG has any significant antipolyomavirus effect *in vivo* is undetermined.

Overall improved graft survival has been reported from centers with vigorous patient screening programs that facilitate an early diagnosis of PVN and therapeutic intervention (362,930,935,985–987,1004,1005). Screening programs are based on the observation that all patients with PVN have evidence of polyomavirus activation/replication in the blood, that is, viremia, and urine, that is, viruria. Most of these patients, however, only transiently activate polyomaviruses and only a small minority actually develops PVN (922,927,986). Nearly all patients with PVN show polyomavirus inclusion-bearing cells in the urine, the so-called decoy cells (Fig. 29.85) (362,928,929,934,986,998,1006–1008). Decoy cells indicate the activation of polyomaviruses in the urinary tract, but not necessarily PVN. Decoy cell analysis as a first-line screening assay is efficient and cost-effective (1008). The threshold of ≥ 10 decoy cells per liquid-based thin prep slide has an excellent negative predictive value of greater than 99%, but a positive

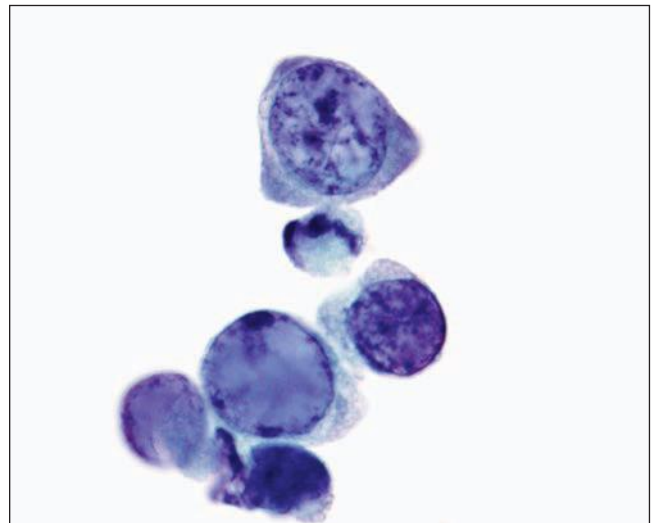


FIGURE 29.85 Polyomavirus inclusion-bearing cells (so-called decoy cells) in the urine. Decoy cells show glassy-appearing intranuclear viral inclusion bodies, sometimes interspersed with dense, granular material. They are a morphologic sign of the activation of polyomaviruses. Liquid-based urine cytology preparation. (Papanicolaou stain, 600 \times original magnification.)

predictive value of only 27% (362,1008). Quantitative urine PCR assays have similar predictive values as decoy cell counts (927). In comparison, quantitative plasma PCR tests have the highest positive predictive value for PVN (986); plasma viral load levels of greater than 10,000 copies per mL predict disease with 74% probability (929). However, these proposed viral load cutoff levels have not been validated in large multi-center studies, and results on viral loads show large interlaboratory variations. We have diagnosed PVN by biopsy in 39% of patients in the setting of BK viremia below 10,000 copies (in 2 patients below 1000 BK copies/mL plasma) (927).

The urine polyomavirus-Haufen test is a novel assay to accurately predict PVN noninvasively (927,1009). It is based on the detection of cast-like, three-dimensional polyomavirus aggregates, that is, "Haufen" (German for heap or stalk) in voided urine samples by negative staining electron microscopy (Fig. 29.86). In PVN, viruses cluster and form cast-like structures in injured renal tubules containing high concentrations of Tamm-Horsfall protein (uromodulin) (Fig. 29.87) (1010). These polyomavirus aggregates are flushed into the bladder and can be detected in voided urine samples as polyomavirus-Haufen.

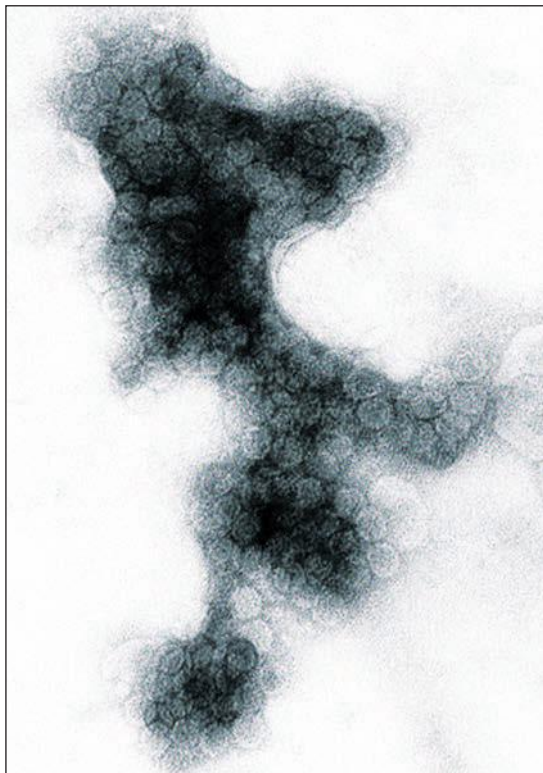


FIGURE 29.86 Negative staining electron microscopy on a voided urine sample from a patient with PVN. In all stages of PVN, large three-dimensional cast-like viral aggregates, the so-called polyomavirus-Haufen, are found in the urine. Polyomavirus-Haufen originate in virally injured renal tubules and are shed into the urine; thus, they are renal disease (=PVN) specific. Aggregated polyomaviruses forming three-dimensional Haufen can easily be identified based on the characteristic polyomavirus capsid surface structure. Polyomavirus-Haufen are pathognomonic urinary biomarkers for PVN with positive and negative predictive values of greater than 90%. ($\times 80,000$.)

Thus, polyomavirus-Haufen detected in the urine are specific biomarkers for intrarenal disease, that is, PVN. The presence of urinary polyomavirus-Haufen has positive and negative predictive values for PVN of greater than 90%, by far exceeding any other currently used screening assay (927). Furthermore, in contrast to commonly used laboratory tests such as quantitative PCR, urinary polyomavirus-Haufen testing can accurately predict the intrarenal polyomavirus burden, that is, the severity of PVN, and identify early disease stages (1011).

Ureteral stenosis might be caused by polyomavirus, as already noted in early reports (1012). Stent placement may be a risk factor for PVN (1013). Urethral stenosis has also been reported (1014).

Cytomegalovirus

CMV is a double-DNA virus of the herpesvirus family. CMV is transmitted via saliva, body fluids, or tissue. Seroprevalence varies; it ranges between 30% and 70% in Western Europe and North America. After a primary infection, CMV establishes latency in myeloid progenitor cells and can be transiently reactivated without causing symptoms or disease, similar to other DNA viruses such as polyomaviruses (1015). CMV is one of the most common and potentially serious pathogens in renal transplant recipients, typically causing a symptomatic infection in the first 2 to 3 months after grafting, manifested by fever, leukopenia, organ dysfunction, and viremia (1016). CMV disease is defined by evidence of virally induced direct tissue injury and, in case of CMV nephritis, by biopsy-proven cytopathic changes (926). Organ invasion in CMV disease can be found in intestine (40%), liver (20%), lungs (10%), kidneys (5%), eyes/brain (1%) (1015,1017), and rare sites such as bladder and ureter with clinical signs of CMV-associated hemorrhagic cystitis (1018). Autopsy studies conducted in patients with CMV disease suggest a higher prevalence of renal involvement (25% to 30%), in particular in renal allograft recipients (1019,1020). Effective patient screening and clinical management strategies have made CMV nephritis of the transplanted kidney exceedingly rare in western countries. However, CMV nephritis seems to be more prevalent in some parts of the world, such as India (993,1021).

Lesions induced by the replication of CMV in the kidneys have been described in renal transplants and native kidneys alike (1019,1020). Cytopathic changes are typically very focal and most often seen in the nuclei and cytoplasm of tubular epithelial cells (proximal tubules, collecting ducts), sometimes in endothelial cells and rarely in podocytes (1019–1021). CMV-infected cells are typically enlarged with nuclei containing a central round inclusion body surrounded by a circumferential halo, that is, the typical "owl's eye" appearance. Also, homogeneous smudgy-appearing intranuclear inclusions are occasionally observed (see Table 29.10). Small basophilic "lumpy" cytoplasmic viral inclusions are frequently (but not always) detected in cells with virally induced intranuclear changes (1020). The replication of CMV in the tubular compartment (seen in 70% of cases in one series (1021)) is usually associated with a nodular, sometimes granulomatous-appearing mononuclear and plasma cell infiltrate and, occasionally, also with cytopathic changes and inclusions in endothelial cells of PTC (1021). Foci of necrosis and microabscesses can occur, but are uncommon (1019,1021). Interstitial inflammation was absent in 2/6 cases of CMV nephritis in one series (1019). Cytopathic changes can also be

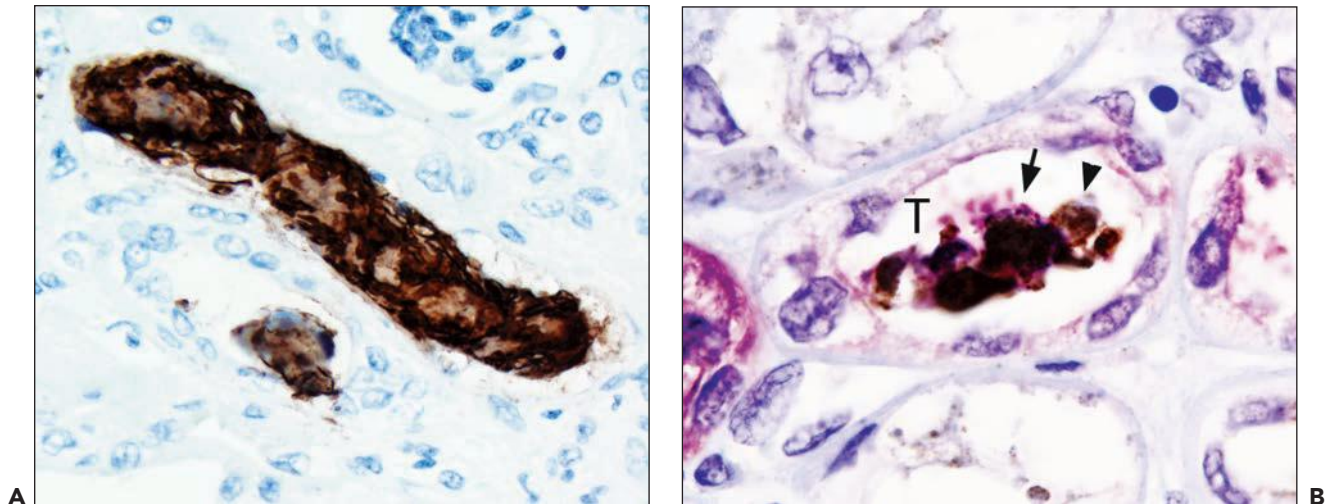


FIGURE 29.87 **A:** In PVN, viruses cluster in injured renal tubules and form dense cast-like viral aggregates staining *dark brown* in this immunohistochemical incubation. The viral aggregates are flushed out of the kidneys and can be found in the urine as PV-Haufen. **B:** Intratubular cast-like aggregation of polyomaviruses requires high concentrations of uromodulin (Tamm-Horsfall protein). A double-labeling study illustrates the close association between Tamm-Horsfall protein (*purple/dark blue arrow*) and aggregated intratubular polyomaviruses (*brown, arrowhead*) in a case of PVN. T, tubule. **A:** IHC antibody directed against polyomavirus capsid proteins (*dark brown*), 400× magnification; **B:** IHC, double labeling with an antibody directed against Tamm-Horsfall protein/uromodulin (*purple/blue*) and a second antibody against polyomavirus capsid protein (*brown*), 600× magnification.

found in the glomeruli, mainly glomerular endothelial cells, either in combination with tubulointerstitial nephritis (3/10 cases) or as an isolated event (4/10 cases) and then often lacking intraglomerular inflammation (1021). Crescent formation and features mimicking an acute glomerulonephritis have rarely been reported (1022–1025). In severe cases of CMV nephritis, also the endothelium of larger vessels might be affected and show viral inclusion bodies (1021). Rare reports suggested an association between CMV disease/nephritis and the development of a TMA (1021,1026); whether this latter feature is, indeed, part of the spectrum of CMV-induced tissue injury (or due to acute AMR, CNI toxicity) remains undetermined.

Diagnostic confirmation of a productive CMV infection can easily be achieved by IHC (e.g., with an antibody directed against the immediate early antigen), by *in situ* hybridization, or by electron microscopy. Ultrastructurally, virions of approximately 150 nm often with a central electron-dense core surrounded by an envelope are found in the nuclei and the cytoplasm. Immunofluorescence microscopy with a standard panel of antibodies detecting immunoglobulins and complement factors is unrevealing (only sometimes minute glomerular IgG deposits are seen) (1020). There is no evidence that a productive intrarenal CMV infection triggers the deposition of the complement factor C4d along PTC; its detection should raise suspicion for concurrent AMR. PCR studies on tissue for the detection of CMV genome do not clearly distinguish between clinically significant productive and clinically insignificant non-productive infections (1027), and it seems doubtful whether these techniques really demonstrate a higher prevalence of “CMV disease” (1028). Similar to the diagnostic approach for PVN, the minimal criteria to establish a diagnosis of CMV disease/nephritis include the demonstration of cytopathic changes or CMV proteins or mRNA, not just the CMV genome.

The differential diagnosis of CMV nephritis includes other types of viral infections, mainly caused by polyoma or adenoviruses (see Table 29.10). Since CMV (in contrast to polyomavirus and adenovirus) often replicates in endothelial and inflammatory cells, a distinction between rejection-induced changes and infection-driven inflammation is difficult. Concurrent AMR or ACR in the setting of CMV nephritis was reported in 30% of cases in one series from India (1021).

CMV infections can stimulate indirect effects on the kidney graft by modulating the immune response and possibly promoting rejection episodes (1017,1029). The most convincing evidence that CMV indirectly causes graft injury was reported by Reinke, who showed that 85% of patients with “late acute rejection” responded to ganciclovir therapy (1030). The outcome with conventional immunosuppression was considerably worse, with 80% graft failure at 1 year. So-called acute allograft glomerulopathy was linked to severe CMV infections in some old literature reports (161); these glomerular lesions, in the absence of intraglomerular virally induced cytopathic changes, are now classified as transplant glomerulitis, that is, rejection-induced changes.

Adenovirus

Productive adenovirus infections of renal allografts are exceptionally rare events (1031). Morphologic changes caused by adenovirus infections have been defined in autopsy studies of native kidneys from severely immunosuppressed patients showing focal necrotizing tubulointerstitial nephritides (983,1032–1036). The major histologic changes include (i) viral inclusion bodies in tubular epithelial cell nuclei (amorphous ground-glass variants, sometimes central inclusion bodies surrounded by halos), (ii) severe tubular destruction with ruptures of basement membranes and foci of necrosis including polymorphonuclear leukocytes, (iii) an interstitial mononuclear

and plasma cell response sometimes with granuloma formation, and (iv) focal interstitial hemorrhage and intratubular red blood cell casts (401,983,1032,1034,1037,1038) (see Table 29.10 and Fig. 29.88). Polymorphonuclear leukocytes can be abundant in areas of necrosis. Glomeruli and blood vessels are generally not affected, except for rare cases with cytopathic changes limited to the parietal epithelial cell layer of the Bowman capsule (983). In kidney transplant recipients, a productive adenovirus infection can in some cases primarily affect the bladder, that is, hemorrhagic cystitis (1039–1041).

Diagnostic confirmation of an adenovirus infection can easily be achieved by IHC or electron microscopy. IHC with antibodies directed against adenovirus antigens shows intranuclear and, to a lesser degree, also intracytoplasmic staining in tubular epithelial cells (see Fig. 29.88D). Positive staining can also be detected in rare inflammatory cells. Ultrastructurally, virions of approximately 75 to 80 nanometers are found in the nuclei and the cytoplasm. The size of adenoviruses is approximately double

that of polyomaviruses and half that of CMV. Free viral particles can typically be detected in the urine by negative staining electron microscopy; however, dense adenovirus aggregates, that is, urinary adenovirus Haufen, do not form. Immunofluorescence microscopy with a standard panel of antibodies directed against immunoglobulins and complement factors is unrevealing. C4d is not deposited along PTC in cases of adenovirus infections, and its detection should raise the possibility of concurrent AMR; experience, however, is limited.

The differential diagnosis includes other types of viral infections, mainly PVN (see Table 29.10). Adenovirus replication can usually be suspected by light microscopy based on a) frank tubular destruction with foci of necrosis, b) granulomatous inflammation including palisading of macrophages around severely injured tubules, and c) interstitial hemorrhage. Predominance of such changes has not been described in PVN or other productive intrarenal viral infections. A superimposed second viral infection in cases of adenovirus-induced nephritis

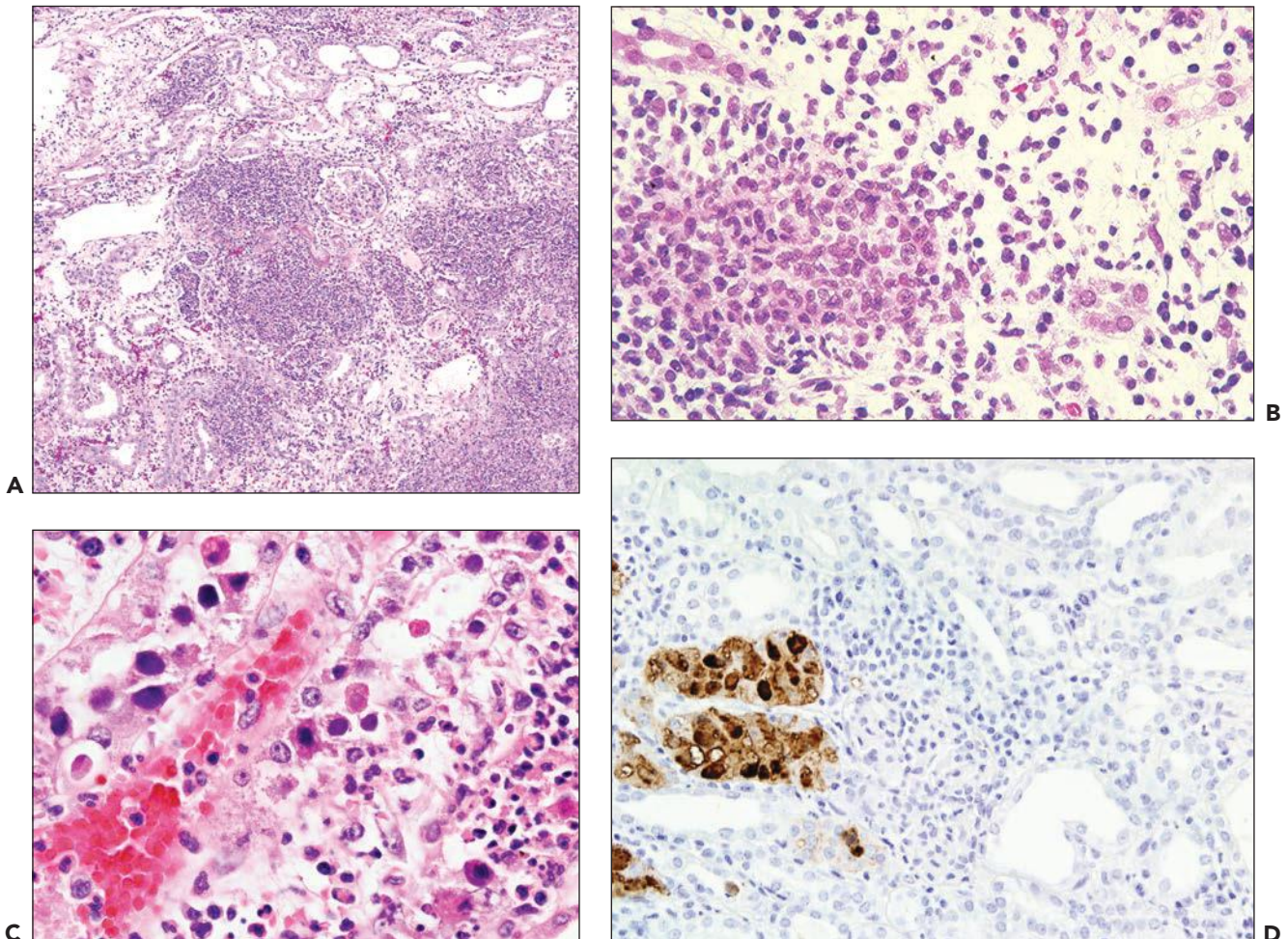


FIGURE 29.88 Adenovirus infection. Characteristic for an adenovirus infection is a focal necrotizing tubulointerstitial nephritis (**A**) that may contain occasional small granulomas (**B**). On high-power examination, (**C**) adenovirus infections demonstrate ground-glass type of intranuclear viral inclusion bodies in tubular epithelial cells, tubular destruction, interstitial hemorrhage, and necrosis. IHC to detect adenovirus antigens (**D**) reveals intranuclear and cytoplasmic staining in tubular epithelial cells. ((A, B, C) H&E, original magnifications 40 \times , 200 \times , and 400 \times ; (D) IHC to detect adenovirus antigens, original magnification 200 \times .)

seems to be rare; in one series, only 1/14 patients demonstrated concurrent focal PVN and no signs of CMV replication (983). We have encountered one exceptional case with concurrent minor evidence of CMV replication detected by immunohistochemistry in few tubular nuclei.

Little is known about the way of transmission; exogenous exposure to adenovirus or possibly transmission via the donor organ has been suggested (401,1042). While adenovirus infections in nontransplant patients are most commonly found in children, the adult population is affected after transplantation (1043). The pathogenesis of adenovirus-induced changes, the severity of clinical symptoms, and organ involvement vary. They are dependent on the adenovirus serotype, patient age, the type and intensity of the underlying immunosuppression, and the type of tissue/organ transplant. Infections are most often caused by adenovirus subgroups B1 and B2 and serotypes 7, 11, 34, 35, and 37. Serotypes 35, 37, and most frequently 11 have been associated with hemorrhagic cystitis and necrotizing interstitial nephritis (983,1032,1035,1043,1044).

Patients suffering from symptomatic adenovirus infections posttransplantation most often present within the first 3 months after transplantation with generalized symptoms (401) including hematuria/pyuria (94%), dysuria (88%), fever (82%), and bilateral testicular pain (44%) (1039). In case of adenovirus-induced nephritis, a rise in serum creatinine levels is usually seen. Treatment strategies for adenovirus allograft infections are not well defined (they include the reduction of the immunosuppression, cidofovir, IVIG, intravenous ribavirin, and ganciclovir (1033–1035,1039,1043–1046). Considering the parenchymal damage and destruction caused by productive intrarenal adenovirus infections outcome is often surprisingly good; some patients present with rapid and profound improvement of renal function and long-term graft survival (1033–1036,1039,1045,1047,1048). Watcharananan and colleagues reported adenovirus clearance from urine and blood in patients with a generalized adenovirus infection with and without renal involvement within less than 7 weeks in a cohort of 17 patients (1039). Friederichs noted viral clearance from a kidney transplant in a repeat graft biopsy taken 26 days after onset of the disease (1044). We have experience with one pediatric renal allograft recipient who first developed PVN and subsequently adenovirus interstitial nephritis; both productive intrarenal viral infections healed (confirmed by repeat biopsy), and graft function in our patient has been stable during long-term follow-up. However, due to the generalized nature of the infection, the disease course can be severe and outcome fatal, in contrast to PVN.

Acute Pyelonephritis

Acute pyelonephritis can present with increase in serum creatinine levels (1049–1051) and affects approximately 10% to 16% of renal allograft recipients (1052–1055). Kidney transplantation by itself is a risk factor for the development of pyelonephritis independent of gender (1054,1056,1057). Long-term prognosis is generally favorable (1053–1055). Pyelonephritis arises most often 1 year or more after grafting (80% of episodes) commonly due to an *E. coli* infection (80%). In rare instances, gas-producing organisms (*E. coli*, *Klebsiella pneumoniae*) have been reported with a potentially fatal form of emphysematous pyelonephritis requiring intensive therapeutic intervention including graft nephrectomies (1051,1058,1059).

As in native kidneys, the diagnosis of acute pyelonephritis is suggested by intratubular polymorphonuclear leukocyte casts associated with polymorphonuclear leukocytes in the surrounding edematous interstitium and between injured and activated tubular epithelial cells. Pyelonephritis is typically a patchy disease process that may be most pronounced in the medulla and can show ill-formed epithelioid granulomas. C4d is not found along PTC. The differential diagnosis includes ATN/ischemia-reperfusion injury, AMR, or TCMR. ATN typically reveals marked and diffuse tubular injury. Although scattered intratubular polymorphonuclear leukocytes may be seen in ATN and ischemia-reperfusion injury, they usually do not form densely packed casts. AMR, typically C4d-positive, often shows peritubular capillaritis that can be rich in polymorphonuclear leukocytes; dense intratubular cellular casts are typically absent. In acute TCMR, scattered polymorphonuclear leukocytes can be found in tubules and the interstitium, possibly due to urinary back leak; typical dense cellular casts are, however, absent.

SURGICAL AND MISCELLANEOUS COMPLICATIONS

Ureteral Obstruction/Leak/Reflux

The proximal ureter derives its blood supply from the renal pelvic vessels and is therefore at risk for ischemic injury after transplantation due to devascularization at time of harvest. Furthermore, the ureterovesical surgical anastomosis must be functional to prevent leakage or reflux. Urine leak can also arise from a ureteropelvic anastomosis. Urologic complications occurred in 6.8% of 1183 consecutive renal transplants performed with bladder anastomoses using various surgical techniques, usually in the first 4 months (84%) (1060). The most common problems were ureterovesical obstruction (4.1%), anastomotic leak (1.0%), and ureteropelvic obstruction (0.4%). Ureteral necrosis was seen in 3.2% of cases (52/1629) in another series (1061). These complications are generally treated with nephrostomy, dilatation stent placement, or surgical reanastomosis; they rarely cause graft loss (0.1%) (1060) and do not impact 10-year patient or graft survival (1061). Postoperative hematuria from bleeding at the site of the ureteral reimplantation site, symptomatic lymphocele formation, and urinary fistula resulting from necrosis of the distal ureter are other well known problems occurring postgrafting (1062). Only very limited data are available on histologic changes of injured ureters. In 25 surgically removed necrotic ureteral segments, vascular thrombosis of periureteral vessels was by far the most common observation (80%) (1061). CMV or BK virus infections of the urothelium can cause ureteral necrosis and stenosis. This seems to play a minor role today under current immunosuppressive protocols. Although ureteral stenosis is mostly a surgical complication, ureteral ischemia and fibrosis can also be caused by severe rejection episodes with transplant endarteritis involving not only intrarenal but also ureteral graft vessels.

Lymphocele

Lymphoceles are collections of lymphatic fluid (i.e., nonsanguinous and nonpurulent) in the perinephric space. Most lymphoceles are small, clinically insignificant, and only detected

by ultrasound. Large lymphoceles can cause obstruction or complications due to infection. The fluid derives from the renal lymphatics at the hilum that are not reanastomosed with the recipient lymphatics during surgery. Intrarenal lymph flow increases during rejection episodes due to increased vascular permeability and intraparenchymal edema formation, thereby promoting the formation of lymphoceles. Among 386 consecutive renal transplants, 35 lymphoceles greater than 50 mL were detected by ultrasonography 2 to 11 years posttransplantation, one third of which were associated with rejection episodes. In an analysis, involving more than 500 patients, 34% demonstrated lymphoceles greater than 2.5 cm in diameter, and 16% required therapeutic intervention. The highest prevalence was noted in patients treated with drug regimens containing mTOR inhibitors; nearly half of them (45%) had perinephric fluid collections; other risk factors were obesity and rejection episodes (1063). Lymphoceles often recur; however, long-term graft survival is unaffected.

Arterial or Venous Thrombosis

Arterial and/or venous thromboses are caused by technical problems with the anastomoses or a hypercoagulable state. They typically develop early posttransplantation and are limited to the large hilar vessels; smaller intraparenchymal arteries and glomeruli are characteristically spared. Thrombus formation in large hilar vessels can cause DGF, anuria, and potentially infarction (1064,1065).

The incidence varies considerably by transplant center. Among 558 consecutive deceased donor kidney recipients, the prevalence of primary renal graft thrombosis was 6% (1.9% arterial, 3.4% venous, and 0.7% both) (1066). In another series, renal artery thrombosis was seen in 0.4% and renal vein thrombosis in 0.1% of patients (1067). The risk factors include surgical technical problems, a history of venous thrombosis and the antiphospholipid syndrome, diabetic nephropathy, recipient hemodynamic status perioperatively (1066), ATN, and placement of graft on the left side (1068,1069).

However, most of these data were collected before the advent of sensitive flow crossmatch technologies. This is crucial to be taken into consideration because thromboses due to surgical complications have to be distinguished from severe acute rejection. The former are limited to the renal artery and/or vein, even in cases of graft infarction. Vascular rejection episodes on the other hand do not generally affect veins but rather large and small intraparenchymal arteries and glomerular capillaries with thrombus formation, fibrinoid necrosis, and inflammation. Cases of acute rejection with thrombosis are nearly always AMR and associated with the deposition C4d in the microcirculation. However, C4d is negative in areas of necrosis, even when due to AMR.

It also needs to be taken into consideration that a mild degree of endarteritis can be seen in autografts undergoing arterial thrombosis. Therefore, it is crucial to validate the presence of DSA in cases with arterial thrombosis for confirming a rejection pathogenesis.

Arterial Stenosis

With increasing age of utilized donors and recipients for renal transplantation, renal artery stenosis in the renal transplant recipient, which presents with hypertension and renal

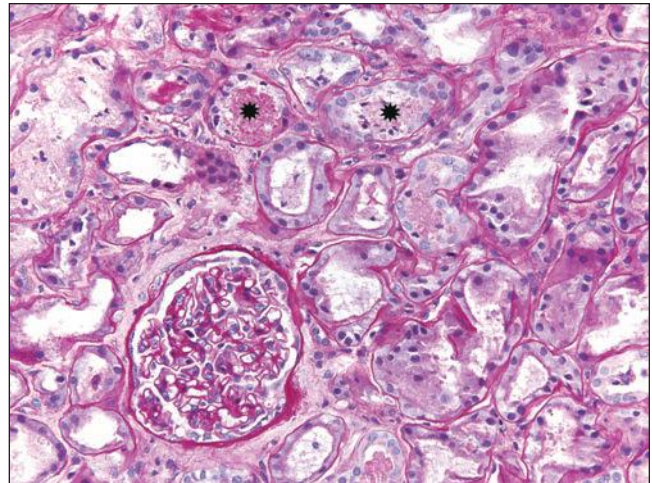


FIGURE 29.89 A patient with central renal artery stenosis and persistent allograft dysfunction only shows focal acute tubular injury and intratubular proteinaceous cast material (*asterisk*) in a graft biopsy. (PAS, original magnification 150 \times .)

dysfunction, can masquerade as rejection or be clinically overlooked (1070,1071). Renal artery stenosis is detected in 1% to 23% of patients, reflecting differences in diagnostic criteria and surgical expertise (1071) (Fig. 29.89). Most of the cases are diagnosed within 3 months and 24 months postsurgery; early or late occurrences, however, are not infrequent. Patients are usually treated with percutaneous angioplasty resulting in a significant, although sometimes only transient improvement of blood flow (1071). In one series, the frequency of rejection episodes was twice as high in the patients with stenosis, raising the possibility that transplant endarteritis and arteriopathy involving major arteries may potentially contribute to vascular stenosis (1072). The pathology in the kidney would be expected to show ischemic atrophy (small, simplified tubules with little interstitial fibrosis). However, we have seen two recent cases that showed acute tubular injury on repeated biopsies over several months so that pattern should raise the question of renal artery stenosis (Fig. 29.89).

Graft Rupture

The classic symptoms of allograft rupture are the sudden onset of severe pain, swelling over the allograft, oliguria, and hypotension. Almost all cases (96%) occur within 3 weeks of transplantation. The frequency in published reports ranges from 4% (1073,1074) to 0.35% in a series of 1682 living donor organs (1075). The usual cause of graft rupture in the past was rejection (accounting for approximately two thirds of the cases), but can be considered nowadays rare after the introduction of sensitive crossmatch technologies reducing the risk for unintentionally induced early hyperacute AMR. Other causes can be ATN (25%), renal vein thrombosis (10%), and trauma (rare) (1073–1077). Rupture is an indication for immediate surgical intervention that can result in graft salvage in about 50% of patients; untreated cases are associated with a high fatality rate.

DE NOVO AND RECURRENT RENAL DISEASES

Virtually all acquired diseases of native kidneys have been detected in renal allografts as de novo or recurrent diseases. Renal transplantation illuminates the early morphologic events during the development of recurrent diseases and can on occasion document the reversibility of preexisting donor diseases such as early diabetic changes or glomerular IgA deposits. The histologic criteria to establish the diagnoses are identical to those described in native kidneys, although the clinical course of the patients may differ due to the baseline immunosuppressive drug regimens administered. Glomerular diseases occurring after transplantation can be superimposed on other changes such as rejection or CNI toxicity.

De Novo Glomerular Diseases

Three de novo glomerular diseases have special significance to the allograft (membranous glomerulopathy [MGN], anti-GBM disease, and recurrent nephrotic syndrome in congenital nephrosis), because the lesions are probably caused by alloantibodies to donor antigens.

Membranous Glomerulopathy

Most cases of MGN in renal allografts occur de novo (67% to 83%) (1078,1079). De novo MGN typically presents with proteinuria 2 to 9 years after transplantation (1 month to over 15 years), sometimes in the nephrotic range. In one recent series, 88% had proteinuria $\geq 1+$, and 30% had nephrotic range proteinuria (1080). Recurrent MGN has an earlier onset (less than 2 years) (1079). The overall prevalence is about 0.3 to 2.1% among adult transplant patients in large series (1081–1083). The risk for MGN seems to be increased in pediatric kidney transplant recipients (9% in one series of 530 grafts (1084,1085) and with HCV (1086). In one series, 18% of allograft biopsies from HCV-positive patients had signs of MGN and decreased graft survival (1087).

Light microscopy often shows rather mild GBM changes accompanied by nonspecific mesangial hypercellularity. Characteristic granular IgG deposits are seen by immunofluorescence (Fig. 29.90). C4d is often present in the deposits (1080). IgG1 is usually more conspicuous than IgG4, in contrast to primary MGN (1080,1088). By electron microscopy, the deposits tend to be smaller and more irregular in distribution than in primary MGN; spike formation is often inconspicuous (1089) likely representing an early stage of the disease development. Endothelial and GBM changes of concurrent transplant glomerulopathy with duplication of the GBM are present in 47% to 50% of cases (1078,1089). Repeat biopsies have shown persistence or progression of the deposits in most patients (1078,1085); resolution of deposits is rare.

Patients with de novo MGN lack autoantibodies to the phospholipase A2 receptor (PLA2R), a feature that distinguishes them from the majority of patients with primary MGN (1090,1091). Evidence of chronic AMR is commonly present. Honda reported that all 5 of recipients with de novo MGN tested by flow cytometry were positive for DSA and 59% (10/17) had C4d deposition in PTC (1080). One case was reported to have colocalization of donor HLA class I and II antigens in deposits, although more needs to be done to substantiate this observation (1080). Collins and

colleagues reported similar findings in 17 patients with de novo MGN: 76% of patients with de novo MGN had C4d+ in PTC, and 58% had DSA, mostly to HLA-DQ (898). The onset of de novo MGN correlated temporally with de novo HLA-DQ DSA in one case (1093). Distinction between recurrent and de novo MGN can be usually achieved by demonstrating granular deposits of PLA2R along the GBM (1094), colocalization of IgG and PLA2R, or serum anti-PLA2R antibodies.

The pathogenesis of de novo MGN is uncertain. It has been suggested that inflammation in the glomerulus leads to an alloimmune response to occult antigens (1095). Because of the association with chronic AMR and the lack of PLA2R antibodies, it is likely that alloantibodies to an antigen on the podocyte contribute. In MHC-identical rat kidney allografts (LEW.1N to BN), de novo MGN develops in the graft but spares the native kidney, elegant evidence that the target is a non-MHC alloantigen (1096). Indeed, HLA-identical sibling grafts develop de novo MGN, perhaps with an increased frequency (this may be related to the longer survival of these grafts) (1097).

Therapy is not well defined in cases of posttransplant MGN (1095). One would expect that agents used in idiopathic MGN, such as rituximab, might be effective, but experience is limited. Retransplantation leads to “recurrent” de novo MGN in the majority of cases (4/7 in one series) (1098). De novo MGN had no effect on outcome in the older literature. However, Truong found that 42% lost their grafts within an average of 3 years of the biopsy, an outcome they attributed in part to chronic rejection (1089).

Anti-GBM Glomerulonephritis in Alport Syndrome (Fig. 29.91)

Anti-GBM antibodies without glomerulonephritis are common after transplantation (10% to 60%) in Alport patients but cause significant glomerulonephritis in a small minority (1099–1101). Alport kidneys fail to express the type IV collagen autoantigen of Goodpasture syndrome (1102), and thus, Alport patients may lack self-tolerance to certain α -chains of type IV collagen. Those can be recognized as a foreign antigen after transplantation and trigger an immune response (1103–1105).

Florid de novo crescentic and necrotizing glomerulonephritis due to anti-GBM antibodies after transplantation is seen in 3% to 5% of male adult renal allograft recipients with typical Alport syndrome (1106,1107). The time of onset of the anti-GBM glomerulonephritis varies from a few days to several months postgrafting. The risk factors for its development are not entirely clear. One factor may be whether the patient expresses enough $\alpha 3$ -chain in the thymus to promote tolerance, perhaps related to the specific mutation. In support of that hypothesis, large *COL4A3* deletions are associated with development of anti-GBM disease (1108), although other mutations have also been implicated (1109). Another factor may be a local inflammatory stimulus, as in a female Alport recipient with a late onset of anti-GBM nephritis associated with acute pyelonephritis (1110).

The morphology of anti-GBM disease occurring posttransplantation is very similar to that observed in native kidneys. It is characterized by the formation of extracellular crescents, segmental fibrinoid glomerular tuft necrosis, and a

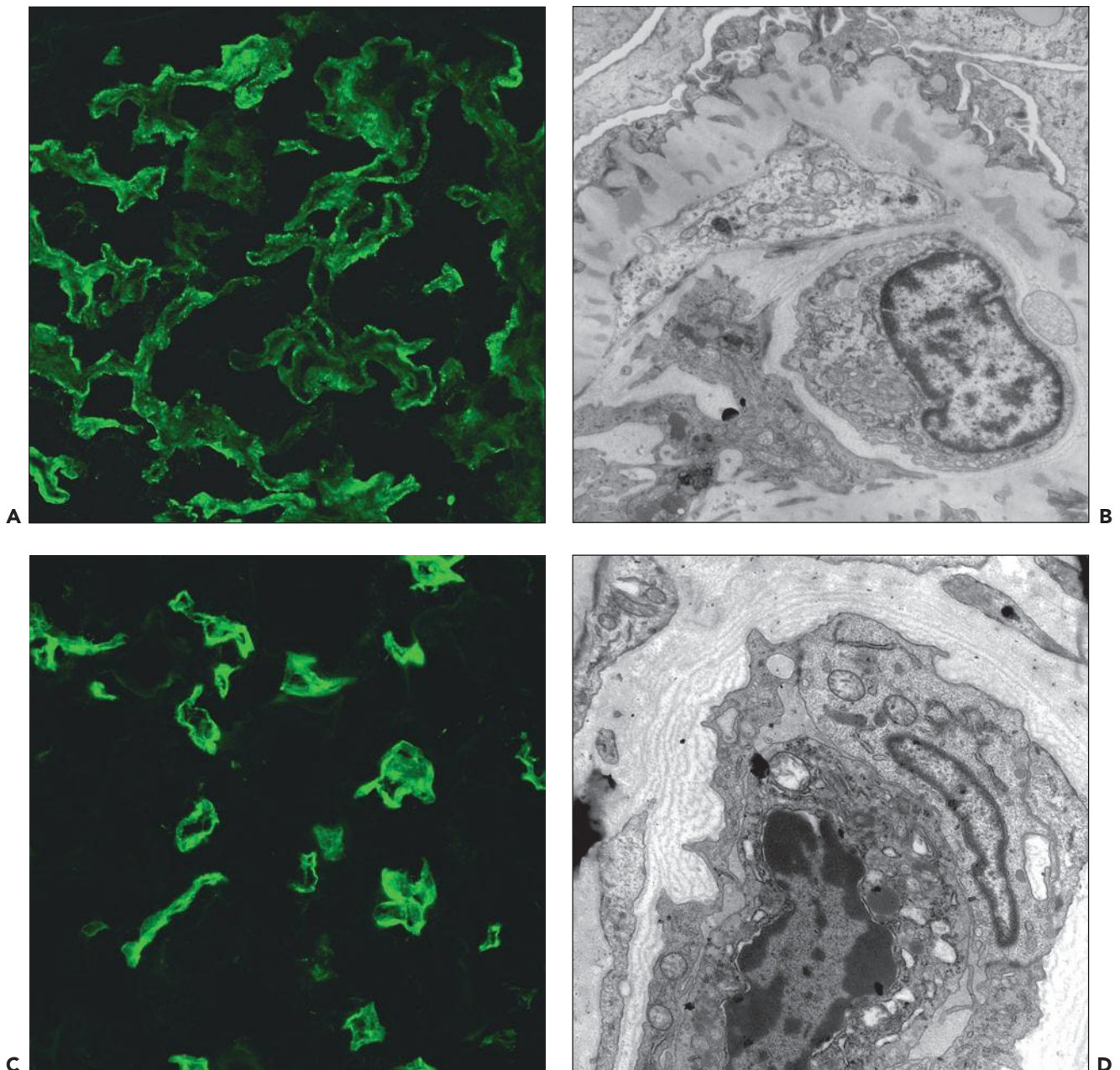


FIGURE 29.90 De novo MGN in a renal transplant. **A:** Granular deposits that stain for IgG are along the GBM. **B:** Electron microscopy reveals subepithelial and intramembranous deposits. **C:** Widespread C4d deposition in PTC which in **(D)** show multilaminated basement membranes. Patients with de novo MGN commonly also have evidence of AMR with C4d deposition in the PTC and DSA (see text).

lack of significant endocapillary proliferation. Tubules show signs of acute injury and intratubular red blood cell casts. By immunofluorescence microscopy, typically bright diffuse and global, linear staining for IgG and less pronounced C3 is detected along peripheral glomerular basement membranes. Fibrin is found in areas of tuft necrosis and extracapillary proliferation.

Even though de novo anti-GBM disease is rare, monitoring these patients for GBM antibodies is recommended

(1111). Anti-GBM antibodies in X-linked Alport transplant recipients differ from those in patients with anti-GBM disease in native kidneys because they bind to the native α 345 NC1 hexamers of the GBM and α 1256 NC1 hexamers of the Bowman capsule (1112,1113). These antibodies are best detected by Western blot rather than enzyme-linked immunosorbent assay (1114).

Three quarters of the grafts with anti-GBM nephritis fail (1106,1107). Anti-GBM nephritis can recur in successive

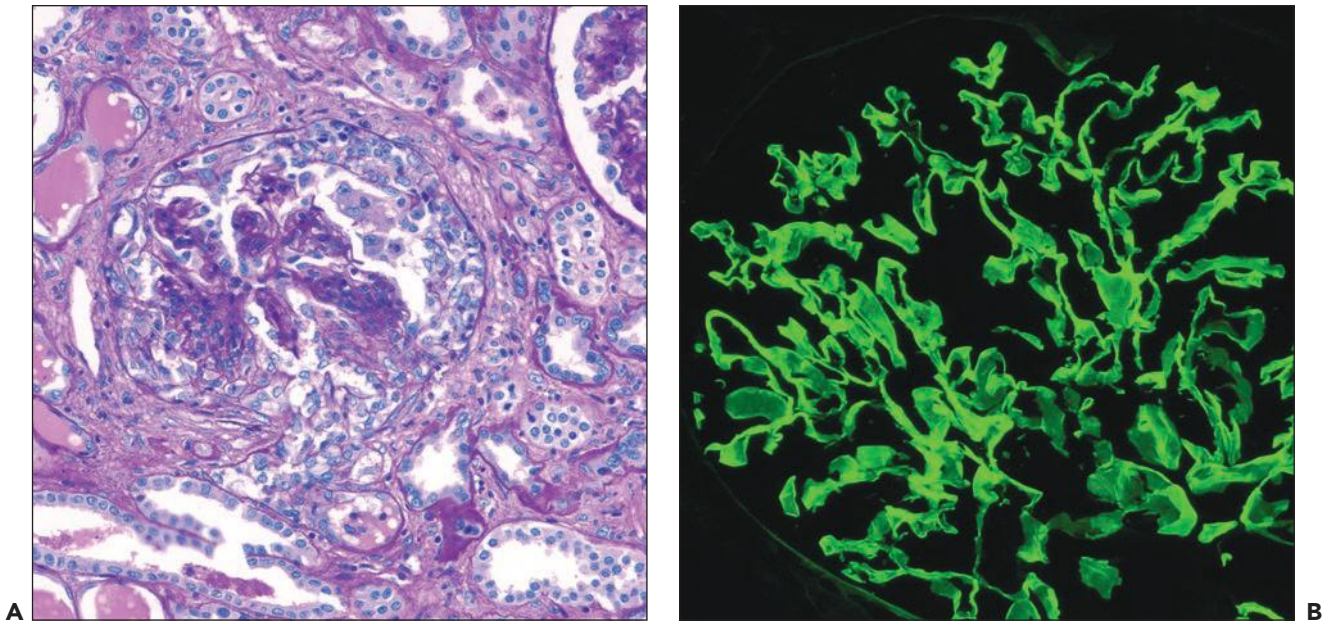


FIGURE 29.91 De novo anti-GBM disease in a 37-year-old woman with X-linked Alport syndrome. Graft was removed after patient returned to dialysis 1 year after second transplant. Her first graft also failed from de novo anti-GBM disease. **A:** Cellular crescents were prominent in the nephrectomy specimen stained with PAS. (200× original magnification.) **B:** Bright linear staining for IgG is seen in the GBM. (400× original magnification.)

allografts (1115–1117) (and personal experience); however, successful retransplantation has been reported in three cases (1118). However, the second recurrence can be accelerated and develop in the immediate postoperative period (1117).

Congenital Nephrotic Syndrome of the Finnish Type

An autosomal recessive disease due to mutations in the nephrin gene *NPHS1*, which paradoxically leads to posttransplant nephrotic syndrome. In a large recent series, 13/65 (20%) recipients developed recurrent nephrotic syndrome (1119). Furthermore, all 6 retransplants developed recurrent nephrotic syndrome. The patients with posttransplant nephrotic syndrome had the Fin-major/Fin-major genotype, leading to complete absence of nephrin (1120). Electron microscopy revealed endothelial swelling of the glomerular capillaries, resembling chronic transplant glomerulopathy, but the GBM is normal. Two grafts had a morphology of minimal change disease (1121,1122) and completely responded to cyclophosphamide as did 7/13 of in a later series. The pathogenesis is believed to be alloantibodies to nephrin. Antinephrin antibodies were detected in 73% of 13 recipients with posttransplant nephrotic syndrome (1119). Plasmapheresis (1119) and rituximab (1123) have been reported to be beneficial.

De Novo Focal and Segmental Glomerulosclerosis (FSGS)

FSGS in allografts has been described in several settings: (i) in long-standing grafts, in which nephron loss and fibrosis lead to glomerular hyperfiltration injury; (ii) in adult recipients of pediatric kidneys, in whom the presumed pathogenesis is hyperfiltration injury; (iii) in grafts with severe vascular disease resulting in presumed glomerular hypoperfusion and (secondary) collapsing FSGS; and (iv) as new onset primary FSGS (rare).

De novo FSGS is frequently seen in late allograft biopsies obtained many months to years after transplantation, associated with nephron loss and glomerular hyperfiltration or, in some cases, potentially even glomerular hypoperfusion (1124). FSGS is often found in cases of late structural CNI-induced toxic changes, nephron loss, and fibrosis. Although certain histologic subtypes of FSGS (i.e., “perihilar”) are more common in secondary FSGS variants, a distinction between “primary” and “secondary” can typically not be rendered based on morphologic grounds. Similar to observations made in native kidneys, glomerular size correlates with the presence of FSGS in allografts (although this phenomenon cannot easily be appreciated by standard light microscopical examination) (1125). In biopsies taken two or more years from the time of transplant, the mean glomerular diameter increased by 37% from 148 μm pretransplant to 203 μm in kidneys with FSGS versus 158 μm in kidneys without FSGS taken at the same time interval. These results further support the hypothesis that FSGS develops in conjunction with glomerular hypertrophy.

The collapsing variant of FSGS can arise de novo posttransplantation (817,1124,1126,1127). Most patients present with modest proteinuria or nephrotic syndrome. The pathology typically shows severe small-vessel disease involving arteriolar hyalinosis related to CNIs and, less commonly, other lesions such as TMA, transplant endarteritis or arteriopathy, or transplant glomerulitis. It is likely that one of the pathogenetic factors is vascular stenosis that leads to glomerular hypoperfusion and collapse. The outcome is poor (1126) with rapid progression to end-stage renal failure seen in 4/5 patients within 2 to 12 months in one series (817). Rare cases have been associated with parvovirus B19 (1128), perhaps related to TMA, which can occur with this infection (1129).

A rare form of rapidly progressive de novo FSGS occurs in adult recipients of kidneys from children less than 3 years old. The first reported case also had an infarcted upper pole due to aberrant arteries, causing further loss of renal mass (1130). All of four patients developed severe hypertension, heavy proteinuria, and ultimate renal failure after 1 to 9 months (1131). Biopsies disclosed focal and segmental glomerulosclerosis with crescents in three patients; the fourth had only mesangial hypercellularity (1131). The authors concluded that severe hypertension and glomerular hyperperfusion promoted glomerular sclerosis and crescent formation in maturing infant kidneys (1131).

De novo Minimal Change Disease

Occasional patients develop nephrotic range proteinuria after renal transplantation due to de novo minimal change disease (MCD). In one series, 7% of recipients (5/67) with nephrotic syndrome had MCD (1132). MCD develops early after transplantation in greater than 90% of the cases (5 days to 4 months); however, one case was 8 years posttransplant (1133). The pathology sometimes differs from MCD in native kidneys by deposition of IgM/C3 in the mesangium and mononuclear cell glomerulitis. Evidence of acute TCMR or acute CNI toxicity may also be present. One patient had an ABOi kidney graft, but there was no evidence of acute AMR (1134). A variety of treatments including high-dose steroids, angiotensin-converting enzyme inhibitors, or angiotensin receptor blockers induced sustained remission in greater than 90% of recipients; plasmapheresis had little effect in one case (1134). The majority of reported cases are in living related kidneys (8/14), which may be a risk factor (1132). The mechanism is not clear, but may be related an alloimmune reaction, analogous to the MCD that sometimes accompanies allergic drug reactions.

Other De Novo Glomerular Diseases

Most acquired glomerular diseases can arise de novo in the allograft. AL amyloidosis was a late complication in 4 patients (16 to 31 years posttransplant), all lambda light chain; bone marrow plasma cells were $\leq 10\%$ (1135). One patient had a stem cell transplant with a complete hematologic response and was retransplanted successfully.

De novo TMA is most often due to CNI toxicity or acute AMR (869). Rare cases have been described associated with CMV infection (1136). Of interest, 29% of the de novo TMA cases (7/24) had mutations in CFH or CFI that were unsuspected prior to transplant, and 25% of the patients had low C3 (1137). Outcome was particularly poor in those with mutations; 86% of the grafts were lost within a year, compared with 6% without mutations. One case responded to eculizumab (1138).

Nodular diabetic glomerulosclerosis has been documented in many patients (1139), typically occurring 6 years after the onset of diabetes and without a prominent effect on graft outcome (1139). Risk factors were not identified. Small numbers of cases have been reported of de novo IgAN (629), fibrillary glomerulopathy (629,1140), and proliferative glomerulonephritis with monoclonal IgG deposits (1141).

Recurrent Glomerular Diseases

Renal transplantation provides unique opportunities for insights into the basic mechanisms of renal disease and its earliest manifestations. Two idiopathic glomerular diseases

were first shown to be caused by blood-borne factors due to their recurrence in the graft (FSGS and dense deposit disease). Conversely, the failure to recur proves that the disease is intrinsic to the kidney (e.g., Alport disease, autosomal dominant polycystic kidney disease) or that the pathogenetic mechanisms are "burnt out" (nephritis due to anti-GBM antibodies).

Recurrent glomerular disease is a significant problem, accounting for 8.4% of graft failure over ten years among patients whose original disease was glomerulonephritis/glomerulopathy (685). That cause of graft loss was exceeded only by chronic rejection and death with a functioning graft.

The precise frequency of recurrence and its contribution to graft failure is difficult to ascertain. Many publications are difficult to interpret due to small numbers, short follow-up, unknown and unclassified native kidney diseases, and lack of definitive pathologic studies. Information provided on graft survival does not always demonstrate whether recurrent disease or other causes (such as rejection) resulted in ultimate transplant failure. At present, however, three diseases clearly have impact on graft survival: primary FSGS, atypical HUS, and forms of membranoproliferative glomerulonephritis (probably mostly C3 nephropathy). Other recurrent diseases are expected to have a greater impact on survival as other causes of graft failure, such as rejection, are reduced.

The diagnosis of recurrence requires the accurate classification of the original kidney disease (either in a biopsy or nephrectomy specimen) and proper diagnostic workup of a subsequent graft biopsy including special stains and immunofluorescence as well as electron microscopical studies. Many different kidney diseases may potentially recur during the lifetime of the graft, for example, glomerulonephritides, diabetic glomerulosclerosis, or hypertension-induced arterionephrosclerosis, all of which present similarly in native and transplanted kidneys. Here, we will focus on few, significant, and informative disease entities.

Focal segmental glomerulosclerosis (FSGS) recurs in about 25 to 40% of recipients with primary (idiopathic) FSGS (1142,1143); in a series of 77, 55% recurred (1144). Patients with recurrence had a lower 5-year graft survival (50% to 72%) than those without recurrence (82% to 86%) (1142,1144). Primary (idiopathic) FSGS accounts for most, if not all, of the recurrences (1142). Secondary FSGS (1142,1145–1147) and familial or genetic FSGS (1142,1148–1150) recur infrequently if at all. However, a few recipients with mutations in the *NPHS2* (podocin) have had recurrent nephrotic syndrome, due to unknown mechanisms (1151). All morphologic patterns of FSGS, as defined by the Columbia classification, recur (1152). The pattern of recurrence reflects the pattern in the native kidneys in 81% of recipients (17/21), although there are exceptions (1152). Early after transplant (less than 1 month), only an MCD-like lesion without the scarring is usually seen (1144,1152) (Fig. 29.92). Furthermore, some transitions have been noted between FSGS, not otherwise specified, and the collapsing or the cellular variants. Another series showed that the Columbia classification categories had a similar recurrence in 77 recipients with idiopathic FSGS (of which 42 developed recurrence). They found no correlation between pre- and posttransplant pathologic variants, and all Columbia variants recurred with similar frequency.

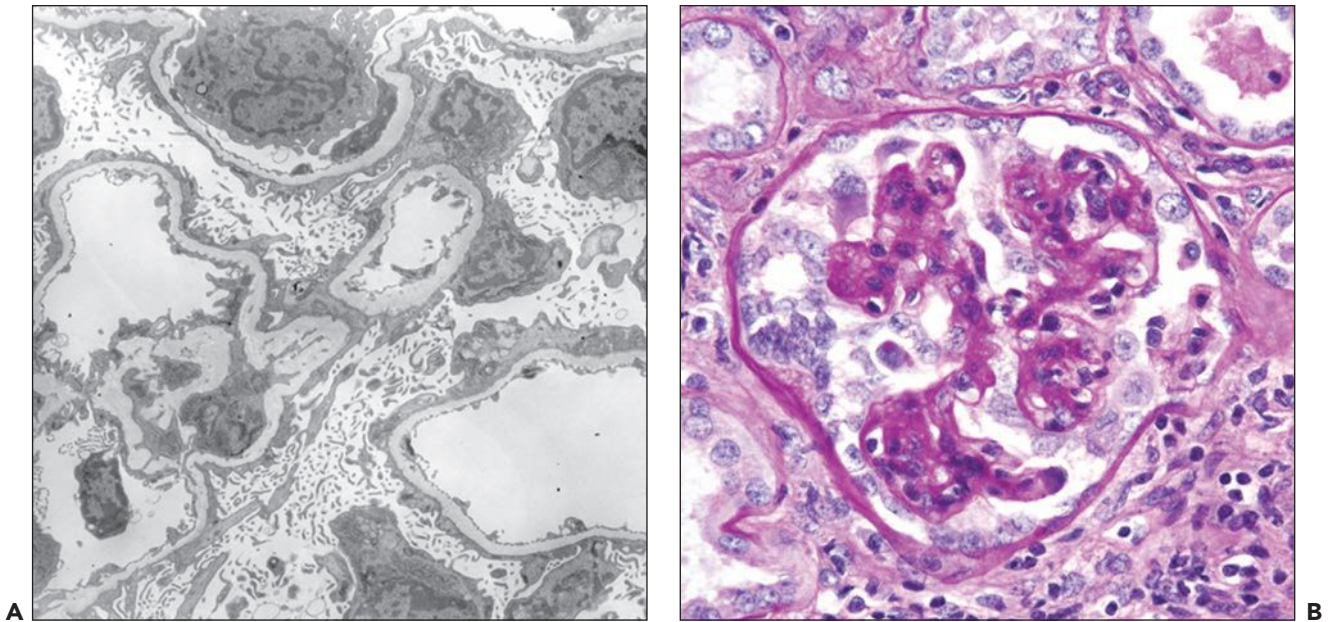


FIGURE 29.92 Recurrent FSGS in a 7-year-old boy who developed nephrotic range proteinuria immediately after transplant. **A:** Electron microscopy of a biopsy taken on day 2 shows a minimal change like lesion with widespread effacement of foot processes and microvillous change in the podocytes. **B:** Graft was removed 1 year later for intractable protein loss. Glomeruli showed FSGS lesions with collapsing features, the same as in his original disease. (PAS stain, original magnification 400 \times .)

The time of recurrence averages 7.5 months in adults (1153) and 2 weeks in children (1154). Occasionally, the recurrence is immediate and dramatic, with proteinuria noted in the first drop of urine emerging from the ureter at surgery, indicating a potent blood-borne factor is responsible. The risk factors for recurrence include low serum albumin at time of diagnosis (1109), rapid progression of the original disease (1148,1153,1155–1158), diffuse mesangial hypercellularity (1148,1157,1159–1161), and young age (1148,1160). Children have a recurrence rate 5 times that of adolescents and adults (50% vs. 11%) (1160). The rate of recurrence seems to be increased in organs of living donation (1162,1163). FSGS recurred in 56% of 16 children who developed renal failure from their native kidney disease within 3 years and in 9% of 11 children with a longer disease course (1155). After a graft is lost to recurrence, the probability of recurrence in a second transplant increases to up to 80% (1153,1157,1164).

The study of renal transplants has allowed insights into the early phase of podocyte injury in FSGS. The pathologic changes in biopsies begin as widespread foot process effacement and villous transformation of the cytoplasm (1 to 2 weeks), followed by podocyte detachment (so-called dropout), segmental tuft sclerosis, and the accumulation of intracapillary foam cells (1 to 2 months) (1165). Displaced slit diaphragms, similar to those in aminonucleoside-treated rats, have been observed (1166). Podocytes show profound changes in adhesion molecules and signs of transdifferentiation into macrophage-like cells (1167,1168). CD44 is up-regulated in both podocytes and parietal epithelium (1169). Sphingomyelin phosphodiesterase acid-like 3b (SMPDL-3b) protein is reduced (1170). In the early phase, podocytes down-regulate $\alpha 5$; $\alpha 3$ - and $\beta 3$ -integrins lose their polarized expression, and the HAR/GP90 receptor is transiently expressed in

a nonpolarized pattern. The loss of adhesion molecules probably is responsible for the podocyte detachment that is characteristic of FSGS (1168). Podocyte foot processes are restored after remission is induced by plasmapheresis (1153). With further evidence of the reversibility, retransplant of a kidney with early recurrence of FSGS on posttransplant day 14 into a second patient (with end-stage diabetic nephropathy) led to a prompt resolution of the disease (1171).

Considerable effort has been made to identify the blood-borne factor responsible for recurrence to provide insights into the mechanisms and therapy and to seek a useful diagnostic test. The nature of the putative molecule is still disputed, with most recent evidence for (1172,1173) and against (1174) soluble urinary plasminogen activator receptor (suPAR). Serum from FSGS patients down-regulates MPDL-3b expressed on cultured podocytes (1170). Proteomic studies of the urine have identified increased levels of apolipoprotein A-1b in 93% (13/14) of recipients with recurrent FSGS and only 3% of patients with other causes of proteinuria (1175). If confirmed, this will be significant as a diagnostic marker and possibly pathogenetically relevant.

Therapy for recurrent FSGS is still evolving and is well summarized in a recent review (1143). Among the current approaches are plasmapheresis and anti-CD20 (rituximab) (1176). Several small case series reported that plasmapheresis could diminish the proteinuria in 50% to 60% of recipients, but had little long-term effect. These studies were uncontrolled and retrospective with the usual publication bias for success (1143). More recently, rituximab therapy has been associated with remission, but controlled trials are lacking. The mechanism is thought to be a cross-reaction of rituximab with SMPDL-3b expressed on podocytes (1170). TNF- α antagonists have also reported individual successes (1177). A pilot

trial of abatacept (CLTA4-Ig) has shown promise in a subset of patients with B7.1 expression on podocytes (1178).

Membranoproliferative glomerulonephritis, type I (MPGN-I), is a pathologic diagnosis due to heterogeneous causes. The historical data lump together those with immunoglobulin deposits, those with pure C3 deposits that would now be classified as C3 nephropathy, and some with monoclonal gammopathies. Overall, MPGN-I has been estimated to recur in the transplant with clinical signs of proteinuria in 20% to 50% of patients and lead to graft failure over several years in 10% to 50% (1179–1183). In a recent large series, 12/29 cases recurred as judged by protocol biopsies from 1 week to 14 months posttransplant (median 3.3 months) (1183). Five of the twelve with recurrence had no IgG in the glomeruli and were probably examples of C3 glomerulopathy. Three had monoclonal immunoglobulins in the serum and light-chain restriction in the biopsy and were presumably examples of glomerulonephritis related to monoclonal gammopathy. The published risk factors for recurrence include low serum complement (C3 or C4) (1183), crescents in the original disease (1184), previous recurrence (1184), and possibly kidneys from living donors (1183).

Recurrent MPGN-I usually presents morphologically as a global and diffuse glomerular disease with signs of endocapillary proliferation, mesangial hypercellularity, GBM duplication, mesangial cell interposition, and accentuation of the tuft lobulation. Some have prominent crescents. The disease is typically milder on protocol biopsies (1183). Immunofluorescence microscopy demonstrates global and diffuse deposition of C3. In a subset, IgG accumulates along glomerular capillary walls and in the mesangium. Ultrastructurally dense, abundant deposits with relatively sharp edges are found most often along the lamina rara interna (associated with the interposition of cell processes and new subendothelial basement membrane formation) and in mesangial regions (1182).

Careful morphologic analyses can usually distinguish MPGN-I from its histologic mimics. The pathologic differential diagnosis includes transplant glomerulopathy due to chronic TCMR, AMR, CNI toxicity, and other forms of TMA (see Table 28.9). In contrast to MPGN-I, the latter lesions show less pronounced endocapillary and mesangial proliferation, and GBM duplication is commonly not associated with prominent cell interposition (160). Chronic AMR- and CNI-induced TMAs usually show minimal immune deposits by immunofluorescence microscopy and electron microscopy (160,1185,1186). The GBM may have a prominent multilayered and wavy appearance (160,1185), which is not found in MPGN-I. Immune complex-mediated glomerulonephritis related to HCV can look very similar to MPGN-I with Ig deposits. The presence of C1q and cryoprecipitates in glomeruli, if present, favors HCV.

No specific treatment strategies for recurrent MPGN-I have been established; most often therapeutic attempts with cyclophosphamide or plasmapheresis are made (1180). Regression of the immune deposits after long-term graft survival has been documented in anecdotal cases (1187).

C3 Glomerulopathies

C3 nephropathies, including dense deposit disease (DDD) and C3 glomerulonephritis, are due to either genetic or acquired systemic abnormalities in the alternative complement activation pathway and usually recur in the transplant.

Treatment has not yet been established. A few cases have been treated with eculizumab, but the long-term efficacy remains to be proved (1188–1191). Eculizumab, a humanized monoclonal antibody, deposits in the glomeruli and TBM giving a granular pattern for IgG2 and IgG4 heavy chains and kappa light chain (1190).

Dense deposit disease recurs in nearly all patients after renal transplantation; however, recurrence is not inevitable (1192–1194). The diagnosis is usually (10/11 patients) established in the first graft biopsy, taken as early as 12 days after surgery (1193). Serum C3 levels are low in approximately 65% of patients with morphologic evidence of recurrent disease (1193,1095). The dense deposits, intensely and exclusively staining for complement factor C3, can either be found in the mesangial regions and/or in glomerular capillary walls (1193). Additional deposits may be seen in tubular basement membranes and the Bowman capsule (1196). Whether C3 deposits can first be noted by immunofluorescence microscopy followed by the subsequent formation of ultrastructurally identifiable dense deposits (1197) or vice versa (1198) is debated. Over time, DDD may persist or even regress (1198). Crescent formation in the native kidney is a risk factor for recurrence (1184), and crescent in the recurrence is a risk factor for graft loss (1193,1195). Outcome in pediatric renal allograft patients with recurrent DDD did not differ from controls (1199). Follow-up biopsies failed to demonstrate a significant increase in global glomerulosclerosis compared to control kidney grafts without recurrent disease (1195).

C3 Glomerulonephritis In addition to the cases of membranoproliferative glomerulonephritis due to C3 abnormalities, isolated examples of C3 glomerulonephritis that recurred have been reported (1190,1200,1201) and, in a few cases, led to graft failure (1201). In two of these cases, patients with mutations in the CFH gene had atypical HUS as the original cause of renal failure, but the recurrences showed C3 glomerulonephritis with prominent mesangial and subepithelial deposits as well as a later biopsy with TMA (1200), arguing that these pathologic patterns are different manifestations of the same underlying abnormality.

ATYPICAL HEMOLYTIC UREMIC SYNDROME

Atypical Hemolytic Uremic Syndrome (aHUS) recurs in most patients in contrast to the rare recurrence of HUS caused by Shiga toxin/*E. coli* infections (1202,1203). Recurrent aHUS typically becomes manifest during the first year postgrafting with symptoms noted as early as the first postoperative day. In a minority of patients (18%), HUS affects the kidney in the absence of overt clinical symptoms (1204). Among 57 patients with aHUS who received kidney transplants, mutations in complement genes were detected in (68%) including CFH, CFI, MCP, C3, and CFB. Genetic abnormalities were a risk factor for recurrence, especially loss of function mutations in CFH and gain of function mutations in C3 and CFB (1205). mTOR inhibitor drugs, but not CNI, increased the risk of recurrence (1205).

The diagnosis of recurrent HUS/TMA is difficult because de novo variants in the transplant have a similar pathology (CNI, sirolimus, or OKT3 therapy; acute AMR). A focal distribution pattern may favor a diagnosis of CNI-induced toxic injury, and the lack of C4d deposition largely excludes acute AMR.

Historically, even using intensive plasmapheresis and fresh frozen plasma, most patients with recurrence lost their graft; among a group of 57 patients, 50% lost their graft within 3 years (1205). Recently, eculizumab was approved for treatment and prevention of aHUS in native kidneys, and small numbers of cases have been treated after transplant with dramatic results. In the largest series of patients, all with mutations of the complement system, prevention of aHUS was achieved in 8/9 and successful reversal of symptomatic recurrent aHUS in 13/13 (1189).

IGA NEPHROPATHY

IgAN recurs with a frequency of 18 to 31% in recent large series (1206–1209). Patients present with microscopic hematuria and less often proteinuria, hypertension, active urinary sediment, or elevated serum creatinine (1210). Additional patients have subclinical recurrence evident only on biopsy. Protocol biopsies detected recurrence in 32% of 65 recipients in the first year as defined by at least 1+ mesangial IgA; 52% of these patients had no urinary abnormalities (1211). Factors, which are associated with increased risk of recurrence, are young recipient, IL-10 genotype, better HLA-DR match, living related donors, crescents in the original disease, and a greater number of rejection episodes (1208–1210). Steroid use reduced risk of recurrence by 50% (1212). Curiously, this effect was specific for IgAN; steroid use increased the risk of recurrence of FSGS and MPGN (1212). Cyclosporine reduced the risk by 43% in a small series (1211), but others have not seen this correlation (1206).

Recurrent glomerular IgA deposits usually present with only minor histologic abnormalities including no or mild mesangial hypercellularity, IgA deposits detected by immunofluorescence microscopy or immunohistochemistry, and mesangial electron-dense deposits observed by electron microscopy. Crescents are rare and are associated with graft failure (90% within 3 years) (1213).

The overall graft survival in patients with IgAN is similar to that in recipients with other primary diseases (1210). However, those with IgAN recurrence have a lower 10-year graft survival than those that did not recur (61% vs. 85%, respectively) (1209). Among 1521 recipients with IgA nephropathy, 54 (12.6%) were lost due to recurrent disease (1212), similar to a 9.4% frequency in another report (18/190) (1207). Paradoxically, among patients with a biopsy for cause, patients whose IgAN does not recur do worse than those with recurrence (51% vs. 74% 10-year graft survival, respectively), suggesting late rejection is worse than recurrence (1214).

HENOCH-SCHÖNLEIN PURPURA

Among 74 grafts, clinical Henoch-Schönlein Purpura (HSP) recurrence developed in 20% and graft failure from recurrence in 12% (1215). Recurrence appears to be associated with a shorter duration of the original disease (i.e., progression of renal failure in less than 30 months) and is not prevented by delay of transplantation of 12 months or more from the time of the original HSP (1215). One patient with hereditary C4 deficiency who had HSP developed recurrent and irreversible IgA nephropathy in the graft (1216).

MEMBRANOUS GLOMERULONEPHRITIS

The overall frequency of recurrence of MGN is about 40% in recent large series (1217). Recurrent MGN can appear within 1 to 2 weeks after transplantation with symptoms of severe

proteinuria (1218), but most commonly has a later onset, and about 50% have subnephrotic range proteinuria (1217). The median time to clinical or protocol biopsy recurrence is about 13 months (1217,1219); 28% develop symptoms and signs within 4 months (1220–1224). Protocol biopsies can reveal the recurrence before proteinuria develops (1217). In the past, no conclusive risk factor was identified, except possibly living related donors and HLA matching (1219).

More recently, assays for PLA2R are being performed with the expectation that they may be predictive (1218,1225). Among 34 recipients with ESRD due to MGN, 23 (67%) were positive for PLA2R antibodies pretransplant. Recurrent MGN developed in 74% of these patients, compared with 32% of the patients without PLA2R antibodies (1226). Median time for recurrence was shorter in patients with high levels of pretransplant PLA2R antibody (11 weeks vs. 51 weeks in those without PLA2R antibody). One dramatic case with monoclonal IgG3κ anti-PLS2R autoantibodies recurred 13 days posttransplant (1227). A minority (10–30%) of MGN in allografts are due to recurrence, and the majority are de novo (1083,1221). Fortunately, serum PLA2R assays can usually distinguish these etiologies, since de novo MGN is uniformly negative for PLA2R autoantibodies and recurrent MGN is usually positive (50% to 70%) (1091).

Protocol biopsies allow early diagnosis and monitoring the effect of treatment (1217). In early cases, light microscopy (including PAS or silver stains) will not demonstrate diagnostic abnormalities, but these can be detected by immunofluorescence microscopy (1228). IgG, kappa, lambda, and C4d are routinely detected. C3 is usually not prominent in the early phase (16/21 were negative or trace) (1228) but does appear on subsequent biopsies (1217). Mesangial deposits are usually absent. Colocalization of IgG and PLA2R is found in most cases (1227,1229). Granular deposits of PLA2R along the GBM by immunofluorescence in paraffin sections help distinguish recurrent from de novo MGN. Most cases (83%, 10/12) of recurrent MGN but few cases of de novo MGN (8%, 1/12) had positive GBM staining for PLA2R (1230). By electron microscopy, the subepithelial deposits lack spikes in about 79% (15/19) of early biopsies, and 42% (8/19) had no detectable subepithelial deposits (1228) (Fig. 29.93). The combination of positive immunofluorescence and negative electron microscopy was proposed to be “stage 0” MGN (1228).

Recent reports have shown encouraging complete or partial remission in the majority of patients treated with rituximab,

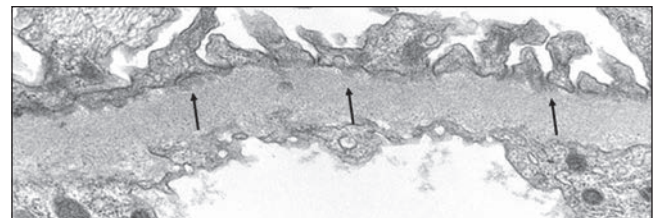


FIGURE 29.93 Recurrent MGN. Electron microscopy reveals tiny subepithelial deposits without spikes (*arrows*) in the early phase of recurrence. Biopsy taken 3 weeks posttransplant. Light microscopy was normal, but granular GBM IgG deposits were detected by immunofluorescence. (Original magnification 11,000×.)

but the reported numbers are small (1219,1231–1233). In the largest series, 6/8 (75%) of patients had a complete or partial remission at one year following rituximab therapy (1233). Postrituximab biopsies in 7 patients showed evidence of resorption of deposits by electron microscopy and loss IgG and C3 by immunofluorescence (43% and 57%, respectively) (1233).

ANTI-GBM DISEASE

Anti-GBM disease recurs if circulating antibodies are present after transplantation. Since the anti-GBM autoantibody response is usually transient, recurrence can be minimized by postponing transplantation for 6 to 12 months after the serum has turned negative for anti-GBM antibodies (1220,1234,1235). Nephrectomy of the native kidneys has no beneficial effect on graft survival (1220,1236). In the early experience, 41% of 68 grafts developed recurrent linear GBM IgG deposition, but only 10% of the grafts failed (642). The most recent series had no recurrence-related graft loss among 10 patients (1237), although individual cases of graft loss are still reported (1238). Recurrent glomerulonephritis and graft failure were observed in an unusual patient with monoclonal IgA antibodies directed against the $\alpha 1/\alpha 2$ (IV)–collagen chains (collagenous domain) (1239). Another case of “recurrence” was diagnosed in a patient 12 years after grafting, potentially representing a second de novo event (1240).

ANTINEUTROPHIL CYTOPLASMIC ANTIBODY-MEDIATED DISEASES

ANCA-associated renal disease recurred in 17% to 19% of patients regardless of the underlying disease entity (Wegener granulomatosis, microscopic polyangiitis, or renal-limited disease forms), the original ANCA type (elevated MPO vs. PR3 antibodies), the presence or absence of circulating ANCAs at the time of transplantation (in clinically asymptomatic patients), the type of graft (living vs. deceased donor organs), or cyclosporine therapy (1241). One recent series of 93 recipients found a recurrence rate of 2% (1242). Recipients with microscopic polyangiitis, but not granulomatous polyangiitis, had almost a twofold increased rate of graft loss or death by 10 years compared to non-ANCA recipients (1242). In a single-center study of 35 recipients, 3 had relapses (8.5%), none involving the transplant, with 5-year graft survival of 94% (1241). Recurrence can arise at any time (5 days to 89 months postgrafting) but rarely causes graft failure (1237,1243–1245). At the time of recurrence, ANCA titers are generally elevated (1246,1247), although sometimes only marginally (1245). Recurrence has also been reported in extrarenal sites, sparing the allograft (1245). Recurrent ANCA disease responds favorably to therapy including cyclophosphamide (1245,1248,1249) and, more recently, rituximab (1250). Recurrent forms of ANCA-associated small-vessel vasculitis and pauci-immune glomerulonephritis are histologically identical to those seen in native kidneys. The complement degradation product C4d is not deposited along PTC.

SYSTEMIC LUPUS ERYTHEMATOSUS

The reported clinical recurrence rate of lupus nephritis was 2.7% among 971 living related recipients (1251). The true recurrence rate is actually higher, because it is often mild or subclinical. Protocol biopsy studies of both living and deceased donor kidneys yield a recurrence rate of 54% (1252). Histologically, recurrent lupus often shows mesangial hypercellularity (class II)

or just mesangial deposits (class I) (1252–1255). Classes I and II would be missed in graft biopsies if special studies were not performed. Goral and colleagues found in 50 transplanted lupus patients an overall recurrence rate of 30% (52% of patients who underwent biopsy). Most common was a mesangioproliferative pattern (class II seen in 8 patients), followed by a focal proliferative pattern (class III, 4 patients), and an MGN (class V, 3 patients). In another series of 177 recipients, recurrence was detected in 11%, and recurrence was a risk factor for graft loss (hazard ratio of 2.48) (1254). Other series are similar. The majority of protocol biopsies had subclinical, class I to II lupus nephritis (1252). In a series of 32 SLE recipients in China, lupus recurred in 19% (50% class I or II, one III, and one IV), without an impact on patient or graft survival (1255).

The risk of recurrence is higher in black recipients (shorter time to recurrence) (1254) and living donors (vs. deceased donors) (1252) and, for unexplained reasons, is less in 2 haplotype-matched living related recipients (vs. 0 haplotype match) (1251). Recurrence is clinically often associated with an increase in ANA and dsDNA antibody titers, a decrease of serum complement levels, hematuria, proteinuria, rash, or Raynaud phenomenon. However, clinical features of pathologic recurrence can be quite bland.

AMYLOIDOSIS

Only a selected group of patients with amyloidosis receive kidney transplants, based in part on the extent of extrarenal involvement. Recurrence depends on the amyloid type and the progression of the underlying disease. In a French series of 59 recipients with AA amyloidosis, recurrence was documented in 14% (8.7% in chronic inflammatory conditions, 20% in familial Mediterranean fever (FMF), 11% in chronic infections) (1256). Recurrence was detected at a median of 10 years post-transplant (8 to 20 years) and commonly associated with proteinuria (75% nephrotic syndrome). The overall 5- and 10-year patient survival was lower than in recipients without amyloidosis; however, graft survival censored for death was similar. The causes of death were largely cardiovascular amyloidosis and infection. Recurrence in the graft and older recipients were the two risk factors for death. In a large series from the UK amyloidosis center, 34% of 128 patients with renal failure due to AA amyloidosis received renal allografts. Recurrence in the graft was detected in 20%, diagnosed a median of 5 years posttransplant (1257). Five- and 10-year graft survival rates were 86% and 59%, respectively. Among 246 patients with renal failure due to AL amyloid, only 10% received kidney transplants (1257). Amyloidosis recurred in 28%, but no graft was lost to recurrent amyloid, and the median graft survival was 5.8 years (1257). Survival was best among those who had achieved at least partial remission before transplantation (8.9 years). Among 10 recipients with hereditary fibrinogen A-chain amyloidosis (AFib) who received a kidney only, recurrence was detected in 70%, and median survival was 7.3 years (1257). In contrast, no recurrence was detected in the 9 patients who also received a liver, but the median survival was 6.4 years (1257). Hereditary apolipoprotein AI amyloidosis has recurred in 30% of those not receiving a liver (one graft lost to recurrence) (1257).

MONOCLONAL IMMUNOGLOBULIN DEPOSITION DISEASE

Monoclonal immunoglobulin deposition disease is a consequence of an uncontrolled production of abnormal light or heavy immunoglobulin chains. Recurrence in renal transplants

heavily depends upon the progression of the underlying condition. If the production of monoclonal immunoglobulins cannot be stopped, disease will recur in the allograft. In one recent series, recurrence was observed in 5/7 patients between 2 and 45 months after transplantation (median 33 months), and all five cases resulted in either death or graft failure (1258). In protocol biopsies, the first evidence of recurrence is positive immunofluorescence for light chains at 1 hour to 3 weeks, followed by deposits by electron microscopy at 6 months (1259). Positive immunofluorescence for light chains has also been noted in grafts that do not appear to progress (1258). In instances of renal disease due to monoclonal immunoglobulins, transplantation is considered only after evidence of remission of the underlying immunoglobulin production (1260).

FIBRILLARY AND IMMUNOTACTOID GLOMERULOPATHIES

Fibrillary and immunotactoid glomerulopathies are rare, and experience is limited. Among 5 recipients with fibrillary glomerulopathy and polyclonal Ig deposits, none recurred (1261). In contrast, 5/7 recipients with light-chain-restricted fibrillary glomerulopathy recurred, and median survival was 3 years (1261). Whereas recurrent fibrillary deposits are noted in 50% (or more) of grafts 2 to 9 years posttransplantation (1262), the rate of decline of renal function seems to be slower than that observed in native kidneys (1262–1264). Graft loss due to recurrent disease is only seen in approximately 20% of patients (1262). Immunotactoid glomerulopathy recurrence has been described in small numbers of recipients (2/4)(1265) and in individual case reports (1266).

DIABETIC NEPHROPATHY

Diabetic nephropathy recurs in most patients with sufficient time, first as arteriolar hyalinosis and later as nodular diabetic glomerulopathy. The study of transplanted kidneys has delineated the sequence of changes in the development of diabetic nephropathy. The first change is an increase in allograft glomerular volume at 6 months (1267), followed by increases in mesangial volume (1268). Thickening of the GBM appears later, with a progressive increase that is first evident after 2 to 3 years (1268,1269). Increased linear staining of GBM and TBM for IgG and albumin appears after about 2 years (1270,1271). Arteriolar hyalinosis follows in a similar time frame and is present in 83% of allografts in diabetics 2 to 5 years posttransplant (1271).

The frequency of recurrent diabetes is easy to underestimate, as a biopsy is required. Among 43 biopsies of diabetic recipients taken 18 months or more after transplantation, 26% had recurrent diabetic nephropathy, arising a mean of 6.7 ± 3.9 years after transplantation. Histologic evidence of diabetic nephropathy developed an average of 8 years after transplantation in another series of 14 patients, most commonly with signs of arteriolar hyalinosis (100%) and GBM thickening (64%); nodular glomerulosclerosis was detected in 14% (1272). Nodular diabetic glomerulosclerosis has been reported 5 to 15 years posttransplant (1270–1273), similar to native kidneys in which the development of nodules usually takes 10 years or more. Graft survival in patients with diabetes is similar to that in nondiabetics if censored for death with a functioning graft (1274). Diabetic glomerulosclerosis was the cause of graft failure in only 1 of 16 patients with biopsies (1274).

The histologic diagnosis of recurrent diabetic nephropathy can be challenging, in particular, if the glomerular disease

is mild. The most important differential diagnoses include arteriolar hyalinosis due to hypertension (either preexisting donor disease or de novo postgrafting) and arteriolar hyalinosis due to CNIs. A diagnosis of recurrent diabetic nephropathy is favored if hyalinosis is in both afferent and efferent arterioles, bright linear IgG and albumin deposits are seen in the GBM and TBM by immunofluorescence, and thickening of the GBM by electron microscopy beyond that normally present in allografts.

Transplantation has shown that diabetic glomerulopathy is potentially reversible. A donor kidney with diabetic glomerulosclerosis was transplanted into two nondiabetic recipients (1275). Loss of proteinuria and mesangial hypercellularity was documented at 7 months; however, the images are difficult to interpret, and no electron microscopy was done. Pancreatic transplantation has shown that diabetic glomerulopathy in the native kidney is potentially reversible (1276). Renal biopsies were taken from 8 patients prior to and 5 and 10 years after pancreatic transplantation. These showed no appreciable effect at 5 years, but a reduction of GBM thickness from 500 to 720 nm to 404 ± 64 nm at 10 years. Reduction of mesangial matrix volume to nearly normal levels was also seen at 10 years, but not at 5 years. Notably illustrated was the loss of Kimmelstiel-Wilson nodules in one case.

GENETIC METABOLIC DISEASES

Metabolic diseases due to genetic abnormalities that cause renal disease in the recipient typically recur unless the metabolic lesions are ameliorated as with a liver transplant or the kidney serves as an important source of the defective molecule.

Primary hyperoxaluria, type I, had a dismal rate of renal graft loss (92%) due to recurrent oxalate deposition in the kidney (1277). Successful renal transplantation has been reported in more recent series (1278–1281). With a strict medical protocol (including extra hemodialysis, diuresis, pyridoxine, and avoidance of graft ischemia), graft survival of 70% was achieved in ten living related allografts. Renal function was good up to 7 years posttransplant, and 60% of patients did not show any evidence of oxalate deposits in their graft biopsies (1279). In cases of oxalosis, transplant biopsies show characteristic birefringent sheaves of oxalate crystals in the tubules, sometimes with tubular cell endocytosis and cell proliferation (1282). Most specific are oxalate deposits in the interstitium and in arterial walls. We have seen a case in consultation in which the diagnosis was initially missed until the transplant nephrectomy was examined, which showed the pathognomonic deposition of oxalate in vascular walls. Combined liver and kidney transplant offers a cure for the enzyme deficiency (1280,1283–1288) and reversal of oxalosis cardiomyopathy (1289). Liver transplantation can delay or prevent the renal damage and may obviate the need for renal transplantation (1285).

Fabry disease is characterized by globoceramide deposits in multiple cell types. These deposits recur in the graft in minor amounts (often detected only by electron microscopy) and usually do not cause renal disease (1290,1291). Biopsies of allografts show the characteristic laminated osmophilic cytoplasmic inclusions in small-vessel endothelium at late intervals (8 to 11 years) (1290,1292). It is likely that these lipids accumulate due to uptake of circulating lipids rather than replacement of the endothelium by recipient cells, as once suggested (1292). On two occasions, a heterozygote was inadvertently

used as a donor (1293,1294). Podocyte deposits were detected on a graft biopsy 11 days after transplantation, but these did not progress in a repeat biopsy 8 years later (1294). In the other case, renal failure developed 5 years after transplantation, and a biopsy showed widespread globoceramide deposits in endothelial cells, podocytes, and mesangial cells, which probably caused the late dysfunction (1293). Rarely, females develop renal failure due to Fabry; one had recurrence in the graft 4 months posttransplant (1295). With the advent of enzyme replacement therapy able to clear deposits from the tissue (1296), more successful transplantation of these patients can be anticipated.

Adenine phosphoribosyltransferase deficiency usually causes urolithiasis and can rarely cause renal failure by accumulation of crystals of the purine metabolite 2,8-dihydroxyadenine in tubules and interstitium, eliciting a chronic interstitial nephritis that resembles oxalosis. One case recurred in an allograft six years posttransplant leading to the correct diagnosis of the original disease (the crystals in the native kidney had been confused with oxalosis or radiocontrast material) (1297). The crystals are insoluble in water and xylene (as oxalate but not uric acid) and form sheaves of needle-shaped crystals, which have an annular appearance with radial striations in polarized light. Definitive identification can be made by infrared microscopy analysis of crystal deposits in thick biopsy sections (1297).

Cystinosis is an autosomal recessive genetic disorder that affects lysosomal cystine efflux, causing cystine accumulation in cells and renal failure (1298). The diagnosis is made pathologically by the electron microscopic demonstration of intracellular hexagonal or rectangular crystals and extremely electron-dense (osmophilic) cytoplasm, especially in macrophages and podocytes. The cytoplasmic changes indelibly mark recipient cells, which retain the metabolic defect. Macrophages with crystals and dense cytoplasm reappear in the infiltrate in grafts in patients with cystinosis, while the parenchymal cells show no abnormality (1299). Cystine crystals (or cytoplasmic crystalline spaces compatible with cystine) occurred in interstitial cells in 96% of biopsies and in the glomerulus in 25% (1300). Macrophages with crystals and a dark cytoplasm can occasionally be found in the graft mesangium, elegant evidence in the human for a bone marrow origin of some mesangial cells (1300). Fortunately, patients with cystinosis generally do well with renal transplantation (1298).

POSTTRANSPLANT LYMPHOPROLIFERATIVE DISORDERS AND OTHER NEOPLASIA

The risk of certain neoplasms is substantially increased in renal allograft recipients compared to the general population and to patients maintained on hemodialysis, in particular for younger age groups (1301–1303). It has been extrapolated that, with continued immunosuppression by the 20th year after transplantation, 70% of patients have one or more malignancies (1301) and that soon mortality from malignancies could exceed that from cardiovascular diseases among transplant recipients (1304). Dr. Israel “Sol” Penn was the first to report on the increased incidence of cancer following organ transplantation. After recognizing the high incidence of malignancies, Dr. Penn started in 1967 the Denver Transplant Tumor Registry, which was renamed into the Cincinnati Transplant Tumor Registry after he moved to the University of Cincinnati

Medical Center and is now named “Israel Penn International Transplant Tumor Registry (IPITTR)” in his honor. More than 15,000 records of the IPITTR provided the transplant community with a substantial resource for research and publication and, through this, positively affected the care of patients with transplant-related malignancies.

Most frequently, allograft recipients suffer from carcinomas (squamous and basal cell) of the skin, lip, vulva, and cervix (occurring many years postgrafting); Kaposi sarcoma; and post-transplant lymphoproliferative disorders (PTLD, commonly seen in the first years after transplantation) (1301,1305,1306). These tumors have in common UV-induced mutations or viral infections that are both less efficiently controlled in immunosuppressed patients. The frequencies of the more common adenocarcinomas (breast, lung, prostate, colon) and melanomas are little affected. Renal transplant recipients also have an increased risk for renal cell carcinoma arising in their end-stage native kidneys (1307). De novo tumors originating from the renal transplant are generally rare, other than PTLT. In a recent French multicenter study, 79 de novo renal tumors were identified in 41,806 recipients (incidence of 0.19%) (1308). The vast majority of the tumors were organ confined, low grade, and papillary carcinomas, so that partial nephrectomy was associated with an excellent prognosis (94% 5-year cancer-specific survival). Curiously, one case of papillary renal carcinoma arising in a kidney allograft was of recipient origin and developed from papillary adenomas (1309). Overall, tumor mortality of renal transplant recipients is not significantly increased compared to the general population, despite the increased incidence of neoplasms (1303). Here, we will limit our discussion to most frequent neoplasms (dermatomalignancies and PTLT) and the features confronting the renal pathologist.

Posttransplant Lymphoproliferative Disorders

According to the WHO Blue Book definition, “post transplant lymphoproliferative disorder is a lymphoid proliferation or lymphoma that develops as a consequence of immunosuppression in a recipient of a solid organ or bone marrow allograft (1310). In organ transplant recipients the risk of lymphoma is increased 20% to 120% compared with the general population with risk dependent in part on the level of immune suppression. In addition, recent data have emerged, including HLA and cytokine gene polymorphisms, regarding genetic susceptibility to PTLT (1311). PTLT comprises a spectrum ranging from early, EBV driven polyclonal proliferations resembling infectious mononucleosis to EBV positive or EBV negative lymphomas of predominately B-cell or less often T-cell type” (summarized in Table 29.11) (1312). B cells are the origin of more than 85% of PTLT in organ transplant recipients (1305). In contrast to the ordinary B-cell lymphomas, clonality of the tumor by immunophenotyping or genotyping is less often demonstrable, in particular in “early” and “polymorphic” PTLT variants. T-cell lymphomas comprise approximately 15% and null cells less than 1% of PTLTs (1305). T-cell PTLTs are often high-grade peripheral lymphomas (1313). Signs of a productive EBV infection are common in B-cell and relatively rare in T-cell proliferations (25% of cases in one series) (1314). There is some evidence that the phenotype and presentation of PTLT have been changing over the last decade with a shift toward monomorphic, EBV-negative, T-cell–dominant tumors.

TABLE 29.11 Histologic categories and subtypes of posttransplant lymphoproliferative disorder (PTLD)

PTLD category and histologic subtype	Frequency	Characteristics
Early Lesions Plasma cell hyperplasia Infectious mononucleosis-like PTLD	<5%	A due to immunosuppression incompletely controlled EBV infection stimulates proliferation in all EBV + B cells, which are at that stage polyclonal. Therefore, morphology and organ architecture are usually preserved, and features of hyperplasia and an infectious mononucleosis-like picture is seen. Early Lesions are found more often in children and seronegative adult transplant recipients.
Polymorphic PTLD	10%–20%	These are biologically advanced stages of early lesions with poly- and oligoclonal B-cell proliferation and partial EBV positivity. Morphology and organ architecture are disturbed or already totally dissolved and show a mixed infiltrate of immunoblasts, plasma cells, and various stages of lymphoid maturation. Polymorphic PTLD is more frequent after primary EBV infection (children!) and more often involves the kidney allograft.
Monomorphic PTLD B-cell PTLD	>60%	Mostly monoclonal and frequently EBV-negative Subtyping is done following the WHO classification of malignant B-cell lymphomas: Most common manifestation is that of a diffuse large B-cell lymphoma, and rarely of Burkitt/Burkitt-like lymphoma, or plasmacytoid B-cell lymphoma.
T-cell PTLD	<5%	Subtyping is done following the WHO classification of malignant T-cell lymphomas, including NK cell lymphomas: The most common manifestation is that of peripheral T-cell lymphoma, not further specified, or of hepatosplenic T-cell lymphoma.
Classic Hodgkin lymphoma	<5%	Presents with typical Hodgkin and/or Reed-Sternberg cells and is more common in renal allograft recipients than in recipients of other types of organ transplants

Rarely, the allograft is involved diffusely by PTLD; if so, the kidneys are swollen with an ill-defined corticomedullary junction and sometimes petechiae, resembling severe acute rejection (Fig. 29.94A). It is not easy to establish a diagnosis of PTLD in a renal allograft biopsy, especially in unsuspected cases (such as those limited to the donor organ (385,1315–1326)). The interstitial compartment typically shows vaguely nodular, expansile, and destructive aggregates of mononuclear cells containing plasma cells, varying numbers of activated lymphocytes, and blasts (see Fig 29.94B and C). Mitotic figures can usually be found and sometimes foci of serpiginous necrosis. The neoplastic mononuclear cells often invade tubules (i.e., tubulitis); they can also infiltrate arterial intimal layers and mimic rejection-induced transplant endarteritis (see Fig. 29.94D and E). Transplant glomerulitis is uncommon. Therefore, the major differential diagnosis in cases of PTLD involving renal allografts is acute cellular rejection (1317,1327). Both in rejection and PTLD, the mononuclear cells have enlarged nuclei with nucleoli, and they can show mitotic activity (although “blasts” and mitoses are typically more prominent in PTLD). Further difficulty arises because rejection can coexist with PTLD (385). Several features should raise the suspicion of PTLD. The most helpful clue is the presence of dense, vaguely nodular expansile aggregates of activated lymphoid cells without an admixture of granulocytes or macrophages and without significant edema. Another potential differential diagnosis is PVN grade 2 or 3 that is usually accompanied by intranuclear viral inclusion bodies; an immunohistochemical stain for polyomavirus replication can resolve the differential diagnosis.

Diagnostic confirmation of PTLD can usually be achieved by immunohistochemistry and in situ hybridization. Most cases of PTLD involving renal allografts are of B-cell lineage and express CD20 (in contrast to cases of cellular rejection

that are CD3 and CD68 dominant). CD20-positive cells cannot only be detected in the interstitial compartment but also in foci of tubulitis and arteries with endothelialitis, thereby identifying these lesions as PTLD induced. Stains or in situ hybridization for kappa and lambda light chains can provide hints toward clonality of the lesion. In situ hybridization for EBV-encoded RNA (EBER) generally shows widespread strong nuclear staining in mononuclear cells (in particular, in B-cell PTLDs; see Fig 29.94F). Immunohistochemical stains for LMP-1 and usually EBNA-2 are expected to be positive in PTLD, except for those cases with marked plasma cell differentiation and the uncommon PTLD variants of T-cell lineage. In a systematic study of 14 cases of PTLD (1321), EBER was detected in all cases by in situ hybridization; 11 were positive for LMP-1 and 9 for EBNA-2 by immunohistochemistry. Molecular tests to detect clonality (e.g., light-chain restriction and/or immunoglobulin gene rearrangement) help to confirm the presence of a monomorphic PTLD; polyclonality, however, does not exclude early and polymorphic PTLD variants. PTLDs of T-cell lineage often present as high-grade monomorphic lymphomas.

EBV-positive PTLDs arise commonly within the first two posttransplant years (in particular, those localized in kidney allografts (1328)), whereas EBV-negative cases have a median onset of 50 to 60 months after grafting (1329). The clinical presentation is heterogeneous and dependent upon the location and extent of the disease. Patients with kidney transplant involvement typically present with graft dysfunction (differential diagnosis: acute rejection) and may sometimes show a “mass lesion” in imaging studies. PTLD rarely involves the peripheral blood, but rather extranodal sites and the bone marrow (in contrast to nontransplant lymphomas). The distribution of EBV-positive PTLDs was documented in

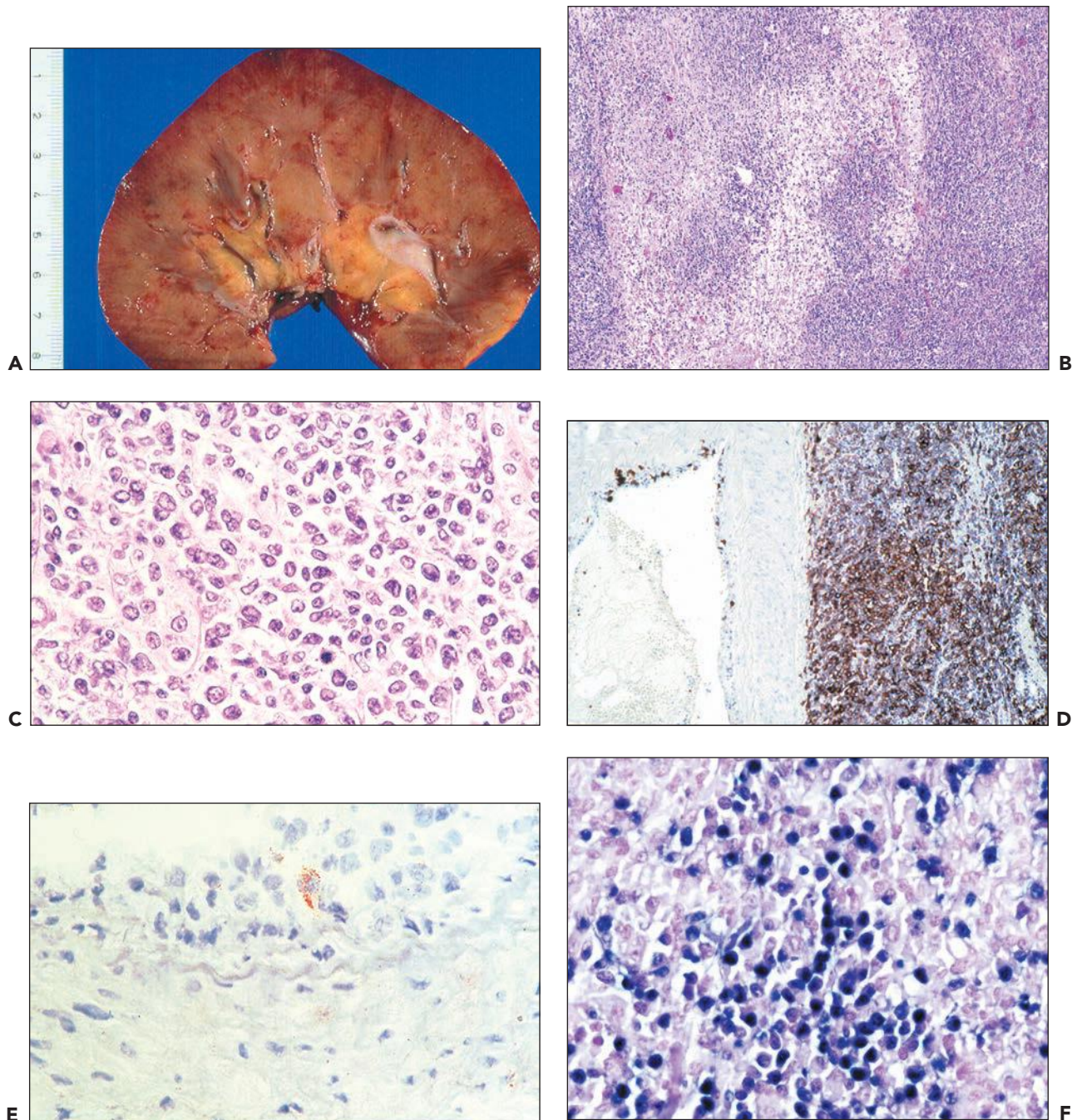


FIGURE 29.94 Posttransplant lymphoproliferative disorder (PTLD), polymorphic and polyclonal variant. **A:** A failed allograft due to PTLD shows marked swelling, an ill-defined corticomedullary junction, and small irregular foci of hemorrhage. Histologically, PTLD often presents with a nodular, destructive-appearing mononuclear cell infiltrate (**B**) that demonstrates on higher-power examination (**C**) activated lymphoid cells and scattered blasts. Most PTLDs are B-cell dominant (**D** shows an immunohistochemical incubation for CD20). The lymphoproliferative disorder can also involve arterial intimal layers (**D and E**) and mimic an acute rejection episode with transplant endarteritis. The majority of PTLDs is promoted by Epstein-Barr virus (EBV) infections that can be detected either by immunohistochemistry (**D** shows in the inflamed intima of an artery a single-cell staining for EBV-LMP in the cytoplasm) or more easily by in situ hybridization detecting EBV (**F** shows EBV staining in many mononuclear cell nuclei). ((**B, C**) H&E, original magnification 40 \times and 300 \times ; (**D**) immunohistochemistry to detect CD20, original magnification 150 \times ; (**E**) immunohistochemistry to detect EBV-LMP, original magnification 400 \times ; (**F**) in situ hybridization to detect EBV, original magnification 400 \times .)

a series of 9 nonhuman primate research animals with kidney transplants that showed involvement of the lymph nodes (100% of cases), liver (56%), lung (44%), heart (44%), renal allograft (44%), and native kidneys (22%) (1330). Overall, the allografts are involved in approximately 25% of all human transplant recipients (heart, lung, liver, kidney, pancreas) (1312). Kidney transplants are affected in more than 30% of patients (385,1331) with restriction of PTLD to the renal allograft in 12% of cases in one series (385). Most cases of PTLD affecting the kidneys are of the polymorphic variant (385,1331). These organ-restricted PTLDs often occur early (on average 5 months) postsurgery, are mostly of donor cell origin, and fare favorably (1332).

A recent paper reported a PTLD prevalence of 1.4% among 25,127 renal allograft recipients transplanted in the United States between 1996 and 2000 (1333) and at the Pittsburgh transplant center of 1.2% in adult and 10.1% in pediatric kidney transplant recipients on tacrolimus therapy (1334). The risk for developing lymphoid neoplasia is estimated to be 20 times that of the normal population for renal allograft, depending on the EBV status of the recipient (1312). The 5-year adult patient and graft survival rates were 86% and 60% in Pittsburgh (1334), whereas 5-year patient survival was less favorable (64%) (1333). Pediatric patients seem to fare favorably (5-year patient survival rate of 100%, 5-year graft survival rate of 89%) (1334). Transplanting an EBV-positive donor organ into seronegative recipient has a higher risk of PTLD, explaining the five- to tenfold higher PTLD incidence in children, who are usually EBV naïve. In general, an inferior prognosis is associated with monoclonality of the PTLD, T-cell PTLD, EBV-negative PTLD, central nervous system involvement, and PTLD manifestation late posttransplantation.

Therapy has typically included reduced immunosuppression, sometimes with added radiation, chemotherapy, and antiviral drugs (acyclovir, ganciclovir, alpha-interferon) (1334,1335). Polymorphic PTLDs respond to antiviral therapy and a reduction in immunosuppression. Surgical resection has been performed for localized disease (limited to the allograft or ureters) with good success (1320,1336,1337). The monomorphic, monoclonal PTLDs that show mutations of the Bcl-6 gene (seen in approximately 90% of cases) require more aggressive therapy and have a poor long-term prognosis (1332). Anti-CD20 (rituximab) therapy is effective in patients with monomorphic or polymorphic B-cell PTLDs, resulting in complete remission (mean duration 18 months) in 53% of patients (1338). However, relapses are frequently observed after rituximab monotherapy in patients with advanced PTLD.

Other malignant neoplasms

The prevalence of oncogenic viruses overall is higher in organ recipients than in the general population. In particular, HPV is found significantly more frequent in (pre)malignancies of the female lower anogenital tract, most likely explaining the three- to sixfold increased risk for cervical carcinoma, the 45- to 50-fold increased risk for vulva carcinoma, and the 10-fold increased risk for anal cancer in renal transplant recipients (1339). High-risk HPV subtypes 16 and 18 are found more frequently in renal transplant recipients. Also, the rate of progression of low-grade to high-grade dysplastic lesions

is greater and more rapid compared to immunocompetent individuals.

Transplant recipients are at particular risk of squamous cell carcinoma and basal cell carcinoma and less for Kaposi sarcoma, Merkel cell carcinoma, and malignant melanoma (1304).

Precursor lesions for skin cancer are more frequent in organ transplant recipients, in particular actinic keratosis. In renal transplant recipients, the prevalence of actinic keratosis is up to 54% (966). Frequently, in transplant recipients, actinic keratosis lesions coalesce to the so-called field cancerization with an increased risk for progression and relapse of invasive squamous cell carcinoma. Another frequent but poorly understood premalignant skin condition in immunosuppressed transplant recipient is porokeratosis. However, as yet no well-documented case series are published describing the rates of progression to invasive squamous carcinoma (1340).

Squamous cell carcinoma (SCC) can develop *de novo* or in the context of preexisting actinic keratosis. Among transplant recipients, SCC of the skin occurs much more commonly than basal cell carcinoma, which is the opposite in the general population. Compared to the general population, transplant patients develop SCC 40 to 250 times more frequently, accounting for 90% of skin cancers in this population. Forty-five percent of all transplant recipients develop at least one SCC within 10 years. SCC is more aggressive in organ recipients with higher rates (4 to 5 times) of recurrence and metastasis, deeper invasion, and occurrence in younger patients. Also, SCC in transplant patients shows more frequently histologic features of human papillomavirus infection, underscoring the role of oncogenic virus for the development of malignancies in transplant patients. Type and duration of immunosuppression is associated with the development of SCC. Heart and lung transplant recipients have a greater risk than renal transplant recipients (965). Accordingly, reduction in immunosuppression and switch to mTOR inhibitors can lead to prolonged disease-free survival.

Basal cell carcinomas are the second most common cancer in renal allograft recipients and affect more often younger patients; occur more often in sun-protected, atypical locations; and show more frequently features of HPV infection and are more commonly multifocal, compared to the general population (1341).

A two- to fourfold increased risk for malignant melanoma is described for transplant patients. In particular, African Americans seem to be exposed to a significantly increased risk (17 times) for developing malignant melanomas after organ transplantation (1342).

Kaposi sarcoma is a vascular neoplasm associated with human herpesvirus 8 (HHV8). Prevalence rates for Kaposi sarcoma in organ recipients vary between 0.5% and 5.3% related to seropositivity for HHV8. High-risk populations are older men in southern Europe, Afro-Caribbean, and Ashkenazi Jews. Similar to other neoplasms, Kaposi sarcomas tend to be more aggressive in immunosuppressed patients with more frequent extracutaneous, visceral involvement (25% to 30%) and multifocal skin involvement including atypical locations (1340).

Merkel cell carcinoma is a rare but highly aggressive cutaneous neoplasm of neuroendocrine origin. In organ recipients,

Merkel cell carcinomas are 5 to 10 times more frequent, occur in younger patients, and metastasize more frequently than in the general population. Recently, viral transcripts derived from polyomaviruses have been detected in Merkel cell carcinomas suggesting a potential pathogenetic role of these in immunosuppressed patients (1343).

Despite strong experimental evidence for the oncogenic potential of various human polyomavirus strains, causation of in human cancers other than Merkel cell carcinoma has not been proved (1344). Several case reports and small case series have been published finding BK polyomaviruses in genitourinary carcinomas occurring in renal allograft recipients. However, no convincing evidence has yet emerged that the detection of viral genome in these malignancies has a causative role and not just a coincidental epiphenomenon. However, molecular virologic data support a potential oncogenic contribution of polyomavirus to carcinogenesis and progression in these cases, in analogy to the Merkel cell polyoma virus. The polyomavirus-induced effects in the context of marked immunosuppression on cell cycle activation and p53 with shift to proliferation and apoptosis inhibition constitute at least an ideal background for malignant transformation (919).

MOLECULAR TRANSPLANTATION PATHOLOGY: METHODS AND APPLICATIONS

Precise, mechanism-based diagnoses are the prerequisite for targeted treatment in the individual patient, that is, personalized medicine (1345). Over the last decade, we are witnessing rapid methodologic advances in molecular biology. The fundamental breakthrough after completion of the human genome project was to expand the scale from studying single genes, transcripts, proteins, or metabolites to studying all molecules simultaneously using array or omics technologies (1346). The expectation is that such approaches will ultimately provide detailed insights into disease mechanisms and through this identify diagnostic, prognostic and theranostic (i.e., predicting response to treatment) biomarkers. However, after a decade of experience, opinions concerning omics studies range from unrealistic hype to excessive skepticism, and many studies are plagued by poor or impenetrable analysis strategies (1347). Consequently, questions concerning platform comparability and irreproducible biostatistics continue to be raised and represent considerable obstacles for integrating these diagnostics into routine practice (1348).

In renal transplants, most experience has been accumulated in studying mRNA expression. Starting with Northern blots on single cases in the 80s (1349,1350) and accelerating in the 90s with the advent of PCR platforms made it feasible to quantify mRNA expression of individual target molecules in transplant biopsies (228,230). More recently, genome-wide expression analysis using cDNA microarray technologies (transcriptomics) became broadly available and reasonably large renal transplant series have been assessed with these omics platforms (184,229,243,690,1351–1353). To date, most comprehensive data sets including clinicopathologic correlations are available for quantitative transcriptomics analysis from renal transplant biopsies and less extensively from urine

or blood. Fewer studies are available describing proteomic and metabolomic testing in renal transplant patients, most likely due to methodologic challenges and the fact that these technologies are less suitable to be applied to tissue biopsies. Furthermore, applying omics technologies to blood specimens is significantly challenged by the huge background noise of detected signals since transplant patients are frequently in a constant “state of inflammation” due to concomitant infections and other metabolic diseases, while simultaneously under systemic immunosuppression (1354). More promising results have been derived from urine specimens. Urine provides a potentially unique, noninvasive window on the graft, especially for those molecules “leaking” into the urine after tubular injury or rejection. Remarkably, urine mRNA can be retrieved reproducibly in sufficient quantities for analysis, as pioneered by Suthanthiran and now standardized in multicenter trials (1355,1356).

Commercially available microarray platforms can also be used for genome-wide assessment of genetic polymorphisms including single nucleotide polymorphisms (SNPs). Many of the cytokines, chemokines, and their receptors have DNA sequence polymorphisms. Therefore, these have been examined for potential clinical or pathologic relevance in the rejection process or response to therapy. For the most part, these studies have been done in single-center cohorts and the validity of the associations is unproved. After initial euphoria (1357), genome-wide association studies have been heavily criticized and are now under significant scrutiny (1358). In addition to established omics platforms for mRNA, protein, or metabolite assessments, new high-throughput technologies are emerging for the assessment of mRNA and regulatory microRNA (miRNA) from formalin-fixed, paraffin-embedded archival specimens (1359) as well as sequencing technologies for DNA and RNA. High-throughput quantitative sequencing technologies based on cDNA in order to get information about a sample's RNA content has already been adopted in cancer studies and will likely also find applications in organ transplantation (1360,1361).

These approaches require sophisticated biostatistics as part of their application. Although the assay platforms are commercially available and fairly easy to operate and the fact that numerous analytical software packages are also commercially available, the interpretation and refinement of the huge amounts of high-dimensional raw data require integrated biostatistical support. The challenge lies in the fact that the number of data points per specimen (tens of thousands) by far exceeds the sample size in all to-date published studies. Thus, any statistical analysis is very susceptible to accidentally finding “significant” associations to clinicopathologic variables while not reflecting true biologic disease mechanisms, that is, to overfit the omics data. The four common mistakes related to microarray data analysis are (1362) as follows:

1. Insufficient exploratory data analysis, for example, to calculate correlations between high numbers of variables (e.g., microarray results with pathologic lesions) that are not linearly related. Standard correlations like Spearman applied to thousands of variables will always find significant correlations even if no true biologic relationship exists.

A visual/graphical exploration can help to guide analyses and also statistical methods like Principal Components analysis (PCA) are very useful in this regard. PCA is a mathematical procedure that converts large sets of observations of possibly correlated variables into a set of values of linearly uncorrelated variables called principal components. The number of principal components is much less than the number of original variables. The first principal component usually captures the largest possible variance from the original data set, and each succeeding component has the highest variance possible under the constraint that it is uncorrelated with the preceding components. Often, PCA is used for revealing the internal structure of the data. Thus, PCA can supply the user with a lower-dimensional picture of a complex data set (Fig. 29.95).

2. Improper use and interpretation of the large variety of clustering algorithms. Clustering samples based on the genes differentially expressed between phenotypes is not supportive evidence for the clinical significance of the genes. Clustering is also not suitable for predicting. Hierarchic clustering generates tree-like relationships within the data even when none truly exists, for example, when the data are randomly generated.

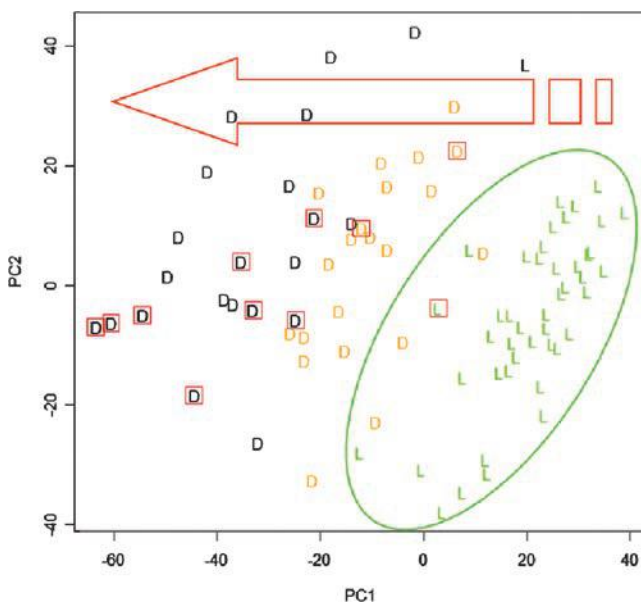


FIGURE 29.95 Principal components analysis: The X- and Y-axis represent the first two principal components in the raw data, PC1 and PC2, explaining most variance observed in the raw data of the microarray experiments in this set of implantation biopsies. A continuity from living donor kidneys (L, green) to low-risk (D, orange) to high-risk (D, black) deceased donor kidneys is observed along PC1, that is, on the X-axis from the right to the left (*large red arrow* at top = risk for DGF. Cases with DGF are highlighted by *red rectangles*). No additional information can be derived from PC2. (Adapted from Mueller TF, Reeve J, Jhangri GS, et al. The transcriptome of the implant biopsy identifies donor kidneys at increased risk of delayed graft function. *Am J Transplant* 2008;8(1):78–85.)

3. Improper validation of results. No information derived from a test set (e.g., differentially expressed genes from a class comparison—rejection vs. no rejection) should leak into the validation procedure. In this regard, cross-validation methods are almost always to be preferred.
4. Weak experimental design. For example, limited challenge bias, meaning evaluating a diagnostic test using nonchallenging samples (e.g., totally normals vs. severely rejecting). By leaving out clinically relevant but diagnostically “difficult” samples (e.g., borderline cases), reported accuracies, sensitivities, etc. are inflated. Limited challenge bias represents by far the most serious and common problem seen in omics studies today (1363).

High-dimensional data outputs from these platforms are not feasible to be integrated into patient care and require postanalytical refinement to become clinically useful. To this end, the Edmonton group developed one approach through generating pathogenesis-based transcript sets (PBTs) for an easy and rapid interpretation of complex cDNA microarray results (1364). The PBT system was developed in cell culture systems, mouse models for kidney transplantation, and human kidney transplant biopsies. The PBTs provide annotation groups of related transcripts (sometimes several hundred) representing discrete biologic events relevant to transplantation, like various subtypes of inflammation (infiltration by T cells, B cells, or macrophages; γ -interferon effects) and the injury-repair response in parenchyma, stroma, or microcirculation (endothelial cells) with increased or decreased expression of respective sets of transcripts. Microarray gene expression results for a PBT can be represented as scores—the geometric mean of fold changes across all probe sets in that PBT. Thus, by the PBT approach, large-scale and cumbersome microarray gene expression results are collapsed into a small number of PBT scores representing molecular measurements of the respective biologic processes in the tissue. Moreover, since the PBTs were developed in transplants, compared to other publically available gene annotations systems (e.g., Gene Ontology) that are frequently derived from cancer-specific experiments, they provide a transplant-specific annotation system.

Significant associations between PBT scores with histopathology lesions (e.g., interstitial or microcirculation inflammation), allograft function, and outcome have been validated by several research groups independently (650,694,1365). A different approach toward high-dimensional omics data is to employ sophisticated biostatistical tools and algorithms for a user-friendly refinement. For class prediction, for example, predicting the diagnosis of a new sample solely from the molecular assessment, frequently classifiers are used. Classifiers are mathematical algorithms/functions that assign probabilities to a new sample based on various input data (e.g., the result of a microarray experiment) regarding its likelihood for belonging to a specific class/diagnosis. Classifiers are usually build using machine learning algorithms and supervised learning, that is, after training on a set of known classes/correctly diagnosed cases with consecutive cross-validation (Fig. 29.96). Building a classifier represents a challenge if no true diagnostic gold standard is available for training, which is frequently the case and represents

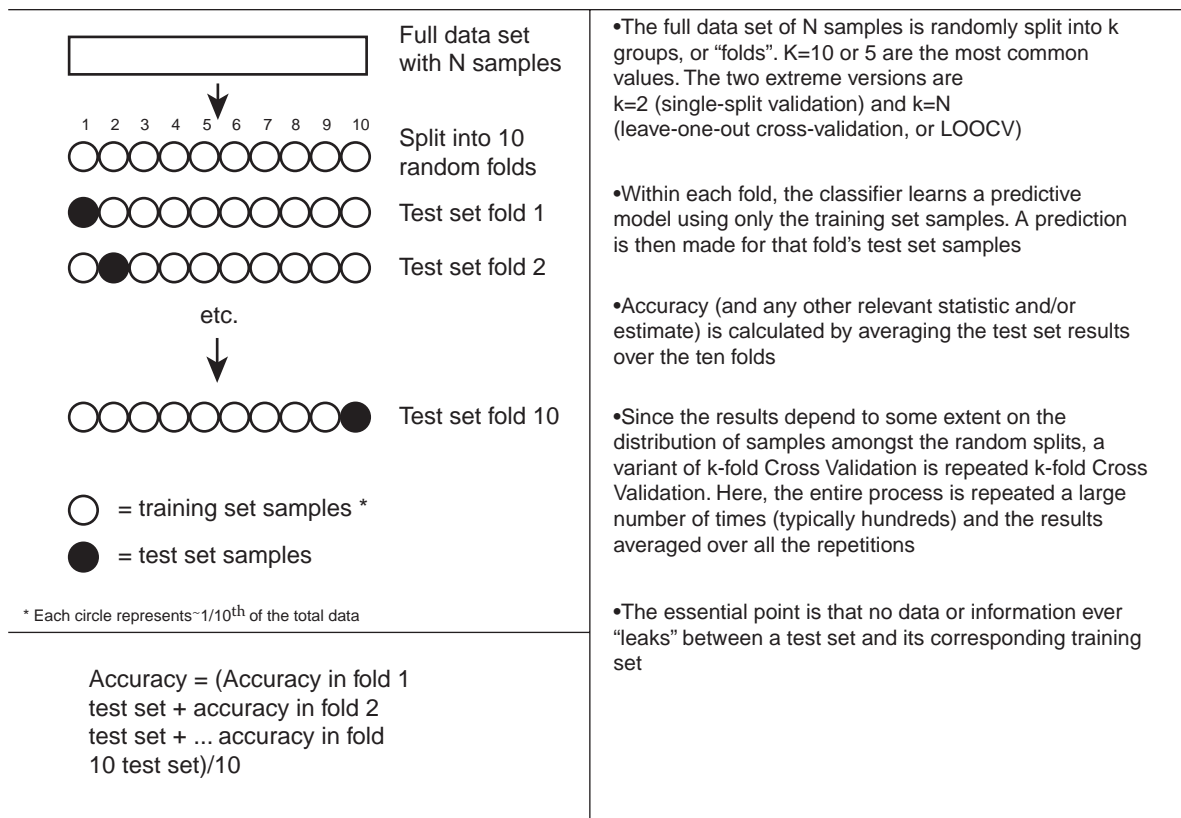


FIGURE 29.96 Building and cross-validating a diagnostic classifier. (Graph designed and provided by Dr. Jeff Reeve, University of Alberta.)

a significant obstacle for validating new “omics” diagnostics in clinical practice (1366). For example, any single classifier’s predictions depends critically on the class labels it is given (i.e., the “gold standard” for training the classifier). In addition, the variability resulting from applying different analytical methods/equations on the same high-dimensional data set can be similar to two pathologists reviewing the same histologic slide (247).

Interestingly, the individual members in a PBT change their expression in a highly correlated, stereotyped fashion and thus move in large groups reflecting the major biologic processes operating in abnormal renal allografts (240,1353,1364). This observation was recently generalized in a comprehensive meta-analysis of human gene expression studies in allograft rejection across all organ types (1367). The authors postulate the Immunological Constant of Rejection hypothesis based on the observation that different immune-mediated tissue destruction processes (i.e., allograft rejection, autoimmunity, infection, cancer, graft versus host disease, acute cardiovascular events, chronic obstructive pulmonary diseases, placental villitis) share common convergent final mechanisms. Molecular features consistently described through all these different immune-mediated tissue destruction processes include the activation of interferon- γ -regulated genes, the recruitment of cytotoxic cell through massive production of respective chemokine

ligands (primarily through CXCR3/CCR5 ligand pathways), and the activation of immune effector function genes (i.e., genes expressed by CD8 cells and NK cells upon activation). Therefore, the molecular constants shared among all these different tissue destruction processes include the coordinated activation of the following pathways: (1) IFN- γ /STAT-1/IRF-1/T-bet/IL-15 pathway; (2) CXCR3 ligand chemokine pathway (CXCL9, 10, 11); (3) CCR5 ligand chemokine pathway (CCL3, 4, 5); and (4) TIA-1 pathway/granzyme A/B/granzyme/perforin pathway. Figure 29.97 shows the networks of related molecules involved in these central pathways jointly representing the Immunological Constant of Rejection theory (1367). Since these biologic pathways operate diffusely in the tissue, respective changes in the transcriptome can be detected frequently in tissue specimens otherwise inadequate for histology.

In this chapter, we describe molecular findings as part of the respective diagnostic entity similar to other ancillary technologies such as IF and EM. However, finding diagnostic specificity in large-scale molecular changes is as challenging as with nonspecific morphologic features like interstitial infiltrates in a kidney biopsy. In some areas, the molecules are likely superior, for example, the assessment of tissue injury, which is essentially invisible to morphology. But, histopathology will carry greater specificity and sensitivity for diseases associated with focal lesions (such as glomerular diseases or isolated

38. Lamb KE, Lodhi S, Meier-Kriesche HU. Long-term renal allograft survival in the United States: a critical reappraisal. *Am J Transplant* 2011;11(3):450–462.
39. Tilney NL. Transplantation between identical twins: a review. *World J Surg* 1986;10:381.
40. Shimmura H, Tanabe K, Ishida H, et al. Long-term results of living kidney transplantation from HLA-identical sibling donors under calcineurin inhibitor immunosuppression. *Int J Urol* 2006;13(5):502–508.
41. de Mattos AM, Bennett WM, Barry JM, et al. HLA-identical sibling renal transplantation—a 21-yr single-center experience. *Clin Transpl* 1999;13(2):158–167.
42. Collins AB, Chicano SL, Cornell LD, et al. Putative antibody-mediated rejection with C4d deposition in HLA-identical, ABO-compatible renal allografts. *Transplant Proc* 2006;38(10):3427–3429.
43. Graff CA, Cornell LD, Gloor JM, et al. Antibody-mediated rejection following transplantation from an HLA-identical sibling. *Nephrol Dial Transplant* 2010;25(1):307–310.
44. Krieger NR, Becker BN, Heisey DM, et al. Chronic allograft nephropathy uniformly affects recipients of cadaveric, nonidentical living-related, and living-unrelated grafts. *Transplantation* 2003;75(10):1677–1682.
45. Legendre C, Thervet E, Skhiri H, et al. Histologic features of chronic allograft nephropathy revealed by protocol biopsies in kidney transplant recipients. *Transplantation* 1998;65(11):1506–1509.
46. Baltzan MA, Shoker AS, Baltzan RB, et al. HLA-identity—long-term renal graft survival, acute vascular, chronic vascular, and acute interstitial rejection. *Transplantation* 1996;61(6):881–885.
47. Danovitch GM, Cecka JM. Allocation of deceased donor kidneys: past, present, and future. *Am J Kidney Dis* 2003;42(5):882–890.
48. Gill J, Bunnapradist S, Danovitch GM, et al. Outcomes of kidney transplantation from older living donors to older recipients. *Am J Kidney Dis* 2008;52(3):541–552.
49. Brook NR, White SA, Waller JR, et al. Non-heart beating donor kidneys with delayed graft function have superior graft survival compared with conventional heart-beating donor kidneys that develop delayed graft function. *Am J Transplant* 2003;3(5):614–618.
50. Bains JC, Sandford RM, Brook NR, et al. Comparison of renal allograft fibrosis after transplantation from heart-beating and non-heart-beating donors. *Br J Surg* 2005;92(1):113–118.
51. Troppmann C, Gillingham KJ, Gruessner RW, et al. Delayed graft function in the absence of rejection has no long-term impact. A study of cadaver kidney recipients with good graft function at 1 year after transplantation. *Transplantation* 1996;61(9):1331–1337.
- 51a. Wilpert J, Fischer KG, Pisarski P, et al. Long-term outcome of ABO-incompatible living donor kidney transplantation based on antigen-specific desensitization. An observational comparative analysis. *Nephrol Dial Transplant* 2010;25(11):3778–3786.
52. John R, Herzenberg AM. Our approach to a renal transplant biopsy. *J Clin Pathol* 2010;63(1):26–37.
53. Waltzer WC, Miller F, Arnold A, et al. Value of percutaneous core needle biopsy in the differential diagnosis of renal transplant dysfunction. *J Urol* 1987;137(6):1117–1121.
54. Matas AJ, Tellis VA, Sablay L, et al. The value of needle renal allograft biopsy. III. A prospective study. *Surgery* 1985;98(5):922–926.
55. Parfrey PS, Kuo YL, Hanley JA, et al. The diagnostic and prognostic value of kidney transplant biopsy. *Transplantation* 1984;38:586–593.
56. Kiss D, Landman J, Mihatsch M, et al. Risks and benefits of graft biopsy in renal transplantation under cyclosporin-A. *Clin Nephrol* 1992;38(3):132–134.
57. Manfro RC, Lee JY, Lewgoy J, et al. The role of percutaneous renal biopsy in kidney transplant. *Rev Assoc Med Brasil* 1994;40(2):108–112.
58. Kon SP, Templar J, Dodd SM, et al. Diagnostic contribution of renal allograft biopsies at various intervals after transplantation. *Transplantation* 1997;63(4):547–550.
59. Pascual M, Vallhonrat H, Cosimi AB, et al. The clinical usefulness of the renal allograft biopsy in the cyclosporine era: a prospective study. *Transplantation* 1999;67(5):737–741.
60. Al-Awwa IA, Hariharan S, First MR. Importance of allograft biopsy in renal transplant recipients: correlation between clinical and histological diagnosis. *Am J Kidney Dis* 1998;31(6 Suppl 1):S15–S18.
61. Colvin RB, Cohen AH, Saiontz C, et al. Evaluation of pathologic criteria for acute renal allograft rejection: reproducibility, sensitivity, and clinical correlation. *J Am Soc Nephrol* 1997;8(12):1930–1941.
62. Sorof JM, Vartanian RK, Olson JL, et al. Histopathological concordance of paired renal allograft biopsy cores. Effect on the diagnosis and management of acute rejection. *Transplantation* 1995;60(11):1215–1219.
63. Gray DW, Richardson A, Hughes D, et al. A prospective, randomized, blind comparison of three biopsy techniques in the management of patients after renal transplantation. *Transplantation* 1992;53(6):1226–1232.
64. Nast CC, Blifeld C, Danovitch GM, et al. Needle biopsy of renal allografts: comparison of two techniques. *Radiology* 1990;174(1):273–275.
65. Mahoney MC, Racadio JM, Merhar GL, et al. Safety and efficacy of kidney transplant biopsy: Tru-Cut needle vs sonographically guided Biopsy gun. *AJR Am J Roentgenol* 1993;160(2):325–326.
66. Hanas E, Larsson E, Fellström B, et al. Safety aspects and diagnostic findings of serial renal allograft biopsies, obtained by an automatic technique with a midsized needle. *Scand J Urol Nephrol* 1992;26(4):413–420.
67. Wilczek HE. Percutaneous needle biopsy of the renal allograft. A clinical safety evaluation of 1129 biopsies. *Transplantation* 1990;50(5):790–797.
68. Furness PN, Philpott CM, Chorbadian MT, et al. Protocol biopsy of the stable renal transplant: a multicenter study of methods and complication rates. *Transplantation* 2003;76(6):969–973.
69. Benfield MR, Herrin J, Feld L, et al. Safety of kidney biopsy in pediatric transplantation: a report of the Controlled Clinical Trials in Pediatric Transplantation Trial of Induction Therapy Study Group. *Transplantation* 1999;67(4):544–547.
70. Merkus JW, Zeebregts CJ, Hoitsma AJ, et al. High incidence of arteriovenous fistula after biopsy of kidney allografts. *Br J Surg* 1993;80(3):310–312.
71. Beckingham IJ, Nicholson ML, Kirk G, et al. Comparison of three methods to obtain percutaneous needle core biopsies a renal allograft. *Br J Surg* 1994;81(6):898–899.
72. Schmid A, Jacobi J, Kuefner MA, et al. Transvenous renal transplant biopsy via a transfemoral approach. *Am J Transplant* 2013;13(5):1262–1271.
73. Schwarz A, Gwinner W, Hiss M, et al. Safety and adequacy of renal transplant protocol biopsies. *Am J Transplant* 2005;5(8):1992–1996.
74. Nicholson ML, Wheatley TJ, Doughman TM, et al. A prospective randomized trial of three different sizes of core-cutting needle for renal transplant biopsy. *Kidney Int* 2000;58(1):390–395.
75. Vidhun J, Masciandro J, Varich L, et al. Safety and risk stratification of percutaneous biopsies of adult-sized renal allografts in infant and older pediatric recipients. *Transplantation* 2003;76(3):552–557.
76. Cohen AH, Gonzalez S, Nast CC, et al. Frozen-section analysis of allograft renal biopsy specimens: reliable histopathologic data for rapid decision making. *Arch Pathol Lab Med* 1991;115(4):386–389.
77. Solez K, Axelsen RA, Benediktsson H, et al. International standardization of criteria for the histologic diagnosis of renal allograft rejection: the Banff working classification of kidney transplant pathology. *Kidney Int* 1993;44(2):411–422.
78. Wilczek HE, Groth CG, Bohman SO. Effect of reduced cyclosporin dosage on long-term renal allograft histology. *Transplant Int* 1992;5(2):65–70.
79. Wang H, Nanra RS, Carney SL, et al. The renal medulla in acute renal allograft rejection: comparison with renal cortex. *Nephrol Dial Transplant* 1995;10(8):1428–1431.
80. Hamburger J. A reappraisal of the concept of organ “rejection,” based on the study of homotransplanted kidneys. *Transplantation* 1967;37(564):564–570.
81. Racusen LC, Solez K, Colvin RB, et al. The Banff 97 working classification of renal allograft pathology. *Kidney Int* 1999;55(2):713–723.
82. Racusen LC, Colvin RB, Solez K, et al. Antibody-mediated rejection criteria—an addition to the Banff 97 classification of renal allograft rejection. *Am J Transplant* 2003;3(6):708–714.
83. Kirk A. CAMPATH path. *Transplantation* 2003;76(1):120–129.
84. Randhawa P. Role of donor kidney biopsies in renal transplantation. *Transplantation* 2001;71(10):1361–1365.
85. Cecka JM. The OPTN/UNOS Renal Transplant Registry 2003. *Clin Transpl* 2003;1–12.
86. Gaber LW, Moore LW, Alloway RR, et al. Glomerulosclerosis as a determinant of posttransplant function of older donor renal allografts. *Transplantation* 1995;60(4):334–339.
87. Seron D, Carrera M, Grino JM, et al. Relationship between donor renal interstitial surface and post-transplant function. *Nephrol Dial Transplant* 1993;8(6):539–543.

88. Taub HC, Greenstein SM, Lerner SE, et al. Reassessment of the value of post-vascularization biopsy performed at renal transplantation: the effects of arteriosclerosis. *J Urol* 1994;151(3):575–577.
89. Randhawa PS, Minervini MI, Lombardero M, et al. Biopsy of marginal donor kidneys: correlation of histologic findings with graft dysfunction. *Transplantation* 2000;69(7):1352–1357.
90. Cahen R, Dijoud F, Couchoud C, et al. Evaluation of renal grafts by pretransplant biopsy. *Transplant Proc* 1995;27:2470.
91. Kaplan C, Pasternack B, Shah H, et al. Age-related incidence of sclerotic glomeruli in human kidneys. *Am J Pathol* 1975;80:227–234.
92. Wang HJ, Kjellstrand CM, Cockfield SM, et al. On the influence of sample size on the prognostic accuracy and reproducibility of renal transplant biopsy. *Nephrol Dial Transplant* 1998;13(1):165–172.
93. Sund S, Reisaeter AV, Fauchald P, et al. Living donor kidney transplants: a biopsy study 1 year after transplantation, compared with baseline changes and correlation to kidney function at 1 and 3 years. *Nephrol Dial Transplant* 1999;14(10):2445–2454.
94. Bago-Horvath Z, Kozakowski N, Soleiman A, et al. The cutting (w) edge—comparative evaluation of renal baseline biopsies obtained by two different methods. *Nephrol Dial Transplant* 2012;27(8):3241–3248.
95. Haas M, Segev DL, Racusen LC, et al. Arteriosclerosis in kidneys from healthy live donors: comparison of wedge and needle core perioperative biopsies. *Arch Pathol Lab Med* 2008;132(1):37–42.
96. Escofet X, Osman H, Griffiths DF, et al. The presence of glomerular sclerosis at time zero has a significant impact on function after cadaveric renal transplantation. *Transplantation* 2003;75(3):344–346.
97. Pokorna E, Vitko S, Chadimova M, et al. Proportion of glomerulosclerosis in procurement wedge renal biopsy cannot alone discriminate for acceptance of marginal donors. *Transplantation* 2000;69(1):36–43.
98. Edwards EB, Posner MP, Maluf DG, et al. Reasons for non-use of recovered kidneys: the effect of donor glomerulosclerosis and creatinine clearance on graft survival. *Transplant* 2004;77(9):1411–1415.
99. Munivenkatappa RB, Schweitzer EJ, Papadimitriou JC, et al. The Maryland aggregate pathology index: a deceased donor kidney biopsy scoring system for predicting graft failure. *Am J Transplant* 2008;8(11):2316–2324.
100. Cecka JM, Gritsch HA. Why are nearly half of expanded criteria donor (ECD) kidneys not transplanted? *Am J Transplant* 2008;8(4):735–736.
101. Foss A, Haldal K, Scott H, et al. Kidneys from deceased donors more than 75 years perform acceptably after transplantation. *Transplantation* 2009;87(10):1437–1441.
102. Segoloni GP, Messina M, Squicciarino G, et al. Preferential allocation of marginal kidney allografts to elderly recipients combined with modified immunosuppression gives good results. *Transplantation* 2005;80(7):953–958.
103. Savoye E, Tamarelle D, Chalem Y, et al. Survival benefits of kidney transplantation with expanded criteria deceased donors in patients aged 60 years and over. *Transplantation* 2007;84(12):1618–1624.
104. Swanson SJ, Hypolite IO, Agodoa LY, et al. Effect of donor factors on early graft survival in adult cadaveric renal transplantation. *Am J Transplant* 2002;2(1):68–75.
105. De Vusser K, Lerut E, Kuypers D, et al. The predictive value of kidney allograft baseline biopsies for long-term graft survival. *J Am Soc Nephrol* 2013;24:1913–1923.
106. Nickeleit V. Foretelling the future: predicting graft outcome by evaluating kidney baseline transplant biopsies. *J Am Soc Nephrol* 2013;24:1716–1719.
107. Farris AB, Chan S, Climenhaga J, et al. Banff fibrosis study: multicenter visual assessment and computerized analysis of interstitial fibrosis in kidney biopsies. *Am J Transplant* 2014;14(4):897–907.
108. Nickeleit V. Pathology: donor biopsy evaluation at time of renal grafting. *Nature Rev Nephrol* 2009;5(5):249–251.
109. Fromer DL, Birkhoff JD, Hardy MA, et al. Bilateral intrarenal adrenal glands in cadaveric donor kidneys resembling renal cell carcinoma on intraoperative frozen section. *J Urol* 2001;166(5):1820–1821.
110. Nalesnik MA, Woodle ES, Dimaio JM, et al. Donor-transmitted malignancies in organ transplantation: assessment of clinical risk. *Am J Transplant* 2011;11(6):1140–1147.
111. Ison MG, Nalesnik MA. An update on donor-derived disease transmission in organ transplantation. *Am J Transplant* 2011;11(6):1123–1130.
112. Curschellas E, Landmann J, Durig M, et al. Morphologic findings in “zero-hour” biopsies of renal transplants. *Clin Nephrol* 1991;36(5):215–222.
113. McCall SJ, Tuttle-Newhall JE, Howell DN, et al. Prognostic significance of microvascular thrombosis in donor kidney allograft biopsies. *Transplant* 2003;75(11):1847–1852.
114. Gaber LW, Gaber AO, Tolley EA, et al. Prediction by postrevascularization biopsies of cadaveric kidney allografts of rejection, graft loss, and preservation nephropathy. *Transplantation* 1992;53(6):1219–1225.
115. Ripple MG, Charney D, Nadasdy T. Cholesterol embolization in renal allografts. *Transplantation* 2000;69(10):2221–2225.
116. Schonermarck U, Guba M, Weiss M, et al. Cholesterol atheroembolic disease in kidney allografts—case report and review of the literature. *Clin Nephrol* 2006;66(5):386–390.
117. Woestenburg AT, Verpooten GA, Ysebaert DK, et al. Fibrous intimal thickening at implantation adversely affects long-term kidney allograft function. *Transplantation* 2009;87(1):72–78.
118. Haas M, Ratner LE, Montgomery RA. C4d staining of perioperative renal transplant biopsies. *Transplantation* 2002;74(5):711–717.
119. Rosenberg HG, Martinez PS, Vaccarezza AS, et al. Morphological findings in 70 kidneys of living donors for renal transplant. *Pathol Res Pract* 1990;186(5):619–624.
120. Cosyns JP, Malaise J, Hanique G, et al. Lesions in donor kidneys: nature, incidence, and influence on graft function. *Transplant Int* 1998;11(1):22–27.
121. Ji S, Liu M, Chen J, et al. The fate of glomerular mesangial IgA deposition in the donated kidney after allograft transplantation. *Clin Transplant* 2004;18(5):536–540.
122. Silva FG, Chandler P, Pirani CL, et al. Disappearance of glomerular mesangial IgA deposits after renal allograft transplantation. *Transplantation* 1982;33(214):214–216.
123. Tolloff-Rubin NE, Cosimi AB, Fuller T, et al. IgA nephropathy in HLA-identical siblings. *Transplantation* 1978;26(6):430–433.
124. Sanfilippo F, Croker BP, Bollinger RR. Fate of four cadaveric donor renal allografts with mesangial IgA deposits. *Transplantation* 1982;33(370):370–372.
125. Parker SM, Pullman JM, Khauli RB. Successful transplantation of a kidney with early membranous nephropathy. *Urology* 1995;46(6):870–872.
126. Nakazawa K, Shimojo H, Komiyama Y, et al. Preexisting membranous nephropathy in allograft kidney. *Nephron* 1999;81(1):76–80.
127. Lipkowitz GS, Madden RL, Kurbanov A, et al. Transplantation and 2-year follow-up of kidneys procured from a cadaver donor with a history of lupus nephritis. *Transplantation* 2000;69(6):1221–1224.
128. Mizuiri S, Shigetomi Y, Sugiyama K, et al. Successful transplantation of a cadaveric kidney with post-infectious glomerulonephritis. *Pediatr Transplant* 2000;4(1):56–59.
129. Brunt EM, Kissane JM, Cole BR, et al. Transmission and resolution of type I membranoproliferative glomerulonephritis in recipients of cadaveric renal allografts. *Transplant* 1988;46(4):595–598.
130. Koppel MH, Coburn JW, Mims MM, et al. Transplantation of cadaveric kidneys from patients with hepatorenal syndrome. Evidence for the functional nature of renal failure in advanced liver disease. *N Engl J Med* 1969;280(25):1367–1371.
131. Kiser RL, Thomas DB, Andreoni K, et al. Preexisting crescentic glomerulonephritis in the renal allograft. *Am J Kidney Dis* 2003;42(5):E20–E26.
132. Mueller TF, Reeve J, Jhangri GS, et al. The transcriptome of the implant biopsy identifies donor kidneys at increased risk of delayed graft function. *Am J Transplant* 2008;8(1):78–85.
133. Hauser P, Schwarz C, Mitterbauer C, et al. Genome-wide gene-expression patterns of donor kidney biopsies distinguish primary allograft function. *Lab Invest* 2004;84(3):353–361.
134. Einecke G, Broderick G, Sis B, et al. Early loss of renal transcripts in kidney allografts: relationship to the development of histologic lesions and allo-immune effector mechanisms. *Am J Transplant* 2007;7(5):1121–1130.
135. Famulski KS, de Freitas DG, Kreepala C, et al. Molecular phenotypes of acute kidney injury in kidney transplants. *J Am Soc Nephrol* 2012;23(5):948–958.
136. Kainz A, Perco P, Mayer B, et al. Gene-expression profiles and age of donor kidney biopsies obtained before transplantation distinguish medium term graft function. *Transplantation* 2007;83(8):1048–1054.
137. Kurian SM, Flechner SM, Kaouk J, et al. Laparoscopic donor nephrectomy gene expression profiling reveals upregulation of stress and ischemia associated genes compared to control kidneys. *Transplantation* 2005;80(8):1067–1071.
138. Kreepala C, Famulski KS, Chang J, et al. Comparing molecular assessment of implantation biopsies with histologic and demographic risk assessment. *Am J Transplant* 2013;13(2):415–426.

139. Sis B, Mengel M, Haas M, et al. Banff '09 meeting report: antibody mediated graft deterioration and implementation of Banff working groups. *Am J Transplant* 2010;10(3):464–471.
140. Matignon M, Muthukumar T, Seshan SV, et al. Concurrent acute cellular rejection is an independent risk factor for renal allograft failure in patients with C4d-positive antibody-mediated rejection. *Transplantation* 2012;94(6):603–611.
141. Nicleleit V. The pathology of kidney transplantation. In: Ruiz P, ed. *Transplantation Pathology*. New York: Cambridge University Press; 2009: 45–110.
142. Nicleleit V, Andreoni K. The classification and treatment of antibody-mediated renal allograft injury: where do we stand? *Kidney Int* 2007; 71(1):7–11.
143. Rao KV, Kasiske BL, Bloom PM. Acute graft rejection in the late survivors of renal transplantation. Clinical and histological observations in the second decade. *Transplantation* 1989;47(2):290–292.
144. Reinke P, Fietze E, Docke WD, et al. Late acute rejection in long-term renal allograft recipients. Diagnostic and predictive value of circulating activated T cells. *Transplantation* 1994;58(1):35–41.
145. Buchmann TN, Wolff T, Bachmann A, et al. Repeat true surveillance biopsies in kidney transplantation. *Transplantation* 2012;93(9):908–913.
146. Morrissey PE, Reinert S, Yango A, et al. Factors contributing to acute rejection in renal transplantation: the role of noncompliance. *Transplant Proc* 2005;37(5):2044–2047.
147. Kasiske B, Gaston RS, Gourishankar S, et al. Long-term deterioration of kidney allograft function. *Am J Transplant* 2005;5:1405–1414.
148. Organ procurement and transplantation network and scientific registry of transplant recipients 2010 annual data report. *Am J Transplantation* 2012;12(Suppl 1):22–23.
149. Gourishankar S, Leduc R, Connett J, et al. Pathological and clinical characterization of the 'troubled transplant': data from the DeKAF study. *Am J Transplant* 2010;10(2):324–330.
150. Nicleleit V, Zeiler M, Gudat F, et al. Detection of the complement degradation product C4d in renal allografts: diagnostic and therapeutic implications. *J Am Soc Nephrol* 2002;13(1):242–251.
151. Herzenberg AM, Gill JS, Djurdjev O, et al. C4d deposition in acute rejection: an independent long-term prognostic factor. *J Am Soc Nephrol* 2002;13(1):234–241.
152. Al-Aly Z, Reddivari V, Moiz A, et al. Renal allograft biopsies in the era of C4d staining: the need for change in the Banff classification system. *Transplant Int* 2008;21(3):268–275.
153. Lefaucheur C, Loupy A, Vernerey D, et al. Antibody-mediated vascular rejection of kidney allografts: a population-based study. *Lancet* 2013;381(9863):313–319.
154. Porter KA, Marchioro TL, Starzl TE. Pathological changes in 37 human renal homotransplants treated with immunosuppressive drugs. *Br J Urol* 1965;37:250–263.
155. Solez K, Colvin RB, Racusen LC, et al. Banff 07 classification of renal allograft pathology: updates and future directions. *Am J Transplant* 2008;8(4):753–760.
156. Nicleleit V, Zeiler M, Gudat F, et al. Histological characteristics of interstitial renal allograft rejection. *Kidney Blood Pressure Res* 1998;21(2–4):230–232.
157. Tuazon TV, Schneeberger EE, Bhan AK, et al. Mononuclear cells in acute allograft glomerulopathy. *Am J Pathol* 1987;129(1):119–132.
158. Axelsen RA, Seymour AE, Mathew TH, et al. Glomerular transplant rejection: a distinctive pattern of early graft damage. *Clin Nephrol* 1985;23(1):1–11.
159. Herrera GA, Alexander RW, Cooley CF, et al. Cytomegalovirus glomerulopathy: a controversial lesion. *Kidney Int* 1986;29(725):725–733.
160. Maryniak RK, First RM, Weiss MA. Transplant glomerulopathy: evolution of morphologically distinct changes. *Kidney Int* 1985;27:799–806.
161. Richardson WP, Colvin RB, Cheeseman SH, et al. Glomerulopathy associated with cytomegalovirus viremia in renal allografts. *N Engl J Med* 1981;305(2):57–63.
162. Katafuchi R, Masutani K, Mizumasa T, et al. A case of persistent acute allograft glomerulopathy with long-standing stable renal function. *Clin Transplant* 2001;15(Suppl 5):2–10.
163. Olsen S, Spencer E, Cockfield S, et al. Endocapillary glomerulitis in the renal allograft. *Transplantation* 1995;59(10):1421–1425.
164. Wiecek G, Bigaud M, Menninger K, et al. Acute and chronic vascular rejection in nonhuman primate kidney transplantation. *Am J Transplant* 2006;6(6):1285–1296.
165. Colvin RB, Cosimi AB, Burton RC, et al. Circulating T-cell subsets in human renal allograft recipients: the OKT4+/OKT8+ cell ratio correlates with reversibility of graft injury and glomerulopathy. *Transplant Proc* 1983;15(1166):1166–1169.
166. Messias NC, Eustace JA, Zachary AA, et al. Cohort study of the prognostic significance of acute transplant glomerulitis in acutely rejecting renal allografts. *Transplantation* 2001;72(4):655–660.
167. Fahim T, Bohmig GA, Exner M, et al. The cellular lesion of humoral rejection: predominant recruitment of monocytes to peritubular and glomerular capillaries. *Am J Transplant* 2007;7(2):385–393.
168. Magil AB. Infiltrating cell types in transplant glomerulitis: relationship to peritubular capillary C4d deposition. *Am J Kidney Dis* 2005;45(6):1084–1089.
169. Trpkov K, Campbell P, Pazderka F, et al. Pathologic features of acute renal allograft rejection associated with donor-specific antibody. Analysis using the Banff grading schema. *Transplantation* 1996;61(11):1586–1592.
170. Bishop GA, Hall BM, Duggin GG, et al. Immunopathology of renal allograft rejection analyzed with monoclonal antibodies to mononuclear cell markers. *Kidney Int* 1986;29(708):708–717.
171. Harry TR, Coles GA, Davies M, et al. The significance of monocytes in glomeruli of human renal transplants. *Transplantation* 1984;37(70): 70–73.
172. Batal I, Lunz JG, III, Aggarwal N, et al. A critical appraisal of methods to grade transplant glomerulitis in renal allograft biopsies. *Am J Transplant* 2010;10(11):2442–2452.
173. Haririan A, Papadimitriou JC. The need for better understanding of transplant glomerulitis. *Am J Transplant* 2011;11(4):866.
174. Papadimitriou JC, Drachenberg CB, Munivenkatappa R, et al. Glomerular inflammation in renal allograft biopsies after the first year: cell types and relationship with antibody-mediated rejection and graft outcome. *Transplantation* 2010;90(12):1478–1485.
175. Nádasdy T, Ormos J, Stiller D, et al. Tubular ultrastructure in rejected human renal allografts. *Ultrastruct Pathol* 1988;12(2):195–207.
176. Marcussen N, Lai R, Olsen TS, et al. Morphometric and immunohistochemical investigation of renal biopsies from patients with transplant ATN, native ATN, or acute graft rejection. *Transplant Proc* 1996;28(1):470–476.
177. Iványi B, Hansen HE, Olsen S. Segmental localization and quantitative characteristics of tubulitis in kidney biopsies from patients undergoing acute rejection. *Transplantation* 1993;56(3):581–585.
178. Mannon RB, Matas AJ, Grande J, et al. Inflammation in areas of tubular atrophy in kidney allograft biopsies: a potent predictor of allograft failure. *Am J Transplant* 2010;10(9):2066–2073.
179. Mengel M, Reeve J, Bunnag S, et al. Scoring total inflammation is superior to the current Banff inflammation score in predicting outcome and the degree of molecular disturbance in renal allografts. *Am J Transplant* 2009;9(8):1859–1867.
180. Scheepstra C, Bemelman FJ, van der Loos C, et al. B cells in cluster or in a scattered pattern do not correlate with clinical outcome of renal allograft rejection. *Transplantation* 2008;86(6):772–778.
181. Sis B, Jhangri GS, Riopel J, et al. A new diagnostic algorithm for antibody-mediated microcirculation inflammation in kidney transplants. *Am J Transplant* 2012;12(5):1168–1179.
182. Hancock WW, Atkins RC. Immunohistological analysis of sequential renal biopsies from patients with acute renal rejection. *J Immunol* 1985;136(2416):2416–2420.
183. Kirk AD, Mannon RB, Kleiner DE, et al. Results from a human renal allograft tolerance trial evaluating T-cell depletion with alemtuzumab combined with deoxyspergualin. *Transplant* 2005;80(8):1051–1059.
184. Sarwal M, Chua MS, Kambham N, et al. Molecular heterogeneity in acute renal allograft rejection identified by DNA microarray profiling. *N Engl J Med* 2003;349(2):125–138.
185. Chang A, Moore JM, Cowan ML, et al. Plasma cell densities and glomerular filtration rates predict renal allograft outcomes following acute rejection. *Transpl Int* 2012;25:1050–1058.
186. Hwang HS, Song JH, Hyoung BJ, et al. Clinical impacts of CD38+ B cells on acute cellular rejection with CD20+ B cells in renal allograft. *Transplantation* 2010;89(12):1489–1495.

187. Tsai EW, Rianthavorn P, Gjertson DW, et al. CD20+ lymphocytes in renal allografts are associated with poor graft survival in pediatric patients. *Transplantation* 2006;82(12):1769–1773.
188. Charney DA, Nadasdy T, Lo AW, et al. Plasma cell-rich acute renal allograft rejection. *Transplantation* 1999;68(6):791–797.
189. Desvaux D, Le Gouvello S, Pastural M, et al. Acute renal allograft rejections with major interstitial oedema and plasma cell-rich infiltrates: high {gamma}-interferon expression and poor clinical outcome. *Nephrol Dial Transplant* 2004;19(4):933–939.
190. Aiello FB, Calabrese F, Rigotti P, et al. Acute rejection and graft survival in renal transplanted patients with viral diseases. *Mod Pathol* 2004;17(2):189–196.
191. David-Neto E, Ribeiro DS, Ianhez LE, et al. Acute interstitial nephritis of plasma cells: a new cause for renal allograft loss. *Transplant Proc* 1993;25:897–899.
192. Meehan SM, Domer P, Josephson M, et al. The clinical and pathologic implications of plasmacytic infiltrates in percutaneous renal allograft biopsies. *Hum Pathol* 2001;32(2):205–215.
193. Danilewicz M, Wagrowska-Danilewicz M. Immunohistochemical analysis of the interstitial mast cells in acute rejection of human renal allografts. *Med Sci Monit*. 2004;10(5):BR151–BR156.
194. Weir MR, Hall-Craggs M, Shen SY, et al. The prognostic value of the eosinophil in acute renal allograft rejection. *Transplantation* 1986;41(6):709–712.
195. Kormendi F, Amend W. The importance of eosinophil cells in kidney allograft rejection. *Transplantation* 1988;45(3):537–539.
196. Nickeleit V, Vamvakas EC, Pascual M, et al. The prognostic significance of specific arterial lesions in acute renal allograft rejection. *J Am Soc Nephrol* 1998;9:1301–1308.
197. Hongwei W, Nanra RS, Stein A, et al. Eosinophils in acute renal allograft rejection. *Transpl Immunol* 1994;2(1):41–46.
198. Almirall J, Campistol JM, Sole M, et al. Blood and graft eosinophilia as a rejection index in kidney transplant. *Nephron* 1993;65(2):304–309.
199. Meleg-Smith S, Gauthier PM. Abundance of interstitial eosinophils in renal allografts is associated with vascular rejection. *Transplantation* 2005;79(4):444–450.
200. Saisu K, Morozumi K, Suzuki K, et al. Significance of interstitial lesions as the early indicator for acute vascular rejection in human renal allografts. *Clin Transplant* 1999;13 Suppl 1:17–23.
201. Colvin RB, Dvorak HF. Basophils and mast cells in renal allograft rejection. *Lancet* 1974;1:212–214.
202. McKenzie I, Colvin RB, Russell PS. Clinical immunopathology of transplantation. In: Miescher PA, Mueller-Eberhard HJ, eds. *Textbook of Immunopathology*, 2nd ed. New York: Grune and Stratton, 1976: 1043–1064.
203. Sibley RK, Rynasiewicz J, Ferguson RM, et al. Morphology of cyclosporine nephrotoxicity and acute rejection in patients immunosuppressed with cyclosporine and prednisone. *Surgery* 1983;94(2):225–234.
204. Schroeder TJ, Weiss MA, Smith RD, et al. The efficacy of OKT3 in vascular rejection. *Transplantation* 1991;51(2):312–315.
205. Kooijmans-Coutinho MF, Hermans J, Schrama E, et al. Interstitial rejection, vascular rejection, and diffuse thrombosis of renal allografts. Predisposing factors, histology, immunohistochemistry, and relation to outcome. *Transplantation* 1996;61(9):1338–1344.
206. Bates WD, Davies DR, Welsh K, et al. An evaluation of the Banff classification of early renal allograft biopsies and correlation with outcome. *Nephrol Dial Transplant* 1999;14(10):2364–2369.
207. Bellamy CO, Randhawa PS. Arteriolitis in renal transplant biopsies is associated with poor graft outcome. *Histopathology* 2000;36(6):488–492.
208. Alpers CE, Gordon D, Gown AM. Immunophenotype of vascular rejection in renal transplants. *Mod Pathol* 1990;3(2):198–203.
209. Aita K, Yamaguchi Y, Horita S, et al. Peritubular capillaritis in early renal allograft is associated with the development of chronic rejection and chronic allograft nephropathy. *Clin Transplant* 2005;19 Suppl 14:20–26.
210. Torbenson M, Randhawa P. Arcuate and interlobular phlebitis in renal allografts. *Hum Pathol* 2001;32(12):1388–1391.
211. Katz JP, Hakki A, Katz SM, et al. Rejection of the ureter: a new component of renal allograft rejection. *Transplant Proc* 1987;19:2200–2202.
212. Paccione F, Enein AA, Shikata T, et al. Changes in the transplanted ureter. *Br J Exp Pathol* 1965;46:519–529.
213. Haber MH, Putong PB. Ureteral vascular rejection in human renal transplants. *JAMA* 1965;192:417–419.
214. Hall BM, Bishop GA, Duggin GG, et al. Increased expression of HLA-DR antigens on renal tubular cells in renal transplants: relevance to the rejection response. *Lancet* 1984;2(8397):247–251.
215. Andrews PA, Finn JE, Lloyd CM, et al. Expression and tissue localization of donor-specific complement C3 synthesized in human renal allografts. *Eur J Immunol* 1995;25(4):1087–1093.
216. Broomann RA, Stegmann AP, van Dorp WT, et al. Interleukin 2 mediates stimulation of complement C3 biosynthesis in human proximal tubular epithelial cells. *J Clin Invest* 1991;88:379–384.
217. McKenzie I, Whittingham S. Deposits of immunoglobulin and fibrin in human renal allografted kidneys. *Lancet* 1968;2(1313):1313–1315.
218. Schwager I, Jungi TW. Effect of human recombinant cytokines on the induction of macrophage procoagulant activity. *Blood* 1994;83(1): 152–160.
219. Mauviyyedi S, Colvin RB. Humoral rejection in kidney transplantation: new concepts in diagnosis and treatment. *Curr Opin Nephrol Hypertens* 2002;11(6):609–618.
220. Wavamunno MD, O'Connell PJ, Vitalone M, et al. Transplant glomerulopathy: ultrastructural abnormalities occur early in longitudinal analysis of protocol biopsies. *Am J Transplant* 2007;7(12):2757–2768.
221. Shimamura T, Gyorky E, Morgen RO, et al. Fine structural observations in human kidney homografts. *Invest Urol* 1966;3:590–598.
222. Cohen AH, Border WA, Rajfer J, et al. Interstitial Tamm-Horsfall protein in rejecting renal allografts. Identification and morphologic pattern of injury. *Lab Invest* 1984;50(5):519–525.
223. Iványi B, Hansen HE, Olsen TS. Postcapillary venule-like transformation of peritubular capillaries in acute renal allograft rejection. An ultrastructural study. *Arch Pathol Lab Med* 1992;116(10):1062–1067.
224. Liapis G, Singh HK, Derebail VK, et al. Diagnostic significance of peritubular capillary basement membrane multilaminations in kidney allografts: old concepts revisited. *Transplantation* 2012;94(6):620–629.
225. Strehlau J, Pavlakis M, Lipman M, et al. Quantitative detection of immune activation transcripts as a diagnostic tool in kidney transplantation. *Proc Natl Acad Sci U S A* 1997;94:695–700.
226. Sharma VK, Bologa RM, Li B, et al. Molecular executors of cell death—differential intrarenal expression of Fas ligand, Fas, granzyme B, and perforin during acute and/or chronic rejection of human renal allografts. *Transplantation* 1996;62(12):1860–1866.
227. Lipman ML, Stevens AC, Strom TB. Heightened intragraft CTL gene expression in acutely rejecting renal allografts. *J Immunol* 1994; 152(10):5120–5127.
228. Strehlau J, Pavlakis M, Lipman M, et al. The intragraft gene activation of markers reflecting T-cell-activation and -cytotoxicity analyzed by quantitative RT-PCR in renal transplantation. *Clin Nephrol* 1996;46(1):30–33.
229. Hoffmann SC, Hale DA, Kleiner DE, et al. Functionally significant renal allograft rejection is defined by transcriptional criteria. *Am J Transplant* 2005;5(3):573–581.
230. Suthanthiran M. Molecular analyses of human renal allografts: differential intragraft gene expression during rejection. *Kidney Int Suppl* 1997;58:S15–S21.
231. Desvaux D, Schwarzinger M, Pastural M, et al. Molecular diagnosis of renal-allograft rejection: correlation with histopathologic evaluation and antirejection-therapy resistance. *Transplantation* 2004;78(5): 647–653.
232. Allanach K, Mengel M, Einecke G, et al. Comparing microarray versus RT-PCR assessment of renal allograft biopsies: similar performance despite different dynamic ranges. *Am J Transplant* 2008;8(5):1006–1015.
233. Einecke G, Melk A, Ramassar V, et al. Expression of CTL associated transcripts precedes the development of tubulitis in T-Cell mediated kidney graft rejection. *Am J Transplant* 2005;5(8):1827–1836.
234. Einecke G, Kayser D, Vanslambrouck JM, et al. Loss of solute carriers in T cell-mediated rejection in mouse and human kidneys: an active epithelial injury-repair response. *Am J Transplant* 2010;10:2241.
235. Hidalgo LG, Einecke G, Allanach K, et al. The transcriptome of human cytotoxic T cells: similarities and disparities among allostimulated CD4(+) CTL, CD8(+) CTL and NK cells. *Am J Transplant* 2008;8(3):627–636.

236. Hidalgo LG, Einecke G, Allanach K, et al. The transcriptome of human cytotoxic T cells: measuring the burden of CTL-associated transcripts in human kidney transplants. *Am J Transplant* 2008;8(3):637–646.
237. Famulski KS, Einecke G, Sis B, et al. Defining the canonical form of T-cell-mediated rejection in human kidney transplants. *Am J Transplant* 2010;10(4):810–820.
238. Famulski KS, Kayser D, Einecke G, et al. Alternative macrophage activation-associated transcripts in T-cell-mediated rejection of mouse kidney allografts. *Am J Transplant* 2010;10(3):490–497.
239. Reeve J, Einecke G, Mengel M, et al. Diagnosing rejection in renal transplants: a comparison of molecular- and histopathology-based approaches. *Am J Transplant* 2009;9(8):1802–1810.
240. Mueller TF, Einecke G, Reeve J, et al. Microarray analysis of rejection in human kidney transplants using pathogenesis-based transcript sets. *Am J Transplant* 2007;7(12):2712–2722.
241. Famulski K, Einecke G, Halloran PF. IFN- γ inducible transcripts are increased in T cell mediated rejection (TCMR), but some are also increased in tissue injury. *Am J Transplant* 2005;5 s11:448–449.
242. Famulski KS, Einecke G, Reeve J, et al. Changes in the transcriptome in allograft rejection: IFN- γ -induced transcripts in mouse kidney allografts. *Am J Transplant* 2006;6(6):1342–1354.
243. Akalin E, Hendrix RC, Polavarapu RG, et al. Gene expression analysis in human renal allograft biopsy samples using high-density oligoarray technology. *Transplantation* 2001;72(5):948–953.
244. Serinsöz E, Bock O, Gwinner W, et al. Local complement C3 expression is upregulated in humoral and cellular rejection of renal allografts. *Am J Transplant* 2005;5(6):1490–1494.
245. Famulski KS, Broderick G, Einecke G, et al. Transcriptome analysis reveals heterogeneity in the injury response of kidney transplants. *Am J Transplant* 2007;7(11):2483–2495.
246. Einecke G, Mengel M, Hidalgo L, et al. The early course of kidney allograft rejection: defining the time when rejection begins. *Am J Transplant* 2009;9(3):483–493.
247. Reeve J, Sellares J, Mengel M, et al. Molecular diagnosis of T cell-mediated rejection in human kidney transplant biopsies. *Am J Transplant* 2013;13(3):645–655.
248. Li B, Hartono C, Ding R, et al. Noninvasive diagnosis of renal-allograft rejection by measurement of messenger RNA for perforin and granzyme B in urine. *N Engl J Med* 2001;344(13):947–954.
249. Afaneh C, Muthukumar T, Lubetzky M, et al. Urinary cell levels of mRNA for OX40, OX40L, PD-1, PD-L1, or PD-L2 and acute rejection of human renal allografts. *Transplantation* 2010;90(12):1381–1387.
250. Suthanthiran M, Schwartz JE, Ding R, et al. Urinary-cell mRNA profile and acute cellular rejection in kidney allografts. *N Engl J Med* 2013;369(1):20–31.
251. Anglicheau D, Suthanthiran M. Noninvasive prediction of organ graft rejection and outcome using gene expression patterns. *Transplantation* 2008;86(2):192–199.
252. Lorenzen JM, Volkman I, Fiedler J, et al. Urinary miR-210 as a mediator of acute T-cell mediated rejection in renal allograft recipients. *Am J Transplant* 2011;11(10):2221–2227.
253. Anglicheau D, Sharma VK, Ding R, et al. MicroRNA expression profiles predictive of human renal allograft status. *Proc Natl Acad Sci U S A*. 2009;106(13):5330–5335.
254. Mas VR, Dumur CI, Scian MJ, et al. MicroRNAs as biomarkers in solid organ transplantation. *Am J Transplant* 2013;13(1):11–19.
255. Rosenberg AS, Mizuochi T, Singer A. Analysis of T-cell subsets in rejection of K^b mutant skin allografts differing at class I MHC. *Nature* 1986;322(829):829–831.
256. Hansen TH, Carreno BM, Sachs DH. The major histocompatibility complex. In: Paul WE, ed. *Fundamental Immunology*. 3rd ed. New York: Raven Press; 1993:577–628.
257. Shiina T, Inoko H, Kulski JK. An update of the HLA genomic region, locus information and disease associations: 2004. *Tissue Antigens* 2004;64(6):631–649.
258. Daar AS, Fuggle SV, Fabre JW, et al. The detailed distribution of MHC Class II antigens in normal human organs. *Transplantation* 1984;38(3):293–298.
259. Fuggle SV, McWhinnie DL, Chapman JR, et al. Sequential analysis of HLA class II antigen expression in human renal allografts: induction of tubular class II antigens and correlation with clinical parameters. *Transplantation* 1985;42:144–150.
260. Hancock WW, Kraft N, Atkins RC. The immunohistochemical demonstration of major histocompatibility antigens in the human kidney using monoclonal antibodies. *Transplantation* 1982;39(430):430–438.
261. Pober JS. Immunobiology of human vascular endothelium. *Immunol Res* 1999;19(2–3):225–232.
262. Maguire JE, Gresser I, Williams AH, et al. Modulation of expression of MHC antigens in the kidneys of mice by murine interferon- α/β . *Transplantation* 1990;49(1):130–134.
263. Skoskiewicz MJ, Colvin RB, Schneeberger EE, et al. Widespread and selective induction of major histocompatibility complex-determined antigens in vivo by gamma interferon. *J Exp Med* 1985;162(5):1645–1664.
264. Matas AJ, Sibley R, Mauer M, et al. The value of needle renal allograft biopsy. I. A retrospective study of biopsies performed during putative rejection episodes. *Ann Surg* 1983;197(2):226–237.
265. Halloran PF, Afrouzian M, Ramassar V, et al. Interferon-gamma acts directly on rejecting renal allografts to prevent graft necrosis. *Am J Pathol* 2001;158(1):215–226.
266. Grusby M, Auchincloss H, Lee R, et al. Mice lacking major histocompatibility complex class I and class II molecules. *Proc Natl Acad Sci U S A* 1993;90:3913–3917.
267. Lee RS, Grusby MJ, Laufer TM, et al. CD8⁺ effector cells responding to residual class I antigens, with help from CD4⁺ cells stimulated indirectly, cause rejection of “major histocompatibility complex-deficient” skin grafts. *Transplantation* 1997;63:1123–1133.
268. Benacerraf B. Antigen processing and presentation. The biologic role of MHC molecules in determinant selection. *J Immunol* 1988;141(7 Suppl):s17–s20.
269. Moreau JF, Bonneville M, Peyrat MA, et al. T lymphocyte cloning from rejected human kidney allografts. Growth frequency and functional/phenotypic analysis. *J Clin Invest* 1986;78(874):874–879.
270. Shinohara N, Bluestone JA, Sachs DH. Cloned cytotoxic T lymphocytes that recognize an I-A region product in the context of a class I antigen. *J Exp Med* 1986;163(972):972–980.
271. Graff RJ, Brown DH. Estimates of histocompatibility differences between inbred mouse strains. *Immunogenetics* 1978;7:367–374.
272. Poindexter NJ, Steward NS, Shenoy S, et al. Cytolytic T lymphocytes from human renal allograft biopsies are tissue specific. *Hum Immunol* 1995;44(1):43–49.
273. Krieger NR, Yin DP, Fathman CG. CD4⁺ but not CD8⁺ cells are essential for allorejection. *J Exp Med* 1996;184(5):2013–2018.
274. Mosmann TR, Cherwinski H, Bond MW, et al. Two types of murine helper T cell clone. I. Definition according to profiles of lymphokine activities and secreted proteins. *J Immunol* 1986;136(7):2348–2357.
275. Yamane H, Zhu J, Paul WE. Independent roles for IL-2 and GATA-3 in stimulating naive CD4⁺ T cells to generate a Th2-inducing cytokine environment. *J Exp Med* 2005;202(6):793–804.
276. Garcia-Zepeda EA, Rothenberg ME, Ownbey RT, et al. Human eotaxin is a specific chemoattractant for eosinophil cells and provides a new mechanism to explain tissue eosinophilia. *Nat Med* 1996;2(4):449–456.
277. Honjo K, Xu XY, Bucy RP. Heterogeneity of T cell clones specific for a single indirect alloantigenic epitope (I-Ab/H-2Kd54-68) that mediate transplant rejection. *Transplantation* 2000;70(10):1516–1524.
278. Hidalgo LG, Urmson J, Halloran PF. IFN- γ decreases CTL generation by limiting IL-2 production: a feedback loop controlling effector cell production. *Am J Transplant* 2005;5(4 Pt 1):651–661.
279. Catalfamo M, Henkart PA. Perforin and the granule exocytosis cytotoxicity pathway. *Curr Opin Immunol* 2003;15(5):522–527.
280. Pinkoski MJ, Waterhouse NJ, Heibein JA, et al. Granzyme B-mediated apoptosis proceeds predominantly through a Bcl-2-inhibitable mitochondrial pathway. *J Biol Chem* 2001;276(15):12060–12067.
281. Schulz M, Schuurman HJ, Joergensen J, et al. Acute rejection of vascular heart allografts by perforin-deficient mice. *Eur J Immunol* 1995;25(2):474–480.
282. Halloran PF, Urmson J, Ramassar V, et al. Lesions of T-cell-mediated kidney allograft rejection in mice do not require perforin or granzymes A and B. *Am J Transplant* 2004;4(5):705–712.

283. Dai Z, Li Q, Wang Y, et al. CD4+ CD25+ regulatory T cells suppress allograft rejection mediated by memory CD8+ T cells via a CD30-dependent mechanism. *J Clin Invest* 2004;113(2):310–317.
284. Walker LS. CD4+ CD25+ Treg: divide and rule? *Immunology* 2004;111(2):129–137.
285. Fahlen L, Read S, Gorelik L, et al. T cells that cannot respond to TGF-beta escape control by CD4(+)/CD25(+) regulatory T cells. *J Exp Med* 2005;201(5):737–746.
286. Segerer S, Bohmig GA, Exner M, et al. Role of CXCR3 in cellular but not humoral renal allograft rejection. *Transpl Int* 2005;18(6):676–680.
287. Segerer S, Cui Y, Eitner F, et al. Expression of chemokines and chemokine receptors during human renal transplant rejection. *Am J Kidney Dis* 2001;37(3):518–531.
288. Ruster M, Spersneider H, Funfstuck R, et al. Differential expression of beta-chemokines MCP-1 and RANTES and their receptors CCR1, CCR2, CCR5 in acute rejection and chronic allograft nephropathy of human renal allografts. *Clin Nephrol* 2004;61(1):30–39.
289. Grandaliano G, Gesualdo L, Ranieri E, et al. Monocyte chemotactic peptide-1 expression and monocyte infiltration in acute renal transplant rejection. *Transplantation* 1997;63(3):414–420.
290. Segerer S, Mac KM, Regele H, et al. Expression of the C-C chemokine receptor 5 in human kidney diseases. *Kidney Int* 1999;56(1):52–64.
291. Eitner F, Cui Y, Hudkins KL, et al. Chemokine receptor (CCR5) expression in human kidneys and in the HIV infected macaque. *Kidney Int* 1998;54(6):1945–1954.
292. Cockwell P, Chakravorty SJ, Girdlestone J, et al. Fractalkine expression in human renal inflammation. *J Pathol* 2002;196(1):85–90.
293. Pattison J, Nelson PJ, Huie P, et al. RANTES chemokine expression in cell-mediated transplant rejection of the kidney. *Lancet* 1994;343(8891):209–211.
294. Schmouder RL, Streiter RM, Wiggins RC, et al. In vitro and in vivo production of interleukin-8 (IL-8) in renal cortical epithelium. *Kidney Int* 1992;41:191–199.
295. Vandembroecke C, Caillat-Zucman S, Legendre C, et al. Differential in situ expression of cytokines in renal allograft rejection. *Transplantation* 1991;51:602–609.
296. Van Kooten C, Boonstra JG, Paape ME, et al. Interleukin-17 activates human renal epithelial cells in vitro and is expressed during renal allograft rejection. *J Am Soc Nephrol* 1998;9(8):1526–1534.
297. Robertson H, Morley AR, Talbot D, et al. Renal allograft rejection: beta-chemokine involvement in the development of tubulitis. *Transplantation* 2000;69(4):684–687.
298. Ali S, Malik G, Burns A, et al. Renal transplantation: examination of the regulation of chemokine binding during acute rejection. *Transplantation* 2005;79(6):672–679.
299. Burdick JF, Beschoner WE, Smith WJ, et al. Characteristics of early routine renal allograft biopsies. *Transplantation* 1984;38(679):679–684.
300. Preffer FI, Colvin RB, Leary CP, et al. Two-color flow cytometry and functional analysis of lymphocytes cultured from human renal allografts: identification of a Leu-2+3+ subpopulation. *J Immunol* 1986;137(9):2823–2830.
301. Sanfilippo F, Kolbeck PC, Vaughn WK, et al. Renal allograft cell infiltrates associated with irreversible rejection. *Transplantation* 1985;40(679):679–685.
302. Sako H, Nakane Y, Okino K, et al. Immunohistochemical study of the cells infiltrating human renal allografts by the ABC and the IGSS method using monoclonal antibodies. *Transplantation* 1987;44(1):43–50.
303. Leskinen R, Häyry P. Topographical distribution of inflammatory leukocyte subsets in acute cellular rejection of a kidney allograft. *Acta Pathol Microbiol Immunol Scand* 1986;94:69–76.
304. Ibrahim S, Dawson DV, Sanfilippo F. Predominant infiltration of rejecting human renal allografts with T cells expressing CD8 and CD45RO. *Transplantation* 1995;59(5):724–728.
305. Raasveld MH, Bloemena E, Surachno S, et al. T gamma/delta lymphocytes in renal transplant recipients. *Nephrol Dial Transplant* 1992;7:530–533.
306. Kirk AD, Ibrahim S, Dawson DV, et al. Characterization of T cells expressing the γ/δ antigen receptor in human renal allografts. *Hum Immunol* 1993;36(1):11–19.
307. Frisman DM, Hurwitz AA, Bennett WT, et al. Clonal analysis of graft-infiltrating lymphocytes from renal and cardiac biopsies. Dominant rearrangements of TcR beta genes and persistence of dominant rearrangements in serial biopsies. *Hum Immunol* 1990;28(2):208–215.
308. Obata F, Yoshida K, Ikeda Y, et al. Clonality analysis of T cells mediating acute and chronic rejection in kidney allografts. *Transpl Immunol* 2004;13(3):233–237.
309. Obata F, Kumano K, Endo T, et al. T-cell receptor variable gene analysis of renal allograft-infiltrating cells in biopsy specimens using a nonradioisotopic micromethod. *Transplantation* 1998;66(10):1389–1392.
310. Douillard P, Cuturi MC, Brouard S, et al. T cell receptor repertoire usage in allotransplantation: an overview. *Transplantation* 1999;68(7):913–921.
311. Hu M, Zhang GY, Walters G, et al. Matching T-cell receptors identified in renal biopsies and urine at the time of acute rejection in pediatric renal transplant patients. *Am J Transplant* 2004;4(11):1859–1868.
312. Kataoka K, Naomoto Y, Shiozaki S, et al. Infiltration of perforin-positive mononuclear cells into the rejected kidney allograft. *Transplantation* 1992;53(1):240–242.
313. Pascoe MD, Marshall SE, Welsh KI, et al. Increased accuracy of renal allograft rejection diagnosis using combined perforin, granzyme B, and Fas ligand fine-needle aspiration immunocytology. *Transplantation* 2000;69(12):2547–2553.
314. Akasaka Y, Ishikawa Y, Kato S, et al. Induction of Fas-mediated apoptosis in a human renal epithelial cell line by interferon-gamma: involvement of Fas-mediated apoptosis in acute renal rejection. *Mod Pathol* 1998;11(11):1107–1114.
315. Kummer J, Wever P, Kamp A, et al. Expression of granzyme A and B proteins by cytotoxic lymphocytes involved in acute renal allograft rejection. *Kidney Int* 1995;47:70–77.
316. Rowshani AT, Florquin S, Bemelman F, et al. Hyperexpression of the granzyme B inhibitor PI-9 in human renal allografts: a potential mechanism for stable renal function in patients with subclinical rejection. *Kidney Int* 2004;66(4):1417–1422.
317. Mengel M, Mueller I, Behrend M, et al. Prognostic value of cytotoxic T-lymphocytes and CD40 in biopsies with early renal allograft rejection. *Transpl Int* 2004;17(6):293–300.
318. Meehan S, McCluskey R, Pascual M, et al. Cytotoxicity and apoptosis in human renal allografts: identification, distribution, and quantitation of cells with a cytotoxic granule protein GMP-17 (TIA-1) and cells with fragmented nuclear DNA. *Lab Invest* 1997;76:639–649.
319. Kurnick JT, Preffer FI, Colvin RB, et al. Functional analysis of lymphocyte subsets and clones infiltrating renal allografts. *J Immunol* 1987;141(4187):4187–4195.
320. Noronha IL, Hartley B, Cameron JS, et al. Detection of IL-1 beta and TNF-alpha message and protein in renal allograft biopsies. *Transplantation* 1993;56(4):1026–1029.
321. Veronese F, Rotman S, Smith RN, et al. Pathological and clinical correlates of FOXP3+ cells in renal allografts during acute rejection. *Am J Transplant* 2007;7:914.
322. Miyajima M, Chase CM, Alessandrini A, et al. Early acceptance of renal allografts in mice is dependent on foxp3(+) cells. *Am J Pathol* 2011;178(4):1635–1645.
323. Lee I, Wang L, Wells AD, et al. Recruitment of Foxp3+ T regulatory cells mediating allograft tolerance depends on the CCR4 chemokine receptor. *J Exp Med* 2005;201(7):1037–1044.
324. Dummer CD, Carpio VN, da Silva Loreto M, et al. Analysis of FOXP3 gene and protein expressions in renal allograft biopsies and their association with graft outcomes. *Ren Fail* 2013;35(4):521–530.
325. Bunnag S, Allanach K, Jhangri GS, et al. FOXP3 expression in human kidney transplant biopsies is associated with rejection and time post transplant but not with favorable outcomes. *Am J Transplant* 2008;8(7):1423–1433.
326. Grimbert P, Mansour H, Desvaux D, et al. The regulatory/cytotoxic graft-infiltrating T cells differentiate renal allograft borderline change from acute rejection. *Transplantation* 2007;83(3):341–346.
327. Bestard O, Cruzado JM, Mestre M, et al. Achieving donor-specific hyporesponsiveness is associated with FOXP3+ regulatory T cell recruitment in human renal allograft infiltrates. *J Immunol* 2007;179(7):4901–4909.

328. Bestard O, Cruzado JM, Rama I, et al. Presence of FoxP3+ regulatory T Cells predicts outcome of subclinical rejection of renal allografts. *J Am Soc Nephrol* 2008;19(10):2020–2026.
329. Bestard O, Cunetti L, Cruzado JM, et al. Intragraft regulatory T cells in protocol biopsies retain foxp3 demethylation and are protective biomarkers for kidney graft outcome. *Am J Transplant* 2011;11(10):2162–2172.
330. Noronha IL, Eberlein-Gonska M, Hartley B, et al. In situ expression of tumor necrosis factor-alpha, interferon-gamma, and interleukin-2 receptors in renal allograft biopsies. *Transplantation* 1992;54:1017–1024.
331. Biancone L, Segoloni G, Turello E, et al. Expression of inducible lymphocyte costimulatory molecules in human renal allograft. *Nephrol Dial Transplant* 1998;13(3):716–722.
332. Grimm PC, McKenna RM, Gospodarek EM, et al. Low frequency of infiltrating cells intensely expressing T cell cytokine mRNA in human renal allograft rejection. *Transplantation* 1995;59(4):579–584.
333. Dugre FJ, Gaudreau S, Belles-Isles M, et al. Cytokine and cytotoxic molecule gene expression determined in peripheral blood mononuclear cells in the diagnosis of acute renal rejection. *Transplantation* 2000;70(7):1074–1080.
334. Waltzer WC, Miller F, Arnold A, et al. Immunohistologic analysis of human renal allograft dysfunction. *Transplantation* 1987;43(1):100–105.
335. Copin MC, Noel C, Hazzan M, et al. Diagnostic and predictive value of an immunohistochemical profile in asymptomatic acute rejection of renal allografts. *Transpl Immunol* 1995;3(3):229–239.
336. Ito H, Kasagi N, Shomori K, et al. Apoptosis in the human allografted kidney. Analysis by terminal deoxynucleotidyl transferase-mediated DUTP-biotin nick end labeling. *Transplantation* 1995;60(8):794–798.
337. Noronha IL, Oliveira SG, Tavares TS, et al. Apoptosis in kidney and pancreas allograft biopsies. *Transplantation* 2005;79(9):1231–1235.
338. August C, Schmid KW, Diedl KH, et al. Prognostic value of lymphocyte apoptosis in acute rejection of renal allografts. *Transplantation* 1999;67(4):581–585.
339. Briscoe DM, Pober JSS, Harmon WE, et al. Expression of vascular cell adhesion molecule-1 in human renal allografts. *J Am Soc Nephrol* 1992;3(5):1180–1185.
340. Wyburn KR, Jose MD, Wu H, et al. The role of macrophages in allograft rejection. *Transplantation* 2005;80(12):1641–1647.
341. Hancock WW, Rickles FR, Ewan VA, et al. Immunohistological studies with A1-3, a monoclonal antibody to activated human monocytes and macrophages. *J Immunol* 1986;136:2416–2420.
342. Wang T, Dong C, Stevenson SC, et al. Overexpression of soluble fas attenuates transplant arteriosclerosis in rat aortic allografts. *Circulation* 2002;106(12):1536–1542.
343. Watschinger B, Sayegh MH. Endothelin in organ transplantation. *Am J Kidney Dis* 1996;27(1):151–161.
344. Ozdemir BH, Ozdemir FN, Haberal N, et al. Vascular endothelial growth factor expression and cyclosporine toxicity in renal allograft rejection. *Am J Transplant* 2005;5(4 Pt 1):766–774.
345. Wang Y, Thompson EM, Whawell SA, et al. Expression and localization of plasminogen activator inhibitor 1 mRNA in transplant kidneys. *J Pathol* 1993;169(4):445–450.
346. Roelofs JJ, Rowshani AT, van den Berg JG, et al. Expression of urokinase plasminogen activator and its receptor during acute renal allograft rejection. *Kidney Int* 2003;64(5):1845–1853.
347. Steinmetz OM, Panzer U, Kneissler U, et al. BCA-1/CXCL13 expression is associated with CXCR5-positive B-cell cluster formation in acute renal transplant rejection. *Kidney Int* 2005;67(4):1616–1621.
348. Andersen CB, Ladefoged SD, Larsen S. Acute kidney graft rejection. A morphological and immunohistological study on “zero-hour” and follow-up biopsies with special emphasis on cellular infiltrates and adhesion molecules. *APMIS* 1994;102(1):23–37.
349. Robertson H, Wheeler J, Kirby JA, et al. Renal allograft rejection—in situ demonstration of cytotoxic intratubular cells. *Transplantation* 1996;61(10):1546–1549.
350. Robertson H, Kirby JA. Post-transplant renal tubulitis: the recruitment, differentiation and persistence of intra-epithelial T cells. *Am J Transplant* 2003;3(1):3–10.
351. Wong WK, Robertson H, Carroll HP, et al. Tubulitis in renal allograft rejection: role of transforming growth factor-beta and interleukin-15 in development and maintenance of CD103+ intraepithelial T cells. *Transplantation* 2003;75(4):505–514.
352. Robertson H, Wong WK, Talbot D, et al. Tubulitis after renal transplantation: demonstration of an association between CD103+ T cells, transforming growth factor beta1 expression and rejection grade. *Transplantation* 2001;71(2):306–313.
353. Yuan R, El-Asady R, Liu K, et al. Critical role for CD103+CD8+ effectors in promoting tubular injury following allogeneic renal transplantation. *J Immunol* 2005;175(5):2868–2879.
354. Robertson H, Wheeler J, Thompson V, et al. In situ lymphoproliferation in renal transplant biopsies. *Histochem Cell Biol* 1995;104:331–334.
355. Wever PC, Aten J, Rentenaar RJ, et al. Apoptotic tubular cell death during acute renal allograft rejection. *Clin Nephrol* 1998;49(1):28–34.
356. Du C, Guan Q, Yin Z, et al. IL-2-mediated apoptosis of kidney tubular epithelial cells is regulated by the caspase-8 inhibitor c-FLIP. *Kidney Int* 2005;67(4):1397.
357. Hagerty DT, Allen PM. Processing and presentation of self- and non-self foreign antigens by the renal proximal tubule. *J Immunol* 1992;126:2324–2332.
358. Niemann-Masanek U, Mueller A, Yard BA, et al. B7-1 (CD80) and B7-2 (CD 86) expression in human tubular epithelial cells in vivo and in vitro. *Nephron* 2002;92(3):542–556.
359. Fuggle SV, McWhinnie DL, Morris PJ. Precise specificity of induced tubular HLA-class II antigens in renal allografts. *Transplantation* 1987;44(2):214–220.
360. Barrett M, Milton AD, Barrett J, et al. Needle biopsy evaluation of class II major histocompatibility complex antigen expression for the differential diagnosis of cyclosporine nephrotoxicity from kidney graft rejection. *Transplantation* 1987;44:223–227.
361. Ozdemir BH, Aksoy PK, Haberal AN, et al. Relationship of HLA-DR expression to rejection and mononuclear cell infiltration in renal allograft biopsies. *Ren Fail* 2004;26(3):247–251.
362. Nickleleit V, Hirsch HH, Zeiler M, et al. BK-virus nephropathy in renal transplants-tubular necrosis, MHC-class II expression and rejection in a puzzling game. *Nephrol Dial Transplant* 2000;15(3):324–332.
363. Alchi B, Nishi S, Kondo D, et al. Osteopontin expression in acute renal allograft rejection. *Kidney Int* 2005;67(3):886–896.
364. Morel D, Normand E, Lemoine C, et al. Tumor necrosis factor alpha in human kidney transplant rejection—analysis by in situ hybridization. *Transplantation* 1993;55(4):773–777.
365. Faull RJ, Russ GR. Tubular expression of intercellular adhesion molecule-1 during renal allograft rejection. *Transplantation* 1989;48(2):226–230.
366. Fuggle SV, Sanderson JB, Gray DW, et al. Variation in expression of endothelial adhesion molecules in pretransplant and transplanted kidneys—correlation with intragraft events. *Transplantation* 1993;55(1):117–123.
367. Brockmeyer C, Ulbrecht M, Schendel DJ, et al. Distribution of cell adhesion molecules (ICAM-1, VCAM-1, ELAM-1) in renal tissue during allograft rejection. *Transplantation* 1993;55(3):610–615.
368. Bukovsky A, Labarrere CA, Carter C, et al. Novel immunohistochemical markers of human renal allograft dysfunction—antithrombin III, Thy-1, urokinase, and alpha-smooth muscle actin. *Transplantation* 1992;54(6):1064–1071.
369. Dvergsten J, Manivel JC, Correa-Rotter R, et al. Expression of clusterin in human renal diseases. *Kidney Int* 1994;45(3):828–835.
370. Murphy BF, Davies DJ, Morrow W, et al. Localization of terminal complement components, S-protein and SP-40,40 in renal biopsies. *Pathology* 1989;21:275–278.
371. Russell PS, Chase CM, Colvin RB. Alloantibody- and T cell-mediated immunity in the pathogenesis of transplant arteriosclerosis: lack of progression to sclerotic lesions in B cell-deficient mice. *Transplantation* 1997;64(11):1531–1536.
372. Visscher D, Carey J, Oh H, et al. Histologic and immunophenotypic evaluation of pretreatment renal biopsies in OKT3-treated allograft rejections. *Transplantation* 1991;51(5):1023–1028.
373. Cosimi AB, Burton RC, Colvin RB, et al. Treatment of acute renal allograft rejection with OKT3 monoclonal antibody. *Transplantation* 1981;32(6):535–539.
374. Hirohashi T, Chase CM, Della Pelle P, et al. A novel pathway of chronic allograft rejection mediated by NK cells and alloantibody. *Am J Transplant* 2012;12(2):313–321.
375. Young-Ramsaran JO, Hruban RH, Hutchins GM, et al. Ultrastructural evidence of cell-mediated endothelial cell injury in cardiac transplant-related accelerated arteriosclerosis. *Ultrastruct Pathol* 1993;17(2):125–136.

376. Woywodt A, Schroeder M, Gwinner W, et al. Elevated numbers of circulating endothelial cells in renal transplant recipients. *Transplantation* 2003;76(1):1–4.
377. Park SY, Kim HW, Moon KC, et al. mRNA expression of intercellular adhesion molecule-1 and vascular cell adhesion molecule-1 in acute renal allograft rejection. *Transplantation* 2000;69(12):2554–2560.
378. Kirveskari J, Paavonen T, Hayry P, et al. De novo induction of endothelial L-selectin ligands during kidney allograft rejection. *J Am Soc Nephrol* 2000;11(12):2358–2365.
379. Alpers CE, Davis CL, Barr D, et al. Identification of platelet-derived growth factor A and B chains in human renal vascular rejection. *Am J Pathol* 1996;148(2):439–451.
380. Bishop GA, Waugh JA, Landers DV, et al. Microvascular destruction in renal transplant rejection. *Transplantation* 1989;48(3):408–414.
381. Watschinger B, Vychytil A, Attar M, et al. Pattern of endothelin immunostaining during rejection episodes after kidney transplantation. *Clin Nephrol* 1994;41(2):86–93.
382. Hiki Y, Leong AY, Mathew TH, et al. Typing of intraglomerular mononuclear cells associated with transplant glomerular rejection. *Clin Nephrol* 1986;26(5):244–249.
383. Ramos EL, Barri YM, Croker BP, et al. Thromboxane synthase expression in renal transplant patients with rejection. *Transplantation* 1995;59(4):490–494.
384. Meehan SM, Josephson MA, Haas M. Granulomatous tubulointerstitial nephritis in the renal allograft. *Am J Kidney Dis* 2000;36(4):E27.
385. Randhawa PS, Magnone M, Jordan M, et al. Renal allograft involvement by Epstein-Barr virus associated post-transplant lymphoproliferative disease. *Am J Surg Pathol* 1996;20(5):563–571.
386. Randhawa PS, Saad RS, Jordan M, et al. Clinical significance of renal biopsies showing concurrent acute rejection and tacrolimus-associated tubular vacuolization. *Transplantation* 1999;67(1):85–89.
387. Mauyyedi S, Crespo M, Collins AB, et al. Acute humoral rejection in kidney transplantation: II. Morphology, immunopathology, and pathologic classification. *J Am Soc Nephrol* 2002;13(3):779–787.
388. Regele H, Exner M, Watschinger B, et al. Endothelial C4d deposition is associated with inferior kidney allograft outcome independently of cellular rejection. *Nephrol Dial Transplant* 2001;16(10):2058–2066.
389. Magil AB, Tinckam K. Monocytes and peritubular capillary C4d deposition in acute renal allograft rejection. *Kidney Int* 2003;63(5):1888–1893.
390. Waiser J, Budde K, Schutz M, et al. Comparison between bortezomib and rituximab in the treatment of antibody-mediated renal allograft rejection. *Nephrol Dial Transplant* 2012;27(3):1246–1251.
391. Mueller A, Schnuelle P, Waldherr R, et al. Impact of the Banff '97 classification for histological diagnosis of rejection on clinical outcome and renal function parameters after kidney transplantation. *Transplantation* 2000;69(6):1123–1127.
392. Macdonald FI, Ashraf S, Picton M, et al. Banff criteria as predictors of outcome following acute renal allograft rejection. *Nephrol Dial Transplant* 1999;14(7):1692–1697.
393. Gaber LW, Moore LW, Alloway RR, et al. Correlation between Banff classification, acute renal rejection scores and reversal of rejection. *Kidney Int* 1996;49(2):481–487.
394. Palomar R, Ruiz JC, Zubimendi JA, et al. Is there any correlation between pathologic changes for acute rejection in kidney transplantation (Banff 97) and graft function? *Transplant Proc* 2002;34(1):349.
395. Haas M, Kraus ES, Samaniego-Picota M, et al. Acute renal allograft rejection with intimal arteritis: histologic predictors of response to therapy and graft survival. *Kidney Int* 2002;61(4):1516–1526.
396. Mihatsch MJ, Nickenleit V, Gudat F. Morphologic criteria of chronic renal allograft rejection. *Transplant Proc* 1999;31(1–2):1295–1297.
397. Kuypers DR, Chapman JR, O'Connell PJ, et al. Predictors of renal transplant histology at three months. *Transplantation* 1999;67(9):1222–1230.
398. Herbertson BM, Evans DB, Calne RY, et al. Percutaneous needle biopsies of renal allografts: the relationship between morphological changes present in the biopsies and subsequent allograft function. *Histopathology* 1977;1(161):161–178.
399. Kiaer H, Hansen HE, Olsen S. The predictive value of percutaneous biopsies from human renal allografts with early impaired function. *Clin Nephrol* 1980;13(58):58–63.
400. Cosio FG, Pesavento TE, Sedmak DD, et al. Clinical implications of the diagnosis of renal allograft infarction by percutaneous biopsy. *Transplantation* 1998;66(4):467–471.
401. Kozlowski T, Nickenleit V, Andreoni K. Donor-transmitted adenovirus infection causing kidney allograft nephritis and graft loss. *Transpl Infect Dis* 2011;13(2):168–173.
402. Solez K, McGraw DJ, Beschoner WE, et al. Reflections on use of the renal biopsy as the “gold standard” in distinguishing transplant rejection from cyclosporine nephrotoxicity. *Transplant Proc* 1985;17 (Suppl 1):123–133.
403. Banfi G, Imbasciati E, Tarantino A, et al. Prognostic value of renal biopsy in acute rejection of kidney transplantation. *Nephron* 1981;28(222):222–226.
404. Hsu AC, Arbus GS, Noriega E, et al. Renal allograft biopsy: a satisfactory adjunct for predicting renal function after graft rejection. *Clin Nephrol* 1976;5(260):260–265.
405. Saad R, Gritsch HA, Shapiro R, et al. Clinical significance of renal allograft biopsies with “borderline changes,” as defined in the Banff Schema. *Transplantation* 1997;64(7):992–995.
406. Schweitzer EJ, Drachenberg CB, Anderson L. Significance of the Banff borderline biopsy. *Am J Kidney Dis* 1996;28:585–591.
407. Meehan SM, Siegel CT, Aronson AJ, et al. The relationship of untreated borderline infiltrates by the Banff criteria to acute rejection in renal allograft biopsies. *J Am Soc Nephrol* 1999;10(8):1806–1814.
408. McWhinnie DL, Thompson JF, Taylor HM, et al. Morphometric analysis of cellular infiltration assessed by monoclonal antibody labeling in sequential human renal allograft biopsies. *Transplantation* 1986;2(352):352–358.
409. Poduval RD, Kadambi PV, Josephson MA, et al. Implications of immunohistochemical detection of C4d along peritubular capillaries in late acute renal allograft rejection. *Transplantation* 2005;79(2):228–235.
410. Hippen BE, DeMattos A, Cook WJ, et al. Association of CD20+ infiltrates with poorer clinical outcomes in acute cellular rejection of renal allografts. *Am J Transplant* 2005;5(9):2248–2252.
411. Bagnasco SM, Tsai W, Rahman MH, et al. CD20-positive infiltrates in renal allograft biopsies with acute cellular rejection are not associated with worse graft survival. *Am J Transplant* 2007;7(8):1968–1973.
412. Schiffer L, Schiffer M, Merkel S, et al. Rationale and design of the RIACT-study: a multi-center placebo controlled double blind study to test the efficacy of Rituximab in Acute Cellular tubulointerstitial rejection with B-cell infiltrates in renal Transplant patients: study protocol for a randomized controlled trial. *Trials* 2012;13:199.
413. Vega J, Goecke H, Carrasco A, et al. Rituximab in the treatment of acute cellular rejection of renal allograft with CD20-positive clusters in the infiltrate. *Clin Exp Nephrol* 2011;15(2):308–311.
414. Nolan CR, Saenz KP, Thomas CA, III, et al. Role of the eosinophil in chronic vascular rejection of renal allografts. *Am J Kidney Dis* 1995;26(4):634–642.
415. Tait BD, Susal C, Gebel HM, et al. Consensus guidelines on the testing and clinical management issues associated with HLA and non-HLA antibodies in transplantation. *Transplantation* 2013;95(1):19–47.
416. Halloran PF, Schlaut J, Solez K, et al. The significance of the anti-class I antibody response. II. Clinical and pathologic features of renal transplants with anti-class I-like antibody. *Transplantation* 1992;53(3):550–555.
417. Scornik JC, LeFor WM, Ciciarelli JC, et al. Hyperacute and acute kidney graft rejection due to antibodies against B cells. *Transplantation* 1992;54(1):61–64.
418. Crespo M, Pascual M, Tolkoff-Rubin N, et al. Acute humoral rejection in renal allograft recipients: I. Incidence, serology and clinical characteristics. *Transplantation* 2001;71(5):652–658.
419. Issa N, Cosio FG, Gloor JM, et al. Transplant glomerulopathy: risk and prognosis related to anti-human leukocyte antigen class II antibody levels. *Transplantation* 2008;86(5):681–685.
420. Pollinger HS, Stegall MD, Gloor JM, et al. Kidney transplantation in patients with antibodies against donor HLA class II. *Am J Transplant* 2007;7(4):857–863.
421. Gloor JM, Sethi S, Stegall MD, et al. Transplant glomerulopathy: sub-clinical incidence and association with alloantibody. *Am J Transplant* 2007;7(9):2124–2132.

422. Sis B, Campbell PM, Mueller T, et al. Transplant glomerulopathy, late antibody-mediated rejection and the ABCD tetrad in kidney allograft biopsies for cause. *Am J Transplant* 2007;7(7):1743–1752.
423. Li L, Chen A, Chaudhuri A, et al. Compartmental localization and clinical relevance of MICA antibodies after renal transplantation. *Transplantation* 2010;89(3):312–319.
424. Sanchez-Zapardiel E, Castro-Panete MJ, Castillo-Rama M, et al. Harmful effect of preformed anti-MICA antibodies on renal allograft evolution in early posttransplantation period. *Transplantation* 2013;96:70–78.
425. Lu J, Luo L, Guo Y, et al. The effect of MICA antigens on transplant outcomes: a systematic review. *J Evid Based Med* 2011;4(2):106–121.
426. Zou Y, Stastny P, Susal C, et al. Antibodies against MICA antigens and kidney-transplant rejection. *N Engl J Med* 2007;357(13):1293–1300.
427. Narayan S, Tsai EW, Zhang Q, et al. Acute rejection associated with donor-specific anti-MICA antibody in a highly sensitized pediatric renal transplant recipient. *Pediatr Transplant* 2011;15(1):E1–E7.
428. Alvarez-Marquez A, Aguilera I, Gentil MA, et al. Donor-specific antibodies against HLA, MICA, and GSTT1 in patients with allograft rejection and C4d deposition in renal biopsies. *Transplantation* 2009;87(1):94–99.
429. Kalil J, Guilherme L, Neumann J, et al. Humoral rejection in two HLA identical living related donor kidney transplants. *Transplant Proc* 1989;21(1 Pt 1):711–713.
430. Sumitran-Karuppan S, Tyden G, Reinholt F, et al. Hyperacute rejections of two consecutive renal allografts and early loss of the third transplant caused by non-HLA antibodies specific for endothelial cells. *Transpl Immunol* 1997;5(4):321–327.
431. Mathew JM, Joyce S, Lawrence W, et al. Evidence that antibodies eluted from rejected kidneys of HLA-identical transplants define a non-MHC alloantigen expressed on human kidneys. *Transplantation* 1991;52(3):559–562.
432. Tan JC, Wadia PP, Coram M, et al. H-Y antibody development associates with acute rejection in female patients with male kidney transplants. *Transplantation* 2008;86(1):75–81.
433. Dragun D, Muller DN, Brasen JH, et al. Angiotensin II type 1-receptor activating antibodies in renal-allograft rejection. *N Engl J Med* 2005;352(6):558–569.
434. Reinsmoen NL, Lai CH, Heidecke H, et al. Anti-angiotensin type 1 receptor antibodies associated with antibody mediated rejection in donor HLA antibody negative patients. *Transplantation* 2010;90(12):1473–1477.
435. Sun Q, Cheng Z, Cheng D, et al. De novo development of circulating anti-endothelial cell antibodies rather than pre-existing antibodies is associated with post-transplant allograft rejection. *Kidney Int* 2011;79(6):655–662.
436. Joosten SA, Sijpkens YW, van Ham V, et al. Antibody response against the glomerular basement membrane protein agrin in patients with transplant glomerulopathy. *Am J Transplant* 2005;5(2):383–393.
437. Dinavahi R, George A, Tretin A, et al. Antibodies reactive to non-HLA antigens in transplant glomerulopathy. *J Am Soc Nephrol* 2011;22(6):1168–1178.
438. Porcheray F, DeVito J, Helou Y, et al. Expansion of polyreactive B cells cross-reactive to HLA and self in the blood of a patient with kidney graft rejection. *Am J Transplant* 2012;12(8):2088–2097.
439. Li L, Wadia P, Chen R, et al. Identifying compartment-specific non-HLA targets after renal transplantation by integrating transcriptome and “antibodyome” measures. *Proc Natl Acad Sci U S A* 2009;106(11):4148–4153.
440. Austen WG Jr, Zhang M, Chan R, et al. Murine hindlimb reperfusion injury can be initiated by a self-reactive monoclonal IgM. *Surgery* 2004;136(2):401–406.
441. Montgomery RA, Lonze BE, King KE, et al. Desensitization in HLA-incompatible kidney recipients and survival. *N Engl J Med* 2011;365(4):318–326.
442. Montgomery RA, Lonze BE, Jackson AM. Using donor exchange paradigms with desensitization to enhance transplant rates among highly sensitized patients. *Curr Opin Organ Transplant* 2011;16(4):439–443.
443. Shapiro-Shelef M, Calame K. Regulation of plasma-cell development. *Nat Rev Immunol* 2005;5(3):230–242.
444. Perry DK, Burns JM, Pollinger HS, et al. Proteasome inhibition causes apoptosis of normal human plasma cells preventing alloantibody production. *Am J Transplant* 2009;9(1):201–209.
445. Noorchashm H, Reed AJ, Rostami SY, et al. B cell-mediated antigen presentation is required for the pathogenesis of acute cardiac allograft rejection. *J Immunol* 2006;177(11):7715–7722.
446. Cascalho M, Platt JL. Novel functions of B cells. *Crit Rev Immunol* 2007;27(2):141–151.
447. Steele DJ, Laufer TM, Smiley ST, et al. Two levels of help for B cell allo-antibody production. *J Exp Med* 1996;183(2):699–703.
448. Gombos P, Opelz G, Scherer S, et al. Influence of test technique on sensitization status of patients on the kidney transplant waiting list. *Am J Transplant* 2013;13:2075–2082.
449. Farkash EA, Colvin RB. Pathology: diagnostic challenges in chronic antibody-mediated rejection. *Nat Rev Nephrol* 2012;8(5):255–257.
450. Zhang X, Reed EF. Effect of antibodies on endothelium. *Am J Transplant* 2009;9(11):2459–2465.
451. Bian H, Harris PE, Reed EF. Ligation of HLA class I molecules on smooth muscle cells with anti-HLA antibodies induces tyrosine phosphorylation, fibroblast growth factor receptor expression and cell proliferation. *Int Immunol* 1998;10(9):1315–1323.
452. Bian H, Reed EF. Alloantibody-mediated class I signal transduction in endothelial cells and smooth muscle cells: enhancement by IFN-gamma and TNF-alpha. *J Immunol* 1999;163(2):1010–1018.
453. Jin YP, Fishbein MC, Said JW, et al. Anti-HLA class I antibody-mediated activation of the PI3K/Akt signaling pathway and induction of Bcl-2 and Bcl-xL expression in endothelial cells. *Hum Immunol* 2004;65(4):291–302.
454. Jin YP, Jindra PT, Gong KW, et al. Anti-HLA class I antibodies activate endothelial cells and promote chronic rejection. *Transplantation* 2005;79(3 Suppl):S19–S21.
455. Jin YP, Singh RP, Du ZY, et al. Ligation of HLA class I molecules on endothelial cells induces phosphorylation of Src, paxillin, and focal adhesion kinase in an actin-dependent manner. *J Immunol* 2002;168(11):5415–5423.
456. Narayanan K, Jaramillo A, Phelan DL, et al. Pre-exposure to saturating concentrations of HLA class I antibodies confers resistance to endothelial cells against antibody complement-mediated lysis by regulating Bad through the phosphatidylinositol 3-kinase/Akt pathway. *Eur J Immunol* 2004;34(8):2303–2312.
457. Yamakuchi M, Kirkiles-Smith NC, Ferlito M, et al. Antibody to human leukocyte antigen triggers endothelial exocytosis. *Proc Natl Acad Sci U S A* 2007;104(4):1301–1306.
458. Jindra PT, Jin YP, Jacamo R, et al. MHC class I and integrin ligation induce ERK activation via an mTORC2-dependent pathway. *Biochem Biophys Res Commun* 2008;369(2):781–787.
459. Chadee DN, Kyriakis JM. MLK3 is required for mitogen activation of B-Raf, ERK and cell proliferation. *Nat Cell Biol* 2004;6(8):770–776.
460. Zhou Q, Heinke J, Vargas A, et al. ERK signaling is a central regulator for BMP-4 dependent capillary sprouting. *Cardiovasc Res* 2007;76(3):390–399.
461. Rotman S, Collins AB, Colvin RB. C4d deposition in allografts: current concepts and interpretation. *Transplant Rev* 2005;19:65–77.
462. Colvin RB, Smith RN. Antibody-mediated organ-allograft rejection. *Nat Rev Immunol* 2005;5(10):807–817.
463. Albrecht EA, Chinnaiyan AM, Varambally S, et al. C5a-induced gene expression in human umbilical vein endothelial cells. *Am J Pathol* 2004;164(3):849–859.
464. Monsinjon T, Gasque P, Chan P, et al. Regulation by complement C3a and C5a anaphylatoxins of cytokine production in human umbilical vein endothelial cells. *FASEB J* 2003;17(9):1003–1014.
465. Nakashima S, Qian Z, Rahimi S, et al. Membrane attack complex contributes to destruction of vascular integrity in acute lung allograft rejection. *J Immunol* 2002;169(8):4620–4627.
466. Hughes J, Nangaku M, Alpers CE, et al. C5b-9 membrane attack complex mediates endothelial cell apoptosis in experimental glomerulonephritis. *Am J Physiol Renal Physiol* 2000;278(5):F747–F757.
467. Kilgore KS, Schmid E, Shanley TP, et al. Sublytic concentrations of the membrane attack complex of complement induce endothelial interleukin-8 and monocyte chemoattractant protein-1 through nuclear factor-kappa B activation. *Am J Pathol* 1997;150(6):2019–2031.
468. Saadi S, Holzkecht RA, Patte CP, et al. Endothelial cell activation by pore-forming structures: pivotal role for interleukin-1alpha. *Circulation* 2000;101(15):1867–1873.

469. Ikeda K, Nagasawa K, Horiuchi T, et al. C5a induces tissue factor activity on endothelial cells. *Thromb Haemost* 1997;77(2):394–398.
470. Saadi S, Holzkecht RA, Patte CP, et al. Complement-mediated regulation of tissue factor activity in endothelium. *J Exp Med* 1995;182(6):1807–1814.
471. Kirby JA, Givan AL, Shenton BK, et al. Renal allograft rejection. Possible involvement of antibody-dependent cell-mediated cytotoxicity. *Transplantation* 1990;50(2):225–229.
472. Akiyoshi T, Hirohashi T, Alessandrini A, et al. Role of complement and NK cells in antibody mediated rejection. *Hum Immunol* 2012;73:1226–1232.
473. Arase N, Arase H, Hirano S, et al. IgE-mediated activation of NK cells through FcγRIII. *J Immunol* 2003;170:3054–3058.
474. Arase N, Arase H, Park SY, et al. Association with FcRγ is essential for activation signal through NKR-P1 (CD161) in natural killer (NK) cells and NK1.1+ T cells. *J Exp Med* 1997;186(12):1957–1963.
475. Lee CY, Lotfi-Emran S, Erdinc M, et al. The involvement of FcR mechanisms in antibody-mediated rejection. *Transplantation* 2007;84(10):1324–1334.
476. Yin D, Zeng H, Ma L, et al. Cutting edge: NK cells mediate IgG1-dependent hyperacute rejection of xenografts. *J Immunol* 2004;172(12):7235–7238.
477. Chen D, Weber M, Lechler R, et al. NK-cell-dependent acute xenograft rejection in the mouse heart-to-rat model. *Xenotransplantation* 2006;13(5):408–414.
478. Sis B, Jhangri GS, Riopel J, et al. A new diagnostic algorithm for antibody-mediated microcirculation inflammation in kidney transplants. *Am J Transplant* 2012;12:1168–1179.
479. Cohen D, Colvin RB, Daha MR, et al. Pros and cons for C4d as a biomarker. *Kidney Int* 2012;81(7):628–639.
480. Kraus ES, Parekh RS, Oberai P, et al. Subclinical rejection in stable positive crossmatch kidney transplant patients: incidence and correlations. *Am J Transplant* 2009;9(8):1826–1834.
481. Haas M, Sis B, Racusen LC, et al. Banff 2013 meeting report: inclusion of c4d-negative antibody-mediated rejection and antibody-associated arterial lesions. *Am J Transplant* 2014;14(2):272–283.
482. Kayler LK, Kiss L, Sharma V, et al. Acute renal allograft rejection: diagnostic significance of focal peritubular capillary C4d. *Transplantation* 2008;85(6):813–820.
483. Fior F, Nacchia F, Minicozzi A, et al. Focal C4d staining in peritubular capillaries and kidney graft survival: results of a retrospective study. *Transplant Proc* 2010;42(4):1095–1097.
484. Kedainis RL, Koch MJ, Brennan DC, et al. Focal C4d+ in renal allografts is associated with the presence of donor-specific antibodies and decreased allograft survival. *Am J Transplant* 2009;9(4):812–819.
485. Kikic Z, Regele H, Nordmeyer V, et al. Significance of peritubular capillary, glomerular, and arteriolar C4d staining patterns in paraffin sections of early kidney transplant biopsies. *Transplantation* 2011;91(4):440–446.
486. Bohmig GA, Exner M, Habicht A, et al. Capillary C4d deposition in kidney allografts: a specific marker of alloantibody-dependent graft injury. *J Am Soc Nephrol* 2002;13(4):1091–1099.
487. Seemayer CA, Gaspert A, Nickleit V, et al. C4d staining of renal allograft biopsies: a comparative analysis of different staining techniques. *Nephrol Dial Transplant* 2007;22(2):568–576.
488. Nadasdy GM, Bott C, Cowden D, et al. Comparative study for the detection of peritubular capillary C4d deposition in human renal allografts using different methodologies. *Hum Pathol* 2005;36(11):1178–1185.
489. Troxell ML, Sibley RK, Higgins JP, et al. Comparison of immunofluorescence and immunohistochemical methods for C4d staining in renal allograft biopsies (Abstr). *Mod Pathol* 2005;18:270A.
490. Mengel M, Chan S, Climenhaga J, et al. Banff initiative for quality assurance in transplantation (BIFQUIT): reproducibility of C4d immunohistochemistry in kidney allografts. *Am J Transplant* 2013;13:1235–1245.
491. Sis B, Jhangri GS, Bunnag S, et al. Endothelial gene expression in kidney transplants with alloantibody indicates antibody-mediated damage despite lack of C4d staining. *Am J Transplant* 2009;9(10):2312–2323.
492. Loupy A, Hill GS, Suberbielle C, et al. Significance of C4d Banff scores in early protocol biopsies of kidney transplant recipients with preformed donor-specific antibodies (DSA). *Am J Transplant* 2011;11(1):56–65.
493. Williams GM, Hume DM, Huson RP, Jr, et al. “Hyperacute” renal-homograft rejection in man. *N Engl J Med* 1968;279(611):611–615.
494. Starzl TE, Boehmig HJ, Amemiya H, et al. Clotting changes, including disseminated intravascular coagulation, during rapid renal-homograft rejection. *N Engl J Med* 1970;283:383–387.
495. Kohler TR, Tilney NL. Microangiopathic hemolytic anemia associated with hyperacute rejection of a kidney allograft. *Transplant Proc* 1982;14(2):444–447.
496. El-Zoghby ZM, Stegall MD, Lager DJ, et al. Identifying specific causes of kidney allograft loss. *Am J Transplant* 2009;9(3):527–535.
497. Gaber LW, Gaber AO, Vera SR, et al. Successful reversal of hyperacute renal allograft rejection with the anti-CD3 monoclonal OKT3. *Transplantation* 1992;54(5):930–932.
498. Myburgh JA, Cohen I, Cecelter L, et al. Hyperacute rejection in human-kidney allografts Shwartzman or Arthus reaction? *N Engl J Med* 1969;281:131–135.
499. Starzl TE, Lerner RA, Dixon FJ, et al. Shwartzman reaction after human renal homotransplantation. *N Engl J Med* 1968;278(642):642–646.
500. Halloran PF, Wadgymar A, Ritchie S, et al. The significance of the anti-class I antibody response. I. Clinical and pathologic features of anti-class I-mediated rejection. *Transplantation* 1990;49(1):85–91.
501. Ahern AT, Artruc SB, DellaPelle P, et al. Hyperacute rejection of HLA-AB-identical renal allografts associated with B lymphocyte and endothelial reactive antibodies. *Transplantation* 1982;33(1):103–106.
502. Jackson AM, Kuperman MB, Montgomery RA. Multiple hyperacute rejections in the absence of detectable complement activation in a patient with endothelial cell reactive antibody. *Am J Transplant* 2012;12(6):1643–1649.
503. Paul LC, van Es LA, de la Rivière GB, et al. Blood group B antigen on renal endothelium as the target for rejection in an ABO-incompatible recipient. *Transplantation* 1989;26:268–272.
504. Chapman JR, Taylor C, Ting A, et al. Hyperacute rejection of a renal allograft in the presence of anti-HLA-Cw5 antibody. *Transplantation* 1986;42(1):91–93.
505. Metzgar RS, Seigler HF, Ward FE, et al. Immunological studies on elutes from human renal allografts. *Transplantation* 1972;13(131):131–137.
506. Ronda C, Borba SC, Ferreira SC, et al. Non-human leukocyte antigen antibodies reactive with endothelial cells could be involved in early loss of renal allografts. *Transplant Proc* 2011;43(4):1345–1348.
507. Jordan SC, Yap HK, Sakai RS, et al. Hyperacute allograft rejection mediated by antivascular endothelial antibodies with a negative monocyte crossmatch. *Transplantation* 1988;46:585–589.
508. Brasile L, Rodman E, Shield CF, et al. The association of antivascular endothelial cell antibody with hyperacute rejection: a case report. *Surgery* 1986;99(5):637–640.
509. Evans PR, Trickett LP, Gosney AR, et al. Detection of kidney reactive antibodies at crossmatch in renal transplant recipients. *Transplantation* 1988;46(6):844–852.
510. Lobo PI, Sturgill BC, Bolton WK. Cold-reactive alloantibodies and allograft malfunction occurring immediately post-transplantation. *Transplantation* 1984;37:76–81.
511. Sturgill BC, Lobo PI, Bolton WK. Cold-reacting IgM antibody-induced renal allograft failure: similarity to hyperacute rejection. *Nephron* 1984;36(125):125–127.
512. Schweitzer RT, Bartus SA, Perkins HA, et al. Renal allograft failure and cold red blood cell autoagglutinins. *Transplantation* 1982;33:77–79.
513. Cross DE, Whittier FC, Cuppage FE, et al. Hyperacute rejection of renal allografts following pulsatile perfusion with a perfusate containing specific antibody. *Transplantation* 1974;17:626–630.
514. Light JA, Annable C, Perloff L, et al. Immune injury from organ preservation: a potential cause of hyperacute rejection in human cadaveric kidney transplantation. *Transplantation* 1975;19:511–514.
515. Colovai AI, Vasilescu ER, Foca-Rodi A, et al. Acute and hyperacute humoral rejection in kidney allograft recipients treated with anti-human thymocyte antibodies. *Hum Immunol* 2005;66(5):501–512.
516. Busch GJ, Martins AC, Hollenberg NK, et al. A primate model of hyperacute renal allograft rejection. *Am J Pathol* 1975;79(1):31–56.
517. Ito S, Camussi G, Tetta C, et al. Hyperacute renal allograft rejection in the rabbit. *Lab Invest* 1984;51(2):148–161.

518. Sedmak DD, Orosz CG. The role of vascular endothelial cells in transplantation. *Arch Pathol Lab Med* 1991;115(3):260–265.
519. Shimizu A, Yamada K, Robson SC, et al. Pathologic characteristics of transplanted kidney xenografts. *J Am Soc Nephrol* 2012;23(2):225–235.
520. Patel R, Terasaki PI. Significance of the positive crossmatch test in kidney transplantation. *N Engl J Med* 1969;280:735–738.
521. Kirkman RL, Colvin RB, Flye MW, et al. Transplantation in miniature swine. VII. Evidence for cellular immune mechanisms in hyperacute rejection of renal allografts. *Transplantation* 1979;28(1):24–30.
522. Eichwald EJ, Shelby J. Serum and cell-mediated responses in tolerance and hyperacute rejection transplanted mouse hearts. *Transplantation* 1987;43(4):520–523.
523. Baid S, Pascual M, Williams WW, Jr., et al. Renal thrombotic microangiopathy associated with anticardiolipin antibodies in hepatitis C-positive renal allograft recipients. *J Am Soc Nephrol* 1999;10(1):146–153.
524. Shimizu T, Ishida H, Tanabe T, et al. A case of transplant glomerulopathy early after kidney transplantation. *Clin Transplant* 2011;25 Suppl 23:34–38.
525. Gloor JM, DeGoey S, Ploeger N, et al. Persistence of low levels of alloantibody after desensitization in crossmatch-positive living-donor kidney transplantation. *Transplantation* 2004;78(2):221–227.
526. Warren DS, Zachary AA, Sonnenday CJ, et al. Successful renal transplantation across simultaneous ABO incompatible and positive crossmatch barriers. *Am J Transplant* 2004;4(4):561–568.
527. Dawson KL, Parulekar A, Seethamraju H. Treatment of hyperacute antibody-mediated lung allograft rejection with eculizumab. *J Heart Lung Transplant* 2012;31(12):1325–1326.
528. Palmer A, Taube DJ, Welsh K, et al. Successful removal of anti-HLA antibodies by extracorporeal immunoadsorption allowing renal transplantation. *Lancet* 1989;1:10–13.
529. Bannett AD, Bensinger WI, Raja R, et al. Immunoadsorption and renal transplantation in two patients with a major ABO incompatibility. *Transplantation* 1987;43(909):909–911.
530. Fuller TC, Forbes JB, Delmonico FL. Renal transplantation with a positive historical donor crossmatch. *Transplantation* 1985;42(1):144–150.
531. Nickleit V, Mihatsch MJ. Kidney transplants, antibodies and rejection: is C4d a magic marker? *Nephrol Dial Transplant* 2003;18(11):2232–2239.
532. Feucht HE, Felber E, Gokel MJ, et al. Vascular deposition of complement-split products in kidney allografts with cell-mediated rejection. *Clin Exp Immunol* 1991;86(3):464–470.
533. Feucht HE, Schneeberger H, Hillebrand G, et al. Capillary deposition of C4d complement fragment and early renal graft loss. *Kidney Int* 1993;43(6):1333–1338.
534. Collins AB, Schneeberger EE, Pascual MA, et al. Complement activation in acute humoral renal allograft rejection: diagnostic significance of C4d deposits in peritubular capillaries. *J Am Soc Nephrol* 1999;10(10):2208–2214.
535. Weinstein D, Braun WE, Cook D, et al. Ultra-late antibody-mediated rejection 30 years after a living-related renal allograft. *Am J Transplant* 2005;5(10):2576–2581.
536. Takemoto SK, Zeevi A, Feng S, et al. National conference to assess antibody-mediated rejection in solid organ transplantation. *Am J Transplant* 2004;4(7):1033–1041.
537. Wiebe C, Gibson IW, Blydt-Hansen TD, et al. Evolution and clinical pathologic correlations of de novo donor-specific HLA antibody post kidney transplant. *Am J Transplant* 2012;12(5):1157–1167.
538. Lorenz M, Regele H, Schillinger M, et al. Risk factors for capillary C4d deposition in kidney allografts: evaluation of a large study cohort. *Transplantation* 2004;78(3):447–452.
539. Marfo K, Lu A, Ling M, et al. Desensitization protocols and their outcome. *Clin J Am Soc Nephrol* 2011;6(4):922–936.
540. Lefaucheur C, Loupy A, Hill GS, et al. Preexisting donor-specific HLA antibodies predict outcome in kidney transplantation. *J Am Soc Nephrol* 2010;21(8):1398–1406.
541. Fan Z, Spencer JA, Lu Y, et al. In vivo tracking of “color-coded” effector, natural and induced regulatory T cells in the allograft response. *Nat Med* 2010;16(6):718–722.
542. Burns JM, Cornell LD, Perry DK, et al. Alloantibody levels and acute humoral rejection early after positive crossmatch kidney transplantation. *Am J Transplant* 2008;8(12):2684–2694.
543. Willicombe M, Roufosse C, Brookes P, et al. Antibody-mediated rejection after alemtuzumab induction: incidence, risk factors, and predictors of poor outcome. *Transplantation* 2011;92(2):176–182.
544. Knechtle SJ, Pirsch JD, H. Fechner J, et al. Campath-1H induction plus rapamycin monotherapy for renal transplantation: results of a pilot study. *Am J Transplant* 2003;3(6):722–730.
545. Knechtle SJ, Pascual J, Bloom DD, et al. Early and limited use of tacrolimus to avoid rejection in an alemtuzumab and sirolimus regimen for kidney transplantation: clinical results and immune monitoring. *Am J Transplant* 2009;9(5):1087–1098.
546. Maignon M, Muthukumar T, Seshan SV, et al. Concurrent acute cellular rejection is an independent risk factor for renal allograft failure in patients with C4d-positive antibody-mediated rejection. *Transplantation* 2012;94:603–611.
547. Sund S, Reisaeter AV, Scott H, et al. Glomerular monocyte/macrophage influx correlates strongly with complement activation in 1-week protocol kidney allograft biopsies. *Clin Nephrol* 2004;62(2):121–130.
548. Herman J, Lerut E, Van Damme-Lombaerts R, et al. Capillary deposition of complement C4d and C3d in pediatric renal allograft biopsies. *Transplantation* 2005;79(10):1435–1440.
549. Higgins R, Zehnder D, Chen K, et al. The histological development of acute antibody-mediated rejection in HLA antibody-incompatible renal transplantation. *Nephrol Dial Transplant* 2010;25(4):1306–1312.
550. Lobo PI, Spencer CE, Stevenson WC, et al. Evidence demonstrating poor kidney graft survival when acute rejections are associated with IgG donor-specific lymphocytotoxin. *Transplantation* 1995;59:357–360.
551. Meehan SM, Kremer J, Ali FN, et al. Thrombotic microangiopathy and peritubular capillary C4d expression in renal allograft biopsies. *Clin J Am Soc Nephrol* 2011;6(2):395–403.
552. Biancone L, David S, Della Pietra V, et al. Alternative pathway activation of complement by cultured human proximal tubular epithelial cells. *Kidney Int* 1994;45(2):451–460.
553. Kanetsuna Y, Yamaguchi Y, Horita S, et al. C4d and/or immunoglobulins deposition in peritubular capillaries in perioperative graft biopsies in ABO-incompatible renal transplantation. *Clin Transplant* 2004;18 Suppl 11:13–17.
554. Regele H, Bohmig GA, Habicht A, et al. Capillary deposition of complement split product C4d in renal allografts is associated with basement membrane injury in peritubular and glomerular capillaries: a contribution of humoral immunity to chronic allograft rejection. *J Am Soc Nephrol* 2002;13(9):2371–2380.
555. Meehan SM, Limsrichamrern S, Manaligod JR, et al. Platelets and capillary injury in acute humoral rejection of renal allografts. *Hum Pathol* 2003;34(6):533–540.
556. Koo DD, Roberts IS, Quiroga I, et al. C4d deposition in early renal allograft protocol biopsies. *Transplantation* 2004;78(3):398–403.
557. Minami K, Murata K, Lee CY, et al. C4d deposition and clearance in cardiac transplants correlates with alloantibody levels and rejection in rats. *Am J Transplant* 2006;6(5 Pt 1):923–932.
558. Haas M, Rahman MH, Racusen LC, et al. C4d and C3d staining in biopsies of ABO- and HLA-incompatible renal allografts: correlation with histologic findings. *Am J Transplant* 2006;6(8):1829–1840.
559. Lawrence C, Willicombe M, Brookes PA, et al. Preformed complement-activating low-level donor-specific antibody predicts early antibody-mediated rejection in renal allografts. *Transplantation* 2013;95(2):341–346.
560. Liptak P, Kemeny E, Morvay Z, et al. Peritubular capillary damage in acute humoral rejection: an ultrastructural study on human renal allografts. *Am J Transplant* 2005;5(12):2870–2876.
561. Lajoie G. Antibody-mediated rejection of human renal allografts: an electron microscopic study of peritubular capillaries. *Ultrastruct Pathol* 1997;21(3):235–242.
562. Nickleit V, Mihatsch MJ. Kidney transplants, antibodies and rejection: is C4d a magic marker? *Nephrol Dial Transplant* 2003;18(11):2232–2239.
563. Thurman JM, Lucia MS, Ljubanovic D, et al. Acute tubular necrosis is characterized by activation of the alternative pathway of complement. *Kidney Int* 2005;67(2):524–530.
564. Artz MA, Steenbergen EJ, Hoitsma AJ, et al. Renal transplantation in patients with hemolytic uremic syndrome: high rate of recurrence and increased incidence of acute rejections. *Transplantation* 2003;76(5):821–826.

565. Lerut E, Kuypers D, Van Damme B. C4d deposition in the peritubular capillaries of native renal biopsies. *Histopathology* 2005;47(4):430–432.
566. Raftery MJ, Seron D, Koffman G, et al. The relevance of induced class II HLA antigens and macrophage infiltration in early renal allograft biopsies. *Transplantation* 1989;48(2):238–243.
567. Dragun D, Philippe A, Catar R. Role of non-HLA antibodies in organ transplantation. *Curr Opin Organ Transplant* 2012;17(4):440–445.
568. Rahimi S, Qian Z, Layton J, et al. Non-complement- and complement-activating antibodies synergize to cause rejection of cardiac allografts. *Am J Transplant* 2004;4(3):326–334.
569. Rother RP, Arp J, Jiang J, et al. C5 blockade with conventional immunosuppression induces long-term graft survival in presensitized recipients. *Am J Transplant* 2008;8(6):1129–1142.
570. Wang H, Arp J, Liu W, et al. Inhibition of terminal complement components in presensitized transplant recipients prevents antibody-mediated rejection leading to long-term graft survival and accommodation. *J Immunol* 2007;179(7):4451–4463.
571. Wahrman M, Bartel G, Exner M, et al. Clinical relevance of preformed C4d-fixing and non-C4d-fixing HLA single antigen reactivity in renal allograft recipients. *Transpl Int* 2009;22(10):982–989.
572. Stegall MD, Diwan T, Raghavaiah S, et al. Terminal complement inhibition decreases antibody-mediated rejection in sensitized renal transplant recipients. *Am J Transplant* 2011;11(11):2405–2413.
573. Stegall MD, Chedid MF, Cornell LD. The role of complement in antibody-mediated rejection in kidney transplantation. *Nat Rev Nephrol* 2012;8(11):670–678.
574. Noone D, Al-Matrafi J, Tinckam K, et al. Antibody mediated rejection associated with complement factor h-related protein 3/1 deficiency successfully treated with eculizumab. *Am J Transplant* 2012;12(9):2546–2553.
575. Wang R, Wang H, Chen J, et al. C4d deposition in allograft renal biopsies is an independent risk factor for graft failure. *Nephrology (Carlton)* 2009;14(5):527–532.
576. Lederer SR, Kluth-Pepper B, Schneeberger H, et al. Impact of humoral alloreactivity early after transplantation on the long-term survival of renal allografts. *Kidney Int* 2001;59(1):334–341.
577. Gloor JM, Winters JL, Cornell LD, et al. Baseline donor-specific antibody levels and outcomes in positive crossmatch kidney transplantation. *Am J Transplant* 2010;10(3):582–589.
578. Sutherland SM, Chen G, Sequeira FA, et al. Complement-fixing donor-specific antibodies identified by a novel C1q assay are associated with allograft loss. *Pediatr Transplant* 2012;16(1):12–17.
579. Yabu JM, Higgins JP, Chen G, et al. C1q-fixing human leukocyte antigen antibodies are specific for predicting transplant glomerulopathy and late graft failure after kidney transplantation. *Transplantation* 2011;91(3):342–347.
580. Roberts DM, Jiang SH, Chadban SJ. The treatment of acute antibody-mediated rejection in kidney transplant recipients—a systematic review. *Transplantation* 2012;94(8):775–783.
581. Pascual M, Saidman S, Tolkoff-Rubin N, et al. Plasma exchange and tacrolimus-mycophenolate rescue for acute humoral rejection in kidney transplantation. *Transplantation* 1998;66(11):1460–1464.
582. Vo AA, Lukovsky M, Toyoda M, et al. Rituximab and intravenous immune globulin for desensitization during renal transplantation. *N Engl J Med* 2008;359(3):242–251.
583. Jordan SC, Toyoda M, Kahwaji J, et al. Clinical aspects of intravenous immunoglobulin use in solid organ transplant recipients. *Am J Transplant* 2011;11(2):196–202.
584. Kaplan B, Jie T, Diana R, et al. Histopathology and immunophenotype of the spleen during acute antibody-mediated rejection. *Am J Transplant* 2010;10(5):1316–1320.
585. Bohmig GA, Wahrman M, Regele H, et al. Immunoabsorption in severe C4d-positive acute kidney allograft rejection: a randomized controlled trial. *Am J Transplant* 2007;7(1):117–121.
586. Wang H, Rollins SA, Gao Z, et al. Complement inhibition with an anti-C5 monoclonal antibody prevents hyperacute rejection in a xenograft heart transplantation model. *Transplantation* 1999;68(11):1643–1651.
587. Pfeiffer S, Zorn GL III, Blair KS, et al. Hyperacute lung rejection in the pig-to-human model 4: evidence for complement and antibody independent mechanisms. *Transplantation* 2005;79(6):662–671.
588. Pratt JR, Jones ME, Dong J, et al. Nontransgenic hyperexpression of a complement regulator in donor kidney modulates transplant ischemia/reperfusion damage, acute rejection, and chronic nephropathy. *Am J Pathol* 2003;163(4):1457–1465.
589. Gueler F, Rong S, Gwinner W, et al. Complement 5a receptor inhibition improves renal allograft survival. *J Am Soc Nephrol* 2008;19(12):2302–2312.
590. Schmidt N, Alloway RR, Walsh RC, et al. Prospective evaluation of the toxicity profile of proteasome inhibitor-based therapy in renal transplant candidates and recipients. *Transplantation* 2012;94(4):352–361.
591. Walsh RC, Everly JJ, Brailey P, et al. Proteasome inhibitor-based primary therapy for antibody-mediated renal allograft rejection. *Transplantation* 2010;89(3):277–284.
592. Bariety J, Oriol R, Hinglais N, et al. Distribution of blood group antigen A in normal and pathologic human kidneys. *Kidney Int* 1980;17(820):820–826.
593. Takahashi K, Saito K. ABO-incompatible kidney transplantation. *Transplant Rev (Orlando, Fla.)* 2013;27(1):1–8.
594. Fuchinoue S, Ishii Y, Sawada T, et al. The 5-year outcome of ABO-incompatible kidney transplantation with rituximab induction. *Transplantation* 2011;91(8):853–857.
595. Ichimaru N, Takahara S. Japan's experience with living-donor kidney transplantation across ABO barriers. *Nat Clin Pract Nephrol* 2008;4(12):682–692.
596. Montgomery JR, Berger JC, Warren DS, et al. Outcomes of ABO-incompatible kidney transplantation in the United States. *Transplantation* 2012;93(6):603–609.
597. Gloor JM, Cosio FG, Rea DJ, et al. Histologic findings one year after positive crossmatch or ABO blood group incompatible living donor kidney transplantation. *Am J Transplant* 2006;6(8):1841–1847.
598. Tobian AA, Shirey RS, Montgomery RA, et al. ABO antibody titer and risk of antibody-mediated rejection in ABO-incompatible renal transplantation. *Am J Transplant* 2010;10(5):1247–1253.
599. Alexandre GPJ, Squifflet JP, De Bruyere M, et al. Splenectomy a prerequisite for successful ABO-incompatible renal transplantation. *Transplant Proc* 1985;17:138–143.
600. Flint SM, Walker RG, Hogan C, et al. Successful ABO-incompatible kidney transplantation with antibody removal and standard immunosuppression. *Am J Transplant* 2011;11(5):1016–1024.
601. Biglarnia AR, Nilsson B, Nilsson Ekdahl K, et al. Desensitization with antigen-specific immunoabsorption interferes with complement in ABO-incompatible kidney transplantation. *Transplantation* 2012;93(1):87–92.
602. Genberg H, Kumlien G, Wennberg L, et al. The efficacy of antigen-specific immunoabsorption and rebound of anti-A/B antibodies in ABO-incompatible kidney transplantation. *Nephrol Dial Transplant* 2011;26(7):2394–2400.
603. Valli PV, Puga Yung G, Fehr T, et al. Changes of circulating antibody levels induced by ABO antibody adsorption for ABO-incompatible kidney transplantation. *Am J Transplant* 2009;9(5):1072–1080.
604. Fidler ME, Gloor JM, Lager DJ, et al. Histologic findings of antibody-mediated rejection in ABO blood-group-incompatible living-donor kidney transplantation. *Am J Transplant* 2004;4(1):101–107.
605. Setoguchi K, Ishida H, Shimmura H, et al. Analysis of renal transplant protocol biopsies in ABO-incompatible kidney transplantation. *Am J Transplant* 2008;8(1):86–94.
606. Abe M, Sawada T, Horita S, et al. C4d deposition in peritubular capillary and alloantibody in the allografted kidney suffering severe acute rejection. *Clin Transplant* 2003;17 Suppl 10:14–19.
607. Toki D, Ishida H, Setoguchi K, et al. Acute antibody-mediated rejection in living ABO-incompatible kidney transplantation: long-term impact and risk factors. *Am J Transplant* 2009;9(3):567–577.
608. Haas M, Segev DL, Racusen LC, et al. C4d deposition without rejection correlates with reduced early scarring in ABO-incompatible renal allografts. *J Am Soc Nephrol* 2009;20(1):197–204.
609. Einecke G, Sis B, Reeve J, et al. Antibody-mediated microcirculation injury is the major cause of late kidney transplant failure. *Am J Transplant* 2009;9(11):2520–2531.
610. Gaston RS, Cecka JM, Kasiske BL, et al. Evidence for antibody-mediated injury as a major determinant of late kidney allograft failure. *Transplantation* 2010;90(1):68–74.

611. Mauyyedi S, Pelle PD, Saidman S, et al. Chronic humoral rejection: identification of antibody-mediated chronic renal allograft rejection by C4d deposits in peritubular capillaries. *J Am Soc Nephrol* 2001;12(3):574–582.
612. Solez K, Colvin RB, Racusen LC, et al. Banff '05 Meeting Report: differential diagnosis of chronic allograft injury and elimination of chronic allograft nephropathy ('CAN'). *Am J Transplant* 2007;7(3):518–526.
613. Zollinger HU, Moppert J, Thiel G, et al. Morphology and pathogenesis of glomerulopathy in cadaver kidney allografts treated with antilymphocyte globulin. *Curr Top Pathol* 1973;57(1):1–48.
614. Freese PM, Svalander CT, Molne J, et al. Renal allograft glomerulopathy and the value of immunohistochemistry. *Clin Nephrol* 2004;62(4):279–286.
615. Hara S, Matsushita H, Yamaguchi Y, et al. Allograft glomerulitis: histologic characteristics to detect chronic humoral rejection. *Transplant Proc* 2005;37(2):714–716.
616. Colvin RB, Dvorak AM, Dvorak HF. Mast cells in the cortical tubular epithelium and interstitium in human renal disease. *Hum Pathol* 1974;5(3):315–326.
617. Roberts IS, Brenchley PE. Mast cells: the forgotten cells of renal fibrosis. *J Clin Pathol* 2000;53(11):858–862.
618. Kerjaschki D, Regele HM, Moosberger I, et al. Lymphatic neoangiogenesis in human kidney transplants is associated with immunologically active lymphocytic infiltrates. *J Am Soc Nephrol* 2004;15(3):603–612.
619. Pardo J, Diaz L, Errasti P, et al. Mast cells in chronic rejection of human renal allografts. *Virchows Arch* 2000;437(2):167–172.
620. Aita K, Yamaguchi Y, Horita S, et al. Thickening of the peritubular capillary basement membrane is a useful diagnostic marker of chronic rejection in renal allografts. *Am J Transplant* 2007;7(4):923–929.
621. Ivanyi B, Kemeny E, Rago P, et al. Peritubular capillary basement membrane changes in chronic renal allograft rejection: comparison of light microscopic and ultrastructural observations. *Virchows Arch* 2011;459(3):321–330.
622. Gibson IW, Gwinner W, Brocker V, et al. Peritubular capillaritis in renal allografts: prevalence, scoring system, reproducibility and clinicopathological correlates. *Am J Transplant* 2008;8(4):819–825.
623. Hidalgo LG, Sis B, Sellares J, et al. NK cell transcripts and NK cells in kidney biopsies from patients with donor-specific antibodies: evidence for NK cell involvement in antibody-mediated rejection. *Am J Transplant* 2010;10(8):1812–1822.
624. Ishii Y, Sawada T, Kubota K, et al. Injury and progressive loss of peritubular capillaries in the development of chronic allograft nephropathy. *Kidney Int* 2005;67(1):321–332.
625. Steegh FM, Gelens MA, Nieman FH, et al. Early loss of peritubular capillaries after kidney transplantation. *J Am Soc Nephrol* 2011;22(6):1024–1029.
626. Basile DP, Donohoe D, Roethe K, et al. Renal ischemic injury results in permanent damage to peritubular capillaries and influences long-term function. *Am J Physiol Renal Physiol* 2001;281(5):F887–F899.
627. Wells AE, Larsson E, Tengblad A, et al. The location of hyaluronan in normal and rejected human kidneys. *Transplantation* 1990;50:240–243.
628. Hill GS, Nochy D, Bruneval P, et al. Donor-specific antibodies accelerate arteriosclerosis after kidney transplantation. *J Am Soc Nephrol* 2011;22(5):975–983.
629. Gough J, Yilmaz A, Yilmaz S, et al. Recurrent and de novo glomerular immune-complex deposits in renal transplant biopsies. *Arch Pathol Lab Med* 2005;129(2):231–233.
630. Olsen S, Bohman SO, Petersen VP. Ultrastructure of the glomerular basement membrane in long term renal allografts with transplant glomerular disease. *Lab Invest* 1974;30(176):176–189.
631. Mauyyedi S, Pelle PD, Saidman S, et al. Chronic humoral rejection: identification of antibody-mediated chronic renal allograft rejection by C4d deposits in peritubular capillaries. *J Am Soc Nephrol* 2001;12(3):574–582.
632. Mroz A, Durlak M, Cieciora T, et al. C4d complement split product expression in chronic rejection of renal allograft. *Transplant Proc* 2003;35(6):2190–2192.
633. Vongwiwatana A, Gourishankar S, Campbell PM, et al. Peritubular capillary changes and C4d deposits are associated with transplant glomerulopathy but not IgA nephropathy. *Am J Transplant* 2004;4(1):124–129.
634. Sijpkens YW, Joosten SA, Wong MC, et al. Immunologic risk factors and glomerular C4d deposits in chronic transplant glomerulopathy. *Kidney Int* 2004;65(6):2409–2418.
635. Loupy A, Hill GS, Jordan SC. The impact of donor-specific anti-HLA antibodies on late kidney allograft failure. *Nat Rev Nephrol* 2012;8(6):348–357.
636. Reed EF, Demetris AJ, Hammond E, et al. Acute antibody-mediated rejection of cardiac transplants. *J Heart Lung Transplant* 2006;25(2):153–159.
637. Jindra PT, Hsueh A, Hong L, et al. Anti-MHC class I antibody activation of proliferation and survival signaling in murine cardiac allografts. *J Immunol* 2008;180(4):2214–2224.
638. Andres GA, Accinni L, Hsu KC, et al. Human renal transplants: III. Immunopathologic studies. *Lab Invest* 1970;22:588–595.
639. Hsu HC, Suzuki Y, Churg J, et al. Ultrastructure of transplant glomerulopathy. *Histopathology* 1980;4(4):351–367.
640. Habib R, Zurowska A, Hinglais N, et al. A specific glomerular lesion of the graft: allograft glomerulopathy. *Kidney Int Suppl* 1993;42:S104–S111.
641. Ivanyi B, Fahmy H, Brown H, et al. Peritubular capillaries in chronic renal allograft rejection: a quantitative ultrastructural study. *Hum Pathol* 2000;31(9):1129–1138.
642. Porter KA. Renal transplantation. In: Heptinstall RH, ed. *The Pathology of the Kidney*, 4th ed. Boston, MA: Little, Brown and Company; 1990:1799–1933.
643. Yamamoto I, Horita S, Takahashi T, et al. Glomerular expression of plasmalemmal vesicle-associated protein-1 in patients with transplant glomerulopathy. *Am J Transplant* 2007;7(8):1954–1960.
644. Haas M, Mirocha J. Early ultrastructural changes in renal allografts: correlation with antibody-mediated rejection and transplant glomerulopathy. *Am J Transplant* 2011;11(10):2123–2131.
645. Monga G, Mazzucco G, Messina M, et al. Intertubular capillary changes in kidney allografts: a morphologic investigation on 61 renal specimens. *Mod Pathol* 1992;5(2):125–130.
646. Mazzucco G, Motta M, Segoloni G, et al. Intertubular capillary changes in the cortex and medulla of transplanted kidneys and their relationship with transplant glomerulopathy: an ultrastructural study of 12 transplantectomies. *Ultrastruct Pathol* 1994;18(6):533–537.
647. Factor SM, Biempica L, Goldfischer S. Intralysosomal lipid in long-term maintenance transplant atherosclerosis. *Arch Pathol Lab Med* 1977;101:474–479.
648. Porter KA, Rendall JM, Stolinski C, et al. Light and electron microscopic study of biopsies from 33 human renal allografts and an isograft 1 3/4 to 2 1/2 years after transplantation. *Ann N Y Acad Sci* 1966;129:615–622.
649. Hidalgo LG, Sellares J, Sis B, et al. Interpreting NK cell transcripts versus T cell transcripts in renal transplant biopsies. *Am J Transplant* 2012;12(5):1180–1191.
650. Dean PG, Park WD, Cornell LD, et al. Intragraft gene expression in positive crossmatch kidney allografts: ongoing inflammation mediates chronic antibody-mediated injury. *Am J Transplant* 2012;12(6):1551–1563.
651. Sellares J, Reeve J, Loupy A, et al. Molecular diagnosis of antibody-mediated rejection in human kidney transplants. *Am J Transplant* 2013;13(4):971–983.
652. Nankivell BJ, Borrows RJ, Fung CL, et al. Evolution and pathophysiology of renal-transplant glomerulosclerosis. *Transplantation* 2004;78(3):461–468.
653. Akalin E, Dinavahi R, Dikman S, et al. Transplant glomerulopathy may occur in the absence of donor-specific antibody and C4d staining. *Clin J Am Soc Nephrol* 2007;2(6):1261–1267.
654. Willicombe M, Brookes P, Sergeant R, et al. De novo DQ donor-specific antibodies are associated with a significant risk of antibody-mediated rejection and transplant glomerulopathy. *Transplantation* 2012;94(2):172–177.
655. Kieran N, Wang X, Perkins J, et al. Combination of peritubular c4d and transplant glomerulopathy predicts late renal allograft failure. *J Am Soc Nephrol* 2009;20(10):2260–2268.
656. John R, Konvalinka A, Tobar A, et al. Determinants of long-term graft outcome in transplant glomerulopathy. *Transplantation* 2010;90(7):757–764.
657. Choi BS, Shin MJ, Shin SJ, et al. Clinical significance of an early protocol biopsy in living-donor renal transplantation: ten-year experience at a single center. *Am J Transplant* 2005;5(6):1354–1360.

658. Cosio FG, Grande JP, Wadei H, et al. Predicting subsequent decline in kidney allograft function from early surveillance biopsies. *Am J Transplant* 2005;5(10):2464–2472.
659. Yakupoglu U, Baranowska-Daca E, Rosen D, et al. Post-transplant nephrotic syndrome: a comprehensive clinicopathologic study. *Kidney Int* 2004;65(6):2360–2370.
660. Fernandez-Fresnedo G, Plaza JJ, Sanchez-Plumed J, et al. Proteinuria: a new marker of long-term graft and patient survival in kidney transplantation. *Nephrol Dial Transplant* 2004;19(Suppl 3):iii47–iii51.
661. Ramanathan V, Suki WN, Rosen D, et al. Chronic allograft nephropathy and nephrotic range proteinuria. *Clin Transplant* 2005;19(3):413–417.
662. Vathsala A, Verani R, Schoenberg L, et al. Proteinuria in cyclosporine-treated renal transplant recipients. *Transplantation* 1990;49(1):35–41.
663. Andresdottir MB, Assmann KJ, Koene RA, et al. Immunohistological and ultrastructural differences between recurrent type I membranoproliferative glomerulonephritis and chronic transplant glomerulopathy. *Am J Kidney Dis* 1998;32(4):582–588.
664. Russell PS, Chase CM, Madsen JC, et al. Coronary artery disease from isolated non-H2-determined incompatibilities in transplanted mouse hearts. *Transplantation* 2011;91(8):847–852.
665. Papadimitriou JC, Drachenberg CB, Ramos E, et al. Antibody-mediated allograft rejection: morphologic spectrum and serologic correlations in surveillance and for cause biopsies. *Transplantation* 2013;95(1):128–136.
666. Topilsky Y, Gandhi MJ, Hasin T, et al. Donor-specific antibodies to class II antigens are associated with accelerated cardiac allograft vasculopathy: a three-dimensional volumetric intravascular ultrasound study. *Transplantation* 2013;95(2):389–396.
667. Ticehurst EH, Molina MR, Frank R, et al. Antibody-mediated rejection in heart transplant patients: long-term follow up of patients with high levels of donor-directed anti-DQ antibodies. *Clin Transpl* 2011:409–414.
668. Isoniemi HM, Krogerus L, von Willebrand E, et al. Histopathological findings in well-functioning, long-term renal allografts. *Kidney Int* 1992;41(1):155–160.
669. Burke BA, Chavers BM, Gillingham KJ, et al. Chronic renal allograft rejection in the first 6 months posttransplant. *Transplantation* 1995;60(12):1413–1417.
670. Smith RN, Kawai T, Boskovic S, et al. Chronic antibody mediated rejection of renal allografts: pathological, serological and immunologic features in nonhuman primates. *Am J Transplant* 2006;6(8):1790–1798.
671. Seron D, Moreso F, Ramon JM, et al. Protocol renal allograft biopsies and the design of clinical trials aimed to prevent or treat chronic allograft nephropathy. *Transplantation* 2000;69(9):1849–1855.
672. de Kort H, Willicombe M, Brookes P, et al. Microcirculation inflammation associates with outcome in renal transplant patients with de novo donor-specific antibodies. *Am J Transplant* 2013;13(2):485–492.
673. Loupy A, Suberbielle-Boissel C, Hill GS, et al. Outcome of subclinical antibody-mediated rejection in kidney transplant recipients with preformed donor-specific antibodies. *Am J Transplant* 2009;9(11):2561–2570.
674. Dickenmann M, Steiger J, Descoedres B, et al. The fate of C4d positive kidney allografts lacking histological signs of acute rejection. *Clin Nephrol* 2006;65(3):173–179.
675. Mengel M, Bogers J, Bosmans JL, et al. Incidence of C4d stain in protocol biopsies from renal allografts: results from a multicenter trial. *Am J Transplant* 2005;5(5):1050–1056.
676. Smith RN, Kawai T, Boskovic S, et al. Four stages and lack of stable accommodation in chronic alloantibody-mediated renal allograft rejection in *Cynomolgus* monkeys. *Am J Transplant* 2008;8(8):1662–1672.
677. Bravou V, Galliford J, McLean A, et al. A case of chronic antibody-mediated rejection in the making. *Clin Nephrol* 2013;80:306–309.
678. Billing H, Rieger S, Ovens J, et al. Successful treatment of chronic antibody-mediated rejection with IVIG and rituximab in pediatric renal transplant recipients. *Transplantation* 2008;86(9):1214–1221.
679. Fehr T, Rusi B, Fischer A, et al. Rituximab and intravenous immunoglobulin treatment of chronic antibody-mediated kidney allograft rejection. *Transplantation* 2009;87(12):1837–1841.
680. Schwaiger E, Regele H, Wahrman M, et al. Bortezomib for the treatment of chronic antibody-mediated kidney allograft rejection: a case report. *Clin Transpl* 2010:391–396.
681. Cecka JM. *The OPTN/UNOS Renal Transplant Registry. Clinical Transplants 2003*. Los Angeles, CA: UCLA Immunogenetics Center, 2004:1–20.
682. Cornell LD, Colvin RB. Chronic allograft nephropathy. *Curr Opin Nephrol Hyperten* 2005;14(3):229–234.
683. Colvin RB. Chronic allograft nephropathy. *N Engl J Med* 2003;349(24):2288–2290.
684. Joosten SA, van Kooten C, Sijpkens YW, et al. The pathobiology of chronic allograft nephropathy: immune-mediated damage and accelerated aging. *Kidney Int* 2004;65(5):1556–1559.
685. Briganti EM, Russ GR, McNeil JJ, et al. Risk of renal allograft loss from recurrent glomerulonephritis. *N Engl J Med* 2002;347(2):103–109.
686. Moreso F, Ibernón M, Goma M, et al. Subclinical rejection associated with chronic allograft nephropathy in protocol biopsies as a risk factor for late graft loss. *Am J Transplant* 2006;6(4):747–752.
687. Sharma VK, Bologa RM, Xu GP, et al. Intra-graft TGF- β 1 mRNA: a correlate of interstitial fibrosis and chronic allograft nephropathy. *Kidney Int* 1996;49(5):1297–1303.
688. Kirk AD, Jacobson LM, Heisey DM, et al. Clinically stable human renal allografts contain histological and RNA-based findings that correlate with deteriorating graft function. *Transplantation* 1999;68(10):1578–1582.
689. Becker BN, Jacobson LM, Becker YT, et al. Renin-angiotensin system gene expression in post-transplant hypertension predicts allograft function. *Transplantation* 2000;69(7):1485–1491.
690. Scherer A, Krause A, Walker JR, et al. Early prognosis of the development of renal chronic allograft rejection by gene expression profiling of human protocol biopsies. *Transplantation* 2003;75(8):1323–1330.
691. Eikmans M, Sijpkens YW, Baelde HJ, et al. High transforming growth factor- β and extracellular matrix mRNA response in renal allografts during early acute rejection is associated with absence of chronic rejection. *Transplantation* 2002;73(4):573–579.
692. Mengel M, Reeve J, Bunnag S, et al. Molecular correlates of scarring in kidney transplants: the emergence of mast cell transcripts. *Am J Transplant* 2009;9(1):169–178.
693. Einecke G, Reeve J, Mengel M, et al. Expression of B cell and immunoglobulin transcripts is a feature of inflammation in late allografts. *Am J Transplant* 2008;8:1434–1443.
694. Einecke G, Reeve J, Sis B, et al. A molecular classifier for predicting future graft loss in late kidney transplant biopsies. *J Clin Invest* 2010;120(6):1862–1872.
695. Keven K, Sengul S. ABO-incompatible kidney transplantation: on-demand strategy. *Nephrol Dial Transplant* 2008;23(5):1773–1774; author reply 4.
696. Bunnag S, Einecke G, Reeve J, et al. Molecular correlates of renal function in kidney transplant biopsies. *J Am Soc Nephrol* 2009;20(5):1149–1160.
697. Ben-Dov IZ, Muthukumar T, Morozov P, et al. MicroRNA sequence profiles of human kidney allografts with or without tubulointerstitial fibrosis. *Transplantation* 2012;94(11):1086–1094.
698. Geyer M, Fischer KG, Drognitz O, et al. ABO-incompatible kidney transplantation with antigen-specific immunoadsorption and rituximab—insights and uncertainties. *Contrib Nephrol* 2009;162:47–60.
699. Kurian SM, Heilman R, Mondala TS, et al. Biomarkers for early and late stage chronic allograft nephropathy by proteogenomic profiling of peripheral blood. *PLoS ONE* 2009;4(7):e6212.
700. Nakorchevsky A, Hewel JA, Kurian SM, et al. Molecular mechanisms of chronic kidney transplant rejection via large-scale proteogenomic analysis of tissue biopsies. *J Am Soc Nephrol* 2010;21(2):362–373.
701. Furness PN, Taub N, Assmann KJ, et al. International variation in histologic grading is large, and persistent feedback does not improve reproducibility. *Am J Surg Pathol* 2003;27(6):805–810.
702. Gough J, Rush D, Jeffery J, et al. Reproducibility of the Banff schema in reporting protocol biopsies of stable renal allografts. *Nephrol Dial Transplant* 2002;17(6):1081–1084.
703. Seron D, Moreso F, Fulladosa X, et al. Reliability of chronic allograft nephropathy diagnosis in sequential protocol biopsies. *Kidney Int* 2002;61(2):727–733.
704. Farris AB, Colvin RB. Renal interstitial fibrosis: mechanisms and evaluation. *Curr Opin Nephrol Hyperten* 2012;21(3):289–300.
705. Farris AB, Adams CD, Brousaides N, et al. Morphometric and visual evaluation of fibrosis in renal biopsies. *J Am Soc Nephrol* 2011;22(1):176–186.

706. Nicholson ML, McCulloch TA, Harper SJ, et al. Early measurement of interstitial fibrosis predicts long-term renal function and graft survival in renal transplantation. *Br J Surg* 1996;83(8):1082–1085.
707. Young EW, Ellis CN, Messana JM, et al. A prospective study of renal structure and function in psoriasis patients treated with cyclosporin. *Kidney Int* 1994;46(4):1216–1222.
708. Grimm PC, Nickerson P, Gough J, et al. Computerized image analysis of Sirius Red-stained renal allograft biopsies as a surrogate marker to predict long-term allograft function. *J Am Soc Nephrol* 2003;14(6):1662–1668.
709. Pape L, Henne T, Offner G, et al. Computer-assisted quantification of fibrosis in chronic allograft nephropathy by picosirius red-staining: a new tool for predicting long-term graft function. *Transplantation* 2003;76(6):955–958.
710. Masseroli M, O'Valle F, Andujar M, et al. Design and validation of a new image analysis method for automatic quantification of interstitial fibrosis and glomerular morphometry. *Lab Invest* 1998;78(5):511–522.
711. Ellingsen AR, Nyengaard JR, Osterby R, et al. Measurements of cortical interstitium in biopsies from human kidney grafts: how representative and how reproducible? *Nephrol Dial Transplant* 2002;17(5):788–792.
712. Sund S, Grimm P, Reisaeter AV, et al. Computerized image analysis vs semiquantitative scoring in evaluation of kidney allograft fibrosis and prognosis. *Nephrol Dial Transplant* 2004;19(11):2838–2845.
713. Yilmaz S, Tomlanovich S, Mathew T, et al. Protocol core needle biopsy and histologic chronic allograft damage index (CADI) as surrogate end point for long-term graft survival in multicenter studies. *J Am Soc Nephrol* 2003;14(3):773–779.
714. Dimeny E, Wahlberg J, Larsson E, et al. Can histopathological findings in early renal allograft biopsies identify patients at risk for chronic vascular rejection? *Clin Transplant* 1995;9(2):79–84.
715. Colvin RB. CADI, Canti, Cavi. *Transplantation* 2007;83(6):677–678.
716. Wilkinson A. Protocol transplant biopsies: are they really needed? *Clin J Am Soc Nephrol* 2006;1:130–137.
717. Rush D. Protocol transplant biopsies: an underutilized tool in kidney transplantation. *Clin J Am Soc Nephrol* 2006;1:138–143.
718. Racusen L. Protocol transplant biopsies in kidney allografts: why and when are they indicated? *Clin J Am Soc Nephrol* 2006;1:144–147.
719. Mengel M, Gwinner W, Schwarz A, et al. Infiltrates in protocol biopsies from renal allografts. *Am J Transplant* 2007;7(2):356–365.
720. Rush DN, Jeffery JR, Gough J. Sequential protocol biopsies in renal transplant patients. Clinico-pathological correlations using the Banff schema. *Transplantation* 1995;59(4):511–514.
721. Shapiro R, Randhawa P, Jordan ML, et al. An analysis of early renal transplant protocol biopsies—the high incidence of subclinical tubulitis. *Am J Transplant* 2001;1(1):47–50.
722. Jain S, Curwood V, White SA, et al. Sub-clinical acute rejection detected using protocol biopsies in patients with delayed graft function. *Transpl Int* 2000;13 Suppl 1:S52–S55.
723. Roberts IS, Reddy S, Russell C, et al. Subclinical rejection and borderline changes in early protocol biopsy specimens after renal transplantation. *Transplantation* 2004;77(8):1194–1198.
724. Schwarz A, Mengel M, Gwinner W, et al. Risk factors for chronic allograft nephropathy after renal transplantation: a protocol biopsy study. *Kidney Int* 2005;67(1):341–348.
725. Rush D, Nickerson P, Gough J, et al. Beneficial effects of treatment of early subclinical rejection: a randomized study. *J Am Soc Nephrol* 1998;9(11):2129–2134.
726. Nankivell BJ, Borrows RJ, Fung CL, et al. The natural history of chronic allograft nephropathy. *N Engl J Med* 2003;349(24):2326–2333.
727. Jain S, Curwood V, Kazi J, et al. Acute rejection in protocol renal transplant biopsies—institutional variations. *Transplant Proc* 2000;32(3):616.
728. Nankivell BJ, Fenton-Lee CA, Kuypers DR, et al. Effect of histological damage on long-term kidney transplant outcome. *Transplantation* 2001;71(4):515–523.
729. Serón D, Moreso F, Bover J, et al. Early protocol renal allograft biopsies and graft outcome. *Kidney Int* 1997;51(1):310–316.
730. Solez K, Vincenti F, Filo RS. Histopathologic findings from 2-year protocol biopsies from a U.S. multicenter kidney transplant trial comparing tacrolimus versus cyclosporine: a report of the FK506 Kidney Transplant Study Group. *Transplantation* 1998;66(12):1736–1740.
731. Rush D, Arlen D, Boucher A, et al. Lack of benefit of early protocol biopsies in renal transplant patients receiving TAC and MMF: a randomized study. *Am J Transplant* 2007;7(11):2538–2545.
732. Kooijmans-Coutinho MF, Bruijn JA, Hermans J, et al. Evaluation by histology, immunohistology and PCR of protocolized renal biopsies 1 week post-transplant in relation to subsequent rejection episodes. *Nephrol Dial Transplant* 1995;10(6):847–854.
733. Park WD, Griffin MD, Cornell LD, et al. Fibrosis with inflammation at one year predicts transplant functional decline. *J Am Soc Nephrol* 2010;21(11):1987–1997.
734. Cosio FG, Grande JP, Wadei H, et al. Predicting subsequent decline in kidney allograft function from early surveillance biopsies. *Am J Transplant* 2005;5(10):2464–2472.
735. Stegall MD, Park WD, Larson TS, et al. The histology of solitary renal allografts at 1 and 5 years after transplantation. *Am J Transplant* 2011;11(4):698–707.
736. Rush DN, Henry SF, Jeffery JR, et al. Histological findings in early routine biopsies of stable renal allograft recipients. *Transplantation* 1994;57(2):208–211.
737. Haas M, Montgomery RA, Segev DL, et al. Subclinical acute antibody-mediated rejection in positive crossmatch renal allografts. *Am J Transplant* 2007;7:576–585.
738. Buehrig CK, Lager DJ, Stegall MD, et al. Influence of surveillance renal allograft biopsy on diagnosis and prognosis of polyomavirus-associated nephropathy. *Kidney Int* 2003;64(2):665–673.
739. Nankivell BJ, Borrows RJ, Fung CL, et al. Calcineurin inhibitor nephrotoxicity: longitudinal assessment by protocol histology. *Transplantation* 2004;78(4):557–565.
740. Gwinner W, Suppa S, Mengel M, et al. Early calcification of renal allografts detected by protocol biopsies: causes and clinical implications. *Am J Transplant* 2005;5(8):1934–1941.
741. Pinheiro HS, Camara NO, Osaki KS, et al. Early presence of calcium oxalate deposition in kidney graft biopsies is associated with poor long-term graft survival. *Am J Transplant* 2005;5(2):323–329.
742. Lachenbruch PA, Rosenberg AS, Bonvini E, et al. Biomarkers and surrogate endpoints in renal transplantation: present status and considerations for clinical trial design. *Am J Transplant* 2004;4:451–457.
743. Lachenbruch PA, Rosenberg AS, Bonvini E, et al. Biomarkers and surrogate endpoints in renal transplantation: present status and considerations for clinical trial design. *Am J Transplant* 2004;4(4):451–457.
744. Nicholson ML, Bailey E, Williams S, et al. Computerized histomorphometric assessment of protocol renal transplant biopsy specimens for surrogate markers of chronic rejection. *Transplantation* 1999;68(2):236–241.
745. Laftavi MR, Stephan R, Stefanick B, et al. Randomized prospective trial of early steroid withdrawal compared with low-dose steroids in renal transplant recipients using serial protocol biopsies to assess efficacy and safety. *Surgery* 2005;137(3):364–371.
746. Cosio FG, Amer H, Grande JP, et al. Comparison of low versus high tacrolimus levels in kidney transplantation: assessment of efficacy by protocol biopsies. *Transplantation* 2007;83(4):411–416.
747. Wilczek H. Percutaneous needle biopsy of the renal allograft. A clinical safety evaluation of 1129 biopsies. *Transplantation* 1990;50:790–797.
748. Lipman ML, Shen Y, Jeffery JR, et al. Immune-activation gene expression in clinically stable renal allograft biopsies: molecular evidence for subclinical rejection. *Transplantation* 1998;66(12):1673–1681.
749. Aquino Dias EC, Veronese FJ, Santos Goncalves LF, et al. Molecular markers in subclinical acute rejection of renal transplants. *Clin Transplant* 2004;18(3):281–287.
750. Oettl T, Halter J, Bachmann A, et al. ABO blood group-incompatible living donor kidney transplantation: a prospective, single-centre analysis including serial protocol biopsies. *Nephrol Dial Transplant* 2009;24(1):298–303.
751. Wahrman M, Schiemann M, Marinova L, et al. Anti-A/B antibody depletion by semiselective versus ABO blood group-specific immunoadsorption. *Nephrol Dial Transplant* 2012;27(5):2122–2129.
752. Midtvedt K, Hartmann A, Sund S. Can a diagnosis of renal allograft rejection be based on histology alone? *Clin Transplant* 1998;12(4):300–302.
753. Shimizu A, Yamada K, Meehan SM, et al. Acceptance reaction: intragraft events associated with tolerance to renal allografts in miniature swine. *J Am Soc Nephrol* 2000;11(12):2371–2380.

754. Russell PS, Chase CM, Colvin RB, et al. Kidney transplants in mice. An analysis of the immune status of mice bearing long-term, H-2 incompatible transplants. *J Exp Med* 1978;147(5):1449–1468.
755. Blancho G, Gianello PR, Lorf T, et al. Molecular and cellular events implicated in local tolerance to kidney allografts in miniature swine. *Transplantation* 1997;63:26–33.
756. Bugeon L, Cuturi MC, Paineau J, et al. Similar levels of granzyme A and perforin mRNA expression in rejected tolerated heart allografts in donor-specific tolerance in rats. *Transplantation* 1993;56(2):405–408.
757. Delikouras A, Hayes M, Malde P, et al. Nitric oxide-mediated expression of Bcl-2 and Bcl-xl and protection from tumor necrosis factor- α -mediated apoptosis in porcine endothelial cells after exposure to low concentrations of xenoreactive natural antibody. *Transplantation* 2001;71(5):599–605.
758. Magee JC, Collins BH, Harland RC, et al. Immuglobulin prevents complement-mediated hyperacute rejection in swine-to-primate xenotransplantation. *J Clin Invest* 1995;96(5):2404–2412.
759. Williams JM, Holzkecht ZE, Plummer TB, et al. Acute vascular rejection and accommodation: divergent outcomes of the humoral response to organ transplantation. *Transplantation* 2004;78(10):1471–1478.
760. Cornell LD, Della Pelle P, Brousiadias N, et al. Endothelial response to rejection: enhanced expression of complement regulatory proteins decay accelerating factor (DAF, CD55) and protectin (CD59) in human renal allografts. *Mod Pathol* 2004;17(Suppl 1):285A.
761. Park WD, Grande JP, Ninova D, et al. Accommodation in ABO-incompatible kidney allografts, a novel mechanism of self-protection against antibody-mediated injury. *Am J Transplant* 2003;3(8):952–960.
762. Sinclair R. Origin of endothelium in human renal allografts. *Br Med J* 1972;4:15–17.
763. Sedmak D, Sharma H, Czajka C, et al. Recipient endothelialization of renal allografts. An immunohistochemical study utilizing blood group antigens. *Transplantation* 1988;46:907–910.
764. Randhawa PS, Starzl T, Ramos HC, et al. Allografts surviving for 26 to 29 years following living-related kidney transplantation: analysis by light microscopy, in situ hybridization for the Y chromosome, and anti-HLA antibodies. *Am J Kidney Dis* 1994;24(1):72–77.
765. Lagaij EL, Cramer-Knijnenburg GF, van Kemenade FJ, et al. Endothelial cell chimerism after renal transplantation and vascular rejection. *Lancet* 2001;357(9249):33–37.
766. Mengel M, Jonigk D, Marwedel M, et al. Tubular chimerism occurs regularly in renal allografts and is not correlated to outcome. *J Am Soc Nephrol* 2004;15(4):978–986.
767. Kerjaschki D, Huttary N, Raab I, et al. Lymphatic endothelial progenitor cells contribute to de novo lymphangiogenesis in human renal transplants. *Nat Med* 2006;12(2):230–234.
768. Strober S, Benike C, Krishnaswamy S, et al. Clinical transplantation tolerance twelve years after prospective withdrawal of immunosuppressive drugs: studies of chimerism and anti-donor reactivity. *Transplantation* 2000;69(8):1549–1554.
769. Gajewski JL, Ippoliti C, Ma Y, et al. Discontinuation of immunosuppression for prevention of kidney graft rejection after receiving a bone marrow transplant from the same HLA identical sibling donor. *Am J Hematol* 2002;71(4):311–313.
770. Kawai T, Sachs DH, Spitzer TR, et al. Combined kidney and bone marrow transplantation for induction of mixed chimerism and renal allograft tolerance in HLA mismatched transplantation. *Am J Transplant* 2004;4(Suppl 8):491.
771. Buhler LH, Spitzer TR, Sykes M, et al. Induction of kidney allograft tolerance after transient lymphohematopoietic chimerism in patients with multiple myeloma and end-stage renal disease. *Transplantation* 2002;74(10):1405–1409.
772. Domenig C, Sanchez-Fueyo A, Kurtz J, et al. Roles of deletion and regulation in creating mixed chimerism and allograft tolerance using a non-lymphoablative irradiation-free protocol. *J Immunol* 2005;175(1):51–60.
773. Sykes M, Shimizu I, Kawahara T. Mixed hematopoietic chimerism for the simultaneous induction of T and B cell tolerance. *Transplantation* 2005;79(3 Suppl):S28–S29.
774. Sellers MT, Deierhoi MH, Curtis JJ, et al. Tolerance in renal transplantation after allogeneic bone marrow transplantation—6-year follow-up. *Transplantation* 2001;71(11):1681–1683.
775. Kawai T, Sachs DH, Sprangers B, et al. Long term results in recipients of combined HLA mismatched kidney and bone marrow transplantation without maintenance immunosuppression. *Am J Transplant* 2014;14 (in press).
776. Yamada Y, Boskovic S, Aoyama A, et al. Overcoming memory T-cell responses for induction of delayed tolerance in nonhuman primates. *Am J Transplant* 2012;12(2):330–340.
777. Brouard S, Mansfield E, Braud C, et al. Identification of a peripheral blood transcriptional biomarker panel associated with operational renal allograft tolerance. *Proc Natl Acad Sci USA* 2007;104(39):15448–15453.
778. Bakr MA, Abbas TM, Mustafa A, et al. Hemolytic anemia after ABO nonidentical living donor kidney transplantation. *Clin Exp Nephrol* 2009;13(2):161–165.
779. Miura M, Fujita H, Suzuki A, et al. A case of progressive thrombotic microangiopathy after ABO-incompatible renal transplantation. *Clin Transplant* 2011;25 (Suppl 23):19–22.
780. Renkens JJ, Rouffart MM, Christiaans MH, et al. Outcome of nonheart-beating donor kidneys with prolonged delayed graft function after transplantation. *Am J Transplant* 2005;5(11):2704–2709.
781. Rudich SM, Kaplan B, Magee JC, et al. Renal transplantations performed using non-heart-beating organ donors: going back to the future? *Transplantation* 2002;74(12):1715–1720.
782. Sanchez-Fructuoso A, Prats Sanchez D, Marques Vidas M, et al. Non-heart beating donors. *Nephrol Dial Transplant* 2004;19(Suppl 3):iii26–iii31.
783. Nicholson ML, Metcalfe MS, White SA, et al. A comparison of the results of renal transplantation from non-heart-beating, conventional cadaveric, and living donors. *Kidney Int* 2000;58(6):2585–2591.
784. Smith KD, Wrenshall LE, Nicosia RF, et al. Delayed graft function and cast nephropathy associated with tacrolimus plus rapamycin use. *J Am Soc Nephrol* 2003;14(4):1037–1045.
785. Perico N, Cattaneo D, Sayegh MH, et al. Delayed graft function in kidney transplantation. *Lancet* 2004;364(9447):1814–1827.
786. Halloran PF, Hunsicker LG. Delayed graft function: state of the art, November 10–11, 2000. Summit meeting, Scottsdale, Arizona, USA. *Am J Transplant* 2001;1(2):115–120.
787. Solez K, Morel-Maroger L, Sraer JD. The morphology of “acute tubular necrosis” in man: analysis of 57 renal biopsies and a comparison with the glycerol model. *Medicine* 1979;58(5):362–376.
788. Hirt-Minkowski P, Amico P, Honger G, et al. Delayed graft function is not associated with an increased incidence of renal allograft rejection. *Clin Transplant* 2012;26(6):E624–E633.
789. Friedewald JJ, Rabb H. Inflammatory cells in ischemic acute renal failure. *Kidney Int* 2004;66(2):486–491.
790. de Vries B, Walter SJ, Peutz-Kootstra CJ, et al. The mannose-binding lectin-pathway is involved in complement activation in the course of renal ischemia-reperfusion injury. *Am J Pathol* 2004;165(5):1677–1688.
791. Nádasy T, Laszik Z, Blick KE, et al. Human acute tubular necrosis: a lectin and immunohistochemical study. *Hum Pathol* 1995;26(2):230–239.
792. Rohr MS. Renal allograft acute tubular necrosis. II. A light and electron microscopic study of biopsies taken at procurement and after revascularization. *Ann Surg* 1983;197(6):663–671.
793. Berry M, Clatworthy MR. Immunotherapy for acute kidney injury. *Immunotherapy* 2012;4(3):323–334.
794. Einecke G, Kayser D, Vanslambrouck JM, et al. Loss of solute carriers in T cell-mediated rejection in mouse and human kidneys: an active epithelial injury-repair response. *Am J Transplant* 2010;10(10):2241–2251.
795. Zhang PL, Rothblum LI, Han WK, et al. Kidney injury molecule-1 expression in transplant biopsies is a sensitive measure of cell injury. *Kidney Int* 2008;73(5):608–614.
796. Schroppel B, Kruger B, Walsh L, et al. Tubular expression of KIM-1 does not predict delayed function after transplantation. *J Am Soc Nephrol* 2010;21(3):536–542.
797. Troppmann C, Gillingham KJ, Benedetti E, et al. Delayed graft function, acute rejection, and outcome after cadaver renal transplantation. The multivariate analysis. *Transplantation* 1995;59(7):962–968.
798. Howard RJ, Pfaff WW, Brunson ME, et al. Increased incidence of rejection in patients with delayed graft function. *Clin Transplant* 1994;8(6):527–531.
799. Merion RM, White DJ, Thiru S, et al. Cyclosporine: five years’ experience in cadaveric renal transplantation. *N Engl J Med* 1984;310(3):148–154.

800. Borel JF, Kis ZL. The discovery and development of cyclosporine (Sandimmune). *Transplant Proc* 1991;23(2):1867–1874.
801. Borel JF, Feurer C, Gubler HU, et al. Biological effects of cyclosporin A: a new antilymphocytic agent. *Agents Actions* 1976;6:468–476.
802. Calne RY, White DJ, Thiru S, et al. Cyclosporin A in patients receiving renal allografts from cadaver donors. *Lancet* 1978;2(8104–8105):1323–1327.
803. Powles RL, Barrett AJ, Clink H, et al. Cyclosporin A for the treatment of graft versus host disease in man. *Lancet* 1978;2(1327):1327–1331.
804. Atkinson K, Biggs JC, Hayes J, et al. Cyclosporin A associated nephrotoxicity in the first 100 days after allogeneic bone marrow transplantation: three distinct syndromes. *Br J Haematol* 1983;54(1):59–67.
805. Pascual J, Marcen R, Burgos FJ, et al. Spanish experience with cyclosporine. *Transplant Proc* 2004;36(2 Suppl):117S–119S.
806. Webster AC, Woodroffe RC, Taylor RS, et al. Tacrolimus versus ciclosporin as primary immunosuppression for kidney transplant recipients: meta-analysis and meta-regression of randomised trial data. *BMJ* 2005;331(7520):810.
807. Kramer BK, Montagnino G, Del Castillo D, et al. Efficacy and safety of tacrolimus compared with cyclosporin A microemulsion in renal transplantation: 2 year follow-up results. *Nephrol Dial Transplant* 2005;20(5):968–973.
808. Mihatsch MJ, Kyo M, Morozumi K, et al. The side-effects of ciclosporine-A and tacrolimus. *Clin Nephrol* 1998;49(6):356–363.
809. Randhawa PS, Tsamandas AC, Magnone M, et al. Microvascular changes in renal allografts associated with FK506 (Tacrolimus) therapy. *Am J Surg Pathol* 1996;20(3):306–312.
810. Stratta P, Canavese C, Quaglia M, et al. Posttransplantation chronic renal damage in nonrenal transplant recipients. *Kidney Int* 2005;68(4):1453–1463.
811. Mihatsch MJ, Thiel G, Spichtin HP, et al. Morphological findings in kidney transplants after treatment with cyclosporine. *Transplant Proc* 1983;15 (Suppl 1):2821–2835.
812. Mihatsch MJ, Ryffel B, Gudat F. The differential diagnosis between rejection and cyclosporine toxicity. *Kidney Int Suppl* 1995;52:S63–S69.
813. Mihatsch MJ, Morozumi K, Strom EH, et al. Renal transplant morphology after long-term therapy with cyclosporine. *Transplant Proc* 1995;27(1):39–42.
814. Mihatsch MJ, Gudat F, Ryffel B, et al. Cyclosporine nephropathy. In: Tisher CC, Brenner BM, eds. *Renal Pathology—with Clinical and Functional Correlations*, 2nd ed. Philadelphia, PA: J.B. Lippincott, 1994:1641–1681.
815. Katari SR, Magnone M, Shapiro R, et al. Tacrolimus nephrotoxicity after renal transplantation. *Transplant Proc* 1997;29(1–2):311.
816. Takeda A, Morozumi K, Uchida K, et al. Is cyclosporine-associated glomerulopathy a new glomerular lesion in renal allografts using CyA? *Transplant Proc* 1993;25(1 Pt 1):515–517.
817. Meehan SM, Pascual M, Williams WW, et al. De novo collapsing glomerulopathy in renal allografts. *Transplantation* 1998;65(9):1192–1197.
818. Mihatsch M, Thiel G, Ryffel B. Cyclosporine nephrotoxicity. *Adv Nephrol* 1988;17:303–320.
819. Kyo M, Gudat F, Dalquen P, et al. Differential diagnosis of kidney transplant rejection and cyclosporine nephrotoxicity by urine cytology. *Transplant Proc* 1992;24(4):1388–1390.
820. Kyo M, Toki K, Nishimura K, et al. Differential diagnosis of kidney transplant rejection and cyclosporin/tacrolimus nephropathy using urine cytology. *Clin Transplant* 2002;16 Suppl 8:40–44.
821. Solez K, Racusen LC, Marcussen N, et al. Morphology of ischemic acute renal failure, normal function, and cyclosporine toxicity in cyclosporine-treated renal allograft recipients. *Kidney Int* 1993;43(5):1058–1067.
822. Messana JM, Johnson KJ, Mihatsch MJ. Renal structure and function effects after low dose cyclosporine in psoriasis patients: a preliminary report. *Clin Nephrol* 1995;43(3):150–153.
823. Lewis RM, Verani RR, Vo C, et al. Evaluation of chronic renal disease in heart transplant recipients: importance of pretransplantation native kidney histologic evaluation. *J Heart Lung Transplant* 1994;13(3):376–380.
824. Yamaguchi Y, Teraoka S, Yagisawa T, et al. Ultrastructural study of cyclosporine-associated arteriopathy in renal allografts. *Transplant Proc* 1989;21(1 Pt 2):1517–1522.
825. Bergstrand A, Bohmann SO, Farnsworth A, et al. Renal histopathology in kidney transplant recipients immunosuppressed with cyclosporin A: results of an international workshop. *Clin Nephrol* 1985;24(3):107–119.
826. Strom EH, Epper R, Mihatsch MJ. Ciclosporin-associated arteriopathy: the renin producing vascular smooth muscle cells are more sensitive to ciclosporin toxicity. *Clin Nephrol* 1995;43(4):226–231.
827. Snanoudj R, Royal V, Elie C, et al. Specificity of histological markers of long-term CNI nephrotoxicity in kidney-transplant recipients under low-dose cyclosporine therapy. *Am J Transplant* 2011;11(12):2635–2646.
828. Brocker V, Schubert V, Scheffner I, et al. Arteriolar lesions in renal transplant biopsies: prevalence, progression, and clinical significance. *Am J Pathol* 2012;180(5):1852–1862.
829. Pei Y, Scholey JW, Katz A, et al. Chronic nephrotoxicity in psoriatic patients treated with low-dose cyclosporine. *Am J Kidney Dis* 1994;23(4):528–536.
830. Strom EH, Thiel G, Mihatsch MJ. Prevalence of cyclosporine-associated arteriopathy in renal transplant biopsies from 1981 to 1992. *Transplant Proc* 1994;26(5):2585–2587.
831. Rossmann P, Jirka J, Chadimova M, et al. Arteriosclerosis of the human renal allograft: morphology, origin, life history and relationship to cyclosporine therapy. *Virchows Arch A Pathol Anat Histopathol* 1991;418:129–141.
832. Fischer G, Wittmann-Liebold B, Lang K, et al. Cyclophilin and peptidyl-prolyl cis-trans isomerase are probably identical proteins. *Nature* 1989;337(6206):476–478.
833. Takahashi N, Hayano T, Suzuki M. Peptidyl-prolyl cis-trans isomerase is the cyclosporin A-binding protein cyclophilin. *Nature* 1989;337(6206):473–475.
834. Borel JF, Baumann G, Chapman I, et al. In vivo pharmacological effects of ciclosporin and some analogues. *Adv Pharmacol* 1996;35:115–246.
835. Kapturczak MH, Meier-Kriesche HU, Kaplan B. Pharmacology of calcineurin antagonists. *Transplant Proc* 2004;36(2 Suppl):25S–32S.
836. Wiederrecht G, Hung S, Chan HK, et al. Characterization of high molecular weight FK-506 binding activities reveals a novel FK-506-binding protein as well as a protein complex. *J Biol Chem* 1992;267(30):21753–21760.
837. Maki N, Sekiguchi F, Nishimaki J, et al. Complementary DNA encoding the human T-cell FK506-binding protein, a peptidylprolyl cis-trans isomerase distinct from cyclophilin. *Proc Natl Acad Sci U S A* 1990;87(14):5440–5443.
838. Liu J, Farmer JDJ, Lane WS, et al. Calcineurin is a common target of cyclophilin-cyclosporin A and FKBP-FK506 complexes. *Cell* 1991;66:807–815.
839. Sigal NH, Dumont F, Durette P, et al. Is cyclophilin involved in the immunosuppressive and nephrotic mechanism of action of cyclosporin A? *J Exp Med* 1991;173(3):619–628.
840. Lo A, Burckart GJ. P-glycoprotein and drug therapy in organ transplantation. *J Clin Pharmacol* 1999;39(10):995–1005.
841. Min SI, Kim SY, Ahn SH, et al. CYP3A5*1 allele: impacts on early acute rejection and graft function in tacrolimus-based renal transplant recipients. *Transplantation* 2010;90:1394.
842. Lemahieu W, Maes B, Verbeke K, et al. Cytochrome P450 3A4 and P-glycoprotein activity and assimilation of tacrolimus in transplant patients with persistent diarrhea. *Am J Transplant* 2005;5(6):1383–1391.
843. Auch-Schwelk W, Bossaller C, Gotze S, et al. Endothelial and vascular smooth muscle function after chronic treatment with cyclosporin A. *J Cardiovasc Pharmacol* 1993;21(3):435–440.
844. Bokemeyer D, Friedrichs U, Backer A, et al. Atrial natriuretic peptide inhibits cyclosporin A-induced endothelin production and calcium accumulation in rat vascular smooth muscle cells. *Clin Sci* 1994;87(4):383–387.
845. Gotze S, Auch-Schwelk W, Bossaller C, et al. Calcium entry blockade may prevent cyclosporin A-induced hypersensitivity to angiotensin II and endothelial dysfunction in the rat aorta. *Eur Heart J* 1993;14(Suppl I):104–110.
846. Bunchman TE, Brookshire CA. Cyclosporine-induced synthesis of endothelin by cultured human endothelial cells. *J Clin Invest* 1991;88(1):310–314.
847. Leszczynski D, Zhao Y, Yeagley TJ, et al. Direct and endothelial cell-mediated effect of cyclosporin A on the proliferation of rat smooth muscle cells in vitro. *Am J Pathol* 1993;142(1):149–155.
848. Haug C, Duell T, Voisard R, et al. Cyclosporine A stimulates endothelin release. *J Cardiovasc Pharmacol* 1995;26(Suppl 3):S239–S241.

849. Takeda Y, Itoh Y, Yoneda T, et al. Cyclosporine A induces endothelin-1 release from cultured rat vascular smooth muscle cells. *Eur J Pharmacol* 1993;233(2-3):299-301.
850. Abassi ZA, Pieruzzi F, Nakhoul F, et al. Effects of cyclosporin A on the synthesis, excretion and metabolism of endothelin in the rat. *Hypertension* 1996;27:1140-1148.
851. Lanese DM, Conger JD. Effects of endothelin receptor antagonist on cyclosporine-induced vasoconstriction in isolated rat renal arterioles. *J Clin Invest* 1993;91(5):2144-2149.
852. Fogo A, Hellings EE, Inagami T, et al. Endothelin receptor antagonism is protective in *in vivo* acute cyclosporine toxicity. *Kidney Int* 1990;42:770-781.
853. Kon V, Hunley TE, Fogo A. Combined antagonism of endothelin A/B receptors links endothelin to vasoconstriction whereas angiotensin II affects fibrosis. Studies in chronic cyclosporine nephrotoxicity in rats. *Transplantation* 1995;60(1):89-95.
854. Fasel J, Kaissling B, Ludwig KS, et al. Light and electron microscopic changes in the kidney of Wistar rats following treatment with cyclosporine A. *Ultrastruct Pathol* 1987;11(4):435-448.
855. Young BA, Burdmann EA, Johnson RJ, et al. Cyclosporine A induced arteriopathy in a rat model of chronic cyclosporine nephropathy. *Kidney Int* 1995;48(2):431-438.
856. Franceschini N, Alpers CE, Bennett WM, et al. Cyclosporine arteriopathy: effects of drug withdrawal. *Am J Kidney Dis* 1998;32(2):247-253.
857. Pichler RH, Franceschini N, Young BA, et al. Pathogenesis of cyclosporine nephropathy: roles of angiotensin II and osteopontin. *J Am Soc Nephrol* 1995;6(4):1186-1196.
858. Neild GH, Rocchi G, Imberti L, et al. Effect of Cyclosporin A on prostacyclin synthesis by vascular tissue. *Thromb Res* 1983;32(4):373-379.
859. Zoja C, Furci L, Ghilardi F, et al. Cyclosporin-induced endothelial cell injury. *Lab Invest* 1986;55(4):455-462.
860. Charba D, Moake JL, Harris MA, et al. Abnormalities of von Willebrand factor multimers in drug-associated thrombotic microangiopathies. *Am J Hematol* 1993;42(3):268-277.
861. Seeber C, Hiller E, Holler E, et al. Increased levels of tissue plasminogen activator (t-PA) and tissue plasminogen activator inhibitor (PAI) correlate with tumor necrosis factor alpha (TNF alpha)-release in patients suffering from microangiopathy following allogeneic bone marrow transplantation (BMT). *Thromb Res* 1992;66(4):373-383.
862. Brown Z, Neild GH, Willoughby JJ, et al. Increased factor VIII as an index of vascular injury in cyclosporine nephrotoxicity. *Transplantation* 1986;42(2):150-153.
863. Slattery C, Campbell E, McMorow T, et al. Cyclosporine A-induced renal fibrosis: a role for epithelial-mesenchymal transition. *Am J Pathol* 2005;167(2):395-407.
864. Mengel M, Mihatsch M, Halloran PF. Histological characteristics of calcineurin inhibitor toxicity—there is no such thing as specificity! *Am J Transplant* 2011;11(12):2549-2550.
865. Satoskar AA, Pelletier R, Adams P, et al. De novo thrombotic microangiopathy in renal allograft biopsies—role of antibody-mediated rejection. *Am J Transplant* 2010;10(8):1804-1811.
866. Tsinalis D, Dickenmann M, Brunner F, et al. Acute renal failure in a renal allograft recipient treated with intravenous immunoglobulin. *Am J Kidney Dis* 2002;40(3):667-670.
867. Haas M, Sonnenday CJ, Cicone JS, et al. Isometric tubular epithelial vacuolization in renal allograft biopsy specimens of patients receiving low-dose intravenous immunoglobulin for a positive crossmatch. *Transplantation* 2004;78(4):549-556.
868. Moreau JF, Droz D, Sabto J, et al. Osmotic nephrosis induced by water-soluble triiodinated contrast media in man: a retrospective study of 47 cases. *Radiology* 1975;115(2):329-336.
869. Mihatsch MJ, Thiel G, Basler V, et al. Morphological patterns in cyclosporine-treated renal transplant recipients. *Transplant Proc* 1985;17(4 Suppl 1):101-116.
870. Markowitz GS, Stokes MB, Radhakrishnan J, et al. Acute phosphate nephropathy following oral sodium phosphate bowel purgative: an underrecognized cause of chronic renal failure. *J Am Soc Nephrol* 2005;16(11):3389-3396.
871. Gonlusen G, Akgun H, Ertan A, et al. Renal failure and nephrocalcinosis associated with oral sodium phosphate bowel cleansing: clinical patterns and renal biopsy findings. *Arch Pathol Lab Med* 2006;130(1):101-106.
872. Hall BM, Tiller DJ, Duggin GG, et al. Post-transplant acute renal failure in cadaver renal recipients treated with cyclosporine. *Kidney Int* 1985;28(2):178-186.
873. Versluis DJ, Ten KFJ, Wenting GJ, et al. Histological lesions associated with cyclosporin: incidence and reversibility in one year old kidney transplants. *J Clin Pathol* 1988;41(5):498-503.
874. English RF, Pophal SA, Bacanu SA, et al. Long-term comparison of tacrolimus- and cyclosporine-induced nephrotoxicity in pediatric heart-transplant recipients. *Am J Transplant* 2002;2(8):769-773.
875. Ojo AO, Held PJ, Port FK, et al. Chronic renal failure after transplantation of a nonrenal organ. *N Engl J Med* 2003;349(10):931-940.
876. Collins BS, Davis CL, Marsh CL, et al. Reversible cyclosporine arteriopathy. *Transplantation* 1992;54(4):732-734.
877. Morozumi K, Thiel G, Albert FW, et al. Studies on morphological outcome of cyclosporine-associated arteriopathy after discontinuation of cyclosporine in renal allografts. *Clin Nephrol* 1992;38(1):1-8.
878. Karthikeyan V, Parasuraman R, Shah V, et al. Outcome of plasma exchange therapy in thrombotic microangiopathy after renal transplantation. *Am J Transplant* 2003;3(10):1289-1294.
879. Hochstetler LA, Flanigan MJ, Lager DJ. Transplant-associated thrombotic microangiopathy: the role of IgG administration as initial therapy. *Am J Kidney Dis* 1994;23(3):444-450.
880. Bren A, Pajek J, Grego K, et al. Follow-up of kidney graft recipients with cyclosporine-associated hemolytic-uremic syndrome and thrombotic microangiopathy. *Transplant Proc* 2005;37(4):1889-1891.
881. Trimarchi HM, Truong LD, Brennan S, et al. FK506-associated thrombotic microangiopathy: report of two cases and review of the literature. *Transplantation* 1999;67(4):539-544.
882. Katafuchi R, Saito S, Ikeda K, et al. A case of late onset cyclosporine-induced hemolytic uremic syndrome resulting in renal graft loss. *Clin Transplant* 1999;13(Suppl 1):54-58.
883. Galli FC, Damon LE, Tomlanovich SJ, et al. Cyclosporine-induced hemolytic uremic syndrome in a heart transplant recipient. *J Heart Lung Transplant* 1993;12(3):440-444.
884. Zarifian A, Meleg-Smith S, O'Donovan R, et al. Cyclosporine-associated thrombotic microangiopathy in renal allografts. *Kidney Int* 1999;55(6):2457-2466.
885. Sommer BG, Innes JT, Whitehurst RM, et al. Cyclosporine-associated renal arteriopathy resulting in loss of allograft function. *Am J Surg* 1985;149(6):756-764.
886. Schwimmer J, Nadasdy TA, Spitalnik PF, et al. De novo thrombotic microangiopathy in renal transplant recipients: a comparison of hemolytic uremic syndrome with localized renal thrombotic microangiopathy. *Am J Kidney Dis* 2003;41(2):471-479.
887. Candinas D, Kusch G, Schlumpf R, et al. Hemolytic-uremic syndrome following kidney transplantation: prognostic factors. *Schweiz Med Wochenschr* 1994;124(41):1789-1799.
888. Dominguez J, Kompatzki A, Norambuena R, et al. Benefits of early biopsy on the outcome of kidney transplantation. *Transplant Proc* 2005;37(8):3361-3363.
889. Langer RM, Van Buren CT, Katz SM, et al. De novo hemolytic uremic syndrome after kidney transplantation in patients treated with cyclosporine-sirolimus combination. *Transplantation* 2002;73(5):756-760.
890. Franco A, Hernandez D, Capdevilla L, et al. De novo hemolytic-uremic syndrome/thrombotic microangiopathy in renal transplant patients receiving calcineurin inhibitors: role of sirolimus. *Transplant Proc* 2003;35(5):1764-1766.
891. Wiener Y, Nakhleh RE, Lee MW, et al. Prognostic factors and early resumption of cyclosporin A in renal allograft recipients with thrombotic microangiopathy and hemolytic uremic syndrome. *Clin Transplant* 1997;11(3):157-162.
892. Young BA, Marsh CL, Alpers CE, et al. Cyclosporine-associated thrombotic microangiopathy/hemolytic uremic syndrome following kidney and kidney-pancreas transplantation. *Am J Kidney Dis* 1996;28(4):561-571.

893. Bolin P, Jr., Jennette JC, Mandel SR. Cyclosporin-associated thrombotic microangiopathy: successful retreatment with cyclosporin. *Ren Fail* 1991;13(4):275–278.
894. Epstein M, Landsberg D. Cyclosporine-induced thrombotic microangiopathy resulting in renal allograft loss and its successful reuse: a report of two cases. *Am J Kidney Dis* 1991;17(3):346–348.
895. Franz M, Regele H, Schmaldienst S, et al. Posttransplant hemolytic uremic syndrome in adult retransplanted kidney graft recipients: advantage of FK506 therapy? *Transplantation* 1998;66(9):1258–1262.
896. Dickenmann M, Oertl T, Mihatsch MJ. Osmotic nephrosis: acute kidney injury with accumulation of proximal tubular lysosomes due to administration of exogenous solutes. *Am J Kidney Dis* 2008;51(3):491–503.
897. Josephson MA, Chiu MY, Woodle ES, et al. Drug-induced acute interstitial nephritis in renal allografts: histopathologic features and clinical course in six patients. *Am J Kidney Dis* 1999;34(3):540–548.
898. Hallgren R, Bohman SO, Fredens K. Activated eosinophil infiltration and deposits of eosinophil cationic protein in renal allograft rejection. *Nephron* 1991;59(2):266–270.
899. Ten RM, Gleich GJ, Holley KE, et al. Eosinophil granule major basic protein in acute renal allograft rejection. *Transplantation* 1989;47(6):959–963.
900. Kahan BD. Sirolimus. In: Morris PJ, ed. *Kidney Transplantation: Principles and Practice*, 5th ed. Philadelphia, London, New York: W.B. Saunders Company, 2001:279–288.
901. Fellstrom B. Cyclosporine nephrotoxicity. *Transplant Proc* 2004;36(2 Suppl):220S–223S.
902. Stallone G, Infante B, Schena A, et al. Rapamycin for treatment of chronic allograft nephropathy in renal transplant patients. *J Am Soc Nephrol* 2005;16(12):3755–3762.
903. Kirken RA, Wang YL. Molecular actions of sirolimus: Sirolimus and mTOR. *Transplant Proc* 2003;35(3 Suppl):227S–230S.
904. Bruns CJ, Koehl GE, Guba M, et al. Rapamycin-induced endothelial cell death and tumor vessel thrombosis potentiate cytotoxic therapy against pancreatic cancer. *Clin Cancer Res* 2004;10(6):2109–2119.
905. Guba M, Yezhelyev M, Eichhorn ME, et al. Rapamycin induces tumor-specific thrombosis via tissue factor in the presence of VEGF. *Blood* 2005;105(11):4463–4469.
906. Guba M, von Breitenbuch P, Steinbauer M, et al. Rapamycin inhibits primary and metastatic tumor growth by antiangiogenesis: involvement of vascular endothelial growth factor. *Nat Med* 2002;8(2):128–135.
907. Letavernier E, Pe'raldi MN, Pariente A, et al. Proteinuria following a switch from calcineurin inhibitors to sirolimus. *Transplantation* 2005;80(9):1198–1203.
908. Sennesael JJ, Bosmans JL, Bogers JP, et al. Conversion from cyclosporine to sirolimus in stable renal transplant recipients. *Transplant* 2005;80(11):1578–1585.
909. Letavernier E, Bruneval P, Mandet C, et al. High sirolimus levels may induce focal segmental glomerulosclerosis de novo. *Clin J Am Soc Nephrol* 2007;2: 326.
910. Straathof-Galema L, Wetzels JF, Dijkman HB, et al. Sirolimus-associated heavy proteinuria in a renal transplant recipient: evidence for a tubular mechanism. *Am J Transplant* 2006;6(2):429–433.
911. Coombes JD, Mreich E, Liddle C, et al. Rapamycin worsens renal function and intratubular cast formation in protein overload nephropathy. *Kidney Int* 2005;68(6):2599–2607.
912. Reynolds JC, Agodoa LY, Yuan CM, et al. Thrombotic microangiopathy after renal transplantation in the United States. *Am J Kidney Dis* 2003;42(5):1058–1068.
913. Sartelet H, Toupance O, Lorenzato M, et al. Sirolimus-induced thrombotic microangiopathy is associated with decreased expression of vascular endothelial growth factor in kidneys. *Am J Transplant* 2005; 5(10):2441–2447.
914. Oyen O, Strom EH, Midtvedt K, et al. Calcineurin inhibitor-free immunosuppression in renal allograft recipients with thrombotic microangiopathy/hemolytic uremic syndrome. *Am J Transplant* 2006;6(2):412–418.
915. Morelon E, Kreis H. Sirolimus therapy without calcineurin inhibitors: Necker Hospital 8-year experience. *Transplant Proc* 2003;35 (3 Suppl):52S–57S.
916. Dean PG, Lund WJ, Larson TS, et al. Wound-healing complications after kidney transplantation: a prospective, randomized comparison of sirolimus and tacrolimus. *Transplantation* 2004;77(10):1555–1561.
917. Geetha D, Tong BC, Racusen L, et al. Bladder carcinoma in a transplant recipient: evidence to implicate the BK human polyomavirus as a causal transforming agent. *Transplantation* 2002;73(12):1933–1936.
918. Nickeleit V, Singh HK, Goldsmith C, et al. BK virus-associated urinary bladder carcinoma in transplant recipients: productive or non-productive polyomavirus infections in tumor cells? *Hum Pathol* 2013;44:2871–2872.
919. Alexiev BA, Randhawa P, Vazquez Martul E, et al. BK virus-associated urinary bladder carcinoma in transplant recipients: report of 2 cases, review of the literature, and proposed pathogenetic model. *Hum Pathol* 2013;44(5):908–917.
920. Kenan DJ, Singh HK, Nickeleit V. High grade urothelial carcinoma associated with BK-polyomavirus in renal allografts. *Mod Pathol* 2013;27(Suppl 2):239A–240A.
921. Roberts IS, Besarani D, Mason P, et al. Polyoma virus infection and urothelial carcinoma of the bladder following renal transplantation. *Br J Cancer* 2008;99(9):1383–1386.
922. Nickeleit V, Mihatsch MJ. Polyomavirus nephropathy in native kidneys and renal allografts: an update on an escalating threat. *Transplant Int* 2006;19(12):960–973.
923. Jennings SH, Wise AG, Nickeleit V, et al. Polyomavirus-associated nephritis in 2 horses. *Vet Pathol* 2013;50(5):769–774.
924. van Gorder MA, Della Pelle P, Henson JW, et al. Cynomolgus polyoma virus infection: a new member of the polyoma virus family causes interstitial nephritis, urethritis, and enteritis in immunosuppressed cynomolgus monkeys. *Am J Pathol* 1999;154(4):1273–1284.
925. Latif S, Zaman F, Veeramachaneni R, et al. BK polyomavirus in renal transplants: role of electron microscopy and immunostaining in detecting early infection. *Ultrastruct Pathol* 2007;31(3):199–207.
926. Ljungman P, Griffiths P, Paya C. Definitions of cytomegalovirus infection and disease in transplant recipients. *Clin Infect Dis* 2002;34(8):1094–1097.
927. Singh HK, Andreoni KA, Madden V, et al. Presence of urinary Haufen accurately predicts polyomavirus nephropathy. *J Am Soc Nephrol* 2009;20(2):416–427.
928. Drachenberg CB, Beskow CO, Cangro CB, et al. Human polyoma virus in renal allograft biopsies: morphological findings and correlation with urine cytology. *Hum Pathol* 1999;30(8):970–977.
929. Nickeleit V, Hirsch HH, Binet IF, et al. Polyomavirus infection of renal allograft recipients: from latent infection to manifest disease. *J Am Soc Nephrol* 1999;10(5):1080–1089.
930. Nickeleit V, Steiger J, Mihatsch MJ. BK virus infection after kidney transplantation. *Graft* 2002;5(December Suppl):S46–S57.
931. Randhawa PS, Finkelstein S, Scantlebury V, et al. Human polyoma virus-associated interstitial nephritis in the allograft kidney. *Transplantation* 1999;67(1):103–109.
932. Drachenberg CB, Papadimitriou JC, Hirsch HH, et al. Histological patterns of polyomavirus nephropathy: correlation with graft outcome and viral load. *Am J Transplant* 2004;4(12):2082–2092.
933. Celik B, Randhawa PS. Glomerular changes in BK virus nephropathy. *Hum Pathol* 2004;35(3):367–370.
934. Drachenberg CB, Hirsch HH, Ramos E, et al. Polyomavirus disease in renal transplantation: review of pathological findings and diagnostic methods. *Hum Pathol* 2005;36(12):1245–1255.
935. Nickeleit V, Mihatsch MJ. Polyomavirus nephropathy in native kidneys and renal allografts: an update on an escalating threat. *Transpl Int* 2006;19:960–973.
936. Kemeny E, Hirsch HH, Eller J, et al. Plasma cell infiltrates in polyomavirus nephropathy. *Transpl Int* 2010;23(4):397–406.
937. Nickeleit V, Mihatsch MJ. Polyomavirus nephropathy: pathogenesis, morphological and clinical aspects. In: Kreipe HH, ed. *Verh Dtsch Ges Pathol, 88 Tagung*. Muenchen, Jena: Urban & Fischer, 2004:69–84.
938. Hever A, Nast CC. Polyoma virus nephropathy with simian virus 40 antigen-containing tubular basement membrane immune complex deposition. *Hum Pathol* 2008;39(1):73–79.
939. Bracamonte E, Leca N, Smith KD, et al. Tubular basement membrane immune deposits in association with BK polyomavirus nephropathy. *Am J Transplant* 2007;7(6):1552–1560.

940. Nickleleit V, Mihatsch MJ. Polyomavirus allograft nephropathy and concurrent acute rejection: a diagnostic and therapeutic challenge. *Am J Transplant* 2004;4(5):838–839.
941. Batal I, Zainah H, Stockhausen S, et al. The significance of renal C4d staining in patients with BK viremia, viremia, and nephropathy. *Mod Pathol* 2009;22(11):1468–1476.
942. Schaub S, Mayr M, Egli A, et al. Transient allograft dysfunction from immune reconstitution in a patient with polyoma BK-virus-associated nephropathy. *Nephrol Dial Transplant* 2007;22(8):2386–2390.
943. Menter T, Mayr M, Schaub S, et al. Pathology of resolving polyomavirus-associated nephropathy. *Am J Transplant* 2013;13(6):1474–1483.
944. Guilbert M, Latour M, Fortin M, et al. Biopsy proven polyoma-JC associated nephropathy eleven years after kidney transplantation. *J Am Soc Nephrol* 2012;23(Abstrac Suppl):882A.
945. Drachenberg CB, Hirsch HH, Papadimitriou JC, et al. Polyomavirus BK versus JC replication and nephropathy in renal transplant recipients: a prospective evaluation. *Transplantation* 2007;84(3):323–330.
946. Rolla D, Giacomazzi CG, Gentile R, et al. Kidney graft loss associated with JC polyomavirus nephropathy. *J Nephrol* 2009;22(2):295–298.
947. Randhawa P, Baksh F, Aoki N, et al. JC virus infection in allograft kidneys: analysis by polymerase chain reaction and immunohistochemistry. *Transplantation* 2001;71(9):1300–1303.
948. Milstone A, Vilchez RA, Geiger X, et al. Polyomavirus simian virus 40 infection associated with nephropathy in a lung-transplant recipient. *Transplantation* 2004;77(7):1019–1024.
949. Kazory A, Ducloux D, Chalopin JM, et al. The first case of JC virus allograft nephropathy. *Transplantation* 2003;76(11):1653–1655.
950. Nickleleit V, Singh HK, Gilliland MGF, et al. Latent polyomavirus type BK loads in native kidneys analyzed by TaqMan PCR: what can be learned to better understand BK virus nephropathy? *J Am Soc Nephrol* 2003;14(Abstrac Issue):424A
951. Nickleleit V, Singh HK, Mihatsch MJ. Polyomavirus nephropathy: morphology, pathophysiology, and clinical management. *Curr Opin Nephrol Hypertens* 2003;12:599–605.
952. Bohl DL, Storch GA, Ryschewitsch C, et al. Donor origin of BK virus in renal transplantation and role of HLA C7 in susceptibility to sustained BK viremia. *Am J Transplant* 2005;5(9):2213–2221.
953. Boldorini R, Veggiani C, Barco D, et al. Kidney and urinary tract polyomavirus infection and distribution: molecular biology investigation of 10 consecutive autopsies. *Arch Pathol Lab Med* 2005;129(1):69–73.
954. Chesters PM, Heritage J, McCance DJ. Persistence of DNA sequences of BK virus and JC virus in normal human tissues and in diseased tissues. *J Infect Dis*. 1983;147(4):676–684.
955. Heritage J, Chesters PM, McCane DJ. The persistence of papovavirus BK DNA sequences in normal human renal tissue. *J Med Virol* 1981;8:143–150.
956. Mackenzie EF, Poulding JM, Harrison PR, et al. Human polyoma virus (HPV)—A significant pathogen in renal transplantation. *Proc Eur Dial Transpl Assoc* 1978;15:352–360.
957. Li YJ, Weng CH, Lai WC, et al. A suppressive effect of cyclosporine A on replication and noncoding control region activation of polyomavirus BK virus. *Transplantation* 2010;89(3):299–306.
958. Gabardi S, Townsend K, Martin ST, et al. Evaluating the impact of pre-transplant desensitization utilizing a plasmapheresis and low-dose intravenous immunoglobulin protocol on BK viremia in renal transplant recipients. *Transpl Infect Dis* 2013;15(4):361–368.
959. Mengel M, Marwedel M, Radermacher J, et al. Incidence of polyomavirus-nephropathy in renal allografts: influence of modern immunosuppressive drugs. *Nephrol Dial Transplant* 2003;18(6):1190–1196.
960. Rocha PN, Plumb TJ, Miller SE, et al. Risk factors for BK polyomavirus nephritis in renal allograft recipients. *Clin Transplant* 2004;18(4):456–462.
961. Brennan DC, Agha I, Bohl DL, et al. Incidence of BK with tacrolimus versus cyclosporine and impact of preemptive immunosuppression reduction. *Am J Transplant* 2005;5(3):582–594.
962. Manipisitkul W, Drachenberg C, Ramos E, et al. Maintenance immunosuppressive agents as risk factors for BK virus nephropathy: a case-control study. *Transplantation* 2009;88(1):83–88.
963. Atencio IA, Shadan FF, Zhou XJ, et al. Adult mouse kidneys become permissive to acute polyomavirus infection and reactivate persistent infections in response to cellular damage and regeneration. *J Virol* 1993;67(3):1424–1432.
964. Sood P, Senanayake S, Sujeet K, et al. Donor and recipient BKV-specific IgG antibody and posttransplantation BKV infection: a prospective single-center study. *Transplantation* 2013;95(6):896–902.
965. Trydzenskaya H, Juerchott K, Lachmann N, et al. The genetic predisposition of natural killer cell to BK virus-associated nephropathy in renal transplant patients. *Kidney Int* 2013;84(2):359–365.
966. Womer KL, Huang Y, Herren H, et al. Dendritic cell deficiency associated with development of BK viremia and nephropathy in renal transplant recipients. *Transplantation* 2010;89(1):115–123.
967. Randhawa PS, Khaleel-Ur-Rehman K, Swalsky PA, et al. DNA sequencing of viral capsid protein VP-1 region in patients with BK virus interstitial nephritis. *Transplantation* 2002;73(7):1090–1094.
968. Gosert R, Rinaldo CH, Funk GA, et al. Polyomavirus BK with rearranged noncoding control region emerge in vivo in renal transplant patients and increase viral replication and cytopathology. *J Exp Med* 2008;205(4):841–852.
969. Dugan AS, Eash S, Atwood WJ. An N-linked glycoprotein with alpha(2,3)-linked sialic acid is a receptor for BK virus. *J Virol* 2005;79(22):14442–14445.
970. Eash S, Querbes W, Atwood WJ. Infection of vero cells by BK virus is dependent on caveolae. *J Virol* 2004;78(21):11583–11590.
971. Eash S, Atwood WJ. Involvement of cytoskeletal components in BK virus infectious entry. *J Virol* 2005;79(18):11734–11741.
972. Jiang M, Abend JR, Tsai B, et al. Early events during BK virus entry and disassembly. *Journal of Virology* 2009;83(3):1350–1358.
973. Jordan JA, Manley K, Dugan AS, et al. Transcriptional regulation of BK virus by nuclear factor of activated T cells. *J Virol* 2010;84(4):1722–1730.
974. Drachenberg CB, Papadimitriou JC, Wali R, et al. BK polyoma virus allograft nephropathy: ultrastructural features from viral cell entry to lysis. *Am J Transplant* 2003;3(11):1383–1392.
975. Ribeiro A, Wornle M, Motamedi N, et al. Activation of innate immune defense mechanisms contributes to polyomavirus BK-associated nephropathy. *Kidney International* 2012;81(1):100–111.
976. Binggeli S, Egli A, Schaub S, et al. Polyomavirus BK-specific cellular immune response to VP1 and large T-antigen in kidney transplant recipients. *Am J Transplant* 2007;7(5):1131–1139.
977. Comoli P, Hirsch HH, Ginevri F. Cellular immune responses to BK virus. *Current Opin Organ Transplant* 2008;13(6):569–574.
978. Mannon RB, Hoffmann SC, Kampen RL, et al. Molecular evaluation of BK polyomavirus nephropathy. *Am J Transplant* 2005;5(12):2883–2893.
979. Dadhania D, Snopkowski C, Ding R, et al. Validation of noninvasive diagnosis of BK virus nephropathy and identification of prognostic biomarkers. *Transplantation* 2010;90(2):189–197.
980. Schmid H, Nitschko H, Gerth J, et al. Polyomavirus DNA and RNA detection in renal allograft biopsies: results from a European multicenter study. *Transplantation* 2005;80(5):600–604.
981. Randhawa PS, Vats A, Zygmunt D, et al. Quantitation of viral DNA in renal allograft tissue from patients with BK virus nephropathy. *Transplantation* 2002;74(4):485–488.
982. Randhawa P, Shapiro R, Vats A. Quantitation of DNA of polyomaviruses BK and JC in human kidneys. *J Infect Dis*. 2005;192(3):504–509.
983. Bruno B, Zager RA, Boeckh MJ, et al. Adenovirus nephritis in hematopoietic stem-cell transplantation. *Transplantation* 2004;77(7):1049–1057.
984. Nada R, Sachdeva MU, Sud K, et al. Co-infection by cytomegalovirus and BK polyoma virus in renal allograft, mimicking acute rejection. *Nephrol Dial Transplant* 2005;20(5):994–996.
985. Hirsch HH, Brennan DC, Drachenberg CB, et al. Polyomavirus-associated nephropathy in renal transplantation: interdisciplinary analyses and recommendations. *Transplantation* 2005;79(10):1277–1286.
986. Hirsch HH, Knowles W, Dickenmann M, et al. Prospective study of polyomavirus type BK replication and nephropathy in renal-transplant recipients. *N Engl J Med* 2002;347(7):488–496.
987. Mayr M, Nickleleit V, Hirsch HH, et al. Polyomavirus BK nephropathy in a kidney transplant recipient: critical issues of diagnosis and management. *Am J Kidney Dis* 2001;38(3):E13.

988. Ahuja M, Cohen EP, Dayer AM, et al. Polyoma virus infection after renal transplantation. Use of immunostaining as a guide to diagnosis. *Transplantation* 2001;71(7):896–899.
989. Jeong HJ, Hong SW, Sung SH, et al. Polyomavirus nephropathy in renal transplantation: a clinico-pathological study. *Transplant Int* 2003;16(9):671–675.
990. Sharif A, Alachkar N, Bagnasco S, et al. Incidence and outcomes of BK virus allograft nephropathy among ABO- and HLA-incompatible kidney transplant recipients. *Clin J Am Soc Nephrol* 2012;7(8):1320–1327.
991. Akazawa Y, Terada Y, Yamane T, et al. Fatal BK virus pneumonia following stem cell transplantation. *Transpl Infect Dis* 2012;14(6):E142–E146.
992. Petrogiannis-Haliotis T, Sakoulas G, Kirby J, et al. BK-related polyomavirus vasculopathy in a renal-transplant recipient. *N Engl J Med* 2001;345(17):1250–1255.
993. Sachdeva MS, Nada R, Jha V, et al. The high incidence of BK polyoma virus infection among renal transplant recipients in India. *Transplantation* 2004;77(3):429–431.
994. Ramos E, Vincenti F, Lu WX, et al. Retransplantation in patients with graft loss caused by polyoma virus nephropathy. *Transplantation* 2004;77(1):131–133.
995. Hirsch HH, Ramos E. Retransplantation after polyomavirus-associated nephropathy: just do it? *Am J Transplant* 2006;6:7–9.
996. Womer K, Meier-Krieschke HU, Patton P, et al. Preemptive retransplantation for BK virus nephropathy: successful outcome despite active viremia. *Am J Transplant* 2006;6:209–213.
997. Mindlova M, Boucek P, Saudek F, et al. Kidney retransplantation following graft loss to polyoma virus-associated nephropathy: an effective treatment option in simultaneous pancreas and kidney transplant recipients. *Transplant Int* 2008;21(4):353–356.
998. Williams JW, Javaid B, Kadambi PV, et al. Leflunomide for polyomavirus type BK nephropathy. *N Engl J Med* 2005;352(11):1157–1158.
999. Kuypers DR, Vandooren AK, Lerut E, et al. Adjuvant low-dose cidofovir therapy for BK polyomavirus interstitial nephritis in renal transplant recipients. *Am J Transplant* 2005;5(8):1997–2004.
1000. Vats A, Shapiro R, Singh Randhawa P, et al. Quantitative viral load monitoring and cidofovir therapy for the management of BK virus-associated nephropathy in children and adults. *Transplantation* 2003;75(1):105–112.
1001. Farasati NA, Shapiro R, Vats A, et al. Effect of leflunomide and cidofovir on replication of BK virus in an in vitro culture system. *Transplantation* 2005;79(1):116–118.
1002. Schaub S, Hirsch HH, Dickenmann M, et al. Reducing immunosuppression preserves allograft function in presumptive and definitive polyomavirus-associated nephropathy. *Am J Transplant* 2010;10(12):2615–2623.
1003. Hirsch HH, Randhawa P. BK polyomavirus in solid organ transplantation. *Am J Transplant* 2013;13(Suppl 4):179–188.
1004. Nicleleit V, Klimkait T, Binet IF, et al. Testing for polyomavirus type BK DNA in plasma to identify renal-allograft recipients with viral nephropathy. *N Engl J Med* 2000;342(18):1309–1315.
1005. Hirsch HH, Drachenberg CB, Steiger J, et al. Polyomavirus associated nephropathy in renal transplantation: critical issues of screening and management. In: Ahsan N, ed. *Polyomaviruses and Human Diseases*, 1st ed. New York, Georgetown, TX: Springer Science + Business Media, Landes Bioscience/Eurekah.com, 2006:160–173.
1006. Drachenberg RC, Drachenberg CB, Papadimitriou JC, et al. Morphological spectrum of polyoma virus disease in renal allografts: diagnostic accuracy of urine cytology. *Am J Transplant* 2001;1(4):373–381.
1007. Nicleleit V, Steiger J, Mihatsch MJ. Re: noninvasive diagnosis of BK virus nephritis by measurement of messenger RNA for BK virus VP1. *Transplantation* 2003;75(12):2160–2161.
1008. Singh HK, Bubendorf L, Mihatsch MJ, et al. Urine cytology findings of polyomavirus infections. In: Ahsan N, ed. *Polyomaviruses and Human Diseases*, 1st ed. New York, Georgetown, TX: Springer Science + Business Media, Landes Bioscience / Eurekah.com, 2006:201–212.
1009. Singh HK, Donna Thompson B, Nicleleit V. Viral Haufen are urinary biomarkers of polyomavirus nephropathy: new diagnostic strategies utilizing negative staining electron microscopy. *Ultrastruct Pathol* 2009;33(5):222–235.
1010. Nicleleit V, Brylawski B, Singh H, et al. Urinary polyomavirus-Haufen shedding in mouse and man: a proof-of-concept study for a non-invasive urine biomarker for polyomavirus nephropathy. *Lab Invest* 2013;93(Suppl 1):390A–391A.
1011. Singh H, Kozlowski T, True K, et al. Urinary polyomavirus-Haufen shedding accurately reflects intrarenal burden of polyomavirus nephropathy (PVN): comparative quantitative analyses of different screening techniques. *Lab Invest* 2011;91(Suppl 1):352A.
1012. Coleman DV, Mackenzie EF, Gardner SD, et al. Human polyomavirus (BK) infection and ureteric stenosis in renal allograft recipients. *J Clin Pathol* 1978;31(4):338–347.
1013. Thomas A, Dropulic LK, Rahman MH, et al. Ureteral stents: a novel risk factor for polyomavirus nephropathy. *Transplantation* 2007;84:433.
1014. Khan H, Oberoi S, Mahvash A, et al. Reversible ureteral obstruction due to polyomavirus infection after percutaneous nephrostomy catheter placement. *Biol Blood Marrow Transplant* 2011;17(10):1551–1555.
1015. Egli A, Binggeli S, Bodaghi S, et al. Cytomegalovirus and polyomavirus BK posttransplant. *Nephrol Dial Transplant* 2007;22(Suppl 8):viii72–viii82.
1016. Giakoustidis D, Antoniadis A, Fouzas I, et al. Prevalence and clinical impact of cytomegalovirus infection and disease in renal transplantation: ten years of experience in a single center. *Transplant Proc* 2012;44(9):2715–2717.
1017. Rubin RH, Colvin RB. Impact of cytomegalovirus infection on renal transplantation. In: Racusen LC, Solez K, Burdick JF, eds. *Kidney Transplant Rejection: Diagnosis and Treatment*, 3rd ed. New York: Marcel Dekker, 1998:605–625.
1018. Ersan S, Yorukoglu K, Sert M, et al. Unusual case of severe late-onset cytomegalovirus-induced hemorrhagic cystitis and ureteritis in a renal transplant patient. *Ren Fail*. 2012;34(2):247–250.
1019. Joshi K, Nada R, Radotra BD, et al. Pathological spectrum of cytomegalovirus infection of renal allograft recipients—an autopsy study from north India. *Indian J Pathol Microbiol* 2004;47(3):327–332.
1020. Battegay EJ, Mihatsch MJ, Mazzucchelli L, et al. Cytomegalovirus and kidney. *Clin Nephrol* 1988;30(5):239–247.
1021. Rane S, Nada R, Minz M, et al. Spectrum of cytomegalovirus-induced renal pathology in renal allograft recipients. *Transplant Proc* 2012;44(3):713–716.
1022. Cozzutto C, Felici N. Unusual glomerular change in cytomegalic inclusion disease. *Virchows Arch A Pathol Anat Histol* 1974;364:365–369.
1023. Beneck D, Greco MA, Feiner HD. Glomerulonephritis in congenital cytomegalic inclusion disease. *Hum Pathol* 1986;17:1054–1059.
1024. Detwiler RK, Singh HK, Bolin P Jr, et al. Cytomegalovirus-induced necrotizing and crescentic glomerulonephritis in a renal transplant patient. *Am J Kidney Dis* 1998;32(5):820–824.
1025. Onuigbo M, Haririan A, Ramos E, et al. Cytomegalovirus-induced glomerular vasculopathy in renal allografts: a report of two cases. *Am J Transplant* 2002;2(7):684–688.
1026. Jeejeebhoy FM, Zaltzman JS. Thrombotic microangiopathy in association with cytomegalovirus infection in a renal transplant patient: a new treatment strategy. *Transplantation* 1998;65(12):1645–1648.
1027. Kadereit S, Michelson S, Mougnot B, et al. Polymerase chain reaction detection of cytomegalovirus genome in renal biopsies. *Kidney Int* 1992;42:1012–1016.
1028. Liapis H, Storch GA, Hill DA, et al. CMV infection of the renal allograft is much more common than the pathology indicates: a retrospective analysis of qualitative and quantitative buffy coat CMV-PCR, renal biopsy pathology and tissue CMV-PCR. *Nephrol Dial Transplant* 2003;18(2):397–402.
1029. Boeckh M, Nichols WG. Immunosuppressive effects of beta-herpesviruses. *Herpes* 2003;10(1):12–16.
1030. Reinke P, Fietze E, Ode-Hakim S, et al. Late-acute renal allograft rejection and symptomless cytomegalovirus infection. *Lancet* 1994;344(8939–8940):1737–1738.
1031. Emovon OE, Chavin J, Rogers K, et al. Adenovirus in kidney transplantation: an emerging pathogen? *Transplantation* 2004;77(9):1474–1475.
1032. Ito M, Hirabayashi N, Uno Y, et al. Necrotizing tubulointerstitial nephritis associated with adenovirus infection. *Hum Pathol* 1991;22(12):1225–1231.

1033. Lim AK, Parsons S, Ierino F. Adenovirus tubulointerstitial nephritis presenting as a renal allograft space occupying lesion. *Am J Transplant* 2005;5(8):2062–2066.
1034. Asim M, Chong-Lopez A, Nickleit V. Adenovirus infection of a renal allograft. *Am J Kidney Dis* 2003;41(3):696–701.
1035. Mathur SC, Squiers EC, Tatum AH, et al. Adenovirus infection of the renal allograft with sparing of pancreas graft function in the recipient of a combined kidney-pancreas transplant. *Transplantation* 1998;65(1):138–141.
1036. Bilic M, Nickleit V, Howell DN, et al. Necrotizing granulomatous tubulointerstitial nephritis due to adenovirus infection in the renal allograft: a characteristic morphologic pattern with major clinical implications (Abstract). *Lab Invest* 2006;86 (Suppl 1):259A.
1037. Nickleit V. Critical commentary to: acute adenoviral infection of a graft by serotype 35 following renal transplantation. *Pathol Res Pract* 2003;199:701–702.
1038. Singh HK, Nickleit V. Kidney disease caused by viral infections. *Curr Diag Pathol* 2004;10:11–21.
1039. Watcharananan SP, Avery R, Ingsathit A, et al. Adenovirus disease after kidney transplantation: course of infection and outcome in relation to blood viral load and immune recovery. *Am J Transplant* 2011;11(6):1308–1314.
1040. Ortiz M, Ulloa C, Troncoso P, et al. Hemorrhagic cystitis secondary to adenovirus infection in a kidney transplant recipient: case report. *Transplant Proc* 2009;41(6):2685–2687.
1041. Yagisawa T, Nakada T, Takahashi K, et al. Acute hemorrhagic cystitis caused by adenovirus after kidney transplantation. *Urol Int* 1995;54(3):142–146.
1042. Watcharananan SP, Junchotikul P, Srichanusmi C, et al. Adenovirus infection after kidney transplantation in Thailand: seasonal distribution and potential route of acquisition. *Transplant Proc* 2010;42(10):4091–4093.
1043. Florescu MC, Miles CD, Florescu DF. What do we know about adenovirus in renal transplantation? *Nephrol Dial Transplant* 2013;28:2003–2010.
1044. Friedrichs N, Eis-Hubinger AM, Heim A, et al. Acute adenoviral infection of a graft by serotype 35 following renal transplantation. *Pathol Res Pract* 2003;199(8):565–570.
1045. Emovon OE, Lin A, Howell DN, et al. Refractory adenovirus infection after simultaneous kidney-pancreas transplantation: successful treatment with intravenous ribavirin and pooled human intravenous immunoglobulin. *Nephrol Dial Transplant* 2003;18(11):2436–2438.
1046. Hoffman JA, Shah AJ, Ross LA, et al. Adenoviral infections and a prospective trial of cidofovir in pediatric hematopoietic stem cell transplantation. *Biol Blood Marrow Transplant* 2001;7(7):388–394.
1047. Sujeet K, Vasudev B, Desai P, et al. Acute kidney injury requiring dialysis secondary to adenovirus nephritis in renal transplant recipient. *Transpl Infect Dis* 2011;13(2):174–177.
1048. Varma MC, Kushner YB, Ko DS, et al. Early onset adenovirus infection after simultaneous kidney-pancreas transplant. *Am J Transplant* 2011;11(3):623–627.
1049. Yang CW, Kim YS, Yang KH, et al. Acute focal bacterial nephritis presented as acute renal failure and hepatic dysfunction in a renal transplant recipient. *Am J Nephrol* 1994;14(1):72–75.
1050. Cartery C, Guilbeau-Frugier C, Esposito L, et al. Systematic kidney biopsies after acute allograft pyelonephritis. *Exp Clin Transplant* 2013;11:239–244.
1051. Alexander S, Varughese S, David VG, et al. Extensive emphysematous pyelonephritis in a renal allograft treated conservatively: case report and review of the literature. *Transpl Infect Dis* 2012;14(6):E150–E155.
1052. Floc'h AP, Buchler M, Bruyere F. [Characteristics of acute pyelonephritis in renal transplant patients]. *Prog Urol* 2012;22(7):397–401. Caracteristiques des pyelonephrites aigues chez les patients transplantés renaux.
1053. Fiorante S, Fernandez-Ruiz M, Lopez-Medrano F, et al. Acute graft pyelonephritis in renal transplant recipients: incidence, risk factors and long-term outcome. *Nephrol Dial Transplant* 2011;26(3):1065–1073.
1054. Kamath NS, John GT, Neelakantan N, et al. Acute graft pyelonephritis following renal transplantation. *Transpl Infect Dis* 2006;8(3):140–147.
1055. Giral M, Pascuariello G, Karam G, et al. Acute graft pyelonephritis and long-term kidney allograft outcome. *Kidney Int* 2002;61(5):1880–1886.
1056. Siliano PR, Rocha LA, Medina-Pestana JO, et al. The role of host factors and bacterial virulence genes in the development of pyelonephritis caused by *Escherichia coli* in renal transplant recipients. *Clin J Am Soc Nephrol* 2010;5(7):1290–1297.
1057. Dunn SP, Vinocur CD, Hanevold C, et al. Pyelonephritis following pediatric renal transplant: increased incidence with vesicoureteral reflux. *J Pediatr Surg* 1987;22(12):1095–1099.
1058. Mohsin N, Budruddin M, Lala S, et al. Emphysematous pyelonephritis: a case report series of four patients with review of literature. *Ren Fail* 2009;31(7):597–601.
1059. Vivek V, Panda A, Devasia A. Emphysematous pyelonephritis in a renal transplant recipient—Is it possible to salvage the graft? *Ann Transplant* 2012;17(3):138–141.
1060. Hakim NS, Benedetti E, Pirenne J, et al. Complications of ureterovesical anastomosis in kidney transplant patients: the Minnesota experience. *Clin Transplant* 1994;8(6):504–507.
1061. Karam G, Maillet F, Parant S, et al. Ureteral necrosis after kidney transplantation: risk factors and impact on graft and patient survival. *Transplantation* 2004;78(5):725–729.
1062. Jefferson RH, Burns JR. Urological evaluation of adult renal transplant recipients. *J Urol* 1995;153(3 Pt 1):615–618.
1063. Goel M, Flechner SM, Zhou L, et al. The influence of various maintenance immunosuppressive drugs on lymphocele formation and treatment after kidney transplantation. *J Urol* 2004;171(5):1788–1792.
1064. Merion RM, Calne RY. Allograft renal vein thrombosis. *Transplant Proc* 1985;17:1746–1750.
1065. Arruda JAL, Gutierrez LF, Jonasson O, et al. Renal-vein thrombosis in kidney allografts. *Lancet* 1973;2:585–586.
1066. Bakir N, Sluiter WJ, Ploeg RJ, et al. Primary renal graft thrombosis. *Nephrol Dial Transplant* 1996;11(1):140–147.
1067. Osman Y, Shokeir A, Ali-el-Dein B, et al. Vascular complications after live donor renal transplantation: study of risk factors and effects on graft and patient survival. *J Urol* 2003;169(3):859–862.
1068. Benedetti E, Troppmann C, Gillingham K, et al. Short- and long-term outcomes of kidney transplants with multiple renal arteries. *Ann Surg* 1995;221(4):406–414.
1069. D'Cruz DP. Renal manifestations of the antiphospholipid syndrome. *Lupus* 2005;14(1):45–48.
1070. Simmons RL, Tallent MB, Kjellstrand CM, et al. Renal allograft rejection simulated by arterial stenosis. *Surgery* 1970;68(5):800–804.
1071. Bruno S, Remuzzi G, Ruggenti P. Transplant renal artery stenosis. *J Am Soc Nephrol* 2004;15(1):134–141.
1072. Wong W, Fynn SP, Higgins RM, et al. Transplant renal artery stenosis in 77 patients—Does it have an immunological cause? *Transplantation* 1996;61(2):215–219.
1073. Heimbach D, Miersch WD, Buszello H, et al. Is the transplant-preserving management of renal allograft rupture justified? *Br J Urol* 1995;75(6):729–732.
1074. Said R, Duarte R, Chaballout A, et al. Spontaneous rupture of renal allograft. *Urology* 1994;43(4):554–558.
1075. Shahrokht H, Rasouli H, Zargar MA, et al. Spontaneous kidney allograft rupture. *Transplant Proc* 2005;37(7):3079–3080.
1076. Soler R, Perez-Fontan FJ, Lago M, et al. Renal allograft rupture: diagnostic role of ultrasound. *Nephrol Dial Transplant* 1992;7(8):871–874.
1077. Chan YH, Wong KM, Lee KC, et al. Spontaneous renal allograft rupture attributed to acute tubular necrosis. *Am J Kidney Dis* 1999;34(2):355–358.
1078. Monga G, Mazzucco G, Basolo B, et al. Membranous glomerulonephritis (MGN) in transplanted kidneys: investigation on 256 renal allografts. *Mod Pathol* 1993;6(3):249–258.
1079. Aline-Fardin A, Riffe G, Martin L, et al. Recurrent and de novo membranous glomerulopathy after kidney transplantation. *Transplant Proc* 2009;41(2):669–671.
1080. Honda K, Horita S, Toki D, et al. De novo membranous nephropathy and antibody-mediated rejection in transplanted kidney. *Clin Transplant* 2011;25(2):191–200.

1081. Hariharan S, Adams MB, Brennan DC, et al. Recurrent and de novo glomerular disease after renal transplantation: a report from Renal Allograft Disease Registry (RADR). *Transplantation* 1999;68(5):635–641.
1082. Charpentier B, Lévy M. Étude coopérative des glomérulonephrites extra-membraneuses de novo sur allogreffe rénale humaine: rapport de 19 nouveaux cas sur 1550 transplantés rénaux du groupe de transplantation de l'Île de France. *Nephrology* 1982;3(158):158–166.
1083. Schwarz A, Krause PH, Offermann G, et al. Recurrent and de novo renal disease after kidney transplantation with or without cyclosporine A. *Am J Kidney Dis* 1991;17(5):524–531.
1084. Heidet L, Gagnadoux ME, Beziou A, et al. Recurrence of de novo membranous glomerulonephritis on renal grafts. *Clin Nephrol* 1994;41(5):314–318.
1085. Antignac C, Hinglais N, Gubler MC, et al. De novo membranous glomerulonephritis in renal allografts in children. *Clin Nephrol* 1988;30(1):1–7.
1086. Morales JM, Pascual-Capdevila J, Campistol JM, et al. Membranous glomerulonephritis associated with hepatitis C virus infection in renal transplant patients. *Transplantation* 1997;63(11):1634–1639.
1087. Cruzado JM, Carrera M, Torras J, et al. Hepatitis C virus infection and de novo glomerular lesions in renal allografts. *Am J Transplant* 2001;1(2):171–178.
1088. Noel LH, Aucouturier P, Monteiro RC, et al. Glomerular and serum immunoglobulin G subclasses in membranous nephropathy and anti-glomerular basement membrane nephritis. *Clin Immunol Immunopathol* 1988;46(2):186–194.
1089. Truong L, Gelfand J, D'Agati V, et al. De novo membranous glomerulonephropathy in renal allografts: a report of ten cases and review of the literature. *Am J Kidney Dis* 1989;14(2):131–144.
1090. Collins AB, Beck LH, Jr., Satoskar AA, et al. De novo MGN is immunologically distinct from idiopathic MGN and associated with C4d deposition. *J Am Soc Nephrol* 2010;(Abstract).
1091. Debiec H, Martin L, Jouanneau C, et al. Autoantibodies specific for the phospholipase A2 receptor in recurrent and De Novo membranous nephropathy. *Am J Transplant* 2011;11(10):2144–2152.
1092. Collins AB, Beck LH, Jr., Satoskar AA, et al. De novo MGN is immunologically distinct from idiopathic MGN and associated with C4d deposition. *J Am Soc Nephrol* 2010. (Abstract).
1093. El Kossi M, Harmer A, Goodwin J, et al. De novo membranous nephropathy associated with donor-specific alloantibody. *Clin Transplant* 2008;22(1):124–127.
1094. Larsen CP, Walker PD. Phospholipase A2 receptor (PLA2R) staining is useful in the determination of de novo versus recurrent membranous glomerulopathy. *Transplantation* 2013;95(10):1259–1262.
1095. Ponticelli C, Glassock RJ. De novo membranous nephropathy (MN) in kidney allografts. A peculiar form of alloimmune disease? *Transpl Int* 2012;25(12):1205–1210.
1096. Thoenes GH, Pielsticker K, Schubert G. Transplantation-induced immune complex kidney disease in rats with unilateral manifestation in the allografted kidney. *Lab Invest* 1979;41(4):321–333.
1097. Pirson Y, Ghysen J, Cosyns JP, et al. Aetiology and prognosis of de novo graft membranous nephropathy. *Proc Eur Dial Transpl Assoc Eur Ren Assoc* 1985;21:672–676.
1098. Kearney N, Podolak J, Matsumura L, et al. Patterns of IgG subclass deposits in membranous glomerulonephritis in renal allografts. *Transplant Proc* 2011;43(10):3743–3746.
1099. Gobel J, Olbricht CJ, Offner G, et al. Kidney transplantation in Alport's syndrome: long-term outcome and allograft anti-GBM nephritis. *Clin Nephrol* 1992;38(6):299–304.
1100. Querin S, Noel LH, Grunfeld JP, et al. Linear glomerular IgG fixation in renal allografts: incidence and significance in Alport's syndrome. *Clin Nephrol* 1986;25(134):134–140.
1101. Nyberg G, Friman S, Svalander C, et al. Spectrum of hereditary renal disease in a kidney transplant population. *Nephrol Dial Transplant* 1995;10(6):859–865.
1102. McCoy RC, Johnson HK, Stone WJ, et al. Absence of nephritogenic GBM antigen(s) in some patients with hereditary nephritis. *Kidney Int* 1982;21(4):642–652.
1103. Kashtan C, Fish AJ, Kleppel M, et al. Nephritogenic antigen determinants in epidermal and renal basement membranes of kindreds with Alport type familial nephritis. *J Clin Invest* 1986;78(1035):1035–1044.
1104. Fleming SJ, Savage CO, McWilliam LJ, et al. Anti-glomerular basement membrane antibody-mediated nephritis complicating transplantation in a patient with Alport's syndrome. *Transplantation* 1988;46(6):857–859.
1105. Kalluri R, Torre A, Shield CF, 3rd, et al. Identification of alpha3, alpha4, and alpha5 chains of type IV collagen as alloantigens for Alport posttransplant anti-glomerular basement membrane antibodies. *Transplantation* 2000;69(4):679–683.
1106. Kashtan CE. Alport syndrome and thin glomerular basement membrane disease. *J Am Soc Nephrol* 1998;9(9):1736–1750.
1107. Kashtan CE. Alport syndrome: renal transplantation and donor selection. *Ren Fail* 2000;22(6):765–768.
1108. Lemmink HH, Schroder CH, Monnens LA, et al. The clinical spectrum of type IV collagen mutations. *Hum Mutat* 1997;9(6):477–499.
1109. Kashtan CE. Renal transplantation in patients with Alport syndrome. *Pediatr Transplant* 2006;10(6):651–657.
1110. de Sandes-Freitas TV, Holanda-Cavalcanti A, Mastroianni-Kirsztajn G, et al. Late presentation of Alport posttransplantation anti-glomerular basement membrane disease. *Transplant Proc* 2011;43(10):4000–4001.
1111. Savige J, Gregory M, Gross O, et al. Expert guidelines for the management of Alport syndrome and thin basement membrane nephropathy. *J Am Soc Nephrol* 2013;24(3):364–375.
1112. Pedchenko V, Bondar O, Fogo AB, et al. Molecular architecture of the Goodpasture autoantigen in anti-GBM nephritis. *N Engl J Med* 2010;363(4):343–354.
1113. Oлару F, Wang XP, Luo W, et al. Proteolysis breaks tolerance toward intact alpha345(IV) collagen, eliciting novel anti-glomerular basement membrane autoantibodies specific for alpha345NC1 hexamers. *J Immunol* 2013;190(4):1424–1432.
1114. Browne G, Brown PA, Tomson CR, et al. Retransplantation in Alport post-transplant anti-GBM disease. *Kidney Int* 2004;65(2):675–681.
1115. Vangelista A, Frasca GM, Martella D, et al. Glomerulonephritis in renal transplantation. *Nephrol Dial Transplant* 1990;1:42–46.
1116. Diaz JJ, Valenzuela R, Gephardt G, et al. Anti-glomerular and anti-tubular basement membrane nephritis in a renal allograft recipient with Alport's syndrome. *Arch Pathol Lab Med* 1994;118(7):728–731.
1117. Goldman M, Depierreux M, De Pauw L, et al. Failure of two subsequent renal grafts by anti-GBM glomerulonephritis in Alport's syndrome: case report and review of the literature. *Transpl Int* 1990;3(2):82–85.
1118. Milliner DS, Pierdes AM, Holley KE. Renal transplantation in Alport's syndrome. Anti-glomerular basement membrane glomerulonephritis in the allograft. *Mayo Clin Proc* 1982;57:35–42.
1119. Kuusniemi AM, Qvist E, Sun Y, et al. Plasma exchange and retransplantation in recurrent nephrosis of patients with congenital nephrotic syndrome of the Finnish type (NPHS1). *Transplantation* 2007;83(10):1316–1323.
1120. Patrakka J, Ruotsalainen V, Reponen P, et al. Recurrence of nephrotic syndrome in kidney grafts of patients with congenital nephrotic syndrome of the Finnish type: role of nephrin. *Transplantation* 2002;73(3):394–403.
1121. Lane PH, Schnaper HW, Vernier RL, et al. Steroid-dependent nephrotic syndrome following renal transplantation for congenital nephrotic syndrome. *Pediatr Nephrol* 1991;5(3):300–303.
1122. Flynn JT, Schulman SL, deChadarevian JP, et al. Treatment of steroid-resistant post-transplant nephrotic syndrome with cyclophosphamide in a child with congenital nephrotic syndrome. *Pediatr Nephrol* 1992;6(6):553–555.
1123. Chaudhuri A, Kambham N, Sutherland S, et al. Rituximab treatment for recurrence of nephrotic syndrome in a pediatric patient after renal transplantation for congenital nephrotic syndrome of Finnish type. *Pediatr Transplant* 2012;16(5):E183–E187.
1124. Nadasdy T, Allen C, Zand MS. Zonal distribution of glomerular collapse in renal allografts: possible role of vascular changes. *Hum Pathol* 2002;33(4):437–441.
1125. Bhatena DB. Glomerular size and the association of focal glomerulosclerosis in long-surviving human renal allografts. *J Am Soc Nephrol* 1993;4(6):1316–1326.
1126. Stokes MB, Davis CL, Alpers CE. Collapsing glomerulopathy in renal allografts: a morphological pattern with diverse clinicopathologic associations. [see comments]. *Am J Kidney Dis* 1999;33(4):658–666.

1127. Goes N, Colvin RB. Renal failure nine years after a heart-lung transplant. *N Engl J Med* 2006;in press.
1128. Moudgil A, Nast CC, Bagga A, et al. Association of parvovirus B19 infection with idiopathic collapsing glomerulopathy. *Kidney Int* 2001;59(6):2126–2133.
1129. Porignaux R, Vuiblet V, Barbe C, et al. Frequent occurrence of parvovirus B19 DNAemia in the first year after kidney transplantation. *J Med Virol* 2013;85(6):1115–1121.
1130. Woolley AC, Rosenberg ME, Burke BA, et al. De novo focal glomerulosclerosis after kidney transplantation. *Am J Med* 1988;84(2):310–314.
1131. Neumayer HH, Huls S, Schreiber M, et al. Kidneys from pediatric donors: risk versus benefit. *Clin Nephrol* 1994;41(2):94–100.
1132. Zafarmand AA, Baranowska-Daca E, Ly PD, et al. De novo minimal change disease associated with reversible post-transplant nephrotic syndrome. A report of five cases and review of literature. *Clin Transplant* 2002;16(5):350–361.
1133. Madhan KK, Temple-Camp CR. Late de novo minimal change disease in a renal allograft. *Saudi J Kidney Dis Transpl* 2009;20(2):266–269.
1134. Mochizuki Y, Iwata T, Nishikido M, et al. De novo minimal change disease after ABO-incompatible kidney transplantation. *Clin Transplant* 2012;26(Suppl 24):81–85.
1135. Qian Q, Nasr SH, Fidler ME, et al. De novo AL amyloidosis in the kidney allograft. *Am J Transplant* 2011;11(3):606–612.
1136. De Keyser K, Van Laecke S, Peeters P, et al. De novo thrombotic microangiopathy induced by cytomegalovirus infection leading to renal allograft loss. *Am J Nephrol* 2010;32(5):491–496.
1137. Le Quintrec M, Lionet A, Kamar N, et al. Complement mutation-associated de novo thrombotic microangiopathy following kidney transplantation. *Am J Transplant* 2008;8(8):1694–1701.
1138. Chandran S, Baxter-Lowe L, Olson JL, et al. Eculizumab for the treatment of de novo thrombotic microangiopathy post simultaneous pancreas-kidney transplantation—A case report. *Transplant Proc* 2011;43(5):2097–2101.
1139. Bhalla V, Nast CC, Stollenwerk N, et al. Recurrent and de novo diabetic nephropathy in renal allografts. *Transplantation* 2003;75(1):66–71.
1140. Isaac J, Herrera GA, Shihab FS. De novo fibrillary glomerulopathy in the renal allograft of a patient with systemic lupus erythematosus. *Nephron* 2001;87(4):365–368.
1141. Albawardi A, Satoskar A, Von Visger J, et al. Proliferative glomerulonephritis with monoclonal IgG deposits recurs or may develop de novo in kidney allografts. *Am J Kidney Dis* 2011;58(2):276–281.
1142. Maas RJ, Deegens JK, van den Brand JA, et al. A retrospective study of focal segmental glomerulosclerosis: clinical criteria can identify patients at high risk for recurrent disease after first renal transplantation. *BMC Nephrol* 2013;14:47.
1143. Cravedi P, Kopp JB, Remuzzi G. Recent progress in the pathophysiology and treatment of FSGS recurrence. *Am J Transplant* 2013;13(2):266–274.
1144. Canaud G, Dion D, Zuber J, et al. Recurrence of nephrotic syndrome after transplantation in a mixed population of children and adults: course of glomerular lesions and value of the Columbia classification of histological variants of focal and segmental glomerulosclerosis (FSGS). *Nephrol Dial Transplant* 2010;25(4):1321–1328.
1145. Bhatena DB, Weiss JH, McMorro RG, et al. Focal and segmental glomerular sclerosis in reflux nephropathy. *Am J Med* 1980;68(886):886–992.
1146. Kiproff DD, Colvin RB, McCluskey RT. Focal and segmental glomerulosclerosis and proteinuria associated with unilateral renal agenesis. *Lab Invest* 1982;46(3):275–281.
1147. Axelsen RA, Seymour AE, Mathew TH, et al. Recurrent focal glomerulosclerosis in renal transplants. *Clin Nephrol* 1984;21(110):110–112.
1148. Weber S, Tonshoff B. Recurrence of focal segmental glomerulosclerosis in children after renal transplantation: clinical and genetic aspects. *Transplantation* 2005;80 (1S Suppl):S128–S134.
1149. Conlon PJ, Butterly D, Albers F, et al. Clinical and pathologic features of familial focal segmental glomerulosclerosis. *Am J Kidney Dis* 1995;26(1):34–40.
1150. Goodman DJ, Clarke B, Hope RN, et al. Familial focal glomerulosclerosis: a genetic linkage to the HLA locus? *Am J Nephrol* 1995;15(5):442–445.
1151. Becker-Cohen R, Bruschi M, Rinat C, et al. Recurrent nephrotic syndrome in homozygous truncating NPHS2 mutation is not due to anti-podocin antibodies. *Am J Transplant* 2007;7(1):256–260.
1152. Ijpeelaar DH, Farris AB, Goemaere N, et al. Fidelity and evolution of recurrent FSGS in renal allografts. *J Am Soc Nephrol* 2008;19(11):2219–2224.
1153. Artero M, Biava C, Amend W, et al. Recurrent focal glomerulosclerosis: natural history and response to therapy. *Am J Med* 1992;92(4):375–383.
1154. Tejani A, Stablein DH. Recurrence of focal segmental glomerulosclerosis posttransplantation: a special report of the North American Pediatric Renal Transplant Cooperative Study. *J Am Soc Nephrol* 1992;2(12 Suppl):S258–S263.
1155. Leumann EP, Briner J, Donckerwolcke RA, et al. Recurrence of focal segmental glomerulosclerosis in the transplanted kidney. *Acta Pathol Microbiol Immunol Scand* 1980;94(69):69–76.
1156. Pinto J, Lacerda G, Cameron JS, et al. Recurrence of focal segmental glomerulosclerosis in renal allografts. *Transplantation* 1981;32(83):83–89.
1157. Striegel JE, Sibley RK, Fryd DS, et al. Recurrence of focal segmental sclerosis in children following renal transplantation. *Kidney Int Suppl* 1986;19:S44–S50.
1158. Broyer M, Gagnadoux MF, Guest G, et al. Kidney transplantation in children: results of 383 grafts performed at Enfants Malades Hospital from 1973 to 1984. *Adv Nephrol* 1987;16:307–333.
1159. Maizel SE, Sibley RK, Horstman JP, et al. Incidence and significance of recurrent focal segmental glomerulosclerosis in renal allograft recipients. *Nephron* 1981;26(180):180–183.
1160. Senguttuvan P, Cameron JS, Hartley RB, et al. Recurrence of focal segmental glomerulosclerosis in transplanted kidneys: analysis of incidence and risk factors in 59 allografts. *Pediatr Nephrol* 1990;4(1):21–28.
1161. Derwiler RK, Falk RJ, Hogan SL, et al. Collapsing glomerulopathy: a clinically and pathologically distinct variant of focal segmental glomerulosclerosis. *Kidney Int* 1994;45(5):1416–1424.
1162. Weber S, Tonshoff B. Recurrence of focal-segmental glomerulosclerosis in children after renal transplantation: clinical and genetic aspects. *Transplantation* 2005;80(1 Suppl):S128–S134.
1163. Schwarz A, Krause PH, Offermann G, et al. Recurrent diseases in the renal allograft. *J Am Soc Nephrol* 1991;2(2):109–121.
1164. Hosenpud J, Piering WF, Garancis JC, et al. Successful second kidney transplantation in a patient with focal glomerulosclerosis A case report. *Am J Nephrol* 1985;5(299):299–304.
1165. Verani RR, Hawkins EP. Recurrent focal segmental glomerulosclerosis: a pathological study of the early lesion. *Am J Nephrol* 1986;6(263):263–270.
1166. Harrison DJ, Jenkins D, Dick J. An unusual interpodocyte cell junction and its appearance in a transplant graft kidney. *J Clin Pathol* 1988;41(2):155–157.
1167. Bariety J, Bruneval P, Hill G, et al. Posttransplantation relapse of FSGS is characterized by glomerular epithelial cell transdifferentiation. *J Am Soc Nephrol* 2001;12(2):261–274.
1168. Kemeny E, Mihatsch MJ, Durmuller U, et al. Podocytes lose their adhesive phenotype in focal segmental glomerulosclerosis. *Clin Nephrol* 1995;43(2):71–83.
1169. Fatima H, Moeller MJ, Smeets B, et al. Parietal epithelial cell activation marker in early recurrence of FSGS in the transplant. *Clin J Am Soc Nephrol* 2012;7(11):1852–1858.
1170. Fornoni A, Sageshima J, Wei C, et al. Rituximab targets podocytes in recurrent focal segmental glomerulosclerosis. *Sci Transl Med* 2011;3(85):85ra46.
1171. Gallon L, Leventhal J, Skaro A, et al. Resolution of recurrent focal segmental glomerulosclerosis after retransplantation. *N Engl J Med* 2012;366(17):1648–1649.
1172. Wei C, Trachtman H, Li J, et al. Circulating suPAR in two cohorts of primary FSGS. *J Am Soc Nephrol* 2012;23(12):2051–2059.
1173. Wei C, El Hindi S, Li J, et al. Circulating urokinase receptor as a cause of focal segmental glomerulosclerosis. *Nat Med* 2011;17(8):952–960.
1174. Bock ME, Price HE, Gallon L, et al. Serum soluble urokinase-type plasminogen activator receptor levels and idiopathic FSGS in children: a single-center report. *Clin J Am Soc Nephrol* 2013;8:1304–1311.
1175. Lopez-Hellin J, Cantarell C, et al. A form of apolipoprotein a-I is found specifically in relapses of focal segmental glomerulosclerosis following transplantation. *Am J Transplant* 2013;13(2):493–500.

1176. Pescovitz MD, Book BK, Sidner RA. Resolution of recurrent focal segmental glomerulosclerosis proteinuria after rituximab treatment. *N Engl J Med* 2006;354(18):1961–1963.
1177. Leroy S, Guignon V, Bruckner D, et al. Successful anti-TNF α treatment in a child with posttransplant recurrent focal segmental glomerulosclerosis. *Am J Transplant* 2009;9(4):858–861.
1178. Yu CC, Fornoni A, Weins A, et al. Abatacept in B7-1-positive proteinuric kidney disease. *N Engl J Med* 2013;369(25):2416–2423.
1179. Andresdottir MB, Assmann KJ, Hoitsma AJ, et al. Recurrence of type I membranoproliferative glomerulonephritis after renal transplantation: analysis of the incidence, risk factors, and impact on graft survival. *Transplantation* 1997;63(11):1628–1633.
1180. Floege J. Recurrent glomerulonephritis following renal transplantation: an update. *Nephrol Dial Transplant* 2003;18(7):1260–1265.
1181. Couser W. Recurrent glomerulonephritis in the renal allograft: an update of selected areas. *Exp Clin Transplant* 2005;3(1):283–288.
1182. Morzycka M, Croker BP, Jr, Siegler HF, et al. Evaluation of recurrent glomerulonephritis in kidney allografts. *Am J Med* 1982;72(588):588–598.
1183. Lorenz EC, Sethi S, Leung N, et al. Recurrent membranoproliferative glomerulonephritis after kidney transplantation. *Kidney Int* 2010;77(8):721–728.
1184. Little MA, Dupont P, Campbell E, et al. Severity of primary MPGN, rather than MPGN type, determines renal survival and post-transplantation recurrence risk. *Kidney Int* 2006;69(3):504–511.
1185. Zollinger HU, Mihatsch MJ. *Renal Pathology in Biopsy*. Berlin, Heidelberg, New York: Springer Verlag; 1978:581.
1186. Croker B, Ramos E. Pathology of the renal allograft. In: Tisher C, Brenner BM, eds. *Renal Pathology—With Clinical and Functional Correlations*. 2nd ed. Philadelphia: JB Lippincott Company; 1989:1591–1640.
1187. Habib R, Malheiros D, Charbit M, et al. Long term results in 70 pediatric renal transplants after more than 10 years. Histological study. *Ann Pediatr (Paris)* 1991;38(6):419–425.
1188. Bomback AS, Smith RJ, Barile GR, et al. Eculizumab for dense deposit disease and C3 glomerulonephritis. *Clin J Am Soc Nephrol* 2012;7(5):748–756.
1189. Zuber J, Fakhouri F, Roumenina LT, et al. Use of eculizumab for atypical haemolytic uraemic syndrome and C3 glomerulopathies. *Nat Rev Nephrol* 2012;8(11):643–657.
1190. Herlitz LC, Bomback AS, Markowitz GS, et al. Pathology after eculizumab in dense deposit disease and C3 GN. *J Am Soc Nephrol* 2012;23(7):1229–1237.
1191. McCaughan JA, O'Rourke DM, Courtney AE. Recurrent dense deposit disease after renal transplantation: an emerging role for complementary therapies. *Am J Transplant* 2012;12(4):1046–1051.
1192. Curtis JJ, Wyatt RJ, Bhatena D, et al. Renal transplantation for patients with type I and type II membranoproliferative glomerulonephritis: serial complement and nephritic factor measurements and the problem of recurrence of disease. *Am J Med* 1979;66:216–225.
1193. Andresdottir MB, Assmann KJ, Hoitsma AJ, et al. Renal transplantation in patients with dense deposit disease: morphological characteristics of recurrent disease and clinical outcome. *Nephrol Dial Transplant* 1999;14(7):1723–1731.
1194. Appel GB, Cook HT, Hageman G, et al. Membranoproliferative glomerulonephritis type II (dense deposit disease): an update. *J Am Soc Nephrol* 2005;16(5):1392–1403.
1195. Braun MC, Stablein DM, Hamiwka LA, et al. Recurrence of membranoproliferative glomerulonephritis type II in renal allografts: the North American Pediatric Renal Transplant Cooperative Study experience. *J Am Soc Nephrol* 2005;16(7):2225–2233.
1196. Beaufils H, Gubler MC, Karam J, et al. Dense deposit disease: long term follow-up of three cases of recurrence after transplantation. *Clin Nephrol* 1977;7(1):31–37.
1197. Jansen JH, Hogasen K, Harboe M, et al. In situ complement activation in porcine membranoproliferative glomerulonephritis type II. *Kidney Int* 1998;53(2):331–349.
1198. Droz D, Nabarra B, Noel LH, et al. Recurrence of dense deposits in transplanted kidneys: I. Sequential survey of the lesions. *Kidney Int* 1979;15(386):386–395.
1199. Muller T, Sikora P, Offner G, et al. Recurrence of renal disease after kidney transplantation in children: 24 years of experience in a single center. *Clin Nephrol* 1998;49(2):82–90.
1200. Boyer O, Noel LH, Balzamo E, et al. Complement factor H deficiency and posttransplantation glomerulonephritis with isolated C3 deposits. *Am J Kidney Dis* 2008;51(4):671–677.
1201. Sethi S, Fervenza FC, Zhang Y, et al. C3 glomerulonephritis: clinicopathological findings, complement abnormalities, glomerular proteomic profile, treatment, and follow-up. *Kidney Int* 2012;82(4):465–473.
1202. Chiurciu C, Ruggenti P, Remuzzi G. Thrombotic microangiopathy in renal transplantation. *Ann Transplant* 2002;7(1):28–33.
1203. Bassani CE, Ferraris J, Gianantonio CA, et al. Renal transplantation in patients with classical haemolytic-uraemic syndrome. *Pediatr Nephrol* 1991;5(5):607–611.
1204. Hebert D, Kim EM, Sibley RK, et al. Post-transplantation outcome of patients with hemolytic-uremic syndrome: update. *Pediatr Nephrol* 1991;5(1):162–167.
1205. Le Quintrec M, Zuber J, Moulin B, et al. Complement genes strongly predict recurrence and graft outcome in adult renal transplant recipients with atypical hemolytic and uremic syndrome. *Am J Transplant* 2013;13(3):663–675.
1206. Kamal Aziz A, Mousson C, Berthoux F, et al. Renal transplantation outcome in selected recipients with IgA nephropathy as native disease: A bicentric study. *Ann Transplant* 2012;17(3):45–51.
1207. Moroni G, Longhi S, Quaglini S, et al. The long-term outcome of renal transplantation of IgA nephropathy and the impact of recurrence on graft survival. *Nephrol Dial Transplant* 2013;28:1305–1314.
1208. Stack A, Campbell E, Browne O, et al. Prevalence and predictors of recurrent IgA nephropathy following renal transplantation. *Irish J Med Sci* 2000;169(4):248–252.
1209. Han SS, Huh W, Park SK, et al. Impact of recurrent disease and chronic allograft nephropathy on the long-term allograft outcome in patients with IgA nephropathy. *Transpl Int* 2010;23(2):169–175.
1210. Bantis C, Heering PJ, Aker S, et al. Influence of interleukin-10 gene G-1082A polymorphism on recurrent IgA nephropathy. *J Nephrol* 2008;21(6):941–946.
1211. Ortiz F, Gelpi R, Koskinen P, et al. IgA nephropathy recurs early in the graft when assessed by protocol biopsy. *Nephrol Dial Transplant* 2012;27(6):2553–2558.
1212. Clayton P, McDonald S, Chadban S. Steroids and recurrent IgA nephropathy after kidney transplantation. *Am J Transplant* 2011;11(8):1645–1649.
1213. Tang Z, Ji SM, Chen DR, et al. Recurrent or de novo IgA nephropathy with crescent formation after renal transplantation. *Ren Fail* 2008;30(6):611–616.
1214. Jeong HJ, Park SK, Cho YM, et al. Progression of renal allograft histology after renal transplantation in recurrent and nonrecurrent immunoglobulin A nephropathy. *Hum Pathol* 2008;39(10):1511–1518.
1215. Meulders Q, Pirson Y, Cosyns J-P, et al. Course of Henoch-Schönlein nephritis after renal transplantation. *Transplantation* 1994;58:1179.
1216. Lhotta K, König P, Hintner H, et al. Renal disease in a patient with hereditary complete deficiency of the fourth component of complement. *Nephron* 1990;56(2):206–211.
1217. Dabade TS, Grande JP, Norby SM, et al. Recurrent idiopathic membranous nephropathy after kidney transplantation: a surveillance biopsy study. *Am J Transplant* 2008;8(6):1318–1322.
1218. Blosser CD, Ayalon R, Nair R, et al. Very early recurrence of anti-Phospholipase A2 receptor-positive membranous nephropathy after transplantation. *Am J Transplant* 2012;12(6):1637–1642.
1219. Sprangers B, Lefkowitz GI, Cohen SD, et al. Beneficial effect of rituximab in the treatment of recurrent idiopathic membranous nephropathy after kidney transplantation. *Clin J Am Soc Nephrol* 2010;5(5):790–797.
1220. Cameron JS. Glomerulonephritis in renal transplants. *Transplantation* 1982;34(237):237–245.
1221. Obermiller LE, Hoy WE, Eversole M, et al. Recurrent membranous glomerulonephritis in two renal transplants. *Transplantation* 1985;40(100):100–102.
1222. Lieberthal W, Bernard DB, Donohoe JF, et al. Rapid recurrence of membranous nephropathy in a related allograft. *Clin Nephrol* 1979;12(5):222–228.

1223. Crosson JT, Wathen RL, Raij L, et al. Recurrence of idiopathic membranous nephropathy in a renal allograft. *Arch Intern Med* 1975;135(8):1101–1106.
1224. Berger BE, Vincenti F, Biava C, et al. De novo and recurrent membranous glomerulopathy following kidney transplantation. *Transplantation* 1983;35(4):315–319.
1225. Stahl R, Hoxha E, Fechner K. PLA2R autoantibodies and recurrent membranous nephropathy after transplantation. *N Engl J Med* 2010;363(5):496–498.
1226. Ayalon R, Beck LH, Jr, Fervenza FC, et al. Do anti-phospholipase A2 receptor antibodies predict recurrence of membranous nephropathy after transplantation? *J Am Soc Nephrol* 2012;abstract FR-OR151.
1227. Debiec H, Hanoy M, Francois A, et al. Recurrent membranous nephropathy in an allograft caused by IgG3kappa targeting the PLA2 receptor. *J Am Soc Nephrol* 2012.
1228. Rodriguez EF, Cosio FG, Nasr SH, et al. The pathology and clinical features of early recurrent membranous glomerulonephritis. *Am J Transplant* 2012;12(4):1029–1038.
1229. Collins AB, Farkash EA, Beck LH Jr, et al. Detection of PLA2R in glomerular deposits in membranous nephropathy cases seronegative for anti-PLA2R. *J Am Soc Nephrol* 2012;Suppl Abstr Annual Meeting:OR008.
1230. Larsen CP, Walker PD. Phospholipase A2 receptor (PLA2R) staining is useful in the determination of de novo versus recurrent membranous glomerulopathy. *Transplantation* 2013;95(10):1259–1262.
1231. Weclawiak H, Ribes D, Guilbeau-Frugier C, et al. Relapse of membranous glomerulopathy after kidney transplantation: sustained remittance induced by rituximab. *Clin Nephrol* 2008;69(5):373–376.
1232. Gallon L, Chhabra D. Anti-CD20 monoclonal antibody (rituximab) for the treatment of recurrent idiopathic membranous nephropathy in a renal transplant patient. *Am J Transplant* 2006;6(12):3017–3021.
1233. El-Zoghby ZM, Grande JP, Fraile MG, et al. Recurrent idiopathic membranous nephropathy: early diagnosis by protocol biopsies and treatment with anti-CD20 monoclonal antibodies. *Am J Transplant* 2009;9(12):2800–2807.
1234. Briggs WA, Johnson JR, Teichman S, et al. Antiglomerular basement membrane antibody mediated glomerulonephritis and Goodpasture's syndrome. *Medicine* 1979;58(348):348–361.
1235. Collins AB, Colvin RB. Kidney and lung disease mediated by glomerular basement membrane antibodies: detection by western blot analysis. In: Rose NR, de Macario EC, Folds JD, Lane HC, Nakamura RM, eds. *Manual of Clinical Laboratory Methods*. Washington, DC: ASM Press; 1997:1008–1012.
1236. Odorico JS, Knechtle SJ, Rayhill SC, et al. The influence of native nephrectomy on the incidence of recurrent disease following renal transplantation for primary glomerulonephritis. *Transplantation* 1996;61(2):228–234.
1237. Deegens JK, Artz MA, Hoitsma AJ, et al. Outcome of renal transplantation in patients with pauci-immune small vessel vasculitis or anti-GBM disease. *Clin Nephrol* 2003;59(1):1–9.
1238. Sauter M, Schmid H, Anders HJ, et al. Loss of a renal graft due to recurrence of anti-GBM disease despite rituximab therapy. *Clin Transplant* 2009;23(1):132–136.
1239. Borza DB, Chedid MF, Colon S, et al. Recurrent Goodpasture's disease secondary to a monoclonal IgA1-kappa antibody autoreactive with the alpha1/alpha2 chains of type IV collagen. *Am J Kidney Dis* 2005;45(2):397–406.
1240. Trpkov K, Abdulkareem F, Jim K, et al. Recurrence of anti-GBM antibody disease twelve years after transplantation associated with de novo IgA nephropathy. *Clin Nephrol* 1998;49(2):124–128.
1241. Gera M, Griffin MD, Specks U, et al. Recurrence of ANCA-associated vasculitis following renal transplantation in the modern era of immunosuppression. *Kidney Int* 2007;71(12):1296–1301.
1242. Tang W, Bose B, McDonald SP, et al. The Outcomes of Patients with ESRD and ANCA-Associated Vasculitis in Australia and New Zealand. *Clin J Am Soc Nephrol* 2013;8(5):773–780.
1243. Nachman PH, Segelmark M, Westman K, et al. Recurrent ANCA-associated small vessel vasculitis after transplantation: a pooled analysis. *Kidney Int* 1999;56(4):1544–1550.
1244. Reaich D, Cooper N, Main J. Rapid catastrophic onset of Wegener's granulomatosis in a renal transplant. *Nephron* 1994;67(3):354–357.
1245. Elmedhem A, Adu D, Savage CO. Relapse rate and outcome of ANCA-associated small vessel vasculitis after transplantation. *Nephrol Dial Transplant* 2003;18(5):1001–1004.
1246. Boubenider SA, Akhtar M, Alfurayh O, et al. Late recurrence of Wegener's granulomatosis presenting as tracheal stenosis in a renal transplant patient. *Clin Transplant* 1994;8(1):5–9.
1247. Le Mao G, Rostaing L, Modesto A, et al. Recurrence of ANCA-associated microscopic polyangiitis after cadaveric renal transplant. *Transplant Proc* 1996;28(5):2803–2804.
1248. van der Woude FJ. Kidney transplantation and ANCA-associated vasculitis. *Cleve Clin J Med* 2002;69(Suppl 2):SII143–SII145.
1249. Lobbedez T, Comoz F, Renaudineau E, et al. Recurrence of ANCA-positive glomerulonephritis immediately after renal transplantation. *Am J Kidney Dis* 2003;42(4):E2–E6.
1250. Geetha D, Seo P, Specks U, et al. Successful induction of remission with rituximab for relapse of ANCA-associated vasculitis post-kidney transplant: report of two cases. *Am J Transplant* 2007;7(12):2821–2825.
1251. Pham PT, Pham PC. Graft loss due to recurrent lupus nephritis in living-related kidney donation. *Clin J Am Soc Nephrol* 2011;6(9):2296–2299.
1252. Norby GE, Strom EH, Midtvedt K, et al. Recurrent lupus nephritis after kidney transplantation: a surveillance biopsy study. *Ann Rheum Dis* 2010;69(8):1484–1487.
1253. Goral S, Ynares C, Shappell SB, et al. Recurrent lupus nephritis in renal transplant recipients revisited: it is not rare. *Transplantation* 2003;75(5):651–656.
1254. Burgos PI, Perkins EL, Pons-Estel GJ, et al. Risk factors and impact of recurrent lupus nephritis in patients with systemic lupus erythematosus undergoing renal transplantation: data from a single US institution. *Arthritis Rheum* 2009;60(9):2757–2766.
1255. Yu TM, Wen MC, Li CY, et al. Impact of recurrent lupus nephritis on lupus kidney transplantation: a 20-year single center experience. *Clin Rheumatol* 2012;31(4):705–710.
1256. Kofman T, Grimbert P, Canoui-Poitrine F, et al. Renal transplantation in patients with AA amyloidosis nephropathy: results from a French multicenter study. *Am J Transplant* 2011;11(11):2423–2431.
1257. Pinney JH, Lachmann HJ, Sattianayagam PT, et al. Renal transplantation in systemic amyloidosis—importance of amyloid fibril type and precursor protein abundance. *Am J Transplant* 2013;13(2):433–441.
1258. Leung N, Lager DJ, Gertz MA, et al. Long-term outcome of renal transplantation in light-chain deposition disease. *Am J Kidney Dis* 2004;43(1):147–153.
1259. Horike K, Takeda A, Otsuka Y, et al. A case of recurrent light chain deposition disease after living-related renal transplantation—detailed process of the recurrence. *Clin Transplant* 2012;26 Suppl 24:64–69.
1260. Canaud G, Audard V, Kofman T, et al. Recurrence from primary and secondary glomerulopathy after renal transplant. *Transpl Int* 2012;25(8):812–824.
1261. Czarnecki PG, Lager DJ, Leung N, et al. Long-term outcome of kidney transplantation in patients with fibrillary glomerulonephritis or monoclonal gammopathy with fibrillary deposits. *Kidney Int* 2009;75(4):420–427.
1262. Samaniego M, Nadasdy GM, Laszik Z, et al. Outcome of renal transplantation in fibrillary glomerulonephritis. *Clin Nephrol* 2001;55(2):159–166.
1263. Brady HR. Fibrillary glomerulopathy. *Kidney Int* 1998;53(5):1421–1429.
1264. Pronovost PH, Brady HR, Gunning ME, et al. Clinical features, predictors of disease progression and results of renal transplantation in fibrillary/immunotactoid glomerulopathy. *Nephrol Dial Transplant* 1996;11(5):837–842.
1265. Korbet SM, Schwartz MM, Lewis EJ. Immunotactoid glomerulopathy. *Am J Kidney Dis* 1991;17(3):247–257.
1266. Sathan S, Khan FN, Ranga KV. A case of recurrent immunotactoid glomerulopathy in an allograft treated with rituximab. *Transplant Proc* 2009;41(9):3953–3955.
1267. Østerby R, Nyberg G, Karlberg I, et al. Glomerular volume in kidneys transplanted into diabetic and non-diabetic patients. *Diabet Med* 1992;9(2):144–149.
1268. Wilczek HE, Jaremko G, Tyden G, et al. Evolution of diabetic nephropathy in kidney grafts. Evidence that a simultaneously transplanted kidney exerts a protective effect. *Transplantation* 1995;59:51–57.

1269. Bohman SO, Tyden G, Wilczek H, et al. Prevention of kidney graft diabetic nephropathy by pancreas transplantation in man. *Diabetes* 1985;34:306–308.
1270. Maryniak RK, Mendoza N, Clyne D, et al. Recurrence of diabetic nodular glomerulosclerosis in a renal transplant. *Kidney Int* 1985;27:799–806.
1271. Mauer SM, Barbosa J, Vernier RL, et al. Development of diabetic vascular lesions in normal kidneys transplanted into patients with diabetes mellitus. *N Engl J Med* 1976;295:916–919.
1272. Hariharan S, Smith RD, Viero R, et al. Diabetic nephropathy after renal transplantation. Clinical and pathologic features. *Transplantation* 1996;62(5):632–635.
1273. Ianhez LE, Saldanha LB, Arap S, et al. Renal biopsy in thirty-one kidney transplant recipients with more than ten years of follow-up. *Transplant Proc* 1989;21:2187–2189.
1274. Kim H, Cheigh JS. Kidney transplantation in patients with type 1 diabetes mellitus: long-term prognosis for patients and grafts. *Korean J Intern Med* 2001;16(2):98–104.
1275. Abouna GM, Al-Adnani MS, Kremer GD, et al. Reversal of diabetic nephropathy in human cadaveric kidneys after transplantation into non-diabetic recipients. *Lancet* 1983;2(8362):1274–1276.
1276. Fioretto P, Steffes MW, Sutherland DE, et al. Reversal of lesions of diabetic nephropathy after pancreas transplantation. *N Engl J Med* 1998;339(2):69–75.
1277. Cameron JS. Recurrent primary disease and de novo nephritis following renal transplantation. *Pediatr Nephrol* 1991;5(4):412–421.
1278. Whelchel JD, Alison DV, Luke RG, et al. Successful renal transplantation in hyperoxaluria. A report of two cases. *Transplantation* 1983;35(2):161–164.
1279. Scheinman JI, Najarian JS, Mauer SM. Successful strategies for renal transplantation in primary oxalosis. *Kidney Int* 1984;25(5):804–811.
1280. Broyer M, Jouve P, Niaudet P, et al. Management of oxalosis. *Kidney Int* 1996;53:S93–S98.
1281. Frei D, Binswanger U, Keusch G, et al. [Intact function of a transplanted kidney 3 years after organ transplantation with primary oxalosis]. *Schweiz Med Wochenschr* 1979;109(26):979–983.
1282. Lieske JC, Spargo BH, Toback FG. Endocytosis of calcium oxalate crystals and proliferation of renal tubular epithelial cells in a patient with type 1 primary hyperoxaluria. *J Urol* 1992;148(5):1517–1519.
1283. Toussaint C, Vienne A, De PL, et al. Combined liver-kidney transplantation in primary hyperoxaluria type 1. histopathology and oxalate body content. *Transplantation* 1995;59(12):1700–1704.
1284. Allen AR, Thompson EM, Williams G, et al. Selective renal transplantation in primary hyperoxaluria type 1. *Am J Kidney Dis* 1996;27(6):891–895.
1285. Latta A, Muller-Wiefel DE, Sturm E, et al. Transplantation procedures in primary hyperoxaluria type 1. *Clin Nephrol* 1996;46(1):21–23.
1286. Cibrik DM, Kaplan B, Arndorfer JA, et al. Renal allograft survival in patients with oxalosis. *Transplantation* 2002;74(5):707–710.
1287. Millan MT, Berquist WE, So SK, et al. One hundred percent patient and kidney allograft survival with simultaneous liver and kidney transplantation in infants with primary hyperoxaluria: a single-center experience. *Transplantation* 2003;76(10):1458–1463.
1288. Lloveras JJ, Dupre-Goudable C, Rey JP, et al. The European experience of liver-kidney transplantation for primary hyperoxaluria type I. Prevention of recurrent intrarenal oxalate deposits. *Presse Med* 1991;20(40):2016–2018.
1289. Detry O, Honore P, DeRoover A, et al. Reversal of oxalosis cardiomyopathy after combined liver and kidney transplantation. *Transplant Int* 2002;15(1):50–52.
1290. Friedlander MM, Kopolovic J, Rubinger D, et al. Renal biopsy in Fabry's disease eight years after successful renal transplantation. *Clin Nephrol* 1987;27:206–210.
1291. Faraggiana T, Churg J, Grishman E, et al. Light- and electron-microscopic histochemistry of Fabry's disease. *Am J Pathol* 1981;103(2):247–262.
1292. Mosnier JF, Degott C, Bedrossian J, et al. Recurrence of Fabry's disease in a renal allograft eleven years after successful renal transplantation. *Transplantation* 1991;51(4):759–762.
1293. Popli S, Molnar ZV, Leehey DJ, et al. Involvement of renal allograft by Fabry's disease. *Am J Nephrol* 1987;7(4):316–318.
1294. Grünfeld JP, le Porrier M, Droz D, et al. La transplantation rénale chez le sujets atteints de maladie de Fabry: transplantation du rein d'un sujet hétérozygote à un sujet sain. *Nouv Presse Med* 1975;4:2081–2083.
1295. Van Loo A, Vanholder R, Madsen K, et al. Novel frameshift mutation in a heterozygous woman with Fabry disease and end-stage renal failure. *Am J Nephrol* 1996;16(4):352–357.
1296. Thurberg BL, Rennke H, Colvin RB, et al. Globotriaosylceramide accumulation in the Fabry kidney is cleared from multiple cell types after enzyme replacement therapy. *Kidney Int* 2002;62(6):1933–1946.
1297. Gagné ER, Deland E, Daudon M, et al. Chronic renal failure secondary to 2,8-dihydroxyadenine deposition: the first report of recurrence in a kidney transplant. *Am J Kidney Dis* 1994;24(1):104–107.
1298. Schneider JA. Therapy of cystinosis. *N Engl J Med* 1985;313:1472–1474.
1299. Spear GS, Gubler MC, Habib R, et al. Dark cells of cystinosis: occurrence in renal allografts. *Hum Pathol* 1989;20(5):472–476.
1300. Bogan ML, Kopecky KK, Kraft JL, et al. Renal allografts in cystinosis and mesangial demography. *Clin Nephrol* 1989;32(6):256–261.
1301. Zeier M, Hartschuh W, Wiesel M, et al. Malignancy after renal transplantation. *Am J Kidney Dis* 2002;39(1):E5.
1302. Birkeland SA, Lokkegaard H, Storm HH. Cancer risk in patients on dialysis and after renal transplantation. *Lancet* 2000;355(9218):1886–1887.
1303. Kiberd BA, Rose C, Gill JS. Cancer mortality in kidney transplantation. *Am J Transplant* 2009;9(8):1868–1875.
1304. Buell JF, Gross TG, Woodle ES. Malignancy after transplantation. *Transplantation* 2005;80(2 Suppl):S254–S264.
1305. Penn I. The changing pattern of posttransplant malignancies. *Transplant Proc* 1991;23:1101–1103.
1306. Penn I. Tumors after renal and cardiac transplantation. *Hematol Oncol Clin North Am* 1993;7(2):431–445.
1307. Neuzillet Y, Lay F, Luccioni A, et al. De novo renal cell carcinoma of native kidney in renal transplant recipients. *Cancer* 2005;103(2):251–257.
1308. Tillou X, Doerfler A, Collon S, et al. De novo kidney graft tumors: results from a multicentric retrospective national study. *Am J Transplant* 2012;12(12):3308–3315.
1309. Verine J, Varna M, Ratajczak P, et al. Human de novo papillary renal-cell carcinomas in a kidney graft: evidence of recipient origin with adenoma-carcinoma sequence. *Am J Transplant* 2013;13(4):984–992.
1310. Swerdlow SH, Campo E. Post-transplant lymphoproliferative disorders. In: Swerdlow SH, Campo E, eds. *WHO Blue Book: Tumors of the Haematopoietic and Lymphoid Tissues*, 4th ed. Geneva: World Health Organization, 2008:343–348.
1311. Jagadeesh D, Woda BA, Draper J, et al. Post transplant lymphoproliferative disorders: risk, classification, and therapeutic recommendations. *Curr Treat Options Oncol* 2012;13(1):122–136.
1312. Harris NL, Swerdlow SH, Frizzera G, et al. Post-transplant lymphoproliferative disorders. In: Jaffe ES, Harris NL, Stein H, et al., eds. *Pathology and Genetics of Tumours of Haematopoietic and Lymphoid Tissues* n Lyon, France: IARC Press, 2001:264–269.
1313. Ross CW, Schnitzer B, Sheldon S, et al. Gamma/delta T-cell posttransplantation lymphoproliferative disorder primarily in the spleen. *Am J Clin Pathol* 1994;102(3):310–315.
1314. Ferry JA, Harris NL. Pathology of posttransplant lymphoproliferative disorders. In: Solez K, Racussen LC, Billingham ME, eds. *Solid Organ Transplant Rejection*. New York: Marcel Dekker, 1996:277–298.
1315. Cockfield SM, Preiksaitis JK, Jewell LD, et al. Post-transplant lymphoproliferative disorder in renal allograft recipients. Clinical experience and risk factor analysis in a single center. *Transplantation* 1993;56(1):88–96.
1316. Citterio F, Lauriola L, Nanni G, et al. Polyclonal lymphoma confined to renal allograft: case report. *Transplant Proc* 1987;19(5):3732–3734.
1317. Jones C, Bleau B, Buskard N, et al. Simultaneous development of diffuse immunoblastic lymphoma in recipients of renal transplants from a single cadaver donor: transmission of Epstein-Barr virus and triggering by OKT3. *Am J Kidney Dis* 1994;23(1):130–134.
1318. Denning DW, Weiss LM, Martinez K, et al. Transmission of Epstein-Barr virus by a transplanted kidney, with activation by OKT3 antibody. *Transplantation* 1989;48:141–144.
1319. Nádasy T, Park CS, Peiper SC, et al. Epstein-Barr virus infection-associated renal disease: diagnostic use of molecular hybridization technology in patients with negative serology. *J Am Soc Nephrol* 1992;2(12):1734–1742.

1320. Weissman DJ, Ferry JA, Harris NL, et al. Posttransplant lymphoproliferative disorders in solid organ recipients are predominately aggressive tumors of host origin. *Am J Clin Pathol* 1995;103:748–755.
1321. Delecluse H-J, Kremmer E, Rouault J-P, et al. The expression of Epstein-Barr virus latent proteins is related to the pathological features of post-transplant lymphoproliferative disorders. *Am J Pathol* 1995;146:1113–1120.
1322. Thomas JA, Hotchin NA, Allday MJ, et al. Immunohistology of Epstein-Barr virus-associated antigens in B cell disorders from immunocompromised individuals. *Transplantation* 1990;49:944–953.
1323. Renoult E, Aymard B, Gregoire MJ, et al. Epstein-Barr virus lymphoproliferative disease of donor origin after kidney transplantation: a case report. *Am J Kidney Dis* 1995;26(1):84–87.
1324. Hjelle B, Evans HM, Yen TS, et al. A poorly differentiated lymphoma of donor origin in a renal allograft recipient. *Transplantation* 1989;47(6):945–948.
1325. Ulrich W, Chott A, Watschinger B, et al. Primary peripheral T cell lymphoma in a kidney transplant under immunosuppression with cyclosporine A. *Hum Pathol* 1989;20(10):1027–1030.
1326. Meduri G, Fromentin L, Vieillefond A, et al. Donor-related non-Hodgkin's lymphoma in a renal allograft recipient. *Transplant Proc* 1991;23(5):2649–2650.
1327. Lager DJ, Burgart LJ, Slagel DD. Epstein-Barr virus detection in sequential biopsies from patients with a posttransplant lymphoproliferative disorder. *Mod Pathol* 1993;6(1):42–47.
1328. Bakker NA, van Imhoff GW, Verschuuren EA, et al. Early onset post-transplant lymphoproliferative disease is associated with allograft localization. *Clin Transplant* 2005;19(3):327–334.
1329. Nalesnik MA. Clinicopathologic characteristics of post-transplant lymphoproliferative disorders. *Recent Results Cancer Res* 2002;159:9–18.
1330. Schmidtko J, Wang R, Wu CL, et al. Posttransplant lymphoproliferative disorder associated with an Epstein-Barr-related virus in cynomolgus monkeys. *Transplantation* 2002;73(9):1431–1439.
1331. Koike J, Yamaguchi Y, Hoshikawa M, et al. Post-transplant lymphoproliferative disorders in kidney transplantation: histological and molecular genetic assessment. *Clin Transplant* 2002;16 Suppl 8:12–17.
1332. Mueller-Hermelink HK, Ott G, Kneitz B, et al. The spectrum of lymphoproliferations and malignant lymphoma after organ transplantation. In: Kreipe HH, ed. *Verhandlungen der Deutschen Gesellschaft fuer Pathologien 88 Tagung*. Muenchen, Jena: Urban & Fischer, 2004:63–68.
1333. Caillard S, Dharnidharka V, Agodoa L, et al. Posttransplant lymphoproliferative disorders after renal transplantation in the United States in era of modern immunosuppression. *Transplantation* 2005;80(9):1233–1243.
1334. Shapiro R, Nalesnik M, McCauley J, et al. Posttransplant lymphoproliferative disorders in adult and pediatric renal transplant patients receiving tacrolimus-based immunosuppression. *Transplantation* 1999;68(12):1851–1854.
1335. O'Brien S, Bernert RA, Logan JL, Lien YH. Remission of posttransplant lymphoproliferative disorder after interferon alfa therapy. *J Am Soc Nephrol* 1997;8(9):1483–1489.
1336. Senel MF, Van BCT, Riggs S, et al. Post-transplantation lymphoproliferative disorder in the renal transplant ureter. *J Urol* 1996;155(6):2025.
1337. Delbello MW, Dick WH, Carter CB, et al. Polyclonal B cell lymphoma of renal transplant ureter induced by cyclosporine: case report. *J Urol* 1991;146(6):1613–1614.
1338. Oertel SH, Verschuuren E, Reinke P, et al. Effect of anti-CD 20 antibody rituximab in patients with post-transplant lymphoproliferative disorder (PTLD). *Am J Transplant* 2005;5(12):2901–2906.
1339. Meeuwis KA, van Rossum MM, Hoitsma AJ, et al. (Pre)malignancies of the female anogenital tract in renal transplant recipients. *Transplantation* 2011;91(1):8–10.
1340. Stoff B, Salisbury C, Parker D, et al. Dermatopathology of skin cancer in solid organ transplant recipients. *Transplant Rev* 2010;24(4):172–189.
1341. Kanitakis J, Alhaj-Ibrahim L, Euvrard S, et al. Basal cell carcinomas developing in solid organ transplant recipients: clinicopathologic study of 176 cases. *Arch Dermatol* 2003;139(9):1133–1137.
1342. Engels EA, Pfeiffer RM, Fraumeni JF Jr, et al. Spectrum of cancer risk among US solid organ transplant recipients. *JAMA* 2011;306(17):1891–1901.
1343. Feng H, Shuda M, Chang Y, et al. Clonal integration of a polyomavirus in human Merkel cell carcinoma. *Science* 2008;319(5866):1096–1100.
1344. Dalianis T, Hirsch HH. Human polyomaviruses in disease and cancer. *Virology* 2013;437(2):63–72.
1345. Mirnezami R, Nicholson J, Darzi A. Preparing for precision medicine. *N Engl J Med* 2012;366(6):489–491.
1346. Ewis AA, et al. A history of microarrays in biomedicine. *Expert Rev Mol Diagn* 2005;5(3):315–328.
1347. Dupuy A, Simon RM. Critical review of published microarray studies for cancer outcome and guidelines on statistical analysis and reporting. *J Natl Cancer Inst* 2007;99(2):147–157.
1348. Rogers S, Cambrosio A. Making a new technology work: the standardization and regulation of microarrays. *Yale J Biol Med* 2007;80(4):165–178.
1349. Halloran PF, Chance H. Genetic regulation of the antibody response to alloantigen Ly-6.2:2. Evidence for a suppressor mechanism. *Transplant Proc* 1982;14(4):682–684.
1350. Halloran PF, Broski AP, Batiuk TD, et al. The molecular immunology of acute rejection: an overview. *Transpl Immunol* 1993;1(1):3–27.
1351. Halloran PF, Einecke G. Microarrays and transcriptome analysis in renal transplantation. *Nat Clin Pract Nephrol* 2006;2(1):2–3.
1352. Stegall M, et al. Gene expression during acute allograft rejection: novel statistical analysis of microarray data. *Am J Transplant* 2002;2(10):913–925.
1353. Halloran PF, de Freitas DG, Einecke G, et al. An integrated view of molecular changes, histopathology and outcomes in kidney transplants. *Am J Transplant* 2010;10(10):2223–2230.
1354. Park WD, Stegall MD. A meta-analysis of kidney microarray datasets: investigation of cytokine gene detection and correlation with rt-PCR and detection thresholds. *BMC Genomics* 2007;8:88.
1355. Muthukumar T, Dadhania D, Ding R, et al. Messenger RNA for FOXP3 in the urine of renal-allograft recipients. *N Engl J Med* 2005;353(22):2342–2351.
1356. Keslar KS, et al. Multicenter evaluation of a standardized protocol for noninvasive gene expression profiling. *Am J Transplant* 2013;13(7):1891–1897.
1357. Hoffmann S, Park J, Jacobson LM, et al. Donor genomics influence graft events: the effect of donor polymorphisms on acute rejection and chronic allograft nephropathy. *Kidney Int* 2004;66(4):1686–1693.
1358. Manolio TA. Genomewide association studies and assessment of the risk of disease. *N Engl J Med* 2010;363(2):166–176.
1359. Geiss GK, et al. Direct multiplexed measurement of gene expression with color-coded probe pairs. *Nat Biotechnol* 2008;26(3):317–325.
1360. Wang Z, Gerstein M, Snyder M. RNA-Seq: a revolutionary tool for transcriptomics. *Nat Rev Genet* 2009;10(1):57–63.
1361. Marguerat S, Wilhelm BT, Bahler J. Next-generation sequencing: applications beyond genomes. *Biochem Soc Trans* 2008;36(Pt 5):1091–1096.
1362. Allison DB, Cui X, Page GP, et al. Microarray data analysis: from disarray to consolidation and consensus. *Nat Rev Genet* 2006;7(1):55–65.
1363. Mengel M, et al. Precision diagnostics in transplantation: from bench to bedside. *Am J Transplant* 2013;13(3):562–568.
1364. Halloran PF, de Freitas DG, Einecke G, et al. The molecular phenotype of kidney transplants. *Am J Transplant* 2010;10(10):2215–2222.
1365. Hayde N, et al. The clinical and molecular significance of C4d staining patterns in renal allografts. *Transplantation* 2013;95(4):580–588.
1366. Waikar SS, et al. Imperfect gold standards for kidney injury biomarker evaluation. *J Am Soc Nephrol* 2012;23(1):13–21.
1367. Spivey TL, Uccellini L, Ascierio ML, et al. Gene expression profiling in acute allograft rejection: challenging the immunologic constant of rejection hypothesis. *J Transl Med* 2011;9:174.

Renal Neoplasms

Pediatric neoplasms 1461

- Wilms tumor 1461
- Congenital mesoblastic nephroma 1463
- Clear cell sarcoma of kidney 1465
- Rhabdoid tumor of the kidney 1465
- Metanephric adenoma 1466
- Translocation carcinomas 1467
- Carcinoma associated with neuroblastoma 1467

Adult neoplasms 1468

Epithelial neoplasms 1468

- Papillary adenoma 1468
- Oncocytoma 1469
- Renal cell carcinoma 1470
- Clear cell renal cell carcinoma 1473
- Papillary renal cell carcinoma 1475
- Chromophobe renal cell carcinoma 1476
- Collecting duct carcinoma 1477
- Medullary carcinoma 1478
- Mucinous tubular and spindle cell carcinoma 1478
- Tubulocystic carcinoma 1479
- Clear cell papillary renal cell carcinoma 1479
- Acquired cystic disease–associated renal cell carcinoma 1480
- Urothelial carcinoma 1480
- Renal cell carcinoma, unclassified 1481
- Neuroendocrine tumors 1482

Mesenchymal neoplasms 1482

- Angiomyolipoma 1482
- Other benign mesenchymal tumors 1484
- Primary sarcoma 1484

Miscellaneous neoplasms 1485

- Cystic nephroma 1485
- Mixed epithelial and stromal tumor 1485
- Juxtaglomerular cell tumor 1486

- Renomedullary interstitial cell tumor 1486
- Lymphoreticular and hematopoietic tumors 1487
- Metastases to the kidney 1487
- Nonneoplastic renal diseases in kidney tumor resection specimens 1488

A diverse array of tumors can arise in the human kidney. In this chapter, these will be covered using an approach that has become a standard one in dealing with this group of tumors. The classification of epithelial tumors of the kidney has in particular undergone substantial progress in the last two decades with major contributions from genetic typing of renal cell carcinomas (RCCs). The role of genotyping and ancillary tools, in particular immunohistochemistry, in correctly classifying these tumors is highlighted in the section on Renal Cell Carcinoma. In 2012, the International Society of Urologic Pathology (ISUP) updated the 2004 World Health Organization (WHO) classification of these tumors; the modified classification is highlighted in Table 30.1 (1). The first section will cover those tumors that characteristically are associated with the pediatric population. This is a somewhat arbitrary designation, as most tumors can develop over a wide age range. This is followed by coverage of neoplasms in the more traditional categories of epithelial, mesenchymal, and other categories. Specific discussions of etiology and pathogenesis are dealt with in each of the sections on individual tumors, rather than as a freestanding section, as is used elsewhere in this text. The purpose of this chapter is to familiarize the reader with the tumor types encountered in the human rather than to provide a comprehensive diagnostic reference, which is better handled in more comprehensive textbooks and monographs.

PEDIATRIC NEOPLASMS

Wilms Tumor

Clinical Findings and Epidemiology

More than 80% of renal tumors of childhood are Wilms tumor (nephroblastoma) (1,2). Neonatal Wilms tumor is rare. Most Wilms tumor occurs in children between the ages of 2 and

TABLE 30.1 Modified 2004 WHO classification of renal tumors**Renal cell tumors**

Clear cell renal cell carcinoma
 Multilocular cystic clear cell renal cell carcinoma
 Papillary renal cell carcinoma
 Chromophobe renal cell carcinoma
 Carcinoma of the collecting ducts of Bellini (collecting duct carcinoma)
 Renal medullary carcinoma
 Translocation-associated carcinomas
 Mucinous tubular and spindle cell carcinoma
 Tubulocystic carcinoma
 Clear cell papillary renal cell carcinoma
 Acquired cystic disease-associated carcinoma
 Carcinoma associated with neuroblastoma
 Papillary adenoma
 Oncocytoma

Metanephric tumors

Metanephric adenoma
 Metanephric adenofibroma
 Metanephric stromal tumor

Nephroblastic tumors

Wilms tumor (nephroblastoma)
 Cystic partially differentiated Wilms tumor (nephroblastoma)

Mesenchymal tumors

Occurring mainly in children
 Clear cell sarcoma
 Rhabdoid tumor
 Congenital mesoblastic nephroma
 Ossifying renal tumor of infancy
 Occurring mainly in adults
 Angiomyolipoma
 Epithelioid angiomyolipoma

Leiomyosarcoma (including the renal vein)
 Angiosarcoma
 Solitary fibrous tumor
 Rhabdomyosarcoma
 Osteosarcoma
 Leiomyoma
 Hemangioma
 Lymphangioma
 Schwannoma
 Juxtaglomerular cell tumor
 Renomedullary interstitial cell tumor

Mixed mesenchymal and epithelial tumors

Cystic nephroma
 Pediatric
 Adult
 Mixed epithelial and stromal tumor
 Synovial sarcoma

Neuroendocrine tumors

Carcinoid
 Neuroendocrine (small cell) carcinoma
 Primitive neuroectodermal tumor
 Neuroblastoma
 Pheochromocytoma

Hematopoietic and lymphoid tumors

Lymphoma
 Leukemia
 Plasmacytoma

Germ cell tumors

Teratoma
 Choriocarcinoma

Metastatic tumors

4 years (3). It is uncommon in the first 6 months of life and after 6 years of age. It is slightly more common in girls than in boys (3). It is bilateral in about 5% of cases (4). Wilms tumor may be associated with hemihypertrophy and aniridia and with genital anomalies, such as cryptorchidism and hypospadias (5). Patients with Beckwith-Wiedemann syndrome and Denys-Drash syndrome have an increased risk of developing Wilms tumor (5,6). Wiedemann-Beckwith syndrome is related to abnormalities on chromosome 11p15 and characterized by multiple craniofacial anomalies, abdominal wall defects, and tumors of the genitourinary tract, liver, adrenal gland, and central nervous system among other abnormalities. Denys-Drash syndrome, due to mutations of the *WT1* gene, is also associated with a congenital nephropathy and disorders of sexual development. Wilms tumor is rare in adults (3). Wilms tumor is believed to arise from embryonic tissues called *nephrogenic rests* that fail to undergo normal involution (7).

Pathology**GENETICS**

The development of Wilms tumor has been linked to mutations of the *WT1* and *WT2* genes located on chromosome 11 at 11p13 and 11p15.5, respectively (8,9).

GROSS

Wilms tumor often is greater than 5 cm in diameter, with an average size of 10 cm (3). The cut surface is typically solid, soft, and gray or pink, with a texture and appearance resembling brain tissue. The tumor is usually circumscribed by a pseudocapsule formed of compressed renal and perirenal tissues. Cysts are common, as are foci of hemorrhage and necrosis (Fig. 30.1). Predominantly cystic Wilms tumor that contains blastema and other Wilms tumor tissues in its septa is called *cystic partially differentiated nephroblastoma* (10).

MICROSCOPIC

Histology remains the most important prognostic indicator of Wilms tumor (11). Wilms tumor is typically composed of a mixture of blastema, epithelium, and stroma; sometimes one or two of these components are absent (Fig. 30.2) (12). Stromal and epithelial predominant Wilms have an excellent prognosis (13). Blastema consists of densely packed small cells randomly arranged in sheets. Blastemal cells have dense nuclei, frequent mitotic figures, and inconspicuous cytoplasm. Aggregates of blastema commonly form serpentine, nodular, and diffuse patterns that have sharp borders with the stromal component.

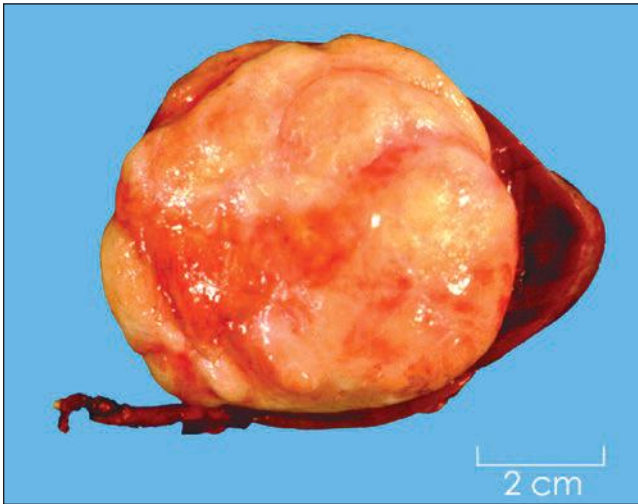


FIGURE 30.1 Wilms tumor. A large, pale, bulging mass in a small kidney.

The epithelium of Wilms tumor usually consists of small tubules or cysts lined by columnar or cuboidal cells. Occasionally, it forms stubby papillae superficially resembling glomeruli or has mucinous, squamous, neural, or endocrine differentiation (12,14).

The stroma of Wilms tumor is variable and may differentiate toward almost any type of mesenchymal tissue. Nondescript myxoid and fibroblastic spindle cell stroma is most common, but smooth muscle, skeletal muscle, fat, cartilage, and bone are present in some tumors (12,14). When diffuse differentiation toward skeletal muscle occurs, the term *fetal rhabdomyomatous nephroblastoma* is applied (15,16). There is evidence that these are more resistant to chemotherapy (16). Complex combinations of differentiated epithelium and stroma are sometimes present. The term *teratoid Wilms tumor* has been applied to these (17,18). These tumors are also resistant to preoperative chemotherapy (18).

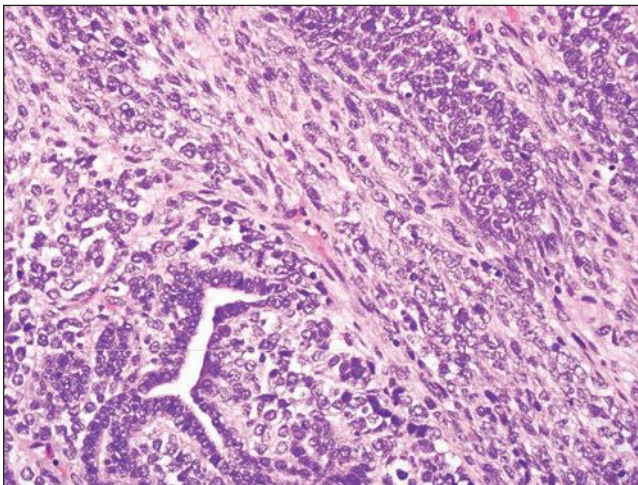


FIGURE 30.2 Wilms tumor. Typical triphasic histology with epithelial, blastemal, and mesenchymal elements. In this case, the mesenchymal component is primitive and undifferentiated.

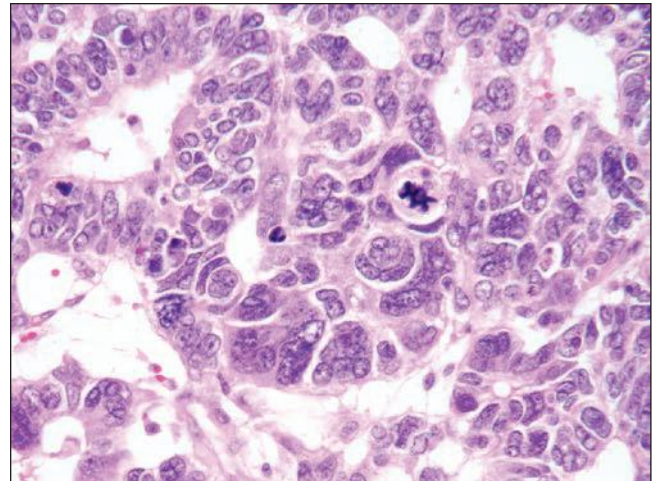


FIGURE 30.3 Wilms tumor. Focus of anaplasia in a Wilms tumor with nucleomegaly, hyperchromasia, and multipolar mitotic figure.

The most important pathologic prognostic feature is the presence or absence of anaplasia (19–21). Anaplasia is defined as the combination of cells with enlarged hyperchromatic nuclei (at least three times as large as typical blastemal nuclei in both axes and having obvious hyperchromasia) and multipolar mitotic figures (Fig. 30.3). Recognition of anaplasia requires proper fixation, sectioning, and staining. The criteria for abnormal hyperdiploid mitotic figures are stringent; not only must there be structural abnormalities but the mitotic figure must also be enlarged as evidence of hyperploidy. Enlarged nuclei in skeletal muscle fibers in the stroma of Wilms tumor are not evidence of anaplasia.

Treatment and Outcome

The progress in the treatment of Wilms tumor is one of the great success stories of oncology. Most cases are treated with surgery and dactinomycin and vinblastine chemotherapy with relatively low toxicity (11). Mortality declined approximately 10% per decade throughout the past century. This owes in large part to the efforts of the National Wilms Tumor Study (NWTs). From the results of the NWTs, Wilms tumor has been classified as having either favorable or unfavorable histology, depending on whether or not anaplasia is present. Approximately 2% of Wilms tumors in patients under 2 years of age have anaplasia, and this increases to 13% in children over age 5 years (9). The staging scheme for Wilms tumor and other pediatric renal malignancies differs somewhat from that used for RCC (Table 30.2) (22). Currently, the overall survival for patients diagnosed with Wilms tumor is approximately 90% (3,11).

Congenital Mesoblastic Nephroma

Clinical Findings and Epidemiology

Congenital mesoblastic nephroma makes up less than 3% of renal neoplasms in children; it is the predominant renal neoplasm in the first 3 months of life and is uncommon after 6 months (23,24). The births of patients with congenital mesoblastic nephroma often are complicated by polyhydramnios and prematurity. The presenting finding is almost always

TABLE 30.2 Staging system for renal tumors of childhood**Stage I**

Tumor is limited to the kidney or surrounded by a fibrous capsule (pseudocapsule)
 Tumor can protrude into the renal pelvis or ureter
 Intrarenal vessel involvement can be present

Stage II

Viable tumor penetrates into perirenal fat but not to the surgical resection margin
 Viable tumor infiltrates the soft tissue of the renal sinus
 Viable tumor infiltrates blood or lymphatic channels outside of the kidney but is completely resected
 Viable tumor infiltrates the renal pelvis or ureter wall
 Viable tumor infiltrates adjacent organs or vena cava, but is completely resected

Stage III

Viable or nonviable tumor extends beyond the resection margins
 Any abdominal lymph nodes are involved
 Tumor ruptures before or intraoperatively (irrespective of other criteria)
 Tumor has penetrated through the peritoneal surface
 Tumor implants are present on the peritoneal surface.
 Tumor thrombi are present at resection margins of vessels or the ureter (or removed piecemeal by the surgeon)
 Tumor has been surgically biopsied (wedge biopsy) prior to preoperative chemotherapy or surgery

Stage IV

Hematogenous metastases (lung, liver, bone, brain, etc.) or lymph node metastases outside the abdominopelvic region

Stage V

Bilateral renal tumors at diagnosis (each side substaged as above)

an abdominal mass. Congenital mesoblastic nephroma was first recognized in 1966 (25), and subsequent studies have shown it to be a morphologically distinct tumor with a good prognosis (24).

Pathology**GENETICS**

Congenital mesoblastic nephroma has genetic similarities to infantile fibrosarcoma with the t(12;15)(p13.q35) translocation common to both (26,27).

GROSS

Congenital mesoblastic nephroma is usually large relative to the infant's kidney. The external surfaces of the tumor and kidney are smooth, and the renal capsule and renal pelvis and caliceal system are stretched over the tumor. Congenital mesoblastic nephroma may be spherical or bosselated. The cut surface resembles leiomyoma: firm, whorled or trabeculated, and pale (28). There is no true capsule. The tumor usually mingles with the surrounding kidney and may extend into perinephric soft tissue. Invasion of the renal vein occurs occasionally. Cysts, necrosis, and hemorrhage may be found occasionally, particularly in cases that are cellular on microscopic examination.

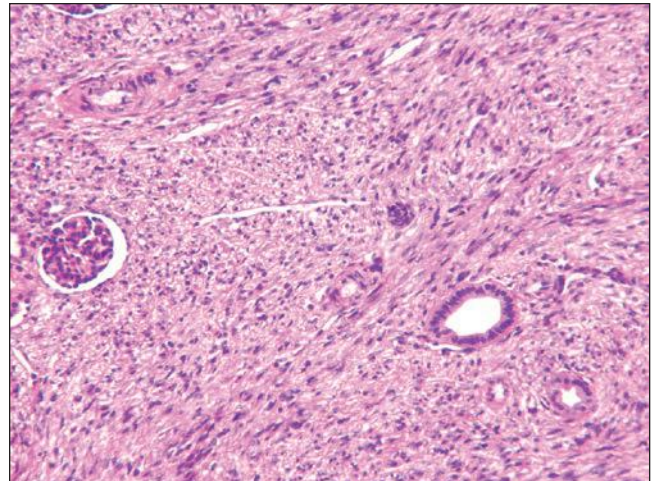


FIGURE 30.4 Congenital mesoblastic nephroma. The tumor is composed of bland, spindle-shaped cells growing in an infiltrative manner; note the invasion between entrapped normal structures.

MICROSCOPIC

Bolande (29) described the classic pattern of congenital mesoblastic nephroma: a moderately cellular neoplasm composed of interlacing bundles of spindle cells with elongate nuclei, usually infiltrating renal and perinephric tissues (Fig. 30.4). In the classic pattern, there is usually either one mitotic figure per 10 high-power fields or less (28). Some tumors contain small islands of cartilage or foci of extramedullary hematopoiesis.

Later, a second, more common, pattern was recognized. This pattern is densely cellular and composed of polygonal cells. Mitotic figures are present in the range of 8 to 30 per 10 high-power fields. Cysts are common in this pattern. Rather than being infiltrative, the borders usually are “pushing.” This pattern is called *cellular congenital mesoblastic nephroma* (28,30). Often both the classic and cellular patterns are mixed in the same tumor.

Congenital mesoblastic nephroma is usually not difficult to diagnose when age and histology are considered. The major differential diagnostic consideration is Wilms tumor with stromal predominance, especially if it has been treated preoperatively with chemotherapy. Identification of blastema, which does not occur in mesoblastic nephroma, usually resolves the issue. Also, the sharply circumscribed borders of Wilms tumor contrast with the infiltrative borders of mesoblastic nephroma.

Treatment and Outcome

Almost all are cured by surgical resection (24). Recurrence and adverse outcome are rare and have mainly occurred in patients older than 3 months when the tumor was discovered. Congenital mesoblastic nephroma has infiltrative borders that the surgical pathologist must carefully study because recurrence may occur if resection is incomplete. Metastasis is exceptional (31,32). It has been suggested that the cellular pattern is prone to recur. Because it is the more common pattern and the great majority of patients are cured, any such tendency must be small, and age and completeness of resection are the prime risk factors.

Clear Cell Sarcoma of Kidney

Clinical Findings and Epidemiology

Clear cell sarcoma occurs in the same age range as Wilms tumor and makes up approximately 6% of renal neoplasms in children (33,34). Most patients are between 1 and 3 years old, and about two thirds are male. Only three cases of bilateral clear cell sarcoma are described, and these may represent metastases rather than two primaries (34).

Pathology

GENETICS

A common translocation $t(10;17)(q22;p13)$ has been identified in some cases (35). This results in fusion of the *YWHAE* and *FAM22* genes (35).

GROSS

Clear cell sarcoma usually is large, is well circumscribed, and often weighs more than 500 g (33). The cut surfaces of clear cell sarcoma have a variable appearance: Some are homogeneous, gray, and lobular; others are variegated and composed of firm gray whorled tissue with light pink soft areas. In some, an abundance of extracellular mucin imparts a glistening slimy appearance. Approximately 33% of tumors have cysts ranging from a few millimeters to several centimeters in diameter.

MICROSCOPIC

The typical appearance of clear cell sarcoma at low magnification is of a monotonous sheet of cells with pale cytoplasm. At higher magnification, the cells are recognized to be organized in cords separated by branching septa composed of spindle cells with dark nuclei and of small blood vessels. The cells of the cords have pale cytoplasm and indistinct cytoplasmic membranes (Fig. 30.5). Although the cytoplasm of the cord cells is pale, it usually is not clear in the same way as that of clear cell RCC, and clarity of cytoplasm is not key to making the diagnosis. Nuclear features are key to the diagnosis. The chromatin is finely dispersed, and the nucleoli are small and inconspicuous. This differs from the dark nuclei of blastema in Wilms tumor and the prominent nucleoli typical of rhabdoid tumor.

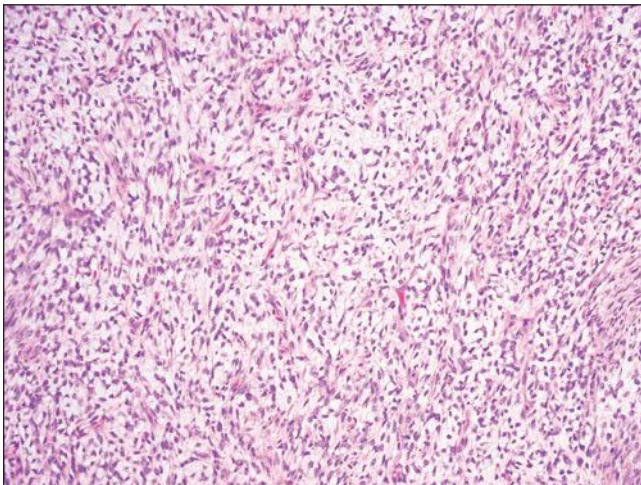


FIGURE 30.5 Clear cell sarcoma of the kidney. The tumor is composed of small, uniform spindle cells with scant pale cytoplasm growing in cords.

Another helpful feature is the infiltrative border in which renal tubules are frequently surrounded by sarcoma; this contrasts with the circumscribed border typical of Wilms tumor. Confusing variations on the classic pattern occur—including spindle cell, cystic, hyaline sclerosis, and palisading (12,33). In such cases, generous sampling often reveals areas in which the pattern of cords and septa indicates the correct diagnosis. Other helpful points that distinguish clear cell sarcoma of the kidney from Wilms tumor include the following: blastema does not occur in clear cell sarcoma, heterologous elements such as cartilage or muscle do not occur in clear cell sarcoma, clear cell sarcoma is neither multicentric nor bilateral, and sclerotic stroma is uncommon in Wilms tumor before therapy. Rarely, clear cell sarcoma contains foci in which the cells have prominent nucleoli, resembling those of rhabdoid tumor of the kidney; in other areas, patterns typical of clear cell sarcoma often clarify the diagnosis.

Treatment and Outcome

Clear cell sarcoma is highly malignant and at least 10 times as likely to metastasize to bone as any other pediatric renal cancer. It was originally called *bone-metastasizing renal tumor of childhood* by Marsden and Lawler (36). It is resistant to conventional therapy for Wilms tumor, but overall survival under chemotherapy with doxorubicin is in the 75% range with excellent survival for children with low-stage disease (33,37).

Rhabdoid Tumor of the Kidney

Clinical Findings and Epidemiology

Rhabdoid tumor is the most aggressive renal neoplasm of childhood and metastasizes widely to cause death in the majority of patients within 3 years of the time of diagnosis (38,39). The NWTS median age at diagnosis is 11 months, and few rhabdoid tumors occur after 3 years. Boys predominate over girls in a ratio of 3:2 (39). Embryonal tumors of the central nervous system (40) and paraneoplastic hypercalcemia (41) occasionally are associated with rhabdoid tumor of the kidney.

Pathology

GENETICS

Almost all cases studied have been found to have a mutation or deletion of the *SMARCB1/INI1* gene located at chromosome 22q.11 (42).

GROSS

Rhabdoid tumor is less well circumscribed than Wilms tumor or clear cell sarcoma. Most tumors are located in the center of the kidney, and it is usual for the renal sinus (the space formed by the medial concavity of the kidney containing fat, loose connective tissue, vascular structures, the renal pelvis, and proximal ureter) and pelvis to be infiltrated (39). The parenchyma of rhabdoid tumor is usually light tan or yellow-gray, solid, and friable with foci of necrosis and hemorrhage.

MICROSCOPIC

Rhabdoid tumor consists of medium or large polygonal cells with abundant eosinophilic cytoplasm and round nuclei with thick nuclear membranes and large nucleoli. The cells are arranged in diffuse sheets (Fig. 30.6). The name was given because the cytoplasm often bears a superficial resemblance to that of differentiating rhabdomyoblasts. The resemblance is

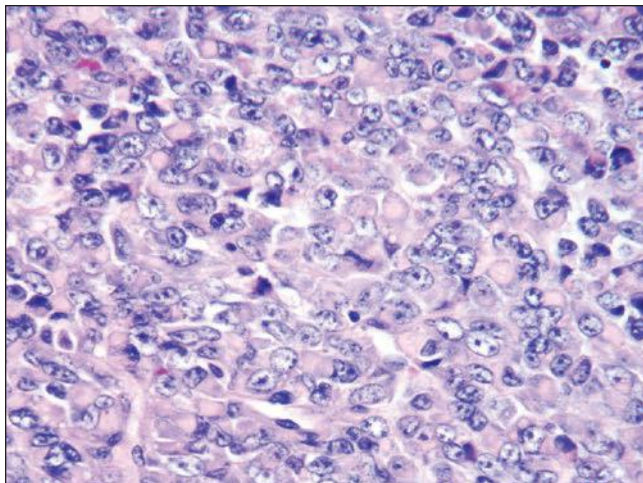


FIGURE 30.6 Rhabdoid tumor. The tumor is composed of a sheet of loosely cohesive cells having vesicular nuclei with prominent nucleoli. Many of the cells have fibrillar eosinophilic cytoplasmic inclusions.

spurious, and if there is definite differentiation toward skeletal muscle, the tumor is not a rhabdoid tumor. The cytoplasm commonly contains a large eosinophilic inclusion that forces the nucleus to one side. At the ultrastructural level, these inclusions are composed of whorled microfilaments (39). A variety of rare patterns have been recognized, including sclerosing, epithelioid, spindle cell, lymphomatoid, vascular, pseudopapillary, and cystic (39). These are usually mixed with the typical pattern and with each other and retain the characteristic nuclear features. It is important to recognize that a number of other primary kidney tumors including medullary carcinoma and RCC can have rhabdoid-like cells (43).

SPECIAL STUDIES

These tumors do not express muscle markers and are positive for vimentin. Loss of INI1 expression can be demonstrated by immunohistochemistry in these tumors (44).

Treatment and Outcome

Rhabdoid tumor of the kidney is not responsive to radiation or chemotherapy, so surgery is the principal treatment. Early and widespread metastasis is common, and approximately 75% of patients die from rhabdoid tumor within 36 months of diagnosis (38,39,45). Survival is better for low-stage tumors and in older (greater than 2 years) patients (46).

Metanephric Adenoma

Clinical Findings and Epidemiology

The rare tumor known as metanephric adenoma has now been described in detail (47–52). Epithelial neoplasms of the kidney are rare in children, but among them metanephric adenoma is the most common. It occurs at all ages but is most common in middle age, with a 2:1 female preponderance. Approximately 50% of metanephric adenomas are incidental findings, with others presenting with polycythemia, abdominal or flank pain, mass, or hematuria. The relationship, if any, of metanephric adenoma to other families of renal neoplasms has been debated. They do not have the chromosomal gains characteristic of papillary renal neoplasia (53), and some consider them to

be related to Wilms tumor (52). Metanephric adenoma is part of a family of neoplasms that includes the even rarer metanephric adenofibroma (54) and metanephric stromal tumor (55). The 2004 WHO classification places these tumors in a family by themselves (1).

Pathology

GENETICS

Gains of chromosome 19 have been detected in some cases by comparative genomic hybridization in one study (56) but not in another (57). In another report, the presence of a tumor suppressor gene at chromosome 2p13-21 was detected (58). Most recently, *BRAF* mutations were detected in 90% of 29 cases studied (59).

GROSS

Metanephric adenoma is well circumscribed, gray or pale tan, and solid or lobular, and its size ranges up to 15 cm. Small cysts and calcifications can be present.

MICROSCOPIC

Metanephric adenoma is composed of small, uniform, round tubules embedded in a loose stroma. It is sharply circumscribed and can have a fibrous capsule. At first glance, Wilms tumor usually comes to mind. Nuclei are small and uniform with absent or inconspicuous nucleoli and scant cytoplasm (Fig. 30.7). Papillary or microcystic architectures are less common. Psammoma bodies are common, as are hemorrhage and necrosis. Wilms tumor stroma and blastema are not found in metanephric adenoma.

SPECIAL STUDIES

Metanephric adenoma cells usually react with antibodies to WT1 (49,51). It is usually nonreactive or only weakly reactive for cytokeratin 7 and epithelial membrane antigen (48,51). The majority do not express alpha-methylacyl-CoA racemase (AMACR) (60).

Treatment and Outcome

Cases reported to date have not recurred or metastasized. There have been two cases with an associated papillary RCC described

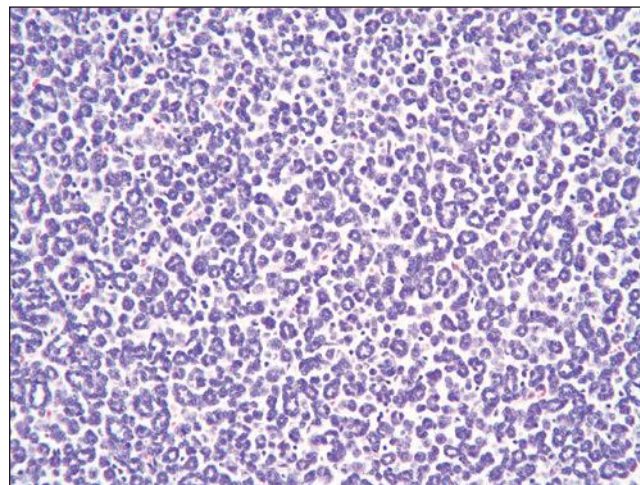


FIGURE 30.7 Metanephric adenoma. The tumor is composed of small uniform cells with scant cytoplasm and forms regular round tubules.

that developed metastases (61,62). Fewer than a handful of metanephric adenomas have been associated with psammoma bodies or even epithelial cells in lymph nodes draining the kidney with the metanephric adenoma; the nature of this process is unclear (63).

Translocation Carcinomas

Over the last several years, a family of renal carcinomas that contain various translocations involving Xp11.2 has been identified (64,65). All of these translocations resulted in gene fusions involving *TFE3*. This family of carcinomas was classified as Xp11 translocation carcinomas in the 2004 WHO classification (1). Subsequently, carcinomas with a t(6;11) producing a fusion with the *TFEB* gene have been identified (66). Since *TFE3* and *TFEB* are members of the MiTF/TFE family of transcription factor genes, some authors have grouped these together as MiT-related RCCs (67).

Clinical Findings and Epidemiology

Although carcinomas make up less than 5% of renal tumors in children (68,69), translocation carcinomas appear to make up at least 20% to 50% of pediatric renal carcinomas (70–72). Translocation carcinomas also occur in adults although their frequency remains unclear (73). Some patients have had histories of chemotherapy for other conditions (71).

Pathology

GENETICS

This group of tumors includes several translocations that result in different gene fusions. These include t(X;1)(p11.2;q21) with *PRCC-TFE3* gene fusion, t(X;1)(p11.2;p34) with *PSF-TFE2* fusion, inv(X)(p11;q12) with *NONO-TFE3* fusion, t(X;17)(p11.2;q25) with *ASPL-TFE3* fusion, t(X;17)(p11.2;q23) with *CLTC-TFE3* fusion, and t(6;11)(p21;q13) with *Alpha-TFEB* fusion (67).

GROSS

Translocation carcinomas are typically nondescript solid tan-yellow neoplasms, often with foci of hemorrhage and necrosis.

MICROSCOPIC

Xp11.2 translocation carcinomas often have large areas of papillary architecture in which the papillae are covered by cells with abundant clear or pale cytoplasm (Fig. 30.8). However, they also have an alveolar or nested architecture, and cells with eosinophilic cytoplasm are common. Psammoma bodies are common and may be quite numerous. There are subtle variations in morphology among carcinomas with the different Xp11 translocations.

The t(6;11) translocation carcinomas consist of nests and microscopic cysts composed of polygonal cells with pale or eosinophilic cytoplasm. Papillae are uncommon. A distinctive component consists of cells with small amounts of cytoplasm and denser chromatin arranged around nodules of hyaline material in large acini. At low magnification, these resemble rosettes (74).

The t(X;17)(p11.2;q25) translocation carcinomas are composed of cells with abundant clear cytoplasm forming papillae and large nests. These tumors also produce prominent hyaline nodules and contain many psammoma bodies (75,76).

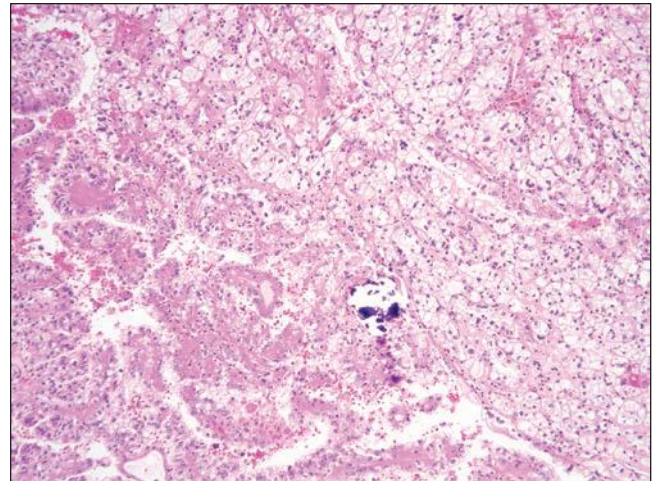


FIGURE 30.8 Xp11.2 translocation carcinoma. The tumor is composed of clear cells forming papillary and solid architectures. Note the large calcification.

There are also very rare tumors considered to belong to this family that produce visible melanin pigment (77,78). These have been reported under the term “*melanotic Xp11 translocation renal cancer*” (77).

SPECIAL STUDIES

Translocation carcinomas with gene fusions involving *TFE3* typically show a positive intranuclear reaction with antibody to TFE3 protein (79). Carcinomas with gene fusions involving *TFEB* typically show positive intranuclear reactions with antibody to TFEB. Xp11 translocation carcinomas characteristically fail to mark or mark weakly with antibodies to epithelial markers, such as epithelial membrane antigen and cytokeratins (64,73,80). Expression of cathepsin-K is present in both *TFE3*- and *TFEB*-related carcinomas (74,81). t(6;11) carcinomas are frequently positive for HMB45 and melan-A (66,74). The hyaline nodules typical of the t(6;11) and t(X;17) tumors react with antibodies to type IV collagen. Ultrastructurally, despite the expression of melanocytic markers, melanosomes or pre-melanosomes are not present in the t(6;11) carcinomas (74).

Treatment and Outcome

Because of the small number of cases studied so far, knowledge of the clinical aspects and outcome of these tumors is limited. Most have been found in children and young adults, but this may reflect a bias in the original populations studied. There may be more female than male patients, but that is not conclusive. Some patients have presented with metastases, yet have had prolonged survival (80,82,83). Tumors in adults appear to behave more aggressively (73).

Carcinoma Associated With Neuroblastoma

Roughly two dozen children and young adults have been diagnosed with RCC after surviving neuroblastoma in the first 2 years of life (84). In 1999, Medeiros et al. (85) published an account of four survivors of neuroblastoma who had histologically distinctive renal tumors and suggested that they constituted a distinct clinicopathologic entity; subsequently, another series of similar tumors in neuroblastoma survivors

was published (86). A few similar looking tumors have also been reported in children treated with chemotherapy for other tumors (87).

Clinical Findings and Epidemiology

The patients had neuroblastoma at the usual age; two of them received neither radiation nor chemotherapy. They were diagnosed with RCC at ages ranging from 5 to 14 years. In one patient, the RCC metastasized to the lymph nodes and liver.

Pathology

GENETICS

There is no information on the genetics of these tumors.

GROSS

The majority tumors have ranged in diameter from 35 to 80 mm; the 20 small tumors in the patient with multiple and bilateral tumors ranged from 1 to 24 mm. Two tumors were invasive of renal capsule, renal vascular system, or peripelvic lymphatics.

MICROSCOPIC

The best-documented postneuroblastoma carcinomas of the kidney contain majority populations of cells with abundant eosinophilic cytoplasm that sometimes is reminiscent of the cytoplasm in oncocytomas (Fig. 30.9). The cells grow in both papillary and solid patterns. Psammoma bodies are infrequently present, as are small clusters of foamy histiocytes. The nuclei often are medium sized and have irregular contours. Nucleoli are easy to find, corresponding to nuclear grade 3. A few mitotic figures are usually present.

SPECIAL STUDIES

All tumors studied have reacted with antibodies to epithelial membrane antigen, vimentin, and cytokeratin Cam 5.2.

Treatment and Outcome

Since so few patients have been reported, little is known of its responsiveness to radiation or chemotherapy, and the long-term outcome of these patients is also not clear (84).

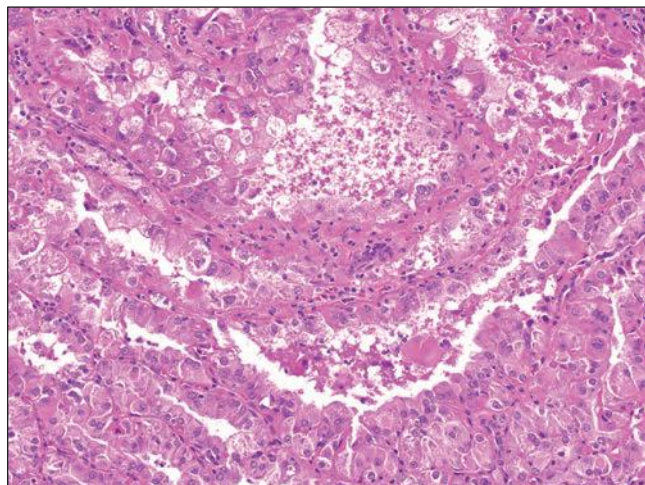


FIGURE 30.9 Postneuroblastoma carcinoma. The tumor is composed of cells with abundant granular eosinophilic cytoplasm.

ADULT NEOPLASMS

EPITHELIAL NEOPLASMS

Papillary Adenoma

Clinical Findings and Epidemiology

All classifications of renal tumors include adenoma as an entity (1,10,88), although criteria for distinguishing adenoma from carcinoma in the kidney remain a significant and unresolved issue in surgical pathology. With increasing numbers of small tumors, including many under 1 cm, being detected with new imaging technology, resolution of this issue is important (89–91). Small cortical epithelial lesions have been found in 7% to 37% of kidneys in autopsy series (92–94). Eble and Warfel (95) evaluated a series of 400 consecutive autopsies in which the kidneys were carefully sectioned and examined; in 83 instances (21%), epithelial cortical lesions were identified. The frequency increased with age (10% in 21- to 40-year-olds vs. 40% in 70- to 90-year-olds). Similar tumors frequently develop in patients on long-term hemodialysis, and papillary adenomas have been reported in up to one third of patients in association with acquired cystic disease (96,97). These are believed to be the precursors of carcinoma in this patient group (96,98)

Pathology

GENETICS

Papillary adenoma has similar cytogenetic changes to papillary carcinoma with trisomy 7 and 17 (99).

GROSS

Papillary adenoma is currently defined as being 5 mm or less in size (1,10). Tumors as small as 1 mm are identifiable with the naked eye. It is well circumscribed, yellow to gray, and located in the cortex. Most are single, but it is not rare for multiple adenomas to be present.

MICROSCOPIC

Adenoma is usually tubular, papillary, or tubulopapillary in architecture, with most corresponding to the chromophil-basophil cell type described by Thoenes et al. (88). The cells have round to oval nuclei with stippled or clumped chromatin, and nucleoli are inconspicuous. Cytoplasm is usually scant and amphophilic to basophilic (Fig. 30.10). Lesions formed by cells with more abundant eosinophilic cytoplasm occur. Nuclear grade is not currently a criterion. All solid clear cell tumors are considered to be clear cell RCC irrespective of size.

SPECIAL STUDIES

The immunohistochemical profile of papillary adenoma is similar to that of papillary RCC including expression of AMACR (98).

Treatment and Outcome

Reliable criteria for distinguishing adenoma from carcinoma remain elusive (50). In 1950, Bell (100) classified all tumors less than 3.0 cm in diameter as adenoma, despite the fact that metastases developed from 3 of 65 tumors (4.6%) in this size range. Small cortical clear cell tumors have repeatedly demonstrated malignant behavior, confirming that size alone is not a reliable diagnostic criterion (101). We agree that these tubulopapillary tumors are the most clearly identified benign

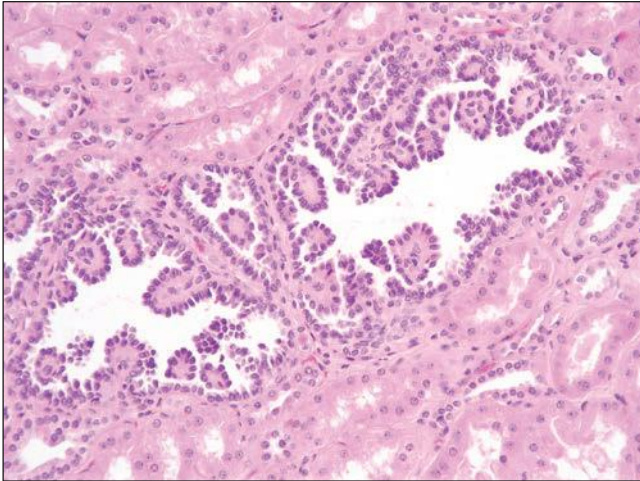


FIGURE 30.10 Papillary adenoma. A small papillary lesion merges imperceptibly with adjacent normal tubules; the cells have small uniform nuclei without significant atypia.

tumor of cortical epithelium and consider all lesions composed of clear cells to be malignant regardless of size (1,10).

Treatment of small cortical epithelial tumors is determined on clinical grounds. A therapeutic decision should not be based on frozen section, which is associated with both false-positive and false-negative results (102). With the popularity of partial nephrectomy for small tumors, the issue of frozen section is less pressing (103,104). Small tumors are also increasingly being managed by surveillance (91,105). Surveillance generally consists of sequential imaging studies (every 3 to 6 months) with reduced frequency if the lesion is slow growing. Intervention is indicated with rapid growth, patient preference, or improvement in the patient's other medical condition(s) if that was the major reason for surveillance.

Oncocytoma

Clinical Findings and Epidemiology

In 1976, Klein and Valensi (106) described a subset of renal tumors in adults composed of oncocytes and having an apparently benign clinical course. This observation, subsequently, was confirmed by several other groups (107–109). Oncocytoma accounts for approximately 4% of renal tumors in adults. Most occur in adults older than age 50 years, with a male-to-female ratio of 2:1. They are most often detected as incidental findings, although oncocytoma may present with hematuria or a palpable mass. They are usually sporadic, but oncocytoma or oncocytoma-like tumors can develop as part of the Birt-Hogg-Dubé syndrome (110). The Birt-Hogg-Dubé syndrome, due to mutation of the *FLCN* gene, is characterized by skin lesions (trichofolliculomas, trichodiscomas, and acrochordons), lung cysts (with increased risk of pneumothorax), and the development of renal tumors.

Radiologic studies may suggest the diagnosis of oncocytoma, although they are not specific. Typical angiographic features include a sharp, smooth margin with the capsule, thereby creating a lucent rim; vasculature without marked disarray, with no pooling of contrast material or arteriovenous shunting; homogeneous capillary pattern, giving a density similar

to normal renal parenchyma; and feeding arteries in a spoke-wheel pattern (111). Radiologic studies are, however, not reliable in making a specific diagnosis of oncocytoma (112,113).

Pathology

GENETICS

Cytogenetic studies have supported the view that oncocytoma is a distinct renal neoplasm. These tumors have a mosaic pattern of normal and aberrant karyotypes and consistently lack abnormalities in the 3p region. The most common abnormality detected is loss or partial loss of chromosome 1 (114–116). Less frequently, translocations involving chromosome 11 are described (117,118).

GROSS

Oncocytoma is well circumscribed, homogeneous, and tan brown or mahogany brown (Fig. 30.11). It sometimes is bilateral or multifocal (119,120), and rarely, innumerable lesions (ranging from 1 to 2 mm up to several centimeters) are present, a process that has been termed *oncocytomatosis* or *oncocytosis* (121,122). There may be areas of hemorrhage, but necrosis is absent. A stellate central zone of edematous connective tissue is common in large tumors, but in smaller tumors, it may be absent. Any tumor with a variegated appearance should be extensively sampled before making a diagnosis of oncocytoma; for this reason, the definitive diagnosis of oncocytoma at frozen section is discouraged.

MICROSCOPIC

Renal oncocytoma is composed of cells with abundant intensely eosinophilic and coarsely granular cytoplasm. Focal cytoplasmic vacuolization and clearing occur in up to 15% of cases (109). The cells are cuboidal to columnar and are arranged in well-defined nests that are closely packed peripherally but often are separated by a loose stroma near the center of the tumor (Fig. 30.12). Tubule formation is common and can predominate in a minority of cases (109). Cysts also occur occasionally and rarely are large enough to be grossly visible.



FIGURE 30.11 Oncocytoma. The tumor is well circumscribed and solid with a golden brown color and central patch of edematous stroma.

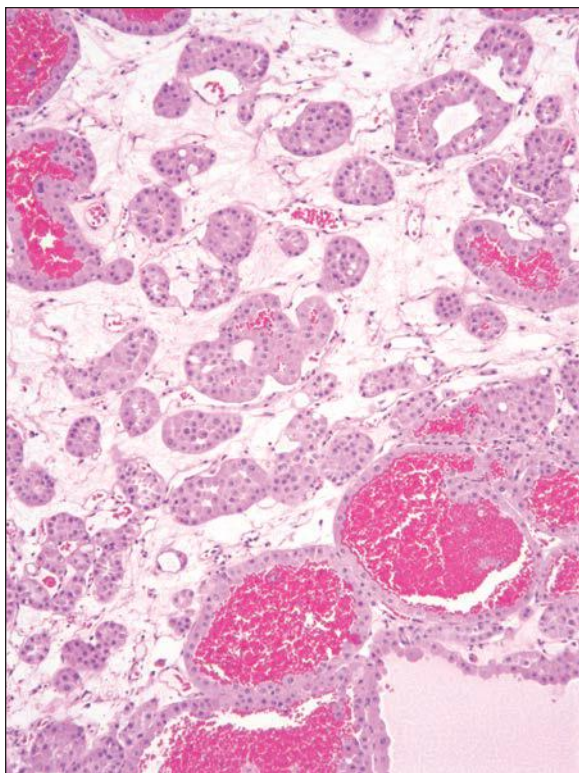


FIGURE 30.12 Oncocytoma. Characteristic histology of oncocytoma, with uniform cells having abundant eosinophilic cytoplasm arranged in well-defined nests and tubules, some of which are becoming microcystic. Note the appearance of the nests in loose, fibrous connective tissue; this pattern is almost pathognomonic for oncocytoma.

Cysts may be associated with hemorrhage. Necrosis is absent. Nuclei are regular and round to oval, with granular chromatin and central nucleoli. The presence of cells with bizarre pleomorphic nuclei is well recognized and believed to be degenerative (Fig. 30.13). Mitotic figures are absent or rare, at most. Evidence suggests that oncocytoma originates from the intercalated cell of the collecting duct (123,124). Distinguishing oncocytoma from chromophobe RCC is important because the latter may show malignant behavior.

SPECIAL STUDIES

Oncocytoma contains low molecular weight cytokeratin but does not contain vimentin (125,126). Cytokeratin 7 is expressed intensely by a few scattered single cells or small groups of cells (125,126). The tumor does not express the RCC antigen (127). The tumors are c-kit (CD117) positive with a membrane pattern (128). Hale colloidal iron stain is negative (positive in chromophobe carcinoma) (129). Some authors will allow staining limited to the luminal surface if tubules are present (109,130). Ultrastructurally, the cells are filled with mitochondria (131).

Treatment and Outcome

It now is accepted that renal oncocytoma is benign. Since oncocytoma is benign, there is no rationale for grading renal oncocytoma. Surgical resection, either by partial nephrectomy or by radical nephrectomy, is curative.

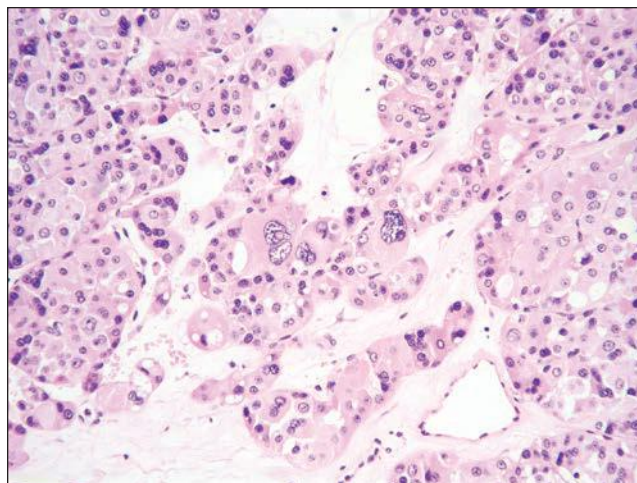


FIGURE 30.13 Oncocytoma. Example of an oncocytoma containing large pleomorphic hyperchromatic nuclei; this pattern is common in oncocytoma and is considered to represent a degenerative phenomenon.

Renal Cell Carcinoma Classification

Today the term *renal cell carcinoma* connotes a group of neoplasms having a common origin from the epithelium of the renal tubules but having distinct morphologic and genetic features. Until the mid-1980s, RCC was most often classified by its cytoplasmic appearance as clear cell or granular cell type (132). In 1976, Mancilla-Jimenez et al. (133) described a subset of papillary tumors that they believed were derived from the collecting ducts (ducts of Bellini). Then, in 1985, the Mainz group reported the first cases of a subtype with distinctive morphologic features that they called the *chromophobe* type (134). In 1986, Thoenes et al. (88) proposed a new classification of renal cell neoplasms that recognized collecting duct carcinoma and chromophobe cell carcinoma as well as clear cell RCC and *chromophil* RCC, also known as *papillary* RCC. Papillary, chromophobe, and collecting duct carcinomas made up 15% to 20% of renal cell neoplasms in surgical series, whereas clear cell RCC accounted for about 70%, with a few rarities and unclassified tumors making up the remainder. These efforts began the development of the currently employed classification system (1,10). Genetic studies validated these approaches to classification by discovering genetic abnormalities that are characteristic for each of the diagnostic groups. The most recent classifications have reaffirmed these changes and have added several newer entities (1,10). In 2012, the ISUP met and updated the 2004 WHO classification to recognize advances since its development. A modified WHO classification is presented in Table 30.1. In the following sections, each of the currently recognized types of RCC is discussed; there are many other described variants that at this point have not been judged to have sufficient evidence to recognize them as distinct. These are not dealt with in this Chapter.

Clinical Findings and Epidemiology

Clear cell RCC comprises a significant majority of RCCs and as such most of the following comments reflect largely on clear cell RCC. Features specific for specific types of RCC are presented

in the relevant sections below. The classic triad of presenting symptoms consists of hematuria, pain, and flank mass, a combination that is generally associated with advanced stage (135). However, approximately 40% of patients lack all of these and present with systemic symptoms. A common constellation is weight loss, abdominal pain, and anorexia, which may suggest carcinoma of the gastrointestinal tract (135). In up to 21% of patients, there is fever without infection (136,137). The erythrocyte sedimentation rate is elevated in approximately 50% of cases (138). Although blood erythropoietin levels are elevated in almost two thirds of patients (139,140), erythrocytosis occurs in less than 2% (140). Hypochromic anemia unrelated to hematuria occurs in about one third of cases (137). Systemic amyloidosis occurs in about 3% to 8% of patients with RCC and is of the AA type (141).

RCC occasionally causes paraneoplastic endocrine syndromes (142), which include pseudohyperparathyroidism, erythrocytosis, hypertension, and gynecomastia. Hypercalcemia occurs in the absence of bone metastases in approximately 10% of patients with RCC (137). Approximately 33% of patients are hypertensive (137); this is commonly associated with elevated renin concentrations (143). Typically, the blood pressure returns to normal after the tumor is resected. Gynecomastia may result from gonadotropin (144) or prolactin (145) production. RCC also is notorious for presenting as metastatic carcinoma of unknown primary, sometimes in unusual sites (146).

RCC occurs almost exclusively in adults, at rates of 10.0 and 4.8 per 100,000 among Caucasian males and females, respectively (147). The rates are significantly higher for African Americans at 11.5 and 5.7 per 100,000 (147). There is significant geographic and ethnic variation in RCC incidence with the lowest rates in Asian and Latin American countries (147,148). In the United States in 2012, approximately 64,770 new cases of cancer of the kidney and renal pelvis were diagnosed, and there were approximately 13,570 deaths attributed to these tumors (RCC accounts for approximately 80% to 90% of these) (149). In the first two decades of life, RCC is rare (68,69). Approximately 10% of cases occur before age 45 (150), but its incidence increases from that age to a peak in the sixth and seventh decades (151). Familial clusters of RCC are rare outside syndromes such as von Hippel-Lindau disease (152). In recent years, a variety of hereditary RCC syndromes have been described; however, overall, these account for a small proportion of tumors (153–157). The hereditary renal cell cancer syndromes are highlighted in Table 30.3.

As much as 30% of RCC is attributed to the carcinogenic effects of smoking (148,158). Obesity also is important, especially in women (148,158). Type 2 diabetes is also a risk factor in women (159). Environmental risk factors include phenacetin and acetaminophen use for long periods (160) and exposure to cadmium (161), petroleum products (161,162), and industrial chemicals (148,161). In most cases, the carcinogenic influence is unknown.

Between one third and one half of patients with von Hippel-Lindau disease develop RCC (156,157,163); metastasis occurs in approximately 50% of these and causes death in up to one half. Approximately 1% to 4% of patients with tuberous sclerosis develop RCC (155,157). Most have no recurrence, but a few cases with metastases have been documented (164). The association of autosomal dominant polycystic kidney disease

TABLE 30.3 Hereditary renal cell carcinoma syndromes

Syndrome	Genetics	Pathology
Von Hippel-Lindau	<i>VHL</i> gene (3p25-26)	Cysts Clear cell RCC
Tuberous sclerosis	<i>TSC1</i> (9q34) <i>TSC2</i> (16p13)	Cysts Angiomyolipoma Clear cell RCC Papillary RCC Chromophobe RCC
Birt-Hogg-Dubé	<i>FLCN</i> (17p11.2)	BHD-associated RCC (so-called hybrid tumor) Clear cell RCC Papillary RCC
Hereditary leiomyomatosis and RCC	<i>FH</i> (1q42-43)	HLRCC-associated papillary RCC
Hereditary papillary RCC	<i>MET</i> (7q31)	Papillary RCC (type 1), papillary adenoma
Chromosome 3 translocation	Unknown	Clear cell RCC
Hereditary paraganglioma	<i>SDHB</i> (1p36) <i>SDHC</i> (1q21) <i>SDHD</i> (11q23)	SDHB-associated RCC Clear cell RCC

with RCC is less well established (165). Acquired renal cystic disease in patients with chronic renal failure is also strongly associated with RCC (166,167).

STAGING

Since there is minimally effective treatment for metastases, the extent of spread of RCC dominates the prognosis (168,169). At present, the American Joint Commission on Cancer tumor-node-metastasis system is recommended for use (170). Tumors confined by the renal capsule are in the most favorable category. Within the most favorable group, the size of the tumor is used to subdivide these into four categories having different prognoses (168,169). Invasion of perinephric or renal sinus adipose tissue defines the pT3a category (171,172). Also included in the pT3a category are tumors that grossly extend into the renal vein or its segmental (muscle-containing) branches. Although the tumor thrombus may extend beyond the site of transection of the renal vein, this is not considered a positive margin unless the thrombus is adherent to the vein wall at the edge. The pT3b and pT3c categories are defined by extension of tumor into the vena cava below or above the diaphragm, respectively. The ipsilateral adrenal is involved by direct invasion or metastasis in about 5% of radical nephrectomy specimens (173). Direct invasion of the adrenal gland is considered to be pT4 (174,175); metastatic involvement is staged as pM1. In 10% to 15% of cases, there is metastasis to regional lymph nodes without distant metastasis (176). However, most regional lymphadenopathy is caused by inflammatory or hyperplastic changes (177). Although radical nephrectomy with regional lymph node dissection has long been the standard operation for RCC, lymph node dissection contributes to accurate staging but does not impact survival (178).

TABLE 30.4 Fuhrman nuclear grading system

Grade	Size (μm)	Shape	Chromatin	Nucleoli
1	<10	Round	Dense	Inconspicuous
2	15	Round	Open	Small, not visible with 10 \times objective
3	20	Round/oval	Open	Prominent
4	>20	Pleomorphic, multilobulated	Open, hyperchromatic	Macro

GRADING

In 1971, Skinner et al. (179) directed attention to the correlation between nuclear features and outcome. Currently, the Fuhrman et al. (180) grading system is most widely used (Table 30.4). Grade 1 and 4 tumors are least common, making up less than 10% of cases each; the middle grades each account for about 40% of cases (Fig. 30.14) (181). Numerous reports have documented that this grading system correlates well with survival in large series of patients with RCC (181–184). Actuarial, 5-year, disease-free survival ranges from around 90% for patients with grade 1 tumors to 18% for patients with grade

4 tumors (181,183,184). The highest grade found is the grade assigned, regardless of extent (181–183). Mitotic figures are not included in this system, but more than one per 10 high-power fields has adverse significance (182). The grading system has repeatedly been shown to be an independent prognostic factor for both clear cell and papillary RCC (181). Nuclear grading is part of almost all prognostic nomograms for RCC (185).

Areas resembling sarcoma are found in approximately 5% of RCCs (186,187). Grossly, these areas are often dense and white and contrast with the rest of the carcinoma (Fig. 30.15). Sarcomatoid areas have been found in association with all of

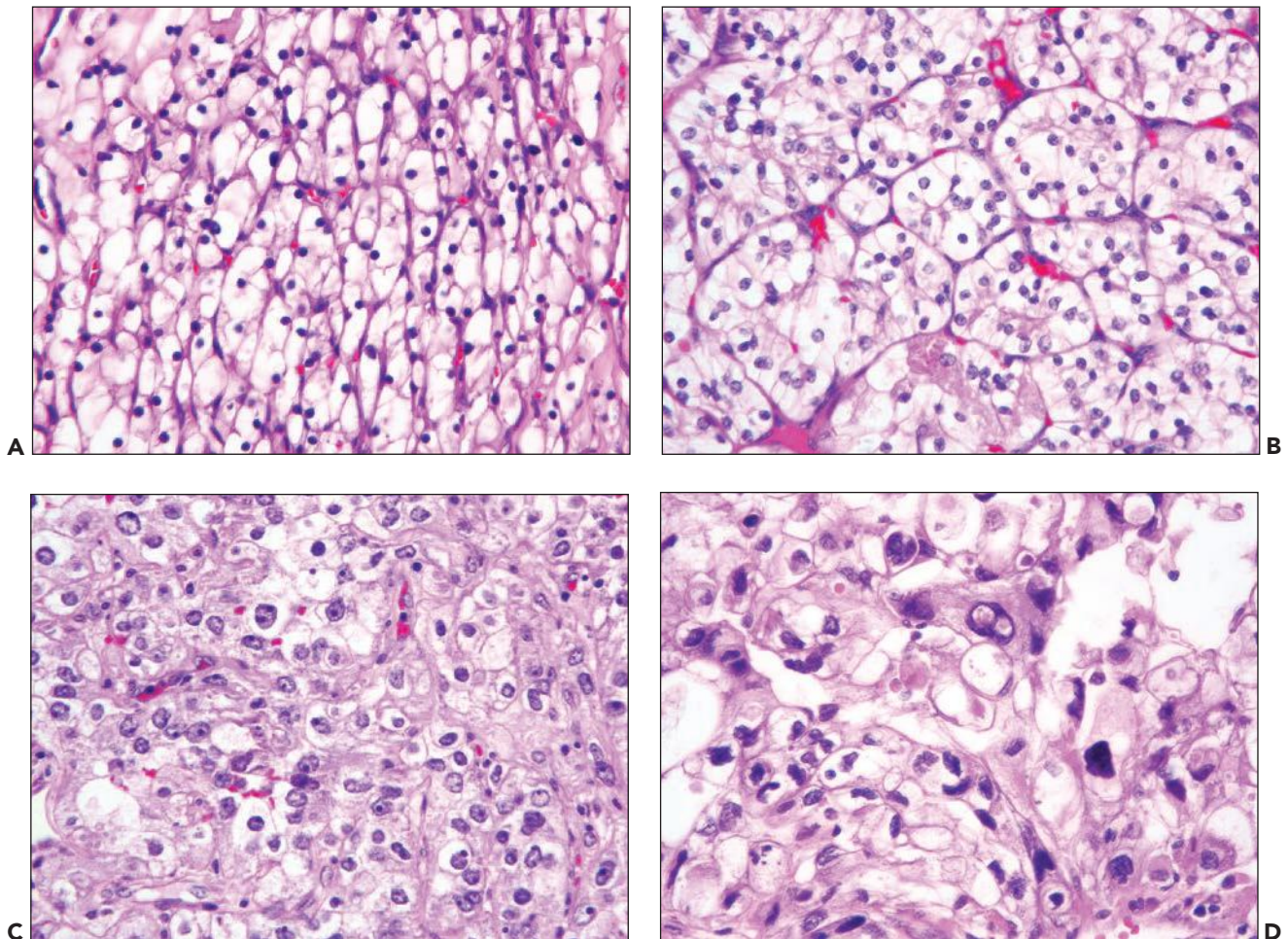


FIGURE 30.14 Clear cell renal cell carcinoma. **A:** Nuclear grade 1 tumor with small, uniform round nuclei and dense chromatin. **B:** Nuclear grade 2 carcinoma with slightly larger nuclei having more open chromatin and inconspicuous (at intermediate magnification, $\times 10$ objective) nucleoli. **C:** Nuclear grade 3 neoplasm has large, open nuclei with prominent nucleoli (readily visible at intermediate magnification). **D:** Nuclear grade 4 carcinoma with large bizarre nuclei.

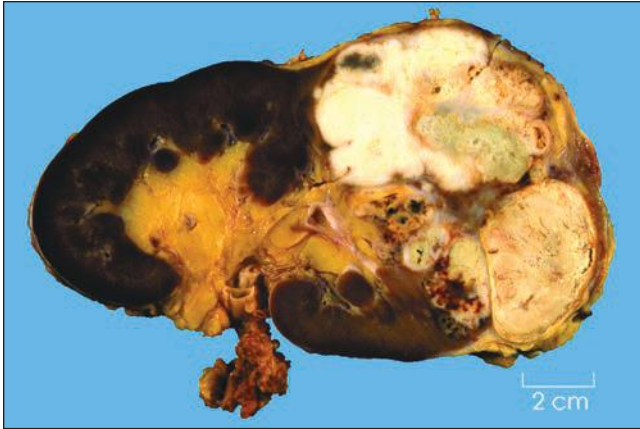


FIGURE 30.15 Sarcomatoid renal cell carcinoma. The tumor is infiltrative with extensive necrosis; the sarcomatoid component is indicated by the fleshy gray-white areas (top left part of the tumor).

the types of RCC. Microscopically, these resemble fibrosarcoma or undifferentiated spindle cell sarcoma (Fig. 30.16) (188). Heterologous differentiation toward osteogenic sarcoma, chondrosarcoma, or rhabdomyosarcoma is uncommon occurring in only 1% to 2% of cases (186,188–190). Patients with even small foci of sarcomatoid carcinoma have a much worse prognosis than those whose tumors do not have such foci (186,188), so thorough sampling of areas with differing gross appearances (especially firm, whitish areas) is important in evaluating RCC.

Treatment and Outcome

The primary treatment of RCC is surgery. In the past, partial nephrectomy was limited to patients with a single kidney or some other specific indication for nephron-sparing surgery (191); however, the last two decades have seen considerable literature supporting the performance of nephron-sparing surgery in a larger patient population. These studies have

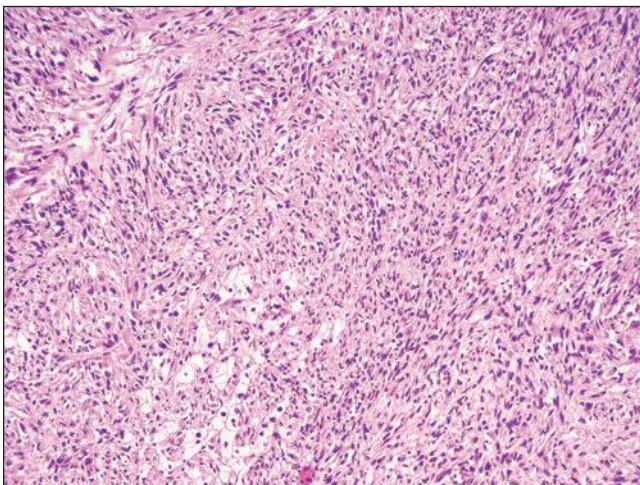


FIGURE 30.16 Sarcomatoid renal cell carcinoma. The tumor is composed of pleomorphic spindle-shaped cells arranged in poorly formed fascicles. Note the few residual clear cell renal cell carcinoma cells in the upper left.

reported excellent long-term results, equivalent to radical nephrectomy, following partial nephrectomy for small tumors (192,193). Emerging data indicate that treatment by partial nephrectomy may improve outcome compared with radical nephrectomy due to a reduction in the development of chronic renal disease (193). The performance of partial nephrectomy has led to the increased use of frozen sections at the time of surgery, with the major role for frozen section being margin control and not diagnosis (194). Frozen-section interpretation of renal masses is associated with both false positives and false negatives, and we would not make an unequivocal diagnosis of oncocytoma or adenoma at the time of frozen section (102,195). Laparoscopic partial or radical nephrectomy is increasingly being performed (196,197). This can result in a morcellated specimen that may make pathologic staging and histologic classification challenging, but in most cases still possible (198,199). Most recently, the use of ablation procedures to treat small renal tumors has become popular with early results indicating equivalent cancer control to surgical approaches (200–202). Lastly, the role of surveillance as an option in selected patients is gaining interest (203–205). The latter two options have resulted in an increasing role for needle biopsy of renal masses (105,206,207). Interpretation of these biopsies can be challenging (208).

For patients with spread of tumor into the renal vein, inferior vena cava, and even the right atrium, surgical resection remains the standard treatment option. Numerous studies have demonstrated the potential curability of such advanced disease (209).

RCC is notorious for its unpredictable clinical course. There are documented cases of spontaneous regression of metastases (210,211). Recurrence, a decade or more after nephrectomy, is found in more than 10% of those who survive so long (212,213), rising to 20% for patients living 20 or more years after surgical resection (212). The resistance of RCC to radiation and chemotherapy gives patients with remote metastases a poor prognosis with a median survival of 1 year (214). Treatment of metastatic disease in the last couple of decades has focused on biologic therapies with limited success (215). Currently, the role of targeted therapies is undergoing intense study with some optimism (216,217). In selected patients, resection of metastases may be beneficial (146,218).

Clear Cell Renal Cell Carcinoma

Clinical Findings and Epidemiology

The clinical and epidemiologic data presented in the previous section are largely based on clear cell RCC, as it makes up almost 75% of RCCs, and will not be repeated here. Clear cell RCC has a worse prognosis than other common types of RCC (108,219).

Pathology

GENETICS

Cytogenetic studies of clear cell RCC have consistently found losses in the short arm of chromosome 3 (3p) (220). RCC arising in patients with von Hippel-Lindau disease also, commonly, has deletion or partial deletion of chromosome 3p (221,222), with a breakpoint in the proximal short arm near the location (3p25) of the von Hippel-Lindau (*VHL*) gene (223). A second commonly involved site is at 3p14, possibly involving the *FHIT* gene (224). In one study, 96% of cases showed a continuous deletion from 3p14.2-p25, including



FIGURE 30.17 Clear cell renal cell carcinoma. The tumor is multicolored and variegated with areas of cyst formation and hemorrhage.

both the *FHIT* and *VHL* genes (225). Although various other genetic abnormalities are common in clear cell RCC, loss in 3p appears to be required for it to develop.

GROSS

A bright yellow or light orange color is the most distinctive aspect of the gross appearance of clear cell RCC. Often its appearance is variegated, mottled by areas of hemorrhage and cream-colored foci of necrosis (Fig. 30.17). Tumors are now frequently discovered incidentally by radiologists and often are less than 3 cm in diameter. Clear cell RCC typically is solid and bulges above the cut surface. Most are roughly spherical and circumscribed by a pseudocapsule, but diffuse infiltration and replacement of the kidney occur occasionally. Sometimes, there are irregularly shaped areas of edematous gray connective tissue at the centers of large tumors. Cysts ranging from a few millimeters to 1 to 2 cm in diameter are common. Occasionally, clear cell RCC is almost completely cystic (226–228). The current classification recognizes multilocular cystic RCC as a specific subtype of clear cell carcinoma (1). Rarely, clear cell RCC arises in the wall of a simple cyst or becomes cystic through necrosis and degenerative changes. Gross features such as hemorrhage and necrosis, solid nodules, and a thick fibrotic capsule indicate a greater likelihood of a cystic lesion being neoplastic. Sampling should be directed to areas of the lesion with these features. Up to 11% of cases are multicentric within the same kidney (229). RCC occurs bilaterally in approximately 2% of patients (230) and can be synchronous (231) or metachronous (232). Multicentricity and bilaterality are much more common in the hereditary RCC syndromes (229).

MICROSCOPIC

The cytoplasm of clear cell RCC is clear because it usually contains much lipid and glycogen, which dissolve during histologic processing. The site of origin of clear cell RCC was controversial until 1960, when Oberling et al. (233) demonstrated apical brush borders, which indicated origin from the proximal

tubule. Although clear cytoplasm has given this carcinoma its name, it does not define it, and other morphologic features are diagnostically important. Clear cell RCC often contains cells with granular eosinophilic cytoplasm and, sometimes, there are areas where most cells do not have clear cytoplasm. In some instances, the cells take on a rhabdoid morphology (234). Such areas may be associated with necrosis and should not be confusing if the other features typical of clear cell RCC are recognized. The nuclei usually are central and nearly spherical, ranging from small hyperchromatic ones lacking visible nucleoli to large and pleomorphic ones with macronucleoli. The mitotic rate is highly variable.

The major architectural patterns are compact (alveolar), tubular, and cystic, occurring alone or in combinations. The vascular pattern, consisting of a conspicuous network of thin-walled blood vessels with little supporting fibrous tissue, is a diagnostically helpful feature of most clear cell RCC. The vascular pattern is most apparent in areas with alveolar architecture (Fig. 30.18). Tubular structures merge with the cystic pattern as they become dilated. The tubules are usually round or oval but may occasionally elongate. Frequently, the small tubules are empty, but larger ones often contain eosinophilic fluid or blood. By definition, *multilocular cystic clear cell RCC* is grossly cystic and consists of fibrous septa with only a small population of carcinoma cells with clear cytoplasm and small, darkly staining nuclei that line the cysts and form small nodules within the septa.

SPECIAL STUDIES

Clear cell RCC frequently expresses both cytokeratins and vimentin; epithelial membrane antigen also, commonly, is present (126,235,236). Most also express the RCC antigen and CD10 (127,237). These findings are especially helpful in evaluating metastases from unknown primaries. Abundant glycogen and lipid are seen in the cytoplasm by electron microscopy. Apical brush borders or microvilli are sometimes present, reflecting this tumor's origin from the epithelium of the proximal tubule.

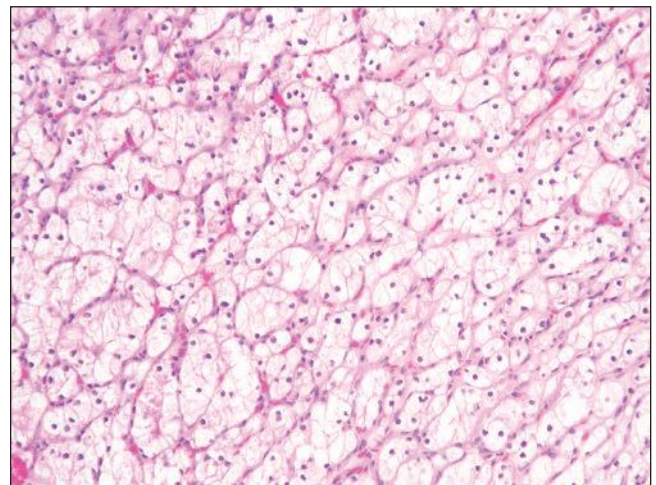


FIGURE 30.18 Clear cell renal cell carcinoma. Characteristic alveolar pattern with nests of clear cells separated by a prominent sinusoidal vascular network.

Papillary Renal Cell Carcinoma

Clinical Findings and Epidemiology

Approximately 10% to 15% of RCC, in surgical series, is papillary RCC (108,133,219,238,239). Males predominate in a ratio of approximately 2:1. Ages range from early adulthood to old age, with the mean between 50 and 55 years. These carcinomas have a mortality of up to 16% at 10 years (219) and sometimes present with metastases (240). Hereditary types of papillary RCC are well described (241). Papillary RCC has a significantly better prognosis than clear cell RCC (108,219,242).

Pathology

GENETICS

Papillary RCC has a characteristic pattern of genetic abnormalities that differs from those of other renal cell neoplasms. The pattern of lesions is one of the chromosomal gains, the most common of which are trisomy or tetrasomy of 17 and 7 (243,244). Most of these tumors in men lose the Y chromosome (243). These results are consistent and have been corroborated by several laboratories (244,245). Trisomy or tetrasomy of only chromosomes 7 and 17 appears to correlate with low-grade tumors, and the development of further trisomy has been suggested to correlate with progression (243).

GROSS

Papillary RCC is usually a well-circumscribed, globular tumor with tan or brown parenchyma (Fig. 30.19). In about 66% of cases, hemorrhage and necrosis are prominent, which may cause the tumor to appear hypovascular radiographically. Many of these tumors are large. Often the cut surface is friable or granular, a reflection of the papillae seen microscopically (Fig. 30.20). The larger tumors are often surrounded by a rim of dense fibrous tissue. In about one third of cases, there are calcifications.



FIGURE 30.19 Papillary renal cell carcinoma. The tumor is well circumscribed, is pale tan, and has a soft, friable surface. The thick capsule is not apparent in this photograph as a result of bulging of the tumor.

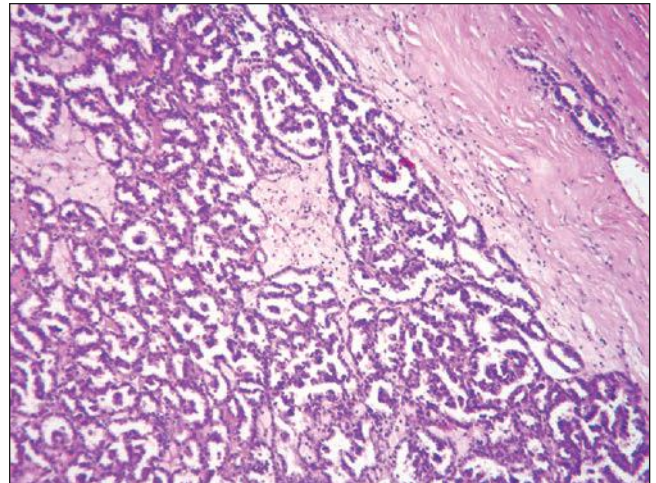


FIGURE 30.20 Papillary renal cell carcinoma. The type 1 tumor has a thick, fibrous capsule (lower right) and is composed of papillary structures. There are abundant foamy macrophages present.

MICROSCOPIC

In more than 90% of papillary RCC, the architecture is predominantly papillary or tubulopapillary (Fig. 30.21). The remaining tumors have a solid growth pattern that is the result of tight packing of papillae (246). The papillae usually have delicate fibrovascular cores covered by a single layer of carcinoma cells. The form of the papillae varies, ranging from complex branching to long parallel arrays. The cores are sometimes expanded by foamy macrophages. Psammoma bodies occasionally are present. Rarely, the papillary cores are wide and collagenous. The tubular architecture consists of small tubules lined by a single layer of cells identical to those covering papillae.

In papillary RCC, the cells range from small ones with inconspicuous cytoplasm to large ones with abundant eosinophilic cytoplasm. Tumors composed of small cells are more

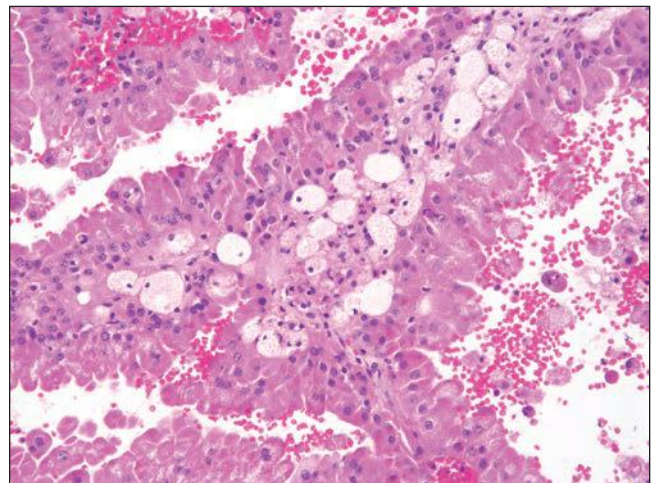


FIGURE 30.21 Papillary renal cell carcinoma. In this type 2 variant, the cells are tall and columnar with abundant eosinophilic cytoplasm; note the pseudostratification of the cells. The papillae also contain foamy histiocytes.

common. The small cells have high nuclear/cytoplasmic ratios because of their small volume of cytoplasm. The cytoplasm of these cells typically is pale and nearly clear. The nuclei are nearly spherical and small, and nucleoli are small or invisible. In the larger cells with eosinophilic cytoplasm, the nuclei tend to be larger and to have prominent nucleoli (Fig. 30.21). Delahunt and Eble (239) proposed subtyping papillary RCC into two groups, type 1 and type 2. There are data to support this distinction from both a clinicopathologic and molecular perspective (239,247–250). In several series, nuclear morphology correlated with stage and outcome (181,251); thus, the nuclear grading system is recommended.

SPECIAL STUDIES

Papillary RCC expresses cytokeratins, including cytokeratin 7, and frequently coexpresses vimentin (126,239). There is also consistent expression of the RCC marker, CD10, and AMACR (127,237,252,253).

Treatment and Outcome

Treatment is the same as for other types of RCC. Papillary RCC has a significantly better prognosis than clear cell RCC (108,219,242).

Chromophobe Renal Cell Carcinoma

Clinical Findings and Epidemiology

Thoenes et al. (134) described the first cases of chromophobe RCC in 1985. The tumor makes up about 5% of all RCCs (219,254–257). In contrast to clear cell RCC and papillary RCC, chromophobe RCC has no gender predilection. Patients range in age from 27 to 86 years, with a mean of approximately 55 years. Prognosis is significantly better than for clear cell and papillary RCC, with 5-year progression-free survival greater than 85% to 95% (219,254,256–258).

Pathology

GENETICS

Losses of multiple entire chromosomes—most often chromosomes 1, 2, 10, 13, 6, 21, and 17—occur in 90% of cases of chromophobe RCC (259–261). The genetic lesions typical of clear cell RCC (loss of 3p) and of papillary RCC (trisomy and tetrasomy of chromosomes 17 and 7 with loss of Y) are not found.

GROSS

The typical chromophobe RCC is solid, beige or light brown, circumscribed, and nearly spherical (Fig. 30.22). Some have small foci of hemorrhage or necrosis. Occasionally, a few small cysts are present. Chromophobe RCC ranges in size from less than 2 cm to larger than 20 cm, and some tumors invade the renal vein.

MICROSCOPIC

In sections stained with hematoxylin and eosin, chromophobe RCC has two variants: *typical* and *eosinophilic*. The former was recognized first (134). Its architecture usually is solid with broad trabeculae, but tubules and microscopic cysts sometimes are present. The cells vary in size and shape, tending to be large and polygonal. Their cytoplasm is abundant and pale staining, with a reticular or flocculent appearance. The cytoplasm is denser at the periphery, which makes the cytoplasmic membranes look thick (Fig. 30.23). Often some of the cells,

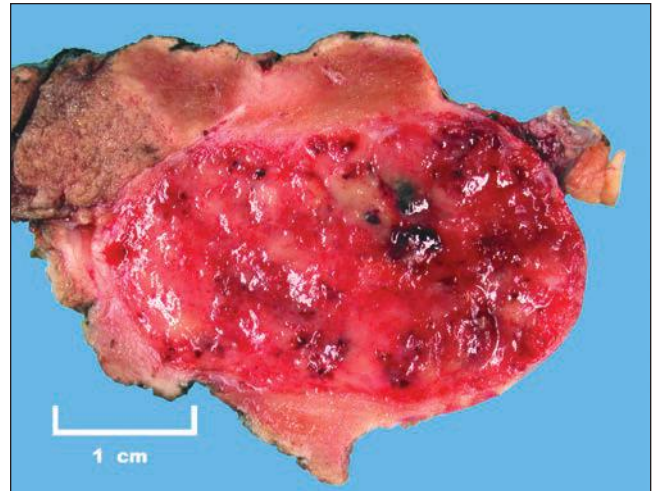


FIGURE 30.22 Chromophobe renal cell carcinoma. The tumor is well circumscribed, pink, and tan with foci of hemorrhage.

particularly the smaller ones, have eosinophilic cytoplasm. The nuclei are of medium size, and many have an irregular “raisinoid” shape. Many have small nucleoli; usually, there are few mitotic figures.

The eosinophilic variant of chromophobe cell RCC was recognized a few years later (262). Its cells have eosinophilic, finely granular cytoplasm. About the nucleus, the cytoplasm often is pale, creating a perinuclear halo (Fig. 30.24). On average, the cells are smaller than those of the typical variant. Architecturally, the cells are arranged in closely packed small nests; tubular structures are infrequent. Tumors having features of both renal oncocytoma and chromophobe RCC have been described, and the term *hybrid tumor* is applied in such cases (122,263,264). We believe that most so-called hybrid

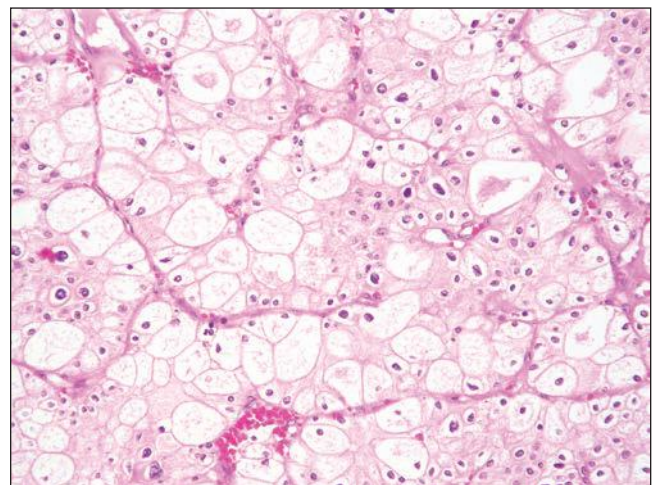


FIGURE 30.23 Chromophobe renal cell carcinoma. In this example of the classic type, there is a mixture of large cells with abundant flocculent cytoplasm and prominent cell borders and smaller cells with more eosinophilic cytoplasm. Many of the nuclei have an irregular “raisinoid” shape.

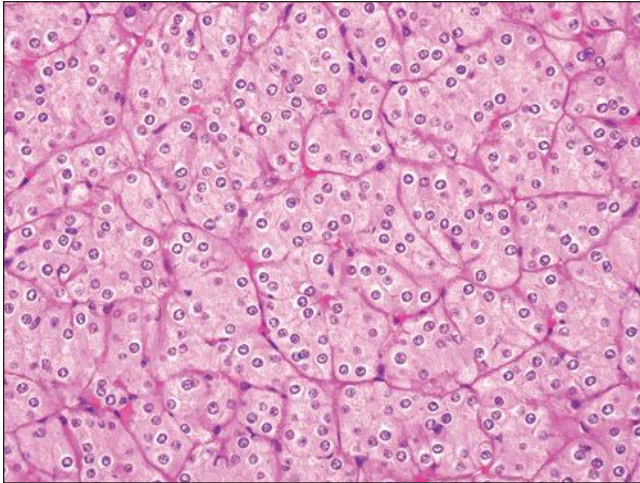


FIGURE 30.24 Chromophobe renal cell carcinoma. The eosinophilic variant of chromophobe renal cell carcinoma has smaller cells than the classic type with granular eosinophilic cytoplasm and prominent perinuclear halos; the cells are arranged in small, closely packed nests and mimic oncocytoma as in this example.

tumors represent tumors unrelated to either oncocytoma or chromophobe RCC but rather represent specific tumors as seen in renal oncocytosis (265) and Birt-Hogg-Dubé syndrome (110).

Sarcomatoid change is seen in 2% to 8% of chromophobe RCCs in large North American series (254,257,258). Heterologous differentiation can be present (266,267). Sarcomatoid change and necrosis are associated with poor outcome (254,257,258).

Although some studies have found nuclear grade to predict outcome in chromophobe RCC (254,258), others have not (268). In general, it is believed that Fuhrman nuclear grading is not validated for chromophobe RCC (269), and alternate grading systems have been proposed (270).

SPECIAL STUDIES

For both variants, the Hale colloidal iron stain is diagnostically helpful, staining the cytoplasm blue (130,134). Hale colloidal iron stain reacts with acid mucosubstances from the characteristic cytoplasmic vesicles. The tumor expresses cytokeratins, including diffuse and strong reactivity for cytokeratin 7, but not for vimentin (125–127). The RCC marker is expressed in about 50% of cases (127,252) and most express *c-kit* (CD117) (128).

Electron microscopy also is valuable. In the typical variant, the cytoplasm is filled with 150- to 300-nm round-to-oval vesicles (131,262). Often, these are invaginated and resemble those of the intercalated cells of the collecting duct (123). In the eosinophilic variant, the cytoplasm contains numerous mitochondria interspersed among the vesicles.

Treatment and Outcome

Treatment is the same as for other RCCs. Prognosis is significantly better than for clear cell and papillary RCC, with 5-year progression-free survival greater than 85% to 95% (219,254,256–258).

Collecting Duct Carcinoma

Clinical Findings and Epidemiology

In a 1976 study of RCC with papillary architecture, Mancilla-Jimenez et al. (133) described three cases with atypical hyperplastic changes in the collecting duct epithelium and postulated that these represented a distinct subset that probably originated from collecting ducts. Since then, several reports have further studied the clinical and pathologic features of this group of tumors (271–275). These are uncommon tumors accounting for less than 1% of RCCs (219). Collecting duct carcinoma often occurs at a younger age than other RCCs and has an aggressive clinical course.

Pathology

GENETICS

Cytogenetic analysis of three examples of collecting duct carcinoma showed loss of chromosomes 1, 6, 14, 15, and 22 (276). Consistent involvement of chromosome 1 has been highlighted in other reports (277–279).

GROSS

Collecting duct carcinoma has its epicenter in the renal medulla, although in larger tumors, this may be impossible to define. It is white or gray-white and has an infiltrative growth pattern; variegation is common, with areas of necrosis frequent.

MICROSCOPIC

These tumors often have a mixed papillary and infiltrative tubular architecture (Fig. 30.25). The infiltrative component is associated with marked stromal desmoplasia. Foci of dysplasia, or carcinoma in situ, can be found in the adjacent collecting ducts in some cases. The tumors are of high nuclear grade, corresponding to Fuhrman grade 3 or 4. Urothelial carcinoma invading the renal parenchyma can mimic collecting duct carcinoma. Some authors have classified tumors like this as collecting duct carcinoma if the urothelial carcinoma component is small (280); we would classify those as urothelial carcinoma.

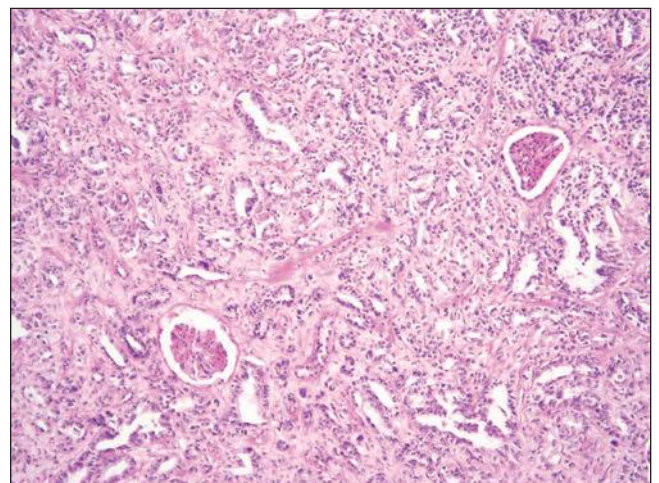


FIGURE 30.25 Collecting duct carcinoma. The tumor is composed of infiltrating ductal structures in a desmoplastic stroma. Individual tumor cells are pleomorphic with irregular chromatin, prominent nucleoli, and frequent mitoses.

Sarcomatoid morphology has been described in collecting duct carcinoma (188,281).

SPECIAL STUDIES

Histochemical stains may help to separate collecting duct carcinoma from other types of RCC. This carcinoma contains relatively small amounts of glycogen and sometimes contains cytoplasmic mucin. By immunohistochemistry collecting duct carcinoma expresses high molecular weight cytokeratin in many but not all cases (280,282). PAX8 is consistently expressed and p63 is not (280,282).

Treatment and Outcome

Treatment has largely been surgical, with a poor overall survival. Of reported cases, 10 died of metastatic disease within 2 years (271,272,275,283). In a series from the M.D. Anderson Cancer Center, the median survival of 10 patients was only 22 months (275).

Medullary Carcinoma

Clinical Findings and Epidemiology

This tumor occurs most often in young African Americans with sickle cell trait or hemoglobin SC disease (133,284). The presentation is similar to other malignant kidney tumors.

Pathology

GENETICS

Inactivation of the *SMARCB1/INI1* gene is demonstrable in most cases (285). A *bcr/abl* gene rearrangement has been demonstrated in one case (286). Molecular profiling has demonstrated that medullary carcinoma clusters closer to urothelial carcinoma than RCC (287).

GROSS

The tumors are located in the medullary region of the kidney. They are gray-white and infiltrative, usually involving the hilar fat. Satellite nodules are often present in the cortex.

MICROSCOPIC

The most characteristic histologic feature is a reticular or yolk sac–like appearance combined with adenoid cystic–like areas. In other areas, tumor cells are in solid nests and sheets. An infiltrate of polymorphonuclear leukocytes is usually present. Individual cells have pleomorphic nuclei with frequent mitoses. In most cases, cells with a rhabdoid morphology are present (Fig. 30.26). There is almost always a prominent desmoplastic stromal response. Sickled erythrocytes may be identified.

SPECIAL STUDIES

These tumors express cytokeratins and in particular cytokeratin 19 (284,288). There is loss of INI1 expression (285). Expression of the germ cell tumor marker OCT 3–4 has been reported (289).

Treatment and Outcome

The cases reported to date have been very aggressive with most patients dying within 1 year of diagnosis (283,284,290).

Mucinous Tubular and Spindle Cell Carcinoma

Clinical Findings and Epidemiology

Mucinous tubular and spindle cell carcinoma is a less common type of RCC that has been postulated to be of collecting

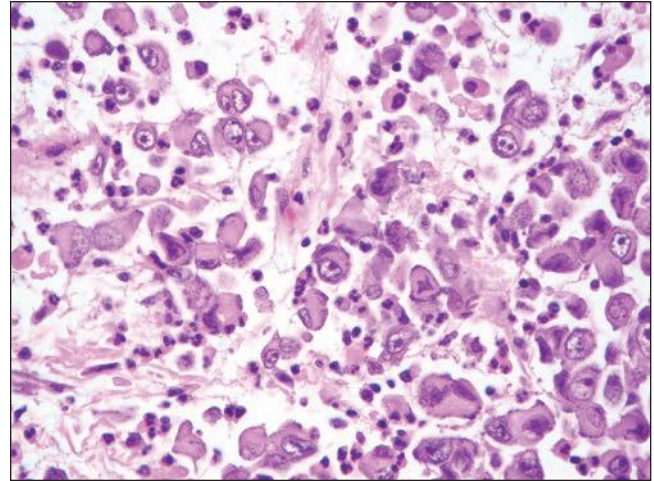


FIGURE 30.26 Medullary carcinoma. In this example, the tumor is composed of loosely cohesive cells with rhabdoid morphology and with neutrophils in the background.

duct and, possibly, loop of Henle origin (291–295). Most cases occur in females and are single although multifocality has been described.

Pathology

GENETICS

Cytogenetic studies have demonstrated consistent losses involving chromosomes 1, 4, 6, 8, 9, 13, 14, 15, and 22, supporting this lesion as being a distinctive entity (292,296,297). These lack the trisomies of 7 and 17 typical of papillary RCC (297).

GROSS

Mucinous tubular and spindle cell tumors are solid, pale tan to yellow to gray-white lesions that may have slight focal areas of necrosis or hemorrhage.

MICROSCOPIC

Histologically, they manifest elongated branching tubules in a bubbly mucinous, myxoid stroma. The collapsed tubules result in a cord-like pattern, and spindle cell areas are also present. The tubules are striking with characteristic long profiles (Fig. 30.27). Any of the three components (mucinous, tubular, spindle cell) can predominate (295). The basal lamina around the tubules is highlighted by PAS staining. The cells are cuboidal with scant clear to pale eosinophilic cytoplasm and low-grade nuclear features. Sarcomatoid change has been described (298,299).

SPECIAL STUDIES

Immunohistochemical studies have had widely varied results, but most tumors express cytokeratins 7, 18, and 19, epithelial membrane antigen, and AMACR (292–294,300). High molecular weight cytokeratin, CD10, RCC marker, and vimentin are less consistently expressed (292–294,300). Immunohistochemical and ultrastructural features of neuroendocrine differentiation have been reported in a few of these tumors (301).

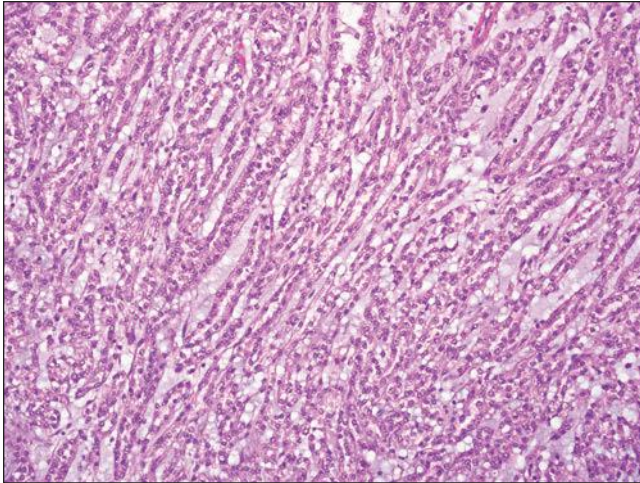


FIGURE 30.27 Mucinous tubular and spindle cell carcinoma. This photomicrograph illustrates the well-formed elongated tubules with bubbly mucin in the background.

Treatment and Outcome

Most of these tumors are low-grade malignancies and only a few examples of lymph node and distant metastases have been described in cases with typical histology (302). Tumors with a high grade or sarcomatoid component are more likely to metastasize (298,299).

Tubulocystic Carcinoma

Clinical Findings and Epidemiology

In the third series AFIP fascicle, Murphy et al. (303) illustrated an unusual tumor with a multicystic gross appearance and striking mixture of tubules and cysts, histologically. This is now recognized as a distinct entity in the ISUP modification of the 2004 WHO classification. These occur over a wide age range with a strong (approximately 8:1) male predominance (304–306). Presentation is as with other RCCs; radiologically, these present as complex multicystic tumors. Over 80% of tumors are pT1 at diagnosis (304–306).

Pathology

GENETICS

Gene expression profiling has demonstrated similarity to papillary RCC with trisomy 7 and 17 being present in many cases (307,308). In another profiling study, trisomy 17 but not trisomy 7 was present (305).

GROSS

These tumors are well circumscribed with a complex, multicystic appearance. The majority are under 4 cm in size though larger tumors are described (304,306). Multifocality occurs but is infrequent (305,306,308).

MICROSCOPIC

The tubules and cysts are lined by cuboidal to columnar cells with eosinophilic cytoplasm (Fig. 30.28). Nuclei are uniform and contain a single prominent nucleolus. Often apocrine-like snouting is present. In some tumors, the cysts are more irregular in shape and are lined by a flattened epithelium. The stroma is typically fibrotic. In some cases, there is an associated

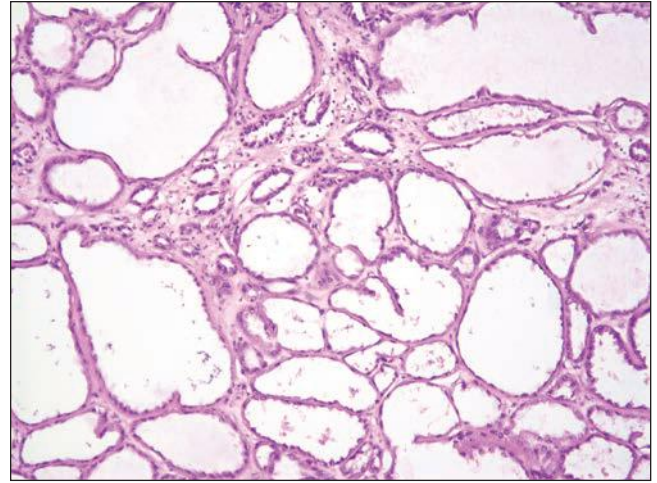


FIGURE 30.28 Tubulocystic carcinoma. This photomicrograph highlights the characteristic architecture with small tubules ranging up to cystic spaces.

papillary RCC (305,308). Sarcomatoid change has been described (309). Whether these truly derive from the collecting system is uncertain.

Treatment and Outcome

The overall survival is excellent; regional lymph node and bone metastases are reported in less than 10% of cases (305,306).

Clear Cell Papillary Renal Cell Carcinoma

Clinical Findings and Epidemiology

This tumor was first described by Tickoo et al. (97) in a study of tumors found in acquired cystic kidney disease. Subsequently, it has been shown that these also develop sporadically (310–313). These are probably not rare tumors, and many cases have likely been included in clear cell RCC and papillary RCC in the past. To date all patients have been adults with a male predominance (approximately 2:1). There are no other specific clinical characteristics.

Pathology

GENETICS

There is limited genetic data available. These do not show the chromosome 3 abnormalities of clear cell RCC or the typical trisomies of papillary RCC (310,311,313). Chromosomal imbalances have not been found by comparative genomic hybridization (312).

GROSS

The tumors typically have a solid and cystic appearance. The majority are small but tumors up to 8.5 cm are described. Most have a visible fibrous capsule.

MICROSCOPIC

In most cases, a tubular architecture predominates with a minor component of papillary architecture. The papillae are distinctive with a short blunt shape, often appearing to grow within elongated ductal structures (Fig. 30.29). Cytoplasm is abundant and clear. In most cases, areas of the tumor have the nuclei located toward the lumen producing a “secretory

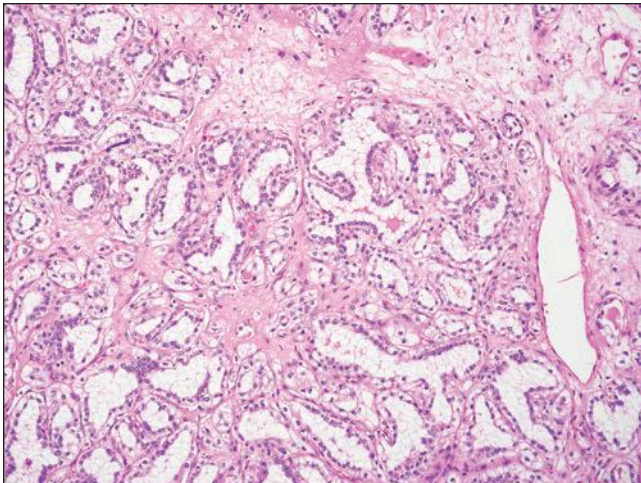


FIGURE 30.29 Clear cell papillary renal cell carcinoma. The tumor is forming tubules and more dilated structures with small papillary infoldings. The cells have clear cytoplasm and in some, the nuclei are located toward the luminal end of the cell.

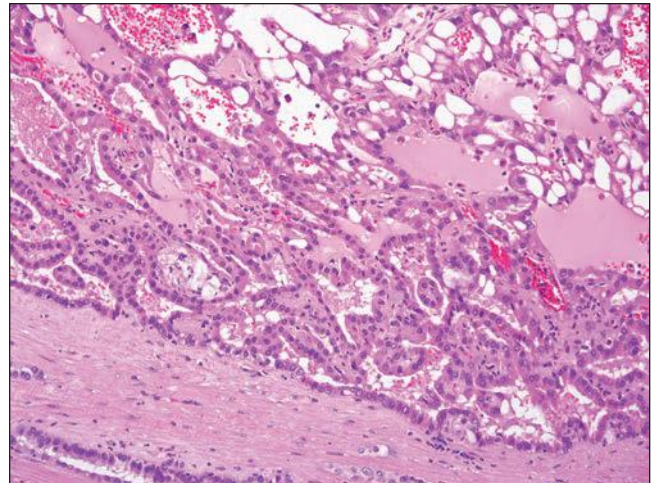


FIGURE 30.30 Acquired cystic disease–associated renal cell carcinoma. The cells have eosinophilic cytoplasm with prominent vacuolization and tubule formation. Note the calcium oxalate crystal deposition (above center).

endometrium-like” appearance. The stroma is fibrotic and can show smooth muscle differentiation. These are almost invariably nuclear grade 1 or 2.

SPECIAL STUDIES

These tumors have a distinctive immunohistochemical profile with diffuse strong immunoreactivity for cytokeratin 7 and carbonic anhydrase IX and no reactivity for CD10 or AMACR (310–313). There is no expression of TFE3 or the RCC marker (311–313).

Treatment and Outcome

The nature of these tumors remains uncertain. The vast majority are small, confined to the kidney and low nuclear grade. At the time of this writing, no case with metastasis has been reported.

Acquired Cystic Disease–Associated Renal Cell Carcinoma

Clinical Findings and Epidemiology

In 2006, Tickoo et al. (97) described a tumor that they considered unique to the setting of acquired cystic kidney disease. It was the most common type of RCC found in that series. Similar tumors had been described earlier in case reports (314,315). To date these tumors have only been found in the native kidneys of patients with end-stage renal disease (316,317).

Pathology

GENETICS

There are limited studies available; abnormalities of chromosome 16 have been described in several cases studied (trisomies and monosomies) (318,319). Trisomy of chromosomes 1, 2, 3, 5, 6, 12, X, and Y have been found less frequently (318,319).

GROSS

These tumors tend to be brown with fibrosis and dystrophic calcification. Some cases are present within cysts. They can be multifocal.

MICROSCOPIC

The tumor is composed of cells with abundant eosinophilic cytoplasm arranged in sheets, nests, and with papillary architecture. Many are partially cystic. The presence of variably sized spaces produces a cribriform or “sieve-like” appearance that is characteristic (Fig. 30.30). Deposition of calcium oxalate crystals within the tumor can be demonstrated in most cases. Sarcomatoid change can occur (97,320). Secondary changes such as fibrosis, hemosiderin deposition, and calcification are common.

SPECIAL STUDIES

These tumors express CD10, CD57, the RCC marker, and AMACR (317,318). They do not express cytokeratin 7 or high molecular weight cytokeratin (317,318).

Treatment and Outcome

Treatment has been as for other types of RCC. There is limited information on the prognosis for these tumors, but some cases have metastasized and resulted in death (97).

Urothelial Carcinoma

Clinical Findings and Epidemiology

Urothelial carcinoma of the renal pelvis accounts for 5% to 10% of renal tumors in adults. Risk factors include advanced age, smoking, exposure to various toxic industrial compounds, analgesic abuse, and Balkan nephropathy (321). These also occur in the Lynch syndrome (also known as the hereditary nonpolyposis colorectal cancer syndrome, is related to multiple genetic abnormalities including *MLH1*, *MSH2*, *MSH6*, and *PMS2* and is best known for increased risk of gastrointestinal tract and endometrial cancers) (322) and the Muir-Torre syndrome (also related to mutations in the *MLH1* and *MSH2* genes, is associated with similar cancers to Lynch syndrome plus cutaneous malignancies in particular sebaceous gland tumors) (323). Synchronous or asynchronous association with urothelial tumors elsewhere in the urinary tract occurs in up to 50% of cases. It is more common in males (3 to 4:1) and occurs

in an older age group (peak in the seventh decade) (324–327). Presentation is typically with gross hematuria (80%); flank pain (20%) and palpable mass are less common (10%).

Staging is based on a modification of the system applied to bladder cancer: pTis, carcinoma in situ; pTa, noninvasive papillary tumors; pT1, invasion of lamina propria; pT2, muscularis propria; pT3, renal pelvic fat or renal parenchyma; and pT4, adjacent structures or through renal parenchyma into perirenal fat (170). Fujimoto et al. (328) suggested that if involvement of the kidney is restricted to intratubular growth without stromal invasion, the prognosis remains favorable, and this is not considered to be pT3 disease when present.

Pathology

GENETICS

The genetics of these tumors is similar to that of urothelial carcinoma of the urinary bladder (329,330). The major genes implicated in the transformation of normal urothelium into low-grade papillary neoplasia include *H-Ras*, *FGFR3*, *PI3K*, and 9p deletion. The major genes implicated in the carcinoma in situ pathway are the tumor suppressor genes *TP53*, retinoblastoma (*RB*), and *PTEN*. Implicated in the 9p abnormalities are the *CDKN2A* and *CDKN2B* genes.

GROSS

Most tumors are papillary, producing an exophytic mass with a fine arborizing surface. In up to one third of cases, there are multiple lesions in the renal pelvis (327). Less often, the tumor forms a solid mass that sometimes extensively infiltrates the kidney or renal sinus soft tissue (Fig. 30.31). In a few cases, there is little if any growth within the renal pelvis, but the kidney is diffusely permeated. Tumors with a sarcomatoid component frequently have an exophytic, polypoid appearance.

MICROSCOPIC

More than 95% of renal pelvic tumors are urothelial, and adenocarcinoma (331,332), squamous cell carcinoma (331,333), and small cell carcinoma (334,335) are rare. Most tumors are composed of papillary fronds covered by urothelium having variable degrees of anaplasia. Most authorities apply the 2004 WHO grading system used in bladder tumors to these lesions.



FIGURE 30.31 Urothelial carcinoma. In this example, the tumor does not form a well-defined mass but is diffusely permeating the kidney parenchyma. The pale, poorly defined areas represent the tumor.

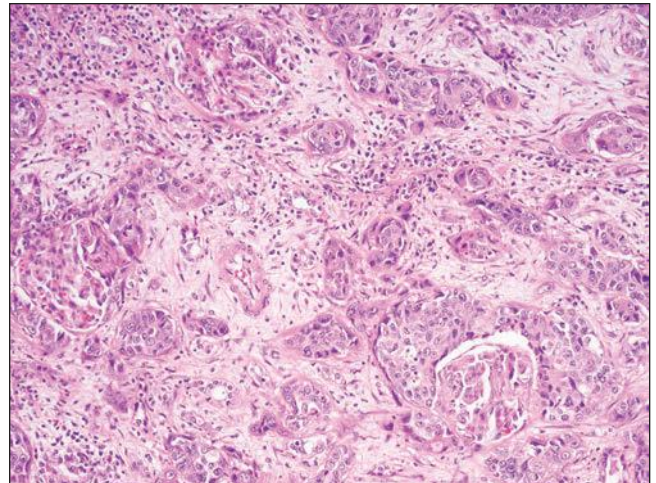


FIGURE 30.32 Urothelial carcinoma. This high-grade tumor is composed of variably sized nests of cells diffusely permeating the renal parenchyma with a desmoplastic and inflammatory tissue response.

High-grade tumors show the same diverse histology associated with urothelial carcinoma of the bladder (Fig. 30.32) (336); squamous or glandular differentiation is found in up to 20% of such tumors (326). These are diagnosed as urothelial carcinoma with squamous or glandular differentiation, and the diagnoses of squamous cell carcinoma and adenocarcinoma are reserved for tumors composed purely of those elements. Less often, areas of small cell or spindle cell differentiation are present (336). Rare examples with human chorionic gonadotropin production and syncytiotrophoblastic morphology have been described (337).

SPECIAL STUDIES

Findings in urothelial carcinoma that help to distinguish it from RCC include mucin demonstrable with the mucicarmine stain (up to 50% of cases). Immunohistochemistry demonstrates expression of cytokeratin 7, cytokeratin 20, high molecular weight cytokeratin, and p63 in a significant percentage (280,338,339). It does not express PAX8 (280,339).

Treatment and Outcome

The standard treatment is surgical resection by nephroureterectomy to prevent the development of additional tumors in the ureter (340). Overall, 5-year survival is in the range of 50%; however, this is strongly influenced by both stage and grade. Low-grade noninvasive tumors are associated with a greater than 90% 5-year survival compared with less than 10% for advanced high-grade carcinomas (324,325,327).

Renal Cell Carcinoma, Unclassified

In approximately 4% to 5% of epithelial kidney tumors, classification into one of the categories defined above is extremely difficult (1,10,108,341). In most cases, the tumors are not undifferentiated but have features that would fit into more than one category of classification. These include lesions with a well-defined differential diagnosis but for which a definitive conclusion cannot be reached. The most frequent problems in classification include the following: (a) separation of oncocytoma from chromophobe RCC; (b) the distinction

of papillary RCC from clear cell RCC with pseudopapillary areas; and (c) the distinction of clear cell RCC from chromophobe RCC (341).

Another large group of these tumors are high-grade carcinomas or sarcomatoid carcinomas, in which the epithelial element cannot be recognized or classified. In sarcomatoid carcinomas, cases may have no identifiable epithelial element, with the diagnosis based on immunohistochemical or ultrastructural evidence of epithelial derivation. Tumors in these groups are associated with an aggressive clinical course (108,342). Additionally, carcinomas with mucin production, mixtures of epithelial and stromal elements, or unrecognizable cell types, not otherwise specified, are included here.

Unclassifiable renal tumors may not, necessarily, have an uncertain prognosis. The poorly differentiated and sarcomatoid carcinomas are predictably aggressive, whether or not they are included in a category of sarcomatoid RCC. Localized tumors lacking significant nuclear atypia are best considered to be low-grade malignancies. For other unusual tumors, pathologic features such as size, stage, and nuclear grade provide important clues to likely future events.

Neuroendocrine Tumors

Clinical Findings and Epidemiology

The full spectrum of neuroendocrine tumors—including carcinoid tumor (343–345), atypical carcinoid (345), and small cell carcinoma (346,347)—occurs in the kidney. Intrarenal pheochromocytoma (348) and neuroblastoma (349) have also been described. Many examples of primitive neuroectodermal tumor have been well documented (350–352). Small cell carcinoma is distinctly uncommon and occurs in older patients, shows no gender predilection, presents with hematuria and abdominal pain, and is usually advanced at diagnosis (346,347). Carcinoid tumors occur at a younger age than RCC and occur roughly equally in males and females. There seems to be a predilection for horseshoe kidneys (344). Carcinoid syndrome and glucagon secretion have been reported with carcinoid tumors (353,354). Primitive neuroectodermal tumors are most common in children and young adults with no gender preference (350–352). Presentation is similar to other renal tumors.

Pathology

GENETICS

Primitive neuroectodermal tumors in the kidney have the *EWS/FLI-1* gene fusion (351,355).

GROSS

Small cell carcinoma is large and bulky, with extensive necrosis and an infiltrative growth pattern. Some are located primarily within the renal parenchyma, whereas others have an epicenter in the renal pelvis. In most cases, it is impossible to be certain of the site of origin. Carcinoid tumors are well circumscribed, red-brown, and hemorrhagic.

MICROSCOPIC

Histologically, these show similar features to neuroendocrine tumors elsewhere. Small cell carcinoma has small to large nuclei with finely distributed chromatin and inconspicuous or absent nucleoli. Cytoplasm is scant. There is prominent nuclear molding. Mitotic figures and individual cell necrosis are frequent (Fig. 30.33). A component of urothelial carcinoma may be present in cases arising in the renal pelvis, similar to small cell

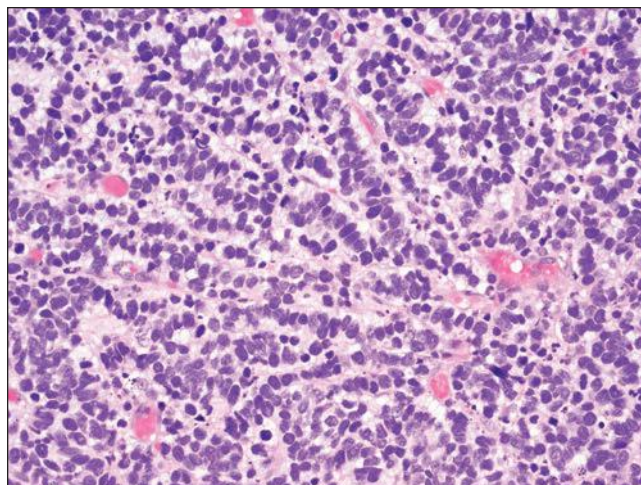


FIGURE 30.33 Small cell carcinoma. The tumor is made up of loosely cohesive cells with hyperchromatic nuclei, inconspicuous nucleoli, nuclear molding, and scant cytoplasm.

carcinoma elsewhere in the urothelial tract. Carcinoid tumors resemble such tumors elsewhere (344); in rare cases, the tumor has been associated with teratoma (345). Primitive neuroectodermal tumors have the typical histology seen elsewhere with cells having scant cytoplasm, small hyperchromatic nuclei, and variable rosette formation. There is great morphologic heterogeneity in these tumors, however (350).

SPECIAL STUDIES

Small cell carcinoma is usually cytokeratin positive, with the characteristic cytoplasmic dot-like pattern of immunoreactivity associated with neuroendocrine carcinoma. Neuroendocrine markers such as synaptophysin, chromogranin, and CD56 are demonstrable in over 50% of cases (346,347). Carcinoid tumors almost always express neuroendocrine markers (344,345). Primitive neuroectodermal tumors express CD99 and Fli-1 and have variable expression of neuroendocrine markers (350–352). Ultrastructural studies on small cell carcinoma and carcinoid tumors show cytoplasmic processes and neurosecretory granules (344,346).

Treatment and Outcome

To date, outcome has been poor for small cell carcinoma with 11 of 13 patients (85%) dead of disease, all within 31 months of diagnosis in a recent series (347). Carcinoid tumors have also been aggressive with metastases in over 50% of patients (344,345). Primitive neuroectodermal tumors are aggressive malignancies (350–352). The primary treatment is surgical resection; the roles of radiation therapy and chemotherapy have not been well defined for any of these.

MESENCHYMAL NEOPLASMS

Angiomyolipoma

Clinical Findings and Epidemiology

Angiomyolipoma is a benign tumor of the kidney, typically composed of smooth muscle, fat, and thick-walled blood vessels. Previously, some have considered it to be a hamartoma,

but genetic studies have shown it to be a clonal neoplastic proliferation (356). These tumors are believed to be derived from perivascular epithelioid cells (357). When tumors believed to be derived from these cells occur outside of the kidneys, they are often referred to as “PEComas.” Some are found as components of the tuberous sclerosis complex, but most are sporadic (358–360). Between 50% and 80% of patients with tuberous sclerosis develop angiomyolipoma (361). In these patients, the tumors are diagnosed earlier (median, 25 years), are smaller, and are less likely to be symptomatic, whereas sporadic cases present later (median, 45 years) with flank pain, mass, hematuria, or a combination of these. The most dangerous complication of angiomyolipoma is retroperitoneal hemorrhage (362).

Lymphangiomyomatosis of the lung occasionally occurs in association with sporadic angiomyolipoma and more frequently in patients with tuberous sclerosis (363,364). Imaging studies may be diagnostic, particularly computed tomography demonstrating fat within a renal tumor (112,113). Angiomyolipoma may also be present in regional lymph nodes or spleen and may extend into the renal vein and vena cava (365,366). Patients with these findings have excellent outcomes, so these should not be misinterpreted as signs of malignancy. In contrast, the epithelioid variant has been shown to have malignant potential (367,368).

Pathology

GENETICS

Angiomyolipoma is related to mutations in either the *TSC1* or *TSC2* genes (369).

GROSS

Angiomyolipoma is circumscribed but not encapsulated. Its cut surface has a variegated appearance (Fig. 30.34). Tumors composed predominantly of smooth muscle tend to have a fleshy, gray-white appearance, mimicking sarcoma or sarcomatoid carcinoma. Necrosis is uncommon, but hemorrhage may be extensive. In patients with tuberous sclerosis, the tumors are typically multiple, bilateral, and small, in contrast to sporadic



FIGURE 30.34 Angiomyolipoma. Large, bulging tumor extending into retroperitoneal soft tissue. The yellow color indicates a large component of fat cells.

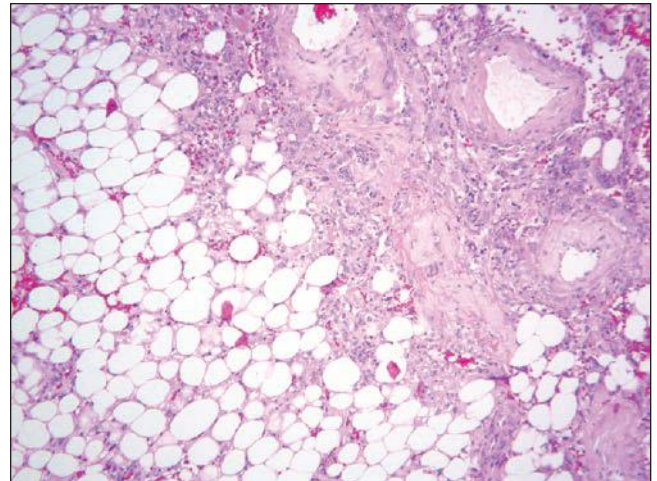


FIGURE 30.35 Angiomyolipoma. Typical example with a mixture of smooth muscle, adipose tissue, and thick-walled blood vessels.

cases that are single, unilateral, and large. RCC occasionally occurs in the same kidney with angiomyolipoma (370).

MICROSCOPIC

Angiomyolipoma has a tripartite composition of smooth muscle, fat, and thick-walled blood vessels in varying proportions (Fig. 30.35). When little fat is present, it may be difficult to decide whether the fat is an intrinsic part of the lesion or whether it represents invasion of perinephric fat by a spindle cell neoplasm. This is particularly problematic in lesions with predominance of smooth muscle when atypical features are present. Recognition of the thick-walled vessels is often the best clue to the true nature of the lesion. Atypical features such as nuclear pleomorphism, mitotic figures, and necrosis can be seen in angiomyolipoma (10,358). The smooth muscle can have an epithelioid appearance with abundant eosinophilic cytoplasm and eccentric large nuclei with prominent nucleoli (Fig. 30.36). Epithelioid angiomyolipoma is now recognized as a distinctive tumor that has malignant potential (367,368,371,372). A clear definition for the diagnosis of epithelioid angiomyolipoma has not been accepted. Features most predictive of malignant behavior are a high percentage ($\geq 70\%$) of atypical epithelioid cells, frequent (≥ 2 per 10 high-power fields) or abnormal mitotic figures, and necrosis (372). Sarcomatous transformation, which is exceedingly rare, is indicated by the presence of unequivocal high-grade sarcoma (373).

SPECIAL STUDIES

The smooth muscle component reacts with antibodies to vimentin, actin, and desmin; interestingly, it also reacts with antibodies to the melanoma-associated markers, including HMB-45, melan A, and microphthalmia transcription factor (359,374), as do other lesions of the tuberous sclerosis complex (375). Cathepsin K is consistently expressed (376).

Treatment and Outcome

Because angiomyolipoma is benign and can often be diagnosed radiographically because of its fat content, most are left in place unless they become symptomatic or exceed 4 cm in

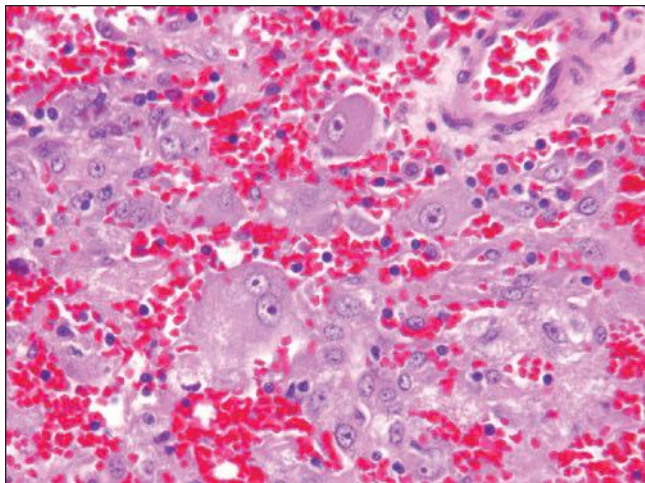


FIGURE 30.36 Epithelioid angiomyolipoma. In this angiomyolipoma, areas of the smooth muscle have a distinctly epithelioid morphology, with cells having abundant eosinophilic cytoplasm and large nuclei with prominent nucleoli producing a ganglion cell–like appearance.

diameter (377). Symptomatic or large tumors can be treated by resection, embolization, or ablative therapies (377). Treatment with mTOR inhibitors has been shown to reduce the size of angiomyolipoma (363,378). Leiomyosarcoma has arisen in angiomyolipoma only twice (373,379). Because of the potential for malignant behavior, epithelioid angiomyolipoma requires close clinical follow-up.

Other Benign Mesenchymal Tumors

Clinical Findings and Epidemiology

Mesenchymal tumors of almost every type have been reported as arising in the kidney (10,358), with leiomyoma (380,381) and hemangioma (382,383) being the most frequent. Other types include lymphangioma (384,385), glomus tumor (386), and lipoma (387,388).

Smooth muscle neoplasms are the most common mesenchymal tumors of the adult kidney (358,381) with leiomyoma being less common than leiomyosarcoma. Leiomyoma is rarely symptomatic (380). Hemangioma is rare, occurs mainly in adults, and has no gender predilection (382,383). It also occurs in association with the Klippel-Trenaunay (associated with multiple vascular lesions including involving the skin and the so-called port-wine stain and the overgrowth of bone and soft tissue) and Sturge-Weber (vascular abnormalities including the port-wine stain plus central nervous system involvement often with seizures) syndromes (389,390). Hematuria can be the presenting symptom, although most are asymptomatic.

Pathology

GROSS

Leiomyoma is well circumscribed, gray-white, and has a bulging lobular cut surface. Necrosis and hemorrhage are absent. Hemangiomas are single, small (less than 1 cm), and spongy red. Large tumors replacing the kidney have been described (391). The most frequent location of hemangioma is the renal medullary pyramids.

MICROSCOPIC

Leiomyoma is composed of spindle-shaped cells with elongate nuclei and eosinophilic cytoplasm. The cells are arranged in intersecting fascicles. No established criteria reliably distinguish benign from malignant renal smooth muscle neoplasms. Most authors have stressed the absence of mitotic figures and nuclear pleomorphism. Grignon et al. (358) indicated that the diagnosis of leiomyoma should be made cautiously; they considered large size, necrosis, nuclear pleomorphism, or one or more mitotic figures per 10 high-powered fields to be indicative of malignancy. In one series of primary renal sarcomas, a leiomyosarcoma with a mitotic rate of less than 2 per 10 high-power fields metastasized and caused the patient's death (392). The vascular spaces of hemangioma range from capillary to cavernous in size and are lined by benign endothelial cells.

Treatment and Outcome

Surgical resection is curative for both leiomyoma and hemangioma.

Primary Sarcoma

Clinical Findings and Epidemiology

Sarcomas account for less than 1% of all kidney tumors in adults (358,393). Leiomyosarcoma is the most frequent type, making up approximately 50% of cases (392–396). Leiomyosarcoma develops in a slightly younger age group than RCC but occurs over a wide age range with a slight female preponderance (397,398). There are no specific presenting symptoms. Abdominal or back pain, hematuria, and weight loss have been most frequent. Virtually, all other types of sarcoma have been reported in the kidney. Among the more frequently described are liposarcoma (399,400), solitary fibrous tumor (401–403), rhabdomyosarcoma (404,405), synovial sarcoma (406–408), chondrosarcoma (409), and osteogenic sarcoma (410,411); vascular sarcomas also occur here (383,412).

Pathology

GROSS

Most sarcomas are large, fleshy, and gray-white. Necrosis is often present. Leiomyosarcoma may be lobulated, bulging, and sharply circumscribed. Origin from the renal capsule, renal vein (413), or renal pelvis can be demonstrated in some cases.

MICROSCOPIC

Leiomyosarcoma is characterized by intersecting fascicles of spindle cells with blunt-ended nuclei and eosinophilic cytoplasm. Nuclear pleomorphism and mitotic rate are variable (Fig. 30.37). Myxoid variants occur here. Grignon et al. (392) recommended a diagnosis of leiomyosarcoma if there was necrosis, nuclear pleomorphism, or one or more mitotic figures in 10 high-power fields of a smooth muscle tumor in the kidney.

SPECIAL STUDIES

The results of immunohistochemical studies of spindle cell tumors of the kidney parallel those of sarcomas arising elsewhere. Vimentin, actin, and desmin should be positive in leiomyosarcoma. Nonreactivity for HMB-45 and melan-A is useful in excluding angiomyolipoma. Although weak reactivity for cytokeratin can be present in smooth muscle tumors, it is usually negative. Primitive cell junctions, focal densities within groups of cytoplasmic microfilaments, pinocytotic vesicles along the cell membrane, and basal lamina are seen ultrastructurally.

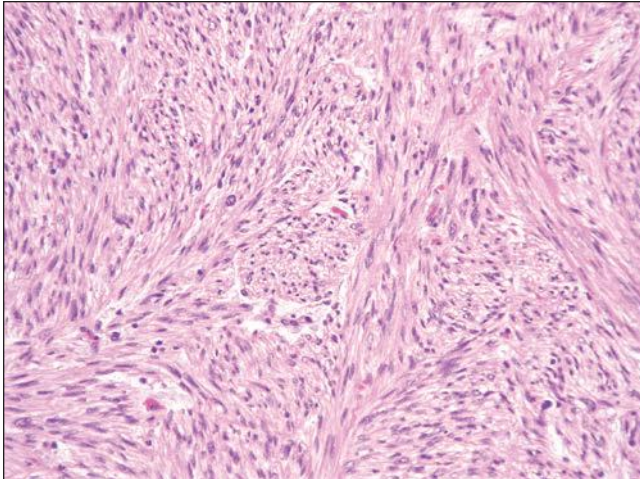


FIGURE 30.37 Leiomyosarcoma. Primary renal leiomyosarcoma composed of spindle-shaped cells in fascicles with mild to moderate nuclear atypia.

Treatment and Outcome

Treatment is primarily surgical, although given the poor prognosis, adjuvant chemotherapy may be appropriate. Outcome has been poor in the major reported series with the 3-year survival in the 20% to 30% range (392,394,396).

MISCELLANEOUS NEOPLASMS

Cystic Nephroma

Clinical Findings and Epidemiology

Cystic nephroma is a tumor that occurs in adults and children. These cases are now considered to represent two distinct tumor types (1,10). In a review of 187 cases, Castillo et al. (414) found a male predominance of nearly 2:1 in children younger than 2 years and a female predominance of more than 3:1 among adults. In children, cystic nephroma is considered by many to represent one end of a spectrum that includes cystic partially differentiated nephroblastoma and Wilms tumor (415). In adults, some pathologists consider cystic nephroma and mixed epithelial stromal tumor to be a single entity (416,417). We disagree and will discuss the two lesions separately.

Pathology

GROSS

Cystic nephroma is a discrete globular mass that is contained by a fibrous capsule. Internally, it is composed of multiple locules with smooth linings and containing clear yellow fluid. The locules do not communicate with one another. The septa range from paper-thin to a few millimeters thick; solid areas are absent or scant.

MICROSCOPIC

The septa are composed of fibrous tissue of variable cellularity and may contain foci of calcification and even ossification. Often the septa are densely collagenous, and many also have areas with increased cellularity producing an ovarian-like stroma. The septa may contain differentiated tubules. Usually the cysts are lined by flat or low cuboidal epithelium with

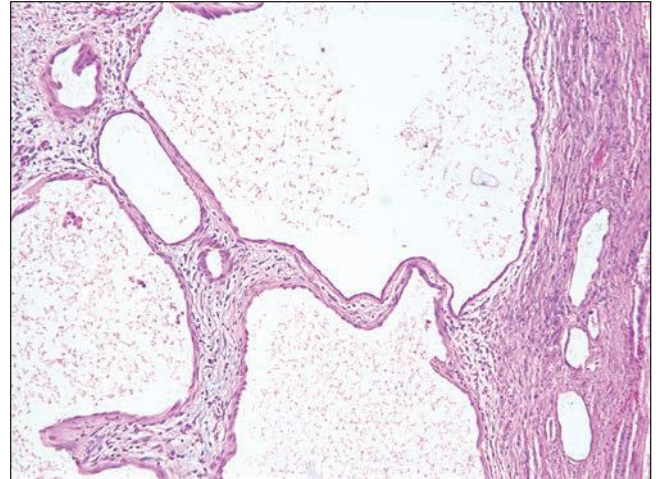


FIGURE 30.38 Cystic nephroma. In this photomicrograph, the septae show variable cellularity with no normal renal elements being present. The cyst lining is a single-cell layer, with some cells being flattened and others having a hobnail morphology.

little cytoplasm; sometimes the lining cells has a hobnail appearance (Fig. 30.38).

Most conditions that produce cysts in the kidneys are easily distinguished from cystic nephroma (418). Cystic Wilms tumor and cystic RCC are the principal differential diagnostic considerations. The predominance of females among adult patients and the rarity of reports of blastema in the septa of tumors from adults are evidence that cystic nephroma is a different entity from cystic partially differentiated nephroblastoma.

Multilocular cystic clear cell RCC differs from cystic nephroma in containing small populations of clear cells lining some of the locules and forming small collections in the septa. These cells are histologically identical to those of clear cell RCC.

Treatment and Outcome

Cystic nephroma is benign and effectively treated by conservative surgery.

Mixed Epithelial and Stromal Tumor

Clinical Findings and Epidemiology

Mixed epithelial and mesenchymal tumors in adults were initially reported under the term “cystic hamartoma of the renal pelvis” (419). The name *mixed epithelial and stromal tumor* is used in the current classification for this lesion (1). These occur more frequently in females (4 to 5:1) and over a broad age range. Because of the consistent expression of estrogen and progesterone receptors in the spindle cells, the possibility of a hormonal influence in the development of these neoplasms has been raised (420,421). Presentation has been similar to other renal neoplasms.

Pathology

GROSS

Some tumors have been well circumscribed and others infiltrative; extensive growth into the renal pelvis, and even into the ureter, has been described. Most cases have a mixture of solid and cystic areas.

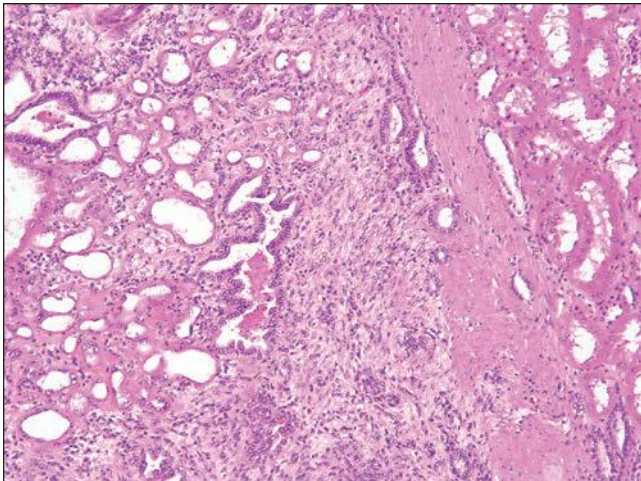


FIGURE 30.39 Mixed epithelial and stromal tumor. The biphasic nature of the tumor is illustrated. Note in particular the heterogeneous morphology of the epithelial element.

MICROSCOPIC

The epithelial component shows striking variability, from small tubules, to complex branching glandular formations, to microcyst and macrocyst formation (Fig 30.39). In some, there are leaf-like structures resembling those seen in phyllodes tumors. Clear cells have also been noted in the tubular component of some cases. The mesenchymal component ranges from hypocellular and fibrotic to more cellular with fibroblastic and myofibroblastic foci to fairly cellular stroma. Smooth muscle differentiation, particular at the outer margin (capsule), can be prominent. A possibly related tumor, with predominantly smooth muscle stroma and a proliferative epithelial component, has been described under the name *renal angioadenomatous tumor* (422).

SPECIAL STUDIES

The spindle cells are positive for vimentin, actin, and desmin. In most, the stromal cells express estrogen and progesterone receptors.

Treatment and Outcome

To date, the reported cases have behaved in a benign fashion. There have been cases described that may represent a malignant counterpart with sarcomatous change in the mesenchymal component (423,424).

Juxtaglomerular Cell Tumor

Clinical Findings and Epidemiology

More than 100 cases of juxtaglomerular cell tumor have been reported (425) since its discovery by Robertson et al. (426) over three decades ago. The tumor occurs in young adults and is more common in females; practically all patients are hypertensive (425,427,428). Detection of elevated plasma renin levels by selective renal vein catheterization is diagnostic. No case of bilateral juxtaglomerular cell tumor has been reported.

Pathology

GROSS

Juxtaglomerular cell tumor is well circumscribed, small (less than 3 cm), and gray-white. Small cysts can be present.

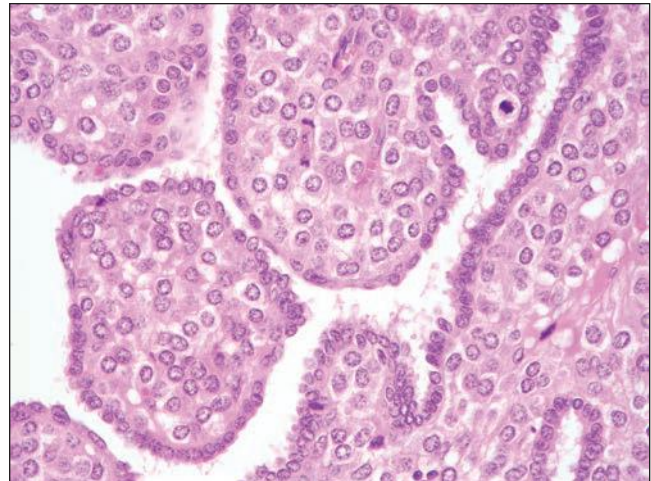


FIGURE 30.40 Juxtaglomerular cell tumor. In this histologic variant, the tumor is composed of broad papillae filled with polygonal cells and covered by a cuboidal epithelium.

MICROSCOPIC

The tumor is composed of small polygonal cells arranged in nests or trabeculae in a myxoid stroma. The histology is, however, quite varied, and solid islands, tubules, cysts, and broad papillae (429) can all be seen (Fig. 30.40). Juxtaglomerular cell tumor is perhaps the most difficult renal tumor to diagnose in routine sections.

SPECIAL STUDIES

Renin can be demonstrated by immunohistochemistry (429), and characteristic rhomboid crystals are seen ultrastructurally (430). The tumors express CD34, vimentin, and actin (428,431).

Treatment and Outcome

Surgical resection results in cure of the hypertension. Juxtaglomerular cell tumor is practically benign, with only a single reported instance of metastasis (432).

Renomedullary Interstitial Cell Tumor

Clinical Findings and Epidemiology

Renomedullary interstitial cell tumor is almost always an incidental finding at autopsy or in kidneys resected for other reasons (433). In one autopsy survey, it was identified in almost 50% of patients older than 20 years of age (434). Rarely it has been seen in needle biopsy specimens (435). It originates from the renomedullary interstitial cell, which is a specialized cell involved in blood pressure regulation.

Pathology

GROSS

The lesions are small and localized to the renal medulla, with most being less than 5 mm in diameter. They are well circumscribed, are gray-white, and do not bulge when cut. In over one half of cases, there is more than one tumor (434).

MICROSCOPIC

Renomedullary interstitial cell tumor is composed of stellate cells embedded in a loose fascicular stroma (Fig. 30.41).

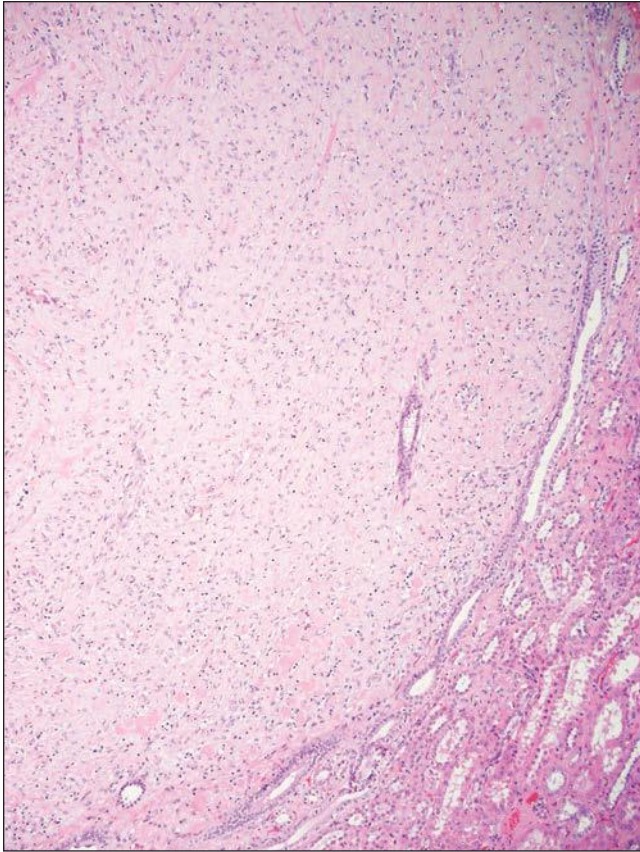


FIGURE 30.41 Renomedullary interstitial cell tumor. The lesion is circumscribed but not encapsulated and is made up of spindle-shaped cells in a dense, collagenized stroma. Note the entrapped tubule toward the periphery.

Tubules are often entrapped at the periphery. Amyloid may be present in the stroma (436).

Treatment and Outcome

These are incidentally found benign lesions, and no specific treatment is required.

Lymphoreticular and Hematopoietic Tumors

Clinical Findings and Epidemiology

Malignant lymphoma infrequently presents as a renal mass, without detectable disease elsewhere (437–440). In most cases of renal involvement by lymphoma, however, systemic disease is discovered soon after the renal mass or the patient already is known to have lymphoma (441). In cases presenting as a renal mass, symptoms are similar to those of other kidney tumors. Diffuse renal involvement can result in presentation with renal failure (442–444). One case of primary MALT lymphoma of the kidney presented with cryoglobulinemia (445).

Pathology

GROSS

Renal lymphoma appears relatively well circumscribed, but close inspection reveals infiltration at its edges. The tumor is soft, gray-white, and homogeneous. There may be a single mass or multiple nodules.

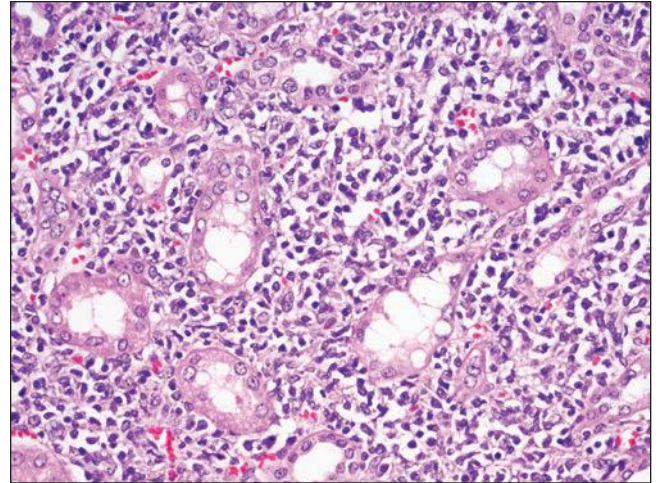


FIGURE 30.42 Lymphoma. In this primary lymphoma of the kidney, the tumor is composed of sheets of small lymphocytes diffusely permeating the parenchyma and sparing some normal structures.

MICROSCOPIC

Most characteristic is diffuse permeation of the renal interstitium by a monotonous population of lymphoid cells, with some degree of sparing of tubules and glomeruli (Fig. 30.42). Specific cytologic features depend on the type of lymphoma with large cell lymphoma of B-cell origin being most common (440). Less commonly, examples of MALT lymphoma (445,446) and plasmacytoma (447,448) have also been described.

SPECIAL STUDIES

Immunohistochemistry reveals positive staining for leukocyte common antigen; in B-cell lymphoma, demonstration of clonality confirms the diagnosis. B- and T-cell gene rearrangement studies, as in lymphoma from any site, can be helpful.

Treatment and Outcome

In most cases, the diagnosis is not made until after surgical resection. Additional treatment depends on the stage and histologic type.

Metastases to the Kidney

Clinical Findings and Epidemiology

In autopsy studies, the kidneys are involved by metastases in up to 7.2% of patients dying with cancer (449,450), with lung being the most common primary site. Much less frequently, tumors present with renal metastasis as the primary manifestation. RCC is the most common host of tumor-to-tumor metastasis (451,452).

Pathology

GROSS

Metastases can be single or multiple with no specific gross features.

MICROSCOPIC

The histology of the tumor reflects its site of origin. In some cases, only microscopic involvement, limited to glomeruli, is present (Fig. 30.43) (453). In the latter instance, presentation with proteinuria or acute renal failure may result (454). Hyperplasia of the Bowman capsule, which rarely occurs in association with carcinoma elsewhere, should not be mistaken for metastasis (455).

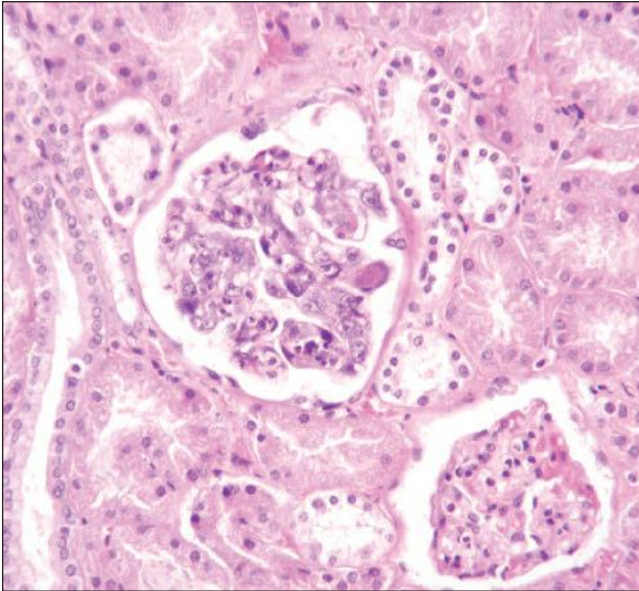


FIGURE 30.43 Intraglomerular metastasis. This is an example of renal metastasis with the kidney involvement limited to glomeruli in a young boy with neuroblastoma.

Treatment and Outcome

As indicated, metastatic involvement of the kidney most often occurs late in the course of the disease. However, in some cases, surgical resection of cancer metastatic to the kidney is indicated to treat intractable hematuria.

Nonneoplastic Renal Diseases in Kidney Tumor Resection Specimens

In the past few years, there has been increasing interest in evaluating the renal parenchyma in nephrectomy specimens for the presence of nonneoplastic diseases (456–459). When reviewed by renal pathologists, the nonneoplastic kidney has been considered “normal” in only 10% of nephrectomy specimens. The most common abnormalities detected are vascular (greater than 50%), and these may or may not have associated parenchymal scarring (456,457). The next most common abnormality has been diabetic nephropathy in almost 25% of studied specimens (456,457). In one report of 110 patients undergoing radical nephrectomy [91] or partial nephrectomy [19], follow-up demonstrated significantly higher serum creatinine levels 6 months after surgery in patients with vascular scarring and/or diabetic glomerulosclerosis (moderate and nodular) (456). Increased awareness of the clinical significance of these findings led the College of American Pathologists to include assessment of the nonneoplastic kidney as a mandatory part of reporting tumor resection specimens.

REFERENCES

- Eble J, Epstein J, Sauter G, et al. *World Health Organization Histologic and Genetic Typing of Tumours of the Kidney, Urinary Bladder, Prostate Gland and Testis*. Lyon, France: IARC Press, 2004.
- Kaatsch P. Epidemiology of childhood cancer. *Cancer Treat Rev* 2010;36:277.
- Ali AN, Diaz R, Shu HK, et al. A Surveillance, Epidemiology and End Results (SEER) program comparison of adult and pediatric Wilms' tumor. *Cancer* 2012;118:2541.
- Owens CM, Brisse HJ, Olsen OE, et al. Bilateral disease and new trends in Wilms tumour. *Pediatr Radiol* 2008;38:30.
- Royer-Pokora B. Genetics of pediatric renal tumors. *Pediatr Nephrol* 2012;28(1):13–23.
- Heppe RK, Koyle MA, Beckwith JB. Nephrogenic rests in Wilms tumor patients with the Drash syndrome. *J Urol* 1991;145:1225.
- Perlman EJ. Pediatric renal tumors: Practical updates for the pathologist. *Pediatr Dev Pathol* 2005;8:320.
- Call KM, Glaser T, Ito CY, et al. Isolation and characterization of a zinc finger polypeptide gene at the human chromosome 11 Wilms' tumor locus. *Cell* 1990;60:509.
- Koufos A, Grundy P, Morgan K, et al. Familial Wiedemann-Beckwith syndrome and a second Wilms tumor locus both map to 11p15.5. *Am J Hum Genet* 1989;44:711.
- Murphy W, Grignon D, Perlman E. *AFIP 4th Series Atlas of Tumor Pathology: Tumors of the Kidney, Bladder, and Related Urinary Structures*. Washington: American Registry of Pathology, 2004.
- Ko EY, Ritchey ML. Current management of Wilms' tumor in children. *J Pediatr Urol* 2009;5:56.
- Sebire NJ, Vujanic GM. Paediatric renal tumours: Recent developments, new entities and pathological features. *Histopathology* 2009;54:516.
- Verschuur AC, Vujanic GM, Van Tinteren H, et al. Stromal and epithelial predominant Wilms tumours have an excellent outcome: The SIOP 93 01 experience. *Pediatr Blood Cancer* 2010;55:233.
- Beckwith JB. Wilms' tumor and other renal tumors of childhood: A selective review from the National Wilms' Tumor Study Pathology Center. *Hum Pathol* 1983;14:481.
- Eble JN. Fetal rhabdomyomatous nephroblastoma. *J Urol* 1983;130:541.
- Pollono D, Drut R, Tomarchio S, et al. Fetal rhabdomyomatous nephroblastoma: Report of 14 cases confirming chemotherapy resistance. *J Pediatr Hematol Oncol* 2003;25:640.
- Inoue M, Uchida K, Kohei O, et al. Teratoid Wilms' tumor: A case report with literature review. *J Pediatr Surg* 2006;41:1759.
- Sultan I, Ajlouni F, Al-Jumaily U, et al. Distinct features of teratoid Wilms tumor. *J Pediatr Surg* 2010;45:e13.
- Bonadio JF, Storer B, Norkool P, et al. Anaplastic Wilms' tumor: Clinical and pathologic studies. *J Clin Oncol* 1985;3:513.
- Zuppan CW, Beckwith JB, Luckey DW. Anaplasia in unilateral Wilms' tumor: A report from the National Wilms' Tumor Study Pathology Center. *Hum Pathol* 1988;19:1199.
- Vujanic GM, Harms D, Sandstedt B, et al. New definitions of focal and diffuse anaplasia in Wilms tumor: The International Society of Paediatric Oncology (SIOP) experience. *Med Pediatr Oncol* 1999;32:317.
- Vujanic GM, Sandstedt B. The pathology of Wilms' tumour (nephroblastoma): The International Society of Paediatric Oncology approach. *J Clin Pathol* 2010;63:102.
- Glick RD, Hicks MJ, Nuchtern JG, et al. Renal tumors in infants less than 6 months of age. *J Pediatr Surg* 2004;39:522.
- England RJ, Haider N, Vujanic GM, et al. Mesoblastic nephroma: A report of the United Kingdom Children's Cancer and Leukaemia Group (CCLG). *Pediatr Blood Cancer* 2011;56:744.
- Kay S, Pratt CB, Salzberg AM. Hamartoma (leiomyomatous type) of the kidney. *Cancer* 1966;19:1825.
- Rubin BP, Chen CJ, Morgan TW, et al. Congenital mesoblastic nephroma t(12;15) is associated with ETV6-NTRK3 gene fusion: Cytogenetic and molecular relationship to congenital (infantile) fibrosarcoma. *Am J Pathol* 1998;153:1451.
- Argani P, Fritsch M, Kadkol SS, et al. Detection of the ETV6-NTRK3 chimeric RNA of infantile fibrosarcoma/cellular congenital mesoblastic nephroma in paraffin-embedded tissue: Application to challenging pediatric renal stromal tumors. *Mod Pathol* 2000;13:29.
- Pettinato G, Manivel JC, Wick MR, et al. Classical and cellular (atypical) congenital mesoblastic nephroma: A clinicopathologic, ultrastructural, immunohistochemical, and flow cytometric study. *Hum Pathol* 1989;20:682.
- Bolande RP. Congenital mesoblastic nephroma of infancy. *Perspect Pediatr Pathol* 1973;1:277.

30. Beckwith JB, Weeks DA. Congenital mesoblastic nephroma. When should we worry? *Arch Pathol Lab Med* 1986;110:98.
31. Vujanic GM, Delemarre JF, Moeslichan S, et al. Mesoblastic nephroma metastatic to the lungs and heart—another face of this peculiar lesion: Case report and review of the literature. *Pediatr Pathol* 1993;13:143.
32. Schlesinger AE, Rosenfield NS, Castle VP, et al. Congenital mesoblastic nephroma metastatic to the brain: A report of two cases. *Pediatr Radiol* 1995;25(Suppl 1):S73.
33. Argani P, Perlman EJ, Breslow NE, et al. Clear cell sarcoma of the kidney: A review of 351 cases from the National Wilms Tumor Study Group Pathology Center. *Am J Surg Pathol* 2000;24:4.
34. Gooskens S, Furtwangler R, Vujanic G, et al. Clear cell sarcoma of the kidney: A review. *Eur J Cancer* 2012;48:2219.
35. O'Meara E, Stack D, Lee C-H, et al. Characterization of the chromosomal translocation t(10;17)(q22;p13) in clear cell sarcoma of kidney. *J Pathol* 2012;227:72.
36. Marsden HB, Lawler W. Bone-metastasizing renal tumour of childhood. *Br J Cancer* 1978;38:437.
37. Kalapurakal J, Perlman E, Seibel N, et al. Outcomes of patients with revised stage I clear cell sarcoma of kidney treated in National Wilms Tumor Studies 1–5. *Int J Radiat Oncol Biol Phys* 2013;85(2):428–431.
38. Reinhard H, Reinert J, Beier R, et al. Rhabdoid tumors in children: Prognostic factors in 70 patients diagnosed in Germany. *Oncol Rep* 2008;19:819.
39. Weeks DA, Beckwith JB, Mierau GW, et al. Rhabdoid tumor of kidney: A report of 111 cases from the National Wilms' Tumor Study pathology center. *Am J Surg Pathol* 1989;13:439.
40. Bonnin JM, Rubinstein LJ, Palmer NF, et al. The association of embryonal tumors originating in the kidney and in the brain. A report of seven cases. *Cancer* 1984;54:2137.
41. Mayes LC, Kasselberg AG, Roloff JS, et al. Hypercalcemia associated with immunoreactive parathyroid hormone in a malignant rhabdoid tumor of the kidney (rhabdoid Wilms' tumor). *Cancer* 1984;54:882.
42. Savla J, Chen TT, Schneider NR, et al. Mutations of the hSNF5/INI1 gene in renal rhabdoid tumors with second primary brain tumors. *J Natl Cancer Inst* 2000;92:648.
43. Weeks DA, Beckwith JB, Mierau GW, et al. Renal neoplasms mimicking rhabdoid tumor of kidney: A report from the National Wilms' Tumor Study pathology center. *Am J Surg Pathol* 1991;15:1042.
44. Sigauke E, Rakheja D, Maddox DL, et al. Absence of expression of SMARCB1/INI1 in malignant rhabdoid tumors of the central nervous system, kidneys and soft tissue: An immunohistochemical study with implications for diagnosis. *Mod Pathol* 2006;19:717.
45. van den Heuvel-Eibrink MM, van Tinteren H, Rehorst H, et al. Malignant rhabdoid tumours of the kidney (MRTKs), registered on recent SIOP protocols from 1993 to 2005: A report of the SIOP renal tumour study group. *Pediatr Blood Cancer* 2011;56:733.
46. Tomlinson GE, Breslow NE, Dome J, et al. Rhabdoid tumor of the kidney in the National Wilms' Tumor Study: Age at diagnosis as a prognostic factor. *J Clin Oncol* 2005;23:7641.
47. Davis CJ, Jr., Barton JH, Sesterhenn IA, et al. Metanephric adenoma. Clinicopathological study of fifty patients. *Am J Surg Pathol* 1995;19:1101.
48. Jones EC, Pins M, Dickersin GR, et al. Metanephric adenoma of the kidney. A clinicopathological, immunohistochemical, flow cytometric, cytogenetic, and electron microscopic study of seven cases. *Am J Surg Pathol* 1995;19:615.
49. Gatalica Z, Grujic S, Kovatich A, et al. Metanephric adenoma: Histology, immunophenotype, cytogenetics, ultrastructure. *Mod Pathol* 1996;9:329.
50. Grignon DJ, Eble JN. Papillary and metanephric adenomas of the kidney. *Semin Diagn Pathol* 1998;15:41.
51. Muir TE, Chevillie JC, Lager DJ. Metanephric adenoma, nephrogenic rests, and Wilms' tumor: A histologic and immunophenotypic comparison. *Am J Surg Pathol* 2001;25:1290.
52. Argani P. Metanephric neoplasms: The hyperdifferentiated, benign end of the Wilms tumor spectrum? *Clin Lab Med* 2005;25:379.
53. Brunelli M, Eble JN, Zhang S, et al. Metanephric adenoma lacks the gains of chromosomes 7 and 17 and loss of Y that are typical of papillary renal cell carcinoma and papillary adenoma. *Mod Pathol* 2003;16:1060.
54. Arroyo MR, Green DM, Perlman EJ, et al. The spectrum of metanephric adenofibroma and related lesions: Clinicopathologic study of 25 cases from the National Wilms Tumor Study Group pathology center. *Am J Surg Pathol* 2001;25:433.
55. Argani P, Beckwith JB. Metanephric stromal tumor: report of 31 cases of a distinctive pediatric renal neoplasm. *Am J Surg Pathol* 2000;24:917.
56. Pan C-C, Epstein JI. Detection of chromosome copy number alterations in metanephric adenomas by array comparative genomic hybridization. *Mod Pathol* 2010;23:1634.
57. Szponar A, Yusenko MV, Kovacs G. High-resolution array CGH of metanephric adenomas: Lack of DNA copy number changes. *Histopathology* 2010;56:212.
58. Pesti T, Sukosd F, Jones EC, et al. Mapping a tumor suppressor gene to chromosome 2p13 in metanephric adenoma by microsatellite allelotyping. *Hum Pathol* 2001;32:101.
59. Choueiri T, Chevillie J, Palescandolo E, et al. *BRAF* mutations in metanephric adenoma of the kidney. *Eur Urol* 2012;62(5):917–922.
60. Olgac S, Hutchinson B, Tickoo SK, et al. Alpha-methylacyl-CoA racemase as a marker in the differential diagnosis of metanephric adenoma. *Mod Pathol* 2006;19:218.
61. Renshaw AA, Freyer DR, Hammers YA. Metastatic metanephric adenoma in a child. *Am J Surg Pathol* 2000;24:570.
62. Drut R, Drut RM, Ortolani C. Metastatic metanephric adenoma with foci of papillary carcinoma in a child: A combined histologic, immunohistochemical, and FISH study. *Int J Surg Pathol* 2001;9:241.
63. Paner GP, Turk TM, Clark JI, et al. Passive seeding in metanephric adenoma: A review of pseudometastatic lesions in perinephric lymph nodes. *Arch Pathol Lab Med* 2005;129:1317.
64. Argani P, Antonescu CR, Couturier J, et al. PRCC-TFE3 renal carcinomas: Morphologic, immunohistochemical, ultrastructural, and molecular analysis of an entity associated with the t(X;1)(p11.2;q21). *Am J Surg Pathol* 2002;26:1553.
65. Argani P, Ladanyi M. Translocation carcinomas of the kidney. *Clin Lab Med* 2005;25:363.
66. Argani P, Lae M, Hutchinson B, et al. Renal carcinomas with the t(6;11)(p21;q12): Clinicopathologic features and demonstration of the specific alpha-TFEB gene fusion by immunohistochemistry, RT-PCR, and DNA PCR. *Am J Surg Pathol* 2005;29:230.
67. Medendorp K, van Groningen JJ, Schepens M, et al. Molecular mechanisms underlying the MiT translocation subgroup of renal cell carcinomas. *Cytogenet Genome Res* 2007;118:157.
68. Helmy T, Sarhan O, Sarhan M, et al. Renal cell carcinoma in children: Single-center experience. *J Pediatr Surg* 2009;44:1750.
69. Selle B, Furtwangler R, Graf N, et al. Population-based study of renal cell carcinoma in children in Germany, 1980–2005: More frequently localized tumors and underlying disorders compared with adult counterparts. *Cancer* 2006;107:2906.
70. Bruder E, Passera O, Harms D, et al. Morphologic and molecular characterization of renal cell carcinoma in children and young adults. *Am J Surg Pathol* 2004;28:1117.
71. Altinok G, Kattar MM, Mohamed A, et al. Pediatric renal carcinoma associated with Xp11.2 translocations/TFE3 gene fusions and clinicopathologic associations. *Pediatr Dev Pathol* 2005;8:168.
72. Rao Q, Chen JY, Wang JD, et al. Renal cell carcinoma in children and young adults: Clinicopathological, immunohistochemical, and VHL gene analysis of 46 cases with follow-up. *Int J Surg Pathol* 2011;19:170.
73. Argani P, Olgac S, Tickoo SK, et al. Xp11 translocation renal cell carcinoma in adults: Expanded clinical, pathologic, and genetic spectrum. *Am J Surg Pathol* 2007;31:1149.
74. Petersson F, Vanecek T, Michal M, et al. A distinctive translocation carcinoma of the kidney; "rosette forming," t(6;11), HMB45-positive renal tumor: A histomorphologic, immunohistochemical, ultrastructural, and molecular genetic study of 4 cases. *Hum Pathol* 2012;43:726.
75. Argani P, Antonescu CR, Illei PB, et al. Primary renal neoplasms with the ASPL-TFE3 gene fusion of alveolar soft part sarcoma: A distinctive tumor entity previously included among renal cell carcinomas of children and adolescents. *Am J Pathol* 2001;159:179.
76. Chen CK, Hsueh C, Lai JY, et al. Renal cell carcinoma with t(X;17)(p11.2;q25) in a 6-year-old Taiwanese boy. *Virchows Arch* 2007;450:215.

77. Argani P, Aulmann S, Karanjawala Z, et al. Melanotic Xp11 translocation renal cancers: A distinctive neoplasm with overlapping features of PEComa, carcinoma, and melanoma. *Am J Surg Pathol* 2009;33:609.
78. Chang IW, Huang HY, Sung MT. Melanotic Xp11 translocation renal cancer: A case with PSF-TFE3 gene fusion and up-regulation of melanogenetic transcripts. *Am J Surg Pathol* 2009;33:1894.
79. Argani P, Lal P, Hutchinson B, et al. Aberrant nuclear immunoreactivity for TFE3 in neoplasms with TFE3 gene fusions: A sensitive and specific immunohistochemical assay. *Am J Surg Pathol* 2003;27:750.
80. Camparo P, Vasiliu V, Molinie V, et al. Renal translocation carcinomas: Clinicopathologic, immunohistochemical, and gene expression profiling analysis of 31 cases with a review of the literature. *Am J Surg Pathol* 2008;32:656.
81. Martignoni G, Gobbo S, Camparo P, et al. Differential expression of cathepsin K in neoplasms harboring TFE3 gene fusions. *Mod Pathol* 2011;24:1313.
82. Geller JI, Argani P, Adeniran A, et al. Translocation renal cell carcinoma: Lack of negative impact due to lymph node spread. *Cancer* 2008;112:1607.
83. Ramphal R, Pappo A, Zielenska M, et al. Pediatric renal cell carcinoma: Clinical, pathologic, and molecular abnormalities associated with the members of the mit transcription factor family. *Am J Clin Pathol* 2006;126:349.
84. Eble JN. Mucinous tubular and spindle cell carcinoma and post-neuroblastoma carcinoma: Newly recognised entities in the renal cell carcinoma family. *Pathology* 2003;35:499.
85. Medeiros LJ, Palmedo G, Krigman HR, et al. Oncocytoid renal cell carcinoma after neuroblastoma: A report of four cases of a distinct clinicopathologic entity. *Am J Surg Pathol* 1999;23:772.
86. Koyle MA, Hatch DA, Furness PD, III, et al. Long-term urological complications in survivors younger than 15 months of advanced stage abdominal neuroblastoma. *J Urol* 2001;166:1455.
87. Dhall D, Al-Ahmadie HA, Dhall G, et al. Pediatric renal cell carcinoma with oncocytoid features occurring in a child after chemotherapy for cardiac leiomyosarcoma. *Urology* 2007;70:178.
88. Thoenes W, Storkel S, Rumpelt HJ. Histopathology and classification of renal cell tumors (adenomas, oncocytomas and carcinomas). The basic cytological and histopathological elements and their use for diagnostics. *Pathol Res Pract* 1986;181:125.
89. Aso Y, Homma Y. A survey on incidental renal cell carcinoma in Japan. *J Urol* 1992;147:340.
90. Gill IS, Kavoussi LR, Lane BR, et al. Comparison of 1,800 laparoscopic and open partial nephrectomies for single renal tumors. *J Urol* 2007;178:41.
91. Jacobs BL, Tan HJ, Montgomery JS, et al. Understanding criteria for surveillance of patients with a small renal mass. *Urology* 2012;79:1027.
92. Xipell JM. The incidence of benign renal nodules (a clinicopathologic study). *J Urol* 1971;106:503.
93. Reis M, Faria V, Lindoro J, et al. The small cystic and noncystic noninflammatory renal nodules: A postmortem study. *J Urol* 1988;140:721.
94. Hiasa Y, Kitamura M, Nakaoka S, et al. Antigen immunohistochemistry of renal cell adenomas in autopsy cases: Relevance to histogenesis. *Oncology* 1995;52:97.
95. Eble JN, Warfel K. Early human renal cortical epithelial neoplasia (abstract). *Mod Pathol* 1991;4:45A.
96. Ishikawa I, Kovacs G. High incidence of papillary renal cell tumours in patients on chronic haemodialysis. *Histopathology* 1993;22:135.
97. Tickoo SK, dePeralta-Venturina MN, Harik LR, et al. Spectrum of epithelial neoplasms in end-stage renal disease: An experience from 66 tumor-bearing kidneys with emphasis on histologic patterns distinct from those in sporadic adult renal neoplasia. *Am J Surg Pathol* 2006;30:141.
98. Wang KL, Weinrach DM, Luan C, et al. Renal papillary adenoma—a putative precursor of papillary renal cell carcinoma. *Hum Pathol* 2007;38:239.
99. Brunelli M, Eble JN, Zhang S, et al. Gains of chromosomes 7, 17, 12, 16, and 20 and loss of Y occur early in the evolution of papillary renal cell neoplasia: A fluorescent in situ hybridization study. *Mod Pathol* 2003;16:1053.
100. Bell E. *Renal Diseases*, 2nd ed. Philadelphia: Lea & Febiger, 1950.
101. Mai KT, Landry DC, Robertson SJ, et al. A comparative study of metastatic renal cell carcinoma with correlation to subtype and primary tumor. *Pathol Res Pract* 2001;197:671.
102. Dechet CB, Sebo T, Farrow G, et al. Prospective analysis of intraoperative frozen needle biopsy of solid renal masses in adults. *J Urol* 1999;162:1282.
103. Lee CT, Katz J, Shi W, et al. Surgical management of renal tumors 4 cm or less in a contemporary cohort. *J Urol* 2000;163:730.
104. Fergany AF, Hafez KS, Novick AC. Long-term results of nephron sparing surgery for localized renal cell carcinoma: 10-year followup. *J Urol* 2000;163:442.
105. Volpe A, Cadeddu JA, Cestari A, et al. Contemporary management of small renal masses. *Eur Urol* 2011;60:501.
106. Klein MJ, Valensi QJ. Proximal tubular adenomas of kidney with so-called oncocytic features. A clinicopathologic study of 13 cases of a rarely reported neoplasm. *Cancer* 1976;38:906.
107. Amin MB, Crotty TB, Tickoo SK, et al. Renal oncocytoma: A reappraisal of morphologic features with clinicopathologic findings in 80 cases. *Am J Surg Pathol* 1997;21:1.
108. Amin MB, Amin MB, Tamboli P, et al. Prognostic impact of histologic subtyping of adult renal epithelial neoplasms: An experience of 405 cases. *Am J Surg Pathol* 2002;26:281.
109. Trpkov K, Yilmaz A, Uzer D, et al. Renal oncocytoma revisited: A clinicopathological study of 109 cases with emphasis on problematic diagnostic features. *Histopathology* 2010;57:893.
110. Pavlovich CP, Walther MM, Eyler RA, et al. Renal tumors in the Birt-Hogg-Dube syndrome. *Am J Surg Pathol* 2002;26:1542.
111. Tikkakoski T, Paivansalo M, Alanen A, et al. Radiologic findings in renal oncocytoma. *Acta Radiol* 1991;32:363.
112. Prasad SR, Surabhi VR, Menias CO, et al. Benign renal neoplasms in adults: Cross-sectional imaging findings. *AJR Am J Roentgenol* 2008;190:158.
113. Pedrosa I, Sun MR, Spencer M, et al. MR imaging of renal masses: Correlation with findings at surgery and pathologic analysis. *Radiographics* 2008;28:985.
114. Junker K, Weirich G, Moravek P, et al. Familial and sporadic renal oncocytomas—a comparative molecular-genetic analysis. *Eur Urol* 2001;40:330.
115. Picken MM, Chyna B, Flanigan RC, et al. Analysis of chromosome 1p abnormalities in renal oncocytomas by loss of heterozygosity studies: Correlation with conventional cytogenetics and fluorescence in situ hybridization. *Am J Clin Pathol* 2008;129:377.
116. Yusenko MV, Kuiper RP, Boethe T, et al. High-resolution DNA copy number and gene expression analyses distinguish chromophobe renal cell carcinomas and renal oncocytomas. *BMC Cancer* 2009;9:152.
117. Fuzesi L, Gunawan B, Braun S, et al. Renal oncocytoma with a translocation t(9;11)(p23;q13). *J Urol* 1994;152:471.
118. Yusenko MV. Molecular pathology of renal oncocytoma: A review. *Int Urol Nephrol* 2010;17:602.
119. Mead GO, Thomas LR, Jr, Jackson JG. Renal oncocytoma: Report of a case with bilateral multifocal oncocytomas. *Clin Imaging* 1990;14:231.
120. Shin LK, Badler RL, Bruno FM, et al. Radiology-Pathology Conference: Bilateral renal oncocytomas. *Clin Imaging* 2004;28:344.
121. Warfel KA, Eble JN. Renal oncocytomatosis. *J Urol* 1982;127:1179.
122. Tickoo SK, Reuter VE, Amin MB, et al. Renal oncocytosis: A morphologic study of fourteen cases. *Am J Surg Pathol* 1999;23:1094.
123. Storkel S, Pannen B, Thoenes W, et al. Intercalated cells as a probable source for the development of renal oncocytoma. *Virchows Arch B Cell Pathol* 1988;56:185.
124. Lyzak JS, Farhood A, Verani R. Intracytoplasmic lumina in a case of bilaterally multifocal renal oncocytomas. *Arch Pathol Lab Med* 1994;118:275.
125. Wu SL, Kothari P, Wheeler TM, et al. Cytokeratins 7 and 20 immunoreactivity in chromophobe renal cell carcinomas and renal oncocytomas. *Mod Pathol* 2002;15:712.
126. Skinnider BF, Folpe AL, Hennigar RA, et al. Distribution of cytokeratins and vimentin in adult renal neoplasms and normal renal tissue: Potential utility of a cytokeratin antibody panel in the differential diagnosis of renal tumors. *Am J Surg Pathol* 2005;29:747.

127. Pan CC, Chen PCH, Ho DMT. The diagnostic utility of MOC31, BerEP4, RCC marker and CD10 in the classification of renal cell carcinoma and renal oncocytoma: An immunohistochemical analysis of 328 cases. *Histopathology* 2004;45:452.
128. Pan CC, Chen PCH, Chiang H. Overexpression of KIT (CD117) in chromophobe renal cell carcinoma and renal oncocytoma. *Am J Clin Pathol* 2004;121:878.
129. DeLong W, Sakr W, Grignon D. Chromophobe renal cell carcinoma: A comparative histochemical and immunohistochemical study. *J Urol Pathol* 1996;4:1.
130. Tickoo SK, Amin MB, Zarbo RJ. Colloidal iron staining in renal epithelial neoplasms, including chromophobe renal cell carcinoma: Emphasis on technique and patterns of staining. *Am J Surg Pathol* 1998;22:419.
131. Tickoo SK, Lee MW, Eble JN, et al. Ultrastructural observations on mitochondria and microvesicles in renal oncocytoma, chromophobe renal cell carcinoma, and eosinophilic variant of conventional (clear cell) renal cell carcinoma. *Am J Surg Pathol* 2000;24:1247.
132. Bennington J, Beckwith J. *Tumors of the Kidney, Renal Pelvis, and Ureter*, 2nd ed. Bethesda: Armed Forces Institute of Pathology, 1975.
133. Mancilla-Jimenez R, Stanley RJ, Blath RA. Papillary renal cell carcinoma: A clinical, radiologic, and pathologic study of 34 cases. *Cancer* 1976;38:2469.
134. Thoenes W, Storkel S, Rumpelt HJ. Human chromophobe cell renal carcinoma. *Virchows Arch B Cell Pathol* 1985;48:207.
135. Lee CT, Katz J, Fearn PA, et al. Mode of presentation of renal cell carcinoma provides prognostic information. *Urol Oncol* 2002;7:135.
136. Szendroi A, Tabak A, Riesz P, et al. Clinical symptoms related to renal cell carcinoma are independent prognostic factors for intraoperative complications and overall survival. *Int Urol Nephrol* 2009;41:835.
137. Ding G, Feng C, Song N, et al. Paraneoplastic symptoms: Cachexia, polycythemia, and hypercalcemia are, respectively, related to vascular endothelial growth factor (VEGF) expression in renal cell carcinoma. *Urol Oncol Semin Invest* 2013;31(8):1820–1825.
138. Sengupta S, Lohse CM, Cheville JC, et al. The preoperative erythrocyte sedimentation rate is an independent prognostic factor in renal cell carcinoma. *Cancer* 2006;106:304.
139. Sakamoto S, Igarashi T, Osumi N, et al. Erythropoietin-producing renal cell carcinoma in chronic hemodialysis patients: A report of two cases. *Int Urol Nephrol* 2003;10:49.
140. Wiesener MS, Munchenhagen P, Glaser M, et al. Erythropoietin gene expression in renal carcinoma is considerably more frequent than paraneoplastic polycythemia. *Int J Cancer* 2007;121:2434.
141. Kirkpantur A, Baydar DE, Altun B, et al. Concomitant amyloidosis, renal papillary carcinoma and ipsilateral pelviclyceal urothelial carcinoma in a patient with familial Mediterranean fever. *Amyloid* 2009;16:54.
142. Palapattu GS, Kristo B, Rajfer J. Paraneoplastic syndromes in urologic malignancy: The many faces of renal cell carcinoma. *Rev Urol* 2002;4:163.
143. Steffens J, Bock R, Braedel HU, et al. Renin-producing renal cell carcinomas—clinical and experimental investigations on a special form of renal hypertension. *Urol Res* 1992;20:111.
144. Mohammed Ilyas MI, Turner GD, Cranston D. Human chorionic gonadotropin-secreting clear cell renal cell carcinoma with paraneoplastic gynaecomastia. *Scand J Urol Nephrol* 2008;42:555.
145. Stanic TH, Donovan J. Prolactin secreting renal cell carcinoma. *J Urol* 1986;136(1):85–86.
146. Antonelli A, Arrighi N, Corti S, et al. Surgical treatment of atypical metastasis from renal cell carcinoma (RCC). *BJU Int* 2012;110:E559–E563.
147. Chow WH, Dong LM, Devesa SS. Epidemiology and risk factors for kidney cancer. *Nat Rev Urol* 2010;7:245.
148. Ljungberg B, Campbell SC, Choi HY, et al. The epidemiology of renal cell carcinoma. *Eur Urol* 2011;60:615.
149. Siegel R, Naishadham D, Jemal A. Cancer statistics, 2012. *CA Cancer J Clin* 2012;62:10.
150. Cao Y, Paner GP, Perry KT, et al. Renal neoplasms in younger adults: Analysis of 112 tumors from a single institution according to the new 2004 World Health Organization classification and 2002 American Joint Committee on Cancer Staging System. *Arch Pathol Lab Med* 2005;129:487.
151. Chow WH, Devesa SS. Contemporary epidemiology of renal cell cancer. *Cancer J* 2008;14:288.
152. Woodward ER, Ricketts C, Killick P, et al. Familial non-VHL clear cell (conventional) renal cell carcinoma: Clinical features, segregation analysis, and mutation analysis of FLCN. *Clin Cancer Res* 2008;14:5925.
153. Malchoff CD, Sarfarazi M, Tendler B, et al. Papillary thyroid carcinoma associated with papillary renal neoplasia: Genetic linkage analysis of a distinct heritable tumor syndrome. *J Clin Endocrinol Metab* 2000;85:1758.
154. Launonen V, Vierimaa O, Kiuru M, et al. Inherited susceptibility to uterine leiomyomas and renal cell cancer. *Proc Natl Acad Sci U S A* 2001;98:3387.
155. Linehan WM, Pinto PA, Bratslavsky G, et al. Hereditary kidney cancer: Unique opportunity for disease-based therapy. *Cancer* 2009;115:2252.
156. Axwijk PH, Kluijdt I, de Jong D, et al. Hereditary causes of kidney tumours. *Eur J Clin Invest* 2010;40:433.
157. Verine J, Pluvinage A, Bousquet G, et al. Hereditary renal cancer syndromes: An update of a systematic review. *Eur Urol* 2010;58:701.
158. Flaherty KT, Fuchs CS, Colditz GA, et al. A prospective study of body mass index, hypertension, and smoking and the risk of renal cell carcinoma (United States). *Cancer Causes Control* 2005;16:1099.
159. Joh HK, Willett WC, Cho E. Type 2 diabetes and the risk of renal cell cancer in women. *Diabetes Care* 2011;34:1552.
160. Baron JA. Epidemiology of non-steroidal anti-inflammatory drugs and cancer. *Prog Exp Tumor Res* 2003;37:1.
161. Pesch B, Haerting J, Ranft U, et al. Occupational risk factors for renal cell carcinoma: Agent-specific results from a case-control study in Germany. MURC Study Group. Multicenter urothelial and renal cancer study. *Int J Epidemiol* 2000;29:1014.
162. McLaughlin JK, Blot WJ, Mehl ES, et al. Petroleum-related employment and renal cell cancer. *J Occup Med* 1985;27:672.
163. Maher ER, Neumann HP, Richard S. von Hippel-Lindau disease: A clinical and scientific review. *Eur J Human Genet* 2011;19:617.
164. Tello R, Blickman JG, Buonomo C, et al. Meta analysis of the relationship between tubular sclerosis complex and renal cell carcinoma. *Eur J Radiol* 1998;27:131.
165. Nishimura H, Ubara Y, Nakamura M, et al. Renal cell carcinoma in autosomal dominant polycystic kidney disease. *Am J Kid Dis* 2009;54:165.
166. Matson MA, Cohen EP. Acquired cystic kidney disease: Occurrence, prevalence, and renal cancers. *Medicine* 1990;69:217.
167. Ishikawa I, Saito Y, Shikura N, et al. Ten-year prospective study on the development of renal cell carcinoma in dialysis patients. *Am J Kid Dis* 1990;16:452.
168. Novara G, Ficarra V, Antonelli A, et al. Validation of the 2009 TNM version in a large multi-institutional cohort of patients treated for renal cell carcinoma: Are further improvements needed? *Eur Urol* 2010;58:588.
169. Kim SP, Alt AL, Weight CJ, et al. Independent validation of the 2010 American Joint Committee on Cancer TNM classification for renal cell carcinoma: Results from a large, single institution cohort. *J Urol* 2011;185:2035.
170. Edge S, Byrd D, Compton C, et al., eds. *AJCC Cancer Staging Manual*, 7th ed. New York: Springer, 2010.
171. Bonsib SM. The renal sinus is the principal invasive pathway: A prospective study of 100 renal cell carcinomas. *Am J Surg Pathol* 2004;28:1594.
172. Thompson RH, Leibovich BC, Cheville JC, et al. Is renal sinus fat invasion the same as perinephric fat invasion for pT3a renal cell carcinoma? *J Urol* 2005;174:1218.
173. Yokoyama H, Tanaka M. Incidence of adrenal involvement and assessing adrenal function in patients with renal cell carcinoma: Is ipsilateral adrenalectomy indispensable during radical nephrectomy? *BJU Int* 2005;95:526.
174. Thompson RH, Leibovich BC, Cheville JC, et al. Should direct ipsilateral adrenal invasion from renal cell carcinoma be classified as pT3a? *J Urol* 2005;173:918.
175. Han KR, Bui MH, Pantuck AJ, et al. TNM T3a renal cell carcinoma: Adrenal gland involvement is not the same as renal fat invasion. *J Urol* 2003;169:899.
176. Giuliani L, Giberti C, Martorana G, et al. Radical extensive surgery for renal cell carcinoma: Long-term results and prognostic factors. *J Urol* 1990;143:468.
177. Studer UE, Scherz S, Scheidegger J, et al. Enlargement of regional lymph nodes in renal cell carcinoma is often not due to metastases. *J Urol* 1990;144:243.

178. Blom JHM, van Poppel H, Marechal JM, et al. Radical nephrectomy with and without lymph-node dissection: Final results of European Organization for Research and Treatment of Cancer (EORTC) randomized phase 3 trial 30881. *Eur Urol* 2009;55:28.
179. Skinner DG, Colvin RB, Vermillion CD, et al. Diagnosis and management of renal cell carcinoma. A clinical and pathologic study of 309 cases. *Cancer* 1971;28:1165.
180. Fuhrman SA, Lasky LC, Limas C. Prognostic significance of morphologic parameters in renal cell carcinoma. *Am J Surg Pathol* 1982;6:655.
181. Lohse CM, Blute ML, Zincke H, et al. Comparison of standardized and nonstandardized nuclear grade of renal cell carcinoma to predict outcome among 2,042 patients. *Am J Clin Pathol* 2002;118:877.
182. Grignon DJ, Ayala AG, el-Naggar A, et al. Renal cell carcinoma. A clinicopathologic and DNA flow cytometric analysis of 103 cases. *Cancer* 1989;64:2133.
183. Chevillet JC, Zincke H, Lohse CM, et al. pT1 clear cell renal cell carcinoma: A study of the association between MIB-1 proliferative activity and pathologic features and cancer specific survival. *Cancer* 2002;94:2180.
184. Ficarra V, Righetti R, Martignoni G, et al. Prognostic value of renal cell carcinoma nuclear grading: Multivariate analysis of 333 cases. *Urol Int* 2001;67:130.
185. Lane BR, Kattan MW. Prognostic models and algorithms in renal cell carcinoma. *Urol Clin North Am* 2008;35:613.
186. Chevillet JC, Lohse CM, Zincke H, et al. Sarcomatoid renal cell carcinoma: An examination of underlying histologic subtype and an analysis of associations with patient outcome. *Am J Surg Pathol* 2004;28:435.
187. Shuch B, Bratslavsky G, Shih J, et al. Impact of pathological tumour characteristics in patients with sarcomatoid renal cell carcinoma. *BJU Int* 2012;109:1600.
188. de Peralta-Venturina M, Moch H, Amin M, et al. Sarcomatoid differentiation in renal cell carcinoma: A study of 101 cases. *Am J Surg Pathol* 2001;25:275.
189. Handoo A, Pai RR, Rao VS, et al. Sarcomatoid renal cell carcinoma with osteosarcomatous differentiation—a case report. *Indian J Pathol Microbiol* 2004;47:528.
190. Li L, Teichberg S, Steckel J, et al. Sarcomatoid renal cell carcinoma with divergent sarcomatoid growth patterns: A case report and review of the literature. *Arch Pathol Lab Med* 2005;129:1057.
191. Novick AC. Partial nephrectomy for renal cell carcinoma. *Urology* 1995;46:149.
192. Kim SP, Thompson RH, Boorjian SA, et al. Comparative effectiveness for survival and renal function of partial and radical nephrectomy for localized renal tumors: A systematic review and meta-analysis. *J Urol* 2012;188:51.
193. Tan HJ, Norton EC, Ye Z, et al. Long-term survival following partial vs radical nephrectomy among older patients with early-stage kidney cancer. *JAMA* 2012;307:1629.
194. Miller DC, Shah RB, Bruhn A, et al. Trends in the use of gross and frozen section pathological consultations during partial or radical nephrectomy for renal cell carcinoma. *J Urol* 2008;179:461.
195. Bielsa O, Lloreta J, Gelabert-Mas A. Cystic renal cell carcinoma: Pathological features, survival and implications for treatment. *Br J Urol* 1998;82:16.
196. Pierorazio PM, Patel HD, Feng T, et al. Robotic-assisted versus traditional laparoscopic partial nephrectomy: Comparison of outcomes and evaluation of learning curve. *Urology* 2011;78:813.
197. Pierorazio PM, Hyams ES, Lin BM, et al. Laparoscopic radical nephrectomy for large renal masses: Critical assessment of perioperative and oncologic outcomes of stage T2a and T2b tumors. *Urology* 2012;79:570.
198. Landman J, Lento P, Hassen W, et al. Feasibility of pathological evaluation of morcellated kidneys after radical nephrectomy. *J Urol* 2000;164:2086.
199. Meng MV, Koppie TM, Stoller ML. Pathologic sampling of laparoscopically morcellated kidneys: A mathematical model. *J Endourol* 2003;17:229.
200. Best SL, Park SK, Yaacoub RF, et al. Long-term outcomes of renal tumor radio frequency ablation stratified by tumor diameter: Size matters. *J Urol* 2012;187:1183.
201. Olweny EO, Park SK, Tan YK, et al. Radiofrequency ablation versus partial nephrectomy in patients with solitary clinical T1a renal cell carcinoma: Comparable oncologic outcomes at a minimum of 5 years of follow-up. *Eur Urol* 2012;61:1156.
202. Venkatesan AM, Wood BJ, Gervais DA. Percutaneous ablation in the kidney. *Radiology* 2011;261:375.
203. Patel NS, Leiblich A, Cranston D, et al. Active surveillance of small renal masses offers short-term oncologic efficacy equivalent to radical and partial nephrectomy. *BJU Int* 2011;108:39.
204. Kim SP, Thompson RH. Approach to the small renal mass: To treat or not to treat. *Urol Clin North Am* 2012;39:171.
205. Jewett MA, Mattar K, Basiuk J, et al. Active surveillance of small renal masses: Progression patterns of early stage kidney cancer. *Eur Urol* 2011;60:39.
206. Lane BR, Samplaski MK, Herts BR, et al. Renal mass biopsy—a renaissance? *J Urol* 2008;179:20.
207. Kummerlin I, ten Kate F, Smedts F, et al. Core biopsies of renal tumors: A study on diagnostic accuracy, interobserver, and intraobserver variability. *Eur Urol* 2008;53:1219.
208. Kummerlin I, ten Kate F, Smedts F, et al. Diagnostic problems in the subtyping of renal tumors encountered by five pathologists. *Pathol Res Pract* 2009;205:27.
209. González J. Update on surgical management of renal cell carcinoma with venous extension. *Curr Urol Rep* 2012;13:8.
210. Nakajima T, Suzuki M, Ando S, et al. Spontaneous regression of bone metastasis from renal cell carcinoma; a case report. *BMC Cancer* 2006;6:11.
211. Lekanidi K, Vlachou PA, Morgan B, et al. Spontaneous regression of metastatic renal cell carcinoma: Case report. *J Med Case Reports* 2007;1:89.
212. Miyao N, Naito S, Ozono S, et al. Late recurrence of renal cell carcinoma: Retrospective and collaborative study of the Japanese Society of Renal Cancer. *Urology* 2011;77:379.
213. Park Y, Baik K, Lee Y, et al. Late recurrence of renal cell carcinoma >5 years after surgery: Clinicopathological characteristics and prognosis. *BJU Int* 2012;110:E553–E558.
214. Leibovich BC, Chevillet JC, Lohse CM, et al. A scoring algorithm to predict survival for patients with metastatic clear cell renal cell carcinoma: A stratification tool for prospective clinical trials. *J Urol* 2005;174:1759.
215. George S, Pili R, Carducci MA, et al. Role of immunotherapy for renal cell cancer in 2011. *J Natl Compr Canc Netw* 2011;9:1011.
216. Singer EA, Gupta GN, Srinivasan R. Targeted therapeutic strategies for the management of renal cell carcinoma. *Curr Opin Oncol* 2012;24:284.
217. Escudier B, Porta CSC, Gore M. Treatment selection in metastatic renal cell carcinoma: Expert consensus. *Nat Rev Clin Oncol* 2012;9:327.
218. Antonelli A, Cozzoli A, Simeone C, et al. Surgical treatment of adrenal metastasis from renal cell carcinoma: A single-centre experience of 45 patients. *BJU Int* 2006;97:505.
219. Chevillet JC, Lohse CM, Zincke H, et al. Comparisons of outcome and prognostic features among histologic subtypes of renal cell carcinoma. *Am J Surg Pathol* 2003;27:612.
220. Anglard P, Tory K, Brauch H, et al. Molecular analysis of genetic changes in the origin and development of renal cell carcinoma. *Cancer Res* 1991;51:1071.
221. Goodman MD, Goodman BK, Lubin MB, et al. Cytogenetic characterization of renal cell carcinoma in von Hippel-Lindau syndrome. *Cancer* 1990;65:1150.
222. Whaley JM, Naglich J, Gelbert L, et al. Germ-line mutations in the von Hippel-Lindau tumor-suppressor gene are similar to somatic von Hippel-Lindau aberrations in sporadic renal cell carcinoma. *Am J Hum Genet* 1994;55:1092.
223. Latif F, Tory K, Gnarr J, et al. Identification of the von Hippel-Lindau disease tumor suppressor gene. *Science* 1993;260:1317.
224. Takahashi M, Kahnoski R, Gross D, et al. Familial adult renal neoplasia. *J Med Genet* 2002;39:1.
225. Sukosd F, Kuroda N, Beothe T, et al. Deletion of chromosome 3p14.2-p25 involving the VHL and FHIT genes in conventional renal cell carcinoma. *Cancer Res* 2003;63:455.
226. Nassir A, Jollimore J, Gupta R, et al. Multilocular cystic renal cell carcinoma: A series of 12 cases and review of the literature. *Urology* 2002;60:421.

227. Suzigan S, Lopez-Beltran A, Montironi R, et al. Multilocular cystic renal cell carcinoma: A report of 45 cases of a kidney tumor of low malignant potential. *Am J Clin Pathol* 2006;125:217.
228. Halat S, Eble JN, Grignon DJ, et al. Multilocular cystic renal cell carcinoma is a subtype of clear cell renal cell carcinoma. *Mod Pathol* 2010;23:931.
229. Shuch B, Singer EA, Bratslavsky G. The surgical approach to multifocal renal cancers: Hereditary syndromes, ipsilateral multifocality, and bilateral tumors. *Urol Clin North Am* 2012;39:133.
230. Blute ML, Itano NB, Chevillet JC, et al. The effect of bilaterality, pathological features and surgical outcome in nonhereditary renal cell carcinoma. *J Urol* 2003;169:1276.
231. Klatte T, Wunderlich H, Patard JJ, et al. Clinicopathological features and prognosis of synchronous bilateral renal cell carcinoma: An international multicentre experience. *BJU Int* 2007;100:21.
232. Klatte T, Patard JJ, Wunderlich H, et al. Metachronous bilateral renal cell carcinoma: Risk assessment, prognosis and relevance of the primary-free interval. *J Urol* 2007;177:2081.
233. Oberling C, Riviere M, Haguenu F. Ultrastructure of the clear cells in renal carcinomas and its importance for the demonstration of their renal origin. *Nature* 1960;186:402.
234. Gokden N, Nappi O, Swanson PE, et al. Renal cell carcinoma with rhabdoid features. *Am J Surg Pathol* 2000;24:1329.
235. Zhou M, Roma A, Magi-Galluzzi C. The usefulness of immunohistochemical markers in the differential diagnosis of renal neoplasms. *Clin Lab Med* 2005;25:247.
236. Ordonez NG. The diagnostic utility of immunohistochemistry in distinguishing between mesothelioma and renal cell carcinoma: A comparative study. *Hum Pathol* 2004;35:697.
237. Avery AK, Beckstead J, Renshaw AA, et al. Use of antibodies to RCC and CD10 in the differential diagnosis of renal neoplasms. *Am J Surg Pathol* 2000;24:203.
238. Amin MB, Corless CL, Renshaw AA, et al. Papillary (chromophil) renal cell carcinoma: Histomorphologic characteristics and evaluation of conventional pathologic prognostic parameters in 62 cases. *Am J Surg Pathol* 1997;21:621.
239. Delahunt B, Eble JN. Papillary renal cell carcinoma: A clinicopathologic and immunohistochemical study of 105 tumors. *Mod Pathol* 1997;10:537.
240. Ronnen EA, Kondagunta GV, Ishill N, et al. Treatment outcome for metastatic papillary renal cell carcinoma patients. *Cancer* 2006;107:2617.
241. Zbar B, Glenn G, Lubensky I, et al. Hereditary papillary renal cell carcinoma: Clinical studies in 10 families. *J Urol* 1995;153:907.
242. Lee JH, Choi JW, Kim YS. The value of histologic subtyping on outcomes of clear cell and papillary renal cell carcinomas: A meta-analysis. *Urology* 2010;76:889.
243. Kovacs G, Fuzesi L, Emanuel A, et al. Cytogenetics of papillary renal cell tumors. *Genes Chromosomes Cancer* 1991;3:249.
244. van den Berg E, van der Hout AH, Oosterhuis JW, et al. Cytogenetic analysis of epithelial renal-cell tumors: Relationship with a new histopathological classification. *Int J Cancer* 1993;55:223.
245. Presti JC, Jr., Rao PH, Chen Q, et al. Histopathological, cytogenetic, and molecular characterization of renal cortical tumors. *Cancer Res* 1991;51:1544.
246. Ngan KW, Ng KF, Chuang CK. Solid variant of papillary renal cell carcinoma. *Chang Gung Med J* 2001;24:582.
247. Delahunt B, Eble JN, McCredie MR, et al. Morphologic typing of papillary renal cell carcinoma: Comparison of growth kinetics and patient survival in 66 cases. *Hum Pathol* 2001;32:590.
248. Leroy X, Zini L, Leteurtre E, et al. Morphologic subtyping of papillary renal cell carcinoma: Correlation with prognosis and differential expression of MUC1 between the two subtypes. *Mod Pathol* 2002;15:1126.
249. Mejean A, Hopirtean V, Bazin JB, et al. Prognostic factors for the survival of patients with papillary renal cell carcinoma: Meaning of histological typing and multifocality. *J Urol* 2003;170:764.
250. Yang XJ, Tan MH, Kim HL, et al. A molecular classification of papillary renal cell carcinoma. *Cancer Res* 2005;65:5628.
251. Sika-Paotonu D, Bethwaite PB, McCredie MR, et al. Nucleolar grade but not Fuhrman grade is applicable to papillary renal cell carcinoma. *Am J Surg Pathol* 2006;30:1091.
252. McGregor DK, Khurana KK, Cao C, et al. Diagnosing primary and metastatic renal cell carcinoma: The use of the monoclonal antibody 'Renal Cell Carcinoma Marker'. *Am J Surg Pathol* 2001;25:1485.
253. Tretiakova MS, Sahoo S, Takahashi M, et al. Expression of alpha-methylacyl-CoA racemase in papillary renal cell carcinoma. *Am J Surg Pathol* 2004;28:69.
254. Amin MB, Paner GP, Alvarado-Cabrero I, et al. Chromophobe renal cell carcinoma: Histomorphologic characteristics and evaluation of conventional pathologic prognostic parameters in 145 cases. *Am J Surg Pathol* 2008;32:1822.
255. Cindolo L, de la Taille A, Schips L, et al. Chromophobe renal cell carcinoma: Comprehensive analysis of 104 cases from multicenter European database. *Urology* 2005;65:681.
256. Peyromaure M, Misrai V, Thiounn N, et al. Chromophobe renal cell carcinoma: Analysis of 61 cases. *Cancer* 2004;100:1406.
257. Przybycin CG, Cronin AM, Darvishian F, et al. Chromophobe renal cell carcinoma: A clinicopathologic study of 203 tumors in 200 patients with primary resection at a single institution. *Am J Surg Pathol* 2011;35:962.
258. Chevillet JC, Lohse CM, Sukov WR, et al. Chromophobe renal cell carcinoma: The impact of tumor grade on outcome. *Am J Surg Pathol* 2012;36:851.
259. Kovacs G. Molecular differential pathology of renal cell tumours. *Histopathology* 1993;22:1.
260. Speicher MR, Schoell B, du Manoir S, et al. Specific loss of chromosomes 1, 2, 6, 10, 13, 17, and 21 in chromophobe renal cell carcinomas revealed by comparative genomic hybridization. *Am J Pathol* 1994;145:356.
261. Brunelli M, Eble JN, Zhang S, et al. Eosinophilic and classic chromophobe renal cell carcinomas have similar frequent losses of multiple chromosomes from among chromosomes 1, 2, 6, 10, and 17, and this pattern of genetic abnormality is not present in renal oncocytoma. *Mod Pathol* 2005;18:161.
262. Thoenes W, Storkel S, Rumpelt HJ, et al. Chromophobe cell renal carcinoma and its variants—a report on 32 cases. *J Pathol* 1988;155:277.
263. Delongchamps NB, Galmiche L, Eiss D, et al. Hybrid tumour 'oncocytoma-chromophobe renal cell carcinoma' of the kidney: A report of seven sporadic cases. *BJU Int* 2009;103:1381.
264. Waldert M, Klatte T, Haitel A, et al. Hybrid renal cell carcinomas containing histopathologic features of chromophobe renal cell carcinomas and oncocytomas have excellent oncologic outcomes. *Eur Urol* 2010;57:661.
265. Gobbo S, Eble JN, Delahunt B, et al. Renal cell neoplasms of oncocytosis have distinct morphologic, immunohistochemical, and cytogenetic profiles. *Am J Surg Pathol* 2010;34:620.
266. Quiroga-Garza G, Khurana H, Shen S, et al. Sarcomatoid chromophobe renal cell carcinoma with heterologous sarcomatoid elements. A case report and review of the literature. *Arch Pathol Lab Med* 2009;133:1857.
267. Anila KR, Mathew APD, Somanathan T, et al. Chromophobe renal cell carcinoma with heterologous (liposarcomatous) differentiation: A case report. *Int J Surg Pathol* 2012;20:416.
268. Delahunt B, Sika-Paotonu D, Bethwaite PB, et al. Fuhrman grading is not appropriate for chromophobe renal cell carcinoma. *Am J Surg Pathol* 2007;31:957.
269. Delahunt B. Advances and controversies in grading and staging of renal cell carcinoma. *Mod Pathol* 2009;22(Suppl 2):S24.
270. Paner GP, Amin MB, Alvarado-Cabrero I, et al. A novel tumor grading scheme for chromophobe renal cell carcinoma: Prognostic utility and comparison with Fuhrman nuclear grade. *Am J Surg Pathol* 2010;34:1233.
271. Kennedy SM, Merino MJ, Linehan WM, et al. Collecting duct carcinoma of the kidney. *Hum Pathol* 1990;21:449.
272. Rumpelt HJ, Storkel S, Moll R, et al. Bellini duct carcinoma: Further evidence for this rare variant of renal cell carcinoma. *Histopathology* 1991;18:115.
273. Chao D, Zisman A, Pantuck AJ, et al. Collecting duct renal cell carcinoma: Clinical study of a rare tumor. *J Urol* 2002;167:71.
274. Peyromaure M, Thiounn N, Scotte F, et al. Collecting duct carcinoma of the kidney: A clinicopathological study of 9 cases. *J Urol* 2003;170:1138.
275. Dimopoulos MA, Logothetis CJ, Markowitz A, et al. Collecting duct carcinoma of the kidney. *Br J Urol* 1993;71:388.

276. Fuzesi L, Cober M, Mittermayer C. Collecting duct carcinoma: Cytogenetic characterization. *Histopathology* 1992;21:155.
277. Polascik TJ, Cairns P, Epstein JI, et al. Distal nephron renal tumors: Microsatellite allelotype. *Cancer Res* 1996;56:1892.
278. Steiner G, Cairns P, Polascik TJ, et al. High-density mapping of chromosomal arm 1q in renal collecting duct carcinoma: Region of minimal deletion at 1q32.1-32.2. *Cancer Res* 1996;56:5044.
279. Antonelli A, Portesi E, Cozzoli A, et al. The collecting duct carcinoma of the kidney: A cytogenetical study. *Eur Urol* 2003;43:680.
280. Albadine R, Schultz L, Illei P, et al. PAX8 (+)/p63 (-) immunostaining pattern in renal collecting duct carcinoma (CDC): A useful immunoprofile in the differential diagnosis of CDC versus urothelial carcinoma of upper urinary tract. *Am J Surg Pathol* 2010;34:965.
281. Baer SC, Ro JY, Ordonez NG, et al. Sarcomatoid collecting duct carcinoma: A clinicopathologic and immunohistochemical study of five cases. *Hum Pathol* 1993;24:1017.
282. Kobayashi N, Matsuzaki O, Shirai S, et al. Collecting duct carcinoma of the kidney: An immunohistochemical evaluation of the use of antibodies for differential diagnosis. *Hum Pathol* 2008;39:1350.
283. Abern MR, Tsivian M, Polascik TJ, et al. Characteristics and outcomes of tumors arising from the distal nephron. *Urology* 2012;80:140.
284. Davis CJ, Mostofi FK, Sesterhenn IA. Renal medullary carcinoma: The seventh sickle cell nephropathy. *Am J Surg Pathol* 1995;19:1.
285. Calderaro J, Moroch J, Pierron G, et al. SMARCB1/INI1 inactivation in renal medullary carcinoma. *Histopathology* 2012;61(3):428-435.
286. Stahlschmidt J, Cullinane C, Roberts P, et al. Renal medullary carcinoma: Prolonged remission with chemotherapy, immunohistochemical characterisation and evidence of bcr/abl rearrangement. *Med Pediatr Oncol* 1999;33:551.
287. Yang XJ, Sugimura J, Tretiakova MS, et al. Gene expression profiling of renal medullary carcinoma: Potential clinical relevance. *Cancer* 2004;100:976.
288. Adsay NV, deRoux SJ, Sakr W, et al. Cancer as a marker of genetic medical disease: An unusual case of medullary carcinoma of the kidney. *Am J Surg Pathol* 1998;22:260.
289. Rao PM, Tannir NM, Tamboli P. Expression of OCT3/4 in renal medullary carcinoma represents a potential diagnostic pitfall. *Am J Surg Pathol* 2012;36:583.
290. Swartz MA, Karth J, Schneider DT, et al. Renal medullary carcinoma: Clinical, pathologic, immunohistochemical, and genetic analysis with pathogenetic implications. *Urology* 2002;60:1083.
291. Parwani AV, Husain AN, Epstein JI, et al. Low-grade myxoid renal epithelial neoplasms with distal nephron differentiation. *Hum Pathol* 2001;32:506.
292. Rakozy C, Schmahl GE, Bogner S, et al. Low-grade tubular-mucinous renal neoplasms: Morphologic, immunohistochemical, and genetic features. *Mod Pathol* 2002;15:1162.
293. Hes O, Hora M, Perez-Montiel DM, et al. Spindle and cuboidal renal cell carcinoma, a tumour having frequent association with nephrolithiasis: Report of 11 cases including a case with hybrid conventional renal cell carcinoma/spindle and cuboidal renal cell carcinoma components. *Histopathology* 2002;41:549.
294. Ferlicot S, Allory Y, Comperat E, et al. Mucinous tubular and spindle cell carcinoma: A report of 15 cases and a review of the literature. *Virchows Arch* 2005;447:978.
295. Fine SW, Argani P, DeMarzo AM, et al. Expanding the histologic spectrum of mucinous tubular and spindle cell carcinoma of the kidney. *Am J Surg Pathol* 2006;30:1554.
296. Brandal P, Lie AK, Bassarova A, et al. Genomic aberrations in mucinous tubular and spindle cell renal cell carcinomas. *Mod Pathol* 2006;19:186.
297. Kuroda N, Hes O, Michal M, et al. Mucinous tubular and spindle cell carcinoma with Fuhrman nuclear grade 3: A histological, immunohistochemical, ultrastructural and FISH study. *Histol Histopathol* 2008;23:1517.
298. Pillay N, Ramdial PK, Cooper K, et al. Mucinous tubular and spindle cell carcinoma with aggressive histomorphology—a sarcomatoid variant. *Hum Pathol* 2008;39:966.
299. Dhillon J, Amin MB, Selbs E, et al. Mucinous tubular and spindle cell carcinoma of the kidney with sarcomatoid change. *Am J Surg Pathol* 2009;33:44.
300. Paner GP, Srigley JR, Radhakrishnan A, et al. Immunohistochemical analysis of mucinous tubular and spindle cell carcinoma and papillary renal cell carcinoma of the kidney: Significant immunophenotypic overlap warrants diagnostic caution. *Am J Surg Pathol* 2006;30:13.
301. Kuroda N, Nakamura S, Miyazaki E, et al. Low-grade tubular-mucinous renal neoplasm with neuroendocrine differentiation: A histological, immunohistochemical and ultrastructural study. *Pathol Int* 2004;54:201.
302. Ursani NA, Robertson AR, Schieman SM, et al. Mucinous tubular and spindle cell carcinoma of kidney without sarcomatoid change showing metastases to liver and retroperitoneal lymph node. *Hum Pathol* 2011;42:444.
303. Murphy WJ, Beckwith J, Farrow G. *AFIP 3rd Series Atlas of Tumor Pathology: Tumors of the Kidney, Bladder, and Related Structures*. Washington: American Registry of Pathology, 1994.
304. Azoulay S, Vieillefond A, Paraf F, et al. Tubulocystic carcinoma of the kidney: A new entity among renal tumors. *Virchows Arch* 2007;451:905.
305. Yang XJ, Zhou MM, Hes O, et al. Tubulocystic carcinoma of the kidney: Clinicopathologic and molecular characterization. *Am J Surg Pathol* 2008;32:177.
306. Amin MB, MacLennan GT, Gupta R, et al. Tubulocystic carcinoma of the kidney: Clinicopathologic analysis of 31 cases of a distinctive rare subtype of renal cell carcinoma. *Am J Surg Pathol* 2009;33:384.
307. Osunkoya AO, Young AN, Wang W, et al. Comparison of gene expression profiles in tubulocystic carcinoma and collecting duct carcinoma of the kidney. *Am J Surg Pathol* 2009;33:1103.
308. Zhou M, Yang XJ, Lopez JI, et al. Renal tubulocystic carcinoma is closely related to papillary renal cell carcinoma: Implications for pathologic classification. *Am J Surg Pathol* 2009;33:1840.
309. Bhullar JS, Thambou T, Esuvaranathan K. Unique case of tubulocystic carcinoma of the kidney with sarcomatoid features: A new entity. *Urology* 2011;78:1071.
310. Gobbo S, Eble JN, Grignon DJ, et al. Clear cell papillary renal cell carcinoma: A distinct histopathologic and molecular genetic entity. *Am J Surg Pathol* 2008;32:1239.
311. Aydin H, Chen L, Cheng L, et al. Clear cell tubulopapillary renal cell carcinoma: A study of 36 distinctive low-grade epithelial tumors of the kidney. *Am J Surg Pathol* 2010;34:1608.
312. Adam J, Couturier J, Molinie V, et al. Clear-cell papillary renal cell carcinoma: 24 cases of a distinct low-grade renal tumour and a comparative genomic hybridization array study of seven cases. *Histopathology* 2011;58:1064.
313. Rohan SM, Xiao Y, Liang Y, et al. Clear-cell papillary renal cell carcinoma: Molecular and immunohistochemical analysis with emphasis on the von Hippel-Lindau gene and hypoxia-inducible factor pathway-related proteins. *Mod Pathol* 2011;24:1207.
314. Rioux-Leclercq NC, Epstein JI. Renal cell carcinoma with intratumoral calcium oxalate crystal deposition in patients with acquired cystic disease of the kidney. *Arch Pathol Lab Med* 2003;127:E89.
315. Sule N, Yakupoglu U, Shen SS, et al. Calcium oxalate deposition in renal cell carcinoma associated with acquired cystic kidney disease: A comprehensive study. *Am J Surg Pathol* 2005;29:443.
316. Nouh MA, Kuroda N, Yamashita M, et al. Renal cell carcinoma in patients with end-stage renal disease: Relationship between histological type and duration of dialysis. *BJU Int* 2010;105:620.
317. Enoki Y, Katoh G, Okabe H, et al. Clinicopathological features and CD57 expression in renal cell carcinoma in acquired cystic disease of the kidneys: With special emphasis on a relation to the duration of haemodialysis, the degree of calcium oxalate deposition, histological type, and possible tumorigenesis. *Histopathology* 2010;56:384.
318. Pan CC, Chen YJ, Chang LC, et al. Immunohistochemical and molecular genetic profiling of acquired cystic disease-associated renal cell carcinoma. *Histopathology* 2009;55:145.
319. Kuroda N, Shiotsu T, Hes O, et al. Acquired cystic disease-associated renal cell carcinoma with gain of chromosomes 3, 7, and 16, gain of chromosome X, and loss of chromosome Y. *Med Mol Morphol* 2010;43:231.
320. Kuroda N, Tamura M, Taguchi T, et al. Sarcomatoid acquired cystic disease-associated renal cell carcinoma. *Histol Histopathol* 2008;23:1327.
321. Colin P, Koenig P, Ouzzane A, et al. Environmental factors involved in carcinogenesis of urothelial cell carcinomas of the upper urinary tract. *BJU Int* 2009;104:1436.

322. Crockett DG, Wagner DG, Holmäng S, et al. Upper urinary tract carcinoma in Lynch syndrome cases. *J Urol* 2011;185:1627.
323. Dores GM, Curtis RE, Toro JR, et al. Incidence of cutaneous sebaceous carcinoma and risk of associated neoplasms: Insight into Muir-Torre syndrome. *Cancer* 2008;113:3372.
324. Olğac S, Mazumdar M, Dalbagni G, et al. Urothelial carcinoma of the renal pelvis: A clinicopathologic study of 130 cases. *Am J Surg Pathol* 2004;28:1545.
325. Novara G, De Marco V, Gottardo F, et al. Independent predictors of cancer-specific survival in transitional cell carcinoma of the upper urinary tract: Multi-institutional dataset from 3 European centers. *Cancer* 2007;110:1715.
326. Gupta R, Paner GP, Amin MB. Neoplasms of the upper urinary tract: A review with focus on urothelial carcinoma of the pelvicalyceal system and aspects related to its diagnosis and reporting. *Adv Anat Pathol* 2008;15:127.
327. Chromecki TF, Cha EK, Fajkovic H, et al. The impact of tumor multifocality on outcomes in patients treated with radical nephroureterectomy. *Eur Urol* 2012;61:245.
328. Fujimoto H, Tobisu K, Sakamoto M, et al. Intraductal tumor involvement and renal parenchymal invasion of transitional cell carcinoma in the renal pelvis. *J Urol* 1995;153:57.
329. Cordon-Cardo C. Molecular alterations associated with bladder cancer initiation and progression. *Scand J Urol Nephrol* 2008;(218):154-165.
330. Knowles MA. Bladder cancer subtypes defined by genomic alterations. *Scand J Urol Nephrol* 2008;(218):116.
331. Busby JE, Brown GA, Tamboli P, et al. Upper urinary tract tumors with nontransitional histology: A single-center experience. *Urology* 2006;67:518.
332. Punia RPS, Mundi I, Arora K, et al. Primary adenocarcinoma of ureter mimicking pyelonephritis. *Urol Ann* 2010;2:42.
333. Holmang S, Lele SM, Johansson SL. Squamous cell carcinoma of the renal pelvis and ureter: Incidence, symptoms, treatment and outcome. *J Urol* 2007;178:51.
334. Miller RJ, Holmäng S, Johansson SL, et al. Small cell carcinoma of the renal pelvis and ureter: Clinicopathologic and immunohistochemical features. *Arch Pathol Lab Med* 2011;135:1565.
335. Ouzzane A, Ghoneim TP, Udo K, et al. Small cell carcinoma of the upper urinary tract (UUT-SCC): Report of a rare entity and systematic review of the literature. *Cancer Treat Rev* 2011;37:366.
336. Perez-Montiel D, Wakely PE, Hes O, et al. High-grade urothelial carcinoma of the renal pelvis: Clinicopathologic study of 108 cases with emphasis on unusual morphologic variants. *Mod Pathol* 2006;19:494.
337. Grammatico D, Grignon DJ, Eberwein P, et al. Transitional cell carcinoma of the renal pelvis with choriocarcinomatous differentiation. Immunohistochemical and immunoelectron microscopic assessment of human chorionic gonadotropin production by transitional cell carcinoma of the urinary bladder. *Cancer* 1993;71:1835.
338. Truong LD, Shen SS. Immunohistochemical diagnosis of renal neoplasms. *Arch Pathol Lab Med* 2011;135:92.
339. Carvalho JC, Thomas DG, McHugh JB, et al. p63, CK7, PAX8 and INI-1: An optimal immunohistochemical panel to distinguish poorly differentiated urothelial cell carcinoma from high-grade tumours of the renal collecting system. *Histopathology* 2012;60:597.
340. Rouprêt M, Zigeuner R, Palou J, et al. European guidelines for the diagnosis and management of upper urinary tract urothelial cell carcinomas: 2011 update. *Eur Urol* 2011;59:584.
341. Reuter VE, Presti JC, Jr. Contemporary approach to the classification of renal epithelial tumors. *Semin Oncol* 2000;27:124.
342. Zisman A, Chao DH, Pantuck AJ, et al. Unclassified renal cell carcinoma: Clinical features and prognostic impact of a new histological subtype. *J Urol* 2002;168:950.
343. Uribe-Uribe N, Gu X, Herrera GA. Primary renal carcinoid tumor. *Pathol Case Rev* 2006;11:187.
344. Hansel DE, Epstein JI, Berbescu E, et al. Renal carcinoid tumor: A clinicopathologic study of 21 cases. *Am J Surg Pathol* 2007;31:1539.
345. Jeung JA, Cao D, Selli BW, et al. Primary renal carcinoid tumors: Clinicopathologic features of 9 cases with emphasis on novel immunohistochemical findings. *Hum Pathol* 2011;42:1554.
346. Tetu B, Ro JY, Ayala AG, et al. Small cell carcinoma of the kidney. A clinicopathologic, immunohistochemical, and ultrastructural study. *Cancer* 1987;60:1809.
347. Si Q, Dancer J, Stanton ML, et al. Small cell carcinoma of the kidney: A clinicopathologic study of 14 cases. *Hum Pathol* 2011;42:1792.
348. Takahashi M, Yang XJ, McWhinney S, et al. cDNA microarray analysis assists in diagnosis of malignant intrarenal pheochromocytoma originally masquerading as a renal cell carcinoma. *J Med Genet* 2005;42:e48.
349. Gohji K, Nakanishi T, Hara I, et al. Two cases of primary neuroblastoma of the kidney in adults. *J Urol* 1987;137:966.
350. Parham DM, Roloson GJ, Feely M, et al. Primary malignant neuroepithelial tumors of the kidney: A clinicopathologic analysis of 146 adult and pediatric cases from the National Wilms' Tumor Study Group Pathology Center. *Am J Surg Pathol* 2001;25:133.
351. Jimenez RE, Folpe AL, Lapham RL, et al. Primary Ewing's sarcoma/primitive neuroectodermal tumor of the kidney: A clinicopathologic and immunohistochemical analysis of 11 cases. *Am J Surg Pathol* 2002;26:320.
352. Thyavithally YB, Tongaonkar HB, Gupta S, et al. Primitive neuroectodermal tumor of the kidney: A single institute series of 16 patients. *Urology* 2008;71:292.
353. Gleeson MH, Bloom SR, Polak JM, et al. Endocrine tumour in kidney affecting small bowel structure, motility, and absorptive function. *Gut* 1971;12:773.
354. Resnick ME, Unterberger H, McLoughlin PT. Renal carcinoid producing the carcinoid syndrome. *Med Times* 1966;94:895.
355. Ellison DA, Parham DM, Bridge J, et al. Immunohistochemistry of primary malignant neuroepithelial tumors of the kidney: A potential source of confusion? A study of 30 cases from the National Wilms Tumor Study Pathology Center. *Hum Pathol* 2007;38:205.
356. Cheng L, Gu J, Eble JN, et al. Molecular genetic evidence for different clonal origin of components of human renal angiomyolipomas. *Am J Surg Pathol* 2001;25:1231.
357. Pea M, Martignoni G, Zamboni G, et al. Perivascular epithelioid cell. *Am J Surg Pathol* 1996;20:1149.
358. Grignon D, Ro J, Ayala A. Mesenchymal tumors of the kidney. In: Eble J, ed. *Tumors and Tumor-like Conditions of the Kidneys and Ureters*. New York: Churchill Livingstone, 1990:123-144.
359. L'Hostis H, Deminiere C, Ferriere J-M, et al. Renal angiomyolipoma: A clinicopathologic, immunohistochemical, and follow-up study of 46 cases. *Am J Surg Pathol* 1999;23:1011.
360. Ryu JH, Hartman TE, Torres VE, et al. Frequency of undiagnosed cystic lung disease in patients with sporadic renal angiomyolipomas. *Chest* 2012;141:163.
361. O'Callaghan FJ, Noakes MJ, Martyn CN, et al. An epidemiological study of renal pathology in tuberous sclerosis complex. *BJU Int* 2004;94:853.
362. Unlu C, Lamme B, Nass P, et al. Retroperitoneal haemorrhage caused by a renal angiomyolipoma. *Emerg Med J* 2006;23:464.
363. Davies DM, de Vries PJ, Johnson SR, et al. Sirolimus therapy for angiomyolipoma in tuberous sclerosis and sporadic lymphangiomyomatosis: A phase 2 trial. *Clin Cancer Res* 2011;17:4071.
364. Mizushima Y, Bando M, Hosono T, et al. Clinical features of lymphangiomyomatosis complicated by renal angiomyolipomas. *Intern Med* 2011;50:285.
365. Govednik-Horny C, Atkins M. Angiomyolipoma with vascular invasion during pregnancy. *Ann Vasc Surg* 2011;25:1138.
366. Ro JY, Ayala AG, el-Naggar A, et al. Angiomyolipoma of kidney with lymph node involvement. DNA flow cytometric analysis. *Arch Pathol Lab Med* 1990;114:65.
367. Eble JN, Amin MB, Young RH. Epithelioid angiomyolipoma of the kidney: A report of five cases with a prominent and diagnostically confusing epithelioid smooth muscle component. *Am J Surg Pathol* 1997;21:1123.
368. Cibas ES, Goss GA, Kulke MH, et al. Malignant epithelioid angiomyolipoma ('sarcoma ex angiomyolipoma') of the kidney: A case report and review of the literature. *Am J Surg Pathol* 2001;25:121.
369. Martignoni G, Bonetti F, Pea M, et al. Renal disease in adults with TSC2/PKD1 contiguous gene syndrome. *Am J Surg Pathol* 2002;26:198.
370. Jimenez RE, Eble JN, Reuter VE, et al. Concurrent angiomyolipoma and renal cell neoplasia: A study of 36 cases. *Mod Pathol* 2001;14:157.

371. Martignoni G, Pea M, Rigaud G, et al. Renal angiomyolipoma with epithelioid sarcomatous transformation and metastases: Demonstration of the same genetic defects in the primary and metastatic lesions. *Am J Surg Pathol* 2000;24:889.
372. Brimo F, Robinson B, Guo C, et al. Renal epithelioid angiomyolipoma with atypia: A series of 40 cases with emphasis on clinicopathologic prognostic indicators of malignancy. *Am J Surg Pathol* 2010;34:715.
373. Ferry JA, Malt RA, Young RH. Renal angiomyolipoma with sarcomatous transformation and pulmonary metastases. *Am J Surg Pathol* 1991;15:1083.
374. Zavala-Pompa A, Folpe AL, Jimenez RE, et al. Immunohistochemical study of microphthalmia transcription factor and tyrosinase in angiomyolipoma of the kidney, renal cell carcinoma, and renal and retroperitoneal sarcomas: Comparative evaluation with traditional diagnostic markers. *Am J Surg Pathol* 2001;25:65.
375. Martignoni G, Pea M, Reghellin D, et al. PEComas: The past, the present and the future. *Virchows Arch* 2008;452:119.
376. Martignoni G, Bonetti F, Chilosi M, et al. Cathepsin K expression in the spectrum of perivascular epithelioid cell (PEC) lesions of the kidney. *Mod Pathol* 2012;25:100.
377. Hadley DA, Bryant LJ, Ruckle HC. Conservative treatment of renal angiomyolipomas in patients with tuberous sclerosis. *Clin Nephrol* 2006;65:22.
378. Franz DN, Bissler JJ, McCormack FX. Tuberous sclerosis complex: Neurological, renal and pulmonary manifestations. *Neuropediatrics* 2010;41:199.
379. Lowe BA, Brewer J, Houghton DC, et al. Malignant transformation of angiomyolipoma. *J Urol* 1992;147:1356.
380. Shum CF, Yip SK, Tan PH. Symptomatic renal leiomyoma: Report of two cases. *Pathology* 2006;38:454.
381. Terada T. Leiomyoma of the kidney parenchyma. *Pathol Int* 2011;61:495.
382. Lee HS, Koh BH, Kim JW, et al. Radiologic findings of renal hemangioma: Report of three cases. *Korean J Radiol* 2000;1:60.
383. Brown JG, Folpe AL, Rao P, et al. Primary vascular tumors and tumor-like lesions of the kidney: A clinicopathologic analysis of 25 cases. *Am J Surg Pathol* 2010;34:942.
384. Nakai Y, Namba Y, Sugao H. Renal lymphangioma. *J Urol* 1999;162:484.
385. Honma I, Takagi Y, Shigyo M, et al. Lymphangioma of the kidney. *Int Urol Nephrol* 2002;9:178.
386. Al-Ahmadie HA, Yilmaz A, Olgac S, et al. Glomus tumor of the kidney: A report of 3 cases involving renal parenchyma and review of the literature. *Am J Surg Pathol* 2007;31:585.
387. Ke H-L, Hsiao H-L, Guh J-Y, et al. Primary intrarenal lipoma: A case report. *Kaohsiung J Med Sci* 2005;21:383.
388. Liu X, Wu X, He D, et al. The first case of renal lipoma in a child. *J Pediatr Surg* 2011;46:1281.
389. Schofield D, Zaatari GS, Gay BB. Klippel-Trenaunay and Sturge-Weber syndromes with renal hemangioma and double inferior vena cava. *J Urol* 1986;136:442.
390. Fligelstone LJ, Campbell F, Ray DK, et al. The Klippel-Trenaunay syndrome: A rare cause of hematuria requiring nephrectomy. *J Urol* 1994;151:404.
391. Yazaki T, Takahashi S, Ogawa Y, et al. Large renal hemangioma necessitating nephrectomy. *Urology* 1985;25:302.
392. Grignon DJ, Ayala AG, Ro JY, et al. Primary sarcomas of the kidney. A clinicopathologic and DNA flow cytometric study of 17 cases. *Cancer* 1990;65:1611.
393. Vogelzang NJ, Fremgen AM, Guinan PD, et al. Primary renal sarcoma in adults. A natural history and management study by the American Cancer Society, Illinois Division. *Cancer* 1993;71:804.
394. Mondaini N, Palli D, Saieva C, et al. Clinical characteristics and overall survival in genitourinary sarcomas treated with curative intent: A multicenter study. *Eur Urol* 2005;47:468.
395. Dotan ZA, Tal R, Golijanin D, et al. Adult genitourinary sarcoma: The 25-year Memorial Sloan-Kettering experience. *J Urol* 2006;176:2033.
396. Wang X, Xu R, Yan L, et al. Adult renal sarcoma: Clinical features and survival in a series of patients treated at a high-volume institution. *Urology* 2011;77:836.
397. Deyrup AT, Montgomery E, Fisher C. Leiomyosarcoma of the kidney: A clinicopathologic study. *Am J Surg Pathol* 2004;28:178.
398. Miller JS, Zhou M, Brimo F, et al. Primary leiomyosarcoma of the kidney: A clinicopathologic study of 27 cases. *Am J Surg Pathol* 2010;34:238.
399. Hora M, Hes O, Reischig T, et al. Tumours in end-stage kidney. *Transplant Proc* 2008;40:3354.
400. Ciccarello G, Mucciardi G, Morgia G, et al. A case of renal capsular liposarcoma with intracaval fat thrombus. *Eur Urol* 2010;57:350.
401. Magro G, Emmanuele C, Lopes M, et al. Solitary fibrous tumour of the kidney with sarcomatous overgrowth. Case report and review of the literature. *APMIS* 2008;116:1020.
402. Hsieh TY, Chang Chien YC, Chen WH, et al. De novo malignant solitary fibrous tumor of the kidney. *Diagn Pathol* 2011;6:96.
403. Guo G, Zhang X, Zhou ZH. Clinical characteristics of malignant solitary fibrous tumors of the kidney with thoracic vertebral metastasis. *Int Urol Nephrol* 2012;19:177.
404. Tsai WC, Lee SS, Cheng MF, et al. Botryoid-type pleomorphic rhabdomyosarcoma of the renal pelvis in an adult. A rare case report and review of the literature. *Urol Int* 2006;77:89.
405. Meir K, Wygoda M, Reichman O, et al. Puerperal renal rhabdomyosarcoma: Case report and review of the literature. *Urol Oncol* 2006;24:40.
406. Argani P, Faria PA, Epstein JI, et al. Primary renal synovial sarcoma: Molecular and morphologic delineation of an entity previously included among embryonal sarcomas of the kidney. *Am J Surg Pathol* 2000;24:1087.
407. Tan YS, Ng LG, Yip SK, et al. Synovial sarcoma of the kidney: A report of 4 cases with pathologic appraisal and differential diagnostic review. *Anal Quant Cytol Histol* 2010;32:239.
408. Pitino A, Squillaci S, Spairani C, et al. Primary synovial sarcoma of the kidney. A case report with pathologic appraisal investigation and literature review. *Pathologica* 2011;103:271.
409. Gomez-Brouchet A, Soulie M, Delisle MB, et al. Mesenchymal chondrosarcoma of the kidney. *J Urol* 2001;166:2305.
410. O'Malley FP, Grignon DJ, Shepherd RR, et al. Primary osteosarcoma of the kidney. Report of a case studied by immunohistochemistry, electron microscopy, and DNA flow cytometry. *Arch Pathol Lab Med* 1991;115:1262.
411. Leventis AK, Stathopoulos GP, Boussiotou AC, et al. Primary osteogenic sarcoma of the kidney—a case report and review of the literature. *Acta Oncol* 1997;36:775.
412. Zenico T, Saccomanni M, Salomone U, et al. Primary renal angiosarcoma: Case report and review of world literature. *Tumori* 2011;97:e6.
413. Imao T, Amano T, Takemae K. Leiomyosarcoma of the renal vein. *Int J Clin Oncol* 2011;16:76.
414. Castillo OA, Boyle ET, Jr, Kramer SA. Multilocular cysts of kidney. A study of 29 patients and review of literature. *Urology* 1991;37:156.
415. van den Hoek J, de Krijger R, van de Ven K, et al. Cystic nephroma, cystic partially differentiated nephroblastoma and cystic Wilms' tumor in children: A spectrum with therapeutic dilemmas. *Urol Int* 2009;82:65.
416. Turbiner J, Amin MB, Humphrey PA, et al. Cystic nephroma and mixed epithelial and stromal tumor of kidney: A detailed clinicopathologic analysis of 34 cases and proposal for renal epithelial and stromal tumor (REST) as a unifying term. *Am J Surg Pathol* 2007;31:489.
417. Zhou M, Kort E, Hoekstra P, et al. Adult cystic nephroma and mixed epithelial and stromal tumor of the kidney are the same disease entity: Molecular and histologic evidence. *Am J Surg Pathol* 2009;33:72.
418. Bisceglia M, Galliani CA, Senger C, et al. Renal cystic diseases: A review. *Adv Anat Pathol* 2006;13:26.
419. Pawade J, Soosay GN, Delprado W, et al. Cystic hamartoma of the renal pelvis. *Am J Surg Pathol* 1993;17:1169.
420. Adsay NV, Eble JN, Srigley JR, et al. Mixed epithelial and stromal tumor of the kidney. *Am J Surg Pathol* 2000;24:958.
421. Michal M, Hes O, Bisceglia M, et al. Mixed epithelial and stromal tumors of the kidney. A report of 22 cases. *Virchows Arch* 2004;445:359.
422. Michal M, Hes O, Nencova J, et al. Renal angiomyoadenomatous tumor: Morphologic, immunohistochemical, and molecular genetic study of a distinct entity. *Virchows Arch* 2009;454:89.
423. Svec A, Hes O, Michal M, et al. Malignant mixed epithelial and stromal tumor of the kidney. *Virchows Arch* 2001;439:700.
424. Nakagawa T, Kanai Y, Fujimoto H, et al. Malignant mixed epithelial and stromal tumours of the kidney: A report of the first two cases with a fatal clinical outcome. *Histopathology* 2004;44:302.

425. Kuroda N, Gotoda H, Ohe C, et al. Review of juxtaglomerular cell tumor with focus on pathobiological aspect. *Diagn Pathol* 2011;6:80.
426. Robertson PW, Klidjian A, Harding LK, et al. Hypertension due to a renin-secreting renal tumour. *Am J Med* 1967;43:963.
427. Eble J. Unusual renal tumors and tumor-like lesions. In: Eble J, ed. *Tumors and Tumor-like Conditions of the Kidneys and Ureters*. New York: Churchill Livingstone, 1990:145–176.
428. Martin SA, Mynderse LA, Lager DJ, et al. Juxtaglomerular cell tumor: A clinicopathologic study of four cases and review of the literature. *Am J Clin Pathol* 2001;116:854.
429. Tetu B, Vaillancourt L, Camilleri JP, et al. Juxtaglomerular cell tumor of the kidney: Report of two cases with a papillary pattern. *Hum Pathol* 1993;24:1168.
430. Mendez GP, Klock C, Nose V. Juxtaglomerular cell tumor of the kidney: Case report and differential diagnosis with emphasis on pathologic and cytopathologic features. *Int J Surg Pathol* 2011;19:93.
431. Dong D, Li H, Yan W, et al. The diagnosis and surgical management of juxtaglomerular cell tumor of the kidney. *J Hypertens* 2010;28:628.
432. Duan X, Bruneval P, Hammadeh R, et al. Metastatic juxtaglomerular cell tumor in a 52-year-old man. *Am J Surg Pathol* 2004;28:1098.
433. Mai KT. Giant renomedullary interstitial cell tumor. *J Urol* 1994;151:986.
434. Warfel K, Eble J. Renomedullary interstitial cell tumors. *Am J Clin Pathol* 1985;83:262.
435. Horita Y, Tadokoro M, Taura K, et al. Incidental detection of renomedullary interstitial cell tumour in a renal biopsy specimen. *Nephrol Dial Transplant* 2004;19:1007.
436. Zimmermann A, Luscieti P, Flury B, et al. Amyloid-containing renal interstitial cell nodules (RICNs) associated with chronic arterial hypertension in older age groups. *Am J Pathol* 1981;105:288.
437. Ferry J, Young R. Malignant lymphoma of the genitourinary tract. *Curr Diagn Pathol* 1997;4:145.
438. Dimopoulos MA, Mouloupoulos LA, Costantinides C, et al. Primary renal lymphoma: A clinical and radiological study. *J Urol* 1996;155:1865.
439. Pervez H, Shaikh M, Potti A, et al. Uncommon presentations of non-Hodgkin's lymphoma: Case 3 primary renal lymphoma. *J Clin Oncol* 2003;21:567.
440. Schniederjan SD, Osunkoya AO. Lymphoid neoplasms of the urinary tract and male genital organs: A clinicopathological study of 40 cases. *Mod Pathol* 2009;22:1057.
441. Da'as N, Polliack A, Cohen Y, et al. Kidney involvement and renal manifestations in non-Hodgkin's lymphoma and lymphocytic leukemia: A retrospective study in 700 patients. *Eur J Haematol* 2001;67:158.
442. Sheil O, Redman CW, Pugh C. Renal failure in pregnancy due to primary renal lymphoma. Case report. *Br J Obstet Gynecol* 1991;98:216.
443. van Gelder T, Michiels JJ, Mulder AH, et al. Renal insufficiency due to bilateral primary renal lymphoma. *Nephron* 1992;60:108.
444. Weng SC, Shu KH, Wen MC, et al. Malignant lymphoma of the kidney mimicking rapid progressive glomerulonephritis. *Clin Nephrol* 2010;74:480.
445. Charitaki E, Liapis K, Moutzouris DA, et al. Primary renal MALT lymphoma presenting with cryoglobulinaemia. *Nephrol Dial Transplant* 2011;26:3819.
446. Tuzel E, Mungan MU, Yorukoglu K, et al. Primary renal lymphoma of mucosa-associated lymphoid tissue. *Urology* 2003;61:463.
447. Fan F, Deauna-Limayo D, Brantley Thrasher J, et al. Anaplastic plasmacytoma of the kidney. *Histopathology* 2005;47:432.
448. Yazici S, Inci K, Dikmen A, et al. Port site and local recurrence of incidental solitary renal plasmacytoma after retroperitoneoscopic radical nephrectomy. *Urology* 2009;73:210.
449. Bracken RB, Chica G, Johnson DE, et al. Secondary renal neoplasms: An autopsy study. *South Med J* 1979;72:806.
450. Wagle DG, Moore RH, Murphy GP. Secondary carcinomas of the kidney. *J Urol* 1975;114:30.
451. Aggarwal N, Amin RM, Chung D, et al. Tumor-to-tumor metastasis: Case report of a pulmonary adenocarcinoma metastatic to a clear cell renal cell carcinoma. *Pathol Res Pract* 2012;208:50.
452. Shin T, Kan T, Sato F, Mimata H. Tumor-to-tumor metastasis to chromophobe renal cell carcinoma: a first report. *Case Rep Urol* 2011;2011:520839.
453. Melato M, Laurino L, Bianchi P, et al. Intraglomerular metastases. A possibly maldiagnosed entity. *Zentralblatt fur Pathologie* 1991;137:90.
454. Naryshkin S, Tomaszewski JE. Acute renal failure secondary to carcinomatous lymphatic metastases to kidneys. *J Urol* 1991;146:1610.
455. Grignon D, Eble J. Adenomatoid metaplasia of the epithelium of Bowman's capsule. *J Urol Pathol* 1993;1:293.
456. Bijol V, Mendez GP, Hurwitz S, et al. Evaluation of the nonneoplastic pathology in tumor nephrectomy specimens: Predicting the risk of progressive renal failure. *Am J Surg Pathol* 2006;30:575.
457. Henriksen KJ, Meehan SM, Chang A. Non-neoplastic renal diseases are often unrecognized in adult tumor nephrectomy specimens: A review of 246 cases. *Am J Surg Pathol* 2007;31:1703.
458. Truong LD, Shen SS, Park M-H, et al. Diagnosing nonneoplastic lesions in nephrectomy specimens. *Arch Pathol Lab Med* 2009;133:189.
459. Bonsib S, Pei Y. The non-neoplastic kidney in tumor nephrectomy specimens: What can it show and what is important? *Adv Anat Pathol* 2010;17:235.

Note: Page numbers followed by “f” indicate figures; page numbers followed by “t” indicate tabular material.

- A**
- Abdominal compartment syndrome, 1205
- Acquired renal cystic disease (ARCD)
 gross pathology, 1306–1307, 1306f
 microscopic pathology, 1307–1308, 1307f
 renal cell tumors, 1308–1309, 1308f
- Actin cytoskeleton, 30f, 177
- α -Actinin 4
 FSGS, 228t, 237
 podocyte adhesion, 32
- Action myoclonus-renal failure syndrome, 238
- Acute postinfectious glomerulonephritis. *See* Poststreptococcal acute glomerulonephritis (PSAGN)
- Acute pyelonephritis
 clinical course, 1046
 clinical presentation, 1041, 1041f
 diffuse suppurative pyelonephritis, 1044–1045, 1044f–1045f
 emphysematous pyelonephritis, 1045–1046, 1045f
 gross pathology and light microscopy, 1042–1044, 1042f–1043f
 prognosis/therapy, 1046
 sepsis and kidney injury, 1046
- Acute tubular injury (ATI), 105–106
 clinical course, 1201, 1201t
 clinical presentation
 antibiotics, 1171–1172
 antineoplastic agents, 1173–1174
 herbal medications, 1175
 immunosuppressive/immunomodulatory agents, 1172–1173
 narcotics, 1175
 radiologic contrast media, 1174–1175
 vancomycin, 1172
- differential diagnosis, 1200–1201
- etiology and pathogenesis
 drug toxicity
 anesthetics, 1200
 antibiotics, 1196–1197
 chemotherapeutic agents, 1199
 herbal medications, 1200
 immunosuppressive/immunomodulatory agents, 1197–1199
 narcotics, 1200
 radiocontrast agents, 1200
- ischemia
 apoptosis and necrosis, 1190–1191
 heat shock protein and chaperones, 1193–1194
 inflammatory response, 1191–1192
 injury and cell death, 1188–1190
 regeneration of tubular injury, 1193
 renal vasculature, 1192–1193
 stem cells and growth factors, 1194–1195
- gross pathology, 1175
 histopathology, 1175–1176, 1176f
 historical background, 1168–1170
 nephrotoxic acute tubular injury, 1181–1182
 aminoglycosides, 1183
 amphotericin, 1183
 anesthetics, 1187
 antibiotics, 1182
 antiviral agents, 1182–1183, 1182f
 cephalosporins, 1183
 chemotherapeutic agents, 1186
 herbal medications, 1187
 immunosuppressive/immunomodulatory agents, 1185–1186, 1185f
 myoglobinuric acute renal failure, 1187, 1187f
 narcotics, 1187, 1187f
 polymyxin/colistin, 1184
 radiocontrast agents, 1186–1187
 vancomycin, 1184–1185
- prognosis, 1201–1202
 syndromic acute tubular injury, 1203–1204
 therapy, 1202–1203
- Acute tubulointerstitial nephritis, 452, 1113–1115, 1113f–1115f, 1402–1403
- Adenine phosphoribosyltransferase (APRT), 1252–1253, 1252f
- Adenovirus infections, 1411–1412
- Adhesion molecules, 78
- ADIKD. *See* Autosomal dominant interstitial kidney disease (ADIKD)
- ADPLD. *See* Autosomal dominant polycystic liver disease (ADPLD)
- Adrenal adenoma, 885–886, 886f
- Adrenal hyperplasia, 885
- Adriamycin nephropathy, 243
- Adult and newborn human kidney, 5f
- Advanced glycation end products (AGEs), 917–919
- Afferent arterioles, 759
- Age-related macular degeneration (AMD), 331, 343
- Aging
 etiology and pathogenesis
 calorie restriction and sirtuins, 1311
 Klotho and FGF23, 1310
 microRNAs, 1310–1311
 mitochondria and autophagy, 1310
 NO deficiency, 1310
 oxidative stress, 1310
 renin-angiotensin system, 1310
 telomeres, 1310
- functional changes
 endocrine and metabolic function, 1293–1294
 fluid and electrolyte balance, 1293
 glomerular filtration rate, 1292–1293
- renal concentrating and diluting ability, 1293
 renal hemodynamics, 1291–1292
- gross pathology, 1294
 hypertension, 870
 microscopic pathology
 glomerulus, 1294–1295
 renal vasculature, 1296–1297, 1296f
 tubules and interstitium, 1295–1296, 1295f
- aHUS. *See* Atypical hemolytic uremic syndrome (aHUS)
- Alagille syndrome, 152t, 1226
- Allografts
 drug-induced disease in
 acute tubulointerstitial nephritis, 1402
 rapamycin-/sirolimus-associated toxic effects, 1402–1403
 reflux nephropathy, 1079
 T-cell mechanisms, 1143
- Alpha 1 antitrypsin deficiency, 331
- Alpha Actinin 4 deficiency, 32, 237
- Alport syndrome (AS)
 anti-GBM Glomerulonephritis, 1415–1417, 1417f
 autosomal dominant inheritance, 538
 autosomal recessive inheritance, 537–538, 538f
 Epstein and Fechtner syndromes, 538–539
 genetic counseling, 539
 mutation study, 539–540, 539f
 pathogenesis of, 525–526
 pathologic findings
 electron microscopy, 526, 528–529, 529f–531f
 extrarenal tissues, 530–532
 gross pathology, 526
 immunofluorescence microscopy, 526
 light microscopy, 526
 renal transplantation, 540–541
 treatment, 540
 type IV collagen, 532, 533f, 534f
 X-linked dominant transmission
 clinical presentation, 532, 534–535
 genetics, 536–537
 immunohistologic study, 535–536, 536f
 phenotype-genotype correlations, 537
- AMD. *See* Age-related macular degeneration (AMD)
- Aminoglycosides, 1171–1172
- Aminonucleoside nephrosis, 176
- 5-Aminosalicylic acid, 1132
- Amphotericin B, 1172
- Amyloid derived from fibrinogen (AFib)
 clinical history, 994
 clinical presentation, 994–995
 gross and microscopic pathology, 995
 laboratory findings, 994–995
 pathogenesis, 995–996, 995f

- Amyloidosis
- AA amyloidosis
 - clinical history, 987
 - clinical presentation, 987–988
 - gross and microscopic pathology, 988
 - laboratory findings, 987–988
 - AL/AH amyloidosis
 - clinical history, 985–986
 - clinical presentation and laboratory findings, 986
 - etiology and pathogenesis, 986–987
 - ALect2, 990–991
 - amyloid deposits, in genitourinary tract, 997–998
 - amyloid immunohistochemistry, 981, 982f, 983
 - amyloid typing, 980, 981f
 - beta-2-microglobulin amyloidosis, 1286–1287, 1286f
 - Aβ₂M, 996–997
 - clinical history, 996–997
 - clinical presentation, 997
 - disease process and prognosis, 997
 - etiology and pathogenesis, 997
 - gross and microscopic pathology, 997
 - laboratory findings, 997
 - treatment, 997
 - C3 nephropathies, 1422
 - classification, 976–977, 976t
 - definition, 976
 - diabetic nephropathy, 932
 - electron microscopy, 984–985
 - familial Mediterranean fever
 - AA amyloidosis, etiology and pathogenesis of, 990
 - clinical presentation and laboratory findings, 989
 - gross and microscopic pathology, 989–990
 - gross pathology, 977
 - hereditary autoinflammatory diseases, 988–989
 - immunofluorescence, 983
 - light microscopy, 977–980, 978f–979f
 - MS with antibody-based amyloid typing, 984
 - nonimmunoglobulin and non-AA amyloidoses
 - AApoAIV, 991–992
 - AFib
 - clinical history, 994
 - clinical presentation, 994–995
 - gross and microscopic pathology, 995
 - laboratory findings, 994–995
 - pathogenesis, 995–996, 995f
 - ALect2, 990–991
 - ATTR, 993–994
 - hereditary amyloidoses, 992–993, 996
 - proteomics, 983–984
 - secondary amyloidosis, 630–631, 630f
 - systemic amyloidosis
 - differential diagnosis, 1000
 - renal transplantation, 999–1000
 - systemic lupus erythematosus, 609
 - Amyloidosis derived from leukocyte chemotactic factor 2 (ALect2), 990–991
 - Amyloidosis derived from transthyretin (ATTR)
 - clinical history, 993
 - clinical presentation and laboratory findings, 993
 - etiology and pathogenesis, 994, 994f
 - gross and microscopic pathology, 993
 - ANA-negative lupus nephritis, 608
 - Analgesic nephropathy
 - 5-aminosalicylic acid, 1132
 - anti-IL-6 agents, 632–633
 - anti-TNF-α agents, 632
 - clinical presentation, 1128
 - cyclosporine-induced nephrotoxicity, 631
 - differential diagnosis, 1130
 - gold salts/penicillamine, 631–632
 - incidence, 1127–1128
 - nonsteroidal anti-inflammatory agents, 631
 - pathogenesis, 1130–1132, 1131f
 - pathologic findings, 1128–1130, 1129f–1130f
 - urothelial cancer and analgesic abuse, 1132, 1132f
 - Anatomy, human kidney development
 - collecting duct system and nephrons, formation of, 72–74, 73f–74f
 - lower renal tract, 74
 - mesonephros, 69–70, 70f
 - metanephros, 70, 71f
 - pronephros, 69
 - renal pelvis and calyces, formation of, 70–72, 71f–72f
 - ANCA. *See* Antineutrophil cytoplasmic autoantibody (ANCA)
 - Angiolympoid hyperplasia, 888
 - Angiomyolipoma
 - clinical findings and epidemiology, 1482–1483
 - pathology, 1483
 - treatment and outcome, 1483–1484
 - Angiotensin-converting enzyme inhibitors, 1266–1267
 - Anti-glomerular basement membrane (Anti-GBM) glomerulonephritis
 - clinical course/clinicopathologic correlation, 680–681
 - clinical presentation, 660t, 661–662, 661t
 - crested glomerulonephritis
 - crested occurrence, 659
 - diagnosis, 658
 - frequency and severity of, 659–660, 660t, 661f
 - glomerular crescent, 658, 658f
 - types of, 658–659, 659f, 660t
 - differential diagnosis, 679–680
 - etiology and pathogenesis, 672–679, 678f
 - pathologic findings
 - blood vessels, 667, 669f
 - electron microscopy, 671–672, 673f–676f
 - glomeruli
 - acute cellular crescents, 658f, 663f, 665, 665f
 - ANCA glomerulonephritis, 664, 667t
 - extensive glomerular necrosis glomerular necrosis, 662, 664f
 - Jones methenamine silver-stained glomerulus, 664, 666f
 - large cellular crescent, 662, 663, 664f
 - macrophages, 664
 - masson trichrome staining, 662, 665, 665f, 670
 - periglomerular interstitial inflammation, 664, 666f
 - segmental fibrinoid necrosis, 662, 663, 663f
 - gross pathology, 662, 663f
 - immunofluorescence microscopy, 671t
 - ELISA, 669
 - glomerular necrosis/cellular crescents, 670, 671f
 - IgG, linear localization, 657, 658f
 - IgM/IgA, linear staining, 669–670
 - membranous glomerulonephritis, 670–671, 671f
 - pulmonary alveolar capillary basement membranes, 671, 673f
 - segmental low-intensity granular staining for C3, 667–668, 670f
 - interstitium, 666–667, 666f, 668f
 - lungs, 667, 669f
 - tubules, 666, 666f, 668f
 - prognosis, 680
 - therapy, 680–681
- Antibiotics
 - acute tubular injury
 - aminoglycosides, 1171–1172, 1196–1197
 - amphotericin B, 1172, 1197
 - antiviral agents, 1171, 1196
 - cephalosporins, 1172, 1197
 - colistin, 1172
 - polymyxin B, 1172
 - nephrotoxic acute tubular injury, 1182
- Antibody/autoantibody
 - ANCA, 99f, 271, 419, 421, 423, 423f, 482, 482f, 608, 619, 667t, 669f, 678f, 698–690, 729, 1422
 - anti-GBM, 657–658, 658f, 663f–665f, 667t, 668f, 675–679
 - anti-PLA₂R, 263, 263f, 596
- Antibody-mediated rejection (AMR)
 - acute AMR
 - ABO-incompatible grafts, 1369, 1370f, 1371
 - clinical course, 1368–1369, 1369f
 - clinicopathologic correlations, 1368–1369, 1369f
 - differential diagnosis, 1366–1367, 1367t
 - electron microscopy, 1365–1366, 1366f
 - gross pathology, 1359, 1360f
 - immunofluorescence microscopy and immunohistochemistry
 - arteries, 1365
 - glomeruli, 1360–1361, 1364f–1365f
 - peritubular capillaries, 1361–1362, 1364–1365, 1365f
 - tubules, 1361
 - light microscopy
 - glomeruli, 1360, 1361f
 - interstitium, 1360, 1363f
 - tubules, 1360, 1362f–1363f
 - vessels, 1360, 1363, 1364
 - pathogenesis, 1367
 - prevalence and clinical presentation, 1359
 - prognosis and therapy, 1368–1369, 1369f
 - risk factors, 1359
 - antigens, 1352–1353
 - B cells and plasma cells, 1353
 - C4d stains, 1354–1356
 - chronic AMR
 - C4d deposition, 1381
 - C4d-negative AMR, 1381
 - electron microscopy
 - arteries, 1379

- glomeruli, 1377–1378, 1377f–1378f
- peritubular capillaries, 1378–1379, 1378f
- etiology and pathogenesis, 1379
- gross pathology, 1372, 1372f
- immunofluorescence microscopy and immunohistochemistry
 - arteries, 1377
 - glomeruli, 1375, 1376f
 - peritubular capillaries, 1376–1377, 1376f
 - tubules, 1376
- light microscopy
 - arteries, 1374–1375, 1375f
 - glomeruli, 1372, 1373f
 - interstitium, 1372f–1373f, 1374f
 - peritubular capillaries, 1373–1374, 1375f
 - tubules, 1372
- natural history, therapy, and outcome, 1381–1382, 1382f
- prevalence, 1371–1372
- prognosis and differential diagnosis, 1379
- risk factors, 1371–1372, 1379–1381
- smoldering/indolent AMR, 1381
- effector mechanisms, 1353–1354, 1355f
- Anticomplement factor H antibodies, 771
- Antimicrobial agents
 - cephalosporins, 1121–1122
 - fluoroquinolones, 1122
 - penicillins, 1122–1123
 - rifampicin, 1123
 - sulfonamides, 1123
 - vancomycin, 1123–1124
- Antineoplastic agents, 1173–1174
- Antineutrophil cytoplasmic autoantibody (ANCA). *See also* Pauci-immune crescentic glomerulonephritis
- anti-GBM disease
 - comparative studies, 667t
 - MPO-ANCA, 662, 662t, 664
 - necrotizing vasculitis, 667, 669f
 - small-vessel vasculitis, 667
- associated granulomatous polyangiitis, 415
- classification, 694–695
- clinical presentation
 - antigen specificity, 687
 - calculated predictive value, 689, 689f
 - cytoplasmic (c-ANCA), 688–689
 - glomerulonephritis, 688
 - incidence, 688
 - MPO-ANCA, 689–690, 690f
 - perinuclear (p-ANCA), 688–689
- definitions, 686, 686t
- electron microscopic finding
 - ANCA IgG incubation, 704, 705f
 - ANCA-induced leukocyte activation, 705
 - PR3-ANCA, 706
- IgA vasculitis nephritis, 501
- lupus nephritis, 608
- necrotizing glomerular lesion, 420, 420f
- prevalence of, 423
- segmental necrotizing lupus glomerulonephritis, 707
- subacute bacterial endocarditis, 419
- Antiphospholipid antibodies, 774–775, 840–841
- Antiphospholipid (APL) syndrome
 - clinical presentation, 575, 576f
 - ELISA, 576–577
 - lupus-like condition, 575
- optimal therapy, 577
- prevalence, 576
- thrombotic microangiopathy, 576
- Antistreptolysin O (ASO), 371, 399
- Antiviral agents, 1171
- Apolipoprotein AIV–derived amyloid (AApoAIV), 991–992
- Apolipoprotein L1 (APOL1), 234t, 240
- Acquired partial lipodystrophy (APL), 343
- Aristolochic acid nephropathy (AAN), 1152, 1153
- Arterial stenosis, 1414, 1389f
- Arterioles
 - calcineurin inhibitor toxicity, 1395, 1397f, 1398
 - efferent, 3f
 - hemolytic-uremic syndrome, 758–760, 758f–760f
 - in rats
 - glomerular efferent, 45f
 - juxtaglomerular portions of afferent, 21f
 - recurrent glomerular diseases, 1422
 - renal corpuscle, 43–44
 - systemic sclerosis (systemic scleroderma), 778–779, 779f–780f
 - thrombotic thrombocytopenic purpura, 758–760, 758f–760f
- Arterionephrosclerosis, 241, 242, 732, 1327
- Atheroembolization, 93t, 96, 208t
- ASO. *See* Antistreptolysin O (ASO)
- Asymptomatic/covert bacteriuria
 - kidney, effects on, 817
 - pregnancy, effects on, 817
- Asymptomatic proteinuria, 788
- Asymptomatic urinary abnormalities, 466, 466t
- Atheroembolic disease, 1208–1209, 1209f
- Atherosclerosis
 - clinical presentation, 179–180
 - complication of, 875
 - development, 877
 - occlusion of lumen, 875, 875f
 - renal artery, 135f
 - severity, 1284
- Atypical hemolytic-uremic syndrome, 361f
 - ADAMTS13 deficiency, 836
 - anticomplement factor H antibodies, 771
 - CFB/C3, 771
 - CFH/CFI, 771
 - clinical classification, 741t, 742–743
 - clinical presentation, 769, 770t
 - C3 nephropathies, 1420–1421
 - complement abnormalities, 769–771, 770f, 770t
 - anticomplement factor H antibodies, 771
 - cobalamin C (cblC) disorder, 743
 - complement factor H, 771
 - epidemiology, 745
 - familial forms, 743, 748
 - membrane cofactor protein, 771
 - recurrences, 748
 - S. pneumoniae* infection, 743
 - thrombomodulin and C3 mutations, 771
 - triggering events, 748
 - complement factor H, 771
 - incidence of, 745
 - membrane cofactor protein, 771
 - pathogenesis, 769, 770
 - thrombomodulin, 771
- Autoimmune thyroiditis, 289–290
- Autophagia, 1310
- Autosomal dominant inheritance, 538
- Autosomal dominant interstitial kidney disease (ADIKD), 120
- Autosomal dominant polycystic kidney disease (ADPKD)
 - clinical presentation, 121–122
 - differential diagnosis, 127
 - early-onset
 - diffuse nephroblastomatosis, 125, 127f
 - gelatinous fluid, 125, 126f
 - isolated cysts, 124–125, 126f
 - renal biopsy, 126, 127f
 - third-hit signaling, 126
 - genetics, 121–122, 140–141
 - incidence of, 120–121
 - malignancy, 124, 125f, 126f
 - pathology
 - human proximal tubule cilia, 124, 125f
 - interstitial fibrosis, 123, 124f
 - PKD2 mutation, 120t, 123, 123t
 - proliferating epithelia, 124, 124f
 - residual renal parenchyma, 123, 123f
 - radiologic evaluation
 - age-specific radiologic analysis, 122–123, 123t
 - bright appearance of cysts, 122, 122f
 - nephromegaly, 122, 122f
- Autosomal dominant polycystic liver disease (ADPLD), 130–131, 132f
- Autosomal recessive Alport syndrome, 537–538, 538f
- Autosomal recessive polycystic kidney disease (ARPKD)
 - clinical presentation, 128
 - genetics, 128, 141
 - incidence of, 127–128
 - pathology
 - degenerating cysts, 129, 130f
 - differential diagnosis, 129
 - diffuse microcysts, 129, 129f
 - renal biopsy, 129, 131f
 - radiologic evaluation, 128, 128f
- Autosomal recessive steroid-resistant nephrotic syndrome
 - CD2-associated protein, 237
 - myosin 1E, 236
 - phospholipase C epsilon, 236
 - podocin, 236
 - protein tyrosine phosphatase receptor type O, 237
- Autotransporter secreted toxins, 1052
- B**
- Balkan endemic nephropathy
 - clinical presentation, 1152
 - pathogenesis, 1152–1153
 - pathologic findings, 1152, 1153f
- Bardet-Biedl syndrome, 141
- Bartter syndrome
 - clinical features, 886
 - pathologic findings, 886, 867f
- Belimumab, lupus nephritis, 604
- Benign hypertension, 788
- Benign mesenchymal tumors, 1484
- Beta-2-microglobulin amyloidosis, 1286–1287, 1286f

- Blood vessels
 anti-GBM glomerulonephritis, 667, 669f
 dense deposit disease, 345
 diabetic nephropathy, 908, 908 f
 end-stage renal disease, 1302–1303, 1303f
 essential hypertension, 858–860, 858f–860f
 juxtaglomerular apparatus, 42–43
 in kidney development
 mechanisms, 84
 renal vasculature, developmental anatomy of, 83–84
 stroma, 84–85
 minimal change disease, 186
 primary membranous glomerulonephritis, 261
 radiation nephropathy, 789, 789f
- Bone morphogenetic protein (BMP), 155–156
 Bowman capsule, 41–42
 Bright, R, 91, 302, 368
 Bucillamine, MGN, 285
- C**
- C3 convertase, 324, 356–357, 357f, 360, 770f
 C5 convertase, 769, 1355f
 C3 glomerulonephritis (C3GN), 1420
 clinical course, 356
 clinical presentation, 350–351
 pathologic finding
 electron microscopy, 351f–355f, 353, 355–356
 glomeruli
 biopsy, 353, 355f
 capillary wall thickening, 351, 353f, 354f
 membranoproliferative pattern, 351, 352f
 mesangial pattern, 351, 351f
 immunohistochemistry, 352f, 353, 361f
 interstitium, 353
 tubules, 353
 prognosis, 356
 treatment, 356
- C3 glomerulopathy
 adenine phosphoribosyltransferase deficiency, 1424
 amyloidosis, 1422
 anti-GBM disease, 1422
 antineutrophil cytoplasmic antibody-mediated disease, 1422
 associated with PSAGN, 395–396
 atypical hemolytic uremic syndrome, 1420–1421
 C3GN. *See* C3 glomerulonephritis (C3GN)
 classification, 301, 304f, 341, 342t
 cystinosis, 1424
 diabetic nephropathy, 1423
 dense deposit disease. *See* Dense deposit disease (DDD)
 Fabry disease, 1423–1424
 fibrillary and immunotactoid glomerulopathies, 1423
 Henoch-Schönlein Purpura (HSP), 1421
 membranous glomerulonephritis, 1421–1422, 1421f
 monoclonal immunoglobulin deposition disease, 1422–1423
 pathogenesis, 324–325
 complement system
 activation, 356–357, 357f
 animal models, 363–364
 biologic effector function, 357, 358f
 C3 nephritic factor (C3NeF), 360
 CFH-CFHR family, 362f, 363
 complement factor H (CFH), 357–360, 359f
 complement factor I (CFI), 357–359, 359f
 genetic and acquired disorders, 359–360
 regulation, 357, 359f
 primary hyperoxaluria, 1423
 systemic lupus erythematosus, 1422
- C3 nephropathies
 amyloidosis, 1422
 antineutrophil cytoplasmic antibody-mediated diseases, 1422
 atypical hemolytic uremic syndrome, 1420–1421
 C3 glomerulonephritis, 1430
 Henoch-Schönlein purpura, 1421
 IgAN nephropathy, 1421
 membranous glomerulonephritis, 1421–1422, 1422f
 systemic lupus erythematosus, 1422
- C5a production, 358f, 364
- Cadmium nephropathy, 1147–1148
- Calcineurin inhibitor toxicity, 751, 116f, 1198
 clinical presentation, 1400–1402, 1401f
 differential diagnosis
 arteriopathy, 1400
 glomerulopathy, 1399–1400, 1400f
 tubular lesions, 1397f, 1400
 electron microscopy, 1398
 etiology and pathogenesis, 1398–1399
 immunofluorescence microscopy, 1398
 immunosuppression, 1391
 light microscopy
 arterioles and arteries, 1395, 1396t, 1397f, 1398
 glomeruli, 1391–1392, 1393f–1396f, 1394
 interstitium, 1394–1395
 tubules, 1394, 1394f
 prognosis and therapy, 1400–1401, 1401f
- Calcium nephrolithiasis
 calcium oxalate stones, 1098
 chloride channel mutations, 1096–1097
 hyperuricosuria
 primary hyperoxaluria, 1097, 1097f
 secondary hyperoxaluria, 1098
 idiopathic hypercalciuria, 1096
 primary hyperparathyroidism, 1096
 randall plaques, 1098
 renal tubular acidosis, 1098
- Calyceal diverticulum, 149, 150f
 Calyces and renal pelvis, 12–13
Candida albicans infection, 1056–1057, 1057f
Candida glabrata infection, 1057, 1057f
 Carbohydrate disorders, 1238–1239, 1238f–1239f
 Cavitory tuberculosis, 1055–1056
 CD2-associated protein (CD2AP), 232t, 237
 C4d-negative antibody mediated rejection, 1381
 Cellular variant focal segmental glomerulosclerosis (FSGS), 219f, 220f, 221, 225, 227
 Cephalosporins, 1121–1122, 1172
 CFHR5 nephropathy, 350, 355f, 356
 CGN. *See* Crescentic glomerulonephritis (CGN)
 C3GN. *See* C3 glomerulonephritis (C3GN)
- Chapel Hill Consensus Conference Classification, 686, 686t, 715, 716t–717t, 720, 721
 Chemokines, 1346
 Cholesterol emboli, 876, 877f
 Chromophobe renal cell carcinoma, 1476–1477, 1476f–1477f
 Chronic pyelonephritis/reflux nephropathy, 93t, 1046
 Chronic tubulointerstitial nephritis, 103, 111–112, 112t, 1115–1118, 1118f, 1150–1151
 Churg, J., 257, 265, 268, 376, 686, 703, 720
 Ciliopathies, 119, 140, 141
 Clear cell renal cell carcinoma
 clinical findings and epidemiology, 1473
 pathology, 1473–1474, 1474f
 CNS. *See* Congenital nephrotic syndrome (CNS)
 Cobalamin C (cblC) deficiency, 1236–1237
 Cobalamin C (cblC) disorder, 743
 Cocaine nephropathy, 870
 Colistin, 1172
 Collagen type III glomerulopathy, 38–39
 clinical presentation, 549
 nature of defect, 549–551
 pathologic findings
 bundles, fibrillar collagen, 548, 550f
 glomerular tuft, 548, 548f
 immunofluorescence study, 548, 551f
 methenamine silver stain, 548, 549f
 Collagen type IV, 38–39
 Collagenofibrotic glomerulopathy
 clinical course, 1031
 clinical presentation, 1029
 differential diagnosis, 1030
 and epidemiology, 1029
 pathogenesis, 1030–1031
 pathologic findings
 electron microscopy, 1030
 light microscopy, 1029, 1030f
 treatment and prognosis, 1031
- Collapsing variant focal segmental glomerulosclerosis (collapsing glomerulopathy), 212, 214f, 218–220, 219f, 220f, 224f, 226, 608, 1261, 1417
- Collecting ducts
 carcinoma, 1477–1478
 human, 55f
 human cortical, 47f
 intercalated cells, 56–58
 nephron and associated, 37f
 principal cells, 52–56
 in rabbit, 55
 in rat, 56f
- Columbia classification of focal segmental glomerulosclerosis, 219f, 221, 222t, 225–227
 Complement factor B (CFB), 771
 Complement factor H (CFH), 486, 771
 Complement factor I (CFI), 771
 Conformeropathy, 677
 Congenital adrenal hyperplasia, 885
 Congenital anomalies of the kidney and urinary tract (CAKUT), 151, 151t
 Congenital mesoblastic nephroma
 clinical findings and epidemiology, 1463–1464
 pathology, 1464
 treatment and outcome, 1464
 Congenital nephrotic syndrome (CNS). *See also* Focal segmental glomerulosclerosis (FSGS)

- Finnish type, 195, 196f
 minimal change disease, 191
 nephrectomy, 195
 nephrin, 195
 transplants, 196
- Connective tissue growth factor (CTGF), 921
- Cortex and medulla
 cortical labyrinth and medullary rays, 13–14
 cortical microvascularization, 14–15
 in human kidney, 7f, 12f, 14f
- Cortical collecting duct
 human, 55f
 in rabbit, 55f
 in rat, 55f
- Cortical interstitium
 human, 58f
 of rat, 59f
- Cortical labyrinth, 13–14
- Cortical necrosis, 836
- Corticosteroids, lupus nephritis, 601–602
- Coxsackievirus infection, 1066
- CIq nephropathy (CIqN)
 clinical presentation, 245–246
 definition, 245
 differential diagnosis, 246
 etiology and pathogenesis, 246–247
 pathological findings, 246, 247f
 treatment and prognosis, 247
- Crescentic glomerulonephritis (CGN)
 crescent occurrence, 659
 diagnosis, 658
 etiology and pathogenesis, 672–675
 frequency and severity of, 659–660, 660t, 661f
 glomerular crescent, 658, 660f
 PSAGN, 400
 types of, 658–659, 659f, 660t
- Cryoglobulinemia
 with acidophilic hyaline thrombi, 329, 329f
 hepatitis C–associated cryoglobulinemic glomerulonephritis, 328–329
 multiple silver-negative hyaline thrombi, 329, 329f
 pathogenesis, 328
 subendothelial and intraluminal electron dense deposits, 329, 330f
- Cryoglobulinemic glomerulonephritis, 99, 328, 329f, 398–399
 acute poststreptococcal glomerulonephritis, 398–399
 electron microscopy, 1024f, 1025
 immunofluorescence microscopy, 1025
 light microscopy, 1024f, 1025
- Cushing syndrome, 885–886
- Cyclosporine, 1172–1173
- Cystic kidney diseases, 119–151
 acquired cystic kidney disease, 148–149, 150f
 ADIKD, 120
 classification, 119, 120t
 clinical presentation, 119–120
 hereditary syndromes
 tuberous sclerosis
 clinical presentation and genetics, 146
 differential diagnosis, 147
 incidence, 145–146
 pathogenesis, 147
 pathology, 146, 146f, 147f
- von Hippel-lindau disease
 clinical presentation and genetics, 144, 144f
 incidence, 144, 144f
 pathogenesis, 145
 pathology, 144–145, 144f, 145f
 prognosis and management, 145
- localized cystic disease, 147–148
- miscellaneous renal cyst
 hygroma renalis, 149, 151, 151f
 perinephric pseudocysts, 149
 pyelocalyceal diverticuli, 149, 150f
- molecular pathogenesis, 139
 autosomal dominant polycystic kidney disease, 140–141
 autosomal recessive polycystic kidney disease, 141
- cilia
 cyclic AMP and DDAVP antagonist therapy, 142–143
 hedgehog signaling, 143–144
 mTOR, 143
 Wnt/planar cell polarity, 143
 fluid flow and calcium, 142
 NPHP, 141
 primary cilia, 141–142, 142f
- multilocular cystic nephroma, 147, 148f
- polycystic kidney disease. *See* Polycystic kidney disease
- renal medullary cyst
 medullary sponge kidney, 120, 139, 140f
 NPHP-MCKD
 clinical presentation and genetics, 136–137
 incidence, 136
 pathology and pathogenesis, 137–139, 137f–139f, 140t
- simple cortical cysts, 148, 149f
- Cystic nephroma, 1485
- Cystinosis
 clinical presentation, 1244
 pathogenesis and treatment, 1246
 pathologic changes, 1244–1246, 1245f–1246f
- Cytomegaloviral infection, 1403t, 1410–1411
- Cytotoxic necrotizing factor 1 (CNF1), 1052
- D**
- DDD. *See* Dense deposit disease (DDD)
- De novo glomerular diseases
 anti-GBM glomerulonephritis, in Alport syndrome, 1415, 1417f
 membranous glomerulopathy, 1415, 1416f
 minimal change disease, 1418
 nodular diabetic glomerulosclerosis, 1418
 TMA, 1418
- Dense deposit disease (DDD)
 classification, 301, 301t, 303f
 clinical presentation, 341–343
 pathologic findings
 blood vessels, 345
 electron microscopy
 electron-dense deposits, 347, 347f
 extraglomerular deposits, 347, 349f
 glomerular intramembranous deposits, 346, 346f
 postinfectious glomerulonephritis, 347, 348f
- segmental distribution of deposits, 346, 347f
- glomeruli
 cellular crescent, 344, 344f
 dense osmiophilic transformation, 342f, 343
 endocapillary proliferative pattern, 343, 344f
 glomerular intramembranous deposits, 344–345, 345f
 mesangial hypercellularity, 343, 343f
 segmental hypercellularity, 344, 344f
- immunohistochemistry, 345–346, 345f
- interstitium, 345
 tubules, 345, 345f
- prognosis, 347, 349
 treatment, 349–350
- Dent disease
 pathogenesis, 1247
 pathologic changes, 1246–1247
- Denys-Drash syndrome, 197–198, 197f, 238
- Descriptive studies, 74–75, 78t–79t
- Developmental kidney defects
 CAKUT, 151, 151t
 cell and molecular biology, 153, 153f
 genes controlling nephrogenesis, 153
 bone morphogenetic protein, 155–156
 forkhead/winged helix transcription factor, 156
 GDNF/RET system, 154
 hepatocyte nuclear factor 1 β , 156
 Hox genes encode homeodomain transcription factors, 156–157
 Osr1 and EYA1, 156
 PAX genes, 154–155
 WNT genes, 155
 WTI genes, 154–155
- genetic renal and urinary tract malformation syndromes, 151, 152t
- pathology
 ectopia and malrotation, 162–163, 163f
 hereditary renal dysplasia, 158, 159f
 renal agenesis and renal aplasia, 158
 renal duplication, 163
 renal dysplasia, 159–161, 159f–161f
 renal fusion, 163, 163f
 renal hypoplasia, 161, 162f
 renal tubular dysgenesis, 163–164, 164f
 supernumerary kidney, 163
 renal malformation, 157
- Diabetes mellitus
 on preexisting renal disease, 841–842
 type 2 diabetes mellitus, 913–914
- Diabetic fibrillitis, 912, 912f
- Diabetic glomerulosclerosis, 99f, 102f, 416, 417f, 900, 904f, 931, 1299–1300, 1423
- Diabetic nephropathy, 1423
 after transplantation, 925–926
 arteriosclerosis and arteriolosclerosis, 936
 clinical course, 924–925
 clinical presentation, 900–901
 clinicopathologic correlation, 930–931, 930f
 differential diagnosis
 amyloidosis, 932
 idiopathic nodular glomerulosclerosis, 933, 934f
 immunoglobulin deposition, 932

- Diabetic nephropathy (*Continued*)
- immunotactoid and/or fibrillary glomerulonephritis, 932, 933f
 - membranoproliferative glomerulonephritis, 933
 - duration of disease, 898
 - electron microscopy
 - diabetic fibrillosis, 912, 912f
 - endothelial cell changes, 910–911
 - foot process detachment, 909–910
 - hyalinosis lesion, 911, 911f
 - Kimmelstiel-Wilson nodule, 911, 912f
 - endothelial dysfunction and structural abnormalities, 923
 - gender, 898
 - genetic factors, 898–899, 898t
 - glomerular lesions, 934
 - glomerulonephritis, 416–417, 417f, 418f
 - gross appearance, 901, 902f
 - hemodynamic changes and hyperfiltration, 914–916
 - immunofluorescence microscopy, 908–909, 908f
 - incidence and prevalence, 897–898
 - inflammation and tubulointerstitial injury, 922–923
 - light microscopy
 - blood vessels, 908, 908 f
 - glomeruli
 - diffuse lesion, 902, 902f–903f
 - miscellaneous glomerular changes, 906–907
 - nodular lesion, 903–906, 904f–905f
 - podocyte loss and hyalinosis lesion, 905–906, 906f
 - interstitium, 907–908, 908f
 - tubules, 907, 907f
 - metabolic control, 924
 - metabolic factors
 - advanced glycation end products, 917–919
 - altered glucose metabolism, 916–917, 916f
 - hyperglycemia, PKC activation by, 919–920
 - oxidative stress–mediated injury, 920
 - resultant renal injury, 917–919
 - transforming growth factor– β , 920–922
 - papillary necrosis
 - clinical aspects, 935
 - pathologic findings, 935, 935f
 - progression factors and renoprotection
 - blood pressure control, 926–928, 927f
 - glycemic control, 928–929, 928f
 - renin-angiotensin system, 929
 - racial and ethnic factors, 898
 - renal and urinary tract infections, 934
 - retinal aneurysms and microvascular changes, 936
 - smoking, 900
 - systemic hypertension, 923–924
 - in type 2 diabetes mellitus, 913–914
- Dialysis, 1267–1268
- Diffuse lupus nephritis
- Chicago group, 592
 - comparative studies, 592–593, 593t
 - diffuse segmental (IV-S) *vs.* diffuse global (IV-G) distribution, 588, 588f
 - electron microscopy, 591, 591f
 - endothelial necrosis, 591, 591f
 - fibrinogen staining, 590–591, 591f
 - hematuria, 591
 - IgG, intense/diffuse staining, 589, 589f
 - membranoproliferative pattern, 590, 590f, 592
 - mesangial and endocapillary proliferation, 589, 589f
 - proteinuria, 591
 - scattered subepithelial deposits, 590, 590f
 - segmental and global glomerulosclerosis, 591
 - severe segmental glomerulonephritis, 589
 - tubular and interstitial lesions, 591, 592f
 - wire-loop deposits, 590, 590f
- Diffuse mesangial sclerosis (DMS)
- case studies, 196, 197f
 - mutation agents, 195t, 196
 - Pierson syndrome, 198
 - Wt1
 - biological functions, 196–197
 - Denys-Drash syndrome, 197–198, 197f
 - Frasier syndrome, 198, 198f
- 2,8-Dihydroxyadenine (2,8-DHA) (Adenine phosphoribosyltransferase), 1252
- DIL. *See* Drug-induced lupus (DIL)
- Diphenylhydantoin, 1132
- Distal tubule, 50–51
- DMS. *See* Diffuse mesangial sclerosis (DMS)
- Donor kidney biopsies
- procurement/harvest biopsies, 1328–1330
 - zero-hour implantation biopsies, 1330–1331
- Drug-induced lupus (DIL)
- clinical presentation, 609–610
 - diagnosis, 609
 - pathogenesis, 610
 - serology, 609
- Drusen, 343, 347
- Dysproteinemias
- laboratory diagnosis, 955–956
 - multiple myeloma and manifestations
 - clinical history, 952
 - immunoglobulin components, 953–955
 - light and heavy chains, metabolism of, 955
- E**
- Eclampsia and preeclampsia
- clinical findings, 819–820
 - course and prognosis, 820–821
 - differential diagnosis, 820
 - etiology and pathogenesis, 832–835
 - focal segmental glomerulosclerosis lesions, 825, 827–832, 830f, 831t
 - HELLP syndrome, 832
 - hypertension, 819
 - pathologic changes, 821–825
- Ectopic adrenocorticotrophic hormone (ACTH) syndrome, 885
- Ecilizumab, 350, 775, 1420
- EGPA. *See* Eosinophilic granulomatosis with polyangiitis (EGPA)
- Ellis, A., 91, 302, 368, 463
- Embolic nonsuppurative focal nephritis, 419
- Embryonal hyperplasia of the Bowman's capsular epithelium (EHBCE), 1301
- End-stage renal disease (ESRD)
- acquired renal cystic disease
 - gross pathology, 1306–1307, 1306f
 - microscopic pathology, 1307–1308, 1307f
 - renal cell tumors, 1308–1309, 1308f
 - beta-2-microglobulin amyloidosis, 1286–1287, 1286f
- cardiovascular system
- atherosclerotic coronary artery disease, 1284
 - calcemic uremic arteriopathy, 1284–1285, 1285f–1286f
 - cardiomyopathies of, 1283–1284
 - valvular calcification, 1284, 1285f
- central nervous system, 1289
- chronic hepatitis and hepatic iron overload, 1289
- CKD-mineral bone disorder and osteodystrophy, 1289–1291, 1290f–1291f
- clinical features, 1283
- etiology and pathogenesis, 1311–1312, 1311f
- gastrointestinal tract and pancreas, 1287–1288
- gross pathology, 1297–1298, 1297f
- hematopoietic system, 1288–1289
- hypertension, 1291
- light microscopy
- blood vessels, 1302–1303, 1303f
 - glomeruli
 - diabetic glomerulosclerosis, 1299, 1300f
 - EHBCE, 1301
 - glomerulonephritis, 1300, 1300f
 - hypertension, 1299, 1299f
 - ischemic glomerular obsolescence, 1299, 1299f
 - ischemic nephropathy, 1299, 1300f
 - pyelonephritis, 1300–1301
 - interstitial nephritis and differential diagnosis, 1303–1305
 - juxtaglomerular apparatus, 1302
 - miscellaneous interstitial changes, 1305–1306, 1306f
 - tubular atrophy, 1305
 - unusual epithelial growth/endothelial metaplasia, 1301–1302, 1301f
- lung, 1286
- management and outcome, 1312–1313
- pericardium, 1285–1286, 1286f
- prevalence of, 121
- secondary parathyroid hyperplasia, 1289
- Eosinophilic granulomatosis with polyangiitis (EGPA)
- clinical presentation, 687
 - comparative studies, 686, 687t, 689, 6690f
 - definitions, 686
 - pathology, 699
- Eosinophils, 112
- Epithelial neoplasms
- acquired cystic disease–associated renal cell carcinoma, 1480, 1480f
 - chromophobe renal cell carcinoma, 1476–1477, 1476f–1477f
 - clear cell papillary renal cell carcinoma, 1479–1480
 - clear cell renal cell carcinoma
 - clinical findings and epidemiology, 1473
 - pathology, 1473–1474, 1474f
 - collecting duct carcinoma, 1477–1478
 - medullary carcinoma, 1478, 1478f
 - mucinous tubular and spindle cell carcinoma, 1478–1479, 1479f
 - neuroendocrine tumors, 1482
- oncocytoma
- clinical findings and epidemiology, 1469
 - pathology, 1469–1470, 1469f–1470f
 - treatment and outcome, 1470
- papillary adenoma, 1468–1469, 1469f

- papillary renal cell carcinoma, 1475–1476, 1475f
- renal cell carcinoma
classification, 1470
clinical findings and epidemiology
grading system, 1472–1473, 1472t
staging, 1471
treatment and outcome, 1473
unclassified, 1481–1482
- tubulocystic carcinoma, 1479, 1479f
- urothelial carcinoma, 1480–1481, 1481f
- Epithelium**
of rat kidney, 50f
renal tubular epithelium, 105–106, 107f
transitional, 12
- Epstein and Fechtner syndromes, 538–539
- Erythropoietin, 1294
- Essential hypertension**
clinical course, 871
clinical features
initial presentation, 852
malignant hypertension, 852–853
clinicopathologic correlation, 872–873
differential diagnosis, 870–871
environmental factors, 851–852
etiology and pathogenesis
glomerular lesions
clinical studies, 866–867, 866f
experimental studies, 865–866
interstitial disease, 870
pathophysiology, 863–865
small vessel changes
hyaline arteriosclerosis, 867
intimal arterial thickening, 867
vascular remodeling, 868–869
- genetic factor, 850–851, 850t
- gross pathology, 854, 854f
- laboratory findings, 853
- pathologic findings, 854–863, 854f–863f
electron microscopy, 861, 863, 861f–863f
gross pathology, 854
immunofluorescence findings, 861, 861f
light microscopy
blood vessels, 858–860, 858f–860f
glomeruli, 854–856, 854f–857f
interstitium, 858
malignant nephrosclerosis, 860–861
thrombotic microangiopathy, 860–861
tubules, 857, 857f
- prevalence, gender, and age, 849–850
- prognosis, 871–872
- racial factors, 852
- therapy, 872
- Extramedullary hematopoiesis, 1464
- Exudative glomerulonephritis, 374
- F**
- Fabry disease**
I-cell disease, 1229, 1231f
pathogenesis, 1234
pathologic changes, 1232–1234, 1233f–1234f
prevalence, 1229
treatment, 1234–1235
- Fahr, T., 91, 208, 302, 463, 658
- Familial benign hematuria (FBH)**
diagnosis, 541–542
genetics, 541
pathologic findings, 541, 541f–543f
- Familial IgA nephropathy**, 495–496
- Familial lecithin-cholesterol acyltransferase deficiency (FLD)**
pathogenesis, 1225
pathologic changes, 1224–1225, 1224f–1223f
- Familial Mediterranean fever (FMF)**, 507, 507t
- AA amyloidosis, etiology and pathogenesis of, 990
- clinical presentation and laboratory findings, 989
- gross and microscopic pathology, 989–990
- Fanconi-Bickel syndrome, 1249
- FBH. *See* Familial benign hematuria (FBH)
- Fibrillary glomerulonephritis**
clinical presentation and epidemiology, 1016–1017
differential diagnosis, 1020–1021
electron microscopy, 1019–1020, 1020f
epidemiology, 1016–1017
gross pathology, 1017
immunofluorescence microscopy, 1018–1019, 1019f, 1020f
light microscopy, 1017–1018, 1019f
pathogenesis, 1021
treatment and prognosis, 1021
- Fibrillosis**
diabetic fibrillosis, 912, 912f
clinical course and prognosis, 1029
clinical presentation and epidemiology, 1026, 1028
differential diagnosis, 1029
electron microscopy, 1028, 1028f
gross pathology, 1028
light microscopy, 1028, 1028f
pathogenesis, 1029
diabetic nephropathy, 912, 912f
- Fibrinoid necrosis**, 758, 759
- Fibromuscular dysplasia (FMD)**
clinical course and therapy, 879–880
pathogenesis, 879
pathologic findings
intimal fibroplasia, 878, 878f
medial dissection, 879
medial fibroplasia with aneurysms, 878, 878f, 879f
medial hyperplasia, 878, 878f
periarterial fibroplasia, 879
perimedial fibroplasia, 878–879, 879f
- Fibronectin glomerulopathy**
clinical presentation, 1026
differential diagnosis, 1026
epidemiology, 1026
pathogenesis, 1026
pathologic findings, 1026, 1027f
treatment and prognosis, 1026
- Fibrosis**, 114, 130–131, 132f
cystic fibrosis, 1093
interstitial fibrosis, 123, 124f
autosomal dominant polycystic kidney disease, 123, 124f
IFTA, 280–282
pathologic classification and diagnosis, 114
Pauca-immune crescentic glomerulonephritis, 698, 699
striped fibrosis, 115
in systemic sclerosis, 785–786
- Finnish congenital nephrotic syndrome**, 31, 93t, 233t
- Fluoroquinolones, 1122
- FMF. *See* Familial Mediterranean fever (FMF)
- Foam cells, 114
- Focal embolic nephritis, 419
- Focal lupus nephritis
class III lupus nephritis, 588
endocapillary proliferation, 586, 586f
glomerular proliferative lesions, 587, 587f
mesangial hypercellularity, 586–587, 587f
segmental subendothelial deposits, 588
wire-loop deposit, 587, 587f
- Focal segmental glomerulosclerosis (FSGS)**, 840
adaptive FSGS
clinical presentation, 241
differential diagnosis, 242
etiology and pathogenesis, 242
glomerular hypertension, 240
pathology
electron microscopy, 228f, 241–242
immunofluorescence microscopy, 241
light microscopy, 241, 241f
podocyte depletion, 242–243
treatment, 243
- clinical history
with lipoid nephrosis, 208, 209f
with minimal change disease, 209
- C1q nephropathy (C1qN)**
clinical presentation, 245–246
definition, 245
differential diagnosis, 246
etiology and pathogenesis, 246–247
pathological findings, 246, 246f
treatment and prognosis, 247
- diagnosis, 191
- discrete segmental scar, 207, 208f
- drug-associated
clinical presentation, 244
pathogenesis, 244
pathologic findings, 244
- etiologic classification, 208, 208t
- glomerular pathology, 198, 198t
- identification of, 192
- incidence of, 181
- lupus podocytopathy, 244–245, 245f
- membranous glomerulonephritis, 282
- PLCE1*, mutation, 195, 195t
- primary FSGS
cellular variant, 212f–214f, 225f
clinical course and prognostic factors, 228, 228f, 229f
clinical-pathologic correlation, 225–227, 222t
collapsing glomerulopathy, 218–220, 219f, 224f
differential diagnosis, 225
epidemiology and clinical presentation
biopsy, 209
incidence, 210
etiology and pathogenesis
cellular phenotypic alterations, 229–230
circulating glomerular permeability factors, 230–231
glomerular filtration barrier, 228–229
morphological variants
cellular lesion, 217
cellular variant, 218, 220f
collapsing glomerulopathy, 217
Columbia classification, 217–218, 218t, 219f, 222t, 223t

- Focal segmental glomerulosclerosis (FSGS)
(*Continued*)
- global glomerular capillary collapse, 218, 220f
 - glomerular tip lesion, 217
 - perihilar variant, 218, 221f
 - tip variant, 218, 220f
 - NOS variant, 221–225
 - pathology
 - acute tubular necrosis, 213, 215f
 - biopsy, 213
 - capillary lumina, 210, 211f
 - classic lesion, 210, 210f
 - endocapillary foam cells, 216, 217f
 - epithelial cell detachment, 216, 216f
 - glomerular capillaries, 212, 214f
 - glomerular tuft, 212, 213f
 - gross pathology, 210
 - hyalinosis lesions, 210, 211f
 - IgM, mesangial staining, 215, 215f
 - nonsclerotic glomeruli, 212, 215, 216f
 - sclerosis/hyalinosis, 215, 215f
 - segmental sclerosis lesion, 211, 212f–214f
 - single segmental lesion, 210–211, 211f
 - tubular atrophy and interstitial fibrosis, 212–213, 214f
 - perihilar variant, 214f, 221f, 221, 227f
 - recurrence, 232
 - tip variant, 221, 224f, 225f
 - treatment
 - cyclosporine A (CsA) therapy, 232
 - glucocorticoids, 231
 - secondary FSGS
 - alleles, 240
 - autosomal dominant FSGS, 237
 - autosomal recessive steroid-resistant nephrotic syndrome
 - CD2-associated protein, 237
 - myosin 1E, 236
 - phospholipase C epsilon, 236
 - podocin, 236
 - protein tyrosine phosphatase receptor type O, 237
 - clinical presentation, 235
 - coenzyme Q10 deficiency, 239–240
 - genetic diseases, 232, 233t–234t
 - mitochondrial tRNA^{Leu}(URR), 239
 - mitochondriopathy, 239
 - pathogenesis, 235–236
 - pathology, 235
 - syndromic FSGS
 - action myoclonus-renal failure syndrome, 238
 - Denys-Drash syndrome, 238
 - Frasier syndrome, 238
 - integrin β_4 , 239
 - Pierson syndrome, 238
 - Schimke immuno-osseous dysplasia, 239
 - virus-associated FSGS
 - clinical presentation and pathogenesis, 243
 - pathologic findings, 243–244
- Foot process effacement (FPE)
- foot processes replacement, 176, 176f
 - glomerular basement membrane, attachment, 176–177
 - podocyte
 - membrane domains, 177
 - motility, 176
 - multiphoton fluorescence imaging, 177
- Foot processes, 25, 25f
- Forkhead/winged helix transcription factor, 156
- FPE. *See* Foot process effacement (FPE)
- Frasier syndrome, 198, 198f, 238
- Free sialic acid storage disorders, 1235
- FSGS. *See* Focal segmental glomerulosclerosis (FSGS)
- Functional studies
 - in vitro, 78
 - in vivo, 78–79
- G**
- Gaucher disease, 1229, 1230t
- GBS. *See* Guillain-Barré syndrome (GBS)
- GCKD. *See* Glomerulocystic kidney disease (GCKD)
- Genetic metabolic diseases, 1423–1424
- Giant cell arteritis, 721
 - clinical course, 736
 - clinical presentation, 733
 - differential diagnosis, 735–736
 - etiology and pathogenesis, 735
 - pathologic findings
 - gross pathology, 733–734
 - immunofluorescence and electron microscopy, 734–735
 - light microscopy, 734, 734f–735f
 - prognosis and therapy, 736
- Glial cell–derived neurotrophic factor (GDNF), 154
- Glomerular basement membrane (GBM)
 - proteins
 - collagen IV, 38–39, 39t
 - entactin, 29, 39
 - fibronectin, 31, 41, 1026
 - laminin, 29, 38, 39
 - nidogen, 29, 38, 40
- Glomerular cells, 36f
- Glomerular diseases
 - collagenofibrotic glomerulopathy. *See* Collagenofibrotic glomerulopathy
 - cryoglobulinemic glomerulonephritis, 1025
 - diabetic fibrillosis
 - clinical course and prognosis, 1029
 - clinical presentation and epidemiology, 1026, 1028, 1028
 - differential diagnosis, 1029
 - electron microscopy, 1028, 1028f
 - gross pathology, 1028
 - light microscopy, 1028, 1028f
 - pathogenesis, 1029
 - electron microscopic evaluation, 98f, 99–101, 101f–103f
 - fibrillary glomerulonephritis
 - clinical presentation, 1016–1017
 - differential diagnosis, 1020–1021
 - electron microscopy, 1019–1020, 1020f
 - epidemiology, 1016–1017
 - gross pathology, 1017
 - immunofluorescence microscopy, 1018–1019, 1019f, 1020f
 - light microscopy, 1017–1018, 1019f
 - pathogenesis, 1021
 - treatment and prognosis, 1021
 - fibronectin glomerulopathy
 - clinical presentation, 1026
 - differential diagnosis, 1026
 - epidemiology, 1026
 - pathogenesis, 1026
 - treatment and prognosis, 1026
- clinical presentation, 1026
- differential diagnosis, 1026
- epidemiology, 1026
- pathogenesis, 1026
- pathologic findings, 1026, 1027f
- treatment and prognosis, 1026
- historical background, 1015–1016
- immunohistologic evaluation, 98–99, 101f
- immunotactoid glomerulopathy
 - clinical presentation, 1021–1022
 - differential diagnosis, 1023–1024, 1024f
 - electron microscopy, 1023
 - epidemiology, 1021–1022
 - gross findings, 1022
 - immunofluorescence microscopy, 1023
 - light microscopy, 1022–1023, 1022f
 - pathogenesis, 1024–1025
 - treatment and prognosis, 1025
- kidney biopsy specimens, diagnoses of
 - native, 96t
- light microscopic evaluation, 97–98, 98f
- systemic lupus erythematosus, 1031–1032
- thrombotic microangiopathies, 753
- ultrastructural findings
 - cellular debris, 1034, 1034f
 - fibrin tactoids, 1034, 1034f
 - glomerular sclerosis, 1033–1034
 - intracellular fibrils, 1034
 - mesangial matrix, 1033, 1033f
 - ultrastructural artifacts, 1034–1035, 1035f
- Glomerular filtration
 - glomerular capillary wall
 - anatomy, 173–174
 - charge-selective barrier, 175
 - size-selective barrier, 174
 - hemodynamic factors, 175
 - molecule properties, 174
 - proteinuria
 - aminonucleoside nephrosis, 176
 - and foot process effacement, 176–177
 - tubules and interstitium, 177
- Glomerular hypertrophy, 241, 241f
- Glomerular lesions, 934
- Glomerular matrix
 - Bowman capsule, 41–42
 - glomerular capillary loop basement membrane
 - collagen type IV, 38–39
 - proteoglycans, 39–41
 - noncollagenous glycoproteins, 39–41
 - mesangium, 41
- Glomerular tuft, 22, 35f
- Glomerular vascular supply, 3f
- Glomerulocystic kidney disease (GCKD)
 - associated diseases, 131–133
 - histological findings, 131, 133t
 - pathogenesis, 135–136
 - pathology and differential diagnosis
 - glomerular cysts, 133, 134, 134f, 135f
 - hyperuricemia, 133, 135f
 - renal artery stenosis, 134, 135f
 - turner syndrome, 134, 135f
 - wedge biopsy, 133, 133f
- Glomerulonephritis
 - acute infective endocarditis
 - causative organisms, 422
 - clinical presentation, 422–423

- pathologic findings
 electron microscopy, 423–424, 424f
 etiology and pathogenesis, 424
 immunofluorescence microscopy, 423
 light microscopy, 423, 423f
 primary/secondary acute form, 422
- anti-GBM glomerulonephritis. *See*
 Anti-glomerular basement membrane
 (Anti-GBM) glomerulonephritis
- Bartonella henselae* infection, 416, 416f
- deep-seated visceral abscesses
 clinical presentation, 417–418
 pathologic findings, 418
 prognosis and outcome, 418
- diabetic nephropathy, 416–417, 417f, 418f
- epidemiology, 405
- infective endocarditis
 pathologic findings, 419
 arteries, 421
 electron microscopy, 421
 etiology and pathogenesis, 421–422
 glomeruli, 420, 420f
 immunofluorescence microscopy, 421
 interstitium, 420
 light microscopy, 420
 treatment, 422
 tubules, 420
 subacute bacterial endocarditis, 418–419
- Klebsiella* infection, 415–416
- Meningococcal infection, 415
- microbial infection, 404, 405t
- Pneumococcal infection, 415
- PSAGN. *See* Poststreptococcal acute
 glomerulonephritis (PSAGN)
- Salmonella typhi* infection, 416
- Staphylococcal infection
 clinical course and outcome, 415
 differential diagnosis, 414–415
 etiology and pathogenesis, 412, 414
- IgA-dominant staphylococcal infection—
 associated glomerulonephritis
 clinical presentation, 405–406
 prevalence, 406–407, 407t, 408t
- pathologic findings
 crescents/necrotizing lesion, capillary
 loops, 409, 411f
 diabetic glomerulosclerosis, 409–410, 412f
 electron microscopy, 409f, 410f, 412,
 413f, 414f
 fibrocellular crescent, 409, 411f
 glomeruli and diffuse endocapillary
 hypercellularity, 409, 409f, 410f
 hyalin thrombi, 409, 411f
 immunofluorescence microscopy,
 409f–411f, 410–412, 413f
 mesangial expansion and mesangial
 hypercellularity, 410, 413f
- ventriculoatrial shunt infection
 causative organisms, 424
 clinical course and outcome, 426
 clinical presentation, 425
 etiology and pathogenesis, 425–426
 pathologic findings, 425, 425f
 shunt nephritis, 425
 virus infection, 416
- Glomerulopathy
 in children, 450
- HIV infection, 449–450, 450t
 pathogenesis, 450
 pathology, 450
 thrombotic microangiopathies, 450–451
- Glomerulus
 cellular components of
 endothelial cell, 33
 mesangial cell, 33, 37
 parietal epithelial cell, 32–33
 podocyte
 and filtration barrier, 29
 molecular domains and filtration
 function, 29–31
 ultrastructure, 25, 27–29
 human glomerulus type IV collagen, 38f
 JGA, of rat kidney, 21f
 normal human, 23f
 with vascular pole, 22f
- Glycogen storage disease
 pathogenesis and treatment, 1239
 pathologic changes, 1238, 1238f–1239f
- Gold therapy
 MGN, 284–285
 proteinuria, 631
- Goodpasture syndrome. *See* Anti-glomerular
 basement membrane glomerulonephritis
- Granulomas, 112
- Granulomatous tubulointerstitial nephritis
 (GIN), 112
- Graves disease, 289
- Growth hormone–insulin–like growth factor axis
 (GH/IGF), 922
- Guillain-Barré syndrome (GBS), 290
- H**
- HAART. *See* Highly active antiretroviral therapy
 (HAART)
- Hantavirus infection, 1064–1065, 1065f
- Hashimoto thyroiditis, 289
- Heavy metal exposure
 cadmium nephropathy, 1147–1148
 lead nephropathy, 1146–1147
 mercury nephropathy, 1148–1149
 miscellaneous heavy metal nephropathy, 1149
- Hematopoietic cell transplantation (HCT),
 1268
- Hematopoietic stem cell transplantation (HSCT)
 animal models, 795–796
 clinical presentation, 794
 etiology and pathogenesis, 795
 pathologic findings, 789f, 794–795, 794f
 treatment, 796
- Hematopoietic tumors, 1487, 1487f
- Hematuria
 clinical presentation, 1259
 treatment of, 1266
- Hemoglobin cast nephropathy, 93t
- Hemolysin toxins, 1052
- Hemolysis, elevated liver enzymes, and low
 platelet count (HELLP) syndrome, 832
- Hemolytic-uremic syndrome (HUS)
 antiphospholipid antibodies, 774–775
 atypical HUS
 cobalamin C (cblC) disorder, 743
 epidemiology, 745
 familial forms, 743, 748
 recurrences, 748
- S. pneumoniae* infection, 743
 triggering events, 748
- classic HUS
 clinical presentation, 745–746
 epidemiology, 745
 incidence, 742
 Shiga toxins, 767–769
- coagulation disturbances, 773
- endothelial damage, 767
- HIV infection, 450–451
- pathologic findings
 arteriolar and arterial changes, 763–764
 clinical findings and prognosis, 766
 differential diagnosis, 761, 763
 electron microscopy, 761, 761f–762f
 gross appearance, 754, 754t
 immunofluorescence microscopy, 760–761,
 761f
 light microscopy
 arteries and arterioles, 758–760,
 758f–760f
 glomerular morphologic features,
 754–758, 754f–758f
 interstitium, 760
 tubules, 760
 microscopic features, 754, 754t
 outcome and prognostic features, 764–766
- platelet activation and aggregation, 773
- secondary HuS, 744
- Shigella dysenteriae* infection, 747
- Streptococcus pneumoniae* infection, 772
- systemic infections, 773
- systemic lupus erythematosus, 574–575
 transmission, 747
- verotoxin-producing *E. coli* infection, 746–747
- Hemosiderin, 105–106, 107f
- Henoch-Schönlein purpura (HSP), 1421. *See also*
 IgA nephropathy
 anaphylactoid purpura, 499
 clinical presentation
 American College of Rheumatology criteria,
 500
 in children, 499–500, 499t
 clinical outcomes, 501–502
 IgA-ANCA, 501
 macroscopic hematuria, 500–501, 500t
 serum IgA level, 501
 clinicopathologic correlation, 508, 508t
 differential diagnosis, 505–506
 pathogenesis
 ACE gene polymorphism, 507
 complement deficiencies, 506–507
 familial Mediterranean fever, 507, 507t
 HLA antigens, 507, 507t
 IgA, glomerular deposits, 506
 pathologic findings
 electron microscopic findings, 504
 extrarenal pathology, 504–505, 504f, 505f
 gross pathology, 502
 immunohistologic findings, 503–504
 light microscopy, 502–503, 502t, 503t
vs. primary IgA nephropathy, 510–511, 510t,
 511t
 prognosis of, 507–508
 recurrence of, 509–510
 secondary IgA vasculitis, 510
 treatment

- Henoch-Schönlein purpura (HSP) (*Continued*)
 in adults, 509
 in children, 509
 prevention, 508–509
- Hepatitis B virus (HBV), 287–288
- Hepatitis C virus (HCV)
 infectious etiologies of MGN, 288
 membranoproliferative glomerulonephritis (MPGN)
 hepatitis C–associated cryoglobulinemic glomerulonephritis, 328–329
 pathogenesis, 328
 prevalence of, 330
 treatment, 329
- Hepatobiliary disease
 clinical presentation and outcome, 497–498
 pathogenesis, 498–499
 pathology, 497, 497f, 498f
- Heptinstall, R.H., 92, 419, 720, 1046
- Hepatocyte nuclear factor 1 β , 156
- Herbal medications, 1175, 1187, 1200
- Hereditary autoimmune diseases, 988–989
- Hereditary diseases, 1150–1151, 1150f
- Hereditary osteoonychodysplasia (HOOD), 543–544
- Hereditary renal adysplasia, 158, 159f
- Hereditary syndromes
 tuberous sclerosis
 clinical presentation and genetics, 146
 differential diagnosis, 147
 incidence, 145–146
 pathogenesis, 147
 pathology, 146, 146f, 147f
 von Hippel-Lindau disease
 clinical presentation and genetics, 144, 144f
 incidence, 144, 144f
 pathogenesis, 145
 pathology, 144–145, 144f, 145f
 prognosis and management, 145
- Heritable tubular defects, 1250, 1251t
- Herpes, 559, 1408, 1427
- Highly active antiretroviral therapy (HAART)
 chronic tubulointerstitial lesions, 453
 HIVAN, 446–447
 renal tubular and interstitial abnormalities, 451
 transplantation, 456
- Hilum, 2
- HIV-associated nephropathy (HIVAN)
 clinical history, 447
 clinical presentation, 438–439
 etiology and pathogenesis, 447–448
 pathology
 electron microscopy
 confronting cylindrical cisternae, 444, 444f
 glomerular podocytes, 442, 443f
 granular transformation, 445, 445f
 granulofibrillar transformation, 445–446, 446f
 nuclear bodies, 444, 435f
 podocyte detachment, 442, 443f
 tubuloreticular structure, 444, 444f, 446–447
 gross pathology, 439
 immunofluorescence and immunohistochemistry, 440, 442, 442f
 light microscopy
 acute tubular cell injury, 440, 442f
 collapse/sclerosis and dilated Bowman spaces, 440, 441f
 dwarf adjacent glomeruli, 440, 441f
 early stage, 439–440, 439f
 solidification of tufts, 440, 440f
 tubular changes, 440, 4441f
- HIVAN. *See* HIV-associated nephropathy (HIVAN)
- HOOD. *See* Hereditary osteoonychodysplasia (HOOD)
- HSP. *See* Henoch-Schönlein purpura (HSP)
- Human collecting ducts, 55f
- Human cortical collecting ducts, 56f
- Human cortical interstitium, 58f
- Human cortical labyrinth, 47f, 48f
- Human glomerulus
 LM-521 stain, 38
 normal, 23f
 with vascular pole, 22f
- Human immunodeficiency virus (HIV)
 HIVAN. *See* HIV-associated nephropathy (HIVAN)
 thrombotic microangiopathies, 749–750
- Human interlobular arteries, 11f
- Human intralobular arteries, 44f
- Human kidneys, 25f
 adult and newborn, 5f
 with aorta, 10f
 hemisected, 5f
 normal, 9f
 outer medulla, 17f
 papillary collecting duct cell of, 56f
 two normal adult, 6f
 vena cava, 10f
- Human leukocyte antigen (HLA)
 haploidentical grafts, 1324–1325
 identical graft, 1324
- Human outer medulla, 52f, 60f
- Human renal cortical labyrinth, 13f
- Human renal pelvis, 7f
- Human renal pyramid, 7
- Hyalinosis lesion, 911, 911f
- Hydronephrosis and obstructive nephropathy
 differential diagnosis
 clinical management and prognosis, 1087–1088
 fibroepithelial polyps, 1084f
 pathogenesis, 1085–1087, 1086f–1087f
 therapy, 1088
 terminology, 1082
 ureteropelvic junction
 gross pathology and light microscopy, 1083–1084, 1083f–1084f
 incidence and clinical presentation, 1082
- Hydroxyurea, 1267
- Hyperacute rejection
 clinical course, 1358–1359
 clinical presentation, 1356
 clinicopathologic correlations, 1358–1359
 etiology and pathogenesis
 antigens, 1357–1358
 differential diagnosis, 1358
 effector mechanisms, 1358
 pathologic changes
 electron microscopy, 1357, 1357f
 gross pathology, 1356, 1356f
 immunofluorescence microscopy and immunohistochemistry, 1356–1357, 1357f
 light microscopy, 1356, 1357f
 prognosis, and therapy, 1358–1359
- Hyperaldosteronism, 884–885, 884t, 885t
- Hypercalcemia
 adrenal disorders, 1093
 calcium oxalate (CaOx) nephropathy, 1093
 calcium phosphate crystals and bowel-cleansing agents, 1092–1093, 1093f
 calcium-sensing receptor (CaR) disorder, 1090–1091
 causes of, 1088
 clinical presentation, 1088
 cystic fibrosis, 1093
 diagnosis, 1089
 granulomatous diseases, 1091
 of malignancy, 1089–1090
 milk-alkali syndrome, 1091
 neonatal/infantile hypercalcemia, 1090
 parathyroid hormone, physiology of, 1089
 pathology, 1089
 primary hyperparathyroidism, 1088–1089
 renal calcification, 1091–1092, 1092f
 renal function, 1089
 renal tubular acidosis, 1093
 treatment and outcome, 1089
 tubular handling defects, 1091
 vitamin A/D excess, 1091
- Hypercholesterolemia, 179, 182
- Hyperlipidemia, 177–179
- Hypersensitivity angitis, 720
- Hypertension
 definition, 849
 essential hypertension
 clinical course, 871
 clinical features, 852–853
 clinicopathologic correlation, 872–873
 differential diagnosis, 870–871
 environmental factors, 851–852
 etiology and pathogenesis, 863–870
 genetic factor, 850–851, 850t
 laboratory findings, 853
 pathologic findings, 854–861, 863, 864f–863f
 prevalence, gender and age, 849–850
 prognosis, 871–872
 racial factors, 852
 therapy, 872
 secondary hypertension
 chronic renal parenchymal disease, 822–883
 prevalence of, 873–874
 renal artery stenosis, 874–882
 tumors and conditions, 883–888
- Hypoalbuminemia, 177
- Hypocomplementemia, 395, 397, 424
- Hypocomplementemic persistent glomerulonephritis, 323
- Hypocomplementemic tubulointerstitial nephritis, 1142
- Hypokalemic nephropathy, 105
- Hypoplasia
 hypoplastic kidney, 161, 162f
 oligomeganephronia, 162
 simple hypoplasia, 162, 162f
- Hyposthenuria, 1258
- Hypotension, 1259

- I**
- I-cell disease
 glomerulus in, 1229, 1231f
 vacuolated podocytes, 1229, 1231f
- Idiopathic crescentic glomerulonephritis, 685
- Idiopathic nodular glomerulosclerosis, 933, 934f
- Idiopathic tubulointerstitial nephritis, 1154
- IFTA. *See* Interstitial fibrosis and tubular atrophy (IFTA)
- IgA1, 483, 483f, 484–485
- IgA-dominant postinfectious glomerulonephritis, 479, 481f, 482f
- IgA glycosylation, 483
- IgA nephropathy, 448, 841. *See also* IgA vasculitis nephritis
 clinical history, 449
 clinical presentation, 449
 etiology and pathogenesis, 449
 familial IgA nephropathy, 495–496
 medical history, 463–464
 pathology, 449
 primary IgA nephropathy
 clinical presentation
 acute renal failure, 467, 467f
 age dependent, 466, 466t
 asymptomatic urinary abnormalities, 466
 c3 complements, 468
 clinical parameters, 468, 469t
 macroscopic hematuria, 466
 proteinuria, 466–467
 review of literature, 466, 467t
 differential diagnosis
 ANCA-associated crescentic glomerulonephritis, 480, 482t
 autopsy study, 479
 dominant/codominant mesangial IgA deposits, 478, 481t
 fibrinoid necrosis and crescent formation, 480, 482f
 IgA-dominant postinfectious glomerulonephritis, 479, 481f, 482f
 membranous nephropathy, 479–480, 482f
 segmental fibrinoid necrosis, 480, 483f
 epidemiology
 diagnosis frequency, 463–464, 464t
 incidence, 465
 U.S. renal biopsy series, 465–466, 465t
 pathogenesis, 480
 circulating and mesangial IgA, 481–483
 complement, 485
 glomerular deposits, 483–484
 human IgA, structure and production, 481, 483f
 mesangial cell proliferation, 485
 mesangial deposits, 484–485
 renin-angiotensin system, 486
 pathologic findings
 diffuse mesangial and endocapillary hypercellularity, 474f
 extraglomerular deposits, 475–476
 focal endocapillary proliferation, 473f
 focal segmental glomerulosclerosis, 472, 472f
 glomerular basement membrane structural abnormalities, 478, 481f
 glomerular fibrinogen deposition, 475, 475f
 glomerular immune complex deposits, 477, 477t
 glomerular immunofluorescence/
 immunohistochemical findings, 473, 475t
 gross pathology, 470
 histopathologic classification, 470–472, 471f, 472f
 IgA, granular staining, 475, 476f
 light microscopy, 470–472, 471f, 472f
 membranoproliferative glomerulonephritis, 473f
 mesangial IgA deposits, 472
 mesangial immune deposits, 477, 477f
 mesangial proliferation, 472, 472f
 residual mesangial hypercellularity, 474f
 severe chronic and active IgA nephropathy, 474f
 subendothelial deposits, 477–478, 479f, 480f
 prognosis, 486
 children *vs.* adults, 492
 original Oxford study cohort, 487, 489t
 Oxford classification, 487, 489–492, 490t
 pregnancy, 492
 renal transplantation, 494–495, 495t
 treatment, 492
 angiotensin-converting enzyme inhibitor therapy, 493–494
 angiotensin receptor antagonists, 494
 corticosteroids, 493
 fish oil, 494
 mycophenolate mofetil, 493
 tonsillectomy, 494
 secondary IgA nephropathy, 496, 496t
 hepatobiliary disease
 clinical presentation and outcome, 497–498
 pathogenesis, 498–499
 pathology, 497, 497f, 498f
 HIV infection, 499
- IgA vasculitis (Henoch-Schönlein Purpura) nephritis
 anaphylactoid purpura, 499
 clinical presentation
 American College of Rheumatology criteria, 500
 in children, 499–500, 499t
 clinical outcomes, 501–502
 IgA-ANCA, 501
 macroscopic hematuria, 500–501, 500t
 serum IgA level, 501
 clinicopathologic correlation, 508, 508t
 differential diagnosis, 505–506
 pathogenesis
 ACE gene polymorphism, 507
 complement deficiencies, 506–507
 familial Mediterranean fever, 507, 507t
 glomerular deposits, 506
 HLA antigens, 507, 507t
 pathologic findings
 electron microscopic findings, 504
 extrarenal pathology, 504–505, 504f, 505f
 gross pathology, 502
 immunohistologic findings, 503–504
 light microscopy, 502–503, 502t, 503t
vs. primary IgA nephropathy, 510–511, 510t, 511t
 prognosis of, 507–508
 recurrence of, 509–510
 secondary IgA vasculitis, 510
 treatment
 in adults, 509
 in children, 509
 prevention, 508–509
- IgA nephropathy (IgAN), 1421
- IgG4-related disease, 290, 1141
- IgG4-related tubulointerstitial nephritis
 clinical presentation, 1137
 diagnostic criteria, 1139–1140, 1140t
 differential diagnosis, 1140
 pathogenesis, 1140–1141
 pathologic findings
 electron microscopy, 1139, 1139f
 immunofluorescence, 1139, 1139f
 light microscopy, 1138–1139, 1138f
 treatment and outcome, 1141
- IgM nephropathy, 190
- Immunotactoid glomerulopathy
 clinical presentation, 1021–1022
 differential diagnosis, 1023–1024, 1024f
 electron microscopy, 1023
 epidemiology, 1021–1022
 gross findings, 1022
 immunofluorescence microscopy, 1023
 light microscopy, 1022–1023, 1022f
 pathogenesis, 1024–1025
 treatment and prognosis, 1025
- Infectious agents, 114, 415–416
- Infective endocarditis
 pathologic findings, 419
 arteries, 421
 electron microscopy, 421
 etiology and pathogenesis, 421–422
 glomeruli, 420, 420f
 immunofluorescence microscopy, 421
 interstitium, 420
 light microscopy, 420
 treatment, 422
 tubules, 420
 subacute bacterial endocarditis, 418–419
- Infliximab, lupus nephritis, 605
- Inherited Fanconi syndrome
 cystinosis
 clinical presentation, 1244
 pathogenesis and treatment, 1246
 pathologic changes, 1244–1246, 1245f–1246f
- Dent disease
 pathogenesis, 1247
 pathologic changes, 1246–1247
- Fanconi-Bickel syndrome, 1249
- idiopathic Fanconi syndrome, 1243
- Lowe syndrome
 pathogenesis, 1249
 pathologic changes, 1248
- mitochondrial disorders
 diagnosis, 1248
 pathologic changes, 1247–1248, 1248f
- Inner medulla, 16, 60f
- Inner stripe, 15–16
- Integrin alpha3 gene (ITGA3), 554
- Integrin β_4 , 233t, 239

- Intercalated cells, 56–58, 56f
 Interlobular artery, 11f
 Interstitial cells
 and cytoarchitecture, 58–61
 lipid-laden, 60f
 Interstitial disease
 acute and chronic tubulointerstitial nephritis, 111, 112t
 edema, 112, 113f
 fibrosis, 114
 granulomas, 112
 immune aggregates, 114
 infectious agents, 114
 interstitial expansion, 114
 leukocytic infiltrates, 112, 113f
 primary and secondary, 111
 renal interstitium, 112
 Interstitial fibrosis and tubular atrophy (IFTA), 280–282
 Interstitium
 human cortical, 58f
 interstitial cells and cytoarchitecture, 58–61
 Intimal fibroplasia, 878, 878f
 Intra-abdominal hypertension, 1205
 Intravenous immunoglobulin (IVIG), 605, 1173
 Inverted formin-2, 237
 Ischemia
 apoptosis and necrosis, 1190–1191
 heat shock protein and chaperones, 1193–1194
 inflammatory response, 1191–1192
 injury and cell death, 1188–1190
 regeneration of tubular injury, 1193
 renal vasculature, 1192–1193
 stem cells and growth factors, 1194–1195
 Ischemic acute tubular injury, 1177–1181, 1177f–1181f
 Ischemic injury
 clinical presentation, 1391
 delayed graft function, 1389–1390
 differential diagnosis, 1390
 molecular correlation, 1390–1391
 pathogenesis, 1390
 pathologic findings, 1390
 prognosis and therapy, 1391
 Isografts, 1324
- J**
 JC virus, 1408
 Juxtaglomerular apparatus (JGA)
 blood vessels and, 42–43
 of rat kidneys, 21f
 Juxtaglomerular cell tumors, 886–887, 887f, 1486, 1486f
- K**
 Kaposi sarcoma, 1427
 Kawasaki disease
 clinical course, prognosis, and therapy, 730
 clinical presentation, 727
 differential diagnosis, 729–730
 etiology and pathogenesis, 728–729
 pathologic findings
 gross pathology, 727
 light microscopy, 727–728, 727f–728f
 Kidney development
 adhesion molecules, 78
- anatomy of human
 human collecting duct system and nephrons, formation of, 72–74, 73f–74f
 human renal pelvis and calyces, formation of, 70–72, 71f–72f
 lower renal tract, 74
 mesonephros, 69–70, 70f
 metanephros, 70, 71f
 pronephros, 69
 angiopoietins (ANGPTs), 77–78, 84
 blood vessels, 83–85
 bone morphogenetic proteins (BMP), 78, 155–156
 cellular events
 cell death, 68
 cell proliferation, 68
 differentiation, 69
 migration, 69
 morphogenesis, 69
 descriptive studies, 74–75, 76t–77t
 diverse miscellaneous molecules, 78
 fibroblast growth factors (FGFs), 78–79
 FOXD1, 84
 functional studies in vitro, 78
 functional studies in vivo, 78–79
 growth factors, 77–78
 hepatocyte growth factor (HGF), 78, 82, 83f
 human malformations and mouse mutants, 79, 79t
 innervation of, 84–85
 insulin-like growth factors (IGFs), 78
 leukemia inhibitory factor (LIF), 78, 81
 LIM1, 80
 metanephric mesenchyme, 79–82
 neurotrophins, 80
 NOTCH1, 78
 PAX2, 77f, 81, 81t
 platelet-derived growth factors (PDGFs), 78
 renal capsule, 84–85
 RET, 78, 82, 154
 sonic hedgehog family (SHH), 78, 83
 transcription factors, 75, 77, 77f
 transforming growth factor- α (TGF α), 78, 81
 transforming growth factor- β (TGF β), 78, 82
 tumor necrosis factor- α (TNF α), 78, 89
 UPII, 83
 UPIII, 79
 ureteric bud-collecting duct development, 82–83
 vascular endothelial growth factor (VEGF), 78, 84
 wingless-type MMTV integration site family members (WNT), 76t, 78, 80
 Kimmelstiel-Wilson nodule, 911, 912f
 Klotho deficiency, 1294
- L**
 Large-vessel vasculitis (LVV), 716t, 720–721
 Late graft biopsies
 causes, 1383t
 differential diagnosis, 1383
 molecular markers, 1384
 morphologic scoring systems, chronic lesions, 1384–1385
 LCAT deficiency
 pathogenesis, 1225
 pathologic changes, 1224–1225, 1224f–1225f
- Lead nephropathy
 clinical presentation, 1146–1147
 etiology and pathogenesis, 1147
 pathologic findings, 1147
 Leflunomide, lupus nephritis, 605
 Leiomyosarcoma, 1450f, 1484–1475
 Leukocytic infiltrates, 112, 113f
 Light chain cast nephropathy
 clinical course, 959
 clinical history, 956–957
 clinical presentation/laboratory findings, 957
 differential diagnosis, 959
 electron microscopy, 958
 etiology/pathogenesis, 958–959
 gross pathology, 957
 immunofluorescence, 958
 light microscopy, 957, 957f
 prognosis, 959
 treatment, 959
 Light chain deposition disease (LCDD)
 clinical presentation/laboratory findings, 965
 electron microscopy, 967, 967f
 etiology/pathogenesis, 968, 970
 gross pathology, 965
 immunofluorescence, 966, 966f
 light microscopy, 966, 966f, 967f
 prognosis, 970
 transplantation, 971
 treatment, 970–971
 Light chain tubulopathy (light chain Fanconi syndrome), 93t
 Lipid disorders
 familial LCAT deficiency
 pathogenesis, 1225
 pathologic changes, 1224–1225, 1224f–1225f
 lipoprotein glomerulopathy
 pathogenesis, 1226–1229
 pathologic changes, 1226
 therapy, 1229
 type III hyperlipoproteinemia, 1228
 Lipid-laden interstitial cells, 60f
 Lipoid nephrosis, 182, 184, 209f
 Lipoprotein glomerulopathy
 pathogenesis, 1226–1229
 pathologic changes, 1226
 therapy, 1229
 Lithium
 clinical presentation, 1132–1133
 pathogenesis, 1133
 pathologic findings, 1133
 Living unrelated grafts, 1325
 Lobar fusion, 3
 Lobular glomerulonephritis. *See* Membranoproliferative glomerulonephritis (MPGN)
 Localized cystic disease, 147–148
 Loop of Henle, 20–21, 53f
 Lowe oculocerebrorenal syndrome, 1248
 Lowe syndrome
 pathogenesis, 1249
 pathologic changes, 1248
 Lower renal tract, 74
 Lupus anticoagulant syndrome. *See* Antiphospholipid (APL) syndrome
 Lupus glomerulonephritis, 244–245, 245f, 608–609

- Lupus nephritis, 840–841. *See also* Systemic lupus erythematosus (SLE)
- Lupus podocytopathy, 244–245, 245f, 608–609
- Lupus vasculitis, 573
- Lupus vasculopathy, 572t, 573, 573f
- Lymphocele, 1413–1414
- Lymphoreticular tumors, 1487, 1487f
- Lymphoreticular and hematopoietic tumors, 1487, 1487f
- Lysosomal storage diseases
- Fabry disease. *See* Fabry disease
 - nephrosialidosis and variants
 - free sialic acid storage disorders, 1235
 - galactosialidosis, 1235
 - pathologic changes, 1235–1236, 1235f
 - sialidosis, 1235
- M**
- M-type phospholipase A₂ receptor (M-type PLA₂R), 279–280, 279f
- Malakoplakia
 - clinical presentation, 1049–1050
 - differential diagnosis, 1050–1051
 - gross pathology and light microscopy, 1050
 - pathogenesis, 1050
- Male genitourinary tract, 2f
- Malignant hypertension, 788, 852–853
- Mammalian target of rapamycin (mTOR), 143, 1327t
- McCluskey, R.T., 91, 583, 1134
- MCN. *See* Multilocular cystic nephroma (MCN)
- MCTD. *See* Mixed connective tissue disease (MCTD)
- Meckel-Gruber syndrome, 139, 139f
- Medial fibroplasia, with aneurysms, 878, 878f, 879f
- Medial hyperplasia, 878, 878f
- Medulla
 - in human kidney, arrangement of cortex and, 7f
 - human outer, 52f, 60f
 - inner medulla (papilla), 16
 - medullary microvascularization, 17–18
 - of mouse, arterial vessels of, 20f
 - outer medulla
 - inner stripe, 15–16
 - outer stripe, 15
- Medullary carcinoma, 1478, 1453f
- Medullary cystic kidney disease (MCKD)
 - ADIKD, 120
 - clinical presentation and genetics, 136–137
 - incidence, 136
 - pathology and pathogenesis, 137–139, 137f–139f, 140t
- Medullary microvascularization, 17–18
- Medullary rays, 12f, 13–14, 13f
- Megalyn, 174, 177, 274, 1196
- Medullary sponge kidney (MSK), 120, 139, 140f
- Megalocytic tubulointerstitial nephritis/ Malakoplakia, 1050–1051
- Membrane cofactor protein (MCP), 771
- Membrane transport disorders
 - acquired Fanconi syndrome, 1249–1250
 - inherited Fanconi syndrome
 - cystinosis
 - clinical presentation, 1244
 - pathogenesis and treatment, 1246
 - pathologic changes, 1244–1246, 1245f–1246f
 - Dent disease
 - pathogenesis, 1247
 - pathologic changes, 1246–1247
 - Fanconi-Bickel syndrome, 1249
 - idiopathic Fanconi syndrome, 1243
 - Lowe syndrome
 - pathogenesis, 1249
 - pathologic changes, 1248
 - mitochondrial disorders
 - diagnosis, 1248
 - pathologic changes, 1247–1248, 1248f
 - specialized heritable tubular defects, 1250, 1251t
- Membranoproliferative glomerulonephritis (MPGN)
 - α1-antitrypsin deficiency, 331
 - acute poststreptococcal glomerulonephritis, 398
 - cryoglobulinemia
 - hepatitis C–associated cryoglobulinemic glomerulonephritis, 328–329, 330f
 - multiple silver-negative hyaline thrombi, 329, 329f
 - numerous acidophilic hyaline thrombi, 329, 329f
 - pathogenesis, 328
 - diabetic nephropathy, 933
 - differential diagnosis, 322–323, 323f
 - etiology and pathogenesis
 - animal models, 327
 - cellular immunity, 326
 - chronic antigenemia and infection, 325
 - complement activation and nephritic factor activation pathways, 323–324
 - C3 nephritic factors (C3NeFs), 324
 - hypocomplementemic persistent glomerulonephritis, 323
 - nephritic factor of the terminal pathway (NeFt), 324
 - complement deficiency, 324–325
 - genetic factors, 327
 - immune complexes and humoral immunity, 325–326
 - platelet activation, 326–327
 - toll-like receptors, 326
 - HBV infection, 330–331
 - HCV infection
 - hepatitis C–associated cryoglobulinemic glomerulonephritis, 328–329
 - pathogenesis, 328
 - prevalence of, 330
 - treatment, 329
 - Lyme disease, 331
 - monoclonal gammopathy, 332
 - MPGN type I, 302, 302t, 304f
 - clinical course, 311–312, 317
 - clinical presentation
 - blood urea nitrogen/serum creatinine, 305
 - hypocomplementemia, 305
 - mild hypertension, 305
 - proteinuria, 305
 - renal biopsy, 304
 - renal vein thrombosis, 305
 - dense deposit disease, 301–303, 302t, 304f
 - epidemiology, 304–305
 - medical history, 302
 - pathologic findings, 301, 302t
 - electron microscopy, 310–311, 311f–316f
 - gross pathology, 306
 - immunofluorescence microscopy, 309–310, 309f
 - light microscopy, 306–309, 306f–309f
 - prognosis, 317–318, 317t
 - therapy, 318–319
 - MPGN type III, 302, 302t, 304f
 - clinical course, 321–322
 - clinical presentation, 319–320
 - pathologic finding
 - electron microscopy, 320–321, 321f–322f
 - immunofluorescence microscopy, 320, 320f
 - light microscopy, 320, 320f
 - prognosis, 321
 - therapy, 322
 - neoplasia, 332
 - nephropathia epidemica, 331
- Membranoproliferative glomerulonephritis (type III of Burkholder), 281, 319, 321f
- Membranoproliferative glomerulonephritis (type III of Strife), 319, 320f, 321f, 322f
- Membranous glomerulonephritis (MGN)
 - definition, 255
 - idiopathic membranous glomerulonephritis, 255–256
 - primary membranous glomerulonephritis
 - clinical course, 256–257
 - clinical presentation, 256–257
 - differential diagnosis, 281
 - etiology, 272
 - pathogenesis
 - bovine serum albumin, 280
 - M-type phospholipase A₂ receptor, 279–280, 279f
 - neutral endopeptidase, 275, 278
 - passive Heymann nephritis, 272, 274
 - tubulointerstitial injury, 280–281
 - pathologic findings
 - electron microscopy, 264–266, 265f–277f, 268–269, 271
 - gross pathology, 257
 - immunopathology, 261–264, 261f–264f, 263t
 - light microscopy, 257–261, 257f–261f
 - prognosis, 282t
 - FSGS, 282
 - hypertension, 283
 - interstitial fibrosis and tubular atrophy, 282
 - proteinuria, 272, 283
 - renal function, 283
 - ultrastructural findings, 282–283
 - recurrence, 1421–1422, 1421f
 - with rheumatoid arthritis, 633
 - secondary membranous glomerulonephritis
 - associated with
 - autoimmune thyroiditis, 289–290
 - bone marrow and stem cell transplantation, 289
 - IgG4-related disease, 290
 - Guillain-Barré syndrome, 290
 - sarcoidosis, 288–289
 - drug-induced etiology
 - bucillamine, 285
 - gold therapy, 284–285

- Membranous glomerulonephritis (MGN)
(*Continued*)
mercury, 286
nonsteroidal anti-inflammatory drugs, 286
penicillamine, 285
incidence, 284
infectious etiology
hepatitis B virus, 287–288
hepatitis C virus, 288
syphilis, 288
malignancy, 286–287
renal transplant, 290–291
renal vein thrombosis, 291
terminology, 255
- Membranous glomerulopathy
gold salt/penicillamine, 631
hepatitis B antigenemia, 330
incidence, 841, 1415
light microscopy, 1022–1023, 1022f, 1415
NSAID therapy, 631
pathogenesis, 1415
prevalence, 1415
thickened GBMs *vs.* glomerulus and cellularity, 99f
- Membranous lupus nephritis
diffuse proliferative and membranous glomerulonephritis, 594, 594f
global mesangial hypercellularity, 594, 594f
granular subepithelial deposits, 595, 595f
idiopathic membranous glomerulonephritis, 596
management, 604
numerous subepithelial electron-dense deposits, 595, 596f
podocytic infolding glomerulopathy, 596
primary membranous glomerulonephritis, 594, 594f, 595
renal insufficiency, 596
renal vein thrombosis, 596–597, 597f
segmental membranous glomerulonephritis, 595
subendothelial immune deposits, 593
- Mercury nephropathy, 1148–1149
- Merkel cell carcinoma, 1427–1428
- Mesangial-endothelial cell interface, 36f
- Mesangial proliferative glomerulonephritis, 472f, 586, 633
- Mesangial proliferative lupus nephritis, 584–586, 585f
- Mesangiocapillary glomerulonephritis. *See* Membranoproliferative glomerulonephritis (MPGN)
- Mesangium (MES), styrene model of rat, 41f
- Mesenchymal neoplasms
angiomyolipoma
clinical findings and epidemiology, 1482–1483
pathology, 1483
treatment and outcome, 1483–1484
benign mesenchymal tumors, 1484
primary sarcoma, 1484–1485, 1485f
- Mesonephros, 69–70, 70f
- Metanephric adenoma, 1466–1467, 1466f
- Metanephric mesenchyme
cell lineages, 80
nephron tubule formation, 80–82, 81t
survival and induction, 79–80
- Metanephros, 70, 71f
- Metastases, 1487–1488, 1463f
- Methicillin sensitive *Staphylococcus aureus* (MSSA) endocarditis, 409, 409f
knee osteomyelitis, 409, 411f
sepsis, 410, 412, 413f
- Methylmalonic acidemia, 1237
- MGN. *See* Membranous glomerulonephritis (MGN)
- Microangiopathic hemolytic anemia, 740
- β_2 -Microglobulin amyloidosis ($A\beta_2M$), 996–997
- Microhematuria, 373, 418, 449
- Microscopic polyangiitis (MPA)
clinical presentation, 687–688
definition, 686, 686t
vs. granulomatosis with polyangiitis, 693
pathology, 699
renal biopsy, 691
- Microscopic polyarteritis, 720
- Microvascularization
cortical, 14–15
and nephrons, 14f
- MIDD. *See* Monoclonal immunoglobulin deposition disease (MIDD)
- Miliary tuberculosis, 1054–1055, 1054f–1055f
- Minimal change disease (MCD). *See also* Nephrotic syndrome (NS); Proteinuria
acute renal failure, 183
clinical course
in adults, 192
in children, 191
clinical presentation
in adults, 183
in children, 182–183
clinico-pathologic correlation
focal global glomerular sclerosis, 193
FSGS, 192–193
glomerular tip lesion, 193
mesangial hypercellularity, 193
de novo MCD, 1418
differential diagnosis
congenital nephrotic syndrome, 191
C1q nephropathy, 190–191
FSGS, 191
IgM nephropathy, 190
laboratory findings, 183
pathogenesis, 188
cell-mediated immunity, 189
epigenetic mechanisms, 190
hemopexin, 189
podocytes, 189–190
T-reg mechanism, 189
- pathology
electron microscopic finding
discrete foot processes, 186–187, 186f–187f
glomerular basement membrane, 187–188, 188f
glomerular epithelial cell vacuoles, 187
immunofluorescence study, 186
immunohistochemical and molecular finding, 188
light microscopy
blood vessels, 186
glomeruli, 184–186, 184f, 185f
interstitium, 186
tubules, 184–186, 185f
prognosis and therapy, 192
secondary causes of
immune response and autoimmune disorders, 194
interferons, 194
lymphoma and neoplasia, 194
nonsteroidal anti-inflammatory drugs, 193
terminology, 182
- Minimal mesangial lupus nephritis, 584, 584f
- Mitochondrial disorders
diagnosis, 1248
pathologic changes, 1247–1248, 1248f
- Mixed connective tissue disease (MCTD)
clinical course, 626
clinical presentation, 624–625
clinico-pathologic correlations, 626
pathologic findings, 625–626, 626f
prognosis, 626
therapy, 626
U1-RNP complex, 624
- Mixed epithelial and stromal tumor, 1485–1486, 1486f
- MMF. *See* Mycophenolate mofetil (MMF)
- Molecular domains and filtration function, 29–31
- Monoclonal gammopathy
clinical presentation, 332
tubulointerstitial nephritis, 1146
- Monoclonal gammopathy of unknown significance (MGUS)
C3 deposits, 974–975
monoclonal IgG deposits, 973, 974f
- Monoclonal immunoglobulin deposition diseases (MIDDs)
adenine phosphoribosyltransferase deficiency, 1424
clinical history, 965
cystinosis, 1424
differential diagnosis
MGUS, glomerulonephritis with C3 deposits, 974–975
monoclonal IgG deposits, 973, 974f
plasma cell dyscrasias, crystalline inclusions in glomeruli, 975–976
Fabry disease, 1423–1424
heavy chain disease
clinical course, 973
clinical presentation/laboratory findings, 971
differential diagnosis, 973
electron microscopy, 972
etiology and pathogenesis, 972–973
gross pathology, 972
immunofluorescence, 972, 972f
light microscopy, 972, 972f
transplantation, 973
prognosis, 973
treatment, 974
identification, 322–323, 323f
light chain deposition disease
clinical presentation and laboratory findings, 965
electron microscopy, 967–968, 968f, 969f
etiology and pathogenesis, 968, 970, 970f
gross pathology, 965
immunofluorescence, 966–967, 967f
light microscopy, 966, 965f, 966
transplantation, 971
prognosis, 970–971
treatment, 970–971
primary hyperoxaluria, type I, 1423
- Moyamoya disease, 881
- MPA. *See* Microscopic polyangiitis (MPA)
- MPGN. *See* Membranoproliferative glomerulonephritis (MPGN)

- MPO-ANCA. *See* Myeloperoxidase (MPO-ANCA)
- MSSA. *See* Methicillin sensitive *Staphylococcus aureus* (MSSA)
- Mucinous tubular and spindle cell carcinoma, 1478–1479, 1479f
- Mucoid intimal hyperplasia, 759
- Multilocular cystic nephroma (MCN), 147, 148f
- Multilocular renal cyst, 147, 148f
- Mycobacterial infections
- aspergillosis, 1057–1058, 1058f
 - blastomycosis, 1059
 - Candida albicans* infection, 1056–1057, 1057f
 - Candida glabrata* infection, 1057, 1057f
 - cavitary tuberculosis, 1055–1056
 - coccidioidomycosis, 1059
 - cryptococcosis, 1058, 1058f
 - histoplasmosis, 1058–1059, 1059f
 - miliary tuberculosis, 1054–1055, 1054f–1055f
 - mucormycosis, 1060, 1060f
 - Mycobacterium leprae*, 1056
 - paracoccidioidomycosis, 1059
 - pathogenesis, 1056
- Mycophenolate mofetil (MMF), 493
- Myeloperoxidase (MPO-ANCA)
- anti-MPO–induced murine model, 705
 - epitope specificity, 689–690
 - vs.* PR3-ANCA, 691, 701, 708
 - statistical analysis, 689, 690f
- Myoglobin cast nephropathy, 93t
- Myosin 1E, 228t, 236
- N**
- Nail-patella syndrome (NPS)
- clinical presentation, 547
 - genetics/nature of defect, 547–548
 - hereditary osteonychodysplasia, 543–544
 - pathologic findings, 544–546, 545f–547f
- Narcotics, 1175, 1200
- Necrotizing arteritis, 718–720, 721f
- Neoplasms
- clinical history, 457
 - clinical presentation, 457
 - etiology and pathogenesis, 457–458
 - pathology, 457
 - renal malignancies, AIDS patients, 457, 457t
- Nephrin, 233t, 235–236
- Nephritic factor of the terminal pathway (NeFt), 324
- Nephritis strain-associated protein (NSAP), 393
- Nephrocalcinosis/nephrolithiasis
- definition, 1088
 - development of, 1244
 - in HIV infection, 451, 1093
 - incidence of, 453, 1093
 - pathology, 1091–1092
 - prevalence of, 451
 - protocol biopsies, 1387
- Nephrolithiasis and crystalline nephropathies
- calcium nephrolithiasis, 1096–1098
 - clinical presentation, 1093–1094, 1094f
 - 2,8-dihydroxyadeninuria deficiency, 1100
 - lithotripsy, treatment, 1100–1101, 1101f
 - non calcium stones, 1098–1100
 - stone formation, mechanisms of
 - CaOx, 1095–1096
 - inhibitors of, 1095
 - innate immunity, 1095–1096
 - nucleation, 1095
 - Oxalobacter formigenes*, 1095
 - urine saturation, 1094–1095
- Nephromegaly, 122, 122f
- Nephronophthisis
- Bardet-Biedl syndrome, 141
 - clinical presentation and genetics, 136–137
 - incidence, 136
 - pathology and pathogenesis, 137–139, 137f–139f, 140t
- Nephronophthisis/medullary cystic disease, 93t, 136–137
- Nephrons
- and associated collecting ducts, 37f
 - metanephric mesenchyme, tubule formation
 - from, 80–82, 81t - microvasculature and, 14f
 - number, 19
 - schematic drawing, 15f
 - types of, 19–21
- Nephropathia epidemica, 331
- Nephrosialidosis
- free sialic acid storage disorders, 1235
 - galactosialidosis, 1235
 - pathologic changes, 1235–1236, 1235f
 - sialidosis, 1235
- Nephrotic syndrome (NS). *See also* Minimal change disease (MCD)
- causes of, 178t
 - disease prevalence
 - children, 180–181, 181t
 - elderly people, 181, 182t
 - geographical differences, 181–182, 182t
 - membranous glomerulonephritis, 182
 - glomerular diseases frequency, 180, 181t - complication, 178f
 - atherosclerosis, 179–180
 - bacterial infection, 179
 - hypercoagulability, 179
 - renal vein thrombosis, 179
- definition, 177
- first year of life, 194
- congenital nephrotic syndrome
 - Finnish type, 195, 196f
 - nephrectomy, 195
 - nephrin, 195
 - transplants, 196 - diffuse mesangial sclerosis. *See* Diffuse mesangial sclerosis (DMS)
 - mutation agents, 194, 195t
- pathophysiology
- edema formation, 178, 178f
 - epithelial sodium channel (ENaC), 178
 - hyperlipidemia, 177–178
 - hypoalbuminemia, 177
- Nephrotoxic acute tubular injury
- aminoglycosides, 1183
 - amphotericin, 1183
 - anesthetics, 1187
 - antibiotics, 1182
 - antiviral agents, 1182–1183, 1182f
 - cephalosporins, 1183
 - chemotherapeutic agents, 1186
 - electron microscopy, 1182
 - extensive coagulative necrosis, 1181–1182
 - herbal medications, 1187
 - immunosuppressive/immunomodulatory agents, 1185–1186, 1185f
 - light microscopy, 1181
 - narcotics and myoglobinuric acute renal failure, 1187, 1187f
 - polymyxin/colistin, 1184
 - radiocontrast agents, 1186–1187
 - swelling and vacuolation, tubular cells, 1181
 - vancomycin, 1184–1185
 - vessels, 1182
- Neuroblastoma, 887, 1467–1468, 1468f
- Neuroendocrine tumors, 1482
- Neurofibromatosis, 881
- Neutral endopeptidase (NEP), 278
- Newborn human kidneys, 5f, 9f
- Nodular diabetic glomerulosclerosis, 1418, 1423
- Nodular lesion, 903–906, 904f–905f
- Non calcium stones
- cystine stones, 1099
 - uric acid stones, 1098–1099, 1098f
 - xanthinuria, 1099–1100
- Noncollagenous glycoproteins and proteoglycans, 39–41
- Noninflammatory necrotizing vasculopathy, 573, 573f, 574f
- Nonneoplastic renal diseases, 1488
- Nonsteroidal anti-inflammatory agents, 1266
- Normal human cortex, 24f
- Novel therapies, 1267
- NPS. *See* Nail-patella syndrome (NPS)
- NSAP. *See* Nephritis strain-associated protein (NSAP)
- O**
- Obesity associated focal segmental glomerulosclerosis (FSGS), 218t, 241f
- Obesity-related glomerulopathy (ORG), 241, 241f
- Obstructive nephropathy and hydronephrosis
- differential diagnosis
 - clinical management, 1087–1088
 - fibroepithelial polyps, 1084f
 - pathogenesis, 1085–1087, 1086f–1087f
 - prognosis, 1087–1088
 - therapy, 1088 - terminology, 1082
 - ureteropelvic junction
 - gross pathology and light microscopy, 1083–1084, 1083f–1084f
 - incidence and clinical presentation, 1082
- Obstructive sleep apnea, 888
- Ocrelizumab, lupus nephritis, 605
- Oligomeganephronia, 162, 241
- Oncocytoma
- clinical findings, 1469
 - clinical outcomes, 1470
 - epidemiology, 1469
 - pathology, 1469–1470, 1469f–1470f
 - treatment, 1470
- ORG. *See* Obesity-related glomerulopathy (ORG)
- Organic acid disorders, 1237
- Outer medulla
- cross section, inner stripe of, 17f
 - human, 52f, 60f
 - inner stripe, 15–16
 - outer stripe, 15
- Oxalosis, 93t, 1097f, 1144, 1284, 1305
- Oxford classification, 470–472, 471f, 472f, 489–492, 490t
- Oxidative stress–mediated injury, 920

- P**
- Pamidronate, 244
- Papillary adenoma, 1468–1469, 1469f
- Papillary collecting duct cell, 56f
- Papillary necrosis
 - clinical aspects, 935
 - pathologic findings, 935, 935f
- Papillary renal cell carcinoma, 1475–1476, 1475f
- Partial lipodystrophy (APL), 343, 575–576
- Parvovirus infection, 1065–1066
- Passive Heymann nephritis (PHN), 272, 274
- Pathologic classification and diagnosis
 - glomerular disease
 - electron microscopy, 99–101
 - immunohistology, 98–99, 101f
 - kidney biopsy specimens evaluation, 96t
 - light microscopy, 97–98, 98f
 - interstitial disease
 - acute and chronic tubulointerstitial nephritis, 111, 112t
 - edema, 112, 113f
 - fibrosis, 114
 - granulomas, 112
 - immune aggregates, 114
 - infectious agents, 114
 - interstitial expansion, 114
 - leukocytic infiltrates, 112, 113f
 - primary and secondary, 111
 - renal interstitium, 112
 - primary site injury, 95
 - renal pathology history, 91–92
 - renal syndromes, 95
 - renal vascular disease, 114–115
 - renal biopsy analysis, 92–93
 - technical considerations
 - pathologic evaluation, 93–94
 - semiquantitation, 94
 - specimen adequacy, 94
 - tubular disease
 - acute tubular injury (ATI), 104–105
 - heavy metal poisoning, 105–106, 107f
 - hemosiderin, 105–106, 107f
 - hyaline droplet change, 105, 107f
 - mitochondrial abnormalities, 110
 - renal tubular epithelium, pigments in, 105–106, 107f
 - tubular atrophy, 109, 110f
 - tubular basement membrane changes, 110–111, 112f
 - tubular casts, 108
 - tubulitis, 108, 109f
 - vacuolar change, 105
 - virial intranuclear inclusions, 106, 108
- Pauci-immune crescentic glomerulonephritis
 - clinical presentation, 707–709
 - ANCA
 - calculated predictive value, 689, 689f
 - cytoplasmic (c-ANCA), 688–689
 - glomerulonephritis, 688
 - incidence, 688
 - MPO-ANCA, 689–690, 690f
 - perinuclear (p-ANCA), 688–689
 - signs and symptoms, 686
 - EGPA, 687
 - MPA, 687–688
 - relapsing polycondritis, 688
 - typical histologic glomerular lesion, 687
 - differential diagnosis, 706–707
 - electron microscopy
 - ANCA IgG incubation, 704, 705f
 - ANCA-induced leukocyte activation, 705
 - anti-MPO–induced murine model, 705, 705f
 - breaks in GBM, 702, 702f
 - cellular crescents, 702, 702f
 - cellular elements removal, 702, 702f
 - glomerular capillary loop, 702, 703f
 - immune complex–type electron-dense deposits, 701
 - marginated neutrophils and monocytes, 702, 703f, 704f
 - PR3-ANCA, 706
 - immunofluorescence microscopy, 700–701, 700f, 701f
 - immunopathologic study, 685, 686f
 - occurrence, 685
 - pathologic findings
 - extrarenal pathology, 699–700
 - glomeruli
 - crescent formation, 691
 - European Vasculitis Study Group (EUVAS) patient cohorts, 694–695
 - fibrinoid necrosis, 690–691, 691f, 692f, 693
 - immune complex glomerulonephritis, 693–694
 - neutrophils, prominent influx and margination, 693, 693f
 - periglomerular granulomatous inflammation, 693
 - segmental/global sclerosis, 694, 694f
 - gross pathology, 690
 - renal vessels
 - extensive necrotizing arteritis, 695
 - fibrotic muscularis, 696f, 697
 - Hilar arteriolar necrosis, 695
 - medullary angitis, 697, 697f
 - perivascular inflammatory infiltrate, 695, 697f
 - subacute arteritis, 695, 696f, 697
 - tubules and interstitium
 - acute tubulointerstitial changes, 697, 697f
 - Bowman capsule, 698, 698f
 - interstitial fibrosis, 698, 699
 - medullary angitis, 697f, 698
 - systemic necrotizing granulomatosis, 698, 698f
 - prognosis, 708
 - renal-limited vasculitis, 685
 - systemic vasculitides, 686
 - therapy, 708–709
- Pediatric neoplasms
 - clear cell sarcoma, 1465, 1465f
 - congenital mesoblastic nephroma
 - clinical findings and epidemiology, 1463–1464
 - clinical outcomes, 1464
 - pathology, 1464
 - treatment, 1464
 - metanephric adenoma, 1466–1467, 1466f
 - neuroblastoma, 1467–1468, 1468f
 - rhabdoid tumor, 1465–1466, 1466f
 - translocation carcinomas, 1467, 1467f
 - Wilms tumor
 - clinical findings and epidemiology, 1461–1462
 - pathology, 1462–1463, 1463f
 - treatment and clinical outcomes, 1463
- Pelvis, corrosion cast of human renal, 7f
- Penicillamine, MGN, 285
- Perfusion-fixed rat kidney, 49f
- Periarterial fibroplasia, 879
- Periarthritis, 719
- Periarthritis nodosa, 719, 720
- Perihilar variant focal segmental glomerulosclerosis (FSGS), 214f, 218, 219f, 221f, 227, 227f, 228f, 241f
- Perimedial fibroplasia, 878–879, 879f
- Peritubular capillaritis, 1359, 1394, 1402
- Peritubular capillary, 45f
- Peroxisomal disorders
 - adult Refsum disease, 1240–1241
 - primary hyperoxaluria, 1241–1243, 1242f
 - Zellweger syndrome, 1240
- Pheochromocytoma
 - clinical features and diagnosis, 883–884
 - familial syndromes and mutations, 883
 - pathologic findings, 884, 884f
- PHN. *See* Passive Heymann nephritis (PHN)
- Phosphate nephropathy, 1092–1093, 1093f
- Phospholipase A₂ Receptor (PLA₂R) antibodies, 1415, 1421
- Phospholipase C epsilon, 233t, 236
- Pierson syndrome
 - clinical presentation, 551
 - genetics/nature of defect, 551, 553
 - LAMB2 gene, mutation, 198, 238
 - pathology, 551, 552f–554f
- Plasma cell dyscrasias
 - light chain cast nephropathy
 - clinical history, 956–957
 - clinical presentation and laboratory findings, 957
 - differential diagnosis, 959
 - electron microscopy, 958
 - etiology and pathogenesis, 958–959
 - gross pathology, 957
 - immunofluorescence, 958
 - light microscopy, 957–958, 957f
 - prognosis, 959
 - treatment, 959
 - multiple myeloma and dysproteinemias, 953–955
 - proximal tubulopathy
 - clinical history, 959–960
 - clinical presentation, 960
 - differential diagnosis, 961–962
 - electron microscopy, 961, 962f
 - etiology and pathogenesis, 962
 - gross pathology, 960
 - immunofluorescence, 960–961
 - laboratory findings, 960
 - light microscopy, 960, 961f
 - prognosis, 963–964
 - treatment, 962–963
 - tubulointerstitial nephritis
 - clinical history, 963
 - clinical presentation, 963
 - differential diagnosis, 964
 - electron microscopy, 964
 - etiology and pathogenesis, 964

- gross pathology, 963
- immunofluorescence, 964
- immunohistochemistry, 964, 964f
- laboratory findings, 963
- light microscopy, 963–964, 963f
- prognosis, 964–965
- treatment, 964–965
- Platelet activation and aggregation, 773
- Platelet-derived growth factor (PDGF), 921–922
- Platinum toxicity, 1149
- Podocin, 233t, 236
- Podocyte
 - and filtration barrier, 29
 - molecular domains and filtration function, 29–31
 - rat, 27f
 - ultrastructure, 25, 27–29
- Podocyte protein
 - α -actinin-4, 32
 - autosomally inherited defects of coenzyme Q10 (CoQ10), 239, 240
 - CD2AP and TRCP6, 32, 237
 - FAT1, 32
 - GLEEP-1, 29, 174
 - inverted formin-2 (INF2), 32
 - LAMB2, 198, 233t, 238
 - leucine transfer RNA (tRNA^{Leu}), 234t, 239
 - myo1E (MYO1E), 236
 - nephrin, 31, 32, 235–236
 - phospholipase C epsilon 1 (PLCE1), 195t, 233t, 236
 - podocalyxin, 29, 30f, 33
 - podocin, 32, 233t, 236
 - podoplanin, 11f, 176
 - protein tyrosine phosphatase receptor type O (PTPRO), 237
 - synaptopodin, 32, 188
 - WT-1, 24, 229, 238
- Podocytic infolding glomerulopathy, 596
- Podocytopeny, 209, 244–245, 247, 608–609
- Podocytopenia, 208, 230
- Polyarteritis nodosa, 719
 - clinical course, 726–727
 - clinical presentation, 721, 722t
 - clinicopathologic correlations, 726–727
 - differential diagnosis, 726, 726f
 - etiology and pathogenesis, 725–726
 - pathologic findings
 - electron microscopy, 725
 - gross pathology, 721–722
 - immunofluorescence, 725
 - light microscopy, 722–725, 723f, 724f
 - prognosis and therapy, 726–727
- Polycystic kidney disease
 - autosomal dominant polycystic kidney disease. *See* Autosomal dominant polycystic kidney disease (ADPKD)
 - autosomal recessive polycystic kidney disease. *See* Autosomal recessive polycystic kidney disease (ARPKD)
 - glomerulocystic kidney disease
 - associated diseases, 131–133
 - histological findings, 131, 133t
 - pathogenesis, 135–136
 - pathology and differential diagnosis, 133–135, 133f–135f
 - hepatic fibrosis, 130–131, 132f
 - polycystic liver disease, 130–131, 132f
- Polycystic liver disease
 - clinical management, 131
 - differential diagnosis, 130
 - liver cirrhosis, 130, 132f
 - liver cysts, 130, 132f
 - pathogenesis, 130–131
 - prognosis and therapy, 131
- Polymyxin B, 1172
- Polyomavirus nephropathy (PVN)
 - clinical presentation, prognosis, and therapy, 1409–1410, 1410f
 - diagnosis, 1403, 1403t
 - differential diagnosis, 1408–1409
 - electron microscopy, 1407–1408, 1405f
 - etiology and pathogenesis, 1408
 - gross pathology, 1404
 - immunofluorescence and immunohistochemistry, 1405, 1407, 1407f
 - light microscopy, 1404–1405, 1404f–1406f
- Postmortem kidney, 724, 724f
- Poststreptococcal acute glomerulonephritis (PSAGN)
 - antibody formation, 371
 - associated with C3 glomerulopathy, 395–396
 - clinical history, 368
 - clinical outcomes, 401, 402t
 - clinical presentation
 - albuminuria, 373
 - anemia, 373
 - hypertension, 372
 - hypertensive encephalopathy, 372
 - microhematuria, 373
 - proteinuria, 372–373
 - synpharyngeal nephritis, 372
 - clinicopathologic correlation
 - ANCAs, 401
 - children, prospective study, 401, 402t
 - crested glomerulonephritis, 400, 401
 - glomerular humps, 399
 - glomerular sclerosis, 404
 - glomerular tuft hypercellularity, 399
 - IgG, linear immunofluorescence, 401
 - immunofluorescence studies, 387
 - initial/persistent nephrotic syndrome, 399–400
 - light and electron microscopy, 400
 - differential diagnosis
 - C3 glomerulopathy, 398
 - class IV lupus nephritis, 399
 - cryoglobulinemic glomerulonephritis, 398–399
 - membranoproliferative glomerulonephritis, 398
 - membranous glomerulonephritis, 399
 - nonstreptococcal origin, 397–398
- epidemiology, 368–369
- etiology and pathogenesis
 - antigen
 - endostreptosin, 392–393
 - nephritis-associated plasmin receptor, 394
 - nephritis strain-associated protein, 393
 - nephritogenic streptococcal antigen, 392, 392t
 - preabsorbing antigen, 393
 - streptococcal M protein, 392
 - circulating immune complexes, 394
 - complement/complement receptors, 394–395
- cryoglobulins, 394
- immune-mediated disease studies
 - foreign protein, parenteral administration, 391
 - glomerular subepithelial electron-dense immune-type deposits, 391
 - pre-absorbing antigen, 392
- nephritogenic strains, 368–369
- pathologic findings
 - altered lymphocyte transformation, 397
 - anti-IgG reactivity, 396
 - antibody production, 396
 - electron microscopic findings, 384, 383f, 385f–391f, 387, 389–391
 - fibrin/fibrinolysis, 397
 - genetic predisposition, 397
 - glomeruli
 - actomyosin, 377
 - chronic latent glomerulonephritis, 377–378
 - diffuse endocapillary hypercellularity, 374, 374f
 - exudative glomerulonephritis, 374
 - incidental healed postinfectious glomerulonephritis, 378
 - intercellular adhesion molecule 1 (ICAM-1) expression, 377
 - Ki-67 expression, 377
 - necrosis, 374, 375f
 - Peanut agglutination lectin, 377
 - polymorphonuclear leukocytes, 377
 - proliferative glomerulonephritis, 376, 377
 - silver stain, 374, 375f
 - trichrome stain, 375, 376f
 - gross pathology, 373–374
 - immunofluorescence findings
 - C3 glomerulonephritis, 383
 - ferritin-conjugated antibodies, 384
 - garland pattern, 379, 380f
 - glomerular capillary wall, 379, 379f
 - lumpy bumpy, 379, 379f
 - membrane attack complex, 384
 - mesangial pattern, 379–380, 381f, 383f
 - starry sky pattern, 379, 381f
 - interleukin, 397
 - interstitium, 378–379, 378f
 - renal biopsy, indication, 373, 374t
 - tubules, 378, 378f
- Posttransplant lymphoproliferative disorders (PTLD)
 - definition, 1424
 - EBV infection, 1061
 - histologic categories and subtypes, 1425t
 - pathology of, 1061–1062, 1062t
 - polymorphic and polyclonal variant, 1425, 1426f
 - prevalence, 1427
 - renal involvement in, 1062–1063, 1062t
- Preeclampsia and eclampsia
 - clinical findings, 819–820
 - course and prognosis, 820–821
 - differential diagnosis, 820
 - etiology and pathogenesis, 832–835
 - focal segmental glomerulosclerosis lesions, 825, 827–832, 830f, 831t
 - HELLP syndrome, 832
 - hypertension, 819
 - pathologic changes, 821–825

- Pregnancy
 acute fatty liver, 836
 acute kidney injury
 acute fatty liver, 836
 cortical necrosis, 836
 eclampsia, 835
 HELLP syndrome, 835
 preeclampsia, 835
 septic abortion, 835
 thrombotic microangiopathy
 clinical findings, 836
 electron microscopic findings, 836
 immunofluorescence findings, 836
 microscopic findings, 836, 837f
 uterine hemorrhage, 835
 functional changes, 816
 hypertensive disorders
 chronic hypertension, 818–819
 gestational hypertension, 819
 preeclampsia and eclampsia
 clinical findings, 819–820
 course and prognosis, 820–821
 differential diagnosis, 820
 etiology and pathogenesis, 832–835
 focal segmental glomerulosclerosis
 lesions, 825, 827–832, 830f, 831t
 HELLP syndrome, 832
 pathologic changes, 821–825
 on preexisting renal disease
 focal segmental glomerulosclerosis, 840
 IgA nephropathy, 841
 kidney transplant, 842
 lupus nephritis, 840–841
 membranous glomerulopathy, 841
 pathogenesis, 839–840
 pregnancy outcome, 839
 reflux nephropathy, 841
 renal cancer, 842
 systemic and genetic diseases
 anti-glomerular basement membrane
 antibody disease, 842
 autosomal dominant polycystic kidney
 disease, 842
 diabetes mellitus, 841–842
 granulomatosis with polyangiitis and
 microscopic polyangiitis, 842
 structural changes, 815–816
 thrombotic microangiopathies, 752–753
 urinary tract infections
 asymptomatic/covert bacteriuria, 817
 incidence and risk factors, 816–817
 symptomatic bacteriuria and pyelonephritis,
 817–818
 Primary crescentic glomerulonephritis, 685
 Proliferative glomerulonephritis with
 monoclonal IgG deposits, 332, 975, 1418
 Protein tyrosine phosphatase receptor type O,
 233t, 237
 Proteinuria. *See also* Nephrotic syndrome (NS)
 acute poststreptococcal glomerulonephritis,
 372–373
 aminonucleoside nephrosis, 176
 caused by, 229
 clinical presentation, 372–373, 408t
 development of, 274
 diffuse lupus nephritis, 591
 and foot process effacement, 176–177
 membranoproliferative glomerulonephritis, 305
 microscopic hematuria, 305
 recurrence, 230, 236
 treatment, 284–285
 tubules and interstitium, 177
 urinary monitoring, 285
 Protocol biopsies
 molecular phenotype, 1388
 nephrocalcinosis, 1387
 subclinical antibody-mediated rejection,
 1386–1387
 subclinical cell-mediated rejection, 1385–1386,
 1386f
 surrogate marker, 1387
 Proton pump inhibitors, 1133
 Proximal tubulopathy
 clinical history, 959–960
 clinical presentation, 960
 differential diagnosis, 961–962
 electron microscopy, 961, 962f
 etiology and pathogenesis, 961
 gross pathology, 960
 immunofluorescence, 960–961
 laboratory findings, 960
 light microscopy, 960, 961f
 prognosis, 962–963
 treatment, 963
 PSAGN. *See* Poststreptococcal acute
 glomerulonephritis (PSAGN)
 Purine metabolism and handling disorders
 acute uric acid nephropathy, 1255
 chronic uric acid nephropathy, 1255–1257,
 1256f–1257f
 hereditary disorders
 enzyme defects
 adenine phosphoribosyltransferase
 deficiency, 1252–1253, 1252f
 glucose-6-phosphatase deficiency, 1253
 hypoxanthine-guanine
 phosphoribosyltransferase deficiency,
 1250, 1252
 5-phosphoribosylpyrophosphate
 synthetase superactivity, 1252
 tubular defects
 hereditary renal hypouricemia, 1253
 uromodulin-associated kidney disease,
 1253–1255, 1254f
 uric acid infarcts, 1255, 1255f
 urolithiasis, 1257–1258
 Puromycin aminonucleoside nephrosis,
 176, 209
 Pyelonephritis
 acute pyelonephritis
 clinical course, 1046
 clinical presentation, 1041, 1041f
 diffuse suppurative pyelonephritis,
 1044–1045, 1044f–1045f
 emphysematous pyelonephritis, 1045–1046,
 1045f
 gross pathology and light microscopy,
 1042–1044, 1042f–1043f
 prognosis/therapy, 1046
 sepsis and kidney injury, 1046
 chronic pyelonephritis
 definition and controversies, 1046
 gross pathology and light microscopy,
 1046–1047, 1046f–1047f
 malakoplakia
 clinical presentation, 1049–1050
 differential diagnosis, 1050–1051
 gross pathology and light microscopy,
 1050
 pathogenesis, 1050
 xanthogranulomatous pyelonephritis
 clinical presentation, 1047
 gross pathology and light microscopy,
 1047–1049, 1049f
 pathogenesis, 1049
 clinical history, 1040–1041
 clinical syndromes, 1040t
 consequences and complications, 817–818
 risk factors, 1054
 terminology, 1039–1040
 treatment, 818
 UTI pathogenesis
 bacteria and host immune defenses,
 1053–1054, 1054f
 bacterial virulence, 1051
 fimbriae, role of, 1051–1052, 1051f
 host-pathogen interactions, 1052–1053,
 1053f
- R**
 Radiation nephropathy
 clinical history, 787
 clinical presentation and clinical course
 acute radiation nephropathy, 787
 asymptomatic proteinuria, 788
 benign hypertension, 788
 chronic radiation nephropathy, 788
 malignant hypertension, 788
 electron microscopy, 790
 etiology and pathogenesis
 experimental studies, 790–791
 hypertension, 791–792
 irradiation, dosage of, 792–793
 gross appearance, 788
 immunofluorescence microscopy, 789
 light microscopy
 blood vessels, 789, 789f
 glomeruli, 788–789, 789f
 tubules and interstitium, 789
 radionuclide therapy, 796–797
 Radiocontrast nephropathy (RN), 1174, 1200
 Rat
 ascending limb of, 54f
 cortical collecting duct in, 55f, 56f
 distal convoluted tubule of, 55f
 glomerular efferent arterioles in, 45f
 glomerulus, 24f, 36f
 mesangium, 41f
 slit diaphragms, 27f, 28f
 with vascular pole, 22f
 inner medulla of, 60f
 intercalated cells in, 57f
 juxtaglomerular portion of afferent arteriole
 in, 21f
 kidney
 arterial cast of, 9f
 perfusion-fixed, 49f
 proximal tubule epithelium of, 50f
 loop of Henle, 53f
 macula densa, 43f
 peritubular capillary in, 45f

- podocyte, 27f
proximal tubule, 51f
Recurrent glomerular diseases
 C3 nephropathies
 amyloidosis, 1422
 antineutrophil cytoplasmic antibody-mediated diseases, 1422
 atypical hemolytic uremic syndrome, 1420–1421
 C3 glomerulonephritis, 1430
 Henoch-Schönlein purpura, 1421
 IgA nephropathy, 1421
 membranous glomerulonephritis, 1421–1422, 1422f
 systemic lupus erythematosus, 1422
 diagnosis of, 1418
 focal segmental glomerulosclerosis, 1419
 membranoproliferative glomerulonephritis, type I, 1420
Reflux nephropathy
 clinical history, 1071, 1072t
 clinical presentation, 1071–1072
 definitions, 1071
 distinct types
 allograft kidney, 1079
 Ask-Upmark kidney, 1075–1076, 1078f
 clinical management, 1081–1082
 hereditary reflux, 1076–1079, 1078t
 pathogenesis, 1079
 in pregnancy, 1079
 prognosis and therapy, 1081–1082
 proteinuria, 1079
 sterile reflux, 1079
 trigone development, 1080–1081
 ureter development, 1079–1080, 1080f
 incidence, 841, 1071–1072
 radiologic evaluation
 bilateral vesicoureteral reflux, 1073, 1074f
 dysplastic kidneys, 1073, 1075f, 1076f
 grading of reflux, 1072, 1074
 segmental cortical scars and dilated pelvis, 1074, 1076f
 unilateral reflux, 1073, 1074f
 unilateral ureter duplication, 1074, 1077f
Relapsing polychondritis, 688
Renal agenesis
 bilateral renal, 158
 unilateral renal, 158
Renal anatomy and histology
 adult and newborn human kidneys, 5f
 cortex
 cortical labyrinth and medullary rays, 13–14
 cortical microvascularization, 14–15
 gross anatomy and macroscopic features of, 2, 10f
 arrangement of cortex and medulla, 7f
 calyces and renal pelvis, 12
 hemisected, 5f
 hilum, 2
 lobar fusion, 3
 multipapillary type of mammalian, 3
 newborn, 2
 papillary collecting duct cell of human, 56f
 perfusion-fixed rat, 49f
 proximal tubule epithelium of rat, 50f
 renal connective capsule, 2
 renal innervation, 11
 renal lymphatic system, 10–11
 renal parenchyma, 4
 renal vasculature, 6–10
 retroperitoneum, 2
 two normal adult, 6f
 venous vessels of rabbit, 20f
medulla
 inner medulla (papilla), 16
 medullary microvascularization, 17–18
 outer medulla
 inner stripe, 15–16
 outer stripe, 15
nephrons
 nephron number, 19
 types of, 19–21
renal corpuscle
 arteries and veins, 43
 arterioles and capillaries, 43–44
 cellular components of glomerulus
 endothelial cell, 33
 mesangial cell, 33, 37
 parietal epithelial cell, 32–33
 podocyte
 and filtration barrier, 29
 molecular domains and filtration function, 29–31
 ultrastructure, 25, 27–29
 general structure and histology, 21–24
 glomerular matrix
 Bowman capsule, 41–42
 glomerular capillary loop basement membrane
 collagen type IV, 38–39
 noncollagenous glycoproteins and proteoglycans, 39–41
 mesangium, 41
 juxtaglomerular apparatus, 42–43
renal interstitium, 58–61
renal tubules
 collecting duct, 52–58
 connecting tubule, 51
 distal tubule, 50–51
 proximal tubule, 46–48
 thin limb of henle, 48–50
Renal artery aneurysms, 880
Renal artery stenosis
 clinical course, 881–882
 clinical features, 874–875
 diagnosis, 875
 differential diagnosis
 fibromuscular dysplasia, 877–880, 878f, 879f
 Moyamoya disease, 881
 renal artery aneurysms, 880
 segmental arterial mediolysis, 881
 Takayasu disease, 880
 etiology and pathogenesis, 876–877
 pathologic findings
 cholesterol emboli, 876, 877f
 ipsilateral kidney, 876, 876f
 renal artery, 875–876, 875f
 prognosis, 881–882
 therapy, 882
Renal cancer, 842
Renal cell carcinoma
 clinical outcomes, 1473
 epithelial neoplasms
 classification, 1470
 clinical findings and epidemiology
 grading system, 1472–1473, 1472t
 staging, 1471
 treatment, 1473
 unclassified, 1481–1482
Renal corpuscle
 arteries and veins, 43
 arterioles and capillaries, 43–44
 cellular components of glomerulus
 endothelial cell, 33
 mesangial cell, 33, 37
 parietal epithelial cell, 32–33
 podocyte
 and filtration barrier, 29
 molecular domains and filtration function, 29–31
 ultrastructure, 25, 27–29
Renal cortical necrosis
 gross pathology, 1205–1207, 1206f, 1207f
 histopathology, 1207–1208, 1208f
 light microscopy, 1206–1207, 1206f
 venous infarction, 1208, 1208f
Renal dysplasia
 dysplastic kidneys, 158, 159f, 160f
 multicystic dysplastic kidney, 159, 159f
 nephrogenic rests, 158, 161f
 renin immunohistochemistry, 161, 161f
 segmental dysplasia, 159, 160f
 unilateral dysplasia, 160
Renal ectopia, 162–163, 163f
Renal fusion, 163, 163f
Renal hypoplasia
 hypoplastic kidney, 161, 162f
 oligomeganephronia, 162
 simple hypoplasia, 162, 162f
Renal infection
 clinical history, 456
 clinical presentation, 454
 etiology and pathogenesis, 456
 pathology
 gross pathology, 454
 microscopic examination, 454–456, 455f, 456f
Renal innervation, 11
Renal interstitium
 fibrotic renal interstitium, 1118, 1118f
 inflammation, 112, 112t
 interstitial cells and cytoarchitecture, 58–61
Renal-limited vasculitis (RLV), 685, 690f
Renal lymphangiectasia, 149, 151f
Renal lymphatic system, 10–11
Renal pelvis
 anterior/posterior direction, 7f
 degree of duplication, 159f, 163
 formation of, 70–72, 72f
 lower urinary tract control, 70–72, 72f
 renal collecting system, 7f, 12–13
 and ureter, 82–83
Renal transplantation
 acute antibody-mediated rejection
 ABO-incompatible grafts, 1369, 1370f, 1371
 chronic antibody-mediated rejection, 1371
 clinical course, 1368–1369, 1369f
 clinical presentation, 1359, 1371
 clinico-pathologic correlations, 1368–1369, 1369f

- Renal transplantation (*Continued*)
- differential diagnosis, 1366–1367, 1367t
 - electron microscopy, 1365–1366, 1366f
 - gross pathology, 1359, 1360f
 - immunofluorescence microscopy and immunohistochemistry
 - arteries, 1365
 - glomeruli, 1360–1361, 1364f–1365f
 - peritubular capillaries, 1361–1362, 1364–1365, 1365f
 - tubules, 1361
 - light microscopy
 - glomeruli, 1360, 1361f
 - interstitium, 1360, 1363f
 - tubules, 1360, 1362f–1363f
 - vessels, 1360, 1363f, 1364f
 - pathogenesis, 1367
 - prevalence, 1359
 - prognosis, 1368, 1369f
 - risk factors, 1359
 - therapy, 1368–1369
- acute ischemic injury
- clinical presentation, 1391
 - delayed graft function, 1389–1390
 - differential diagnosis, 1390
 - molecular correlation, 1390–1391
 - pathogenesis, 1390
 - pathologic findings, 1390
 - prognosis, 1391
 - therapy, 1391
- acute pyelonephritis, 1413
- acute T-cell-mediated rejection
- clinical course, 1350–1351
 - clinicopathologic correlations, 1350–1351, 1350f
 - differential diagnosis
 - glomerular lesions, 1350
 - tubulointerstitial inflammation, 1348–1350
 - vascular lesions, 1349–1350, 1349f
 - electron microscopy
 - glomeruli, 1341–1342, 1342f–1343f
 - interstitium, 1342
 - tubules, 1342, 1344f
 - vessels, 1342–1343
 - etiology and pathogenesis
 - antigens, 1344–1346
 - chemokines, 1346
 - pathogenetic mechanisms, 1346–1348
 - gross pathology, 1332, 1332f
 - immunofluorescence microscopy
 - glomeruli, 1340
 - interstitium, 1341
 - tubules, 1341, 1341f
 - vessels, 1341
 - light microscopy, 1322
 - glomeruli, 1333–1334, 1333f
 - interstitium, 1335–1336, 1336f, 1337f
 - tubules, 1334–1335, 1335f, 1336f
 - ureter and pelvis, 1340, 1340f
 - vessels, 1336–1370, 1337f–1340f
 - molecular studies, 1343–1344
 - prognosis, 1351
 - therapy, 1350–1351
- adenovirus infections, 1411–1413, 1412f
- allografts, drug-induced disease in
- acute tubulointerstitial nephritis, 1402
 - rapamycin-/sirolimus-associated toxic effects, 1402–1403, 1402f
- biopsies
- diagnosis
 - adequacy, 1326
 - Banff criteria and scoring system, 1326–1327, 1327t
 - pathologic classification, 1326, 1326t
 - value of, 1325
 - donor biopsies, 1327–1328
 - late graft biopsies, 1383–1385, 1383t
 - protocol biopsies, 1385–1389, 1386f, 1389f
 - safety, 1326
 - sensitivity and specificity, 1325–1326
- calcineurin inhibitor toxicity
- clinical presentation, 1400–1402, 1401f
 - differential diagnosis
 - arteriopathy, 1400
 - glomerulopathy, 1399–1400, 1400f
 - tubular lesions, 1397f, 1400
 - electron microscopy, 1398
 - etiology and pathogenesis, 1398–1399
 - immunofluorescence microscopy, 1398
 - immunosuppression, 1391
 - light microscopy
 - arterioles and arteries, 1395, 1396f, 1397f, 1398
 - glomeruli, 1391–1392, 1393f–1396f
 - interstitium, 1394–1395
 - tubules, 1394, 1394f
 - prognosis, 1400
 - therapy, 1400–1401
- chronic antibody-mediated rejection
- C4d deposition, 1381
 - C4d-negative AMR, 1381
 - clinical presentation, 1371–1372
 - clinical outcomes, 1381–1382
 - differential diagnosis, 1379–1381
 - electron microscopy
 - arteries, 1379
 - glomeruli, 1377–1378, 1377f–1378f
 - peritubular capillaries, 1378–1379, 1378f
 - etiology and pathogenesis, 1379
 - gross pathology, 1372, 1372f
 - immunofluorescence microscopy/immunohistochemistry
 - arteries, 1377
 - glomeruli, 1375, 1376f
 - peritubular capillaries, 1376–1377, 1376f
 - tubules, 1376
 - light microscopy
 - arteries, 1374–1375, 1375f
 - glomeruli, 1372–1373f
 - interstitium, 1372f–1373f, 1374
 - peritubular capillaries, 1373–1374, 1375f
 - tubules, 1372
 - molecular studies, 1379
 - natural history, 1381–1382
 - prevalence, 1371–1372
 - prognosis, 1379
 - risk factors, 1371–1372, 1379–1381
 - therapy, 1381–1382
 - smoldering/indolent AMR, 1381
- chronic T-cell-mediated rejection
- antigens, 1352–1353
 - B cells and plasma cells, 1353
 - C4d stains, 1354–1356
 - effector mechanisms, 1353–1354
 - clinical history, 1322–1323
 - clinical outcome
 - deceased donors, 1325
 - factors, graft survival, 1325
 - living donors, 1324–1325
 - cytomegaloviral infection, 1403, 1410–1411
 - de novo glomerular diseases
 - anti-GBM glomerulonephritis, in Alport syndrome, 1415, 114f
 - membranous glomerulopathy, 1415, 1416f
 - minimal change disease, 1418
 - nodular diabetic glomerulosclerosis, 1418
 - TMA, 1418
 - hyperacute rejection
 - clinical course, 1358–1359
 - clinical presentation, 1356
 - clinicopathologic correlations, 1358–1359
 - etiology and pathogenesis
 - antigens, 1357–1358
 - differential diagnosis, 1358
 - effector mechanisms, 1358
 - pathologic changes
 - electron microscopy, 1357, 1357f
 - gross pathology, 1356, 1356f
 - immunofluorescence microscopy and immunohistochemistry, 1356–1357, 1357f
 - light microscopy, 1356, 1357f
 - prognosis, 1358–1359
 - therapy, 1358–1359
 - Kaposi sarcoma, 1427
 - Merkel cell carcinoma, 1427–1428
 - molecular transplantation pathology, 1428–1431, 1429f–1431f
 - polyomavirus nephropathy
 - clinical presentation, 1409–1410, 1410f
 - diagnosis, 1403, 1403t
 - differential diagnosis, 1408–1409
 - electron microscopy, 1405f, 1407–1408
 - etiology and pathogenesis, 1408
 - gross pathology, 1404
 - immunofluorescence and immunohistochemistry, 1405, 1407, 1407f
 - light microscopy, 1404–1405, 1404f–1406f
 - prognosis, 1409–1410
 - therapy, 1409–1410
 - posttransplant lymphoproliferative disorders
 - definition, 1424
 - histologic categories and subtypes, 1425t
 - polymorphic and polyclonal variant, 1425, 1426t
 - prevalence, 1427
 - pregnancy, 842
 - recurrent glomerular diseases
 - C3 nephropathies
 - amyloidosis, 1422
 - antineutrophil cytoplasmic antibody-mediated diseases, 1422
 - atypical hemolytic uremic syndrome, 1420–1421
 - C3 glomerulonephritis, 1430
 - Henoch-Schönlein purpura, 1421
 - IgA nephropathy, 1421
 - membranous glomerulonephritis, 1421–1422, 1422f
 - systemic lupus erythematosus, 1422

- diagnosis of, 1418
 focal segmental glomerulosclerosis, 1419
 membranoproliferative glomerulonephritis, type I, 1420
 SCN, 1267–1268
 squamous cell carcinoma, 1427
 standard immunosuppression, 1323–1324
 surgical and miscellaneous complications
 arterial stenosis, 1414, 1412f, 1414f
 arterial/venous thrombosis, 1414
 graft rupture, 1414
 lymphocele, 1413–1414
 ureteral obstruction/leak/reflux, 1413–1414
 surgical procedure, 1323
 Renal tubular dysgenesis (RTD), 163–164, 164f
 Renal tubular epithelium, 105–106, 107f
 Renal tubules
 collecting duct, 52–58
 connecting tubule, 51
 distal tubule, 50–51
 proximal tubule, 46–48
 thin limb of Henle, 48–50
 Renal vascular disease, 114–115, 115t, 116f
 Renal vasculature, 6–10, 83–84
 Renal vein thrombosis (RVT)
 incidence of, 179
 membranoproliferative glomerulonephritis, 305
 membranous glomerulonephritis, 291
 membranous lupus nephritis, 596–597, 597f
 Renin-angiotensin system, 929
 Renomedullary interstitial cell tumor, 1486–1487, 1487f
 Retroperitoneum, 2
 Rhabdoid tumor, 1465–1466, 1466f
 Rhabdomyolysis, 452, 1170, 1200
 Rheumatoid arthritis (RA)
 anticitrullinated peptide antibodies, 629
 associated renal disease, 629, 631
 focal necrotizing and crescentic glomerulonephritis, 633–634
 membranous glomerulonephritis, 633
 mesangial proliferative glomerulonephritis, 633
 renal amyloidosis and crescentic glomerulonephritis, 634
 diagnosis, 629
 pathologic finding
 analgesic nephropathy
 anti-IL-6 agents, 632–633
 anti-TNF- α agents, 632
 cyclosporine-induced nephrotoxicity, 631
 gold salts/penicillamine, 631–632
 nonsteroidal anti-inflammatory agents, 631
 immune complex glomerulonephritis, 633
 secondary amyloidosis, 630–631, 630f
 Rifampicin, 1123
 Rituximab, lupus nephritis, 604
 RTD. *See* Renal tubular dysgenesis (RTD)
 RVT. *See* Renal vein thrombosis (RVT)
- S**
 Sarcoidosis, associated with MGN, 288–289
 Schimke immuno-osseous dysplasia, 239
 Secondary hypertension
 chronic renal parenchymal disease, 882–883
 obstructive sleep apnea, 888
 oral contraceptive agents, 888
 prevalence of, 873–874
 renal artery stenosis
 clinical course, 881–882
 clinical features, 874–875
 diagnosis, 875
 differential diagnosis
 fibromuscular dysplasia, 877–880, 878f, 879f
 Moyamoya disease, 881
 renal artery aneurysms, 880
 segmental arterial mediolysis, 881
 Takayasu disease, 880
 etiology and pathogenesis, 876–877
 pathologic findings
 cholesterol emboli, 876, 877f
 ipsilateral kidney, 876, 876f
 renal artery, 875–876, 875f
 prognosis, 881–882
 therapy, 882
 tumors and associated conditions
 adrenal cortical lesions
 congenital adrenal hyperplasia, 885
 Cushing syndrome, 885
 hyperaldosteronism, 884–885, 884t
 pathologic findings, 885–886, 886f
 angiolymphoid hyperplasia with eosinophilia, 888
 Bartter syndrome
 clinical features, 886
 pathologic findings, 886
 Juxtaglomerular cell tumors, 886–887, 887f
 miscellaneous tumors, 888
 nephroblastoma (Wilms tumor), 887
 neuroblastoma, 887
 pheochromocytoma
 clinical features and diagnosis, 883–884
 familial syndromes and mutations, 883
 pathologic findings, 884, 884f
 renal cell carcinoma, 887–888
 Segmental arterial mediolysis, 881
 Segmental membranous glomerulonephritis, 595
 Shiga toxins, 767–769
 Sialidosis, 1235
 Sicking disorders
 clinical course and prognosis
 chronic renal failure, 1266
 multifactorial/pleiotropic genes, 1265–1266
 clinical presentation
 acute renal failure, 1259
 altered glomerular function, 1258
 hyperfunctioning proximal tubules, 1259
 hyposthenuria, 1258
 hypotension, 1259
 incomplete renal tubular acidosis, 1259
 drug therapy
 angiotensin-converting enzyme inhibitors, 1266–1267
 dialysis and renal transplantation, 1267–1268
 hematopoietic cell transplantation, 1268
 hydroxyurea, 1267
 nonsteroidal anti-inflammatory agents, 1266
 novel therapies, 1267
 etiology and pathogenesis
 renal cortical alterations, 1265
 renal medullary alterations, 1264–1265
 sickling cells, 1264
 gross pathology, 1259–1260, 1260f
 hematuria
 clinical presentation, 1259
 treatment of, 1266
 malignancies
 differential diagnosis, 1264
 pathologic change, 1262–1264, 1264f
 microscopic pathology
 glomerular abnormalities, 1261–1262, 1261f
 tubulointerstitial abnormalities, 1260, 1260f
 vascular abnormalities, 1260
 mouse models of, 1268
 Silent lupus nephritis, 608
 Sirolimus, 1173
 Sjögren syndrome (SS)
 associated diseases, 627
 characterization, 626, 1141
 clinical renal presentation, 627
 diagnosis, 627
 pathologic findings
 IgG, semilinear tubular basement membrane deposits, 628, 628f
 membranoproliferative glomerulonephritis, 628, 629
 tubulointerstitial nephritis, 627–628, 628f
 prognosis, 629
 therapy, 629
 SLE. *See* Systemic lupus erythematosus (SLE)
 Smith-Lemli-Opitz syndrome, 144
 Solid organ transplantation
 antibody-mediated rejection, 751
 calcineurin inhibitors, 751
 clinical-laboratory features, 752
 complement regulatory abnormalities, 751
 incidence of, 752
 recurrence rate, 752
 viral infection, 752
 Soluble urinary plasminogen activator receptor (suPAR), 231, 1419
 Squamous cell carcinoma (SCC), 286, 1427, 1481
 Standard immunosuppression, 1323–1324
Streptococcus pneumoniae infection, 743, 772
Streptococcus pyogenes
 causes of, 369–370
 identification, 370
 M proteins, 370–371
 pathology, 370
 Striped fibrosis, 115
 Stroma, of kidney development, 84–85
 Sulfonamides, 1123
 Symptomatic bacteriuria, 817–818
 Syndecan, 45–46, 47f
 Syndromic acute tubular injury
 cardiorenal syndrome, 1204
 hepatorenal syndrome, 1203–1204
 sepsis, in ARF, 1203
 Sympyaryngeal nephritis, 372
 Syphilis, 288
 Systemic karyomegaly, 1151
 Systemic lupus erythematosus (SLE)
 activity and chronicity index, 598–600, 599t
 amyloidosis, 609
 ANA-negative lupus nephritis, 608
 ANCA, 608
 clinical course, 605–607

- Systemic lupus erythematosus (SLE) (*Continued*)
- clinical presentation
 - arthralgias/arthritides, 601
 - cardiovascular/neurologic manifestations, 601
 - constitutional symptoms, 600
 - discoid skin lesions, 600–601
 - hematologic abnormalities, 601
 - pleuritis, 601
 - renal complication, 560
 - dialysis and transplantation, 607–608
 - drug-induced lupus
 - clinical presentation, 609–610
 - diagnosis, 609
 - pathogenesis, 610
 - serology, 609
 - HIV infection, 610
 - lupus podocytopathy, 608–609
 - medical history, 559–560
 - pathogenesis, 610
 - cross-reactivity
 - coagulation abnormalities, 624
 - complement system, 621
 - immune cells and soluble factors, 621–624
 - lupus autoantibodies, 621
 - defective apoptosis, 617
 - exogenous factors, 616–617
 - genetic factors, 612, 613t–614t, 615–616
 - immunologic abnormalities
 - antibody specificities, 618–619
 - autoantibodies, 617–618
 - immune complex deposition
 - mechanisms, 620
 - immunoglobulin characteristics, 619–620
 - Mendelian risk factors, 616
 - murine model
 - BXSB/MpJ model, 611–612
 - chronic graft *vs.* host disease model, 612
 - MRL/lpr model, 611–612
 - NZB/W and NZW models, 611
 - SNF1 model, 611
 - susceptibility genes, 612
 - sex hormones, 617
 - in situ immune complex formation, 620–621
 - transcriptomal studies, 616
 - pathologic findings
 - electron microscopy
 - diffuse proliferative glomerulonephritis, 579, 579f
 - discrete crater-like deformities, 581, 581f
 - fingerprint substructure, 579, 580f, 581
 - fingerprint-whorled, lamellated substructure, 579, 580f
 - glomerular proteinuria, 582–583
 - hematoxylin body, 581–582, 582f
 - interferon footprints, 582
 - intracellular tubuloreticular inclusions, 582, 582f
 - glomeruli
 - cellular crescents, 567–568, 568f
 - endocapillary hypercellularity, 566, 567f
 - global subendothelial fuchsinophilic deposits, 564, 564f
 - glomerular scarring, 568–569, 568f
 - glomerular thrombi, 566
 - hematoxylin bodies, 567, 568f
 - hyaline thrombi, 565–566, 565f, 566f
 - mesangial hypercellularity, 566
 - necrosis, 566–567, 567f
 - numerous subendothelial deposits, 564, 565f
 - wire loops, 564, 564f
 - gross pathology, 563
 - immunofluorescence microscopy
 - different antisera, 577–578, 577t
 - properdin, 578, 578f
 - tubular antinuclear antibody reactivity, 578–579, 578f
 - light microscopy, 563
 - tubulointerstitial immune deposits
 - class IV and class III lupus nephritis, 569
 - electron microscopy, 570–571, 570f, 571f
 - immunofluorescence study, 570, 571f
 - infiltrating mononuclear leukocytes, 569–570
 - tubular atrophy, 571
 - vascular lesions
 - hemolytic uremic syndrome, 574–575
 - lupus anticoagulant/APL syndrome. *See* Antiphospholipid syndrome
 - morphologic forms, 571–572, 572t
 - noninflammatory necrotizing vasculopathy, 573, 573f
 - renal vasculitis, 577
 - thrombotic microangiopathy, 573–574, 575f
 - thrombotic thrombocytopenic purpura, 574–575
 - uncomplicated vascular immune deposits, 572, 572f, 573f
 - prognosis, 605–607
 - recurrence, 1421, 1421f
 - renal biopsy, 561–563
 - silent lupus nephritis, 608
 - therapeutic management
 - abatacept, 604–605
 - belimumab, 604
 - corticosteroids, 601–602
 - focal and diffuse lupus nephritis
 - advanced sclerosing lupus nephritis, 604
 - induction therapy, 602–603
 - maintenance therapy, 603–604
 - membranous lupus nephritis, 604
 - infliximab, 605
 - intravenous immunoglobulin, 605
 - leflunomide, 605
 - mesangial lupus nephritis, 602
 - ocrelizumab, 605
 - plasmapheresis, 605
 - rituximab, 604
 - TMA, 750
 - TMB, 120
 - WHO classification
 - fluorescence and electronmicroscopic study, 561, 562t
 - immune deposits distribution, 561, 563f
 - ISN/RPS classification, 561, 562t
 - advanced sclerosing lupus nephritis, 597, 597f
 - diffuse lupus nephritis, 588–593, 588f–592f, 593t
 - focal lupus nephritis, 586–588, 586f–588f
 - histologic patterns, 583, 583t
 - membranous lupus nephritis, 593–597, 594f–597f
 - mesangial proliferative lupus nephritis, 584–586, 585f
 - minimal mesangial lupus nephritis, 584, 584f
 - reproducibility, 600
 - transformations, 597–598, 597t
 - modified WHO classification, 560–561, 561t
 - original WHO classification, 560, 560t
- Systemic sclerosis (systemic scleroderma)
- abnormal microvasculature, 784
 - animal models, 786
 - arterial intimal hyperplasia, 784
 - chronic forms, 777, 780–782
 - classification, 775–776
 - clinical presentation, 776
 - electron microscopy, 780, 781f
 - epidemiology, 776
 - genetic and epigenetic factors, 783
 - gross appearance, 777, 777f
 - hypertension and morphologic vascular changes, 782
 - immunofluorescence microscopy, 780, 781f
 - inflammation and immune factors, 784–785
 - light microscopy
 - arteries and arterioles, 778–779, 779f–780f
 - glomeruli, 778, 778f
 - interstitium, 779–780, 780f
 - tubules, 779
 - renal involvement, 776–777
 - vascular abnormalities
 - endothelial damage, 783
 - functional vasoconstriction, 784
 - permeability, 783–784
 - platelet activation and intravascular coagulation, 784
- Systemic vasculitis, 715–717, 715t–717t
- T**
- T-regulatory cells (T-regs), 189
 - Takayasu arteritis
 - clinical course, 733
 - clinical presentation, 731
 - differential diagnosis, 732–733
 - etiology and pathogenesis, 732
 - pathologic findings
 - gross pathology, 731
 - light microscopy, 731–732, 732f
 - prognosis, 733
 - therapy, 733
 - Takayasu disease, 880
 - Temporal arteritis, 721
 - Tetraspanin, 229, 233t, 553
 - Thin glomerular basement membrane lesion, 542–543, 544f
 - Thin limb of henle, 48–50
 - Thrombotic microangiopathy (TMA)
 - classification, 741–745, 741t–742t
 - de novo glomerular diseases, 1418
 - drugs, 750–751
 - fibrin/fibrinolysis, 397
 - glomerular diseases, 753
 - hematopoietic stem cell transplantation
 - animal models, 795–796
 - clinical presentation, 794

- etiology and pathogenesis, 795
- pathologic findings, 789f, 794–795, 794f
- treatment, 796
- hemolytic uremic syndrome, 134, 450–451
- historical background and nomenclature, 740–741
- human immunodeficiency virus, 749–750
- HUS. *See* Hemolytic-uremic syndrome (HUS)
- ischemic glomerulosclerosis, 573–574, 575f
- malignancy, 753
- malignant hypertension, 753
- microangiopathic hemolytic anemia, 745
- pathologic findings
 - antiphospholipid antibody syndrome, 763–764
 - arteriolar and arterial changes, 763
 - clinical findings and prognosis, 766
 - clinical outcomes, 764–766
 - differential diagnosis, 761, 763
 - electron microscopy, 761, 762f–765f
 - gross appearance, 754
 - immunofluorescence microscopy, 760–761, 760f, 761f
 - light microscopy
 - arteries and arterioles, 758–760, 758f–760f
 - glomeruli, 754–758, 754f–758f
 - interstitium, 760
 - tubules, 760
 - renal morphologic features, 754, 754t
- pregnancy, 752–753
- radiation nephropathy
 - clinical presentation and clinical course
 - acute radiation nephropathy, 787
 - asymptomatic proteinuria, 788
 - benign hypertension, 788
 - chronic radiation nephropathy, 788
 - malignant hypertension, 788
 - electron microscopy, 790
 - etiology and pathogenesis
 - experimental studies, 790–791
 - hypertension, 791–792
 - irradiation, dosage of, 792–793
 - gross appearance, 788
 - historical review, 787
 - immunofluorescence microscopy, 789
 - light microscopy
 - blood vessels, 789, 789f
 - glomeruli, 788–789, 789f
 - tubules and interstitium, 789
 - radionuclide therapy, 796–797
- solid organ transplantation, 751
 - antibody-mediated rejection, 751
 - calcineurin inhibitors, 751
 - clinical-laboratory features, 752
 - complement regulatory abnormalities, 751
 - recurrence rate, 752
 - viruses, 752
- systemic infections, 749
- systemic lupus erythematosus, 750
- systemic sclerosis (systemic scleroderma)
 - abnormal microvasculature, 784
 - animal models, 786
 - arterial intimal hyperplasia, 784
 - chronic forms, 777, 780–782
 - classification, 775–776
 - electron microscopy, 780, 781f
 - epidemiology and clinical presentation, 776
 - genetic and epigenetic factors, 783
 - gross appearance, 777, 777f
 - hypertension and morphologic vascular changes, 782
 - immunofluorescence microscopy, 780, 781f
 - inflammation and immune factors, 784–785
 - light microscopy
 - arteries and arterioles, 778–779, 779f–780f
 - glomeruli, 778, 778f
 - interstitium, 779–780, 780f
 - tubules, 779
 - renal involvement, 776–777
 - vascular abnormalities
 - endothelial damage, 783
 - functional vasoconstriction, 784
 - permeability, 783–784
 - platelet activation and intravascular coagulation, 784
- thrombocytopenia, 745
- thrombotic thrombocytopenic purpura
 - antiphospholipid antibodies, 774–775
 - clinical features, 748
 - clinical signs and symptoms, 749
 - coagulation disturbances, 773
 - complement abnormalities, 773
 - endothelial damage, 767
 - vs.* HUS, 744–745
 - platelet activation and aggregation, 773
 - relapses and recurrences, 749
 - systemic infections, 773
 - triggering events, 749
 - von Willebrand factor and AdAMTS13 abnormalities, 772
- treatment, 775
- Thrombotic thrombocytopenic purpura (TTP)
 - antiphospholipid antibodies, 774–775
 - clinical features, 748
 - clinical signs and symptoms, 749
 - coagulation disturbances, 773
 - complement abnormalities, 773
 - endothelial damage, 767
 - vs.* HUS, 744–745
 - platelet activation and aggregation, 773
 - pathologic findings
 - arteriolar and arterial changes, 763–764
 - clinical findings and prognosis, 766
 - differential diagnosis, 761, 763
 - electron microscopy, 761, 763f–765f
 - gross appearance, 754, 754t
 - immunofluorescence microscopy, 760–761, 760f
 - light microscopy
 - arteries and arterioles, 758–760, 758f–760f
 - glomeruli, 754–758, 754f–758f
 - interstitium, 760
 - tubules, 760
 - microscopic features, 754, 754t
 - outcome and prognostic features, 764–766
 - relapses and recurrences, 749
 - systemic lupus erythematosus, 574–575
 - triggering events, 749
 - von Willebrand factor and AdAMTS13 abnormalities, 772
- Thymic stromal lymphopoietin (TSLP), 327
- Thyroiditis, 289–290
- TMA. *See* Thrombotic microangiopathy (TMA)
- TNF-like weak inducer of apoptosis (TWAK), 624
- Tonsillectomy, 494
- Transforming growth factor- β 1, 920–921
- Transient receptor potential cation channel, 233t, 237
- Transitional epithelium, 12
- Translocation carcinomas, 1467, 1467f
- Transplantation. *See* Renal transplantation
- Tubulointerstitial nephritis and uveitis (TINU), 1143–1144, 1144f
- TRIs. *See* Tubuloreticular inclusions (TRIs)
- True inflammatory vasculitis, 577, 577f
- TSC. *See* Tuberos sclerosis (TSC)
- TSLP. *See* Thymic stromal lymphopoietin (TSLP)
- TTP. *See* Thrombotic thrombocytopenic purpura (TTP)
- Tuberos sclerosis (TSC)
 - clinical presentation and genetics, 146
 - differential diagnosis, 147
 - incidence, 145–146
 - pathogenesis, 147
 - pathology, 146, 146f, 147f
- Tubular and interstitial abnormalities
 - acute
 - clinical history, 452
 - clinical presentation, 451
 - etiology and pathogenesis, 452, 453t
 - pathology
 - gross pathology, 451
 - intratubular crystals, 451, 452f
 - tenofovir-induced mitochondrial injury, 451, 453f
 - chronic
 - clinical history, 454
 - clinical presentation, 453
 - etiology and pathogenesis, 454
 - pathology, 453–454
- Tubular atrophy, 109, 110f
- Tubular basement membrane (TBM)
 - changes, 110–111, 112f
 - deposits, 111f
- Tubular casts, 104t, 108, 442f
- Tubular disease
 - acute tubular injury, 104–105
 - heavy metal poisoning, 105–106, 107f
 - hemosiderin, 105–106, 107f
 - hyaline droplet change, 105, 107f
 - mitochondrial abnormalities, 110
 - renal tubular epithelium, pigments in, 105–106, 107f
 - tubular atrophy, 109, 110f
 - tubular basement membrane changes, 110–111, 112f
 - tubular casts, 108
 - tubulitis, 108, 109f
 - vacuolar change, 105
 - viral intranuclear inclusions, 106, 108
- Tubular dysgenesis. *See* Renal tubular dysgenesis
- Tubulitis, 108, 109f
- Tubulocystic carcinoma, 1479, 1479f
- Tubulointerstitial nephritis (TIN)
 - anti-TBM antibody disease
 - etiology and pathogenesis, 1136
 - pathologic findings, 1136
 - secondary, 1134–1136

- Tubulointerstitial nephritis (TIN) (*Continued*)
- aristolochic acid (Chinese herb) nephropathy, 1153–1154, 1153f
 - Balkan endemic nephropathy
 - clinical presentation, 1152
 - pathogenesis, 1152–1153
 - pathologic findings, 1152, 1153f
 - causes/etiologic agents, 1112
 - classification, 1112
 - with drug reactions
 - analgesic nephropathy
 - 5-aminosalicylic acid, 1132
 - clinical presentation, 1128
 - differential diagnosis, 1130
 - incidence, 1127–1128
 - pathogenesis, 1130–1132, 1131f
 - pathologic findings, 1128–1130, 1129f–1130f
 - urothelial cancer/analgesic abuse, 1132, 1132f
 - antimicrobial agents
 - cephalosporins, 1121–1122
 - fluoroquinolones, 1122
 - penicillins, 1122–1123
 - rifampicin, 1123
 - sulfonamides, 1123
 - vancomycin, 1123–1124
 - clinical course, 1121
 - clinical features, 1119
 - diphenylhydantoin, 1132
 - electron microscopy, 1120
 - etiology and pathogenesis, 1120–1121
 - gross findings, 1119
 - immunopathology, 1120
 - light microscopy
 - glomeruli, 1119–1120
 - interstitium, 1120, 1120t
 - tubules, 1120
 - vessels, 1120
 - lithium, 1132–1133
 - NSAIDs
 - clinical presentation, 1125
 - incidence, 1124–1125
 - pathogenesis, 1126–1127
 - pathology, 1126
 - risk factors, 1125–1126
 - protease inhibitors, 1133
 - proton pump inhibitors, 1133
 - heavy metal exposure
 - cadmium nephropathy, 1147–1148
 - lead nephropathy, 1146–1147
 - mercury nephropathy, 1148–1149
 - miscellaneous heavy metal nephropathy, 1149
 - hereditary diseases, 1150–1151, 1150f
 - idiopathic TIN, 1154
 - immune complexes
 - pathogenesis, 1142–1143
 - pathology, 1142
 - primary, 1136–1137
 - secondary
 - dense deposit disease, 1141–1142
 - familial immune complex tubulointerstitial nephritis, 1142
 - giant cell tubulitis, 1142
 - hypocomplementemic urticarial vasculitis syndrome, 1142
 - IgG4-related disease, 1137–1141, 1138f, 1139f, 1140t
 - membranoproliferative glomerulonephritis, 1141–1142
 - membranous glomerulonephritis, 1142
 - mixed cryoglobulinemia, 1142
 - Sjögren syndrome, 1141
 - systemic lupus erythematosus, 1141
 - incidence, 1112
 - metabolic disorders/monoclonal gammopathies, 1146
 - monoclonal light chain mediated
 - clinical history, 963
 - clinical presentation, 963
 - differential diagnosis, 964
 - electron microscopy, 964
 - etiology and pathogenesis, 964
 - gross pathology, 963
 - immunofluorescence, 964
 - immunohistochemistry, 964, 964f
 - laboratory findings, 963
 - light microscopy, 963–964, 963f
 - prognosis, 964–965
 - treatment, 964–965
 - pathogenesis, 1118, 1119f
 - primary tubulointerstitial nephritis
 - clinical presentation, 1112–1113
 - pathology
 - acute TIN, 1113–1115, 1114f–1115f
 - chronic TIN, 1115–1117, 1116f–1118f
 - T-cell mechanisms, 1143–1146, 1143f
 - secondary, 1112, 1145
 - systemic karyomegaly, 1151
 - terminology, 1111–1112
 - Tubulointerstitial nephritis and uveitis (TINU), 1143–1144, 1144f
 - Tubuloreticular inclusions (TRIs), 582, 582f, 596
 - Turner syndrome, 134, 135f
 - Type III hyperlipoproteinemia, 1228
 - Type IV collagen diseases, 543
- U**
- Unipapillary kidney, 16f
 - Ureteric bud-collecting duct development
 - branching morphogenesis, 82
 - renal pelvis and ureter, 82–83
 - Urinary tract infections
 - asymptomatic/covert bacteriuria, 817
 - incidence and risk factors, 816–817
 - symptomatic bacteriuria and pyelonephritis, 817–818
 - Uromodulin (Tamm–Horsfall protein)
 - nephropathy, 108, 137, 1253–1255, 1254f
 - Urothelial carcinoma, 1480–1481, 1481f
 - Urothelium, 12, 74f, 1481
- V**
- Vancomycin, 1123–1124, 1172
 - Vascular endothelial growth factor (VEGF)
 - characteristics, 921
 - endothelial cell function, 33
 - endothelial fenestration, 174
 - GVHD, 795
 - mouse kidney defects, 76t
 - preeclampsia, 833
 - renal blood vessels, 84
 - TMA, 750–751
 - Vena cava, human kidneys with, 10f
 - Ventriculoatrial shunt
 - causative organisms, 424
 - clinical course and outcome, 426
 - clinical presentation, 425
 - etiology and pathogenesis, 425–426
 - pathologic findings, 425, 425f
 - shunt nephritis, 425
 - Verotoxin-producing *E. coli* infection, 746–747
 - VHL. *See* von Hippel-lindau disease (VHL)
 - Viral nephropathies
 - actinomycosis, 1066
 - AKI, in H1N1 infection, 1066
 - amoebiasis, 1070
 - clinical course, 1070
 - clinical presentation, 1068
 - Coxsackievirus infection, 1066
 - cytomegalovirus nephritis, 1063, 1063f
 - echinococcal infection (hydatid disease), 1070
 - Epstein-Barr virus infection, 1061
 - etiology and pathogenesis, 1069
 - filariasis, 1070
 - Hantavirus infection, 1064–1065, 1065f
 - leishmania, 1070–1071
 - leptospirosis, 1067–1068
 - malarial infection, 1068
 - microsporidiosis, 1070
 - nocardiosis, 1066
 - parasitic infections, 1068
 - Parvovirus infection, 1065–1066
 - pathogenesis and tropism, 1060–1061
 - pathologic findings, 1068–1069, 1068f
 - posttransplant lymphoproliferative disorders, 1061–1063, 1062f
 - prognosis and therapy, 1070
 - rickettsial infections, 1066–1067, 1067f
 - schistosomiasis, 1069–1070
 - syphilis, 1066
 - viral hemorrhagic fever, 1065
 - Vitamin disorders, 1236–1237
 - von Hippel-lindau disease (VHL)
 - incidence, clinical presentation and genetics, 144, 144f
 - pathogenesis, 145
 - pathology, 144–145, 144f, 145f
 - prognosis and management, 145
 - von Willebrand factor, 772
- W**
- Waldenström macroglobulinemia (WM)
 - clinical history, 1000
 - clinical presentation and laboratory findings, 1000–1001
 - differential diagnosis, 1002
 - electron microscopy, 1002
 - gross pathology, 1001
 - immunofluorescence, 1002
 - light microscopy, 1001–1002, 1001f
 - transplantation, 1002
 - prognosis, 1002
 - treatment, 1002
 - Williams syndrome, 1090
 - Wilms tumor
 - clinical findings and epidemiology, 1461–1462
 - pathology, 1462–1463, 1463f
 - treatment and outcome, 1463
 - tumor gene, 154–155
- Z**
- Zero-hour implantation biopsies, 1327–1331